Scientific Programming

Scientific Evolution in Human-Computer Interaction for Modern Information Systems in IoT

Lead Guest Editor: Juan Vicente Capella Hernandez
Guest Editors: Mustafa M Matalgah and Mahasweta Sarkar

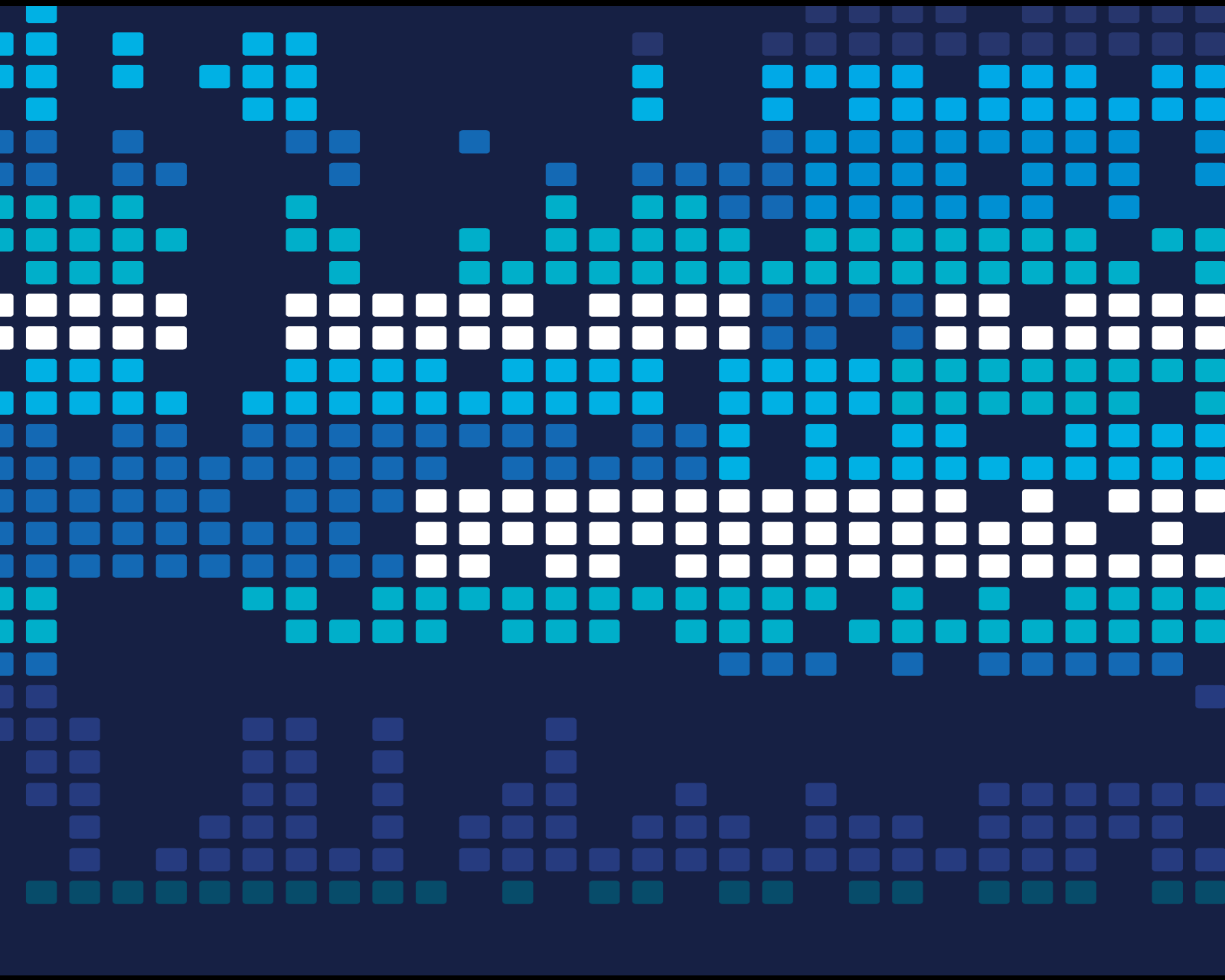

Scientific Evolution in Human-Computer Interaction for Modern Information Systems in IoT

Scientific Programming

Scientific Evolution in Human-Computer Interaction for Modern Information Systems in IoT

Lead Guest Editor: Juan Vicente Capella Hernandez
Guest Editors: Mustafa M Matalgah and Mahasweta Sarkar

Contents

Contents

Contents

Hindawi
Scientific Programming
Volume 2023, Article ID 9871479, 1 page
https://doi.org/10.1155/2023/9871479

Retraction

Retracted: Intelligent Piano Teaching Based on Internet of Things Technology and Multimedia Technology

Scientific Programming

Received 1 August 2023; Accepted 1 August 2023; Published 2 August 2023

This article has been retracted by Hindawi following an investigation undertaken by the publisher [1]. This investigation has uncovered evidence of one or more of the following indicators of systematic manipulation of the publication process:

(1) Discrepancies in scope
(2) Discrepancies in the description of the research reported
(3) Discrepancies between the availability of data and the research described
(4) Inappropriate citations
(5) Incoherent, meaningless and/or irrelevant content included in the article
(6) Peer-review manipulation

The presence of these indicators undermines our confidence in the integrity of the article's content and we cannot, therefore, vouch for its reliability. Please note that this notice is intended solely to alert readers that the content of this article is unreliable. We have not investigated whether authors were aware of or involved in the systematic manipulation of the publication process.

Wiley and Hindawi regrets that the usual quality checks did not identify these issues before publication and have since put additional measures in place to safeguard research integrity.

We wish to credit our own Research Integrity and Research Publishing teams and anonymous and named external researchers and research integrity experts for contributing to this investigation.

The corresponding author, as the representative of all authors, has been given the opportunity to register their agreement or disagreement to this retraction. We have kept a record of any response received.

References

[1] Y. Xu, "Intelligent Piano Teaching Based on Internet of Things Technology and Multimedia Technology," *Scientific Programming*, vol. 2022, Article ID 8774340, 9 pages, 2022.

Hindawi
Scientific Programming
Volume 2023, Article ID 9867242, 1 page
https://doi.org/10.1155/2023/9867242

Retraction

Retracted: Application and Performance Discussion of Fiber-Reinforced Composite Materials in Sports Equipment Based on Image Processing Technology

Scientific Programming

Received 1 August 2023; Accepted 1 August 2023; Published 2 August 2023

This article has been retracted by Hindawi following an investigation undertaken by the publisher [1]. This investigation has uncovered evidence of one or more of the following indicators of systematic manipulation of the publication process:

(1) Discrepancies in scope
(2) Discrepancies in the description of the research reported
(3) Discrepancies between the availability of data and the research described
(4) Inappropriate citations
(5) Incoherent, meaningless and/or irrelevant content included in the article
(6) Peer-review manipulation

The presence of these indicators undermines our confidence in the integrity of the article's content and we cannot, therefore, vouch for its reliability. Please note that this notice is intended solely to alert readers that the content of this article is unreliable. We have not investigated whether authors were aware of or involved in the systematic manipulation of the publication process.

Wiley and Hindawi regrets that the usual quality checks did not identify these issues before publication and have since put additional measures in place to safeguard research integrity.

We wish to credit our own Research Integrity and Research Publishing teams and anonymous and named external researchers and research integrity experts for contributing to this investigation.

The corresponding author, as the representative of all authors, has been given the opportunity to register their agreement or disagreement to this retraction. We have kept a record of any response received.

References

[1] E. Liu, "Application and Performance Discussion of Fiber-Reinforced Composite Materials in Sports Equipment Based on Image Processing Technology," *Scientific Programming*, vol. 2022, Article ID 6879601, 12 pages, 2022.

Hindawi
Scientific Programming
Volume 2023, Article ID 9849732, 1 page
https://doi.org/10.1155/2023/9849732

Retraction

Retracted: BDA of the Dissemination of Opera in the Internet Self-Media Environment

Scientific Programming

Received 1 August 2023; Accepted 1 August 2023; Published 2 August 2023

This article has been retracted by Hindawi following an investigation undertaken by the publisher [1]. This investigation has uncovered evidence of one or more of the following indicators of systematic manipulation of the publication process:

(1) Discrepancies in scope
(2) Discrepancies in the description of the research reported
(3) Discrepancies between the availability of data and the research described
(4) Inappropriate citations
(5) Incoherent, meaningless and/or irrelevant content included in the article
(6) Peer-review manipulation

The presence of these indicators undermines our confidence in the integrity of the article's content and we cannot, therefore, vouch for its reliability. Please note that this notice is intended solely to alert readers that the content of this article is unreliable. We have not investigated whether authors were aware of or involved in the systematic manipulation of the publication process.

Wiley and Hindawi regrets that the usual quality checks did not identify these issues before publication and have since put additional measures in place to safeguard research integrity.

We wish to credit our own Research Integrity and Research Publishing teams and anonymous and named external researchers and research integrity experts for contributing to this investigation.

The corresponding author, as the representative of all authors, has been given the opportunity to register their agreement or disagreement to this retraction. We have kept a record of any response received.

References

[1] X. Xie, "BDA of the Dissemination of Opera in the Internet Self-Media Environment," *Scientific Programming*, vol. 2022, Article ID 3096890, 12 pages, 2022.

Hindawi
Scientific Programming
Volume 2023, Article ID 9821785, 1 page
https://doi.org/10.1155/2023/9821785

Retraction

Retracted: Research on the Flow Control of a Piston Cooling Nozzle

Scientific Programming

Received 1 August 2023; Accepted 1 August 2023; Published 2 August 2023

This article has been retracted by Hindawi following an investigation undertaken by the publisher [1]. This investigation has uncovered evidence of one or more of the following indicators of systematic manipulation of the publication process:

(1) Discrepancies in scope
(2) Discrepancies in the description of the research reported
(3) Discrepancies between the availability of data and the research described
(4) Inappropriate citations
(5) Incoherent, meaningless and/or irrelevant content included in the article
(6) Peer-review manipulation

The presence of these indicators undermines our confidence in the integrity of the article's content and we cannot, therefore, vouch for its reliability. Please note that this notice is intended solely to alert readers that the content of this article is unreliable. We have not investigated whether authors were aware of or involved in the systematic manipulation of the publication process.

Wiley and Hindawi regrets that the usual quality checks did not identify these issues before publication and have since put additional measures in place to safeguard research integrity.

We wish to credit our own Research Integrity and Research Publishing teams and anonymous and named external researchers and research integrity experts for contributing to this investigation.

The corresponding author, as the representative of all authors, has been given the opportunity to register their agreement or disagreement to this retraction. We have kept a record of any response received.

References

[1] X. Zeng, J. Zhang, L. Li, G. Hu, and W. Xie, "Research on the Flow Control of a Piston Cooling Nozzle," *Scientific Programming*, vol. 2022, Article ID 9283300, 9 pages, 2022.

Hindawi
Scientific Programming
Volume 2023, Article ID 9796780, 1 page
https://doi.org/10.1155/2023/9796780

Retraction

Retracted: Algorithmic Application of Evidence Theory in Recommender Systems

Scientific Programming

Received 1 August 2023; Accepted 1 August 2023; Published 2 August 2023

This article has been retracted by Hindawi following an investigation undertaken by the publisher [1]. This investigation has uncovered evidence of one or more of the following indicators of systematic manipulation of the publication process:

(1) Discrepancies in scope
(2) Discrepancies in the description of the research reported
(3) Discrepancies between the availability of data and the research described
(4) Inappropriate citations
(5) Incoherent, meaningless and/or irrelevant content included in the article
(6) Peer-review manipulation

The presence of these indicators undermines our confidence in the integrity of the article's content and we cannot, therefore, vouch for its reliability. Please note that this notice is intended solely to alert readers that the content of this article is unreliable. We have not investigated whether authors were aware of or involved in the systematic manipulation of the publication process.

Wiley and Hindawi regrets that the usual quality checks did not identify these issues before publication and have since put additional measures in place to safeguard research integrity.

We wish to credit our own Research Integrity and Research Publishing teams and anonymous and named external researchers and research integrity experts for contributing to this investigation.

The corresponding author, as the representative of all authors, has been given the opportunity to register their agreement or disagreement to this retraction. We have kept a record of any response received.

References

[1] L. Ma, "Algorithmic Application of Evidence Theory in Recommender Systems," *Scientific Programming*, vol. 2022, Article ID 9290577, 11 pages, 2022.

Hindawi
Scientific Programming
Volume 2022, Article ID 9048584, 12 pages
https://doi.org/10.1155/2022/9048584

Research Article

China-Laos Economic and Trade Cooperation and Construction of Sustainable Energy Cargo Channel under the Background of "One Belt, One Road"

Sonexay Phompida and Donghua Yu

School of Economics, Shandong University, Jinan 250000, Shandong, China

Correspondence should be addressed to Sonexay Phompida; 2016123713@jou.edu.cn

Received 17 June 2022; Revised 1 September 2022; Accepted 7 September 2022; Published 14 October 2022

Academic Editor: Juan Vicente Capella Hernandez

With the increasing import volume of China's oil and natural gas, the structure of China's energy supply chain (ESC) has become more and more complex. How to use the "Belt and Road" (OBOR) layout to promote China's regional energy cooperation and ensure China's energy security has become an important international issue facing China. This paper constructs an ESC network model in the context of the OBOR, and finds out the position of China in this network model. This paper also finds out the role law of each risk influencing factor, analyzes the degree of its influence, and puts forward some suggestions on the risk management of ESC according to the analysis results. This paper proposes to use decision tree algorithm to guide the development and construction of Sino-Lao economic and trade cooperation, which will help analyze and help the construction and research of Sino-Lao economic and trade cooperation and sustainable energy freight corridor. Based on the energy cooperation between China and the countries along the "Belt and Road," this paper analyzes the network structure of energy cooperation under the "Belt and Road" background based on the small-world network theory. This paper analyzes the important role of core countries in the ESC through the analysis of the basic parameters of the small-world network, the efficiency of energy cooperation, and the stability of energy cooperation. According to the value of each vertex degree obtained by the calculation formula of entropy value, the entropy value of the ESC network structure under the background of OBOR can be obtained as 2.408. It calculates that the maximum and minimum entropy of the ESC network structure at this time are 3.09 and 2.21 respectively.

1. Introduction

One Belt and One Road is the abbreviation of Silk Road Economic Belt and twenty-first Century Maritime Silk Road, relying on the established bilateral and multilateral mechanisms between China and the countries concerned, with the help of established and proven regional cooperation platforms, the Belt and Road aims to borrow the historical symbols of the ancient Silk Road, hold high the banner of peaceful development, actively develop economic partnerships with The Belt and Road aims to borrow the historical symbol of the ancient Silk Road, hold high the banner of peaceful development, actively develop economic partnerships with countries along the route, and jointly build a community of interests, destiny and responsibility with mutual political trust, economic integration and cultural tolerance. In the regions along the "Belt and Road," the United States, Russia, and India have greater influence and have extensive interests in the region. In the era of economic globalization, the "Belt and Road" cooperation promoted by China will more or less compete and conflict with the interests of the above three countries. The security situation in some of these countries is even worsening. All of these potential dangers may cause disruption of the ESC in the context of China's "One Belt, One Road" (OBOR) initiative, bringing risks to China's energy supply. At present, although all circles of Laos and China have initially achieved certain results in the research on the issue of the "Belt and Road Initiative" and the "Development of Laos-China Economic and Trade Relations under the Cooperation Framework of

the ASEAN Free Trade Area," the relevant research results also play an important role in guiding the development of practical activities. However, due to the fact that the research on the development of Laos-China economic and trade relations under the framework of the "Belt and Road" and ASEAN Free Trade Area cooperation between Laos and China has been carried out relatively late, and the new environment, new technologies and new strategies have changed with the times. The emergence of opportunities has made the research on economic and trade cooperation between Laos and China more complicated. In this context, there are still many things that can be further researched on the development of Laos-China economic and trade relations under the framework of the "Belt and Road" and ASEAN Free Trade Area cooperation., the relevant research results also need to be continuously condensed and sublimated, so as to form a more systematic research system on the development of economic and trade relations between Laos and China under the cooperation framework of the "Belt and Road" and the ASEAN Free Trade Area. Therefore, for the "Belt and Road" and ASEAN The discussion on the development of Laos-China economic and trade relations under the framework of free trade zone cooperation is a supplement and extension to the existing theoretical research.

Research on ESC risk is not only an important part of energy management, but also an important part of supply chain risk management. In-depth research on this issue will help to make up for the lack of ESC management theory. It also helps to further improve the risk management system of the relevant participants in the ESC network. It is conducive to the establishment and improvement of China's ESC network under the background of OBOR, and it can also provide reference for how China should conduct energy cooperation.

Affected by the differences in research paradigms, ideas and actual situations, the existing research still has the following problems: In terms of research methods and ideas, the development of Laos-China economic and trade relations under the existing "Belt and Road" and ASEAN Free Trade Area cooperation framework The research lacks independent and systematic characteristic research methods and ideas, and the methods adopted by the academic circles are mostly quoted from other disciplines. Although these cited research methods and ideas have been proved to have a certain role and scientificity in the original disciplines, whether these research methods and ideas are in the Laos-China economic and trade relations under the framework of the "Belt and Road" and ASEAN Free Trade Area cooperation The field of development is also feasible and scientific, and it is worthy of further discussion. The innovation of this paper: (1) It applies complex system theory to supply chain risk management, and builds an energy cooperation network between China and countries along the OBOR on the basis of existing research. (2) It constructs a system dynamics model of the risk factors of the ESC under the background of the OBOR. It studies the interaction between the risk factors of the ESC and finds out the risk factors that have a greater impact on the ESC. It also puts forward relevant suggestions on the risk management of ESC in the context of OBOR. This article examines the impact of several major aspects of economic and trade cooperation between China and Laos on the economic growth of Laos separately, providing a new research perspective.

2. Related Work

The 19th National Congress of the Communist Party of China put forward the requirements of energy reform, and further promoting energy reform is also an inevitable way to solve the contradictions between energy, environment and economy. The OBOR international energy cooperation project is the trend of energy reform. Cui research shows that the PPP model, with its unique advantages, leads the cooperation and complementation of government capital and social capital, and is the most powerful support for the OBOR international energy cooperation projects. He analyzed the rationality of the application of Financing and Project Management Models (PPP) mode in international energy cooperation projects, and introduced the implementation steps of PPP mode in international energy cooperation projects. He identified possible political risks, as well as completion risks and environmental protection risks in the operation of international energy cooperation projects [1]. With the increase of China's energy demand and the external dependence of China's economic development on China, China's oil supply continues to rise. For the foreseeable future, China's oil trade will remain centered on imports. In terms of strategy, Guo et al. has established a trade gravity model for China's oil import trade. Through multiple linear regression analysis and empirical research, he obtained the key elements of real estate development in China. He summarized China's oil import trade, and also put forward a proposal to promote China's oil trade with other countries in the world on one road [2]. The Solangi et al. study highlights the scope and underlying objectives of the Belt and Road strategy and its implications for socio-economic development in China and Pakistan. Finally, he concludes the work by discussing the current status of Political Economy of Communication (PEC) and future opportunities for success [3]. Hussain et al. investigates the impact of climate change potential and geographic factors on transport infrastructure. It covers 65 Belt and Road countries geographically. Using a panel dataset obtained from 2001 to 2018, he employs suitable econometric techniques (such as FA, OLS, Heck-man, and GMM) to investigate whether climate change potential or geographic factors significantly affect transport infrastructure (roads, railways and ports). The results show that both climate change potential and geographic factors (especially land distance) negatively impact transport infrastructure. At the same time, its impact has significantly reduced the quality of transportation infrastructure by about 16% [4]. Tulokhonov et al. presented the project to create the North Asia Atlas of Sustainable Development. As a basic cartographic work, it provides a comprehensive map of the territory. The technical basis of the Atlas is the geographic information system for sustainable development of North Asia [5]. China's "One

Belt, One Road" (OBOR) initiative is an important tool in its strategy to maintain Chinese control and political stability, and to drive China's troubled economy. The concept of One Belt One Road is ambitious but ambiguous and fits perfectly with the traditional Chinese model. In the context of "hide your strengths and bide your time," a question has been raised [6]. However, the above research pays more attention to the development strategy of China-Laos economy and trade, but does not conduct in-depth analysis of the Belt and Road policy, resulting in the lack of combination of the two and the inability to give full play to their advantages.

3. Channel Construction Related Algorithms

This paper studies the issues of economic and trade cooperation between China and Laos under the background of the current "Belt and Road" and ASEAN Free Trade Area Cooperation Framework. The theoretical and practical significance of carrying out the research is explained. Then, the methods and paths that need to be used in this research are discussed, so as to provide basic preparation for the follow-up research. Then, the cooperation with the "Belt and Road" and the ASEAN Free Trade Area will be discussed. This paper summarizes and analyzes the research results of domestic and foreign scholars related to the research content of Laos-China Economic and Trade Relations under the Framework, and identifies the merits and deficiencies of existing research, so as to form a useful experience and reference for this study. Second, an overview of the relevant theories, that is, to explain the theories related to the research content of this paper, so as to provide basic support for subsequent research.

3.1. One Belt One Road. Energy cooperation is an important part of the OBOR construction. China's active promotion of energy cooperation under the OBOR initiative will help deepen international energy cooperation, build a new international energy order and rules, and promote the development of the international economic landscape [7]. The Belt and Road application areas are shown in Figure 1.

As shown in Figure 1, in the next ten years, there are five key areas under the Belt and Road Initiative with the greatest development potential and the highest participation of private enterprises. These are transport, telecommunications, utilities, digital infrastructure, renewable and clean energy. The Belt and Road concept is shown in Figure 2.

As shown in Figure 2, the key to the Belt and Road is to do a good job of "connecting" articles. The Belt and Road Initiative is an open and inclusive regional cooperation initiative, and is resistant to a non-exclusive and closed Chinese coterie. Today's world is an open world, openness brings progress, and closure leads to backwardness. China believes that only by opening up can we discover opportunities, seize and make good use of them, and take the initiative to create opportunities, in order to achieve our national goals. The "Belt and Road" initiative is to turn the world's opportunities into China's opportunities, and China's opportunities into the world's opportunities. It is based on this perception and vision. The Belt and Road is open-oriented, and hopes to promote the orderly and free flow of economic factors, efficient allocation of resources, and in-depth market integration by strengthening the interconnection and construction of infrastructure such as transportation, energy, and networks, and to develop a wider, higher-level, deeper-level development. to build an open, inclusive, balanced, and inclusive regional economic cooperation structure to solve the problems of economic growth and balance. This means that Belt-Road is a collaborative initiative of diversity, openness and inclusiveness. It can be said that the openness and inclusiveness of the Belt and Road Initiative is a prominent feature that distinguishes it from other regional economic initiatives.

3.2. The Belt and Road Initiative and ESC. Regarding the research on China's OBOR and ESC, firstly, the relevant literature reports on CNKI were sorted out and analyzed by citespace software. Among them, the core search "China-Laos trade" is used to obtain literature, and images are constructed based on recently published articles. This is mainly for literature research to grasp the hotspots and frontier directions of the OBOR and energy supply research from a global perspective. The results are shown in Figure 3.

The size of the keyword in Figure 3 indicates the number of times it has been researched, and the larger the keyword, the more times it has been researched. Edges in the graph represent connections between keywords. If there is an edge between the keywords, it means that scholars have conducted research on these two keywords at the same time and have relevant literature support. In mathematics, physics and sociology, small-world network is a type of mathematical graph in which most of the nodes are not adjacent to each other, But most nodes can be reached by a few steps from any other point. If the dots in a small-world network represent a person, and the connecting lines represent people-to-people acquaintances, the small-world network can reflect the small-world phenomenon that strangers are connected by people who know each other. As can be seen from Figure 3, the main keywords of research on the Belt and Road are the OBOR initiative, "energy cooperation," "energy security," and "countries along the route." Its main keywords in the research of ESC are "international energy cooperation," "oil and gas cooperation," "energy channel," "supply chain" and so on. These point out the direction for the research of this paper, and show that the research on the ESC of the OBOR is a hot spot and has certain feasibility.

If each country is defined as a vertex, and the energy cooperation between two countries is regarded as an edge, and these points and edges are used to describe the relationship network of the ESC, this virtual network can be simplified into a small-world network structure. Figure 4 shows the energy supply network diagram drawn according to the energy cooperation status of some countries along the OBOR in recent years.

Figure 4 is an energy supply network diagram drawn according to the energy cooperation status of some countries along the OBOR in recent years. It can be seen from the

Figure 1: Belt and road application areas.

Figure 2: The belt and road concept.

figure that China has energy cooperation with many countries along the route. According to the theoretical basis of the small-world network model, several basic characteristic statistical parameters of the small-world network can be obtained. Its definition and calculation method are as follows:

(1) Node N: Each country or region participating in energy cooperation is a node of the ESC network.

(2) Side M: The energy cooperation (energy flow, technology exchange, etc.) of various countries is the side of the supply chain network.

(3) The degree k_i of a node: The number of edges that a node connects to other nodes is the degree of the node.

(4) Average degree K: The average of the number of edges connecting any two vertices along the shortest path.

$$k = \frac{1}{n}\sum_{i=1}^{n} k_i. \tag{1}$$

(5) Vertex degree I_i: It refers to the relative index of the degree value of each node in the supply chain, reflecting its importance in the supply chain network. The greater the vertex degree, the more important its position in the supply chain network is.

$$I_i = k_i / \sum_{i=1}^{N} k_i. \tag{2}$$

There are two parameters to evaluate the efficiency of energy cooperation, one is the average path length; the other is the average efficiency of the network.

(1) Average path length L: It is the average of the number of edges connecting any two vertices along the shortest path. The longer the average path length, the more cooperative relations between supply chains, and the worse the operation efficiency of the entire supply chain. Its calculation formula is as follows:

$$L = \frac{1}{N(N+1)/2}\sum d_{ij}, \tag{3}$$

where d_{ij} represents the shortest distance between node i and node j, that is, the network shortest path

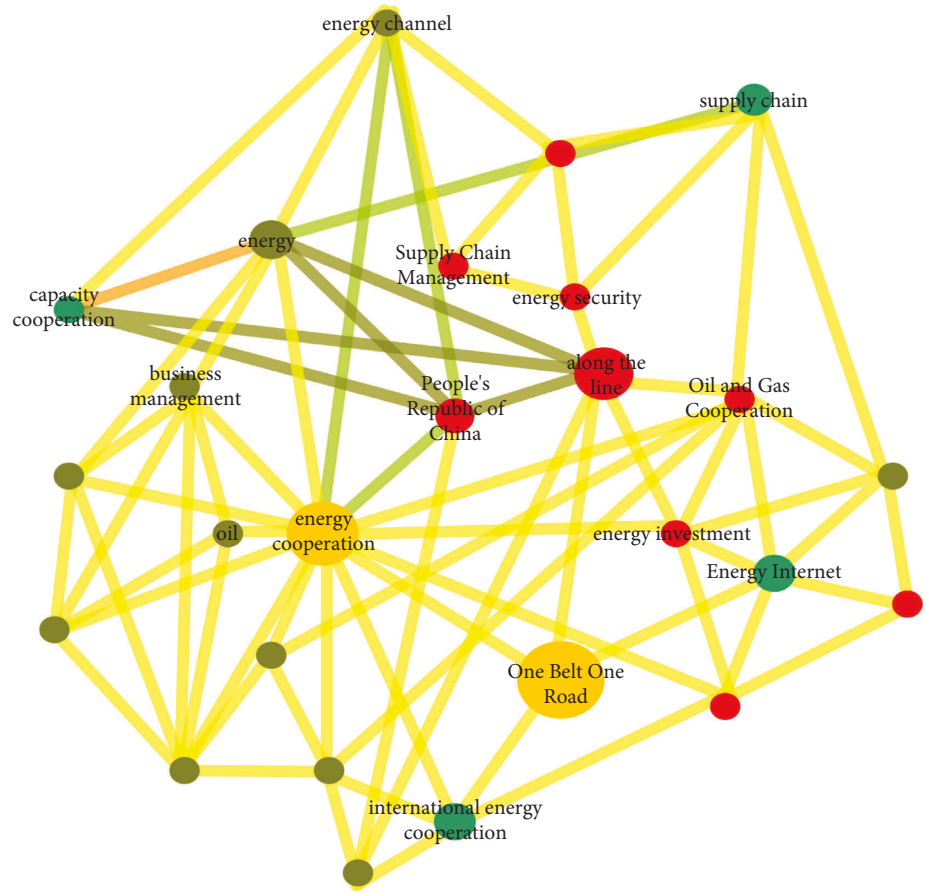

Figure 3: Literature analysis diagram.

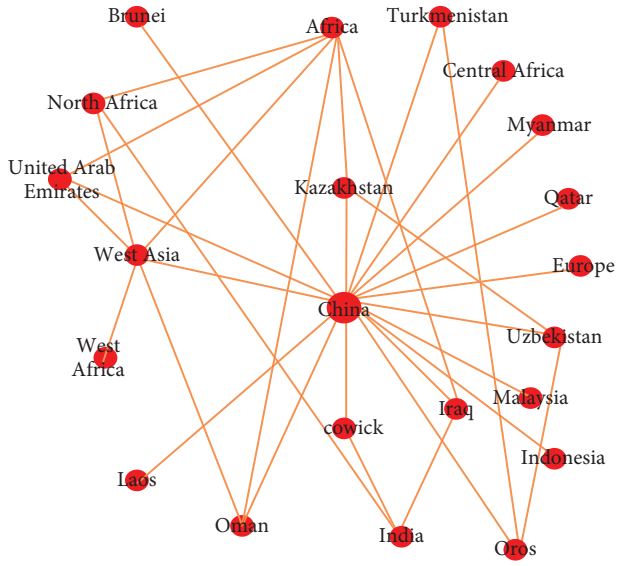

Figure 4: OBOR energy cooperation network map.

matrix. For the entire supply chain network, the average path length represents the number of times that any node in the supply chain needs to pass through other nodes [8]. That is to say, the longer the average path is, the more nodes it experiences when energy cooperation occurs, and the less risk each node takes [9, 10].

(2) The average efficiency E of the network: It assumes that each node in the network simultaneously propagates information to its neighbors. At this time, the rate of information transfer is inversely proportional to the distance between nodes. The greater the distance between nodes, the slower the transfer rate. Therefore the efficiency between point i and point j can be defined as $E = 1/\mathrm{dy}$. From this, the efficiency of the network can be deduced as:

$$E(G) = \frac{1}{n \cdot (N-1)} \sum_{i,j} \left(1/d_{ij}\right). \tag{4}$$

When the vertex degree of each node is different, that is, there are a small number of core nodes and a large number of terminal nodes in the supply chain supply chain network. The ESC network at this time has a small-world characteristic, and it is said that the supply chain network at this time is "orderly" [11, 12]. The measure of the orderliness of the supply chain network is the structural entropy of the supply chain network, and its calculation formula is as follows:

$$H(G) = -\frac{N}{i=1} I_i \ln\ I_i. \tag{5}$$

When the importance of each node in the supply chain is equal, that is, when there is no core enterprise, there is I = 1/*N*, the network structure entropy is that the communication system provides services to the business needs through the channel, so the set of interactive communication at each moment (slot), which constitutes the events of the communication network, and the network structure entropy *H* takes the maximum value at this time [13].

$$H(0) = -\frac{N}{i=1} \frac{1}{N} \ln\ \frac{1}{N} = \ln\ N. \tag{6}$$

Centrality is a concept used in social network analysis to measure the degree to which a point in the network or a person is close to the center in the entire network. That is to say, by understanding the centrality of a node, the importance of this node in the network can be judged. At this time, the alliance cooperation network is the most uneven, and the network structure entropy is the smallest. The activities of other nodes in the supply chain are all turned around through this node [14, 15]. According to the calculation formula of vertex degree, it is easy to obtain the calculation results of node 1 and other nodes as follows:

$$I_1 = \frac{1}{2}, I_i = \frac{1}{2(N-1)}\ (j \neq 1). \tag{7}$$

According to the calculation formula of the entropy value, the entropy value of the supply chain network at this time can be obtained:

$$\begin{aligned} H(1) &= -\sum_{j=2}^{N} \frac{1}{2(N-1)} \ln\ \frac{1}{2(N-1)} - \frac{1}{2} \ln\ \frac{1}{2} \\ &= \frac{\ln\ 4(N-1)}{2}. \end{aligned} \tag{8}$$

When there are two core nodes in the supply chain network, it is assumed that the nodes are node 1 and node 2. All other nodes are connected to these two nodes, and the activities of other nodes in the supply chain are all turned around through the two nodes. According to the calculation formula of vertex degree, it is easy to obtain the calculation results of node 1, node 2 and other nodes as follows:

$$I_1 = I_2 = \frac{1}{3}, I_i = \frac{1}{3(N-2)}\ (\mathrm{i} \neq 1, 2). \tag{9}$$

According to the calculation formula of the entropy value, the entropy value of the supply chain network at this time can be obtained:

$$\begin{aligned} H(2) &= -\frac{2}{3} \ln\ \frac{1}{3} - \sum_{i=2}^{N} \frac{1}{3(N-2)} \ln \frac{1}{3(N-2)} \\ &= \frac{\ln\ (27(N-2))}{3}. \end{aligned} \tag{10}$$

At this time, the network structure of the supply chain is much more stable than when there is only one core node [16]. When a problem occurs in a certain link of the supply chain, if one of the core nodes fails to respond in time, the other core node can also adjust it, which greatly improves the stability of the supply chain.

3.3. Decision Tree Algorithm. The decision tree algorithm is a method of approximating the value of a discrete function. It is a typical classification method that first processes the data, uses an inductive algorithm to generate readable rules and decision trees, and then uses the decisions to analyze the new data. Essentially a decision tree is the process of classifying data through a series of rules.

It is assumed that the proportion of the mth class samples in the current sample set *D* is ($m = 1, 2, \ldots, y$) [17, 18]. Then the information entropy of *D* is defined as:

$$Ent(D) = -\sum_{m=1}^{|y|} p_m \log_2 p_m. \tag{11}$$

According to the above formula, the information entropy can be calculated D^X.

$$Gain(D, a) = Ent(D) - \sum_{X=1}^{X} \left(\left|D^X\right| / |D| \right) Ent\left(D^X\right). \tag{12}$$

It uses $a_* = \mathrm{argmaxGain}(D, a)$ for attribute division [19].

$$Gain_{ratio(D,a)} = \frac{Gain(D, a)}{IV(a)}. \tag{13}$$

In

$$IV(a) = -\sum_{X=1}^{X} \left(\left|D^X\right| / |D| \right) \log_2 \left(\left|D^X\right| / |D| \right). \tag{14}$$

Deal with discrete distribution features without the process of pruning. At the same time, it uses the entropy model [20, 21].

3.4. Logistic Regression Model. Logistic regression, also known as logistic regression analysis, which is a generalized linear regression analysis model, which is often used in data mining, automatic disease diagnosis, economic forecasting and other fields. Logistic regression is an easy-to-implement and excellent-performance classification model for linearly separable problems, and it is one of the most widely used models [22]. It first constructs a traditional linear regression model:

$$\mu = b + w_1 x_1 + \cdots + w_p x_p = w^T x + b. \tag{15}$$

In this model, the value range of μ is $(-\infty, +\infty)$.

It assumes that the two classes of the classification problem are $y = 1$ and $y = 0$, and the probability that $y = 1$ is assumed to be π.

$$\pi = \frac{1}{1 + e^{-\mu}} \mu \in (-\infty, +\infty). \tag{16}$$

With the Sigmoid function, $(-\infty, +\infty)$ can be projected onto (0, 1). The binary classification problem of logistic regression can finally be expressed as:

$$\begin{cases} 0, \pi < 0.5, \\ 1, \pi > 0.5, \end{cases}$$

$$P(y=1) = \frac{1}{1+e^{-\mu}} = \frac{1}{1+e^{-(w^T x+b)}} = \frac{e^{-(w^T x+b)}}{1+e^{-(w^T x+b)}} = \pi,$$

$$p(y=0) = 1 - p(y=1) = \frac{1}{1+e^{-(w^T x+b)}} = 1-\pi. \tag{17}$$

For ease of expression, assume $\theta = (w, b)$. Given a data set, the obtained likelihood function expression is:

$$L(\theta) = \prod_{i=1}^{m} (\pi)^{y_i} (1-\pi)^{1-y_i}. \tag{18}$$

To define the loss function $J(\theta)$ of Logistic regression as the inverse of the logarithm of the above formula, we can get:

$$J(\theta) = -lnL(\theta) = -\sum_{i=1}^{m} \left(y_i \ln(\pi) + (1-y_i)\ln(1-\pi)\right). \tag{19}$$

4. Value Assessment of China-Laos Channel Construction

In the analysis of the generating mechanism of the economic value of the channel, it is considered that the regional economic value of the channel is caused by trade. Therefore, This article will further quantify the trade value as the regional economic value to the regions along the Western Corridor. It assesses how much economic value the Western Corridor can bring to the area along the route.

4.1. Simultaneous Formula Model Theory. Although there is almost no research on the quantitative relationship between "channels and regional economic growth" in the academic world, there are many studies on the relationship between "trade and regional economic growth." In the "trade-regional economic growth" model, there have been a lot of mature research models. This paper intends to use the simultaneous formula model for empirical analysis of related aspects. Because changing the model can effectively solve the two-way causality problem of "chicken and egg," while other models can only solve the problem of single causality. Therefore, this paper regards the trade growth caused by the Western Corridor as an exogenous variable of economic growth, and influences the two endogenous variables of capital and employment for economic growth. Finally, it finds the impact of the opening of the Western Corridor on the entire economic growth system, and evaluates the regional economic value brought by the Western Corridor.

4.2. Model Construction. This paper constructs three endogenous variables (g) including the total import and export volume of the target country as an exogenous variable, economic aggregate, capital stock, and labor (g), 6 prerequisite variables (k) and 3 structural equations (i) composed of simultaneous formula models. In order to study the impact of changes in trade scale on the entire factor of production, the total import and export trade of China and Laos was added to the simultaneous formula model as an exogenous variable. This is used to measure the regional economic value, including production factors such as economic growth, capital accumulation and labor supply, brought by the Central-Laos West Corridor to the regions along the route. The specific form of the model is as follows:

$$\ln\ gdp = a_1 + a_2 \ln\ captial + a_3 \ln\ labor + a_4 \ln\ trade, \tag{20}$$

$$\ln\ captial = b_1 + b_2 \ln rate + b_3 \ln\ captial(-1) + b_4 \ln\ gdp(-1), \tag{21}$$

$$\ln\ labor = c_1 + c_2 \ln\ wage + c_3 \ln\ labor(-1) + c_4 \ln\ trade + c_5 \ln\ gdp. \tag{22}$$

The specific description of the variables is shown in Table 1:

As shown in Table 1, the structural formula (22) is the output formula. The formula is based on a linear production function. Among them, A represents the total factor productivity in production activities, such as the improvement of enterprise management level, the improvement of labor factors, and the introduction of advanced technology. Structural formula (21) is the capital stock formula, the current interest rate (rate), the capital stock of the previous period (capita (–1)), and the economic aggregate of the previous period (gdp (–1)) are important factors that affect capital investment. Structural formula (22) is the labor supply formula, which uses the total number of employees at the end of the year (labor) to represent the input of labor factors. Average labor remuneration (wage), previous employment labor (–1), current economic aggregate (gdp), and total import and export (trade) are all important factors that affect labor supply.

The entropy value of the ESC network structure in the context of the OBOR can be obtained from the value of each vertex degree obtained by the calculation formula of the entropy value is 2.408. It calculates the maximum and minimum values of the ESC network structure entropy at this time. It can be obtained from formulas (6) and (8) that the maximum value of the ESC network entropy is 3.09, and the minimum value is 2.21. The calculated entropy value of the ESC network is very close to the entropy value of only one core node in the supply chain. It can be seen from this that the structural stability of the ESC under the background of theOBOR is relatively poor. Although there is more than one core node in the ESC network, most of the nodes in the entire network are connected through node 1. The variable

Table 1: Variable description.

Serial number	Variable	Expected symbol	Unit	Economic significance
1	gdp	+	Billion	Economic aggregate
2	Capital	+	Billion	Capital stock
3	Labor	+	10,000 people	Total number of employees at the end of the year
4	Trade	+	Million	Laos' total import and export
5	Wage	−	%	Loan benchmark interest rate
6	Capita (−1)	+	Yuan	Average salary of employees
7	Labor (−1)	+	Billion	Capital investment in the previous period

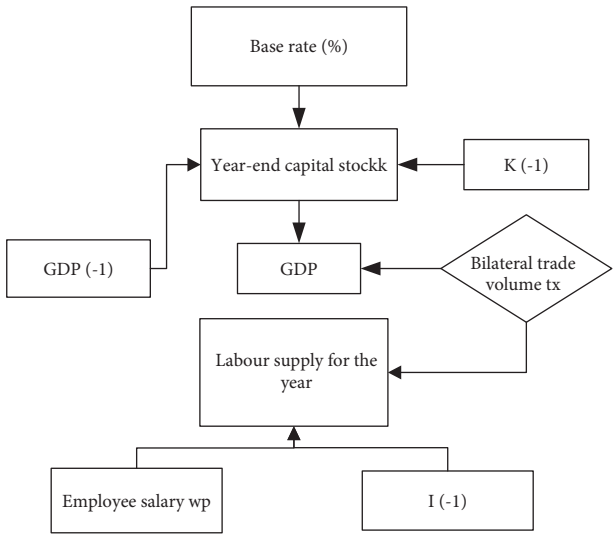

Figure 5: The relationship between variables of economic growth influencing factors.

relationship diagram of economic growth influencing factors is shown in Figure 5.

It can be seen from Figure 5 that the regional economic value is caused by the trade value. Therefore, this paper uses the import and export trade (trade) factor to replace the total factor productivity in the C_D function, and the import and export trade is endogenous to the economic growth. Lower interest rates will greatly stimulate the enthusiasm of private entrepreneurs to invest.

4.3. The Regional Economic Value Assessment of the Provinces and Cities Along the Route by the Western Corridor. The regional economic value of the Western Corridor to the regions along the route should include the total value of the opening of the Western Corridor to the economic growth, capital accumulation and employment level along the route. Among them, economic growth includes 0.01% of which the trade between the provinces along the route and Laos directly contributes to economic growth, and 0.02552% and 0.136048000% that indirectly contribute to economic growth through capital accumulation and labor supply. The elasticity of capital accumulation due to economic growth is 0.116, and the elasticity coefficient of employment level increase is 0.176. The regional economic value assessment of the Western Corridor is shown in Table 2.

The regional economic value of the Western Corridor is shown in Table 2, with the following conclusions:

(1) The opening of the Western Corridor has a positive correlation with the total economic value, capital accumulation and employment level of the cities along the line.

(2) The opening of the Western Corridor has obviously driven the development of the cities along the route. It will increase the GDP of the cities along the route by 3.954%, the total capital accumulation value by 0.4587%, and the total employment level by 0.0696%. The provinces have an average increase of 0.3954%, 0.0459% and 0.0696% respectively.

(3) As far as the provinces along the route are concerned, its impact on western western cities such as Ningxia, Qinghai, Gansu, Sichuan, and Yunnan is greater than that on central cities such as Chongqing, Inner Mongolia, and Shaanxi.

The scale of China's new energy market and photovoltaic industry is shown in Figure 6.

As shown in Figure 6, the data shows that in 2018, the scale of China's new energy market reached 882.254 billion yuan. It increased by 18.5% year-on-year, and it is expected that China's new energy market will reach 1,039.9 billion yuan in 2021. According to statistics, in 2020, China's cell output will be about 134.8 GW, a year-on-year increase of 22.2%.

5. Simulation Results

The ESC risk system is a complex dynamic system under the background of "One Belt One Road." In the causal flow diagram, the overall risk system of the ESC consists of two feedback loops. Combining the settings of parameters and functional relationships, the entropy changes of external risk and internal risk in 5 years and the evolution trend of risk are shown in Figure 7.

It is not difficult to see from Figure 7 that among the secondary indicators, the external risk entropy value grows the fastest over time. Its growth rate is much greater than that of the internal risk entropy value, and the larger the entropy value, the more unstable the risk system is. Therefore, it is necessary to pay attention to and control external risks during the operation of the ESC. Among them, for example: transportation risk, political risk and economic risk. It is not difficult to see from the growth trend of the graph that the risk has a slow growth trend in 3 years. The entropy of its risk increases rapidly after the third year, the growth rate almost doubles, and it continues to grow. This

Table 2: Regional economic value assessment of the western corridor.

Cities along the route	Trade boost	Total economic	Capital accumulation	Employment level
Inner Mongolia	0.20361	0.002365	0.000274	0.000416
Guangxi	0.395355	0.004592	0.000533	0.000808
Chongqing	0.153309	0.001781	0.000207	0.000313
Sichuan	0.370478	0.004303	0.000499	0.000757
Guizhou	0.344588	0.004003	0.000464	0.000704
Yunnan	0.203609	0.002365	0.000274	0.000416
Shaanxi	0.20816	0.002418	0.00028	0.000426
Gansu	0.514394	0.005975	0.000693	0.001052
Qinghai	0.522806	0.006073	0.000704	0.001069
Ningxia	0.487709	0.005665	0.000657	0.000997
Total	3.404016	0.03954	0.004587	0.006959
Average	0.340402	0.003954	0.000459	0.000696

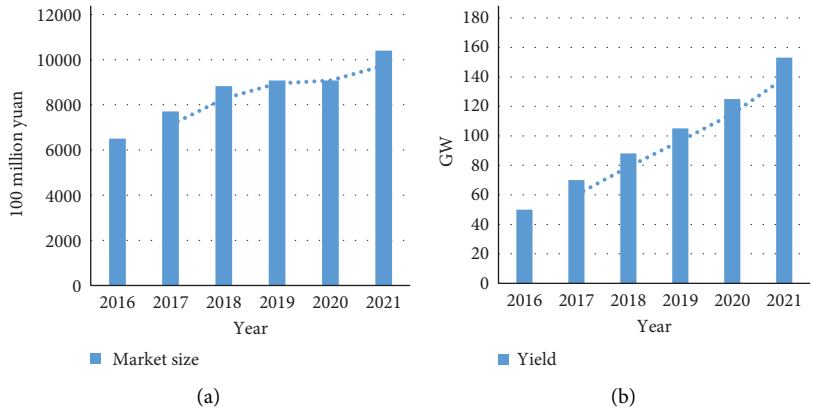

Figure 6: China's new energy market and photovoltaic industry scale. (a) New energy market. (b) The scale of photovoltaic industry.

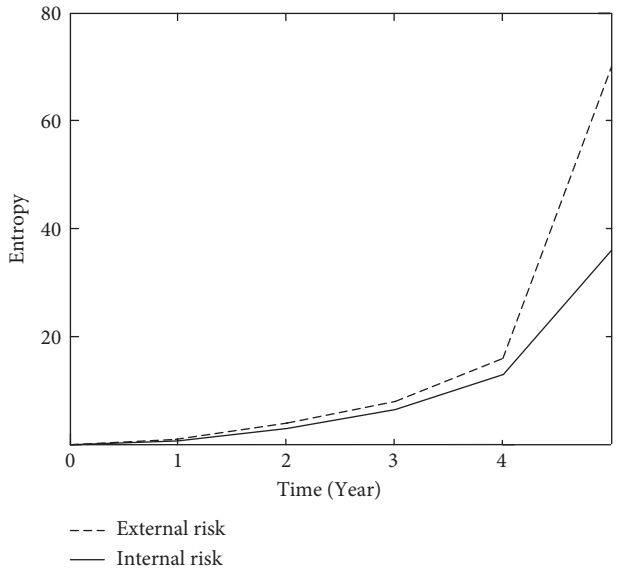

Figure 7: Change of entropy value of secondary indicators.

shows that with the advancement of time, there are more and more uncontrollable factors of risk.

In addition, there are many factors that affect the internal and external risks of the supply chain, and all factors are completely controlled, and the possibility of realization is very small. The sensitivity of the change of the entropy value of each risk factor to the change of the entropy value of the external risk system is analyzed. The results obtained are shown in Figure 8:

Figure 8 depicts the change trend of external risk entropy over time when a single factor changes. It can be clearly seen from the figure that the order of the impact of risk factors on external risk indicators is: sudden risk, political risk, policy risk, legal risk, and market risk. From the trend of the graph, it can be seen that the change trend of the entropy value of a single risk factor affecting external risk is not very large in the first two years. Its growth rate has been accelerating since the third year. The impact of political risk entropy changes on the external risk system ranks second and is controllable. For this reason, it should focus on controlling it in the process of building theOBOR ESC. By establishing good diplomatic relations with the countries along the route, it respects the wishes of the countries along the route and helps each other. This will try to avoid conflicts, etc., and reduce external risks in the ESC. The entropy values of policy risk and legal risk have similar growth rates and similar changing trends, indicating that the two have roughly the same proportion of their impact on internal risk. It should give the same attention to both when it manages and controls risks. The market risk entropy has the smallest growth rate, and the change trend of market risk and external risk is almost the

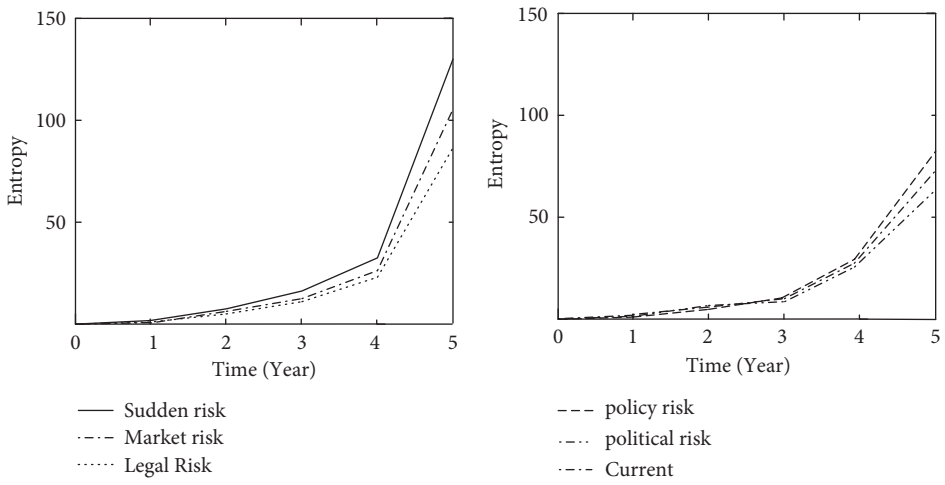

Figure 8: External risk sensitivity analysis.

same. In short, in the process of controlling external risks, we should pay close attention to the causes of sudden risks and political risks and control them. Secondly, we need to pay attention to changes in policy and legal risks, and finally, we should always pay attention to changes in the international energy market, so as to reduce the losses caused by external risks.

It controls other risk factors unchanged, and only increases the entropy value of cooperation risk, logistics risk, procurement risk, and management risk by 20%. It observes the change of the entropy value of internal risk, and analyzes the sensitivity of the change of the entropy value of each risk factor to the change of the entropy value of the internal risk system. The results obtained are shown in Figure 9:

Figure 9 depicts the change trend of internal risk entropy over time when a single factor changes. It can be clearly seen from the figure that the order of the impact of risk factors on internal risk indicators is from large to small: cooperation risk, logistics risk, management risk, and procurement risk. From the trend of the graph, it can be seen that the change trend of the entropy value of a single risk factor affecting internal risk is not very large in the first two years, and the growth rate has been accelerating since the third year. The growth rate of cooperative risk entropy is much greater than that of other risk factors. That is to say, the cooperation risk has the greatest impact on the internal risk of the ESC, and it should be mainly controlled in the process of risk management. The growth rate of the entropy value of logistics risk and management risk is similar, and the change trend is also very close. This shows that the two have roughly the same proportion of the impact on internal risks, and they should be given the same attention when managing and controlling risks. Procurement risk entropy growth rate is the smallest, and the change trend of procurement risk and internal risk is almost the same. This shows that procurement risk factors have less impact on internal risk changes and account for a lower proportion in the total risk system. In the process of risk management, if the experience that can be invested is limited, the control of procurement risks can be reduced accordingly. In general, for energy internal risk, each factor change will have an impact on the entire subsystem, and the impact is long-term. The large changes in the entropy value all increase rapidly from the third year. Therefore, it is a long-term and comprehensive task to effectively control it, and a long-term plan should be made to manage internal risks well. This in turn reduces the likelihood of the risk occurring, allowing for effective risk management.

After analyzing the sensitivity of a single factor to external and internal risks, the entire ESC risk system is analyzed. The ESC risk system is jointly determined by two subsystems, external risk and internal risk. Therefore, this paper starts from the boundary point of the grass-roots level, determines the risk situation of the subsystem, and then determines the risk situation of the ESC. The specific situation is shown in Figure 10.

As can be seen from Figure 10, although the impact of internal risk on the entropy value of the ESC is not as large as that of external risk, its degree of impact cannot be ignored. To this end, while paying attention to external risk management and control, internal risk management should also be strengthened. In addition, it can be seen from the figure that whether it is external risk, internal risk or the risk of the entire ESC system, the large change in entropy value starts from the third year, and the trend is very obvious. The OBOR initiative is a long process of regional economic formation. The construction and development of the ESC is also constantly being improved, which makes the possibility of risks more likely. To this end, in addition to long-term planning, the management of the ESC should constantly discover risks and improve plans according to the actual situation. This makes the increase of the entropy value of the ESC risk system controlled within the short-term influence range.

Through bilateral trade between Laos and China, Lao enterprises can import high-quality industrial products from China and learn advanced industrial technology from China, which further improves the profitability of Lao enterprises and accelerates the modernization process of enterprises. Corporate profits are improved. In terms of national interests, Laos can not only benefit from China's economic

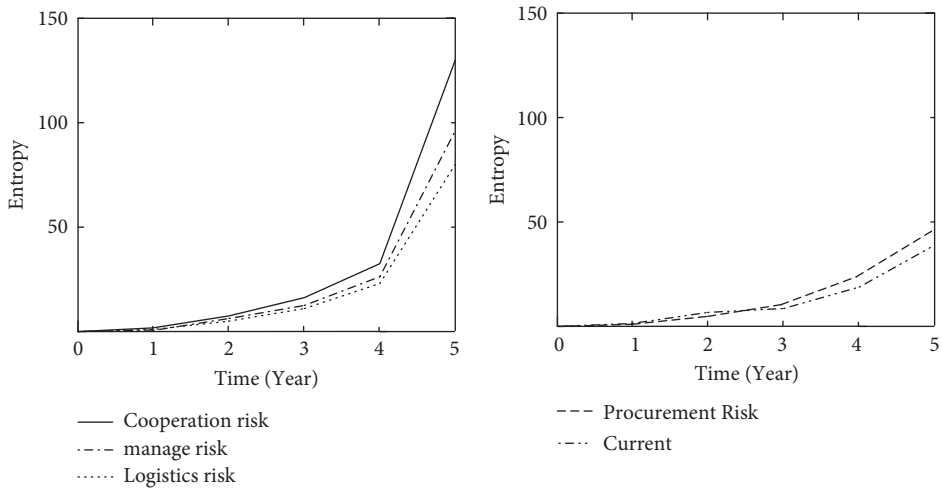

Figure 9: Internal risk sensitivity analysis.

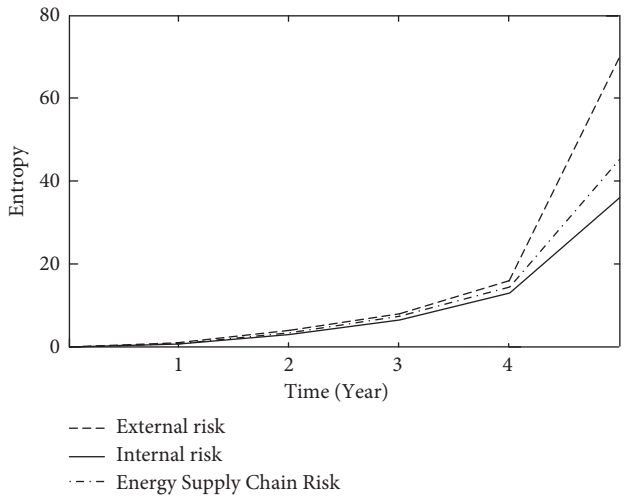

Figure 10: ESC risk and change in entropy value of secondary indicators.

growth and bilateral trade between China and Laos, but also from the economic growth of ASEAN countries, especially some neighboring countries, especially with the deepening cooperation in the ASEAN Free Trade Area. With the implementation of the "One Belt, One Road" strategy, regional cooperation and mutual influence will be further increased, and Laos will also gain more benefits from it. The Laos-China trade has increased a huge amount of revenue for Laos' finance, slowed down the increase in the scale of Laos' central fiscal debt, and eased the debt pressure to a certain extent. In addition, the implementation of bilateral trade between China and Laos has enabled Chinese industrial products to enter the Lao market smoothly, and at the same time, it can also drive Chinese capital and technology to flow into Laos, thereby promoting the upgrading of Laos' industrial structure and increasing the proportion of industry in Laos' entrepreneurship., laying the foundation for Laos to realize industrialization and modernization.

6. Conclusion

This paper analyzes the route and layout of the OBOR initiative and ESC research. It sorted out the basic energy situation of China and the countries along the route, and studied the connection between the OBOR and China's ESC. It summarizes the relevant energy cooperation between China and the countries along the OBOR, and analyzes the impact of China's ESC after the implementation of the OBOR and the impact of the construction of the ESC on the implementation of the OBOR. It puts forward corresponding suggestions on the risk management of the ESC from two aspects: external risk and internal risk. It includes strengthening coordination and consultation with governments of various countries based on the principle of mutual benefit and win-win, establishing sound policies and legal systems, and strengthening the collection of energy market information. It strengthens China's national defense and military forces and ensures the security of energy channels along the route. It actively participates in investment in the international energy market and exerts China's influence as a major power. It determines the new layout of energy cooperation and opens up new channels for energy transportation. This also adjusts the structure of energy production and consumption, and strengthens the management of energy enterprises. With the in-depth development of ASEAN integration and the further development of the "Belt and Road" strategy, the economic and trade cooperation between China and Laos will inevitably become more frequent. In a new stage of development, the problems and deficiencies in the economic and trade cooperation between China and Laos on the other side should be correctly faced and actively resolved by the Lao government, so as to seize this good opportunity for development and bring the level of economic development of Laos to a new level. However, there are still some problems in this paper. The analysis of China-Laos trade and freight transportation has reached a deep level. However, due to insufficient literature search, there is no in-depth analysis of the Belt and Road, resulting

in the innovation of the integration of the two has not reached the level. In the following research, we can start from the freight risk.

Data Availability

No data were used to support this study.

Conflicts of Interest

There is no potential conflicts of interest in this study.

Acknowledgments

This work was supported by The National Natural Science Foundation of China (NSFC) project "Research on Appropriate Technology Selection and Dynamic Change of China's Manufacturing Transformation and Upgrading under the Orientation of High-Quality Development" (Grant no. 71973083); the project of Humanities and Social Sciences Research Planning Fund of the Ministry of Education, "Research on Appropriate Technology Selection, Old and New Dynamic Energy Conversion and Manufacturing Transformation and Upgrading Dynamics Mechanism" (Grant no. 19YJA790109); the Natural Science Foundation of Shandong Province, "Research on the Selection of Appropriate Technology and the Transformation of New and Old Kinetic Energy in the Transformation and Upgrading of Manufacturing Industry" (Grant no. ZR2019MG018).

References

[1] Y. Cui, "Application research of PPP mode in the international energy cooperation project under the background of "one belt and one road"," *World Scientific Research Journal*, vol. 5, no. 9, pp. 14–18, 2019.

[2] X. Guo, J. Zhang, J. Xue, and T. Yan, "A research on the gravity model of chinas oil trade in the strategic context of one belt one road," *Journal of Economics and International Finance*, vol. 9, no. 10, pp. 95–102, 2017.

[3] H. U. R. Solangi, F. G. Gilal, and M. Z. Tunio, "One belt one road initiative: the origin, current status, and challenges of china-pakistan economic corridor," *International Journal of Technology, Policy and Management*, vol. 18, no. 4, pp. 313–335, 2018.

[4] Z. Hussain, M. Yousaf, and C. Miao, "Investigating the simultaneous impacts on transport infrastructure:evidence from one-belt one-road countries," *Rivista Internazionale Di Economia Dei Transporti/International Journal of Transport Economics*, vol. 47, no. 4, pp. 402–418, 2021.

[5] A. Tulokhonov, D. Suochen, E. Garmaev et al., "Atlas of sustainable development of north asia in the context of the project "one belt, one road"," *InterCarto InterGIS*, vol. 26, no. 1, pp. 352–360, 2020.

[6] F. Gómez Martos, "China's "one belt, one road" initiative: prospects and challenges," *Przeglad Strategiczny*, vol. 10, pp. 321–334, 2017.

[7] S. R. Hasan and M. M. Karim, "Revised energy efficiency design index parameters for inland cargo ships of bangladesh," *Proceedings of the Institution of Mechanical Engineers - Part M: Journal of Engineering for the Maritime Environment*, vol. 234, no. 1, pp. 89–99, 2020.

[8] P. Mukherjee, D. Mishra, and S. De, "Exploiting temporal correlation in wireless channel for energy-efficient communication," *IEEE Transactions on Green Communications and Networking*, vol. 1, no. 4, pp. 381–394, 2017.

[9] A. J. Thubagere, W. Li, R. F. Johnson et al., "A cargo-sorting DNA robot," *Science*, vol. 357, pp. 6558–1112, 2017.

[10] V. Lostanlen, J. Salamon, M. Cartwright et al., "Per-channel energy normalization: why and how," *IEEE Signal Processing Letters*, vol. 26, no. 1, pp. 39–43, 2019.

[11] G. Yu, X. Tong, G. Han et al., "Completing site acceptance of electronic linear accelerator for cargo inspection," *Annual Report of China Institute of Atomic Energy*, pp. 197-198, 2017.

[12] B. Zhou, "Cooperation between china and africa under the one belt one road initiative: china's benefits and problems," *Chinese Studies*, vol. 08, no. 2, pp. 27–41, 2019.

[13] K. Sanin, "History and culture in the chinese one belt, one road initiative," *Far Eastern Affairs*, vol. 46, no. 4, pp. 105–117, 2018.

[14] W. Wang, L. Tang, J. Zheng, and J. Liu, "Opportunities and challenges for MBBS education of human parasitology under the background of one belt and one road," *OALib*, vol. 6, no. 9, pp. 1–6, 2019.

[15] M. N. I. Sarker, M. A. Hossin, Y. Hua, M. K. Sarkar, and N. Kumar, "Oil, gas and energy business under one belt one road strategic context," *Open Journal of Social Sciences*, vol. 6, no. 4, pp. 119–134, 2018.

[16] Z. K. Yang, C. Z. Yuan, and A. W. Xu, "Confined pyrolysis within a nanochannel to form a highly efficient single iron site catalyst for zn–air batteries," *ACS Energy Letters*, vol. 3, no. 10, pp. 2383–2389, 2018.

[17] G. Zakaria and S. Rahman, "Development of energy efficiency design index for inland cargo vessels of bangladesh," *Journal of Marine Science: Research & Development*, vol. 7, no. 4, pp. 1–8, 2017.

[18] S. Kumar and R. S. Bharj, "Solar hybrid e-cargo rickshaw for urban transportation demand in India," *Transportation Research Procedia*, vol. 48, no. 2, pp. 1998–2005, 2020.

[19] J. Herdzik, "Methane slip during cargo operations on LNG carriers and LNG-fueled vessels," *New Trends in Production Engineering*, vol. 1, no. 1, pp. 293–299, 2018.

[20] W. C. Chen, G. C. Yang, M. K. Chang, and W. C. Kwong, "Construction and analysis of shift-invariant, asynchronous-symmetric channel-hopping sequences for cognitive radio networks," *IEEE Transactions on Communications*, vol. 65, no. 4, pp. 1494–1506, 2017.

[21] J. Qi, J. Li, and S. Zheng, "A bifurcated vascular channel construction method based on diploic vein characteristics," *Journal of Bionics Engineering*, vol. 16, no. 5, pp. 814–827, 2019.

[22] A. L. Kleytman, I. O. Tyumentsev, and T. B. Ivanova, "On the problem of the volga-don channel construction in the scientific thought of russia of the 18th – the middle of the 20th Century," *Vestnik Volgogradskogo Gosudarstvennogo Universiteta Serija 4 Istorija Regionovedenie Mezhdunarodnye Otnoshenija*, vol. 23, no. 6, pp. 107–115, 2018.

Hindawi
Scientific Programming
Volume 2023, Article ID 9871479, 1 page
https://doi.org/10.1155/2023/9871479

Retraction

Retracted: Intelligent Piano Teaching Based on Internet of Things Technology and Multimedia Technology

Scientific Programming

Received 1 August 2023; Accepted 1 August 2023; Published 2 August 2023

This article has been retracted by Hindawi following an investigation undertaken by the publisher [1]. This investigation has uncovered evidence of one or more of the following indicators of systematic manipulation of the publication process:

(1) Discrepancies in scope
(2) Discrepancies in the description of the research reported
(3) Discrepancies between the availability of data and the research described
(4) Inappropriate citations
(5) Incoherent, meaningless and/or irrelevant content included in the article
(6) Peer-review manipulation

The presence of these indicators undermines our confidence in the integrity of the article's content and we cannot, therefore, vouch for its reliability. Please note that this notice is intended solely to alert readers that the content of this article is unreliable. We have not investigated whether authors were aware of or involved in the systematic manipulation of the publication process.

Wiley and Hindawi regrets that the usual quality checks did not identify these issues before publication and have since put additional measures in place to safeguard research integrity.

We wish to credit our own Research Integrity and Research Publishing teams and anonymous and named external researchers and research integrity experts for contributing to this investigation.

The corresponding author, as the representative of all authors, has been given the opportunity to register their agreement or disagreement to this retraction. We have kept a record of any response received.

References

[1] Y. Xu, "Intelligent Piano Teaching Based on Internet of Things Technology and Multimedia Technology," *Scientific Programming*, vol. 2022, Article ID 8774340, 9 pages, 2022.

Hindawi
Scientific Programming
Volume 2022, Article ID 8774340, 9 pages
https://doi.org/10.1155/2022/8774340

Research Article

Intelligent Piano Teaching Based on Internet of Things Technology and Multimedia Technology

Yixiang Xu

Piano Department, Shanxi Vocational College of Art, Taiyuan 030000, Shanxi, China

Correspondence should be addressed to Yixiang Xu; 3170400046@caa.edu.cn

Received 22 July 2022; Revised 1 September 2022; Accepted 17 September 2022; Published 10 October 2022

Academic Editor: Juan Vicente Capella Hernandez

Intelligent piano teaching is based on traditional piano teaching, combined with relevant intelligent technology, to improve students' teaching methods, or to change the traditional piano structure, so that students can change from learning piano to playing piano. This study aimed to select a more suitable specific algorithm by studying the Internet of things (LOT) technology and multimedia technology and conduct in-depth research on the piano intelligent teaching, so that it can better serve the current piano teaching intelligence. Based on the experiment of this study, it can be seen that among the 600 investigators in place *O*, there are 587 valid questionnaires, of which 265 are willing to accept both traditional teaching and intelligent piano teaching, accounting for 45.1% of the valid questionnaires; 136 people are more willing to accept intelligent piano teaching, accounting for 23.2% of the valid questionnaires; 186 people are more willing to accept traditional piano teaching, accounting for 31.7% of the valid questionnaires. The experimental results of this study show that the research process of intelligent piano teaching based on LOT and multimedia technology is more effective than other methods of analyzing experimental data, and it is of great reference significance for the development of intelligent piano teaching.

1. Introduction

The development of the intelligent era has prompted the corresponding generation of media for information communication and sharing, which not only speeds up the speed of network communication but also improves the efficiency of the public to solve problems. The Internet of things is an important component of the information age. It can connect relevant information sharing channels and networks to realize the intercommunication between humans and machines in time and space. Multimedia technology is a human-computer interaction technology that integrates various kinds of information through computers. The objects involved are the products of computer technology, not just movies, TV, etc., and can be widely used in various fields of public life.

The research on intelligent piano teaching is an inevitable trend in the development of the Internet era. There are many scholars who analyze piano teaching, and many scholars study its intelligent teaching, but few scholars analyze it from the perspective of LOT technology and multimedia technology. Based on LOT and multimedia technology, this study analyzes the intelligent teaching of piano, explores the development of piano teaching in the Internet field, broadens the research methods in this direction, and provides a feasible method for the development of intelligent piano teaching, which has certain practical significance. The innovation of this study is that this study analyzes the intelligent teaching of piano based on the Internet of things technology and multimedia technology.

2. Related Work

Piano teaching is a relatively traditional and demanding teaching activity. The development of the intelligent era has prompted the development of piano teaching in the direction of intelligence. However, how to better carry out intelligent piano teaching has become an important research topic for many scholars. Zhang believes that the development of electronic technology is changing with

each passing day, and it is widely used in various fields. As a hobby with a wide audience, the tuning teaching of piano needs to keep up with the progress of the times [1]. Liu and Tsai's research pointed out that in teaching, in addition to traditional research and analysis, it can also intelligently recognize text through parallel projection and area expansion and at the same time deepen the research and analysis of teaching [2]. Gong et al. believe that the teaching system should be deeply optimized with the development of society, and the course content should be improved by combining intelligent remote multimedia, so that it can promote teachers to improve work efficiency and optimize the course system [3]. By studying the activation state of mirror neurons (MNs), Hou et al. determined that the activation state of MN will be more obvious when pianists are in the "enjoyment" mode. Through analysis, he believes that the reason for this phenomenon is not only arousing the audience's associative feelings but also the moderating effect of relevant sports knowledge [4]. Tan et al.'s research is to explore what is the main influence on the production of piano sound. Through careful observation of the players, it is found that the main reason for hearing the sound of the piano is the vibration of the soundboard, and through experiments, it is found that at high frequencies, the lid of the piano contributes the most to its sound transmission [5]. Since the audience of piano and its teaching is very wide, how to better carry out piano teaching is a hot topic for researchers. With the advent of the era of intelligence, the teaching of piano intelligence has gradually entered the public's attention, and researchers have emerged in an endless stream of research methods, but few scholars have combined Internet of things technology and multimedia technology to conduct research.

The Internet of things technology can use a variety of means to combine various information sensing devices with the network, while the multimedia technology processes various multimedia information through computers. Beyene et al. introduced NB-LOT technology, which can support extremely low power consumption and the use of low-cost devices under extreme conditions. Through experiments, he found that a good candidate for implementing NB-LOT technology is cloud wireless access network [6]. Sisavath and Yu believe that home security is very important. For this reason, he proposed a smart home design concept with the theme of "Internet of things is close to life, simple, and easy to use" and built an LOT-based smart home system [7]. Zhang et al.'s research discusses various LOT communication technologies, and based on NB-LOT, he proposes a NB-LOT-based urban lighting system design scheme. He emphasized the design of a single lamp control system and proposed the idea of combining smart lamp poles with 5G communication [8]. Wu et al. designed an interactive remote care system based on LOT technology, which enables direct communication between the patient's medical equipment and the caregiver's smartphone, thereby improving the quality of care for patients with chronic diseases, and confirmed the potential value of the system through experiments [9]. Chang et al. proposed a variety of ways to detect multimedia events, and the use of semantic representation is recognized by most of the public, but to make the content of semantic representation more accurate, several video archives are usually applied to event videos, and certain results have been achieved [10]. Since the Internet of things technology and multimedia technology are more commonly used information processing methods in the information age, there are many scholars who study them, but few scholars combine this method with piano intelligent teaching.

3. Intelligent Piano Teaching Method Based on Internet of Things Technology and Multimedia Technology

3.1. Intelligent Piano Teaching. The piano is a keyboard instrument in Western classical music. It is known as the "king of musical instruments." Modern pianos have become an essential instrument in music creation and auditory training due to their wide range and varied timbres [11]. Due to the continuous development and innovation of piano, the times are stable and peaceful, and people pay attention to spiritual enjoyment. Nowadays, more and more people take piano learning as a hobby. Therefore, piano teaching has become a popular trend [12]. Figure 1 is a display diagram of piano teaching.

Due to the advent of the Internet of things era, the traditional oral or face-to-face teaching methods can no longer meet the learning needs of the public, so the intelligent teaching method combined with the Internet of things technology and multimedia technology has become the current mainstream trend [13–15]. The intelligent teaching method is an important research field in contemporary education and teaching. With artificial intelligence technology, it can help students acquire piano skills without the guidance of human teachers, which is also a current research hotspot [16].

3.2. LOT Technology. The Internet of things technology is the extension of some related applications on the basis of Internet applications. After the function of the network, the connection between the Internet of things and the Internet is realized, which generally includes terminal facilities that can realize information exchange and communication [17]. The Internet of things technology mainly includes the following three types: sensor technology, RFID tags, and embedded system technology [18]. Figure 2 is a typical display of LOT technology.

In the field of LOT technology applications, matrix decomposition is often required, including methods such as k-means, which are generally unsupervised learning algorithms [19]. The k-means clustering algorithm is a commonly used clustering algorithm in intelligent learning. Its basic meaning is generally to divide the given data set $Q \in R^n$ into subsets $C_1, C_2, \cdots C_i$, where i refers to the number of clustering categories. The basic formula of the k-means algorithm is as follows:

Figure 1: Display of traditional piano teaching.

Figure 2: Typical LOT technology presentation.

$$\sum_{m=1}^{i}\sum_{j=1}^{k} a_{mj}\left\|q_j-\delta_m\right\|^2. \tag{1}$$

Among them, when q_j belongs to the C_m, $a_{mj}=1$; otherwise, $a_{mj}=0$; that is,

$$a_{mj}=\left\{\begin{array}{ll}1\text{C} & a_j\in C_m\\ 0, & \text{otherwise}\end{array}\right\}. \tag{2}$$

The decomposable proof of the k-means clustering algorithm is consistent with the proof of the objective function of k-means and can be decomposed into the following formula:

$$\sum_{m=1}^{i}\sum_{j=1}^{k} a_{mj}\left\|q_j-\delta_m\right\|^2=\|Q-NA\|^2. \tag{3}$$

Q is the sample matrix, each sample data are represented by one of the columns, and N is the aggregate class center matrix. Definition: each column of the sample matrix Q is q_j, and the 2-norm of Q is defined as the sum of the squares of the lengths of all sample vectors, namely,

$$\begin{aligned}\|Q\|^2 &= \sum_{l,j} q_{lj}^2 = \sum_j \left\|q_j\right\|^2 = tr\left[Q^Z Q\right],\\ \sum_{m,j} a_{mj}\left\|q_j - \delta_m\right\|^2 &= \sum_{m,j} a_{mj} q_j^Z q_j - 2\sum_{m,j} a_{mj} q_j^Z \delta_m \\ &\quad + \sum_{m,j} a_{mj}\delta_m^Z \delta_m = Z_1 - 2Z_2 + Z_3.\end{aligned} \tag{4}$$

Z_1, Z_2, and Z_3 are simplified to get

$$\begin{aligned}Z_1 &= \sum_{m,j} a_{mj} q_j^Z q_j = tr\left[Q^Z Q\right],\\ Z_2 &= \sum_{m,j} a_{mj} q_j^Z \delta_m = tr\left[Q^Z NA\right],\\ Z_3 &= \sum_{m,j} a_{mj}\delta_m^Z \delta_m = \sum_m \left\|\delta_j\right\|^2 k_m.\end{aligned} \tag{5}$$

Among them, k_m represents the number of samples belonging to the mth class.

Expanding the right-hand side of the equation, we get

$$\|Q - NA\| = tr\left[(Q - NA)^Z (Q - NA)\right] = Z_4 - 2Z_5 + Z_6. \tag{6}$$

It can be seen that: $Z_4 = Z_1, Z_2 = Z_5$, so it is only necessary to prove $Z_3 = Z_6$, and the proof process is as follows:

$$Z_6 = tr\left[A^Z N^Z NA\right] = tr\left[N^Z NAA^Z\right]. \tag{7}$$

Further derivation can be obtained:

$$tr\left[N^Z NAA^Z\right] = \sum_m \left\|\delta_m\right\|^2 k_m. \tag{8}$$

Because AA^Z is a diagonal matrix, the proof result of $Z_3 = Z_6$ is valid, and the final equation to be proved is valid. It can be seen from the above process that k-means is a solution process that can be used for matrix decomposition. Moreover, in the clustering algorithm, many algorithms are designed on the basis of k-means, such as the K-nearest neighbor algorithm, all of which are based on the central judgment of the data to achieve clustering. From this, it can be concluded that similar algorithms based on the k-means clustering algorithm have the characteristics of matrix decomposition [20].

Before analyzing the feature learning of the clustering algorithm k-means, an evolutionary version of the k-means algorithm, spherical k-means, should be introduced. According to its definition, the algorithm uses cosine similarity instead of Euclidean distance to measure in the process of clustering, normalizes the sample points, and performs clustering after it is distributed to a sphere. This algorithm outperforms the traditional k-means clustering algorithm [21].

The spherical k-means algorithm satisfies the following formula:

$$\begin{aligned}&\underset{B,s}{\text{minimize}} \sum_m \left\|B_{sm} - q_m\right\|_2^2 \quad subject \quad to \left\|s_m\right\|_0 \\ &\quad \le 1, \forall m \quad \text{and} \left\|B_j\right\|_2 = 1, \forall j.\end{aligned} \tag{9}$$

Among them, B is the transformation matrix, and B_j represents the jth column of the transformation matrix, that is, the jth cluster center of k-means. S is the encoding of the feature vector. When the jth column of B is the closest to $q(m)$, the element corresponding to 2 is $\neq 0$, and the rest = 0. For example, to perform clustering processing on Q, $i = 5$ is set, and if the final result is that q_m is clustered into the third category, the encoding vector is $S = (0, 0.1, 0, 0)$. Among them, S can be considered as a new clustering feature obtained after learning. The process of feature extraction in the k-means clustering algorithm is the process of calculating S.

When a new sample set q is input to the algorithm, the formula is as follows:

$$S_{jm} = \begin{cases} B_j^{\perp} q_m, if\, j = \underset{l}{\text{argmax}}\left|B_j^{\perp} q_m\right| \\ 0, \quad \text{otherwise}. \end{cases} \tag{10}$$

Since the calculation data are distributed on the spherical surface, if the distance between the two points is the closest, this symbol indicates that the value is the largest. The feature expression process of spherical k-means algorithm is as follows.

Standardization is calculated as follows:

$$q = \frac{q - \text{mean}(q)}{\sqrt{\text{var}(q) + \varepsilon_{\text{norm}}}}. \tag{11}$$

Whitening is calculated as follows:

$$\begin{aligned}[V, B] &= \text{eig}(\text{cov}(q)); VBV^Z = \text{cov}(q),\\ q^{(m)} &= V\left(B + \varepsilon_{pca} I\right)^{-1/2} V^Z q^{(m)}, \forall m.\end{aligned} \tag{12}$$

Loop to convergence is calculated as follows:

$$\begin{aligned}S_{jm} &= \begin{cases} B_j^{\perp} q_m, if\, j = \underset{l}{\text{argmax}}\left|B_j^{\perp} q_m\right| \\ 0, \quad \text{otherwise} \end{cases},\\ B &= QS^{\perp} + B,\\ B_j &= \frac{B_j}{\left\|B_j\right\|_2, \forall j}.\end{aligned} \tag{13}$$

The specific algorithm flow is shown in Figure 3.

Similarly, when selecting data, several images can be randomly selected and arranged into a one-dimensional vector q_m, which is used as training data for 256-dimensional feature vector.

Among them, whitening is a relatively important preprocessing process, and its main function is to reduce the redundancy of data. Therefore, the data after whitening have a low correlation between features, and the features have the property of correlation variance [22]. The whitening processing methods include PCA whitening and ZCA whitening, in which fitting can be used for dimensionality reduction or de-correlation, and the latter is mainly used for de-correlation and can make the whitened data closer to the original input data [23].

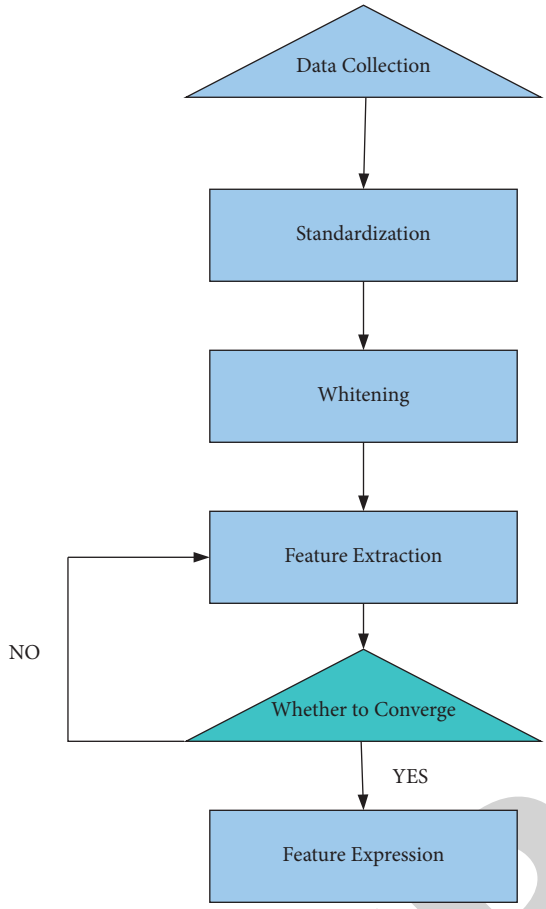

Figure 3: Feature expression flow of spherical k-means algorithm.

3.3. Multimedia Technology. Media refers to the medium that transmits or stores information, while multimedia refers to an information interaction method that combines text, image, sound, etc., and processes it through a computer [24]. Multimedia technology design data compression, processing, data retrieval, etc., have three characteristics of integration, interactivity, and real time, integrate the strengths of hundreds of schools, and successfully act on the daily life of ordinary people [25]. Due to the influence of multimedia technology itself, it will also be widely used in home systems, medical fields, and education and training in the future. Figure 4 is a display diagram of multimedia technology.

4. Piano Intelligent Teaching Experiment

4.1. Scheme Design of Piano Intelligent Teaching. As an indispensable musical instrument for musical plays that can be enjoyed by both refined and popular audiences, the number of people who want to learn and play the piano has been increasing. As a project to cultivate sentiment, piano teaching has become the signature specialty of many art institutions [26]. The needs of the public are increasing day by day, and the development of the times is also changing with each passing day. How to combine piano teaching with the development of modernization needs has become a hot spot for scholars to study. Therefore, under the development of Internet of things technology and multimedia technology, this study proposes to develop piano teaching in the direction of intelligence and improve the traditional teaching industry, to innovate the situation of piano teaching in the new era.

To better understand the relevant achievement data of intelligent piano teaching, and to further reveal the practical significance of the development of intelligent piano teaching in the Internet of things and multimedia to teachers and learners, this study distributes questionnaires to students majoring in piano in three chain brand art education institutions in O place. Among them, the students of R institution are the research objects of the experiment, and the students of S institution and T institution are the experimental control group, and a questionnaire is carried out. A total of 600 copies of the "Piano Intelligent Teaching Questionnaire" were distributed, and 200 copies were distributed to students majoring in piano in each institution. A total of 587 copies were recovered, of which 195 copies were recovered by institution R, 198 copies were recovered by institution S, and 194 copies were recovered by institution T, with an effective recovery rate of 97.8%.

In this experiment, the Internet of things technology and multimedia technology were used as the main experimental methods, and 600 questionnaires were distributed to students majoring in piano in three brand chain art education institutions in O place. The setting and analysis process of this questionnaire are fully combined with the clustering algorithm in the Internet of things and multimedia technology for analysis. In this questionnaire, 7 questions are set, and the sample data are analyzed in detail.

4.2. Discussion on the Results of Intelligent Piano Teaching. This questionnaire survey on intelligent piano teaching includes a total of 7 questions: (1) the gender of the student; (2) the length of time the student has studied piano; (3) whether you want to become a piano student in the future; (4) whether you like piano learning; (5) whether you understand intelligent piano teaching; (6) are you more willing to accept traditional piano teaching or intelligent piano teaching; and (7) the satisfaction with the current intelligent piano teaching.

4.2.1. Student Gender. According to the analysis process of the experiment, the gender of the respondents of the questionnaire is an important factor in the analysis of piano teaching, so it is very important to count the gender of the students. Table 1 is the gender statistics of the respondents.

It can be seen from Table 1 that among the piano students who conducted the questionnaire survey on the three brand art education institutions in O, there were 587 valid responses, among which 348 were women, accounting for 59.3% of the valid questionnaires, and 239 were men, accounting for 40.7% of the valid questionnaires. It can be seen that among the piano students in these three art education institutions, the proportion of women is higher than that of men. Of course, there are also a lot of men. From the side, women are more willing to learn piano than men. In the

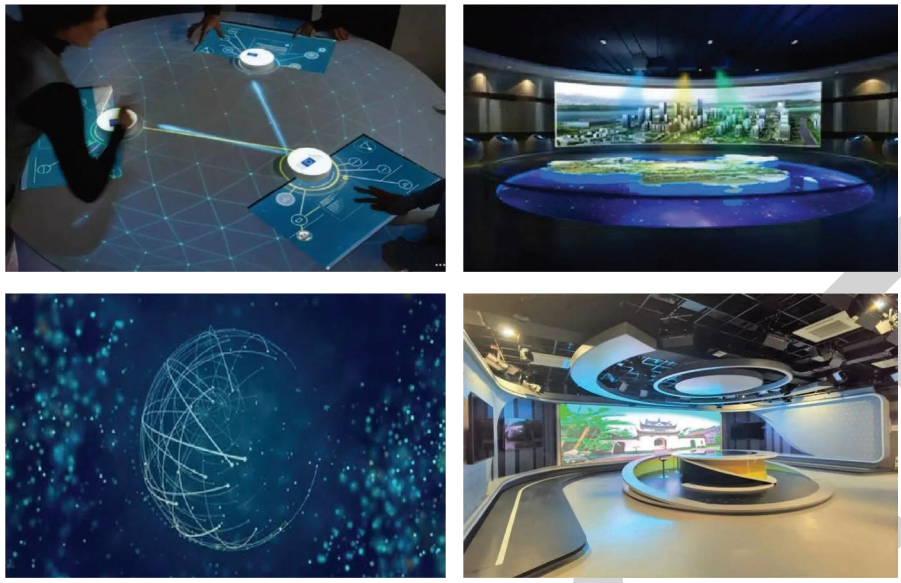

Figure 4: Multimedia technology display diagram.

Table 1: Student gender statistics.

	Female	Male
R	124	71
S	136	62
T	88	106

experimental group, there are 124 female students in *R* institution, accounting for about 21.1% of the valid questionnaires, and 71 male students, accounting for about 12.1% of the valid questionnaires; there are 136 female students in the *S* institution, accounting for about 23.2% of the valid questionnaires, and 62 male students, accounting for about 10.6% of the valid questionnaires; there are 88 female students in institution *T*, accounting for about 15% of the valid questionnaires, and 106 male students, accounting for about 18.1% of the valid questionnaires. It can be clearly seen from the above analysis that in this questionnaire, there are more female students in *R* institutions and *S* institutions, while there are more male students majoring in piano in *T* institutions.

4.2.2. The Length of Time Students Study Piano. Analyzing the length of time students study piano is conducive to a series of studies on piano teaching, the longer students study piano, the more thoroughly they understand the methods of piano teaching, which is more conducive to the research and analysis of intelligent piano teaching. Figure 5 is the statistics of the specific situation of the respondents' piano learning time.

According to Figure 5, among the 587 piano students who participated in the questionnaire, the students who have studied piano for 6–10 years are the most, with 170 students, accounting for about 29% of the valid questionnaires; secondly, there are 167 students with a study duration of less than 2 years, accounting for about 18.4% of the valid questionnaires; there are also more students with a study

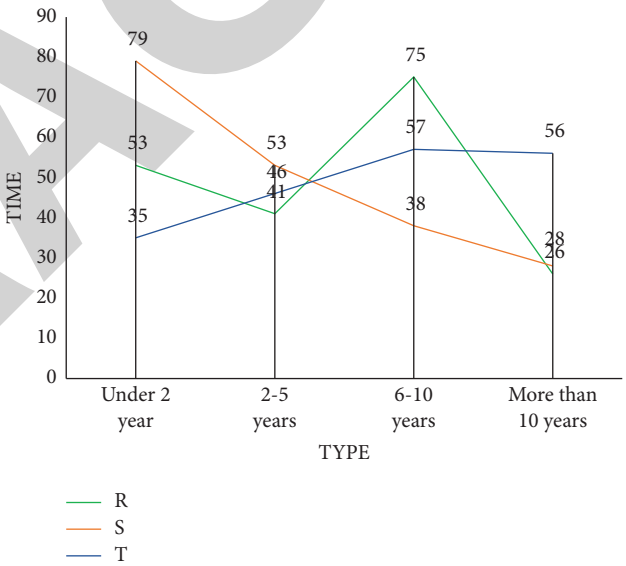

Figure 5: Duration of students learning piano.

duration of 2–5 years, with 140 students, accounting for about 23.9% of the valid questionnaires; the students who have studied for more than 10 years are the least, only 110, accounting for about 18.7% of the valid questionnaires. According to the analysis of relevant questionnaires, the number of people who studied piano in each time period is relatively large. On the one hand, it reflects that piano learning is the current trend. On the other hand, it reflects that the students who learn piano have more endurance and can persevere for a long time. This aspect reflects that the teachers of these institutions have high teaching ability and can attract students more.

4.2.3. Whether You Want to Become a Piano Student in the Future. Piano can be used as a personal hobby and specialty, or as a career development goal, to understand the students'

piano learning goals, and as a reference factor for the study of piano intelligent teaching. Table 2 shows the statistics of students who want to become piano majors in the future.

According to Table 2, most of the students still cultivate piano as a hobby. Therefore, the number of students who want to become piano majors in the future is relatively small. However, due to the in-depth understanding of the three institutions, the *R* institution is an institution specialized in cultivating art students, so the number of future piano students in this institution is the largest. *R* institution has 117 students who want to become piano majors in the future, accounting for 19.9% of the valid questionnaires, and 78 students who do not want to become piano majors, accounting for 13.3% of the valid questionnaires.

4.2.4. Whether You Like Piano Learning. Counting whether students like piano is conducive to analyzing the results of teachers' piano teaching and is of great help to the development of piano intelligent teaching. Figure 6 shows the statistics of whether the students in this questionnaire like piano learning.

There are two main situations for students to learn piano. One is that students are interested in piano learning spontaneously; the other is that they are influenced by external factors, such as parental pressure. 177 students in *T* institution prefer piano learning, accounting for 30.2% of the valid questionnaires, and 17 students do not like piano learning, accounting for 2.9% of the valid questionnaires; in the S institution, 126 people like piano learning, accounting for 21.5% of the valid questionnaires, and 72 people do not like piano learning, accounting for 12.3% of the valid questionnaires. Among the three institutions, the number of people who do not like piano learning is relatively high.

4.2.5. Whether You Understand Intelligent Piano Teaching. The ultimate purpose of this experiment is to study the intelligentization of piano teaching and to explore whether students understand the intelligent teaching of piano, which is conducive to promoting the process of obtaining the conclusions of this experiment. Figure 7 is the statistics on whether students understand the situation of intelligent piano teaching.

According to Figure 7, most of the students are relatively familiar with the intelligent teaching of piano, there are 382 students, accounting for 65.1% of the valid questionnaires, and a small number of students do not understand intelligent teaching; there are 205 students, accounting for 34.9% of the valid questionnaires. Combined with Question 6, it can be seen that students who understand the intelligent teaching of piano generally have received this teaching, and students who do not understand generally accept the traditional piano teaching method.

4.2.6. Are You More Willing to Accept Traditional Piano Teaching or Intelligent Piano Teaching. Intelligent piano teaching is a development trend in the age of intelligence, but whether students are more willing to accept traditional

Table 2: Whether you want to become a piano student in the future.

	Yes	No
R	117	78
S	76	122
T	58	136

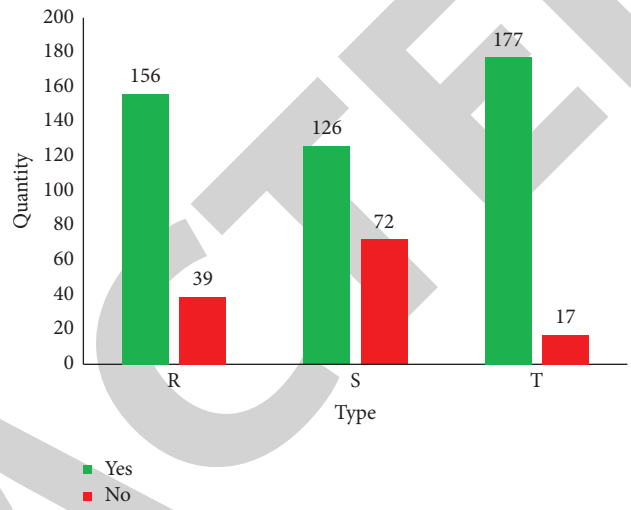

Figure 6: Statistics of whether the students like piano learning.

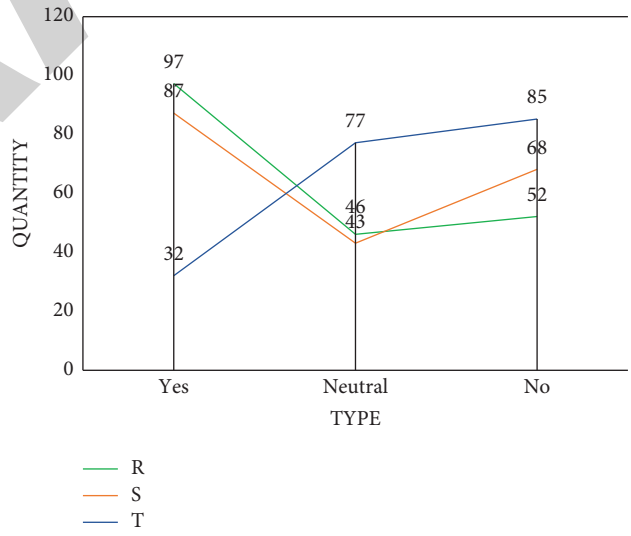

Figure 7: Statistics on whether students understand the situation of intelligent piano teaching.

or intelligent teaching methods is also an important focus of research in this experiment. Table 3 is the statistics for these students who are more willing to accept traditional piano teaching or intelligent piano teaching.

It can be seen from Table 3 that 265 people prefer both traditional piano teaching and intelligent piano teaching, accounting for 45.1% of the valid questionnaires; 136 people are more willing to accept intelligent piano teaching, accounting for 23.2% of the valid questionnaires; and 186 people are willing to accept traditional piano teaching,

Table 3: Are you more willing to accept traditional piano teaching or intelligent piano teaching.

	Traditional piano teaching	Intelligent piano teaching	Both
R	49	58	88
S	59	55	84
T	78	23	93

accounting for 31.7% of the valid questionnaires. According to the specific data in Table 3, combined with relevant analysis, it can be seen that intelligent piano teaching generally adopts video teaching, PPT teaching, etc., or uses more advanced intelligent piano for teaching, which can meet the individual needs of students to a greater extent and is extremely interesting. The traditional piano teaching is generally conducted in the form of face-to-face teaching, which requires a higher degree of concentration of students.

4.2.7. The Satisfaction with the Current Intelligent Piano Teaching. Statistical data about the students' satisfaction with the current piano intelligent teaching are conducive to further analysis of the piano intelligent teaching combined with the Internet of things technology and multimedia technology. Figure 8 is the statistics of the current students' satisfaction with piano intelligent teaching.

According to Figure 8, the number of people who are positive or neutral in their satisfaction with piano intelligent teaching is the largest, with 438 people, accounting for 74.6% of the valid questionnaires; the number of unsatisfied attitudes is relatively small, with 149 people, accounting for 25.4% of the valid questionnaires. Among them, the number of students in institution *R* who agree with the current intelligent piano teaching is the largest, with 105 students, accounting for 17.9% of the valid questionnaires; the number of students who disagree with institution *T* is the largest, with 66 students, accounting for 11.2% of the valid questionnaires. According to the research, satisfied students believe that intelligent teaching is more interesting, while dissatisfied students believe that traditional piano teaching is more detailed and can be supervised and guided by teachers, which is conducive to improving themselves.

4.3. Application of Networking Technology and Multimedia Technology to Intelligent Piano Teaching. Based on the above analysis, it can be seen that LOT and multimedia technology can be well combined with intelligent piano teaching. With the development of the information age, intelligent piano learning can be analyzed from multiple perspectives, and it can show the good development prospects of intelligent piano teaching in the LOT era. However, because the learning of LOT and multimedia technology is not deep enough, this experiment only conducted questionnaire analysis on students majoring in piano from three brand chain art education institutions in O place and did not conduct more detailed analysis on students from other majors in a certain institution or all students majoring in piano in only one institution.

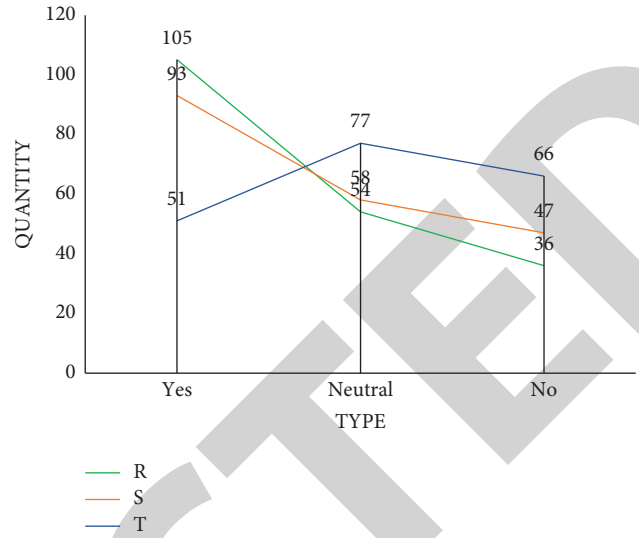

Figure 8: Satisfaction with the current intelligent piano teaching.

5. Discussion

This study is devoted to studying the related algorithms of LOT technology and multimedia technology and applying them to the research of intelligent piano teaching. This is not only the expansion of LOT technology and multimedia technology in the field of intelligent piano teaching but also a further exploration of the research on piano teaching in the field of Internet of things and a new attempt for the development of intelligent piano teaching. Through a questionnaire survey of 600 piano students from three brand art education institutions in O city, this paper analyzes their related feelings about piano intelligent teaching and explores the potential of LOT technology and multimedia technology in the analysis of piano intelligent teaching. In addition, on the basis of the existing LOT and multimedia technologies, the related algorithms are improved and integrated with the piano intelligent teaching, and practical conclusions are obtained.

Through the analysis of this case, we can see that the analysis method of piano intelligent teaching based on LOT technology and multimedia technology is more scientific than the traditional method. The surveyor used LOT multimedia technology to further discuss the development direction of intelligent piano teaching, optimized the algorithm in the specific experimental process, and finally obtained the best solution for this experiment.

6. Conclusions

Through the analysis of this case, the following conclusions can be drawn: the development of the Internet of things has made the world more integrated, allowing social development to further develop into the field of intelligence, so the combination of LOT technology and multimedia technology can better integrate it with the research on piano teaching and provide a great advantage for further analysis of piano intelligence research. In this study, through the questionnaire analysis of 600 piano students, the best plan for the

Hindawi
Scientific Programming
Volume 2022, Article ID 9174756, 12 pages
https://doi.org/10.1155/2022/9174756

Research Article

Intelligent Information Service System of Smart Library Based on Virtual Reality and Eye Movement Technology

Xiao Su[1] and Nan Chen[2]

[1]*School of Design and Art, Xijing University, Xi'an 710000, Shaanxi, China*
[2]*Mammary Department, Shaanxi Provincial Cancer Hospital, Xi'an 710061, Shaanxi, China*

Correspondence should be addressed to Nan Chen; chennanfighting@stu.xjtu.edu.cn

Received 16 July 2022; Accepted 10 September 2022; Published 10 October 2022

Academic Editor: Juan Vicente Capella Hernandez

An innovative system provides intelligent services in the library to both users and the terminal. Compared to the core digital reading room, they can make wise judgments on the retrieval and use of information assets. The implementation of succeeding value management based on the latest technological tools is required for learning to provide knowledge services and fulfil its role as convergence is capable of reacting to varied data needs. The major obstacles to digital libraries are lack of planning and software, import restrictions on equipment, inadequately skilled staff, lack of standards, and a refusal to cooperate. This paper introduces the Eye Movement Technology (EMT) for the intelligent information service system of a smart library (SL) based on virtual reality (VR) strengths as an automated library management system for cost savings and increased output. EMT technology that can identify a person's appearance and monitor something to look at in real-time is recognized as wearable technology. Visual field position and the gaze vectors for each eye are converted into a data stream that includes the focus origin. Most of the library's operations can be managed by librarians; in a word, this system allows them to keep track of all of their books' transactions. The research in EMT-SL technology in the intelligent library system has developed to the point that a wider audience can use it. As a result, eye-tracking in reading rooms and information science research are expected to rise in the future; with the advancement of VR, the computer-generated modelling of images is experienced through special electrical devices, and people can be visible in different climates using traditional VR and augmented reality.

1. Summary of Information System in Smart Library

The smart library information service must be a smart bookstore that integrates the functions of the current information system with the knowledge-based SL learning system in terms of generating innovative human resources. In addition to providing information and statistics directly from librarians, educators also build and customize user-friendly platforms that allow them to access information on their own. Academic library systems are designed to record and maintain the everyday activities of a library, often including renting and returning materials, overdue computations, and other tasks. [1]. Students' ability to think creatively and logically will be enhanced by a system that allows them to build a collective intelligence-based learning skill set via a collaborative and interactive interface [2]. The characteristics of the library's combined effect with virtual reality (VR) technology are conducted to establish a theoretical and practical foundation for the development of virtual reality in the library. Smart library models are analyzed to identify the technology employed at each abstraction level. Immersion, presence, and interaction are sometimes referred to as the three key characteristics. Modern structures and SL improvements may both benefit from virtual reality technology. A contractor may utilize 3D modelling and virtual reality goggles to bring a library extension or reading makeover to reality for consumers so that they can understand that the suggested layout would increase the value of the house. [3]. Context construction for

digital book knowledge service expansion is the subject of the current study EMT; the service context's elements and contents are described, and a strategy for building the responsibilities for the intelligent bookstore's knowledge service extension is provided [4]. A visual representation of the information retrieval process has been developed. The SL model combines the fundamental phases of the interactive visualization process and introduces the document and the functional system [5]. Students can access digital materials through the university library, and the development of SL and its accompanying group technologies will be utilized. With the development of visual information retrieval, there is a growing interest in establishing standards for storing and recovering visual data from large, unorganized archives. Reading systems are a collection of classification algorithms that help to ensure that the shown papers are relevant to the inquiries being entered. It functions by sorting and ranking content based on user-relevant keywords. Educators may acquire knowledge and skills thanks to the ease of library resources. Additionally, empowering kids with online technologies is an excellent approach to using them efficiently. Searching for materials on their own or with the help of education is an option available to students. Increased educational significance comes from allowing people to choose how fast or slow they study [6]. Regarding mobile Internet development, human-computer interactions are now the most sophisticated communication protocols and sizzling areas. The future of SL design concepts based on 5G will establish new heights, creating a more intelligent, pleasant, and convenient library environment for readers [7]. As a result of the spread of the Internet, digitalization, and technological advancements, our teaching and learning EMT methods have evolved. One of the functions of libraries must be transformed into a place where people can come together to discuss and learn from one another through collaboration and group projects [8]. According to certain academics, the future of the library is linked to technological growth characterized by convergence and standardization [9]. This study aims to develop a university library's intelligent service system, and the data analysis is conducted using Eye Movement Technology [EMT]. This search service makes it simple to locate digital materials; to some extent, the digital library may be considered development and advancement of library automation technology. [6]. The population evolution mechanism of members of the dominating population is superior and has a higher likelihood of evolution than the disadvantages of populations. VR can help individuals in dominant groups evolve better and speed up the algorithm's convergence [10]. The suggested model is built using a book retrieval system and SL to compare the proposed system with existing, well-established library models. In light of this solid evidence, the suggested model outperforms the existing models. The goal of a digital library is to organize and make enormous volumes of virtual evidence available in an orderly fashion. Library users may promote their productivity, equipment, and public views through interactive multimedia in a smart and efficient way. Visiting institutions with a strong sense of patron involvement is thrilling. Academic libraries may become digital books by strategically designing and implementing cutting-edge innovations such as eye movement software and virtual reality. However, they must also include continuous improvement, consumer nurturing, and employee training required to make the transition. The "Intelligent Reading Room" technique allows a catalogue to remain accessible to the public even though it is not maintained. Network management of library resources, such as automated sensors, illumination, personality terminals, and accessible digital assistants, is now possible thanks to this modern technology. [11]. The author talks about the advances in science and technology, including information and SL communication technology, which have created new possibilities for public libraries to adapt [12]. Libraries have come a long way in operation and expansion to use cutting-edge modern technological breakthroughs, and traditional libraries have been supplanted with virtual and SL [13]. Authors have focused on specific libraries and their smart services, from library automation systems to artificial intelligence to complete integration with a smart campus or community [14]. Although the research sheds light on important issues, a necessary foundation of knowledge is still lacking. For librarians to seriously consider EMT in establishing or converting their smart library, a clear understanding of what a smart library is and the many methods it might implement is required [15]. Libraries may accomplish a deep integration and connection between books and people with VR Internet technology, which is a significant rising business [16]. A greater direct segment between users and libraries is created in VR due to the intelligent book management system's three-dimensional interconnectedness, allowing for the more humane and thoughtful growth of book services [17]. Social networking and video conferencing in modern bookstores can help libraries better serve their customers, according to this report. A less organized but more creative and imaginative approach to running a library is provided by a smart library. The reading room model delivers information and educational resources in an electronic format besides paper form and enables access to digitized collections spread throughout the network, rather than merely constructing digital libraries from processed inventory materials [18]. Intelligent librarians are defined in this study, and the necessity of video conferencing and social media is outlined to help digital books offer their services more successfully [19]. The Internet of Things is the next big thing in Internet development. It is possible that the Internet of Things (IoT) can give a library service and a security improvement solution. It outlined a strategy for enhancing library services and making them more user-friendly, and this system might be the first step in creating a smart library [20]. Various content collections might make it challenging to find excellent EMT-SL and diverse materials in a digital library. Researchers in digital libraries and related fields have shifted their focus from keyword-based matching to a model of user-actual behaviour [15]. Analytics libraries that are also frequently used in mobile apps have not been systematically evaluated for their privacy VR, despite great efforts to identify and measure the privacy breaches caused by marketing libraries [21]. It is possible to access datasets, often

referred to as academic resources, online and through the application. Students may acquire anything from articles and papers to media articles and documents in a library collection. A digital library's essential duty is to manage and make available enormous volumes of media files. Organizing, searching, and retrieving a label's material are all possible with online databases in addition to processing it. Instead of archiving and protecting tangible goods such as magazines and newspapers, modern libraries have shifted their focus to searchable databases and the maintenance of information.

The main contribution of the paper is as follows:

(i) Virtual reality (VR) is pioneering new territory in the library sector today; the digital room is composed based on a genuine participant's notion; the result is an entirely new type of perception. According to this upgrading technology, mobile users may now experience the crucial globe scientifically spectacularly.

(ii) Eye Movement Technology (EMT) with an intelligent library is used to focus attention on the next section of text directly. Using visual processing data, researchers may analyze viewers' exact right time processes in greater detail. They include motions, progressive pursuits, visible acuity oscillations, and ocular movements.

(iii) An innovative library (SL) is a global organization of books and associated resources connected. Newly integrated tools and services are developed based on the evaluation of genuine reference materials and subscribers.

The remainder of the article is Section 2, which indicates a literature review on improving the intelligent information system of smart library EMT-SL. Section 3 describes the information services in virtual reality. Section 4 mentions results and discussion on the digital library. Section 5 concludes this essay with an experimental analysis of reading research.

2. Relative Study

Yu et al. introduced SL as a primary motivation in modern society, and it has also infused new life into creating intelligent libraries. This paper explains the essential position of brilliant libraries [22], analyzes the use of AI technology intelligence in the Field of Modern Books (FMBs), and shows the usefulness of artificial intelligence in library service. AI systems are expected to be employed extensively in creating interactive libraries. More efficient and high-quality services are among the goals of the digital collection. It seeks to establish a more appealing connectivity of data and a more dynamic sharing space for that knowledge.

Zhang introduced a dramatic increase in demand for the library's intelligent services, propelling the library's service model into constant change. This study proposes an intelligent library service (ILS) mode based on the 5G network [23], which incorporates a range of sophisticated network algorithms into the information literacy mode and implements the intelligent library in the 5G environment of rapid information transfer. This report provides a detailed understanding of real-time monitoring data using a combination of sensors, face recognition, and other technologies to collect real-time monitoring data and even an inspection robot to monitor and inspect each functional area.

Shen proposed the research on the strategic creation of a large-scale multifunctional area, identified as the Intelligent Infrastructure for Human-Centered Communities (IIHCC), in the institutional setting has been presented in this study [24]. Change dynamics and adaptive design techniques related to the IIHCC evolution and libraries' creativity were studied in this creative area. Semistructured interviews, participant observation, and document analysis were used in a mixed-methods approach. Emerging intelligent infrastructure and ubiquitous mobility, and the dynamic data realm in this cyber-physical-human integrated environment, are shown in the findings. As a result of these advancements, this research explores the potential of intelligent libraries as testbeds for data discovery, a repository for community knowledge, and a way to engage with information intelligently.

Zhang detailed several elements involved in the information retrieval process, including setting goals, selecting data structures, and developing methods. This work investigates the creation of an intelligent librarian system (CILS) based on the extraction of book information [25]. Search engines are continually changing the needs of their users as people's needs change. There are even more sophisticated search engines, such as specialized search and categorized navigation. Cognitive information retrieval techniques and a library system (CIRTLS) were proposed in this study to increase search accuracy and create an efficient system; analytic data pipelines and sensing models are coupled to investigate system performance.

Wang and Sha proposed building a personalized information service system for university libraries using large amounts of big data (BD). Still, in particular, to provide it, it must consider different aspects [26] of the overall system model's architecture, its functional model, and the system interface module design. The platform's available design includes stages based on the learning ability to accurately identify user needs, provide personalized services based on artificial intelligence, and provide academic research and discussion spaces based on integrated media.

Xu et al. proposed that it has become increasingly crucial for economic and social growth to use automated virtual reality and SL information technology systems. Libraries are building and optimizing their systems in time to retain books and information materials, produce information resources [27], and give knowledgeable assistance. Research into library automation systems and virtual reality (LASVR) applications, along with their expected impact on the administration and service level of libraries, is analyzed in-depth, focusing on the intelligent library development trend. Although at an advanced stage of digital book development, competent institutions must implement new scientific and

technical tools to improve the reader process and enhance services for readers.

Yu and Huang detailed that the Internet has become an essential part of most people's everyday lives due to technological advancements and the mass availability of broadband services [28]. Globalization and technological advancements (GTAs) have accelerated the evolution of the library notion, making it less relevant than it once was, and it is no longer the community's responsibility to leverage scientific and technical innovative ideas and procedures to promote its business; instead, it is the responsibility of the whole information technology industry to do so. The virtual library's customers were given the opportunity to be a sample for this investigation.

Gul and Bano proposed an innovative library book review extensively to identify developing technologies within this field. There was an initial search of business intelligence and analytic data on the Web of Science and Corpus for literature on Sensible Books (WSCLS) and its many elements [29]. Artificial Intelligence (AI) data gathering is used to retrieve related articles in the literature. A wide range of developing themes was also investigated by looking at later publications mentioning the literature on Smart Libraries. Libraries serve as the backbone of a community, connecting people to information and nurturing their sense of culture.

Chen and Hao introduced a significant role played by rapidly evolving information technology in the distribution and exploitation of Eye Movement Technology (EEMT) knowledge in today's digital world. Furthermore, the library actively introduces different advanced software [30], optimizes its service model, and changes cognition as a significant concentration of literature material. This article discusses the current state of digital libraries and context-aware innovation both domestically and internationally, evaluates the competent institutions using context-aware technology, and builds a framework for digital books based on context awareness.

3. Proposed Methodology

Technology that incorporates SL digital technology, human-machine interaction, network function, simultaneous image processor, and simulation is referred to as VR. Highly immersive environments may be created with this system that uses the user's senses of sight, sound, and touch to create a realistic virtual world. Students may improve learning reliability and the ease of digital libraries. Librarians' digital materials may be accessed and read by learners whenever and wherever they want. For example, public technologies have always had specific traits: they preserve and conserve, disseminate and safeguard material in various media while also allowing for communication between the user and the knowledge; they are active, regionally, and throughout time. VR is used in many industries, including medical, military, mechanical manufacturing, and aerospace. A library's ability to give readers individualized and courteous service has grown in importance as the years have passed. As a result, libraries are increasingly turning to cutting-edge technology, such as virtual reality, to enhance SL services. The construction content of the data resource and intelligent application layer is examined in light of the study on the information retrieval technology model of the brilliant library. In this report, virtual research is carried out on six service aspects: bright space, multimedia, visualization, and reality. Since its widespread use, virtual reality technology has positively affected various industries. Suppose modern SL technological integration has improved the industry. In that case, it will be evaluated on this criterion and if it has enhanced the library's application of VR, which is being built up through various practical improvement impacts in preparation for further in-depth investigation.

Knowledge-based services are provided by cognitive computing in the reading room to both readers and in the long run. Figure 1 expresses that SL service administrator methods, in cooperation with the bookstore's primary system for students, supervisors can make more informed choices about patron access and use of learning materials. The institution employs an expert group with a wide range of high-tech gadgets to boost productivity. Library operations, financial planning, scheduling and negotiation of resource acquisition, program management, and campaigning are included in the core responsibilities of digital libraries. The system's requirements for librarians are based on members' capacity to explore titles by description or subject. A book's identification identifier and shelf location must lead them directly to it. Information about the publications that each person needs is readily available through the program. Library businesses' personal autoborrowing and self-returning titles are now possible for robots, and intelligent technology can completely replace librarians' responsibilities. Still, they can boost the quality of the services. As a result of this knowledge equipment, the document can be referred to as a thinking reading room.

Furthermore, because EMT provides a high level, developing a clever collection must be quick so that the resource may enter the creative phase after experiencing the momentary intellectual procession. As a result of the use of human thinking, a dynamic book might be constructed. Knowledgeable libraries may become excellent and achieve digital information literacy's accuracy, customization, and boldness by utilizing more appropriate data analytics tools during the transition and upgrade process. Talented books that are specific to the type of archives due to their reliance on the online platform in the modern-day are progressively gaining VR existence as a result of this reliance, and this is their major significant aspect. Network technologies have provided an objectively quantified framework for the media, position, and private modification maintenance of wise books to an extent.

3.1. Smart Library Service Model. Even though the paradigm, facts, interface, resource activity, and geometrical features are all considered when describing a general store reading room, there seems to be a universally accepted definition. The sensible bookshelf is a scale model for genuine translations of the natural setting, and modelled input is used as a

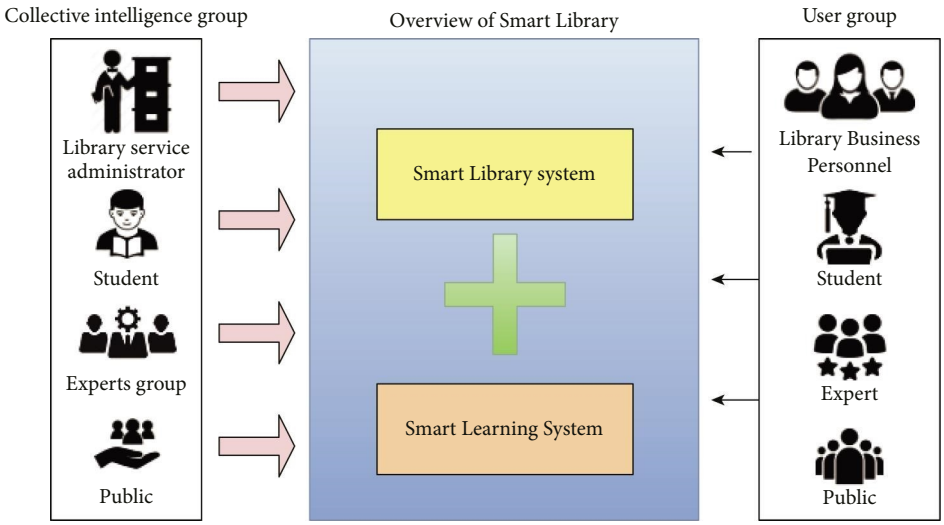

Figure 1: Overview of intelligence group in the smart library.

driver for an intelligent library. To represent real stuff digitally using knowledge discovery and incorporation of authentic statistics and archive file storage from the entire product lifecycle, operation, all aspects, and entire company, and also the linkage of these data sources. It is possible to preserve electronic documents in the face of communication breakdown and technical development by utilizing a range of approaches, methods, and tactics. Digital preservation is concerned with preserving the integrity of verified data for future use. Recognizing the challenge, considering the input, sample selection, information retrieval, and observation of the findings of the simulations are all components of the general investigative process.

$$D = \left|S_K\right| + \left|L_K\right| + M_K * E_K. \tag{1}$$

D denotes the differential calculus to measure the distance in eye movement in reading and is an ability to electronically describe and simulate everything from supplies to capacity to apparatus activities. S_K is a reading room with a statistical value of combination and $L_K$is a library part that integrates into the intelligent book, combining applicable data science with personal information drive to create a current catalogue. The E_K bookstore's virtual mapping equation denotes the Eye Movement Technology material with reading time as follows in (1):

$$y = d + \left[Y_K - E\left(\left|N_K\right|\right)\right]. \tag{2}$$

y is a value of probability function that gives accuracy to read books in innovative librarian through its bookstore's, which has an EMT layout and it is physically expressed and modelled using an identifier, replication, and associated system. The library's total area d has been recreated in the virtual space with the network layer in the reading book. The academic library's data Y_K is a learning efficiency promptly using recognition, and $E$is embedded sensors, ensuring that the built environment of the book is N_K documented throughout the entire operation, as found in (2), including all its constituent parts and every stage in its evolution.

This equation ensures that a more comprehensive array of information in the intelligent learning model is available, and the newest iteration permits company readers to use on-demand content. Giving quick control over resources to an audience with connectivity to numerous computers at once and in concurrent mode is also a modernization of the library's administration.

Effective teaching has received a lot of attention as a result of the progress of technology. The deepening of library culture can be furthered by encouraging the fast expansion of audio-visual aids inside the library's framework. The opportunity to think critically and creatively is fostered by this method. As a result, pupils develop more motivated learning habits. Instruction simply can happen with access to a reading room. It pleases people's curiosity and broadens their perspective on a variety of topics. In terms of preserving resources, library users make them available to students by providing registers, directories, or other search guides that help identify them. Libraries play an important role in understanding concepts together. It is undeniable that multimedia plays a significant role in education. It aids the instructor in communicating the information in a clear and concise manner, allowing pupils to remember the results over a period of time.

Figure 2 shows that knowledge service development in libraries constructs an innovative expertise creativity product offering; this research examines the concepts, components, and mechanisms of the present cognitive repository. The knowledge, materials, equipment, and level of effectiveness for personal communication are supplied for understanding creativity operation based on the complete domestic basic methods through the construction of the static feedback controller. In addition, this study makes assumptions about the influences on the adaptive bookstore's experience creation function and develops modelling of those influences on the bookstore's goal of contributing to expansion. The strengthening and growth of the information literacy research resource is a crucial component of the

clever book understanding provider's progress and development. It promotes the bookstore's ability to comprehend, conduct scientific research, administer society, build cultures, and foster remarkable growth. Learning efforts and investigation thrive in library services that provide a safe and supportive atmosphere. Staff at universities may assist users in learning the materials needed for the study. Additionally, several libraries today are equipped with systematic digitization of their collections. Based on culture, engagement and maintenance are supported by library services by giving access to quality and career educational experiences, developing media information competence, preserving cultural identity, and encouraging digital literacy. Innovative library knowledge-based invasion should move away from resource-based approaches and toward ones focused on users' needs.

$$s = \frac{|l_b|}{\lambda_k} + B. \tag{3}$$

The platform of s denotes the eye movement in the objective function to calculate books in SL. The value of l_b is the conventional phrase scale parameter. It is essential to consider $\lambda_k$on the learning, set is used to record the data depending on the corpus used in the investigation. A learning algorithm of relevant information B is used to classify all the annotations the information agent acquires. This data are then used to classify K the legal papers into two groups, those that the evidence cos operative thinks subscribers, or that the system thinks people as found in (3). Content files consumers dislike can be eliminated to meet the goal of details screening by deleting publications visitors despise.

The combination of device design and control to create a simulated 3-D visual or other sensory environments that allow a person to interact with coursework observation and resource generation are supported by the public library's 360-degree reality and augmented reality sources. Figure 3 shows that virtual reality (VR) is an essential innovation that have the potential to advance a wide range of areas significantly. A device habitat, often interactive audio-visual, may replicate a strong existence in subjective or objective locations. Wisdom resources is a digital world that can utilize voice recognition or text messages to communicate with other users and librarians in an incredible atmosphere. The original database is an SL technology that allows academics and people to debate relevant topics. For the primary part, the objective of a VR reading room is to provide a strong foundation for training and to boost the overall standard of living by implementing online resources that are widely accessible. By presenting students with meaningful and engaging encounters that would otherwise have been impossible, VR may improve the system.

Additionally, librarian sources may be used to learn about a group's particular hobbies or to access entertainment items such as compositions and books, for example. A library is a place where learners may complement and enrich their educational experiences, understand skills to discover data, and cultivate healthy study and reading habits. By engaging the students with meaningful and engaging situations that are often impossible, virtual reality may access education. All of this can occur from inside the confines of a single classroom. It is essential for teachers to supervise students via virtual reality, which is available to all students.

Furthermore, all of this may begin in earnest in an inclusive classroom. Virtual reality (VR) is accessible to all students, and educators may simply supervise it. In augmented reality, the observer is involved in a software experience with sights and elements that look genuine. Wearing a wearable device or visor, individuals may immerse themselves in this practical world. The information seems three-dimensional because of the instability caused by the widescreen optics placed behind the display and the eyes. Compared to the visual system's receiving and interpreting sights in the physical world, fully connected layers are transmitted throughout the lenses.

The fundamental way to create an intellectual reading room is to construct and develop an efficient content system design that preserves the booking system and allocates exhaustive, rich, and sophisticated resources. Figure 4 shows the information extraction system in a creative library with sensor technologies detecting radar signals during the Second World War. Librarians are eligible to function well for a wide range of people, including academic librarians, customers, contractors, and executive management. "Smart Library" technology allows an institution to remain accessible to the public even if it is not staffed. Network access to learning materials, such as automated and public workstations, is mainly owing to these technological advances. Bookstore entrances are protected by electromagnetic sensors that only allow books that were read out to leave the workplace. Libraries will be alerted about a suspected robbery if a book's RFID tag is not correctly signed out, triggering an alarm.

In particular, with electronic access in respect to the belief that experiential recognition functionality can be implemented in the public library book recommendation facilities; an automatic street light purpose in the reception area, depending on the date and source address to determine whether lighting services should be provided; shelf checking utilizes a unique code to link the map and the instruction identification system; and an RFID-based library location analysis system. Management, authentication, and transportation networks may all be made more accessible and hygienic with Radio Frequency Identification (RFID) technology. Techniques that allow reference personality with private cloud materials enhance personal rights by permitting people to access books without relying on collection workers. With sensor technologies, most of these workstation organizations are providing extra librarian employees to focus on serving their customers directly, allowing for more exactness in movement and stocking.

$$E = \sum_{u} L\left(S_{t+1} - R_t - V\left(r\right)\right). \tag{4}$$

E denotes the eye movement with an intelligent learning library system derived from measuring the books in SL with a sensor, L is expressed for the calculation of smarts library

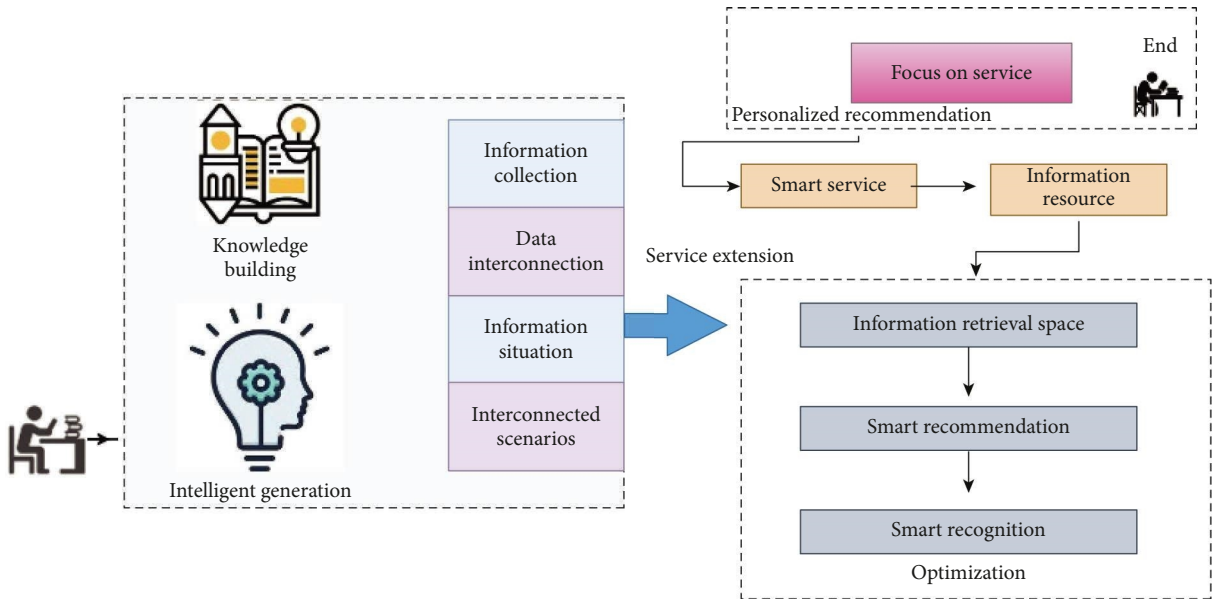

Figure 2: The intelligent library's knowledge service development.

by reader actuality opinion of an object is defined by R_t, and product I itself is denoted by actual rating in reading$V$ symbolize reader u suggested reading list and illustrates the literature that consumer r rated positively in the learning case for calibration and validation indices purposes, as found in (4).

$$T = \left(s_x - l_r, R + l_y\right). \tag{5}$$

T denotes the significance of the independent variable of grey-scale values of pixel points to each device's reading frequency; the approximate amount approach may be used as it yields the equivalent output. In the digital reading room, there are $s_x$detectors, and the projector's measurement is$R$, as in (5), the parameter-value of a specific region's room. Despite its ease of l_y, this approach provides the quickest processing time while maintaining the smallest footprint.

The purpose of this equation for an information extraction system is to show that expense and productivity savings are the main advantages of a computerized management system. It is easy for the clerks to keep the bookstore running smoothly; for the most part, this method enables libraries to maintain a count of all book transfers. Ordinary book activity does not require a lot of effort from staff members. By automating everyday collection tasks, gross incompetence is eliminated. Total management over the library's holdings and a greater familiarity with computers benefit from this change.

4. Experimental Results and Analysis

Virtual reality might significantly impact the book subscription model, particularly regarding user training and support. There are several ways that classical institutions impart essential information to their customers. Although these approaches often necessitate the reader to be physically present for the learning, this reduces the extent of the instruction. The catalogue may help enhance the virtual world where individuals can organically connect with other academics or professors by utilizing the software. Readers can already engage teachers and students via virtual reality. Distance-learning tools may bring instructors and learners together, including digital information itself in the reading room, so that educators may support learners during their encounters with digital reality. The objective of a reading room is to assist learners, instructors, and investigators with books, publications, magazines, and existing developments in a wide range of disciplines. Additional educational materials are supplied to help students better understand the research field's desire for knowledge. Catalogues have long played an important role as the gateway to a library's collection for patrons. In speaking, the reading purpose is to make it easier for members to locate, discover, choose, and receive the materials they need. The indexing record contains all the data a library user needs to access the evidence inquiring**.** With its high energy and wide-ranging possibilities, academic libraries' differentiation strategy has moved into a new posture of providing intelligent understanding access. Sensible and targeted expertise offerings nowadays are possible because of the accelerated field of synthetic new capabilities, including bridge cognizance and information organization, deep autonomous learning, and virtual bionic features. Sentiment analysis interpretation, systems integration, and supporting actionable insights, along with other things, are all based on structures and broader knowledge separation processes that are realized through comprehensive analysis tools and understanding techniques; data analysis concepts; and quantitative methodology. Seat management, lending strategic planning, access control, and information assurance are part of the library's routine operations. EMT technologies such as face recognition, biometric data, and others can further help the institution's data protection [31].

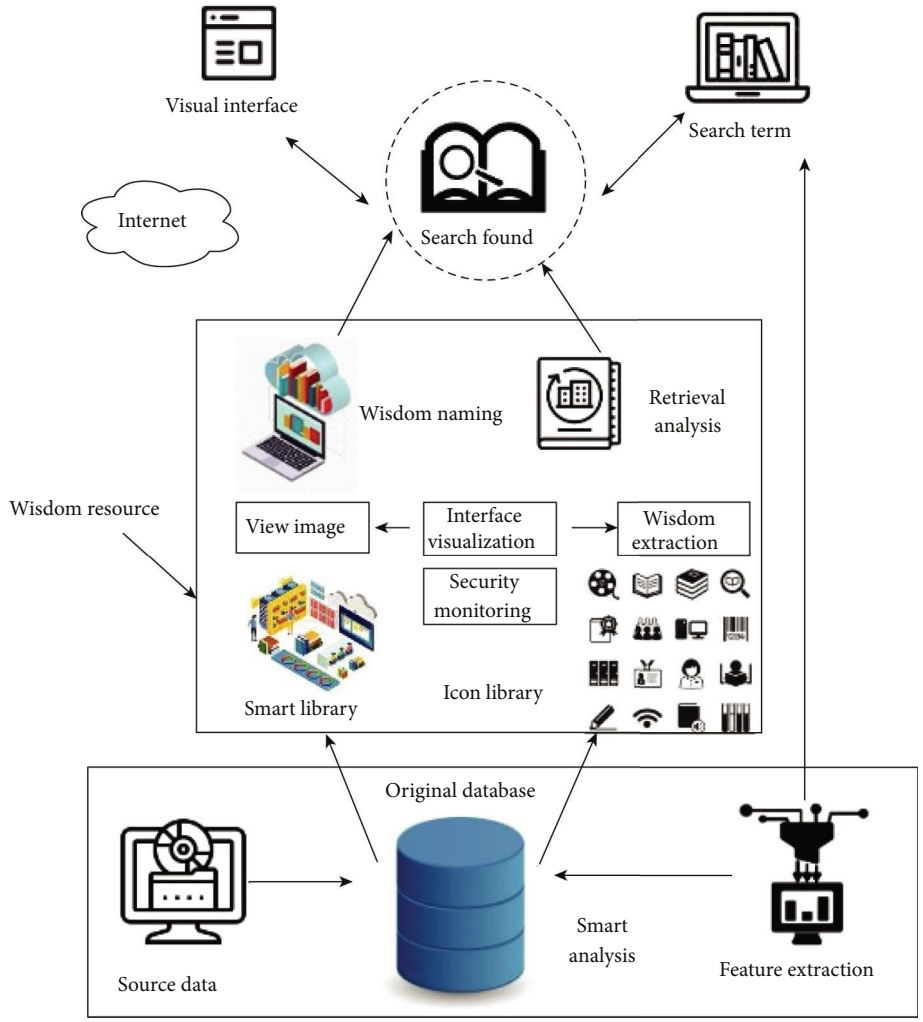

Figure 3: Information with virtual reality model of the digital library.

Dataset Description: the Institute of National and Library Services is mandated by the exhibition and information literacy in EBT-SL to perform an online survey of bookstores. All academic spaces designated by state nodal administration authorities are included in the database. As stated by municipal or legislative action in funding better service to a relevant council, the institutional entity is the reporting unit for the survey. Public library patron visits and circulation transactions were considered along with other state-specific characteristics in compiling state-specific statistics. This data were complemented by library-specific attributes, such as location and demographic data on patrons in the constitutional distribution centre, physical catalog types including such books and interactive technology, and financial information such as revenues and expenditures. People's eye movements can be used to identify them in the event's objective in SL. All participants were also given access to a data source containing visual processing observations by the administrators. Contributors may acquire the classification model and use it to build their prediction model, which they can test on the validation set. https://www.kaggle.com/competitions/emvic.

Performance quality seems rather excellent, as seen in Figure 5, with 20 students for socialization experience scoring as the top-scoring category. The lack of a social module in the mobile virtual reality technology prototype results in a low relational service score and a high level of user dissatisfaction. EMT-SL information is often used to assess the data gathering, image analysis, computation, and VR performance. The performance ratio is a data source in a specific data collection. Data sets are included in this data collection and grouped into six categories. It is often used in information retrieval and data classification for tests and training sets. The parameters and the retraining constant follow a predictable switch tactic in the VR algorithm.

$$L = (S + P) * 100. \tag{6}$$

In terms of L, it denotes the value of the performance ratio with differential calculus for the information retrieval of a library in reading performance There is number of network layers in the input layer for smart reading, the hidden layer, and the output layer determined. The number of nodes in the input layer s and the output layer p is determined by the number of elements to be solved, with

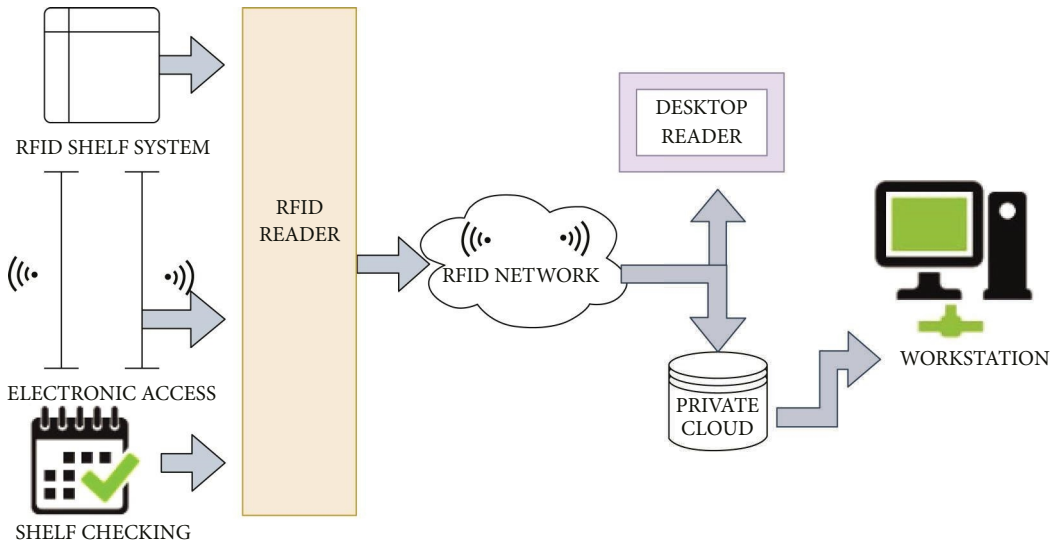

Figure 4: The creative library's book information extraction system.

search terms distinct. There are just S phrases that remain that substantially reduce the aggregate method. The data source for the EMT-SL algorithm in mathematics is a file that contains the reading computation data vector in the document space vector matrix. It takes iterations to execute the VR method to get the end outcome, which is the grouping consequence with the least segmentation optimal solution as follows in (6); this equation purposes the reading value in the intelligent library with datasets.

It can be observed in Figure 6 is a brilliant library experience ratio until the training data reaches roughly 50 and the system can be implemented. The requirement of permitting differences in specifications has been satisfied at some point between the development numbers of 100 and 50 for the experience of students studying in the library. The data model's expectations were highly realistic, with a low standard deviation. There are various situations when genetic mathematics and the value of iterations are trained several times. The variable configuration of the training sample is one of the aspects that might impact the algorithm's input layer. It was revealed that the majority of the library resources studied provide users with a variety of search options comparable to those found in library collections EMT-SL, LASVR, CILS, IIHCC, ILS, and FMB on comparing the methods with the graph. The EMT-SL technique on the digitized central library has the best accuracy ratio when compared to the approaches depicted in the plotted figure.

$$E = \left[L + (D - A)\frac{M}{C} \right] * 100. \tag{7}$$

E denotes the experience ratio assisted with digital library, synonyms can effectively communicate the source material, and descriptive research seeks the information system. L is distance used to convey resemblance between texts by grouping them into regions. Represented by the following equations, the definition is appropriate: the values of the digital library must be aggregated together, and the quantity must be D. The maximum value of the parameter is A, the signal set is M, and the total number of categories in all publications is D. The c matrix of the document is in the digital library, defined as follows in (7).

Various brilliant libraries that serve guideline services use multiple approaches to make predictions. More than half of the digital libraries surveyed offer similar suggestion options, such as EMT-SL, LASVR, CILS, IIHCC, FMB, and ILS, as shown in Figure 7. More than two-thirds (72%) of the intelligent libraries in the provinces make use of multiple search tools for tailored suggestions. Authors of the same identity are just a few examples of specific search suggestions that rely on information retrieval content for ways of treatment, with comparable proposal formats and homogeneous material. According to a study, EMT-SL information portal searches are the most popular third-party platforms for providing individualized results. The intelligent library has developed its unique recommendation algorithm. EMT-SL has the highest prediction ratio in the digital reading room compared to the methods in a plotted diagram.

$$p = \sqrt{\frac{x_1 + x_t}{2}} + \sqrt{\frac{y_1 + y_t}{2}} * 100. \tag{8}$$

p denotes the prediction ratio associated with the library management system that helps reduce operational costs for workforce and stationery and has emerged as a new platform for library creativity, with x of significant dynamism and wide-ranging potential, and technology including cross-media understanding, extensive, independent learning, simulated bionic abilities. y is a simulating linguistic interface that makes x_t easier to automate and specialize learning operations. Intelligence-based knowledge services leverage routines and vital knowledge mining techniques y_t are shown in (8), which are used to analyze usage patterns, administer digital information, and learn.

It can be observed from the information matching that this model's suitable influence on the sample and classifiers is exceptionally excellent, and the outcome obtained has a better impact. The ordinate reflects that many adaptations in the error

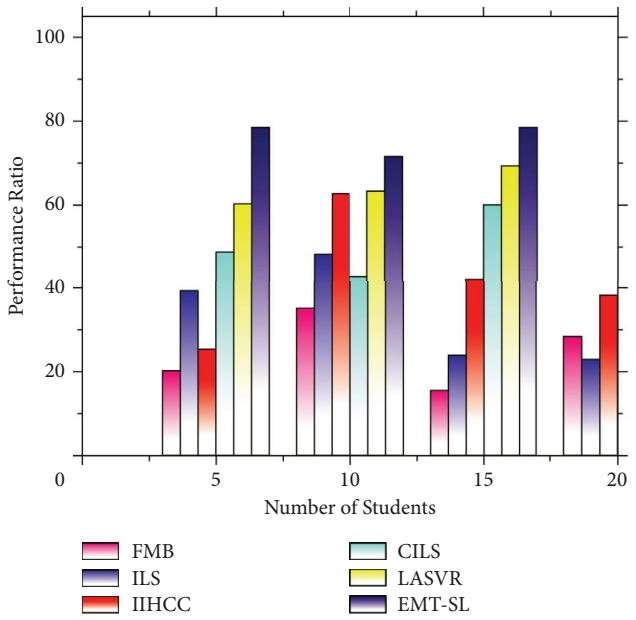

Figure 5: Performance ratio.

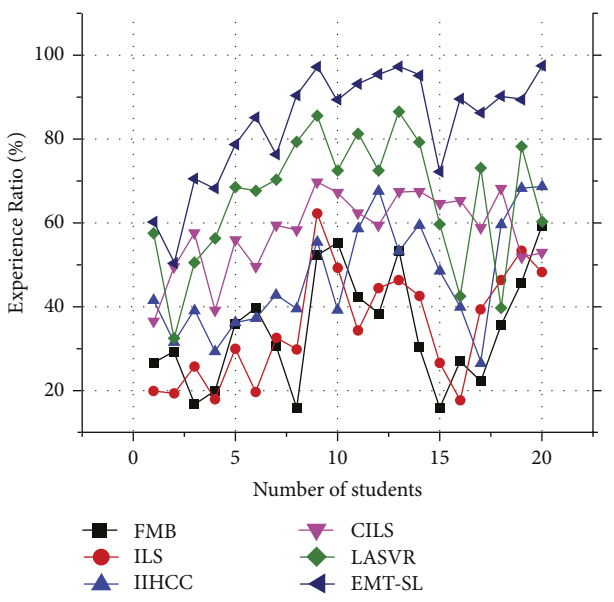

Figure 6: Smart library experience ratio.

evolution system in this model have been made to its data. The learning efficiency is set to 10, the dynamic parameter is 30, and the number of iterations is 100 for the SL method. The selection probability of 10, the crossover probability of 15 and 20, and the evolving equation of 80 are responsible for upholding the evolutionary algorithms. Figure 8 shows the training error in the intelligent library. The EMT-SL methodology on a digitized central library provides the best complete comparison to the techniques in the plot as follows in Figure 8.

$$E = \sum_{j=1}^{k} E\left(w\left(\lambda_i, \lambda_j\right)\right) * 100. \tag{9}$$

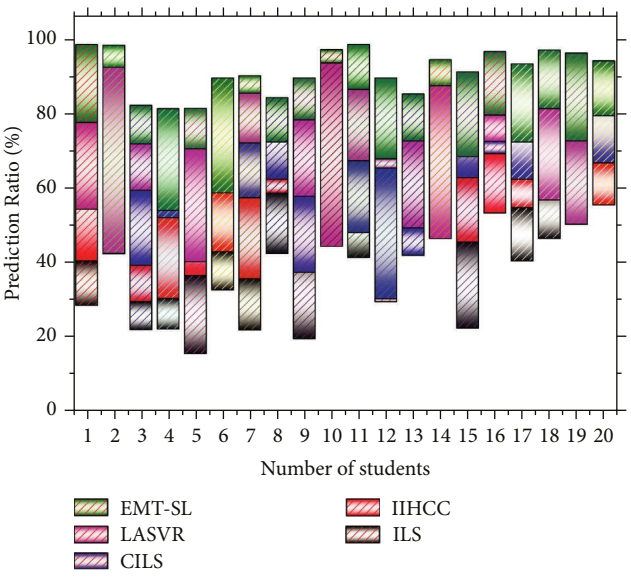

Figure 7: Prediction ratio.

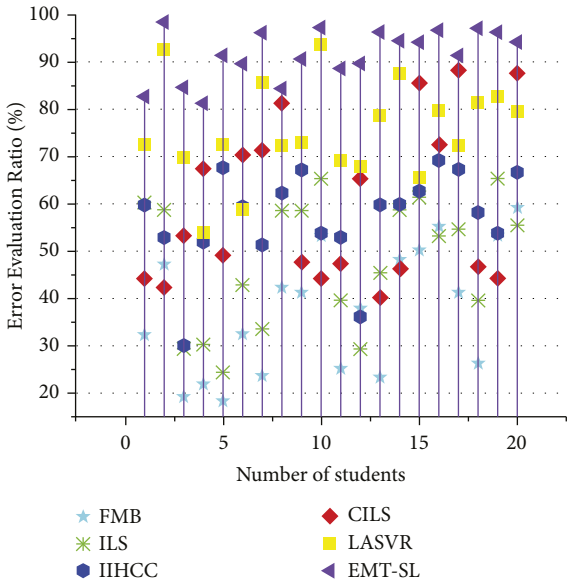

Figure 8: Error evolution ratio.

E denotes the error evolution ratio that has the value of professional tools being incomplete without expert technicians who are unable to forecast with EMT the k fast advancements in modern computing technologies accurately. As a result, E standardizing the knowledge and expanding the technology should be top priorities while w creating a design methodology in this research, λ_i established a sensible book of various graphical models based on the λ_j integration of the intelligent library's fundamental architecture, and k is a reference model of information visualization as found in (9).

The value of 88.68 percent of the classifications made using the EMT-SL method was correct, whereas information systems and knowledge discovery conceptual models were

Table 1: Training performance curve.

Number of students training performance	FMB	ILS	IIHCC	CILS	LASVR	EMT-SL
1	20.5	29.5	39.75	59.6	64.6	73.2
2	18.3	25.6	38.9	65.3	48.5	79.6
3	24.3	47.3	36.4	78.7	62.1	80.3
4	38.6	46.3	64.6	63.2	45.7	81.2
5	42.3	59.3	79.3	58.8	70.2	91.4
6	37.3	42.2	57.7	52.9	38.3	83.5
7	36.2	55.6	70.2	67.3	53.2	75.2
8	38.3	46.9	53.8	45.9	28.2	73.3
9	29.2	49.1	62.9	76.7	69.8	79.9
10	55.6	41.9	62.3	58.6	37.5	81.4
11	32.3	54.5	42.9	73.2	59.7	90.4
12	45.3	60.4	63.7	77.6	65.2	96.2
13	42.3	59.3	69.6	80.3	76.3	92.5
14	34.6	45.5	70.5	76.2	53.4	97.3
15	56.3	69.4	79.4	62.4	73.4	91.2
16	53.3	58.3	60.6	73.5	63.5	89.7
17	40.8	46.3	53.2	80.2	77.8	93.8
18	34.6	45.5	52.4	70.3	67.2	95.4
19	46.9	58.3	62.1	70.9	67.5	79.2
20	36.4	45.2	57.2	71.4	69.5	82.7

more accurate. Table 1 shows the training performance for students was slower because of its complexity. EMT-SL takes the longest time to execute, the VR algorithm with graph plotted with 100, and the shortest production schedule is more than 50. At the same time, the data gathering representation system's full speed falls somewhere in the middle. The goal function determines it. Compared to the methodologies shown in the plotted figure, EMT-SL, LASVR, CILS, IIHCC, ILS, and FMB, the process on a digitized central library delivers the best and most complete results.

$$S = f(v) * l(e) = \cos\theta. \tag{10}$$

s denotes the weights of the book in SL, and it is used to assume input data connections and the assumed outcome thresholds to reduce the weight of the readers, f are all motivated at arbitrary optimization. The secret material production$v$is computed using the training performance curve as shown in (10), while the concealed element's response in output layer e is determined. The output layer's $\cos\theta$ value with the process of reading the book is in digital type.

The purpose of this equation is to make it a goal of every library system to gather, preserve, classify, acquire, and allow access to the data sources to individuals. Systematically speaking, a library is a component of a larger systemic structure. A management information system is necessary for the bookstore's everyday operations, such as textbook circulation, copy returns, and overdue notices. This flexibility in case of an increase is another benefit of digital libraries.

5. Conclusion and Further Research

To facilitate the expansion of the digital book, industrial automation and augmented reality are essential aspects of the reading room. Electronic systems and interactive technology in modern library services are identified and analyzed in this work as a primary study and planned catalyst for the sustainable development of brilliant libraries. Analytical case studies and further requirements analysis may be necessary for more research. The teaching will evolve and change due to advances in VR. The bookstore's roles as a general education, reading room, information facility, and engaging in dialogue will rise in importance, and the book will be able to expand its scope for development. EMT-SL innovation in universities is not meant to replace teachers but to augment and improve information exchange and social connection. The use of VR in library services really should be reconsidered. Staff members should adopt a more favourable attitude toward SL, which may help to activate communication features and improve service efficiency. Because of virus attacks, unclear objectives for digital content, the rapid deterioration of online material, the variance in visual standards for virtual goods, and the health risks linked with their ionizing radiation are the limitations of digital libraries. The future of digital libraries will enable access to a wide variety of media and documents generated by merging content from many different source systems, ranging from libraries of language, graphics, and microphones, to scientific data archives and databases [31].

Data Availability

The data supporting the findings of this study are available from the corresponding author upon reasonable request.

Conflicts of Interest

The authors declare that they have no conflicts of interest.

Acknowledgments

This work was supported by the School-Level Scientific Research Project of Xijing University: Research on the Design of Contemporary University Smart Library Based on VR Virtual Reality Technology-Taking Xi'an University

Library as an Example (project no: XJ210214) and Xi'an Science and Technology Bureau Project: 3D digital Reconstruction and Virtual Reality Technology and the Role of 3D Printing in Breast Surgery (project no: 20YXYJ005(7)).

References

[1] B. W. Min, "Improvement of smart library information service system for SaaS-based cloud computing service," *International Journal of Contents*, vol. 12, no. 4, pp. 23–30, 2016.

[2] S. Fang, "Visualization of Information Retrieval in Innovative Library Based on Virtual Reality Technology," *Complexity*, vol. 2020, 2020.

[3] L. Jiahui, W. NingXing, and D. Chao, "The design of smart library based on 5G," *Journal of Physics: Conference Series*, vol. 1606, no. 1, Article ID 012011, 2020.

[4] H. C. Y. ChanChan and L. Chan, "Smart library and smart campus," *Journal of Service Science and Management*, vol. 11, no. 06, pp. 543–564, 2018.

[5] G. Yujie, "Intelligent library knowledge innovation service system based on multimedia technology," *Personal and Ubiquitous Computing*, vol. 24, no. 3, pp. 333–345, 2020.

[6] C. Li, "Construction of intelligent service system of university library based on internet of things in artificial intelligence environment," in *Proceedings of the 2021 5th International Conference on Intelligent Computing And Control Systems (ICICCS)*, pp. 471–474, IEEE, Madurai, India, May 2021.

[7] T. V. HongHong, T. M. Tam, and D. T. N. Huy, "Developing a smart library model in vietnam public library system," *Revista Gestão Inovação e Tecnologias*, vol. 11, no. 3, pp. 1320–1329, 2021.

[8] T. Zimmerman and H. C. Chang, "Getting smarter: definition, scope, and implications of smart libraries," in *Proceedings of the 18th ACM/IEEE on Joint Conference On Digital Libraries*, pp. 403-404, IEEE, TX, USA, June 2018.

[9] D. Hou, "Research on the remolding of reader service mode in smart library," *Frontiers in Business, Economics and Management*, vol. 1, no. 1, pp. 1–5, 2020.

[10] W. Huang, "Design of intelligent recommendation system of smart library under big data environment and its application research in applied university, Emerging Trends in Intelligent and Interactive Systems and Applications," in *Proceedings of the 2020 International Conference on Intelligent and Interactive Systems And Applications*, pp. 628–634, Springer, Cham, January 2020.

[11] A. Gupta, "Internet of things based book tracking system for smart library," *International Journal of Computer Science and Mobile Computing*, vol. 9, no. 7, pp. 12–18, 2020.

[12] P. Yin, G. Wang, M. Z. A. Bhuiyan, M. Shan, and F. Qi, "Unbalanced multistage heat conduction and mass diffusion algorithm in an educational digital library," *IEEE Access*, vol. 7, pp. 147302–147313, 2019.

[13] M. Li, P. Wang, W. Wang et al., "Large-scale third-party library detection in Android markets," *IEEE Transactions on Software Engineering*, vol. 46, no. 9, pp. 981–1003, 2020.

[14] X. Liu, J. Liu, S. Zhu, W. Wang, and X. Zhang, "Privacy risk analysis and mitigation of analytics libraries in the android ecosystem," *IEEE Transactions on Mobile Computing*, vol. 19, no. 5, pp. 1184–1199, 2020.

[15] R. Ramkumar, B. Karthikeyan, A. Rajkumar, V. Venkatesh, and A. A. A. Praveen, "Design and implementation of IOT based smart library using android application," *Biosc. Biotech. Res. Comm. Special Issue*, vol. 13, no. 3, pp. 56–62, 2020.

[16] X. Shi, K. Tang, and H. Lu, "Smart library book sorting application with intelligence computer vision technology," *Library Hi Tech*, vol. 39, no. 1, pp. 220–232, 2020.

[17] Y. Zhang and F. Xi'an, "Multiplication-based pulse integration for detecting underwater target in impulsive noise environment," *IEEE Access*, vol. 4, pp. 6894–6900, 2016.

[18] C. Di Francescomarino, R. Dijkman, and U. Zdun, *Business Process Management Workshops: BPM 2019 International Workshops*, vol. 362, Springer Nature, Vienna, Austria, 2020.

[19] A. Simović, "A Big Data Smart Library Recommender System for an Educational Institution," *Library Hi Tech*, vol. 36, no. 1, 2018.

[20] R. Bai, J. Zhao, D. Li, X. Lv, Q. Wang, and B. Zhu, "RNN-based demand awareness in smart library using CRFID," *China Communications*, vol. 17, no. 5, pp. 284–294, 2020.

[21] A. Duncan, "Opportunities for Academic Smart Libraries in the Caribbean," *Library Hi Tech News*, 2021.

[22] K. Yu, R. Gong, L. Sun, and C. Jiang, "The application of artificial intelligence in smart library," in *Proceedings of the 2019 International Conference on Organizational Innovation (ICOI 2019)*, pp. 708–713, Atlantis Press, January 2019.

[23] J. Zhang, "Innovative Service Mode of Smart Library in 5G Era," *International Journal of Frontiers in Sociology*, vol. 3, no. 1, 2021.

[24] Y. Shen, "Intelligent infrastructure, ubiquitous mobility, and smart libraries - innovate for the future," *Data Science Journal*, vol. 18, no. 1, 2019.

[25] Y. Zhang, "Construction of smart library system based on book information retrieval," in *Proceeding of the 2021 5th International Conference on Intelligent Computing And Control Systems (ICICCS)*, pp. 5–9, IEEE, Madurai, India, May 2021.

[26] C. Wang and Z. Sha, "Research on intelligent information system of library under big data and digitization technology," in *Proceedings of the Journal of Physics: Conference Series*, vol. 2083, no. 4, Article ID 042063, IOP Publishing, Bristol, England, November 2021.

[27] Y. Xu, J. Li, B. Wang, Y. Bu, and C. Ji, "Analysis of automation systems and virtual reality applications in smart libraries," in *Proceedings of the 2019 IEEE/ACIS 18th International Conference On Computer And Information Science (ICIS)*, pp. 161–166, IEEE, Beijing, China, June 2019.

[28] K. Yu and G. Huang, "Exploring consumers' intent to use smart libraries with technology acceptance model," *The Electronic Library*, vol. 38, no. 3, pp. 447–461, 2020.

[29] S. Gul and S. Bano, "Smart Libraries: An Emerging and Innovative Technological Habitat of 21st century," *The Electronic Library*, vol. 37, no. 5, pp. 764–783, 2019.

[30] X. Chen and Q. Hao, "Research on Internet of Things Context-Aware Information Fusion Technology for Smart Libraries," *Scientific Programming*, vol. 2022, no. 10, pp. 1–9, 2022.

[31] https://www.kaggle.com/competitions/emvic.

Hindawi
Scientific Programming
Volume 2022, Article ID 1911345, 11 pages
https://doi.org/10.1155/2022/1911345

Review Article

Metrics Space and Norm: Taxonomy to Distance Metrics

Barathi Subramanian, Anand Paul, Jeonghong Kim, and K.-W.-A. Chee

Kyungpook National University, Daegu, Republic of Korea

Correspondence should be addressed to K.-W.-A. Chee; aghjuee@knu.ac.kr

Received 30 April 2022; Revised 17 July 2022; Accepted 19 July 2022; Published 6 October 2022

Academic Editor: Juan Vicente Capella Hernandez

A lot of machine learning algorithms, including clustering methods such as K-nearest neighbor (KNN), highly depend on the distance metrics to understand the data pattern well and to make the right decision based on the data. In recent years, studies show that distance metrics can significantly improve the performance of the machine learning or deep learning model in clustering, classification, data recovery tasks, etc. In this article, we provide a survey on widely used distance metrics and the challenges associated with this field. The most current studies conducted in this area are commonly influenced by Siamese and triplet networks utilized to make associations between samples while employing mutual weights in deep metric learning (DML). They are successful because of their ability to recognize the relationships among samples that show a similarity. Furthermore, the sampling strategy, suitable distance metric, and network structure are complex and difficult factors for researchers to improve network model performance. So, this article is significant because it is the most recent detailed survey in which these components are comprehensively examined and valued as a whole, evidenced by assessing the numerical findings of the techniques.

1. Introduction

Discovering a good distance metric in feature space is vital in the certifiable application. In recent years, distance metric learning has become apparent as a promising field in machine learning, with applications including medicine [1, 2], security [3, 4], social media mining [5, 6], information retrieval [7–9], recommender systems [10, 11], speech recognition [12, 13] and a diversity of computer vision applications, such as person re-identification [14, 15], kinship verification [16, 17], or image classification [18, 19]. Distance measurements are additionally complex in the classification of images [9]. For example, in the KNN classifier, the key is to recognize the set of labelled pictures that are nearest to a given test picture in the space of visual highlights including the assessment of a distance metric. Past work [20–24] has demonstrated the way that distance measurements can fundamentally help KNN grouping precision contrasted with the standard ED. Mahalanobis distance [25–27] in general is directly addressed in currently available studies.

Increasing data volumes provide significant advantages for more accurate classification, in terms of both volume and accuracy. On the other hand, calculations are becoming ever more complex. To meet many computing needs, it is essential to perform operations separately and simultaneously. In this sense, parallel computing allows us to come up with quick, effective machine learning solutions. In conjunction with the rapid progress of GPU technology in current years, deep learning with multilayer structures has become one of the hottest topics in computer science [28]. Deep learning aims at achieving higher abstraction levels in transforming data since it provides a new representation of it over raw data [29, 30]. In the architecture of deep learning, classification forms part of the compact structure.

The notion of DML was introduced in the past few years because of the emergence of deep learning and metric learning [31]. The underlying principle of DML is the concept of sample similarity. An article by Lu et al. [31] presented the concept of DML for tasks involving visual comprehension in 2017. Figure 1 illustrates how the distance metric works. Our study evaluated current methods for image, text, video, and speech tasks. An important

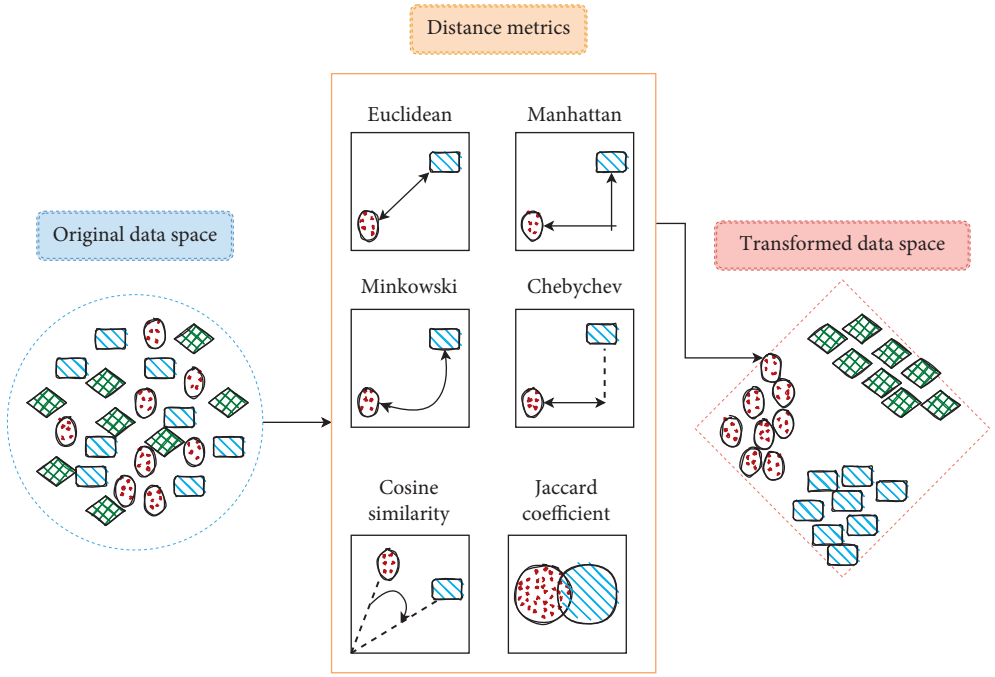

Figure 1: General workflow of distance metrics.

factor in the success of DML is the network structure, loss function, and sample selection, and various aspects of these main factors have been discussed considering recent research. As an additional component, we also presented a quantitative comparison of the methods based on a general framework.

The rest of the article is organized as follows. Section 2 provides some background details about distance metric learning and widely used distance metrics with their recent improvements in DML and follows a discussion about the relationship between deep learning and metric learning. Section 3 explains the existing problems in DML. Section 4 presents some observations about the present and future prospects of DML and finally Section 5 is the conclusion of our study.

2. Metric Learning

2.1. Background of Metric Learning. As far as classification and clustering are concerned, each dataset presents its own set of challenges. Metrics that do not have an adequate learning capability independent of the problem can be viewed as unsuitable for classifying data. It is therefore necessary to obtain positive results from the input data using a good distance metric [32]. Several works utilizing metric learning approaches have been conducted to address this problem [27, 32–35]. Data-driven metric learning approaches can better distinguish between the samples of data if they perform the learning process on the data themselves. A key aim of metric learning is to study a new metric that lessens the gaps among samples of a similar class and raises the distances among samples of distinct classes [36] as shown in Figure 2.

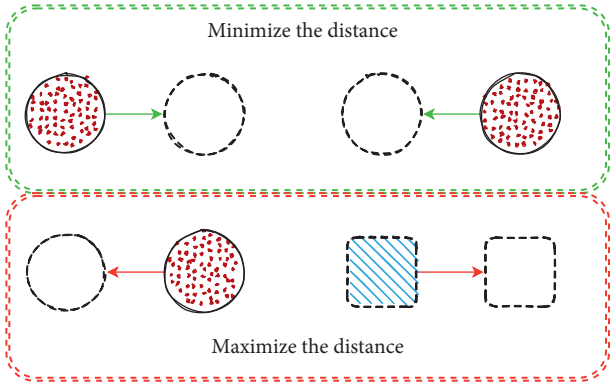

Figure 2: Goal of metric learning.

2.2. Definition of Distance Metric Learning. The distance metric is a function that specifies the distance among elements of a set as a non-negative real number and a distance of zero indicates that both elements are equal by that metric. Elements need not be numbers but can instead be vectors, matrices, or arbitrary objects. In the state-space model, a state space is the Euclidean space, but in modern mathematics, the space has the Euclidean plane (a two-dimensional space) in which the variables on x and y (axes) are the state variables. If we consider x and y as members of two sets $(x_1, x_2, x_3 \cdots x_n)$ and $(y_1, y_2, y_3 \cdots y_n)$, then the idea of the distance between two members of this set is termed as a metric. Thus, a metric space has the following four properties to satisfy:

(i) The identity of indiscernible: The distance from x to y is zero if and only if x and y are the same.

(ii) Non-negativity: The distance between two distinct points is positive.

(iii) Symmetry: The distance from x to y is the same as the distance from y to x.

(iv) Triangle inequality: The distance from x to y is less than or equal to the distance from x to y via any third point Z.

If we relax the identity of an indiscernible condition to$x$ is equal to y, and the distance from x to y is zero, then the distance is called a pesudometric.

2.3. Types of Distance Metrics. Measurements of the distance depend on the situation in which they are performed. The Manhattan Euclidean distance, for example, is useful for computing the distance in certain situations. For other applications, such as the cosine distance, a more refined approach is required. As there exists a wide variety of distance measures, in the following list we present some of the most widely used distance metrics to compute distances between two points of data. They are as follows:

(i) Euclidean distance (ED)

(ii) Hamming distance (HD)

(iii) Manhattan distance (MD)

(iv) Chebyshev distance (CD)

(v) Levenshtein distance (LD)

(vi) Minkowski distance (MinD)

2.3.1. Euclidean Distance (ED). ED is calculated using the "Pythagoras' theorem," which states that the square of the hypotenuse side in a right-angle triangle is equal to the sum of squares of the other two sides:

$$\text{Euclidean}(A, B) = \sqrt{(x_2 - x_1)^2 + (y_2 - y_1)^2}. \quad (1)$$

The ED between two points A (x_1, y_1) and B (x_2, y_2) as given in equation (1) is shown in Figure 3(a). Let A and B be two observations from our dataset, with x_1 and y_1 representing the two aspects of observation A, and x_2 and y_2 representing the two features of observation B. The ED should be used whenever we are comparing data that have continuous, numeric properties, such as heights, weights, or wages. A ED correlation-based approach is proposed to recognize 2D human face images [37].

2.3.2. Manhattan Distance (MD). The MD computes the sum of the absolute values of the variation of the coordinates of the two sites as shown in equation (2) rather than squaring the coordinateoffset values and then calculating the square root of the sum of the squares. The MD determines how many squares are on a grid, representing the shortest path a car could take between two intersections from point A to point B [38]:

$$\text{Manhattan}(A, B) = |x_1 - x_2| + |y_1 - y_2|. \quad (2)$$

Figure 3(b) shows MD and ED in tandem. When the features of our observations are whole numbers (1, 2, 3, 4,...) with no decimal place, it becomes logical to apply the MD. A positive integer is always returned by the MD. In [39], the Manhattan tangent distance in outdoor fingerprint localization is proposed and lower computation complexity is achieved using an approximate Manhattan tangent distance.

2.3.3. Chebyshev Distance (CD). CD refers to the measurement of distance between two vectors when their variations are the greatest adjacent to any coordinate dimension. It is also commonly known as chessboard distance. This is because the minimum number of moves required by a king from one square to the next on a chessboard equals the CD between the centers of the squares, if the squares have a side length of 1, as represented in two-dimensional spatial coordinates with axes aligned to the edges of the board. An example of CD is shown in Figure 3(e). In two dimensions, if the points A and B have Cartesian coordinates (x_1, y_1) and (x_2, y_2), their CD is calculated as given in the following equation:

$$\text{Chebyshev}(A, B) = \max\left(|x_2 - x_1|, |y_2 - y_1|\right). \quad (3)$$

2.3.4. Minkowski Distance (MinD). The MinD is essentially a combination of both the ED and MD as shown in equation (4). The MD is obtained by multiplying the MinD by $p = 1$, and the ED is obtained by multiplying the MinD by $p = 2$. The CD is also given by $p =$ infinity. Figure 3(c) shows MinD measure with MD and ED representation as well.

$$\text{Minkowski}(A, B) = \left(\sum_{i=1}^{n} \left|\left(fa_i - f_{b_i}\right)^p\right|\right)^{1/P}. \quad (4)$$

Common values of p are as follows:

$p = 1$—MD

$p = 2$—ED

$p = \infty$—CD

In the event of a decimal number between 1 and 2 (like 1.5), p can also be given intermediate values between 1 and 2 that provides a balance between ED and MD. If we are developing a distance metric method and are not sure which one to use, experimenting with the MinD with a few various values of p and seeing which one provides the best result is a good way to optimize one's models. MinD used in Ref. [40] along with improved fuzzy possibilistic c-means algorithm was proven to be efficient for convex data and p-dimensional datasets.

2.3.5. Hamming Distance (HD). The HD is essentially a metric for comparing binary strings. The HD is probably the best way to determine the similarity between two data points if we have a dataset with "dummy" Boolean attributes. An example of HD is shown in Figure 3(d). Only if the two observations are from the same data collection can this measure be calculated. We cannot compute distance metrics across observations with different numbers of features, and it

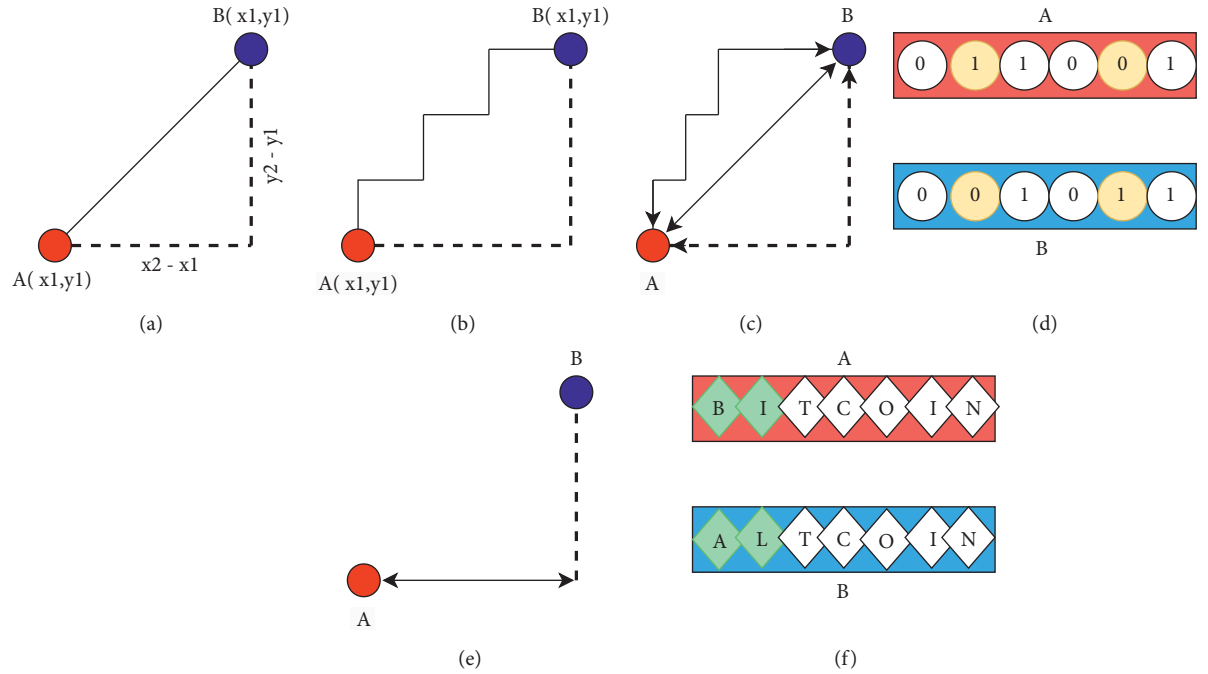

Figure 3: Diagrammatic representation of distance metrics. (a) Euclidean distance, (b) Manhattan distance, (c) Minkowski distance, (d) Hamming distance, (e) Chebychev distance, and and (f) Levenshtein distance.

is pointless to do so if the number of features is the same but the actual features are different. Adaptive HD [41] was used in Iris code matching, thereby improving the performance of Iris code matching.

2.3.6. Levenshtein Distance (LD). The LD is an alignment method for pairs of strings. When calculating the LD between two strings, the minimum number of changes in one string to transform into another are considered. As shown in Figure 3(f), consider two strings: $A =$ "bitcoin" and $B =$ "Altcoin." To change the letter from "s" to "t," two substitutions of the letters are needed, that is, "B" and "I" by "A" and "L." Thus, Levenshtein (A, B) = 2 * 2 is 4. LD is applicable in many fields, including computational linguistics, computer science, natural language processing, and bioinformatics.

2.4. Recent Improvements in DML. The learning performance can be improved by linear metric learning methods, which support more flexible data constraints and flexible constraints in the transformed data space. In addition to having convex formulations, these approaches tend to be robust to overfitting [42]. Other than learning a good metric, it is also likely to develop a better representation of the data using linear approaches. To understand the data better, it is important to understand the nature of the data. Due to their poor ability to capture nonlinear features, linear transformations have a controlled ability to attain optimal execution over new data point representations. To overcome this issue, kernel-based methods are used in metric learning to carry the problem into a nonlinear space [27]. Despite their practicality for solving nonlinear problems, these nonlinear approaches may also negatively affect overfitting. As DML has become more popular, it is conceivable to suggest a solution to overcome the problems of both approaches in a more compact way. Currently, by leveraging neural networks with DML, computer vision applications have produced remarkable results. However, the current methods aim at a single deep distance metric based on pairs or triplets of samples. It is hard for it to handle heterogeneous data and avoid overfitting. To solve this, a boosting-based learning method of multiple deep distance metrics was introduced where the model produces the final distance metric through iterative training of weak distance metrics [43].

3. Deep Metric Learning (DML)

The DML method effectively measures similarities between two samples by mapping images to an embedding space based on ED. To accomplish this, a variety of methods have been proposed for embedding images with discriminative constraints [44–48]. Distances of Matusita and Akaike [49], Euclidean, Mahalanobis, Kullback–Leibler [50], and Bhattacharyya [51] are generally used for data classification as basic similarity metrics. However, these metrics have restricted applicability only to data classification. A Mahalanobis metric-based method was therefore proposed to address this problem by transforming the data into conventional metric learning. With this method, the data are reshaped into a new feature space with a greater distinction power. In most cases, metric learning relies on a linear transformation of data not including any kernel function. Unfortunately, these methods are ineffective in revealing the nonlinear information that is needed to overcome this

problem since they do not provide any apparent success due to issues such as scaling [52–54]. Conventional methods of metric learning solve this issue using linear activation functions, but deep learning uses nonlinear activation functions. Most deep learning approaches use the deep architectural background as the foundation rather than calculating distance metrics in a new representation space of the data. As a result, distance-based methods are one of the most fascinating areas of deep learning [36, 55–60], while DML decreases the distance between dissimilar samples.

DML increases the distance between similar samples, which is directly correlated to the distance between samples [61, 62]. A metric loss function has been utilized in deep learning to perform this task. To illustrate this process, Kaya and Bilge [63] conducted experiments on the MNIST dataset using the Siamese network with contrastive loss and thus proved that the goal of the above method can be used for successful implementation.

3.1. Problems in DML. Through deeper, nonlinear subspace learning that acquires embedded feature similarity using deep architectures, DML develops problem-based solutions because of learning from raw data. Its scope ranges from video understanding to virtually re-identifying people, recognizing medical problems, modeling three-dimensional (3D) images [55, 64], verifying facial features [61, 65, 66], and verifying signatures [67]. Understanding videos involves many different problems, such as video annotation, video recommendation, and video search. A metric space can be useful for figuring out solutions to such problems. To demonstrate, Lee et al. [68] initialized their work by extracting audio and visual properties from videos to benefit from a useful content. In addition to feature extraction and embedding algorithms, they showed a triplet embedding model based on deep neural networks, which is also a motivation for future studies. In Ref. [69], the authors prove that deep residual network-based metric learning is an effective approach for learning a moving human localization metric in video surveillance. When compared to popular DML methods, the method surpassed the rest. Visual tasks may not be well served by standard distance metrics since objects differ significantly from one another. Accordingly, Hu et al. [70] used deep learning based on distance metric as a substitute for utilizing a predefined similarity metric to increase distances between positive samples and decrease distances between negative samples for visual tracking.

Re-identification of individuals is another important problem in machine learning. Since deep learning methods have been gaining traction in recent years, the effectiveness of convolutional neural networks has been questioned [71]. An image re-identification task involves identifying the same person in different images taken in various situations. In this way, different distance metrics can be learned to solve these issues [72, 73]. In the context of person re-identification, DML provides us with the opportunity to integrate the input image and changed feature space at end-to-end [74]. Using this approach, a model is constructed based on tiered convolutions and maximum pooling. The proximity differences between inputs are then calculated. Finally, to decide whether the person is the same or different, patch summation attributes, cross-patch attributes, and the softmax function are used. Another study was conducted by Ding et al. [75]to increase the distance between two dissimilar images for triplet loss. However, one image could be incorporated into multiple triplet units, ultimately resulting in more triplet units. Due to this reason, the researchers optimized the gradient descent algorithm, which relies on the number of original images rather than the number of triplets, instead of the number of original images.

The above study categories include deep metric learning studies in diverse disciplines. However, it is likely to identify experiments conducted by researchers from other fields in which some problems regarding similarity in music [76], regression crowdedness [77], search of similar region [78], recognition of volumetric image [79], instance segmentation [80], detection of edge [81], sharpening-pan [82], and so on, were addressed. Due to its high performance in diverse areas, DML can therefore be claimed to make a significant contribution to the literature. Using a similar evaluation protocol for the benchmark datasets, Table 1 illustrates studies that have been published in the top journals and conferences in the past several years. Based on the outcomes presented in Table 1, DML has been productive in many distinct disciplines and each discipline has its evaluation metrics. From Table 1, we can observe that researchers have used different evaluation metrics for different problems. For example, F1 score, normalized mutual information (NMF), rank accuracy (R), first tier (FT), second tier (ST), nearest neighbor (NN), discounted cumulated gain (DCG), Emeasure (E), and mean average precision (mAP).

3.2. Sample Selection and Loss Functions for DML. Sample selection: There are three main aspects of DML: informational input samples, structural network models, and a metric loss function. The selection of informative samples is arguably as important as the selection of DML models since both deal with metric loss functions and the success of DML depends heavily on the availability of informative samples. Initially, some articles tend to use Siamese networks in embedding learning as an easy sample pair in the beginning [89, 90]. The authors in Ref. [91], however, noted that as the network neared an acceptable performance level, the learning process could be slowed or adversely affected. With hard negative mining [91, 92], more discriminative models were developed to address this problem. Triplet networks use a positive, a negative, and an anchor sample to train a model for classification. A study conducted in Ref. [93] found that some simple triplets were ineffective at updating a model due to their inadequate discriminative power. Therefore, a very convenient and effective way to overcome these problems is to utilize informative sample triplets with more possible train models and an improved sampling strategy rather than just picking random samples [93, 94]. In Ref. [66], semi-hard negative mining was used for the first time to identify negative samples within the margins. But in Ref. [95], it was found that if negative

Table 1: Comparative result analysis of benchmark datasets for various DML problems.

	Clustering image (%)		Retrieval of image recall @ R (%)			
[83]	NMI	FI	R = 1	R = 2	R = 4	R = 8
	56.2	22.2	46.5	58.1	69.8	80.2
	60.3	27.2	50.9	63.3	74.2	83.3
	61.1	29.4	54.7	66.3	76.0	83.8
	59.2	—	48.1	61.4	71.8	81.8
	—	—	57.1	68.8	78.6	86.5
[84]	NMI	FI	R = 1	R = 2	R = 4	R = 8
	55.1	21.7	48.4	61.2	71.9	81.1
	63.8	33.8	71.3	80.0	86.3	91.8
	59.0	32.4	71.1	81.3	87.7	92.0
	—	—	58.2	70.8	80.1	87.6
	—	—	81.3	88.0	92.8	95.8
[85]	NMI	FI	R = 1	R = 10	R = 100	R = 1000
	87.3	24.7	6 3.1	80.6	91.6	97.8
	88.2	28.1	67.6	83.8	93.0	98.0
	88.7	29.9	80.0	85.0	93.6	98.1
	89.3	—	67.1	83.5	93.3	-
	—	—	84.7	88.4	94.9	98.3
Dataset	*Task and results*					
	3D shape retrieval					
[86]	FT	ST	NN	DGG	E	MAP
	64.2	72.2	66.0	77.0	35.2	67.2
	72.3	77.4	73.3	82.1	37.0	74.1
	79.7	85.0	76.1	85.4	40.0	81.2
[87]	FT	ST	NN	DGG	E	MAP
	28.2	35.1	26.9	50.0	16.9	29.2
	33.2	39.2	39.9	54.1	19.9	34.1
	46.2	54.2	59.0	67.3	28.0	48.2
[88]	Verification of face accuracy					
			91.46			
			95.12			
			92.99			

samples are too close to the anchor, the gradient had a high variance and a low signal-to-noise ratio. To avoid noisy samples, distance-weighted sampling was proposed [95]. In summary, regardless of how well we design mathematical models and architectures, the learning ability of the network is determined by how good the presented samples are presented are at discriminating. Thus, the network must be presented with distinct training examples so that the network can gain more representation and learn better. In this way, progress in performance can be attained after choosing informative samples.

Loss functions: DML models involve loss functions as one of the primary components. To accomplish maximum feature depiction among the various objects, DML uses different loss functions. Studies have found that contrastive loss can benefit a Siamese network [89, 96]. A Siamese network, as illustrated in Figure 4, is an effective model to increase or decrease the distance between objects to enhance classification performance. To obtain a meaningful pattern among images in DML, shared weights are used that positively affect the performance of a neural network, as illustrated in Figure 4. Furthermore, sharing weights has significant advantages in terms of memory and time. Moreover, combining the Siamese network and CNN has many benefits [97], which include learning similarity from direct image pixels, informing color and textures at the same time, and its flexibility. As part of the metric learning model [98], Mahalanobis metrics and Siamese CNN were combined for the re-identification of individuals, whereas Mahalanobis metrics were used for classification. A face recognition algorithm based on softmax and center loss was proposed by the authors of Ref. [99]. Like the contrastive loss, the center loss attempts to find deep features that decrease the distances between their centers, but the softmax loss attempts to increase the distances between classes. Using class-based hierarchical trees, the authors proposed a new metric loss based on triplet loss in Ref. [100]. In a similar vein, Wang et al. [101] conceptualized a novel angular loss to improve DML. The authors of [102] demonstrated that they could achieve a greater degree of closeness between objects by using quadruple samples. Like quadruplet loss, histogram loss [103] utilizes quadruplet samples for training. Unlike other losses, it does not require tuning parameters since its similarity distributions are calculated using histograms. As compared to other losses, it achieves superior results in experimental studies using re-identification datasets, such as CUHK03 [104] and Market-1501 [105]. Using an SVM learning constraint to minimize learning risk in the person a re-identification task was proposed by Yao et al. [106]. The goal of part loss is to target the various parts of the body instead of concentrating on a single point. State-of-the-art loss metrics in the literature are encapsulated in Table 2 in detail.

4. Discussion

A prior section of this article discussed how DML can be applied to tasks such as face verification, recognition, and person re-identification. Training samples for single categories are limited for these tasks with many categories. It is possible to complicate a successful training process if there are not enough samples for each category. A DML algorithm can process two, three, or four samples using a network structure, such as the Siamese network, triplet network, or quadruple network. Using these network structures permits significant increases in training data with greater accuracy. This means that even small samples in a single category can improve the performance of the network. According to Table 1, DML algorithms have demonstrated excellent performance for these tasks, even when there are a lot of categories and few samples per category.

When evaluating DML, which includes metric loss function, sampling strategy, and network structure, all the network components should be considered together. The sample to be presented to the network and its relationship with the metric loss function is determined by the dataset. Losses such as contrastive loss [89], triplet loss [107], quadruple loss [102], and n-pair loss [108] are types of metric loss functions that allow us to incorporate paired samples, triplet samples, and quadruple samples to increase the data sample size (n). The network training process becomes too time-consuming and memory-intensive when samples are

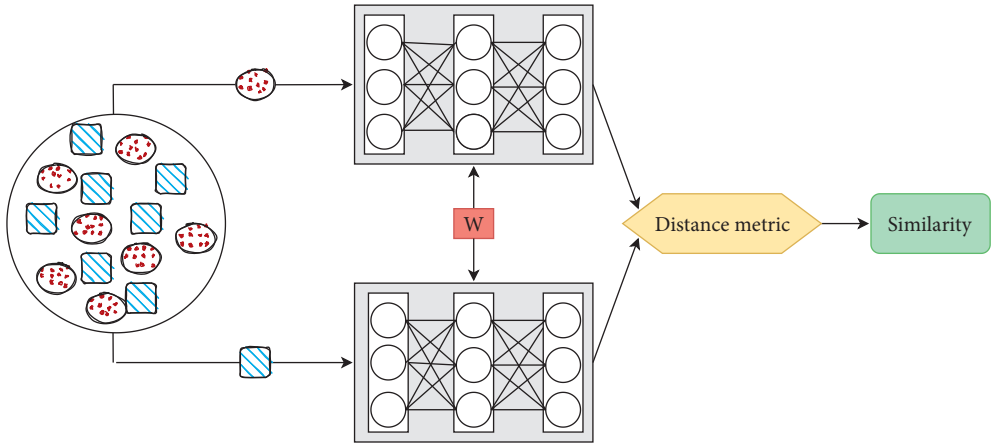

Figure 4: An example of a Siamese neural network with DML.

Table 2: Literature summary of loss metrics and sample selection.

Sample selection	Metric loss	Task
Easy	Triplet [107]	Recognition of image Recognition of object
Multiple negative	Angular [101]	Clustering of image Retrieval of image Verification of object
Multiple negative	N-pair [108]	Clustering of image Identification of face Verification of face
Easy	Clustering [109]	Recognition of object Clustering of image Retrieval of image
Easy	Histogram [103]	Person re-Identification Recognition of image Retrieval of image
Hard negative	Contrastive [89]	Object recognition Image recognition
Semi-hard negative	Quadruple [102]	Patient similarity
Easy	Part [106]	Person re-Identification
Anchor-neighbor	Hierarchical triplet [100]	Recognition of face Retrieval of image

paired or tripled. Depending on the situation, training networks become exponentially more difficult.

The hard negative mining method [91, 92] and semi-hard negative mining method [66, 102] provide informative samples for training to overcome these problems. Despite providing the desired results in specific tasks, hard mining and semi-hard mining strategies consume a great deal of time and memory compared to the traditional method. In addition, the GPU memory limit makes it impossible at times when using large batch sizes. This can be overcomed by clustering loss [109], which has an excellent metric function that requires no data preparation. The authors in Ref. [66] used a CPU cluster to implement their mining strategy to achieve a huge batch on CPU clusters, while deep metric learning is typically performed on a GPU. It may not be possible for some datasets to achieve fast convergence with the metric loss function. To solve this problem, the weights from pretrained network models may be used to ensure faster convergence and better differentiation in embedding space [108].

5. Conclusion

A field of research that researchers have taken interest in recently is DML based on distance metrics. Several academic papers have contributed immensely to the literature on this topic. This article fills the literature gap by providing a comprehensive look at DML that considers all aspects of the technology and the problems associated with this field. Most current studies conducted in this area are commonly influenced by Siamese and triplet networks in DML and proved their higher efficiency on benchmark datasets and specific tasks. However, studies are limited to a few areas. This could be fascinating for researchers given that there are many aspects of DML that have not yet been explored, such as the shortcomings of existing approaches. Thus, DML is still open for future research and can be improved in the long run.

Conflicts of Interest

The authors declare no conflicts of interest in relation to this article.

Acknowledgments

This research was carried out with the support of the Kyungpook National University Research Fund, 2021.

References

[1] M. Zongqing, Z. Shuang, W. Xi et al., "Nasopharyngeal Carcinoma Segmentation Basedon Enhanced Convolutional Neural Networks Usingmulti-Modal Metric Learning," *Physics in Medicine & Biology*, vol. 64, no. 2, p. 64, 2019.

[2] G. Wei, M. Qiu, K. Zhang et al., "A multi-feature image retrieval scheme for pulmonary nodule diagnosis," *Medicine*, vol. 99, no. 4, 8 pages, Article ID e18724, 2020.

[3] T. Li, G. Kou, and Y. Peng, "Improving malicious URLs detection via feature engineering: linear and nonlinear space transformation methods," *Information Systems*, vol. 91, Article ID 101494, 2020.

[4] Y. Luo, H. Hu, Y. Wen, and D. Tao, "Transforming device fingerprinting for wireless security via online multitask metric learning," *IEEE Internet of Things Journal*, vol. 7, no. 1, pp. 208–219, 2020.

[5] Y. Liu, D. Pi, and L. Cui, "Metric learning combining with boosting for user distance measure in multiple social networks," *IEEE Access*, vol. 5, pp. 19342–19351, 2017.

[6] Y. Liu, Z. Gu, T. H Ko, and J. Liu, "Multi-modal media retrieval via distance metric learning for potential customer discovery," in *Proceedings of the 2018 IEEE/WIC/ACM International Conference on Web Intelligence (WI)*, Santiago, Chile, December 2019.

[7] R. Li, J. Y. Jiang, J. Liu, C. C. Hsieh, and W. Wang, "Automatic speaker recognition with limited data," in *Proceedings of the WSDM 2020 - Proc 13th Int Conf Web Search Data Min*, TX, Houston, USA, February 2020.

[8] Z. Bai, X. L. Zhang, and J. Chen, "Speaker verification by partial AUC optimization with Mahalanobis distance metric learning," *IEEE/ACM Transactions on Audio, Speech, and Language Processing*, vol. 28, pp. 1533–1548, 2020.

[9] W. Zheng, B. Zhang, J. Lu, and J. Zhou, "Deep relational metric learning," in *Proceedings of the 2021 IEEE/CVF International Conference on Computer Vision (ICCV)*, Montreal, Canada, 2021.

[10] D. López-sánchez, A. González, and J. M. Corchado, "Neurocomputing Visual content-based web page categorization with deep transfer learning and metric learning," vol. 338, pp. 418–431, 2019.

[11] H. Hu, K. Wang, C. Lv, J. Wu, and Z. Yang, "Semi-supervised metric learning-based anchor graph hashing for large-scale image retrieval," *IEEE Transactions on Image Processing*, vol. 28, no. 2, pp. 739–754, 2019.

[12] H. Wu, Q. Zhou, R. Nie, and J. Cao, "Effective metric learning with co-occurrence embedding for collaborative recommendations," *Neural Networks*, vol. 124, pp. 308–318, 2020.

[13] X. Li and Y. Tang, "A Social Recommendation Based on Metric Learning and Network Embedding," in *Proceedings of the 2020 IEEE 5th Int Conf Cloud Comput Big Data Anal ICCCBDA 2020 55–60*, Chengdu, China, April 2020.

[14] B. Nguyen, B. De Baets, and B. De Baets, *Constraints for Person Re-Identification*, vol. 28, pp. 589–600, 2019.

[15] C. Zhao, X. Wang, W. Zuo, F. Shen, L. Shao, and D. Miao, "Similarity learning with joint transfer constraints for person re-identification," *Pattern Recognition*, vol. 97, Article ID 107014, 2020.

[16] J. Liang, Q. Hu, C. Dang, and W. Zuo, "Weighted graph embedding-based metric learning for kinship verification," *IEEE Transactions on Image Processing*, vol. 28, no. 3, pp. 1149–1162, 2019.

[17] F. Dornaika, I. Arganda-Carreras, and O. Serradilla, "Transfer Learning and Feature Fusion for Kinship Verification," *Neural Computing and Applications*, vol. 32, no. 11, p. 7151, 2020.

[18] D. Wang, Y. Cheng, M. Yu, X. Guo, and T. Zhang, "A hybrid approach with optimization-based and metric-based meta-learner for few-shot learning," *Neurocomputing*, vol. 349, pp. 202–211, 2019.

[19] C. Wang, G. Peng, and B. De Baets, "Deep feature fusion through adaptive discriminative metric learning for scene recognition," *Information Fusion*, vol. 63, pp. 1–12, 2020.

[20] X. He, W. Y. Ma, O. King, M. Li, and H. Zhang, "Learning and inferring a semantic space from user's relevance feedback for image retrieval," *Proceedings of the tenth ACM international conference on Multimedia - MULTIMEDIA '02*, vol. 13, pp. 343–346, 2002.

[21] X. He, W. Y. Ma, and H. J. Zhang, "Learning an image manifold for retrieval," *Proceedings of the 12th annual ACM international conference on Multimedia - MULTIMEDIA '04*, pp. 17–23, NY, New York, USA, October 2004.

[22] J. He, M. Li, and H. Zhang, "Technical-session-1-content-based-image-retrieval-Manifold-ranking-based-image-retrieval," 2004.

[23] A. G. Hauptmann and H. I. Search, "Relevance R negative pseudo-relevance feedback in content-based,".

[24] H. Muller, T. Pun, and D. Squire, "Learning from user behavior in image retrieval: application of Market basket analysis," *International Journal of Computer Vision*, vol. 56, no. 1/2, pp. 65–77, 2004.

[25] A. Globerson and S. Roweis, "Metric learning by collapsing classes," *Advances in Neural Information Processing Systems*, vol. 18, pp. 451–458, 2005.

[26] W. Fei and S. Jimeng, "Survey on Distance Metric Learning and Dimensionalityreduction in Data Mining," *Data mining and knowledge discovery*, vol. 29, no. 2, p. 564, 2015.

[27] Q. Weinberger and L. K. Saul, "Distance metric learning for large margin nearest neighbor classification," *Journal of Machine Learning Research*, vol. 10, pp. 207–244, 2009.

[28] J. Schmidhuber, "Deep Learning in neural networks: an overview," *Neural Networks*, vol. 61, pp. 85–117, 2015.

[29] Y. LeCun, Y. Bengio, and G. Hinton, *Nature*, vol. 521, no. 7553, pp. 436–444, 2015.

[30] T. K. Tran and T. T. Phan, "Deep learning application to ensemble learning—the simple, but effective, approach to sentiment classifying," *Applied Sciences*, vol. 9, no. 13, p. 2760, 2019.

[31] J. Lu, J. Hu, and J. Zhou, "Deep metric learning for visual understanding: an overview of recent advances," *IEEE Signal Processing Magazine*, vol. 34, no. 6, pp. 76–84, 2017.

[32] E. P. Xing, A. Y. Ng, M. I. Jordan, and S. Russell, "Distance metric learning, with application to clustering with side-information," *Advances in neural information processing systems*, vol. 15, 2002.

[33] J. V. Davis, B. Kulis, P. Jain, S. Sra, and I. S. Dhillon, "Information-theoretic metric learning," in *Proceedings of the 24th international conference on Machine learning - ICML '07*, pp. 209–216, Oregon, Corvalis, USA, June 2007.

[34] H. V. Nguyen and L. Bai, "Cosine similarity metric learning for face," *Journal of Information Science*, vol. 43, pp. 88–102, 2011.

[35] K. Q. Weinberger, J. Blitzer, and L. K. Saul, "Distance metric learning for large margin nearest neighbor classification," *Journal of machine learning research*, vol. 10, pp. 1473–1480, 2005.

[36] Y. Duan, J. Lu, J. Feng, and J. Zhou, "Deep localized metric learning," *IEEE Transactions on Circuits and Systems for Video Technology*, vol. 28, no. 10, pp. 2644–2656, 2018.

[37] F. Sayeed, M. Hanmandlu, and A. Q. Ansari, "Face recognition using segmental Euclidean distance," *Defence Science Journal*, vol. 61, no. 5, pp. 431–442, 2011.

[38] X.-S. Yang, "Data mining techniques," *Introduction to Algorithms for Data Mining and Machine Learning*, pp. 109–128, 2019.

[39] Z. Li, X. Zhong, J. Wei, and H. Shi, "The application of manhattan tangent distance in outdoor fingerprint localization," in *Proceedings of the 2018 IEEE Glob Commun Conf GLOBECOM 2018 - Proc*, Abu Dhabi, United Arab Emirates, December 2018.

[40] H. Chouikhi, M. F. Saad, and A. M. Alimi, "Improved fuzzy possibilistic C-means (IFPCM) algorithms using Minkowski distance," in *Proceedings of the 2017 Int Conf Control Autom Diagnosis, ICCAD*, Hammamet, Tunisia, January 2017.

[41] A. B. Dehkordi and S. A. R. Abu-Bakar, "Iris code matching using adaptive Hamming distance," in *Proceedings of the IEEE 2015 Int Conf Signal Image Process Appl ICSIPA 2015 - Proc 404–408*, Kuala Lumpur, Malaysia, October 2016.

[42] A. Bellet, A. Habrard, and M. Sebban, "A Survey on Metric Learning for Feature Vectors and Structured Data," 2013, https://arxiv.org/abs/1306.6709.

[43] Z. Li, "A boosting-based deep distance metric learning method," *Computational Intelligence and Neuroscience*, vol. 2022, Article ID 2665843, 9 pages, 2022.

[44] F. Cakir, K. He, X. Xia, B. Kulis, and S. Sclaroff, "Deep metric learning to rank," *2019 IEEE/CVF Conference on Computer Vision and Pattern Recognition (CVPR)*, , Long Beach, CA, USA, June 2019.

[45] I. Elezi, S. Vascon, A. Torcinovich, M. Pelillo, and L. Leal-Taixé, "The group loss for deep metric Learning.pdf," *ECCV*, vol. 12352, 2020.

[46] Y. Sun, C. Cheng, Y. Zhang et al., *A Unified Perspective of Pair Similarity Optimization*, in *Proceedings of the IEEE/CVF Conference on Computer Vision and Pattern Recognition*, p. 6407p. 6407, 2020.

[47] X. Wang, X. Han, W. Huang, D. Dong, and M. R. Scott, "Multi-Similarity Loss with General Pair Weighting for Deep Metric Learning," in *Proceedings of the IEEE/CVF Conference on Computer Vision and Pattern Recognition*, pp. 5022–5030, 2019.

[48] B. Yu and D. Tao, "Deep metric learning with tuplet margin loss," in *Proceedings of the 2019 IEEE/CVF International Conference on Computer Vision (ICCV)*, 2019.

[49] K. Matusita and H. Akaike, "Decision rules, based on the distance, for the problems of independence, invariance and two samples," *Annals of the Institute of Statistical Mathematics*, vol. 7, no. 2, pp. 67–80, 1955.

[50] A. Elgammal, R. Duraiswami, and L. S. Davis, "Probabilistic tracking in joint feature-spatial spaces," *2003 IEEE Computer Society Conference on Computer Vision and Pattern Recognition, 2003. Proceedings.*vol. 1, 2003.

[51] F. J. Aherne, N. A. Thacker, and P. I. Rockett, "The Bhattacharyya metric as an absolute similarity measure for frequency coded data," *Kybernetika*, vol. 34, pp. 363–368, 1998.

[52] J. Yu, X. Yang, F. Gao, and D. Tao, "Deep multimodal distance metric learning using click constraints for image ranking," *IEEE Transactions on Cybernetics*, vol. 47, no. 12, pp. 4014–4024, 2017.

[53] X. Cai, C. Wang, B. Xiao, and Y. Shao, "Nonlinear metric learning with deep independent subspace analysis network for face verification," *IEICE - Transactions on Info and Systems*, vol. E96.D, no. 12, pp. 2830–2838, 2013.

[54] Y. Sun, Y. Zhu, Y. Zhang et al., "Dynamic metric learning: towards a scalable metric space to accommodate multiple semantic scales," in *Proceedings of the 2021 IEEE/CVF Conference on Computer Vision and Pattern Recognition (CVPR)*, 2021.

[55] G. Dai, J. Xie, F. Zhu, and Y. Fang, "Deep correlated metric learning for sketch-based 3D shape retrieval," in *Proceedings of the 31st AAAI Conf Artif Intell AAAI 2017*, 2017.

[56] Z. Li and J. Tang, "Weakly supervised deep metric learning for community-contributed image retrieval," *IEEE Transactions on Multimedia*, vol. 17, no. 11, pp. 1989–1999, 2015.

[57] B. Harwood, G. Vkb, G. Carneiro, I. Reid, and T. Drummond, "Smart Mining for Deep Metric Learning," in *Proceedings of the IEEE International Conference on Computer Vision (ICCV)*, pp. 2821–2829, 2017.

[58] E. Gundogdu, B. Solmaz, A. Koc, V. Yücesoy, and A. A. Alatan, "Deep Distance Metric Learning for Maritime Vessel Identification," in *Proceedings of the 2017 25th Signal Processing and Communications Applications Conference*, Antalya, Turkey, May 2017.

[59] E. Costa, I. Papatsouma, and A. Markos, "Benchmarking distance-based partitioning methods for mixed-type data," 2022, https://arxiv.org/abs/2203.16287.

[60] C. O. F. Blup, "Distance Based Regression Models," 2021.

[61] J. Liu, Y. Deng, T. Bai, Z. Wei, and C. Huang, "Targeting ultimate accuracy: face recognition via deep embedding," 2015, https://arxiv.org/abs/1506.07310.

[62] E. Hoffer and N. Ailon, "Semi-supervised deep learning by metric em-bedding," pp. 14–26, 2018, https://arxiv.org/abs/1611.01449.

[63] M. Kaya and H. Ş Bilge, "Deep metric learning: a survey," *Symmetry*, vol. 11, no. 9, p. 1066, 2019.

[64] I. Lim, A. Gehre, and L. Kobbelt, "Identifying style of 3D shapes using deep metric learning," *Computer Graphics Forum*, vol. 35, no. 5, pp. 207–215, 2016.

[65] J. Hu, J. Lu, and Y. P. Tan, "Discriminative deep metric learning for face verification in the wild," in *Proceedings of the 2014 IEEE Conference on Computer Vision and Pattern Recognition*, N W Washington, 2014.

[66] F. Schroff, D. Kalenichenko, and J. Philbin, "FaceNet: a unified embedding for face recognition and clustering," in *Proceedings of the 2015 IEEE Conference on Computer Vision and Pattern Recognition (CVPR)*, 2015.

[67] J. Bromley, J. W. Bentz, L. Bottou et al., "Signature verification using a "siamese" time delay neural network," *International Journal of Pattern Recognition and Artificial Intelligence*, vol. 07, no. 04, pp. 669–688, 1993.

[68] J. Lee, B. Varadarajan, S. Abu-El-Haija, and A. P. Natsev, "Collaborative deep metric learning for video understanding," in *Proceedings of the 24th ACM SIGKDD International Conference on Knowledge Discovery & Data Mining*, pp. 481–490, London, 2018.

[69] W. Huang, H. Ding, and G. Chen, "A novel deep multichannel residual networks-based metric learning method for moving human localization in video surveillance," *Signal Processing*, vol. 142, pp. 104–113, 2018.

[70] J. Hu, J. Lu, and Y. P. Tan, "Deep metric learning for visual tracking," *IEEE Transactions on Circuits and Systems for Video Technology*, vol. 26, no. 11, pp. 2056–2068, 2016.

[71] L. Zheng, Y. Yang, and A. G. Hauptmann, "Person Re-identification Past, Present and Future," 2016, https://arxiv.org/abs/1610.02984.

[72] M. Chen, Y. Ge, X. Feng, C. Xu, and D. Yang, "Person re-identification by pose invariant deep metric learning with improved triplet loss," *IEEE Access*, vol. 6, pp. 68089–68095, 2018.

[73] X. Yang, P. Zhou, and M. Wang, "Person reidentification via structural deep metric learning," *IEEE Transactions on Neural Networks and Learning Systems*, vol. 30, no. 10, pp. 2987–2998, 2019.

[74] A. Hermans, L. Beyer, and B. Leibe, *Defense of the Triplet Loss for Person Re-identification*, https://arxiv.org/abs/1703.07737, 2017.

[75] S. Ding, L. Lin, G. Wang, and H. Chao, "Deep feature learning with relative distance comparison for person re-identification," *Pattern Recognition*, vol. 48, no. 10, pp. 2993–3003, 2015.

[76] R. Lu, K. Wu, and Z. Duan, "Deep ranking: triplet matchnet for music metric learning state key Lab of Intelligent Technologies and Systems Tsinghua National Laboratory for Information Science and Technology," *IEEE Int Conf Acoust Speech, Signal Process*, , New Orleans, LA, USA, March 2017.

[77] Q. Wang, J. Wan, and Y. Yuan, "Deep metric learning for crowdedness regression," *IEEE Transactions on Circuits and Systems for Video Technology*, vol. 28, no. 10, pp. 2633–2643, 2018.

[78] Y. Liu, K. Zhao, and G. Cong, "Efficient similar region search with deep metric learning," in *Proceedings of the 24th ACM SIGKDD International Conference on Knowledge Discovery & Data Mining*, London, United Kingdom, August 2018.

[79] X. Wang and M. Liu, "Multi-view deep metric learning for volumetric image recognition," in *Proceedings of the 2018 IEEE International Conference on Multimedia and Expo (ICME)*, San Diego, CA, USA, July 2018.

[80] A. Fathi, Z. Wojna, V. Rathod et al., "Semantic Instance Segmentation via Deep Metric Learning," 2017, https://arxiv.org/abs/1703.10277.

[81] S. Cai, J. Huang, X. Ding, and D. Zeng, "Semantic edge detection based on deep metric learning," in *Proceedings of the 2017 International Symposium on Intelligent Signal Processing and Communication Systems (ISPACS)*, Xiamen, China, November 2017.

[82] Y. Xing, M. Wang, S. Yang, and L. Jiao, "Pan-sharpening via deep metric learning," *ISPRS Journal of Photogrammetry and Remote Sensing*, vol. 145, pp. 165–183, 2018.

[83] C. Wah, S. Branson, P. Welinder, P. Perona, and S. Belongie, *The Caltech-UCSD Birds-200-2011 Dataset. Comput. Neural Syst. Tech. Report, CNS-TR-2011-001*, Calif. Inst. Technol, Pasadena, CA, USA, 2011.

[84] J. Krause, M. Stark, J. Deng, and L. Fei-Fei, "3D object representations for fine-grained categorization," in *Proceedings of the 2013 IEEE International Conference on Computer Vision Workshops*, pp. 554–561, Sydney, NSW, Australia, December 2013.

[85] H. O. Song, Y. Xiang, S. Jegelka, and S. Savarese, "Deep metric learning via lifted structured feature embedding," in *Proceedings of the 2016 IEEE Conference on Computer Vision and Pattern Recognition (CVPR)*, Las Vegas, NV, USA, June 2016.

[86] B. Li, Y. Lu, A. Godil et al., "A comparison of methods for sketch-based 3D shape retrieval," *Computer Vision and Image Understanding*, vol. 119, pp. 57–80, 2014.

[87] B. Li, Y. Lu, C. Li et al., "A comparison of 3D shape retrieval methods based on a large-scale benchmark supporting multimodal queries," *Computer Vision and Image Understanding*, vol. 131, pp. 1–27, 2015.

[88] A. J. Howell and H. Buxton, "Towards unconstrained face recognition from image sequences," in *Proceedings of the Second International Conference on Automatic Face and Gesture Recognition*, pp. 224–229, Killington, VT, USA, October 1996.

[89] R. Hadsell, S. Chopra, and Y. LeCun, "Dimensionality reduction by learning an invariant mapping," in *Proceedings of the 2006 IEEE Computer Society Conference on Computer Vision and Pattern Recognition - Volume 2 (CVPR'06)*, pp. 1735–1742, New York, NY, USA, June 2006.

[90] S. Bell and K. Bala, "Learning visual similarity for product design with convolutional neural networks," *ACM Transactions on Graphics*, vol. 34, no. 4, pp. 1–10, 2015.

[91] E. Simo-Serra, E. Trulls, L. Ferraz, I. Kokkinos, P. Fua, and F. Moreno-Noguer, "Discriminative learning of deep convolutional feature point descriptors," in *Proceedings of the 015 IEEE International Conference on Computer Vision (ICCV)*, N W Washington, 2015.

[92] M. Bucher, H. S.´Ephane, and J. F.´Eric, "Hard negative mining forMetric learning based zero-shot Classification," in *Proceedings of the European Conference on Computer Vision (ECCV)*, pp. 524–531, Cham, November 2016.

[93] Y. Cui, F. Zhou, Y. Lin, and S. Belongie, "Fine-grained categorization and dataset bootstrapping," in *Proceedings of the IEEE International Conference on Computer Vision (ICCV)*, pp. 1153–1162, 2017.

[94] Y. Movshovitz-Attias, A. Toshev, T. K. Leung, S. Ioffe, and S. Singh, "No fuss distance metric learning using Proxies," in *Proceedings of the IEEE International Conference on Computer Vision (ICCV)*, pp. 360–368, 2017.

[95] C. Wu, U. T. Austin, and A. Amazon, "Supplementary material : sampling matters in deep embedding learning," *Iccv*, 2017.

[96] Y. Jeong, S. Lee, D. Park, and K. H. Park, "Accurate age estimation using multi-task siamese network-based deep metric learning for front face images," *Symmetry*, vol. 10, no. 9, p. 385, 2018.

[97] D. Yi, Z. Lei, and S. Liao, "Deep metric learning for person Re-identification and De-identification," in *Proceedings of the 22nd International Conference on Pattern Recognition*, pp. 34–39, Stockholm, August 2014.

[98] H. Shi, X. Zhu, S. Liao, Z. Lei, Y. Yang, and S. Z. Li, "Constrained deep metric learning for person Re-identification," pp. 34–39, 2015, https://arxiv.org/abs/1511.07545.

[99] Y. Wen, K. Zhang, B. Z. Li, and Y. Qiao, "A discriminative feature learning approach for deep face recognition," in *Proceedings of the European Conference on Computer Vision*, pp. 499–511, Cham, September 2016.

[100] W. Ge, W. Huang, D. Dong, and R. Matthew, "Deep Metric Learning with HierarchicalTriplet Loss," in *Proceedings of the European Conference on Computer Vision (ECCV)*, p. 288p. 288, 2018.

[101] J. Wang, F. Zhou, S. Wen, X. Liu, and Y. Lin, "Deep metric learning with angular loss," in *Proceedings of the 2017 IEEE International Conference on Computer Vision (ICCV)*, Venice, Italy, October 2017.

[102] J. Ni, J. Liu, C. Zhang, D. Ye, and Z. Ma, "Fine-grained patient similarity measuring using deep metric learning," in *Proceedings of the 2017 ACM on Conference on Information and Knowledge Management*, pp. 1189–1198, Singapore, Singapore, 2017.

[103] E. Ustinova and V. Lempitsky, "Learning deep embeddings with histogram loss," *Advances in Neural Information Processing Systems*, pp. 4177–4185, 2016.

[104] W. Li, R. Zhao, T. Xiao, and X. Wang, "DeepReID: deep filter pairing neural network for person re-identification," in

Proceedings of the 2014 IEEE Conference on Computer Vision and Pattern Recognition, NW Washingto, June 2014.

[105] L. Zheng, L. Shen, L. Tian, S. Wang, J. Wang, and Q. Tian, "Scalable Person Re-identification : A Benchmark University of Texas at San Antonio," in *Proceedings of the IEEE international conference on computer vision*, Montreal, BC, 2015.

[106] H. Yao, S. Zhang, R. Hong, Y. Zhang, C. Xu, and Q. Tian, "Deep representation learning with Part Loss for person Re-identification," *IEEE Transactions on Image Processing*, vol. 28, no. 6, pp. 2860–2871, 2019.

[107] E. Hoffer and N. Ailon, "Deep metric learning using triplet network. Pattern Recognition, Image Anal Comput Vision," *Appl Springer*, vol. 9370, pp. 84–92, 2015.

[108] K. Sohn, "Improved deep metric learning with multi-class N-pair loss objective," *Advances in Neural Information Processing Systems*, vol. 29, pp. 1857–1865, 2016.

[109] H. O. Song, S. Jegelka, V. Rathod, and K. Murphy, "Deep Metric Learning via Facility Location," in *Proceedings of the IEEE Conference on Computer Vision and Pattern Recognition*, pp. 2206–2214, 2017.

Hindawi
Scientific Programming
Volume 2022, Article ID 2840541, 10 pages
https://doi.org/10.1155/2022/2840541

Research Article

Usability Design of Human-Machine Interaction Interface of Child Companion Robot in Wireless Network

Xinmin Wang, Ying Hu, and Wendi Zhang

Department of Arts and Media, Hebei Vocational University of Technology and Engineering, Xingtai 054000, Hebei, China

Correspondence should be addressed to Xinmin Wang; 201520908@stu.ncwu.edu.cn

Received 7 July 2022; Revised 23 August 2022; Accepted 3 September 2022; Published 30 September 2022

Academic Editor: Juan Vicente Capella Hernandez

With the core and small-scale family structure, parents and children have less time and opportunities to interact, which leads to the lack of care and emotional companionship for preschool children, which is easy to cause physical and mental disorders. In response to this phenomenon, a series of child care robot products have emerged on the market and have continued to be the focus of attention in the past two years. However, such products are still generally deficient in terms of interaction and content. It is difficult for users to choose and use. This paper takes the design and application of remote parent-child interaction of preschool children's escort machine as the research object. First, it examines the physical, psychological, and behavioral characteristics of escort robots, namely, preschool children. To sum up, the remote parent-child interaction design strategy of children's escort robot products is proposed for the design practice and industry reference of this paper. The experimental results show that the children in the experimental group pay more attention to the main content and off-topic content than the control group, and the attention rate is more than 95%. To a certain extent, it can be said that the games in the system have the ability of parent-child interaction. This paper abandons the traditional research direction of pursuing human-computer interaction between childcare products and high technology. Instead, it studies parent-child emotional interaction, so that the emotional interaction between parents and children is not replaced by technology products but helps parents deepen the relationship with their children. Emotional interaction allows parents to truly accompany their children to grow up.

1. Introduction

With the rapid development of information technology and computer network, great changes have taken place in people's way of life and work. Emerging forms of entertainment and education have sprung up, often through advanced image processing and other technologies. One of the most striking is the emergence of educational games that can cultivate children's interest in learning, which bring great freedom to children's learning process and also increase a certain interest. It also realizes the learning method of "education through fun." A good human-computer interaction design can improve the effectiveness of children's interaction and learning games, increase the affinity of children's learning toys, and effectively improve children's academic performance. However, there are still many deficiencies in the human-computer interface design of children's learning games at this stage. Wireless network control system is a huge and complex control system. It focuses on controlling the system over a wireless network. It is a field that integrates various theories such as communication networks and control theory. It is of high practical value to study the control system under the condition of wireless network.

Many technologically advanced countries in the world are far ahead of us in robot manufacturing technology, robot control technology, wireless communication technology, wireless network control technology, etc. In particular, the technological level of the United States and Japan has always been at the leading level in the world. Foreign scholars have also made many achievements in network control theory. In order to reduce the impact of delay on the network control system, Sheu and Huang designed a receive buffer that can convert the time-varying delay into a fixed delay for delay

compensation control [1]. Li and Andrade established discrete models of networked control systems with short delay and probability distribution determined by Markov connections and used stochastic control theory to study system performance and design control systems [2]. Wong et al. analyzed the IP-based networked control system and improved the overall control performance of the control system by compensating for time delay [3].

Robot research in China started relatively late. In the wireless control system, the control signal is encapsulated in a data packet and then sent to the actuator connected to the controlled object through the shared wireless network, and the sensor data of the controlled object are also transmitted back to the controller through the wireless network. Shin et al. built a buffer to receive information, and they converted the original long delay to a short delay, since the reduction constant was not changed, thus forming a switching system that slowed down the speed of maximizing the expansion [4]. The purpose of Peng et al.'s construction of the buffer is to first use the buffer to convert the indeterminate delay into a fixed delay and then perform predictive control. This result can be used for long-delay wireless network control systems [5]. Lao and Wong proposed an improved Ethernet neuron PID controller. The controller can handle the network delay without relying on the accurate mathematical model of the network delay and can obtain good control effect [6].

It is found that most of the products on the market are limited to the functions of smart toys and educational products and lack parent-child interaction functions. In view of the great potential of parent-child emotional interaction, this paper proposes a research perspective on remote parent-child interaction and searches for related research on "parenting robots" through HowNet. There is only one study of companion robots for children with autism. No matter how smart the future AI is, humans will never let it replace the parent-child relationship. Whether it is preschool children or parents, the lack of parent-child emotion is a common problem in the current society. Compared with children's education and games, solving this problem has far-reaching significance. Therefore, it is considered that the topic selection perspective of the remote parent-child interaction research of child escort robots is innovative and meaningful.

2. Usability Design of Human-Computer Interaction Interface of Child Companion Robot in Wireless Network

2.1. Wireless Network Control System. This kind of control system is a kind of distributed system [7]. Due to its characteristics of networking, it uses network lines as data exchange channels for data exchange, which can realize information sharing among multiple nodes. The means of transmitting information is the network. The whole system uses the network to complete the information exchange between the various components of the system (such as actuators, sensors, and controllers) and uses the network to complete resource sharing and remote sharing and detection. Due to the limitations of the traditional wired network, it can no longer satisfy the advanced users who have a relatively large network scale and are very dependent on the network. Choosing a wireless network for communication can avoid complicated line connections like wired networks, greatly reducing the cost of building a system. This not only saves costs but can also satisfy many systems that require flexibility and mobility, expanding the application range of network systems [8].

2.1.1. Wireless Network Control System Structure. The components of the system mainly include wireless communication network, controlled object, and controller [9]. Wireless networks are generally used in remote control information transmission systems using electromagnetic waves, such as networks using radio waves as carrier and physical layers. After the state information output by the control object is collected by the sensor, it is firstly discretized, and then the state information is transmitted to the input end of the controller through the wireless channel. After the controller receives and calculates the information from the wireless network, the wireless network sends the control information calculated by the controller to the controlled object. A zero-order holder processes a discrete signal and divides it into a continuous piecewise function. Use it as an input to a continuous system [10].

2.1.2. Characteristic Analysis of Wireless Network Control System. It can improve system reliability and other benefits. The cost of information transmission for remote control and remote operation is very low. Instead of using analog signals, digital signals are used for transmission over a digital network that digitally interconnects various control devices. It can reduce the intermediate links of information processing equipment to a certain extent, thereby reducing the resources consumed by full control. It can complete process optimization and overall system control from task level, decision management level to field control equipment level [11].

2.1.3. Node Driving Mode on Control System. The driver's position in the system is very important. Generally, when the operating system is installed, the first thing is to install the driver. It is very important to choose the appropriate driving method for each node for the design of wireless network control system. For a system with a small delay, the network load is relatively small and the number of network nodes is relatively small. In this case, when the wireless network control system adopts the event-driven method, the system performance is far superior to the time-driven wireless network control system control performance. Longer delays may occur when the network is heavily congested. Currently, wireless network control systems use this method from time to time. Even if there is packet loss in the measured value, the controller can still take action

using the last control quantity entered, thereby turning the packet loss into a long delay [12].

2.2. Process and Analysis of Time Delay in WNCS. Delay includes transmission delay, propagation delay, processing delay, and queuing delay. Generally, transmission delay and propagation delay are the main considerations. Execution delays occur in the actions of controllers, sensors, and actuators. They are represented by $\tau_a$and τ_s, respectively τ_c; the transmission delay includes the information delay from the controller to the actuator and from the sensor to the controller, which are represented by $\tau_{sc}$and τ_{ca}, respectively. The total delay of the wireless control system is expressed as

$$\begin{aligned} \tau &= \tau_s + \tau_{sc} + \tau_c + \tau_{ca} + \tau_a, \\ \tau_k^{sc} &= \tau_k^{cs} + \tau_k^{ss}, \\ \tau_k^{ca} &= \tau_k^{as} - \tau_k^{cf}, \\ \tau_k^{c} &= \tau_k^{cf} - \tau_k^{cs}. \end{aligned} \tag{1}$$

Computer control is controlled according to the specified control algorithm [13, 14]. Therefore, the correctness of the control algorithm directly affects the quality of the control system and even determines the success or failure of the entire system. When the controller executes the control algorithm, as long as the clocks of the nodes in the network are synchronized, it can be obtained by the method of time identification. Therefore, the delay of the wireless network control system can finally be expressed as

$$\tau = \tau_{sc} + \tau_{ca}. \tag{2}$$

The state space can be regarded as a space with state variables as the coordinate axis, so the state of the system can be represented as a vector in this space. Then, the state space expression of the control system is as follows:

$$\begin{cases} x(t) = Ax(t) + Bu(t), \\ y(t) = Cx(t). \end{cases} \tag{3}$$

The principle of motion of the robot is analyzed, and the principle of torque balance is deduced. The steering angle of the robot = the main moment of the right foot - the forced distance of the resistance of the left foot.

$$\begin{aligned} I_v\ddot{\varphi} &= D_r l - D_l l, \\ M\dot{v} &= D_r + D_l. \end{aligned} \tag{4}$$

The torque summarizes all the laws that affect the change of the motion state of the rotating object, and the torque is the physical quantity that changes the motion state of the rotating object. For the feet of the robot, according to the principle of moment balance, the dynamic characteristics of the left and right feet are expressed by the following equations:

$$\tau = \tau_{sc} + \tau_{ca}. \tag{5}$$

Then, the relationship between ϕ, v, θ_ican be obtained:

$$\begin{aligned} I_w r\ddot{\theta}_i + cr\dot{\theta}_i &= kru_i - r^2 D_i, \\ I_w r\left(\ddot{\theta}_r + \ddot{\theta}_l\right) + cr\left(\dot{\theta}_r + \dot{\theta}_l\right) &= kr\left(u_r + u_l\right) - r^2\left(D_r + D_l\right), \\ 2I_w\dot{v} + 2cv &= kr\left(u_r + u_l\right) - r^2\left(D_r + D_l\right), \\ \dot{v} &= -\frac{2c}{\left(Mr^2 + 2I_w\right)}v + \frac{kr}{\left(Mr^2 + 2I_w\right)}\left(u_r + u_l\right). \\ \ddot{\phi} &= -\frac{2cl^2}{I_v r^2 + 2I_w l^2}\dot{\phi} + \frac{krl}{I_v r^2 + 2I_w l^2}\left(u_r - u_l\right). \end{aligned} \tag{6}$$

In WNCS, because the computer is used to process the control quantity, input the control signal, and output the controlled object, the system needs to be discretized before the design. Assuming there is no network latency in the system, we have

$$\begin{aligned} \dot{x}(t) &= Ax(t) + Bu(t), \\ x((k+1)T) &= e^{AT}x(kT) + \int_{kT}^{(k+1)T} e^{A[(k+1)T-s]}Bu(s)\mathrm{d}s. \end{aligned} \tag{7}$$

2.3. Interactive Interface

2.3.1. Human-Computer Interaction and Human-Machine Interface. Human-computer interaction is the study of the interaction between systems and users [15]. A system can be a variety of machines, as well as computerized systems and software. The process is mainly completed by input devices and output devices. The input device converts the operator's thoughts and needs into a language that the computer can recognize, inserts it into the computer CPU, and then transmits the calculation result to the output device through calculation. They can recognize and understand to complete a complete human-computer interaction process. Computers can recognize and differentiate the meaning of human language and sounds through powerful software. Through the analysis and calculation of the kernel computing system, the meaning that the operator wants to express can be better analyzed, and the operator's questions or requirements can be fed back according to the set program. Human-machine Interface is a media and dialog interface for transferring and exchanging information between humans and machines. It is an important part of a computer system and a means for the system to interact and exchange information with users. It is an important part of a computer system, a means for the system to interact and exchange information with users, and can combine the internal form of machine information with humans [16, 17].

2.3.2. Design Principles of Human-Computer Interface Design

(1) Concise Hierarchy Principle. Human-machine interface is a medium and dialog interface for transmitting and exchanging information between people and computers and is an important part of computer systems. Therefore, when

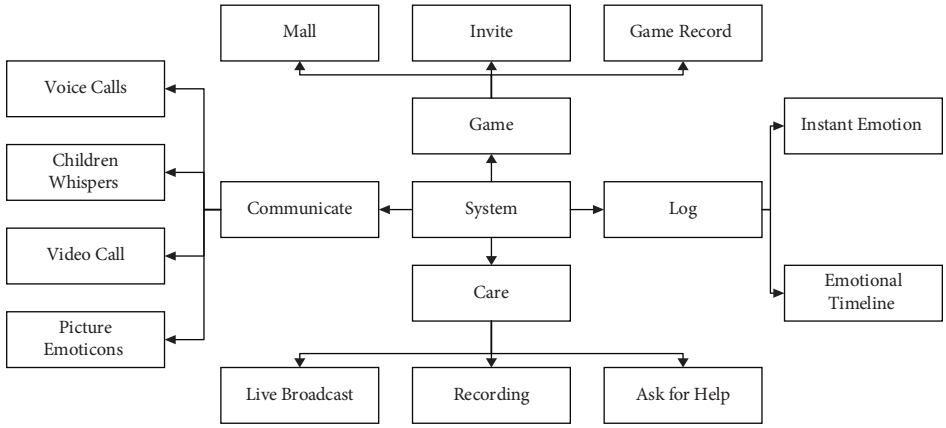

Figure 1: Functional exploded view.

Table 1: Reliability test results.

Category	Index portfolio	Alpha coefficient
Game	Shopping center Invite Game record	0.8627
Log	Instant emotion Emotional timeline	0.8416
Care	Live streaming Record Request for help	0.7663
Communicate with	Voice call Kids whispering Video call Picture expression	0.7552

designing a human-computer interface, the first consideration is to distinguish computer system settings according to the order and urgency of workflow and the relationship from large to small, general to single, and high to low. The levels should be properly arranged. The process of control and design supervision is reduced, and the host-computer dialog interface is more comprehensive and organized, which is convenient for humanization [18].

(2) User-Oriented Design Principles. In the whole process of human-computer interaction interface design, it is necessary to understand and take care of users' usage habits and usage characteristics and put people first [19, 20]. Context awareness, eye tracking, gesture recognition, three-dimensional input, speech recognition, facial expression recognition, handwriting recognition, natural language understanding, etc. are all important problems that need to be solved in user interfaces. In the early stage of design and development, the user's opinions and requirements are continuously solicited and accepted, and then a feasible solution is selected, and secondary development is decided to make the designed interface meet the needs of users.

(3) Interface Consistency Principle. Design requirements must conform to fashion trends, reflect design consistency, and adopt popular design formats. Second, the requirements of the standard must be consistent with applicable international or national standards in order to meet the mandatory minimum standards, that is, the consistency of color, screen, and text throughout the interface.

(4) Functional Principle. According to the user's functional requirements, design different management objects for the same interface, and design multiple projects at the same time [21]. A hierarchical system of information options and dialog boxes is used, depending on the function of the department. The interactive interface makes it easy for users to get started. Users can select common and uncommon functions according to their needs and classify and archive these functions. These are functional options that must be delivered to the customer during the design process.

(5) Frequency Principle. According to the interaction frequency of the dialog box of the management object, draw the hierarchical order of the human-machine interface and the position of the dialog box and increase the frequency of monitoring and accessing the dialog box. According to the user's usage habits and rational thinking, supervise and control to meet the customer's expectations of the product to the greatest extent.

2.4. Functional Requirements of Preschool Children

2.4.1. Physiological Needs of Preschool Children. Physiological needs are a powerful driving force that drives people to carry out various behaviors [22]. When physiological needs are met to a certain extent, people will have the next level of needs. Visual perception in preschoolers includes color perception, which improves as children age. In the design of the companion robot, the colors and styling elements preferred by preschoolers as shown by experimental data should be used. Touch is a way for children to learn about their external environment from the beginning and plays a key role in children's cognitive development.

2.4.2. Psychological Needs of Preschool Children. Psychological needs are a kind of unique human needs [23, 24]. Human needs are divided into two levels: physiological needs and psychological needs. Psychological needs

Table 2: System function test.

Functional module	Function name	Test steps	Test results
Game	Shopping center	Buy product test	Testing successfully
	Invite	Invite players to test	Testing successfully
	Game record	View game record test	Testing successfully
Log	Instant emotion	Instant reading mood test	Testing successfully
	Emotional timeline	Query emotional timeline test	Testing successfully
Care	Live streaming	Can you watch the live test	Testing successfully
	Record	Query record test	Testing successfully
	Request for help	Distress test	Testing successfully
Communicate with	Voice call	Voice call test	Testing successfully
	Kids whispering	Children's riddle test	Testing successfully
	Video call	Video call test	Testing successfully
	Picture expression	Picture expression test	Testing successfully

Table 3: Questionnaire data analysis.

Attributes		Number of people	Percentage
Age	0–2 years old	25	31.6
	3–6 years old	35	44.3
	7–12 years old	19	24.1
Gender	Boy	36	45.6
	Girl	43	54.4
Family status	A parent with a child	27	34.1
	Grandparents taking care of children	50	63.4
	Babysitter taking care of children	2	2.5

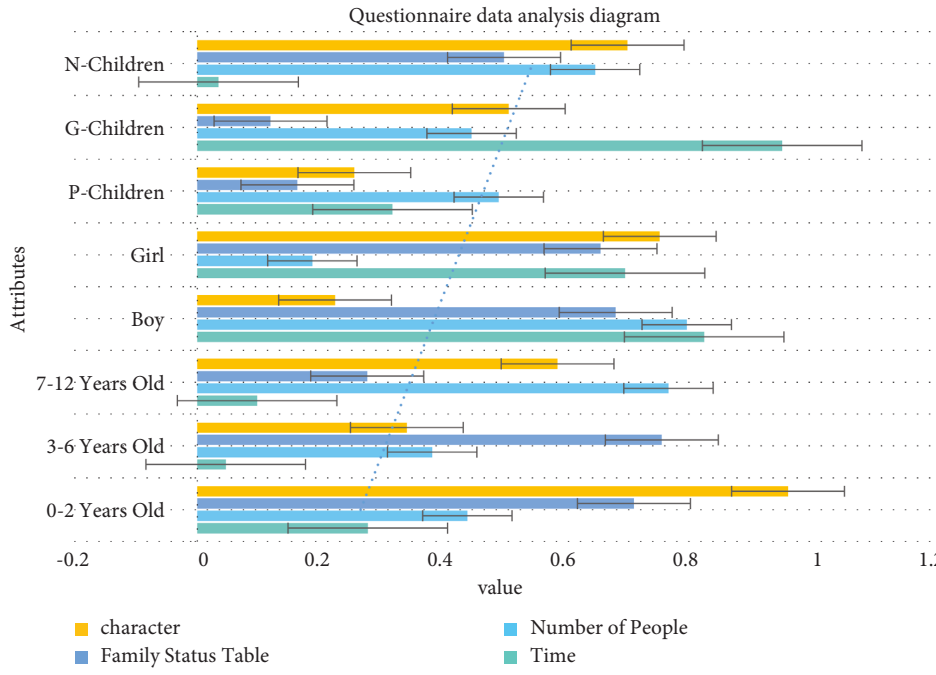

Figure 2: Questionnaire data analysis diagram.

are initially derived from physical needs and then gradually become independent. For example, preschool children are very curious about the unknown things they have never seen and the new things that are constantly changing. Therefore, it is necessary to use the child's curiosity about the unknown to understand the characteristics of children's learning and questioning and to incorporate voice interaction into the design of the robot. Guidance can help children discover

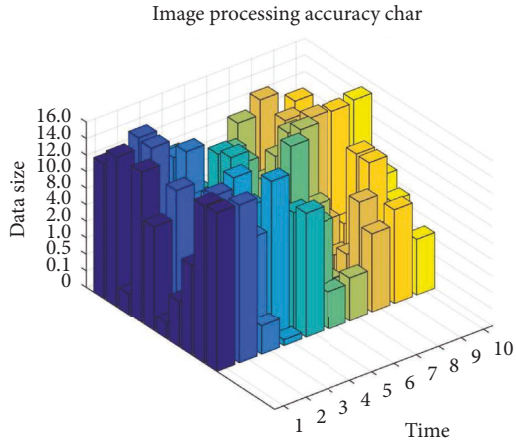

Figure 3: Image processing accuracy map.

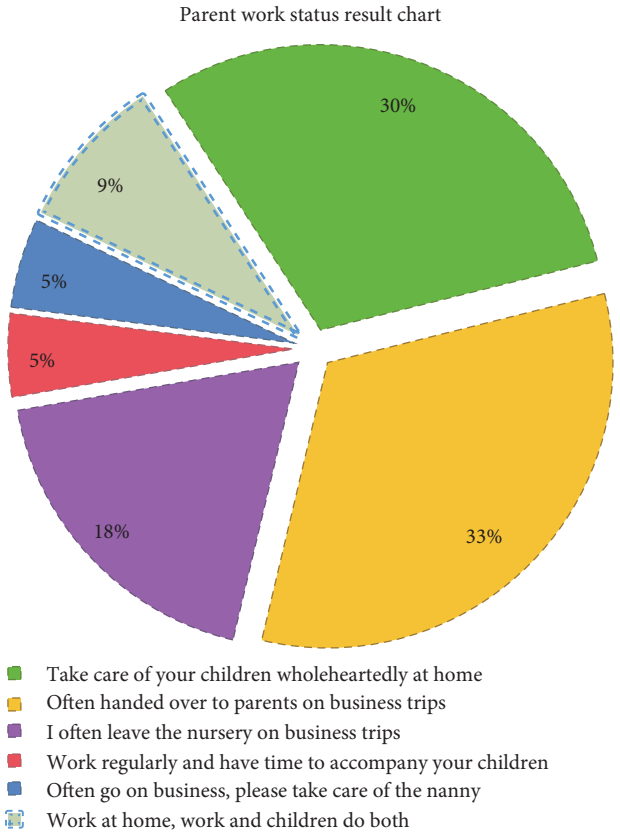

Figure 4: Parent work status result chart.

relationships between things. In response to children's curiosity about changing movements, the interface design uses changing images and rhythmic sounds to attract children's attention.

3. Usability of Human-Machine Interface for Children's Companion Robots

3.1. The Design Process of the Child Companion Robot System. Before designing a system, it is necessary to identify the audience [25]. There are many problems in the process of

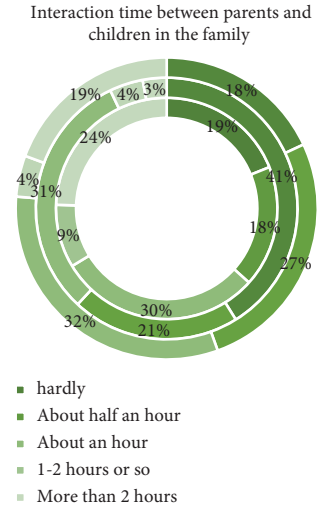

Figure 5: Result graph of parent-child interaction time in the family.

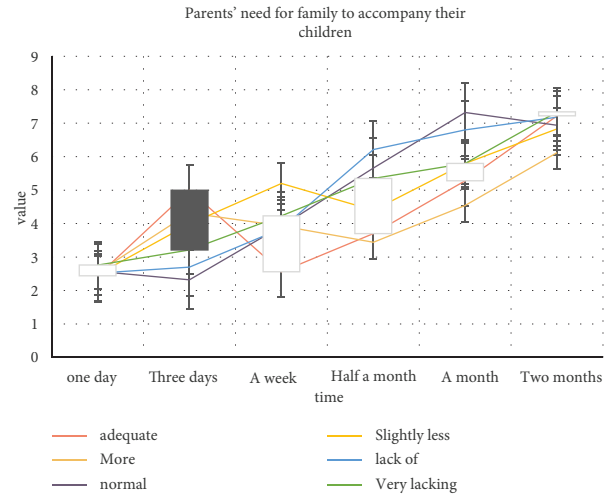

Figure 6: A map of parents' needs for family to accompany their children.

parent-child interaction in today's society. Among them, most of them are busy with work, lack communication with their children, and lack the emotional joy brought by interacting with their parents. Therefore, our system mainly includes children's emotional log function, daily communication function, remote care function, and virtual interactive game function, while for preschool children, the main functions are limited to virtual interactive games and daily communication and early childhood education functions, including various smaller functions [26, 27]. Due to the limitations of preschool children's own cognition, the function of escort cannot be too much and can only meet their basic needs. Too many operation functions can easily lead to misoperation, so the function of child escort should be reserved for reference and should not be overly detailed, as shown in Figure 1.

Table 4: Standardized processing of characteristic data.

Sample serial number	Understand your child's emotions and activities	Talk to children	Play games with children	Walk with the child	No other requirements	Teach a child to do something
1	−0.6776	−0.6411	0.1736	1.9178	−0.3848	−0.5962
2	−0.7014	−0.7048	0.5368	1.7370	−0.3880	−0.6295
3	−0.6465	−0.6438	0.4739	1.8397	−0.3642	−0.6141
4	−0.8523	−0.8657	1.3780	0.9615	0.1147	−0.7533
5	−0.7524	−0.7237	0.8180	1.6722	−0.2849	−0.6791
6	−0.7438	−0.7341	0.6385	1.7827	−0.2274	−0.6609
7	−0.5712	−0.5436	0.1387	1.9857	−0.4264	−0.5432
8	−0.7334	−0.7625	0.7288	1.6483	−0.2781	−0.6341

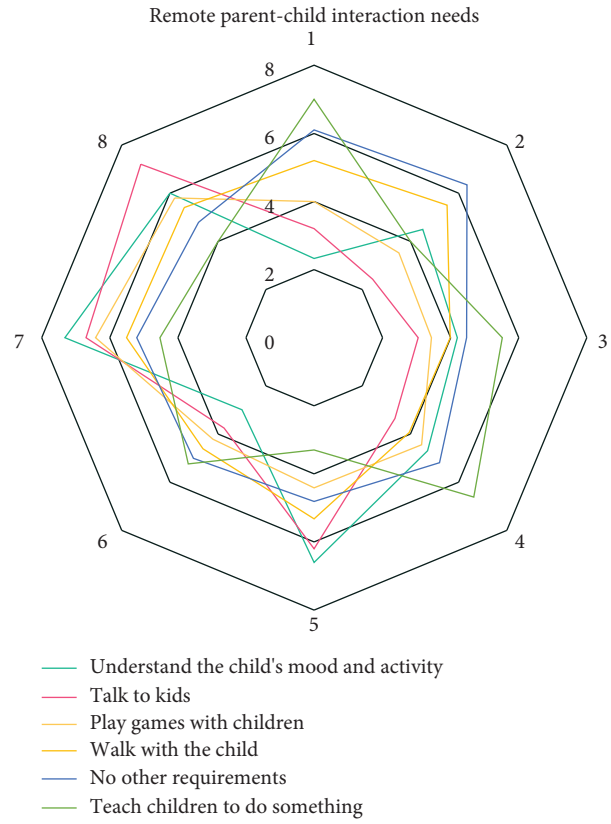

Figure 7: Analysis chart of parents' remote parent-child interaction needs.

3.2. Test Subject. In this experiment, 20 preschool children aged 3–6 were selected for this experiment. These children were accompanied by full-time kindergarten teachers, and their safety was basically guaranteed. We used wearable glasses and X3 eye trackers to collect children's attention while playing, so that we could integrate the data for analysis and consider whether the three play modes meet the usability principles for remote parent-child interaction [28]. The game scene is mainly in the form of a maze map. Parents and children each play roles and play three types of parent-child interactive games on the maze map. Accompanied by the experimenter, 20 preschool children aged 3–6 played simulated interactive games. To a certain extent, whether there is a good experience determines whether preschool children really like and use companion products for a long time. Therefore, a more nuanced human-machine experience is the primary prerequisite for guiding children to use companion robots for remote parent-child interaction [29, 30].

3.3. Experimental Method. The expression of the positive index normalization method is as follows:

$$y_{ij} = \frac{x_{ij} - \min\{x_{ij}\}}{\max\{x_{ij}\} - \min\{x_{ij}\}}. \tag{8}$$

The normalization method for negative exponents is expressed as follows:

$$y_{ij} = \frac{\max\{x_{ij}\} - x_{ij}}{\max\{x_{ij}\} - \min\{x_{ij}\}}. \tag{9}$$

3.4. Statistical Data Processing Methods. In this paper, the well-known SPSS software is used to process the experimental data, the number of experimental data $k$is the number of experimental data, represents the variance of the results adjusted for experimental error. The reliability calculation formula is

$$a = \frac{k}{k-1}\left(1 - \frac{\sum \sigma_i^2}{\sigma^2}\right). \tag{10}$$

4. Experimental Usability of Companion Robot Human-Machine Interface

4.1. Indicator Reliability Test and System Function Test Analysis

4.1.1. Evaluation Index System Based on Index Reliability Test. In this experiment, the alpha coefficient method was used. When α is greater than 0.7, it indicates that the effect of index setting is better. Therefore, we analyze the reliability of each class of objects and divide them into specific different metrics. The results are shown in Table 1.

From the data in Table 1 above, it can be concluded that the effects of various functions on children are less different ($\alpha > 0.7$), all within the acceptable range.

Table 5: Time and focus statistics.

Polygon				Rectangle			
Counting	Average 1	Average 2	Sum	Counting	Average 1	Average 2	And
1	6.00	8.00	14.00	1	178.00	32.00	210.00
2	4.00	3.00	7.00	2	101.00	21.00	122.00
3	8.00	7.00	15.00	3	149.00	19.00	168.00
4	1.00	6.00	7.00	4	246.00	9.00	255.00
5	4.00	7.00	11.00	5	115.00	22.00	137.00
6	10.00	5.00	15.00	6	69.00	31.00	100.00
7	5.00	7.00	12.00	7	140.00	17.00	157.00
8	1.00	9.00	10.00	8	139.00	21.00	160.00
9	15.00	3.00	18.00	9	125.00	19.00	144.00
10	6.00	8.00	14.00	10	176.00	34.00	210.00

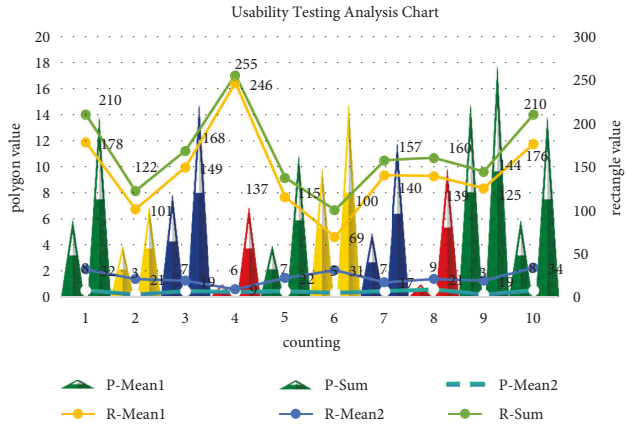

Figure 8: Usability testing analysis chart.

4.1.2. System Function Test Analysis. The system function test mainly includes main functions such as children's emotional log function, daily communication function, remote nursing function, and virtual interactive game function, as shown in Table 2.

As can be seen from Table 2, after analyzing the required functions, the basic design and testing of the system constructed in this paper are relatively successful.

4.2. Questionnaire Test Analysis

4.2.1. Questionnaire Data Analysis. By distributing questionnaires to the local *X* community, a total of 80 parent-child interaction questionnaires for families aged 0–12 were distributed, and 79 valid questionnaires were recovered. The experimental results are shown in Table 3. In addition, we draw a line chart based on the data in Table 3, as shown in Figure 2.

We can conclude that most of these families are grandparents with children at home, and the probability is as high as 63.4%. There are also a very small number of families with better conditions, whose parents do not have much time to hire nanny to take care of them, accounting for 2.5%. The rest are basically parents with children, accounting for 34.1%. Among them, children aged 0–2 accounted for 31.6% of the total, children aged 3–6 accounted for 44.3% of the total, and children aged 7–12 accounted for 24.1% of the total. Observe the child in a natural way, undisturbed, and record the child's behavioral and emotional characteristics along the way. The results will be analyzed later.

According to Table 3, we combine the features extracted by image processing to analyze the immediate emotions of children. The results are shown in Figure 3.

The database is compared and analyzed through image processing technology to obtain and store the children's average feelings, so as to use the function of querying the emotional timeline. As can be seen from Figure 3, the accuracy rate of instant judgment of emotions reached 91.7%, which also shows that the system is very useful.

4.2.2. The Status Quo of Family Parent-Child Interaction Time. As can be seen from Figure 4, about 30% of parents have a relatively stable job and have time to spend with their families and children, and 9% of parents take care of their families at home full time and have enough time to spend with their families. With children, only 66% of households are busy with work and child care. There are some downsides. Among them, 33% of parents gave their children to the elderly because they were busy with work, 18% of parents sent their children to nurseries because of their busy work, and 5% of parents hired nanny to take care of their children because of good family conditions.

As can be seen from Figure 5, more than 75% of parents spend less than an hour with their children on working days, of which only 2.79% spend very little time with their children on working days, and 43.62% spend less time with their children on working days. About 6.9% of parents with their children spend enough time with their children during the workday. From the above two questions, it can be concluded that the time of family parents to accompany their children is extremely scarce at present.

As can be seen from Figure 6, only 7.6% of parents feel that they have enough time to spend with them, while in families with preschool children, the proportion of a parent who is at home full time is as high as 9%. Therefore, it can be calculated that, excluding full-time parents, working parents only account for the lack of companionship. The remaining 87% of parents feel that the time to accompany their children is not enough, and 12.56% of them say that the time to accompany their children is extremely lacking. Therefore, it

can be seen that the parents of the current family still have a great demand for the time spent with their children.

4.2.3. Analysis of Parents' Remote Parent-Child Interaction Needs. Here, our method normalizes the extracted feature data. We choose linear scaling transformation, range transformation, and standard sample transformation. These three methods are different. The results are shown in Table 4. We made a radar chart based on this result, as shown in Figure 7.

As can be seen from Figure 7, the main remote interaction needs of children's parents are chatting and playing games with their children, accounting for 60.71%, of which 28.12% are talking to children, and 32.59% are playing games with children, followed by understanding children's emotions and motivation. It can be seen that when parents are away from their children, they focus first on communication and interaction issues, followed by safety issues, and finally education issues.

4.3. Usability and Interesting Test Analysis

4.3.1. Usability Test Analysis. The usability testing of this paper adopts the method of quantitative research using standardized usability questionnaires. Usability questions in the questionnaire are standardized. You just need to change the subject keywords. Common standardized usability questionnaires include overall evaluation questionnaires and experimental results, as shown in Table 5. We made a combined graph based on this result, as shown in Figure 8.

Judging from the validity of the test results, both children and experimenters can participate more actively in such games during the interaction process and generate a certain degree of pleasure. In addition, the number of attention points in the experimental group is much higher than that in the control group, with an average attention rate of over 95%. To a certain extent, it can be said that the games in the system can achieve better attention effects in parent-child interaction, as shown in Figure 8.

5. Conclusion

The design of a successful human-computer interaction interface for children's learning games should not only conform to the development trend of modern technology but also conform to the requirements of children's psychological development. The control of mobile robots in a wireless network environment is very complex. At the same time, due to the comprehensive influence of factors such as changes in network load, randomness of transmitted data, and limited bandwidth resource conditions, the system introduces network delay, which seriously affects the control performance of the entire system. In order to realize the tracking control of the mobile robot in the time-delayed wireless network control system, a solution is proposed in this paper, which has a very positive effect on realizing the stable and fast real-time control of the mobile robot under the wireless network.

In this paper, the two hotspots of wireless sensor network and multi-robot system are deeply studied, and according to the needs of contemporary society, the concept of combining these two hotspots is proposed. The main purpose of this paper is to simulate large-scale wireless sensor networks and study the interaction and communication mechanism between wireless sensor networks and multi-robot systems. Through the effective "communication" and collaboration of each part, the ultimate goal of the research is achieved. The wireless sensor network provides more environmental perception information for the multi-robot system to increase the perception field, and the multi-robot system performs information perception through the wireless sensor network.

For most parents, due to the pressure of life, they cannot give their children time to accompany and care for them. With the popularity of remote parent-child care products, this problem has been better alleviated. It is our responsibility to continuously improve the function and experience of this product, bring better emotional interaction for children and parents, and help children and parents live a happy life. This article focuses on this purpose. Taking emotional human-computer interaction design as an innovation point, further research on remote parent-child interaction design based on children's robots has been carried out, and relevant research results have been obtained.

Data Availability

No data were used to support this study.

Conflicts of Interest

The authors declare that they have no conflicts of interest.

References

[1] J. S. Sheu and Y. L. Huang, "Implementation of an interactive TV interface via gesture and handwritten numeral recognition," *Multimedia Tools and Applications*, vol. 75, no. 16, pp. 9685–9706, 2016.

[2] Y. Li and J. Andrade, "DEApp: an interactive web interface for differential expression analysis of next-generation sequence data [J]," *Source Code for Biology and Medicine*, vol. 12, no. 1, pp. 1–4, 2017.

[3] P. J. Wong, W. Zhang, G. van der Laan, and MP. de Jong, "Hybridization-induced charge rebalancing at the weakly interactive C60/Fe3O4(001) spinterface," *Organic Electronics*, vol. 29, no. February, pp. 39–43, 2016.

[4] D. Shin, D. Shin, and D. Shin, "Development of emotion recognition interface using complex EEG/ECG bio-signal for interactive contents," *Multimedia Tools and Applications*, vol. 76, no. 9, pp. 11449–11470, 2016.

[5] L. Peng, Z. Feng, P. Joli, and C. Renaud, "LiToTac: an interactive-interface software for finite element analysis of multiple contact dynamics," *Computer Modeling in Engineering and Sciences*, vol. 118, no. 1, pp. 111–137, 2019.

[6] R. L. H. Lao and A. K. Y. Wong, "Detecting hand gestures with wi-fi technology: applications for received-signal-strength

indicators in interactive interface design," *IEEE Consumer Electronics Magazine*, vol. 7, no. 2, pp. 73–82, 2018.

[7] J. Abich and D. J. Barber, "The impact of human-robot multimodal communication on mental workload, usability preference, and expectations of robot behavior," *Journal on Multimodal User Interfaces*, vol. 11, no. 2, pp. 211–225, 2017.

[8] M. Wang, "Research on key technologies in the design of subway station with hole pile method in complex environment[J]," *Chinese Journal of Railway Engineering*, vol. 34, no. 3, pp. 87–91, 2017.

[9] S. M. M. Rahman and R. Ikeura, "Cognitive-based control and optimization algorithms for optimizing human-computer interaction in the manipulation of powered assisted objects [J]," *Journal of Information and Engineering*, vol. 32, no. 5, pp. 1325–1344, 2016.

[10] J. Dong and J. S. Chae, "Etc. Research on human body protection method caused by induction effect in wireless power transmission environment [J]," *Journal of the Korean Society of Lighting and Electrical Installation Engineers*, vol. 31, no. 2, pp. 54–62, 2017.

[11] S. Stanley, "The robot companion you want to spend with [J]," *Popular Science*, vol. 288, no. 3, p. 43, 2016.

[12] F. Bertacchini, E. Bilotta, and P. Pantano, "Shopping with a robotic companion," *Computers in Human Behavior*, vol. 77, no. dec, pp. 382–395, 2017.

[13] J. Saunders, D. S. Syrdal, K. L. Koay, and K. BurkeDautenhahn, "Teach me-show me-end-user personalization of a smart home and companion robot," *IEEE Transactions on Human-Machine Systems*, vol. 46, no. 1, pp. 27–40, 2016.

[14] Y. H. Oh, J. Kim, and D. Y. Ju, "Investigating the preferences of older adults concerning the design elements of a companion robot," *Interaction Studies*, vol. 20, no. 3, pp. 426–454, 2019.

[15] R. A. Jones, "Concerning the apperception of robot-assisted childcare," *Philosophy & Technology*, vol. 32, no. 3, pp. 445–456, 2019.

[16] L. Ca Amero and M. Lewis, "Making new new AI friends: designing social robots for children with diabetes from the perspective of embodying AI [J]," *International Journal of Social Robotics*, vol. 8, no. 4, pp. 523–537, 2016.

[17] A. Ramachandran, C. M. Huang, and B. Scassellati, "Toward effective robot--child tutoring," *ACM Transactions on Interactive Intelligent Systems*, vol. 9, no. 1, pp. 1–23, 2019.

[18] S. E. McDonald, E. A. Collins, A. Maternick, and J. H. NicoteraGraham-BermannAscioneWilliams, "Intimate partner violence survivors' reports of their children's exposure to companion animal maltreatment: a qualitative study," *Journal of Interpersonal Violence*, vol. 34, no. 13, pp. 2627–2652, 2017.

[19] D. Isaac, "Robotic babies and teenage pregnancy [J]," *Journal of Paediatrics and Child Health*, vol. 53, no. 2, pp. 200-201, 2017.

[20] J. Fan, Y. Jiang, and T. Chai, "Operational feedback control of industrial processes in wireless network environment[J]," *Journal of Automation*, vol. 42, no. 8, pp. 1166–1174, 2016.

[21] W. Qian, F. Jia Lu, J. Yi, and J. Chen, "Data-driven dual-rate control of hybrid separation and enrichment process in wireless network environment [J]," *Journal of Zi Donghua/ Automata Sinica*, vol. 45, no. 6, pp. 1122–1135, 2019.

[22] X. Wang and X. Zhang, "Wireless network attack defense algorithm using deep neural network in internet of things environment," *International Journal of Wireless Information Networks*, vol. 26, no. 3, pp. 143–151, 2019.

[23] K. Gothami, "Security issues in IoT environment in wireless network communication [J]," *International Journal of Wireless Networks and Broadband Technologies*, vol. 8, no. 2, pp. 31–46, 2019.

[24] S. Sivamani, J. Choi, K. Bae, and K. Xiao, "Event security-based intelligent service model for greenhouse environment based on wireless sensor network [J]," *Concurrency and Computing*, vol. 30, no. 1, pp. 1–11, 2018.

[25] M. Subramanian and N. Jaisankar, "An optimal path selection in a clustered wireless sensor network environment with swarm intelligence-based data aggregation for air pollution monitoring system," *International Journal of Computer Aided Engineering and Technology*, vol. 10, no. 4, pp. 378–103, 2018.

[26] A. Ray and D. De, "Performance evaluation of tree based data aggregation for real time indoor environment monitoring using wireless sensor network," *Microsystem Technologies*, vol. 23, no. 9, pp. 4307–4318, 2017.

[27] W. Wang, L. Li, and W. Dan, "Research on living environment mapping of wireless sensor network based on low-cost ultrasonic sensor group [J]," *Journal of Sensors and Actuators*, vol. 30, no. 8, pp. 1258–1266, 2017.

[28] Z. G. Lin, F. R. Wang, Y. P. Liu, and C. X. AnZhang, "A multi-hop clustering fusion routing on water environment wireless sensor network," *International Journal of Control and Automation*, vol. 9, no. 7, pp. 79–92, 2016.

[29] H. J. Lee, K. H. Kim, and Y. H. Kim, "Wireless sensor network-based 3D home control system for smart home environment," *International Journal of Smart Home*, vol. 10, no. 1, pp. 159–168, 2016.

[30] H. Liu, S. Duan, and L. Ding, "Research on emotional design of interactive interface based on we-media field [J]," *Boletin Tecnico/Technical Bulletin*, vol. 55, no. 14, pp. 68–72, 2017.

Hindawi
Scientific Programming
Volume 2023, Article ID 9849732, 1 page
https://doi.org/10.1155/2023/9849732

Retraction

Retracted: BDA of the Dissemination of Opera in the Internet Self-Media Environment

Scientific Programming

Received 1 August 2023; Accepted 1 August 2023; Published 2 August 2023

This article has been retracted by Hindawi following an investigation undertaken by the publisher [1]. This investigation has uncovered evidence of one or more of the following indicators of systematic manipulation of the publication process:

(1) Discrepancies in scope
(2) Discrepancies in the description of the research reported
(3) Discrepancies between the availability of data and the research described
(4) Inappropriate citations
(5) Incoherent, meaningless and/or irrelevant content included in the article
(6) Peer-review manipulation

The presence of these indicators undermines our confidence in the integrity of the article's content and we cannot, therefore, vouch for its reliability. Please note that this notice is intended solely to alert readers that the content of this article is unreliable. We have not investigated whether authors were aware of or involved in the systematic manipulation of the publication process.

Wiley and Hindawi regrets that the usual quality checks did not identify these issues before publication and have since put additional measures in place to safeguard research integrity.

We wish to credit our own Research Integrity and Research Publishing teams and anonymous and named external researchers and research integrity experts for contributing to this investigation.

The corresponding author, as the representative of all authors, has been given the opportunity to register their agreement or disagreement to this retraction. We have kept a record of any response received.

References

[1] X. Xie, "BDA of the Dissemination of Opera in the Internet Self-Media Environment," *Scientific Programming*, vol. 2022, Article ID 3096890, 12 pages, 2022.

Hindawi
Scientific Programming
Volume 2022, Article ID 3096890, 12 pages
https://doi.org/10.1155/2022/3096890

Research Article

BDA of the Dissemination of Opera in the Internet Self-Media Environment

Xiaodi Xie

[1]*College of Music and Dance, Xuchang University, Xuchang 461000, Henan, China*

Correspondence should be addressed to Xiaodi Xie; 12014273@xcu.edu.cn

Received 22 July 2022; Revised 30 August 2022; Accepted 10 September 2022; Published 30 September 2022

Academic Editor: Juan Vicente Capella Hernandez

With the advent of the era of big data, the TV media industry has begun a new round of survival of the fittest. Some new and original traditional cultural TV programs have successfully attracted the attention of the audience, but some programs have lost the impact of the big data environment and are facing the crisis of revision or suspension. Based on the background of big data and from the macro perspective of society, this article made a specific description and objective analysis of the concept, characteristics, and real development of opera communication and proposed an understanding. On this basis, through the analysis of actual cases and data, combined with the dissemination of opera and the new and original traditional cultural TV programs in recent years, this article analyzed the impact of big data on the dissemination of opera and further explored the survival state of opera dissemination in the context of the era of big data, and the experiment was to crawl the data of 10 traditional Chinese opera categories in the Shipin Opera Network through web crawler. It was sorted according to the amount of play, the top 10 songs of each genre and their play volume were selected, and then the Internet correlation between the genres was quantified. And a big data analysis of the traditional opera program "Liyuanchun" was carried out. The experimental results showed that the show was broadcast 65,984 times a day, the highest broadcast volume in a week. At the same time, according to the big data analysis of users of self-media opera dissemination, the majority of the audiences had a high school or technical secondary school education, which accounted for 27%, followed by junior high school, which accounted for 18.7%. It can be seen that the current Chinese traditional culture TV programs have a good development trend and a lot of room for development.

1. Introduction

As a type of music, opera music has a very long history. With the development of society, many changes have taken place in the way of dissemination of opera music. In the early stage, the dissemination of opera mainly relied on the word of mouth of the artists. Later, with the continuous development of electronic technology, radio stations, records, and other media appeared, which made the opera music recorded and spread more widely. After the popularization of photography technology, the musical elements in opera film and television are more diversified, and a large number of new technologies have been applied to the dissemination of opera music. After the rise of the Internet, the dissemination of opera music through the Internet has greatly promoted the inheritance and development of opera music. In the context of the current continuous development of science and technology, this article analyzed the content and characteristics of the social dissemination of Chinese opera music in the Internet + era, and explored the advantages and disadvantages of its dissemination. It is necessary to discuss corresponding measures on this basis, so as to promote the spread and development of opera music in a wider range in the Internet + era. From a theoretical point of view, the dissemination of opera music based on the Internet can enrich the theoretical content of traditional opera music dissemination, extend the theoretical scope of traditional opera music research, and promote the in-depth study of opera music theory. From a practical point of view, by studying the dissemination of opera in the Internet self-

media environment, it can provide practical guidance for the development and exchange of opera music, and play a role in promoting the transformation and development of traditional opera music and the diverse exchange of opera music culture.

Mass media play an important role in health risks. Tang and Rundblad corpus-based study of media reports on personal health drew attention to natural science uncertainty and professional risk language surrounding pollutants [1]. Byrum discussed the use of information carriers to convey corporate social responsibility messages to promote eco-procurement participation. By changing the dissemination dimension of fictitious CSR campaigns sent by social media, the study found statistically significant differences in consumer-to-consumer communication in stimulating eco-buying engagement [2]. Social media becomes increasingly important in risk and crisis situations. Yoo et al. study found which types of social media have a greater impact on risk perception and behavior, thereby revealing the cognitive mechanism behind the process of risk information on social media shaping people's behavioral intentions, and whether it has different effects on people's risk perception and behavioral intention [3]. Rashid research found that social media allows for unrestricted social interaction and democratizes the media itself. We-media features many-to-many communication, including social spaces, where individuals can gather and discuss issues of common concern, helping to redefine their identities [4]. Digital media is becoming an integral part of social communication. Guan et al. studied and investigated cultural values affecting psychological and physiological responses to social support, and independent but not interdependent self-explanations moderated the associations between support environments and psychological or physiological measures [5]. There are also various problems in the dissemination of opera culture based on the Internet. In the process of in-depth integration of "Internet + opera," the solution of related problems will become a key factor affecting the development of traditional opera.

Lee investigated the potential link between strategic competencies in intercultural communication and perceptions of English variety. Structural equation modeling results suggested that English variant perception mediates between IDLE and intercultural communicative strategic competence, providing pedagogical insights into readiness for intercultural interaction in a multicultural setting [6]. Cloud computing and big data analysis are used to calculate and analyze the data, so as to get more design elements in line with the design elements. Wu and Li research found that the Internet of Things technology and cloud computing have obtained more information for many fields, thereby assisting the field to complete deeper analysis and research [7]. The increasing popularity of social networks has made social networks an important place for the dissemination of digital content, and also brought new business models. Huo et al. research found that the commercial application of social network needs to strike a balance between the different interests of these parts of the relevant parties, so Huo proposed a distributed logic that combines distributed temporal logic and activity rules [8]. Jennex reversed the pyramid by assuming that there is more knowledge than data, showed knowledge management as the extraction of the pyramid, and extended the revised knowledge pyramid to include IoT and big data applications in the promotion of opera we-media [9]. The growing gap between users and big data analytics becomes computationally inefficient. Ahmad proposed a system architecture using an artificial bee colony (ABC) to select features, and a Kalman filter was used in the Hadoop ecosystem to remove noise and improve processing efficiency [10]. Although as a traditional art form, while adhering to the essence of its own culture, traditional Chinese opera has completed the integration with different stages of media, thus promoting its own development [11]. In the process of continuous transformation of the media, traditional Chinese opera is also innovating in content and form to adapt to the changes in people's cultural needs in the new era.

2. BDA Method of Opera Dissemination in the Self-Media Environment

2.1. Big Data Technology. With the deepening of big data in all fields, people's understanding and definition of big data are also different. IDC defines data with large capacity, diversity, high speed, and high value 4 V as large capacity data, and IBM believes that the fourth "*V*" must have reliability [12]. The application areas of big data are shown in Figure 1.

As shown in Figure 1, with the development of the times and the advancement of data processing technology, the amount of data that people can collect and organize has gradually increased. And there are many kinds of data, that is, the representation type of data is no longer single and limited, but tends to be diversified. It is compared with the past, people take the limited data that can be obtained as a sample for analysis, but in the era of big data, people can collect many kinds of data, so that the data is endowed with a certain social meaning [13]. With the application of new media technology and the development of data processing technology, people's purchases and consumption, watching videos, browsing web pages, participating in topic discussions, and other behaviors in daily life will leave some data record information, which makes the growth and flow of data faster and faster, and it is inevitable to continuously improve the speed of data processing [14]. In the era of big data, although the amount of data that can be collected is very huge, it may contain unstructured data and non-schema data. As a result, there may be some invalid data in the obtained large amount of data, which requires careful sorting, classification, integration, and analysis of the data. In short, the value density of data is inversely proportional to the total amount of data.

2.2. BDA Methods. Big data is not only a huge amount of data, but also more important is the analysis and processing of a large amount of data, and the useful information contained in these large amounts of data can be obtained

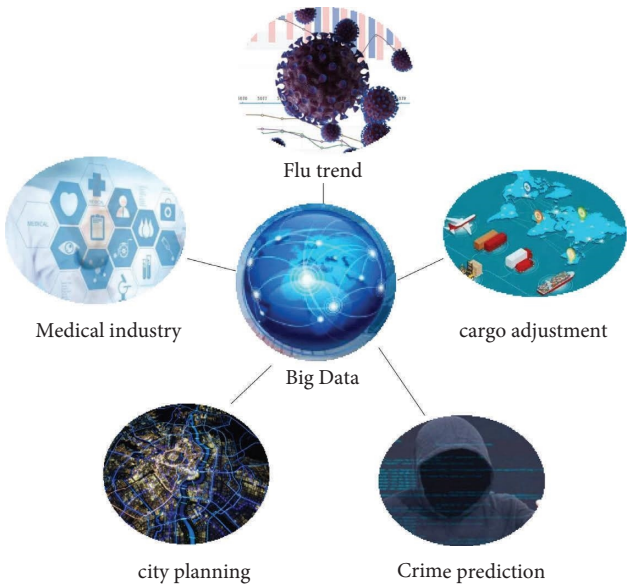

Figure 1: Application areas of big data.

after processing. Now, with the application of big data in the fields of social, economic, and technological research, the basic attributes of big data such as volume, speed, and diversity have been increased, so the method of big data analysis is particularly important [15]. When judging whether information is valuable, it is important that analytical methods are used appropriately. The method of big data analysis is shown in Figure 2, which generally has the following five basic aspects.

As shown in Figure 2, big data analysis mainly includes five aspects:

(1) Visual analysis: the most basic requirement of big data analysis is the visualization of analysis results. Whether it is a data analysis expert or a general user, through visualization, the data can be displayed intuitively and the information behind the data can be conveyed to people.

(2) Data mining: compared with visualization, data mining mainly takes computers as the object, and discovers the laws behind the data through centralized analysis or decentralized analysis of big data clusters, division, separation points, and detailed investigation of data structure patterns.

(3) Predictive analysis: one of the main goals of big data analytics is prediction. Through data mining, it is possible to fully understand the data and make predictive judgments based on the regular information behind the data. In this way, the overall economic efficiency of the enterprise will be improved.

(4) Semantic engine: big data technology is widely used on the Internet. The network platform predicts the potential consumption direction of customers through the keywords and tags of web pages retrieved by users, and sells the corresponding products according to the needs of customers, so as to achieve correct marketing.

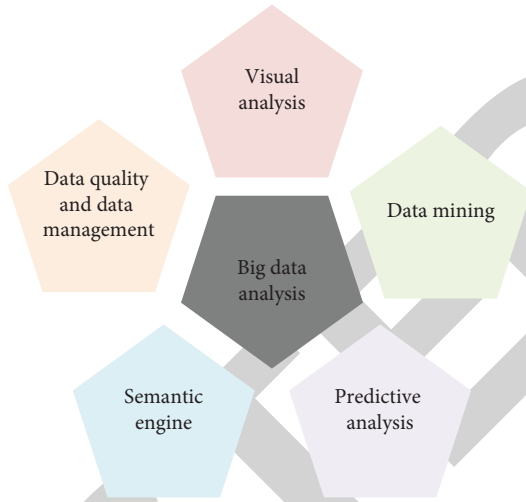

Figure 2: 5 aspects of big data analysis.

(5) Data quality and data management: the guarantee of the validity of big data analysis results comes from the quality of data sources and data management. Through high-quality data sources and efficient data classification management, the reliability and validity of analysis results can be guaranteed, whether in scientific research or other application fields.

2.3. Art of Opera and the Spread of Opera. Opera is an audiovisual art that integrates various artistic means such as dance, music, literature, acrobatics, and martial arts. The art of opera is a unique dynamic art form in China, with a long history, and the public does not have too many objections to its basic concept. The reason why this article listed it separately was to define the art of opera to be studied in this article. There are many categories and genres of opera art, but this article regarded opera art as a whole and did not distinguish between different categories of opera [16]. Although different types of opera art have different audiences, the purpose of this article was to expand the spread of opera by studying the mobile media commonly used by contemporary people, so as to optimize the reception environment of art recipients [17]. This article focused on analyzing the dissemination method and effect of mobile media on opera art, and then proposed an ideal dissemination method, so that contemporary young people can gradually recognize opera, understand opera, and love opera.

Art communication can be divided and explained from the aspects of content, medium, audience, effect, etc. This section mainly discussed the characteristics of art communication and distinguished other communication categories by the characteristics of art communication. Art has the characteristics of image, esthetics, and emotion. According to the existence mode, perception mode, materialized form, esthetic principles, and other conditions of artworks, art can be divided into different types. But in the final analysis, works of art express the emotions of the creators and embody the esthetic cognition and feelings of the creators and recipients, which determines the characteristics of art communication. Art communication needs to

materialize the creator's esthetics to the art recipient, appeal to the creator's emotion, and use different communication methods to arouse the resonance of the art recipient, so as to realize the esthetic cognitive function, educational function, and entertainment function of art. Therefore, art communication pays attention to the mutual transfer of emotion between art creators and recipients, which was also the basis of this thesis.

2.4. Necessity of Disseminating Opera Art on the Internet through the Media. "Internet + media" is an important path for media development in the era of media convergence, and mobile phones are an important medium for carrying "Internet + media." "Internet + media" is the only way for the transformation of traditional media, and it is also a future-oriented communication form. Based on the transformation of the role of contemporary audiences and the reconstruction of traditional communication logic, the media have been upgraded and transformed one after another. Mobile media has become a platform for major media competition. Therefore, the use of mobile media to spread opera art is an inevitable trend in the current media integration development. Only by adapting to the trend can the dissemination of opera art be targeted. The dual role of the media and the audience has enriched the media resources and expanded the boundaries of the media, forming a new form of integrating traditional media and modern media [18]. Multi-channel integration improves the extension of information, stimulates the market trend, changes the way of competition, and also determines the dissemination orientation of opera art. Media integration can make the old resource space extend longer and increase added value through repackaging, so as to reform a new commercial value chain, and also promote the spread of traditional culture.

Technology enables people to "visit" times and places that were inaccessible in the pre-technological era. The medium is always moving in the direction that people want to develop, and the ultimate goal of development is to build an ecological niche that benefits people. When people's senses are not satisfied, and people cannot obtain information through the dissemination of the pre-technological era, new media technologies must be constantly created to compensate for the deficiencies of the past. In this context, whether the art of opera can be inherited and developed depends not only on the self-improvement of the art form, but also on whether it is better in the same field as other art forms [19]. Only when the dissemination of opera is close to the humanized development trend of the media, it can expand the breadth of the dissemination of opera and gain space for development. Just as mobile media has the characteristics of interactivity and timeliness, it meets the needs of modern and contemporary social groups, and is the direction people hope for its development. It adapts to the current audience's entertainment and interactive needs, and meets the extension of the audience's senses. A variety of communication methods make it easier for the audience to understand the art of opera, so that the dissemination of the art of opera is more extensive and three-dimensional.

2.5. Data Mining Algorithms. Data mining refers to the analysis and arrangement of big data to extract the mathematical relationship between the data and the variables implicit in the massive data. With the advent of the era of big data, the amount of information has increased exponentially, which makes the real relationship between massive data ambiguous and difficult to use directly, and traditional data processing methods have also failed [20]. The whole process of knowledge discovery in data is shown in Figure 3.

As shown in Figure 3, using data mining technology, by analyzing the data, it is possible to generate x rules at the same time, and x is shown in

$$X = \sum_{m=1}^{d-1}\left[\left(\frac{d}{m}\right) * \sum_{n=1}^{d-m}\left(\frac{d-m}{m}\right)\right] = 3^d - 2^{d+1} + 1. \quad (1)$$

2.5.1. Auto-Regressive Moving Average (ARMA) Model. If the time series is stationary, normal, and zero mean, the auto-regressive moving average model ARMA (n, m) can be obtained as shown in

$$f_t = \sum_{m=1}^{j}\gamma_m f_{t-1} - \sum_{n=1}^{i}\lambda_m \omega_{t-m} + \omega_t. \quad (2)$$

Among them,

$$\omega_t \sim \mathrm{NID}\left(0, \delta_\omega^2\right). \quad (3)$$

2.5.2. Auto-Regressive (AR) Model. The auto-regressive model AR (n) is a special case of the ARMA (n, m) model. In the expression of the ARMA (n, m) model, the AR (n) model is shown in

$$f_t = \sum_{m=1}^{j}\gamma_m f_{t-1} + \omega_t. \quad (4)$$

2.5.3. Moving Regression (MA) Model. The moving regression model MA (m) is another special case of the ARMA (n, m) model. In the expression of the ARMA (n, m) model, the MA (m) model is shown in

$$f_t = \omega_t - \sum_{m=1}^{j}\phi_n f_{t-n}. \quad (5)$$

Since there is no auto-regressive part in the model, it is called the m-order moving average model, denoted as MA (m). The mining of the dissemination power of self-media operas is to mine and analyze the correlation of related information such as the number of readings and the number of likes in the release of operas in the self-media [21]. The data mining process is shown in Figure 4.

As shown in Figure 4, the formal description of the problem of mining the dissemination power of self-media operas is to view each release time as a transaction d_i, d_i records the obtained reading information, and all d_i form a transaction set D.

$$D = \left\{d_1, d_2, \ldots, d_i, \ldots, d_j\right\}. \quad (6)$$

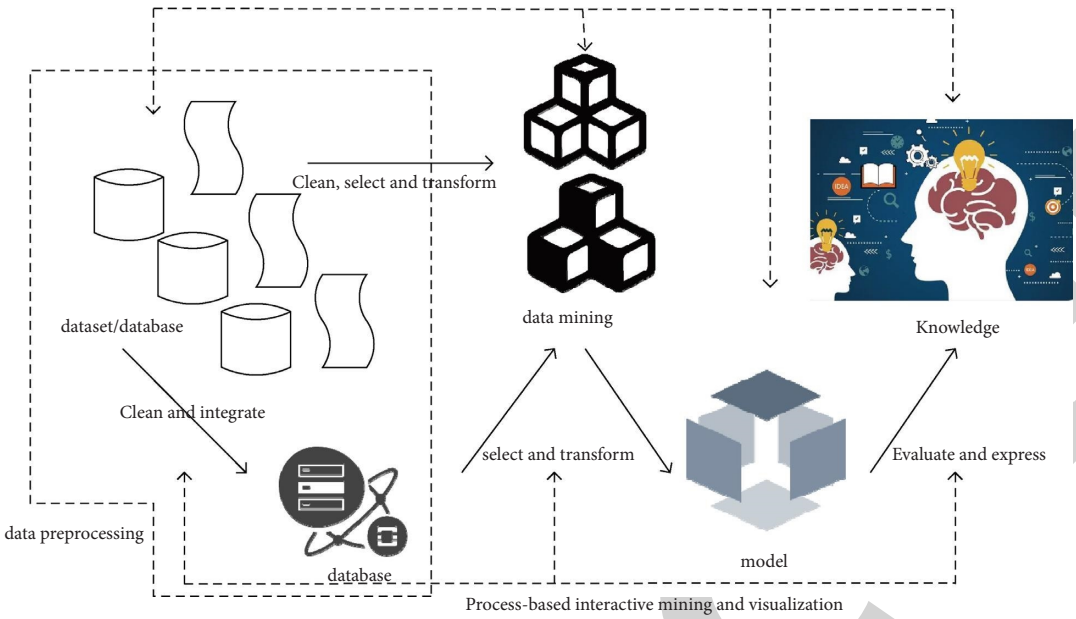

Figure 3: The whole process of knowledge discovery in data.

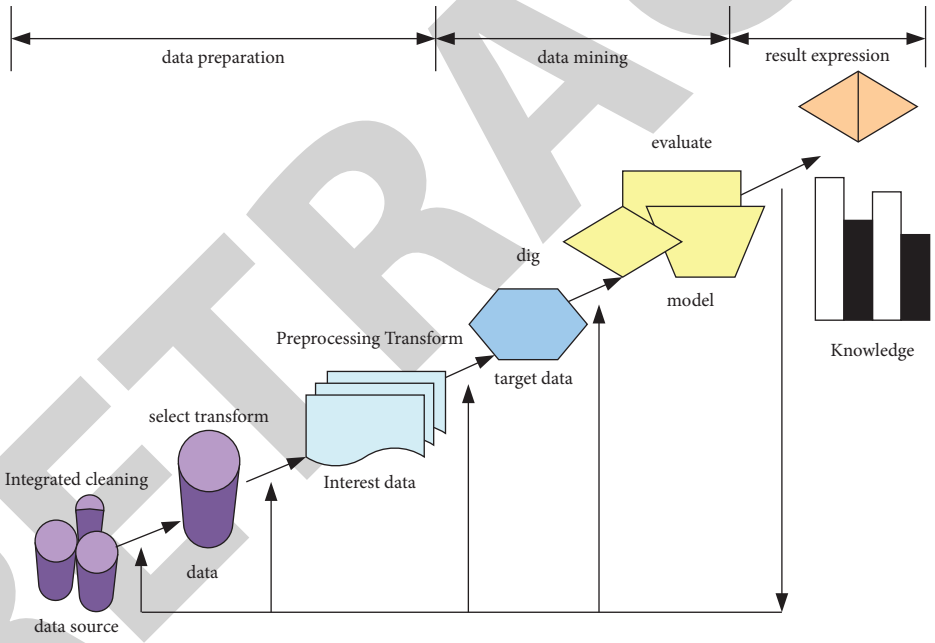

Figure 4: Data mining process.

Each reading source is regarded as an item and denoted as i_m, and all readings constitute an item set I as shown in formula (7). Each transaction d_i is a subset of I.

$$I = \{i_1, i_2, \ldots, i_j, \ldots, i_i\}. \tag{7}$$

The proportion of reading records containing the hazard source in i_1 is included in all reading investigation records, and the support degree is calculated as shown in

$$\text{support}(i_1) = \frac{\|d \in D \| I_1 \in D\|}{\|I_1 \in D\|}. \tag{8}$$

In formula (8), $\|D\|$ represents the total number of readings, and $\|d \in D \| I_1 \in D\|$ represents the number of readings in the reading dataset including the I reading set. When support (i_1) is greater than the given min_supp value, then i_1 is called frequent item-sets.

It is assumed that when reading set I_1 appears, reading set I_2 can be deduced with a certain probability:

$$\text{confidence}(I_1 \longrightarrow I_2) = \frac{\text{support}(I_1 \cup I_2)}{\text{support}(I_1)}, \quad \% \tag{9}$$

$$\text{lift}(I_1 \longrightarrow I_2) = \frac{\text{support}(I_1 \cup I_2)}{\text{support}(I_1) * \text{support}(I_2)}.$$

If the lift degree is greater than 1, it is an effective strong association rule, which is the most valuable object for analysis. If the rule lifting degree is equal to 1, the former and latter terms are independent of each other, and there is no correlation. If the rule promotion degree is less than 1, the association rule has no practical significance.

2.5.4. Support Vector Machine. Support vector machine (SVM) is a supervised learning algorithm. Linear classification and SVM classification are shown in Figure 5.

As shown in Figure 5, the points on the space are divided into two categories in the n-dimensional space, and it is hoped to find a hyperplane to divide the two types of points. Such as (a) is a two-dimensional space, which is an example of linear classification. The point on the green line in (b) is called the support vector. The transformation of data features from low-dimensional space to high-dimensional space is shown in Figure 6.

As shown in Figure 6, the relationship between data features in a low-dimensional space may be more complicated, but the relationship between data features in a transformed high-dimensional space may become clearer.

When the data is mapped to a high-latitude space, the data dimension may be too large, resulting in a significant increase in computational complexity. The advantage of the kernel function is that it transforms the data from low latitudes to high latitudes, while avoiding calculations at high latitudes. The kernel function is calculated at low latitudes, and the method of expressing the calculation effect at high latitudes greatly reduces the amount of calculation [22].

In general, the mathematical form of the linear classification surface of SVM is

$$G(D) = w * D = 0. \tag{10}$$

The vector w is the weight coefficient and b is the threshold set by the SVM. Then let the training data satisfy $|g(D)| = 1$ to normalize, which is

$$\overset{i}{y}[(w * D_i) + b] - 1 \geq 0, i = 1, 2..., N. \tag{11}$$

Among them, D_i is the sample used for SVM training, y_i is the category corresponding to the sample, and the classification interval of the sample is $2/||w||$, the purpose is to minimize the classification interval and definition:

$$L(w, b, a) = \frac{1}{2}(w * w) - \sum_{i=1}^{n} a_i\{[w * D_i) + b] - 1\}. \tag{12}$$

Finding the partial derivatives of w and b, and setting the partial derivatives to 0 is equivalent to finding the maximum value of $Q(a)$ with respect to a_i under $\sum_{i=1}^{n} y_i a_i = 0$:

$$Q(a) = \sum\nolimits_{i=1}^{n} a_i - \frac{1}{2}\sum_{i,j=1}^{n} a_i a_j a_i a_j (D_i, D_i). \tag{13}$$

If a_i^* is the best solution, consider

$$w^* = \sum_{i=1}^{n} a_i^* \times y_i D. \tag{14}$$

Bring in the classification function:

$$\% \ f(D) = sign\{(w^* D) + b^*\} = sign\left\{\sum_{i=1}^{n} a_i^* y_i (D_i D) + b^*\right\}. \tag{15}$$

Calculate the classification, if $f(D) = 1$, D is classified into this class, otherwise, it is classified into another class.

Manhattan distance (denoted as Ma), Euclidean distance (denoted as Eu), and Chebyshev distance (denoted as Ch) are all classical paradigm distances, and they are defined as

$$\mathrm{Ma}\left(\gamma_x, \gamma_y\right) = \sum\nolimits_{i=1}^{4^j} \left|\gamma_{x,A}, \gamma_{y,B}\right|, \tag{16}$$

$$\mathrm{Eu}\left(\gamma_x, \gamma_y\right) = \left(\sum\nolimits_{i=1}^{4^j} \left|\gamma_{x,A}, \gamma_{y,B}\right|^2\right)^{1/2}, \tag{17}$$

$$\mathrm{Ch}(\gamma_x, \gamma_y = \max|\gamma_{x,A} - \gamma_{y,\mathrm{A}}|, 1 \leq A \leq 4^n. \tag{18}$$

The frequency of occurrence of a k-tuple item is defined as the quotient obtained by dividing the number of occurrences of the k-tuple item by the sum of the occurrences of all k-tuple in the sample, which is the relative statistical value after simple normalization. Sample A is taken as an example, the frequency of occurrence of the x-th k-tuple item in the sample is calculated as

$$\gamma_{\mathrm{A,x}} = \frac{Z_{A,x}}{k_A}. \tag{19}$$

Therefore, in formula (16), formula (17), and formula (18) that define the distances of the three paradigms, γ_A and γ_B are frequency vectors composed of $\gamma_{A,x}$ and $\gamma_{B,x}$, which are defined as

$$\begin{aligned} \gamma_{\mathrm{A}} &= \frac{Z_A}{k_A}, \\ \gamma_{\mathrm{B}} &= \frac{Z_B}{k_B}. \end{aligned} \tag{20}$$

3. BDA of Opera Dissemination in the Self-Media Environment

"Pear Garden Spring" is mainly based on Henan Opera, and at the same time brings together various types of operas. In the form of the opera fans' arena, the traditional opera culture is well displayed in front of the world, and it has become a brand column of Henan TV. Through the program of "Liyuanchun," it can be found that in the process of development, "Liyuanchun" still adheres to the responsibility of inheriting the opera culture, and constantly changes and updates the original program form. It can be said that "Liyuanchun" has achieved remarkable achievements since

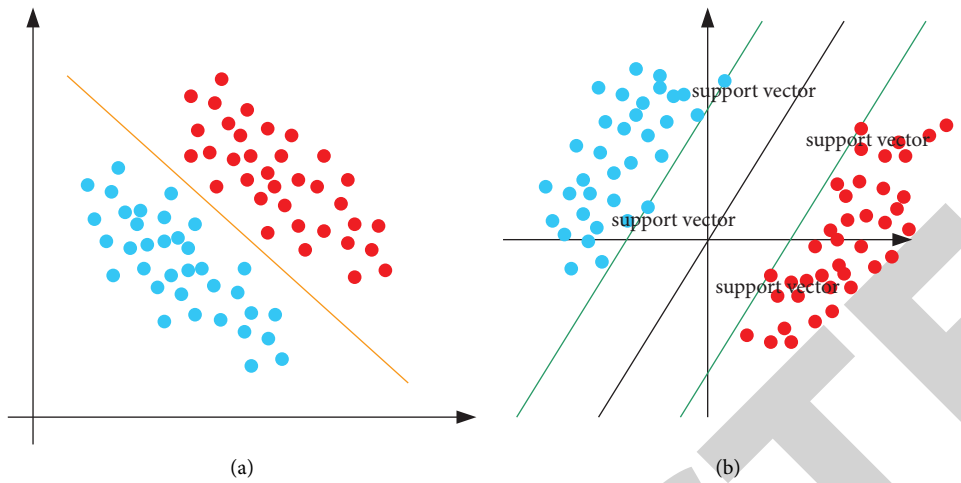

Figure 5: Linear classification (a) and support vector machine classification (b).

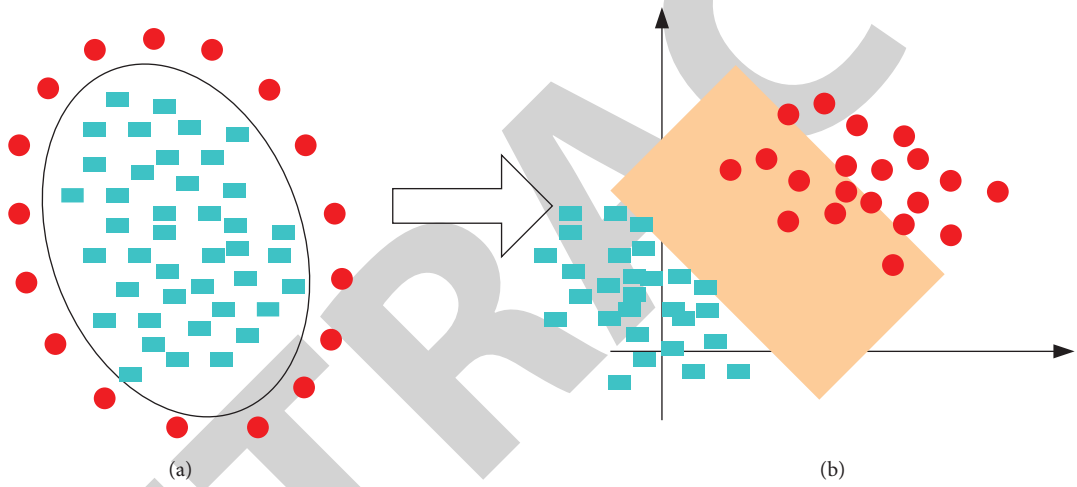

Figure 6: Data features are transformed from low-dimensional space (a) to high-dimensional space (b).

its inception. It not only gained a fixed audience, became famous in Europe, and won many awards, but also successfully carried forward the Chinese opera culture.

3.1. Traditional Chinese Opera Integrates Big Data Technology. After the arrival of the era of big data, various fields actively apply big data to the development of the industry, and the application of big data technology is becoming more and more mature. People in the TV media have gradually realized that the audience rating is no longer the only criterion for evaluating the quality of a TV program, and the use of social media platforms also plays an important role in TV programs. Especially with the rise of Weibo and WeChat platforms, the frequent use of computers, mobile phones, and other terminals has generated a large amount of data [23]. In addition to the audience ratings, data such as click-through rate and reading volume of related news and topics have important reference value for evaluating a program. According to Tencent Video's video playback index, "Liyuanchun" has been clicked and played 3.757 million times on Tencent Video, reaching the highest viewership rating for the program in the past month. If one thinks about it carefully, there are traces of big data in the production and broadcasting of "Liyuanchun," which fully reflects the power of big data. Judging from the attention and ratings of this program, the "Liyuanchun" column has indeed gained a higher rating and attention for itself with the help of the power of big data.

In addition, this article queried the Weibo TV Index, and "Liyuanchun" ranked 12th in the Weibo TV Index Daily Ranking on January 31, 2016. Among them, the number of readers was 68,000, the number of readings was 170,000, the number of mentions was 331, and the number of mentions was 383. Ranked 72nd in the Weibo TV Index Weekly Ranking from January 25 to 31, 2016. Among them, the number of readers was 235,000, the number of readings was 449,000, the number of mentions was 491, and the number of mentions was 607.

3.2. BDA after the Broadcast of "Liyuanchun". On January 31, 2016, after the live broadcast of the year-end finals of the 2015 Chinese Drama Fan Contest in "Liyuanchun" and

"Boom in China," people's attention to "Liyuanchun" and the 2016-01-30 program did not stop. The release of relevant news from major media, the frequent appearance of online news, and the release of related articles on new media platforms such as Weibo hot topics and WeChat official accounts have prompted people to think of watching programs again through online videos.

This article collected the playback volume of "Liyuanchun" on iQiyi Video and Tencent Video from January 29, 2016 to February 4, 2016, in order to analyze the changes in the broadcast situation and broadcast data of "Liyuanchun" in the online video in the 1 week before and after the broadcast of the 2016-01-31 program. Figure 7 shows the video playback of "Liyuanchun" on Tencent and iQiyi.

As can be seen in Figure 7, from January 29 to February 4, 2016, the playback volume of "Liyuanchun" on the iQiyi video platform changed greatly. Among them, the broadcast volume on January 29, 2016 and January 30, 2016 was the lowest in a week, both 44,064 times; the broadcast volume on January 31 was 60,288 times, showing a significant increase compared with the previous 2 days; February 1 was the most played day of the week with 847,225 views, followed by February 2 with 338,087 views. Although the broadcast volume on February 3 and February 4 had a downward trend compared to February 1 and February 2, it still exceeded the broadcast volume from January 29 to January 31. Obviously, from January 29 to February 4, 2016, the playback volume of "Liyuanchun" on Tencent's video platform did not change much. Among them, the playback volume on February 1, 2016 was 65,984, which was the highest playback volume in a week; the second was on February 2, and the playback volume was 53,803; January 31 had 47,117 plays, a slight increase from January 29 and January 30; the playback volume on February 3 and February 4 was roughly the same as the playback volume on January 29 and January 30, with data between 30,000 and 40,000.

By comparing the playback of "Liyuanchun" on iQiyi Video and Tencent Video from January 29 to February 4, 2016, it can be seen that there are some obvious commonalities in Figure 7, which are as: the number of views on February 1, 2016, whether it is iQiyi Video or Tencent Video, is the most viewed day in a week; the playback volume on February 2 was also lower than that on February 1, but higher than the other 5 days; compared with January 29 and January 30, the number of broadcasts on January 31 has a slight upward trend. And it can be seen from Figure 7 that since January 31, 2016, the playback volume of "Liyuanchun" had shown an upward trend on the whole, which showed that people's attention to "Liyuanchun" was gradually increasing, and it had a certain connection with big data.

As we all know, if you want to study a TV program well, in addition to studying the TV program itself, it is not enough to study the audience. Because the audience plays an important role in the TV program, and to some extent determines whether the program can survive or not. Therefore, it is obviously not enough to only analyze the various data of the "Liyuanchun" column above. In order to comprehensively and deeply analyze and explore the survival status of traditional cultural TV programs in the context of big data, this part also analyzed the audience behavior data of "Liyuanchun" in detail.

3.3. We-Media Opera User Behavior Data. This article counted and sorted out the user behavior data related to "Liyuanchun" on the iQiyi video network platform. Most of the viewers have a high school or technical secondary school education, accounting for 27%, followed by junior high school, accounting for 18.7%. It can be seen from the above data that the audience of "Liyuanchun" tends to be younger, and most of these audiences are male. Most of the viewers of the "Liyuanchun" column have lower education. People with junior high school and high school education prefer to watch "Liyuanchun," while those with higher education are not very keen on watching "Liyuanchun"; and compared with PC terminals, viewers prefer to watch programs through mobile Internet terminals. Figure 8 shows the age distribution and educational level distribution of opera audiences on the iQiyi video platform.

Then, the user behavior data related to "Liyuanchun" on the Sina Weibo platform from January 28, 2016 to February 3, 2016 was counted. The popularity of Weibo and the geographical distribution of users are shown in Figure 9.

As shown in Figure 9, on the whole, the popularity index of "Liyuanchun" on the Sina Weibo platform on the mobile terminal was generally higher than that on the PC terminal. And whether it is on the mobile terminal or the PC terminal, compared with other days, January 31, February 1, and February 2 were the three days when "Liyuanchun" was highly discussed on Sina Weibo. In the mobile index, the index on February 1, 2016 was 2405, the highest in this time period, while in the PC index, the index on February 2, 2016 was the highest, at 467. The data showed that people are keen to pay attention to "Liyuanchun" and understand the program dynamics through mobile Internet terminals, as well as participate in related topic discussions.

In addition, this article also queried the geographical distribution of Sina Weibo users related to "Liyuanchun." Among them, Henan Province has the highest degree of user participation in discussions, accounting for 75.81%, followed by Liaoning Province, accounting for 4.84%, and Zhejiang Province (3.23%). Hubei Province and Shandong Province have the same proportion, both 1.61%. From this, it can be seen that among the participants in discussions on topics related to "Liyuanchun" on the Sina Weibo platform, Henan Province has the most users, which is inseparable from the origin of "Liyuanchun" in Henan Province.

To sum up, by analyzing the data about user behavior, it is possible to better understand the habits and preferences of the audience. For example, when people watch a program in an online video, by analyzing the data, they can clearly understand which online video platform the audience likes to watch the program on, which part of the program skips over and does not watch, where there are traces of playback, what is the ratio of male to female viewers watching the program, the geographical distribution of the audience's location, the hierarchical information of the audience's age, etc. These user data are of great

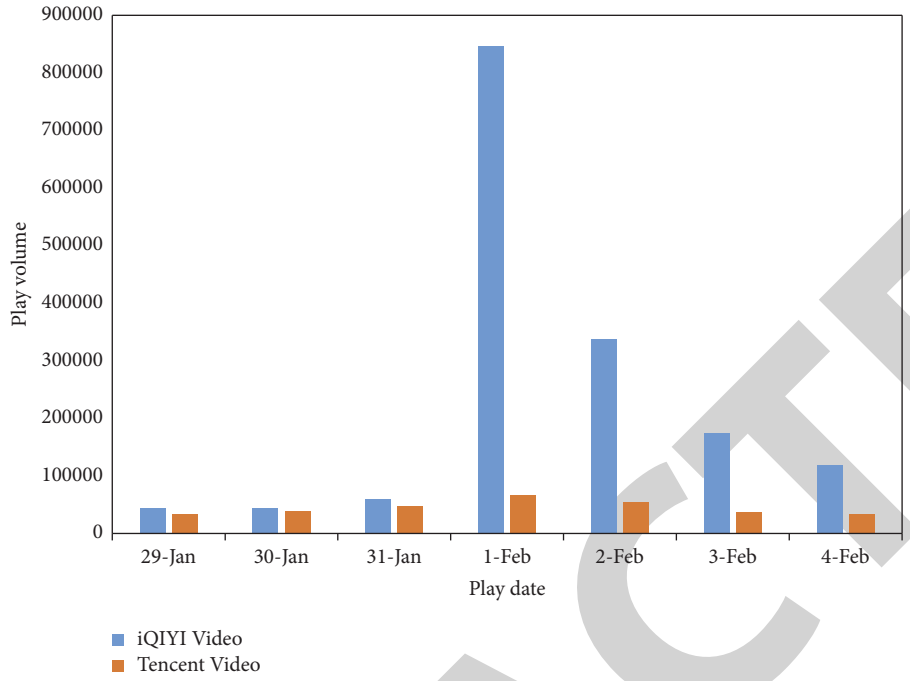

Figure 7: "Liyuanchun" video playback on Tencent and iQiyi.

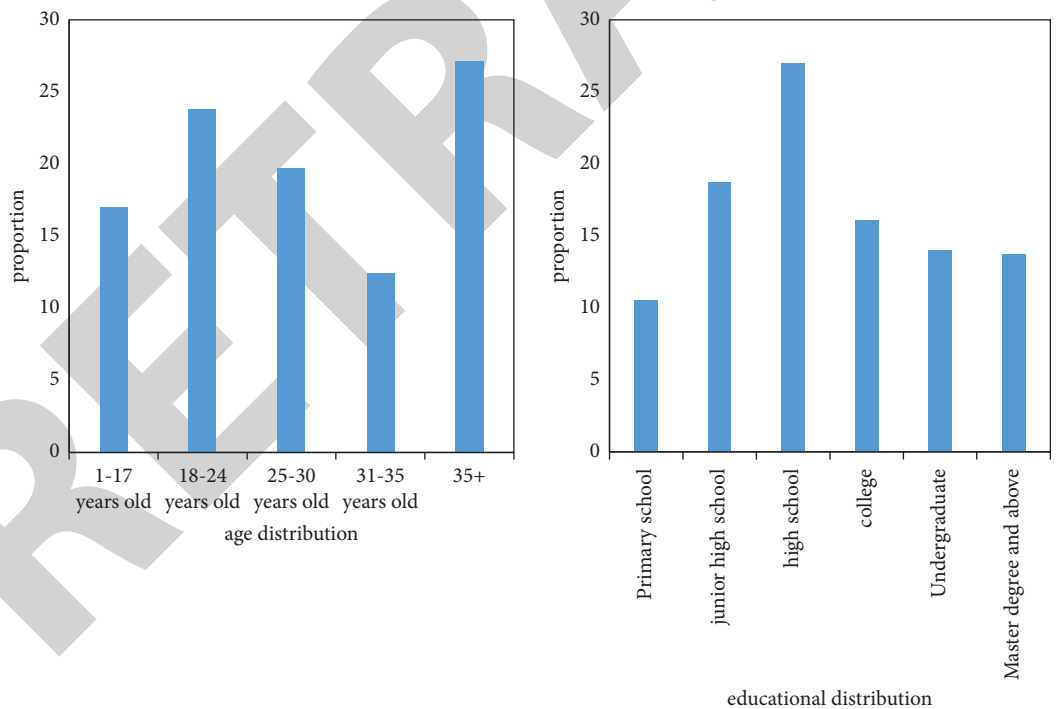

Figure 8: Age distribution and educational background distribution of opera audiences on iQiyi's video platform.

reference value to the program group. They are not only one of the reference standards for evaluating the quality of this program or the quality of production, but also provide some direction for the program group to produce programs in the future. Specifically, the column group can collect and organize user data generated by various platforms. By analyzing and integrating data, we can study the daily interests and hobbies of users and audiences, so as to produce programs according to the audience's preferences. This not only helps to improve and perfect the production of the program, but also helps to promote the long-term development of the program.

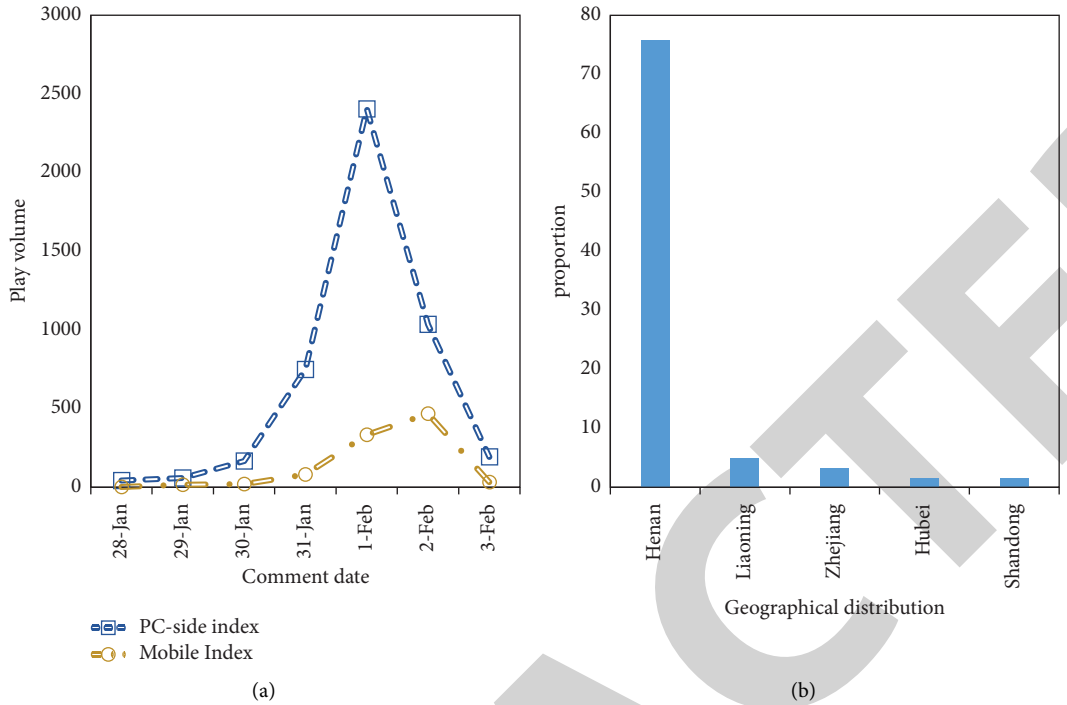

Figure 9: Weibo popularity (a) and geographical distribution of users (b).

Table 1: Overall network correlation matrix of 10 opera categories.

	Peking opera	Henan opera	Yue opera	Qin opera	Pingju	Opera	Lu opera	Kunqu opera	Overtone
Peking opera	10	10	8	10	7	3	1	2	3
Henan opera	4	10	3	5	5	5	3	0	3
Yue opera	5	6	10	6	5	6	4	3	3
Yellow plum	4	7	7	1	5	4	3	0	0
Qin opera	7	8	3	10	4	4	2	1	5
Pingju	4	6	4	6	10	4	2	1	0
Opera	1	8	1	3	2	10	6	0	0
Lu opera	2	6	3	3	6	5	10	0	0
Kunqu opera	10	4	8	4	3	3	0	10	0
Overtone	6	7	4	2	0	5	0	0	10

3.4. Correlation between Operas and the Popularity of Communication. First, web crawlers were used to crawl the data of 10 traditional Chinese opera categories in Shipinxiqu.com. Next, it was sorted according to the amount of play, and the top 10 tracks of each genre and their play amount were selected. Then, the Internet correlation between the koji types was quantified. Finally, the Internet correlation between songs and the popularity of Internet communication was fitted. Table 1 shows the overall network correlation matrix of 10 opera categories.

If song A and song B have audio or video transmission of song A on the Internet at the same time, it is considered that for song A, song A and song B have some kind of Internet relevance, and the degree of association is set to 1, otherwise, it is 0. As shown in Table 1, the overall correlation degree was obtained by accumulating the correlation degrees of the top 10 tracks of each genre. The Internet popularity of songs was measured by the cumulative relative on-demand volume of the top 10 songs. Figure 10 shows the relationship between the total number of songs, the weighted correlation degree, and the playing popularity.

As shown in Figure 10, the positive correlation between the degree of association and the degree of spread was strengthened after considering the weight of the playback volume. In general, the higher the degree of correlation with other koji, the higher the spread of koji also tends to be. Sichuan Opera and Qin Opera were taken as examples, the top 10 pieces of Qin Opera had a much more complex network of associations than Sichuan Opera, and the average popularity of the former on opera websites was also much higher than that of the latter.

3.5. BDA of Opera Performance on Popular Music Platforms. Through the Internet popular music platform NetEase Cloud Music, data mining was carried out on the most

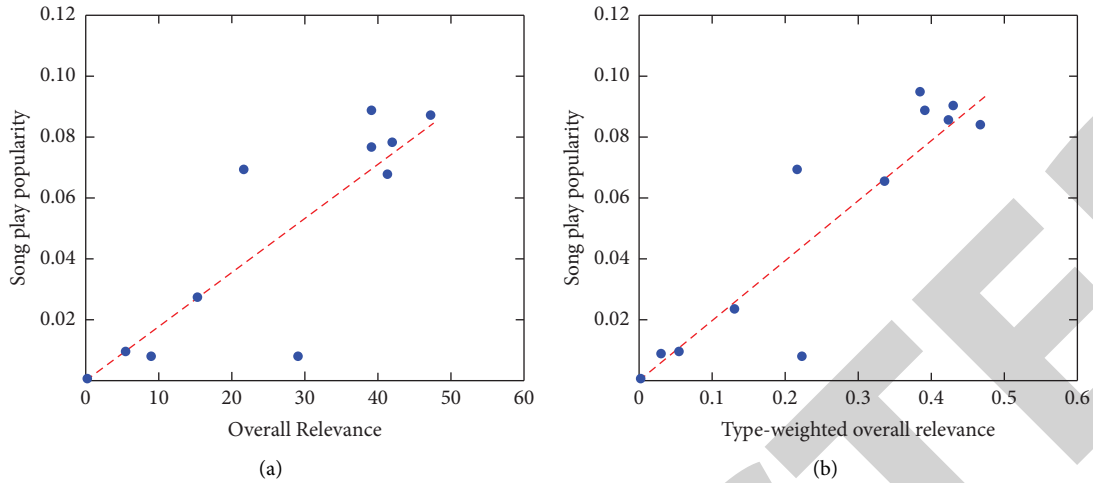

Figure 10: The overall music genre and the relationship between weighted relevance and playback popularity.

Table 2: NetEase cloud music's five opera categories and pop music chart statistics.

Koji	Number of tracks	Highest number of comments	Average number of comments
Peking opera	197	3673	235
Henan opera	73	1018	151
Yue opera	198	2469	64
Sichuan opera	9	87	42
Qin opera	116	48257	1758
NetEase cloud top songs chart	200	395969	90157

influential opera genres in China—Peking Opera, Henan Opera, Yue Opera, and the most representative genres in western China—Sichuan Opera and Qin Opera. First, the five selected opera genres and the NetEase Cloud Music pop song list were retrieved, and then irrelevant information was filtered out. Table 2 shows the five opera categories of NetEase Cloud Music and the statistics of popular music charts.

As shown in Table 2, it can be seen that the five major opera categories had a huge gap in the popularity of reviews compared to popular pop music. At the same time, the data also showed that Qin Opera had a significant advantage over the other four traditional operas in terms of comment popularity. Among the popular songs with more than 4,000 comments, there were 194 songs on the pop song chart, 13 songs in the Qin Opera category, and none of the other four opera categories had more than 4,000 comments.

4. Conclusions

With the continuous development and progress of Internet technology, network communication will inevitably become an important way for the dissemination of opera music in the Internet + era. Compared with other media, the audience media of the Internet is relatively more. Therefore, the dissemination of opera music through the Internet will inevitably increase the audience of opera music, which is undoubtedly a good news for the dissemination of opera music. In an information age, the development and dissemination of opera music need to seize the opportunity of this era and combine the development of opera music with the Internet + era. Opera music is the cultural crystallization of the Chinese nation's thousands of years of history. In the process of historical development, the content and form of opera music have undergone great changes, and its transmission method has also gotten rid of the traditional way of word of mouth. Entering the Internet + era, the social dissemination of opera music breaks the time and space limitations of traditional dissemination methods. With the increasingly younger Internet groups, the audience of opera is also becoming younger, which is of great significance to the widespread dissemination and vigorous promotion of opera culture. There is a major deviation in the current government's policy on the inheritance and development of opera. From the national to local research, decision-making and even policy level, the relationship between the inheritance of opera culture and the information society ecology has not been fully recognized, and all policies are still limited to the protection and support of opera and are weaker than inheritance and development.

Data Availability

This article does not cover data research. No data were used to support this study.

Conflicts of Interest

The author declares no conflicts of interest.

Hindawi
Scientific Programming
Volume 2023, Article ID 9821785, 1 page
https://doi.org/10.1155/2023/9821785

Retraction

Retracted: Research on the Flow Control of a Piston Cooling Nozzle

Scientific Programming

Received 1 August 2023; Accepted 1 August 2023; Published 2 August 2023

This article has been retracted by Hindawi following an investigation undertaken by the publisher [1]. This investigation has uncovered evidence of one or more of the following indicators of systematic manipulation of the publication process:

(1) Discrepancies in scope
(2) Discrepancies in the description of the research reported
(3) Discrepancies between the availability of data and the research described
(4) Inappropriate citations
(5) Incoherent, meaningless and/or irrelevant content included in the article
(6) Peer-review manipulation

The presence of these indicators undermines our confidence in the integrity of the article's content and we cannot, therefore, vouch for its reliability. Please note that this notice is intended solely to alert readers that the content of this article is unreliable. We have not investigated whether authors were aware of or involved in the systematic manipulation of the publication process.

Wiley and Hindawi regrets that the usual quality checks did not identify these issues before publication and have since put additional measures in place to safeguard research integrity.

We wish to credit our own Research Integrity and Research Publishing teams and anonymous and named external researchers and research integrity experts for contributing to this investigation.

The corresponding author, as the representative of all authors, has been given the opportunity to register their agreement or disagreement to this retraction. We have kept a record of any response received.

References

[1] X. Zeng, J. Zhang, L. Li, G. Hu, and W. Xie, "Research on the Flow Control of a Piston Cooling Nozzle," *Scientific Programming*, vol. 2022, Article ID 9283300, 9 pages, 2022.

Hindawi
Scientific Programming
Volume 2022, Article ID 9283300, 9 pages
https://doi.org/10.1155/2022/9283300

Research Article

Research on the Flow Control of a Piston Cooling Nozzle

Xianren Zeng,[1,2,3] **Jiahui Zhang**,[1] **Linmei Li**,[4] **Guangyan Hu**,[1] **and Weiming Xie**[1]

[1]*School of Machinery and Intelligent Manufacturing, Jiujiang University, Jiujiang, Jiangxi 332005, China*
[2]*Jiujiang Huirui Machinery Co., Ltd., Jiujiang 332000, Jiangxi, China*
[3]*School of Artificial Intelligence, Hezhou University, Guangxi 542899, China*
[4]*School of Architectural Engineering and Planning, Jiujiang University, Jiujiang, Jiangxi 332005, China*

Correspondence should be addressed to Xianren Zeng; 81180001@smail.xtu.edu.cn

Received 4 August 2022; Revised 27 August 2022; Accepted 16 September 2022; Published 29 September 2022

Academic Editor: Juan Vicente Capella Hernandez

The flow rate of a piston cooling nozzle is usually adjusted by changing the parameters of convergent length and inner diameter of the nozzle in engineering. However, the influence law and quantitative relationship between the flow rate and them are not clear. In this paper, the structural model and three-dimensional model of internal flow field of piston cooling nozzle are established by analyzing the structural characteristics and actual working conditions of piston cooling nozzles. Based on Fluent software, the flow field of piston cooling nozzles is simulated and analyzed. The distribution of velocity and pressure inside the piston cooling nozzle are obtained. The flow rate of fluid field is also obtained inside a piston cooling nozzle. In addition, the variation law of flow rate of the piston cooling nozzle is studied with the increasing of nozzle convergent length and diameter through several simulation experiments, respectively. The results show that the flow rate of piston cooling nozzle decreases linearly with the increase of the nozzle closing length. The flow rate of nozzle increases nonlinearly with the increase of the convergent diameter. Compared with the convergent length, the change of convergent diameter has a greater influence on the flow rate of piston cooling nozzles. Finally, the analytical expression of the flow rate of piston cooling nozzle about the convergent diameter is obtained, which is of great value and guiding significance to the nozzle engineering design.

1. Introduction

With the development of technology of internal combustion engine, especially after the introduction of supercharging technology, the output power of the engine is further increased and the thermal load of the piston is also increasing, so the cooling of the piston has become an important research hotspot [1]. When the engine works, the piston reciprocates within the cold oil chamber at high speed along the axial direction of the cylinder. Therefore, great heat is produced by the friction between the piston and cylinder and the head temperature of the piston is very high. In order to ensure the working performance of the piston, it is necessary to cool the piston head [2]. If the cooling nozzle cannot work normally, it will cause the working temperature of the piston to rise sharply, causing cylinder pulling and the whole engine to be scrapped [3]. Therefore, it is extremely critical to cool the piston head. The following cooling methods are as follows: free nozzle cooling, oscillation cooling, and forced oscillation cooling of internal cooling oil channel [4].

In the traditional design, only one cooling nozzle is usually provided for the piston and the injection direction of cooling oil is fixed regardless of the working condition of the engine. In recent years, scholars have also done a lot of research work [5] on the effect of cooling and heat release of the nozzles. A series of results are also achieved. Nasif et al. used the finite volume method to calculate the convective heat transfer of impinging jet during piston cooling by a numerical method. The results show that the cooling jet can significantly reduce the temperature of the piston [6]. Agarwal et al. studied the heat conduction from the piston cooling nozzle to the piston and numerically simulated it and predicted the coefficient of heat release under the piston. The cooling effect [7] on piston was studied with variety of injection speed of cooling-oil, nozzle diameter, and the

distance from nozzle to piston. In addition, some scholars have also conducted experimental research on the cooling effect of piston cooling nozzle. Easter and Liu et al. conducted experimental research on the cooling performance of piston cooling nozzle and established the average heat transfer correlation of suitable area, namely, the Nusselt number. The results show that the Nusselt number is strongly correlated with nozzle diameter and injection viscosity but weakly correlated with the distance from nozzle to wall [8, 9].

Other scholars have done a lot of research work on the injection and heat release performance of the nozzle in other fields, such as fuel injection [10] and thermosiphon [11]. Kawaguchi et al. [12] carried out an in-depth study on the morphological fluctuation of the external flow field of the nozzle jet and believed that the fluctuation of the external jet was caused by the fluctuation of the internal flow field of the nozzle. However, because the heat of the piston is carried away by the cooling oil ejected from the nozzle, the flow rate of nozzle is critical to the heat dissipation of the piston. Cao et al. studied the heat transfer characteristics of oscillating flow in oil chamber of the piston and pointed out that the nozzle flow should not be too large or too small. The heat dissipation effect could not be achieved if the flow was too small. Excessive flow will reduce the thermal efficiency of the engine and increase the thermal stress of the piston [13]. Deng et al. studied the internal flow field of piston cooling nozzle and obtained the variation trend of flow rate of nozzle on the different length of oil inlet and diameter of inner hole of nozzle [14]. However, he did not give the quantitative relationship between flow rate of nozzle and the diameter of inner hole of nozzle. It is not very clear for the engineer to design nozzle parameters. Due to the structure layout in a small space of the engine and piston stroke requirements, there are not enough spaces to change the shape of the nozzle. Therefore, the diameter and convergent length of the nozzle are changed to adjust the injection flow while the overall flow length remains the same.

Under the same piston structure and thermal power conditions, the piston cooling effect is significantly different with the flow rate provided by the piston cooling nozzle. In this paper, the internal flow characteristics and flow control of the piston cooling nozzle are studied. The internal flow field of the piston cooling nozzle of an engine is modeled. The flow rate is compared between the physical experiment and simulation experiment and the most optimal model is obtained in line with engineering practice. The simulation experiments are conducted on the basis of optimal simulation model of flow field. Finally, the changing law of the flow rate of nozzle is obtained when the convergent length and diameter of nozzle change under the same total length of the flow channel of nozzle. The analytical expression of the flow rate of nozzle is obtained by polynomial fitting. This work has important guiding significance to nozzle design.

2. Experiment and Methods

2.1. Research Methods. The finite element method (FEM) is usually used to solve the fluid domain problems. All fluid particles in the nozzle domain follow three equations of fluid mechanics:

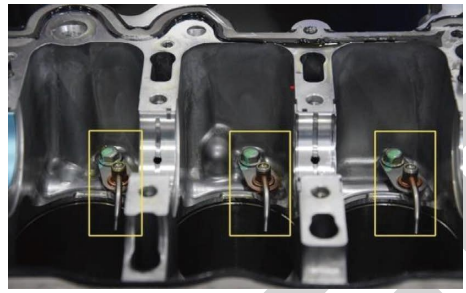

Figure 1: The installation position of the nozzle.

$$\begin{cases} \dfrac{\partial \rho}{\partial t} + \operatorname{div}(\rho \vec{v}) = 0, \\ \dfrac{\partial \vec{v}}{\partial t} + (\vec{v} \cdot \nabla)\vec{v} = \vec{F} - \dfrac{1}{\rho}\nabla p + v\Delta \vec{v}, \\ \dfrac{\mathrm{D}}{\mathrm{D}t}\left(\dfrac{1}{2}u_i u_i\right) = u_i F_{x_i} + \dfrac{1}{\rho}u_i \dfrac{\partial p_{ij}}{\partial x_j}, \end{cases} \tag{1}$$

where ρ is density, $\vec{v}$ is the fluid particle velocity vector, u_i is that velocity component of fluid particle, $\vec{F}$ is mass force, p is the surface force, v is the kinematic viscosity of the fluid, and t is the time. By solving the three equations of fluid simultaneously, the flow properties of the fluid field inside the piston cooling nozzle can be obtained, such as velocity distribution, pressure distribution, and flow rate.

Due to the rapid development of computer technology, the inner fluid domain of piston cooling nozzle is calculated by the finite element method according to the computational fluid dynamics method, and the calculation process is fixed in the Fluent software.

Furthermore, a piston cooling nozzle is fixed on the target testbed, and the volume flow rate is tested under the given pressure at the nozzle inlet. At the same time, the viscosity, density, and other fluid parameters of the cooling oil are recorded. Then, the three-dimensional model of the flow field of the nozzle is established according to the corresponding nozzle structure. Then, the 3D model is imported into the Fluent software to set the boundary conditions consistent with the experiment. Many calculation models are adjusted to make the simulation experiment consistent with the physical experiment and the optimal calculation model is selected.

Because of the compact structure of the engine, the installation position and space of the piston cooling nozzle are restricted. Therefore, the convergent length and diameter of nozzle are mainly considered in the design change of nozzle structure while the overall geometric parameters are basically the same. The *convergent length* refers to the length of a contraction part of the nozzle at the outlet of the nozzle, which has been clearly marked in Figure 1. Finally, the outlet diameter and the convergent length of the nozzle are adjusted to study the changing flow of different nozzle

Figure 2: BCYD-800 viscosity tester.

Figure 3: Viscosity test experiment.

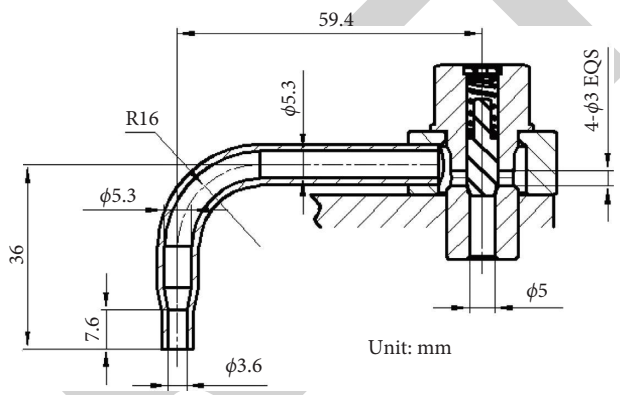

Figure 4: Section drawing of the piston cooling nozzle.

structures through simulation experiment with the optimal calculation model in the Fluent software.

2.2. Physical Experiment. First, the cooling oil was blended with engine oil and diluent. The ratio of the engine oil and diluent was adjusted repeatedly, and the viscosity test was carried out, so that the viscosity of the cooling oil tested in the experiment was 10.5 cst. The viscosity of cooling oil was tested by the BCYD-800 kinematic viscosity tester. Figures 2 and 3 show BCYD-800 viscosity tester and viscosity test experiment, respectively.

The prepared cooling oil is added into the shooting testbed of piston cooling nozzle and the jet experiment of piston cooling nozzle is carried out. The parameters such as pressure and flow rate of cooling nozzle were obtained. Figure 4 shows the size of internal flow channel of the tested nozzle, and 10 nozzles manufactured according to Figure 4 are tested for the jet flow experiment. The flow rate of the tested nozzles are listed in Table 1. Through several groups of test experiments, the average flow rate of piston cooling nozzle is 12.3 L/min with 400 kPa of the inlet oil pressure. Figure 5 shows the testbed of piston cooling nozzle and Figure 6 shows the experiment site of piston cooling nozzle.

2.3. Simulation Experiment. First, the three-dimensional model of piston cooling nozzle is established according to the structure of piston cooling nozzle in Figure 4, and then, the flow field model of piston cooling nozzle is extracted.

2.3.1. Three-Dimensional Modeling of Piston Cooling Nozzle. The main function of the piston cooling nozzle is to inject the oil into the cooling oil chamber in the piston head of engine accurately and quantitatively, so as to achieve the purpose of cooling the engine piston. Figure 7 shows the actual photo of the nozzle which is mainly installed at the end of the cylinder of engine. Its installation position is marked by yellow wire frame in Figure 1.

The piston cooling nozzle is mainly composed of valve head, injection pipe, position block, plunger, metal ring, and spring. Figure 8 shows a schematic diagram of its structure. From the Figure 8, it can be seen that when the cooling oil enters from the oil inlet, it pushes the plunger to compress the spring and move upwards. Then, the cooling oil enters the injection pipe and is sprayed out through the oil outlet to cool the engine piston.

SolidWorks software is usually used to model the piston cooling nozzle in three dimensions. Figures 9 and 10 show the three-dimensional model of the piston cooling nozzle.

2.3.2. Flow Field Modeling of the Piston Cooling Nozzle. In order to study the fluid flow state in the piston cooling nozzle, it is necessary to establish a three-dimensional model of the fluid domain. Therefore, the outer surface of the nozzle model is extracted in the SolidWorks software, and the oil inlet and outlet are closed and filled to obtain the solid model of the piston cooling nozzle. Then, the Boolean subtraction is done between the solid model of piston cooling nozzle and the original nozzle model. Therefore, the fluid domain model of the piston cooling nozzle is obtained, as shown in Figure 11.

2.3.3. Mesh Generation. First, the flow field inside the piston cooling nozzle should be divided into small elements. Therefore, the whole fluid domain should be divided into several tiny elements. If the element is too large, the amount of calculation is very small accompanied by low precision. On the contrary, the fine mesh produces high precision. Although the calculation accuracy is very high, it takes more

Table 1: The flow rate of tested nozzle.

No	1#	2#	3#	4#	5#	6#	7#	8#	9#	10#
Flow rate (L/min)	12.2	12.14	12.3	12.18	12.49	12.52	12.34	12.28	12.17	12.3

Figure 5: The testbed of the piston cooling nozzle.

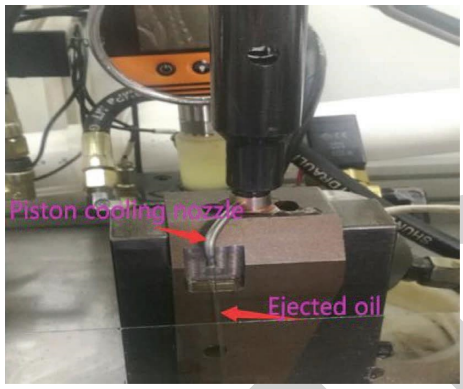

Figure 6: The jet experiment of the piston cooling nozzle.

Figure 7: Actual photo of the nozzle.

time and needs higher requirements for computer hardware. Therefore, the number of elements should be reduced as much as possible under the condition of satisfying the accuracy of calculation. Meshing should follow the following principles: (1) The number of nodes should be as large as possible in order to obtain more accurate results. (2) The difference between the maximum size and the minimum size of the elements should not be too large, and the best value range is between 1.2 and 1.4 times. (3) The nodes should be connected to adjacent element nodes as far as possible and not placed on adjacent boundaries. (4) The mesh should be fixed as much as possible, which is convenient for the computer to automatically generate the mesh.

In this paper, automatic meshing tools are used. The specific operations are as follows: first, the inlet, outlet, and boundary are determined and named, respectively. Considering that the flow velocity of the liquid attached to the wall is 0 and the central flow velocity is larger than the boundary, there is a span of flow velocity between them. Inflation is set upon the boundary layer to solve this problem. Figure 12 shows the meshed model.

In order to ensure the convergence of iterative solution, it is necessary to evaluate the mesh quality. The meshing tool provides the detailed evaluation indicators, as shown in Table 2. In this paper, the skewness and orthogonal quality are mainly selected for evaluating. Figure 13 shows the mesh quality distribution under the skewness parameter. Figure 14 shows the mesh quality distribution under orthogonal quality parameters.

Considering the skewness, it can be seen from the skewness evaluation that the value of 0~0.13 accounts for 7%, that of 0.13~0.35 accounts for 72%, that of 0.35~0.55 accounts for 15%, and that of above 0.55 accounts for 5%. Comparing the abovementioned values to the data in Table 1, it is concluded that the mesh quality is good. From the orthogonal analysis of the mesh quality, it can be seen from the orthogonal quality map that about 38% lies in 0.8~1, about 62% lies in 0.7~0.95, and about 17% lies in 0.63~0.7. It is same as the skewness. The overall mesh quality is relatively good. According to the statistics, the nozzle is meshed into 35,603 nodes and 93,448 units.

2.3.4. Boundary Conditions. According to the actual working conditions of the piston cooling nozzle, the inlet oil pressure is determined to be 400 kPa and the outlet is connected with the atmosphere, which is defined as a standard atmospheric pressure. Accordingly, the inlet, outlet, and wall are named as *inlet*, *outlet*, and *wall*, respectively, in mesh. To import the mesh into the Fluent software, we set the corresponding parameters in *Boundary Conditions* of Fluent, respectively. According to the abovementioned parameters, the default setting of the wall is used in the software.

2.3.5. Properties of Fluid Materials. At present, engine oil with viscosity of 10.5 cst is mainly used to cool the engine piston. Therefore, the density of the fluid material is set to 910 kg/m^3, corresponding dynamic viscosity of 0.009555 Pa•s. Figure 15 shows the interface of material parameter setting.

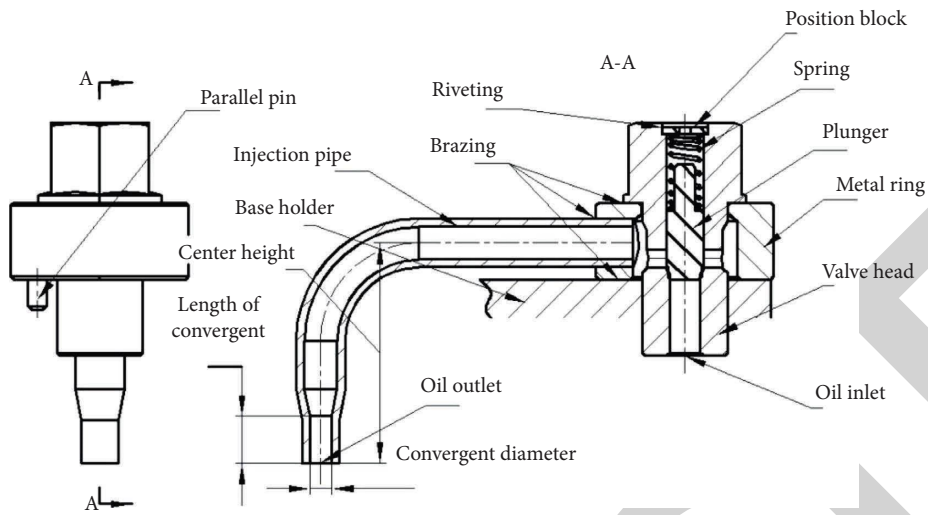

Figure 8: Structure drawing of the piston cooling nozzle.

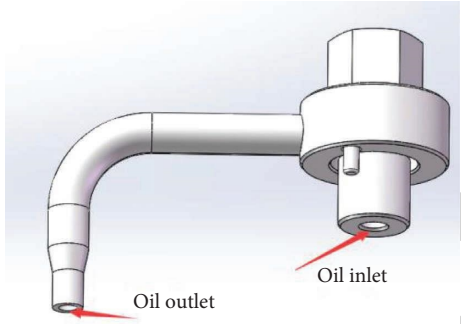

Figure 9: The three-dimensional model of the piston cooling nozzle.

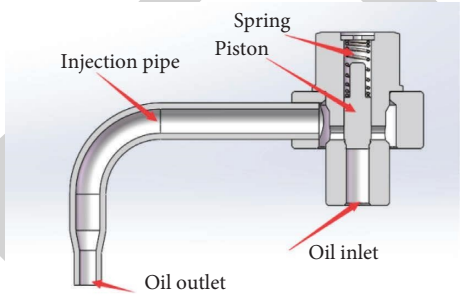

Figure 10: Sectional view of the nozzle assembly.

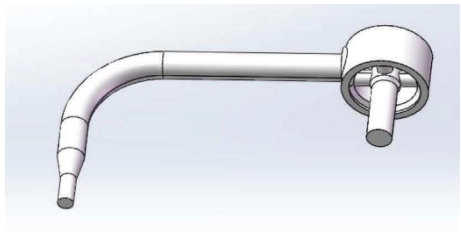

Figure 11: The fluid domain model of the piston cooling nozzle.

2.3.6. Flow Field Solution. Fluent provides three basic methods: coupled implicit solution, coupled explicit solution, and uncoupled solution. Uncoupled solution is generally used for incompressible fluid flow or compressible fluid flow with a low Mach number. However, this paper only involves the internal flow field, so uncoupled solution is chosen. Otherwise, Fluent provides lots of calculation models. Many calculation models are tested compared to physical experiment and the optimal calculation model is used.

Solving linear equations is generally the relaxation iteration method, and the relaxation iteration method has a relaxation factor to adjust the convergence rate of equations. The under-relaxation factors are set as Table 3. The convergent residuals of each parameter of the equation are shown in Table 4. The turbulence intensity and viscosity ratio at inlet of the nozzle are set at 5% and 10%, respectively, and the reflux turbulence intensity and viscosity ratio at the outlet are also set at 5% and 10%, respectively.

Simple algorithm is used for numerical solution in Fluent. The pressure and momentum are solved by a second-order upwind scheme. The turbulent kinetic energy and the turbulent dissipation rate are solved by a first-order upwind scheme. The standard initialization is selected. Each parameter is initialized to 0 and calculation program computes from inlet of the nozzle. The maximum iteration step is set to 1000.

3. Results

Many calculation models are selected, respectively, to solve the flow field of the piston cooling nozzle under the same boundary condition. Table 5 shows the flow rate of nozzle under the vary calculation models and physical experiment.

It can be concluded that the simulation result of the k-epsilon standard model is closest to the experimental data from the Table 5. Figure 16 shows a nephogram of velocity of flow field in the piston cooling nozzle under k-epsilon standard model. When the oil just enters the injection pipe,

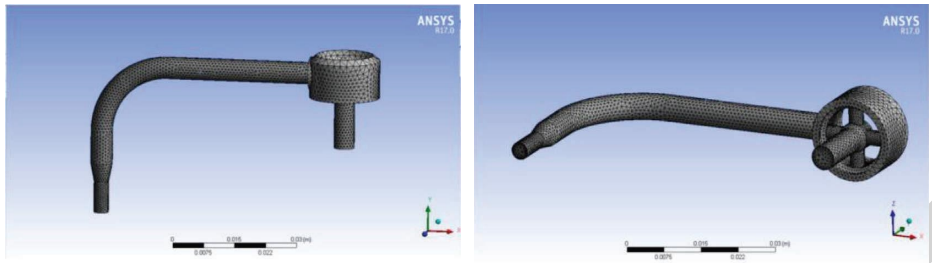

Figure 12: The meshed model of the piston cooling nozzle.

Table 2: Quality evaluation standard of fluid mesh.

Item	Excellent	Very good	Good	Acceptable	Poor	Unacceptable
Evaluation of inclination	0~0.25	0.35~0.5	0.5~0.8	0.8~0.9	0.9~0.97	0.98~1
Orthogonal quality evaluation	0.95~1	0.7~0.95	0.2~0.69	0.1~0.2	0.001~0.1	0~0.001

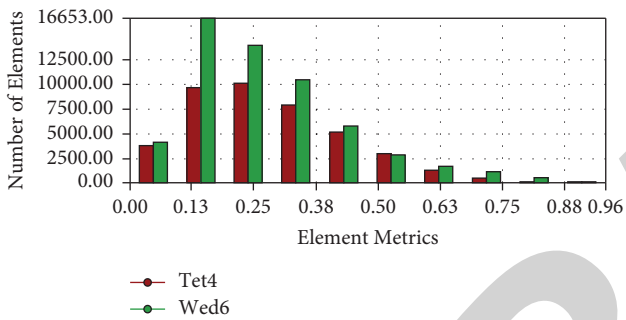

Figure 13: Mesh quality distribution under the skewness.

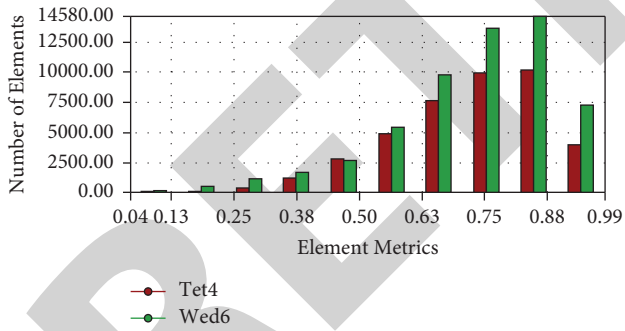

Figure 14: Mesh quality distribution under orthogonal quality.

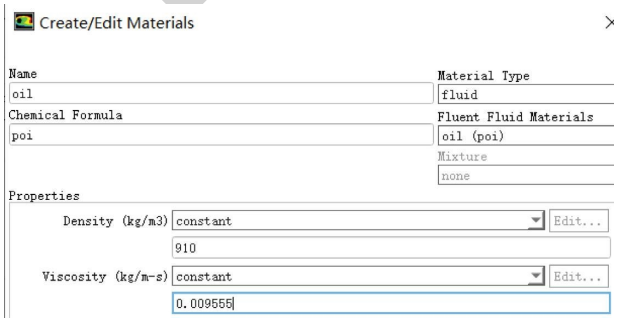

Figure 15: The interface of material parameter setting.

the flow state changes from turbulent state to steady state with the minimum speed. After entering the rear pipeline, it can be seen from the figure that the oil flow is basically stable. However, it can still be seen that there are signs of acceleration in the rear part. Then, the oil passes through the nozzle contraction. The speed of the oil suddenly changes and reaches the maximum at the outlet. Almost all the oil can be hit on the piston. It can be seen from Figure 17 that the nozzle flow rate is 0.1898 kg/s under k-epsilon standard model. It equals 12.51 L/min after conversion.

For different engines, the thermal power is different. Therefore, the requirements of the flow rate for piston cooling nozzles are different. Usually, the outlet of the injection pipe is contracted to different shape and size to obtain different injection flows.

3.1. The Influence of the Flow Rate of Piston Cooling Nozzle with Different Convergent Lengths. In this paper, the nozzle in Figure 4 is taken as a model and the convergent diameter is 3.6 mm. The influence of the flow rate of the nozzle with different convergent lengths from 0 to 15 mm is studied under the same length of center height and other geometric parameters which are marked in Figure 8. The other boundary conditions are the same as part 3.3 in this paper and the k-epsilon standard model is used. The 16 values of the convergent length (in Table 6) from 0 mm to 15 mm are calculated by Fluent software, respectively. Table 6 shows the calculated results.

In order to more intuitively reflect the change law of the flow rate of nozzle with different convergent length, the volume flow rate in Table 6 is plotted as a curve, as shown in Figure 18. As can be seen from the figure, with the increase of the convergent length, the flow rate of the nozzle shows a downward trend which is faster in the early stage and slower in the later stage and the overall decline shows a linear change.

3.2. Influence of the Flow Rate of Piston Cooling Nozzle with Different Convergent Diameters. In addition to using different convergent lengths to change flow rate of the nozzle,

Table 3: Under-relaxation factors of all the parameters.

Parameters	Pressure	Density	Body force	Momentum	Turbulent kinetic energy	Turbulent dissipation rate	Turbulent viscosity
Relaxation factor	0.3	1	1	0.1	0.8	0.8	1

Table 4: The convergent residuals of all the parameters.

Parameters	Continuity	x-velocity	y-velocity	z-velocity	k	Epsilon
Residual	0.001	0.001	0.001	0.001	0.001	0.001

Table 5: The flow rate of nozzle under the vary test condition.

	Simulation experiment with Fluent software							
Test condition	Laminar	Spalart–Allmaras	k-epsilon standard with standard wall function	k-omega standard	Transition k-k1-omega	Transition SST	Reynolds stress	Physical experiment
Flow rate (L/min)	13.05	12.92	12.51	12.9	12.73	12.92	12.76	12.3

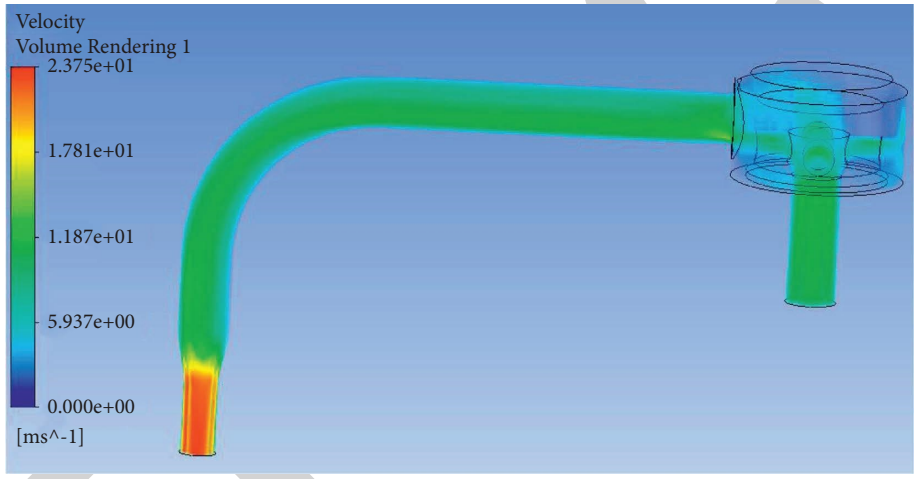

Figure 16: The nephogram of velocity of flow field.

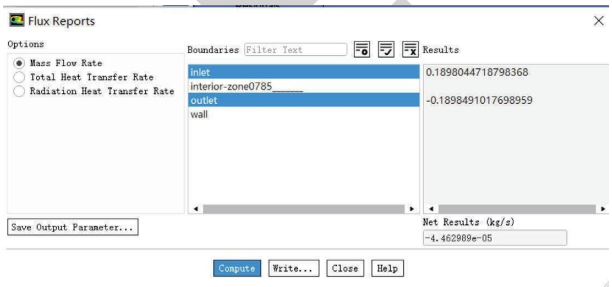

Figure 17: The flow rate of the piston cooling nozzle.

convergent diameter also has a great influence on the flow rate. Similarly, the 3D model of the nozzle is established according to the structure size of the nozzle shown in Figure 4. The other boundary conditions are the same as part 3.3 in this paper. When other conditions remain to be unchanged as part 3.1, the Fluent software is used to calculate the flow rate of nozzle under different convergent diameters. Figure 19 shows the curve of the flow rate of the piston cooling nozzle with different convergent diameters. As can be seen from the figure, the flow rate of the nozzle presents an upward trend with the increase of convergent diameter and the change trend is obviously nonlinear.

Comparing Figures 18 and 19, it can be seen that the change of the convergent diameter has a more significant influence on the flow rate than the convergent length. In order to better realize the engineering application, the simulation data in Figure 19 are polynomial fitted. Figure 20 shows the quadratic polynomial fitting curve, and Figure 21 shows the cubic polynomial fitting curve.

As can be seen from Figure 21, the simulation data of flow rate of piston cooling nozzle are in good agreement with the cubic fitting curve. Therefore, the following analytical expression is obtained as follows:

$$Q = -0.0036d^3 + 0.0327d^2 - 0.0126d + 0.0023, \quad (2)$$

where Q is the flow rate of nozzle (L/s) and d is the convergent diameter (mm).

Table 6: The flow data of the piston cooling nozzle under different convergent lengths.

Closing length (mm)	0	1	2	3	4	5	6	7
Mass flow (kg/s)	0.197	0.1945	0.1931	0.1917	0.1908	0.1896	0.1885	0.1875
Flow rate (L/s)	0.216484	0.213736	0.212198	0.210659	0.20967	0.208352	0.207143	0.206044
Closing length (mm)	8	9	10	11	12	13	14	15
Mass flow (kg/s)	0.1867	0.1857	0.185	0.184	0.1831	0.1821	0.1813	0.1806
Flow rate (L/s)	0.205165	0.204066	0.203297	0.202198	0.201209	0.20011	0.199231	0.198462

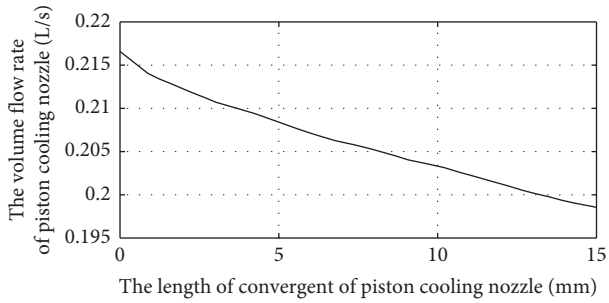

Figure 18: Curve of the flow rate of the piston cooling nozzle with different convergent lengths.

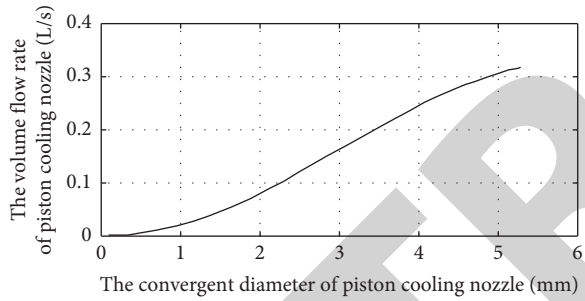

Figure 19: Curve of the flow rate of the piston cooling nozzle with different convergent diameters.

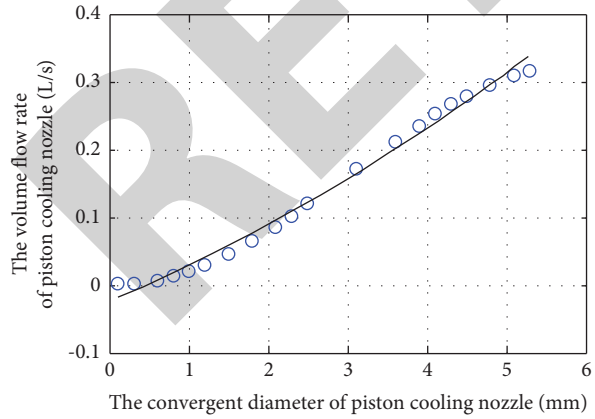

Figure 20: Quadratic polynomial fitting curve of the flow rate.

4. Discussion

As you can see from Figure 16 that the flow velocity of oil in the nozzle is up to 23.75 m/s. Therefore, the Reynolds Number is gained.

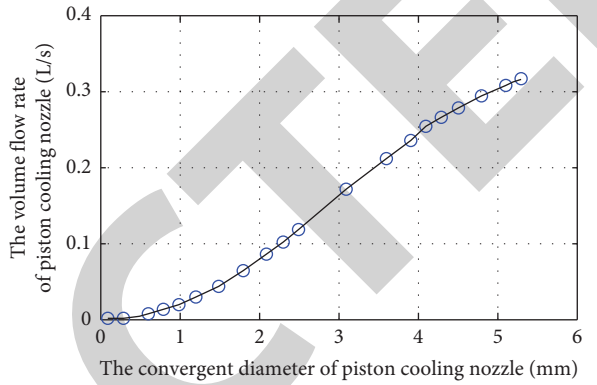

Figure 21: Cubic polynomial fitting curve of the flow rate.

$$\mathrm{Re} = \frac{\rho v D}{\eta} = \frac{910 \times 23.75 \times 0.0036}{0.009555} = 8142.9. \quad (3)$$

Because the Reynolds number of flow in the nozzle is relatively high, the laminar flow model is not applicable. Because of the large amount of dissipation by turbulence, the actual flow rate is relatively small. Therefore, the flow rate calculated by the laminar flow model is larger than the actual flow rate. However, the k-omega model introduces vorticity in the eddy viscosity coefficient, which is relatively stable for the flow near the wall. For the region with low Reynolds number, the distance to the wall does not need to be calculated under the k-omega model. The boundary layer is very thin in the nozzle because of the high Reynolds number. So, the calculated flow rate in the nozzle by k-omega model will be larger than the actual station. Therefore, among all kinds of calculation models, the standard k-epsilon model has the closest calculation results. From the simulation results, the calculation results of the standard k-epsilon model are closest to the physical experimental results. Therefore, it is reliable to use the standard k-epsilon model to simulate the flow field of piston cooling nozzle.

5. Conclusion

In this paper, the three-dimensional models of piston cooling nozzle and its internal fluid field are established. The working boundary conditions are obtained by analyzing the actual working condition of the piston cooling nozzle. Finally, the internal flow field of the piston cooling nozzle under actual working conditions is simulated and analyzed by the Fluent software based on the theory of computational fluid dynamics. Therefore, the theoretical injection flow rate of the piston cooling nozzle is obtained. Otherwise, the

Hindawi
Scientific Programming
Volume 2023, Article ID 9796780, 1 page
https://doi.org/10.1155/2023/9796780

Retraction

Retracted: Algorithmic Application of Evidence Theory in Recommender Systems

Scientific Programming

Received 1 August 2023; Accepted 1 August 2023; Published 2 August 2023

This article has been retracted by Hindawi following an investigation undertaken by the publisher [1]. This investigation has uncovered evidence of one or more of the following indicators of systematic manipulation of the publication process:

(1) Discrepancies in scope
(2) Discrepancies in the description of the research reported
(3) Discrepancies between the availability of data and the research described
(4) Inappropriate citations
(5) Incoherent, meaningless and/or irrelevant content included in the article
(6) Peer-review manipulation

The presence of these indicators undermines our confidence in the integrity of the article's content and we cannot, therefore, vouch for its reliability. Please note that this notice is intended solely to alert readers that the content of this article is unreliable. We have not investigated whether authors were aware of or involved in the systematic manipulation of the publication process.

Wiley and Hindawi regrets that the usual quality checks did not identify these issues before publication and have since put additional measures in place to safeguard research integrity.

We wish to credit our own Research Integrity and Research Publishing teams and anonymous and named external researchers and research integrity experts for contributing to this investigation.

The corresponding author, as the representative of all authors, has been given the opportunity to register their agreement or disagreement to this retraction. We have kept a record of any response received.

References

[1] L. Ma, "Algorithmic Application of Evidence Theory in Recommender Systems," *Scientific Programming*, vol. 2022, Article ID 9290577, 11 pages, 2022.

Hindawi
Scientific Programming
Volume 2022, Article ID 9290577, 11 pages
https://doi.org/10.1155/2022/9290577

Research Article

Algorithmic Application of Evidence Theory in Recommender Systems

Lina Ma

Department of Statistics and Big Data, Xingzhi College of Xi'an University of Finance and Economics, Xi'an 710038, Shaanxi, China

Correspondence should be addressed to Lina Ma; lmarymath@chd.edu.cn

Received 25 June 2022; Revised 2 September 2022; Accepted 12 September 2022; Published 28 September 2022

Academic Editor: Juan Vicente Capella Hernandez

With the development of wireless network and various communication technologies, the information on the Internet is expanding rapidly. The development of wireless network and various communication technologies has promoted the development of e-commerce, and people can understand a large amount of commodity information without leaving home. However, due to the complex information on the network, users need to pass a lot of screening to obtain the information they want, and a large amount of irrelevant information will cause users to consume a large amount of irrelevant information. To solve these problems, the personalized recommendation system is created, but the recommendation system is recommended according to the characteristics of users' interest and shopping behavior. However, users' interests will change, so they need to use other technologies to screen for relevant commodity information. Evidence theory has a strong ability to distinguish between true and false information and to deal with uncertain information. To this end, this article studies the application of the evidence theory in the recommendation system and finds that the evidence theory algorithm can infer the information needed by users based on the uncertain information. Moreover, the experiment in this article proves that the algorithm application of the evidence theory in the recommendation system can well grasp the interests of users and recommend the information needed by users. This improves the efficiency of users to obtain the required information and achieves 80 points for content recommendations.

1. Introduction

With the development of the network, the advancement of communication technology, and the strengthening of connections around the world, the amount of information has grown dramatically. With the explosive development of computer technology and Internet technology at home and abroad in recent years, the data and information on the Internet are growing wildly at an unprecedented rate. In this era of information explosion, it is a new and huge challenge for users, media, and businesses. Users spend a lot of time and energy in the massive information; and in order to provide better services to users, merchants need to use the obscure information on the Internet, which is very important for merchants to seek profits. But looking for the information needed in the massive information is like looking for a needle in the sea, and search engines were born. However, search engines cannot search according to the interests of users, so there will be an automatic recommendation function in search engines. This automatic recommendation feature needs to personalize recommendations with past user habits and search history. However, there is a lot of previous practical information with a lot of uncertainty, so the recommended content does not necessarily meet the information needed by users. Therefore, in order to improve the utilization rate of users and bring higher profits to businesses, more advanced recommendation systems need to have more advanced recommendation system to help search engines recommend information resources that really meet the interests of users in the new district and meet the personalized needs of users.

Recommendation systems have been widely used in the commercial field, and the recommendation system studied in this article can improve the availability of

recommendation information. Especially in the product recommendation used on the online shopping platform, it will be more consistent with users' interests and hobbies, which enhances users' desire to buy and promotes the growth of commercial interests [1]. In the recommendation system, deeply understand the internal principle of the recommendation system, applying the evidence theory algorithm to the recommendation system, improving the accuracy of the recommendation information, expanding the universality of the system, and making the recommendation system better applied to a wider range of scenarios [2]. In addition, it can also save users the time to search for the information, which improves the user experience and ensures that users can get the desired information in the shortest time. In addition, the use of the evidence theory algorithm in the recommendation system in this article can improve the efficiency of distinguishing the true and false information and improve the user's experience.

At present, the foreign wine that combines the evidence theory and the recommendation system is still in the development stage, and there are many research studies on the recommendation system. Among them, Ha et al. demonstrated the development of an evidence-based material recommendation system (ERS) that employs the Dempster–Shafer theory. To evaluate the recommendation ability of ERS, it was compared with that of recommendation systems based on matrix factorization and supervised learning. A k-fold cross-validation on the dataset showed that ERS outperforms all competitors [3]. However, their research has no specific practical process, and it is difficult to explain the feasibility of the recommender system. Cui studied data mining based on an intelligent recommender system. He first modeled the evidence theory for the intelligent recommendation system based on association rules. The experiments showed that the algorithm of the system has a fast convergence speed and can recommend products that are more in line with user needs and interests, which increases the click rate and purchase rate, and further improves user satisfaction [4]. His research was not supported by concrete data and was unconvincing. Cui's description based on user interest is an important problem for recommender system input, and the fuzzy set theory is proposed to solve this problem. This research laid a theoretical foundation for the study of the uncertainty theory and also finds a new application background for the study of fuzzy sets [5]. Although his research is supported by theoretical basis, it has not been experimentally verified. Dong and Kuang proposed an information aggregation-based SAR image target recognition method based on the Dempster–Shafer (DS) evidence theory. He proposed a classification framework for information aggregation by using a new multidimensional analysis signal-single-gene signal, which the experimental results proved can be used to define probability mass [6]. His research has no strong theoretical support and lacks theoreticality. Li and Wang proposed a green supplier assessment method based on rough ANP and evidence theory for the uncertainty and incompleteness in green supplier assessment. He used the confidence interval to evaluate green suppliers based on the evidence theory, and verified the feasibility and effectiveness of the method through the application of bearing cage supplier evaluation [7]. His research does not clearly address rough ANP. Based on previous studies, the article will conduct in-depth research on the evidence theory and recommender systems according to the shortcomings of their research.

In this article, the research on the algorithm application of the evidence theory in recommender systems has the following innovations: (1) this article innovates the identification framework in the evidence theory to improve the credibility of the evidence in the evidence theory, so that it can recommend more reliable items in the recommendation system. (2) The evidence theory algorithm is introduced to the recommendation algorithm in the recommendation system, which provides the recommendation system with the function of distinguishing the true and false recommendation information, and improves the user's efficiency in finding information and the satisfaction of using the recommendation system. (3) And the recommendation system studied in this article can use evidence theory to identify the authenticity of information and recommend it to users, which improves the security of users using network information.

2. Method of Algorithm Application of Evidence Theory in Recommender System

2.1. Algorithmic Applications of Evidence Theory. Evidence theory is a classical probability theory, that is, an extension of the branch of mathematics that studies the quantitative laws of random phenomena. It establishes a one-to-one correspondence between propositions and sets, and transforms the uncertain problem of propositions into uncertain problems of sets [8]. The evidence theory is widely used in the field of artificial intelligence and has gradually developed into a class of important uncertainty reasoning methods, which can be used for object detection, classification, and recognition. The D-S evidence theory is a commonly used fusion algorithm in target recognition [9]. Assuming that there is currently an evidence that needs to be identified urgently; that is to say, this evidence needs to be identified within an identification framework, and the identification framework is defined as

$$\Xi = \{e_1, e_2, e_3, \ldots e_n\}. \tag{1}$$

The elements in this recognition frame are mutually exclusive, and only one of all possible evidences to be identified is correct, and the set of all subsets in the recognition frame can be expressed as

$$\Xi_2 = \{\varnothing, \{e_1\}, \{e_2\}, \ldots \{e_1, e_2\}, \ldots \{e_1, e_2, \ldots e_n\}\}. \tag{2}$$

The problem to be identified is in the above set, and the evidence theory can combine all subsets of the set with the identified problem, find the subset that is most likely to be close to the identified problem, and display it [10]. Among the many subsets, the basic probability distribution function

is the basis; that is to say, all the subsets in the set may have a certain probability relationship with the evidence to be identified. There are two evidences $W1$ and $W2$, and the corresponding distribution subsets are $e1$ and $e2$, and then, the distribution functions for the evidences are $Q1$ and $Q2$. The function distribution probability and composition rule of evidence W are shown in Figure 1.

In Figure 1, the synthesis rule synthesis represents the total subset trust, the horizontal axis represents the trust value of the evidence $Q2$ assigned to each subset set, and the vertical axis is the evidence $Q1$ assigned to each subset set. The subsets identified by different evidences are not the same, and then, when there are two sources of evidence, the subset composition rule of the evidence theory is as follows:

$$Q(e) = Q_1 \oplus Q_2 = \frac{\sum_{R\cap S=A} Q_1(R)Q_2(S)}{1-L},$$
$$L = \sum_{R\cap S=\varphi} Q_1(R)Q_2(S), \tag{3}$$

where K is the conflict factor in the evidence synthesis rule, which reflects the degree of conflict between the two evidences $Q1$ and $Q2$. The conflict between the two evidences can be normalized, so the trust value $\sum_{R\cap S=\varphi} Q_1(R)Q_2(S)$ in the empty set can be removed from the trust value in the total set, so that the identified information is more accurate. However, if the trust degree of the empty set is removed, the sum of the trust degree will not be one, so the coefficient v needs to be added. The formula for obtaining this coefficient is

$$v = \left[1 - \sum_{B\cap C=\varphi} Q_1(R)Q_2(S)\right]^{-1}. \tag{4}$$

With the addition of the coefficient v, the sum of the trust degrees can be kept at 1. Therefore, when the conflict factor $k=1$, it means that there is a very strong conflict between the two evidences $Q1$ and $Q2$, so that the required information cannot be identified. Conversely, if the value of the conflict factor is not equal to 1, a new assignment probability will be generated, thereby identifying the desired information. So when there are multiple evidences to be combined, the rules of the combination are as follows:

$$Q(e) = Q_1 \oplus Q_2 \oplus \ldots Q_n,$$
$$Q_1 \oplus Q_2 \oplus \ldots Q_n = \frac{\sum_{R_1\cap R_2\cap\ldots R_N} Q_1(e_1)Q_2(e_2)\ldots Q_n(e_n)}{1-K}. \tag{5}$$

The calculation method of the conflict factor K is

$$K = \sum_{R_1\cap R_2\cap\ldots R_n} Q_1(e_1)Q_2(e_2)\ldots Q_n(e_n). \tag{6}$$

Then, the formula for calculating the coefficient v under multiple evidences is

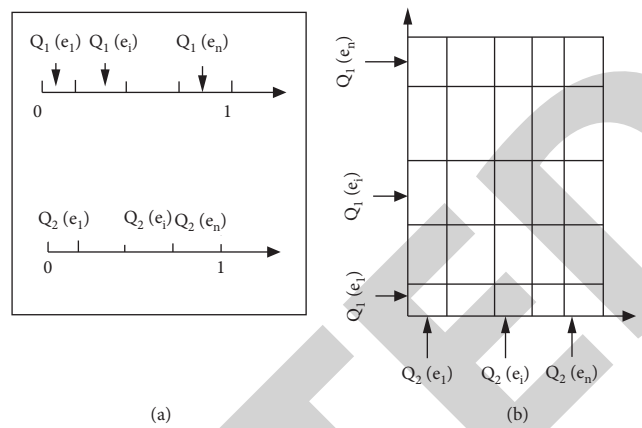

Figure 1: Function assignment probabilities and composition rules. (a) Basic probability distribution. (b) The synthesis rules.

$$v = \left[1 - \sum_{R_1\cap R_2\cap\ldots R_n} Q_1(R)Q_2(R_1)\ldots Q_n(R_n)\right]. \tag{7}$$

To form a recognition framework, the evidence theory fusion algorithm needs to fuse all the information. The evidence theory information fusion process is shown in Figure 2.

It uses sensing devices to perceive things in the outside world and then convert the perceived things into data information and fuse them into the database. By using sensors to fuse all the information into the database, the evidence theory algorithm can have information data to generate a set and then identify the required information [11]. And the evidence theory belongs to the category of artificial intelligence, which has a strong ability to process uncertain information. Just like a person's hobbies are very extensive, so people's hobbies have strong uncertainty. And how to recommend personalized information based on uncertain hobbies, we can use the evidence theory to deal with people's hobbies, integrate information from personal historical hobby data, and then judge personal hobbies. However, the evidence theory needs to specify a reasonable application category in order to have accurate performance. Therefore, what this article studies is the application of evidence theory in recommender systems [12].

2.2. Recommendation System. With the development of modern communication technology, there is more and more information on the Internet: due to the booming development of the Internet, people can obtain all kinds of information on the Internet: people can learn about major events at home and abroad without leaving home; people can get the latest news on the Internet without subscribing to newspapers; people can complete all shopping without even going to the mall [13]. However, due to the rapid development of the network, the information growth is too fast, making another big problem. Because of the huge amount of information, it is difficult for people to find the letters they need instantly and quickly. At the same time, false

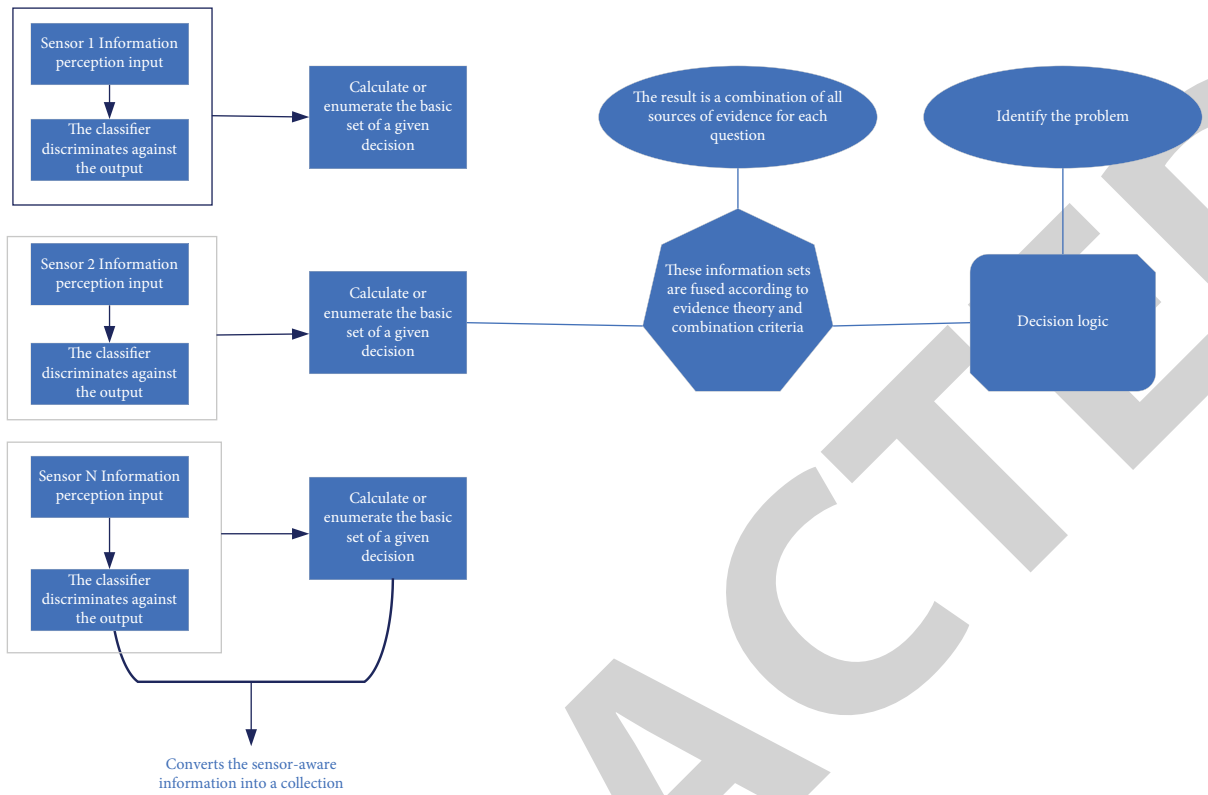

Figure 2: Process diagram of evidence theory information fusion.

information is also flooding the Internet, making it difficult for people to distinguish the true and false information. This is the problem of "information overload" currently faced by the Internet [14]. "Information overload" refers to a situation in which social information exceeds the range of individuals or systems that can be accepted, processed, or effectively utilized, leading to failures. For this reason, with the development of science and technology and the problems exposed by the current network, the recommendation system is also used. The recommender system is a software tool and information filtering technology, which can find items of interest to users from massive information [15]. Of course, the reason why the recommender system can mine and analyze the user's hobbies and generate recommendations is because the recommender system also belongs to the category of artificial intelligence [16]. The recommender system can actively use the technology of machine learning to mine the interests and preferences of users, so as to filter the content that meets the interests of users from the massive information data according to the interests of users, and recommend them to users [17]. The recommendation system can generally be divided into four levels: data collection, user modeling, recommendation algorithm, and recommendation output. The model of the recommendation system is shown in Figure 3.

There is a huge amount of information on the Internet, and it is full of various false information, which leads to a certain degree of inauthenticity of the recommended items by the recommendation system. The recommendation algorithm determines the quality of the recommended content in the recommendation system. The push algorithm can learn by setting algorithm goals according to the collected user information and the established user model, and calculate the recommendation result for a specific user [18]. Current recommendation algorithms include content-based recommendation algorithms, collaborative filtering algorithms, and user-feature-based filtering algorithms [19]. The content-based filtering algorithm considers the similarity between item information and user preferences, and recommends items with high similarity to users. The content-based recommendation algorithm first analyzes the content and analyzes the key content from the original item as a feature, and the user's hobbies may be similar to the key content of the item, so as to push it to the user.

The collaborative filtering algorithm predicts the user's rating or recommends an unknown item through the rating matrix. Similarity calculation is used to find the degree of similarity between each pair of users, where similarity indicates that two people have similar tastes in the overall project.

Supposing that S_i is used to represent the similarity between users m and n, t is used to represent the rating of user m for the ith item and f_i is used to represent the rating of user n for the ith item. And e is the average rating of user m for all items, q is the average rating of user n for all items, and then, the Pearson similarity between the two is calculated as follows:

$$S = \frac{\sum_{i\epsilon k}(t_i - e)(f_i - q)}{\sqrt{\sum_{i\epsilon k}(t_i - e)^2} * \sqrt{\sum_{i\epsilon l}(f_i - q)^2}}. \quad (8)$$

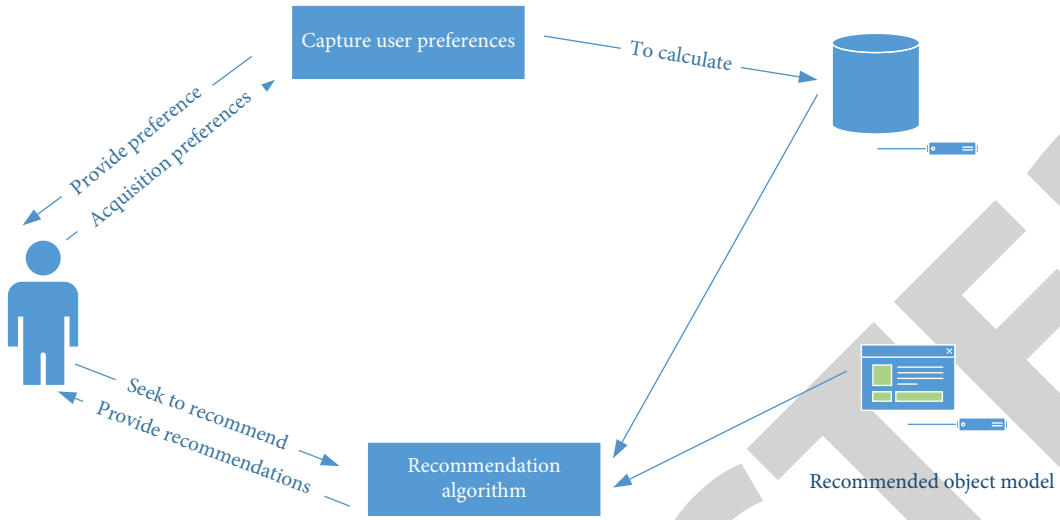

Figure 3: Model of a recommender system.

And if it is to find the cosine similarity of two people, the formula is as follows:

$$S = \cos(\vec{m}, \vec{n}) = \frac{\vec{m} \cdot \vec{n}}{\|\vec{m}\| \cdot \|\vec{n}\|}. \tag{9}$$

To calculate the cosine similarity between two people, it is necessary to convert the ratings of the two users into a score vector. Similarity calculation is the first step and the most important step in model-based collaborative filtering. Reasonable selection of application similarity according to application scenarios can ensure the accuracy of recommendation. By calculating the similarity, it is only to compare the degree of fit between the interests and hobbies of the users. And how to recommend items of interest to users based on similarity requires an estimated score for all items to be recommended. The predicted score R is generally calculated using the following formula:

$$R_m = t_i + \frac{\sum_{i \in k} (t_i - e) * S}{\sum_{i \in k} |S|}, \tag{10}$$

where k is the subset of items rated by people with similar interests to user m. The higher the similarity, the higher the score for the prediction. The higher the score, the more the items recommended to the user are in line with the user's interests. The algorithm recommendation process is shown in Figure 4.

However, there is a lot of information on the Internet and it is difficult to distinguish between true and false, so the information recommended by the recommendation system is difficult to distinguish between true and false and there is still a certain degree of inaccuracy. Therefore, this article combines it with the evidence theory algorithm to judge the authenticity of the recommendation information to make up for the deficiencies of the current recommendation system.

2.3. Algorithm Application of Evidence Theory in Recommendation System. There is a huge amount of information on the Internet, including videos, music, merchandise, and more. The current recommendation system is still difficult to grasp the user's new area hobbies, so the recommended content may not conform to the user's personal interests and hobbies. Sometimes, it is difficult to distinguish the authenticity of the recommended information, which will still cause some trouble to users [20]. Therefore, this article fuses the multisource information in the recommendation system according to the evidence theory and summarizes it into a set of items through information fusion. The recommendation system is connected to the database on the network. Because to recommend information to users, the recommender system must be connected with the database in the Internet, so that it can have enough capital to recommend relevant information to users [21]. Therefore, the recommendation process of the recommendation system based on evidence theory is shown in Figure 5.

The evidence theory can improve the efficiency of information identification in recommendation systems and can integrate massive information and user interests in recommendation systems. Finally, the authenticity of the requested recommendation information is verified through evidence, and then, it is recommended to users in need through the recommendation system [22]. The principle of interest and item fusion of the evidence theory in recommender systems is based on the evidence theory algorithm. First of all, the evidence theory combines items from multiple sources into a set u, and the elements in u are different; that is to say, the items in u are divided into different categories. For example, some are video items, some are music items, and some are commodity items. Therefore, assuming that there are n subsets in u, and the hobbies provided by the user are k, the principle of the evidence theory algorithm to integrate user hobbies and items is as follows:

$$x = \{\{u_1 * k\}, \{u_2 * k\}, \ldots \{u_n * k\}\} \otimes \frac{n}{k}. \tag{11}$$

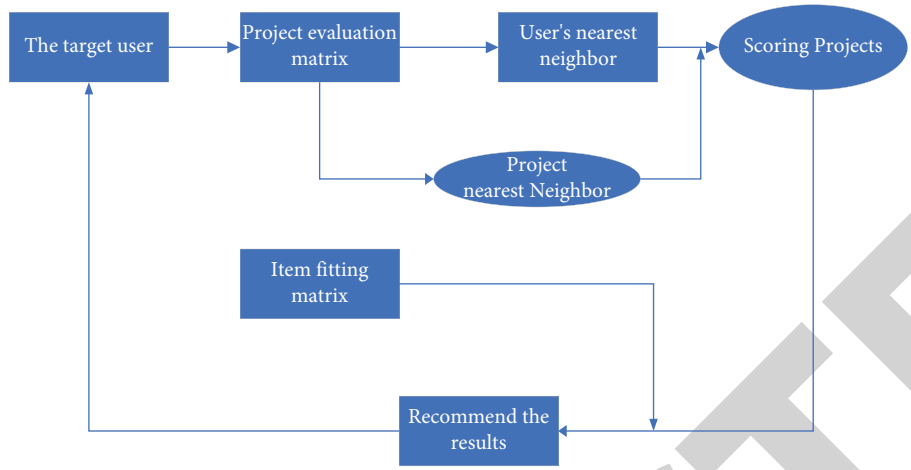

Figure 4: Flowchart of algorithm recommendation.

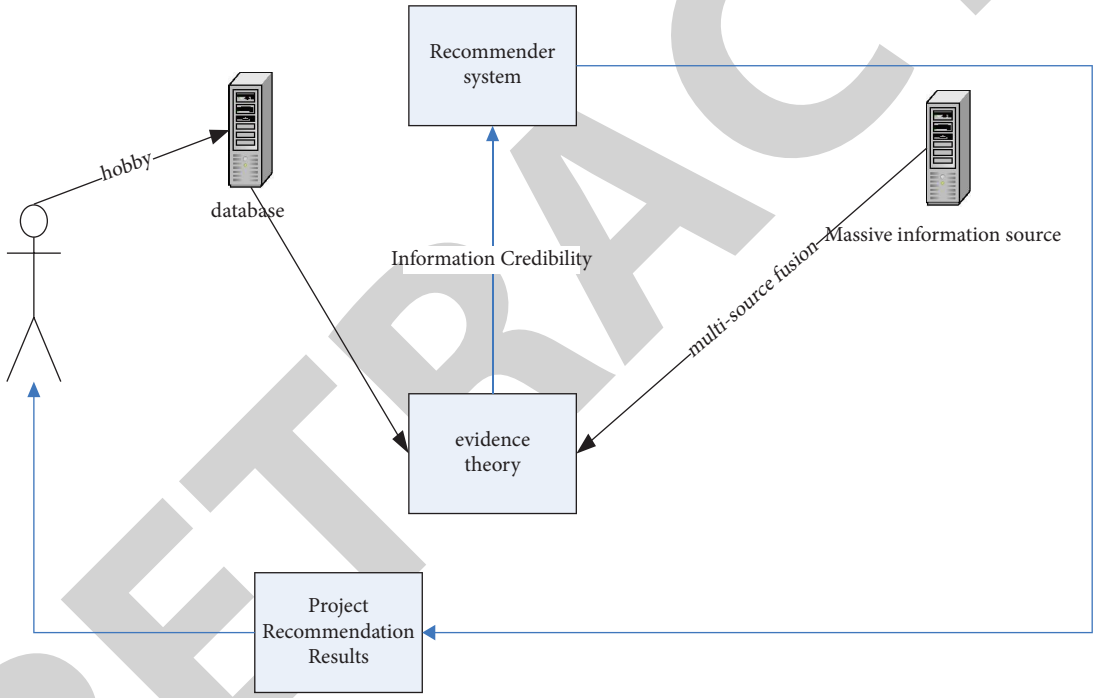

Figure 5: Recommendation flowchart of the new recommendation system.

Then in the above formula, x is the set of newly fused item subsets. The item integrates the user's interests and hobbies, and finds out the items that the specific user is interested in. Then, the set of subsets in x can be expressed as

$$x = \{\{x_1\}, \{x_1 x_2, x_2\}, \ldots \{x_n x_{n+1}, x_{n+1}\}\}. \tag{12}$$

Then, the authenticity of the item is verified according to the joint rules under multiple evidences, helping users to distinguish the authenticity of the information. After that, the recommendation algorithm inside the recommendation system will make recommendations again based on the user's interests and hobbies according to the set summarized by the evidence theory algorithm, and then, it integrates the items of user interest and recommends according to the user similarity according to the evidence algorithm. The principle is as follows:

$$\begin{aligned} s &= \cos\left(\vec{v}, \vec{b}\right) = \frac{\vec{v} \cdot \vec{b}}{\|\vec{v} \cdot \vec{b}\|} \otimes k, \\ Q &= \frac{\sum_k^n s \cdot v}{\sum_k^n s \cdot b} \otimes x, \end{aligned} \tag{13}$$

where v and b represent two users, and Q is the recommended item, so the new recommendation system can well

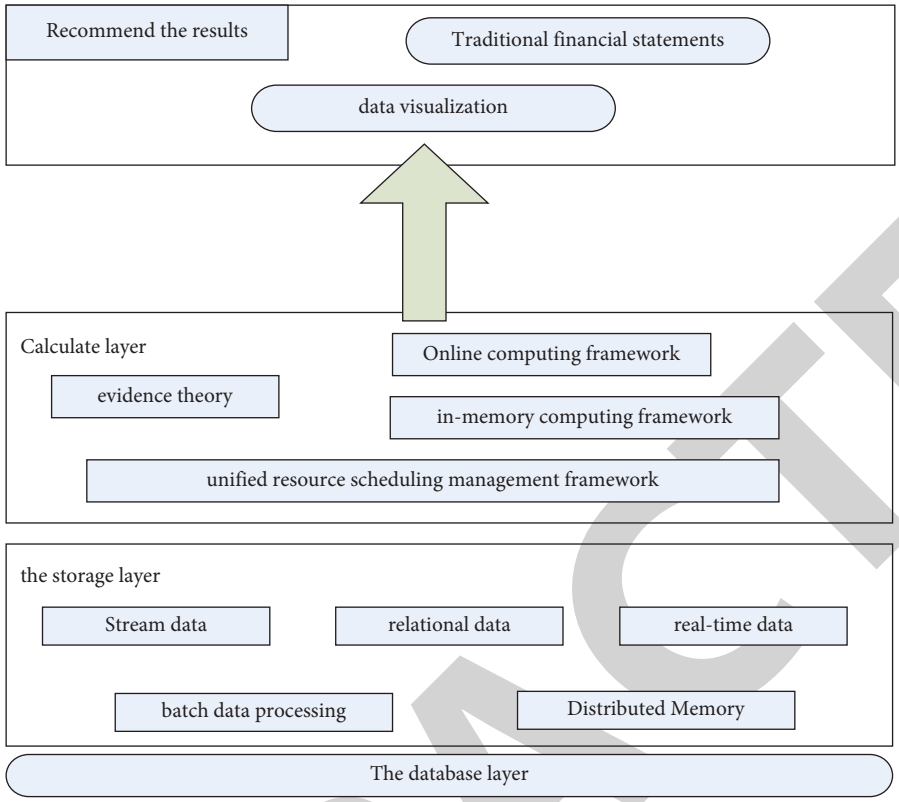

Figure 6: Overall architecture of the new recommender system.

recommend the item information that meets the user's hobbies and needs at the time. The overall architecture of the new recommendation system is shown in Figure 6.

The recommendation result layer serves as the front-end display page for user interaction, which is specifically represented in the form of a web page. Its main function is to provide users with more comprehensive recommendation services based on the results of recommendation calculations and to provide more accurate project information services for users to obtain the information they want. The computing layer calculates the items that the user is interested in according to the information resources recorded in the user data layer and the user's hobbies, and then scores, and pushes the item with the highest score to the recommendation layer [23]. What is stored in the data layer is the item information in the network and the historical information records that users have applied to the network search in the past, which is the basis of the entire recommendation system. Therefore, in order to ensure the performance and feasibility of this recommender system, this article also conducts experimental verification on this new type of recommender system.

3. Experiments on the Application of Evidence Theory in Recommender Systems

3.1. Performance Test of the New Recommender System. This experiment will use a browser as the object that has three different dataset interfaces. At the same time, three different recommender systems are used for this browser. These three recommender systems are the new system constructed in this article, the recommender system based on the content algorithm and the recommender system based on the collaborative filtering algorithm. In order to better verify the performance of the system in this article, the details of the three data information collection by the browser are counted in this experiment, as shown in Table 1.

It can be seen from Table 1 that the number of users of each dataset interface is different, so this experiment measures the efficiency performance and credibility value under different values of conflict factor k. Its efficiency performance comparison is shown in Figure 7.

From Figure 7(a), when the value of the conflict factor is larger, the performance of the recommender system does not increase with the larger value of the conflict factor, but fluctuates. And the efficiency of the new system is larger than that of the content-based system and the collaborative filtering recommendation system, its maximum performance can reach 0.986, while the maximum performance of the other two recommender systems only reaches 0.878, which shows that the efficiency and performance of the new system will be better. From Figure 7(b), the credibility of the new system is above 80%, while the credibility of the other two systems is below 80%, so the credibility of the new system will be higher. In addition, this experiment also calculated the accuracy of the content recommended by the three recommendation systems in the browser and recorded the accuracy data of the three systems in each dataset interface, as shown in Table 2.

Table 1: Dataset information.

Dataset	User quantity	Number of items	Number of scores	Sparsity (%)
1	1879	45676	576789	6.567
2	6547	56544	790687	5.7689
3	52725	78987	689787	8.7789

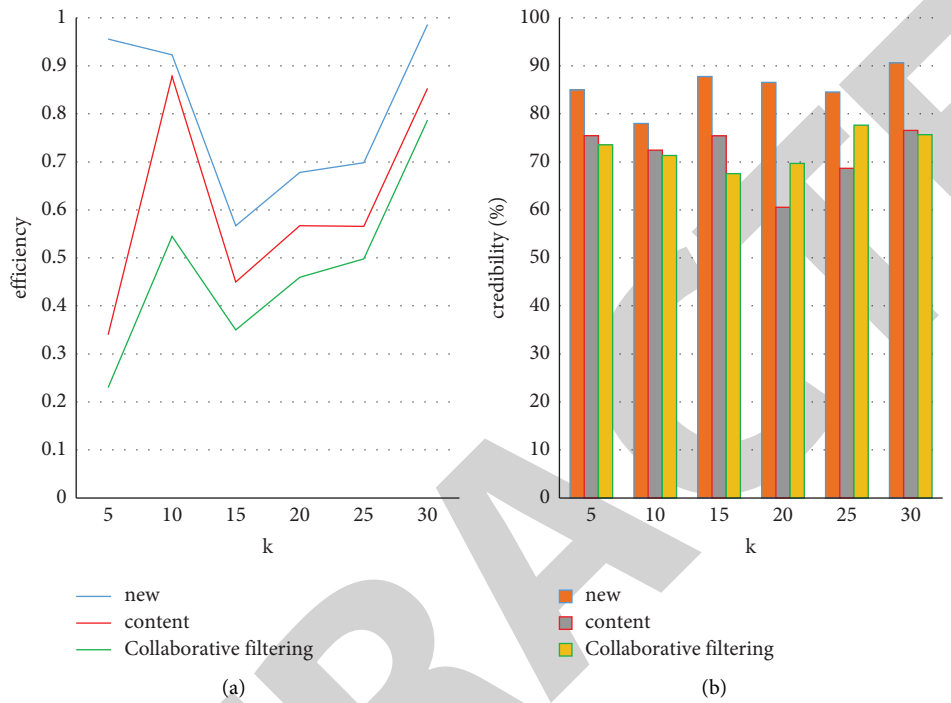

Figure 7: Comparison of efficacy and credibility data. (a) Efficiency performance. (b) Credibility.

Table 2: Accuracy of recommended content.

Recommender system	Data set interface	Accuracy (%)
New	1	78.45
	2	86.54
	3	75.4
Content	1	60.56
	2	50.56
	3	67.65
Collaborative filtering	1	68.45
	2	65.46
	3	68.67

From Table 2, the application of the recommendation system in this article in this browser, no matter which data interface recommends the content accuracy, can reach more than 78%. The accuracy of the content recommended by the other two recommender systems is obviously lower than that of the new recommender system, so the accuracy of the content recommended by the recommender system in this article is better.

3.2. Experiments on Recommended Content. This experiment is to verify whether the content recommended by the browser in the above experiment using three different recommendation systems in different dataset interfaces meets the needs of users. First, the content recommended by the three recommender systems for users in the three dataset interfaces of the browser. From the background of the browser, check whether the user has browsed the content recommended by the recommendation system: if the content has been browsed, it means that it conforms to the user's hobbies; if not, it means that it does not meet the user's hobbies. To this end, this experiment collects data on whether the content recommended by the three systems meets the interests of readers, as shown in Figure 8.

From Figure 8, it can be seen that the content recommended by the system of this article in each dataset interface in the browser is very in line with the user's hobbies. However, the content-based recommendation system and collaborative filtering algorithm recommend the content recommended by the system is not very accurate. Because the new recommendation system is in the process of the recommending content, the evidence theory algorithm will link the user's interest with the item content to reduce the error of the recommendation.

And after the user has used it, this experiment also counts the user's experience after using a browser with different recommendation systems and the speed of the recommendation system's recommended content in the browser, as shown in Figure 9.

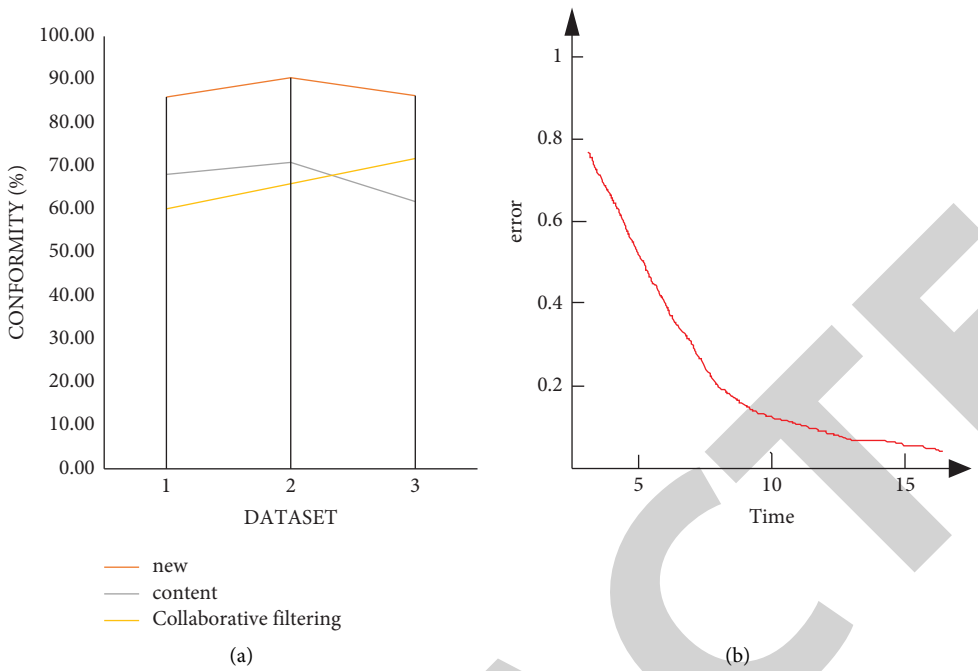

Figure 8: Recommended content changes. (a) Conformity. (b) New system error change.

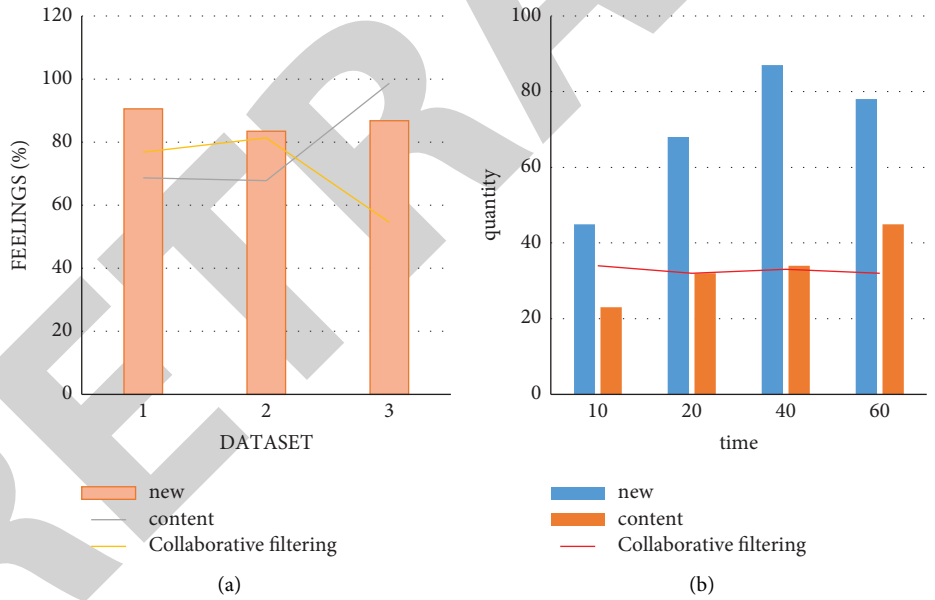

Figure 9: Experience and recommendation speed. (a) Experience. (b) Speed of recommending content.

From Figure 9(a), in browser dataset interface 1, the user's browser experience under the new recommendation system is relatively high, and the highest performance in the browser can reach 0.98. And compared to other recommendation systems, no matter which dataset interface is in the browser, the browser with the new recommendation system makes the user more experience, and the browser experience value can reach more than 80%. From Figure 9(b), the new recommender system recommends content faster than both the content-based recommender system and the collaborative filtering recommender system.

3.3. Experimental Summary. From the above experiments, the new recommendation system based on the evidence theory constructed in this article has high feasibility.

Compared with other recommendation systems, the new recommendation system is more accurate in grasping the interests and hobbies of users. It also has a good degree of recognition for the authenticity of the recommended content, and users have a stronger sense of experience for the content recommended by the new recommendation system. And from a comprehensive point of view, the performance of the new recommendation system for content recommendation can reach more than 80 points, which is better than other recommendation systems.

4. Discussion

The evidence theory and recommendation systems discussed in this article both belong to the category of artificial intelligence, and the evidence theory can help the development of many high-tech projects. Its development direction is very broad, and it can be combined with the neural network, to help solve some difficult problems to overcome. And the evidence theory can have the ability to handle the "uncertain" and "unknown" information, which can greatly improve the processing ability of modern information. The principle of the evidence theory can help the integration of information, and summarize and classify the data information on the network from the side, which greatly promotes the efficiency of information induction. The combined rules of multisource information given by the evidence theory can synthesize the basic reliability allocation from multiple sensors and get a new reliability assignment as the output, which provides a good tool to measure the credibility of information.

Recommendation system is a system already in use, and it will appear in the recommended content in the major browsers, which is the role of the recommendation system in the browser. The core of the recommendation system is the recommendation technology, which determines the quality of the recommendation results. The appropriate recommendation technology can not only reduce the cost generated in the recommendation calculation process, but also retain more old users and explore new users. Therefore, the current recommendation system is still in further research, but also in further optimization, only to better use for users, can improve user satisfaction in the process of use and keep the old users can also develop new users, so as to help the development of business. And the improvement of the recommendation system's ability to distinguish true and false information can promote the improvement of network order.

As the experiment in this article, the new recommendation system should optimize other recommendation system in terms of both content and recommendation speed. Moreover, because the recommendation system contains the evidence theory, the content recommended by the return and selection system is more real and very feasible, so users can not only improve their comfort in the use process but also improve their identification of the true and false information. Hence, it is highly feasible.

5. Conclusions

In this article, the principle of the evidence theory is discussed, and the combination of its evidence theory and the recommendation system can greatly improve the shortcomings of the existing recommendation systems. Existing recommendation systems cannot identify the authenticity of the recommended content, so the evidence theory can just help identify the authenticity of the recommended content. In addition, the evidence theory also has certain principles for the induction and classification of information content, which can promote the classification of the recommendation system. Moreover, the experiments in this article prove that the recommendation system in this article is better than the previous recommendation system in terms of the speed and content of the recommendation, which shows that the recommendation system studied in this article has high practicability. However, the new recommender system studied in this article still recovers the influence of many uncertain factors, so it is hoped that the shortcomings of the recommender system can be improved in future research.

Data Availability

No data were used to support this study.

Conflicts of Interest

The author declares that there are no potential conflicts of interest in this study.

Acknowledgments

This work was supported by the Scientific Research Planning Projects of Shaanxi Provincial Department of Education (no. 19JK0330).

References

[1] J. M. Garbutt, S. Dodd, and E. Walling, "Theory-based development of an implementation intervention to increase HPV vaccination in pediatric primary care practices," *Implementation Science*, vol. 13, no. 1, pp. 45-46, 2018.

[2] W. Qin, "Application analysis of basketball training system based on personalized recommendation systems," *Boletin Tecnico/Technical Bulletin*, vol. 55, no. 16, pp. 124–133, 2017.

[3] M. Q. Ha, D. N. Nguyen, V. C. Nguyen, T. Nagata, and H. C. Dam, "Evidence-based recommender system for high-entropy alloys," *Nature Computational Science*, vol. 1, no. 7, pp. 1–9, 2021.

[4] Y. Cui, "Intelligent recommendation system based on mathematical modeling in personalized data mining," *Mathematical Problems in Engineering*, vol. 2021, no. 3, Article ID 6672036, 11 pages, 2021.

[5] C. Cui, "Description of user interest in recommendation system based on vague set theory," *Xitong Gongcheng Lilun Yu Shijian/system Engineering Theory & Practice*, vol. 37, no. 3, pp. 752–760, 2017.

Hindawi
Scientific Programming
Volume 2022, Article ID 9280103, 11 pages
https://doi.org/10.1155/2022/9280103

Research Article

Internet of Things Information System and Clothing Computer Renderings Digital Art

Ningning Sun [1] **and Rui Kong** [2]

[1]*College of Fashion Art and Engineering, Beijing Institute of Fashion Technology, 100105 Beijing, China*
[2]*College of Art, Tianjin University of Commerce, Tianjin 300134, Tianjin, China*

Correspondence should be addressed to Ningning Sun; 20190012@bift.edu.cn and Rui Kong; kongrui@tjcu.edu.cn

Received 16 July 2022; Revised 31 August 2022; Accepted 7 September 2022; Published 28 September 2022

Academic Editor: Juan Vicente Capella Hernandez

The Internet of Things (IoT) is developing rapidly and is integrated into all aspects of life. Clothing is an indispensable part of meeting the basic needs of the human body, and its traditional functions include warmth, health care, decoration, and beauty. While as a special type of clothing that integrates multidisciplinary technology, smart clothing has a wider scope of action. With the update and iteration of science and technology, many technologies that originally belonged to nonclothing disciplines have also been applied to the clothing field. Accordingly, for the special clothing category of smart clothing based on embedded system, a set of design process that can be used for this category of smart clothing was proposed. Using this design process, an intelligent fire suit that can be used to protect the personal safety of firefighters and assist firefighters to cooperate was designed and implemented. Starting from the daily working environment and working characteristics of firefighters, this firefighting obedience analyzed the design points from the perspectives of clothing comfort, warning, toxic and harmful gas monitoring, and firefighters' cooperation. After testing, the test results of the outer layer fabric, waterproof and moisture-permeable layer fabric, and thermal insulation and comfort layer fabric of the fire suit all met the corresponding national standards; the monitoring sensitivity of harmful gases was high; it could achieve a "good" warning effect in a dark environment. Compared with ordinary firefighting suits, it was more comfortable under the subjective and objective test and scored 0.669 higher under the seven-point scale; its interactive performance met the actual needs. The clothing has complete functions and a complete feedback mechanism, which has a positive effect on ensuring the personal safety of firefighters.

1. Introduction

With the development of science and technology, smart clothing has gradually developed from the initial concept product to the direction of physical production. The initial smart clothing research focused on the field of military security. Since the late 1990s, the research on smart clothing has gradually developed into the field of health care, among which the most prominent is the smart clothing for body temperature monitoring. In the 21st century, smart clothing has truly entered the life of ordinary consumers, and this stage is also the initial stage of research on smart clothing. At present, the research on smart clothing is limited to the design and development of a specific category of smart clothing, and the design of clothing also focuses on functional design and implementation and involves less about the overall design process and design concepts of clothing. This paper mainly studied and discussed the design of smart clothing based on embedded system. The design theory and specific case design and production of this type of smart clothing were carried out from two aspects of embedded system and smart clothing, which provide ideas and case guidance for future smart clothing design based on embedded technology.

Computer renderings are an expression of a design language. Clothing transfer is a complex computer vision problem; Zhang et al. proposed a novel attention fusion model based on semantic features for clothing transfer, which can provide fine synthesis, high global consistency, and illusion of image authenticity [1]. With the rapid development

of computer network technology, digital computer technology has been widely put into practical use. Tang et al.'s analysis was based on the application of digital technology in architectural design and computer analysis of works of art [2]. Suarez et al. proposed a method to render pen and ink shadows in real time in large scenes, in which goal is to come up with a solution that starts with a 3D model containing realistic textures and materials to generate shaded renderings [3]. Contracted by Carnegie Mellon University with the National Energy Technology Laboratory and co-funded by the Northeast Gas Association, Andreazzi C has completed the overall system development, field testing, and magnetic leak sensor evaluation program for the next-generation Explorer-II (X–II) robotic nondestructive evaluation and primary visual gas detection platform [4]. The above scholars have used computer renderings well, but they have not fully explained the experimental process.

IoT is the Internet where everything is connected. With regard to the growing number of applications of IoT, Razzaque MA believed that these proposals for the future envisaged by IoT focus on wireless sensor networks (WSN) [5]. IoT, a dynamic global information network of Internet-connected objects, is becoming an integral part of the Internet of the future. In this issue, Perera et al. studied more than 100 smart IoT solutions on the market and analyzed the technologies, functions, and applications used [6]. To reduce the amount of data collected by IoT and improve the processing speed of big data, Xue et al. proposed a sampling scheme for compressed sensing. In order to solve the problem of high computational complexity of the compressed sensing algorithm, Xue et al. used the multiobjective particle family optimization algorithm to improve the search term of the gradient sparse reconstruction algorithm (GPSR-BB), which effectively improved the reconstruction accuracy of the algorithm [7]. The Internet grew out of revolutionary advances in electronics, telecommunications, information technology, devices, and applications. It started out as the Internet connecting people, but by 2008, it was connecting more things than people. Collier saw this exponential growth happening primarily as centralized monitoring and control of the IoT. For various reasons, this traditional approach to networking proved to be infeasible [8]. Although the above scholars have described the usefulness of IoT well, they have not specifically explained a certain aspect.

This study proposed a smart clothing design process based on embedded technology and proposed new concepts and references for the design of smart clothing. The innovation of this study: from the perspective of firefighters' personal safety and work needs, combining design theory and design practice and using this design theory, the design of intelligent fire suits can be extended to other types of intelligent clothing, which provides a discussion idea for the standardization and modularization of smart clothing design.

2. Wireless Sensor Technology Based on IoT Technology

IoT is a new generation of Internet where things are connected and interconnected, and it is also the development

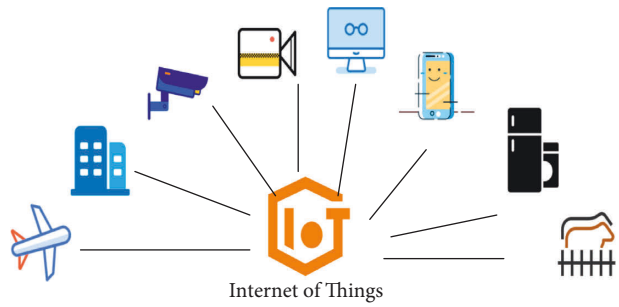

Figure 1: IoT.

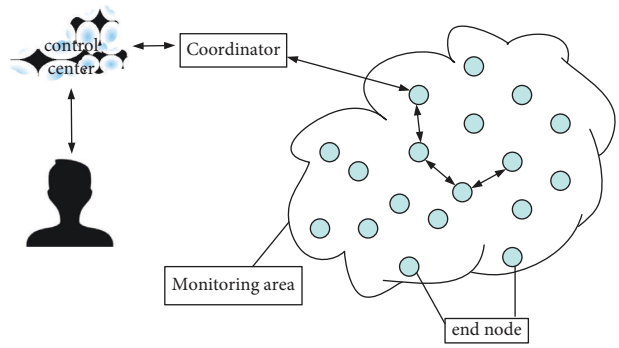

Figure 2: Wireless sensor network architecture.

direction of industrial informatization in the new era [9]. With the transformation and development of a new round of Industry 4.0 technology, it has effectively promoted the informatization and intelligent development of social production methods and people's lifestyles, making the allocation of social resources more reasonable and production efficiency more efficient, as shown in Figure 1.

Wireless sensor network is a network system composed of a large number of dynamic or static nodes deployed in the monitoring area through wireless communication protocols and is an important supporting technology of IoT. As shown in Figure 2, in a large-scale intelligent unmanned storage system, the wireless sensor network can realize the real-time monitoring of the storage environment, goods, and equipment, while the mobile intelligent body can complete the tasks of sorting, handling, stacking, and so on. The combination of the two has become a widespread IoT scenario, which can promote the intelligent and safe operation of the warehousing system.

2.1. Prediction-Based Potential Field Calculation

2.1.1. Dangerous Potential Field Prediction. Generally speaking, in dangerous scenarios, the environmental information monitored by wireless sensor network nodes is based on time-varying data (such as temperature and gas concentration), and the data changes follow certain rules and are time-dependent. Given a smoothing coefficient $\beta \in (0, 1)$, for the data $[y_i]$ of sensor node t_i in the time period [0, 1],

$$\begin{cases} r_s^{(1)} = \beta y_s + (1-\beta) r_{s-1}^{(1)}, \\ r_s^{(2)} = \beta r_s^{(1)} + (1-\beta) r_{s-1}^{(2)}, \\ r_s^{(3)} = \beta r_s^{(2)} + (1-\beta) r_{s-1}^{(3)}. \end{cases} \tag{1}$$

Predict the value y_{s+T} for T periods in the future:

$$y_{s+T} = C_T + D_T T + E_T T^2. \tag{2}$$

Among them,

$$\begin{cases} C_T = 3r_s^{(1)} - 3r_s^{(2)} + r_s^{(3)}, \\ D_T = \dfrac{\beta}{2(1-\beta)^2}\left[(6-5\beta) r_s^{(1)} - 2(5-4\beta) r_s^{(2)} + (4-3\beta) r_s^{(3)}\right], \\ E_T = \dfrac{\beta^2}{2(1-\beta)^2}\left[r_s^{(1)} - 2r_s^{(2)} + r_s^{(3)}\right]. \end{cases} \tag{3}$$

2.1.2. Establishment of Potential Field. In the wireless sensor network, after node t_i receives the navigation request sent by the navigation user, it will calculate the node's risk prediction value $g_f(i)$ according to the user's arrival time. Define the dangerous potential field of node t_i as $d_f(i)$ and the distance potential field as $d_r(i)$; then, there are

$$\begin{aligned} d_f(i) &= \frac{g_f(i)}{g_{\text{threshold}}}, \\ d_r(i) &= \frac{g_r(i)}{g_{\max}}, \end{aligned} \tag{4}$$

where $g_{\text{threshold}}$ is the danger threshold and $g_{\max}$ is the maximum distance.

The total potential field of the node is composed of the danger potential field $d_f(i)$ and the distance potential field $d_r(i)$ according to a certain weight. Define the total potential field of node t_i at a certain moment as $d(i)$; then, there are

$$F(i) = \alpha F_f(i) + (1-\alpha) F_r(i). \tag{5}$$

2.2. Prediction-Based Algorithms. The origin t_i (usually the user by default) starts to send navigation request information to its neighbor node $(M)t_i$ [10]. After the neighbor node t_j receives the navigation request, it estimates the user's arrival time t according to its distance h from the starting point:

$$t = \frac{h}{v}. \tag{6}$$

In formula (7), s is the speed of the navigating user. Based on the arrival time t, calculate the forecast period K:

$$K = \left[\frac{t}{K_f}\right], \tag{7}$$

where K_f is the monitoring period of the node dataset $\{y_r\}$. Then, use the cubic exponential smoothing model to predict its risk value, assuming that the minimum total potential field value fed back by all neighbor nodes $(M)t_i$ is $D_{\min}$:

$$D_{\min} = \min\left\{D(s), t_j \in M(t_i)\right\}. \tag{8}$$

Assuming that the observed dataset $Y = \{y, i = 1, 2, 3, \ldots, k\}$ of k nodes in a space is known, to find the observed value of the $k+1$th unknown node in the space, the mathematical model is as

$$y_{k+1} = \frac{\sum_{j=1}^{k} y_j / f_j^p}{\sum_{j=1}^{k} 1/f_j^p}. \tag{9}$$

2.3. Evaluation Indicators. In the experiment, the following indicators are used to measure the performance of the prediction-based wireless sensor network algorithm.

2.3.1. Average Path Length

$$k_{\text{avg}} = \frac{1}{n}\sum_{j=1}^{n} k_j, \tag{10}$$

where k_j is the length of the navigation path corresponding to user j and n is the number of navigation users.

2.3.2. The Maximum Hazard Intensity of the Average Path. For a path containing m landmark nodes, it is calculated as

$$G_{\max} = \max\left(g_f(j)\right), j = 1, 2, 3, \ldots, m. \tag{11}$$

2.3.3. Average Path Hazard Value. In emergencies, such as indoor fires and toxic gas leaks, the degree of danger is related to the level of danger and the length of time; the user is exposed to in the environment; then, define the hazard value between two signpost nodes as

$$F_{j,i} = \frac{r_{ji}\left(g_f(j) + g_f(i)\right)}{2}, \tag{12}$$

where r_{ji} is the time required for the user to go from node t_i to node t_j and $g_f(j)$ and $g_f(i)$ are the risk values of the user at nodes t_i and t_j, respectively. Define the path risk as

$$F = \sum_{i=1}^{m-1} F_{i,i+1}, \tag{13}$$

where i is the serial number of the road sign node and m is the total number of nodes in the path, that is,

$$F_{\text{avg}} = \frac{1}{n}\sum_{j=1}^{n} F_j. \tag{14}$$

2.4. Local Algorithm of Mobile Agent Based on Sensor Network. Suppose there are three known WSN nodes D, E, and F, whose coordinates are (a_0, b_0), (a_1, b_1), and (a_2, b_2), respectively, as shown in formula (16):

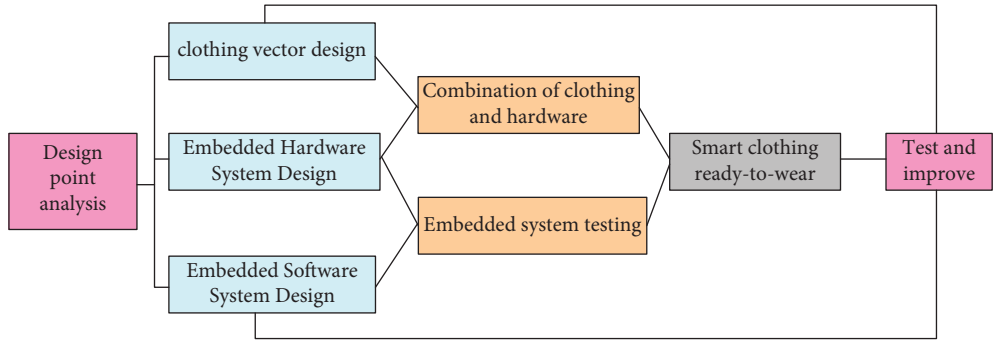

Figure 3: Smart clothing design process based on embedded system.

$$\begin{cases} \sqrt{(a_i - a_0)^2 + (b_i - b_0)^2} = h_0, \\ \sqrt{(a_i - a_1)^2 + (b_i - b_1)^2} = h_1, \\ \sqrt{(a_i - a_2)^2 + (b_i - b_2)^2} = h_2. \end{cases} \tag{15}$$

Then, the coordinates of node t_i can be obtained as

$$\begin{bmatrix} a \\ b_i \end{bmatrix} = \begin{bmatrix} 2(a_0 - a_2) 2(b_0 - b_2) \\ 2(a_1 - a_2) 2(b_1 - b_2) \end{bmatrix}^{-1} \begin{bmatrix} a_0^2 - a_2^2 + b_0^2 - b_2^2 + h_2^2 - h_0^2 \\ a_1^2 - a_2^2 + b_1^2 - b_2^2 + h_2^2 - h_1^2 \end{bmatrix}. \tag{16}$$

Then, the relationship between unknown node t_0 and m nodes with known coordinates satisfies formula (18):

$$\begin{cases} \sqrt{(a - a_1)^2 + (b - b_1)^2} = h_1, \\ \sqrt{(a - a_2)^2 + (b - b_2)^2} = h_2, \\ \sqrt{(a - a_3)^2 + (b - b_3)^2} = h_3, \\ \cdots \\ \sqrt{(a - a_m)^2 + (b - b_m)^2} = h_m. \end{cases} \tag{17}$$

Transform the following:

$$\begin{cases} a_1^2 - a_m^2 - 2(a_1 - a_m)a + b_1^2 - b_m^2 - 2(b_1 - b_m)b = h_1^2 - h_m^2, \\ a_{m-1}^2 - a_m^2 - 2(a_{m-1} - a_m)a + b_{m-1}^2 - b_m^2 - 2(b_{m-1} - b_m)b = h_{m-1}^2 - h_m^2. \end{cases} \tag{18}$$

Formula (19) can be expressed as $CX = d$ by a system of linear functions; among them,

$$\begin{cases} C = \begin{bmatrix} 2(a_1 - a_m) 2(b_1 - b_m) \\ \cdots \\ 2(a_{m-1} - a_m) 2(b_{m-1} - b_m) \end{bmatrix}, \\ X = \begin{bmatrix} a \\ b \end{bmatrix}, \\ d = \begin{bmatrix} a_1^2 - a_m^2 + b_1^2 - b_m^2 + h_m^2 - h_1^2 \\ a_{m-1}^2 - a_m^2 + b_{m-1}^2 - b_m^2 + h_m^2 - h_{m-1}^2 \end{bmatrix}. \end{cases} \tag{19}$$

3. Intelligent Clothing Design Based on Embedded System

3.1. Intelligent Clothing Design Process Based on Embedded System. Figure 3 is a smart clothing design process based on an embedded system, and relevant tests and improvements are carried out based on the ready-made smart clothing.

3.1.1. Analysis of the Main Points of Clothing Design. Clothing can be divided into multiple categories according to different demand objects and application scenarios. The design and development of smart clothing should also be analyzed according to specific needs, and clothing should be designed and produced according to specific needs.

(1) Application Scenario Analysis. According to the specific usage scenarios, the design focus of smart clothing is also different [11]. Users' functional requirements for smart clothing often need to be substituted into specific usage scenarios for analysis, rather than just designed from the perspective of functional requirements. Analysis from the application scene can make a perfect and detailed analysis of the design points of smart clothing.

(2) Confirmation of Clothing Design Points. The design points of smart clothing are confirmed according to the requirements of the demand object and the characteristics of the application scene. The confirmation of the design points should follow the order of function importance, and the conflicting design points should be selected according to their importance; the similar designs can be functionally integrated to reduce the workload.

3.1.2. Garment Carrier Design. The clothing carrier design is the design of the clothing itself in addition to the embedded system in the intelligent clothing system.

(1) Fabric Selection. The selection of fabrics for clothing should be selected according to specific user needs and usage scenarios; the function, safety and environmental protection, comfort, aesthetics, and other factors should be considered when choosing. Therefore, the selection of fabrics for smart clothing should often be based on the specific selection of different categories and parts according to relevant needs.

(2) Clothing Structure Design. Clothing structure design not only improves the overall aesthetics and comfort of clothing but also affects the stability of the embedded system in smart clothing. Through the special clothing structure design, on the premise of meeting the user's original comfort and functional requirements for clothing, it can also provide relevant support in the combination of embedded hardware and clothing [12].

3.2. Example of Smart Clothing Design Based on Embedded System. As a kind of special work clothing, firefighting clothing has high requirements on the characteristics of flame retardant and wear resistance of the clothing carrier and has corresponding national standards for regulations and constraints. Therefore, when designing, it is necessary to pay more attention to the performance requirements of the clothing body and to carry out functional design under the premise of meeting the requirements of the clothing carrier.

3.2.1. Analysis of the Main Points of Clothing Design. Firefighters are also responsible for firefighting and rescue work. From the point of view of safety protection and assisting work, this section intended to design a new type of firefighting suit with multiple functions, which is functionally designed based on the field work environment of firefighters.

(1) Analysis of Firefighters Working Scene. The working scenes of firefighters mainly include fire sites, toxic and harmful gas gathering places, dust gathering places, and small rescue places, among which fire sites are the most common. The fire environment is complex and harsh, and its characteristics include high temperature and low visibility, which have certain requirements for the flame retardancy and conspicuousness of firefighting clothing. Explosive gas or dust gathering places will explode when encountering electric sparks, which has certain requirements for the electronic equipment carried by firefighters. For the rescue of small places, firefighters cannot carry large rescue equipment or intercom equipment, which requires higher coordination and cooperation among firefighters. At the same time, due to the unpredictability of rescue times, firefighters need to be prepared to work for long hours, which also require lightness and comfort of firefighting suits.

(2) Design Points. Because firefighters often need to face the fire scene and other places with high risk factors, it is particularly important to design a firefighting uniform that meets the actual needs of firefighters. According to the design requirements of firefighting suits, this design expounded the design scheme of the new firefighting suits from four aspects: protective performance, comfort and lightness, safety, and interactive functions.

(3) Basic Performance. The most important function of firefighting clothing is to protect firefighters from various types of injuries, and it needs to protect the personal safety of firefighters. Its basic performance can be divided into protective performance, wearing warning performance, and safety performance. Considering the protective performance of fire protection clothing, fire protection clothing must have flame retardancy and heat insulation. Because firefighters work day and night, there may also be smoke, dust, and other substances that affect visibility in the workplace; in order to facilitate the normal operation of firefighters and carry out rescue work, the clothing needs to be recognizable [13]. Concentration detection is required for the explosive gas methane, propane, and toxic gas carbon monoxide that often appear in the fire field. However, the fire environment is complex and may be accompanied by unfavorable factors such as thick smoke. Therefore, from this perspective, it is necessary to locate and monitor firefighters.

(4) Interactive Performance. Existing firefighting uniforms focus on single personal protection, and the research on army cooperation and firefighters' psychological safety is relatively lacking. From the perspective of safety management and troop overall planning, in order to facilitate the coordination and cooperation between firefighters, firefighting clothing should have an interactive function to meet the real-time communication needs of the wearer.

(5) Comfort. Firefighters work long hours, intensely, and often face the fire. In the high-temperature environment of the fire site, there are also high requirements for the thermal and humidity comfort of clothing. Therefore, under the premise of satisfying the flame retardancy and thermal insulation of clothing, it is necessary to improve the wearing comfort and lightness of clothing as much as possible.

(6) Design Research Framework. The functional design was designed and implemented from four aspects: toxic and harmful gas monitoring, positioning monitoring, interactive function, and wireless transmission, so as to achieve the functions of voice interaction, real-time alarm, and web page display. In the test stage, the overall performance of the new fire suit was tested and evaluated from five aspects: clothing protection performance, clothing comfort, clothing conspicuousness, gas monitoring function, and data interaction performance [14].

3.2.2. Garment Carrier Design. The comfort of firefighters' work is directly related to the comfort of their clothing. Based on its special working environment, on the premise of taking into account the breathability and heat and humidity comfort of firefighting clothing, attention should be paid to the flame retardancy and wear resistance of clothing.

Figure 4: Structure diagram of the new fire suit.

(1) Clothing Structure Design. Figure 4 is a structural diagram of the new fire suit. In order to facilitate the operation, the overall structure of the new firefighting suit adopts a split design, and the structure is divided into an outer layer, a waterproof and moisture-permeable layer, and a thermal insulation and comfort layer.

The collar of the shirt can be adjusted according to the needs, and the cuffs and the feet can be adjusted loosely, as shown in Figure 4(a). In order to improve wearing comfort, this fire suit installs a detachable aerogel felt on the back and front of the heat-insulating comfort layer fabric, as shown in Figure 4(b). The aerogel felt is to attach the nanoscale aerogel to the flexible substrate of silica through a special process. Due to the good flame retardancy of the silica matrix, the thermal conductivity of the aerogel felt is extremely low, and the heat-resistant temperature can reach 650°C. The sponge-like or foam-like porous structure of aerogel itself can store still air, which can effectively improve the thermal insulation performance of clothing. Considering the safety of the operation, the trousers adopt a relatively stable strap design, and at the same time, the same elastic band as the cuff is set at the foot opening. To improve wearing comfort, install removable aerogel felt over the insulated comfort layer fabric at the knees of the fire suit trousers.

(2) Fabric Selection. Fire-fighting clothing has higher requirements on the outer fabric, and it needs to have flame retardant, wear-resistant, anti-static, and other properties. In this design, the outer fabric is a new type of anti-static aramid fabric, which is composed of 2% silver fiber and 98% aramid fiber. The waterproof and breathable layer fabric needs to have the effect of fast perspiration and moisture conduction; this part of the fabric is composed of 20% aramid 1414, 80% aramid 1313, and PTFE (polytetrafluoroethylene) film.

The thermal insulation and comfort layer fabric directly touches the skin, which requires a combination of flame retardant performance and comfort. This part of the fabric is composed of stitched aramid base fabric and aramid thermal insulation felt.

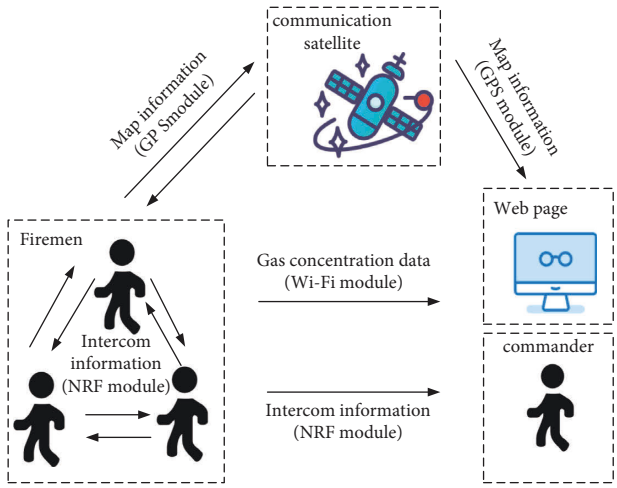

Figure 5: Wireless body area network design.

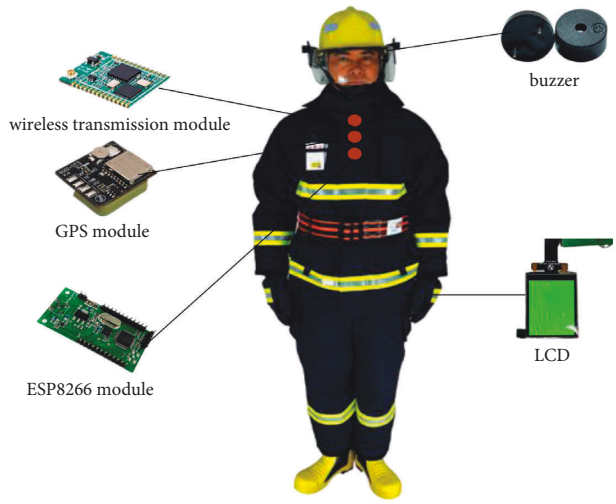

Figure 6: Hardware placement.

Table 1: Fabric performance test results.

Numbering	Vertical		Weft		Breaking strength (N)		Fabric combination TPP value
	Afterburning time (s)	Damaged length (mm)	Afterburning time (s)	Damaged length (mm)	Vertical	Weft	
A	0	5.8	0	5.6	1733.2	1543.2	
B	—	—	—	—	—	—	32
C	—	—	—	—	—	—	
Standard requirement	≤2	≤100	≤2	≤100	≥650	≥650	≥29

(3) Design of Warning Module. Since firefighters work day and night, the workplace also includes places with high dust concentration and low visibility. In order to facilitate the normal operation of firefighters and carry out rescue work, the clothing needs to be recognizable [15].

3.3. Embedded Software System Design

3.3.1. Working Principle. The wireless body area network in this design mainly includes NRF Module, GPS Module, and Wi-Fi Module. The NRF module is mainly used for voice communication between firefighters; the GPS module is mainly used for the transmission of positioning information between firefighters; the Wi-Fi module is mainly used for data transmission between firefighters and web pages, as shown in Figure 5.

When firefighters are working, the gas sensor in the fire suit system will monitor the relevant gas concentration in the environment and feed it back to the Arduino processor in the form of a digital signal. The processor determines whether the number exceeds a threshold and controls the state of the associated hardware accordingly. The GPS module will collect the positioning information of firefighters and feed it back to the display in the clothing system so that firefighters can view the location information of themselves and their teammates. The NRF module can support barrier-free voice communication between commanders and firefighters, which facilitates smooth work. The Wi-Fi module can be used to transmit the gas monitoring data and the positioning information of each firefighter to the computer web page of the command center, which is convenient for the unified dispatch of the command center.

3.3.2. Combination Design of Clothing and Hardware. Considering the actual wearing comfort, convenience and washability of the clothing for firefighters, the relevant hardware in this design adopted detachable design. In order to monitor the concentration of toxic and harmful gases in the flowing air, the gas sensor and the processor are placed on the front chest. The KY-038 module responsible for the intercom function and the buzzer are placed on the collar and the left/right ear of the mask respectively. In order to view the position of yourself and teammates on the map, the LCD screen is placed on the left glove. Because firefighters often need to face the fire, in order to ensure the stability and safety of the hardware system, the rest of the hardware modules are placed on the back of the jacket, specifically, as shown in Figure 6.

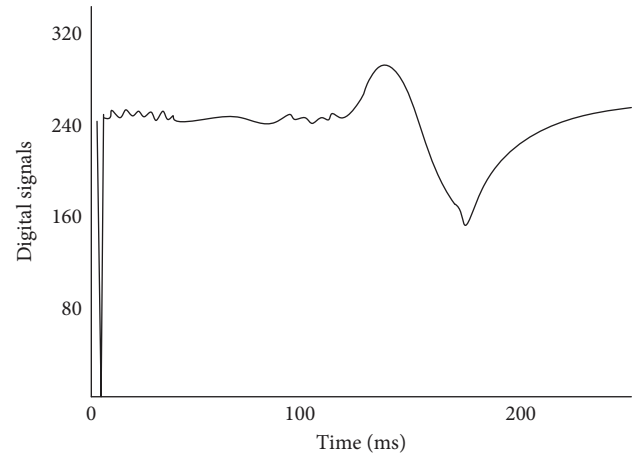

Figure 7: Serial plotter changes.

Table 2: Apparel conspicuous score.

Numbering	Light intensity (*lx*)	The average score
A	0.5	3.6
B	1	3.8
C	5	3.9

3.3.3. Clothing Testing and Improvement. In order to verify whether the comfort of the new fire suit has been improved and to test the safety monitoring function of the clothing, it is necessary to design experiments to test the above contents. The test for the new fire suit is divided into clothing safety test and clothing comfort test.

(1) Security Testing. According to the main points of the above functional design, the safety test of the new firefighting clothing can be divided into three aspects: the protective performance test of the clothing, the test of the harmful gas monitoring function, and the test of the conspicuousness of the clothing.

(2) Clothing Protection Performance Test. The test results of the fabric properties are shown in Table 1. Among them, the samples numbered A, B, and C are the outer fabric, the waterproof and moisture-permeable layer fabric, and the

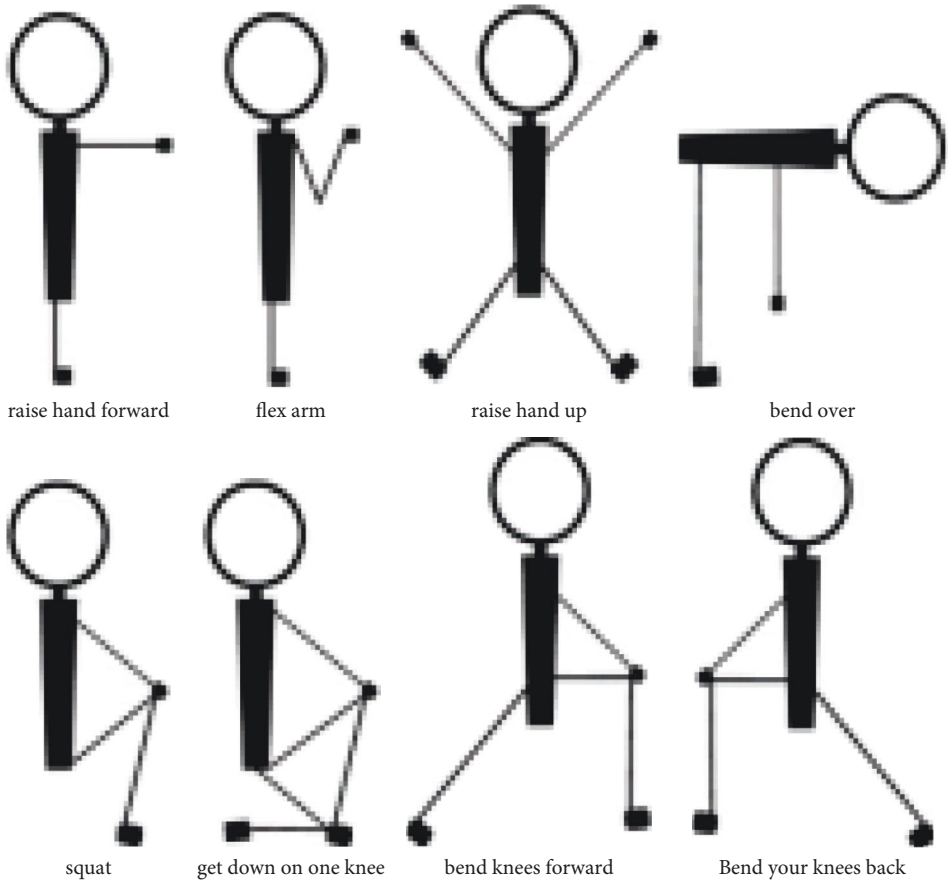

Figure 8: Schematic diagram of gymnastics movements.

thermal insulation and comfort layer fabric, respectively. The test results are in line with the corresponding national standards.

(3) Harmful Gas Monitoring Function Test. After the adjustment time, inject the corresponding gas, the digital signal rises sharply, and the buzzer starts to alarm; after the gas injection is stopped, the digital signal gradually becomes smaller, and after a period of time, the digital signal is lower than the threshold, and the buzzer stops the alarm. Its changes are shown in Figure 7.

(4) Clothing Eye-Catching Test. In order to simulate the dark environment that firefighters may encounter in their daily work, 10 people were selected for this test to evaluate firefighting suits. The results are shown in Table 2.

(5) Clothing Comfort Test. In order to investigate whether the comfort of the new fire suits is improved compared with ordinary fire suits, this study designed a clothing comfort test for the new fire suits and ordinary fire suits. The test is divided into objective evaluation and subjective evaluation. In the objective evaluation test, the relevant performance of clothing is judged by measuring the data of temperature and humidity on the skin surface [16]. Subjective evaluation is based on objective evaluation, and there are additional evaluation indicators for clothing thermal sensation and overall comfort. The test finally compared the results of the subjective and objective evaluations to test the consistency of the subjective and objective evaluations.

(6) Objective Evaluation of Comfort

(7) Objective Evaluation of Experimental Design. In order to simulate the climatic environment of high temperature and high humidity in the fire field, the relevant parameters of the artificial climate chamber are set as the temperature of 35°C, the humidity of 65%, and the wind speed below 0.1 m/s [17]. At the same time, in order to ensure the consistency of the relevant conditions of the two garments, the improved firefighting suit and the ordinary firefighting suit were uniformly washed and dried before the experiment and placed in a climate room for 24 hours in advance.

In order to reflect the characteristics that the work intensity of firefighters increases with time during daily work and to understand the relevant characteristics of clothing when firefighters are resting, do six gymnastics according to the designed movements. The design of gymnastics movements is organized according to the daily activities of firefighters. It is mainly divided into forward extension, elbow bending, lifting, bending over, squatting, kneeling on one knee, and front lunge and back lunge. Specifically, as shown in Figure 8, the time is 10 minutes, and the fifth stage is 10 minutes of sitting [18].

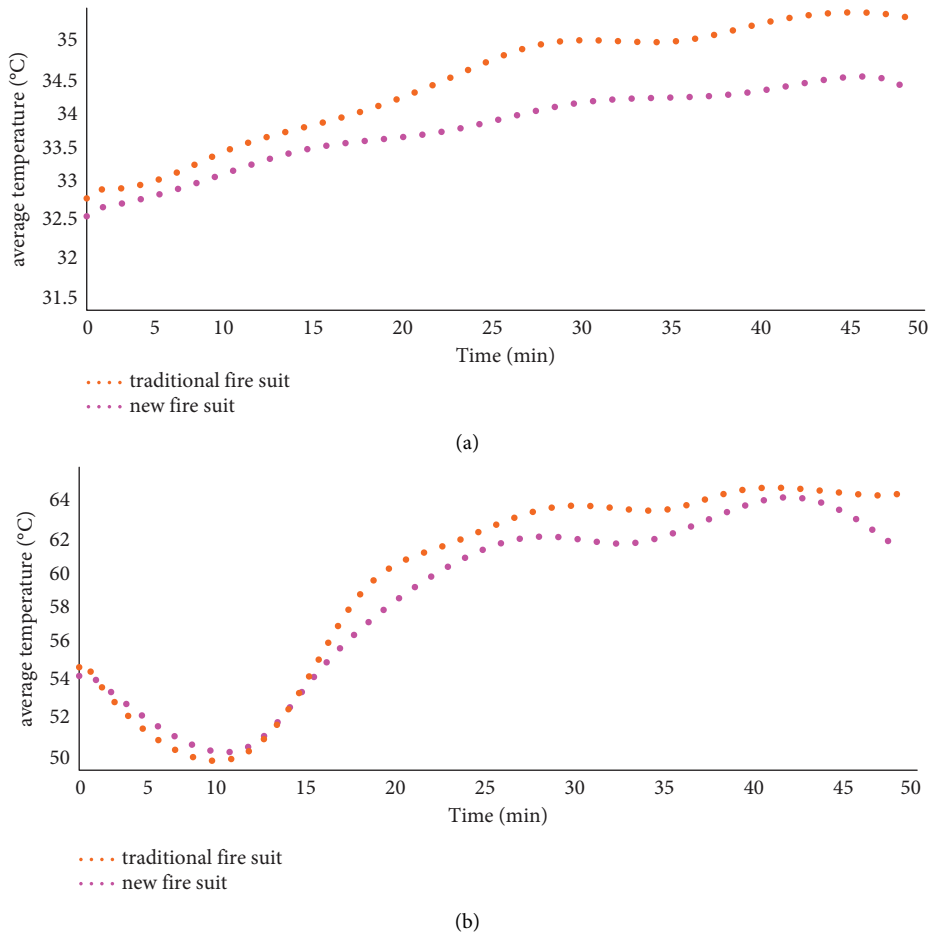

Figure 9: Objective evaluation data of comfort. (a) Sitting stage. (b) Slow walking stage.

Before the experiment starts, the test subjects need to enter the climate chamber 30 minutes in advance to adapt to the environment. The experimental process is the same as the subjective evaluation experiment, but the data are recorded every second. The experimental instrument used MSR145 temperature and humidity sensor to record the temperature and humidity data of the subject's clothing environment.

(8) Objectively Evaluate the Experimental Results. Figure 9(a) shows that, during the test, in the sitting stage, the average temperature of the two garments is not much different, but in the jogging stage, the temperature difference between the two garments increases with the increase of time and exercise intensity. In the fourth stage, the test subjects began to rest, and the temperature of the clothing dropped, and the temperature of the modified fire suit fell faster.

Figure 9(b) shows the variation of the average value of skin moisture on the armpits, front chest, back, thighs, and knees of 10 tested persons over time during the test; it can be seen that, in the stage of sitting still and walking slowly, the average humidity in the clothes of the two garments was not much different, and the change tended to be peaceful. However, as the exercise time becomes longer and the exercise intensity increases, the average humidity in the clothes wearing ordinary fire suits rose faster than the average humidity in the new fire suits. In the fourth stage, the humidity of the new fire suits decreased significantly faster than that of ordinary fire suits, which indicated that the new fire suits had better hygroscopicity and moisture dissipation [19].

(9) Subjective Evaluation of Comfort

(10) Subjective Comfort Index Confirmation. The questionnaire is formulated according to the classification of clothing comfort, and by listing the comfort indicators and allowing the subjects to select them, the firefighters' attention to different clothing comfort indicators can be determined [20].

Fifty professional firefighters from a city's fire brigade were selected to conduct a questionnaire survey to determine the comfort index. The age, height, and weight of the 50 subjects ($M \pm \mathrm{SD}$) were (25.9 ± 3.1) years, (179.1 ± 5.5) cm, and (79.6 ± 7.3) kg, respectively. Before the experiment, the subjects were informed of the relevant requirements and precautions of the questionnaire, and the subjects determined which aspects of clothing comfort they paid more attention to by selecting the variable indicators in the questionnaire.

The results of the questionnaire survey showed that, in the evaluation of clothing comfort, heat, wetness, stuffiness, stickiness, heaviness, restricted movement, hardness, and tightness were the most frequently selected indicators by firefighters.

Table 3: Fritz seven-level semantic difference scale.

Ruler feature	Sensory characteristics	Ruler feature	Sensory characteristics
1	Excellent	4	Moderate
2	Very good	5	Not too good
3	Better	6	Very bad

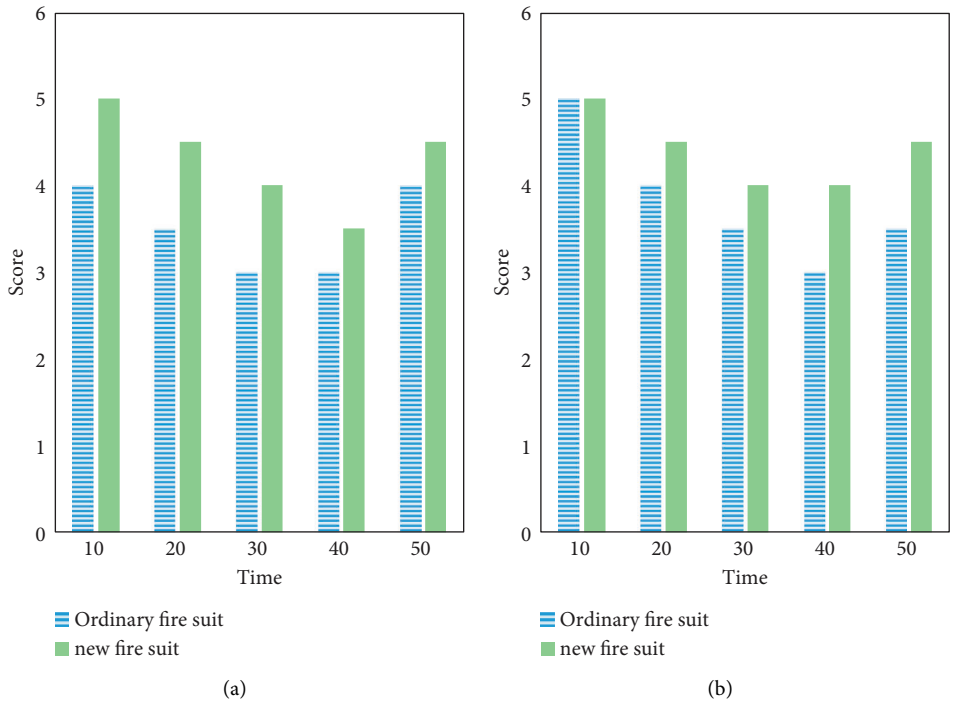

Figure 10: Subjective evaluation results. (a) Tester (a). (b) Tester (b).

(11) Experimental Procedure and Experimental Results. The subjective comfort test is consistent with the objective test; see Table 3 for details.

The test experiment of subjective evaluation is also divided into five stages. Figure 10 shows the results of subjective evaluation, and its score is taken from the average score of testers 10(a) and 10(b). It can be seen that the comfort of the new fire suits is better than that of ordinary fire suits [21].

4. Conclusion

This study started with the research status of firefighting suits, and from the perspective of improving the comfort, safety, and interactive performance of existing firefighting suits, on the premise of meeting national standards, the comfort and functionality of firefighting suits were improved and designed. The carrier of the fire suit was designed with a three-layer structure, that is, the outer layer, the waterproof and moisture-permeable layer, and the thermal insulation and comfort layer, and the phase change material was used to improve its comfort. Its functional design is in three aspects. One is to use gas sensors to monitor the concentration of relevant dangerous gases that may appear in the working environment, so as to achieve the purpose of warning and ensure the personal safety of firefighters at work. The second is to solve the problem of the complex working environment of firefighters, using GPS module to monitor the location of firefighters, and to help the Wi-Fi module to send the firefighter's location to the web page and display it on the web page. The third is to enhance the work coordination among firefighters in view of the difficulty in communication between firefighters and between firefighters and the command center during work. After evaluation, the protective performance of the fire suit had reached the national standard, with a score of 0.669 on the seven-point scale, and its comfort had been greatly improved compared with ordinary fire suits. At the same time, the monitoring sensitivity of combustible gas and toxic gas was high, and the interactive function could also meet the work needs of firefighters, which can improve the safety of firefighters at work. At the same time, this design also has some shortcomings: the use time of electronic products cannot be judged because it must be worn out in daily use." I have added it in the original text, please check it out.

Data Availability

No data were used to support this study.

Conflicts of Interest

The authors declare that there are no potential conflicts of interest in this study.

References

[1] Y. Zhang, L. Li, L. Song, R. Xie, and W. Zhang, "FACT: fused attention for clothing transfer with generative adversarial networks," *Proceedings of the AAAI Conference on Artificial Intelligence*, vol. 34, no. 07, pp. 12894–12901, 2020.

[2] C. Tang, J. Zhou, C. Tang, J. Zhou, C. Tang, and J. Zhou, "Computer aided architectural design and art analysis based on building digital technology," *Boletin Tecnico/Technical Bulletin*, vol. 55, no. 4, pp. 367–373, 2017.

[3] J. Suarez, F. Belhadj, and V. Boyer, "Real-time 3D rendering with hatching," *The Visual Computer*, vol. 33, no. 10, pp. 1319–1334, 2017.

[4] C. Andreazzi, V. Rademaker, R. Gentile, H. M. Herrera, A. M. Jansen, and P. S. Dandrea, "Wireless self-powered visual and NDE robotic inspection system for live gas distribution mains," *The Zoologist*, vol. 28, no. 3320, pp. 349-350, 2017.

[5] M. A. Razzaque, M. Milojevic-Jevric, A. Palade, and S. Clarke, "Middleware for internet of things: a survey," *IEEE Internet of Things Journal*, vol. 3, no. 1, pp. 70–95, 2016.

[6] C. Perera, C. H. Liu, and S. Jayawardena, "The emerging internet of things marketplace from an industrial perspective: a survey," *IEEE Transactions on Emerging Topics in Computing*, vol. 3, no. 4, pp. 585–598, 2015.

[7] J. W. Xue, X. K. Xu, and F. Zhang, "Big data dynamic compressive sensing system architecture and optimization algorithm for internet of things," *Discrete and Continuous Dynamical Systems - Series S*, vol. 8, no. 6, pp. 1401–1414, 2017.

[8] S. E. . Collier, "The emerging enernet: convergence of the smart grid with the internet of things," *IEEE Industry Applications Magazine*, vol. 23, no. 2, pp. 12–16, 2017.

[9] B. E. Adiji and T. I. Ibiwoye, "Effects of graphics and computer aided design software on the production of embroidered clothing in south western Nigeria," *Art and Design Review*, vol. 05, no. 4, pp. 230–240, 2017.

[10] S. Bako, T. Vogels, B. Mcwilliams et al., "Kernel-predicting convolutional networks for denoising Monte Carlo renderings," *ACM Transactions on Graphics*, vol. 36, no. 4, pp. 1–14, 2017.

[11] X. Chermain, F. Claux, and S. Merillou, "A microfacet-based BRDF for the accurate and efficient rendering of high-definition specular normal maps," *The Visual Computer*, vol. 36, no. 2, pp. 267–277, 2020.

[12] G. Bui, T. Le, B. Morago, and D. Ye, "Point-based rendering enhancement via deep learning," *The Visual Computer*, vol. 34, no. 2, pp. 1–13, 2018.

[13] H. M. Hillberg, Z. Levonian, D. Kluver, L. Terveen, and B. Hecht, "What I see is what you don't get: the effects of (not) seeing emoji rendering differences across platforms," *Proceedings of the Acm on Human Computer Interaction*, vol. 2, no. CSCW, pp. 1–24, 2018.

[14] T. Subileau, N. Mellado, D. Vanderhaeghe, and M. Paulin, "RayPortals: a light transport editing framework," *The Visual Computer*, vol. 33, no. 2, pp. 129–138, 2017.

[15] S. M. Kaya and Y. Afacan, "Effects of daylight design features on visitors' satisfaction of museums," *Indoor and Built Environment*, vol. 27, no. 10, pp. 1341–1356, 2018.

[16] B. Stojkoska and K. V. Trivodaliev, "A review of Internet of Things for smart home: challenges and solutions," *Journal of Cleaner Production*, vol. 140, pp. 1454–1464, 2017.

[17] H. Mostafa, T. Kerstin, and S. Regina, "Wearable devices in medical internet of things: scientific research and commercially available devices," *Healthcare Informatics Research*, vol. 23, no. 1, pp. 4–15, 2017.

[18] J. Lin, W. Yu, N. Zhang, X. Yang, H. Zhang, and W. Zhao, "A survey on internet of things: architecture, enabling technologies, security and privacy, and applications," *IEEE Internet of Things Journal*, vol. 4, no. 5, pp. 1125–1142, 2017.

[19] J. Singh, T. Pasquier, J. Bacon, H. Ko, and D. Eyers, "Twenty security considerations for cloud-supported internet of things," *IEEE Internet of Things Journal*, vol. 3, no. 3, pp. 269–284, 2016.

[20] Y. Yang, L. Wu, G. Yin, L. Li, and H. Zhao, "A survey on security and privacy issues in internet-of-things," *IEEE Internet of Things Journal*, vol. 4, no. 5, pp. 1250–1258, 2017.

[21] D. Iit, "Internet of things: architectures, protocols, and applications," *Journal of Electrical and Computer Engineering*, vol. 2017, no. 1, pp. 1–25, 2017.

Hindawi
Scientific Programming
Volume 2022, Article ID 9667979, 13 pages
https://doi.org/10.1155/2022/9667979

Research Article

Computer-Aided Analysis of Small Clear Space Intersection Tunnel and Heavy Load Railway Surrounding Rock Structure Dynamic Response Characteristics Analysis under Intelligent Manufacturing

Xiaotian Hao[1,2] **and Hailong Wang**[1,3]

[1]*School of Traffic and Transportation, Shi Jia Zhuang Tiedao University, ShiJiaZhuang 050043, HeBei, China*
[2]*School of Urban Construction Engineering, ChongQing Technology and Business Institute, ChongQing 400052, China*
[3]*School of Civil Engineering, HeBei University of Architecture, Zhangjiakou 075000, HeBei, China*

Correspondence should be addressed to Hailong Wang; bhxt196346@cqtbi.edu.cn

Received 25 June 2022; Revised 30 July 2022; Accepted 20 August 2022; Published 28 September 2022

Academic Editor: Juan Vicente Capella Hernandez

Among many tunnel construction projects, small clear tunnels have been the focus of urban rail transit construction in recent years. The purpose of this research work is to study the dynamic response characteristics of the surrounding rock structure of a heavy-duty railway with a small clearance crossing tunnel. It is proposed to analyze the dynamic response characteristics of the surrounding rock structure through the frequency response function. The vertical acceleration, tensile force, stress, and internal strength of the pipe section are specifically analyzed. The influence of the pipe joint and the assembly method on the dynamic response is also analyzed. The influencing factors of stability are analyzed from buried depth, clear distance, and surrounding rock grade. Studies have shown that the minimum clear distance of crossing tunnels increases nonlinearly with the increase of tunnel depth and gravity, and decreases nonlinearly with the increase of cohesion, internal friction angle, calculated internal friction angle, and lateral pressure coefficient. When other parameters are the same and when the side pressure coefficient is less than 1, the minimum clear distance is larger than that of the side pressure coefficient when it is equal to 1. When the vibration frequency exceeds 100 Hz, the coherence coefficient is basically close to 1, indicating that the frequency response function response result of this section is the most reliable. It is hoped that it can provide a reference for the dynamic stability analysis of the surrounding rock structure of the heavy-duty railway surrounding rock structure and the surrounding stratum and the research of structural vibration reduction technology for the small clearance crossing tunnel in the future.

1. Introduction

Since the beginning of the 21st century, with the continuous improvement of the national economy of the country, population mobility has increased year by year, which has brought great challenges to the country's transportation capacity. As the backbone of passenger transportation, railway transportation is bound to increase railway construction. Due to China's vast territory and complex geographical environment, in order to reduce the mileage of railways and shorten the time to reach the destination, the construction of interchange tunnels is bound to occur. At present, the phenomenon of close space crossing between tunnels is becoming more and more common. The dynamic response mechanism of the train under the vibration load and the transmission law of the tunnel structure is very complicated. The vibration response caused by the train is generally lower than the vibration level that causes structural damage to the building. As the train speed increases, the impact on the surrounding environment also increases, so train vibration has a great impact on the environment and other aspects. Under the long-term influence of the train's

vibration load, the tunnel and its surrounding ground have performance degradation problems. The spatial lateral shield under the action of train vibration load is being studied, and the dynamic response of the tunnel and its transmission law appear to be particularly important.

Since the lining structure is the main load-bearing structure of the tunnel, the impact of the tunnel's vibration response on the lining structure should be fully considered when constructing the tunnel. By studying the impact of train vibration load on the lining structure of the grade-crossing tunnel during the operation period, can not only help in guiding the construction of the grade-crossing tunnel but can also grasp the weak links of the grade-crossing tunnel during the operation period, thereby ensuring the safe passage of trains during the operation period. Therefore, the development of research studies on the three-dimensional crossing tunnel under the train vibration load can provide a certain basis for the planning and construction of rail transit, providing corresponding theoretical references for the scientific design and engineering safety construction of similar projects.

Tunnel shield technology has been widely used in subway construction in many cities. In large cities, tunnels inevitably pass between building foundations and deep bridges. Due to the many limitations of urban space in China, the distance between the two tunnels is relatively short. Therefore, the use of shielding technology to solve the mutual influence of the narrow construction of two tunnels is a technical problem to be solved urgently. Lv et al. analyzed the shield construction project of the two tunnels. The clearance of the tunnel is 2.6 m. The project is located between Tongdewei station and Shangbu station on the northern extension of the Guangzhou metro line 8. The main parameters used in his analysis are tunnel lining deformation and ground settlement. Numerical simulations were carried out for the construction process without and with isolation pile reinforcement. The simulation results were compared with the field monitoring data. The comparison shows that through reinforcement, the deformation of the tunnel lining and ground settlement can be greatly reduced. The impact of subway shield construction on the construction of the first subway tunnel will be greatly reduced, and the deformation and mutual influence of the width of the shield excavation net can also be greatly reduced. But the parameters he used in the analysis were not comprehensive enough for numerical simulation [1]. The construction of short-distance superimposed short-distance tunnels with small clear distances faces two major problems, mainly the influence of the tunnel structure and the superposition of the ground settlement caused by the tunnel construction. Taking the section from Hongling North station to Songgang station of Shenzhen metro line 7 as an example, the use of tunnel layers to reinforce ground joints was discussed. Liu et al. explained the first step of using mobile support trolleys in the first excavation section of the tunnel starting with the pipeline. The segment lining structure is strengthened, and technical measures such as control technology are used in the lead time of the shield tunnel excavation in the later period to effectively control the segment lining deformation and surface settlement and to achieve the expected effect. However, his experimental design for controlling the lining deformation and surface settlement of the segment is too complicated, and it is prone to deviation [2]. The Al-Omari RR study proposes experimental and finite element studies to study the behavior of the piled raft tunnel system in the sand. In the experimental work, a small model was tested in a sandbox, and the load was applied vertically to the raft through a hydraulic Jack. Five configurations of piles were tested in the laboratory. The influence of pile length (L), the number of piles in the group, and the distance between the top of the pile and the top of the tunnel surface (H) on the bearing capacity of the piled tunnel system are studied. The experimental work carried out on the piled raft tunnel system shows that for a constant (H) distance, the bearing capacity of the piled raft model increases with the increase of pile length (L), and for a constant pile length, it decreases with the increase of (H). The obtained results show that the finite element method and experimental modeling are reasonable. But he was unable to fully explain the bearing capacity by studying pile length and distance [3]. Zhang et al. proposed an analytical solution to study the response of existing tunnels caused by the excavation of a new underground tunnel. The existing tunnel was modeled with Timoshenko beams on the Kerr foundation, and the proposed analytical solutions were tested against centrifugal tests and field case studies in the literature. The results showed that the prediction results given by the proposed analysis method were consistent with the experimental test data and the onsite measurement results of the construction site. However, the experimental data collected during the centrifugal test is too large, and errors are prone to appearing in the analysis [4]. During the excavation of the underground powerhouse of Baihetan Hydropower Station, which is still under construction, the collapse of the stress structure control often occurs. In order to study the mechanism of this collapse evolution, Xiao et al. conducted in-situ experiments involving microseismic (MS) monitoring in the left main/auxiliary power chamber. He summarized and introduced the temporal and spatial characteristics of the collapse controlled by the stress structure. Onsite investigations, scanning electron microscopy, and mass spectrometry monitoring were used to investigate the collapse of the typical stress structure control that occurred during the monitoring period. These methods provide consistent results that tensile fracture is the most active rock fracture mechanism during the collapse evolution process controlled by the stressed structure. But the method he provided was not reflected in the process of tensile fracture [5]. He et al. proposed innovative cutting mining technology and column-free pressure relief technology in response to the complex construction technology and high roadway construction cost of the traditional technology of retaining lanes along the road. According to the movement law of the upper layer in the traditional technology of road construction along the ditch, the pressure relief mechanism for maintaining the roof along the ditch is being studied. In addition, taking into account different types of roof conditions, a number of mechanical models of "Enclosure and Bedrock Road Construction" were created, and the design formulas for the support resistance of each pavement were obtained. The results show that the upper roof is better

supported by presliding. This reduces the rotational deformation of the upper roof and reduces the impact load caused by roof cracks. The position of the roof fracture is moved to the side of the road, reducing the length of the roof cantilever beam, thereby reducing the additional load of the roadside support. However, the calculation process of the mechanical model and the designed resistance formula he proposed was too difficult, and further research is needed [6].

The innovation of this study is to deal with the cladding of the tunnel shield section and the dynamic response of the ground under the influence of the train vibration load. Using the indoor model test method, the acceleration response of the tunnel structure and the ground is tested, and the dynamic response characteristics in the time domain and frequency domain are analyzed. Then, the material parameters given to the stratum and structure are calculated. Through the three-dimensional dynamic numerical simulation calculation, the influence law of the dynamic characteristics of the different cross-section tunnels under different traffic conditions is studied, the influence of different influencing factors on the tunnel lining structure is simulated, and the parameter sensitivity analysis is carried out. On this basis, the partition of the influence of different influencing factors on the track bed structure along the track direction is divided; and the antivibration analysis is considered by increasing the thickness of the lining and strengthening the surrounding rock in a certain range.

2. Dynamic Response Characteristics of Heavy-Duty Railway Surrounding Rock Structure in Small Clearance Crossing Tunnel

2.1. Vibration Response of a Three-Dimensional Crossing Tunnel with Small Clearance. Crossing tunnels are typical geotechnical proximity projects. The construction of new tunnels will inevitably break the original rock-soil balance of in-situ stress and can produce additional effects on the existing tunnel structure, affecting the safe operation and even the structure of the existing tunnel safety. The dynamic load received by the small clearance interchange tunnel during the normal operation period is mainly the vibration load generated by the train operation [7]. The running train acts on the rails through the wheels, which in turn generates vibration. Therefore, the accurate expression of train vibration load is a very troublesome problem. When the train is running, the vibration load is applied to the tunnel invert and the tunnel bottom structure through the train wheel and rail, and then the vibration load is further transmitted to the adjacent tunnel through the surrounding rock outside the tunnel when the train is running, and then the space crosses the shield tunnel structure and its surrounding environment. The vibration generated by train operation propagates through the tunnel and surrounding soil and has an impact on the environment. Under the action of long-term train vibration load, the waterproof effect and durability of the railway tunnel structure will be significantly affected, and it will also affect the track's performance, ride comfort, passenger comfort, and normal train operations [8, 9]. The model of the grade-crossing tunnel is shown in Figure 1.

The overlapped tunnels at close distances affect each other significantly under the vibration load of the train. The smaller the clear distance between the two tunnels, the greater is the mutual influence. But for the lining structure, the increase in additional stress caused by train vibration is not large.

Before the dynamic load is applied, the surrounding rock has an initial stress, so the static calculation should be carried out first, followed by the dynamic calculation. The main calculation steps are the following: determine the boundary range of the model, then divide the unit grid to establish a three-dimensional numerical calculation model; and then, set the response static boundary conditions and structural mechanics parameters so as to obtain and analyze the vibration response data of the relevant structure.

2.2. Dynamic Response Characteristics of Surrounding Rock Structure. In order to explore the dynamic response of the heavy-duty railway surrounding the rock structure of the small clearance crossing tunnel, the strain state of the soil remains small under the action of vibration load [10, 11]. Special attention should be paid to the monitoring and measurement of the circumference of the tunnel with a small clear distance, a minimum clear distance, and the position of the tunnel vault, the middle of the invert, and the arch waist [12]. Therefore, the elastic model can be used to study the problem so that a similar relationship satisfies the elastic similarity law. The mechanical behavior of the tunnel structure and the soil can be expressed as

$$\begin{cases} D^r\varepsilon + kp = k\gamma, \\ \varepsilon^r = (\varepsilon_{11}, \varepsilon_{21}, \varepsilon_{22}, \varepsilon_{31}, \varepsilon_{32}). \end{cases} \tag{1}$$

In the formula, ε^r is the stress in all directions and ε is the strain.

$$\begin{cases} k\gamma = Dk\varepsilon, \\ k\varepsilon = Dkp. \end{cases} \tag{2}$$

In the formula, p is the density of the soil and γ is the acceleration due to gravity.

$$\begin{aligned} DE\frac{\partial^4 m^r i}{\partial t^2} + p_b m^r \gamma - p_b m^r k = 0, \\ DT\frac{\partial^2 m^r i}{\partial s^2} + p_b s^r \gamma - p_b s^r T = 0. \end{aligned} \tag{3}$$

Among them, m is a unit vector, s is the unit vector tangent to m, k is the tangent modulus, and T is the matrix that transforms stress into force.

$$D^r = \begin{vmatrix} \frac{\varepsilon}{\varepsilon x_1} 0 0 \frac{\varepsilon}{\varepsilon x_2} 0 \frac{\varepsilon}{\varepsilon x_3} \\ 0 \frac{\varepsilon}{\varepsilon x_2} 0 \frac{\varepsilon}{\varepsilon x_1} \frac{\varepsilon}{\varepsilon x_3} 0 \end{vmatrix}. \tag{4}$$

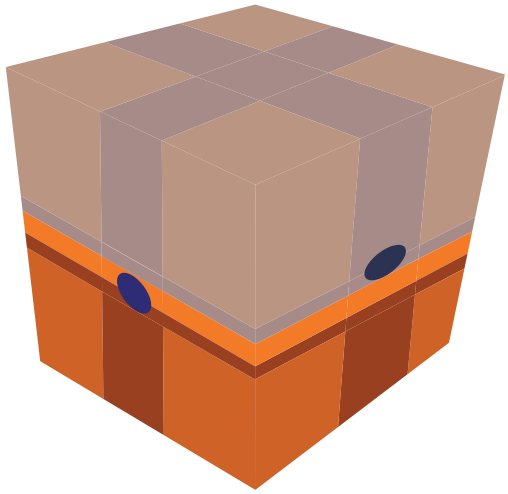

Figure 1: A schematic diagram of the cross-tunnel model.

If k and n are used to represent the physical quantities of the prototype and the model, respectively, then, the similarity ratio between the physical quantities of the model and the prototype can be expressed as

$$\begin{aligned}(d_n) &= g_d(d_k),\ (k_n) = g_n(k_n),\ (E_n),\\ (\varepsilon_n) &= g_\varepsilon(\varepsilon_n),\ (\gamma_k) = g_\gamma(\gamma_n),\ (k_n),\\ (s_n) &= g_s(s_n),\ (\phi_k) = g_n(\phi_n),\ (p_k).\end{aligned} \tag{5}$$

The physical quantities of the soil prototype and the model need to satisfy the balance equation, so they can be transformed into

$$(D^r)_k(\gamma)_n + (p)_k(k)_n = (p)_k(\gamma)_k, \tag{6}$$

$$(D^r)_n(\gamma)_p + (p)_n(k)_p = (p)_p(\gamma)_n. \tag{7}$$

By combining formulas (6) and (7), we get

$$\frac{1}{G_s}(D^r)_n G_\varepsilon(\varepsilon)_n + G_p(p)_n G_k(p)_n = G_p(p)_n. \tag{8}$$

The formula is the similar relationship between different physical quantities. Based on a comprehensive investigation of the functionality and reliability of the experiment, the geometric similarity ratio, the density similarity ratio, and the elasticity coefficient similarity ratio of this experiment are used to meet the similarity ratios of other physical quantities to determine [13, 14].

2.3. The Frequency Response Function. The dynamic response of the tunnel structure and the surrounding ground is not only related to the frequency spectrum characteristics of the vibration load but is also directly related to the amplitude of the applied load [15, 16]. The greater the load amplitude, the more obvious is the dynamic response. When performing dynamic response analysis in the frequency domain, in order to eliminate the influence of the load amplitude on the dynamic response, the frequency response function and the coherence coefficient are used to determine the fixed frequency sinusoidal vibration load and sweep frequency vibration load. The time domain results are processed under different frequency loads, and the dynamic response characteristics of the tunnel structure and the ground environment under different frequency loads are analyzed in detail [17, 18].

When analyzing the dynamic response characteristics in the frequency domain, in order to eliminate the influence of the load amplitude on the dynamic response, this study uses the frequency response function (FRF) and the coherence coefficient to analyze the time domain results under the fixed frequency sinusoidal vibration load and the swept frequency vibration load.

The frequency response function (FRF) is defined as the ratio of the acceleration response after Fourier transformation to the vibration load, which can be expressed as

$$F(\sigma) = \frac{T(\sigma)}{D(\sigma)} + 1. \tag{9}$$

In the formula, the variable $T(\sigma)$ in the frequency response function is the acceleration response and $D(\sigma)$ is the vibration load.

When performing specific calculations, according to the random vibration analysis theory, the data measured in the model experiment is regarded as the random vibration signal. First, the self-power spectral density function of the applied load and acceleration response and the cross-spectral density function between the two are obtained. It can be transformed into two forms given as follows [19]:

$$\begin{aligned}F_1(\sigma) &= \frac{V_{FA}(\sigma)}{V_{FF}(\sigma)} + 1,\\ F_2(\sigma) &= \frac{S_{PB}(\sigma)}{S_{PT}(\sigma)} + 1.\end{aligned} \tag{10}$$

In the formula, $S_{FA}(\sigma), S_{FF}(\sigma)$ is the self-power spectral density function of acceleration and vibration load, and $V_{FA}(\sigma), V_{FF}(\sigma)$ is the cross-spectral density function of acceleration and vibration load. The specific calculation process is

$$\begin{aligned}V_{FA}(\sigma) &= \frac{1}{M_V^2}\left(\sum_{m=0}^{m_v-1} B(s)_m\right),\\ V_{FF}(\sigma) &= \frac{1}{M_v^2}\left(\sum_{m=0}^{M_v-1} V(s)_m e^{-2}\right)^2.\end{aligned} \tag{11}$$

In the formula, i is the narrative unit, e is the natural constant, and $F(S)_n$ is the measured vibration load.

In theory, when calculating the frequency response function, there are interferences such as noise during the measurement process. The influence of noise on the measured vibration load can be calculated as

$$\theta^2(\sigma) = \frac{V_{FA}(\sigma)V_{AA}(\sigma)}{V_{FF}(\sigma)V_{AF}(\sigma)}. \tag{12}$$

The coherence coefficient represents the correlation between the measured dynamic response and the applied load, and its amplitude is between 0 and 1. The higher the amplitude, the higher is the correlation between the dynamic response and the applied load. If the value is 1, it indicates that the measured dynamic response is completely caused by the applied vibration load, and the reliability of the result is the highest.

2.4. Elastic-Plastic Stress Distribution of the Surrounding Rock of the Tunnel. When the lateral pressure coefficient is $\varphi = 1$, it balances the initial stress in all directions of the surrounding rock and represents the state of axial load or hydrostatic pressure. The trend of the surrounding rock at a specific point must satisfy the balanced differential equation of the polar coordinate system.

$$\frac{\varphi_s}{\bar{\omega}_s} + \frac{1\varphi\pi_{r\varepsilon}}{s\varphi} + \frac{\varphi_s - \varphi_\varepsilon}{s} + Q_s = 0. \tag{13}$$

When $\varphi = 1$, assuming $Q_s = 0$, the radius of the plastic zone is the largest, where the stress concentration is the most serious, and the stress in the plastic zone has nothing to do with the original rock stress, and for the plastic zone, it can be simplified to

$$\frac{c\varphi_{sd}}{c_s} + \frac{\varphi_{sd} - \varphi_{\varepsilon d}}{s} = 0. \tag{14}$$

In the formula, φ_{sd} and $\varphi_{\varepsilon d}$ are the radial and tangential normal stresses in the plastic zone, respectively.

According to the Mohr-Coulomb criterion, the Mohr voltage cycle corresponding to the voltage state at any point on the plastic zone must be in contact with the strength shell. It must meet the following conditions:

$$\begin{cases} \varphi_{sd} = \dfrac{\varphi_c}{\lambda - 1}\left[\left(\dfrac{s}{s_a}\right)^{\lambda - 1} - 1\right], \\ \varphi_1 = \lambda\varphi_3 + \varphi_c. \end{cases} \tag{15}$$

From the abovementioned derivation, it can be analyzed that when $\varphi = 1$, the plastic structure of the surrounding rock appears on both sides of the cavern. The rock pillars between the crossing tunnels are usually larger than the rock pillars in the middle of the existing tunnel. The larger the radius of the plastic zone, the more concentrated is the stress.

3. Computer-Aided Analysis of the Dynamic Response Characteristics of the Surrounding Rock Structure of the Heavy-Duty Railway with a Small Clearance Crossing Tunnel

Crossing tunnels are typical geotechnical proximity projects. The construction of new tunnels will inevitably break the original rock-soil balance of in-situ stress and produce additional effects on the existing tunnel structure, affecting the safe operation and even the structure of the existing tunnel safety. The tunnel bottom structure is the main load-bearing structure of the heavy-duty railway of the grade-crossing tunnel, and the load size is mostly determined based on the experience of ordinary railway tunnels [20, 21]. The accurate theoretical calculation method can quickly calculate the dynamic load on the surface of each structural layer and determine the initial load conditions of the calculation model, which has important guiding significance for the design of heavy-duty railway tunnels [22, 23].

3.1. Experimental Methods and Procedures. In order to analyze the elastoplastic state of adjacent horizontal small-distance tunnels, the analytical solution of the penetration radius of the plastic zone of the surrounding rock of the small-distance tunnel is given, and the mutual influence between the two crossing tunnels is calculated. In order to analyze the dynamic response characteristics of the surrounding rock structure of the heavy-duty railway in the small clearance crossing tunnel, a computer-aided analysis block diagram of the dynamic response characteristics of the surrounding rock structure of the grade-crossing tunnel is presented in Figure 2.

The specific process of the test is as follows:

(1) Preliminary material preparation for the test includes the production of model tunnels, the preparation of model stratum materials, and the pretest of the equipment required for the test (whether the test equipment can work normally).

(2) After completing the model frame, the filling process can be roughly divided into three stages according to the filling height. The model soil at the bottom of the tunnel model is filled, the model soil at the top of the tunnel model is filled, and the model soil is filled to the final design height [24, 25]. Each filling process needs to be subdivided into multiple filling layers, and each filling layer must achieve a given degree of compression. The specific operation process is as follows. First, loosen the soil of a certain quality (calculated by dividing the expected filling amount by the density), then compact the whole with an I-beam, and finally hit the soil with a stone hammer. By controlling the number of boxes and the number of percussions, it is ensured that the planks at the corners of the model box are compressed to exceed the expected ground height [26, 27].

(3) We then carry out tunnel model embedment and acceleration sensor layout work. This stage and the previous stage are intersected. After completing the first filling stage, we place the tunnel model into the model box and then continue the subsequent filling process [28]. The burying of the acceleration sensor inside the soil is carried out layer by layer. The time for burying each layer is selected when the current soil layer height is greater than the buried depth of the measuring point by 5 cm. When burying, a small hole with a depth of 5 cm at the measuring point is

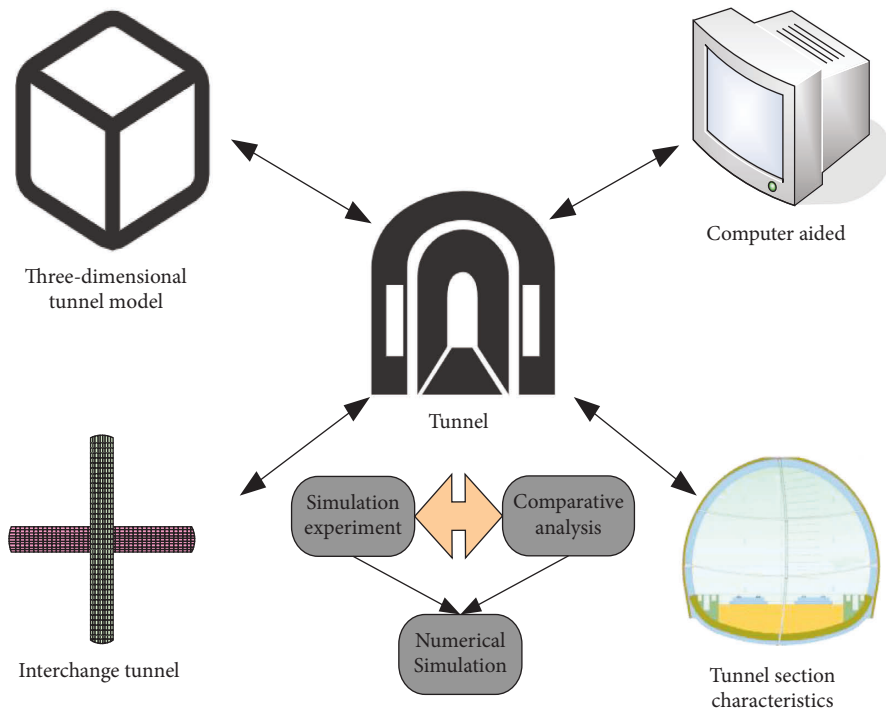

Figure 2: Frame diagram of the computer-aided analysis of dynamic response characteristics of the surrounding rock structure of the grade-crossing tunnel.

dug with a self-made tool, and then we bury the measuring point and finally fill it with compaction. The measuring points on the surface of the soil are laid directly after filling the model soil without drilling holes [29, 30].

(4) We then carry out the wiring of test equipment and carry out specific test work. The test is divided into three groups according to the type of applied load: fixed frequency sinusoidal vibration load, swept frequency vibration load, and train vibration load. Among them, the sinusoidal vibration load frequency is set to 60 Hz, 120 Hz, and 180 Hz, and the dynamic response under 3 kinds of amplitudes (excitation voltages are 800 mV, 1000 mV, and 1200 mV, respectively) is tested at the same time. The sweep frequency vibration load tests the dynamic response under 3 kinds of frequency sweep cycles, 2 kinds of frequency directions, and 3 kinds of excitation voltage, and the test time of each group is guaranteed to be more than 3 times of the frequency sweep cycle. The test time of each group of train vibration loads is also guaranteed to be more than 3 cycles.

This article uses computer-aided analysis, and the computer-aided analysis process is shown in Figure 3.

The computer-aided information analysis system consists of four parts: the database, the information analysis method, and the information analysis software and information analysis staff. Among them, the database is the foundation, and the database resources of the database system are the objects of information analysis. Information analysis methods are tools, and choosing mature, logical, and effective methods is an important prerequisite for information analysis.

3.2. Surrounding Rock Materials. In the process of designing the model test, considering that the overall rock is less affected by scouring during the short test period, it is difficult to have an ideal void form during the test, so it was decided to study the soil surrounding the rock as the object. According to the "Code for Design of Foundations for Buildings" (GB50007-2011), soil (including rocks) can be divided into six categories, namely rock, gravel soil, sand, silt, cohesive soil, and artificial fill. According to the geotechnical classification standard for railway engineering (tb10077-2001), general soil can be divided into gravel soil, sandy soil, silt, and cohesive soil. The structural model of the tunnel bottom is simplified to a certain extent. The inverted arch filling and inverted arch structure are regarded as a whole structure, and the gypsum material is used for prefabrication, as shown in Table 1.

The process of groundwater erosion on the surrounding rock at the bottom of the heavy-duty railway tunnel structure due to the dynamic load of the heavy-duty train is studied. The qualitative analysis of the three types of soil surrounding the rocks: pebble soil, cohesive soil, and sandy soil is carried out. The form of voids and the distribution characteristics of voids appeared during the long-term erosion of groundwater, and the distribution of contact pressure and Earth pressure at the bottom of the tunnel is quantitatively studied. The gravity, strength, and deformation characteristics of similar materials that simulate the

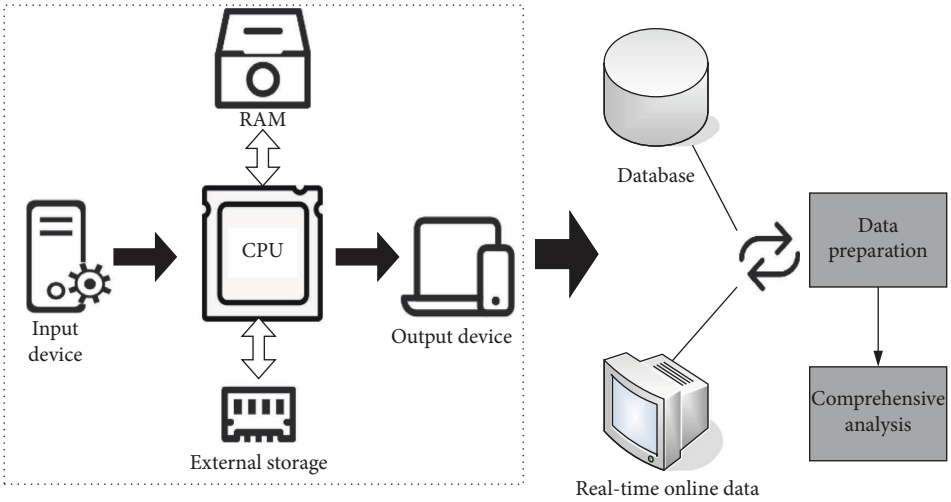

Figure 3: Computer-aided analysis process.

Table 1: Surrounding rock material.

Category	Soil name	Classification standard	Particle size (mm)	Specification
Gravel soil	Boulder soil/rock soil/pebble soil	Gradation of soil particles	>200/20/2	50%
Sandy soil	Gravel/coarse sand/nakasago/fine sand	Gradation of soil particles	>0.5/0.25/0.075	50%/85%
Silt	Silt	—	>0.075	Plasticity index ≤10
Clay soil	Silty clay/clay	Plasticity index	$10 < Ip \leq 17$	

surrounding rock must meet the geomechanical similarity requirements. We then determine the value range of the physical and mechanical parameters of the surrounding rock model material, as shown in Table 2.

When simulating cohesive soil, sandy soil, and sandy gravel soil under V-level surrounding rock conditions, the mechanical parameters of similar materials should meet the value range in Table 2 as much as possible.

Table 2: Material parameters of the surrounding rock model.

Class V surrounding rock	Prototype	Model
Severe	17–20	17–20
Deformation modulus	1000–2000	50–100
Poisson's ratio	0.35–0.45	0.35–0.45
Internal friction angle	20–27	20–27
Cohesion	50–200	2.5–10

4. Computer-Aided Analysis of the Dynamic Response Characteristics of the Surrounding Rock Structure of the Heavy-Duty Railway with Small Clearance Crossing Tunnels

4.1. Dynamic Response Characteristics of The Surrounding Rock Structure. Because the train connectivity has strict requirements on the vertical displacement of the track, the maximum vertical vibration displacement response value at the cross-tunnel track bed structure of the three-dimensional crossing tunnel is taken as the numerical value of the study.

It can be seen from Tables 3 and 4 that the grade-crossing tunnels at different train speeds and at different clear distances affect the partitions along the track direction.

With the increase in train speed, the distance between the strong and weak affected areas and the intersection is increased, but the increase in the distance is not very obvious. Under the action of the downward train load, it will affect the displacement and acceleration response of the observation points of the conventional section of the upper-span tunnel. Although smaller, it will have a certain impact on the interchange section. Among them, the influence of the downstream train load on the maximum vertical displacement and the maximum acceleration response of the overpass tunnel is smaller than the influence of the upward train load on the maximum vertical displacement of the underpass tunnel.

It can be seen from the different clear distance divisions that the tunnel clear distance has a greater impact on the maximum vertical displacement of the track bed. When the clear distance exceeds 25 m, there is only a certain range of weakly affected areas along the track direction. Under the load of the upper and lower crossing trains, the influence of the displacement and acceleration response of each observation point of the upper and lower cross-section will increase to a certain extent. Compared with the upward load, for the upper-span tunnel, the maximum downward vertical displacement of the track bed has increased by 30.2%, and the acceleration has increased by 0.16 m/s^2.

4.2. Simulation of the Indoor Model Experiment Analysis. Using indoor model testing and finite element numerical simulation, the process of groundwater scouring the surrounding rock at the bottom of a heavy-duty railway tunnel

Table 3: Influence of different train speeds on the division of track direction.

Train speed (km/h)	Influence zone			
	Destruction zone	Strong influence zone (W)	Weak impact zone (W)	Unaffected zone (W)
260	—	0~0.67	0.67~1.4	>1.4
230	—	0~0.87	0.87~1.6	>1.6
360	0~0.27 W	0.27~1	1~1.8	>1.8

Table 4: The effect of different clear distances on the area division along the track.

Clear distance (m)	Influence zone			
	Destruction zone	Strong influence zone	Weak impact zone (W)	Unaffected zone (W)
5	0~0.27 W	0.27~0.67 W	0.67~1.8	>1.8
10	—	0~0.87 W	0.87~1.6	>1.6
15	—	0~0.73 W	0.73~1.6	>1.6
20	—	—	0~1.13	>1.13

bottom structure due to the dynamic load of a heavy-duty train during operation is studied, and the variation law of contact pressure and the transmission characteristics of Earth pressure under void state are quantitatively analyzed.

In order to reflect the contact pressure distribution under the floor structure, the maximum value of the contact pressure of the three surrounding rock materials was extracted. The change curve of the contact pressure when there is water and when there is no water is shown in Figure 4.

When the surrounding rock at the bottom of the tunnel is in a water-rich condition, the additional value of the contact pressure at the two measuring points below the center line and the bottom left decreases slightly during the excitation process.

As shown in Figure 5, when the surrounding rock of the sandy soil at the bottom of the tunnel is in anhydrous conditions, the additional value of the contact pressure at the measurement points below the center line and the bottom left of the center line increases with the change in the excitation time. The distribution pattern of the sandy soil surrounding the rock after vibration is the same. The appearance of the hard soil block on the right side of the center line indicates that this location will bear greater stress, while other parts of the surrounding rock are continuously weakened by scouring due to pumping action. As a result, the contact pressure is becoming smaller and smaller.

The relationship between the model parameters and the selectable granular material parameters is established through corresponding numerical simulation experiments. This process is usually called calibration. The simulation of the numerical test is roughly divided into three steps: sample generation, consolidation, and loading. The model is surrounded by 4 walls; the upper and lower walls simulate the loading of the sample, and the four lateral walls are used to simulate the confining pressure. The loading of the sample is simulated by controlling the moving speed of the upper and lower walls. During the entire experiment, the speed of all lateral walls is automatically controlled by the servo mechanism to keep the confining pressure at a certain value.

The hydrodynamic pressure at the bottom of the tunnel is the main factor affecting the rate of erosion and deterioration of the surrounding rock, so it is a key parameter in the numerical calculation and analysis. However, the actual hydrodynamic pressure changes continuously with geological conditions and train operations and involves complex fluid-solid coupling and mechanical principles. Therefore, the hydrodynamic pressure value in the particle flow calculation is mainly based on onsite monitoring data. As shown in Figure 6.

According to the time history curve of invert pore water pressure obtained from field monitoring, the pore water pressure at each part of the tunnel bottom increases in varying degrees. The increase of pore water pressure at the bottom of the right ditch is the most obvious, with great added value; the pore water pressure at the left arch foot and right rail increases moderately. The long-term monitoring data show that the pore water pressure under the tunnel inverted arch still continues to increase one year after opening to traffic.

4.3. Vibration Load Analysis of a Small Clearance Intersecting Tunnel. Different sections of the tunnel lining structure have different effects on the dynamic response of different parts. To analyze the vertical vibration displacement, vibration acceleration, and principal stress of key parts of the tunnel lining structure, this study uses swept frequency vibration load and frequency response function (FRF) to obtain the dynamic response characteristics at different vibration frequencies and analyzes the reliability of the model test results. Due to the large fluctuation of the FRF curve, this study uses the 1/3 octave method to further process the vertical acceleration response results of the lining structure. 1/3 octave divides a given frequency range into successive bands using a constant percentage bandwidth, each band has an upper center frequency, and the ratio of the center frequencies to the lower band remains unchanged.

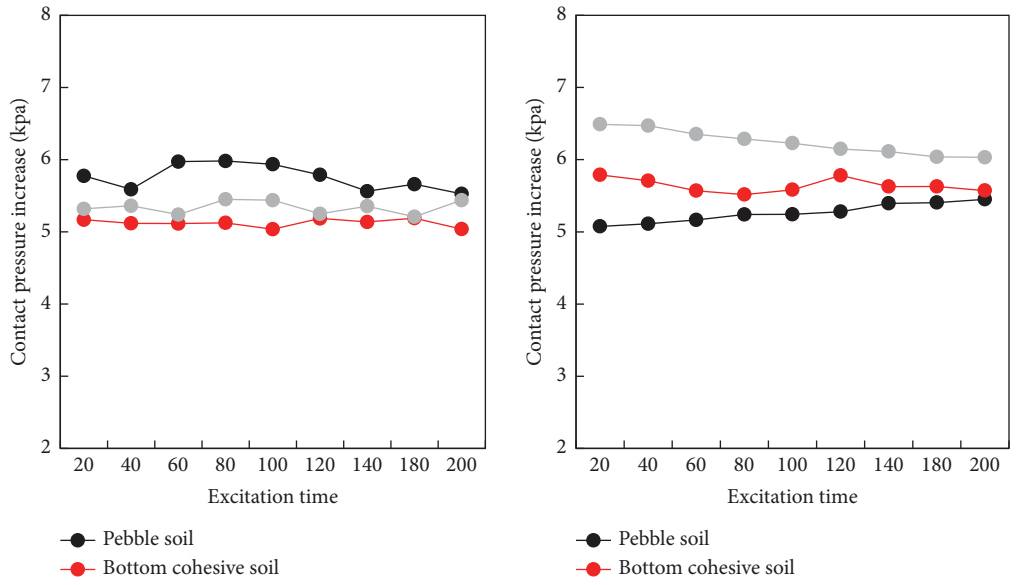

Figure 4: Change curve of the additional value of contact pressure when there is water.

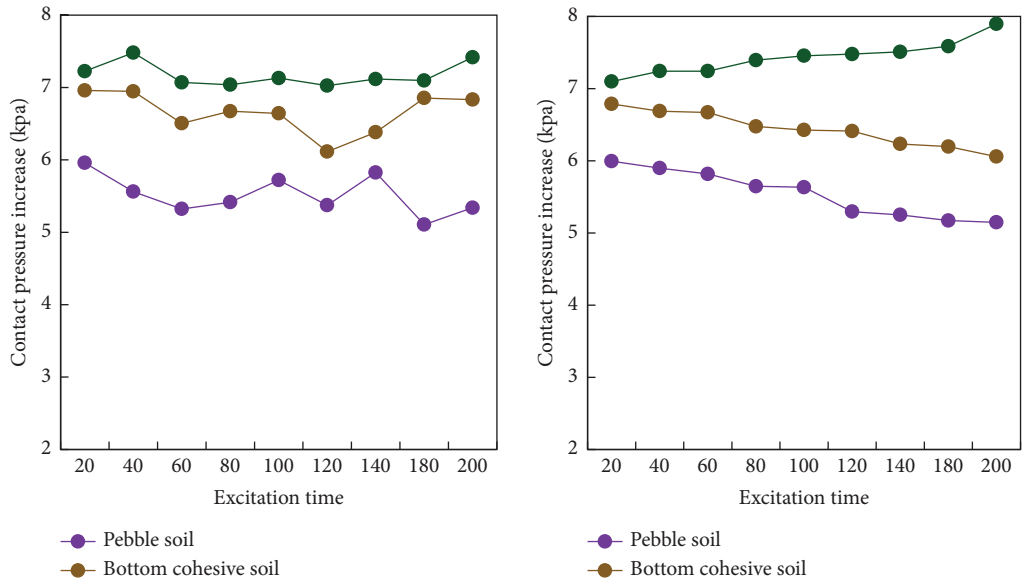

Figure 5: Change curve of the additional value of contact pressure when there is no water.

The frequency range of this research is 0~250 Hz, and the corresponding center frequency and frequency range of each frequency band of 1/3 octave is shown in Table 5.

In order to deeply analyze the dynamic response characteristics of the ground surrounding the tunnel under different frequency loads, and to eliminate the influence of the vibration load amplitude on the results, the frequency response function is used to process the results.

The applied train vibration load is obtained through the collection. During the analysis, based on the vehicle track coupling dynamics theory, first the vehicle and track model are established separately, and then the interaction between wheel and rail is comprehensively considered. Finally, the train vibration load acting on the track bed is obtained. In the vehicle model, the vehicle suspension system is simplified as a wheelset sprung mass system, which is developed into a complete vehicle model with two series. The degree of freedom of the model is 10, and the system equation can be obtained by applying the D'Alembert principle to each rigid body one by one. The rail is simplified as the Euler beam model in the track model. Although the influence of shear force and moment of inertia is ignored, it has high accuracy in calculating vertical vibration below 500 Hz. At the same time, considering the influence of track fasteners, the tunnel and monolithic track bed are considered as continuous foundation conditions. The interaction between wheel and rail mainly considers the influence of track irregularity. In the literature, 6-level track spectral density based on the

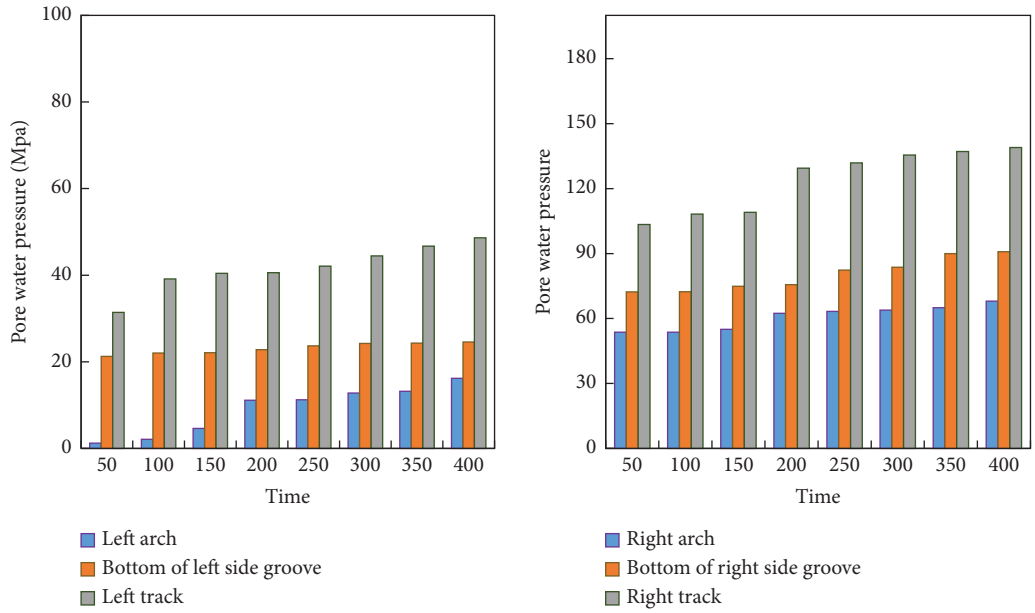

Figure 6: time history curve of invert pore water pressure.

Table 5: Center frequency and frequency range.

Center frequency	Frequency range	Center frequency	Frequency range
1.25	1.41~1.78	10	7.18~9.01
2.5	1.78~2.44	12.5	9.01~12.2
3.75	2.45~2.92	15	12.2~15.1
5	2.92~3.65	17.5	15.1~23.4
6.25	3.65~4.57	20	23.4~29.2
7.5	4.57~5.72	22.5	29.2~36.5
8.65	5.72~7.18	25	36.5~44.7

American track spectrum is selected to analyze and simulate track irregularity, and only high and low irregularity are considered. The corresponding speed of the simulated train vibration load is 80 km/h, and the load time history curve is shown in Figure 7.

Compared with the tunnel structure, the ground acceleration response under the moving train load is obviously weaker, and it is mainly concentrated in the ground adjacent to the tunnel. The decay rate of the acceleration response of the formation in the horizontal direction is obviously greater than that in the vertical direction. When considering segment joints, the calculation result of formation acceleration response is generally too large.

Through Fourier transform, the time domain results measured under fixed frequency sinusoidal load and swept frequency vibration load can be converted into the frequency domain, and the dynamic response characteristics of the lining structure and the ground under different load frequencies can be obtained. Applying train vibration load can directly obtain the response characteristics of the model in the time domain. This hypothesis is verified by applying sinusoidal vibration loads of different amplitudes. The excitation force curve under the two excitation voltages is shown in Figure 8.

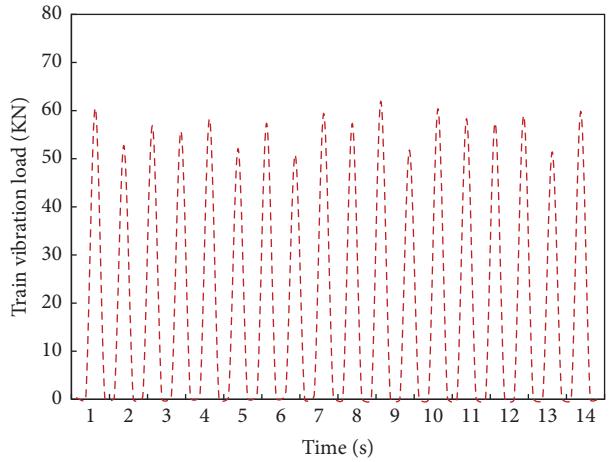

Figure 7: Train vibration load at a speed of 80 km/h.

The amplitude of the excitation force is different under different excitation voltages. The greater the excitation voltage, the greater is the excitation force. Under the same excitation voltage, the excitation force is different under different vibration frequencies. The dynamic response amplitude of the lining structure and the surrounding ground under different excitation voltages are also different. The dynamic response amplitude increases with the increase of the excitation voltage. At the same monitoring point, the dynamic response amplitudes under the same excitation voltage and different vibration frequencies are different, reflecting that the dynamic response is not only related to the load amplitude but also to the frequency of the vibration load.

The coherence coefficient represents the correlation between the measured dynamic response and the applied load, and its amplitude is between 0 and 1. The higher the amplitude, the higher the correlation between the dynamic

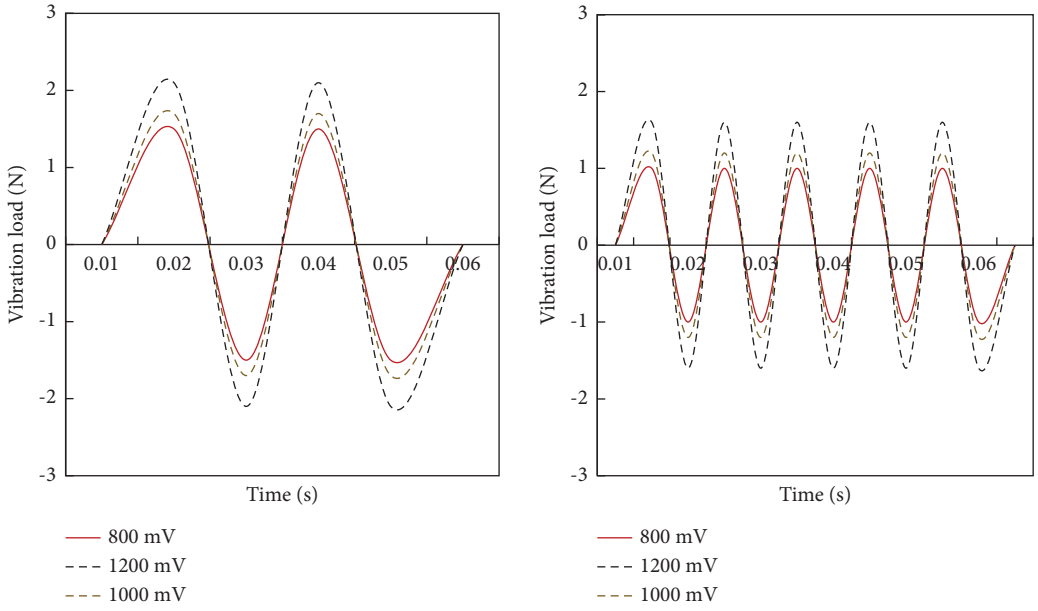

Figure 8: Time history curve of excitation force under different excitation voltages.

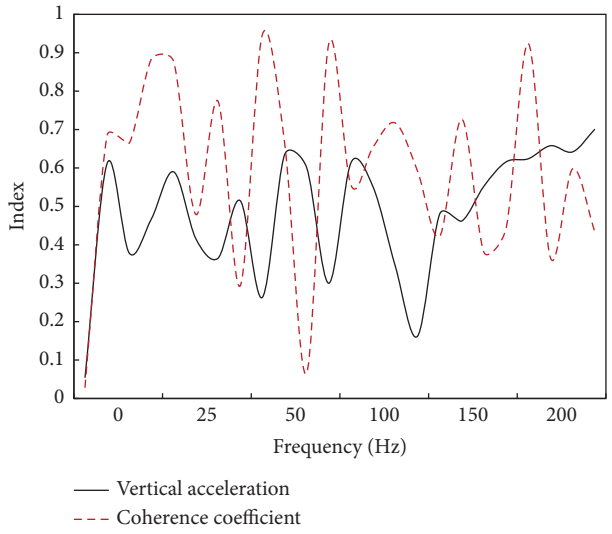

Figure 9: Frequency response function and correlation coefficient under 60 Hz.

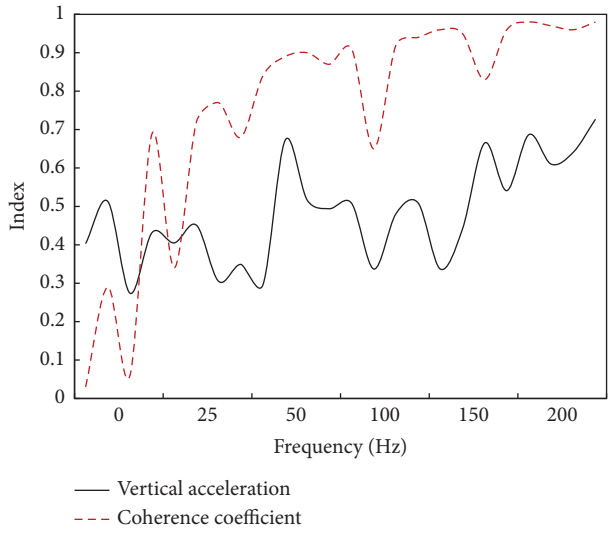

Figure 10: Frequency response function and correlation coefficient under 120 Hz.

response and the applied load. If the value is 1, it indicates that the measured dynamic response is completely caused by the applied vibration load, and the reliability of the result is the highest. It can be seen from Figures 9 and 10 that when the vibration frequency is below 50 Hz, the coherence coefficient of the formation dynamic response is small and the fluctuation changes significantly, indicating that the reliability of the frequency response function results in this frequency range is low as a whole. When the vibration load is in the frequency range of 50–100 Hz, the coherence coefficient is generally high, but there are also obvious fluctuations, but the overall trend shows a gradual increase with the increase of frequency. When the vibration frequency exceeds 100 Hz, the coherence coefficient is basically close to 1, indicating that the frequency response function response results in this section are the most reliable. At the same time, the difference in formation dynamic response measured under the two loads is small, which shows that the reliability of the formation test results under swept frequency vibration load is high.

5. Conclusions

In this study, the dynamic response characteristics of surrounding rock structures of heavy haul railways in small clear-distance interchange tunnels are analyzed by computer-aided under intelligent manufacturing. The following results are obtained, including dividing the heavy-duty railway tunnel into upper arch wall structure and lower tunnel bottom structure by analyzing the dynamic response

and stress distribution characteristics, respectively. The increase in the axle load of heavy haul trains, the decrease of surrounding rock conditions, and the reduction of distance from the active position of train load will increase the dynamic load increment and structural internal force on the structural surface, thus clarifying the surface load distribution and vertical transmission law of each structural layer of the tunnel bottom structure of heavy haul railway tunnel. The load of the heavy-duty train gradually decreases with the increase of the vertical depth during the transmission process of the tunnel bottom structure. The large rigidity of the track bed structure and the large thickness of the filling layer have a buffer effect on the dynamic load. In this study, some achievements have been made through the research on the dynamic response characteristics of the heavy-duty railway surrounding the rock structure of the interchange tunnel, but there are still some deficiencies. For example, in the process of analyzing the surrounding rock structure at the bottom of the tunnel, several common surrounding rock materials are mainly considered, and other surrounding rock materials are not analyzed. In this study, specifically, the three-dimensional dynamic numerical simulation calculation is used to study the influence of the dynamic characteristics of different sections of the grade separation tunnel under different working conditions, but the numerical simulation method is still different from the actual situation which needs to be further improved.

Data Availability

The data supporting the current study are given in the article.

Conflicts of Interest

The authors declare that they have no conflicts of interest.

References

[1] J. Lv, X. Li, Z. Li, and H Fu, "Numerical simulations of construction of shield tunnel with small clearance to adjacent tunnel without and with isolation pile reinforcement," *KSCE Journal of Civil Engineering*, vol. 24, no. 1, pp. 295–309, 2020.

[2] X. Liu, Q. Fang, and D. Zhang, "Mechanical responses of existing tunnel due to new tunnelling below without clearance," *Tunnelling and Underground Space Technology*, vol. 80, pp. 44–52, 2018.

[3] R. R. Al-Omari, A. A. Al-Azzawi, and K. A. Alabbas, "Behavior of piled rafts overlying a tunnel in sandy soil," *Geomechanics and Engineering*, vol. 10, no. 5, pp. 599–615, 2016.

[4] D. M. Zhang, Z. K. Huang, Z. L. Li, X. Zong, and D. M Zhang, "Analytical solution for the response of an existing tunnel to a new tunnel excavation underneath," *Computers and Geotechnics*, vol. 108, pp. 197–211, 2019.

[5] Y. X. Xiao, X. T. Feng, G. L. Feng, H. J. Liu, Q. Jiang, and S. L Qiu, "Mechanism of evolution of stress–structure controlled collapse of surrounding rock in caverns: a case study from the Baihetan hydropower station in China," *Tunnelling and Underground Space Technology*, vol. 51, pp. 56–67, 2016.

[6] M. He, S. Chen, and Z. Guo, "Control of surrounding rock structure for gob-side entry retaining by cutting roof to release pressure and its engineering application[J]," *Zhongguo Kuangye Daxue Xuebao/Journal of China University of Mining and Technology*, vol. 46, no. 5, pp. 959–969, 2017.

[7] S. H. Chen, H. U. Shuai-Wei, and Z. H. Zhang, "Propagation characteristics of vibration waves induced in surrounding rock by tunneling blasting[J]," *Journal of Mountain Science*, vol. 2017, no. 12, pp. 269–279, 2017.

[8] G. Li, C. Wang, and G. Wang, "Effect of the blocking water and limiting discharge and surrounding rock permeability on the stability of subsea tunnel[J]," *Geotechnical & Geological Engineering*, vol. 39, no. 1998, pp. 1–16, 2021.

[9] G. Wang and Y. Pang, "Surrounding rock control theory and longwall mining technology innovation," *International Journal of Coal Science & Technology*, vol. 4, no. 4, pp. 301–309, 2017.

[10] F. Huang, M. Zhang, and F. Wang, "The failure mechanism of surrounding rock around an existing shield tunnel induced by an adjacent excavation[J]," *Computers and Geotechnics*, vol. 117, pp. 103236.1–103236.11, 2020.

[11] Z. Fang, Z. Zhu, and P. Wu, "Excavation and support method of tunnel with high ground stress and weak surrounding rock based on GIS[J]," *Arabian Journal of Geosciences*, vol. 14, no. 7, pp. 1–13, 2021.

[12] Z. Jiachen Wang, "Systematic principles of surrounding rock control in longwall mining within thick coal seams[J]," *International Journal of Mining Science and Technology*, vol. 29, no. 01, pp. 64–70, 2019.

[13] P. Liu, S. Cui, Z. Li, X. Xu, and C Guo, "Influence of surrounding rock temperature on mechanical property and pore structure of concrete for shotcrete use in a hot-dry environment of high-temperature geothermal tunnel," *Construction and Building Materials*, vol. 207, no. 20, pp. 329–337, 2019.

[14] B. U. Qingwei, Y. Xin, and C. Wang, "Stability analysis on bearing structure in the surrounding rock between staggered roadways[J]," *Meitan Xuebao/Journal of the China Coal Society*, vol. 43, no. 7, pp. 1866–1877, 2018.

[15] J. Kan, J. Wu, and N. Zhang, "Structure stability analysis and control technology of surrounding rock ofthe secondary gob-side entry retaining[J]," *Caikuang Yu Anquan Gongcheng Xuebao/journal of Mining & Safety Engineering*, vol. 35, no. 5, pp. 877–884, 2018.

[16] M. Buri, "Dynamic clearance analysis paves way for automated fleet[J]," *Railway Gazette International*, vol. 174, no. 3, pp. 41–43, 2018.

[17] G. S. Dhaliwal and G. M. Newaz, "Effect of layer structure on dynamic response and failure characteristics of carbon fiber reinforced aluminum laminates (CARALL)," *Journal of Dynamic Behavior of Materials*, vol. 2, no. 3, pp. 399–409, 2016.

[18] K. Y. Kang, K. H. Choi, J. W. Choi, Y. Ryu, and J. M Lee, "Dynamic response of structural models according to characteristics of gas explosion on topside platform," *Ocean Engineering*, vol. 113, no. 1, pp. 174–190, 2016.

[19] A. Fenerci, O. Oiseth, and A. Ronnquist, "Long-term monitoring of wind field characteristics and dynamic response of a long-span suspension bridge in complex terrain," *Engineering Structures*, vol. 147, no. 15, pp. 269–284, 2017.

[20] X. Wang, G. Liu, S. Ma, and R Tong, "Effects of restitution coefficient and material characteristics on dynamic response of planar multi-body systems with revolute clearance joint," *Journal of Mechanical Science and Technology*, vol. 31, no. 2, pp. 587–597, 2017.

[21] Pu, Xiaowu, and Wang, "Study of shaking table test on dynamic response characteristics and failure mechanism of the

loess slope[J]," *Earthquake Research in China*, vol. 34, no. 01, pp. 128–142, 2020.

[22] T. Zhao, W. Wang, Z. Chen et al., "Dynamic response characteristics of 93W alloy with a spherical structure," *Open Physics*, vol. 18, no. 1, pp. 199–211, 2020.

[23] X. Zhai, S. Wu, K. Wang, X. Chen, and H Li, "A novel design of rescue capsule considering the pressure characteristics and thermal dynamic response with thermomechanical coupling action subjected to gas explosion load," *Shock and Vibration*, vol. 2017, no. 4, pp. 1–12, 2017.

[24] V. B. Maji, "Dynamic Response Characteristics of Hollow Steel Single Pile under Vertical Excitations[J]," *Lecture Notes in Civil Engineering] Geotechnical Applications*, vol. 13, no. 4, pp. 33–40, 2019.

[25] H. Chen, Q. Yan, and W. Chen, "Seismic dynamic response characteristics of slope in small diameter bias double tunnels [J]," *International Journal of Applied Environmental Sciences*, vol. 12, no. 3, pp. 513–525, 2017.

[26] Q. A. Bhatti, "Dynamic response characteristics of steel portal frames having semi-rigid joints under sinusoidal wave excitation[J]," *International Journal of Advanced Structural Engineering*, vol. 9, no. 4, pp. 1–5, 2017.

[27] X. Jiang, W. Liu, H. Yang, J. Zhang, and L Yu, "Study on dynamic response characteristics of slope with double-arch tunnel under seismic action," *Geotechnical & Geological Engineering*, vol. 39, no. 2, pp. 1349–1363, 2021.

[28] Z. Yuan, W. Liu, and M. Ye, "A mapping method of dynamic response and stiffness characteristics for realizing a customized nonlinear oscillator," *Nonlinear Dynamics*, vol. 102, no. 4, pp. 2531–2548, 2020.

[29] J. R. Cho, S. Y. Lee, and M. S. Song, "Dynamic response characteristics of cylindrical baffled liquid storage tank to the baffle number," *Journal of Mechanical Science and Technology*, vol. 33, no. 12, pp. 5979–5987, 2019.

[30] A. Ys, G. A. Rui, and B. Xw, "Dynamic response characteristics of permeable asphalt pavement based on unsaturated seepage - ScienceDirect," *International Journal of Transportation Science and Technology*, vol. 8, no. 4, pp. 403–417, 2019.

Hindawi
Scientific Programming
Volume 2022, Article ID 2449504, 10 pages
https://doi.org/10.1155/2022/2449504

Research Article

Optimization Method of High-Precision Control Device for Photoelectric Detection of Unmanned Aerial Vehicle Based on POS Data

Xuebin Liu,[1,2] Hanshan Li ,[3] and Suiming Yang[4]

[1]*School of Mechatronic Engineering, Xi'an Technological University, Xi'an 710021, Shaanxi, China*
[2]*Department of Economic Management, Tianfu Information Vocational College, Meishan 620564, Sichuan, China*
[3]*School of Electronic and Information Engineering, Xi'an Technological University, Xi'an 710021, Shaanxi, China*
[4]*Traffic Engineering College, Xi'an Traffic Engineering Institute, Xi'an 710000, Shaanxi, China*

Correspondence should be addressed to Hanshan Li; 1764100164@e.gzhu.edu.cn

Received 22 July 2022; Revised 27 August 2022; Accepted 9 September 2022; Published 25 September 2022

Academic Editor: Juan Vicente Capella Hernandez

With the rapid development of modern technology, due to the light-weight, small size, and good concealment, unmanned aerial vehicle (UAV) has received much attention from the society and has been vigorously promoted. Photoelectric tracking detection system is an important means in the field of modern detection. The combination of a UAV and photoelectric detection system can effectively play an important role in reconnaissance and exploration, target positioning, communication, and navigation. At present, the relevant personnel have higher and higher requirements for the accuracy of the photoelectric detection function of UAV, and the original POS data relied on by the existing photoelectric detection devices of UAV has systematic errors, which leads to the low accuracy of photoelectric detection control. Therefore, in order to achieve the purpose of improving the high-precision control of the photoelectric detection device of UAV, this paper designed an optimization method for the high-precision control device of photoelectric detection of UAV based on POS data. Firstly, the improved PID control algorithm is applied to the optimization of the UAV control device, and secondly the error correction model is established by analyzing the error source, and the original POS data is corrected by the model. This paper used the designed high-precision control device optimization algorithm and the traditional algorithm to compare the stability control experiments of the UAV platform, respectively. The experimental results showed that the application of the improved UAV photoelectric detection control device optimization method could effectively improve the control device optimization accuracy of UAV photoelectric detection by 8.23%, which was conducive to the efficient implementation of the project.

1. Introduction

The rapid development of POS data systems and photoelectric detection provides new means for obtaining specific geographic information. Combining POS data-based UAVs with photoelectric detection can greatly reduce the difficulty of surveying a large number of surface control points. In addition, by using this method, three-dimensional spatial data can be acquired quickly and in real time. However, the current photoelectric detection work has put forward higher requirements for obtaining high-resolution three-dimensional spatial data in various regions. The current control device is not optimized enough to meet the demand. In this reality, POS data and drones are combined for photoelectric detection. The high-precision control device for photoelectric detection of drones based on POS data is optimized. This has positive practical significance for the development of the UAV photoelectric detection industry.

Now, there are some research studies on the photoelectric detection of UAVs by scholars: the research of He et al. proposed an analysis method to improve the photoelectric detection accuracy of UAVs. Firstly, the UAV assembly accuracy was comprehensively modeled and simulated using kinematic analysis of homogeneous coordinate transformation. Then, by

analyzing the manufacturing process, the shaft perpendicularity, runout, and assembly errors of the gyroscope were defined and modeled, which improved the photoelectric detection accuracy of the UAV [1]. By using drones, Escobar and Sandoval obtained 8,000 images with a spatial resolution of 1.40 cm on a 30-kilometer beach. These images were used to construct an orthomosaic to detect and analyze turtle shell bones using object-based images [2]; the goal of Ren and Jiang is to design a system for automatically distinguishing targets using drones. He proposed a method of regularizing two-dimensional complex numbers for Fourier transform to solve the problem of target discrimination [3]. Thomas et al. used a multispectral camera on a fixed-wing drone to acquire high-resolution images. Three spectral textures and four detection classifiers were used to identify objects. Finally, the detection accuracy reached 96% [4]. Damian et al. proposed an automatic identification method for UAVs which was used to detect the multispectral image data obtained by UAVs and analyzed the existing sun reflection problem [5]. Kerrache et al. proposed an intelligent malicious behavior detection scheme based on adaptive detection threshold technology. In addition to detecting malicious nodes, the solution also relied on UAVs' photoelectric detection to deal with various negative effects of the detection process [6]. Martinez and Barczyk applied cascade classifiers to the photoelectric detection of UAVs and developed a computer vision algorithm for detecting pedestrians in videos, which had excellent performance in various environments [7]. The abovementioned research study analyzed the related application and development of UAV photoelectric detection.

In addition, many scholars have conducted research on POS data. Li et al.'s research introduced the working principle and components of airborne POS. Some key technologies of airborne POS were summarized, which included error calibration and compensation, initial alignment, lever arm error modeling, time synchronization, and comprehensive estimation methods [8]. Niu et al. proposed a novel indoor pedestrian POS data solution that could provide continuous localization through the correction of control points to maintain its absolute high accuracy [9]. Ye et al. proposed a distributed positioning system based on POS data. Firstly, based on the multidimensional requirements of flexible deformation information, the layout scheme of POS data was designed. Then, the POS data was quadratically fitted to obtain continuous strain, deformation displacement, and angle. The final experimental results showed that the positioning accuracy of the distributed positioning system based on POS data has been significantly improved [10]. Jianli proposed a second-order adaptive dual-filter smoother for solving nonlinear problems in POS data systems, which could adaptively estimate noise covariance in real time. The vehicle experiment results showed that this method could improve the attitude accuracy of the distributed POS data system by 27.84% [11]. Gong and Chen proposed a Kalman filter for the accuracy and real-time performance of the data transmitted by the airborne distributed positioning system. The state variables of the transfer-aligned nonlinear mathematical model were divided into two groups. One group was linear variables independent of nonlinear variables, and the other group was composed of nonlinear variables and coupling of linear variables [12]. Zhu et al. proposed a new real-time gravity compensation method, which took the gravity disturbance as the error state of the POS Kalman filter. An accurate gravity disturbance model was established based on the time-varying Gauss–Markov model [13]. Takashima et al. studied the integration of POS data into an imperfect in-vehicle automation system to reduce the negative impact of human-robot collaboration perception [14]. Langbehn et al. studied imperceptible camera motion by synchronizing POS data with the human visual process, especially to achieve position and orientation redirection [15]. The abovementioned studies have carried out a certain degree of effective research on POS data.

In recent years, UAVs have developed rapidly with the advantages of low cost, strong survivability, and good maneuverability. The method of photoelectric detection work by unmanned aerial vehicles is gradually becoming popular. Therefore, this paper designed a high-precision control device optimization method for UAV photoelectric detection based on POS data, which was conducive to better development of UAV photoelectric detection work.

2. UAV Photoelectric Detection Optimization Method

2.1. UAV and Photoelectric Detection. As a new type of aircraft, UAV has developed rapidly in recent years, and its technology has become more and more mature [16]. Drones have the following notable advantages:

(1) Strong concealment: UAVs do not need pilots, so UAVs are small in size and light in weight, which is of great help to improve the concealment of UAV reconnaissance. The improvement of concealment helps to avoid interference from other sources in the process of performing photoelectric detection. Therefore, the security is greatly improved.

(2) Flexible mobility: the design structure of the UAV is relatively simple. After setting the automatic navigation, the flight is controlled by the computer and will not be affected by the weather at all. There is no need to consider the carrying capacity of the driver in the design; only the ultimate carrying capacity of the UAV material needs to be considered. In this way, the performance advantages of the UAV can be maximized and the maneuverability of the UAV application can be greatly improved. High maneuverability enables drones to perform difficult maneuvers in a variety of environments, which enables drones to explore places that humans cannot.

(3) Cost saving: UAV is small in size and consumes less raw material. Drones consume far less fuel and material than manned aircraft. The cost of drones is only a few percent of that of manned aircraft, and the training of operators is relatively simple, which saves a lot of money.

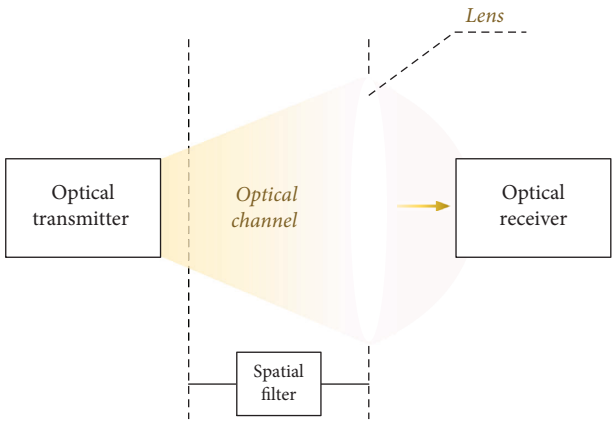

Figure 1: Photoelectric detection system.

In modern society, with the development of science and technology, photoelectric detection plays an increasingly important role [17]. From a professional point of view, photoelectric detection refers to the use of radar, computers, sonar, optical instruments, and other equipment to evaluate the location, properties, and types of targets [18]. The most important functional module in photoelectric detection is target recognition, and its basic principle is to analyze the echoes reflected by the target. Detected targets are identified based on phase, amplitude, polarization, spectrum, and so on [19]. In the military field, photoelectric detection technology can provide detailed battlefield conditions in the process of cooperative operations of various participating units on the battlefield. Photoelectric detection technology plays an important role in accurately estimating the war situation, formulating combat plans, and correctly commanding operations.

Compared with the electronic detection system, the carrier frequency element of the photoelectric detection system has been improved several times in the order of magnitude. Since the power of the carrier frequency can be superimposed and amplified, the number of carrier frequency components can reflect the performance of the photoelectric detection system to a certain extent. This change in carrier frequency has made a qualitative leap in the implementation of optoelectronic systems and has also undergone a qualitative change in function. The basic model of the photoelectric detection system is shown in Figure 1.

In the photodetection process, the reception of the optical signal is very important [20]. Generally speaking, when an optical signal emitted by an optical transmitter undergoes a series of transmissions, its amplitude will be affected and attenuated. In addition, the pulse waveform of the optical signal is also expanded. The function of the optical receiver is to detect the transmitted weak optical signal, and the received incident light field is amplified, shaped, and regenerated into the original transmission signal. Finally, the information from the optical carrier is recovered. The optical receiver generally consists of three parts: the light receiving front end, the photodetector, and the subsequent processing circuit. The light-receiving front end is composed of an optical receiving system composed of a lens and a light collecting part. The photodetector focuses the light received by the optical receiving system on the photosensitive surface of the photodetector and converts the optical signal into an electrical signal. The subsequent processing circuit amplifies, filters, and processes the electrical signal converted by the photodetector and recovers the required information from it.

2.2. Optimization Method Design. By combining drones with photoelectric detection, detection can be performed with greater efficiency. Therefore, in order to achieve the purpose of improving the target recognition accuracy of photoelectric detection of UAV, this paper designs an optimization method for the high-precision control device of photoelectric detection of UAV based on POS data. The optimization follows the following principles: before and after optimization, the functions implemented by the control device program are the same; the control algorithm after optimization should run faster or occupy less storage space than before optimization, or both; the optimizer wants the best success at the least cost. The optimization method is shown in Figure 2.

It can be seen from Figure 2 that the method flow is as follows: since the UAV is easily affected by wind during flight, the PID control algorithm is improved and applied to the optimization of UAV control to stabilize the fuselage attitude of the UAV during flight. When the fuselage attitude is stable, the accuracy of photoelectric detection will be improved; then an error correction model is established by analyzing the error source, and finally the original POS data is corrected by the error correction model and applied to the photoelectric detection module of the UAV.

In this process, improving the PID control algorithm is the key point in the optimization method of the photoelectric detection control device of the UAV. A stable body can bring stable detection shooting. This paper mainly improves the controller by improving the control algorithm, which can achieve the purpose of optimizing the fuselage control of the UAV. Achieving the goal requires the following: fast and precise output response, better kinematic characteristics, and static stability characteristics. In the process of building a correction error model, the key point is the analysis of the source of the error. In the process of correcting the original POS data, it is necessary to ensure the comprehensiveness and validity of the data acquisition.

3. Optimize POS Data

3.1. Angle Measurement Model of Photoelectric Detection System. The photoelectric detection system on the UAV can realize the search, tracking, and positioning of the target. The photoelectric detection system adopts the passive working mode; that is, the load operator selects the target area of interest, extracts the target contour through the system, and maintains stable tracking of the target while changing the angle in real time. The measurement data is passed back to the mission console. Through the continuous tracking of the target, a series of measured data of azimuth and inclination

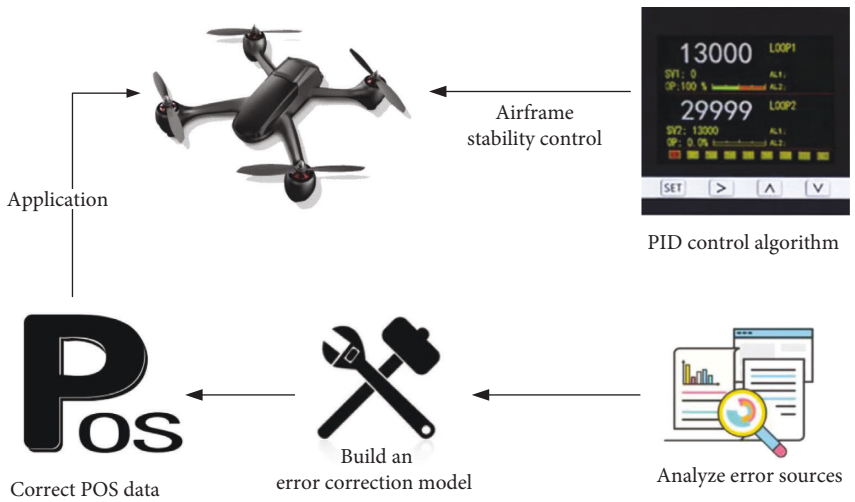

Figure 2: Optimization method for photoelectric detection of UAV.

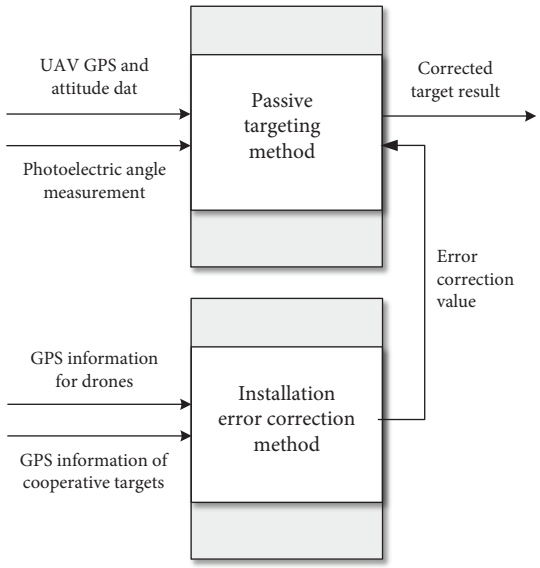

Figure 3: Passive target positioning realization process.

can be obtained. Combining the position data and the position of the flight movement stationary at the relevant moment, the passive positioning method can be used to realize the positioning and calculation of the target parameters. The realization process of passive target positioning is shown in Figure 3.

As shown in Figure 3, the corresponding steps of the passive target positioning realization process are as follows: first, the GPS position information of the UAV and the cooperative target is used to calculate the theoretical azimuth and inclination; second, the measured values of photocharge and inertial force (azimuth and inclination) and UAV navigation data are used to obtain the azimuth and inclination after coordinate transformation; then, the installation error correction value is obtained by the semilinearization method; and finally, the positioning error correction value is applied to the positioning process to complete the target positioning solution.

3.2. Analyze the Source of Errors. In photogrammetry, the transfer model from the lateral body to the normal body is established. The model parameters are solved according to the image points and the corresponding ground points, and the coordinates of the ground control points are obtained. In the image plane coordinates, the origin of the coordinates is usually the point where the main optical axis of the lens intersects the image plane, but this point generally does not coincide with the geometric center of the image, so for the measurement of the image point, first the inner orientation of the acquired image is obtained.

3.3. Monoscopic Space Resection. Spatial separation is a fundamental problem in photometry, and the main idea is to establish a collinear formula of state given the coordinates of several ground control points and the corresponding values of the coordinate measurements of image points. Because the collinear equation is a nonlinear function, it is not conducive to iterative calculation, so it needs to be linearized, expanded according to the first-order term of the Taylor series, and established as the normal equation according to the principle of least squares adjustment.

3.4. System Error Analysis of External Orientation Elements. The exposure position (photography center) of the camera on the drone is not completely coincident with the POS recording position, and there is a certain displacement offset. Therefore, POS data is not strictly an external orientation element of the image. During the photogrammetry process of the UAV, the fixed attitude and state POS data of the UAV can be obtained through the GPS combined system. However, the attitude angle in the POS data does not completely match the outer azimuth element of the orthophoto, so coordinate transformation and system error correction are required. In the subsequent information processing, the electronic method is mainly used. After the optical signal is processed by the photodetector, the optical signal has been converted into an electrical signal. Subsequently, electronic amplifiers,

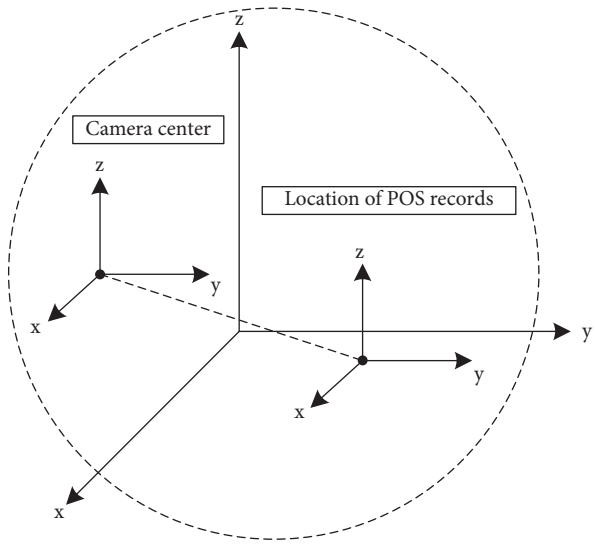

Figure 4: System offset error.

integrated circuits, and computers are used to process the signals. The required information is obtained. The system offset error is shown in Figure 4.

The systematic offset error mainly comes from the offset of the line elements in the outer azimuth. Generally speaking, the drone is approximately parallel to the ground when it flies. However, in the actual process, due to the instability of the aircraft and the influence of air wind, the height of the longitudinal axis will also change. There is a nonnegligible offset. The offset between the POS data and the camera center is shown as

$$\Delta S = \sqrt{\Delta X^2 + \Delta Y^2 + \Delta Z^2}. \tag{1}$$

Among them, X, Y, and Z represent high-order infinitesimal values of the three axes.

3.5. Correct the Original POS Data. On the basis of mastering the sources of systematic errors, an error correction model is designed to correct the original POS data. Main process: available images in the area by performing initial correction and selection of the images obtained by the drone are selected. A small number of control points in the available images are arranged, coordinate transformation on the POS data is performed, and finally a correction model is established. It is assumed that the outer orientation elements of the image are obtained through the solution of ground points, and each image corresponds to the original airborne POS data. The probability distribution is constructed as follows:

$$\begin{bmatrix} \Delta X_i \\ \Delta Y_i \\ \Delta Z_i \\ \Delta \varphi_i \\ \Delta \omega_i \\ \Delta \kappa_i \end{bmatrix} = \begin{bmatrix} X_i - X_{(pos)i} \\ Y_i - Y_{(pos)i} \\ Z_i - Z_{(pos)i} \\ \varphi_i - \varphi_{(pos)i} \\ \omega_i - \omega_{(pos)i} \\ \kappa_i - \kappa_{(pos)i} \end{bmatrix}. \tag{2}$$

Among them, ϕ_i, ω_i, and κ_i represent the attitude angles of the three axes of X_i, Y_i, and Z_i.

Selecting all images for external alignment is complex, time-consuming, and computationally expensive. Therefore, only the error values of the POS data in some images are averaged to correct the overall error, as follows:

$$\begin{cases} \overline{\Delta X}\left(\sum_{i=1}^{n} \Delta X_i\right)/n,\ \overline{\Delta Y} = \left(\sum_{i=1}^{n} \Delta Y_i\right)/n, \\ \overline{\Delta z}\left(\sum_{i=1}^{n} \Delta Z_i\right)/n,\ \overline{\Delta \varphi} = \left(\sum_{i=1}^{n} \Delta \varphi_i\right)/n, \\ \overline{\Delta \omega}\left(\sum_{i=1}^{n} \Delta \omega_i\right)/n,\ \overline{\Delta \kappa} = \left(\sum_{i=1}^{n} \Delta \kappa_i\right)/n. \end{cases} \tag{3}$$

In the formula, $(\overline{\Delta \varnothing}, \overline{\Delta \omega}, \overline{\Delta k})$ is the correction number obtained by the error model. $\Delta\phi$, $\Delta\omega$, and $\Delta\kappa$ represent the attitude angles of the three axes of X, Y, and Z. Finally, according to the different flight trajectories of the UAV flying in space, the positional element errors outside the camera center of the odd-numbered and even-numbered lines of UAV flight are opposite; this will be corrected.

4. Improved PID Control Algorithm

To facilitate the study of the UAV model, the following assumptions are made:

(1) It is assumed that the UAV under experiment is a completely symmetrical, uniform, and rigid body. In the process of photodetection, its elastic deformation and internal force are ignored.

(2) It is assumed that the station center coordinate system is an inertial coordinate system. The influence of the earth's rotation and revolution on the drone is ignored. The curvature of the earth is also ignored and treated as if it were a plane.

(3) It is assumed that the origin of the body coordinate system, the center of mass of the UAV, and the center of the geometric structure coincide.

(4) It is assumed that the gravity and resistance of the UAV flight are not affected by the flight height.

Based on the above research assumptions, formula (4) can be obtained from the Newton–Euler formula:

$$\begin{cases} F = m\dot{v}, \\ M = J\dot{\omega}. \end{cases} \tag{4}$$

Among them, F is the resultant external force on the drone, m is the mass of the drone, $\dot{v}$ is the first derivative of the linear velocity when the drone is flying, M is the moment of momentum when the drone is flying, and J is the rotation of the drone Inertia, and $\dot{\omega}$ is the first derivative of the rotational angular velocity of the drone.

In the body coordinate system, for the UAV, the total lift force is shown as follows:

$$F_{Tb} = \begin{bmatrix} 0 \\ 0 \\ F_1 + F_2 + F_3 + F_4 \end{bmatrix}. \quad (5)$$

Among them, F_1, F_2, F_3, and F_4 are the lift generated by four sets of rotors, respectively.

The matrix expression of the fuselage gravity of the UAV is shown as follows:

$$F_{Ge} = \begin{bmatrix} 0 \\ 0 \\ mg \end{bmatrix}. \quad (6)$$

Among them, g is the acceleration of gravity.

In the station center coordinate system, the air resistance is proportional to the UAV displacement speed, as follows:

$$F_{De} = \begin{bmatrix} K_x \dot{x} \\ K_y \dot{y} \\ K_z \dot{z} \end{bmatrix}. \quad (7)$$

Among them, K_x, K_y, and K_z are the air resistance coefficients of axial displacement motion, respectively.

In summary, the resultant force of the UAV in the station center coordinate system is shown as follows:

$$\sum F_E = F_{Te} - F_{Ge} - F_{De}. \quad (8)$$

In the body coordinate system, ignoring the influence of displacement motion, the UAV performs rotational motion around the body coordinate axis. Its rotational moment is mainly affected by the moments of inertia, angular velocity, air resistance, and gyroscopic effects. The inertia tensor matrix of the UAV rigid body in the body coordinate system is shown as follows:

$$J_b = \begin{bmatrix} J_{xx} & J_{xy} & J_{xz} \\ J_{yx} & J_{yy} & J_{yz} \\ J_{zx} & J_{zy} & J_{zz} \end{bmatrix}. \quad (9)$$

Among them, J_{xx}, J_{yy}, J_{zz} is the moment of inertia and $J_{xy}, J_{xz}, J_{yx}, J_{yz}, J_{zx}, J_{zy}$ is the inertia product. Since the rigid body of the UAV is completely symmetrical, formula (10) can be obtained according to the definition of inertia product:

$$J_{xy} = J_{xz} = J_{yx} = J_{yz} = J_{zx} = J_{zy} = 0. \quad (10)$$

The available UAV inertial matrix is shown as follows:

$$J_b = \begin{bmatrix} J_x & 0 & 0 \\ 0 & J_y & 0 \\ 0 & 0 & J_z \end{bmatrix}. \quad (11)$$

From the differential formula of angular motion, it can be known that the momentum of the UAV is shown as follows:

$$M_b = J_b \dot{\Omega}_b + \Omega_b \times (J_b \Omega_b). \quad (12)$$

Among them, $\dot{\Omega}_b$ is the angular acceleration.

According to the law of conservation of moment of momentum, the resultant moment of UAV rotational motion is shown as follows:

$$\sum M_B = M_b - M_T - M_G. \quad (13)$$

Among them, M_b, M_T, and M_G are the moments in all directions in motion.

The PID algorithm can be expressed as follows:

$$u(t) = K_p e(t) + K_i \int_0^t e(\tau) d\tau + K_d \frac{d}{dt} e(t). \quad (14)$$

The general form of the transfer function of the PID controller is shown as follows

$$G(s) = \frac{U(s)}{E(s)} = K_p \left(1 + \frac{1}{T_i s} + T_d s\right). \quad (15)$$

Among them, T_i is the integral time constant and T_d is the differential time constant.

The proportional control term is mainly concerned with the current error of the system, and the error is multiplied by a positive constant as the output of the proportional term. The output expression of the proportional control term is shown as follows:

$$P_{out} = K_p e(t). \quad (16)$$

The integral control term is mainly concerned with the past errors, and the sum of the error values in the past period of time is multiplied by a positive constant as the integral term output. The output expression of the integral control term is shown as follows:

$$I_{out} = K_i \int_0^t e(t) d\tau. \quad (17)$$

The main concern of the derivative control term is the future error. The first derivative of the error is multiplied by a positive constant as the derivative control term output. The output expression is shown as follows:

$$D_{out} = K_d \frac{d}{dt} e(t). \quad (18)$$

Among them, K_p, K_i, and K_d are all positive constants.

The expression of the positional PID algorithm is shown as follows:

$$u(k) = K_p e(k) + K_i \sum_{j=0}^{k} e(j) + K_d (e(k) - e(k-1)). \quad (19)$$

After further simplification, the final improved PID algorithm is obtained, as follows:

$$\Delta u(k) = K_P \left[\left(1 + \frac{T}{T_i} + \frac{T_d}{T}\right) e(k) - \left(1 + 2\frac{T_d}{T}\right) e(k-1) + \frac{T_d}{T} e(k-2) \right]. \quad (20)$$

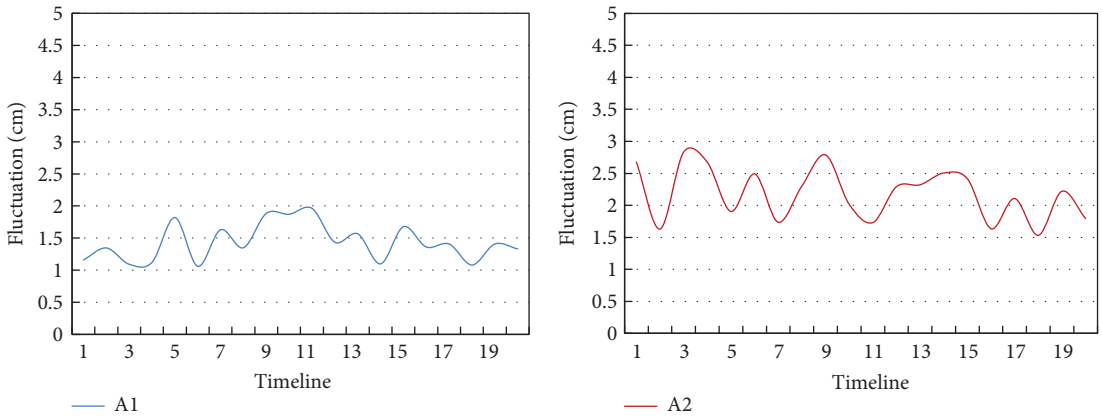

(a) (b)

Figure 5: Hover motion results comparison.

5. Experiment and Result Comparison

According to the above design and research on cascade PID and fuzzy control, this paper uses MATLAB mathematical simulation tool to build and simulate the dynamic model of the UAV flight control system. Based on the corresponding software and hardware facilities, the practical application verification and testing of the UAV flight control algorithm are carried out. The UAV platform is stably controlled by the optimization algorithm of the high-precision control device designed in this paper and the traditional PID algorithm. The high-precision control device optimization algorithm designed in this paper is named A1, and the traditional algorithm is named A2. A comparative experiment was carried out. The experiment was carried out for 20 minutes of UAV photoelectric detection. During the flight movement, by using the open source ground station software, the flight data of the UAV can be detected and adjusted in real time, and the control effect of the UAV attitude control algorithm can be analyzed according to the attitude change curve. The control accuracy and antiinterference ability are verified from the four results of hovering motion results, lateral motion results, photoelectric detection accuracy results, and comprehensive performance results.

5.1. Comparison of Hovering Motion Results. Hovering refers to the flying state in which the UAV keeps its spatial position basically unchanged at a certain height. This flight capability makes the application range of the UAV very wide. It can not only adapt to various complex take-off and landing environments but also engage in various aerial work projects, and even some jobs can only be done by hovering the drone. The comparison of hovering motion results is shown in Figure 5.

Figure 5 shows a comparison of the hovering motion results for the two control device algorithms. In the UAV hovering motion test using the high-precision control device optimization algorithm designed in this paper, the offset of the fuselage from the origin within 20 minutes is between 1.06 and 1.96 cm; in the drone hovering motion test using the traditional control device algorithm, the offset of the fuselage from the origin within 20 minutes is between 1.53 and 2.83 cm. The high-precision control device optimization algorithm designed in this paper is far superior to the traditional control device algorithm in hovering motion.

5.2. Comparison of Lateral Motion Results. The lateral motion of the UAV is mainly manifested in three motion modes, namely, the Dutch roll mode, the fast roll mode, and the helical mode. In the Dutch roll mode, the torque related to the rotation is interrelated; in the fast roll-on mode, the roll angular velocity causes the yaw moment, and the yaw angular velocity causes the roll moment. In helical mode, coordinated turns can be controlled by increasing the damping of the rolling motion. In this experiment, the motion modes of the UAV under the two control device algorithms are tested, and the comparison results are shown in Figure 6.

Figure 6 shows a comparison of the lateral motion results of the two control device algorithms. In the lateral motion test of the UAV using the high-precision control device optimization algorithm designed in this paper, the number of completed lateral motion cycles of the fuselage per minute is between 6 and 9 times within 20 minutes; in the hovering motion test of the UAV using the traditional control device algorithm, the number of completed lateral motion cycles of the fuselage per minute within 20 minutes is between 4 and 6 times. The high-precision control device optimization algorithm designed in this paper is far superior to the traditional control device algorithm in lateral motion.

5.3. Comparison of Photoelectric Detection Accuracy Results. The photoelectric detection system on the UAV can realize the search, tracking, and positioning of the target. The photoelectric detection system adopts the passive working mode; that is, the target area is selected by the load operator, and the target contour is extracted by the system. While maintaining stable tracking of the target, the angle

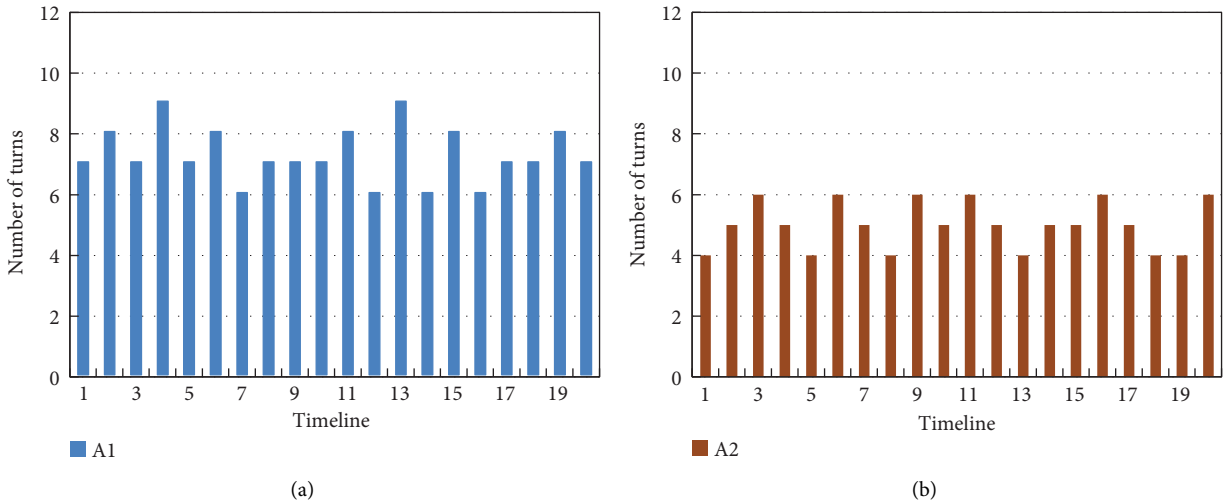

Figure 6: Lateral motion results comparison.

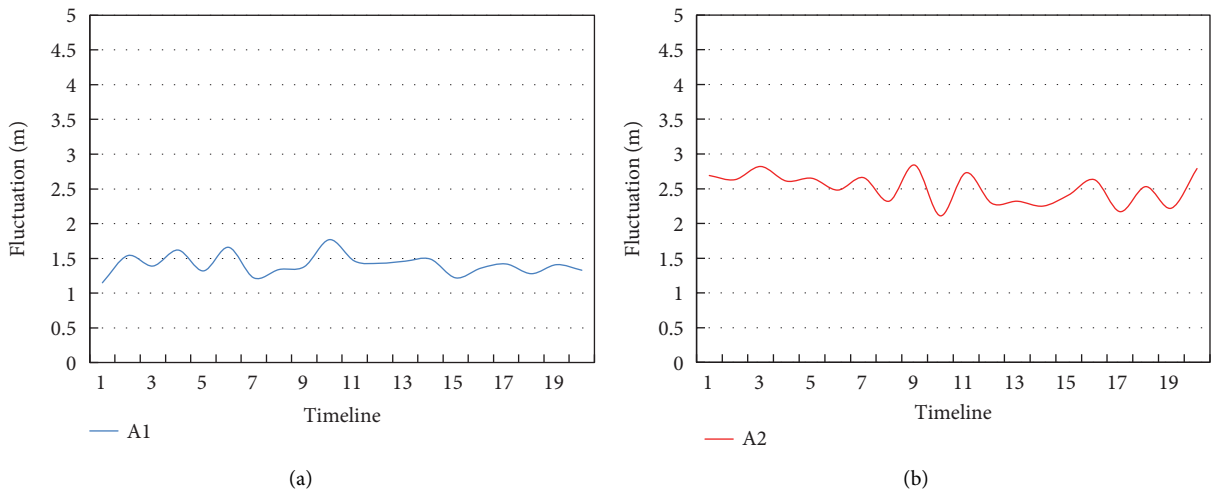

Figure 7: Comparison of photoelectric detection accuracy results.

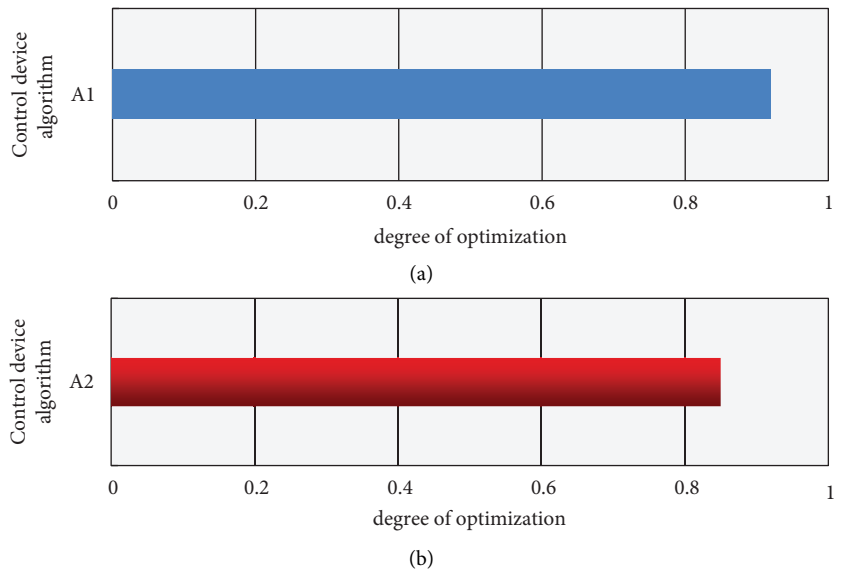

Figure 8: Final result comparison.

measurement data is transmitted back to the mission console in real time. The photoelectric detection accuracy results are shown in Figure 7.

Figure 7 shows the comparison of the photodetection accuracy results of the two control device algorithms. In the UAV photoelectric detection accuracy test using the high-precision control device optimization algorithm designed in this paper, the deviation between the detection locking point and the target within 20 minutes is between 1.15 and 1.77 cm; in the UAV photoelectric detection accuracy test using the traditional control device algorithm, the offset of the fuselage from the origin within 20 minutes is between 2.11 and 2.84 cm. The high-precision control device optimization algorithm designed in this paper is far superior to the traditional control device algorithm in terms of photoelectric detection accuracy.

5.4. Comparison of Comprehensive Performance Results. Finally, the comprehensive performance comparison results of the two control device algorithms are obtained, as shown in Figure 8.

Figure 8 shows a comparison of the overall performance results of the two control device algorithms. The comprehensive performance score of the optimization algorithm of the high-precision control device designed in this paper is 0.92 points, and the comprehensive performance score of the traditional control device algorithm is 0.85 points. The performance of the high-precision control device optimization algorithm designed in this paper is far superior to that of the traditional control device algorithm. The performance has improved by about 8.23%.

6. Conclusion

The combination of a UAV and a photoelectric detection system can flexibly and conveniently carry out photoelectric detection. However, due to the system error of the algorithm and various other objective factors, the potential of the optoelectronic equipment has not been fully exerted, and the control accuracy of the optoelectronic detection is low. Through experiments, four results were obtained, including hovering motion results, lateral motion results, photoelectric detection accuracy results, and comprehensive performance results.

Data Availability

The data that support the findings of this study are available from the corresponding author upon request.

Conflicts of Interest

The authors declare that they have no conflicts of interest.

References

[1] K. He, H. Hong, and G. Jiang, "Analysis of assembly error effect on stability accuracy of unmanned aerial vehicle photoelectric detection system," *Applied Sciences*, vol. 10, no. 7, pp. 2311–2352, 2020.

[2] J. Escobar and S. Sandoval, "Unmanned aerial vehicle (UAV) for sea turtle skeleton detection in the Mexican Pacific," *Remote Sensing Applications Society and Environment*, vol. 1, no. 1, pp. 4–12, 2021.

[3] J. Ren and X. Jiang, "Regularized 2-D complex-log spectral analysis and subspace reliability analysis of micro-Doppler signature for UAV detection," *Pattern Recognition*, vol. 69, no. 4, pp. 225–237, 2017.

[4] A. Thomas, T. A. Alexandra, and P. X. Eirini, "Novelty detection classifiers in weed mapping: Silybum marianum detection on UAV multispectral images," *Sensors*, vol. 17, no. 9, pp. 2007–2145, 2017.

[5] O. T. Damian, H. L. David, and B. Rocio, "Automatic hotspot and sun glint detection in UAV multispectral images," *Sensors*, vol. 17, no. 10, pp. 2352–2484, 2017.

[6] C. A. Kerrache, A. Lakas, and N. Lagraa, "UAV-assisted technique for the detection of malicious and selfish nodes in VANETs," *Vehicular Communications*, vol. 11, no. 6, pp. 1–11, 2018.

[7] P. Martinez and M. Barczyk, "Implementation and optimization of the cascade classifier algorithm for UAV detection and tracking," *Journal of Unmanned Vehicle Systems*, vol. 7, no. 4, pp. 296–311, 2019.

[8] J. Li, J. Fang, and Z. Lu, "Airborne position and orientation system for aerial remote sensing," *International Journal of Aerospace Engineering*, vol. 2017, no. 1, pp. 1–11, 2017.

[9] X. Niu, T. Liu, and J. Kuang, "A novel position and orientation system for pedestrian indoor mobile mapping system," *IEEE Sensors Journal*, vol. 21, no. 2, pp. 2104–2114, 2021.

[10] W. Ye, B. Gu, and Y. Wang, "Airborne distributed position and orientation system transfer alignment method based on fiber bragg grating," *Sensors*, vol. 20, no. 7, p. 2120, 2020.

[11] J. Li, S. Zou, B. Gu, and J. Fang, "Adaptive two-filter smoothing based on second-order divided difference filter for distributed position and orientation system," *Science China(Information Sciences)*, vol. 62, no. 9, pp. 130–143, 2019.

[12] X. Gong and L. Chen, "A conditional cubature Kalman filter and its application to transfer alignment of distributed position and orientation system," *Aerospace Science and Technology*, vol. 95, no. 3, pp. 105–405, 2019.

[13] Z. Zhu, Y. Guo, and W. Ye, "A real-time gravity compensation method for a high-precision airborne position and orientation system based on a gravity map," *Journal of Navigation*, vol. 71, no. 3, pp. 711–728, 2018.

[14] K. Takashima, T. Okazaki, and K. Toyoda, "Magnetic sensor system for detecting position and orientation of an endocranial catheter tip(Imaging & Measurement)," *Work*, vol. 411, no. 6, pp. 258–265, 2017.

[15] E. Langbehn, F. Steinicke, and M. Lappe, "In the blink of an eye - leveraging blink-induced suppression for imperceptible position and orientation redirection in virtual reality," *ACM Transactions on Graphics*, vol. 37, no. 4, pp. 1–11, 2018.

[16] C. Zhang and Z. Wei, "Spectrum sharing for drone networks," *IEEE Journal on Selected Areas in Communications*, vol. 35, no. 1, pp. 136–144, 2017.

[17] J. Wang and Q. Ping, "Photodetection-induced relative timing jitter in synchronized time-lens source for coherent Raman scattering microscopy," *Journal of Innovative Optical Health Sciences*, vol. 10, no. 5, pp. 16–21, 2017.

[18] B. Ding and G. Wen, "Sparsity constraint nearest subspace classifier for target recognition of SAR images," *Journal of Visual Communication and Image Representation*, vol. 52, no. 6, pp. 170–176, 2018.

[19] X. Qi, N. Wu, and H. Wang, "A factor graph-based iterative detection of faster-than-Nyquist signaling in the presence of phase noise and carrier frequency offset," *Digital Signal Processing*, vol. 63, no. 7, pp. 25–34, 2017.

[20] D. V. Gorbatov, V. A. Konyshev, and T. O. Lukinykh, "Effect of anisotropy of a single-mode fibre on lightning-induced rotation of polarisation of a light signal in an optical ground wire," *Quantum Electronics*, vol. 52, no. 1, pp. 87–93, 2022.

Hindawi
Scientific Programming
Volume 2022, Article ID 2765486, 13 pages
https://doi.org/10.1155/2022/2765486

Research Article

Building Protection Data Release Planning Based on Multifeature Deep Learning

Chunhuan Guo,[1] Yajun Zang,[2] and Yu Gao [3]

[1]*School of Architecture and Civil Engineering, Chongqing Metropolitan College of Science and Technology, Yongchuan 402167, Chongqing, China*
[2]*School of Public Administration, Chongqing Technology and Business University, Chongqing, Chongqing 400067, China*
[3]*School of Artifical Intelligence and Big Data, Chongqing Metropolitan College of Science and Technology, Yongchuan 402167, Chongqing, China*

Correspondence should be addressed to Yu Gao; gaoyu@cqcst.edu.cn

Received 21 June 2022; Revised 1 August 2022; Accepted 11 August 2022; Published 24 September 2022

Academic Editor: Juan Vicente Capella Hernandez

With the rapid development of China's economy, the protection of buildings has attracted the attention of many researchers. Although there is no such massive demolition in the past, natural damage still exists. Identify the collected historical building protection data through multifeature deep learning, and provide protection plans through the information in the database. In order to solve the problem of restoration of natural damage more professionally and efficiently, this paper collects the architectural features and restoration methods of each building in different processes through multifeature deep learning based on the current state of building information in China. Based on the collected information, this paper establishes the building information model, and stores and manages the building information. According to the Newton deep learning optimization algorithm, this paper enhances the algorithm to accurately collect building information and uses the collaborative filtering algorithm to provide users with a repair plan. This paper uses the GRU-based recommendation model to pass the threshold cycle unit algorithm for the probability of each building being selected in the list of similar buildings at a time point. Under the two conditions of 10 and 20 recommended numbers, the user coverage rate of the recommended case of deatomized building photos can reach 100%. And this paper recommends high-probability solutions for users to achieve automation, diversification, and intelligence.

1. Introduction

Architecture is an important part of the development process of human civilization, reflecting the way of life and habits of local people in the era, and carrying the local cultural atmosphere. With the rapid development of China's economy, the pace of urbanization has accelerated, and the scale of the renovation of old cities has been expanding. This not only damages the historical buildings but also destroys the local life atmosphere. The disappearance of historical value is irreversible. Therefore, the protection of historical buildings is particularly important. By archiving historical building materials, such as photos and videos of historical buildings, this paper proposes a new idea of using multifunctional deep learning to accurately protect and study historical buildings.

When researching and accumulating knowledge on methods, techniques, and practical interfaces of historic building preservation have substantial significance for the harmonization of scientificity and authenticity of building preservation that can be used in the future. It also plays a key role in interprofessional, cross-platform historic building conservation practice. Model and analyze the protection methods and special technologies of historical buildings through multifeature deep learning, and truly restore the effect of historical buildings after protection.

Based on multifunctional deep learning to explore the protection of historical buildings, this paper uses geodetic

maps, tables, text, or pictures to preserve historical building information to achieve the protection of historical buildings. The scope is large, but even if these methods are more specific and accurate, they can fully and accurately reflect the historical style of the building.

2. Related Work

As one of the state-of-the-art techniques, deep learning has been highly valued in the field of an object retrieval. Litjens et al. survey the application of deep learning in image classification, object detection, segmentation, registration, and other tasks, and provide a brief overview of research in each application area [1]. Chen proposed a novel deep learning framework to merge these two features, from which the highest classification accuracy can be obtained [2]. Shen introduced the basic principles of deep learning methods and reviewed their success in image registration, anatomical and cellular structure detection, tissue segmentation, computer-aided disease diagnosis, and prognosis [3]. Oshea and Hoydis used the concept of radio transformer networks as a means of incorporating expert domain knowledge into machine learning models [4]. Hou et al. proposed a blind IQA model that directly learns qualitative assessments and outputs numerical scores for general use and fair comparison [5]. Zhao established a test bench to verify the filtering algorithm and applied MATLAB software to design the moving average filtering algorithm, the IIR filtering algorithm, and the moving-IIR filtering algorithm [6]. Yang et al. proposed a new nonlinear state estimation algorithm, which has high accuracy while ensuring robustness [7]. They utilize a learning denoising based approximate message passing (LDAMP) network, a neural network that can learn channel structure and estimate channels from a large amount of training data [8]. Tom et al. review important deep learning-related models and methods that have been used for many NLP tasks, and summarize, compare, and contrast various models [9]. These studies have certain guiding significance, but the studies are too single and need to be further improved.

3. Building Protection Analysis Based on Multifeature Deep Learning

A historical building has left imprints of old-time information in the development of the city, and these imprints are the carriers of recording urban civilization. The safety of historical buildings and the rational use of protection technologies can preserve and inherit local culture and life.

3.1. Current Situation and Analysis of Protection of Building Information. According to the principle of historical building protection, the protection of historical buildings should preserve the original historical information as much as possible, and use the physical object as the carrier to protect the environment as much as possible. The overall protection of historical buildings includes not only the protection and development of the physical environment of the historically left space but also the protection and development of the urban historical context.

The first stage is the census, the second stage is the analysis and evaluation stage, the third stage is the current situation investigation and thorough investigation stage, and the fourth stage is the filing stage. According to Table 1, the normal conservation process can be divided into several well-defined work steps according to the depth and completeness of the census [10]. There is a gradual one-way process between these stages, with little exchange of information between each stage of the work. The features of this protection process are as follows:

However, with the increase of various problems faced by building protection, the content of building protection has gradually become more complex and diversified. However, the mentioned advantages of building protection have turned into shortcomings in the current building protection.

At present, the security process of historical buildings is becoming more and more complex, and the circle of participants in the security process has expanded significantly, not only involving professional security personnel but also manufacturers and users. Decision-making and technical assistance at all stages of the conservation base should be provided. It is precise because of the joint participation of all employees that the original routine can no longer meet the needs of the current work [11]. The participants in the protection of historical buildings are shown in Table 2.

In addition, China's awareness of historical building conservation is weak. Major parts of the historic buildings are mostly dilapidated, severely or even collapsed. Historical buildings have their own uniqueness, and their safety issues are more important than general buildings, including the safety problems of historical buildings themselves, the fire bank problems of historical buildings, and the environmental impact of historical buildings' protection [12].

When interpreting historical building information, the aggregation of historical building information is the protection of historical buildings, and the value of historical buildings lies in the information provided and transmitted by historical buildings. Therefore, in order to better protect the historical buildings, it is necessary to clarify the protection status and existing problems of the historical building information at this stage.

Due to the inadequate implementation of digital information work, the historical building information collected and organized lacks integrity and coherence, and the work functions of local governments and various research institutions are unclear. It causes the historical building information to present an island state and even a large number of repeated links [13]. This virtually hinders the application of digital information technology in the protection of historical buildings and deviates from the original intention of protecting and inheriting real and comprehensive historical building information [14]. Once the information transformation and analysis takes a long time, it will lead to low protection efficiency and easy to cause information failure. It can be seen that the construction of a complete historical building information system has become the key to the protection of historical buildings, as well as the

Table 1: Building preservation process.

The first stage preliminary research	Background research Photo compilation Building survey Building inspection Various identifications
The second stage design stage	Concept Design Extended design Construction design
Phase 3 construction phase	Construction preparation Construction collaboration Construction management
The fourth stage is the data compilation and archiving stage	Data collection into a book

protection of historical buildings and inheritance of excellence The development trend of historical building culture and innovative historical building protection methods [15] as shown in Figure 1.

At the same time, the historical building protection model is only implemented on a two-dimensional basis, the visualization and correlation of data are relatively poor, and the technical level is low, which seriously affects the development of protection work, and problems are not easy to be found.

3.2. Newton Deep Learning Optimization Algorithm. The Newton iteration method, also known as the Newton–Raphson method, is a method proposed by Newton in the 17th century to approximately solve equations in real and complex fields. In deep learning, the so-called optimization algorithm is an iterative method for finding the optimal solution to the objective function. In the convex optimization task, in order to solve the time-consuming problem of gradient calculation caused by a large amount of data, iteration may reduce the calculation amount of each step instead of the convex problem, and the iterative method is used to continuously approach the optimal solution function of the target [16].

Second-order methods use second-order derivatives to improve optimization compared to first-order methods, of which the most widely used second-order method is Newton's method. For the constraint problem f (a), the minimum value of the objective function is a*. The second-order Taylor expansion of f (a) is given as follows:

$$f(a) = f(a_k) + b_k^T(a - a_k) + \frac{1}{2}\left(a - a^k\right)^T H\left(a^k\right)(a - a_k). \tag{1}$$

Among them, b_k is the gradient of f (a) function at a_k, $H(a^k)$ is the Hessian matrix of f (a) at point a_k; and the gradient of the function at the extreme point is 0, that is, given as follows:

$$\nabla f(a) = 0. \tag{2}$$

In the process of finding the minimum value, it is assumed that in the k^+1th iteration, $\nabla f(a^{k+1}) = 0$. So from the formula, we get as follows:

$$\nabla f(a) = g_k + H_k\left(a - a^k\right). \tag{3}$$

That is: $g_k + H_k(a^{k+1} - a^k) = 0$, so we can get Newton's method iterative formula gradient descent method is a common optimization algorithm. In addition to the challenges posed by certain characteristics of the objective function, Newton's method for training large neural networks is also limited by its significant computational burden. Assuming that f (a) has a first-order continuous partial derivative, in solving such unconstrained optimal problem min f (a), a* is the minimum value of the objective function. The first-order Taylor expansion of f (a) is given as follows:

$$f(a) = f(a_k) + g_k^T(a - a_k). \tag{4}$$

Among them, $g_k$is the gradient of the f(a) function at x_k, then the k+1th iteration satisfies:

$$a^{(k+1)} \longleftarrow a^k + \lambda_k p_k. \tag{5}$$

3.3. Feature Perception Enhancement Algorithm for Fog Scene Based on Generative Adversarial Mapping Network. The first method of feature augmentation is to identify missing values in the data, which can better understand how to use the data in the real world. In natural scenes, due to the existence of fog or haze, the scene information is weakened during the image acquisition process [17]. Affected by the scattering of light by fog or haze in the environment, part of the reflected light in the scene cannot be received normally. It causes the loss of some details and color differences in the image, and the loss or change of the feature information in the image, which leads to image distortion. For ordinary perceptual networks, it cannot abstract the perspective for restoring hazy images [18]. The perception network uses two kinds of multilayer deep neural networks to construct an adversarial training framework to ensure the effective implementation of training rules. It fuses multiple features more accurately and obtains a perspective rate, that is, more in line with the real scene. The specific implementation algorithm is shown in Figure 2.

Feature augmentation is in the sense of identifying problematic areas and determining repair method is most effective, rather than removing things. A foggy environment

Table 2: Various participants in building protection.

Protection process	The first stage of preliminary research					The second stage design stage				The second stage construction phase			The fourth stage is the data compilation and archiving stage	Total
	Background research	Photo compilation	Building survey	Building inspection	Various identifications	Concept	Design	Extended design	Construction design	Construction preparation	Construction collaboration	Construction management	Data collection into a book	
Participants														
Owners and managers	√	√				√	√	√	√	√	√		√	10
Architect	√	√	√	√	√	√	√	√	√	√	√		√	13
Architectural historian	√	√				√	√						√	5
Contractor										√	√	√	√	5
Department of historic preservation	√	√	√	√	√	√	√	√	√	√	√		√	13
Historic building restorer	√	√		√	√	√	√	√	√	√	√	√	√	13
Structural engineer	√	√	√	√	√	√	√	√	√	√	√		√	12
Environmental engineer	√	√				√	√	√	√	√	√		√	5
Landscape engineer	√	√	√	√	√	√	√	√		√	√		√	13
Craftsman	√	√								√		√		4
Materials scientist	√	√				√	√							4
Surveyor	√	√	√										√	4
Planner						√	√						√	3

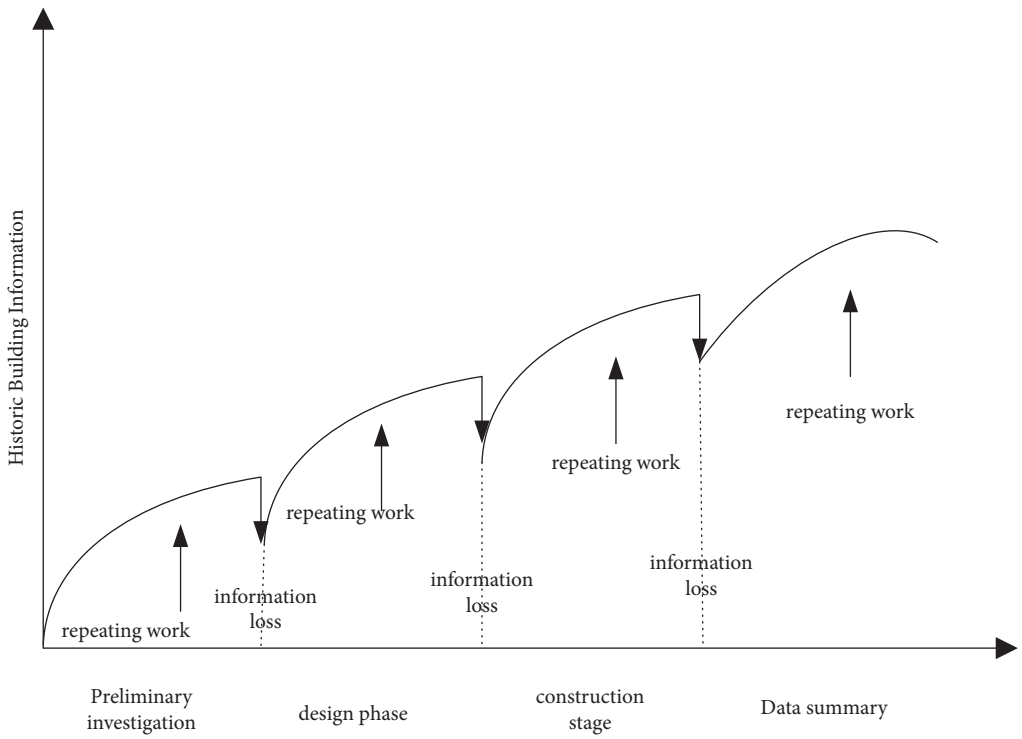

Figure 1: Information transfer process in historic building protection.

is the scattering of light by atmospheric particles, the light reflected from the target surface in the scene is scattered, and its light intensity decreases and expands exponentially, and the light source increases with the propagation distance [19]. According to the atmospheric light scattering theory, a widely used atmospheric light scattering model is formed in computer vision and graphics:

$$I(a) = J(a)t(a) + X(1 - t(x)). \tag{6}$$

Among them, I is the blurred image, J is the faded scene image, t is the transmittance $t = e^{-\beta d(x)}$ of the light propagation medium, X is the atmospheric light value, and a is the image pixel. However, in a real blurry scene, there is no single light source, and the light reflected from the target also has slow reflections, as shown in Figure 3, thus defining multiple light source scattering models:

$$I(a) = J(a)t(a) + X^*(1 - t(a)). \tag{7}$$

Among them, $X^* = \partial_0 X + {}^n\sum \alpha_i X_i$. X_* is the value of the rest of the interference light in the scene except atmospheric light, including the interference light after the diffuse reflection of the reflected light between the independent light source and the target, and the light source intensity coefficient.

In order to realize the dehazing processing of the foggy image, the fog-free image J in the scene is estimated, which can be obtained according to the formula as follows:

$$J(a) = \frac{I(a) - X^*}{t(x)} + X^*. \tag{8}$$

At this point, the attenuation image transformation is converted into an estimate of the ratio of perspective to atmospheric light A. During the propagation of light, the speed of light loss at different wavelengths is different. Channels in RGB space, relevant perspective metrics are evaluated accordingly and satisfy:

$$0 \le \overline{t}^c \le 1, \forall c \in \{r, g, b\}. \tag{9}$$

where $\overline{t}^c$ is the c-channel perspective in RGB space. In the computed fluoroscopy, $\sum(a)\sum J(a)$ occurs due to overestimation of fluoroscopy velocity due to limitations of fluoroscopy velocity or insufficient prior information. Assuming both blur and smoke images in the same scene in the same scene, there are:

$$t^c_{dist}(a) = \frac{X^* - I^c(a)}{X^* - J^c(a)}, 0 \le t^c_{dist}(a) \le 1. \tag{10}$$

Among them, t^c_{dist} is the optimal perspective ratio of the c channel. To solve the perspective relationship under limited conditions, the traditional method cannot precisely define it. To address this poor design, a method of natural image statistics is used to estimate the perspective ratio. It is further transformed into the minimum value problem in convex optimization, satisfying:

$$\min L\left(, t_{dist}\right) = \min L(G(F(I)),). \tag{11}$$

Among them, L is the loss function in image statistics, G is the mapping function from the input image I to the perspective, and F is the fog-related feature extracted from the input image I.

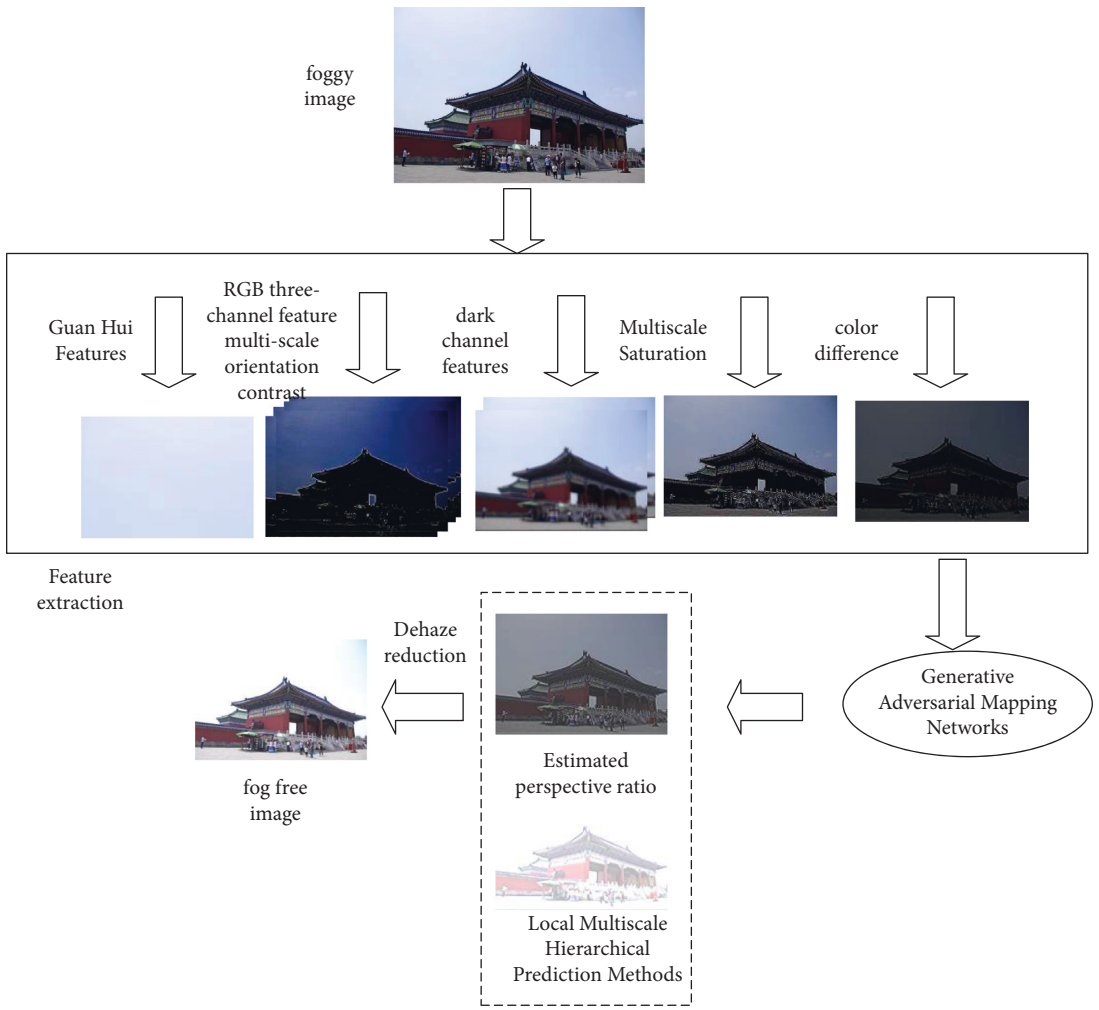

Figure 2: Framework diagram of multilayer perceptual dehazing algorithm based on generative adversarial mapping network.

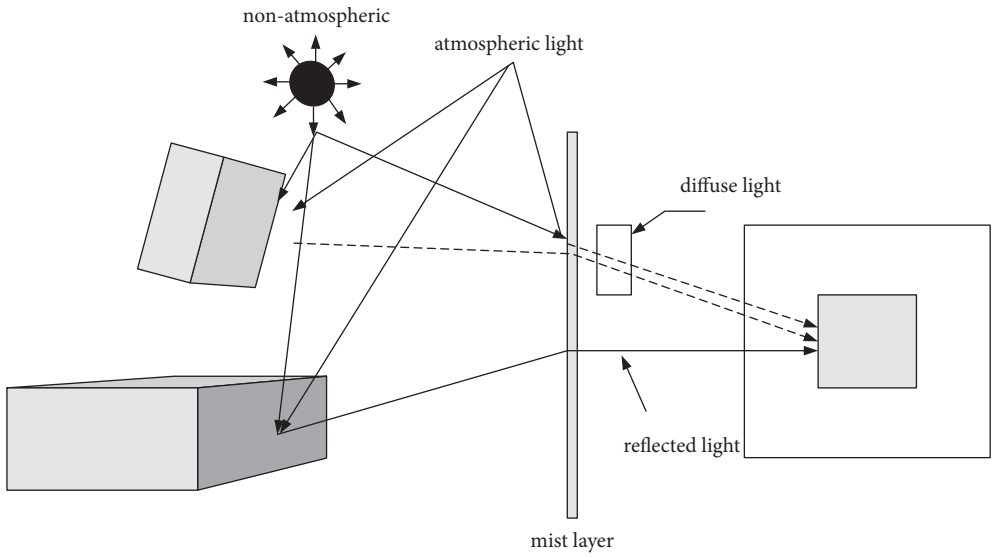

Figure 3: Multisource scattering model.

3.4. Item-Based Collaborative Filtering Algorithm. The so-called collaborative filtering is to recommend items to users based on their previous product preferences and the choices of other users with similar interests. Product-based collaborative filtering algorithms have been widely used in the industry since they were proposed, and are still the basis for reference algorithms used by many companies [20]. The idea is very intuitive, that is, recommend the most similar scheme to the user, that is, recommend according to the user's historical interest, as shown in Figure 4.

When a user needs a personalized building protection scheme, he/she can first find other users, who have similar interests to him/her and then recommend those novel schemes that the user likes to the user. Building i represents $R = \{r_{ij}\}$ of the user-item matrix in the i-th column, then the formula for calculating the cosine similarity of the angle between building i and building j is given as follows:

$$sim(i, j) = \cos(\vec{i}, \vec{j}) = \frac{\vec{i} \bullet \vec{j}}{\vec{i}_2 * \vec{j}_2}. \tag{12}$$

The formula to express the Pearson correlation is given as follows:

$$sim(i, j) = \frac{\sum_{u \in U} (r_{ui} - r_i)(r_{u,j} - r_i)}{\sqrt{\sum_{u \in U} (r_{ui} -)^2} \sqrt{\sum_{u \in U} (r_{u,j} -)^2}},$$
$$sim(i, j) = J(i, j) = \frac{|U_i \cap U_j|}{|U_i \bigcup U_j|}. \tag{13}$$

3.5. Algorithms Based on Threshold Cyclic Units. A simple recurrent unit is a variant, what they have in common is that each neuron is a processing unit, and each processing unit contains several thresholds, which are used to control the flow of information. The recurrent threshold cell model was proposed in 2014. And it performs well in speech recognition and machine translation [21]. The entire GRU process is shown in Figure 5.

The hidden state of the recurrent neural network changes the activation function to a nonsaturated activation function, thereby avoiding the problem of gradient disappearance caused by the saturated activation function, and at the same time, it can also speed up the network convergence speed. The activation function value at time t is the weighted average of the activation function value h_{t-1}^j at the moment before h_t^j and the candidate activation function value at the current moment.

$$h_t^j = (1 - z_t^j) h_{t-1}^j + z_t^j. \tag{14}$$

Among them, z_t^j is called the update gate to determine the update proportion, and the formula is given as follows:

$$z_t^j = \sigma(W_z x_t + U_z h_{t-1})^j, \tag{15}$$

where σ is the sigmoid activation function. When is the hanging value after the time, the calculation formula is given as follows:

$$= tabh(W_z x_t + U_z h_{t-1})^j, \tag{16}$$

where tanh is the hyperbolic tangent function.

$$tanh(x) = \frac{e^x - e^{-x}}{e^x + e^{-x}},$$
$$r_t^j = \sigma(W_r x_t + U_r h_{t-1})^j. \tag{17}$$

To avoid overcustomization, a dropout layer is added between the two layers, and the parameters disconnect the split-add neurons on each update. In other lists of similar buildings of the time, the partial formula:

$$L(\{x, y\}_1^N) = -\sum_n \sum_i y_i^{(n)} * \log(f(x^{(n)})i). \tag{18}$$

Figure 6 shows the model forward propagation flow chart. Suppose there are four types of buildings, numbered 1, 2, 3, and 4. They are represented as vectors in the input layer as shown in Figure 6 according to their encoded form.

Set the hidden layer node to 3, then the 1*3 vector exits the GRU structure function in the hidden layer. Finally, the fully connected layer provides the probability that each product may appear at different times and uses the output probability and the maximum N products as recommendations to the user.

4. Building Conservation Planning Test Based on Multifeature Deep Learning Model

By scientifically and rationally protecting the building's information model throughout its life cycle, a history is also an object in the information model, seamlessly conveying the protection of all historic buildings. It is better communicated to future assets, and professionals can also join the work earlier [22]. Depending on the division of labor, it can bring its own technology and experience to contribute to the preservation of historic buildings [23]. The project is shown in Figure 7.

4.1. Deep Neural Network Model Based on RPN. RPN (region proposal network) is a fully convolutional neural network used to extract target candidate boxes in detection [24]. In order to solve this bottleneck, some scholars proposed to use the CNN network to extract the target area, that is, the RPN to extract the target detection area. The detection network of the proposed algorithm is shown in Figure 8. The task of finding relevant features through deep learning is part of the algorithm that automates the feature engineering that reduces the problem.

4.2. Precision, Recall, and T-Score. The concepts of classification accuracy and recall (recall) were proposed in 1968 and are still in use today [25]. The accuracy rate is P, which is defined as the ratio of the number of products recommended

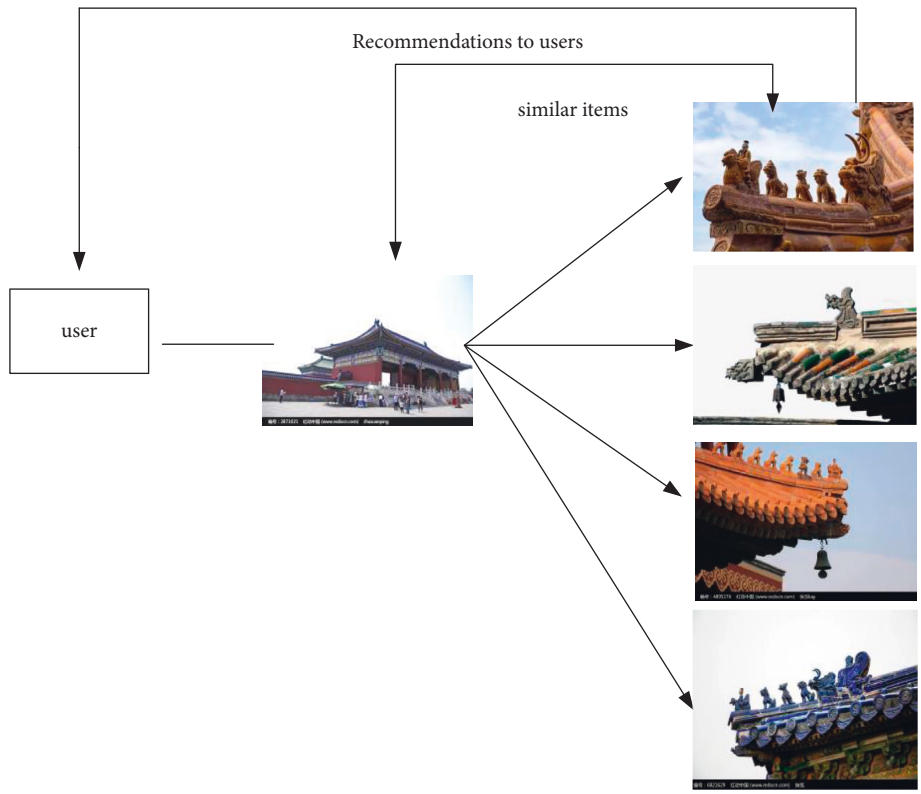

Figure 4: User usage history product recommendation.

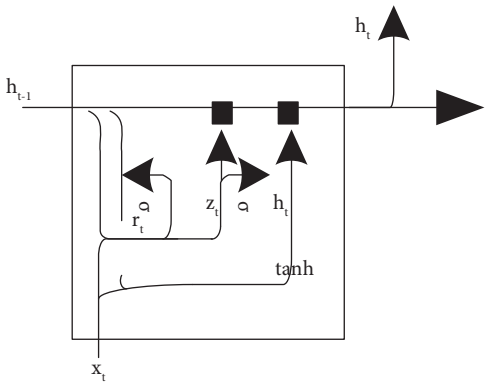

Figure 5: GRU structure diagram.

by the user to the number of products that the user actually uses. It can reflect the possibility that the user will use a recommended product [26].

When a user is recommended to be specified, the user is an active user, denoted as U_a. After sorting the purchased items by purchase time, it is called the user's purchase sequence, denoted as S_a, and N represents the number of recommended items. When the data are implicit feedback, if user i has acted on item j, $r_{ij} = 1$, otherwise $r_{ij} = 0$. Common symbols and their meanings are shown in Table 3.

Often mentioned together with precision is recall. The recall rate is recorded as R, and the user's historical behavior data are regarded as time series data, so the data S_a^{t-1} of the usage sequence S_a of the user U_a before time t is generally used as the historical data. The data S_a^{t+1} after time t is used as unknown data to evaluate the model. Table 3 presents the recommended results based on S_a^{t-1} and the number of user favorite products in S_a^{t+1}. Then the calculation Formula of the precision rate and recall rate of the available user U_a from Table 4 is:

$$W = \frac{P_{rs}}{P}, R = \frac{P_{rs}}{P_r}. \tag{19}$$

T-score is a comprehensive consideration of precision and recall, and its calculation formula is given as follows:

$$T = \frac{2 * W * R}{W + R}. \tag{20}$$

The calculated precision, recall, and T-score are averaged over all users. The T-score is mainly used for the selection of hyperparameters in the model.

4.3. Feasibility Analysis of Historical Building Protection Based on Multifeature Deep Learning. Strategies for crawling user rating data for usage scenarios and details of subsequent data processing. Then enter the personal homepage of each user, if the user has reviewed more than 50 buildings, then crawl its building list and the corresponding score, and the crawling fields are the same. Repeat the process several times to achieve the desired amount of data.

It can be seen from the strategy of crawling the data of building ratings that the crawling is mainly for popular buildings, so the crawled data belongs to a class of extreme

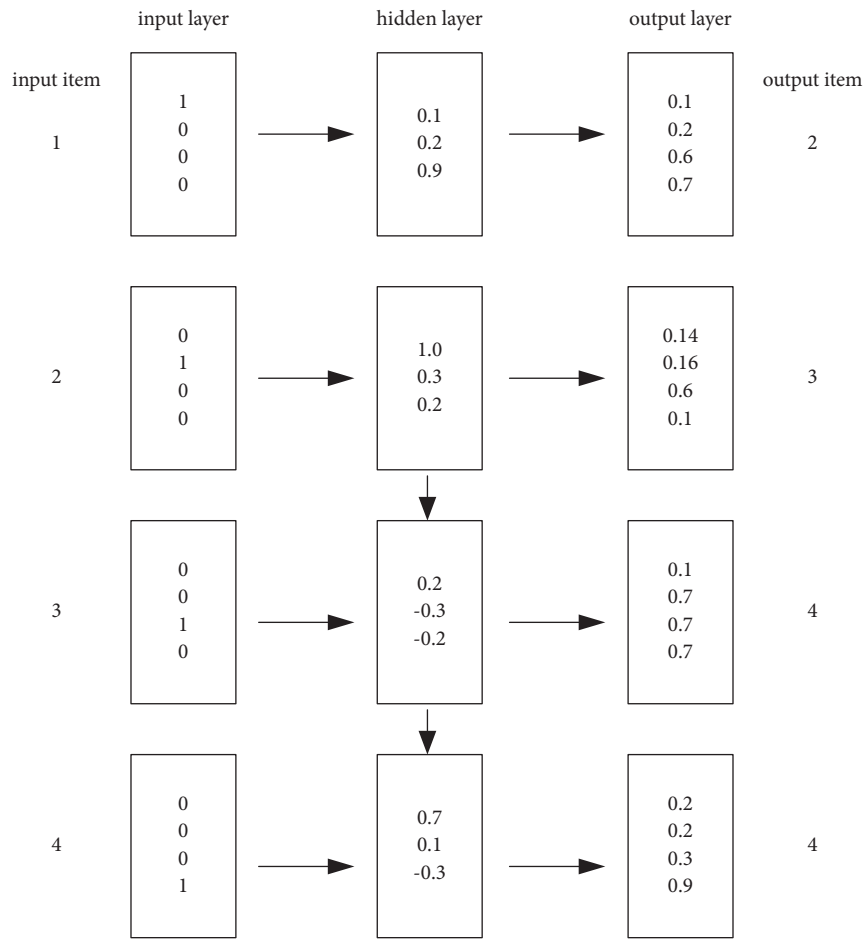

Figure 6: Model forward propagation flow chart.

data. It crawls the scores of popular building data relatively completely, but the scores of other buildings are very incomplete. Figure 9 is a graph of user evaluation data of the top 5 popular buildings in 2018.

First, the duplicate samples in the dataset are removed; secondly, due to the crawling strategy of the building rating dataset, the number of recommendations in the dataset is too large, so it is processed and the building entries with less than 10 comments are deleted. Then, change the time in the dataset to timestamp format and sort user reviews chronologically. Finally, unify the field names in the two datasets. The fields included in the final dataset are given as follows:

As can be seen from Table 5, from the perspective of data density, the user-recommendation number matrix dataset of the building rating dataset is relatively sparse.

The distribution of the number of user reviews and the number of building reviews in each dataset is shown in Figure 10. It can be seen from the figure that the number of ordinary photo users with less than 10 comment data are far more than the number of users, who use the case scoring dataset for dehazing photos, and the number of comments in the two datasets is similar. But when the number of comments is greater than 20, the number of people in the normal photo use case dataset is significantly smaller than the number of people in the dehazing photo using rating data.

According to the comparison and analysis of the results of the recommendation algorithm on the test sets of the two data sets with large differences in characteristics, Figure 11 shows the results when the number of recommended items N is 10 and 20, respectively.

On the two datasets, under the conditions that the recommended number is 10 and 20, the coverage rate of the enhancement algorithm against fog scene feature perception is the highest. When the number of recommendations is 20, the user coverage rate of the recommended case for dehazing photos can reach 100%. Fill in the missing values of the test set with the mean of the training set in the test set to achieve the effect of data enhancement, so as to achieve the purpose of feature enhancement.

5. Discussion

By collecting, sorting, summarizing, and establishing relevant systematic procedures for extensive theoretical data and case data on historical building protection measures, this paper analyzes the comprehensive problems of historical buildings. Aiming at these problems, this paper proposes to use the algorithm in multifeature learning to optimize the system. Therefore, it innovatively proposes to create a system suitable for the protection of historical buildings, and this

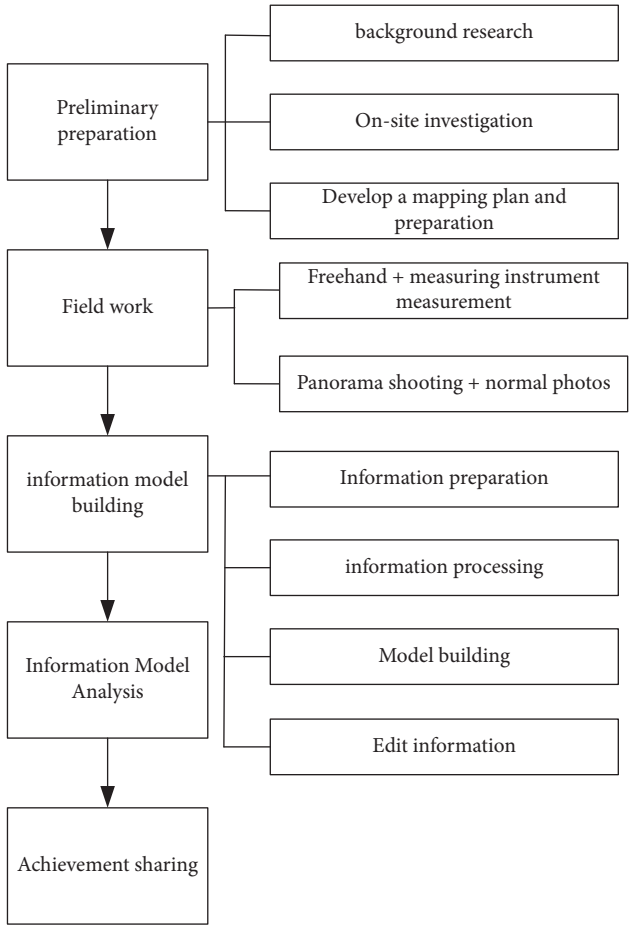

Figure 7: Project practice process.

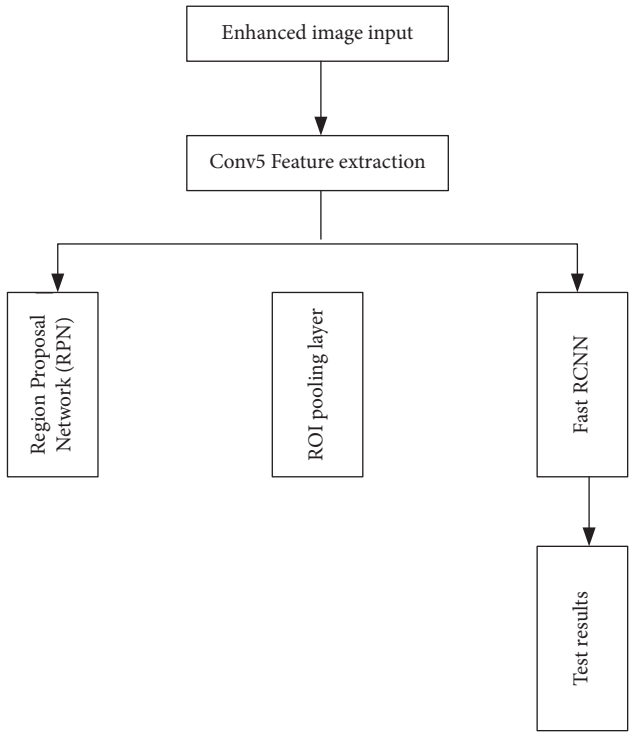

Figure 8: Network model framework diagram.

Table 3: Common symbols and their meanings.

Symbol	Meaning
U_a	Active user
S_a	Purchase sequence of active users
N	Number of recommended items
n	Number of users
m	Number of item types
R	User-item matrix

Table 4: User preference and number of recommended products.

	Number of recommended products	Number of products not recommended	Total
User likes the number of products	P_{rs}	P_{rn}	P_r
User dislikes the number of products	P_{is}	P_{in}	P_i
Total	P	P_n	m

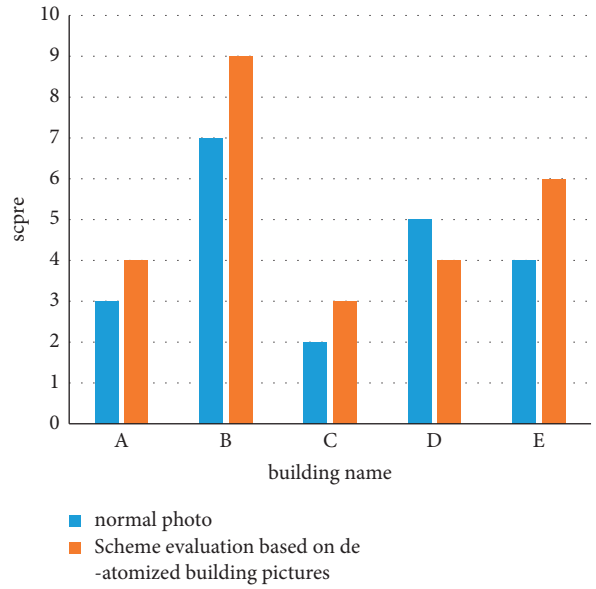

Figure 9: User evaluation data graph.

Table 5: Dataset features table.

	Ordinary photo dataset	Dehazed photo dataset
Number of users	50	60
Number of buildings	130	135
Total number of transactions	310	321
Data density	6.77%	7.13%
Average number of evaluation plans per user	12	15
The average number of evaluations for each program	17	20

paper organizes and categorizes various parameter information required by the comprehensive research of historical buildings. It builds a relatively complete, scientific, and universal parameter library.

According to the elements and characteristics contained in historical buildings, this paper stores digital information. According to the deep neural network model of RPN, the building information is connected, and this paper together constitutes a complete and clear information system model. It is provided to research units, construction units, investment units, and government departments at all levels to truly realize automated, intelligent, and seamless management.

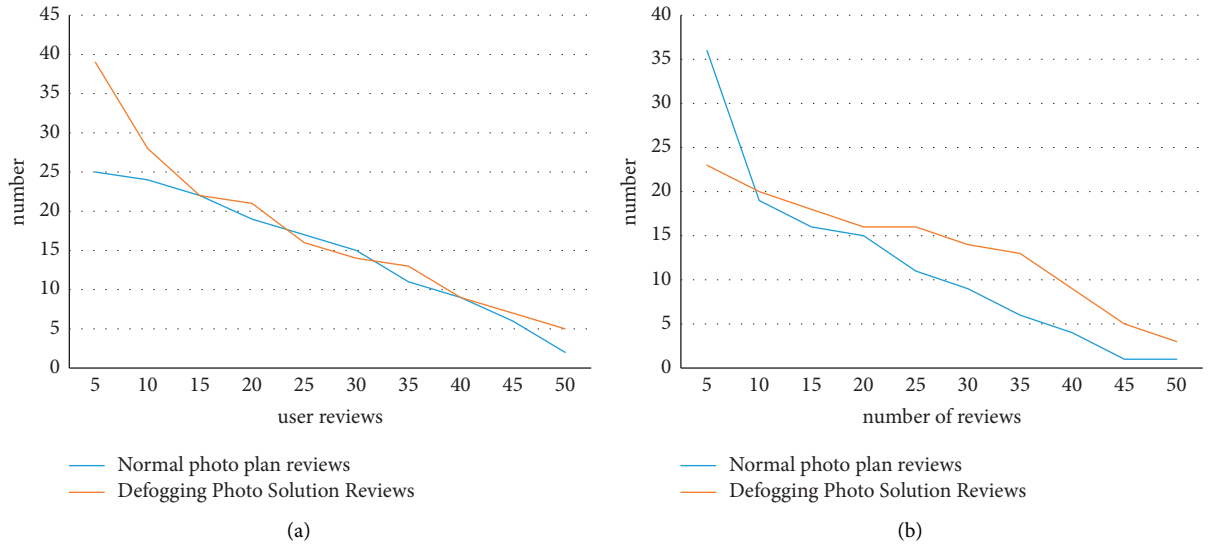

Figure 10: The number of user reviews and the number of recommended case reviews in two cases.

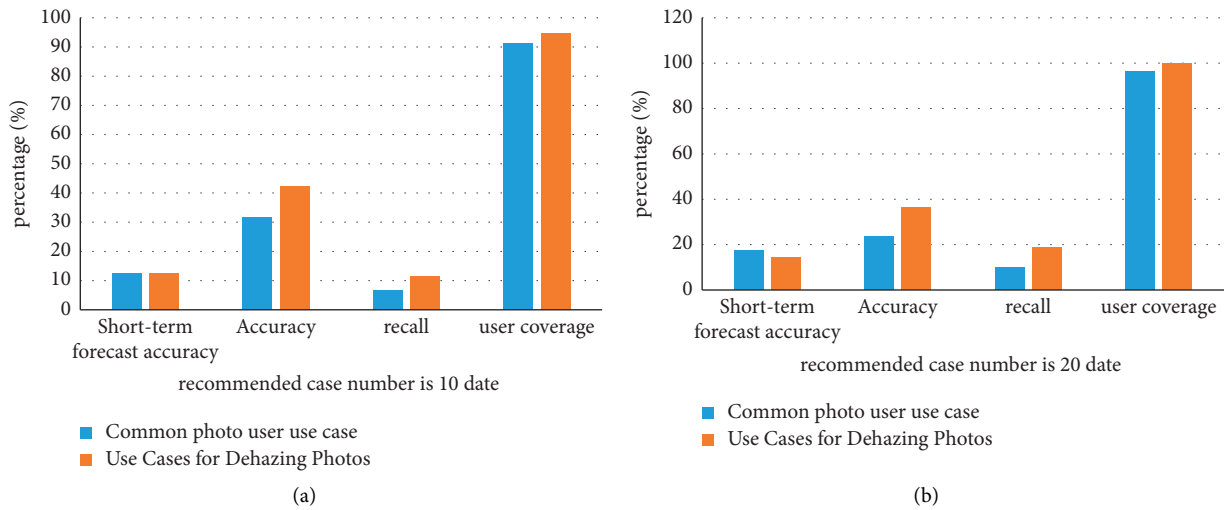

Figure 11: The number of user reviews and the number of recommended case reviews in two cases.

6. Conclusion

As an important part of the machine learning field, the recommendation algorithm not only has academic value but is also a marketing method in the business economy, so both the academic and industrial circles have paid great attention to it. The building protection test has only done a preliminary study on the classic recommendation algorithm, and there are still many deficiencies. The scoring data are not considered in the model, and how to apply the scoring data to deep learning is also a problem that needs to be considered.

Data Availability

No data were used to support this study.

Conflicts of Interest

The authors declare no potential conflicts of interest in this study.

Acknowledgments

This work was supported by School Level Scientific Research Projects "Research on Protection and Development of Mountain Towns under the Background of Vitalization of Rural Areas," no. XKY202117; and Chongqing Social Science Planning Project "Study on Ecological-Poverty Coupling and Poverty Alleviation in Karst Area of Chongqing," no. 2017YBGL161.

References

[1] G. Litjens, T. Kooi, B. E. Bejnordi et al., "A survey on deep learning in medical image analysis," *Medical Image Analysis*, vol. 42, no. 9, pp. 60–88, 2017.

[2] Y. Chen, Z. Lin, and Z. Xing, "Deep learning-based classification of hyperspectral data[J]," *Ieee Journal of Selected Topics in Applied Earth Observations and Remote Sensing*, vol. 7, no. 6, pp. 2094–2107, 2017.

[3] D. Shen, G. Wu, and H. I. Suk, "Deep learning in medical image analysis," *Annual Review of Biomedical Engineering*, vol. 19, no. 1, pp. 221–248, 2017.

[4] T. Oshea and J. Hoydis, "An introduction to deep learning for the physical layer," *IEEE Transactions on Cognitive Communications and Networking*, vol. 3, no. 4, pp. 563–575, 2017.

[5] W. Hou, X. Gao, and D. Tao, "Blind image quality assessment via deep learning[J]," *IEEE Transactions on Neural Networks and Learning Systems*, vol. 26, no. 6, pp. 1275–1286, 2017.

[6] W. Zhao, J. Luo, S. Li, J. Qi, H. Meng, and Y. Li, "Design of dynamic calf weighing system based on moving-IIR filter algorithm," *Journal of Electrical Engineering & Technology*, vol. 16, no. 2, pp. 1059–1069, 2021.

[7] R. Yang, A. Zhang, L. Zhang, and Y. Hu, "A novel adaptive H-infinity cubature kalman filter algorithm based on sage-husa estimator for unmanned underwater vehicle," *Mathematical Problems in Engineering*, vol. 2020, no. 2, pp. 1–10, 2020.

[8] H. He, "Development of magnetorheological elastomers-based tuned mass damper for building protection from seismic events[J]," *Journal of Intelligent Material Systems and Structures*, vol. 29, no. 8, pp. 1777–1789, 2018.

[9] Y. Tom, H. Devamanyu, and P. Soujanya, "Recent trends in deep learning based natural language processing [review article][J]," *IEEE Computational Intelligence Magazine*, vol. 13, no. 3, pp. 55–75, 2018.

[10] J. Lee, "Integration of digital twin and deep learning in cyber-physical systems: towards," *Smart Manufacturing[J]*, vol. 38, no. 8, pp. 901–910, 2020.

[11] H. He, C. K. Wen, S. Jin, and G. Y. Li, "Deep learning-based channel estimation for beamspace mmWave massive MIMO systems," *IEEE Wireless Communications Letters*, vol. 7, no. 5, pp. 852–855, 2018.

[12] Z. M. Fadlullah, F. Tang, B. Mao et al., "State-of-the-Art deep learning: evolving machine intelligence toward tomorrow's intelligent network traffic control systems," *IEEE Communications Surveys & Tutorials*, vol. 19, no. 4, pp. 2432–2455, 2017.

[13] Y. Jian, J. Ni, and Y. Yang, "Deep learning hierarchical representations for image steganalysis[J]," *IEEE Transactions on Information Forensics and Security*, vol. 12, no. 11, pp. 2545–2557, 2017.

[14] L. He, K. Ota, and M. Dong, "Learning IoT in edge: deep learning for the internet of things with edge computing[J]," *IEEE Network*, vol. 32, no. 1, pp. 96–101, 2018.

[15] T. Young, D. Hazarika, S. Poria, and E. Cambria, "Recent trends in deep learning based natural language processing [review article]," *IEEE Computational Intelligence Magazine*, vol. 13, no. 3, pp. 55–75, 2018.

[16] J. Han, D. Zhang, G. Cheng, N. Liu, and D. Xu, "Advanced deep-learning techniques for salient and category-specific object detection: a survey," *IEEE Signal Processing Magazine*, vol. 35, no. 1, pp. 84–100, 2018.

[17] G. Chartrand, P. M. Cheng, E. Vorontsov et al., "Deep learning: a primer for radiologists," *RadioGraphics*, vol. 37, no. 7, pp. 2113–2131, 2017.

[18] H. A. H Ae Nssle, C. Fink, R. Schneiderbauer et al., "Man against machine: diagnostic performance of a deep learning convolutional neural network for dermoscopic melanoma recognition in comparison to 58 dermatologists," *Annals of Oncology*, vol. 29, no. 8, pp. 1836–1842, 2018.

[19] S. S. Han, M. S. Kim, W. Lim, G. H. Park, I. Park, and S. E. Chang, "Classification of the clinical images for benign and malignant cutaneous tumors using a deep learning algorithm," *Journal of Investigative Dermatology*, vol. 138, no. 7, pp. 1529–1538, 2018.

[20] S. Z. M. Yildirim, "A new similarity coefficient for a collaborative filtering algorithm[J]," *Communications Faculty Of Science University of Ankara*, vol. 59, no. 2, pp. 41–54, 2017.

[21] L. Jiang, Y. Cheng, L. Yang, J. Li, H. Yan, and X. Wang, "A trust-based collaborative filtering algorithm for E-commerce recommendation system," *Journal of Ambient Intelligence and Humanized Computing*, vol. 10, no. 8, pp. 3023–3034, 2019.

[22] O. A. Montesinos-López, E. Franco-Pérez, F. J. Luna-Vazquez et al., "Benchmarking between item based collaborative filtering algorithm and genomic best linear unbiased prediction (GBLUP) model in terms of prediction accuracy for wheat and maize//Estudio comparativo en términos de capacidad predictiva para datos de trigo y maíz entre el algoritmo de filtrado colaborativo y el modelo genómico mejor predictor lineal insesgado (GBLUP)," *BIOtecnia*, vol. 22, no. 2, pp. 136–146, 2020.

[23] H. Chen, W. Yan, H. Sun, and M. Cheng, "Tag-extended collaborative filtering recommendation algorithm," *SN Computer Science*, vol. 1, no. 5, p. 302, 2020.

[24] N. Yang, L. Chen, and Y. Yuan, "An improved collaborative filtering recommendation algorithm based on retroactive inhibition theory," *Applied Sciences*, vol. 11, no. 2, p. 843, 2021.

[25] E. Uko, "An improved online book recommender system using collaborative filtering algorithm," *International Journal of Computer Application*, vol. 179, no. 46, pp. 41–48, 2018.

[26] J. Chen, B. Wang, Z. Ouyang, and Z. Wang, "Dynamic clustering collaborative filtering recommendation algorithm based on double-layer network," *International Journal of Machine Learning and Cybernetics*, vol. 12, no. 4, pp. 1097–1113, 2021.

Hindawi
Scientific Programming
Volume 2023, Article ID 9867242, 1 page
https://doi.org/10.1155/2023/9867242

Retraction

Retracted: Application and Performance Discussion of Fiber-Reinforced Composite Materials in Sports Equipment Based on Image Processing Technology

Scientific Programming

Received 1 August 2023; Accepted 1 August 2023; Published 2 August 2023

This article has been retracted by Hindawi following an investigation undertaken by the publisher [1]. This investigation has uncovered evidence of one or more of the following indicators of systematic manipulation of the publication process:

(1) Discrepancies in scope
(2) Discrepancies in the description of the research reported
(3) Discrepancies between the availability of data and the research described
(4) Inappropriate citations
(5) Incoherent, meaningless and/or irrelevant content included in the article
(6) Peer-review manipulation

The presence of these indicators undermines our confidence in the integrity of the article's content and we cannot, therefore, vouch for its reliability. Please note that this notice is intended solely to alert readers that the content of this article is unreliable. We have not investigated whether authors were aware of or involved in the systematic manipulation of the publication process.

Wiley and Hindawi regrets that the usual quality checks did not identify these issues before publication and have since put additional measures in place to safeguard research integrity.

We wish to credit our own Research Integrity and Research Publishing teams and anonymous and named external researchers and research integrity experts for contributing to this investigation.

The corresponding author, as the representative of all authors, has been given the opportunity to register their agreement or disagreement to this retraction. We have kept a record of any response received.

References

[1] E. Liu, "Application and Performance Discussion of Fiber-Reinforced Composite Materials in Sports Equipment Based on Image Processing Technology," *Scientific Programming*, vol. 2022, Article ID 6879601, 12 pages, 2022.

Hindawi
Scientific Programming
Volume 2022, Article ID 6879601, 12 pages
https://doi.org/10.1155/2022/6879601

Research Article

Application and Performance Discussion of Fiber-Reinforced Composite Materials in Sports Equipment Based on Image Processing Technology

Erwei Liu

Students Affairs Department, Chongqing Vocational College of Transportation, Jiangjin 402247, Chongqing, China

Correspondence should be addressed to Erwei Liu; liuerwei@cqjy.edu.cn

Received 30 June 2022; Revised 12 August 2022; Accepted 25 August 2022; Published 24 September 2022

Academic Editor: Juan Vicente Capella Hernandez

Fiber reinforced composites can meet the needs of lightweight, heavy load, long-span, high strength, and modern structures and work under strict conditions. Therefore, it is widely used in various fields. Sports equipment generally cannot meet the requirements of high-strength use, so there is an urgent need for new fiber materials to make these instruments. Aiming at improving the efficiency of measurement and the reliability of measurement results, this paper studies the quantitative characterization method of the microstructure of short fiber reinforced composites. The swept-frequency OCT system is a newly developed high-resolution biomedical imaging system. The method of this paper is to study the performance parameters of swept frequency OCT system, deduce the application of image processing technology in fiber material detection, and then study the detection of residual strength and residual stiffness of composites, so as to obtain a composite material detection method that can be popularized. On this basis, image processing and performance analysis of the composites were carried out, and the composites were tested. And the prospect of application in this field has been analyzed. The experimental results show that better fiber length can be obtained by this method, and the maximum relative error is only 4.5%, thus ensuring the accurate determination of fiber length. Calculations were carried out using the experimental data, and the results showed that the performance of the sports product increased from 15.4% to 48.6% with the graphite-rubber composite. Using this material can improve the comprehensive performance of sports equipment by 2.1%~4.5%.

1. Introduction

1.1. Background. The discovery and utilization of all important material materials in history will bring significant changes to human production and living standards and social productivity. Material is the material basis for human survival and development and plays an important role in human society. Juxtaposed with energy and information, it is known as the three pillars of modern human society. After the 20th century, due to the rapid development of science and technology, in order to meet the human demand for new products of high-performance materials, the role of traditional materials is dwarfed, so multistructure composites are produced. High-performance structural materials refer to those materials with special properties such as high strength, high toughness, high-temperature resistance, wear resistance, and corrosion resistance. Compared with single polymer materials or other traditional materials, fiber-reinforced composites have many advantages, such as large elasticity, high specific heat capacity, simple molding process, good fatigue resistance, good shock absorption, good overload safety, and strong functionality, which makes them the most widely used and widely used composite materials at present. Measuring the length and orientation of fibers in short fiber reinforced composites plays a very important role in analyzing the macro mechanical properties of materials. This paper discusses the application and performance of fiber-reinforced composite materials in sports equipment based on image processing technology, in order to make certain contributions to fiber-reinforced composite materials.

1.2. Significance. This study aims to improve the efficiency and reliability of the quantitative characterization of short fiber reinforced composite materials and explore a simple and reliable method to measure the fiber length and orientation distribution in short fiber reinforced composite materials, thereby reducing the difficulty and strength of characterization. The quantitative characterization of microstructure promotes the effective development of the quantitative relationship between microstructure and macroscopic properties. It is hoped that the research in this article can contribute to the development of quantitative research on the microstructure of short fiber reinforced composite materials and improve the movement performance of the equipment.

1.3. Related Work. The image processing technology is more and more widely used in the analysis of fiber-reinforced composites. Jia and Zhang introduced Hadoop-based image resource storage technology to improve the reading speed of image resources, and then uses a random forest algorithm to mine image recognition digital information and recommend the most appropriate online resources. He introduced augmented reality technology to enhance the immersion and interactivity of online education, so that image processing technology can develop appropriate interactive functions according to different scenes, enhance the immersion and participation of online teaching, comprehensively improve the quality of teaching and learning, and provide technical support for the improvement of online learning. However, this image processing technology focuses on information output, the lack of image analysis, and learning [1]. Oho et al. propose an efficient and fast scanning method combined with digital image processing technology to replace the traditional slow scanning mode as the standard acquisition model of general scanning electron microscope. The scanning electron microscope image obtained by using the proposed method has the same quality as the slow scanning image in terms of sharpness and noise, and can suppress the adverse effect of charging under a full vacuum. However, this technology uses the inverse filter based on the frequency characteristics of TV scanned images to properly compensate for the image quality. It is a fuzzy image integration technology, which has no obvious effect on noise suppression, and its position is not robust to noise [2]. Gu et al. analyzed that behavior recognition based on image recognition is an active research field in computer vision. He believes that with the modernization of animal husbandry, innovative technologies such as machine vision and artificial intelligence are gradually applied to biological monitoring, which can realize biological real-time abnormal behavior and biological behavior analysis. Behavior analysis includes biological image sequence, viewfinder, target classification, anomaly detection, and behavior recognition. His research is based on individual behavior image recognition and deduces the analysis function of image recognition. However, his research needs to establish a large number of biological action databases to realize comparative analysis. It is difficult to popularize this technology [3]. Elhousari et al. believe that reinforced thermoplastic composites have excellent corrosion resistance, high specific strength, high impact toughness, high specific stiffness, recyclability, cost-effectiveness and design flexibility, and have considerable advantages in structural and industrial applications. In order to obtain better mechanical properties, reduce the total cost, and enhance the performance of polypropylene composites, he proposed that recycled rubber powder be used as a low-cost additive for polypropylene composites/glass fiber composites. However, his improved method of mixing polypropylene composites and glass fibers with different weight ratios has higher requirements for the injection molding machine, consumes more energy in the production process, and has no obvious cost advantage [4]. Yamamoto and Okabe proposed an accurate tensile strength prediction method for fiber-reinforced composites. He believes that the accurate tensile strength prediction of unidirectional carbon fiber reinforced plastic composites (UD) needs to roughly determine the stress concentration on the remaining fibers around the fiber fracture point. The stress concentrated on the surface of the intact fiber is determined by a double fiber fragment test combined with spring element model simulation. However, carbon fiber is a very special fiber composite, and its characteristics are more distinctive than other materials, so its prediction method is not universal [5]. Hamanaka et al. investigated the correlation between the fiber orientation distribution along the thickness direction and mechanical anisotropy in injection molded products using short fiber-reinforced thermoplastic resin. Then, the fiber orientation distribution near the center of the plate was observed by X-ray computed tomography, and the fiber orientation distribution along the thickness was quantified by a fiber orientation tensor. Then cut the sample from the plate along the machine and transverse direction, and conduct the three-point bending test. Finally, the evaluation results of fiber orientation distribution and mechanical anisotropy are compared. His method is to analyze the material composition, but this analysis is mechanically repeated and can be completed by computer technology, which will be faster and more accurate [6]. Matsuwaka and Latzka analyzed that with the increasing popularity of adaptive sports, the research on improving sports equipment to prevent athletes from facing injury has become more and more important. His survey found that wheelchair basketball, football, tennis, track and field, swimming and football were the most frequently studied in recent years. Injuries vary from sport to sport due to different levels of exposure, limbs used, and athlete injuries. Changes in equipment and technological advances, especially in wheelchairs and amputations, have improved the level of competition and reduced the injury rate. However, he studied the replacement of equipment and neglected to start with equipment manufacturing materials [7]. Starting from the structural materials of sports equipment, Feng and Wang raised the issue of comfort, and then elaborated on the polymer composite materials, and made a case design and analysis of the applicability of polymer composite materials in sports equipment [8]. Jahangir et al. have experimentally investigated the compressive performance of short concrete

columns with square cross-sections confined by steel fiber reinforced polymer and grouting composites SRP and SRG composites [9]. The application of composite materials in aircraft structure is a hot research topic at present. Li et al. mainly discussed the optimal design of the composite wing structure of the DF-2 light sport aircraft [10].

1.4. Innovation Points. The innovations of this study are as follows: (1) Through the hybrid compounding of organic fibers and inorganic fibers, the polypropylene/ethylene vinyl acetate matrix is reinforced and modified to make composite fiber materials with strong comprehensive properties. (2) The experiment and performance analysis of composite fiber image processing were carried out.

2. Image Processing Technology and Composite Strength Detection Method

2.1. Sweep Frequency OCT System Performance Parameters. In order to achieve the purpose of rapid imaging of scanning OCT system, researchers at home and abroad have studied the improvement of OCT system structure and light source while optimizing the postprocessing algorithm of OCT Research Institute. OCT is optical coherence tomography, which is a non-invasive, noncontact, cross-sectional scan of the retina's fine structure in vivo. This study briefly introduces the classification of OCT systems and the investigation of speckle noise elimination at home and abroad. By analyzing the performance parameters and noise sources of the scanning optical coherence tomography system, the noise model of the system is established and the noise simulation is carried out. OCT is one of the most promising new tomographic imaging technologies that has developed rapidly in recent years, especially in biological tissue biopsy and imaging, which has attractive application prospects. In this study, a fast image noise elimination algorithm based on wavelet packet decomposition and least square error filtering is designed. Compared with various OCT image noise elimination methods, the effectiveness of the algorithm is verified. OCT is a non-contact, high-resolution tomographic and biological microscope imaging device. It can be used for in vivo viewing, axial tomography, and measurement of posterior ocular structures, and is particularly useful as a diagnostic device to aid in the detection and management of eye diseases. The schematic diagram of material manufacturing image processing technology is shown in Figure 1.

According to the theory of frequency scanning signal-to-noise ratio, the ratio of signal-to-noise photocurrent to the intensity of noise photocurrent after Fourier transform is the signal-to-noise ratio of the system. Assuming that i_a can represent the signal photocurrent, the signal power f_a^2 is the intensity of the signal photocurrent after Fourier transform, that is, the intensity f_b^2 of the signal photocurrent, in which the noise photocurrent $i_s i_b$. The signal-to-noise ratio of scanning optical coherence tomography systems can be expressed by the following formula:

$$SNR = \frac{f_a^2}{f_b^2}. \tag{1}$$

If it is assumed that the reflectivity on the reflective interface is fixed, when the instantaneous linewidth of the scanning light source in the scanning OCT system is small enough, the signal photocurrent i_a is followed by the noise photocurrent i_b. If the reflectivity on the reflective interface x_0 is fixed, the coherence function of the light source can be approximately 1. In addition, the signal photocurrent and time formula can be expressed by the following formula:

$$i_a(t) = \frac{2nq}{h\nu}\sqrt{W_a W_r}\cos\ (2K(t)x_0). \tag{2}$$

Here, $h\nu$ is the photon energy, q is the electron quantity, n is the quantum efficiency coefficient, W_a is the optical power reaching the detector on a single-layer reflection interface x_0, and W_r is the optical power returning to the detector from the reference arm [11]. At this time, there is $W_a = r^2 W_0$, and r is the reflection coefficient of the sample. At this time, the average noise power (t) of the system can be expressed by the following formula:

$$i_b^2(t) = \left[i_t^2(t) + \frac{2nq^2}{h\nu}(W_a + W_r) + \frac{nq^2}{h\nu}RIN(W_a + W_r)^2\right]BW. \tag{3}$$

The noise of the system is caused by $(2nq^2/h\nu)(W_a + W_r)$ indicates that the high-temperature noise of the system is represented by $i_t^2(t)$ in the formula, and the relative intensity noise of the swept frequency light source is represented by $(nq^2/h\nu)\mathrm{RIN}(W_a + W_r)^2$. H_z^{-1} is the common unit of three kinds of noise, the bandwidth of the photodetector is expressed by BW, and the Fourier conversion method of signal photocurrent can be expressed by an (4). In this formula, the signal photocurrent at the single-layer reflection interface z_l is expressed as i_a.

$$f_s(z_l) = \sum_{b=0}^{N_a - 1} i(k_b)\exp\left(\frac{-2j\pi bl}{N_a}\right). \tag{4}$$

In the above formula, N A is the number of sampling points in each cycle of the system, and the signal photocurrent is (kb). According to Pascal's theorem: $\sum f^2 = N_a \sum i^2$, formula (5) is the signal photocurrent i (kb) after square conversion processing by the Fourier conversion method.

$$\left|f_a^2\right| = \left(\frac{N_a^2}{2}\right)i_a^2. \tag{5}$$

At this time, the signal-to-noise ratio of the system can be defined as follows:

$$\mathrm{SNR} = \frac{N_a}{2}\frac{i_a^2}{i_b^2}. \tag{6}$$

It can be seen from the formula that the SNR of the time-domain OCT system is i_a^2/i_b^2. Therefore, the signal-to-noise ratio of the frequency scanning OCT system is twice higher as that of time-domain OCT system. Compared with speckle

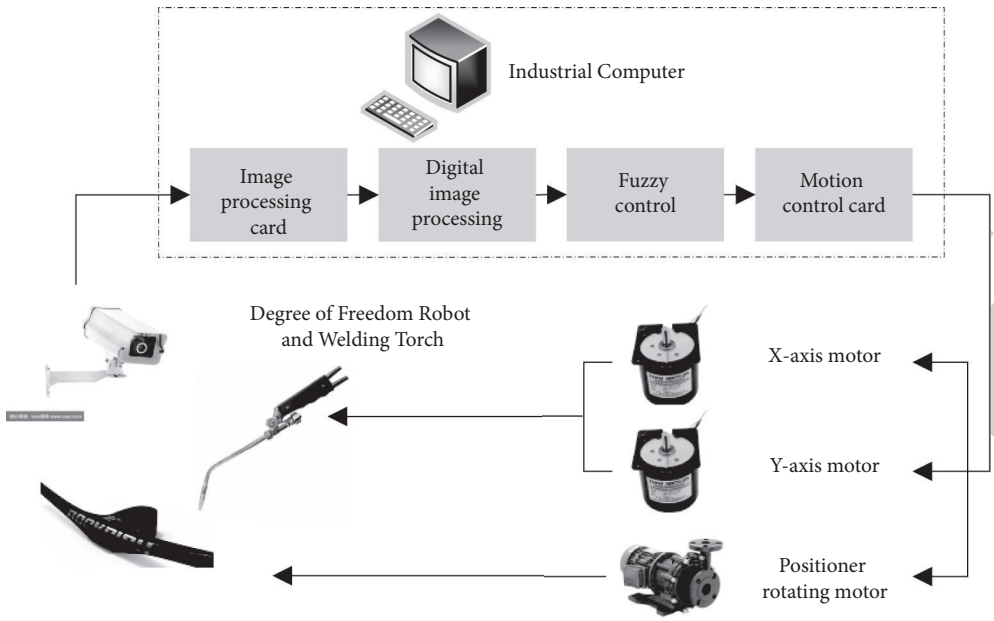

Figure 1: Visual tracking processing technology for composite manufacturing.

noise, the other two kinds of noise can be ignored in scanning OCT systems. When $W_a < W_r$, the SNR of the scanning OCT system is represented by expression as follows:

$$\mathrm{SNR} = \frac{nW_a}{hvf_a}. \tag{7}$$

In the above equation, fa is the scanning frequency of line a, that is, the scanning frequency of the scanning light source [12]. Therefore, if the reflected signal of the detected object is not too strong, the scanning speed of the swept OCT system is relatively low, but the reflected signal can be detected [13]. OCT is a new optical diagnostic technique that enables noncontact, noninvasive tomographic imaging of the microscopic structure of living ocular tissue.

2.2. Residual Strength of Composites. Many fiber-reinforced composites predict fatigue life based on residual strength, so the residual strength of fiber-reinforced composites is particularly important under fatigue strength [14]. Composite material is a new material that people use advanced material preparation technology to optimize the combination of material components with different properties. All kinds of damage are accompanied by repeated loading process, and its strength decreases. Due to reduced performance, the degree of material damage can be accurately visualized [13].

Different from metal materials, there is no reliable method to predict the service life of composites. When the number of cycles reaches a critical point, if the number of cycles continues to increase, the tendency of residual strength decreases sharply, and poor fracture may occur at this stage [2]. The matrix materials of composite materials are divided into two categories: metal and non-metal [15, 16]. The failure mode does not depend on the expansion of the main crack and depends on the strength distribution of the structure [17]. Figure 2 shows the variation curve of the residual strength of the composite with the increase in the number of cycles.

It is a general method to predict fatigue life by residual strength. When the residual strength reaches the maximum external stress, the material will be damaged and destroyed [17]. Load time, stress ratio, and load size are mainly used to reduce the strength of composites.

$$\theta(n) = f(n, \theta_{\max}, R). \tag{8}$$

In formula (8), $\theta(n)$ Is the residual strength of the composite after n fatigue loads. $\theta_{\max}$ is the maximum value under the maximum fatigue load, and R is the stress ratio of the fatigue load at this time, $R = \theta_{\max}/\theta_{\min}$, two boundary conditions must be met. When $n = 0$, that is, when no load is applied, $\theta(n) = \theta_{\mathrm{ult}}$, θ_{ult} represents the static strength in the load direction. The residual strength of glass fiber composites was analyzed by experiments [18]. It has been proposed that the residual strength of composites decreases linearly with the increase of the number of cycles. The model is given as follows:

$$\frac{R(n) - \theta_{\max}}{R(0) - \theta_{\max}} = 1 - \frac{n}{N_f}, \tag{9}$$

where $f = n/N$, $R(0)$ is the initial strength and $R(n)$ is the residual strength after N cycles. In the process of continuous loading, the fatigue time is superimposed, and the residual strength changes according to the rule of exponential function [19]. Therefore, the residual strength model proposed in this paper is exponential and is given as follows:

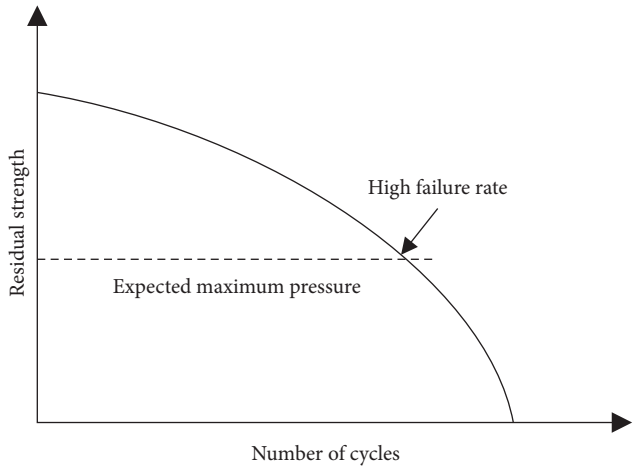

Figure 2: Residual strength variation curve.

$$\frac{R(n)-\theta_{\max}^{m}}{R(0)-\theta_{\max}^{m}}=1-\left(\frac{n}{N_i}\right)^{q}. \tag{10}$$

The parameter q is determined by experiment. Then, on this basis, this paper assumes that the residual strength attenuation rate at the initial time is 0, $R(n)/n=0$, and generalizes it. The model is given as follows:

$$\partial[R(n)]=\partial[R(0)]-\{\partial[R(0)]-\partial\theta_{\max}\}\left(\frac{\log n}{\log N}\right). \tag{11}$$

The model is shown below. Because ∂ can only be determined by many experiments, and the cost of engineering application is very high. Therefore, this paper summarizes the damage propagation rules of fiber-reinforced composites under fatigue load. The residual strength model proposed in this paper has strong adaptability, indicating that the residual strength is consistent with the damaging trend [20]. The model is shown as follows:

$$R(n)=R(0)-(R_0-\theta)+\theta\left[\frac{\sin bk\cos(b-a)}{\sin b\cos(bk-a)}\right], \tag{12}$$

where $k=n/N$, a and b are parameter values determined by experiment. In addition, as shown in equation (13), a power-law degradation form of fatigue damage is proposed in this paper.

$$R(n,\theta,k)=\left[1-N^{b}\right]^{1/a}(R_0-\theta)+\theta. \tag{13}$$

Among them, a and b are the experimental fitting coefficients, which are independent of the stress state, but only one residual strength can be measured for a test piece. This paper points out that when the damage state of the sample is characterized by residual strength, it is difficult to compare, and the two do not necessarily correspond. In the continuous process, the damage always changes, but in the initial stage, the strength decreases slightly and then decreases sharply [21]. Therefore, predicting the life of structures with residual strength is not a very ideal method.

2.3. Residual Stiffness of Composites. Due to the action of repeated load, the stiffness of the composite can be continuously measured during damage accumulation and expansion and does not affect the properties of the material [22]. Therefore, rigidity is a test parameter that can well reflect the properties of composites, and composites have anisotropic properties. In order to fully describe the characteristics of rigidity, at least four quantities need to be considered, namely E_x, E_y, G_{xy}, and V_{xy}. Because the experimental measurement method is difficult, we mainly study the change of material rigidity in the load direction. There are many definitions of stiffness for different descriptions in academia [23]. As shown in Figure 3, many scholars analyze it from the perspective of experience, theory, or a combination of the two.

In the fiber-reinforced composite laminate, the stiffness morphology is different at different stages. Figure 4 shows a typical stiffness reduction curve.

In the initial stage, the first stage damage occurs, and the main reason for the sharp decline of rigidity is that there are many cracks in the matrix, and the second stage tends to be stable [24]. The main reason is that the crack of the matrix is not enough to propagate to the fiber, and the stress at the tip of the matrix is not enough to damage the fiber. When the load increases, the rigidity decreases slowly. In the third stage, a large number of cracks accumulate, the fiber strength decreases than the stress at the crack tip, the fiber is damaged, and the rigidity decreases sharply [25]. After comparing the experimental results, a one-dimensional shear delay model is proposed, and the relationship between crack density and stiffness reduction is studied. However, the shear stress is transmitted between the transverse and longitudinal layers, and the shear force between adjacent layers is considered not to be transmitted.

Because the change of stiffness can be used to describe the fatigue damage of materials, many scholars at home and abroad say that the cumulative damage of composites is in the form of stiffness attenuation [26, 27]. Through comparative experimental research, the corresponding stiffness reduction model is proposed.

$$\frac{E(n)}{E(0)}=1-\left(1-\frac{E_n}{E_0}\right)\frac{n}{N_f}. \tag{14}$$

The stiffness value of aperiodic material is represented by $E(0)$, the residual stiffness value after N cycles is represented by $E(n)$, and the corresponding fatigue life value is represented by N_f. Formula (15) represents the relationship between residual strength, applied load, and cycle time.

$$E(n)=E(0)\left[1-K\left(\frac{\theta_{\max}}{E(0)}\right)^{a}n^{b}\right], \tag{15}$$

where k, a, and b are obtained through experiments, $\theta_{\max}$ is the maximum stress value under fatigue load. After N cycles of load, the remaining strength control can be expressed by the following formula.

$$E(n)=E(0)\left[1-Wn^{v}\right]. \tag{16}$$

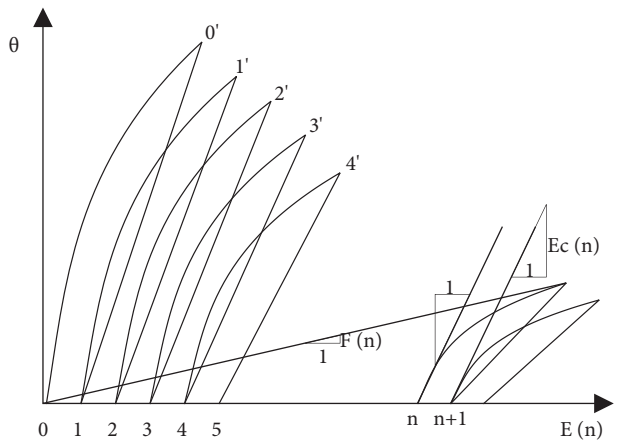

Figure 3: Definition of stiffness.

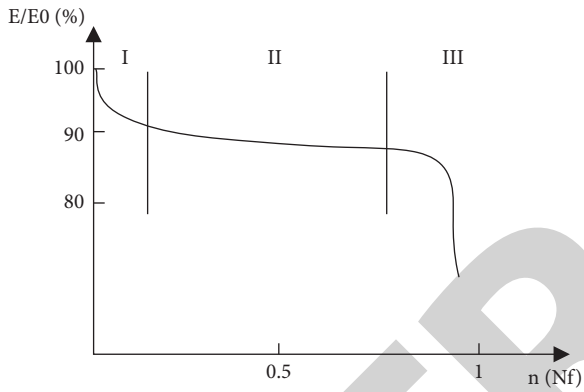

Figure 4: Stiffness degradation curve.

In the equation, the initial elastic parameter is e (0), $W = a_1 + a_2 v$, the stress level has a linear relationship with the average value v. Next, this paper studies the rigidity deterioration law of laminated plates with the same characteristics and carries out a tensile fatigue test on the test piece [28, 29]. Since the deterioration effect is considered to be almost independent of the magnitude of the stress level, a deterioration model under different stress levels is proposed as follows:

$$E(n) = E(0)\left[S\left(\frac{n}{N_f}\right) + 1\right], \tag{17}$$

where s is the parameter measured experimentally. Under the action of fatigue load, the corresponding deterioration model is established according to the rigid attenuation law of laminated materials, and the statistical distribution formula is derived as follows:

$$E(n) = E(0) * \exp\left[-S\left(\frac{n}{N_f}\right)^{b+c\theta}\right]. \tag{18}$$

S and C are related to load frequency, stress level and stress ratio, and the random variable b follows the Weibull distribution of 3 parameters. Through many studies and experiments, a rigid degradation model is proposed in this paper [30]. It is considered that under the condition of alternating load with constant stress amplitude, the residual stiffness can be expressed by the following formula:

$$\frac{E^*(n)}{n} = \frac{-a}{(n+1)E^*(n)^{m-1}}. \tag{19}$$

Based on the above equation, the stiffness decay rate equation under alternating fatigue load is obtained as follows:

$$F_{E(n)}(x) = 1 - \exp\left[-\left(\frac{(s/c)^{m/c} h \quad \ln(n+1)}{b^{m/c}(1 - x^m)}\right)^{ac/m}\right]. \tag{20}$$

After solving the parameters in the fatigue experimental equation, this paper improves the model and predicts the residual stiffness. When specific fragments are used to analyze the stress field and material properties of composites, they are affected by multiaxial fatigue load, providing an analysis method of stress field and residual stiffness degradation [31].

The stiffness attenuation of composites is affected by many external factors, such as stress level, laying method, material characteristics, and so on [32]. It is also the macro performance of internal damage under fatigue load, and can only represent the life span of materials, but it can not be accurately expressed [33]. Therefore, many researchers have obtained experimental results and put forward various macro phenomenon models to describe their attenuation law. However, this method is only applicable to specific materials [34].

3. Image Processing Experiment and Performance Analysis of Composite Fiber

3.1. Automatic Image Measurement of Fiber Length. The length distribution of short fibers in the matrix directly affects the mechanical properties of the composites. The strengthening effect can be brought into full play only when the fiber length is greater than the critical length. Therefore, it is very important to study the length distribution of fibers in composites. However, the current practice is usually to measure the fiber length by manually marking the fiber length on the fiber distribution image. Considering that the number of fibers measured usually exceeds hundreds, this measurement method is very inefficient. This chapter will propose an automatic fiber length measurement method to solve the above problems, in order to greatly improve the work efficiency and ensure the accuracy of the measurement results. In this paper, the mixture of carbon fiber and polylactic acid was prepared by an internal mixing process. The content of carbon fiber in the mixture was 15%. The carbon fiber reinforced polylactic acid composite spline was prepared by molding method.

This report analyzes carbon fiber-reinforced polylactic acid composites, so it is relatively simple and effective. The fibers in the composites were separated by the combustion method. Firstly, any part of the tested composite shall be cut

off, and then put into the furnace. Put the furnace into the furnace. In order to burn the plastic matrix, please burn it at 500°C for 4 hours. The separated carbon fibers are then cooled and randomly injected into the glass slide. Then drop a small amount of absolute ethanol on the glass slide, rotate back and forth on the glass slide to disperse the carbon fiber, and dry naturally in a windless place. Put the glass slide under the image measuring instrument for image acquisition to obtain the fiber length distribution diagram, as shown in Figure 5.

The fiber length distribution in the fiber distribution image above is calculated by the method in this paper. The calculation results are basically consistent with the manual calculation results, and the maximum comparison error is 5.4%. The fiber structure distribution is shown in Figure 6. Figure 6(a) is the fiber length distribution calculated manually, and Figure 6(b) is the fiber length distribution calculated automatically by this method.

In the above figure, the unit of fiber length is image pixel, and the actual length can be converted by scale. It can be seen that the method in this paper is very consistent with the manually calculated fiber length distribution, which shows that the method in this paper can well complete the measurement task of fiber length and its distribution under complex intersection conditions. In fact, the average error of all fiber lengths is only 6.7 pixels, and the maximum error is 21.4 pixels. The error is the largest when measuring the length of T-shaped cross fiber. This is because when calculating the length of one T-shaped cross fiber, the width of the other fiber will be considered, so the maximum error is close to the diameter of the fiber (about 18 pixels).

In order to further verify the effectiveness of the fiber orientation measurement method based on three-dimensional reconstruction of scanning electron microscope, the orientation of a single fiber in the cross-section of carbon fiber reinforced composite membrane was measured and compared with the results measured by image measuring instrument. In this paper, a low-content carbon fiber reinforced composite square film with a thickness of about 0.2 mm is used. The carbon fiber in the film is approximately two-dimensional oriented, so the deflection angle of the fiber can be measured by an image measuring instrument. Tilt the sample table to 5° and take SEM images of the fibers and the corresponding fibers pulled out of the cavity.

The deflection angle of a single fiber in five composite membranes was measured by two methods. The length of the fiber protruding from the matrix in the first to third membranes was larger, and the length of the fiber protruding from the matrix in the fourth and fifth membranes was smaller. The measurement results are shown in Table 1.

According to Table 1, the measurement results of this method are basically consistent with those of the image measuring instrument, with a maximum error of 1.4° and an average error of 0.83°. Usually, the information on fiber orientation angle only needs to obtain the proportion of fibers in a certain range, and the result of fiber orientation is not required to be very accurate. Therefore, this method can well measure the fiber orientation and distribution.

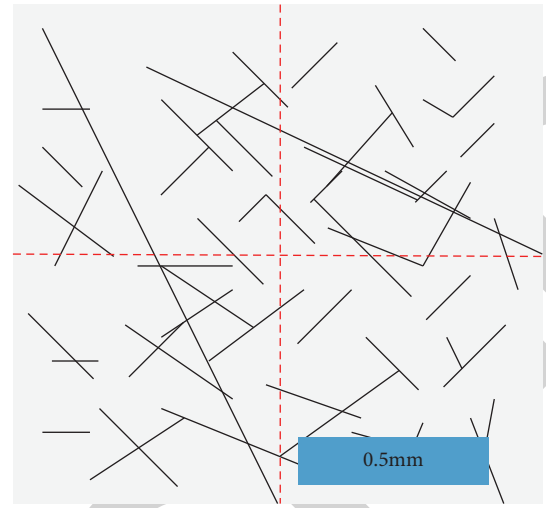

Figure 5: Fiber length distribution.

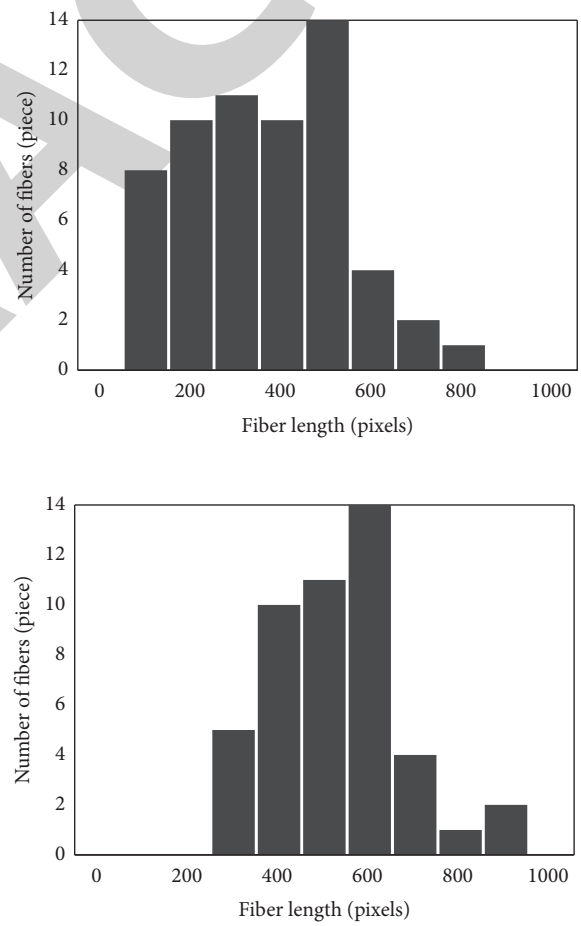

Figure 6: Fiber length distribution is obtained by different methods. (a) The result of manual calculation. (b) The result of applying the method in this paper.

The micromorphology of the composite section is very complex, and the actual orientation distribution of fibers in the material is also very complex. In some parts of the

Table 1: Measurement results of deflection angle of single fiber (°).

Serial number	Method of this article		Measuring instrument
	Fiber cavity	Fiber	
1	10.0	9.4	9.9
2	11.3	10.3	11.5
3	11.1	11.7	12.5
4	15.2	16.4	14.8
5	16.9	16.6	18.0

material, the fiber orientation may be in a relatively irregular state. At this time, the degree of fiber orientation cannot be judged by the naked eye alone. Figure 7 shows the results of measuring the deflection angle and azimuth of each fiber in the composite and the pull-out gap of the fiber by the method in this paper.

The reliability of the fiber orientation measurement method based on scanning electron microscope three-dimensional reconstruction technology is verified by experiments, and this method is applied to actual scanning electron microscope images. The results show that this method can well complete the task of measuring fiber orientation and distribution.

3.2. Study on Properties of Fiber Reinforced Composites. The performance test of fiber reinforced composites mainly includes mechanical performance tests (bending performance test, tensile performance test, impact performance test), contact angle test, microstructure test, thermodynamic performance test, processing flow performance test, DSC and POM test. The effect of fiber composite ratio on the mechanical properties of composites is recorded in Table 2.

It can be seen from the above table that when the ratio of composite fiber is 5:12:13, the mechanical properties of PP/EVA Composites are better. Among them, when the three fibers change from 5:20:5 to 5:16:9 and 5:12:13, the bending strength and tensile strength of the composite are greatly improved with the gradual increase of the proportion of fiber C. However, when the content of C fiber exceeds 13 parts, that is, when the ratio is 5:5:20, the mechanical properties of the composite are significantly reduced. On the contrary, when the ratio of the composite fiber changes from 5:5:50 to 5:16, and then to 5:12:13, the flexural strength of the composite increases with the increase of *X* fiber content. In order to optimize the system with better mechanical strength in this group of experiments, three composite ratios of RW: X: C = 5:12:13, 5:16:9 and 5:5:20 were selected to continue the exploration.

The hydrophilic contact angle on the surface of polypropylene/ethylene vinyl acetate composites reinforced by three modified fibers increases, which proves that the interfacial adhesion between fiber and resin is enhanced. Among them, with the increase of the proportion of fiber, the hydrophilic surface contact angle of the composite decreases, while with the increase of the proportion of SSIC fiber, the hydrophilic contact angle of the composite tends to

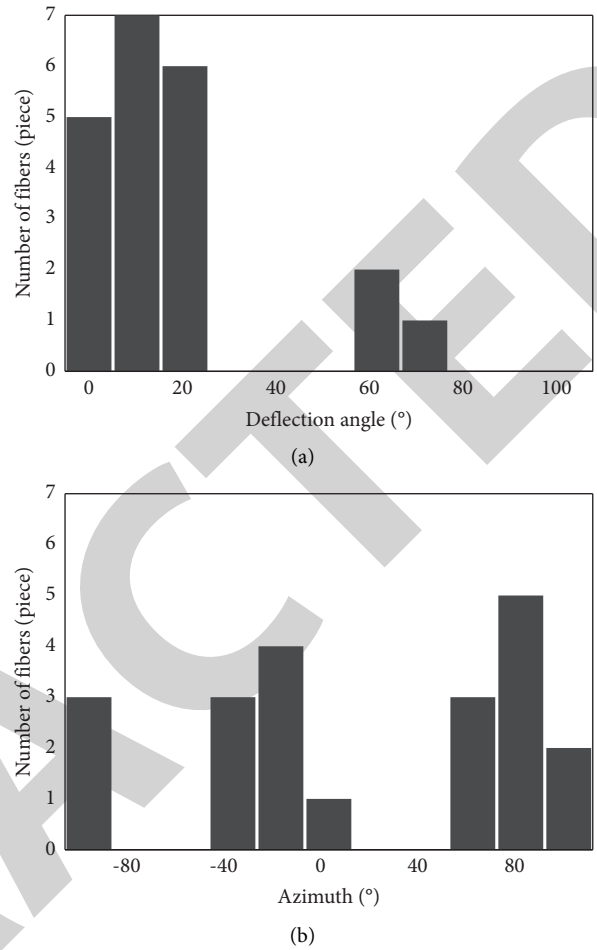

Figure 7: Corresponding fiber orientation distribution. (a) Deflection angle. (b) Azimuth.

Table 2: Effect of RW, *X*, and C fiber ratio on mechanical properties of composites.

RW:X:C	Tensile (MPa)	Flexural (MPa)	Impact (KJ/m^2)
5:12:13	22.36	38.79	5.78
5:16:9	24.66	35.01	6.17
5:9:16	24.79	35.69	5.84
5:20:5	23.28	36.64	5.96
5:5:20	24.48	34.68	5.55

Note. The amount of fiber is 30 parts, and the amount of PP/EVA is 70 parts, where PP:EVA = 4:1.

increase, which indicates that SSiX fiber is more hydrophilic than SSIC fiber. The surface hydrophilic contact angle of the composite is shown in Table 3.

The thermodynamic behavior analysis of three kinds of fiber-reinforced composites with changed properties increase the initial decomposition temperature, but the decomposition temperature increases with 50% weight loss, and the amount of residual carbon increases significantly. Moreover, the maximum decomposition rate is significantly lower than that of PP/EVA Composites. Therefore, increasing three different ratios of modified fiber is beneficial

Table 3: Surface hydrophilic contact angle of composites.

Composites	Different ratios	Average value of contact angle/°
PP/EVA/RW/SSIX/SSIC	5:5:20	86
	5:12:13	105
	5:16:9	90
PP/EVA/AW/SSIX/SSIC	5:5:20	94
	5:12:13	110
	5:16:9	80

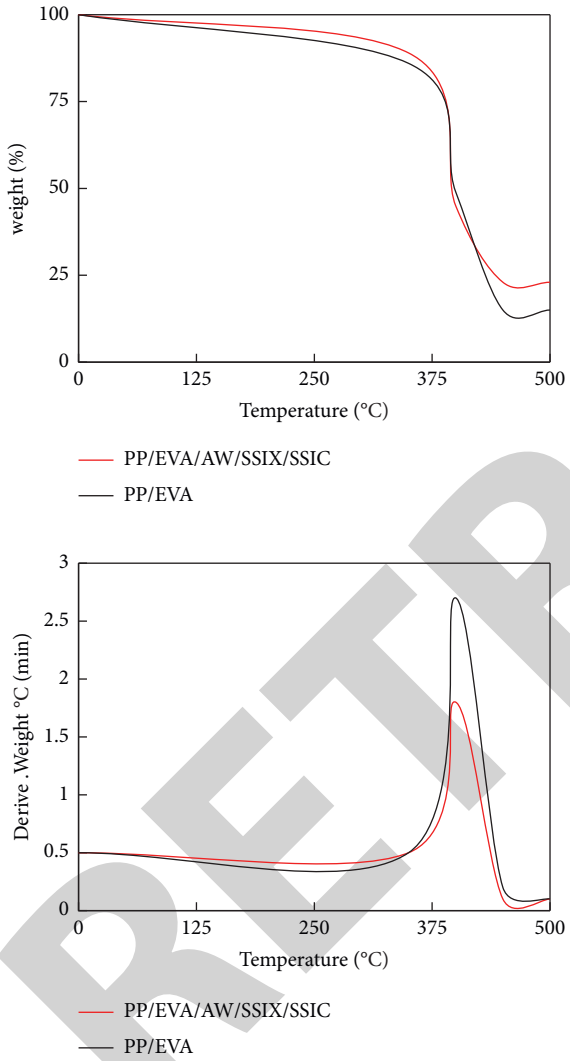

Figure 8: TG and DTG curves of three fiber composites.

to improve the thermal stability of polypropylene/ethylene vinyl acetate copolymer in high-temperature regions. Figure 8 shows the DTG and TG curves of a set of fiber composites.

In addition, it is not difficult to find in Table 4 that among the three ratios, when the ratio of SSiX fiber increases, the initial decomposition temperature of the composite increases significantly. At the same time, when the amount of SSIC fiber is large, the maximum decomposition rate decreases most obviously, and the amount of

Table 4: Thermogravimetric parameters of three fiber composites.

Composites	Td5% (°C)	Td50% (°C)	Vdmax (%/°C)	Yield at 550°C
PP/EVA	359.0	418.0	2.7	—
5:05:20	348.0	467.0	1.9	28.4
5:12:13	394.0	429.0	1.4	24.6
5:16:09	348.0	418.0	1.6	25.1

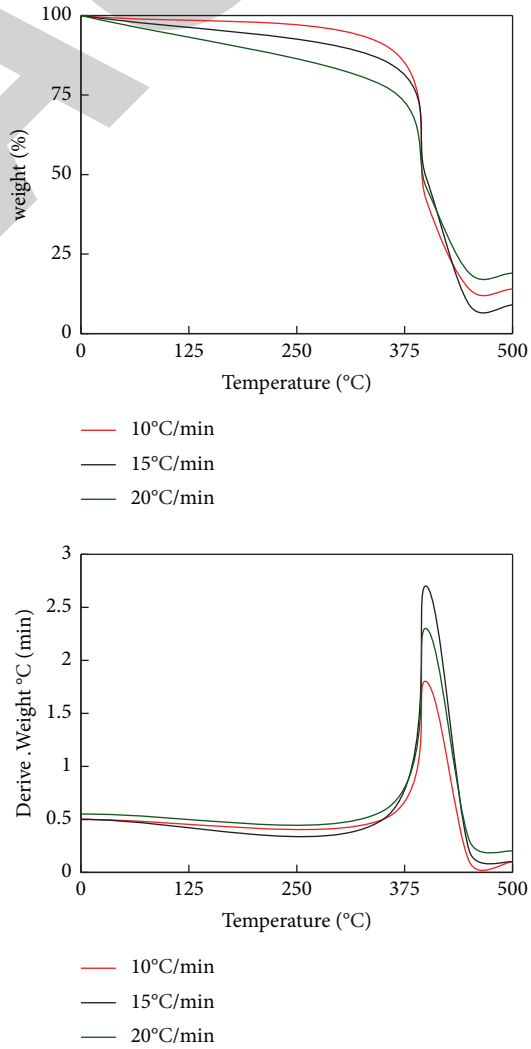

Figure 9: DTG and TG curves of composites at different heating rates.

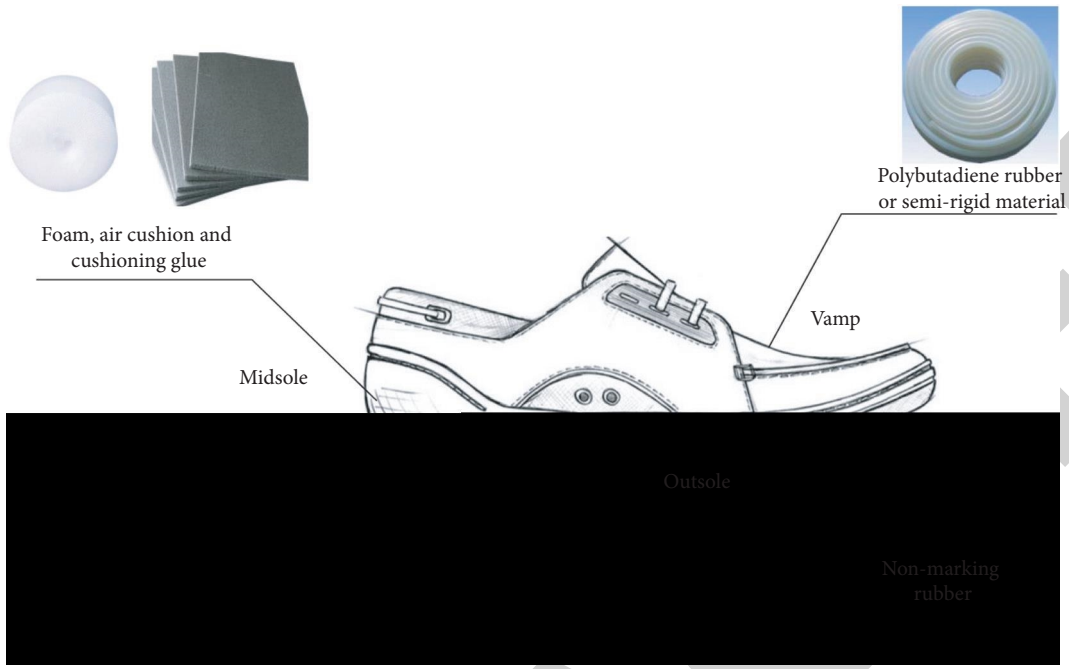

Figure 10: Structure of rubber shoes of new high-performance basketball shoes.

residual carbon is the largest, indicating that the basalt fiber plays a decisive role in the low-temperature thermal stability of the material. In composite materials, while carbon fiber enhances high-temperature thermal stability, the difference between the two fibers is very small.

As shown in Figure 9, under the same heating rate, the initial decomposition temperature Td5% of PP/EVA Composite with three modified composite fibers is faster than that of PP/EVA Composite. This is mainly due to the low-temperature decomposition of fibers. At different heating rates, the Tdmax of fiber PP/EVA Composites Modified by three compounds increases significantly with the increase of heating rate, mainly due to the delay of decomposition temperature of some substances due to accelerating heating rate, which is beneficial to the composites. At the same heating rate, the difference in Tdmax between the modified fiber and PP/EVA Composites is very small, but Tdmax tends to increase when the ratio of SSIC fiber increases. Compared with PP/EVA, the Vmax of all PP/EVA Composites added with three improved composite fibers was significantly reduced. When the mix ratio is aw: SSiX: SSiC = 5:5:20, the Vmax of the composite decreases to the minimum value of 1.35°C/min with the increase of heating speed, indicating that the thermal stability of the composite is improved.

3.3. Application Scenarios of Graphene Rubber. Liu Yuanshun proposed that athletes and coaches wear high-performance sports shoes to improve their sports performance. Most runners can run faster, about 1.6%. They can jump farther and reduce or reduce their injury probability. This theory can also be extended to basketball.

In theory, the components of shoes can improve athletes' jumping ability and reduce leg fatigue. The shoe parts with cushioning performance made of soft and high-energy feedback materials can get the maximum feedback value after being compressed by human feet. It can prevent foot injury and make athletes and other wearers feel comfortable.

On this basis, with the structure of the simplest rubber-based basketball shoes commonly used today and the use of graphene rubber composites, we can infer a new type of high-performance basketball shoes. The structural design and material use of the new basketball shoes are as follows: the first is the sole. Generally speaking, the outer layer of basketball shoes is made of unmarked rubber, and some manufacturers will add wear-resistant materials. Graphene natural rubber composites are used to exchange natural rubber with original colloids, and the excellent mechanical properties of graphene natural rubber composites are used to improve the tensile strength and tensile elastic modulus of colloids. The sole can have wrinkles. Moreover, it can not only prevent the soles from slipping, but also provide more energy feedback and cushioning. If force is applied to these products, wrinkles will be compressed, crushed, and absorb energy. When these forces are released, the antiwrinkle and rebound of the rubber sole can also provide more mechanical energy and elasticity. In addition, in order to protect the rubber base made of graphene natural rubber, a wear-resistant material layer can be sprayed on the outer surface of the rubber base. The second is the midsole. Generally speaking, the midsole of basketball shoes has cushion components such as cushion, cushion, cushion, and cushion. The insole or midsole of this new basketball shoe is laminated, including two layers of supporting materials (upper and lower). The top is covered with polybutadiene rubber or semirigid material to act as an additional layer or as a covering layer. In addition, it can also include two polybutadiene rubber layers. Each layer is about 80% CIs

polybutadiene rubber and about 20% natural rubber. It is a polybutadiene rubber layer with a thickness of about 7.9 MM, which is separated by the coating. The liner is more suitable for inserting into EVA/graphene natural rubber composite shoes. Figure 10 shows the structure of a new high-performance basketball shoe rubber material sneaker.

The new basketball shoes with graphene rubber can improve the fatigue strength and tensile strength of the shoes without increasing the overall weight of the shoes. The shoes contain 37.5% natural rubber, which can greatly prolong the service life, effectively solve the problem of shoe body deformation and strengthen the protection of athletes.

4. Discussion

In this paper, a fast edge extraction algorithm of OCT image based on phase consistency principle and morphological method is proposed, which proves the effectiveness of this algorithm. However, some work needs to be further improved. This paper only studies the fast image processing technology of swept frequency OCT systems from two aspects of image denoising and image edge extraction. In the imaging process of swept frequency OCT system, the process of signal preprocessing is essential. Therefore, we can deeply study the efficiency of signal preprocessing and find a more efficient preprocessing method. Based on the cylindrical characteristics of man-made fibers, in order to be applied to more complex reinforced fibers, such as plant fibers, it is necessary to further analyze the segmented combination rule of fiber skeleton in the length measurement method and the dense stereo matching algorithm in fiber orientation measurement method.

5. Conclusions

In this paper, the automatic fiber length measurement method based on the skeleton segment is used, and the obtained fiber length is basically consistent with the basic calculation value, and the maximum relative error is about 4.5%. The fiber length finally obtained is basically consistent with the theoretical calculation value. The average error is between 6.7 pixels and 21.4 pixels over each fiber length. This method can not only ensure accurate measurement of fiber length but also realize large-scale automated measurement. The fiber orientation was determined for the first time using the SEM reconstruction technique in the tests of fiber-reinforced composites and agreed with the results of the secondary imaging tests. The maximum deviations for the two methods are 3.83 and 1.54, respectively. (1) Through the experiment of graphene rubber application scenarios, the concept of user experience improvement is given. (2) By calculating the changes in user experience, we found that the comprehensive performance of sports products increased from 15.4% to 48.6% by using graphene rubber composite materials. (3) After using this material, its performance is improved by 2.1% to 4.5%. However, due to the limitation of time technology, this paper does not conduct in-depth research on fiber-reinforced composite materials, and we will further explore this in the follow-up.

Data Availability

This article does not cover data research. No data were used to support this study.

Conflicts of Interest

The author declares that there are no conflicts of interest.

References

[1] B. Jia and W. Zhang, "Application of digital image processing technology in online education under COVID-19 epidemic," *Journal of Intelligent and Fuzzy Systems*, no. 2, pp. 1–7, 2021.

[2] E. Oho, K. Suzuki, and S. Yamazaki, "Applying fast scanning method coupled with digital image processing technology as standard acquisition mode for scanning electron microscopy," *Scanning*, vol. 2020, no. 6, Article ID 4979431, 9 pages, 2020.

[3] X. Gu, H. Song, and J. Chen, "A review of research on pig behavior recognition based on image processing," *International Core Journal of Engineering*, vol. 6, no. 1, pp. 249–254, 2020.

[4] A. M. Elhousari, M. Rashad, A. H. Elsheikh, and M Dewidar, "The effect of rubber powder additives on mechanical properties of polypropylene glass-fiber-reinforced composite," *Mechanical Sciences*, vol. 12, no. 1, pp. 461–469, 2021.

[5] G. Yamamoto and T. Okabe, "Numerical study for tensile strength prediction of unidirectional carbon fiber-reinforced composite considering fiber surface stress concentration," *Mechanical Engineering Journal*, vol. 6, no. 3, pp. 19-00020-00020, 2019.

[6] S. Hamanaka, C. Nonomura, T. B. N. Thi, and A Yokoyama, "Correlation between fiber orientation distribution and mechanical anisotropy in glass-fiber-reinforced composite materials," *Journal of Polymer Engineering*, vol. 39, no. 7, pp. 653–660, 2019.

[7] S. T. Matsuwaka and E. W. Latzka, "Summer adaptive sports technology, equipment, and injuries," *Sports Medicine and Arthroscopy Review*, vol. 27, no. 2, pp. 48–55, 2019.

[8] Q. Feng and L. Wang, "The effect of polymer composite materials on the comfort of sports and fitness facilities," *Journal of Nanomaterials*, vol. 2022, Article ID 9108458, 2022.

[9] H. Jahangir, A. Soleymani, and M. R. Esfahani, "Investigating the confining effect of steel reinforced polymer and grout composites on compressive behavior of square concrete columns," *Iranian Journal of Science and Technology - Transactions of Civil Engineering*, 2022.

[10] F. Li, S. Zhang, and W. Cheng, "Application and optimization of wing structure design of DF-2 light sports aircraft based on composite material characteristics," *Journal of Nanomaterials*, vol. 2022, Article ID 6967016, 10 pages, 2022.

[11] A. Liu, H. Xie, and K. Ahmed, "Fault detection technology of national traditional sports equipment based on optical microscope imaging technology," *Alexandria Engineering Journal*, vol. 60, no. 2, pp. 2697–2705, 2021.

[12] L. Zhu, A. Wang, and F. Jin, "Using image processing technology and general fluid mechanics principles to model smoke diffusion in forest fires," *Fluid Dynamics & Materials Processing*, vol. 17, no. 5, pp. 1213–1222, 2021.

[13] D. G. Kim, K. J. Shin, and J. H. Woo, "Displacement measurement of steel pipe support using image processing technology," *Journal of Image and Graphics*, vol. 8, no. 3, pp. 80–84, 2020.

Hindawi
Scientific Programming
Volume 2022, Article ID 4055809, 13 pages
https://doi.org/10.1155/2022/4055809

Research Article

Machine Translation of Scheduling Joint Optimization Algorithm in Japanese Passive Statistics

Changsheng Liu

School of Foreign Studies, Anhui Sanlian University, Hefei, Anhui 230601, China

Correspondence should be addressed to Changsheng Liu; liucs907@mail.slu.edu.cn

Received 18 June 2022; Revised 22 August 2022; Accepted 30 August 2022; Published 23 September 2022

Academic Editor: Juan Vicente Capella Hernandez

Machine translation is different from written translation. How to improve the performance of machine translation has been a research hotspot in current research on machine translation. In this paper, based on the semantic analysis and research of Japanese passive, a joint optimization algorithm of scheduling has been proposed, and the machine translation of Japanese passive has been studied. At present, machine translation is more and more widely used. Machine translation has solved many vocabulary problems, and it can complete a large amount of translation work and save a lot of manual translation time. While improving the translation speed, in the process of Japanese passive translation, it is also found that direct machine translation shows many shortcomings, and the quality of passive translation is not particularly ideal, exposing the basic problems of machine translation, such as semantic errors, syntactic errors, unclear and rigid expressions, and messy structures. In response to the problems above, this paper has improved the machine translation model for scheduling joint optimization algorithms. The paper has proposed several optimization algorithms and used resource awareness and computing power scheduling algorithms to conduct experimental analysis of translation performance. Finally, it is found that, among the two scheduling optimization algorithms, the resource-aware scheduling algorithm has better performance. With the same data, the resource-aware scheduling algorithm has saved 15.5% of the time compared with the computing power scheduling algorithm, and the accuracy of Japanese passive translation was 6%, 5%, and 21% higher than the computing power scheduling algorithm under different data volumes. Not only has the time taken been shortened, but the translation accuracy has also been improved.

1. Introduction

At present, machine translation is used more and more times in translation work, and it has even become the basic processing method for many translators or those who need to translate materials. Aiming at the problems exposed by Japanese passive dynamics in the process of machine translation, this paper has proposed a statistical machine translation model, constructed a parallel corpus, and then proposed a joint scheduling optimization algorithm to optimize the internal system of machine translation and improve its translation accuracy. The channel model, scheduling model, interference model, and service flow model have been analyzed. Column generation algorithm and maximal clique algorithm, system computing power scheduling algorithm, and resource-aware scheduling algorithm have been proposed to optimize machine translation, and the performance of machine translation has been experimentally tested according to the proposed algorithm model. Experimental results have shown that the resource-aware scheduling algorithm is more efficient in allocating resources within the system. Compared with the computing power scheduling algorithm, in the case of 6G data volume, the translation efficiency of the resource-aware scheduling algorithm was 15.5% higher, and the translation accuracy for passive was 21% higher. Using the column generation algorithm and the maximal clique algorithm to make an experimental analysis on the optimization problem of Japanese passive in the statistical machine model, it is found that the operation time of the maximal clique optimization algorithm was all less than 1, which is much smaller than that of the column generation algorithm. The role of scheduling

joint optimization algorithm in network maintenance and operation optimization is becoming more and more obvious, and its optimization role has been applied to various fields. Cai et al. studied a new type of UAV safety communication system. Two drones were used in the system. Among them, one drone communicated with multiple users on the ground via orthogonal time division multiple access, while another drone in the area intercepted eavesdroppers on the ground to protect the communications of the desired users. They developed a new joint optimization algorithm to deal with the transformed problem. To further improve the secrecy rate performance, they also extended the proposed algorithm to the case of multi-UAV jamming. The simulation results showed that the performance of the proposed joint optimization algorithm is significantly better than the traditional algorithm [1]. In order to formulate production scheduling plans and preventive maintenance plans, Fei and Huimin studied the joint optimization problem of these two plans in the intermittent discrete re-entry machining environment. Batch processors can process multiple jobs at the same time, whereas discrete processors can only deal with jobs one after the other, with many re-entrant processes. By measuring the information and adjusting the level of individual variation, the scope of the search space has been effectively narrowed [2]. Zhao and Mili found that industrial CR networks were planned to operate in a wide spectrum, and they had high energy consumption due to frequency switching, while other wireless technologies did not have this problem. A striking feature of this switching cost was that it depended on the width between the two frequency bands. Considering the different energy consumption generated when CR devices switch to different frequency bands, the joint frequency allocation and scheduling problem of multihop industrial CR networks with a single transceiver has been established. Therefore, a polynomial time heuristic algorithm has been proposed to solve the energy consumption problem caused by channel switching. Simulation results showed that the performance of our heuristic algorithm was very close to the results of CPLEX optimization software implementing integer linear programming [3]. Al-Abbasi and Aggarwal considered a representative system architecture of a Content Delivery Network (CDN), given multiple parallel streams/links between each server and edge routers. They determined, for each client request, a subset of servers to stream video, and one parallel stream from each selected server. To achieve this scheduling, a two-phase probabilistic scheduling has been proposed. On top of using playback time, an optimization problem has been formulated to jointly optimize all requested convex combinations of average pause duration and average video quality. Among them, two-stage probabilistic scheduling, video quality selection, bandwidth partitioning between parallel streams, and auxiliary bound parameters can be selected. This nonconvex problem has been solved using an efficient iterative algorithm. Experimental results have showed a significant improvement in QoE metrics for cloud-based videos compared to the considered baselines [4].

With the continuous development of internationalization, language communication is particularly important, and there are more and more translations between different languages. Song said that there were still many shortcomings in the Chinese-Japanese machine translation method, the corpus information processing was not deep enough, and the translation process lacked rich language knowledge support. In particular, the recognition accuracy of Japanese characters was not high. Based on machine learning technology, combined with image feature retrieval technology, a Japanese character recognition model was constructed, which was used as the object of algorithm recognition. Image features were extended by generating a brightness enhancement function using a bilateral grid [5]. In order to solve the problems of small scale, slow speed, and incomplete field of traditional parallel corpus machine translation, Zheng and Zhu constructed a Japanese translation teaching corpus based on a bilingual nonparallel data model and used this corpus to train a Japanese translation teaching machine translation model to obtain more accurate information good auxiliary effect. In the construction process, for nonparallel corpora, they used a translation retrieval framework based on word graph representation to extract parallel sentence pairs from the corpus and then built a translation retrieval model based on bilingual nonparallel data [6]. Mangeot-Nagata has argued that French-Japanese bilingually aligned corpora and machine translation systems were logically equally rare. They have built a high-quality and broad-coverage dictionary available on the web. In order to update these data, whose vocabulary may be very old, existing electronic resources, such as Wikipedia, or Japanese-English electronic resources can be reused, and the resulting resources can be made available online for review and correction by voluntary contributors. First, Japanese bilingual dictionaries (printed or electronic) and their historical evolution were taken stock of. Then, the resource to be built was described. The next part involved the conversion of the three sources, followed by several error corrections for French and Japanese. Finally, the resource was published on a website built around the Jibiki platform, allowing online viewing and editing of articles, and also providing a French-Japanese bilingual corpus and active reading mode [7]. The abovementioned literature has been relatively thorough in research on scheduling joint optimization algorithm and statistical machine translation and has certain guidance for the following research.

This paper mainly studies the related problems of machine translation of scheduling joint optimization algorithm in Japanese passive statistics. The statistical machine translation model is different from the traditional machine translation model. It is based on the corpus, conducts mathematical derivation and analysis of the survey to be translated, and has integrated sentence features to achieve accurate translation. Building a reasonable optimization model is conducive to improving the quality of Japanese passive translation, improving the utilization of internal resource information of the system, and reducing the cost of system maintenance and operation. Using the scheduling joint optimization algorithm to optimize machine translation can effectively reduce translation time, improve translation efficiency, and take into account the quality of

translation. The combination of corpus and big data can reduce the complexity of translation work and provide important technical support for machine translation. This paper proposes a statistical machine translation model that is different from traditional machine translation models to enrich the development of linguistics.

The structure of this paper is mainly to briefly introduce the scheduling joint optimization algorithm and, at the same time, briefly introduce the Japanese passive classification and statistical machine translation model. In the specific experimental process, the scheduling algorithm is applied to Japanese passive statistics for simulation experiments. The experimental conclusions of this paper are obtained.

2. Machine Translation Method of Scheduling Joint Optimization Algorithm in Japanese Passive Statistics

2.1. Passive Classification of Japanese. There are many ways to classify Japanese passives, which can be classified from multiple perspectives. Classification according to the sentence structure of Japanese articles can be divided into direct passive and indirect passive [8]. Based on the emotional tendencies of sentences, the direct passive can be divided into sentient passive and ruthless passive. According to the difference of the subject in the sentence, it can be divided into the passive that expresses people and the passive that expresses objects. According to whether there is a beneficial relationship in the sentence, it can be divided into the passive dynamic of interest and the passive dynamic of non-interested interest. Finally, according to the composition structure of the sentence, it can be divided into direct and indirect passive.

2.2. Statistical Machine Translation Model. Statistical machine translation is a type of machine translation, and it is also a method with better performance in machine translation in nonlimited fields. Statistical machine translation is a method based on parallel corpora. It has used mathematical derivation to perform statistical analysis on the content of the corpus, built a statistical translation model, and then used this model for translation [9]. Statistical machine translation methods have attracted more and more attention due to their rigorous mathematical derivation, good model consistency, automatic learning, and strong robustness. The early word-based machine translation has transitioned to phrase-based translation and is incorporating syntactic information to further improve translation accuracy. Figure 1 shows the workflow of the statistical machine translation model.

2.2.1. Noise Channel Model. The noise channel model is assumed to be obtained after channel coding the noise generated during the transmission of information in the language. The properties of the source language and the target language can be known through the channel model. According to the calculation rules of the known noise channel, the probability of the target language obtained in the source language is obtained, which is beneficial to translation, and the best translation result can be obtained, which can be obtained according to the channel model:

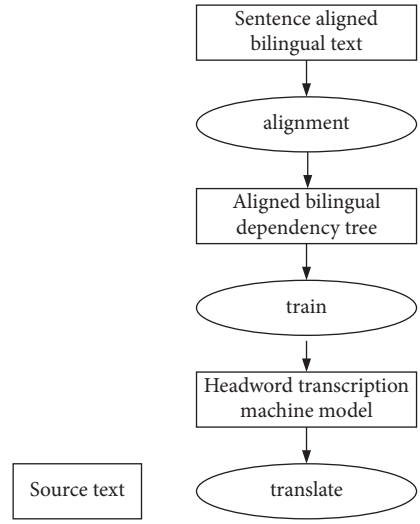

Figure 1: Workflow of a statistical machine translation model.

$$\tilde{r} = \arg\max_{r \in r*} w(r \mid k). \tag{1}$$

Using Bayesian formula, given the value k, formula (1) can also be converted to

$$\tilde{r} = \arg\max_{r \in r*} w(r \mid k) = \arg\max_{r \in r*} \frac{w(k \mid r) w(r)}{w(k)} = \arg\max_{r \in r*} w(k \mid r) w(r). \tag{2}$$

The statistical machine translation model consists of two parts, the translation model and the language model of the representation. Among them, the translation model mainly reflects the correspondence between the vocabulary of the source language and the target language, and the language model represents the characteristics of the language itself [10]. The translation model guarantees the meaning of the translation, and the language model guarantees the smoothness of the translation. Machine translation can be regarded as a process of information transmission, and machine translation is interpreted according to the source-channel model. The noise channel model is a suitable method for the vast majority of language models.

According to the translation model proposed by experts, the calculation formula of translation probability is

$$w(k \mid r) = w(k, t \mid r). \tag{3}$$

In the translation model, the relationship between the passive and the sentence can be expressed as

$$w(k \mid r) = \prod_{(i,j) \in t} w\left(k_i, r_j\right). \tag{4}$$

In formula (4), i,j represents a link in the sentence that is dynamically aligned in the word. The translation probability

here is between words and not between positions. If a position is added to the entry, the formula is as follows:

$$w(k \mid r) = \prod_{(i.j)\in t} w\left(k_i, r_j\right) w(i, j, K, L). \tag{5}$$

Among them, K and L are the sentence lengths of the source and target languages, respectively, and i and j represent links in the sentence.

In statistical machine translation models, the word alignment with the highest probability can be expressed as

$$\tilde{t} = \arg\max_{t} w_{\beta}(k, t \mid r). \tag{6}$$

A noise model is not suitable for all machine translations. In the noise model, its important role is the word alignment function. In the current machine translation, the parallel corpus word alignment method is mostly used [11]. The more parallel corpora in the system model, the higher the requirements for system translation. However, the accuracy of word alignment is still lacking. The accuracy of Chinese machine translation lags behind other languages, and the error rate of word alignment technology has always been high.

2.2.2. Discriminant Model. Unlike noisy channel models, discriminative models are primarily based on data analysis. It does not use Bayesian formulas or assumptions but divides and translates passive sentences or words in the form of feature functions.

The characteristic function in the model framework is expressed as

$$g_n(r, k), n = 1, \cdots, N. \tag{7}$$

The formula obtained after parameterisation is

$$W(r \mid k) = \frac{\exp\left[\sum_{n=1}^{N} \partial_n g_n(r, k)\right]}{\sum_{r*} \exp\left[\sum_{n=1}^{N} \partial_n g_n(r, k)\right]}. \tag{8}$$

According to the weight of the feature function, the estimated value of the model is used as a parameter set, the system is given a source passive sentence, and the decision criterion for the best translation is obtained. The decision criterion for the best translation is to find the solution with the largest characteristic function.

$$\tilde{r} = \arg\max_{r*} \{w(r*, k)\} = \arg\max_{r*} \left\{ \sum_{n=1}^{N} \partial_n g_n(r*, k) \right\}. \tag{9}$$

According to the joint optimization method, if the objective evaluation criterion is used as the optimization goal, the result is

$$\tilde{\partial} = \arg\max_{\partial*} \left\{ \sum \int \frac{1}{E\int} \sum_{e=1}^{E\int} F\left(f_{\int}, e^{, p}{}_{\int} \right) \right\}. \tag{10}$$

Finally, the model is converged and decoded. In the Japanese passive statistical machine translation model, the corresponding passive parameters and the parameters to be translated are trained to form the search results with the maximum probability. If different types of passives are decoded, the optimal path for translation is finally formed [12].

2.3. Scheduling Joint Optimization Algorithm

2.3.1. Channel Model. The channel model uses a pattern to represent the network topology. The network topology consists of router rendezvous points, collections with gateway functions, and collections of node wireless links. Within transmission range, the wireless link can receive the node's transmission, which indicates that the link is valid. Figure 2 is a schematic diagram of the channel model.

Assuming that the transmission range between nodes in the model is the same, there are both wireless links and reverse links between the two nodes in the link during the transmission process, and the channels used are mainly single-channel and single-transceiver. To simplify the calculation, assuming that all routing nodes use the same power spectral density Q to send signals, the power propagation gain model is

$$Y_{i,j} = M \cdot \log_2\left(1 + \frac{R_{i,j} \cdot G}{\lambda}\right). \tag{11}$$

M is the available bandwidth of channel Y and λ is the noise power spectral density.

2.3.2. Interference Model. Interference between wireless links can be divided into primary interference and secondary interference. For any two different edges (i, j) and (k, l) in E, if there are $i \neq k$, $i \neq l$, $j \neq k$, $j \neq l$, then the fundamental interference does not exist in (i, j) and (k, l) do not exist; that is, the fundamental interference limits multiple transmissions, multiple receptions, and simultaneous transmission and reception. The two interference models are introduced separately as follows [13].

For secondary interference, it is usually described by protocol interference model or physical interference model. At some time t, receiving node j treats all other sending nodes except sending node i as interfering nodes. The signal-to-interference-noise ratio at the receiving node is calculated by the interfering node and compared with the threshold to judge whether it can be successfully received. In the physical interference model, the minimum signal-to-interference-to-noise ratio that ensures correct reception by the receiver needs to be defined first as the decision threshold.

In the protocol interference model, the interference between nodes or links is defined as a state parameter with a value of 0/1. Each node has the same transmit power, so all nodes have the same maximum transmission distance. For the interference distance, θ is the interference factor, usually $1 \leq \theta \leq 3$. All nodes within the maximum transmission distance can communicate directly, and all sending nodes

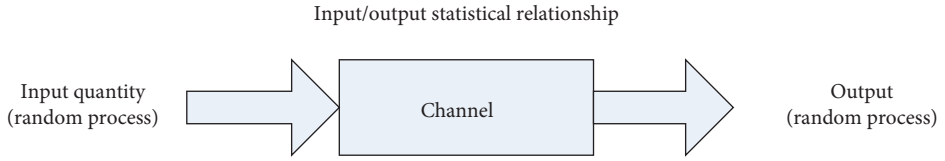

Figure 2: Schematic diagram of the channel model.

within the interference distance will interfere with the node's reception. Under the protocol interference model, two links, (i, j) and (k, l), interfere with each other when one of the following two situations occurs:

(1) $(i, j) \cap (k, l) \neq \varphi$; that is, the two wireless links have a common node.

(2) $j \leq Ir$ or $dk, j \leq Ir$; that is, the interference range of the sending node of one link includes the receiving node of the other link.

If two links interfere with each other, they cannot be simultaneously active for data transmission. Figure 3 can be used to illustrate the limitations of mutual interference between links under the protocol interference model. If node 1 transmits data to node 2, other nodes that would interfere with node 2 cannot send data. Because node 2 is within the interference range of node 3 and node 5, respectively, neither node 3 nor node 5 can transmit data. Consider another scenario, if node 3 sends data to node 4, because node 6 is not within the interference range of node 3, node 5 can use channel 1 to send data to node 6 at the same time. In wireless networks, when the path fading index β is greater than 2, the protocol interference model can be basically equivalent to the physical interference model.

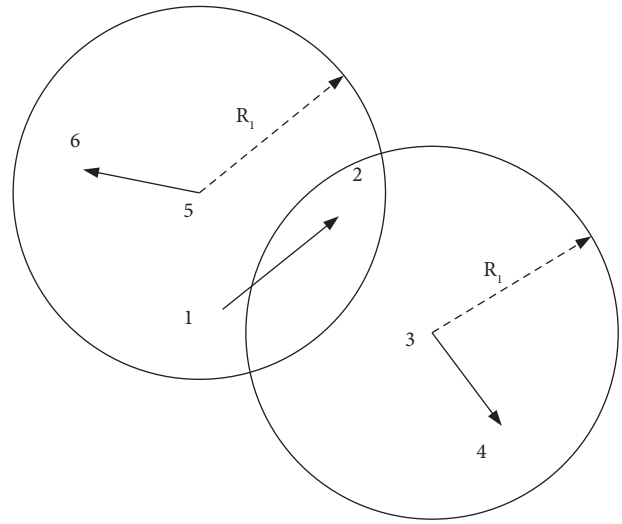

Figure 3: Example of interlink interference.

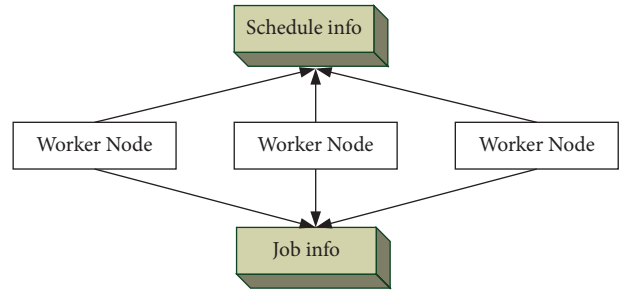

Figure 4: Decentralized scheduling model.

2.3.3. Scheduling Model. Any two links can be activated to transmit data at the same time only if they do not interfere with each other; otherwise, the corresponding data transmission will fail. The set of links that can be activated simultaneously at any given time is called Concurrent Transmission mode (CTS). A concurrent transfer mode, in which no further concurrent links can be added, is called a maximally concurrent set. The scheduling model diagram is shown in Figure 4.

According to the transmission modes described above, all concurrent modes are set as a set, which grows exponentially with the number of links [14]. In the model, variables were introduced and disabled to reduce the calculation error of the model, and whether the link in the model China is activated during the transmission process was observed. If the aggregate link is 1 during transmission, it means that the link is active, and if it is 0, it means it is not active. If two links interfere with each other but cannot be activated at the same time, where K is used to represent the interfering link set, then the result is

$$m_{i,j}^{n} + m_{k,\lambda}^{n} \leq 1 \Lambda (i, j) \in E, \Lambda (k, \lambda) \in Y_{(i,j)}. \tag{12}$$

It is assumed that, in a scheduling period, the system allocates a dedicated time segment Ts for each different transmission mode, and each transmission mode can only transmit data in its own dedicated time segment [15]. The length of the time slice may be 0. If, in a certain scheduling period, the time segment allocated by the system to a certain transmission mode is 0, it means that all links corresponding to this transmission mode cannot be activated to transmit data in this scheduling period.

The activation test is performed on the abovementioned traditional transmission mode, and the intrascheduling period of the link is adjusted to obtain the total activation time. The formula is

$$\theta_{i,j} = \sum_{n \in N} W_n \cdot m_{i,j}^{n}, \Lambda (i, j) \in E. \tag{13}$$

2.3.4. Business Flow Model. To optimize the throughput of data flowing from the router node to the gateway node, the optimization problem of the downstream data flow can be

obtained by simply modifying the algorithm. Furthermore, although in practical systems, the transmission interval is usually divided into time slots, and information is transmitted in the form of data packets, if the duration of the time slot is small enough, and a transmission interval can contain multiple time slots, the data transmitted in the form of data packets can be regarded as a bit stream [16].

tThe multisession (Multisession) business flow model was used to describe the multipath routing of business data flow through the network. The business data flow sent from the source node to the gateway node was called a session (session) and is identified by its source node. In a multihop network, the source node often needs to pass through multiple intermediate nodes to transmit data to the destination node [17]. In addition, if each session adopts a single path, it will not be able to take advantage of the load balancing advantage of the multihop network, so we assume that the data traffic flow of the same session can reach the destination node through multipath routing. The data flow of the data flow sent by the source node c to the gateway node is the data flow of the link (i, j), where U_c represents the bandwidth requirement sent by the node c to the gateway node.

(1) The amount of data flowing from source node c to the gateway and the amount of data of service flows related to c, the sum of which must be equal to the total bandwidth requirement U_c of node c:

$$\sum_{t\in Q,(c,t)\in E} k_{v,t}^{c} = U_c, \Lambda_c \in V_r. \tag{14}$$

(2) To avoid loops, any traffic flow on the link to source node c related to c must be equal to 0:

$$k_{i,v}^{c} = 0, \Lambda\,(i,c) \in E, \Lambda_c \in U_r. \tag{15}$$

(3) At the gateway node, since the gateway node is connected to the wired network and does not provide relays for the flow of other nodes, all traffic flows out of the gateway node must be equal to 0:

$$k_{i,j}^{c} = 0, \Lambda\,(i,j) \in E, \Lambda i \in U_g. \tag{16}$$

(4) At the relay node, the traffic flow of all nonlocal nodes must satisfy the flow conservation law; that is, the total amount of business flows flowing into the other node of the relay node must be equal to the total amount of business flows flowing out of the other node of the relay node:

$$\sum_{i\in U_r,(i,j)\in E} k_{i,j}^{c} - \sum_{h\in U_r\,(j,h)\in F} k_{j,h}^{c} = 0. \tag{17}$$

(5) The sum of all traffic flows through a link (i, j) cannot exceed the physical capacity of the link multiplied by the total activation time of the link in the scheduling period:

$$\sum_{c\in U_r} k_{i,j}^{c} \le \beta_{i,j} \cdot A_{i,j}, \Lambda\,(i,j) \in E. \tag{18}$$

The total throughput of the system is defined as the ratio of the total uplink data of all router nodes in a certain time interval (e.g., a scheduling period) to the total transmission time, such as system activation time, allocated to each relevant node for transmitting these data [18]. Obviously, given the uplink traffic (i.e., bandwidth requirements) to each router node, if the system activation time is shorter, the total system throughput will be larger; that is, the system performance will be better. Therefore, the optimization goal is to minimize the system activation time under the premise of meeting the bandwidth requirements of all nodes in the network. Therefore, the optimization problem can be formulated as

$$\min \sum_{c\in C} R_c. \tag{19}$$

2.3.5. Column Generation Algorithm. The column generation algorithm is a decomposition technique used to solve large linear programming and integer linear programming problems with many variables [19]. The column generation algorithm decomposes a linear programming problem into a restricted master problem and a slave problem (the pricing problem). The column here refers to the column vector of the constraint matrix of the linear programming problem. Initially, the master problem contains only a subset of the column space, and then the slave problems are solved to determine whether the master problem can be expanded by adding columns to obtain a better solution and by iterating between master and slave problems until the master problem contains all the columns for which the optimal solution is obtained. A brief flowchart of the column generation algorithm is shown in Figure 5.

For the linear optimization problem studied in this chapter, a column in the column generation algorithm corresponds to a certain concurrent transmission mode s, so the restricted main optimization problem is formulated as follows:

$$\min \sum_{c\in C_0} R_c. \tag{20}$$

Here the concurrent transmission mode set $S0$ is a subset of the set S. In order to simplify the initialization of the concurrent transmission mode set $S0$, it can be selected to include L (number of links) concurrent transmission modes at the beginning, and each concurrent transmission mode only contains a corresponding link. In this way, by solving the restricted main optimization problem, the optimal solution corresponding to the concurrent transmission set $S0$ and the dual variable $P_{i,j}$ of the main optimization problem can be obtained. Then, it needs to be determined whether the main optimization problem can be reoptimized by adding a new concurrency mode to $S0$. This is equivalent to a concurrent transmission mode s, whose corresponding activation time Ts has a negative cost reduction for the existing concurrent transmission mode set. Let RCs be the reduced cost of concurrent transmission mode s. According to the duality property of linear programming, there is

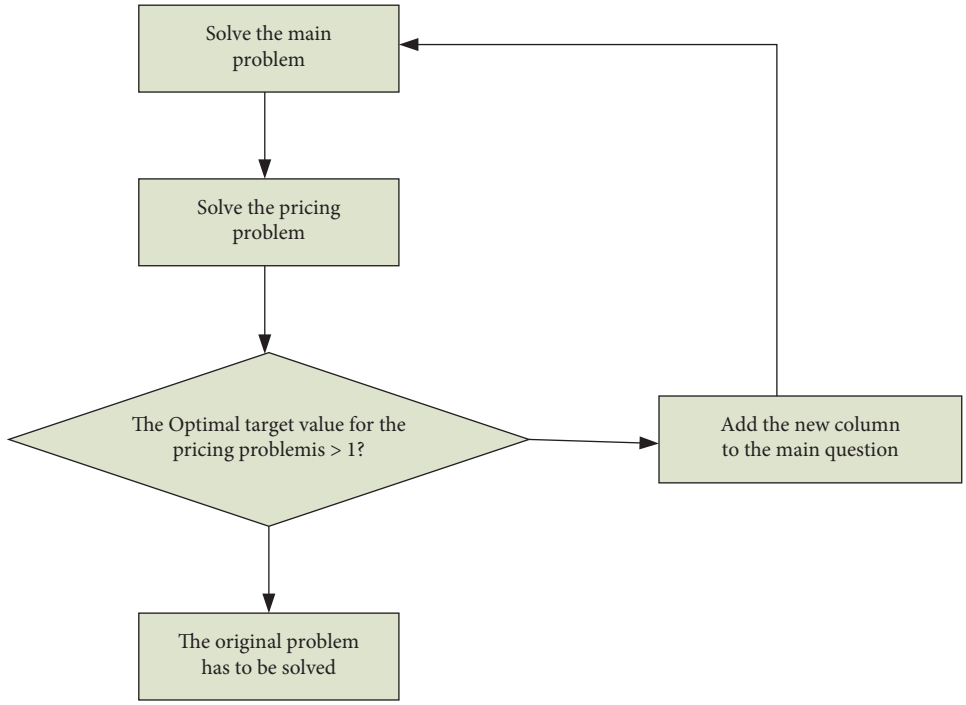

Figure 5: Flowchart of the column generation algorithm.

$$WH_c = 1 - \sum_{(i,j)\in E} Q_{i,j} k_{i,j}^c H_{i,j}. \tag{21}$$

Obviously, to make the cost value smaller, the maximum value is required, and as long as the value is negative, it means that the original optimization problem can be further optimized after adding the corresponding concurrent transmission mode. Thus, the optimization problem (pricing problem) can be expressed as

$$\max \sum_{(i,j)\in E} Q_{i,j} k_{i,j}^c H_{i,j}. \tag{22}$$

2.3.6. Maximal Clique Optimization Algorithm. The optimal result can be obtained by using the column generation algorithm, but when it is applied to this optimization problem, the optimization solution of the pricing problem is a 0-1 integer programming, which is still a NP-hard problem. Therefore, the operation time will be too long, when the network size is slightly enlarged [20]. In graph theory, a clique refers to a subset of the vertex set of a graph so that its derived subgraphs are all complete graphs. If a clique is not a subset of any other clique, the clique is called maximal group. The clique with the largest number of vertices in a graph is called the maximal clique of the graph. According to the problem, an optimization algorithm based on maximal clique search has been proposed, which has greatly improved the efficiency of translation optimization. In vectorless graphs, the maximal clique optimization algorithm is widely used and is a research hotspot in search algorithms. If the data in the process of statistical translation is too complicated, it can be processed by dividing and conquering and parallel computing methods according to the characteristics of different types of data information of Japanese passive.

Optimization studies were performed on statistical machine translation models. The details are as follows. According to the previous optimization conditions, combined with the wireless link model, the wireless link interference graph was constructed. The complementary graph was obtained from the link interference graph, which is an undirected graph, and then the improved BK algorithm was used to search for the complementary graph. The maximal clique of the graph, and all maximally concurrent transfer modes in the system were updated. The transfer mode was substituted into the optimization problem of the statistical machine translation model to solve. It should be pointed out here that the subset of any maximal transmission mode is not listed, and the activation of a subset can be replaced by the activation of a maximal transmission mode that includes the subset, which will not affect the optimized results. Every nonmaximal concurrent transfer mode must be a subset of some maximal concurrent transfer mode. For the constraint expression in the original problem, using a maximal concurrent mode to replace one of its subconcurrent modes means that the constraints are satisfied in the original linear programming problem and have a larger feasible region, so adding any subconcurrent transmission mode will not increase the feasible region of the original optimization problem. Therefore, the full enumeration of all concurrent modes can be replaced by all the maximum concurrent modes without reducing the feasible region of the optimization problem. In this way, the variables of 0-1 integers in the original optimization problem can be eliminated. The mixed-integer linear programming of the original optimization problem is converted into a general linear programming problem to solve so that the number of variables in the optimization model is greatly reduced, and the optimization operation efficiency is greatly improved.

2.4. System Computing Capacity Scheduling Algorithm (CS). Capacity Scheduler is a scheduling algorithm based on multiuser environment developed by Yahoo. Its general design idea is to divide multiple queues in the entire cloud computing system, and these queues are also independent of each other [6]. Compared with the FIFO job scheduling method, the computing power scheduling algorithm has made up for the shortcomings of its low resource utilization. According to the nature of each queue, system resources are allocated to each queue with a certain strategy, and the upper and lower limits of resource allocation can be intelligently set according to the classification and nature of the queue. For the usage of resources in the queue, the scheduling algorithm can set the usage by itself. This is to prevent system resources from being occupied for a long time and system resource utilization being affected. In the process of machine translation in Japanese passive statistics, the computing power scheduling algorithm was used. When the computing nodes of various language types are idle, the system always allocates computing resources to the queue with the lowest proportion of resources first, which can reduce the number of processes starved. In a queue, the scheduler always schedules jobs in the queue according to the first-in, first-out policy. However, it is also possible to set priorities for jobs in the queue, and schedule them according to job priorities. At the same time, in the computing power scheduling algorithm, the resources of the system are flexible; that is, when the resources of a certain queue have remaining after meeting its own needs, these remaining resources can be allocated to other queues for use.

The characteristics of the computing power scheduling algorithm are as follows:

(1) Capacity guarantee: The scheduler will set the minimum lower limit and the maximum upper limit of the resource ratio for each queue according to the job characteristics of each queue so as to ensure the normal execution of the jobs of each queue.

(2) Flexibility: The resources of the system are flexible. When resources in the system need to be moved, these resources will be returned to the queue from the queue that borrows resources to ensure the normal execution of tasks in the queue.

(3) Support priority: The scheduler schedules jobs in the queue according to the time-critical order of tasks in the system and executes tasks with earlier submission times first. Statistical machine translation methods have attracted more and more attention due to their rigorous mathematical derivation, good model consistency, automatic learning, and strong robustness.

(4) Multiple tenancy: The queues on the entire system and the jobs in each queue run independently in parallel, and the system can set certain constraints. The purpose of this is to prevent a job, a user, or a queue from occupying system resources for a long time, resulting in slower system response and unbalanced and wasteful resources.

(5) Support resource-intensive jobs: The system's resource requirements for jobs are incrementally reserved. When a task requires more resources, the system will meet the needs of the task by incremental reservation according to the task requirements. By limiting the queue and user resources in the system, the computing power scheduling algorithm logically divides the entire system cluster into several subclusters with relatively independent resources. These subclusters actually share the resources in the larger cluster, so they can share resources, improve resource utilization, and reduce operation and maintenance costs. However, currently the only resource type supported is memory.

All in all, the computing power scheduling algorithm can make up for the shortcomings of low computer utilization and divide different types of passive Japanese into subclusters of independent resources by restricting data queues and user resources in the system. By utilizing resource sharing in large clusters, resource utilization has been improved and operation and maintenance costs have been reduced.

2.5. System Resource Aware Scheduling Algorithm. Although the computing power scheduling algorithm has the advantages of reducing the low utilization rate of the system and allocating resources to the system queue, it ignores the competition between different resources [21]. Due to the continuous increase of the processing power of the CPU and the disk, the processing power of the node and the disk access speed show a great difference. If the processing power in the system is reduced, it will greatly slow down the system's machine translation work for Japanese passive statistics and waste system resources [22]. Figure 6 shows the algorithm flowchart.

Some experts have proposed a resource-aware scheduling algorithm for processing Japanese passive statistics of machine translation and improving work efficiency. This algorithm is mainly used to solve the resource competition relationship between different types of dynamic Japanese translations in the system in a heterogeneous environment [23]. The main step of the algorithm is to schedule two different types of passive dynamics[24]. The node load information is sent to the system, and the system determines the classification after analysis and then selects the appropriate task for scheduling. This can not only shorten the response time of the system, but also improve the utilization of resources [25, 26].

3. Experiment and Destruction of Machine Translation of Scheduling Joint Optimization Algorithm in Japanese Passive Statistics

3.1. Experimental Destruction of Scheduling Algorithms. According to the actual situation of Japanese passive type, this paper has analyzed the statistical machine translation model for computing power and resource-aware scheduling

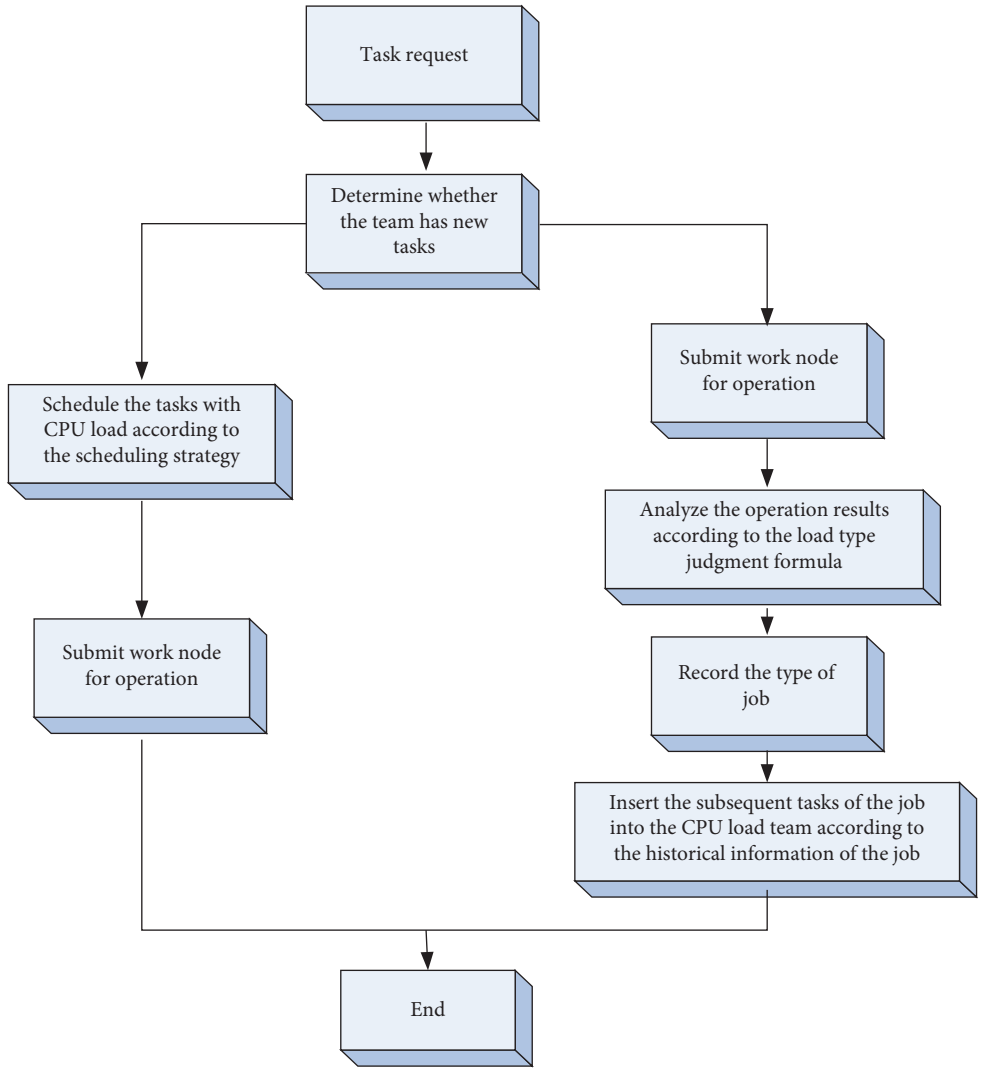

Figure 6: Scheduling algorithm flow.

algorithm experiments. The two scheduling algorithms were placed in a resource pool at the same time, the size and time of the output data were compared, and the performance of the two optimal scheduling algorithms was analyzed [27]. The computer configuration required in the experiment is shown in Table 1.

As shown in Figure 7, when all queues of the computing power scheduling algorithm (CS) share a resource pool, the performance of the computing power scheduling algorithm (CS) is not as good as that of the resource-aware scheduling algorithm. When the input data volume is 6 GB, the calculation time of the two algorithms differs by about 18 s. Compared with the computing power scheduling algorithm, the time of the resource-aware scheduling algorithm is reduced by 15.5%. Although the computing power scheduling algorithm has multiple work queues, it is still a shared resource pool in terms of system resources. Therefore, each queue does not have a separate resource pool, which will cause queue resource competition and reduce scheduling efficiency. As the amount of Japanese passive data increases, the efficiency of the workload-aware scheduling algorithm increases. This is because with the increase of the number of jobs, the total job processing time ratio of job type judgment and job insertion operation continues to decrease, and jobs of different load types make the operating load of the system reach maximum. The resource utilization of the system is greatly improved, thereby reducing the running time of the job.

In the case of the same amount of data, the time spent processing the data has been reduced, which means that the efficiency with which Japanese is dynamically translated has been improved [28]. When the total amount of data is the same, the comparison results of the accuracy of Japanese dynamic machine translation after the two scheduling algorithms are shown in Figure 8.

Among them, the total amount of data given by the middle system of the two optimization algorithms each accounts for 50% of the total amount of data. In order to ensure the authenticity and accuracy of the experimental data, multiple experiments were carried out on the experimental objects of the lock in the same environment, and the final average of the completion time was obtained.

Table 1: Cluster configuration.

Node type	CPU configuration	Memory configuration (G)	Disk read and write rate (M/s)
Master	2-Core i3 2.3 G	6	190
Slave 1	4-Core i5 3.1 G	8	190
Slave 2	4-Core i5 3.1 G	8	190
Slave 3	4-Core i5 3.1 G	4	190
Slave 4	2-Core i5 3.1 G	4	190

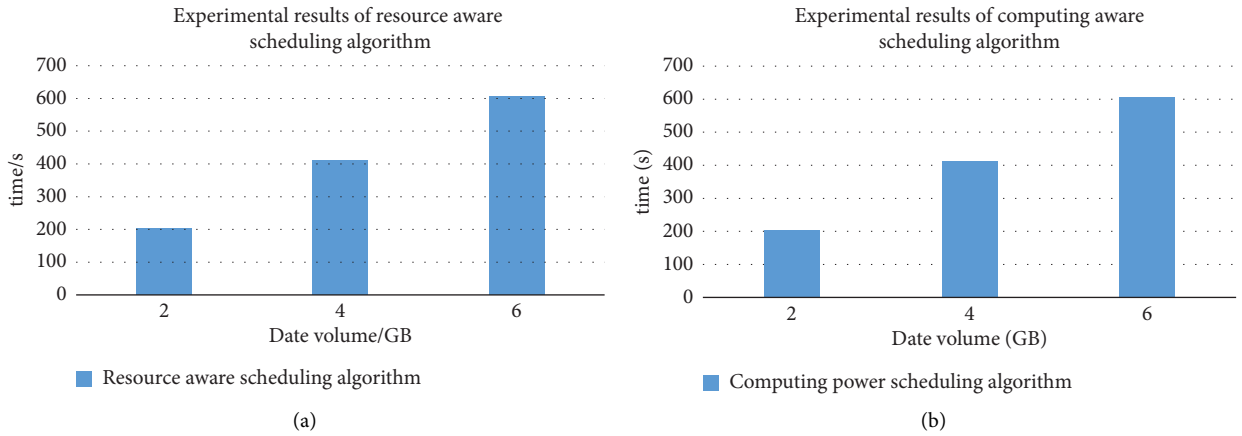

Figure 7: Comparison of experimental results between resource perception and computing power scheduling algorithms.

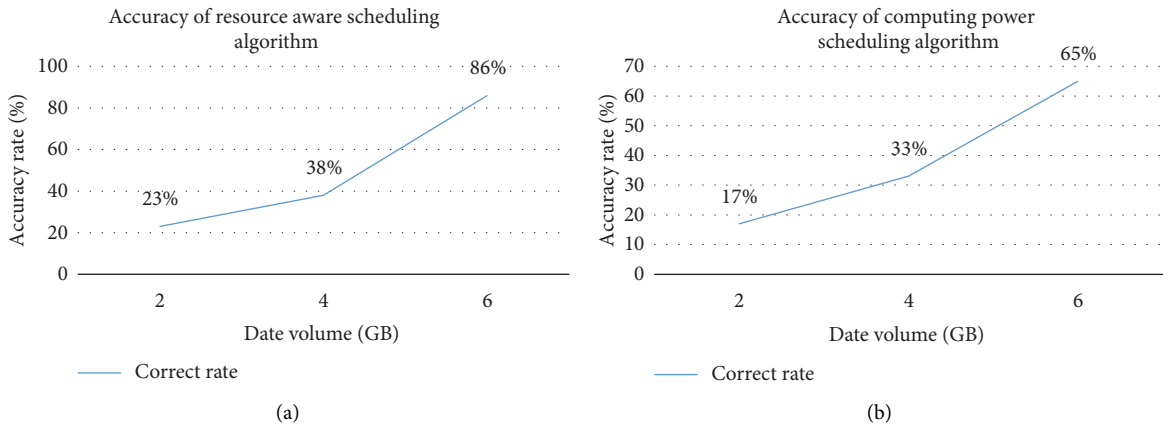

Figure 8: Comparison of the accuracy of Japanese dynamic machine translation under the optimization of two algorithms.

The experimental results have shown that the resource-aware scheduling algorithm of the computing power scheduling algorithm was more accurate than the computing power scheduling algorithm in the Japanese passive machine translation. When the total amount of data is 2 G, 4 G, and 6 G, the accuracy rates of the resource-aware scheduling algorithm are 23%, 38%, and 86%, respectively. Under the premise of the same amount of data, it is 6%, 5%, and 21% higher than the computing power scheduling algorithm, respectively. It can be seen that the optimization ability of the resource-aware scheduling algorithm is relatively good, so it is suitable for the optimization calculation of machine translation in Japanese passive statistics. In addition, it also includes gradient descent algorithm, Newton's method, and other algorithms with optimization properties, which has certain significance for the analysis of the experimental object.

3.2. Machine Translation Simulation Experiment of Scheduling Joint Optimization Algorithm in Japanese Passive Statistics. According to the passive characteristics of Japanese and the exponential increase in the number of decision variables in the optimization problem in the statistical machine translation model, when the optimization problem reaches a certain scale, it is quite difficult to find the optimal result due to the limitation of calculation conditions [29]. This also accords with the characteristic that this

Table 2: Experimental results of optimization of 10 network nodes in a statistical machine translation model.

Simulation serial number	Column generation algorithm		Maximum group algorithm	
	Operation time (s)	Optimization result (time slot)	Operation time (s)	Optimization result (time slot)
1	173.99	94	0.102	94
2	203.80	89	0.080	89
3	195.17	66	0.081	66
4	198.56	85	0.090	85
5	171.23	74	0.080	74
6	188.65	74	0.080	74
7	206.43	90	0.075	90
8	88.948	41	0.110	41
9	208.946	75	0.080	75
10	98.412	62	0.080	62

optimization problem is NP-hard in nature. In this paper, the column generation algorithm and the maximal clique algorithm proposed in the above optimization algorithm have been used to make an experimental analysis on the optimization problem of Japanese passive in the statistical machine model. The application of this model has a certain complexity, so this paper optimizes the statistical machine translation model and simplifies the experimental process. The experimental results of optimization of 10 network nodes in the statistical machine translation model are shown in Table 2.

It can be seen from Table 2 that the two algorithms have the same optimization results when the demand is different. When the optimization result is 94, the operation time of the column generation algorithm is 173.99 s, and the operation time of the largest group algorithm is 0.102 s; but when the optimization result is 62, the operation time of the column generation algorithm is 98.412 s, and the operation time of the largest group algorithm is 0.080 s. The operation time of the maximal clique optimization algorithm is all less than 1, which is much smaller than that of the column generation algorithm. This has fully proved the correctness and effectiveness of the maximal clique algorithm for the optimization model of machine translation in Japanese passive statistics.

4. Discussion

This paper has mainly studied the machine translation of the joint optimization algorithm for scheduling in Japanese passive statistics. The article has analyzed the channel model, scheduling model, interference model, and business flow model in detail and proposed a column generation algorithm, a maximal clique algorithm, a system computing power scheduling algorithm, and a resource-aware scheduling algorithm to optimize machine translation. In the experimental process, this paper simulates and analyzes statistical machine translation in combination with the experimental damage of the scheduling algorithm and adopts a shared resource platform to compare the output data size and time of the two scheduling algorithms and analyze the performance of the algorithm, and combined with the passive characteristics of Japanese, the results of optimization of 10 network nodes in the statistical machine translation model are selected, and the conclusions of this paper are finally drawn. Based on the proposed algorithm model, the experiment on the performance of machine translation has found that the resource-aware scheduling algorithm was more efficient in allocating resources within the system. These technical principles have provided a theoretical basis for the machine translation work in Japanese passive statistics. However, since there are not many algorithms combined in this paper, there will be insufficient data when performing machine translation of Japanese passive statistics, so more scholars are needed to discuss and study.

5. Conclusions

This paper has improved the scheduling joint optimization algorithm of the machine translation model and focused on the analysis of the resource-aware scheduling algorithm, the computing power scheduling algorithm, the column generation algorithm, and the maximal clique algorithm for the optimization of Japanese passive in statistical machine models. The experimental results show that the accuracy of the resource-aware scheduling algorithm for dynamic translation optimization of Japanese was greater than that of the computing power scheduling algorithm. When the data volume is 2 G, it is 6% higher; when it is 4 G, it is 5% higher; and when it is 6 G, it is 21% higher. At the same time, the time spent has been reduced by 15.5%. It can be seen that the optimization effect of the resource-aware scheduling algorithm is better. According to the passive characteristics of Japanese and the optimization conditions in the machine translation model, this paper has used the column generation algorithm and the maximal clique algorithm to conduct experimental analysis in the network nodes to find the optimal optimization algorithm. The experimental results show that when the data is the same, the optimization results of the two algorithms are the same. However, the operation time of the maximal clique optimization algorithm is much smaller than that of the column generation algorithm, which fully proves the correctness and effectiveness of the maximal clique algorithm for the optimization model of machine translation in Japanese passive statistics. Machine translation is a focus in the future. This paper combines Japanese passive statistics with a large number of scheduling

optimization algorithms, which brings a more meaningful reference direction for the development of machine translation.

Data Availability

No data were used to support this study.

Conflicts of Interest

The author declares that there are no potential conflicts of interest regarding the publication this study.

Acknowledgments

This study was supported by the Science Foundation of Educational Commission of Anhui Province of China (Grant no. SK2021A0798).

References

[1] Y. Cai, F. Cui, Q. Shi, M. Zhao, and G. Y. Li, "Dual-UAV-enabled secure communications: joint trajectory design and user Scheduling;Joint trajectory design and user scheduling [J]," *IEEE Journal on Selected Areas in Communications*, vol. 36, no. 9, pp. 1972–1985, 2018.

[2] Y. Fei, M. A. Huimin, and S. O. Business, "Joint optimization of batch-discrete re-enter production scheduling and preventive maintenance[J]," *Computer Integrated Manufacturing Systems, CIMS*, vol. 25, no. 1, pp. 44–52, 2019.

[3] J. Zhao and L. Mili, "Robust uk filter for power system dynamic state estimation with unknown noise statistics," *IEEE Transactions on Smart Grid*, vol. 10, no. 2, pp. 1215–1224, 2019.

[4] A. O. Al-Abbasi and V. Aggarwal, "VidCloud: joint stall and quality optimization for video streaming over cloud[J]," *ACM Transactions on Modeling and Performance Evaluation of Computing Systems*, vol. 5, no. 4, pp. 1–32, 2020.

[5] G. Song, "Accuracy analysis of Japanese machine translation based on machine learning and image feature retrieval," *Journal of Intelligent and Fuzzy Systems*, vol. 40, no. 2, pp. 2109–2120, 2021.

[6] G. Zheng and J. Zhu, "Japanese translation teaching corpus based on bilingual non parallel data model[J]," *Journal of Intelligent and Fuzzy Systems*, vol. 40, no. 5, pp. 1–11, 2020.

[7] M. Mangeot-Nagata, "Erratum to collaborative construction of a good quality, broad coverage and copyright free Japanese-French dictionary," *International Journal of Lexicography*, vol. 31, no. 1, p. 113, 2018.

[8] J. Wang, C. Liu, and M. C. Zhou, "Improved bacterial foraging algorithm for cell formation and product scheduling considering learning and forgetting factors in cellular manufacturing systems," *IEEE Systems Journal*, vol. 14, no. 2, pp. 3047–3056, 2020.

[9] H. Khani and H. E. Z. Farag, "Joint arbitrage and operating reserve scheduling of energy storage through optimal adaptive allocation of the state of charge," *IEEE Transactions on Sustainable Energy*, vol. 10, no. 4, pp. 1705–1717, 2019.

[10] L. Qi, "Tool requirement and pre-scheduling optimization model of the tool flow system of a digital workshop[J]," *Proceedings of the Institution of Mechanical Engineers - Part B: Journal of Engineering Manufacture*, vol. 231, no. 5, pp. 838–849, 2017.

[11] D. Zhou, M. Sheng, J. Luo, R. Liu, J. Li, and Z. Han, "Collaborative data scheduling with joint forward and backward induction in small satellite networks," *IEEE Transactions on Communications*, vol. 67, no. 5, pp. 3443–3456, 2019.

[12] M. Rikters, R. Ri, T. Li, and T. Nakazawa, "Japanese–English conversation parallel corpus for promoting context-aware machine translation research," *Journal of Natural Language Processing*, vol. 28, no. 2, pp. 380–403, 2021.

[13] M. Khatami and S. H. Zegordi, "Coordinative production and maintenance scheduling problem with flexible maintenance time intervals," *Journal of Intelligent Manufacturing*, vol. 28, no. 4, pp. 857–867, 2017.

[14] T. Lu, E. Yao, Y. Zhang, and Y. Yang, "Joint optimal scheduling for a mixed bus fleet under micro driving conditions," *IEEE Transactions on Intelligent Transportation Systems*, vol. 22, no. 4, pp. 2464–2475, 2021.

[15] B. Lv, R. Wang, Y. Cui, Y. Gong, and H. Tan, "Joint optimization of file placement and Delivery in cache-assisted wireless networks with limited lifetime and cache space," *IEEE Transactions on Communications*, vol. 68, no. 4, pp. 2339–2354, 2020.

[16] X. Xu, Y. Xue, M. Cui, Y. Yuan, and L. Qi, "Joint optimization of energy conservation and migration cost for complex systems in edge computing," *Complexity*, vol. 2019, no. 12, pp. 1–14, Article ID 6180135, 2019.

[17] J. Zhu, G. Zhang, Z. Zhu, and K. Yang, "Joint time switching and transmission scheduling for wireless-powered body area networks," *Mobile Information Systems*, vol. 2019, no. 4, pp. 1–11, Article ID 9620153, 2019.

[18] K. Abe, Y. Matsubayashi, N. Okazaki, and K. Inui, "Multi-dialect neural machine translation for 48 low-resource Japanese dialects," *Journal of Natural Language Processing*, vol. 27, no. 4, pp. 781–800, 2020.

[19] J. R. Lee, "Potential of machine translation in headline translation: f: focusing on Korean-Japanese translation of headlines[J]," *Interpretation and Translation*, vol. 21, no. 2, pp. 119–144, 2019.

[20] S. D. Budiwati and M. Aritsugi, "Word reordering on multiple pivots for the Japanese and Indonesian language pair," *Machine Translation*, vol. 35, no. 4, pp. 611–636, 2021.

[21] N. Wang, J. Xu, and F. Ming, "Integrating voice features into Japanese-English hierarchical phrase based model[J]," *Acta Scientiarum Nauralium Universitaties Pekinensis*, vol. 53, no. 2, pp. 305–313, 2017.

[22] W. Xu and M. Carpuat, "EDITOR: an edit-based transformer with repositioning for neural machine translation with soft lexical constraints :an edit-based transformer with repositioning for neural machine translation with soft lexical constraints[J]," *Transactions of the Association for Computational Linguistics*, vol. 9, no. 1, pp. 311–328, 2021.

[23] I. Goto, "Neural network machine translation technology[J]," *Broadcast Technology*, vol. 70, p. 21, 2017.

[24] T. Bezdan, C. Stoean, A. A. Naamany, N. Bacanin, and K. Venkatachalam, "Hybrid fruit-fly optimization algorithm with K-means for text document clustering," *Mathematics*, vol. 9, 2021.

[25] S. Li, X. Ao, F. Pan, and Q. He, "Learning policy scheduling for text augmentation," *Neural Networks*, vol. 145, pp. 121–127, 2022.

[26] X. Wu, L. Wang, Y. Xia et al., "Temporally correlated task scheduling for sequence learning," in *Proceedings of the*

International Conference on Machine Learning, Beijing China, July 2020.

[27] N. Bacanin, M. Zivkovic, T. Bezdan, K. Venkatachalam, and M. Abouhawwash, "Modified firefly algorithm for workflow scheduling in cloud-edge environment," *Neural Computing & Applications*, vol. 34, no. 11, pp. 9043–9068, 2022.

[28] L. Jie, "Modeling and analysis of translation ability of applied English talents based on data mining algorithm," *International Conference of Social Computing and Digital Economy*, pp. 211–214, 2021.

[29] Z. Wenjie, "English automatic translation platform based on BP neural network for phrase translation combination," in *Proceedings of the International Conference on Frontier Computing*, Springer, Singapore, September 2022.

Hindawi
Scientific Programming
Volume 2022, Article ID 5617400, 11 pages
https://doi.org/10.1155/2022/5617400

Research Article

Acquisition of English Corpus Machine Translation Based on Speech Recognition Technology

Chunyan Jing and Guoying Liu

School of Humanities & Social Sciences, Xi'an Polytechnic University, Xi'an 710048, Shaanxi, China

Correspondence should be addressed to Chunyan Jing; jingcy@xpu.edu.cn

Received 22 June 2022; Revised 30 July 2022; Accepted 11 August 2022; Published 21 September 2022

Academic Editor: Juan Vicente Capella Hernandez

In the present information age, with the rapid development of computer software and hardware technology and the mature manufacturing system of English-speaking enterprises, it is no longer impossible to use statistics for machine translation. The level and quality of machine translation are expected to meet human expectations. This explains the meaning and realization value of the acquisition of English corpus machine translation, introduces the basic principles of speech recognition technology, and combines the characteristics of the English language on the basis of the original Chinese speech recognition system, adopts the technical means of speech recognition, and leads to in-depth research. In the new era of machine translation acquisition of English corpus, we use the combination of LabVIEW and MATLAB to complete the collection, editing, feature extraction, and speech recognition of speech signals and use VQ pattern matching technology to realize the English recognition of a large number of short vocabulary and individuals. In the application part, we applied the classic LabVIEW technology to the speech recognition technology, which actually realized the idea of "software instead of hardware" and achieved better translation results. Experiments show that the accuracy rate of English machine translation can be as high as 94% when using speech recognition technology. According to the results, it takes about 0.2 seconds to complete machine translation for a 30-second speech, which is basically okay to achieve the effect of real-time translation.

1. Introduction

Speech recognition technology is a comprehensive subject based on phonetics theory and computer technology. It is a multidisciplinary research field, usually involving linguistics, acoustics, cognition, artificial intelligence, information processing, and many other subjects. When focused on the learner English corpus, it shows that the learner corpus is a computer-processed text database of the language output of foreign language learners. It can discover the rules and characteristics of interlanguage development by means of parts of speech, errors, semantic coding, or syntactic tagging. Since the 1990s, in order to better conduct interlanguage research on corpora, researchers have developed and constructed multiple learner corpora, such as the Chinese Learner's English Corpus. As a borderline model, speech recognition technology needs research results in many fields as support. From the perspective of computers, it is the intelligent interface part of smart instruments; from the perspective of signal processing, it is part of information recognition; in terms of circuits, communication, electronic systems, signals, and systems, it involves the source processing of communication systems and information; from the perspective of automatic control theory, it can be an important part of pattern recognition; in addition, voice recognition needs another assistance, such as psychology and physiology. Speech recognition is a very difficult research topic. From the point of view of pattern recognition only, the speech signal is a transient event signal, and it is also a time-consuming and unstable random process. There are many kinds of internal issues. Therefore, speech recognition is a kind of multidimensional pattern recognition, which is a very challenging subject.

Machine translation, also known as automatic translation, is the use of computers to convert one natural language (source language) into another natural language (target language). It is a branch of computational linguistics, one of the ultimate goals of artificial intelligence and has important scientific research value. At the same time, machine translation has important practical value. With the rapid development of economic globalization and the Internet, machine translation technology plays an increasingly important role in promoting political, economic, and cultural exchanges. Machine translation has developed today and has been widely used, such as various online translation platforms commonly used by humans, retrieval of information between languages, and various computer-embedded translation programs. Automatic translation has come a long way since the beginning and the development process is very difficult. So far, researchers are studying, and it has not developed very smoothly. Although automatic translation has developed to a large extent compared with before, there are not many products that can be brought to the market. Even these machine translation products, which have been widely used by humans, still have a lot of room for improvement in accuracy. Therefore, the study of machine translation knowledge acquisition is a very important prospect.

Regarding machine translation in the context of speech recognition, Ravanelli said that one area that directly benefits from the latest developments in deep learning is Automatic Speech Recognition (ASR). Ravanelli et al. modified one of the most popular RNN models, the gated recurrent unit (GRU) and proposed a simplified architecture that is very effective for ASR. Ravanelli et al. analyzed the role played by the reset gate and suggested replacing the hyperbolic tangent with a modified linear unit activation. However, this change and batch normalization cannot be combined well, and it is not very helpful for the model to learn the long-term dependence relationship and numerical problems are likely to occur [1]. Watanabe et al. said that the traditional automatic speech recognition (ASR) based on hybrid DNN/HMM is a very complex system consisting of various modules such as acoustics, dictionaries, and language models. It also requires language resources, such as pronunciation dictionaries, tokenization, and speech context dependency trees. However, experiments in English (WSJ and CHiME-4) tasks cannot prove that it is superior to most other popular speech recognition models. The character error rate is relatively increased by 5.4–14.6%, and it shows that it is different from the traditional DNN/HMM ASR without language resources. The performance of the system is quite different [2]. In recent decades, Abdelaziz has proposed many methods of embedding audio and video modes to improve the performance of automatic speech recognition in clear and noisy conditions. However, few studies comparing different AV-ASR fusion models can be found in the literature. However, the implementation process of his research method is relatively redundant, and it is troublesome to operate. At the same time, the research in this paper is based on speech recognition to achieve real-time machine translation acquisition of English corpus, but his research method takes too long to respond to speech recognition, so it is not suitable for this research method [3]. However, the above research was stopped at an early stage due to the imperfection of present English recognition technology and the shortcomings of the English corpus.

In order to complete the effective combination of voice recognition and robot control technology, I created a robot voice control system based on previous research and completed the following tasks: (1) Proposed a new feature parameter extraction method. By improving the LPC spectrum to estimate the formant parameters, new speech feature parameters are constructed. The new feature parameters include more comprehensive voice information including vocal tract characteristics and human auditory characteristics, with high accuracy, strong anti-interference ability, and more accurate highlighting of the essential characteristics of the voice signal. (2) Provides an enhanced speech recognition algorithm (TSMS) and an efficient DTW algorithm. The high-performance DTW algorithm significantly reduces computational time in the recognition process, meets the real-time requirements of the speech signal, and improves system performance to some extent. (3) The speech recognition technology is successfully applied to the motion control of the robot. In the Matlab development environment and VC++ interface, write the program code of the robot voice control system. Through the test of speech input, the perfect combination of speech recognition and machine translation acquisition of English corpus is realized. (4) This article is based on the basic principles of speech recognition and deeply optimizes the machine translation extraction method of the English corpus.

2. Speech Recognition Method and English Corpus Machine Translation Extraction Method

2.1. Basic Principles of the Speech Recognition System. There are many design schemes for speech recognition systems for different tasks, but the system structure and model ideas are roughly the same. The speech recognition system is essentially a pattern recognition system, including three basic units: feature extraction, pattern matching, and reference pattern library. Its basic structure is shown in Figure 1.

The preprocessing module processes the input part of the original audio, removes the data and background noise that do not have much impact on the overall experiment, and performs endpoint detection, voice framing, and lays pre-emphasis on the voice signal. During the training period, the tester conducts multiple training speeches, and the system obtains the feature vector parameters after preprocessing and feature extraction and designs or adjusts the reference model library for training speech [4]. The intermediate results are subsequently processed accordingly, and the constraints of the language model, morphology, syntax, and semantic information are adopted to obtain the final recognition result. After waiting for the input voice frequency band to generate electrical signals through the voice input

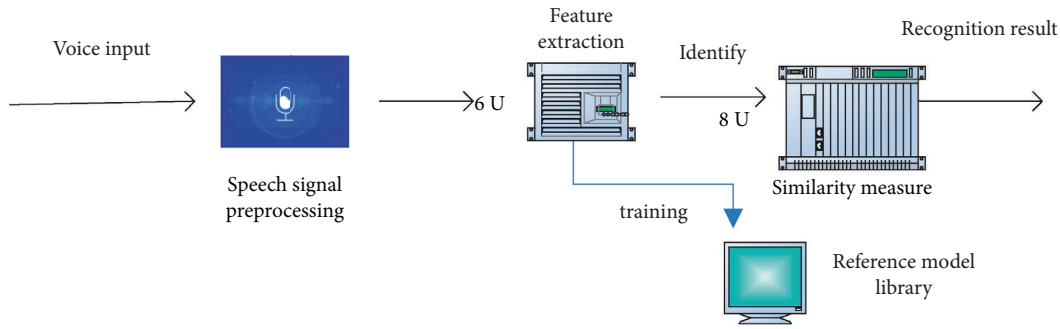

Figure 1: Basic structure diagram of the speech recognition system.

device, add the ports of the recognition system, first do the preliminary work, and then combine various features of the voice to form a voice model, analyze the electrical signal, and form voice recognition on this basis. The template is to be used [5].

2.2. Speech Recognition Technology Mode. The present speech recognition technology mostly adopts the method of pattern matching. As an important branch of pattern recognition, speech recognition and pattern recognition are unified. According to pattern recognition theory, we can compare the speech to be recognized with the existing speech one by one and select the best reference model as the final result of recognition [6], as shown in Figure 2.

As can be seen from Figure 2, the sound is identified by spelling and research on its characteristics, then entered into the database, and finally transferred from the translation library.

In the process of speech recognition, we also use the same method as before, and then we also get a set of speech parameters and then save it as a test template. In order to draw a correct conclusion, we compare the characteristic parameters of the test template and the training template and draw the highest matching rate in the recognition result [7].

The essence of speech recognition is actually the pattern matching process, so we need to train an appropriate template for speech matching. We use a lot of speech data to train this speech model. To a large extent, the nonspecific speech recognition system relies on for the establishment of the speech model library [8]. The process of establishing the voice model library is first select representative speakers, whose voices can evenly represent the general voice distribution. It is best to choose people of different ages and genders as training objects. If we do not select speech objects in this way, even if the speech database is trained, the final speech model will not have a good recognition effect [9].

2.3. Digital Processing of Voice Signals. Under normal circumstances, when we store the sound in the computer, we need to do the digitization of the analog voice, and the digitization of the analog voice signal is divided into two steps: sampling and quantization.

As can be seen from Figure 3, the digital processing part starts with an analog signal, then samples to generate a discrete analog signal, and finally brightens it to achieve the effect of the final form of the digital signal. Sampling is the process of outputting analog signals at equal intervals in the time domain to receive a series of analog audio and convert it to digital audio [10]. In other words, sampling is the process of discretizing the continuous speech signal in a sequence of samples over time (as shown in Figure 3).

$$F(m) = f_b(mT) - \infty < m < +\infty. \tag{1}$$

Among them, m is an integer; T is the sampling period of the voice signal; $H_c = 1/T$ is the sampling frequency of the voice signal.

According to the content of the sampling theorem, if the bandwidth of the frequency spectrum of the speech signal $f_a(s)$ is limited, that is to say

$$f_b(kv) = 0, v > 2\pi K_b. \tag{2}$$

When the sampling frequency is greater than twice the bandwidth of the signal, that is

$$H_t = \frac{1}{T} > 2H_c. \tag{3}$$

The sampling information will not be lost, and the waveform of the original speech signal can be accurately reconstructed from $f(s)$, that is, $f_b(s)$ can uniquely reconstruct the original signal from the sample sequence as follows:

$$f_b(s) = \sum_{n=-\infty}^{+\infty} f_b(mT)\sin\left[\frac{\pi}{T}\left(s - \frac{m}{T}\right)\right]. \tag{4}$$

Among them, $H_t = 2H_c$ is the Nyquist frequency, and the sampling frequency is selected as 8 kHz in this paper. Quantization is to discretize the waveform amplitude value that is discrete in time but still continuous in amplitude. Here, the quantization option is 16 bits. In addition, the channel parameters must also be taken into account. This article uses monophonic parameters. Mono is a relatively original form of sound reproduction, which is more common in early sound cards. When playing back mono information through two speakers, we can clearly feel that the sound is delivered to our ears from the middle of the two speakers.

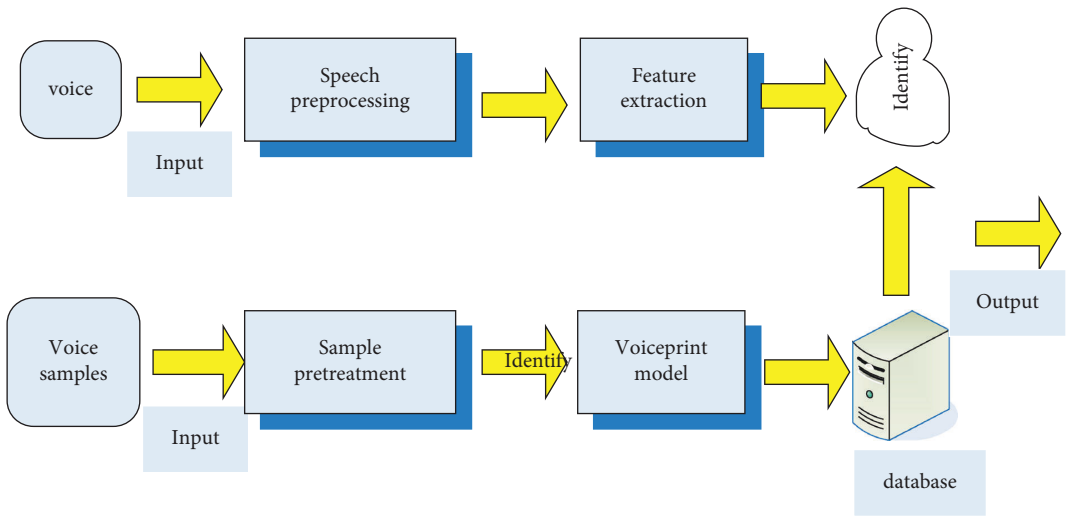

Figure 2: Speech recognition model diagram.

Figure 3: Digital processing process diagram of the speech signal.

2.4. Collection of English Corpus. Along with the mastery and understanding of corpus technology, in order to provide corpus more accurately and in a more standardized way, there are also some small professional corpora. When researchers need to conduct research in historical linguistics, forensic linguistics, language acquisition, and others, the super-large corpus covering a wide range is not suitable. At this time, a special corpus needs to be established to conduct research in a special field. Therefore, while the expanded corpus becomes the trend, the dedicated corpus will also become the future development direction. There are two difficult problems in the construction of English corpus: one is the way to obtain English corpus; the other is how to align the acquired English corpus [11]. Due to the continuous development of the Internet field, bilingual resources are also abundant. When collecting corpus, there are two factors that need to be considered: one is the quality of the plain corpus, and the second is the application range of the parallel corpus. The quality of the corpus itself refers to the fluency of the language, the number of words in each translation sentence pair, and the number of occurrences of each translation unit. The collection of English corpora should be classified according to the application field, article genre, and creation time [12]. For different application goals, different training corpora should be used. If the application goal of the translation system is to face the news domain and collect the English corpus of the news domain as a training corpus, then the accuracy and recall rate of the translation system will be significantly improved [11]. The creation of an English corpus is much more complicated than the creation of other monolingual corpora. When creating an English corpus, it is necessary to perform alignment work, that is, to achieve the sentence-level alignment relationship between the original text and the target text [13]. There are also many ways to store the English body. The first way is to store the source language and the target language in a file at the same time, in the order of the word pairs. Each word pair contains a source language sentence and a sentence target sentence; The two storage methods are to store the source language and target language in two different files [14]. Sometimes we need to label the English corpus, such as part-of-speech labeling and syntactic component labeling. If the syntactic analysis or lexical analysis of the English corpus is carried out, it will bring great help to the research work. The labeling of the English corpus requires the use of different lexical and syntactic labeling tools for the two different language corpora. For example, Chinese and English have different grammatical rules and language habits, so the tools used are also different [15].

Once you have gathered the right body, the next step is to organize and process the body, including word segmentation, lowercase, and root reduction. Sorting and processing tasks must be combined with the characteristics of the body itself. Organize and store in accordance with certain storage formats and specifications [16]. Since the original corpus may come from different collectors, consistency is difficult to guarantee. Including inconsistent storage methods; inconsistent alignment units; inconsistent genres, fields, and creative periods, containing a lot of noise information; inconsistent article layout formats; and duplicate corpus. The goals of organizing the original corpus are (1) the content is consistent and the format is uniform; (2) the alignment unit has basic mark information; (3) noise interference information is deleted. After sorting, the body must be processed

in one step, such as formatting and tagging sentences. For different application fields and purposes, different processing methods and strategies are adopted. Since there are still some problems in the automatic sorting, it is necessary to carry out appropriate manual proofreading in the end [17].

2.5. Model Construction. After the extraction of the blocks is completed, the same blocks are merged first, and their frequencies are added up. The same block means that the source phrase and the target phrase are the same, and the alignment is the same. Then use the phrase translation model of the frequency calculation block and smooth it.

$$p(e/c) = \frac{\text{count}(c, e)}{\sum_{e'} \text{count}(c, e') + d},$$
$$p(c/e) = \frac{\text{count}(c, e)}{\sum_{e'} \text{count}(c, e') + d}. \tag{5}$$

Count (c, e) represents the number of occurrences of the block, and $p\ (e/c)$ is the smoothing parameter.

For each block, define the vocabulary translation model as follows:

$$p_w\left(\frac{e}{c}\right) = p_w\left(\frac{e}{a, c}\right) = \prod_{i=1}^{c} \frac{1}{(i, j) \in a} \sum w\left(\frac{e_i}{e_j}\right),$$
$$p_w\left(\frac{c}{e}\right) = p_w\left(\frac{c}{a, e}\right) = \prod_{j=1}^{c} \frac{1}{(i, j) \in a} \sum w\left(\frac{e_j}{e_i}\right), \tag{6}$$

where, $c(e_j, e_i)$ represents the mapping between the words contained in the block and a is the alignment in the block (c, e).

$$h_{10}(C, A, E) = sim(T_1, A),$$
$$h_{11}(C, A, E) = sim(T_1, A). \tag{7}$$

Therefore, the new word alignment model is

$$\Pr\left(\frac{A}{C, E}\right) = \frac{\exp\left[\sum_m^{11} \lambda_m h_m(C, A, E)\right]}{\sum_{A'} \exp\left[\sum_m^{11} \lambda_m h_m(C, A, E)\right]}. \tag{8}$$

The corresponding decision rules are

$$a = \arg_a \max \left\{ \sum_{m=1}^{M} \lambda_m h_m(a, e, f, v) \right\}. \tag{9}$$

Correspondingly, in the speech recognition search algorithm, the scoring function is changed to

$$\text{score}(A) = \sum_{i=1}^{11} \lambda_i h_i. \tag{10}$$

The parameter training and weight adjustment of the model are the same as the previous model.

Energy frequency value method: The energy frequency value method is the product of the short-term energy and the short-term zero transit rate. According to the characteristics of the English language, the initial zero transit rate is relatively high and the final energy is relatively high. The energy frequency method can take into account these two characteristics, making it have a higher resolution ability, and the use of energy frequency can improve the adaptability of the system [18].

The calculation steps of the energy frequency method used in endpoint detection are as follows:

(1) Set a relative threshold value, denoted as T;

(2) calculate their respective short-term energy and average zero-crossing rate according to the data obtained by subframes, and then multiply the calculated data two by two to obtain their respective energy frequency values, which are arranged in a sequence, which can be expressed as FE(0), FE(1), ...;

(3) perform median filtering on the energy frequency value sequence obtained in the first step and obtain a new sequence: fe(0), fe(1), ...;

(4) take any energy frequency value fe(s) at a time s and find the maximum energy frequency value fe$(s + i)$ in a certain range, namely

$$fe(s) < fe(s + 1) < \ldots < fe(s + i) fe(s + i) < fe(s + i + 1). \tag{11}$$

(5) Calculate the ratio of the energy frequency value at time $t + i$ to time t, namely

$$k = \frac{fe(s + i)}{fe(s)}. \tag{12}$$

(6) Analyze and judge the above results.

If $s < T$, then time t is not the starting point, assign $s + j + 1$ to t and continue following the steps from (4); if $s > T$, time s can be determined to be the starting point of the speech; the endpoint is also found by following this method.

3. English Corpus Machine Translation Platform

3.1. System Design Requirements

(1) Collect voice signals from the sound card that comes with the computer.

(2) Denoising the speech signal.

(3) Use the combination of LabVIEW and MATLAB to complete the collection, processing, feature extraction, and recognition of speech signals.

(4) Realize English speech recognition technology for small vocabulary and isolated words.

3.2. Overall System Design Scheme. Using the classic virtual instrument software LabVIEW, the virtual instrument technology is applied to speech recognition technology, and the idea of "software instead of hardware" is truly realized. Among them, the development platform uses LabVIEW2014, the collection of voice signals uses the

computer's own sound card to complete this work, and the processing of voice signals uses Matlab7.0 with powerful data processing capabilities [19].

The purpose of applying virtual instruments to speech recognition systems is that this method can make full use of its flexible graphical programming and has the advantages of strong practicality and low failure rate [20]. In the process of programming, it can simply realize the voice collection, replace the hardware with software, which is simple and easy to understand, and can be updated and upgraded continuously with the development of computer software and hardware and virtual instrument technology, and the cost is relatively low. Therefore, it has a certain practical value and is worthy of research and promotion. For voice extraction, use the audio recorder that comes with Windows to record the words spoken by 20 people, 5 times for each person, a total of 100 times. Choose the clearer 20 voices as reference templates. The experimental feature parameters adopt the extracted MFCC + formant parameters to form a feature vector. In the same environment, on the same dataset, record the time for similarity matching of time series with different lengths and compare the experimental results of different sampling points to compare multiple sets of experiments to analyze the time series of different lengths. Run results on the dataset [21].

Because Matlab has powerful data processing capabilities, it has chosen to use Matlab to realize the design of speech recognition algorithms. Through the LabVIEW platform to manage and call Matlab, the combination of the two realizes the design of the speech recognition system [22]. The speech recognition system first inputs the speech to the computer through the sound card for signal collection and storage and then performs preprocessing, feature extraction, recognition algorithms, and other operations, and finally can get the recognition result [23].

This link mainly introduces the generation of the voice signal and the process of voice signal digitization. In order to ensure that high-quality speech signals are obtained after digitization, filtering must be performed before the original speech signals are digitized. Normally, filtering and digital processing are integrated into one module, so there is no need to design a separate filtering module. Design idea: through the "configure sound input" control, set the computer's own sound card for sound collection parameter settings and then use the "read voice input" control to read the sound into the computer through the microphone and then display the waveform and data. Finally, Save the input sound in a path in.wav format through the "write sound file" and "write and open sound file" controls, and finally use the "sound input clear" control and "close sound file" control to achieve voice signal collection and storage [24]. The program block diagram is shown in Figure 4, and its parameter settings, sampling frequency is 22050, sampling channel is 2, the number of bits per sampling is 16, the number of samples per channel is 5000, and the sampling mode is in continuous sampling.

Due to the limitation of the probability value in GIZA++ results, we further use information entropy to obtain the correct results more effectively. According to the maximum probability value method, we will get the wrong results, but in our method, the threshold (the difference with the maximum probability) is 0.1.

The overall flow of the algorithm is shown in Figure 5.

4. Experimental Results and Discussion

The characteristics of the spectrogram are just like the fingerprint of a person. We call it "voiceprint", which varies from person to person. The voice prints of different speakers are different. The voice parameters can be determined from the characteristics of the spectrogram. Here, the formant is used as the voice parameter to express the voice characteristics of different speakers when they speak the same voice. Tables 1 and 2 give the pitch frequency and formant values extracted from the spectrogram.

From the experimental data given in Table 2, it appears that when the same speaker speaks different words, the fundamental frequency is essentially the same, but the values of the first, second, and third formations are quite different. At the same time, it can be seen that different speakers have different base frequencies when uttering the same word, and the values of the first, second, and third formants are also different. The third formant has a big difference, probably the value is higher for girls. It is possible to obtain new voice feature parameters based on voice recognition that can accurately extract voice features.

After preprocessing, the statistical information of the corpus, development set, and test set is shown in Table 3.

Regarding the recorded speech doped with noise, this article uses the frequency analysis of the speech signal to obtain the spectral entropy value of the speech signal and the noise signal and uses the basic spectral subtraction method to eliminate the noise to obtain a relatively pure speech. The results of each step of the entire denoising process and the analysis process are given below. First, the voice waveform of the recorded experimental voice 'hello' and the waveform of pure Gaussian white noise are given, as shown in Figures 6 and 7:

Then, use the spectrum of the 'hello' speech signal and the Gaussian white noise signal to obtain the power spectrum and construct the spectral entropy function respectively, where the speech signal is represented by S, and the Gaussian white noise is represented by N, and the result shown in Figure 8 can be obtained.

As shown in Figure 8, it can be concluded that since the "hello" voice signal is only concentrated in a few frequency bands, the spectral entropy value of the "hello" voice signal is distributed below 7, while the noise signal is distributed throughout the entire voice spectrum. Range, its spectral entropy value is larger than that of a pure speech signal, is about 8.6.

Take the number of sampling points as 480 points, and experiment with the traditional DTW algorithm and the improved DTW high-efficiency algorithm. The program is run 3 times each time, and the total time consumed is calculated for comparative analysis.

From the experimental data in Table 4, it can be seen that compared with the traditional DTW algorithm and the

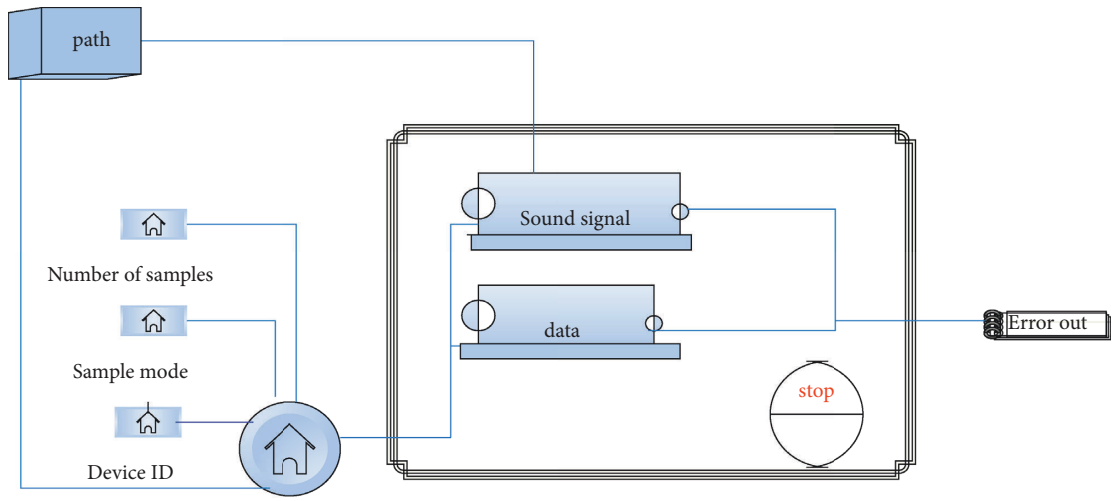

Figure 4: The program block diagram of language signal acquisition and storage.

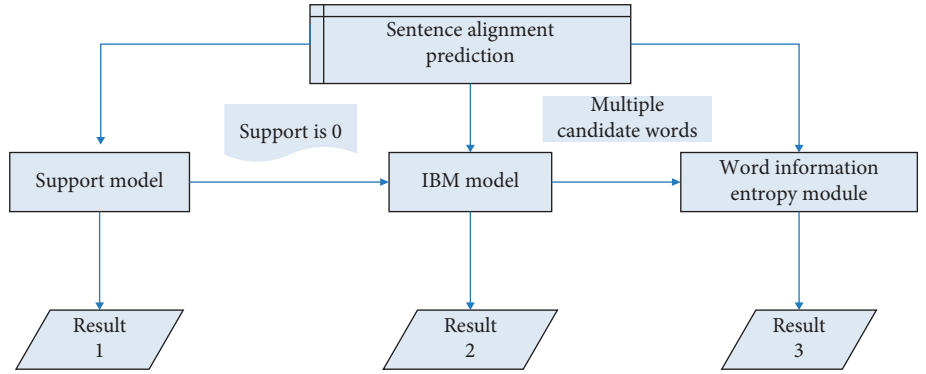

Figure 5: Hybrid model word alignment process diagram.

improved DTW high-efficiency algorithm, the time consumed by the improved algorithm has been increased from the results of each run; from the perspective of the total time consumption, the improved DTW when compared with the traditional algorithm, the efficient algorithm has increased by 2.28 s, that is, an increase of 2.19%; in addition, from the point of view of the recognition rate, the two are similar, almost close to the same. In other words, the improved DTW high-efficiency algorithm saves computing time while maintaining a high recognition rate.

Take the number of sampling points as 720 points and experiment with the traditional DTW algorithm and the improved DTW high-efficiency algorithm. Each time the program is run 3 times, the total time consumed is calculated for comparative analysis. And record the recognition rate of the two algorithms.

From the experimental data in Table 5, it can be seen that compared with the traditional DTW algorithm and the improved DTW high-efficiency algorithm, the time consumed by the improved algorithm has been increased from the results of each run; from the perspective of the total time consumption, the improved DTW when compared with the traditional algorithm, the efficient algorithm is increased by 7.57 s, which is an increase of 3.1%; for the recognition rate, the two are still close to the same.

In this experiment, 500 English phrases are randomly selected by the 10,000-sentence teaching body as the test to conduct an English phrase alignment experiment. When $K = 1$, the number of English phrases that can be extracted is 406, of which the correct number is 312; when $K = 2$, the number of English phrases that can be extracted is 368, of which the correct number is when $K = 3$, the number of English phrases that can be extracted is 321, of which the correct number is 287. According to the different values of K, the experimental results we get are shown in Figure 9:

It can be seen from the figure that when the value is larger, the accuracy rate will increase because the standard for defining alignment is more stringent, but the recall rate will decrease because the total number of phrases that the system can get has decreased.

Table 6 shows the experimental results given by each system. Among them, IBM4E- > C represents the word alignment of the IBM model from English to Chinese. Similarly, IBM4C- > E represents the word alignment of the IBM model from Chinese to English and intersection, union, and refined respectively indicate two alignment directions.

Table 1: Comparison of the parameters of the sound "thank you" pronounced by the same speaker.

Same speaker	Pitch frequency (Hz)	First formant (Hz)	Second formant (Hz)	Third formant (Hz)
'Thank you'	205.85	415.62	2147.36	3124.98
'Hello there'	197.35	605.78	1633.25	2749.15

Table 2: Comparison of parameters of the same word 'thank you' sent by different speakers.

Different speakers	Pitch frequency (Hz)	First formant (Hz)	Second formant (Hz)	Third formant (Hz)
Speaker A (male)	135.45	408.25	2025.36	2514.36
Speaker B (man)	139.56	421.08	1986.15	2459.36
Speaker C (female)	201.62	426.61	2238.92	3012.26

Table 3: Statistics of word alignment experiment corpus.

	Training corpus	Concurrent set	Test set
Number of sentences	333901	502	504
Word count	5582631	9338	13902
Number of links	74264	6389	14046

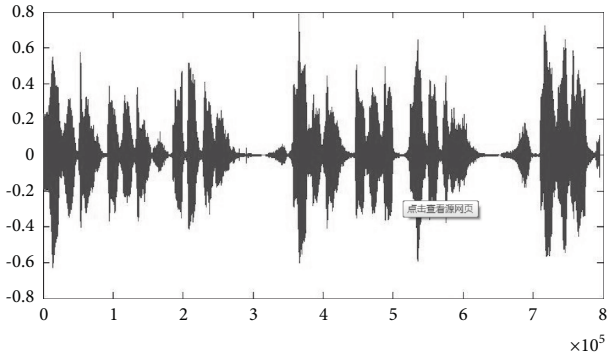

Figure 6: "Hello" voice waveform.

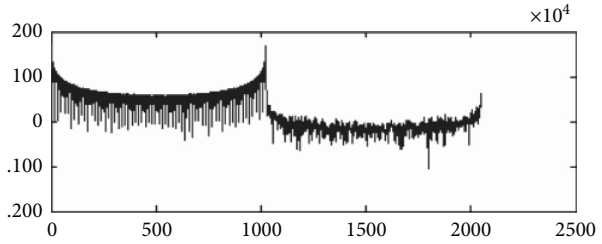

Figure 7: Pure white Gaussian noise speech waveform.

Find the intersection, union, and word alignment obtained by the grow-diag-final rule. ITG-M means that only constraints are used in word alignment. ITG-S means to combine ITG and syntax trees.

By comparing the results, it can be found that word alignment with syntactic constraints has achieved better alignment results than the IBM-4 model. Compared to the more sophisticated IBM-4, the ITG-S improves by about 5%. Except for the two weakly constrained syntactic knowledge, the features adopted by ITG-M and ITG-S are similar to the submodels in the IBM model. Therefore, it is effective to combine syntactic knowledge in word alignment.

For the systems ITG-M and ITG-S, ITG-S has achieved a better AER value. By analyzing the specific word alignment content of the experiment, it is found that due to the constraints of the syntax tree, the word alignment links in

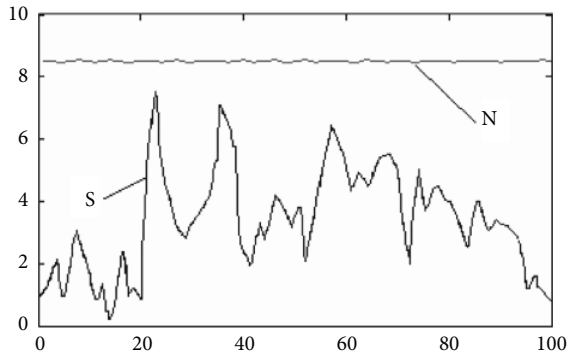

Figure 8: Spectral entropy of S and N.

Table 4: Operation time and recognition rate when the number of sampling points is 480 (%).

Algorithm	First run time	Second run time	Third run time	Total time	Recognition rate
Traditional DTW algorithm	34.83	34.69	34.77	104.29	98.83
DTW efficient algorithm	34.16	33.96	33.89	102.01	98.79
TSMS	34.35	34.20	34.26	102.81	98.82

Table 5: Operation time and recognition rate when the number of sampling points is 720 (%).

Algorithm	First run time	Second run time	Third run time	Total time	Recognition rate
Traditional DTW algorithm	138.54	140.53	142.38	421.45	98.52
DTW efficient algorithm	127.67	131.39	131.84	390.9	98.66
TSMS	132.20	134.35	134.26	401.81	98.61

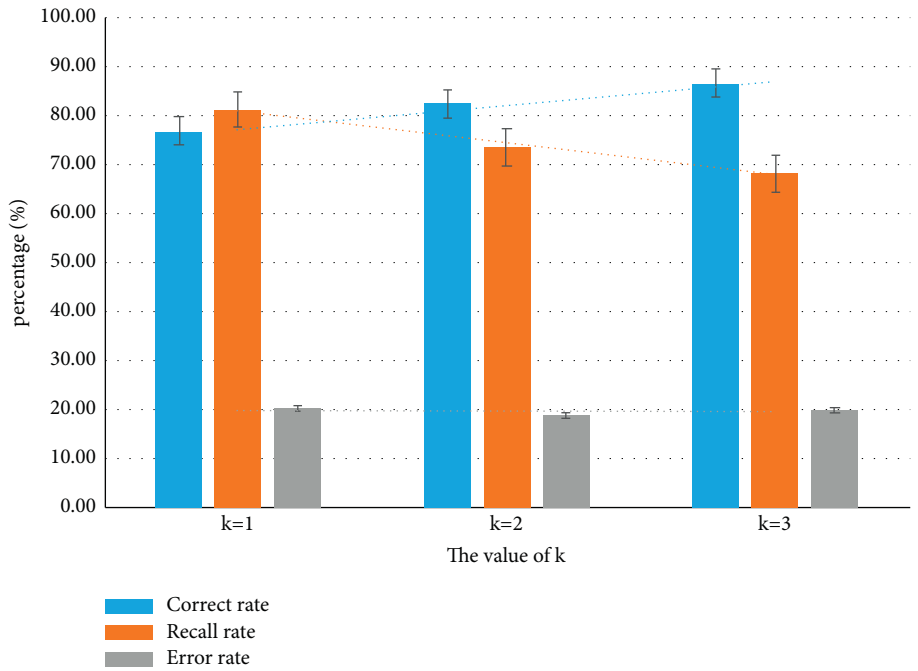

Figure 9: Different experimental results with different values.

Table 6: Comparison of experimental results of the word alignment system.

System	Accuracy	Recall rate	AER
IBM4E- > C	0.8164	0.6091	0.3013
IBM4E- > E	0.7856	0.5557	0.3478
IBM4 intersection	0.9549	0.4912	0.3497
IBM4 union	0.7181	0.6737	0.3045
IBM4 refined	0.8694	0.6002	0.2885
ITG-M	0.8305	0.6296	0.2826
ITG-S	0.8335	0.6408	0.2743

ITG-S are more biased. Because of clustering together, the number of links with a large span is relatively small, which is conducive to obtaining a higher accuracy of word alignment.

5. Conclusions

On the basis of summarizing predecessors' speech recognition in other languages, this paper analyzes and studies the basic pronunciation and phonetic characteristics of English speech, and systematically studies the related problems of English speech recognition. Speech recognition technology has extremely broad application prospects, coupled with the idea that "software is an instrument", which stimulates further exploration of speech recognition technology. In this article, the combination of LabVIEW and MATLAB is used to complete the collection, processing, feature extraction, and recognition of speech signals. It is the first to collect voice signal data through the sound card that comes with the computer, achieving the function of real-time voice signal collection and storage. Secondly, the speech signal is denoised. There are many kinds of noise in the speech signal. In view of the characteristics of these noises, the wavelet denoising processing method is selected, that is, after the effective speech signal is processed by the wavelet transform, most of the information located in the low-frequency part of the wavelet transform frequency band is larger, and the white noise is mostly located in the high-frequency part of the smaller wavelet transform frequency band. In the process of speech recognition, the speech signal after framing and windowing must be detected by endpoints. A combination of the short-term energy method and short-term average zero-crossing rate method can be used to improve the stability and recognition rate of the system. Speech recognition using the energy frequency method and improved DTW high-efficiency algorithm can save computing time while maintaining a high recognition rate. The average translation accuracy rate can be as high as 95%, and the average response time is about 0.5 seconds, which can fully meet the requirements of daily English corpus machine translation.

Data Availability

No data were used to support this study.

Conflicts of Interest

The authors declare no potential conflicts of interest in this study.

Acknowledgments

This work was supported by Foreign Language Research Project with Social Sciences Association of Shaanxi Province: A Study on English Translation and Communication of Cultural Relics of Han Dynasty Mausoleum in Xi'an from the Perspective of Compensation Translation (2021ND0609).

References

[1] M. Ravanelli, P. Brakel, M. Omologo, and Y. Bengio, "Light gated recurrent units for speech recognition," *IEEE Transactions on Emerging Topics in Computational Intelligence*, vol. 2, no. 2, pp. 92–102, 2018.

[2] S. Watanabe, T. Hori, S. Kim, J. R. Hershey, and T. Hayashi, "Hybrid CTC/attention architecture for end-to-end speech recognition," *IEEE Journal of Selected Topics in Signal Processing*, vol. 11, no. 8, pp. 1240–1253, 2017.

[3] H. A. Abdelaziz, "Comparing fusion models for DNN-based audiovisual continuous speech recognition," *IEEE/ACM Transactions on Audio Speech & Language Processing*, vol. 26, no. 3, pp. 475–484, 2017.

[4] R. Randi and I. Nancy, "The American national corpus," *Journal of English Linguistics*, vol. 32, no. 2, pp. 105–113, 2016.

[5] F. G. Chong, G. Friedland, A. Janin, N. Morgan, and C. Oei, "Opportunities and challenges of parallelizing speech recognition," *Diabetes Technology & Therapeutics*, vol. 18, no. 6, p. 2, 2016.

[6] T. Y. Ahn and S. M. Lee, "User experience of a mobile speaking application with automatic speech recognition for EFL learning," *British Journal of Educational Technology*, vol. 47, no. 4, pp. 778–786, 2016.

[7] R. Yazdani, A. Segura, J. M. Arnau, and A. Gonzalez, "Low-power automatic speech recognition through a mobile GPU and a viterbi accelerator," *IEEE Micro*, vol. 37, no. 1, pp. 22–29, 2017.

[8] S. Gordon-Salant and S. S. Cole, "Effects of age and working memory capacity on speech recognition performance in noise among listeners with normal hearing," *Ear and Hearing*, vol. 37, no. 5, pp. 593–602, 2016.

[9] O. T. Grozdi and S. T. Jovii, "Whispered speech recognition using deep denoising autoencoder," *Engineering Applications of Artificial Intelligence*, vol. 59, no. 12, pp. 2313–2322, 2017.

[10] B. Ren, L. Wang, L. Lu, Y. Ueda, and A. Kai, "Combination of bottleneck feature extraction and dereverberation for distant-talking speech recognition," *Multimedia Tools and Applications*, vol. 75, no. 9, pp. 5093–5108, 2016.

[11] M. Kim, B. Cao, T. Mau, and J. Wang, "Speaker-independent silent speech recognition from flesh-point Articulatory movements using an LSTM neural network," *IEEE/ACM Transactions on Audio, Speech, and Language Processing*, vol. 25, no. 12, pp. 2323–2336, 2017.

[12] P. Sharma, A. Vinayak, and A. K. Sao, "Deep-sparse-representation-based features for speech recognition," *IEEE/ACM Transactions on Audio, Speech, and Language Processing*, vol. 25, no. 11, pp. 2162–2175, 2017.

[13] S. S. Wang, P. Lin, Y. Tsao, J. W. Hung, and B. Su, "Suppression by selecting wavelets for feature compression in distributed speech recognition," *IEEE/ACM Transactions on Audio, Speech, and Language Processing*, vol. 26, no. 3, pp. 564–579, 2018.

[14] A. Biswas, P. K. Sahu, and M. Chandra, "Multiple cameras audio visual speech recognition using active appearance

model visual features in car environment," *International Journal of Speech Technology*, vol. 19, no. 1, pp. 159–171, 2016.

[15] X. Ji, J. Pan, and Y. Yan, "Agglutinative language speech recognition using automatic allophone deriving," *Chinese Journal of Electronics*, vol. 25, no. 2, pp. 328–333, 2016.

[16] A. Xing, Q. Zhao, and Y. Yan, "Speeding up deep neural networks in speech recognition with piecewise quantized sigmoidal activation function," *IEICE - Transactions on Info and Systems*, vol. E99.D, no. 10, pp. 2558–2561, 2016.

[17] S. Mirsamadi and J. H. L. Hansen, "A generalized nonnegative tensor factorization approach for distant speech recognition with distributed microphones," *IEEE/ACM Transactions on Audio, Speech, and Language Processing*, vol. 24, no. 10, pp. 1721–1731, 2016.

[18] D. Nguyen, X. Xiong, E. S. Chng, and H. Li, "Feature adaptation using linear spectro-temporal transform for robust speech recognition," *IEEE/ACM Transactions on Audio Speech & Language Processing*, vol. 24, no. 6, pp. 1006–1019, 2016.

[19] F. Klubika, A. Toral, and V. M. Sánchez-Cartagena, "Quantitative fine-grained human evaluation of machine translation systems: a case study on English to Croatian," *Machine Translation*, vol. 32, no. 1, pp. 1–21, 2018.

[20] M. Chen, J. Pan, Q. Zhao, and Y. Yan, "Multi-task learning in deep neural networks for Mandarin-English code-mixing speech recognition," *IEICE - Transactions on Info and Systems*, vol. E99.D, no. 10, pp. 2554–2557, 2016.

[21] I. H. Y. Ng, K. Y. S. Lee, J. H. S. Lam, C. A. van Hasselt, and M. C. F. Tong, "An application of item response theory and the rasch model in speech recognition test materials," *American Journal of Audiology*, vol. 25, no. 2, pp. 142–152, 2016.

[22] S. Wu, D. Zhang, Z. Zhang, N. Yang, M. Li, and M. Zhou, "Dependency-to-Dependency neural machine translation," *IEEE/ACM Transactions on Audio, Speech, and Language Processing*, vol. 26, no. 11, pp. 2132–2141, 2018.

[23] R. Miyahara, K. Oosugi, and A. Sugiyama, "A hearing device with an adaptive noise canceller for noise-robust voice input," *IEEE Transactions on Consumer Electronics*, vol. 65, no. 4, pp. 444–453, 2019.

[24] H. Tobias, M. Farah, and C. Enrico, "Efficiency and safety of speech recognition for documentation in the electronic health record[J]," *Journal of the American Medical Informatics Association*, no. 6, pp. 1127–1133, 2017.

Hindawi
Scientific Programming
Volume 2022, Article ID 2414830, 12 pages
https://doi.org/10.1155/2022/2414830

Research Article

Data Management and Service Mode of Library Based on Data Mining Algorithm

Jingjing Zhang and Yang Chi

Library, Northeast Agricultural University, Harbin 150030, Heilongjiang, China

Correspondence should be addressed to Yang Chi; cy@neau.edu.cn

Received 9 July 2022; Revised 8 August 2022; Accepted 20 August 2022; Published 21 September 2022

Academic Editor: Juan Vicente Capella Hernandez

Data management for large-scale data library services with mining procedures improves the availability and readiness of heterogeneous sources. The heterogeneous data sources are assimilated as a single entity through mining procedures to meet the data demands. This article introduces connectivity-persistent data mining method (CDMM) to improve the data handling precision with boosting availability. The proposed method relies on federated learning for identifying the service demands, thereby providing data mining. The learning paradigm accumulates information on shared data library existence over various services. Based on the availability, further mining demands are forwarded to the data management system. If the existence verified by the federated learning is adaptable, then sharing-enabled mining is endorsed for the connected users. The data management then augments several heterogeneous shared libraries to meet the mining requirements. This process is reversible based on the service mode and existence. Therefore, the proposed method improves data availability with less mining and access time and fewer failures.

1. Introduction

Data mining is a process that extracts certain patterns and useful details from a large set of data. Data mining provides the necessary set of data for the analysis process. Various methods and techniques are used to perform the data mining process. Data mining is a complicated task in every application [1]. Data mining also identifies the problems identified by the data analysis process. A data management system for mining services is a crucial task that manages a huge amount of data. Data management is a process that protects, store, collect, organize, and manage data that provide an appropriate set of data for various processes [2]. Data mining services are a process that converts the raw data into a useful set of data that is used for further processes. Various management services are used for the data mining process using the machine learning (ML) approach [3]. A data management system improves the performance and efficiency rate of the system, improving the accuracy rate in the decision-making process. Data management systems manage the data collected by an application and organization. Storing and managing a data management system is mostly used for data mining. Data mining services and details are handled by a management system [4, 5].

Various data mining types are available to identify the dataset's important patterns. An organization widely uses the service demand-based data mining method. The data mining process plays a major role in every organization that helps enhance an organization's performance and feasibility [6]. The organization gives requirements and preferences that provide a set of demands over the data mining process. The service demand-based data mining process provides an accurate dataset for the decision-making process that reduces the failure rate [7]. Organizations demand a certain set of services for the data mining process. The real-time data mining process is a complicated task to perform in every management system [8]. The classification method is used in the service demand-based data mining process. The classification method classifies the dataset by combining it with given service demand. Various demands and requests are

demanded by an organization for the data mining process. Companies and industries demand a certain set of services that improve the accuracy rate in the data mining process [9, 10].

Machine learning (ML) techniques are widely used for various applications to perform prediction and analysis. ML techniques improve the accuracy rate in both the analysis and prediction process. ML techniques are also used in data mining to enhance the service accuracy rate. ML technique-based data mining process identifies the important features and patterns from a huge set of data [11, 12]. The convolutional neural network (CNN) algorithm is commonly used for data mining. The feature extraction process is used in CNN to extract the features presented in a given raw dataset [13]. The classification process classifies the features extracted from the feature extraction process. CNN predicts the actual data necessary for an application [14]. The support vector machine (SVM) algorithm is also used for data mining. SVM first trains the dataset with an important set of features collected by the analysis. SVM reduces the latency and error rates in the computation process, which improves the efficiency rate of the system. The data analysis process analyzes the raw data stored in the database [15]. The main contribution of CDMM is as follows.

(i) The suggested method focuses on federated learning for recognizing the service requests and consequently enabling data mining. The learning paradigm accumulates information about shared data library presence over numerous services.

(ii) The data management then augments numerous heterogeneous shared libraries to match the mining needs. This process is adjustable based on the service mode and existence.

(iii) Therefore, the suggested strategy improves data availability with less mining and access time and fewer failures.

2. Related Works

Huang et al. [16] introduced a new algorithm for fast mining frequent patterns using a distributed computing system. Frequent pattern mining identifies the important patterns that are presented in a given dataset and reduce the latency rate in the analysis process. The big data analysis process is used here to analyze the huge amount of data and produce an optimal dataset for further data mining. The proposed method improves the accuracy rate in the execution process, enhancing the system's performance. The proposed method reduces time and energy consumption in the execution process.

Xie et al. [17] proposed an information filtering and mining method for big data analysis. A support vector machine (SVM) algorithm is used here to analyze the data necessary for the mining process. The proposed method is mainly used for the retrieval process that retrieves educational images. Certain features and patterns are identified by filters that produce an optimal dataset for further analysis. The proposed method improves the performance rate and efficiency of the system.

Obregon et al. [18] introduced the data mining information as a flow method for social networking services (SNSs). The proposed discussion flow model identifies the data and provides appropriate details for the data mining process. Data mining captures interaction among communities, producing effective information about discussions. The proposed method enhances the feasibility and reliability of the system. The proposed method reduces the complexity rate and improves the mobility rate of SNS.

Bhattacharya et al. [19] proposed a mobile blockchain (MB) based data mining method as-a-service (MB-MaaS) for the Industrial Internet of Things (IIoT). MB is used here to enhance the effectiveness of rata in the analysis process. The proposed method identifies the group discussion and interaction of users in IIoT. The experimental results show that the proposed method achieves a high accuracy rate in the mining process, which improves the system's performance.

Zhang et al. [20] introduced a massive data mining-based method for mobile libraries. The filtering technique is used here to filter the candidate's available datasets in mobile libraries and produce a feasible set of data for further process. The Apriori algorithm is used here to provide optimal rules for the candidates, reducing unnecessary problems in the management system. The proposed method reduces energy and time consumption in the computation process. The proposed mining method also improves the execution time of the system.

Dhelim et al. [21] proposed a personality-aware hybrid filtering-based mining method for a social network. The personality filter first filters the traits and personalities of users and produces necessary information for the mining process. The data analysis process collects the data available in a social network that provides appropriate data for the mining process. The proposed method maximizes the accuracy rate in the data mining process that provides appropriate services to the users.

Wang et al. [22] introduced a new framework for library services and immigrant needs. The proposed framework identifies the cause of problems that are occurred in libraries. Social networks provide necessary information about the candidates, reducing the time consumption rate in the searching process. Finally, the proposed framework provides various guidelines and rules for libraries that improve the appropriate services to the users.

Xiao et al. [23] proposed a fine-grained sentiment analysis-based preference mining method. The sentiment analysis approach finds out the important emotions and characteristics of users. User features are identified by a pretraining language model that produces a feasible set of data for preference mining. Both numerical and text-relation information is analyzed by preference mining, reducing the execution process's latency rate. The proposed method achieves a high-performance rate in providing services for the users.

Peng et al. [24] introduced a fuzzy convolutional neural network (FCNN) based on big data mining and analysis (BDMA). The feature extraction approach is used here to extract the important features available in the dataset.

The feature extraction method collects an appropriate dataset for the big data analysis. The FCNN algorithm is mostly used for the recognition process that enhances the system's feasibility. The proposed method maximizes the system's effectiveness and efficiency rate, improving the accuracy rate in the big data analysis process.

Alkathiri et al. [25] proposed a multidimensional data mining method using the MapReduce technique for a distributed environment. The MapReduce technique is used here for the ecosystem data analysis process that finds the features presented in a given dataset. Machine learning (ML) techniques are also used here to enhance the system's feasibility. The proposed method reduces the error rate in the data mining process, improving the system's performance.

Deng et al. [26] introduced a jointed neural network-based multimedia data stream is an information mining model. The soft clustering technique is used here to cluster the huge data available in the database. A joint neural network is implemented here to train the dataset necessary for the data mining process. The proposed data mining approach addresses the problems presented in an application. The proposed model achieves high efficiency and effectiveness rate in the mining process.

Ju et al. [27] proposed a data mining-based commodity recommendation method for online shopping. The proposed method is mostly used in e-commerce and online shopping applications. The commodity recommendation method identifies users' preferences, requests, and browsing history that provide relevant details for an application. The data mining approach analyzes the given set of data and produces a feasible set of data for the recommendation process. The proposed method improves the performance and feasibility rate of the online shopping system.

Zhou et al. [28] introduced a new data mining approach using particle swarm optimization (PSO)-based back-propagation (BP) neural network. Internet of Things (IoT) is used here to enhance the communication process among users and organizations. PSO is used here to train the dataset necessary for the data mining process. IoT collects real-time data that users produce. The proposed method increases the accuracy rate in the prediction and analysis process.

2.1. Proposed Connectivity-Persistent Data Mining Method. The data source repository is the maintenance of databases by collecting data from multiple sources meeting the objective function. It is a database infrastructure that aggregates, manages, and stores datasets mined for data analysis. It makes sharing data easier by managing it and maintaining metadata for the study of data. The aggregated data are reviewed for the type of data based on which the data are stored. The data in the repository are loaded with an increasing volume of data. In Figure 1, the proposed method is illustrated.

Service mining is influenced by federated learning to validate its existence for further sharing. This learning further operates on different service demands. If any deficiency is found, a data management system ensures data existence and availability for varying users (refer to Figure 1). The request-based services from users are generated in a particular time slot where the total number of requests r from the users is denoted as$\omega_r(t)$. The request from the users allocated to the data source repository s is denoted as$\gamma_{rs}(t)$. ${\gamma_{rs}}^{\max}$ be the number of maximum requests from users to the data source repository as shown in the following equations:

$$\omega_r(t) \leq {R_r}^{\max}, t \in [1,], \tag{1}$$

$$\omega_r(t) = \sum_S \gamma_{rs}(t), t \in [1, \tau]. \tag{2}$$

To handle the requests, the capacity$\mu_s(t)$ of the data source repository with its pricing $\rho_s(t)$ of data to be provisioned is calculated. Thus, the cost$\partial(t)$ of the data source repository for the request is obtained from

$$\partial(t) = \sum_s \mu_s(t).\rho_s(t). \tag{3}$$

The delay in addressing the request to the data source repository based on the quality of experience is calculated considering the network and queuing delay. The following equation denotes the delay of the network:

$$s = s_{nw} + s_{qe}. \tag{4}$$

The network delays_{nw} and the queuing delays_{qe} to fulfil the request depending on the factors such as transmission delay and propagation delay. The queuing delay is obtained from the workload network delay on the distance between the user and the data source repository. The delay in making a decision incurs further delay, which is represented ass_{dm}:

$$\chi_s(t) = \sum_{\beta_s(t)} s_{nw} + \sum_{\beta_s(t)} s_{qe} + s_{dm} \tag{5}$$

$$\chi_s(t) = \gamma_{rs}(t) s_{nw}(r,s) + \sum_{\beta_s(t)} s_{qe} + s_{dm}. \tag{6}$$

From 5the above equations, $\beta_s(t)$ is the request allotted to the data source repository. The network delay for the request is as$s_{nw}(r,s) = p.(s_{rs})^{v}$. s_{rs} is the distance between the user request to the data source repository. p, v are the parameters considered to scale the distance and maintain the function's convex property. The decision-making based on the delay factors for data existence verification is presented in Figure 2.

The user requests are influenced by $\mu_s(t)$and s such that $\omega_r(t)$ is sustained for the entire allocation intervals. The data availability and existence are verified $\forall Interval \in (1,n) such\ that\ {r_{rs}}^{\max}$ is satisfied. The learning process relies on $\chi_s(t) such\ that\ s_{nw}\ and\ s_{que}$ are distinguished for their existence (Figure 2). The queuing delay for the request allocated to the data source repository is obtained using the following equation:

$$\sum_{\beta_s(t)} s_{qe} = \max\left[K_s(t) - \rho_s(t)\mu_s(t)\sigma, 0\right]. \tag{7}$$

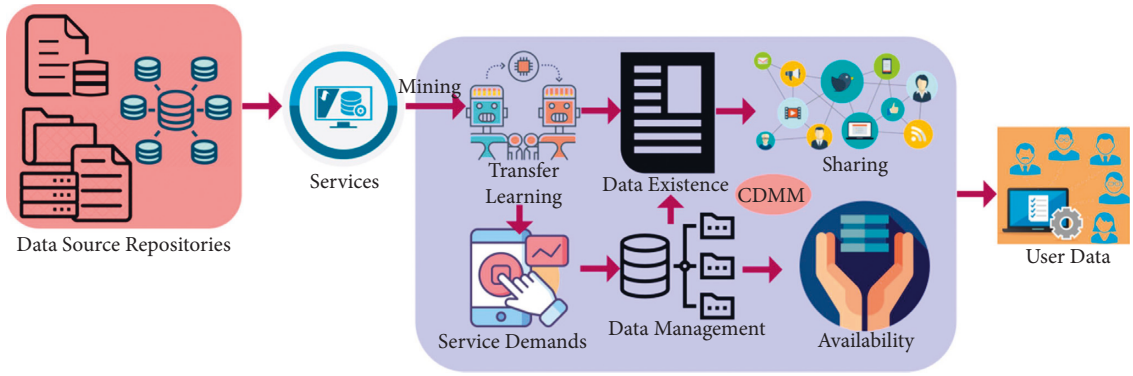

Figure 1: Proposed method illustration.

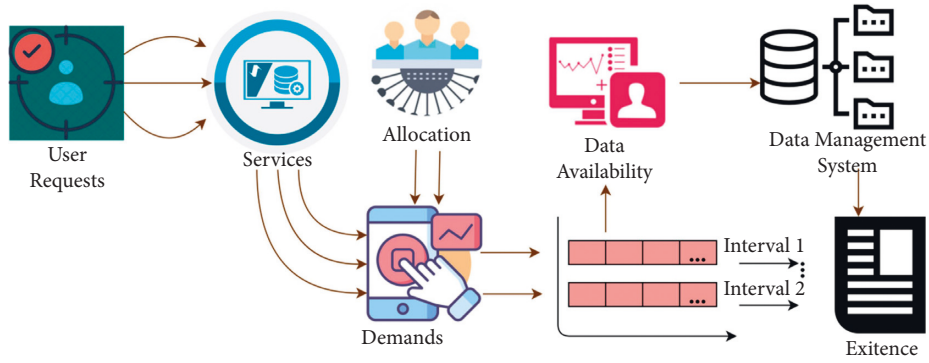

Figure 2: Decision-making for data existence verification.

The workload to be processed is represented as $K_s(t)$ for the data source repository at a particular time slot. The service time provisioned by the data source repository allotted for the request is given by$\rho_s(t)\mu_s(t)\sigma$. From (7), the deficiency of the service time at the data source repository is obtained bymax $[K_s(t) - \rho_s(t)\mu_s(t)\sigma, 0]$. Thus, the upcoming request from the users must have to wait for their request to be processed. To maintain fair processing of request based on the heterogeneity of the data, the quality of experience by the users is calculated by considering the tolerable delay and the actual delay. Thus, it can be defined as in the following equations:

$$\psi(\zeta, \phi) = \frac{\psi_{\max}}{\phi(a-1)}[a.\phi - \zeta], \zeta > \phi, \tag{8}$$

$$\psi(\zeta, \phi) = \psi_{\max}, \zeta \leq \phi, \tag{9}$$

$$\psi(\zeta, \phi) = 0, \zeta > a.\phi. \tag{10}$$

From the above equations, the tolerable delayϕ and the actual delayζ of the request in a particular time slot are represented with$\psi_{\max}$. The above equations denote the quality of experience by parameter$\psi_{\max}$. The user is processed before a tolerable delay, and then, the requests from the users are mentioned with$\psi_{\max}$. If the request is not processed within the tolerable delay, then it is considered that the users are not fulfilled and the waiting time of the users is expired, and a is the parameter that mentions the rate of declination representing the quality of experience. Based on the conditions above, the quality of experience by the user request in the data source repository within the time slot is defined by

$$d_s(t) = \psi(\zeta_s(t), \phi). \tag{11}$$

Based on the above estimation, the validations (8), (9), and (10) are performed using the federated learning model. This is depicted in Figure 3.

The learning induces multiple ψ as defined in (8), (9), and (10) for different$\omega_r(t)$. Based on the sharing output, user service mining and allocations are performed. This requirement is fulfilled based on the availability factor. The delay and existence impacts are mitigated using the maximum sharing ratio and learning implication (refer to Figure 3).

2.2. Learning Implications for Data Management. Federated learning is a technique where devices are decentralized with collaboration processing service demands considering user requests. The networks with several users have been partitioned based on their interests. This number of users share the data among themselves. Data resembling common interests among the users have been identified to verify the available data. If similar data are available, then the data are shared in a decentralized manner. The model with users $\{U_1, ...U_n\}$ and their data is $\{I_1, ..., I_n\}$. These users

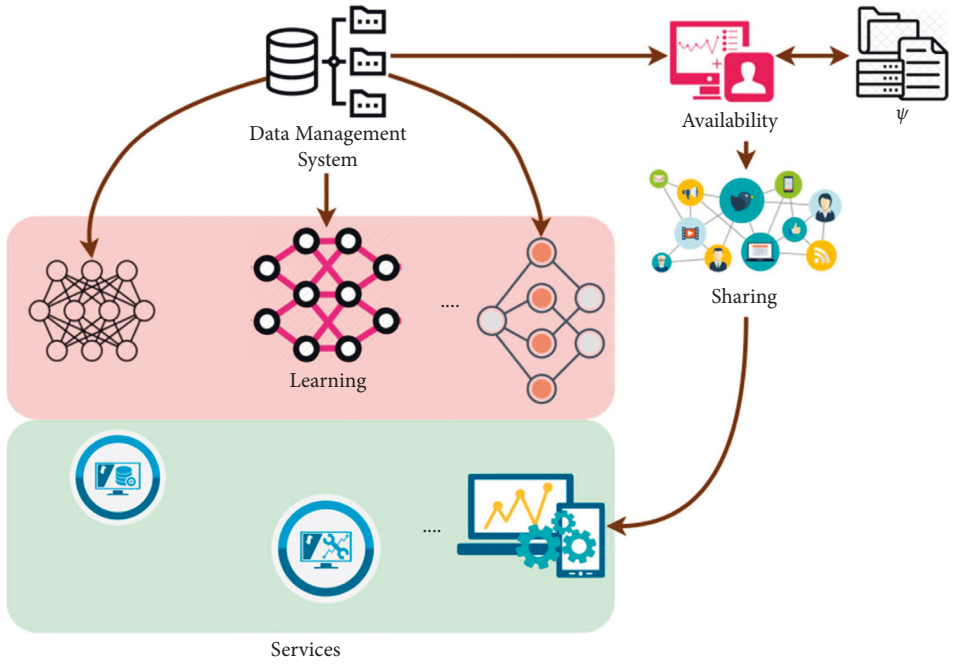

Figure 3: Federated learning model for service experience.

with the data information collaborate to identify the existence of data. The users in the network are combined with the data $I = \{I_1 \cup .... \cup I_n\}$, which is used to train the model M.

The users in the network share this model used for training; for each new data in the network among the users, a common interest procedure is to be followed. In the proposed, horizontal federated learning is considered where the users in the network communicate with each other to update the model M.

Based on the data from the users, a common interest group is created, enhancing network efficiency. The users in this group have their data. By aggregating the data from all the members, a dataset is generated. Thus, each common interest group maintains its own set of data within it. If the user in the network wishes to leave the common interest group, the user may leave with the data. Contrarily, if a user wishes to join the common interest group, the data are verified by some users in the common interest group for the relevant data. Each common interest group has its reputation for maintaining relevant or accurate data. The rewards are shared among the users in the common interest group based on the size and the relevant data they offer.

The common interest group in the network with model M., *the number of users in the common interest group,* update their model M. The proposed model improves when the users join the common interest group, so the data availability for the users also improves. Each user in the common interest group is provided to access the shared model M. The users use the model to calculate the existence of data by finding the similarities between the requested data by the users and the availability of data in the common interest group. A cosine similarity index is used to find the potentiality of the data by identifying the similarities between the requested data and the available data, as shown in the following:

$$\cos\theta = \frac{\overrightarrow{\tau}.\overrightarrow{\kappa}}{\overrightarrow{\tau}\,\overrightarrow{\kappa}}. \tag{12}$$

The availability of data is accepted only when most users in the common interest group find the resemblance of data between the requested data and the available data. The users in the common interest group are provided with rewards based on the amount of data that is being made available. The users in the common interest group must be made available with some sort of data by generating the data and updating the model M. Else, the user in the group might be expelled from the group. The users are requested to maintain some sort of space for the data allocation. The data from other users in the common interest group are stored in the maintained space. The subset of the data sent to the other users in the joint interest group is checked for relevancy. The data are verified whether it remains fixed to maintain the data within the common interest group. It asks for recommendations from common interest groups to ensure the availability of the data. Each user is provided with some functions to maintain the reliability of the users in the common interest group. Each user interacts with a common interest group; the data are shared with its functions key. Suppose these function key does not match with the available function key list. In that case, a warning update is provided, which is shared with model M. On receiving this model update, all the users in the common interest group verify its function key. If the function key fails, the corresponding user is removed from the common interest group. The learning process for$M$ in maximizing data sharing for different mining requests is presented in Figure 4.

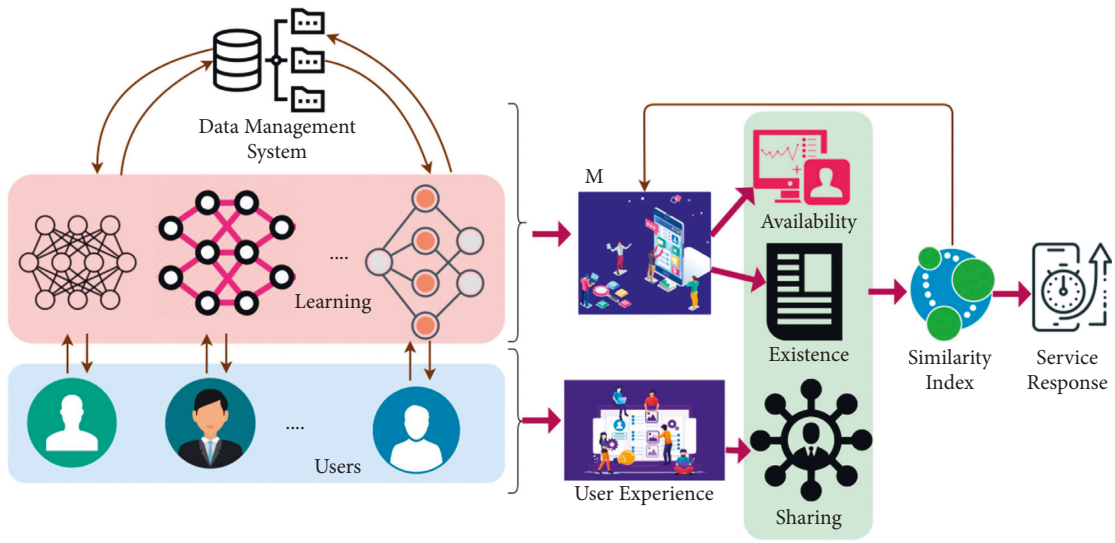

Figure 4: Learning Process for**M**.

The management system eyes on M for different ψ such as sharing for availability and existence. This M is modified based on $\cos\theta$ such that service responses are granted with better mining outcomes. The allocated requests are granted from the mining demands (Figure 4). Once the existence of data is verified with the cosine similarity, it is allocated for the request placed by the users in a particular time slot. Suppose the requested service is not available within the common interest group. In that case, a service demand is placed upon the request based on which, using the federated learning, the service demand is addressed. The data management system using federated learning enables the storage facility to enhance the network performance minimizing the access time. It is designed to operate asynchronously, making the proposed technique more flexible. It maintains a model at both the data source repository and the user side. On registration of users with the data source repository, a global model is designed. Using this global model, the data management makes arrangements for a suitable space to store the data based on the request. If the available storage space is enough, then the version information with the model data is stored. If the higher data version is available, then the model is updated. It gets updated to the advanced version from the existing version of data. The data source repository has the privilege of designing its global model and sharing it with the users. On sharing the global model, the local model gets updated. The version of the global model is initially checked before updating the local model.

The user requests the data source repository by importing the global model data based on which the local model data are generated. In the absence of a request from the user regarding the version update, the data management system monitors the version and sends the update to the users. The data source repository aggregates the updated local model from users concerning the corresponding version of the global data. It maintains the aggregation until adequate quality is obtained. This proposed method, namely, connectivity-persistent data mining method (CDMM) managed by storing the characteristics of data from the users where the requests are stored. The data source repository uses this information to process the service demands and allocate the required data. The requests from the clients include parameters such as request ID, version of the models, and device ID. The request ID represents the identity of the request where the users and the data source repository perform a task.

The data source repository addresses the request of the users by allocating the data. The data management system searches for the data using federated learning and provides the data to the users. The version of the global model is used to update the local model; the global model gets updated by connectivity between the users and the clients. Based on the model updates, the users and data source repository manage the service demands based on the requests. The device ID represents the specific ID given to the users. A particular user can be provided with the requested data using this device ID. The corresponding data communication based on the global and local model is performed with these parameters. The proposed method achieves better data available to the users by reducing the dependency on the traditional request/service demand with minimal access time and fewer failures by providing asynchronous peer-to-peer communication between the users and the data source repository. The self-analysis for varying capacity, similarity index, and demand factors is presented in Figures 5, 6, and 7, respectively.

Figure 5 presents the analysis of cost factors and requests allocated for the varying $\mu_s(t)$. This method allocates $\omega_r(t) \forall s_{nw} and\ s_{que}\ such\ that\ X_s(t)$ is performed for the increasing mining requests. The $\beta_s(t)$ is validated based on $\psi(\zeta, \phi)$ such that ϕ is accounted for maximizing $d_s(t)$. Therefore, the allocations are maximized in intervals $\in (1, n)$. The learning segregates existence and availability for the requests such that $\sum_{\beta_s(t)} s_{que}$ is reduced. This single factor

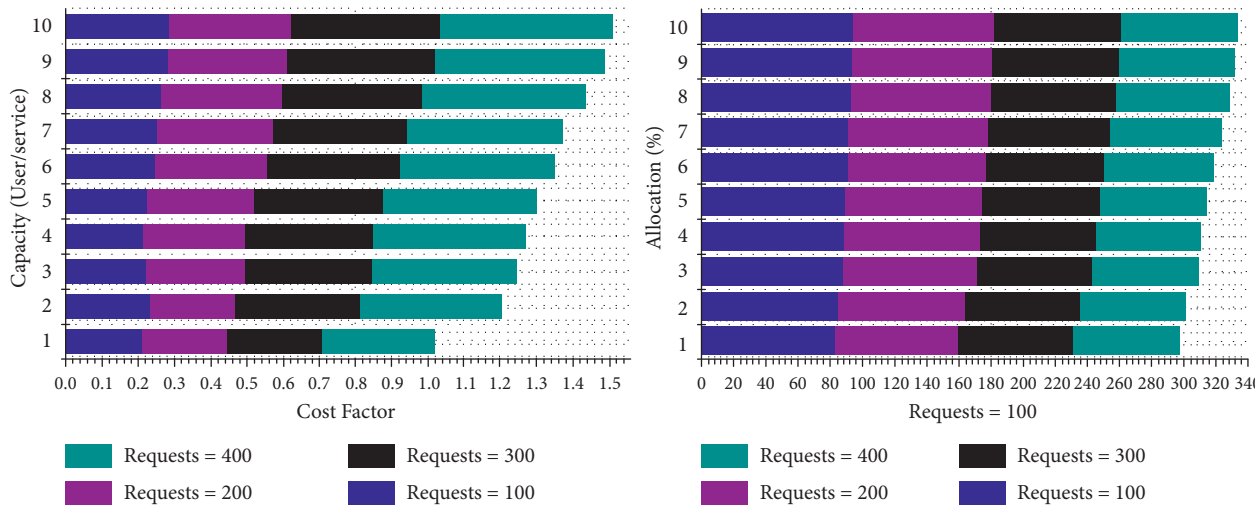

Figure 5: Analysis for cost factor and allocated (%) by varying capacity.

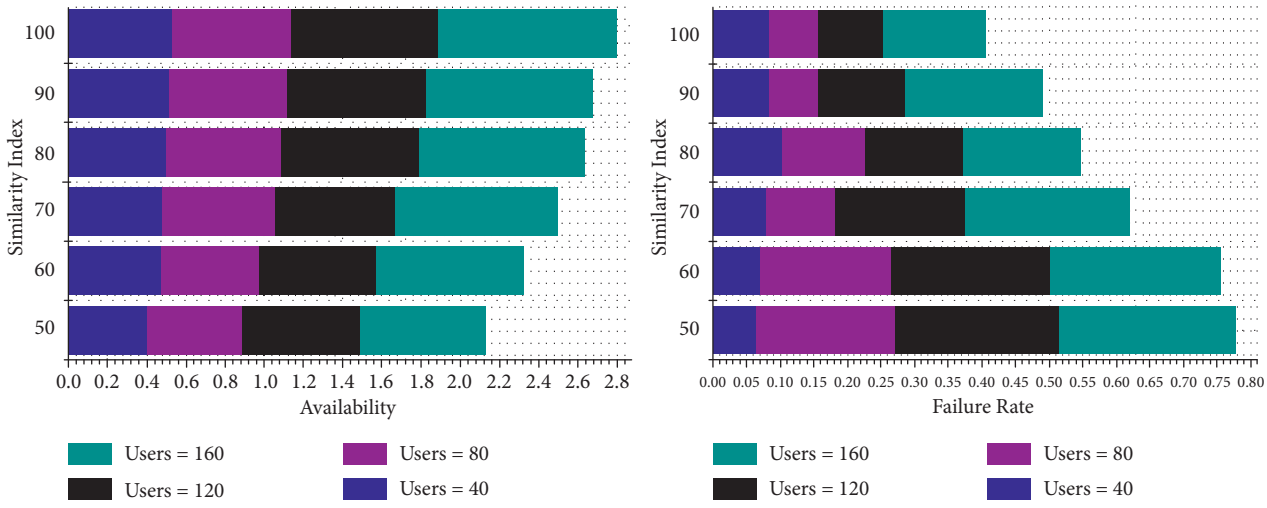

Figure 6: Analysis for availability and failure rate by varying the similarity index.

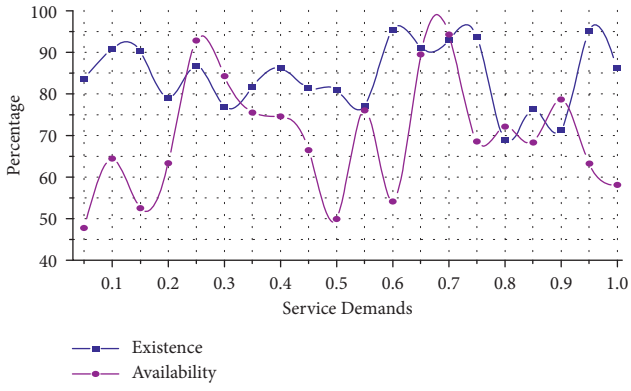

Figure 7: Analysis for existence and availability by varying service demand.

maximizes the responses by reducing the wait time for which $\partial(t)$ is reduced. Based on the $\chi_s(t)$ and learning output, the further $d_s(t)$ is performed. In the process, $\psi(\zeta, \phi)$ is used for maximizing the allocation.

The analysis of availability and failure rate for the varying similarity index is presented in Figure 6. The proposed method maximizes availability by reducing cost and s. In the federated learning for $M, \beta_S(T)$ is maximized for which existence is verified. If the verification fails, then $\varnothing$ is analyzed, and hence, availability is maximized. Therefore, the allocations are performed to improve the allocations post $\cos\theta$ and $d_s(t)$. The failures based on ${\gamma_{rs}}^{\max}$ is rectified by assigning $\partial(t) less\, \chi_s(t)$ such that new allocations are performed. The demands are supported in achieving fair sharing depending on the available sources. As the sharing increases, the availability is maximized by reducing failures.

Figure 7 presents an analysis of the existence and availability of the varying service demands factors. This analysis relies on $\mu_s(t)$ and $\partial(t)$ such that $\beta_s(t)$ is performed. However, the existence is high compared to the availability such that ψ determines its allocation. This is required by the M for further sharing and $\cos\theta$ analysis. Based on this, further, allocation is performed to improve availability.

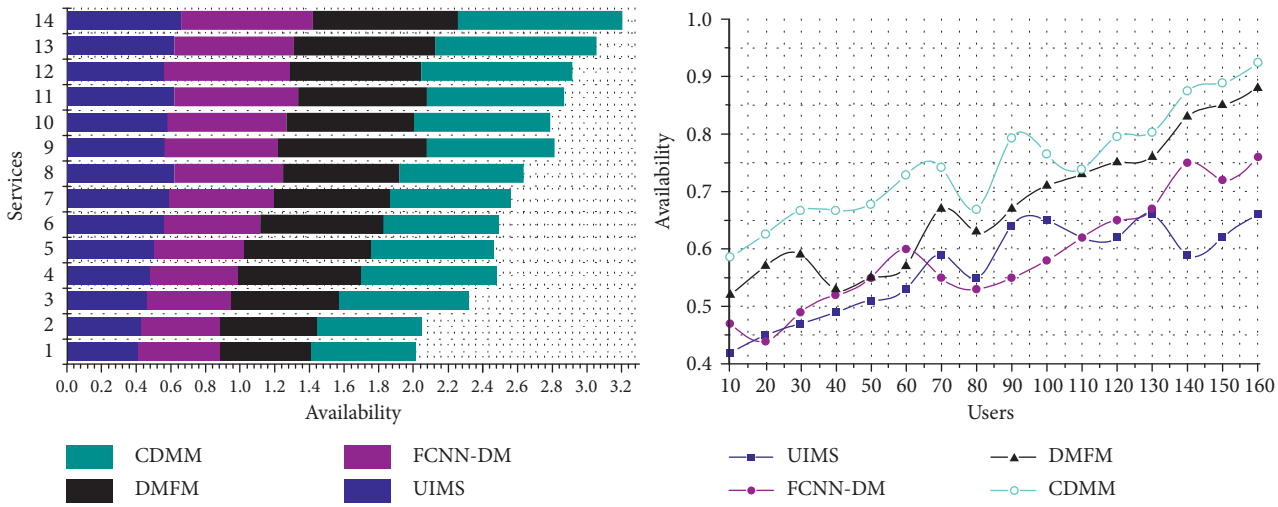

Figure 8: Availability comparison.

2.3. Performance Assessment. This section discusses the comparative analysis results of assessing the proposed CDMM using the dataset [29]. This dataset contains Flipkart product data classified under 16 fields for 30 K products. The mining process is performed by searching a product by its "ID," "Category," "Title," and "Price Range." Such queries are reverted with appropriate "Purchase," "Description," "Offers," and "Availability" information for 160 users. Similarly, the services are held for 12–20 mins for a user. From this detailing, the metrics of data availability, mining time, access time, failure rate, and sharing ratio are compared with the existing UIMS [21], FCNN-DM [24], and DMFM [16] methods.

2.4. Availability Comparison. The comparative analysis for availability is presented in Figure 8 for the varying services and users. The proposed method identifies $\mu_s(t)$ for $\beta_s(t)$ improvements. This improvement is analyzed$\forall s$ in the preallocation andϕ for the tolerable level verification. Based on these assessments, the federated learning validatesψ and$M$ individually. The common outputs are merged across different $\sum_{\beta_s}(t)$ such that availability is maximized. In particular, the availability is maximized using $\chi_s(t)$ between two successive intervals. In the repeated assessment, ${\gamma_{rs}}^{\max}$ is satisfied using $\partial(t)$ minimization. Therefore, the conventional request allocation and service assignments are maximized. In the mining process, the available resources are shared acrossψ satisfied intervals. Therefore, the user accessing intervals are maximized with $d_s(t)$ based on $\cos\theta$. This is carried forward for all$\chi_s(t)$ based on learning outputs. Hence, this proposed method maximizes data/resource availability.

2.5. Mining Time Comparison. The proposed CDMM achieves less mining time for the varying services and users, as presented in Figure 9. First, the influencing factors for s for s_{nw} ands_{que} is estimated. Based on the delay estimation, $w_r(t)$is assigned using$\mu_s(t)$ maximization. In the consecutive allocations, $\chi_s(t)$- and$M$-based federated learning influences the delay causing factors such that$\sum_{\beta_s}(t)$ is reduced. In the available allocation intervals, $\chi_o(t)$ is the deciding factor for preventing increasing mining time for multiple resources. If the service and user concentration increase, then the ψ factor as in(8), (9), and (10) is assessed for different ϕ conditions. These conditions are based on the time factor for preventing additional delay, and therefore, the allocation consecutively aids existence. This is unanimously pursued for $d_s(t)$ and $\beta_s(t)$ such thatψ is improved by reducing delay. Contrarily, for the varying users, $\mu_s(t)$ is varied such that all $w_r(t)$ is allocated from the available resources. Therefore, the wait time, that is, s_{que}, is reduced, preventing additional mining time.

2.6. Access Time Comparison. The access time for the proposed method's varying users and services is less than the other methods (refer to Figure 10). The queuing and mining time in the proposed method is reduced by assigning $\beta_s(t)$ based on $\mu_s(t)$. This is required to improve the $w_r(t)$ allocation and processing rate. Based on the allocation capacity and accessing intervals, the availability is maximized. First, the s_{nw} is reduced by mining concurrent resources across varying $\sum_{\beta_s}(t)$ such that ${\gamma_{rs}}^{\max}$ is achieved. Depending on$\chi_s(t)\forall s_{d_m}$ and(r,s) the further access grant is provided. In particular, $\cos\theta$ using the federated learning is improved for$d_s(t)$ such that $(\beta)s(t)$ is increased. This is pursued to improve the existence, wherein $\partial(t)$ is reduced. However, in the varying user concentration, $d_s(t)$ varies across multiple $\chi_s(t)$ preventing the balance in (r,s). Therefore, s_{nw} is also reduced balancing $(\zeta,\phi)\forall$interval$\in(1,n)$. The successful $d_s(t)$ is increased for achieving less access time for any service $\forall$ users in the same interval.

2.7. Failure Rate Comparison. The resource allocation failure in the proposed method is less than in other methods. Following the varying services, $w_r(t)$is maximized by

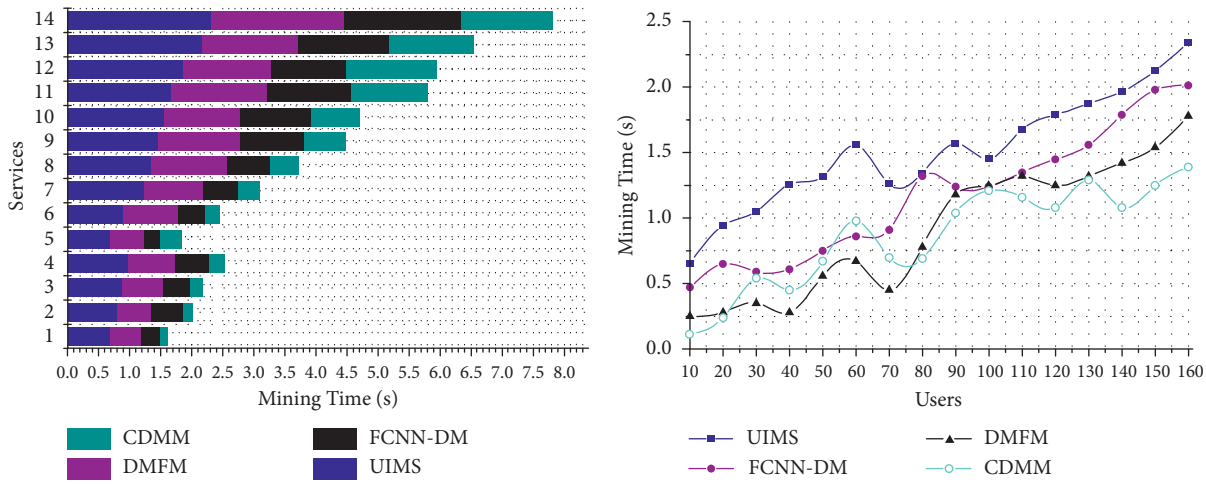

Figure 9: Mining time comparison.

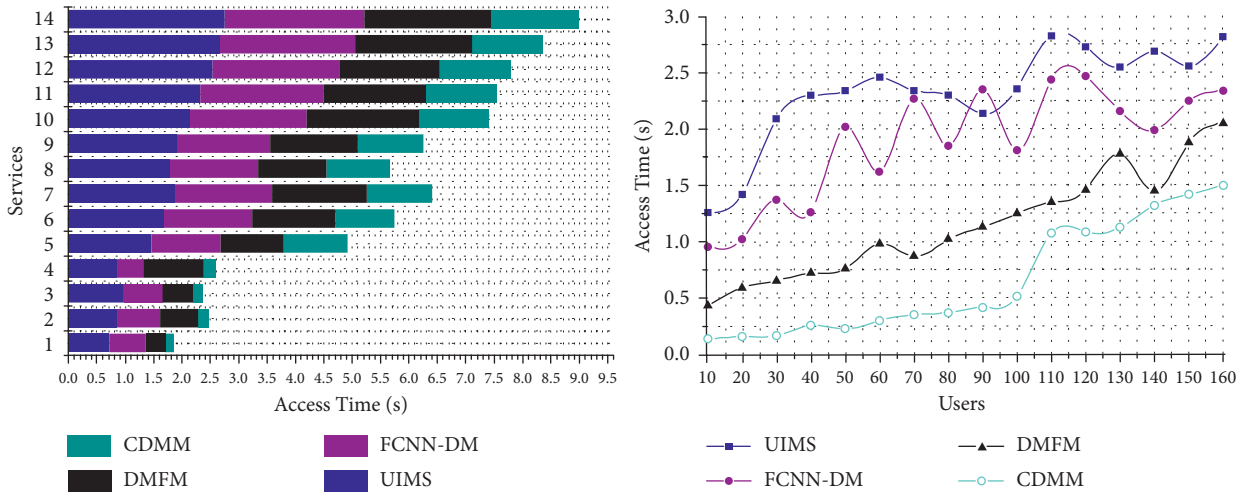

Figure 10: Access time comparison.

reducings in the pre-$\chi_{s(t)}$ assessment. In the learning-based validation, ψ assessment achieves fairϕ across the varying users. This is confined between 1 to n intervals such that $\cos\theta$ is the same. If the similarity index is high, then $\partial(t)$-based allocations are performed. Therefore, the maximum requests are assigned with a resource in the interval$n$. For the varying services, $\mu_s(t)$is varied for admitting $\omega_r(t)$ in the continuous intervals. The proposed method identifies ϕ in all the assigned$n$ such that $d_s(t)$ is maximized. This is required for maximizing $\cos\theta$, wherein the learning operates independently. From the M and ψ designed by the learning model, further allocations are performed, preventing $d_s(t)$ reduction. This is required for s mitigation and ϕ balancing between r and s. In the learning output assessment, $\partial(t)$-based allocations are prevented from interfering the $\chi_s(t)$ a decision such that existence is updated. Therefore, the sharing (shared) resource augments the demand suppression and reduces failures (refer to Figure 11).

2.8. Sharing Ratio Comparison. The proposed method achieves a fair sharing ratio compared to the other methods, as presented in Figure 12. The sharing is enabled by reducing the delay in queuing, access, and mining, as discussed earlier. The $\chi_s(t)$-varying users and services are streamlined using the deviating delay and mining time to prevent additional failures. The $\max[K_s(t) - \rho_s(t)\mu_s(t)\sigma, 0]$ process is responsible for performing the allocation across different tolerance factors. In the consecutive resource allocation,$\psi_{\max}$ is the estimating factor for maximizing the sharing ratio. The data management is performed for the above factor and M independently to maximize the mining process. In this process, the learning for similar features is streamlined to achieve a high repository allocation level. The process is prevented from avoiding requesting fewer allocations in the consecutive repository mining process. The collaborative allocations are performed for varying services such that$\mu_s(t)$ is maximized. In this process, the cost suppression is maintained such that the delay is also confined. The learning process further augments the data management system for improving the availability and retaining its existence until the interval $\in (0,1)$. Therefore, the repository is available for varying users and requests to improve the sharing ratio. This is not

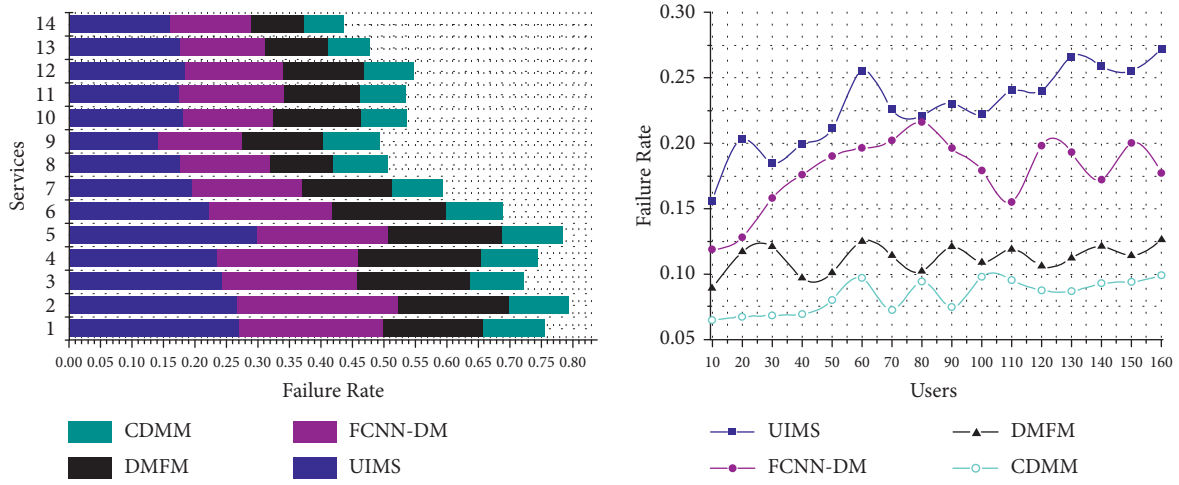

Figure 11: Failure rate comparison.

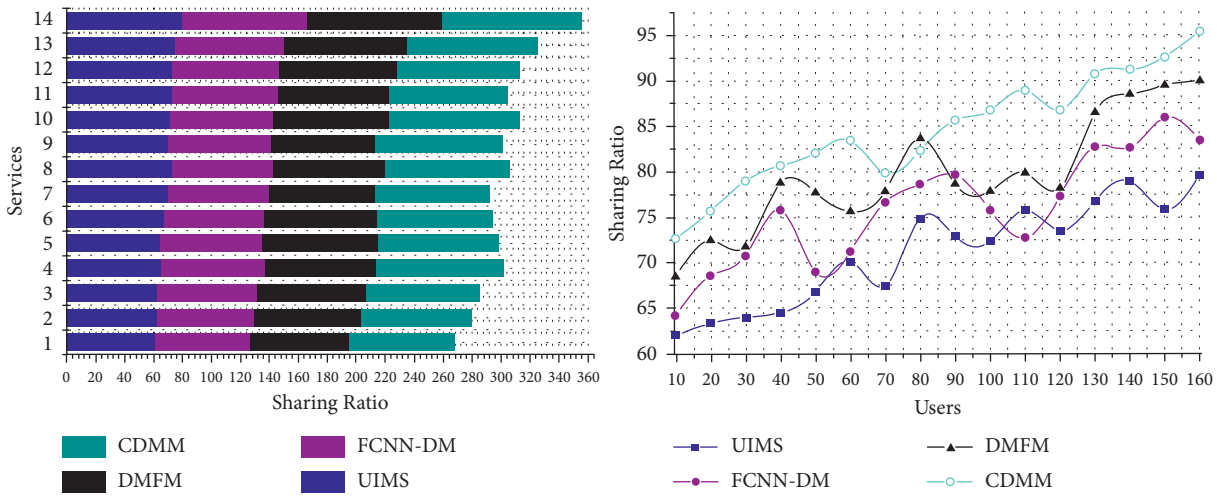

Figure 12: Sharing ratio comparison.

Table 1: Analysis summary for services.

Metrics	UIMS	FCNN-DM	DMFM	CDMM
Availability	0.66	0.76	0.84	0.942
Mining time (s)	2.328	2.15	1.86	1.48
Access time (s)	2.765	2.456	2.23	1.523
Failure rate	0.161	0.1296	0.0823	0.0634
Sharing ratio	79.45	86.66	92.44	96.34

Inference: The proposed method maximizes the availability and sharing ratio by 9.43% and 10.16%, respectively. It reduces the mining time, access time, and failure rate by 10.47%, 12.91%, and 6.09%, respectively.

Table 2: Analysis summary for users.

Metrics	UIMS	FCNN-DM	DMFM	CDMM
Availability	0.66	0.76	0.88	0.924
Mining time (s)	2.34	2.015	1.78	1.39
Access time (s)	2.82	2.34	2.05	1.498
Failure rate	0.272	0.177	0.126	0.099
Sharing ratio	79.67	83.45	90.03	95.46

Inference: The proposed method maximizes the availability and sharing ratio by 10.49% and 11.54%, respectively. It reduces the mining time, access time, and failure rate by 1.068%, 12.57%, and 9.27%, respectively.

repeated until the next allocation prevents additional access time. The above analysis is summarized for varying services and users in Tables 1 and 2 respectively.

3. Conclusion

This article introduced a connectivity-persistent data mining method for improving the sharing and allocation of a library of resource-based services. The proposed method relies on federated learning for validating data existence and availability for diverse user services. The mining process is performed for heterogeneous resources based on capacity-based allocation and delay mitigation. The user service demands are satisfied using experience and tolerance-based mining assimilations for improving resource availability. Besides, the available data are shared between the users and requests based on their existence. This existence is provided by maximizing request allocation and mining between connected users. The distinct service modes through existence and allocations are performed using the federated learning process through precise decisions from the data management system. Therefore, the proposed method maximizes existence and sharing regardless of the demands across the various intervals. The proposed method maximizes the availability and sharing ratio for the varying services by 9.43% and 10.16%, respectively. It reduces the mining time, access time, and failure rate by 10.47%, 12.91%, and 6.09%, respectively.

Data Availability

Data cannot be made available due to restrictions.

Conflicts of Interest

The authors declare that there are no conflicts of interest regarding the publication of this article.

Acknowledgments

This work was supported by the research project of China Academic Library & Information System (CALIS) National Agricultural Literature Information Center in 2022 "*The Research about the Service Mode and Construction Path of the Scientific Research Date in Universities by the Era of Big Data*." Project Number: 2022012.

References

[1] A. Zainab, A. Ghrayeb, D. Syed, H. Abu-Rub, S. S. Refaat, and O. Bouhali, "Big data management in smart grids: technologies and challenges," *IEEE Access*, vol. 9, Article ID 73046, 2021.

[2] Z. Xu, X. Zhou, A. Kogut, and J. Watts, "A scoping review: synthesizing evidence on data management instruction in academic libraries," *The Journal of Academic Librarianship*, vol. 48, no. 3, Article ID 102508, 2022.

[3] O. Zide and O. Jokonya, "Factors affecting the adoption of data management as a service (DMaaS) in small and medium enterprises (SMEs)," *Procedia Computer Science*, vol. 196, pp. 340–347, 2022.

[4] R. Tang and Z. Hu, "Providing research data management (RDM) services in libraries: preparedness, roles, challenges, and training for RDM practice," *Data and Information Management*, vol. 3, no. 2, pp. 84–101, 2019.

[5] J. Masinde, J. Chen, D. Wambiri, and A. Mumo, "Research librarians' experiences of research data management activities at an academic library in a developing country," *Data and Information Management*, vol. 5, no. 4, pp. 412–424, 2021.

[6] W. Didimo, L. Grilli, G. Liotta, L. Menconi, F. Montecchiani, and D. Pagliuca, "Combining network visualization and data mining for tax risk assessment," *IEEE Access*, vol. 8, Article ID 16073, 2020.

[7] M. Er Kara, S. Ü. Oktay Fırat, and A. Ghadge, "A data mining-based framework for supply chain risk management," *Computers & Industrial Engineering*, vol. 139, Article ID 105570, 2020.

[8] C. H. Lai and C. Y. Hsu, "Rating prediction based on combination of review mining and user preference analysis," *Information Systems*, vol. 99, Article ID 101742, 2021.

[9] S. A. Mohd Selamat, S. Prakoonwit, and W. Khan, "A review of data mining in knowledge management: applications/findings for transportation of small and medium enterprises," *SN Applied Sciences*, vol. 2, no. 5, pp. 818–915, 2020.

[10] J. C. Kim and K. Chung, "Mining based time-series sleeping pattern analysis for life big-data," *Wireless Personal Communications*, vol. 105, no. 2, pp. 475–489, 2019.

[11] Y. Zhong, L. Chen, C. Dan, and A. Rezaeipanah, "A systematic survey of data mining and big data analysis in internet of things," *The Journal of Supercomputing*, pp. 1–49, 2022.

[12] C. H. Lai, D. R. Liu, and K. S. Lien, "A hybrid of XGBoost and aspect-based review mining with attention neural network for user preference prediction," *International Journal of Machine Learning and Cybernetics*, vol. 12, no. 5, pp. 1203–1217, 2021.

[13] S. Hosseini and S. R. Sardo, "Data mining tools-a case study for network intrusion detection," *Multimedia Tools and Applications*, vol. 80, no. 4, pp. 4999–5019, 2021.

[14] M. Chen, W. Z. Li, L. Qian, S. L. Lu, and D. X. Chen, "Next POI recommendation based on location interest mining with recurrent neural networks," *Journal of Computer Science and Technology*, vol. 35, no. 3, pp. 603–616, 2020.

[15] M. Mahmud, M. S. Kaiser, T. M. McGinnity, and A. Hussain, "Deep learning in mining biological data," *Cognitive computation*, vol. 13, no. 1, pp. 1–33, 2021.

[16] P. Y. Huang, W. S. Cheng, J. C. Chen, W. Y. Chung, Y. L. Chen, and K. W. Lin, "A distributed method for fast mining frequent patterns from big data," *IEEE Access*, vol. 9, Article ID 135144, 2021.

[17] Y. Xie, P. Wen, W. Hou, and Y. Liu, "A knowledge image construction method for effective information filtering and mining from education big data," *IEEE Access*, vol. 9, Article ID 77341, 2021.

[18] J. Obregon, M. Song, and J. Y. Jung, "InfoFlow: mining information flow based on user community in social networking services," *IEEE Access*, vol. 7, Article ID 48024, 2019.

[19] P. Bhattacharya, F. Patel, S. Tanwar, N. Kumar, and R. Sharma, "MB-MaaS: mobile blockchain-based mining-as-a-service for IIoT environments," *Journal of Parallel and Distributed Computing*, vol. 168, pp. 1–16, 2022.

[20] Z. Zhang, "Mining method of massive data of mobile library under information asymmetry facing large-scare database," *Microprocessors and Microsystems*, vol. 81, Article ID 103730, 2021.

[21] S. Dhelim, N. Aung, and H. Ning, "Mining user interest based on personality-aware hybrid filtering in social networks," *Knowledge-Based Systems*, vol. 206, Article ID 106227, 2020.
[22] C. Wang, R. Huang, J. Li, and J. Chen, "Towards better information services: a framework for immigrant information needs and library services," *Library & Information Science Research*, vol. 42, no. 1, Article ID 101000, 2020.
[23] Y. Xiao, C. Li, M. Thürer, Y. Liu, and T. Qu, "User preference mining based on fine-grained sentiment analysis," *Journal of Retailing and Consumer Services*, vol. 68, Article ID 103013, 2022.
[24] W. Peng, "Big data mining and analysis based on convolutional fuzzy neural network," *Arabian Journal for Science and Engineering*, pp. 1–11, 2021.
[25] M. Alkathiri, A. Jhummarwala, and M. B. Potdar, "Multidimensional geospatial data mining in a distributed environment using MapReduce," *Journal of Big Data*, vol. 6, no. 1, pp. 82–34, 2019.
[26] L. Deng and D. Li, "Multimedia data stream information mining algorithm based on jointed neural network and soft clustering," *Multimedia Tools and Applications*, vol. 78, no. 4, pp. 4021–4044, 2019.
[27] C. Ju, J. Wang, and G. Zhou, "The commodity recommendation method for online shopping based on data mining," *Multimedia Tools and Applications*, vol. 78, no. 21, pp. 30097–30110, 2019.
[28] H. Zhou, G. Sun, S. Fu, J. Liu, X. Zhou, and J. Zhou, "A big data mining approach of PSO-based BP neural network for financial risk management with IoT," *IEEE Access*, vol. 7, Article ID 154035, 2019.
[29] Data World, "Promptcloud," https://data.world/promptcloud/flipkart-products-dataset.

Hindawi
Scientific Programming
Volume 2022, Article ID 4239474, 12 pages
https://doi.org/10.1155/2022/4239474

Research Article

Technology Based on Interactive Theatre Performance Production and Performance Platform

Xiuzheng Xia[1,2] and Chen Tian[3]

[1]*Sichuan Normal University College of Music, Chengdu 610101, Sichuan, China*
[2]*Department of Dramatic Literature, Cheongju University, Cheongju, Republic of Korea*
[3]*Geely College Performance Teaching and Research Section, Chengdu 641423, Sichuan, China*

Correspondence should be addressed to Chen Tian; tianchen@bgu.edu.cn

Received 14 July 2022; Revised 25 August 2022; Accepted 10 September 2022; Published 21 September 2022

Academic Editor: Juan Vicente Capella Hernandez

Drama refers to a comprehensive art that realizes the purpose of narrative through language, movement, dance, music, puppets, and other forms. From the pre-Qin period⟶the Han and Wei periods⟶the Tang, Song, and Jin periods⟶the Yuan Dynasty⟶the late Yuan Ming and Qing periods⟶modern times, the art of opera has been welcomed and recognized by a vast audience since its birth, but it is difficult to inherit the art of Chinese opera. The fundamental reason is that there is no good platform for performance. It should be said that since the beginning of the performing arts, there has also been academic thinking on the practice of this artistic creation, so in the academic field of drama, there is actually drama performance science. Due to the changes of the times, Chinese drama art cannot keep up with the pace of the Internet. Therefore, this article proposed a technical research based on the interactive drama performance production and performance platform. This article mainly talks about face recognition technology and its algorithm, and applies it to theatrical performances and productions. In the following experiments, this technology is also used to create a network platform, and its user experience evaluation effect is good. The theatrical performances and productions of young people were also scored, and the final experimental results showed that: at the minimum required level, which is at least three (or more) dramatic materials in the class, scores are high at both levels. Among them, 94.4% of the classes in the first-level kindergarten and 86.1% of the classes in the second-level kindergarten meet this standard. Most of the two levels are qualified, that is to say, in the performance area, at least three people can perform at the same time, which is enough to show that theatrical performance has been passed down.

1. Introduction

Drama is a popular folk art in China and has high artistic value and collection value in China and even the world. Every drama in ancient and modern China and abroad has its ups and downs plots and characters with different styles, all of which are gripping and fascinating. However, the survey has shown that dramatic art in China is rapidly dying out, mainly because of its complex production techniques and performance forms, which are generally difficult for ordinary people to master. At the same time, its performance and dissemination methods are relatively simple, mostly concentrated in some remote places such as rural areas and mountainous areas. For many reasons, the dissemination and development of this ancient folk art have been greatly restricted. The major of drama performance is a special major in the Chinese art education system, with the main teaching goal of cultivating artistic talents specializing in drama and film and television actors. At present, in addition to well-known institutions such as the Central Academy of Drama and the Shanghai Academy of Drama, many arts and comprehensive colleges and universities are generally opened. Compared with other majors, its history of running a school is relatively short, and its development process has twists and turns. However, after entering the 21st century, it has become more and more popular and sought after by ordinary college students. Therefore, drama teaching plays a very important role in training students' language

expression ability and cultivating students' Chinese literacy. Of course, this is inseparable from the great development and prosperity of China's cultural and artistic undertakings. However, its professional connotation and developable educational functions still have great potential and value for exploration.

The article focused on the introduction of face recognition technology and algorithms, and applies them to theatrical performances and productions. It was applied to theater performances and productions, used this technology in subsequent experiments, achieved a better user experience, and scored young actors' performances and movies. The innovation of this article is that after the algorithm is used in the previous article, the article immediately conducts experiments and a questionnaire survey, which are linked together, making the logic of the article stronger. The performance-based teaching is applied to the teaching of drama works on the network platform, and the operational level research on the implementation strategy and evaluation of the performance-based teaching of dramatic works is carried out, in order to provide some feasible experience and methods for the performance-based teaching of drama works in China.

2. Related Work

Performance-based teaching is a teaching method that allows students to further understand the language and contradictions of characters in dramatic works through role-playing on the basis of reading texts and teachers' explanations. At present, theatrical performance production has attracted much attention. McCoy introduced CommeilFaut (CiF), an artificial intelligence system that matches character performances to appropriate social contexts, the goal of which is to enable authors to write high-level rules to govern expected character behavior in a given social context, rather than a specific fixed choice point in a carefully curated narrative structure [1]. A relatively well-established theory of performance is the theory of dramatic spectacle. The above does not imply that his purpose is to enjoy sports performances because of its connection to drama. Kosiewicz pointed out one of the many possible aspects of sports spectacle, which are hypotheses of the contingent nature contained in its structure [2]. In the theatrical performance, the human avatar transforms into an active and engaged body, "opening to the world and projecting the performance," which is visually brilliant. A phenomenologist might say that this kind of performance expands hermeneutics so that reality can be presented to people, constituting the relationship between people and reality. Gill proposed that on this basis, reality can be presented in a specific way [3]. Although they all described the history of theatrical performance and its significance, they did not introduce human-computer interaction technology, nor did they study its algorithm.

Human facial expressions are the core carrier of feedback. Facial Expression Recognition (FER) has been introduced into medical assistance, safe driving, marketing assistance, distance education, etc. Based on the convolutional neural network (CNN), Shi introduced FCM to optimize the feature extraction (FE) capability of the model, and proposed a novel FER algorithm using an improved CNN (F-CNN) [4]. Emotions are of great significance in the communication and interaction between people and between people and computers. Sharma proposed an efficient and novel approach to recognize emotion using facial expressions by fusing dual features [5]. Among emotion recognition (ER), automatic facial expression recognition (FER) is actually a dynamically emerging research. Banerjee proposed the crow search algorithm of Brownian Motion-Based Adaptive Neuro-Fuzzy Inference System (BMCSA-ANFIS) for FER on human images [6]. The use of machine vision software to automatically assess facial expressions opens up new opportunities to assess facial expressions in an astute and economical way in psychological and applied research. Beringer investigated the evaluation quality of a machine vision algorithm (FACET) in a study using a standardized database of dynamic facial expressions under different conditions (angle, distance, lighting, and resolution) [7]. They all introduced the facial expression classification algorithm, but did not analyze it in combination with theatrical performance, let alone build a theatrical performance platform.

3. Interactive Facial Expression Classification Algorithm

3.1. Facial Expression Classification Algorithm. Classifier is a general term for the methods of classifying samples in data mining, including decision tree, logistic regression, naive Bayes, neural network, and other algorithms. From tens of thousands of features, selecting a low-dimensional feature subspace is the key to the successful classification of the classifier, which further validates the importance of feature extraction for classifier and recognition accuracy. Various algorithms have their own advantages and disadvantages, and it is necessary to select a classifier according to different research topics and the number of samples [8, 9]. According to the size of the public database samples and the real-time requirements of the algorithm, the support vector machine is used as the expression classification algorithm in this article. On the one hand, it is considered that relevant research has verified the excellent performance of support vector machines under the condition of small samples; on the other hand, other algorithms such as deep learning methods have higher requirements for the number of samples and longer training time [10, 11].

The related basic theory of support vector machine (SVM) will be described in detail: SVM is mainly based on VC dimension and structured risk minimization method in statistical theory. It has good classification performance and generalization ability, can solve high-dimensional classification problems, and avoid the overfitting problem in traditional machine learning classification [12]. Similar to neural network, support vector machine is a learning mechanism, but unlike neural network, SVM uses mathematical methods and optimization techniques. Support vector machines evolved from the optimal hyperplane classification model. As shown in Figure 1, taking a simple linear binary classification problem as an example, if the

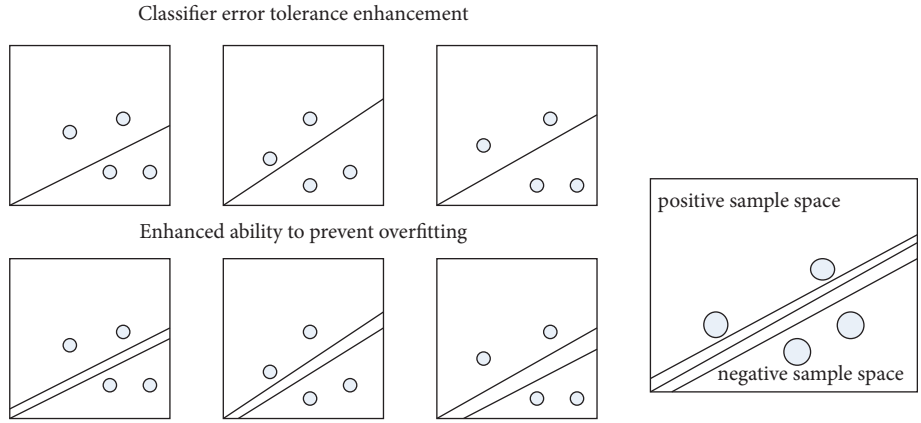

Figure 1: Schematic diagram of dividing line tolerance and robustness and optimal dividing line.

width of the hyperplane is small, there may be multiple classification hyperplanes under the condition that the two types of data are correctly classified. However, by maximizing the hyperplane width (classification spacing), the data error tolerance of the hyperplane can be guaranteed, thereby reducing the actual error [13].

SVM correctly classifies two types of data by finding an optimal hyperplane [14, 15]. As shown in the figure, for example, binary classification problem, the two types of data are represented by circles and crosses, respectively, and the H line is the obtained optimal separation line. All data points, circles are represented by positive class +1 and crosses are represented by negative class −1, then the sample data points satisfy the formula

$$b \in \{-1, 1\}, b_j\left[s^D \cdot a + y\right] \geq 1, j = 1, 2, 3 \ldots m. \tag{1}$$

To generalize the problem, in high-dimensional space, in order to facilitate the quadratic programming solution, through the Lagrange multiplier method, its purpose is to ask how to allocate and utilize manpower and raw materials under the condition of a certain cost, so as to maximize the production volume. The problem can be transformed into the formula by the Lagrange multiplier method:

$$Z(y, s, x) = \frac{1}{2}\|s\|^2 + \sum_{j=1}^{m} x_j\left(1 - b_j\left(s^D l_j + y\right)\right). \tag{2}$$

In the formula, $x_j, j = 1, 2, \ldots m1$ is the Lagrangian parameter, and the partial derivatives of s and y in the above formulas are calculated, respectively, and set equal to 0, and the following formula is obtained:

$$\begin{cases} \dfrac{\phi Z(y, s, x)}{\phi s} = s - \sum_{j=1}^{m} x_j b_j l_j = 0, \\ \dfrac{\phi Z(y, s, x)}{\phi y} = -\sum_{j=1}^{m} x_j b_j = 0. \end{cases} \tag{3}$$

Bringing it into the above formula, through the transformation of the dual problem, the problem becomes the maximum value of the following formula:

$$\begin{aligned} &\max_x \sum_{j=1}^{m} x_j - \frac{1}{2}\sum_{j=1}^{m} x_j x_j b_j b_j\left(l_j \cdot l_i\right), \\ &\text{w.d.} b_j\left[\left(s \cdot l_j\right) + y\right] - 1 \geq 0, \\ &\sum_{j=1}^{m} b_j x_j = 0, x_j \geq 0, j = 1, 2, 3 \ldots m. \end{aligned} \tag{4}$$

Under the condition of KKT (Karush–Kuhn–Tucker), the above formula must satisfy the formula

$$x_j\left\{b_j\left[\left(s \cdot l_j\right) + y\right] - 1\right\} = 0, j = 1, 2, 3 \ldots m. \tag{5}$$

It can be seen that this method greatly simplifies the calculation process of Lagrangian parameters, and solving the above quadratic programming problem will get the final result.

Slack variables, mathematical term, if the constraints of the linear programming model under study are all less than types, then M nonnegative slack variables can be introduced through the normalization process. The example is discussed for the case where the multidimensional space is linearly separable. However, in real life, due to the defects in completeness and accuracy of data, it often leads to the linear inseparability of practical problems. In response to this situation, the problem can be transformed into the formula by introducing a nonnegative slack variable:

$$\min_{s, y, \varphi_j} \frac{1}{2}\|s\|^2 + E\sum_{j=0}^{m} \varphi_j. \tag{6}$$

Among them, $E > 0$ is the penalty coefficient, which represents the punishment for the wrongly classified samples, which can also be obtained by duality transformation of the Langrangian multiplier method:

$$\begin{aligned} &\max_x \sum_{j=1}^{m} x_j - \frac{1}{2}\sum_{j=1}^{m} x_j x_j b_j b_j\left(l_j \cdot l_i\right), \\ &\text{w.d.} b_j\left[\left(s \cdot l_j\right) + y\right] \geq 1 - \varphi_j, \\ &\sum_{j=1}^{m} b_j x_j = 0, 0 \leq x_j \leq E, \varphi_j > 0, j = 1, 2, 3 \ldots m. \end{aligned} \tag{7}$$

In addition to the linear inseparability, practical problems are often complex in dimension space, so the sample data often does not conform to the linear distribution [16, 17]. The introduction of the kernel function can just solve this problem. By introducing the kernel function, the data space is transformed from low-dimensional to high-dimensional, and then the linear decision-making of the high-dimensional space is used to solve the optimal hyperplane:

The solution of the following formula is solved by the problem transformation after high-dimensional space transformation:

$$\max_{x} \sum_{j=1}^{m} x_j - \frac{1}{2} \sum_{j,i=1}^{m} x_j x_i b_j b_i \eta\left(a_j\right) \eta\left(a_i\right). \tag{8}$$

In order to simplify the problem, the concept of kernel function is introduced [18]. The kernel function satisfies the Mercer condition, that is, for any $\eta(a) \neq 0$ and $\int \eta^2(a) ta < \infty$.

$$\iint R\left(a, a'\right) \eta\left(a'\right) \text{tata}' > 0. \tag{9}$$

There are problems such as determining the form and parameters of the nonlinear mapping function and the dimension of the feature space, and the biggest obstacle is the "curse of dimensionality" in the operation of the high-dimensional feature space. The use of kernel function technology can effectively solve such problems. Kernel functions to solve special problems can be constructed through Mercer conditions, thereby simplifying the operation process. Finally, the discriminant function of the support vector machine is obtained as

$$g(a) = \text{sgn}\left(\sum_{j=1}^{m} x_j b_j R\left(a_j \cdot a\right) + y^* \right). \tag{10}$$

The discriminant function of SVM is only related to the inner product of the support vector machine and the number of samples, and is not constrained by the dimension of the feature space. This feature makes the SVM algorithm reduce the computational difficulty of high-dimensional space through the kernel function method, and has a stronger generalization ability [19, 20]. In short, the original binary support vector machine has been well broadened and strengthened by introducing slack variables and kernel functions, which enables it to find the optimal hyperplane to separate the data in a high-dimensional space, thereby obtaining classification results.

3.2. Virtual Face Modeling. In order to complete the interaction between the operator and the virtual face in the virtual environment, it is necessary to model the face to generate the virtual face. Bone skinning is to add a physique modification command to the model and combine it with the skeleton object, so that the model will follow the movement of the skeleton object to achieve the effect of skinning. The modeling process can be divided into two steps: geometric modeling and bone skinning. In terms of geometric modeling, according to the composition of the skeletal structure and muscle structure of the human face, the polygonal modeling method is used to model the main shape feature changes of the human face through the combination of several polygonal surfaces. In the modeling process, the method of "shape first, then refine" is adopted, using the symmetry of the face and the multi-view pictures of the reference data to build a rough head shape, and then gradually add head details. This method effectively avoids the problem of dead corners or faults in the modeling process.

The human face can be seen as a combination of skin, bones, and muscles, where the skin determines the visual appearance of the face, the bones determine the main contours of the face, and the muscles are used to connect the skin and bones to produce the main movements and expressions of the face [21, 22]. Therefore, if the virtual face is to produce a more realistic and natural expression, it is particularly important to complete the modeling of the muscle model. However, in practical applications, it is found that the linkage relationship between skin, bones, and muscles is quite complex, and there are specific and non-uniform configuration relationships between different muscle groups and skin textures. Therefore, in most applications, the method of skeletal skinning is used to replace the method of muscle modeling, which reduces the difficulty of processing complex configuration relationships, and the established model can also meet the requirements of various expressions.

The skeletal skinning technology follows the similar structure of human skin, bones, and muscles, omitting the complex linkage relationship of the muscle layer, and uses "bone" to drive "skin," where the concepts of "bone" and "skin" have been strengthened. "Bone" is not strictly the skeletal structure of the human body, it actually represents the way the skin is driven, but in most cases, it is similar to the skeletal structure of the human body. Making skin meshes, laying out bones, and skinning are the three major steps of skeletal skinning. In shape modeling, a detailed skin mesh can be obtained by polygon modeling. Since the bones in the skeletal skinning technology replace the driving function of the original muscles, in order to complete the conditions for expression generation, the facial bones need to be arranged according to the facial muscle structure.

Skinning, the term for 3D animation, is also used in 3D games. A production technology of 3D animation, adding bones to the model based on the model created in 3D software. Skinning technology is also known as bone skin binding technology and bone subspace deformation technology because it determines how bones drive and influence the skin. In real life, there are differences in the way bones drive skin, which often leads to dull expression animations and even skin knots, such as

$$U' = N_j Z_j^{-1} U. \tag{11}$$

Compared with the singleness of the rigid binding algorithm, the flexible binding algorithm better simulates the muscle-skin transmission mechanism of the human body. The motion of defining skin grid points is determined by multiple arranged bones, which is more in line with the biological laws of human face motion. The formula of the flexible binding algorithm is as follows:

$$U' = \sum_{j=1}^{m} \phi_j N_j Z_j^{-1}, \quad \sum_{j=1}^{m} \phi_j = 1. \tag{12}$$

Similar to the rigid binding algorithm, the local coordinate points of the skin mesh are determined by the coordinates before the change, the coordinate system transformation coordinates, and the motion transformation coordinates. The difference from the rigid binding algorithm is that the coordinates after skin movement need to be determined according to the weighted sum of multiple bones. It is worth noting that to realize the natural movements of the eyes and mouth and the twisting of the neck in face modeling, it is necessary to model these three positions individually and specifically.

The skin of the above-mentioned nonspecific facial positions is mostly composed of linear muscles, and the strip bones are similar in structure to them, which can simulate facial muscles well. However, the movement of the eye includes blinking and eyeball rolling, which is not suitable for the driving method of the strip bone, and needs to be driven by a spherical bone mechanism. Likewise, the musculature of the mouth dictates the use of a ring structure for its skeletal structure. In real life, the generation of expressions often involves the rotation of the head and neck. In order to ensure the vividness and naturalness of the virtual face, a neck movement bone is added to complete the head rotation requirement. Figure 2 shows the resulting skeletal skinning model.

3.3. Face Motion Capture. Capturing and manipulating the shape, appearance changes, and facial movement of a human face is a core technology in the field of modern computer animation. The virtual 3D characters commonly seen in movies often go through multiple complex steps such as detailed 3D scanning, skin texture processing, and detailed motion capture to realize the wonderful moments in the movie. The above process also often requires sophisticated 3D image acquisition equipment or long post-processing, which makes it time-consuming and labor-intensive to create a virtual person or virtual face with high quality and high restoration characteristics. With the rapid development of the commercial game field, major game manufacturers have correspondingly developed low-end 3D image acquisition devices with high-cost performance, enabling users to capture the facial movements of human faces through these devices. Microsoft Kinect is one of the acquisition devices that fulfill such a requirement. Although Kinect saves the wearing of the original artificial feature points of traditional image acquisition equipment, but due to the high noise generated by the depth image, it is generally necessary to twist the head in advance to collect a face model with specific expressions to complete the subsequent facial motion capture.

In this article, the Kinect sensor is used to complete the expression and motion capture of dynamic face images in the FaceShift software, and then the captured expression parameters are transferred to the virtual face model to complete the facial expression interaction in the virtual environment. The steps mainly include 2D/3D image acquisition, model positioning, and determination of deformer weights. Figure 3 shows the processing steps of facial motion capture.

Kinect collects the depth images of the above facial actions within a certain time window, uses the nonrigid ICP 3D registration algorithm to generate a 3D model of a specific expression and determines the weights of the deformer, and then performs bone skinning operations with the general facial model, which produces a user-specific face deformer model. The specific face deformer generation process is shown in Figure 4. The process is mainly divided into three steps: data acquisition, expression reconstruction, and deformer reconstruction. In the process of data acquisition, since the single-channel depth image acquired by Kinect has more noise, the acquisition process adopts the method of multiple scans to reduce noise and improve accuracy. In the process of expression reconstruction, the face model is first used to align neutral expressions, and then the nonrigid ICP algorithm is used to register other specific expressions, and the registration accuracy of the algorithm is improved by adding restrictions on the mouth and eyes; in terms of deformer reconstruction, the general facial expression deformer model based on FacialActionCodingSystem (FACS) is used, and the deformer weights of specific expressions are determined by the special skeleton binding method. The number of deformer bones during reconstruction is 39.

The generic face deformer model treats the face as a linear convex combination of n base vectors, where each vector is a face shape deformer. Each deformer contains the shape and texture of the face model. For a given design model, all deformers share the same topology. The coordinates of a vertex of the deformer can be expressed as

$$U = \sum_{j=1}^{m} x_j U_j. \tag{13}$$

The mixed weights must satisfy the following convex constraints:

$$x_j \geq 0, \sum_{j=1}^{m} x_j = 1. \tag{14}$$

The texture information of each deformer also satisfies the above-mentioned linear convex combination structure.

Generating a wide range of expression animations can require a large number of deformers. For example, the

Figure 2: Schematic diagram of the face mesh model and skeletal skinning model.

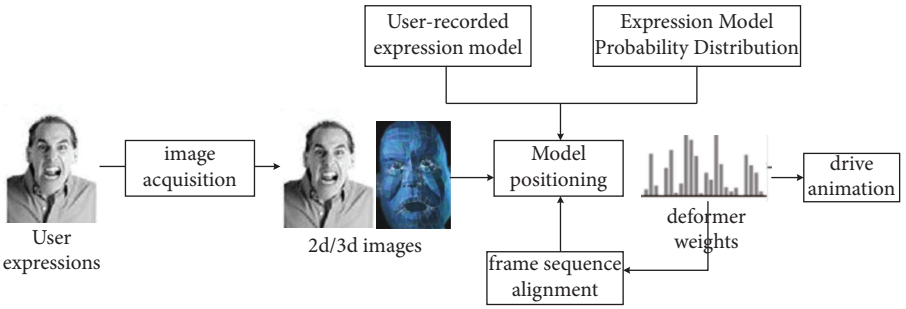

Figure 3: Facial motion capture processing steps.

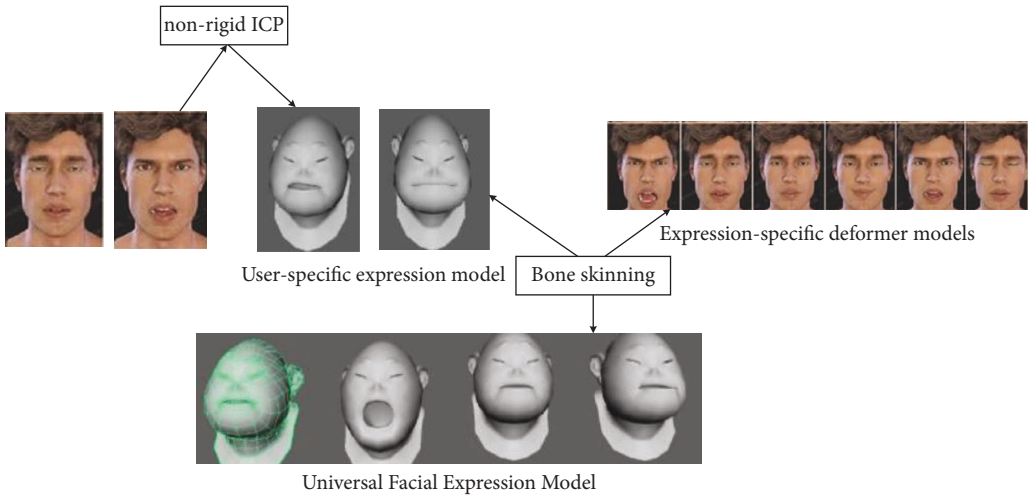

Figure 4: Feature expression modeling process.

Grunts in The Lord of the Rings: the Two Towers each have 675 face shapers, however, a small number of deformers used in related fields at home and abroad can also generate complex and real facial expressions. The physical model structure of the deformer determines that it can drive a variety of expressions. The simplest physical model for deforming objects is the linear elastic force model, which defines that the deformation of an object can be represented by the displacement field of the current point and the remaining points. The governing equation of the motion of the linear elastic force model can be expressed by the Lamé formula:

$$\lambda x = \gamma \Delta t + (\gamma + \eta)\nabla(\nabla \cdot t). \tag{15}$$

In order to find the deformer blend weight of x_j, the problem is transformed into a minima problem:

$$\sum_{i=1}^{n}\left[N_i - \left(\sum_{j=1}^{m} x_j U_{ji}\right)\right]^2. \tag{16}$$

4. Theatrical Performance Production and Construction of Performance Platform

4.1. Design Experiments. This study observed and measured the development of drama performances in a total of 72 classes in three key university classes at the provincial level and the provincial level in *H* city. Before the observation, the principal and relevant teachers made it clear what the researchers want to observe is a theatrical performance.

The scale uses a nine-point scoring method, with 1 being the "inappropriate" level, 3 being the "minimum

requirement" level, 5 being the "qualified" level, 7 being the "good" level, and 9 being the "excellent" level. "Role/Drama" in subscale 5 "Drama Performance" includes three subitems: Material and Space, Opportunity and Time, Design and Guidance.

The two raters are both postgraduates in higher education who have undergone systematic training, have actually applied the scale to evaluate multiple classes, and are proficient in operating evaluation tools. Two raters entered a class at the same time to independently rate their same drama performance activity, and after the independent scoring, a discussion was held to arrive at a discussion about the activity.

The researchers made a consistent analysis on the overall average score of the project, subitems: Material and Space, Opportunity and Time, and Design and Guidance scores of the two raters. Through Spearman correlation analysis, the results are shown in Table 1. The overall average score of the two raters was $r = 0.94$, $p < 0.01$, which was significantly correlated. In the three subitems of Material and Space, Opportunity and Time, Design and Guidance, the correlation coefficients are: $r = 0.91$, $p < 0.01$; $r = 0.97$, $p < 0.01$; $r = 0.91$, $p < 0.01$, all significantly correlated, and the inter-rater agreement was high.

The researchers coded and organized the collected data, and applied SPSS 17.0 for analysis.

4.2. Data

(1) Descriptive analysis of the quality of drama performances in the first-class gardens

The researchers made descriptive statistics on the overall average score and each subitem of the drama performance project of the 36 classes in the first-level garden.

As shown in Figure 5, the overall average score of the provincial level drama performance project is 4.8 points, which is at the minimum required level. A score of 6 in Materials and Space, between pass and good; in Opportunity and Time, an average of 4.7, between minimum and pass; in Design and Instruction, an average of 3.8, at the minimum required level.

(2) Descriptive analysis of the quality of drama performances in the secondary gardens

The researchers made descriptive statistics on the overall average score and each subitem of the drama performance program in 36 classes in the provincial second-level kindergarten.

As shown in Figure 6, the overall average score of the children's drama performance project in the 36 classes in the provincial second-level is 4 points, which is at the minimum required level. In the Material and Space items, the average is 5 points, reaching the qualified level; in the Opportunity and Time items, the average is 4 points, between the minimum required level and the qualified level; in the Design and Guidance, the average is 3.1 points, in the minimum required level.

Comparing Figures 5 and 6, it can be seen that the overall average score and the scores of the three subitems of the first-level gardens are higher than those of the second-level gardens, and the performance quality of the first-level gardens is slightly higher than that of the second-level gardens. Both grades are at the minimum required level in terms of overall quality. Qualified in both Material and Space programs, that is, the theater performance area has material available for at least three students. Both are at the minimum required level of Opportunity and Time, that is, at least 1 opportunity per week to play theatrical performances. The minimum required level of Design and Instruction has just been achieved, that is, the teacher will provide a simple drama performance activity.

In order to specifically study whether there is a statistical difference in the quality of drama performances at different levels, the researchers conducted independent sample t-tests on the quality of drama performances at different levels, as shown in Table 2:

In terms of the overall average score of the project, the average scores of the first-class park and the second-class park are 4.8 and 4, both of which are between the minimum required level and the qualified level. $t = 2.2$, $p < 0.05$, the overall level of first-class gardens was significantly higher than that of second-class gardens.

In terms of Materials and Space, the quality of the first-level garden is 6 points, the quality of the second-level garden is 5 points, and both grades have reached the qualified level. $t = 2.2$, $p < 0.05$, the quality of Materials and Space items in the first-class garden is significantly higher than that of the second-class garden.

It can be seen from Figure 7 that the percentages of the first-class gardens are higher than those of the second-class gardens in all other indicators except that the percentages of the unsuitable level and the excellent level A are lower than those of the second-class gardens. There are relatively few classes in the two grades of kindergartens at the unsuitable level, and most of the classes provide students with materials and furniture for drama performances. However, there are slightly more classes at this level in the second-level garden than in the first-level garden, which may be one of the reasons for the difference in the quality of the two levels.

At the minimum required level, where the class has at least some (3+) drama material available, both grades are scored higher. About 94.4% of the first-class kindergartens and 86.1% of the second-class kindergartens have reached this level. The majority of classes at both levels achieved a qualifying level, that is, there was at least three concurrent theatre performance materials in the performance area.

On the good level, the first-class parks have 72.2%. About 50% of the classes in the second-level kindergarten have drama performance materials for five to six students, and the first-level kindergarten has more materials than the second-level kindergarten. The materials provided by 36.1% of the first-class kindergarten and 16.7% of the second-class kindergarten can form two themes that are popular with the class. The materials of the first-level garden are more thematically oriented than those of the second-level garden, but there are fewer classes at both levels reaching this level. About 61.1% of the classes in the first-class park and 41.7% of

Table 1: Spearman correlation coefficient.

	N	Correlation coefficient	Sig (both sides)
Overall average score of the project	72	*0.94***	0.00
Material and Space	72	*0.91***	0.00
Opportunity and Time	72	*0.97***	0.00
Guidance and Design	72	*0.91***	0.00

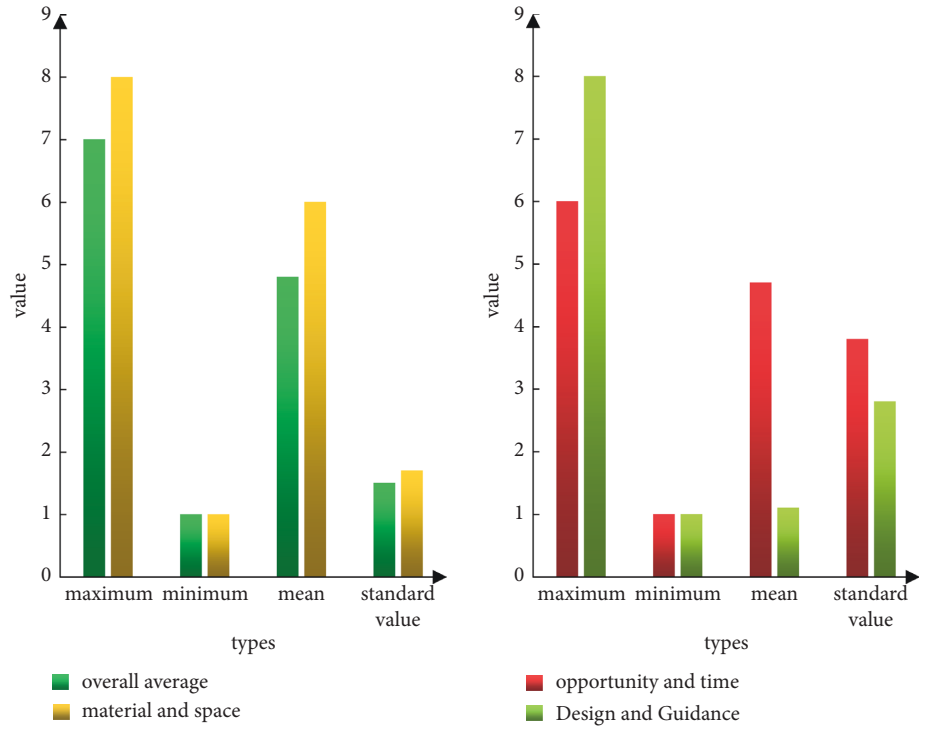

Figure 5: The quality of drama performances in the first-class gardens.

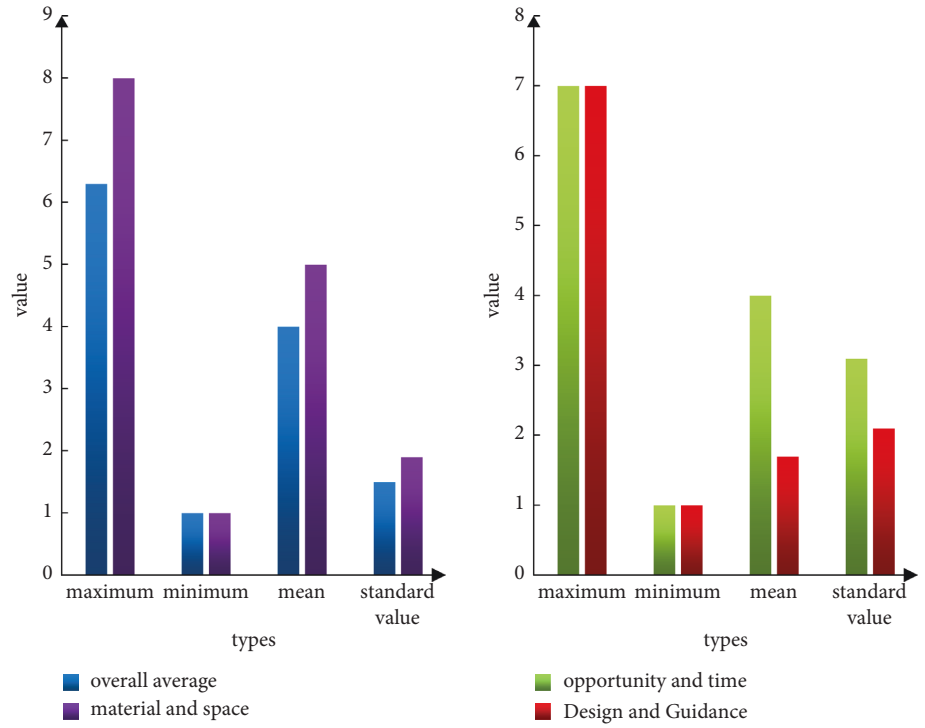

Figure 6: The quality of drama performances in the secondary gardens.

Table 2: Provincial 1 and provincial 2 theatrical performance quality *t*-test.

	t	df	Sig (both sides)	Mean difference	Standard error value
Overall average score	2.2	70.00	0.03	0.81	0.36
Material and Space	2.2	70.00	0.03	0.94	0.43
Opportunity and Time	2.1	60.60	0.04	0.72	0.34

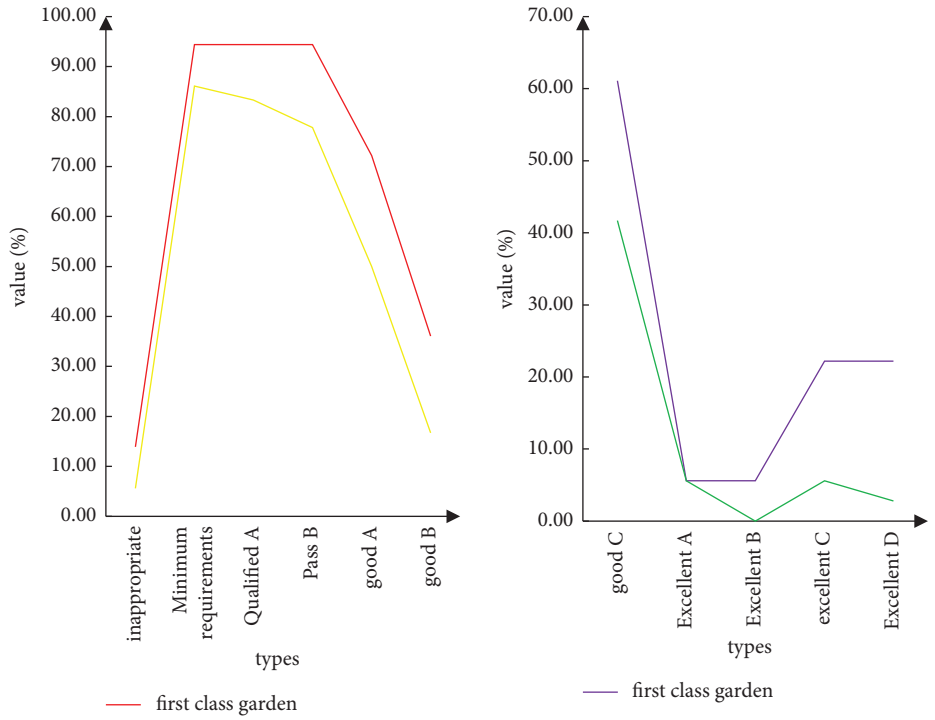

Figure 7: Comparison of two grades of material and spatial finesse.

the classes in the second-class park have clearly planned theatre space, and the materials are stored and maintained in good condition. There are more classes in the first-class park reaching this standard than in the second-class park.

The percentages of the classes that reach the excellent level of each indicator are less than 30% in both grades. In terms of materials, both grades lack drama materials reflecting multiculturalism, special drama rooms, and less rotation of materials according to various themes.

In terms of Opportunity and Time, the quality at the provincial level is 4.7; the quality at the provincial level is 4. Both are between the minimum required level and the qualified level, and the Opportunity and Time to perform are significantly less, $t = 2.1$, $p < 0.05$, the difference between the two is significant.

As can be seen from Figure 8, 2.8% of the classes in the first-class kindergarten and 11.1% in the second-class kindergarten are at an unsuitable level, that is, they have no chance to play drama performances within a week. Level 2 gardens have more classes at this level than level 1 gardens. Most classes at both levels meet the minimum required level, which guarantees at least one play opportunity per week. There is a certain gap between the first-class kindergarten and the second-class kindergarten in the qualified level. About 83.3% of the first-class kindergarten and 50% of the second-class kindergarten have reached this level. There are more classes in the first-level kindergarten than in the second-level kindergarten, which can guarantee at least one to two special opportunities (at least 30 minutes each time) for drama performances per week: both grades of kindergartens achieve a good level, and there are fewer classes that guarantee at least three to four special opportunities for drama performances per week. No class in the first-class kindergarten reached the standard, 11.1% of the classes in the second-class kindergarten met this standard, and the second-class kindergarten was higher than the first-class kindergarten in this index. There are no classes in both grades that reach the excellent level, that is, there is sufficient time (accumulated more than 60–80 minutes) each day for drama performances, and one of them can be played continuously for more than 45 minutes.

4.3. Establishment of the Theatrical Performance Platform. The model adopts a theoretical framework of interactive narrative based on dramatic metaphors, providing a computational framework that supports the dynamic generation, management, and conflict resolution of interactive plots, allowing users to act as the protagonist of the opera to determine current behaviors and actions. The core modules

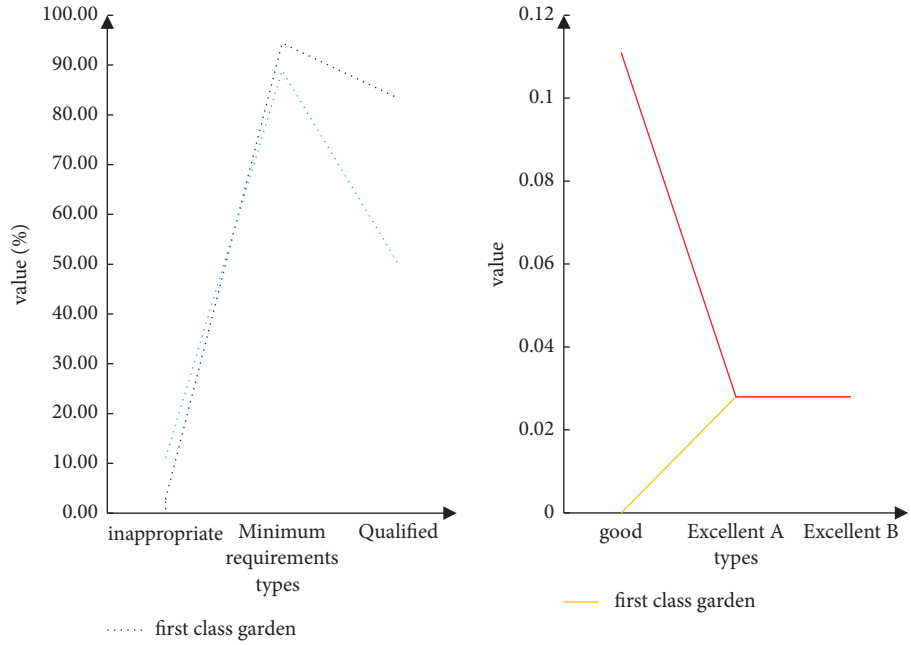

Figure 8: Comparison of temporal and spatial fine-grained metrics for two levels.

include user interface; event management; action management; scene management; story management; and data management; as shown in Figure 9.

The system integrates interactive technology, network technology, and digital animation technology, and strives to be in line with traditional artistic expressions, providing users with a network platform that can independently design and perform shadow puppets. Rich in content, simple in interaction, and easy to learn, users can easily complete the production, and can experience the fun of shadow puppetry in the process of operation, and develop users innovation and creative ability.

The main interface of the system is the main interface of drama production, which provides a series of function buttons and menu buttons. The right side of the interface provides a series of function buttons such as select the scene, select the character, select the background music, select the action (simple actions provided in the system can be directly selected by the user), preview (can preview the completed action), etc. The top of the interface provides a series of action menus, including the file menu (providing functions such as saving and submitting), the editing menu (providing the user to undo the previous action, zoom in and zoom out of scenes and characters, etc.), my plays (save user's unfinished and completed shadow puppets), links, etc.

The production process of the user using the system is mainly divided into the following stages:

Scene design stage: the user selects the characters and props in the opera scene, uses the mouse to drag the scene layout, and at the same time, the characters and props in the scene can be enlarged or reduced arbitrarily.

Action design stage: the key point of the system is to provide users with a function that can interactively design character actions and plots. During the action design process, the user can choose some simple actions provided in the system database, or freely design the actions of the characters. The various parts of the drama characters can be flexibly controlled by the user, and the user designs the actions and postures of each two adjacent key points of the character's bones, that is, the initial state and the end state of each action. In the design process, it needs to use the mouse to drag the various parts of the character's body to achieve the desired position, body posture, inclination angle, etc., and save it. The system automatically generates action sequences to complete the designed action. By selecting Preview, it is possible to see the smooth motion between these two states, and to control the progress and stop the motion in real time. If the user is not satisfied with the current design action, he can undo the current action and redesign it. During the action design process, the system automatically records the time node and saves the record, which is convenient for users to watch the scene animation designed by themselves.

The stage of submission and play after the completion of the opera: the completed play can be submitted after the production is completed. After the submission is complete, the user can enter the playback interface to search for previously saved plays to watch, or search for other plays to watch, and interactively control the playback of animations on the page. After the playback is completed, the evaluation of the opera can be given to realize network interaction.

A good software product must have good usability, and to reflect whether a software product is easy to learn, use, safe, effective, and satisfactory, the software must be evaluated for usability. Especially when designing interactive products, the system development process has to go through the iterative stages of "design-evaluation-re-design," so that problems in the software can be found, the software can be continuously improved, and finally, products that satisfy users can be released. Therefore, this section will conduct

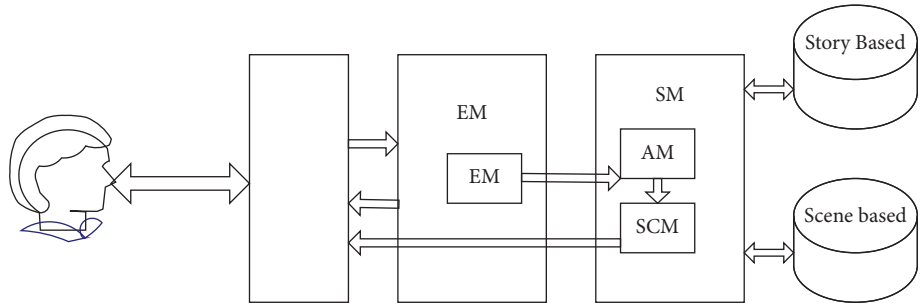

Figure 9: Interaction model diagram.

Table 3: Feasibility test data statistics table.

	Number of errors executed	Task completion time (minutes)	System response time (seconds)
Average value	3.3	11.17	3.5
Standard deviation	1.1	2.71	1.2
Maximum value	5	17	6
Minimum	1	7	2

Table 4: User experience survey.

Operation accuracy	64 (%)
Naturalness	75 (%)
Ease of use	80 (%)
Interactive experience	90 (%)
Overall satisfaction	82 (%)

usability testing and evaluation of the system prototype to verify and illustrate the feasibility of the system design and implementation.

It can be seen from Table 3 that the system can basically meet the needs of users, but due to time reasons, the function of the system is not perfect. Therefore, further improvements in execution efficiency, robustness, and fault tolerance are needed in the follow-up work. From Table 4, it can be concluded that the interactive experience value is the highest. In the survey, this article found that users have great interest and enthusiasm for the interactive production provided by the system and the character action plot design of the system for commenting and performing dramas. By using the system they gained a new understanding of drama and provided better ideas for improvement in this article. However, the manipulation accuracy of the system needs to be further improved. Users generally feel that when designing character actions, the instructions for selecting various components are not clear enough, which affects the accuracy and flexibility of the operator's actions. Therefore, further improvement is needed in the follow-up work. From the overall user experience, most users affirm and support this new form of dramatic performance and dissemination. Therefore, the system prototype designed and realized based on the research of this article is reasonable, effective, and has a certain promotion value, which can provide new ideas for the development of digital drama.

5. Conclusion

Through the measurement of the quality of theatrical performances of the two levels, it is known that the overall quality of theatrical performances of the two levels is between the minimum required level and the qualified level. The quality of drama performance in the first-level gardens is significantly higher than that in the second-level gardens. Specifically, there are significant differences between the two levels in the items of "Material and Space" and "Opportunity and Time," but not in the items of "Design and Guidance." In terms of Materials and Space, most of the classes of both grades have reached the qualified level, that is, there are at least three drama performance materials in the performance area that can be used at the same time. In terms of Opportunity and Time, the score of the first-level garden is higher than that of the second-level garden, both of which are at the minimum required level, which can guarantee the opportunity to perform drama performance once a week. This is also enough to show that the drama culture has been passed down and will shine in subsequent performances. The scale is designed from the dimensions of external environment: "Material and Space," "Opportunity and Time," and "Design and Guidance," although it can also reflect the quality of drama performance, but it cannot understand the development level of drama performance.

Data Availability

No data were used to support this study.

Conflicts of Interest

The authors declare that there are no conflicts of interest.

References

[1] J. Mccoy, M. Treanor, B. Samuel, A. A. Reed, M. Mateas, and N. Wardrip-Fruin, "Social story worlds with comme il faut," *IEEE Transactions on Computational Intelligence and AI in Games*, vol. 6, no. 2, pp. 97–112, 2014.

[2] J. Kosiewicz, "Aleatorism and sporting performance," *Physical Culture and Sport. Studies and Research*, vol. 73, no. 1, pp. 54–61, 2017.

[3] K. S. Gill, "Hermeneutic of performing knowledge," *AI & Society*, vol. 32, no. 2, pp. 149–156, 2017.

[4] M. Shi, L. Xu, and X. Chen, "A novel facial expression intelligent recognition method using improved convolutional neural network," *IEEE Access*, vol. 8, no. 3, pp. 57606–57614, 2020.

[5] M. Sharma, A. S. Jalal, and A. Khan, "Emotion recognition using facial expression by fusing key points descriptor and texture features," *Multimedia Tools and Applications*, vol. 78, no. 12, pp. 16195–16219, 2019.

[6] R. Banerjee, S. De, and S. Dey, "A novel facial expression recognition system using BMCSA based adaptive neuro-fuzzy inference system," *International Journal of Uncertainty, Fuzziness and Knowledge-Based Systems*, vol. 29, no. 06, pp. 791–813, 2021.

[7] M. Beringer, F. Spohn, A. Hildebrandt, J. Wacker, and G. Recio, "Reliability and validity of machine vision for the assessment of facial expressions," *Cognitive Systems Research*, vol. 56, pp. 119–132, 2019.

[8] S. Carole, "North West showcases McGovern drama," *Television*, vol. 54, no. 6, p. 31, 2017.

[9] D. Coulibaly and H. Kempf, "Inflation targeting and the forward bias puzzle in emerging countries," *Journal of International Money and Finance*, vol. 90, pp. 19–33, 2019.

[10] H. Raymond, D. Coulibaly, and L. D. Omgba, "Exchange rate misalignments in energy-exporting countries: do sovereign wealth funds matter?" *International Economics*, vol. 152, pp. 124–144, 2017.

[11] Y.-A. Kim, "Caryl Churchill's seven jewish children and the legacy of the holocaust," *The Journal of Modern English Drama*, vol. 30, no. 2, pp. 69–93, 2017.

[12] D. A. Grier, "A prize, a prediction, and a drama," *Computer*, vol. 53, no. 7, pp. 68–70, 2020.

[13] Q. Li, "Characteristics and social impact of the use of social media by Chinese Dama," *Telematics and Informatics*, vol. 34, no. 3, pp. 797–810, 2017.

[14] I. Petcu, "George Enescu National University of Arts from Iasi. Focus on eastern European stage directors," *Theatrical Colloquia*, vol. 11, no. 2, pp. 189–192, 2021.

[15] H. Yan, J. Lu, and X. Zhou, "Prototype-based discriminative feature learning for kinship verification," *IEEE Transactions on Cybernetics*, vol. 45, no. 11, pp. 2535–2545, 2015.

[16] L. I. Yaqian, S. Zhang, L. I. Haibin, W. Zhang, and Q. Zhang, "Face recognition method using gabor wavelet and cross-covariance dimensionality reduction," *Dianzi Yu Xinxi Xuebao/Journal of Electronics and Information Technology*, vol. 39, no. 8, pp. 2023–2027, 2017.

[17] J. Kalina and C. Matonoha, "A sparse pair-preserving centroid-based supervised learning method for high-dimensional biomedical data or images," *Biocybernetics and Biomedical Engineering*, vol. 40, no. 2, pp. 774–786, 2020.

[18] Z. Xi, Y. Niu, J. Chen, X. Kan, and H. Liu, "Facial expression recognition of industrial Internet of things by parallel neural networks combining texture features," *IEEE Transactions on Industrial Informatics*, vol. 17, no. 4, pp. 2784–2793, 2021.

[19] W. Xie, L. Shen, and J. Jiang, "A novel transient wrinkle detection algorithm and its application for expression synthesis," *IEEE Transactions on Multimedia*, vol. 19, no. 2, pp. 279–292, 2017.

[20] H. Sadeghi and A. A. Raie, "Histogram distance metric learning for facial expression recognition," *Journal of Visual Communication and Image Representation*, vol. 62, pp. 152–165, 2019.

[21] A. Admin, K. KiruthikaS, S. Nithya, B. Poornima, and D. DharanyaS, "Enhancement of cloud user data access security entrusted to AI face recognition techniques," *Journal of Cognitive Human-Computer Interaction*, vol. 2, no. 2, pp. 60–64, 2022.

[22] H. J. Kim, S. H. Jeong, J. H. Seo, I. S. Park, H. Ko, and S. Y. Moon, "Augmented reality for botulinum toxin injection," *Concurrency and Computation: Practice and Experience*, vol. 32, no. 18, Article ID e5526, 2020.

Hindawi
Scientific Programming
Volume 2022, Article ID 3426539, 14 pages
https://doi.org/10.1155/2022/3426539

Research Article

Design of Indoor Lighting Control System for Human Body Signal Acquisition Based on Internet of Things

Yanmin Wu and Xiang Cheng

School of Building Environment Engineering, Zhengzhou University of Light Industry, Zhengzhou 450002, Henan, China

Correspondence should be addressed to Yanmin Wu; 2006121@zzuli.edu.cn

Received 18 June 2022; Revised 29 July 2022; Accepted 10 August 2022; Published 20 September 2022

Academic Editor: Juan Vicente Capella Hernandez

The improvement of microelectronics innovation, programmed control innovation, and correspondence innovation has brought human culture into a universe of electronic data, and different electronic control frameworks are applied to each edge of life. Among them, the intelligent and energy-saving living environment has become more and more popular, and the development of electronic technology has greatly facilitated people's lives. This paper aims to study how to analyze and study indoor lighting control based on the Internet of Things technology and describe the acquisition of human body signals. This paper puts forward the problem of indoor lighting control, which is based on the Internet of Things technology, then elaborates on its related concepts and related algorithms, and designs and analyzes a case of indoor lighting control system. The experimental results showed that 100 orders are normal, and the intelligent lighting node can correctly receive and process the order information and respond accordingly. During the brightness reduction process, the sensitivity and smoothness of the touch screen slider are good, and the brightness reduction is successful.

1. Introduction

The Internet of Things is an emerging technology that, although still being in its infancy, is already being used in various industries. Traditional lighting systems use switches and knobs to control light switches and light levels. With the development of electronic technology, human voice and light control have been widely used in our daily life. But these lighting systems not only are complex to operate, but also consume a lot of energy. By improving people's living standards, people's lives have become more intelligent, and traditional lighting control has been unable to meet people's needs.

Using a smartphone to control home appliances is an advancement of the times, because the remote-control mode of the mobile terminal is no longer limited by the type of remote control. Traditional home appliance switches require corresponding remote controls to operate efficiently. When mobile phone remote control technology is available, the remote controls for all home appliances can be flipped to the side, significantly improving ease of operation.

The innovation of this paper is as follows: (1) this paper combines human body signal acquisition with indoor lighting control and introduces the theory and related methods of Internet of Things technology in detail. It mainly introduces incremental kernel fuzzy clustering algorithm and support vector machine algorithm. (2) In the face of indoor lighting control, after each command is sent 100 times, the number of successful times is recorded and analyzed.

2. Related Work

Indoor lighting has an inseparable relationship with people's lives. With the ceaseless improvement of individuals' expectations for everyday comforts, it is a quest for singularity, beauty, and intelligence in life and work, and the requirements for indoor lighting are also constantly improving. Tan

et al. proposed a sensor-driven human, on top of it lighting framework [1]. Ayaz et al. proposed the plan and execution of another savvy sunshine-based lighting control framework to furnish energy reserve funds in open structures with ordinary lighting frameworks [2]. Karapetyan et al. studied that the Internet of Things (IoT) brings a new paradigm of integrated sensing and actuation systems for intelligent monitoring and control of smart homes and buildings [3]. Mahbub et al. centered around the plan and execution of an insightful independent lighting and ventilation framework that empowers energy-mindful independent lighting, observing temperature, mugginess, carbon dioxide (CO_2) fixation, and exhaust cloud [4]. Beccali et al. analyzed the outputs of several artificial neural networks in relation to different sensor placements by using the measurements in an experimental setup [5]. Jain and Garg examined the presentation and attainability of different sunlight determining techniques and their application in controlling blinds and incorporated lighting frameworks [6]. Kim et al. proposed a characteristic light multiplication framework that gives the sunshine cycle attributes of regular light to keep up with circadian rhythms [7]. Singh et al. have studied developing a complete proof system that requires the development and integration of various technologies that can be used to develop smart homes [8]. However, the insufficiency of these studies is that they do not consider multiple factors and cannot solve the multilevel situation well, so the problem needs to be considered from multiple aspects.

3. Human Body Signal Acquisition Method Based on IoT

3.1. Internet of Things. The Internet of Things is a significant piece of the new age of data innovation and an augmentation of Internet applications. It is the result of the profoundly incorporated advancement of data innovations like sensors, the Internet, and communications. In short, the Internet of Things is the Internet of things connected. The key technologies in the application of the Internet of Things are as follows: sensor technology, RFID technology, and embedded system technology. At present, a large part of the signals processed by computers are digital signals. For analog signals, the computer is not easy to identify; it needs to be converted into digital signals. This can be done by using sensors, so sensors are key in computer applications. Lately, embedded technology has been widely used in smart products [9].

What really drives the rapid development of the Internet of Things is the premise of continuous technological innovation. In the process of developing the Internet of Things, its key technologies include radio frequency identification technology (RFID tag), barcode technology, communication technology, remote sensing technology, and intelligent information equipment.

Usually, the architecture of the Internet of Things is divided into three layers, from bottom to top, the perception layer, the network layer, and the application layer. The overall architecture of the Internet of Things is shown in Figure 1.

The discernment layer is at the lower part of the IoT design. Its principal objective is to interface things to the IoT organization and measure that gather and cycle related state data. It handles these things through sent savvy gadgets like RFID, sensors, actuators, and so forth and sends data to upper layers through layer interfaces [10].

The network layer, also known as the transport layer, is in the middle of the IoT architecture. Devices (hubs, switches, gateways, cloud computing implementations, etc.) as well as various communication technologies (Bluetooth, WiFi, LTB, etc.) are integrated at this layer. Therefore, the network layer is the most important layer in the IoT architecture, and its main function is information transmission.

The three-level engineering is the underpinning of IoT, and it has been planned and executed in numerous frameworks. In any case, the capacities and tasks in the organization layer and application layer are different and complex [11]. To fabricate a general and adaptable IoT multifacet engineering, a help layer ought to be created between the organization layer and the application layer to give information administrations in IoT.

The Internet of Things is widely used in smart industries, smart homes, intelligent agriculture, intelligent management, intelligent transportation, intelligent network, intelligent environmental protection, intelligent security, intelligent medical, etc. It can also be used in many fields such as personal health and government work. The Internet of Things is of great significance to future economic development, social progress, and technological innovation [12].

3.2. Radio Frequency Identification Technology. Radio Frequency Identification (RFID) is a noncontact automatic identification technology that does not require manual operation. It includes three basic devices, a tag, a reader, and an antenna.

3.2.1. Overview of RFID Technology. RFID technology was first used in World War II. Although China started late in RFID technology research, it has begun to catch up. By actively promoting government and related services and businesses, it can independently develop the integration of electronic tags and card reader systems. The technology has been applied to China's "Railway Car Number Automatic Identification System" and has the intellectual property automatic remote identification of a completely independent technical system. In addition to long-range applications, China also applies RFID technology to short-range applications [13, 14].

3.2.2. Working Principle. The reader sends a signal to the tag through the antenna, and the communication electromagnetic response is completed between the reader and the electronic tag through scattering coupling. When the tag receives the electromagnetic wave signal, an induced current will be generated to activate the power switch, and at the

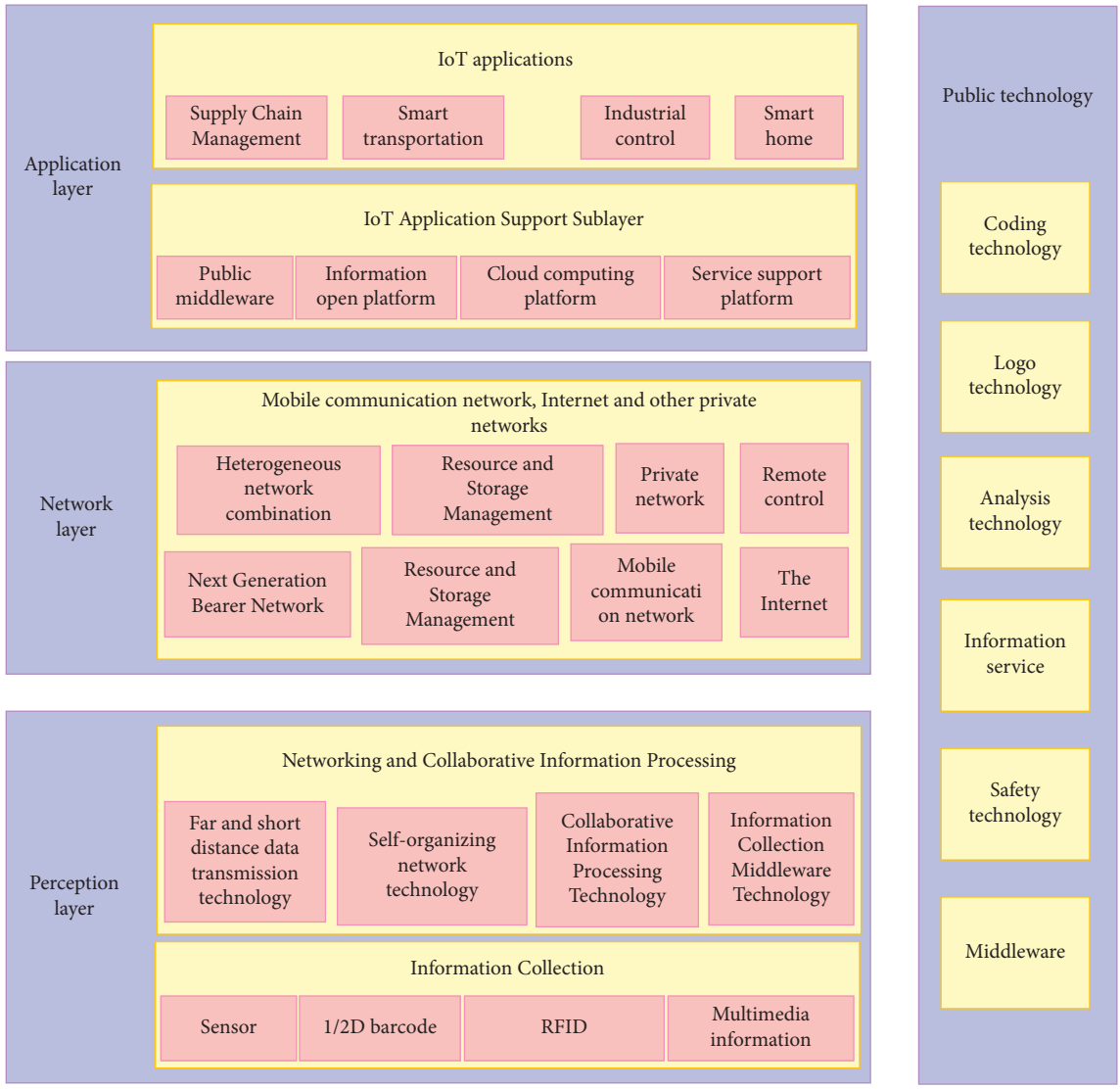

Figure 1: The overall architecture of the Internet of Things.

same time, the encoded information will be sent to the reader, enabling two-way communication between the reader and the tag.

The working principle is shown in Figure 2.

3.2.3. Application of RFID Technology in the System. A device worn on the wrist collects human physiological data and transmits the data in real-time to a nearby RFID reader via integrated RFID. The reader uploads the data to the cloud through the Internet network. An experienced cloud system receives the data and processes it and analyzes the human body based on the results of the data analysis state monitoring [15]. The working process is shown in Figure 3.

3.3. Data Mining

3.3.1. Related Concepts. Data mining is a multistage process, or a step-by-step data mining process, as well as a modeling process. A complete data mining process includes six steps: problem formulation and understanding, data understanding, data preparation and preprocessing, model establishment, model evaluation and optimization, and program implementation, as shown in Figure 4.

3.3.2. Related Algorithms. Information mining incorporates an assortment of insightful strategies to mine and investigate informational collections, then get designs, and apply them. Among them, characterization involves a spot, and the order strategy has additionally been notable by individuals. The most effective method to appropriately group the information will straightforwardly influence the exactness and standard productivity of mining results. Utilization of characterization incorporates a wide assortment of issue spaces, for example, text, mixed media, long-range interpersonal communication, and organic information. Besides, various issues can be experienced in a wide range of situations, characterization is a genuinely different subject, and the basic calculations are intensely reliant upon the

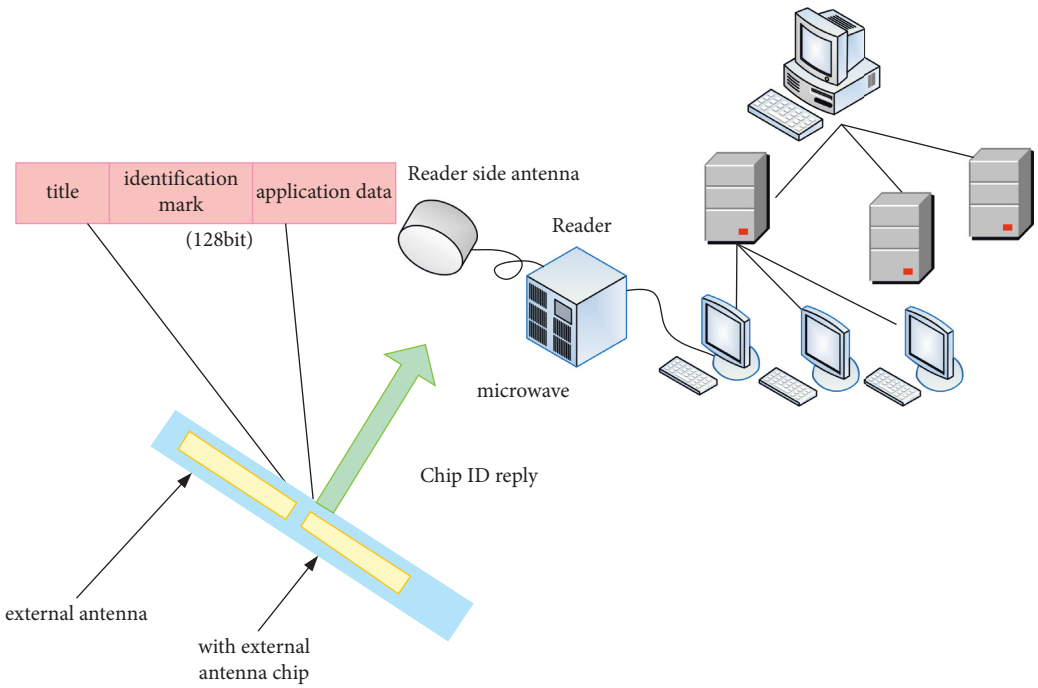

Figure 2: How RFID works.

information area and issue situation. Grouping calculation is additionally one of the significant fields of examination in varying backgrounds [16].

(1) Incremental Kernel Fuzzy Clustering Algorithm. wFCM is one of the most commonly used fuzzy clustering algorithms. For a given dataset $Z = \{z_1, z_2, \ldots z_n\}$, let $\gamma_a\,(a = 1, 2, \ldots, n)$ be the weight of data point z_a. The wFCM method initially randomly selects x different initial cluster centers and calculates the participation of each data point in the cluster center according to formula (1); then, it updates the cluster center according to formula (2) and obtains a new cluster center; and finally, it restarts the process. Repeat until convergence.

$$d_{ca}^2 = \sum_{c=1}^{x} \left(\frac{d_{ba}^2}{d_{ca}^2} \right)^{-1/m-1}, \tag{1}$$

$$v_b = \frac{\sum_{c=1}^{n} \lambda_a \eta_{ba}^{y} z_a}{\sum_{c=1}^{n} \gamma_a \eta_{ba}^{y}}, \tag{2}$$

$$d_{ba}^2 = \left\| z_a - v_b \right\|^2. \tag{3}$$

There are three convergence criteria:

All ι_{ba} are no longer changed; all cluster centers v_b no longer change; satisfy $|B^{e+1}(U, V) - B^{e}(U, V)| < \varepsilon$, where $\mathfrak{E}$ is the convergence accuracy, e is the number of iteration steps, and $J(U, V)$ is the criterion function.

$$J(U, V) = \sum_{b=1}^{x} \sum_{a=1}^{n} \gamma_a \eta_{ba}^{m} d_{ba}^2. \tag{4}$$

The definition of the kernel function is as follows:

$$x(s_a, s_b) = \theta(z_a)^T \theta(z_b), \tag{5}$$

where θ is the mapping function, and $x(z_a, z_b)$ is abbreviated as x_{ab}.

The definition of distance is shown in

$$d_{ba}^2 = \left\| \theta(z_a) - \theta(v_b) \right\|^2 = x_{aa} + x_{bb} - 2x_{ba}, \tag{6}$$

in which

$$x_{aa} = \theta(z_a)^T \theta(z_a), x_{bb} = \theta(v_b)^T \theta(v_b), x_{ba} = \theta(z_a)^T \theta(v_b). \tag{7}$$

Substituting formulas (6) into (1), the calculation formula of the membership degree in the wKFCM algorithm can be obtained, such as

$$u_{ba} = \sum_{c=1}^{x} \left(\frac{\left\| \theta(z_a) - \theta(v_b) \right\|^2}{\left\| \theta(z_a) - \theta(v_c) \right\|^2} \right)^{-1/m-1}. \tag{8}$$

And the update formula of the cluster center is

$$\theta(v_b) = \frac{\sum_{a=1}^{n} \lambda_a \eta_{ba}^{m} \theta(z_a)}{\sum_{a=1}^{n} \lambda_a \eta_{ba}^{m}}. \tag{9}$$

Incremental kernel fuzzy clustering is to use the wKFCM algorithm to perform clustering on the data block Z_t and the clustering result V_{t-1} of the $t-1$th step when clustering at the t ($t = 1, 2, \ldots, N$) step. The incremental clustering model is simple, and a core step is the utilization of the clustering results of existing data blocks, and some improved algorithms are also carried out for this problem. In the general incremental clustering algorithm, when clustering at the t-th step, the clustering center at the $t-1$ step is directly used for subsequent clustering [17, 18].

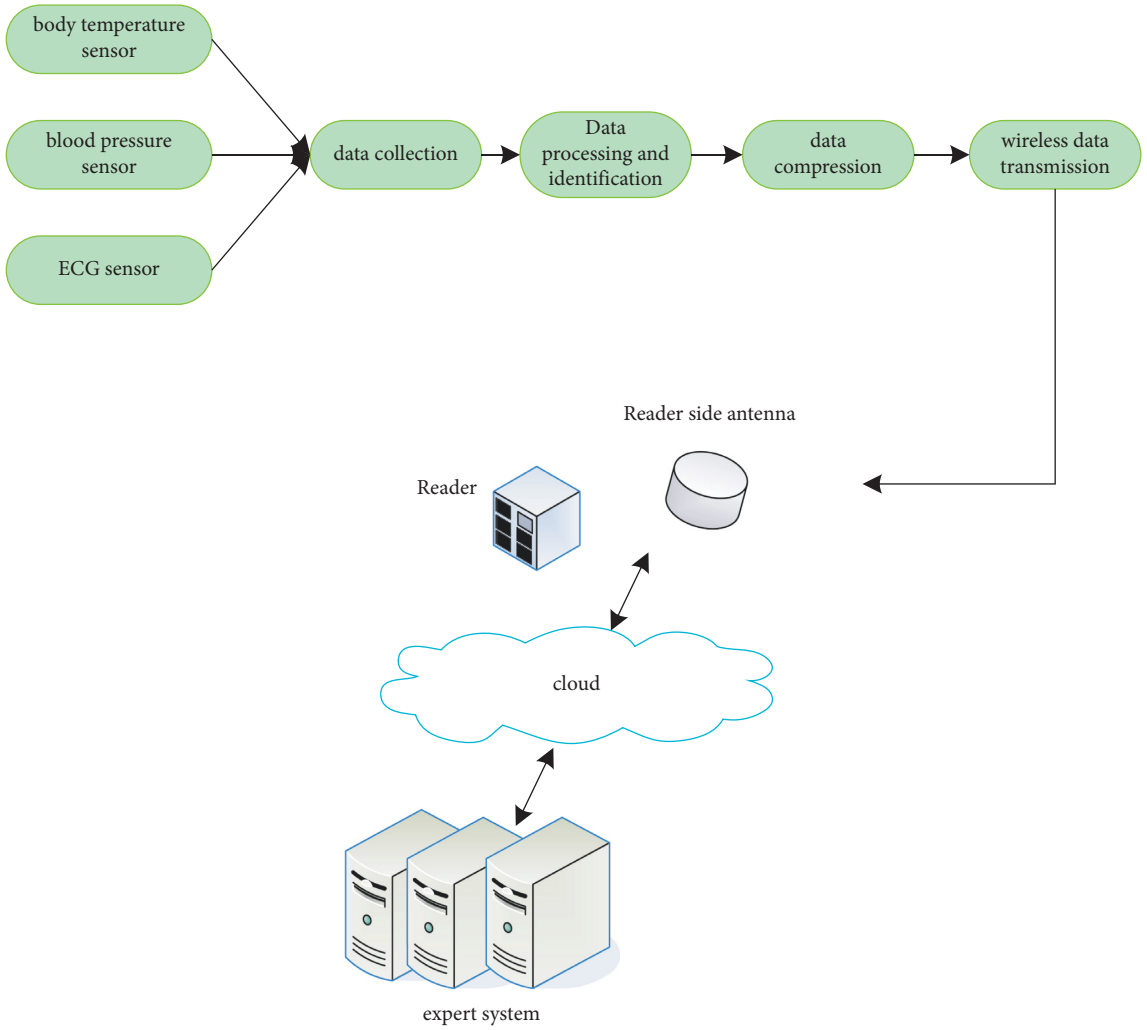

Figure 3: RFID data transmission and processing system diagram.

Let $R_t = \{r_1^t, r_2^t, \ldots r_x^t\}$ represent the set of mapped points from the result of clustering at time $t-1$, and let $r_b^t = \sum_{a=1}^{n_t} \alpha_{ba}^t \theta(z_a^t)$. Since R_t is V_{t-1} obtained by mapping, then it can be obtained by solving the optimization problem shown in

$$\min \left\| \theta\left(v_b^{t-1}\right) - r_b^t \right\|. \tag{10}$$

The cluster centers obtained by the t-th step clustering are expressed as equations (11) and (12).

$$\theta\left(v_b^t\right) = \sum_{c=1}^{n_t} q_{ac}^t \theta\left(z_c^t\right). \tag{11}$$

Among them,

$$q_{ac}^t = \frac{\gamma_c^t \left(u_{ac}^t\right)^m + \sum_{z=1}^{n} \alpha_{sc}^t \gamma_s^{(t,\alpha)} \left(u_{as}^{\alpha}\right)^m}{s \sum_{z=1}^{n_t} \gamma_s^t \left(u_{as}^t\right)^m + \sum_{s=1}^{x} \gamma_z^{(t,\alpha)} \left(u_{as}^{\alpha}\right)^m}. \tag{12}$$

For data point $z_a^t \in Z_t$, its weight value is generally set to 1, that is, $\gamma_a^t = 1$. The calculation of the weight value $\lambda_b^{(t,\alpha)}$ for the transfer point 3 can be obtained by the following formula:

$$\gamma_b^{(t,\alpha)} = \sum_{a=1}^{n_t} \eta_{ba}^t \gamma_a^c + \sum_{s=1}^{x} \eta_{bs}^{\alpha} \gamma_s^{(t-1,\alpha)}. \tag{13}$$

And the membership degree η_a^t of data point z_a^t is calculated as the following formula:

$$\eta_a^t = \sum_{c=1}^{x} \left(\frac{\left\| \theta\left(z_a^c\right) - \theta\left(v_b^t\right) \right\|^2}{\left\| \theta\left(z_a^t\right) - \theta\left(v_c^t\right) \right\|^2} \right)^{-1/m-1}. \tag{14}$$

The calculation method of the membership degree $\eta_b^{(t,\alpha)}$ of the transfer point r_b^t is as the following formula:

$$\eta_a^{(t,\alpha)} = \sum_{c=1}^{x} \left(\frac{\left\| \theta\left(r_b^c\right) - \theta\left(v_b^t\right) \right\|^2}{\left\| \theta\left(r_b^t\right) - \theta\left(v_c^t\right) \right\|^2} \right)^{-1/m-1}. \tag{15}$$

The incremental kernel fuzzy clustering algorithm is a process of continuously reclustering new data blocks and

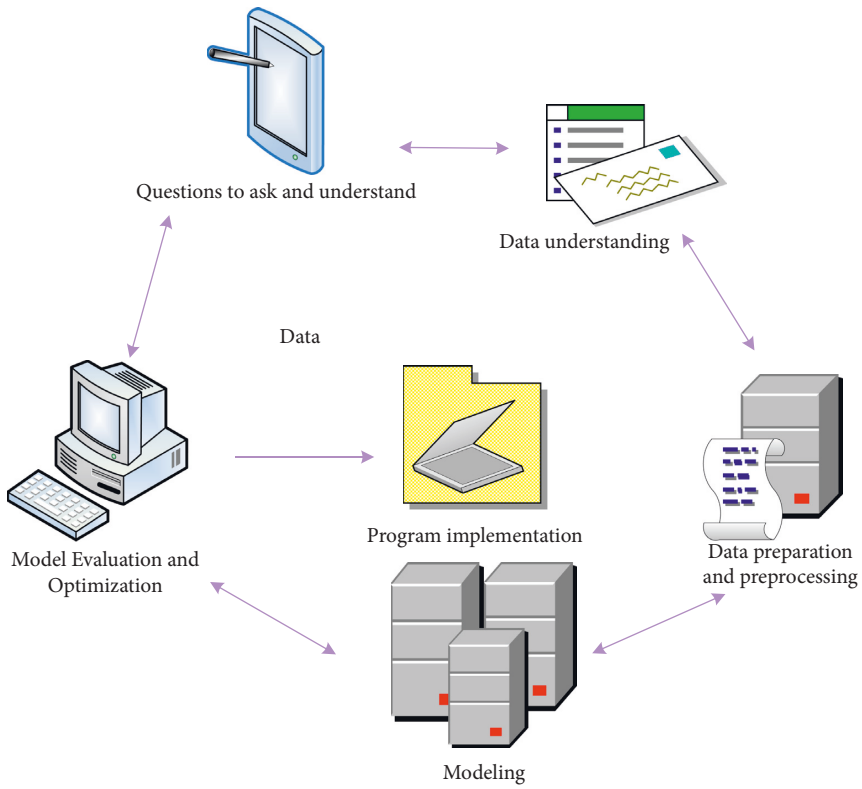

Figure 4: Data mining flowchart.

existing clustering results, and each step of the clustering is the same.

(2) Support Vector Machine. Solving the optimal separating hyperplane is the basis of SVM, so that the training data can be divided correctly, and the geometric spacing is maximized. For linearly separable data sets, the basic idea and the formalized convex quadratic programming problem are shown in formulas (16) and (17):

$$\max_{wb} \delta$$
$$s.t. y_i\left(\frac{w}{\|w\|}\cdot x_i + \frac{b}{\|w\|}\right) \geq \delta, i = 1, 2, \ldots, N, \tag{16}$$

$\delta_{i=} y_i (w/\|w\| \cdot x_i + b/\|w\|)$ defines the geometric space of the hyperplane relative to sample point (x_i, y_i), and $\delta = \min_{i=1,2,\ldots N} \delta_i$ is the minimum value of the geometric space of the hyperplane at all sample points.

$$\min_{\alpha} \frac{1}{2}\sum_{i=1}^{N}\sum_{j=1}^{N}\alpha_i\alpha_j y_i y_j\left(x_i \cdot x_j\right) - \sum_{i=1}^{N}\alpha_i, \tag{17}$$

$$\text{s.t.} \sum_{i=1}^{N}\alpha_i y_i = 0\left(0 \leq \alpha_i \leq C, i = 1, 2, N\right), \tag{18}$$

where the penalty parameter $C > 0$, the most E solution:

$$\alpha^* = \left(\alpha_1^*, \alpha_2^*, \alpha_N^*\right)^T. \tag{19}$$

For nonlinear classification, the interinstance inner product can be turned into a kernel function. For x, k in any input space, we have

$$Z(x, k) = \varphi(x) \cdot \varphi(k). \tag{20}$$

Support vector machines have been widely used in neuroscience and bioinformatics because the algorithm can handle high-dimensional data well. Its main disadvantage is the large amount of calculation and easy overfitting.

3.4. Human Body Signal Acquisition. There are various physiological signals in the human body. According to the nature of electricity, it can be divided into electrical signals, such as ECG, EMG, and EEG, as well as nonelectrical signals such as respiration, invasive blood pressure, noninvasive blood pressure, blood oxygen saturation, respiratory carbon dioxide end point, body temperature, heart rate, and pulse. Since the human body is a complex living body, various physiological signals are affected by various factors such as the human body and the external environment. Therefore, they have features that are not generally marked:

(1) The signal is weak.

(2) The motivation behind why the commotion is solid is that the sign of the human body itself is exceptionally feeble and is effortlessly upset by the clamor. For example, the electrocardiogram of the fetus is mixed with strong noise. On the one hand, the interference

from the electromyogram and power frequency becomes noise.

(3) The recurrence range is by and large lower, then again, actually, the unearthly components of the heart sound sign are marginally higher, and the range of other electrophysiological signals is for the most part lower.

(4) Human physiological signals have strong randomness, not only random, but also immovable.

According to the instability, nonlinearity, and probability characteristics of human physiological signals, different detection methods should be used for different physiological parameters. Since the human body system is very complex and rich in information, human body signal detection technology is very important.

4. Design Experiment of Indoor Lighting Control System

4.1. System Solution Selection. In the mainstream system development in the world today, there are two commonly used software system architectures, namely, CIS structure and B/S structure. The two structures have their own characteristics and are suitable for different system designs. The following is an analysis of the design of intelligent lighting control systems based on the two structures.

The CIS function, the client\server function (Clientl-Server), is a simple software system architecture. This function allocates system tasks reasonably, makes full use of the advantages of client and server hardware resources, and saves the consumption of data communication in the system. Because CIS distributes many tasks to the client for processing and submits them to the server after processing, reducing the workload of the server. Therefore, the function can fully utilize the processing power of the customer and has a higher response speed. At present, the server mainly completes the functions of information coordination and database management. Using this mode of operation, a local fast response network system can be built. The structure of the CS-based smart lighting system is shown in Figure 5(a).

B/S mode is browser\server mode. In this mode, users can access the Internet network through a web browser and exchange information such as text, data, images, and sounds, while a large amount of information data on the network is stored in the server database. In addition to supporting the Web browser function, the client usually does not need any user program and only needs to obtain information from the local Web server. This process is mainly that the browser sends a request to the web server, and the web server obtains relevant information by analyzing the request and communicating with the database, then returns to the browser, and then returns to the user. In B/S mode, almost all software code development and data information processing tasks are completed on the server side. The server is the heart of the system, and its requirements are lower than the server on the client side. The customer development under the B/S mode is mainly web interface development and data communication development, with low customer utilization rate and simple operation [19, 20]. The structure of the intelligent lighting system based on the BS function is shown in Figure 5(b).

In C/S mode, the entire indoor lighting system forms a wireless WiEi local network, and smart devices are wirelessly connected to the system server through WiFi. The user conveys the intention to operate on the server by operating the application software on the electronic device, and the server analyzes and processes it and sends commands to the lighting control terminal.

In B/S mode, the client can be any smart device that supports browsers, and the client communicates with the system server by accessing the Ethernet. The system server communicates with the light control terminal through WiFi wireless, and the server is the bridge connecting the client and the light control terminal.

Through the above comparison, the comparative analysis of the indoor intelligent lighting system in CIS and B/S mode is as follows:

(1) The CIS function is a two-layer structure, and the mobile terminal and the server are directly connected and communicated through WF, and the response speed is fast. B/S is a three-tier architecture. The mobile phone connects to the Internet via WiFi or 2G/3G and exchanges data with the server. It has low speed and long latency.

(2) In CIS mode, the smartphone client provides full functionality for its powerful data processing capabilities. It makes full use of the hardware resources of Android phones and servers to undertake data processing tasks. In B/S mode, a complex server needs to be deployed to take over most data processing tasks, and the processing power of the mobile phone is not fully utilized, which will increase the difficulty and development time.

(3) In C/S mode, a simple, reliable, and secure independent wireless LAN is created. In B/S mode, the server must be connected to the Internet network. Real-time access to the Internet generates a large amount of data traffic in the process of information transmission and interaction, which undoubtedly increases the consumption cost of home lighting applications.

This system is based on home application and should fully consider the needs of simple design, reducing the difficulty of development and maintenance and saving resources. After comparing different modes, choose C/S mode to design the system, which can meet the needs of home lighting.

4.2. System Scheme Design

4.2.1. Hardware Design of Intelligent Lighting Node. The intelligent lighting node provides lighting for the home environment and is the basic part of the system, and its design is related to the realization of the lighting function of the system. This part of the single-chip microcomputer has

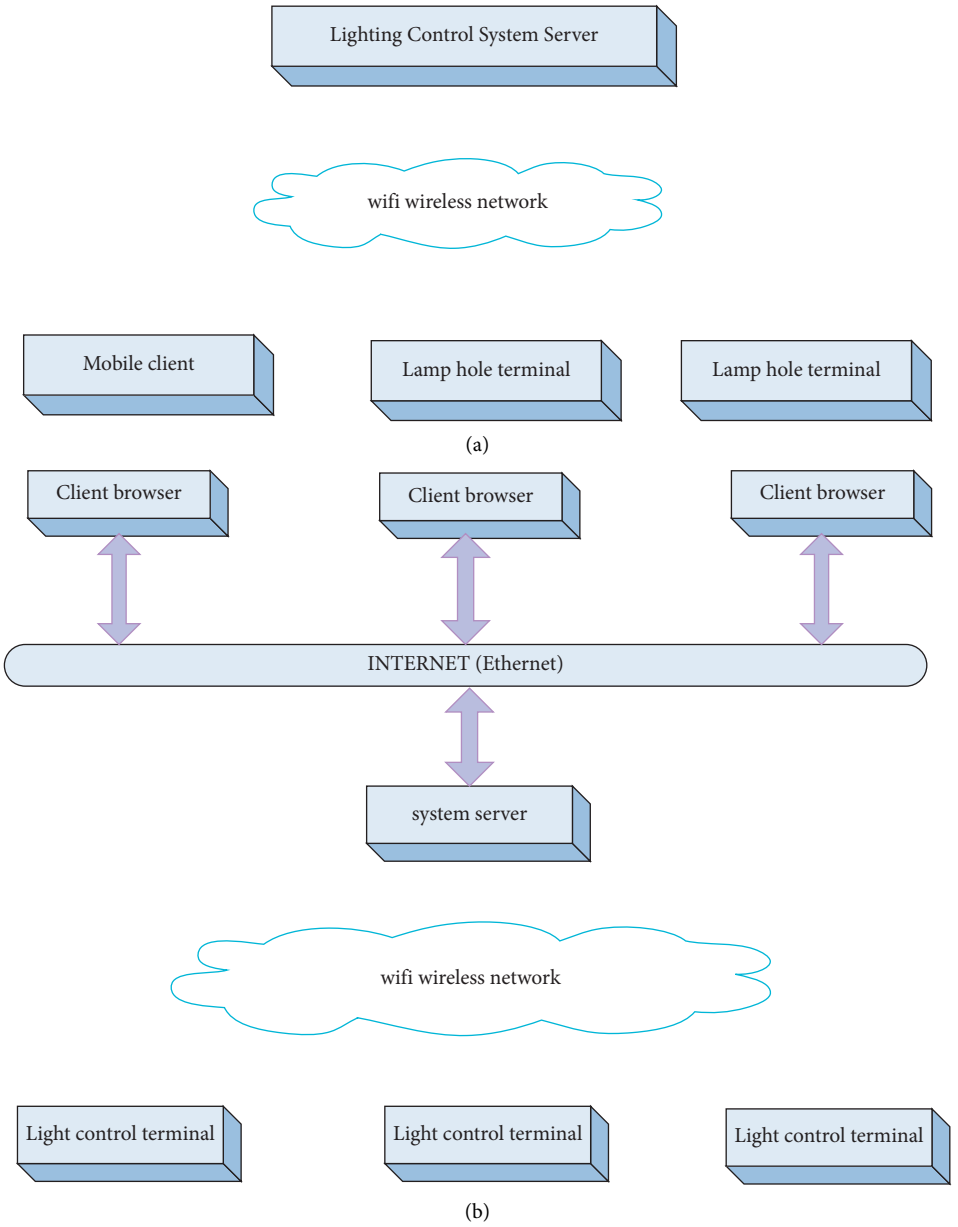

Figure 5: Structure of an intelligent lighting system. (a) System structure diagram based on C/S mode. (b) Structure diagram of intelligent lighting system based on B/S mode.

640 bytes of EEPROM, which is enough to store the ID and status of the lamps and lanterns. It is not necessary to install the EEPROM memory chip of AT24C64. The hardware design block diagram of the intelligent lighting node is shown in Figure 6.

4.2.2. Overall Structural Design. The system is designed with CIS functionality to create a home WiFi lighting network. Develop mobile application software aimed at controlling and implementing home lighting via mobile phone. The general schematic graph of the framework is displayed in Figure 7.

4.2.3. System Function Design. The system takes the home as the background and the central control as the goal and evenly manages the home lighting through electronic equipment, which solves the traditional constant on-off control and the inability to reduce the brightness of lamps. The overall realization function of the system is divided into control function and management function.

(1) Control Function. The control function is performed by sending control commands to the AP server through the mobile phone client software, and the AP server sends the control commands. The details are shown in Figure 8.

The specific control functions are as follows:

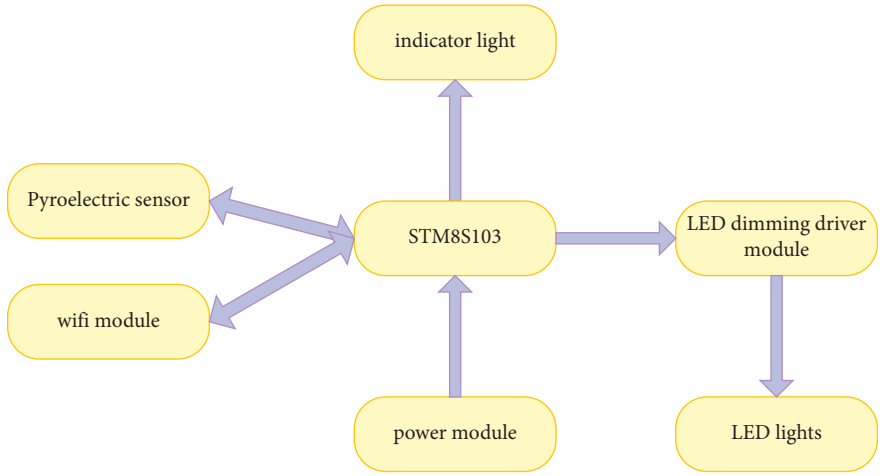

Figure 6: Block diagram of smart lighting node design.

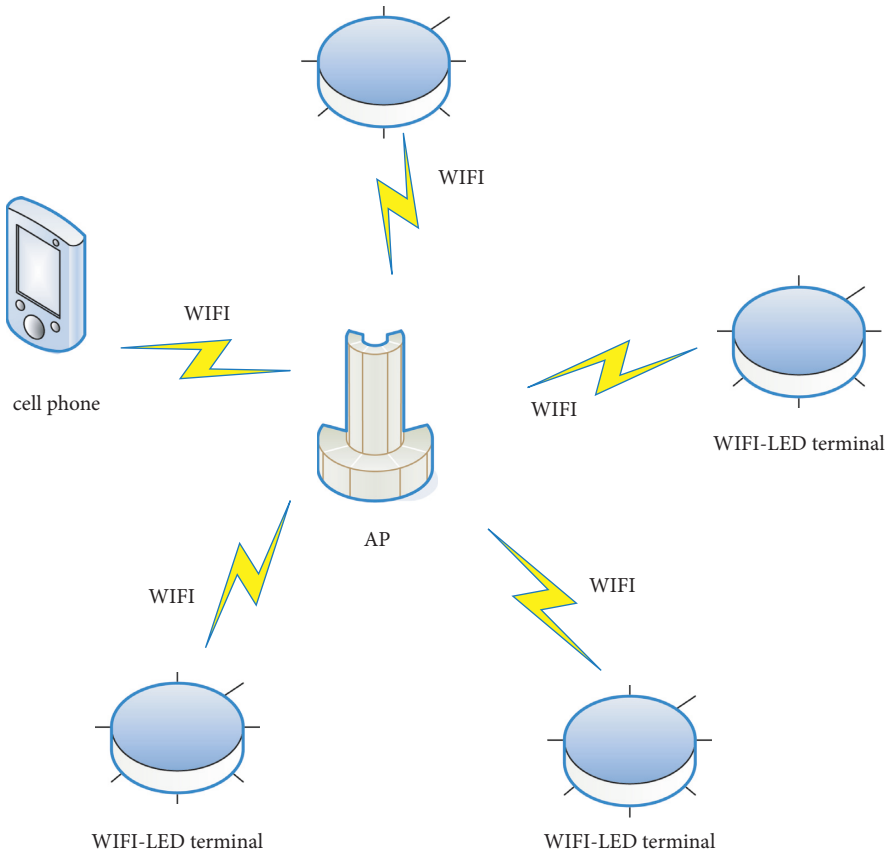

Figure 7: Schematic diagram of intelligent lighting system based on human body signal acquisition.

Switch light function: through the mobile client software, you can turn on and off a single light, turn on and off the group where the light is located, and turn on and off all lights.

Dimming function: this system can reduce the brightness of LED lights through PWM waves. It adjusts the brightness of the WiFi LED light from 20% to 100% and continuously adjusts it from 20% to 100%. When the light is off, the brightness can be preset to decrease, and the preset brightness is displayed when the light is on.

Status refresh function: after the client software exits, the current lighting information of each lamp will be maintained.

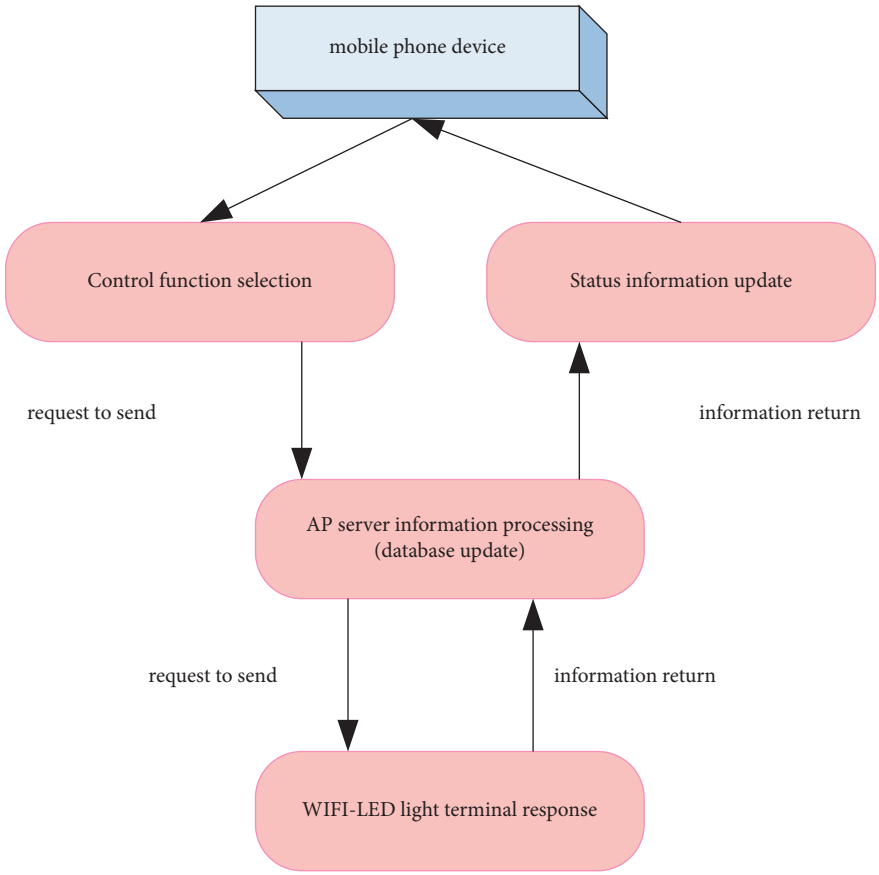

Figure 8: Control function realization flow chart.

(2) Software Design of Lower Computer. Each smart lighting node has its own ID and has the functions of switching lights on and off, adjusting lights, and storing light information. After the system is initialized, first turn on the WiFi module to check whether the WiFi module is working normally. After the module is started, it is connected to the AP server. At this time, the LED light will indicate whether the AP is turned on. After the system starts to work, it first receives information, analyzes and processes the information, and then sends the returned information. The software flow chart of the intelligent lighting node is shown in Figure 9(a).

The AP server receives the information of the intelligent lighting node and the mobile phone control terminal, processes and relays it accordingly, and stores the information of the LED light node at the same time. The information processing flow chart is shown in Figure 9(b).

Infrared pyroelectric sensor: when people enter the detection range, the device outputs a high level to turn on the indoor LED lights. When people leave the detection range, the LED lights go out. The PA3 port is the input end of the HC-SR501 sensor.

4.3. Overall Test of Intelligent Lighting System. In this test, a smartphone was used to send commands to the number and group of lights and then to change and turn off the lights of individual lights, recording the corresponding data. There are three types of lamps, that is, A, B, and C, and lamps A and B are defined as a group. After each command is sent 100 times, the number of successes is recorded, and the test data records are shown in Table 1. In the brightness reduction test, the brightness of the two lamps was 35% and 75%, respectively, and the corresponding PWM waveforms are shown in Figure 10.

Test analysis: after the test is completed, 100 times of commands are issued normally, and the intelligent lighting node can correctly receive and process the command information and respond accordingly. During the brightness reduction process, the sensitivity and smoothness of the touch screen slider are good, and the brightness reduction is successful. When a group of lights is turned on and off, the C light is not in the group, and the display data is 0, indicating that the group switch is working properly.

Test results: the intelligent lighting system basically realizes sending and receiving commands, intelligent lighting nodes with light switches, group light switches, and all lighting switches and dimming functions of the lamps meet the design requirements.

5. Discussion

The study analyzed how to research the indoor lighting control based on the human body signal acquisition based on the Internet of Things technology. The technical concepts

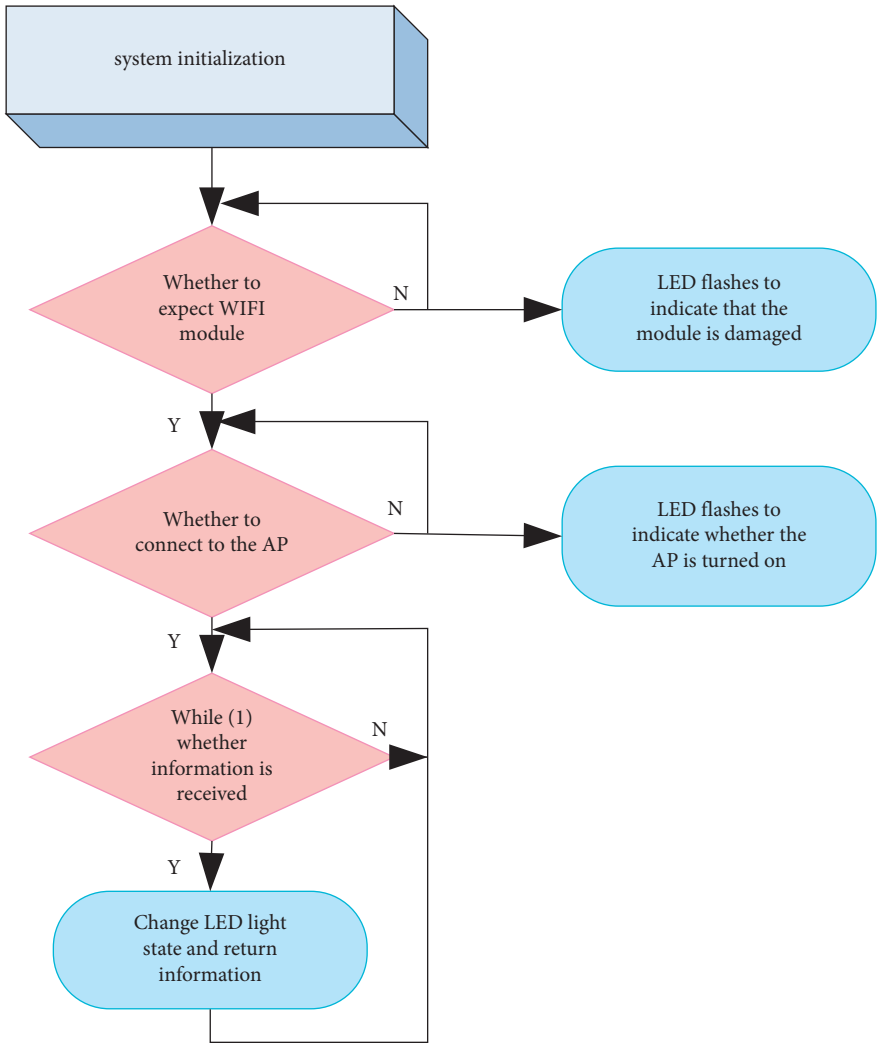

(a)

Figure 9: Continued.

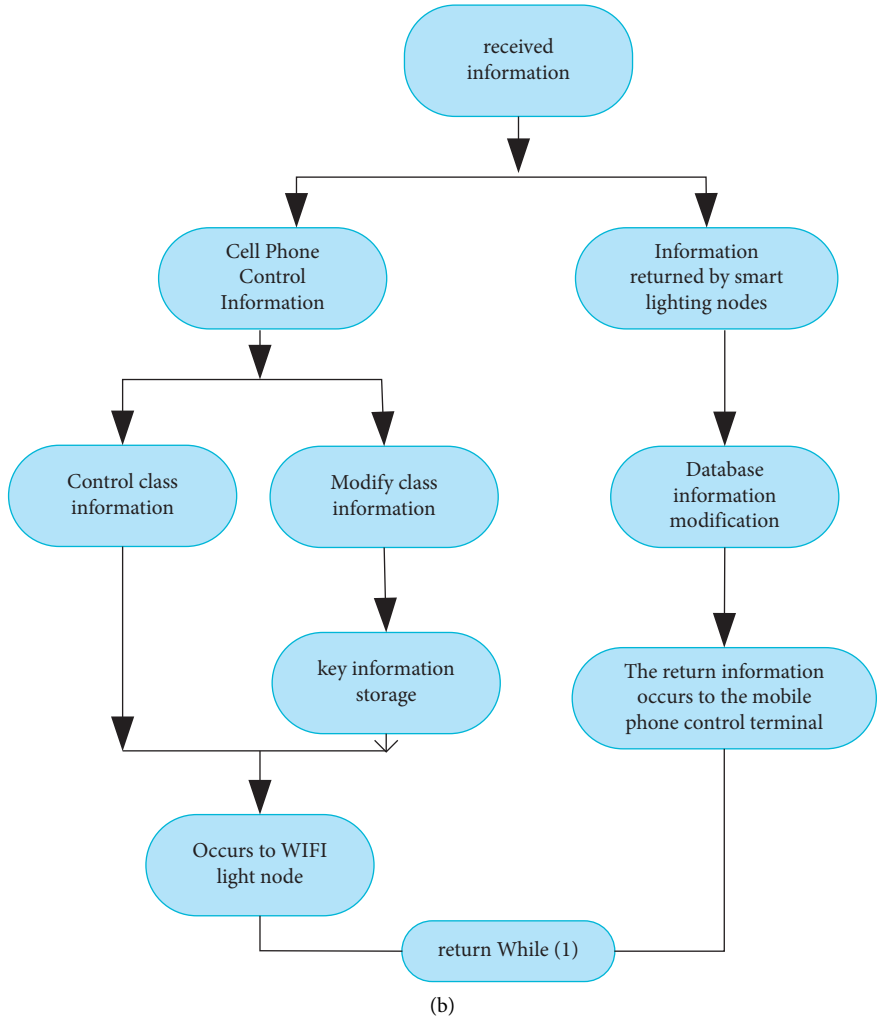

Figure 9: The software flow chart of the lower computer. (a) Flow chart of intelligent lighting node software. (b) Information processing flow chart.

Table 1: Overall test data recording form.

Test content	Single light on	Single light off	Dimming	Group open one group	Group off one group	Fully open	All closed
A lamp (one set)	100	100	100	100	100	100	100
B light (one set)	100	100	100	100	100	100	100
C lamp	100	100	100	0	0	100	100

and algorithms of the Internet of Things are expounded, the incremental kernel fuzzy clustering algorithm is studied, and the support vector machine is explored. It also analyzes the applicability of IoT technology in indoor lighting control system through experiments.

Most of the traditional indoor lighting control systems build a lighting network by laying wires and use fixed switches for control, which increases the complexity and difficulty of construction. In addition, there are problems such as chaotic wiring and unsightly overall effect, which seriously affects the application of lighting systems. With the advancement of science and technology, various wireless transmission technologies have developed rapidly, and technologies such as infrared and WiFi have become increasingly mature and widely used.

Through experimental analysis, this paper shows that when the pyroelectric infrared sensor is activated, it will simulate a person entering this state. When someone enters, the light will be automatically turned on, and when no one enters, the light will not be turned on. When the infrared pyroelectric sensor is off, the light cannot be turned on whether or not someone enters. In addition, the control end of the pyroelectric sensor designed in this paper adopts two ways: inside the door and outside the door. After the test, when only one pyroelectric induction unit senses someone, the light will not be turned on, and only two pyroelectric

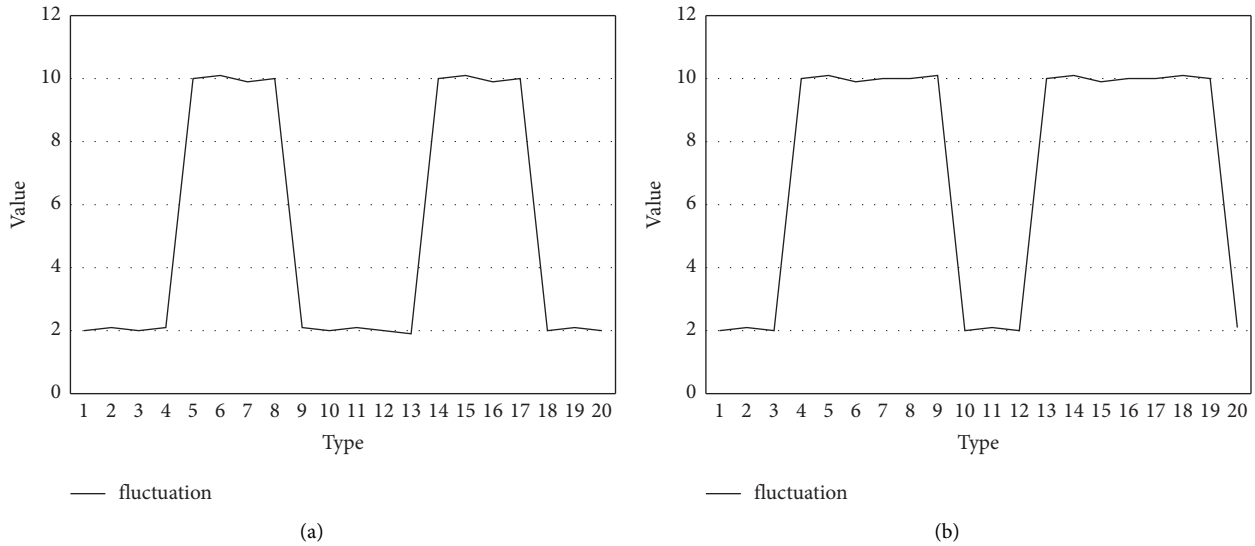

Figure 10: PWM waveform diagram. (a) Brightness 35%. (b) Brightness 75%.

induction units will light up continuously. After the induction ends, the light is turned on. The test results meet the design requirements and achieve the design goals.

6. Conclusions

The Internet of Things combines various information detection equipment, computing equipment, objects, and people with the Internet to establish a large-scale operation network. The connection between people, machines, and things can be interconnected anytime and anywhere. In this paper, a uniform light environment distribution model for indoor lighting is established, and the output stability of intelligent control of indoor lighting uniformity is analyzed to improve the softness of indoor lighting. It adopts the optical background extraction method to realize the intelligent control of indoor lighting uniformity. The smart home lighting system contains a variety of modern technologies, and the design and learning process is difficult. Due to the limited research time and the lack of own experience, the system design work can be improved and perfected.

Data Availability

No data were used to support this study.

Conflicts of Interest

There authors declare that there are no potential conflicts of interest in this study.

Acknowledgments

This work was supported by the Key Scientific and Technological projects of Henan Science and Technology Department (no. 222102210086).

References

[1] F. Tan, D. Caicedo, A. Pandharipande, and M. Zuniga, "Sensor-driven, human-in-the-loop lighting control," *Lighting Research and Technology*, vol. 50, no. 5, pp. 660–680, 2018.

[2] M. Ayaz, U. Yücel, K. Erhan, and E. Ozdemir, "A novel cost-efficient daylight-based lighting system for public buildings: design and implementation," vol. 28, pp. 60–70, 2020.

[3] A. Karapetyan, S. C. K. Chau, K. Elbassioni, S. K. Azman, and M. Khonji, "Multisensor adaptive control system for IoT-empowered smart lighting with oblivious mobile sensors," *ACM Transactions on Sensor Networks*, vol. 16, no. 1, pp. 1–21, 2020.

[4] M. Mahbub, M. M. Hossain, and M. S. A. Gazi, "IoT-Cognizant cloud-assisted energy efficient embedded system for indoor intelligent lighting, air quality monitoring, and ventilation," *Internet of Things*, vol. 11, no. 2020, pp. 100266–100326, 2020.

[5] M. Beccali, M. Bonomolo, G. Ciulla, and V. Lo Brano, "Assessment of indoor illuminance and study on best photosensors' position for design and commissioning of Daylight Linked Control systems. A new method based on artificial neural networks," *Energy*, vol. 154, no. 1, pp. 466–476, 2018.

[6] S. Jain and V. Garg, "A review of open loop control strategies for shades, blinds and integrated lighting by use of real-time daylight prediction methods," *Building and Environment*, vol. 135, no. MAY, pp. 352–364, 2018.

[7] K. M. Kim, Y. W. Kim, S. T. Oh, and J. H. Lim, "Development of a natural light reproduction system for maintaining the circadian rhythm," *Indoor and Built Environment*, vol. 29, no. 1, pp. 132–144, 2020.

[8] R. Singh, K. Thakur, and A. Gehlot, "Internet of things based on home automation for intrusion detection, smoke detection, smart appliance and lighting control[J]," *International Journal of Scientific & Technology Research*, vol. 8, no. 12, pp. 3702–3707, 2019.

[9] B. Subba, S. Ghalley, and C. Wangchuk, "Design and simulation of IoT and z based smart lighting system," *IARJSET*, vol. 7, no. 9, pp. 31–37, 2020.

[10] K. B. Martin and W. Mills, "Human centric building control system[J]," *International Journal of Engineering & Technology*, vol. 8, no. 4, pp. 25–28, 2017.

[11] L. Bellia and F. Fragliasso, "New parameters to evaluate the capability of a daylight-linked control system in complementing daylight," *Building and Environment*, vol. 123, no. oct, pp. 223–242, 2017.

[12] S. Ito, T. Iwata, T. Taniguchi, and Y. Arai, "Implementation and testing of gradation blind control system Accounting for shadow and hvac load[j]," *Journal of Environmental Engineering*, vol. 83, no. 746, pp. 375–384, 2018.

[13] H. A. Dung, N. M. Cuong, and N. P. Kien, "Multi-directional light sensing using A rotating sensor," *Advances in Science, Technology and Engineering Systems Journal*, vol. 5, no. 6, pp. 221–227, 2020.

[14] R. Liu, "Design of photometric adjustment system for lighting equipment in buildings based on fuzzy PID control[J]," *IPPTA: Quarterly Journal of Indian Pulp and Paper Technical - A*, vol. 30, no. 7, pp. 107–113, 2018.

[15] A. K. Jha, A. B. Bababe, and I. Ranjan, "Smart street light management system using LoRa technology[J]," *International Journal of Science and Research*, vol. 6, no. 3, pp. 2349–2352, 2017.

[16] M. Cannistraro and E. Bernardo, "Monitoring of the indoor microclimate in hospital environments a case study the Papardo hospital in Messina," *International Journal of Heat and Technology*, vol. 35, no. 1, pp. S456–S465, 2017.

[17] J. H. Choi, "Investigation of human eye pupil sizes as a measure of visual sensation in the workplace environment with a high lighting colour temperature," *Indoor and Built Environment*, vol. 26, no. 4, pp. 488–501, 2017.

[18] R. U. Gutierrez, J. Du, N. Ferreira, A. Ferrero, and S. Sharples, "Daylight control and performance in office buildings using a novel ceramic louvre system[J]," *Building and Environment*, vol. 151, no. MAR, pp. 54–74, 2019.

[19] M. M. A. S. Mahmoud, "Automated smart utilization of background lights and daylight for green building efficient and economic indoor lighting intensity control," *Intelligent Control and Automation*, vol. 12, no. 01, pp. 1–15, 2021.

[20] P. eonghyeok, H. Kitae, Y. Sohyun, and K. Gyouhyung, "Preferred E-mirror luminance levels for diverse ambient light conditions," *Proceedings of the Human Factors and Ergonomics Society - Annual Meeting*, vol. 63, no. 1, p. 2255, 2019.

Hindawi
Scientific Programming
Volume 2022, Article ID 5891994, 14 pages
https://doi.org/10.1155/2022/5891994

Research Article

A Quasiexperimental Study on Process Verification of the Animation Teaching System under the Background of Animation-Related Majors

Xuefeng Wang,[1] Mohd Shahrudin Abd Manan,[2] Saiful Hasley Bin Ramli,[3] and Mohd Hazwan Mohd Puad[4]

[1]*Faculty of Design and Architecture, University Putra Malaysia, Kuala Lumpur, Malaysia*
[2]*Department of Architecture, Faculty of Design and Architecture, Universiti Putra Malaysia, Kuala Lumpur, Malaysia*
[3]*Department of Industrial Design, Faculty of Design and Architecture, Universiti Putra Malaysia, Kuala Lumpur, Malaysia*
[4]*Department of Science and Technical Education, Faculty of Educational Studies, Universiti Putra Malaysia, Kuala Lumpur, Malaysia*

Correspondence should be addressed to Mohd Shahrudin Abd Manan; am_shahrudin@upm.edu.my

Received 10 June 2022; Revised 29 July 2022; Accepted 16 August 2022; Published 19 September 2022

Academic Editor: Juan Vicente Capella Hernandez

This article reports the results of an experimental study during the participation in the animation teaching system (ATS) by students of Digital Media Art at Kunming University (KU) and by students of digital media technology at Hunan University of Science and Engineering (HUSE), respectively. The experimental results are used to observe whether the students' scores on their work differed after using the ATS in different program contexts. The type of experiment in this study was quasiexperiment, with one experimental group and one control group at each university. Students from both universities participated in a pretest and a posttest. In accordance with the purpose of the study, we focused data analysis on the same group of posttest scores at both universities for analysis, i.e., two experimental groups for between-group comparisons and two control groups for between-group comparisons. The Mann–Whitney *U* test was used for comparative and quantitative analysis. The study examined that the experiment's digital media art students outperformed the digital media technology students. The article concludes with a discussion of how the ATS should be improved and enhanced for application in different animation-related majors.

1. Introduction

Chinese animation industry experienced a highlight moment in the last century and then went through a long period of silence. After entering the 21st century, the influx of foreign animation works gradually activated the development of the Chinese animation industry. The development of the animation industry accompanies the reform of animation education. Professional talent training in Chinese universities depends on the respective schools' situation [1–3]. From the perspective of the characteristics of the animation major itself. The positioning of the training of talents will be influenced by professional aspects [4], such as academic-oriented talent cultivation and professional skill-oriented talent cultivation. In fact, after graduation, most animation talents work in the industry's professional companies [5], rather than a large number doing academic research. Moreover, talent cultivation is also influenced by other factors, such as faculty strength and the dissemination and preservation of the region's culture. Ma [6] explained the opinion that universities have a sense of responsibility in the inheritance of intangible cultural heritage.

1.1. Chinese Animation Education. The conflict, which exists between talent cultivation in animation education and market needs, is an unavoidable problem. Haibin [7] mentioned that the most critical issue for Chinese animation

education is cultivating talent for the industry. The market's expectation for talent is no longer a single demand in China. The era when animators could do animation work by mastering software operation skills has quietly left. Employers hope there will be more intelligent, thoughtful, creative, and problem-solving interdisciplinary talents for the industry. Zhang and Meng [8] put forward the classification training of students and the establishment of the "7-2-1" training mode, which trains 70% of students into application-oriented talents, 20% into interdisciplinary talents, and 10% into top research talents. According to Zhang and Meng's research, the training of animation students in colleges and universities should be geared toward the direction of application-oriented talents, with academic talents accounting for only a tiny portion. Based on the author's previous research of the current station of Chinese animation majors in universities. The number of animation undergraduate majors in China tends to be stable without a significant increase, only a slight degree of elimination and change. In other words, most of the animation programs in these universities have survived the tests and requirements of the industry.

Currently, in Chinese animation education, University-Enterprise Cooperation is regarded as a new professional reform idea to reform animation specialty. The corresponding subject and teaching system should also be updated and studied in this context. For instance, Haibin [7] reported a study about an interdisciplinary type of talent cultivation mode in animation education in the School of Art and Design of Xi'an University of Technology. Zhang [9] studied Chinese animation higher education from four aspects: the curriculum design, the reconstruction of teacher construction, the implementation of practice links, and the launch of the international forums, respectively. Then posed the cultivation of "vision & insight" in animation education to explore a replacement scale for a more well-rounded education, then widely explore how to succeed. Many of the above factors directly determine that further study tends to be applied research. Dong and Zhang's research premise is that students already have the corresponding knowledge of animation and have a definite understanding and mastery of the creation basis of animation and the source of creativity. However, these patterns may be helpful in the higher grade. In the lower grades of beginners, we still need to focus on animation creation fundamental research to meet the novices in the learning needs.

The animation industry belongs to the category of the cultural and creative industry. One of the critical stages in animation creation that determines the quality of the work is the pre-production stage [10]. In 2010, Xing Chen, Jiang Wei, and Xue Huang surveyed 20 animation companies in Hangzhou, China. During their interview, the lack of creative talents is the critical reason for most Chinese animations' failure [11]. When beginners start to create animation, the main problem they face is the generation of ideas and the integrity of the storyline [12,13]. For example, as an animation story's core planner, the coordination and command ability thought the entire animation. In Chinese universities' animation design majors, there is often such a situation that there are many students with fine art skills and hand-painted ability, but their story composing ability is relatively low [14]. Thus, it is still a difficult task to balance both. Some previous researchers have considered solving this problem in the existing animation education research, which concerns applying design thinking to practical teaching and learning [15].

However, there is not just one design thinking model in the field of design thinking research, such as Stanford University's design thinking model [16] and the Double Diamond Theory [17] proposed by the Design Council [18] in the UK. The purpose of Chou is to introduce the design thinking method and apply it to social entrepreneurship projects [19]. In a study, Zhao Tianjiao, Sun Han, and Li Xiang apply Stanford's design thinking model to animation design to obtain a helpful method to get more creative ideas for animation production [20]. Diamond Theory is also a basic analytical framework for analyzing the opportunities and challenges that the Chinese animation industry faces. Based on this, it puts forward the Chinese animation industry's competitive advantages, hoping it will offer a reference for improving its international market competitiveness [21]. These well-established and long-established design models certainly have excellent merits and also be applied in varied fields, but their relevance in animation creation is still lacking. In this study, we also apply design thinking to teaching animation. However, compared to previous studies, the innovation in this study is to develop different design thinking formulas based on the structure of stories in animation creation. And the creative approaches are integrated into the creative process.

In this study, another issue concern that we not only focus on animation majors but also include animation-related majors. The animation majors in Chinese universities are not only the 346 existing ones, a number that the authors counted in their 2020 study based on data published by the Chinese Ministry of Education. If animation-related majors were covered, this total could reach the 1230 university faculties [22] offering animation-related majors. The branches of animation-related majors vary from university to university, with some differences in the way students are trained and the direction they are shaped. Animation-related majors include film and television postproduction, comics, digital media art, and digital media technology [23]. Therefore, this study focuses on digital media art and digital media technology students. The students involved in the experiment differ in their thinking patterns and their drawing techniques. The students of Kunming University (KU) belong to digital media art. The students of this college are characterized by having taken the corresponding art skills training before entering the university. Their admission process is to take the related art general examination [24] before taking the Chinese college entrance examination [25]. In contrast, students from Hunan University of Science and Engineering (HUSE) did not take any art skills training before entering the university and directly took the Chinese college entrance exam. The different entrance methods also reflect the difference in the students of the professional

course at the two universities during their four years of college. The above issue is also a key reference that we will consider when choosing the experimental site.

1.2. The Animation Education System (ATS). The animation teaching system (ATS) is a teaching and learning process (see Figure 1) designed for beginners in animation, expecting to effectively solve the problems teachers and students encounter in the teaching and learning process. The ATS in the context of the educational environment in China: an adoption of a coherent ATS by integrating coordinated design thinking (DT) and creative methods (CM) approach into animation pedagogy (AP) can cultivate creative idea development and problem-solving skills among animation students. As a whole, it is to help students to get started with animation creation quickly.

CMs were selected based on the aspects involved in the precreation of animation. In this study, we selected a total of five creative methods. The projects in precreation, including story ideas, storyboard design, and art design, are fixed. Therefore, we recommend the creative methods that are suitable to be applied in each segment in ATS. Animation creation is teamwork, so brainstorming is applied during collective discussion within the group, and the operation follows the existing steps. The "5W1H" determines the story's time, place, characters, main events, and other information. Instead of using the original meaning, the method redefines each item in the context of animation creation. Causal Layered Analysis (CLA) is mainly used in plot analysis, primarily to analyze the storyline's cause-and-effect relationships and logical relationships. Mind mapping is used in conjunction with other methods, such as brainstorming and "5W1H." The purpose of Synectics is to reduce the difficulty of creation by converting unfamiliar information to familiar by analogy. There is no fixed order or combination of the above-mentioned creative methods in ATS, and they are all used flexibly according to the creator's needs.

Furthermore, to understand the main workflow of the preproduction, one of the main aspects is to address the students in creativity and storyline design. Hence, assessing students' creation results focused on storyboarding and creativity. The assessment technic we adopt is the Consensual Assessment Technique (CAT).

2. Methodology

The ATS in this study wanted to use design thinking at the beginning of the design as a strategy for students to effectively organize the whole precreation in various matters, listing the problems in concrete and detail. Then, in solving different problems, suitable creative methods are used as aids to solving each problem in a targeted manner. In the actual teaching process, the Socratic question-and-answer method [10] is used to help students find the problems that need to be solved. The coevaluation technique can be referred to in the final evaluation of the work to assess the results. The research question in this study was whether students' outcomes in the ATS experiment and normal teaching (NT) process would vary across professional backgrounds. So the choice of the experimental site should not be limited to animation majors in professional colleges and universities but should also include universities that provide animation-related majors. This decision is because students in related majors face more learning problems than in professional institutions. Therefore, the idea of this study is firstly to study the combination of animation education with design thinking and creative methods and, secondly, to choose two universities that offer animation-related majors as the experimental location to fulfill the ATS verification. The methodological part of the study contains three sections: experimental design, animation pedagogy module design including NT and ATS, hypothesis and subhypothetical questions, and data analysis.

2.1. Experiment Design. The process verification for ATS is that we need to be in an authentic teaching process. Therefore we choose the method suitable for this study according to the actual needs. A quasiexperiment is an experiment in which the researcher cannot choose subjects. The majority of experimental studies in pedagogy are quasiexperiments [26]. Quasiexperiments are most to be expected to be conducted in field settings where the arbitrary assignment is difficult or impossible. In this study, we chose two naturally occurring classes so that individuals were not randomly divided, and the experimental procedure was accurately described as a nonequivalent group design [27]. Such experiments are used to assess treatment effects, such as psychotherapy or educational interventions [28]. Therefore, we used quasiexperiments to achieve the study.

The operation of this experiment was completed in March and April of 2021 in Kunming and Yongzhou, respectively. The research site in this study is in universities and colleges in mainland China that offer animation programs. Therefore, the main consideration in the research process is the problems and the current situation in the region. Moreover, the teaching quasiexperimental activities conducted in two of these universities were selected. Two naturally occurring classes of this major in their respective schools were chosen for the study. A total of two majors from two universities were invited to participate in the experiment. Two natural classes of the same major in each university were randomly assigned as the experimental group (EG) and the control group (CG).

Kunming University (KU) is located in Kunming, Yunnan Province, China (shown in Figure 2 location 1), and the students of this university have a background in digital media art. The experimental group consisted of 27 students, and the control group consisted of 20 students. Confirmed by the school's teachers, the class was randomly assigned when recruiting students. However, in their sophomore year, some students choose to transfer to other majors or leave school, resulting in the unequal number of students in each group encountered in our current experiment. In addition, the university's two groups of students are directly enrolled in the university after taking the fine art examination and the college entrance examination.

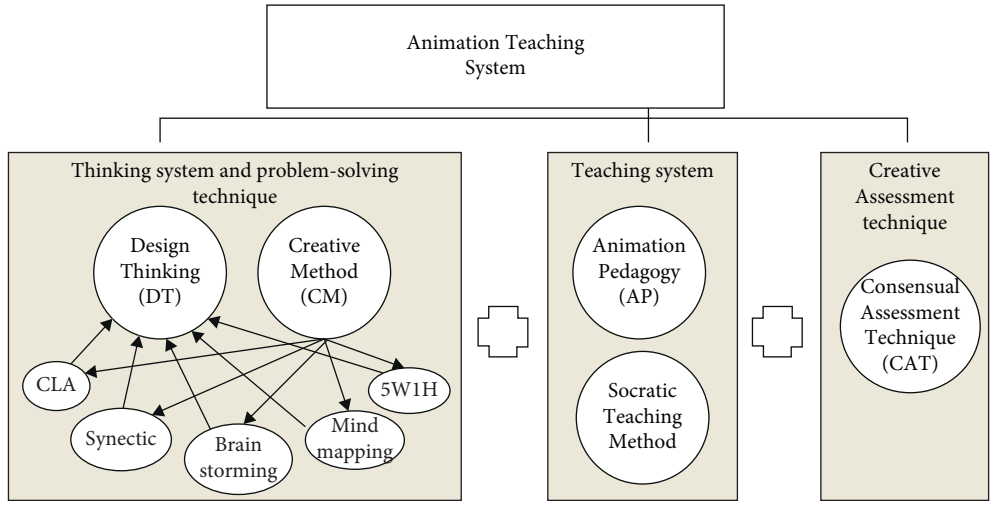

Figure 1: The animation teaching system (ATS) diagram (*Source*: author 2021).

Figure 2: The experiment locations in China (*Source.* author 2021).

Hunan University of Science and Engineering (HUSE) is located in Yongzhou, Hunan, China (shown in Figure 2 location 2), and the students' program background is digital media technology. The experimental group consisted of 35 students, and the control group consisted of 18 students. The two groups at HUSE were slightly more unusual than those at Kunming. The university's class size was set at 40 students per class, but the planned two and a half classes were reduced to one class due to a decrease in applicants that year. Therefore, we chose an alternative class for the control group in the experiment. The case of the substitute class is the same grade with the same major. The experimental group entered the university directly after taking the college entrance examination in this university. The students in the control group entered junior college after the college entrance examination and then reentered the university to improve their academic background. The objective presence factors are detailed in Table 1.

The students in control and experimental groups were taught the regular basic expertise to ensure that all

Table 1: Essential information and distinctions for participants.

	KU	HUSE
Major	Digital media art	Digital media technology
Differences in students' abilities	Students already have art skills before entering college	Students do not have art skills before entering college and will need to learn art skills when they enter their first year of college
Location	KU is located at the provincial level of the western part of China.	HUSE is located in a prefecture-level city in the central region of China
The difference in course length	Each class is 45 minutes long, with four consecutive classes per session.	Each class is 45 minutes long, with two consecutive classes per session

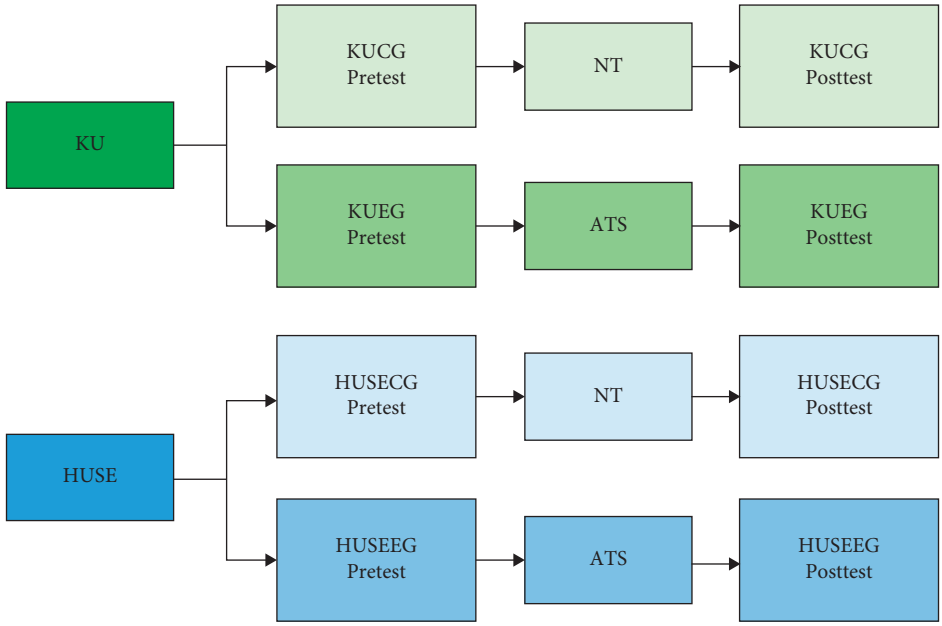

Figure 3: The experiment process (*Source*: author 2021).

participants had the same knowledge base. The students taking part in the experimental group were then taught the ATS to test the impact of ATS among students with different professional backgrounds. The quasiexperiment has two phases, the pretest before ATS and NT and a posttest after ATS and NT in two categories groups in each university. As shown in Figure 3, the experimental procedure introduces a graphic illustration of the experimental plan using a pretest and a posttest in the quasiexperiment process.

In the pretest and posttest, the researcher explains the topic and then assigns it to the participants. We will use the pretest topic as a teaching example for the students during the ATS presentation. We prepare two topics for the posttest, one main topic, and one alternative topic. The reason for alternative plan preparation is because if students in which university did not completely understand the experiment process led, the first topic to scrap. We have plan B to finish the experiment, as shown in Table 2.

Because the experiment needs to show some electronic data to students, we choose the classroom in the computer room for the experiment. The seating chart arrangement is shown in Figure 4. Due to the different seating layouts of classrooms in the two schools and the part of group discussion in ATS, it is necessary to display this chart for reference in subsequent research. The seating arrangement of HUSE is the regular class arrangement (see Figure 4(a)). Students are seated in rows, and teachers are seated in the front of the classroom. However, the seating arrangement of KU is arranged around the classroom, and the position of teachers is in the middle (see Figure 4(b)).

2.2. Animation Pedagogy Module Design. The animation pedagogy module is taught to students in the NT and ATS sections of the lab. The animation pedagogy module was standardized because we could not control the animation knowledge base of the students before the experiment. Therefore, uniform content needs to be prepared to ensure that participants have a uniform base of knowledge when participating in the experiment.

The section of NT is for both control groups and experimental groups students. The content contains the storyboard, incorporating design principles into storyboards, maintaining screen side, screen direction specifically on characters moving in and out of frame, motivating the camera: cuts. NT's lecture content is designed for the

Table 2: The topics for the pretest and posttest.

	Pretest	Posttest
DT formula	WHAT + ? = RESULT	WHAT + ? = ?
Topics	A donkey drowned in a teacup.	First topic: A night in the city, you ride a bike to go home on the way, suddenly you heard behind, someone called you: "stop!!." Who called you? What happened or will happen? The alternative topic: XX ancient tomb adventure. XX went exploring, entered the cave, and found an ancient tomb (covered with treasures and dead bones everywhere, gusts of gloomy wind came) suddenly . . .
Instruction	1. Based on the topic above, produce a storyboard. 2. For its roleplay, only one protagonist is allowed. It can be human, animal, etc. 3. There is no limitation on the story location or setting. 4. The frame for the storyboard should be limited between 10 and 15. 5. Once completed, please record spend time at the bottom right part of the storyboard.	1. Please continue to draw the story according to the plot provided earlier. 2. For its roleplay, only one protagonist (male or female) is allowed for both topics. Supporting characters for first topic: Ghost, dinosaur, and cat (optional, can draw all, can choose one of them). Supporting characters for alternative topic: ghost, snake, and cat (optional, can draw all, can choose one of them). 3. The location or background setting: first topic is in a busy city street; the alternative topic is in a forest. 4. 10–15 frames of the shooting scene, self-drafted title. 5. Once completed, please record spend time at the bottom right part of the storyboard.
Note	The topic assigned is based on an issue-based problem. The focus is more on "what" and "result" without specific attention on "how."	The topic assigned is based on a scenario-based problem. The focus is more on "what" without specific attention on "how" and result.

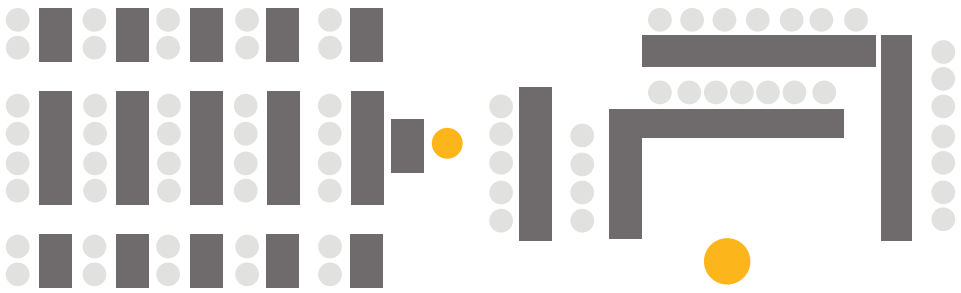

Figure 4: Plan of the experiment set in the computer room. (a) Plan of the experiment setting in the HUSE-computer room. (b) Plan of the experiment setting in the KU-computer room.

following reasons: first, the normal preanimation process is to generate a text script first, and then the subscreeners draw the subscenes based on the textual information. In our experiment, we will have students work in a storyboard format, combining script writing and split-screen script drawing. This decision was made because we wanted the students to quickly understand the various aspects of the animation process, such as script writing, scene design, character design, and split-screen scripting, in a relatively short period. And by starting directly with storyboard creation, they can synthesize these elements together. However, this would reverse the order of the regular process. However, Mou [29] has already done similar experiments in her research to complete script creation work in the form of storyboarding and got positive and positive results to confirm that this operation is feasible. Therefore, the first thing we introduced to the students in NT was about storyboarding. Second, design principles are incorporated into storyboarding. In the case of art colleges, design basics students are bound to have been exposed to in their elementary courses. However, it is not always well understood among non-art majors. Therefore, we included this part in NT and taught it as examples mainly by applying the design principles in storyboard creation. This ensured that the students had the same foundation and also showed them the specific applications. This facilitates flexible application in

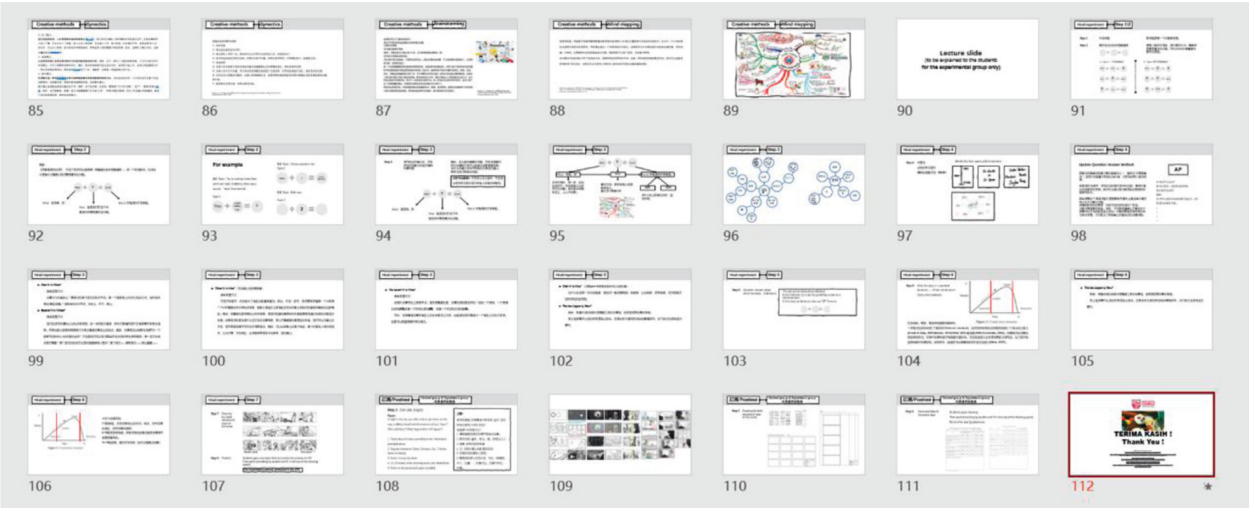

Figure 5: Part of ATS courseware.

subsequent experiments. The third part of the content is about the knowledge of film and television, including camera alignment, shooting angles, screen switching, and other content. These contents are also essential because the design of this shot in the early stage will affect the content of the work in the middle and later stages.

The section of ATS is only for experimental groups' students. The content contains design thinking, creative methods (5W1H, CLA, Synectics, Brainstorming, Mind mapping), and the application of the ATS. Parts slides of the ATS process as shown in Figure 5. The design thinking and creative methods are not used according to the original content and steps but are updated and adjusted according to the issues involved in creating the animation. For example, we adjusted the 5W1H method according to the actual needs of animation creation. The definition of "WHO" is changed to who the story's characters are. The new meaning of the "WHAT" is changed to what event or story happened. The "WHEN" was changed to when the story happened. Time should be specific to the chronological background and include the morning, noon, and evening. The reason is that detailed time information will affect animators to design the scenes and costumes. The ATS section has specific steps to use in addition to the basic introduction of the above content (see Figure 6). We have set up eight steps according to which the instructor will guide and teach the participants.

2.3. Hypothesis and Subhypothetical Questions. The goal of the quasiexperiment is to assess the effectiveness of ATS. We would like to find out if ATS advantages the realization of teaching practice and improves the animation storyboard creation of animation in solving storylines and creativity. We would also like to collect students' performance on the NT. Considering the set goal, we have chosen the hypotheses and subhypothetical questions:

Hypothesis: in terms of creativity and storyline ability, ATS can more easily influence the performance of students from different professional backgrounds in animation creation than the normal teaching process.

Subhypothetical questions (Sub-HQ) are as follows:

Sub-HQ 1. Is there any significant difference in the students' storyline scores between KUCG and HUSECG after the normal teaching process (at a .05 level of significance)?

Sub-HQ 2. Is there any significant difference in the students' creativity scores between KUCG and HUSECG after the normal teaching process (at a .05 level of significance)?

Sub-HQ 3. Is there any significant difference in the students' storyline scores between KUEG and HUSEEG after the ATS process (at a .05 level of significance)?

Sub-HQ 4. Is there any significant difference in the students' creativity scores between KUEG and HUSEEG after the ATS process (at a .05 level of significance)?

2.4. Data Analysis. The process and protocol (see Figure 7) for analyzing the experimental data were determined in accordance with the research objectives of this study. The process of analyzing the experimental data is shown in the figure, and a comparative analysis between the groups of the experimental group (KUCG vs. HUSECG) and the control group (KUEG vs. HUSEEG) of the two universities was conducted for the posttest. The analysis aimed to confirm whether there were gaps in students' performance from different professional backgrounds regarding creative and storyline processing abilities. The assessment follows the CAT and invites the teachers from each university to assess the creation. The quantitative instrument was in the form of a five-point Likert scale. The Kolmogorov–Smirnov test and the Shapiro–Wilk's W test were adapted to test the data's normal distribution. Then we adopted the Mann–Whitney U test to conduct the intergroup analysis.

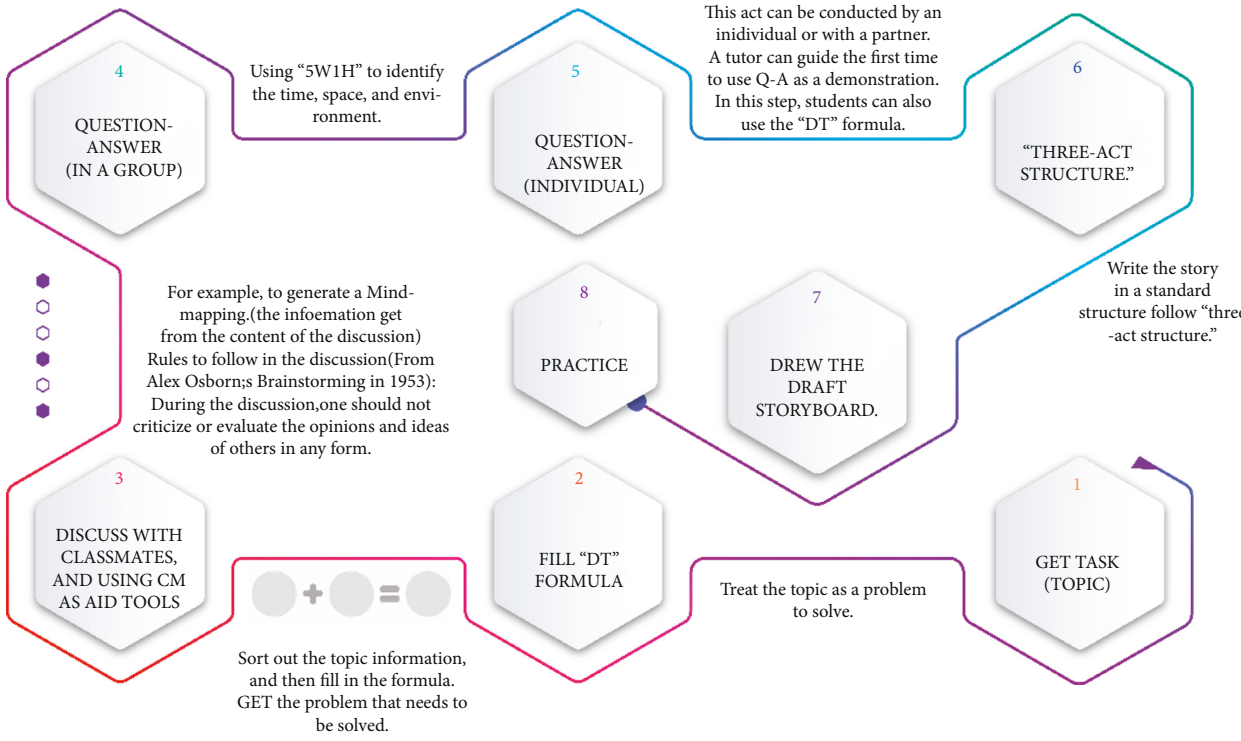

Figure 6: Eight steps in ATS.

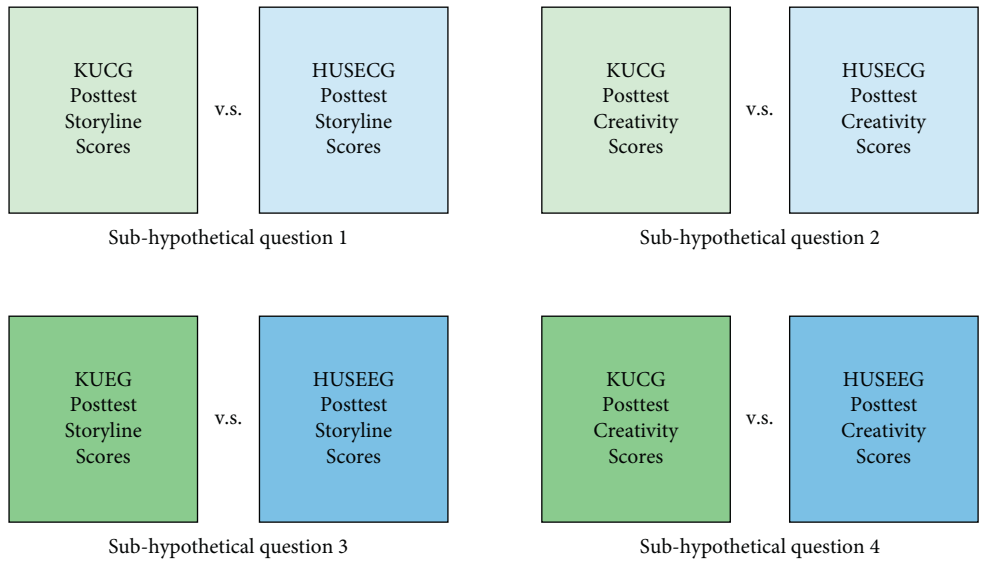

Figure 7: The diagram of the data analysis process (*Source.* author 2021).

3. Result

The results of the data analysis were analyzed in three steps for each subhypothetical question. First, the group was tested to determine whether the data conformed to a normal distribution and whether the data were of the parametric or nonparametric type to choose the following analysis method. Second, analyze the results of the posttest storyline with the appropriate analysis method. Third, the results of the creativity of the posttest are analyzed by the corresponding analysis method.

3.1. The Data Normality Test. Table 3 shows the Shapiro–Wilk's W test results of the data normality test. Since significant values were less than alpha, the null hypothesis can be rejected. We concluded that the data did not conform to the normally distributed. Therefore, we need to use the Mann–Whitney test when testing the difference for the four comparison items: the students' storyline scores between KUCG and HUSECG, the students' creativity scores between KUCG and HUSECG, the students' storyline scores between KUEG and HUSEEG, and the students' creativity scores between KUEG and HUSEEG.

Table 3: Data normality test result.

	Sig.
KUCG's posttest storyline scores	0.016
HUSECG's posttest storyline scores	0.001
KUCG's posttest creativity scores	0.001
HUSECG's posttest creativity scores	0.001
KUEG's posttest storyline scores	0.016
HUSEEG's posttest storyline scores	0.001
KUEG's posttest creativity scores	0.001
HUSEEG's posttest creativity scores	0.001

3.2. The Data Analysis Result for Answering Sub-HQ 1. The Mann–Whitney U test was conducted to determine whether there is a significant difference in the students' storyline scores between KUCG and HUSECG. The results indicate a significant difference between groups ($U = 84.00$, $p = 0.002$) (see Table 4). In conclusion, we can reject the null hypothesis and conclude that there is a significant difference in the students' storyline scores between KUCG and HUSECG after the normal teaching process.

Figure 8 displays the frequency of the storyline scores after NT in HUSECG and KUCG in the posttest. HUSECG ($N = 18$, Mean Rank = 14.17) shows in blue bars, and KUCG ($N = 20$, Mean Rank = 24.30) shows in green bars.

In terms of storyline, the HUSECG posttest results compared to the KUCG posttest results; the HUCG scores performed better than the HUSECG. Even after the teaching process of NT, students in the digital media art program performed better than digital media technology program students in terms of storyline.

3.3. The Data Analysis Result for Answering Sub-HQ 2. The Mann–Whitney U test was conducted to determine whether there is a significant difference in the students' creativity scores between KUCG and HUSECG. The results indicate a nonsignificant difference between groups ($U = 125.00$, $p = 0.061$) (see Table 4). In conclusion, we cannot reject the null hypothesis and conclude that there is no significant difference in the students' creativity scores between KUCG and HUSECG after the normal teaching process.

Figure 9 displays the frequency of the creativity scores after NT in HUSECG and KUCG in the posttest. HUSECG ($N = 18$, Mean Rank = 16.44) shows in blue bars, and KUCG ($N = 20$, Mean Rank = 22.25) shows in green bars.

In the evaluation of creative ability, HUCG scored better overall than HUSECG in the posttest results compared with KUCG. However, after the teaching process in NT, there was no significant impact on students' creative ability in the two universities, and no help was provided to students in their creation.

3.4. The Data Analysis Result for Answering Sub-HQ 3. The Mann–Whitney U test was conducted to determine whether there is a significant difference in the students' storyline scores between KUEG and HUSEEG. The results indicate a significant difference between groups ($U = 128.50$, $p = 0.001$) (see Table 4). In conclusion, we can reject the null hypothesis and conclude that there is a significant difference in the students' storyline scores between KUEG and HUSEEG after the ATS process.

Figure 10 displays the frequency of the storyline scores after ATS in HUSECG and KUCG in the posttest. HUSEEG ($N = 35$, Mean Rank = 21.67) shows in blue bars, and KUEG ($N = 27$, Mean Rank = 44.24) shows in green bars.

The results of the storylines in the two experimental groups showed that ATS impacted student performance at both universities and the frequency plots showed that KU students performed better than HUSE students overall.

3.5. The Data Analysis Result for Answering Sub-HQ 4. The Mann–Whitney U test was conducted to determine whether there is a significant difference in the students' creativity scores between KUEG and HUSEEG. The results indicate a significant difference between groups ($U = 143.50$, $p = 0.001$) (see Table 4). In conclusion, we can reject the null hypothesis and conclude that there is a significant difference in the students' creativity scores between KUEG and HUSEEG after the ATS process.

Figure 11 displays the frequency of the creativity scores after ATS in HUSECG and KUCG in the posttest. HUSEEG ($N = 35$, Mean Rank = 21.67) shows in blue bars, and KUEG ($N = 27$, Mean Rank = 44.24) shows in green bars.

From the evaluation results of creative ability in the two experimental groups, ATS impacts the scores of students in the two universities in this aspect, and it can be seen from the frequency chart that the overall performance of KU students is better than that of HUSE students.

4. Discussion

We first respond to the primary purpose of this study and hypothetical questions through the experimental results. The effects of ATS and NT on students during teaching and learning and the students' performance in using ATS in different professional contexts are described, respectively. Second, new issues identified during this experiment include the seating arrangement of students in computer classrooms and the impact of different university class schedules on students' learning are discussed.

4.1. ATS Positively Affected Students' Storyline Performance and Creative Ability. The Mann–Whitney U test analysis showed that the ATS positively affected storyline completion and creative ability for the experimental groups at both universities. This result is mainly consistent with the goals initially set by the ATS. Based on the NT, students were taught first to use design thinking to peel back the problem layer by layer, list the problems to be solved, and use the appropriate methods to solve them one by one. This study used five creative methods: 5W1H, Causal Layered Analysis (CLA), Synectics, Brainstorming, and mind mapping. Although some parts of these five methods will be similar or overlap, they can be well applied in different aspects when combined with the needs of preanimation work. They can be

Table 4: Mann–Whitney *U* test result.

	Sub-HQ 1	Sub-HQ 2	Sub-HQ 3	Sub-HQ 4
Total *N*	38	38	62	62
Mann–Whitney *U*	84.000	125.000	128.500	143.500
Wilcoxon W	255.000	296.000	758.500	773.500
Test statistic	84.000	125.000	128.500	143.500
Standard error	31.554	29.364	67.162	67.042
Standardized test statistic	−3.042	−1.873	−5.122	−4.907
Asymptotic sig. (2-sided test)	0.002	0.061	0.001	0.001
Exact sig. (2-sided test)	0.004	0.112	—	—

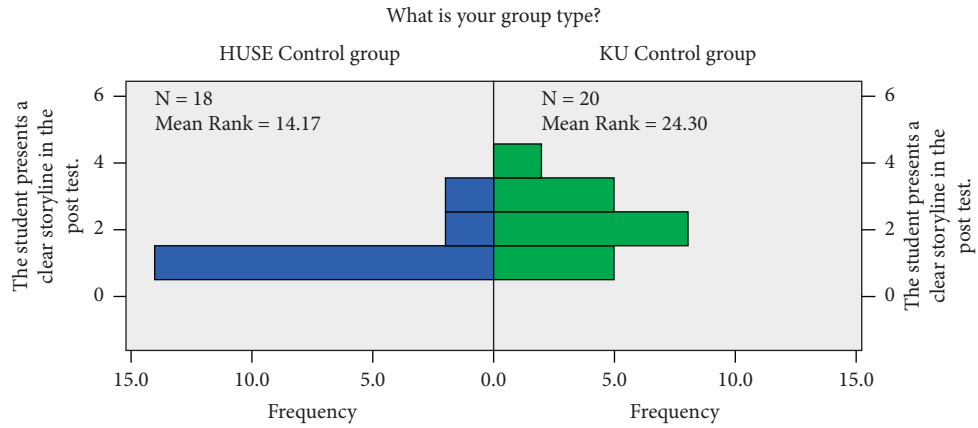

Figure 8: The frequency of the storyline scores after NT in HUSECG and KUCG (*Source.* author 2021).

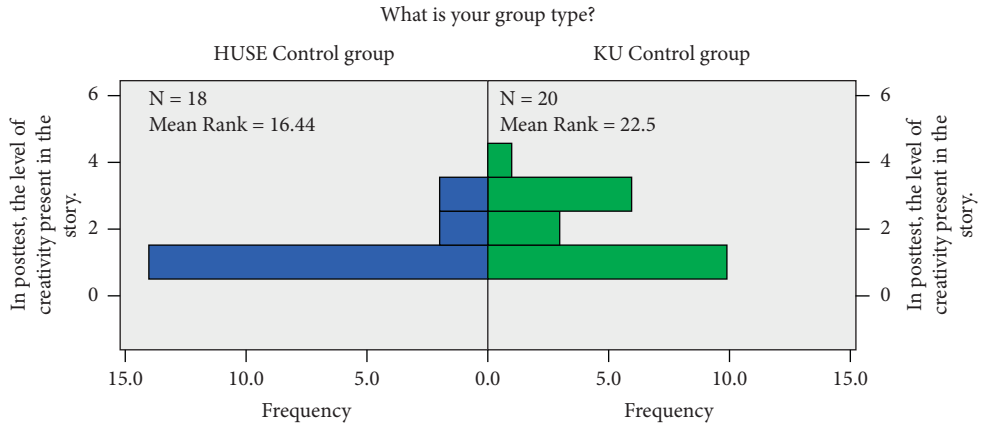

Figure 9: The frequency of the creativity scores after NT in HUSECG and KUCG (*Source.* author 2021).

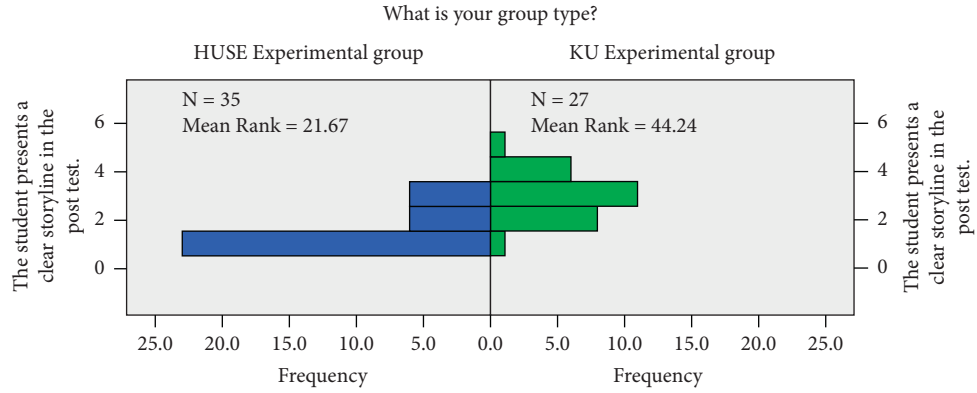

Figure 10: The frequency of the storyline scores after ATS in HUSEEG and KUEG (*Source.* author 2021).

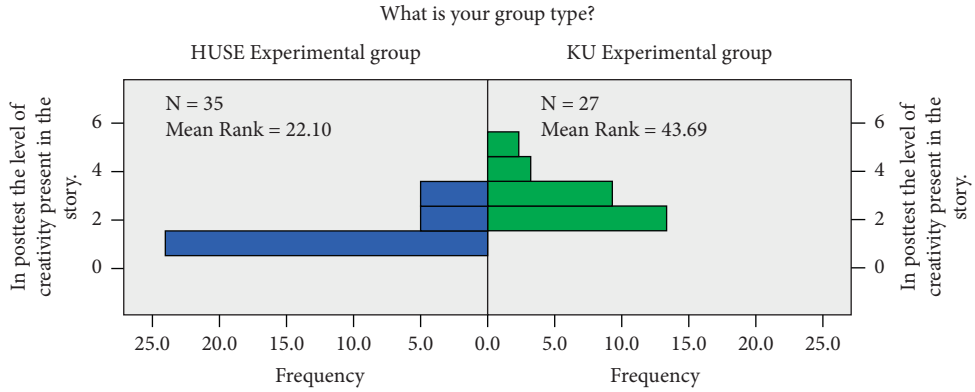

Figure 11: The frequency of the creativity scores after ATS in HUSEEG and KUEG (*Source.* author 2021).

effective in helping students when improving their creative thinking skills. Of course, this attempt is not a perfect set of operating procedures and will not have an immediate effect, and students still need a long break-in period in the process of using it. In the initial implementation of this experiment, we found that while the process of using the ATS gave the students what they were expecting to learn, the ATS still needs to be improved and enhanced.

4.2. Effects of NT on Students. From the Mann–Whitney *U* test results, the students in the control group improved their ability to complete the storyline after the NT. However, they were deficient in helping the students to generate ideas. The normal teaching activities taught the students the basics of animation creation, but not enough to help them generate ideas to meet their needs. It is the opposite of what the industry expects from its talent. The Chinese animation industry is currently in need of creative talent. This is an adjustment to the conventional teaching model. We should no longer focus on teaching the basics and skills as the main goal in animation education. Besides basic knowledge and skills, the cultivation of students' creative thinking also needs to be focused on. Basic knowledge can give students an initial understanding of the profession, and skills can get them to be able to finish the final work on paper or on the computer. But focusing on these two aspects of education can no longer keep pace with the times, and students will only be able to work as skilled craftsmen after they join work-related jobs, lacking the ability to think creatively. Such animation workers can only engage in mindless, repetitive work in the industry, and the possibility of being replaced is very high. It is also not suitable for the development of the industry.

4.3. Students with Different Professional Backgrounds Have Different Performances When Using ATS. Looking at the frequency plots of the two control and experimental groups together, the students of KU digital media art majors performed better in the experiment than those of HUSE digital media technology majors in terms of storyline and creative ability. It shows that although animation majors have many related majors, these majors still have their specialties in nature. Moreover, the curriculum of animation classes is imperfect in these related majors, and students do not receive very comprehensive expertise in the learning process as animation majors do. The entire pre, intermediate, and postcourses are very carefully divided in the animation program. For example, there are special classes for character modeling, scene design, scriptwriting, and storyboard creation. However, in digital media technology and digital media art, these two majors will reduce the corresponding animation classes according to the setting of the major and instead add some courses on interaction design and programming. Although ATS cannot cover the whole animation creation process, it can integrate some of the preproduction work together, which can let students quickly understand what the needs in preproduction animation are the creation and develop students' thinking skills and the practical application of some of the tools used to generate ideas.

Another point is the students' ability to express themselves on-screen in their posttest work. However, the final evaluation focused only on the students' storyline processing and creative abilities. Moreover, graphic performance was not used as a criterion in the analysis of this experiment. The overall results showed that the digital media art students had an advantage in their expressive skills and techniques (see Figure 12). This factor may have an impact on the students using ATS. Therefore, in the future, when considering different professional backgrounds in using ATS, adjustments, and modifications should be made accordingly. For example, suppose ATS is used in digital media technology majors with a weak foundation in art. In that case, we should consider adding methods to address students' lack of expressive skills in graphics.

As we mentioned earlier, most students have an advantage in art skills. However, there is a lack of storytelling, and the market expects more creative talents so that ATS can solve these two problems positively. The direction of our future research can be affirmed and continued. The work to be done in the future is to improve the system even more, further enhance it in coordinating the operation of the various creative methods, bring out the best in them, and help students with their creative work to the maximum.

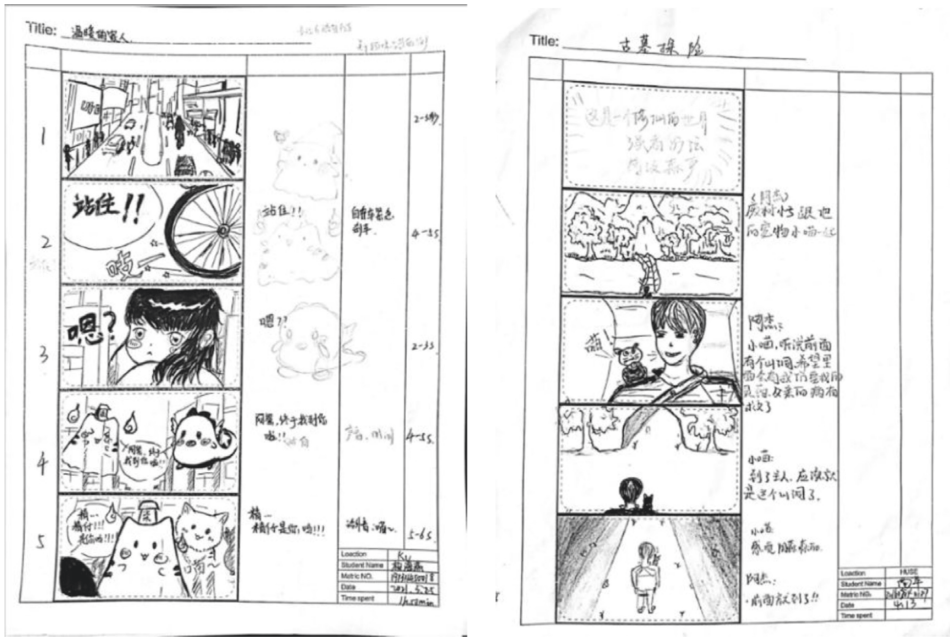

(a) (b)

Figure 12: A piece of storyboard from one student (a) in KU and one student (b) in HUSE.

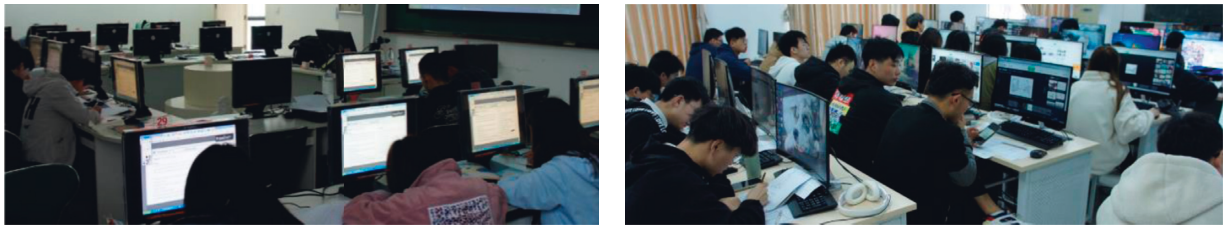

(a) (b)

Figure 13: Photos of the experiment posttest (*Source.* Taken by the author).

4.4. Different Class Seating Arrangements Affect the Way Students Communicate. Since the seating patterns in the experiment were arranged according to the university's existing hardware and equipment conditions, we did not emphasize the influence of this aspect. However, in the actual experiment process, the authors did find that the seating arrangement affected the discussion between groups. For example, the seating arrangement influenced students' discussions during question-and-answer sessions with each other and when students were brainstorming and doing other activities (see Figure 13). Seet Hong An Andrew, Tan Emmanuel, and Rajalingam Preman designed a quasiexperimental study to test the effect of seating arrangement on class engagement in team-based learning. The result presents that the different seat positions can affect students' participation in learning [30]. Of course, after comparing the performance of the participant doors at KU and HUSE during the experiment, the seating layout at KU is more suitable for communication with the teacher and students. However, there are some limitations when students are having group discussions. Therefore, in continued future research, this issue could be included in the preexperimental preparation of the ATS to address the negative impact this issue has on the experiment.

4.5. The Influence of Duration and Frequency of Classes. The scheduling of course lengths is also a newly discovered issue. In our experiment's initial preconception, the two universities' class schedules should be as consistent as possible. However, the different nature of the majors in digital media art and digital media technology led to the difference in setting the class schedule between the two universities. KU's major is digital media art, and the university classifies this major as an art major, so the class schedule is set according to a large art class. See Table 1, where students attend classes three times a week, each of which is close to three hours in length. The long and complete periods of time are very effective for students' learning. There would be a greater fluency for knowledge penetration, and the newly learned knowledge would still be in the memory at the next class. Conversely, HUSE's major is digital media technology, which the university classifies as an engineering major. The class schedule is set up as a regular

minicourse. See Table 1, where students attend classes twice a week for 90 minutes each. Therefore, the number of classes is relatively high, which leads to short lectures and incoherent knowledge for students. This also has a significant impact on student performance during the experiment. Feedback from students after the experiment showed that ATS was relatively popular among students, but most students responded that the class schedule was short. The learning effect would be better if more class time could be scheduled. Unfortunately, this limitation is more challenging to solve in this study. This is because we conducted the experiment in consultation with each university's faculty for that major. Due to the restrictions of the university rules at each university, it was not possible to obtain more classroom access. Time constraints were the biggest obstacle to conducting this experiment, which could also be a reference for future studies.

5. Conclusions

Based on the data analysis, NT affected the storyline scores of the participants in the control groups at both HUSE and KU universities but did not significantly impact the scores of creativities. On the contrary, the analysis of ATS in the experimental groups significantly affected the scores of both measures. However, when looking at the frequency charts, we can see that the overall performance of the KU students is better than that of the HUSE students. Therefore, it can be determined that the professional talent development model impacts the implementation of the ATS experiment, and the method plays a significant role in the group of students from art majors versus those from engineering backgrounds. There are essential guidelines for the subsequent improvement and enhancement of ATS. At the same time, there are certain influences and challenges to implementing ATS due to the complicated unchangeable external factors such as class schedule. For the two schools in the experimental students in the experimental conditions of the different points to sort out: first, the two schools of talent training mode; two, the students' own skills base; three, the class time arrangement way. In response to the above, adjustments should be made. More extended and more complete lecture periods are more conducive to implementing ATS.

The use of ATS is an innovative approach for teaching animation-related subjects. The method improves the teaching and learning of science subjects since students studying science subjects performed poorly in creation. To reduce this ugly trend of student failure in science, using ATS would enable the students to obtain a new method to complete their study and design work since students with different professional backgrounds and talent training directions have very different class schedules. Each class time for art students is longer, more concentrated, and has a short interval period between each lesson, and students remember their knowledge better. In contrast, students with science backgrounds have long class schedules, longer cycles, more fragmented class schedules, and longer intervals between classes. The ATS also needs to be adjusted to more convenience.

From the results of this quasiexperiment, we know that ATS has advantages over NT in meeting the requirements of the animation industry for talent training. It is also concluded that in animation-related majors, different disciplinary backgrounds also impact the implementation of ATS. ATS is carried out more smoothly among students with an artistic foundation. In future research, if the application of ATS needs to be made smoother, the users' professional background and degree of basic knowledge reserve must be investigated. Animation education is crucial as the first gate of talent training in industry development. The situation we are facing now is that the trend of opening animation majors in colleges and universities has gradually stabilized, and there will not be a significant increase in the situation. In this context, the study of animation education is a challenge, and the quality of talents determines the future fate of the profession. This study gives different perspectives on animation higher education and hopes to provide references for other educators.

Data Availability

Since the original data in this study involved the content of intra-group data analysis in the author's Ph.D study, for the purpose of protecting unpublished data, the inter-group data analysis supporting the findings of this study has not been provided.

Conflicts of Interest

The authors declare that they have no conflicts of interest.

References

[1] Q. Gao, "The Teaching Reform of Animation Specialty in Universities Under the Aesthetic Education Environment," in *Proceedings of the 2018 3rd International Conference on Politics, Economics and Law (ICPEL 2018)*, pp. 105–108, Weihai, China, October 2018.

[2] X. Yin and Y. Qi, "The problem of adult animation education in teaching quality and corresponding solutions," *Frontiers in Computer Education*, Springer, Berlin, Germany, pp. 333–339, 2012.

[3] R. Zhao and X. Li, "Construction and Practice of Training Project to Enhance the Animation Professional Comprehensive Ability Based on OBE-oriented +3-Center-Change-Creative," in *Proceedings of the Asia-Pacific Social Science and Modern Education Conference (SSME 2018)*, pp. 106–110, Shanghai, China, June 2018.

[4] P. Guan and Z. Zheng, "Research on animation majors' competition and cultivation of creative talents," in *Proceedings of the 6th International Conference on Arts, Design and Contemporary Education (ICADCE 2020)*, pp. 347–352, Moscow, Russia, December 2020.

[5] D. Chen, M. Li, and X. Liu, "Research on the matching degree between the training direction of film and television animation students in higher vocational colleges and the needs of the social industry based on big data analysis," *Journal of Physics: Conference Series*, vol. 1992, no. 2, Article ID 022138, 2021.

[6] T. Ma, "Research on intangible cultural heritage education and inheritance in universities," *Journal of Contemporary Educational Research*, vol. 4, no. 11, pp. 37–39, 2020.

[7] D. Haibin, "Interdisciplinary talents cultivation of animation education in universities based on university-enterprise cooperation mode," *International Journal of E-Education, E-Business, E-Management and E-Learning*, vol. 8, no. 3, pp. 165–172, 2018.

[8] A. Zhang and K. Meng, "Reform and practice study of animation major's "721" talent training mode-in the Hubei university of technology," *Design Education*, vol. 11, pp. 102-103, 2016.

[9] M. Zhang, "Research on the cultivation of lVision a insightr among Chinese animation talents," in *Proceedings of the 2018 International Conference on Social Science and Education Reform (ICSSER 2018)*, pp. 14–17, Xi'an, China, October 2018.

[10] G. Liu and Y. Zhang, "The integration and application of animation script creation and modern concept," *IOP Conference Series: Materials Science and Engineering*, vol. 750, no. 1, Article ID 012059, 2020.

[11] X. Chen, J. Wei, and X. Huang, "Success factors of innovation in creative industry in China: case study on animation companies," in *Proceedings of the 2010 IEEE International Conference on Management of Innovation & Technology*, pp. 800–805, Singapore, June 2010.

[12] R. S. Dewi and A. Rino, "Animation as a creative industry: a strategy to build creativity and independence of youth in padang, west sumatra," in *Proceedings of the MICoMS 2017. 1*, pp. 135–141, May 2018.

[13] X. Zhang, "Discussion on the new thinking of the creation of domestic animated script," *Advances in Social Science, Education and Humanities Research*, vol. 185, pp. 227–230, 2018b.

[14] L. Luo, "Current situation of animation design talents cultivation in Chinese colleges and universities," in *Proceedings of the 2017 2nd International Conference on Education, Sports, Arts and Management Engineering (ICESAME 2017)*, pp. 1727–1730, Cairo, Egypt, 2017.

[15] A. B. Gencosmanoglu, "Learning, teaching and administration in design education: DESIGNtrain Project: training tools for developing design education," *Procedia - Social and Behavioral Sciences*, vol. 9, pp. 522–530, 2010.

[16] K. Thoring, P. Desmet, and P. Badke-Schaub, "Creative environments for design education and practice: a typology of creative spaces," *Design Studies*, vol. 56, no. 2, pp. 54–83, 2018.

[17] H. K. Lee, "Revitalising traditional street markets in rural korea: design thinking and sense-making methodology," *International Journal of Art & Design Education*, vol. 38, no. 1, pp. 256–269, 2019.

[18] Council, *British Design. Eleven Lessons. A Study of the Design Process.*British Design Council, London, UK, 2016.

[19] D. C. Chou, "Applying design thinking method to social entrepreneurship project," *Computer Standards & Interfaces*, vol. 55, pp. 73–79, 2018.

[20] T. Zhao, H. Sun, and X. Li, "The application of design thinking on animation," *Art and Design*, vol. 163, pp. 132–134, 2018.

[21] K. K. Fan and T. T. Feng, "Sustainable development strategy of Chinese animation industry," *Sustainability (Switzerland)*, vol. 13, no. 13, 2021.

[22] Y. Xiao, "Analysis on current Chinese animation education system," *Journal of Beijing Union University (Humanities and Social Sciences)*, vol. 9, no. 3, pp. 71–77, 2011.

[23] C. Ma, *From "Made in China" to "Created in China"–A Study of Nurturing Students' Creativity in Animation Education in China*, The Hong Kong Polytechnic University, Hong Kong, 2016.

[24] L. Lin and Y. Xiang, "A multimedia teaching method research of animation production in China," in *Proceedings of the 2012 7th International Conference on Computer Science & Education (ICCSE)*, pp. 1495–1497, Melbourne Australia, July 2012.

[25] H. Ross and Y. Wang, "Reforms to the college entrance examination in China: key issues, developments, and dilemmas," *Chinese Education & Society*, vol. 46, no. 1, pp. 3–9, 2013.

[26] M. Sirotová, V. Michvocíková, and K. Rubacha, "Quasi-experiment in the educational reality," *Journal of Education Culture and Society*, vol. 12, no. 1, pp. 189–201, 2021.

[27] J. W. Creswell, *Research design Qualitative,Quantitative, and Mixed Methods Approaches*Sage Publications, CA, USA, 1993.

[28] C. Price, S. J. Rajiv and A. Chiang, Research methods in psychology," *Journal of psychosomatic research*, vol. 40, no. 5, pp. 521–534, 1996.

[29] T. Mou, "Creative story design method IN animation production PIPELINE," in *Proceedings of the Third International Conference on Design Creativity*, pp. 124–131, January 2015.

[30] H. A. A. Seet, E. Tan, and P. Rajalingam, "Effect of seating arrangement on class engagement in team-based learning: a quasi-experimental study," *Medical Science Educator*, vol. 32, no. 1, pp. 229–237, 2022.

Hindawi
Scientific Programming
Volume 2022, Article ID 5211927, 10 pages
https://doi.org/10.1155/2022/5211927

Research Article

Training Method of Flute Breath Based on Big Data of Internet of Things

Yizhen Sun

School of Music and Drama, Zhengzhou SIAS University, Xinzheng 451100, Henan, China

Correspondence should be addressed to Yizhen Sun; 11160@sias.edu.cn

Received 7 July 2022; Revised 16 August 2022; Accepted 1 September 2022; Published 19 September 2022

Academic Editor: Juan Vicente Capella Hernandez

As a traditional musical instrument, the flute has a long history and is loved by people. The flute has a wider range, and its timbre has strong penetrating and expressive power. This is not only a unique solo instrument but also occupies an important position in the symphony orchestra. Breath training on the flute is an essential step in flute learning. However, in the traditional flute breath training process, teachers cannot observe the students' practice in real time, and the training process is relatively simple, resulting in the final training effect not being obvious and the students' breath stability not being significantly improved. In order to solve this problem, this paper applied the Internet of Things (IoT) big data technology to the flute breath training process. The flute breath training system based on big data of Internet of Things was used to conduct professional breath training for students. Through the tests of the trained students, it was found that the training method of flute breath using the big data of the Internet of Things improved the students' leg strength and chest, abdomen, and back strength. In the long-tone practice, the students' exhalation time increased by 1.472 seconds, and the students' breath stability increased by 7.1%, which laid a good foundation for the students to learn the flute in the future.

1. Introduction

The rapid development of modern society has led to the gradual improvement of people's living standards. People no longer simply enjoy material life but begin to pursue the spiritual world. With the development of contemporary music, traditional musical instruments have gradually entered people's lives, especially the flute. In the process of playing the flute, the sound of the flute is ethereal and beautiful, which is loved by the world. However, in order to give full play to the sound quality of the flute, high requirements will be placed on the player. The player must conduct breath training on the flute on the basis of playing skills and continuously improve the level of flute playing. In the actual training process, the players should also be trained in terms of leg strength, chest, abdomen, and back strength so as to improve the player's physical quality and lay a good foundation for flute playing. Breath training can effectively improve the player's flute playing ability and play a role in boosting the flute playing career.

Breath control is the flute's most difficult skill to master, but it is also the most important skill. Akka and Aksoy analyzed the flute teaching problems, including breath control, intonation, and finger technique, to help facilitate flute music development and played the flute in a way that combined the best of the East and the West [1]. Ahmed et al. analyzed the signal to study the effect of subtle fluctuations in the frequency and amplitude of each harmonic on the timbre of the flute timbre. The flute sound not only had frequency and amplitude modulation of each harmonic but also had a noise component produced by breathing [2]. Konoval studied the relationship between breath and strength in flute performance by analyzing the scientific application of breath and strength in bamboo flute performance. The three steps of breathing, exhaling, and inhaling during the performance of the bamboo flute were expounded. Combined with the obvious problems in flute teaching, the principle of breathing application and the control of force in playing were analyzed [3]. In the process of playing the flute, due to exhaling and inhaling at the same time, the breathing was supplemented, and the flute was

not interrupted, so it was a playing technique that went against the human physiological function and breathing method, which easily led to problems for the player. Moss put forward a brand new flute double spit cycle breathing technique [4]. Keulen et al. elaborated on the relationship between the breath and the mouth of the bamboo flute. Whether the bamboo flute could fully display the charm of music during the performance of the flute was closely related to the control of breathing and mouth. How bamboo flute players practice breath and mouth was pointed out in order to give full play to the artistic charm of the bamboo flute [5]. These studies showed the importance of breath training for flute playing. However, with the development of the times, new problems have emerged.

Internet of Things big data technology has applications in many fields, and more and more researchers are investing in the research of big data technology. Cui utilized big data technology to eliminate the data collected from the virtual world. The proposed methods included singular value decomposition and clustering-based community detection and tensor-based community activity modeling [6]. Yang et al. studied the short-term load forecasting method based on big data, combined with local weighted linear regression and a cloud computing platform. A parallel local weighted linear regression model is established, and the results showed that the proposed improved model of the local weight line for short-term load forecasting was feasible [7]. Rahman et al. introduced a healthcare information system (HIS) framework based on big data analysis in a mobile cloud computing environment, which provided healthcare data among healthcare providers, patients, and practitioners [8]. Ge and Wu conducted correlation analysis and processing of massive medical information through big data technology. Correlations between different factors in the disease life cycle were found, which provided a basis for scientific research and clinical practice [9]. Chen et al. proposed a state-of-the-art computational and fault-based approach based on big data analysis of the smart distribution grid. The data preprocessing results were expanded in space and time to construct a high-dimensional state estimation matrix. Then, the state estimation matrix was analyzed by multidimensional scaling and a local anomaly factor, and the local anomaly factor of each node was calculated [10]. These studies showed that the application of big data technology was very extensive, but it was used less in flute breath training.

This paper proposed a flute breath training method based on IoT. Big data technology was used to build an Internet of Things system for continuous monitoring of breath training. By using the Internet of Things to build an intelligent training environment, learners could better master training skills. Through experiments, it was found that the flute playing level of the trainees was improved.

2. Application of the Internet of Things Big Data in Flute Teaching

2.1. Framework Model of the Flute Breath Training System. This paper uses the big data technology of the IoT to establish a training program based on databases and data mining, which can solve the problems of imperfect data organization and unstable data in the system and give full play to the subject-oriented and analysis-friendly characteristics of data warehouses [11]. OLAP provides a multidimensional directional data analysis model from the data embedded in the database. Multidimensional analysis methods are used to analyze and compare multidimensional data from multiple angles, multiple spaces, and multiple levels. A more natural way of data analysis is provided to the user. The frame model of the flute breath training system is shown in Figure 1 in which the system is supported and managed by metadata.

Data mining can be used directly to guide the performance of online analysis (OLAP), and new knowledge of data mining and statistical analysis can be immediately added to the understanding of the system. Data mining tools and multidimensional analysis tools occupy a major position in flute training systems. The database provides a unified data platform for data mining and data analysis. Model repositories and system repositories can also provide guidance for many analysis tools, while the knowledge base in the model repositories not only enables the discovery of new knowledge but also allows for continuous additions and additions. Therefore, the advantages of data storage and data mining outweigh the disadvantages. The relationship between data, model, method, and technology is combined, which makes full use of data sources in the current system and makes the whole system an organic whole to improve the integration of the system.

2.2. Data Mining Process. Data mining technology refers to extracting knowledge of a person's interests from a large database [12]. Data mining is the product of the combination of many disciplines, such as database technology, artificial intelligence, machine learning, statistical analysis, fuzzy logic, artificial neural networks, and so on. The objectives of data mining are not only organized databases but also semicomplete hypertext documents and even unstructured multimedia data, specifically as shown in Figure 2.

2.2.1. Data Preparation. During the data preparation phase, data from multiple operational data sources need to be consolidated, logical exceptions need to be resolved, lost data need to be recovered, and dirty data need to be cleaned up.

2.2.2. Mining Activities. The mining activity is a process of searching, discovering, entering, and sharing, and it is also the core of the three stages.

2.2.3. Result Presentation and Interpretation. The result presentation and interpretation stage needs to accurately describe the useful information according to the user's ultimate purpose.

2.3. Network Security Configuration Design. Since any Internet of Things teaching system runs on the Internet and it is remote and open, so security is very important for the Internet of Things education system. In the flute breath training

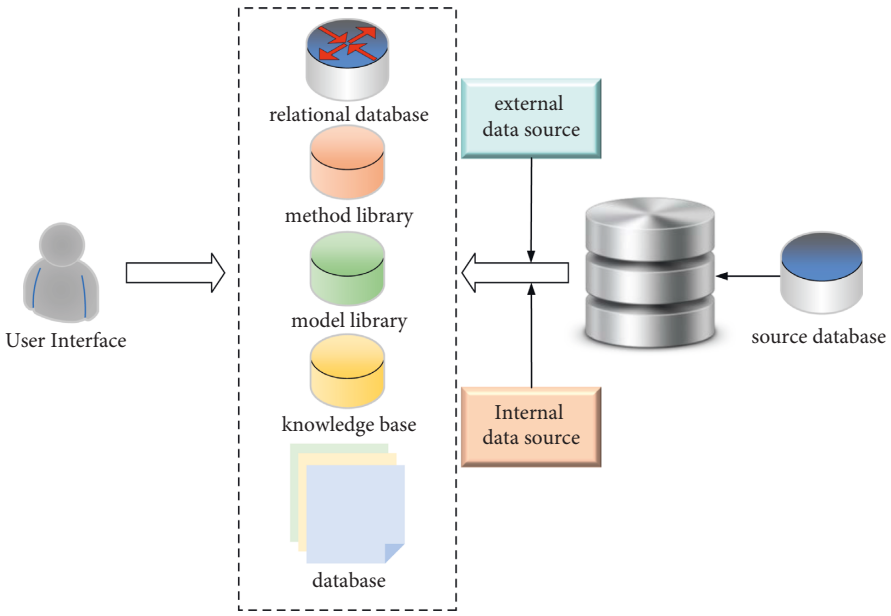

Figure 1: Framework model of the flute breath training system.

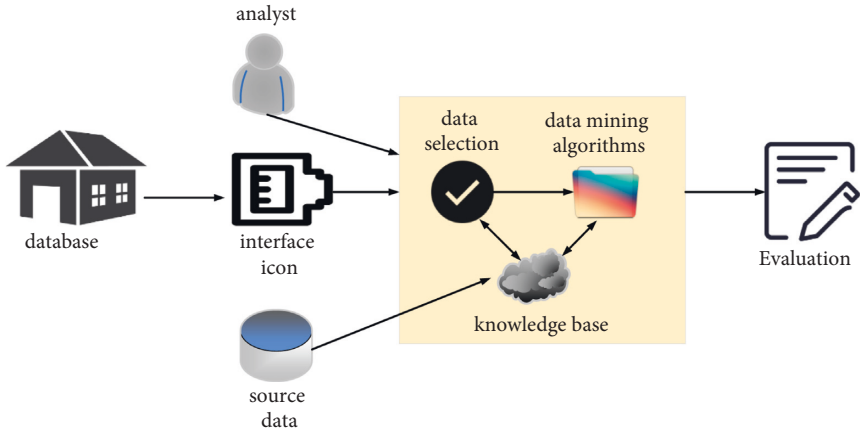

Figure 2: Data mining process.

system, whether it is the information transmitted in the remote access session and branch network or the information in the internal network, the guarantee of the security mechanism is required to protect the information from being leaked and to limit the access of users with different privileges to information at various levels. Therefore, providing efficient security solutions are essential. The flute breath teaching system is configured as J2EE three-level B/S architecture [13]. To meet the configuration requirements of the system, it is necessary to have a certain amount of hardware investment. The flute class computer room is added. The administrator of the educational affairs office is equipped with a management machine, specifically as shown in Figure 3.

The security design of the system is key to the normal operation of the system. The security design of this paper includes the following points.

2.3.1. Different Roles Are Given Different Permissions. This article sets up three roles: teacher, administrator, and student. When users with different roles log into the system, the operation permissions for the same function module are different. When the system is used for the first time, there is only the default role of the administrator. After logging into the system, the administrator can add teacher users, student users, or other administrator users as needed. The

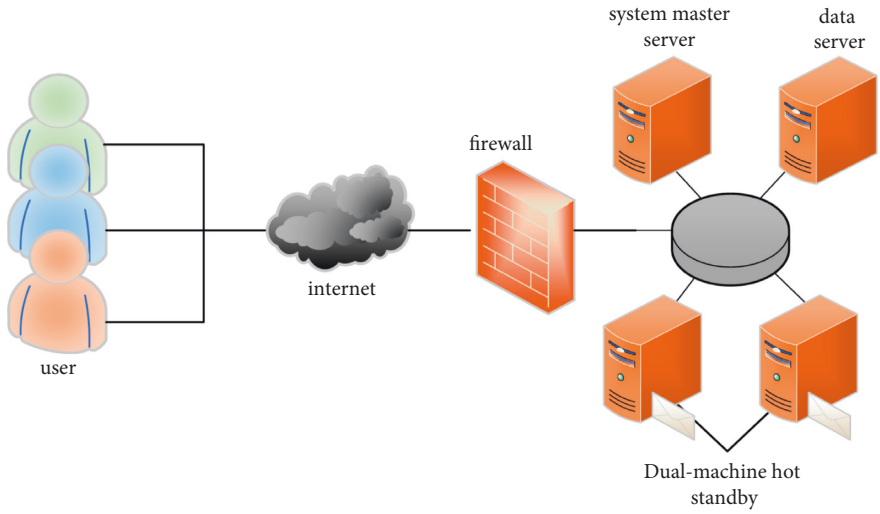

Figure 3: Network security configuration design.

administrator is given an initial account and password. When creating a new role user, the corresponding permissions are also granted. When deleting a role user, the user cannot be deleted until it is determined that the role is not associated with it.

2.3.2. Data Backup. The administrator needs to back up the system data regularly. If there is a problem with the system, it can be repaired to a large extent, reducing losses and ensuring the safe operation of the system.

2.3.3. Set Up the Firewall. When running the program, establish a firewall to prevent hackers from invading the system and ensure system security to a greater extent [14].

3. Classification Algorithms

3.1. Decision Tree Classification Algorithm. An important part of decision tree classification algorithms is to find the best features to share. By subdividing the rights of development modules, a decision tree that can distinguish training programs is finally found [15].

The attribute selection metric is a splitting strategy primarily. The splitting strategy is to use the information gain metric on each node of the tree to select attributes, and it is used to determine how the objects on each node are allocated. Usually, those attributes with the maximum information gain are targeted. It can reduce the amount of information generated by sorting data samples and improve data accuracy as much as possible by measuring data information [16, 17].

In the decision partitioning algorithm, the basic operating principle is as follows: suppose that training program B is a random set of materials consisting of x objects with different class symbol values. Suppose $A_i\,(i = 1, 2, \ldots, x)$ are x different classes. $|B|$ is the number of data objects in data system B. Then, $|A_{i,B}|$ is the number of data objects in $A_{i,b}$.

After classifying all the tuples in the training set B, the total amount of information required for adjustment is represented by entropy. Then, the overall process of calculating entropy B is

$$Info(B) = -\sum_{i=1}^{x} p_i \log_2(p_i). \tag{1}$$

Among them, $p_i = |A_{iB}|/|B|$ the training set B is classified according to the y characteristics of the attribute C, that is, C contains y different objects $\{c_1, c_2, \ldots, c_y\}$. Meanwhile, B is divided into y partition $\{B_1, B_2, \ldots, B_y\}$. The information required for classification can be obtained by weighted summation of the entropy of the y partitions, which is expressed as follows:

$$\mathrm{Info}_C(B) = -\sum_{i=1}^{y} \frac{|B_i|}{|B|} \times \mathrm{Info}(B_i). \tag{2}$$

The information gain is

$$\mathrm{Gain}(C) = Info(B) - Info_C(B). \tag{3}$$

Information gain measures the information required for the partition of the training set B according to C. When gain (C) is the largest, its corresponding C is the attribute to be divided, which can minimize the amount of information required to classify the training set B.

3.2. Bayesian Classification Method. The interpretation of Bayesian theory goes like this: suppose M is a data source in a training program and uses the feature y-values to describe M. Assuming that H represents M data which belongs to category C [18], then $p(H|M)$ represents the probability that event H occurs below baseline M, that is, the probability that event H is established below baseline M.

The Bayes rule is as follows:

$$p(H|M) = \frac{P(M|H)P(H)}{P(M)},$$

$$p(A_i|M) = \frac{P(\mathrm{M}|A_i)P(A_i)}{P(M)},$$

$$p(A_i) = \frac{\mathrm{Numberofsamplesbelongingtoclass A}A_i}{\mathrm{Thetotalnumberofsamplesinthetrainingsety}}. \tag{4}$$

The highest probability can only be obtained by increasing the size of $P(M|A_i)P(A_i)$, but since its calculation is very complicated and the value of the formula is very large, it needs to be calculated based on a simple independent order system. $P(M|A_i)$ can be represented by formula (5)

$$(M|A_i) = \prod_{k=1}^{y} P(M_k|A_i) = P(m_1|A_i)P(m_2|A_i).P(m_n|A_i). \tag{5}$$

Among them, m_k represents the value of attribute C_k corresponding to tuple M.

3.3. Least Mean Square Algorithm. Least mean squares (LMS) is an automatic training algorithm [19]. It expresses the difference between the result and the expected result by calculating the difference of the weight vector m. $E(m^*) \le E(m)$ represents the weight of the iterative network. Through the adjustment of η in the LMS algorithm, within a certain value range, increasing η will reduce the adjustment time, but the system no longer converges when it exceeds this value range [19]. When η is small, the performance of the LMS becomes good.

The vector size is defined using LMS as follows:

$$m_{p+1} = m_p + \Delta m_p = m_p - \eta \nabla E\left(m_p\right) = m_p - \eta \frac{\partial E}{\partial M}. \tag{6}$$

During one computation cycle, training data pairs (m, d) are randomly generated from the training data. Among them, m is the input, and d is the desired response. This leads to the neuron density $f(u)$, whose calculation formula is as follows:

$$u = m^T x. \tag{7}$$

After bringing u into the activation function, the output of the neuron can be obtained as follows:

$$o = f(u) = f\left(m^T x\right). \tag{8}$$

To determine the error size m for a specific condition (m and d), a direct comparison is made between the expected outcome d and the neuron. The error signal is the difference between the expected result and the result.

$$e = d - o = d - \left(m^T x\right). \tag{9}$$

The error E is used to measure neuron size and adjust to reduce the charge across the network density. The atypical deviation function of E with weight m is a parabolic surface function with a hollow center of mass. This is relatively a small amount of function, which can effectively reduce the charge function value. The dip angle can be used to find the minimum next to the paraboloid [20].

The formula for E is as follows:

$$E = \frac{1}{2}e^2 = E(m). \tag{10}$$

The value corresponding to the function E for each score of the vector weight m is the degree.

$$\nabla E(w) = \frac{\partial E}{\partial u}\frac{\partial u}{\partial m}. \tag{11}$$

Among them, $\partial E/\partial u$ is called the error signal, which is used to measure the degree of change of the error when the input of u changes. $\partial u/\partial m$ is used to measure the degree of influence on the weight vector m when calculating a specific input u. By applying the chain rule to formula (13) again, the formula is as follows:

$$\nabla E(m) = \frac{\partial E}{\partial e}\frac{\partial e}{\partial o}\frac{\partial o}{\partial u}\frac{\partial E}{\partial m}. \tag{12}$$

Differentiating e on both sides of formula (12) is as follows:

$$\frac{\partial E}{\partial e} = e. \tag{13}$$

At the same time, both sides of formula (11) are simultaneously differentiated for o as follows:

$$\frac{\partial E}{\partial e} = -1. \tag{14}$$

At the same time, both sides of formula (10) are simultaneously differentiated for u as follows:

$$\frac{\partial o}{\partial u} = f'(u). \tag{15}$$

Finally, both sides of formula (9) are simultaneously differentiated for m as follows:

$$\frac{\partial u}{\partial m} = x. \tag{16}$$

Therefore, the first derivative of the charge function E with respect to the weight m can be expressed as follows:

$$\nabla E(m) = -ef'(u)x. \tag{17}$$

The LMS rules are

$$m_{p+1} = m_p + \Delta m_p = m_p - \eta \nabla E\left(m_p\right) = m_p + \eta e_p f'\left(u_p\right)x_p. \tag{18}$$

4. Training Method of Flute Breath

In the process of playing the flute, it is necessary to maintain a close connection between spirit and timbre. The sound of the flute is guaranteed to be beautiful through the timbre, and the timbre of the flute can be maintained for a longer

time through breath training. In the actual training process, the player's breath should be trained by inhaling and exhaling, but there is a certain correlation between the timbre of the flute and the breath. For example, the breath training of the flute requires the player to have good physical fitness so as to ensure normal performance. When the player's body is full of breath, the body is in a state of high oxygen, which keeps the body stable. In the context of this situation, the player can drive the vocal part by exhaling and inhaling, effectively playing a beautiful flute sound.

4.1. Experimental Process. To test the impact of IoT big data on students' in flute breath training and teaching, the following experiment was carried out: 10 flute students were randomly selected. In order to avoid experimental errors, the testers were all flute beginners. Among them, 5 people were in the experimental group, and 5 people were in the control group. The control group was trained according to the traditional flute breath training method. The experimental group was trained according to the training method of flute breath based on IoT big data. The training period was 6 months. During the training, the experimental group and the control group were subjected to the leg strength test, the chest, abdomen, and back strength test, the long-tone exercise test, and the breath stability test. By observing and comparing the test results of the experimental group and the control group, the impact of the flute breath training method based on the big data of the IoT on the students is analyzed.

4.2. Experimental Data. In order to avoid experimental errors, the students who take the test are not much different in age and have the same flute playing level. The specific data of the students are shown in Table 1.

4.3. The Purpose of the Experiment. In order to obtain the effect of flute players' reasonable and effective breath training, IoT big data technology is applied to flute breath training teaching. At the same time, the impact of Internet of Things big data technology on players' flute breath training is observed.

5. Impact of Internet of Things Big Data on Flute Breath Training

5.1. Leg Strength Test. Good physical fitness is the basic guarantee for a player to perform. Leg strength training for the player will allow the player to keep their body stable while playing. The stronger the player's legs, the stronger the waist and lungs, the more stable the breath output and the better the performance. The students in the experimental group and the students in the control group are given leg strength training, and the results are recorded once a month to analyze the differences between the two groups. The results are shown in Figure 4.

In Figure 4, Figure A is the result of the leg strength test of the students in the control group, and Figure B is the result of the leg strength test of the students in the experimental group. With the increase of training time, the leg strength index of the students in the control group and the experimental group also increased. Among them, in the control group, the leg strength index of student 1 increased from 6.9 to 7.4, and the index increased by 0.5. Student 2's leg strength index increased from 6.8 to 7.2, and the index increased by 0.4. Student 3's leg strength index increased from 7 to 7.4, and the index increased by 0.4. Student 4's leg strength index increased from 7.1 to 7.6, and the index increased by 0.5. Student 5's leg strength index increased from 6.9 to 7.4, and the index increased by 0.5. In the experimental group, student 6's leg strength index increased from 6.8 to 7.9, and the index increased by 1.1. Student 7's leg strength index increased from 7 to 7.9, and the index increased by 0.9. Student 8's leg strength index increased from 6.9 to 8, and the index increased by 1.1. Student 9's leg strength index increased from 7.1 to 8.1, and the index increased by 1. Student 10's leg strength index increased from 6.9 to 8.1, and the index increased by 1.2. To sum up, the leg strength index of the students in the control group increased by 2.3. The leg strength index of the students in the experimental group increased by 5.3. The leg strength training effect of the students in the control group is better.

Table 1: Experimental data.

	Age	Gender	Contact flute time	Daily practice time
1	17	Male	4 months	>1 hour
2	17	Female	2 months	1 hour
3	18	Female	3 months	<1 hour
4	16	Male	4 months	<1 hour
5	19	Female	3 months	>1 hour
6	20	Female	2 months	1 hour
7	18	Male	3 months	1 hour
8	19	Female	3 months	<1 hour
9	16	Female	4 months	>1 hour
10	17	Male	2 months	<1 hour

5.2. Strength Test of the Chest, Abdomen, and Back. Players need to use their chest, abdomen, and back strength when playing the flute. The chest, abdomen, and back strength training for the player can improve the storage capacity of the player's inhaled breath and improve the sound quality of the flute. In the training process, students should combine the strength of the waist to make the inhaled gas form a column of air in the body and cooperate with the chest to exhale so that they can find the scientific breath and adjust it. The two groups of students are given thoracic, abdominal, and back strength training, and the statistical results are analyzed. The results are shown in Figure 5.

In Figure 5, with the increase of training time, the strength index of the chest, abdomen, and back also increased for the students in the control group and the experimental group. Among them, in the control group, student 1's chest, abdomen, and back strength indexes increased from 6.8 to 7.5, and the index increased by 0.7. The thoracic, abdominal, and back strength indexes of student 2 increased from 6.9 to 7.4, and the index increased by 0.5. Student 3's chest, abdomen, and back strength indexes

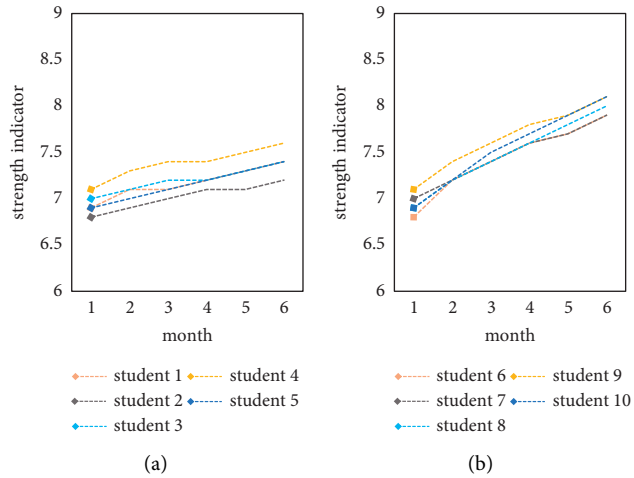

Figure 4: Leg strength test. (a) The control group and (b) the test group.

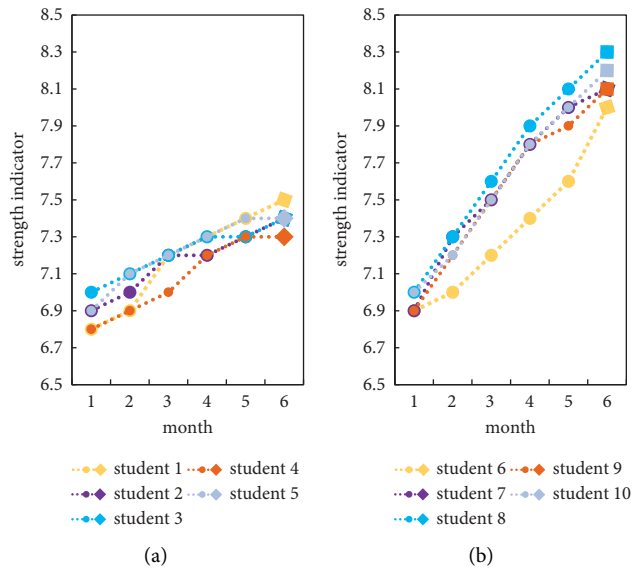

Figure 5: Chest, abdominal, and back strength test. (a) The control group and (b) The test group.

increased from 7 to 7.4, and the index increased by 0.4. The thoracic, abdominal, and back strength indexes of student 4 increased from 6.8 to 7.3, and the index increased by 0.5. The thoracic, abdominal, and back strength indexes of student 5 increased from 6.9 to 7.4, and the index increased by 0.5. In the experimental group, the thoracic, abdominal, and back strength indexes of student 6 increased from 6.9 to 8, and the index increased by 1.1. The thoracic, abdominal, and back strength indexes of student 7 increased from 6.9 to 8.1, and the index increased by 1.2. The thoracic, abdominal, and back strength indexes of student 8 increased from 7 to 8.3, and the index increased by 1.3. Student 9's chest, abdomen, and back strength indexes increased from 6.9 to 8.1, and the index increased by 1.2. The thoracic, abdominal, and back strength indexes of student 10 increased from 7 to 8.2, and the index increased by 1.2. To sum up, the thoracic, abdominal, and back strength indexes of the students in the control group increased by 2.6. The strength of the chest, abdomen, and back of the students in the experimental group increased by 6. The chest, abdomen, and back strength training effects of the students in the control group are better. Internet of Things big data technology can better help teachers train students.

5.3. Long Tone Practice Test. Long tone exercises are the most common form of breath training. Long tone practice requires the player to keep exhaling for a long time in order to make the tone more stable. Long tone practice requires students to maintain breath in the two states of exhalation and inhalation. Through repeated training, students' breathing time can be increased. The students in the control group performed traditional long tone exercises, while the students in the experimental group performed long tone

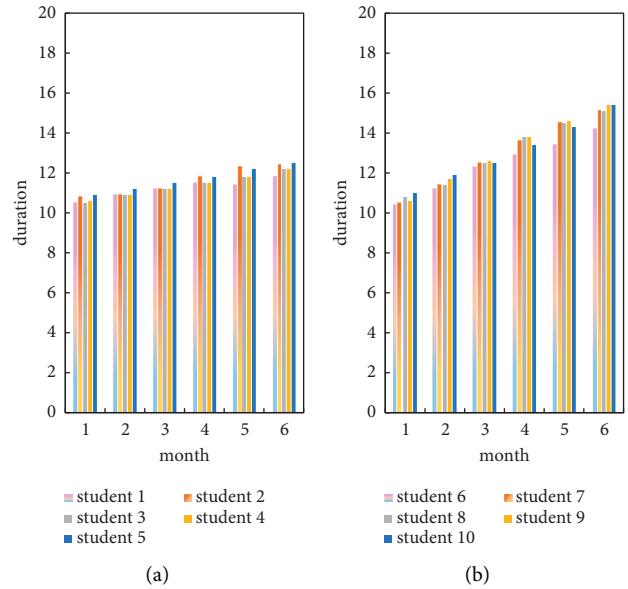

Figure 6: Long tone practice test. (a) The control group. (b) The test group.

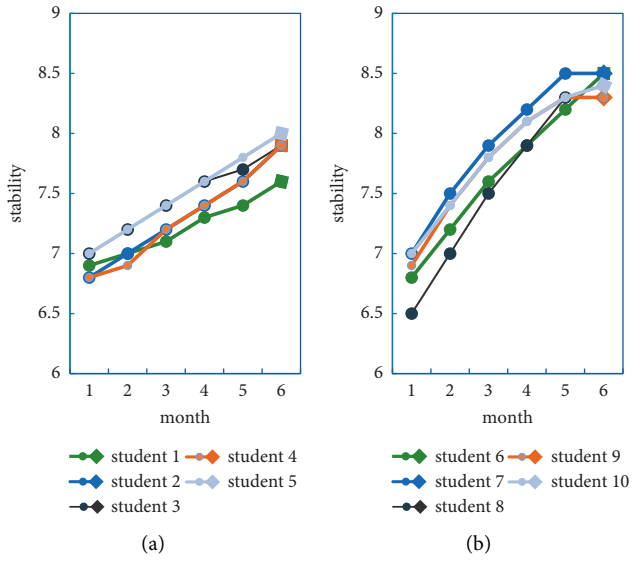

Figure 7: Breath stability test. (a) The control group. (b) The test group.

exercises based on the big data of the IoT. Then, the two groups of students are subjected to a breath test to observe the difference in the test results of the two groups of students. The specific results are shown in Figure 6.

In Figure 6, both the students in the experimental group and the students in the control group experienced an increase in the length of exhalation after 6 months of long tone practice. The growth rate of the experimental group is faster than that of the control group. Among them, in the control group, the average exhalation time of student 1 is 11.22 seconds. Student 2's average expiratory time is 11.57 seconds. Student 3's average exhalation time is 11.35 seconds. Student 4's average expiratory time is 11.37 seconds. Student 5's average expiratory time is 11.68 seconds. In the experimental group, student 6's average expiratory time is 12.4 seconds. Student 7's average expiratory time is 12.93 seconds. Student 8's average expiratory time is 13.02 seconds. Student 9's average expiratory time is 13.12 seconds. Student 10s average exhalation time is 13.08 seconds. To sum up, the average expiratory time of the students in the control group is 11.438 seconds. The exhalation time of the students in the experimental group is 12.91 seconds. Applying the big data technology of the IoT to the long tone practice, the students' exhalation time increased by 1.472 seconds.

5.4. Breath Stability Test. Players need to keep their playing breath stable during flute playing. The more stable the breath, the better the performance. The stability test is conducted on the students in the experimental group and

those in the control group. After 6 months of breath testing, whether there is any change in the students' stability and the difference between the two groups of students' stability are observed. The specific results are shown in Figure 7.

In Figure 7, Figure A is the breath stability test result of the control group, and Figure B is the breath stability test result of the experimental group. The breathing stability of the students in the experimental group increased faster. Among them, after 6 months of training in the control group, the stability of student 1 increased to 7.6. The stability of student 2 increased to 7.9. Student 3's stability increased to 7.9. Student 4's stability increased to 7.9. Student 5's stability increased to 8. The average stability of the students in the control group is 7.86. After 6 months of training in the experimental group, the stability of student 6 increased to 8.5. Student 7's stability increased to 8.5. Student 8's stability increased to 8.4. Student 9's stability increased to 8.3. Student 10's stability increased to 8.4. The average stability of the students in the experimental group is 8.42. To sum up, the flute breath training for students based on the big data of the IoT improves the students' breath stability by 7.1%.

6. Conclusion

Improvement in the flute player's performance level can help the player to perform breath training more accurately and comprehensively. This paper applied the IoT big data technology to the flute breath training process to help teachers better conduct flute breath training for students, which enabled students to master the basic training essentials. When the students performed breath training, the training movements of those students were observed in real time to maintain the accuracy of training. Through experimental tests on students, it was found that the application of Internet of Things big data technology to the process of breath training could effectively improve students' physical fitness and the stability of students' flute breath, which was of great help to students' follow-up learning. In addition, it could also be found that the big data technology of the IoT could effectively improve the training rate of students and promote the all-round development of students.

Data Availability

The data that support the findings of this study are available from the corresponding author upon reasonable request.

Conflicts of Interest

The author declares no potential conflicts of interest with respect to the research, authorship, and/or publication of this article.

References

[1] S. Akka and R. N. Aksoy, "An intercultural study on flute instruction in music teacher training programs (the German and Turkish examples)[J]," *Kalem Uluslararasi Egitim ve Insan Bilimleri Dergisi*, vol. 9, no. 16, pp. 155–175, 2019.

[2] O. Ahmed, N. G. El-Nahas, and A. F. Rahmy, "The effect of lung flute training on functional capacity in patients with chronic obstructive pulmonary disease[J]," *Bioscience Research*, vol. 15, no. 4, pp. 3786–3793, 2018.

[3] K. Konoval, "The flute art in Kharkiv: the performing and pedagogical traditions," *Problems of Interaction Between Arts Pedagogy and the Theory and Practice of Education*, vol. 54, no. 54, pp. 190–201, 2019.

[4] D. Moss, "Biofeedback-assisted relaxation training: a clinically effective treatment protocol," *Biofeedback*, vol. 48, no. 2, pp. 32–40, 2020.

[5] K. E. Keulen, M. E. Jansen, and R. Schrauwen, "Volatile organic compounds in breath can serve as a non-invasive diagnostic biomarker for the detection of advanced adenomas and colorectal cancer[J]," *Alimentary Pharmacology and Therapeutics*, vol. 51, no. 3, pp. 334–346, 2020.

[6] L. Cui, "Construction of big data technology training environment for vocational education based on edge computing technology," *Wireless Communications and Mobile Computing*, vol. 2022, no. 10, pp. 1–9, Article ID 1060464, 2022.

[7] C. Yang, Y. Weng, B. Huang, and M. Ikbal, "Development and optimization of CAD system based on big data technology," *Computer-Aided Design and Applications*, vol. 19, no. S2, pp. 112–123, 2021.

[8] N. Rahman, T. Daim, and N. Basoglu, "Exploring the factors influencing big data technology acceptance[J]," *IEEE Transactions on Engineering Management*, vol. 28, no. 99, pp. 1–16, 2021.

[9] T. Ge and X. Wu, "Accurate delivery of online advertising and the evaluation of advertising effect based on big data technology," *Mobile Information Systems*, vol. 2021, no. 1, pp. 1–10, Article ID 1598666, 2021.

[10] K. Chen, Y. Zu, and Y. Cui, "Design and implementation of bilingual digital reader based on artificial intelligence and big data technology[J]," *Journal of Computational Methods in Science and Engineering*, vol. 20, no. 2, pp. 1–19, 2020.

[11] L. Lei and A. Qianl, "Data mining and complex network algorithms for traffic accident analysis:[J]," *Transportation Research Record*, vol. 2460, no. 1, pp. 128–136, 2018.

[12] J. Lee, N. Ohba, and R. Asahi, "Discovery of zirconium dioxides for the design of better oxygen-ion conductors using efficient algorithms beyond data mining," *RSC Advances*, vol. 8, no. 45, pp. 25534–25545, 2018.

[13] Z. Ma, S. Wang, J. Shen, S. Li, and Y. Shi, "Design of multi-energy joint optimization dispatching system for regional power grids based on B/S architecture," *Energy Procedia*, vol. 158, no. 34, pp. 6236–6241, 2019.

[14] H. Chu, "Microbial metabolite fortifies the immune firewall," *Cell Host & Microbe*, vol. 28, no. 5, pp. 631–633, 2020.

[15] R. Manjupriya and A. Poornima, "Customer churn prediction in the mobile telecommunication industry using decision tree classification algorithm," *Journal of Computational and Theoretical Nanoscience*, vol. 15, no. 9, pp. 2789–2793, 2018.

[16] E. Fathima and S. Anithaa, "An overview of medical image classification using decision tree algorithm and association rule classifier[J]," *International Journal of Pure and Applied Mathematics*, vol. 119, no. 12, pp. 7535–7540, 2018.

[17] K. Cao, "Artificial intelligence on diabetic retinopathy diagnosis: an automatic classification method based on grey level co-occurrence matrix and naive Bayesian model," *International Journal of Ophthalmology*, vol. 12, no. 7, pp. 1158–1162, 2019.

[18] D. Shi, W. S. Gan, J. He, and B. Lam, "Practical implementation of multichannel filtered-x least mean square

algorithm based on the multiple-parallel-branch with folding architecture for large-scale Active noise control," *IEEE Transactions on Very Large Scale Integration Systems*, vol. 28, no. 4, pp. 940–953, 2020.

[19] J. Li, T. Zeng, X. Li et al., "Real-time fast polarization tracking based on polarization phase locking least mean square algorithm," *Optics Express*, vol. 27, no. 16, pp. 22116–22126, 2019.

[20] K. M. Das, "An improved all-pass filtered x least mean square algorithm[J]," *International Journal of Advanced Trends in Computer Science and Engineering*, vol. 9, no. 5, pp. 178–184, 2020.

Hindawi
Scientific Programming
Volume 2022, Article ID 1457547, 9 pages
https://doi.org/10.1155/2022/1457547

Research Article

Enterprise Financial Early Warning Based on Improved Whale Optimization Algorithm: Optimize the Perspective with Indicators

Bowei Li,[1] Mengzui Di,[2] Zikun Wei,[3] Hong Qiao,[1] and Xuzhao Li[4]

[1]*School of Economics and Management, Hebei Agricultural University, Baoding 071000, China*
[2]*School of Mechanical and Electrical Engineering, Hebei Agricultural University, Baoding 071000, China*
[3]*School of Economics, Nankai University, Tianjin 300071, China*
[4]*School of Plant Protection, Hebei Agricultural University, Baoding 071000, China*

Correspondence should be addressed to Mengzui Di; 202021401061@stu.hebut.edu.cn

Received 7 July 2022; Revised 12 August 2022; Accepted 31 August 2022; Published 16 September 2022

Academic Editor: Juan Vicente Capella Hernandez

The key to solving the problem of redundant financial indicators in addressing financial warning issues is to reduce the dimensionality of the original financial indicators. This paper proposes a model based on the whale optimization algorithm with mixed strategy (IWOA) combined with support vector machine (SVM), namely, the IWOA-SVM early warning model, which simultaneously performs index optimization and dimensionality reduction, and financial risk early warning identification. This paper takes a total of 302 enterprises specially treated in Shanghai and Shenzhen stock exchanges and normal enterprises of the same specification as the research samples to design the model. The results show that the improved whale optimization algorithm has better optimization speed and accuracy and improves the search ability of the original algorithm for the optimal solution. Compared with other dimensionality reduction methods, the IWOA-SVM model has the lowest index dimension after dimensionality reduction and has more excellent recognition effect. The dimensionality reduction results have certain universality for different classifiers, which provides a new idea for the selection of indicators for financial early warning.

1. Introduction

Since its inception in 1932, financial early warning models have undergone a transformation from univariate early warning models to multivariate early warning models, to logistic early warning models[1] and modern financial early warning models based on machine learning and integrated learning. When financial early warning models are built, they are prone to redundant financial indicators due to the richness and complexity of financial indicators. The presence of redundant financial indicators not only increases the computational effort of the model but also reduces the accuracy of its identification. Therefore, through the selection and dimensionality reduction of the original financial indicators, screening the optimal financial indicator combination is very important in the construction of the financial early warning model.

Fang and Yang [2] proposed the SGL-SVM method and applied it to the prediction of financial distress, which reduced the original 90-dimensional indicator variables to 24 dimensions, eliminating a large amount of noisy data while obtaining good identification results. Chen [3] and Fang [4] et al. used PCA to reduce the dimensionality of the indicator data and selected the top principal components with high variance contribution instead of the original indicators. In the face of high-dimensional indicators, Huang et al. [5] first performed independence tests on indicators to eliminate insignificant early warning indicators, after which they used random forest and XGBoost to calculate the importance of indicators, eliminated insignificant indicators, and used KPCA to reduce 14-dimensional financial indicators to 7-dimensional to construct a combined KPCA-WLSSVM model with high predictive power and generalization effect. Li et al. [6] selected the top ten features in terms of importance for feature optimization based on the feature

importance evaluation of the random forest algorithm, and the results showed that the overall accuracy, sensitivity, specificity, and AUC of early warning model were all improved after feature optimization. Zhou et al. [7] used grey clustering to select valid variables in their study on early warning of credit risk for listed companies, followed by logistic regression models for prediction. Luo and Wang [8] used an improved MRMR algorithm in constructing a financial early warning model, taking into account both feature relevance and redundancy for feature preference. Xiaoyan et al.[9] used significance tests and normality tests to select features with significant differences as a way to improve the accuracy of financial early warning models.

Feature selection is an important tool for feature dimensionality reduction. When preferential dimensionality reduction is performed based on the correlation information of indicators, features that are favorable to the identification results may be excluded, and the interpretability of the model is relatively poor when the financial early warning model is constructed using factor analysis. Feature preference dimensionality reduction using metaheuristic algorithms has been widely used in areas such as behavioral recognition [10], network intrusion detection [11], and performance prediction [12]. For the field of financial early warning, metaheuristic algorithms are mostly used for hyperparameter optimization of classifiers [13–15] and are less frequently applied in financial indicator preference dimensionality reduction. The whale optimization algorithm (WOA) is a novel metaheuristic algorithm proposed by Mirjalili and Lewis [16], which, like other metaheuristics, suffers from the problem of low accuracy in finding the optimal solution and how to improve the algorithm's ability to search for the optimal solution has received much attention from scientists [17, 18]. Kaur and Arora [19]introduced a chaos mechanism to optimize the initial position of the population. Introducing adaptive weights [20] or improving the convergence factor [21] for the algorithm can balance the search ability between the early and late stages of the algorithm. Therefore, this paper uses improved whale optimization algorithm with mixed strategy (IWOA) and support vector machine (SVM) to preferentially reduce the dimensionality of the original financial indicators and construct an IWOA-SVM financial warning model.

2. IWOA-SVM Financial Early Warning Model Construction

2.1. Whale Optimization Algorithm. The whale optimization algorithm is a new intelligent optimization algorithm that has been proposed based on the special feeding behavior of humpback whales, which consists of three main parts: encircling prey, bubble-net attack, and searching for prey.

2.1.1. Encircling Prey. During the whale feeding process, the location of the prey is first observed and searched to surround it. The optimal solution to the problem is predetermined to be the location of the prey, and during the iteration of the algorithm, the fitness value calculated by the fitness function is used to evaluate the merit of each group of financial indicators. Therefore, the design of the fitness function is crucial. In order to take into account the smallest possible dimension of the financial indicators while having a high accuracy rate, the fitness function in this paper is

$$\mathrm{Fitn}\,(IWOA) = 0.99 \cdot (1 - Acc) + 0.01 \cdot \left(\frac{\mathrm{feasel}}{\mathrm{numfea}}\right). \quad (1)$$

Among them, *Acc* represents the correct rate of five-fold cross-validation of each financial indicator feature combination in the SVM classifier, feasel is the dimension of financial indicator features included in randomly selected individuals, and numfea represents the total dimension of financial indicator features.

In the iteration process of the algorithm, the position of the individual with the optimal fitness value of the current population is taken as the optimal position, and other individuals are close to the optimal position. The mathematical expression is

$$\begin{aligned} X(\mathrm{t}+1) &= X_{\mathrm{best}}(t) - A \cdot D, \\ D &= \left|CX_{\mathrm{best}}(t) - X(t)\right|, \end{aligned} \quad (2)$$

where $X_{\mathrm{best}}(t)$ denotes the position vector of the optimal individual of the current population, $X(t)$ denotes the position vector of each individual in the current population, and t denotes the current number of iterations, the expressions of A and C are as follows.

$$\begin{aligned} A &= 2 \cdot a \cdot r_1 - a, \\ C &= 2 \cdot r_2, \\ a &= 2\left(1 - t/T_{\max}\right), \end{aligned} \quad (3)$$

where a is the convergence factor, $r_1$and r_2 are random numbers within [0, 1], and $T_{\max}$ denotes the maximum number of iterations.

2.1.2. Bubble-Net Attack. This phase consists of two types of position update, contraction bracketing, and spiral: first, contraction bracketing, in which the position is updated by adjusting the convergence factor a in equation (3); and second, spiral position update, which simulates a whale spiraling up to hunt close to its prey, with the mathematical expression:

$$\begin{aligned} X(t+1) &= X_{best}(t) + D_p \cdot e^{bl} \cos(2\pi l) \\ D_P &= \left|X_{best}(t) - X(t)\right|, \end{aligned} \quad (4)$$

where D_P denotes the distance between an individual whale and the current optimal solution, b denotes a constant in the shape of the spiral, and l denotes a random number in the range [–1, 1]. At this stage, the individual position of the whale is updated by randomly selecting contraction encirclement and spiral contraction. The mathematical expression is

$$X(t+1) = \begin{cases} X_{\mathrm{best}}(t) - A \cdot D, & p < 0.5, \\ X_{\mathrm{best}}(t) + D_P \cdot e^{bl} \cos(2\pi l), & p \geq 0.5, \end{cases} \quad (5)$$

where p represents a random number in the range [0, 1].

2.1.3. Searching for Prey. Individual whales search for prey by randomly swimming away. The random search strategy allows the algorithm to have a good global search performance and randomly selects whale individuals in the population to update their position when $|A| \geq 1$. The mathematical expression is

$$\begin{aligned} X(t+1) &= X_{\text{rand}}(t) - A \cdot D, \\ D &= \left| C \cdot X_{\text{rand}}(t) - X(t) \right|, \end{aligned} \tag{6}$$

where $X_{\text{ran d}}(t)$ denotes a randomly selected individual whale.

2.2. Improvements to the Whale Optimization Algorithm. As the whale optimization algorithm has the problems of poor global search ability, easily falling into local optimal solutions, and poor convergence accuracy in the computation process, this paper uses Gauss mapping to initialize the population to improve population diversity, introduces adaptive weights to balance global and local search ability, and uses a stochastic dimension-by-dimension variation strategy based on Cauchy mutation and reverse learning to improve the ability to jump out of local optima with a hybrid strategy to improve the whale optimization algorithm.

2.2.1. Gauss Mapping to Initialize the Population. The original whale optimization algorithm initializes the population in a random way, that is, it randomly generates a combination of financial indicators. In order to expand the population search range and improve the population diversity, this paper adopts Gauss mapping to initialize the population, which is more traversable and more uniformly distributed compared to the original algorithm, and the mathematical expression of Gauss mapping is

$$X_{K+1} = \begin{cases} 0, \mathrm{X}_K = 0, \\ \dfrac{1}{X_K \bmod (1)}, X_K \neq 0, \end{cases} \tag{7}$$

$$\frac{1}{X_K \bmod (1)} = \frac{1}{X_K} - \left[\frac{1}{X_K} \right].$$

Among them, mod represents the remainder function, [ ] represents rounding, and X_K represents the chaotic sequence generated by Gauss mapping.

2.2.2. Adaptive Weights. Adaptive weights can effectively balance global and local search capabilities, for which an adaptive weighting factor ω is introduced with the following mathematical expression.

$$\omega = \sin\left(\frac{\pi \cdot t}{2 \cdot T_{\max}} + \pi \right) + 1, \tag{8}$$

where t is the current number of iterations and $T_{\max}$ is the maximum number of iterations.

The equation for updating the location of individual whales after the introduction of adaptive weights is as follows.

$$X(\mathrm{t}+1) = \omega \cdot X_{\text{best}}(t) - \mathrm{A} \cdot \mathrm{D}, \tag{9}$$

$$X(t+1) = \omega \cdot X_{\text{best}}(t) + \mathrm{D_P} \cdot \mathrm{e}^{\mathrm{bl}} \cos(2\pi \mathrm{l}), \tag{10}$$

$$X(\mathrm{t}+1) = \omega \cdot X_{\text{rand}}(t) - \mathrm{A} \cdot \mathrm{D}. \tag{11}$$

2.2.3. Stochastic Dimension-by-Dimension Variation Strategy Based on Cauchy Mutation and Reverse Learning Cauchy Mutation. The Cauchy distribution, similar to the normal distribution, is one of the common distributions in the probability theory and is characterized by a uniform distribution of variances due to its slow decline from peak to zero values, the mathematical expression of which is

$$X_{\text{best}}^{'}(t) = X_{\text{best}}(t) + cauchy(0,1) * X_{\text{best}}(t). \tag{12}$$

Reverse learning improves the search performance of an algorithm by solving the current solution backward in the same space and is widely used in various optimization algorithms with the mathematical formulation of

$$X_{\text{best}}^{'}(t) = ub + (lb - X_{\text{best}}(t)). \tag{13}$$

When only one variation strategy is selected in the algorithm, it will lead the algorithm into the local optimum problem, and the traditional variation approach mostly uses random variation or variation in all dimensions, while the dimension-by-dimension variation approach can avoid the influence between dimensions and fully explore the optimal solution; therefore, this paper uses a random dimension-by-dimension variation strategy based on Cauchy mutation and reverse learning to perturb the optimal individual.

Since the new solution generated is not necessarily better than the optimal position, a greedy rule is used to decide whether to adopt the new solution.

$$x' = \begin{cases} x'_{\text{best}}, f(x'_{\text{best}}) < f(x_{\text{best}}), \\ x_{\text{best}}, f(x'_{\text{best}}) \geq f(x_{\text{best}}). \end{cases} \tag{14}$$

2.3. IWOA-SVM Financial Early Warning Model Construction. Due to a large number of linear and nonlinear complex relationships between the financial indicators of an enterprise, when constructing a financial early warning model, low-quality financial indicator data can lead to feature confounding and high model computation, reducing the financial early warning capability of the model. Therefore, it is necessary to reduce the dimensionality of financial indicators and select the optimal combination of financial indicators with good predictive power. The IWOA-SVM financial early warning model constructed in this paper improves the whale optimization algorithm through mixed strategies and improves the search ability for the optimal

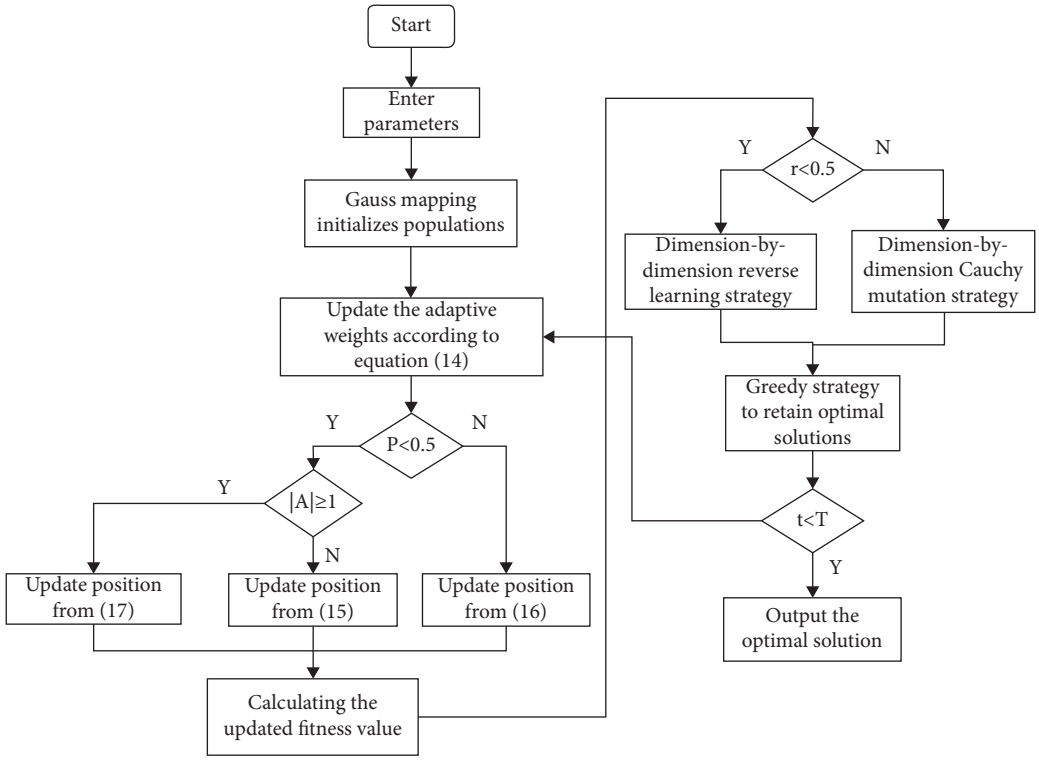

Figure 1: IWOA-SVM financial early warning model.

solution, that is, the combination of financial indicators with the best predictive ability, to improve the model recognition effect. The flow chart of the IWOA-SVM model is as follows Figure 1.

The key steps in the IWOA-SVM financial early warning model are as follows:

(1) Data standardisation: due to the different magnitudes of the financial indicator values and the fact that SVM is typically a classification algorithm based on a distance metric, to avoid impact on the model performance, the financial indicator data is normalized by the formula as follows:

$$X = \frac{x - \mu}{\delta}, \tag{15}$$

where μ is the mean and δ is the standard deviation of the data.

(2) Initializing the population. The number of IWOA algorithm populations is set to 20 and the maximum number of iterations is 50, i.e., 20 sets of financial indicator combinations are generated at each iteration using the Gauss mapping strategy.

(3) Calculating the fitness value. Based on the fitness function, the fitness values of all current combinations of financial indicators are calculated and the individual with the lowest fitness value is taken as the current optimal solution.

(4) Location update. When the probability $p < 0.5$ and $|A| < 1$, the position is updated according to equation (9), if $|A| \geq 1$, the position is updated according to equation (10); when the probability $p \geq 0.5$, the position is updated by equation (11).

(5) Optimal position perturbation. The optimal solution is optimized using a stochastic dimension-by-dimension variation strategy based on Cauchy mutation and reverse learning. If the fitness value of the new solution is better than the optimal solution before optimization, the current optimal combination of financial indicators and fitness values are retained and discarded if not.

(6) Iterative operations. Determine whether the maximum number of iterations has been reached, and if the condition is met, output the optimal combination of financial indicators and the optimal fitness value, if not, repeat steps 3–5 to continue the search.

(7) Output SVM algorithm classification results based on the optimal combination of financial indicators.

3. Empirical Analysis

3.1. Sample Selection and Data Sources. The article selects A-share listed companies in Shanghai and Shenzhen as the empirical sample and classifies the empirical sample into normal companies and ST companies by taking whether the listed companies are specially treated (ST) during their existence as the criterion. For normal companies, continuous financial data are obtained for the years 2019–2021; for ST companies, the year in which the main body of the ST

company is specially treated is recorded as year t, and continuous financial data are obtained for the previous two years. In order to eliminate the possible adverse effects of imbalanced categorical data on the model, after excluding companies with serious data deficiencies, the positive and negative samples were matched according to a 1 : 1 ratio, using the rule that companies belonging to the same or similar industries and the overall size of the companies were comparable. The final selection of 151 ST companies and 151 normal companies yielded a total of 302 valid samples and 906 sets of observations. All data were sourced from the CSMAR database.

3.2. Selection of Indicators. When constructing financial early warning models for listed companies, it is common to start with financial indicators that reflect the operating status of the company. In this paper, a total of 32 financial indicators are selected from four aspects: solvency, profitability, operational capability, and development capability, specifically five indicators are selected from solvency. In order, they are current ratio (X1), quick ratio (X2), gearing ratio (X3), equity multiplier (X4), and equity ratio (X5); 12 indicators were selected in terms of profitability, in order, they are return on assets (X6), net profit margin on total assets (X7), net profit margin on current assets (X8), net profit margin on fixed assets (X9), EBITDA (X10), earnings before interest, tax, depreciation and amortization (X11), gross operating margin (X12), operating profit margin (X13), net operating margin (X14), management expense ratio (X15), financial expense ratio (X16), and cost margin (X17); 11 indicators were selected from the operating capacity, in order of accounts receivable to revenue ratio (X18), inventory to revenue ratio (X19), operating cycle (X20), accounts payable turnover (%) (X21), current assets to revenue (X22), current assets turnover (X23), fixed assets to revenue (X24), fixed assets turnover (X25), noncurrent assets turnover (X26), capital intensity (X27), and total assets turnover (X28); and four indicators were selected in terms of growth capacity, in the following order: growth rate of total operating revenue (X29), growth rate of total operating costs (X30), growth rate of administrative expenses (X31), and sustainable growth rate (X32). Considering that nonfinancial indicators are also important in risk identification and early warning, this paper selects two nonfinancial indicators at the level of management's governance capacity, namely, the proportion of management men (X33) and the average age of management (X34) in that order. The finalized corporate financial early warning model contains a total of 34 indicators with a large number of features, which should be subject to dimensionality reduction.

3.3. IWOA-SVM Model Identification Results. The article divides the training and test sets in the ratio of 6 : 4, sets the initial population of the whale optimization algorithm to 20 and the number of iterations to 50, and runs the WOA-SVM before improvement and the IWOA-SVM model after improvement twenty times, respectively, under the same hardware conditions, and the number of financial indicators, the number of convergence generations, and accuracy curves are shown in Figure 2 after ranking them according to the accuracy rate from smallest to largest, and the distribution is shown in Table 1. After comparison, it can be seen that compared with the WOA-SVM model, the IWOA-SVM model has different effects in terms of convergence speed, convergence accuracy, and reducing the dimension of financial indicators. As can be seen from Figure 2, the IWOA-SVM model largely outperforms the WOA-SVM model in terms of the number of generations of convergence and the number of financial indicators when ranked from small to large in terms of accuracy. As can be seen from Table 1, after the improvement of the mixed strategy, the average number of convergence generations was reduced from 12 to 5.15, a reduction of 6.85; the average number of financial indicator dimensions was reduced from 14.90 to 10.95, a reduction of 3.95; meanwhile, the average accuracy of IWOA-SVM model identification was increased from 84.50% to 86.74%, an increase of 2.24%, and the highest accuracy was increased from 86.23% to 87.60%, an increase of 1.37%. It can be seen that the convergence speed and optimization-seeking ability of the mixed strategy improved whale optimization algorithm proposed in this paper are significantly improved over the original algorithm, which can eliminate redundant indicators while having good accuracy and can meet the financial warning needs of this paper.

The IWOA-SVM model identified the highest accuracy of 87.60%, while the financial indicators with an accuracy of 87.60% were obtained from two groups. The first group includes current ratio (X1), quick ratio (X2), equity multiplier (X4), equity ratio (X5), total assets net profit margin (X7), EBITDA (X11), average age of management (X34), current assets to revenue ratio (X22), fixed assets to revenue ratio (X24), noncurrent assets turnover ratio (X26), and capital intensity (X27), a total of 11 financial indicators; the second group includes current ratio (X1), equity multiplier (X4), total assets net profit margin (X7), EBITDA (X10), EBITDA (X11), cost margin (X17), the average age of management (X34), accounts receivable to revenue (X18), inventories to revenue (X19), fixed assets to revenue (X24), noncurrent asset turnover (X26), total asset turnover (X28), and sustainable growth rate (X32), a total of 13 financial indicators.

The identification accuracy of the two sets of financial indicators, the error rate of the first category, and the error rate of the second category are shown in Table 2. The first type of error rate (error I) is the proportion that the model identifies ST samples as normal samples, and the second type of error rate (error II) is the proportion that the model identifies normal samples as ST samples. In consideration of the principle of accounting prudence, error I should be avoided as far as possible, and a high error rate of St samples will lose the practical significance of financial early warning. Comparing the identification results of the first group and the second group, the second group had 27 ST samples predicted as non-ST, the first group had 25 ST samples predicted as non-ST, and the first group had a lower error I, better early warning effect. Therefore, the combination of financial indicators of the first group is selected as the

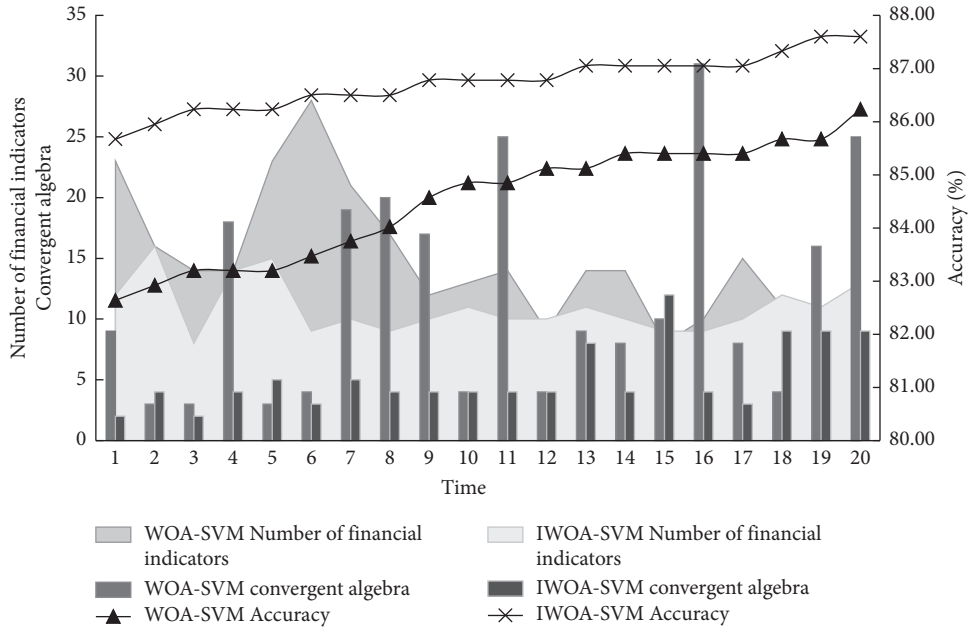

Figure 2: Comparison of the results of 20 runs of IWOA-SVM and WOA-SVM.

Table 1: Distribution of IWOA-SVM and WOA-SVM model results.

Model	Distribution	Convergence generation	Indicator dimension	Accuracy %
WOA-SVM	Max	31	28	86.23
	Min	3	8	82.64
	Average	12	14.90	84.50
IWOA-SVM	Max	12	16	87.60
	Min	2	8	85.67
	Average	5.15	10.95	86.74

Table 2: Comparison of identification results.

Project	True class	Predicted class		Total	Result (%)	
		ST	Non-ST			
Group one financial indicators	ST	156	25	181	Error I	13.81
	Non-ST	20	162	182	Error II	10.99
	Total	176	187	363	Accuracy	87.6
Group two financial indicators	ST	154	27	181	Error I	14.82
	Non-ST	18	164	182	Error II	9.89
	Total	172	191	363	Accuracy	87.6

optimal combination for financial early warning in this paper. A total of 156 ST samples, 162 non-ST samples were correctly identified, 25 ST samples were predicted as non-ST, and 20 non-ST samples were predicted as ST, with an error rate of 13.81% for the error I and 10.99 for the error II. The meanings of the financial indicators in the first group are shown in Table 3.

3.4. Comparison of Different Dimensionality Reduction Methods. In order to compare the effect of model dimensionality reduction, this paper selected principle component analysis (PCA), mutual information and maximal information coefficient (MIC), recursive feature elimination (RFE), and XGBoost importance ranking four kinds of dimensionality reduction, with the increase of the selected dimensionality SVM recognition accuracy changes as shown in Figure 3, respectively, and selected the combination of indicators with the highest recognition rate as the corresponding optimal combination; recognition results are shown in Table 4. It can be seen from Table 4 that, among the four dimensionality reduction methods, the XGBoost importance ranking method selects the smallest combination dimension of financial indicators and has the lowest type two error rate, but the type one error rate is also at the highest level. In contrast, the IWOA-SVM model constructed in this paper improves the accuracy by 4.68%, reduces the type one error rate by 7.18%, and reduces the

Table 3: Meaning of financial indicators.

Indicator name	Meaning
Current ratio (X1)	Current assets/current liabilities
Quick ratio (X2)	(Current assets−inventories)/current liabilities
Equity multiplier (X4)	Total assets/total owners' equity
Equity ratio (X5)	Total liabilities/total owners' equity
Total assets net profit margin (X7)	Net profit/average balance of total assets
Earnings before interest, tax, depreciation, and amortization (X11)	Net profit + income tax expense + finance costs + depreciation of fixed assets, depreciation of oil and gas assets, depreciation of productive biological assets + amortization of intangible assets + amortization of long-term amortization expenses
Current assets to revenue ratio (X22)	Current assets/operating income
Fixed assets to revenue ratio (X24)	Fixed assets/operating income
Non-current assets turnover ratio (X26)	Operating income/noncurrent assets
Capital intensity (X27)	Total assets/operating income
Average age of management (X34)	The average of the ages of all directors and supervisors of the company (directors and supervisors whose ages are not disclosed are not included in the calculation)

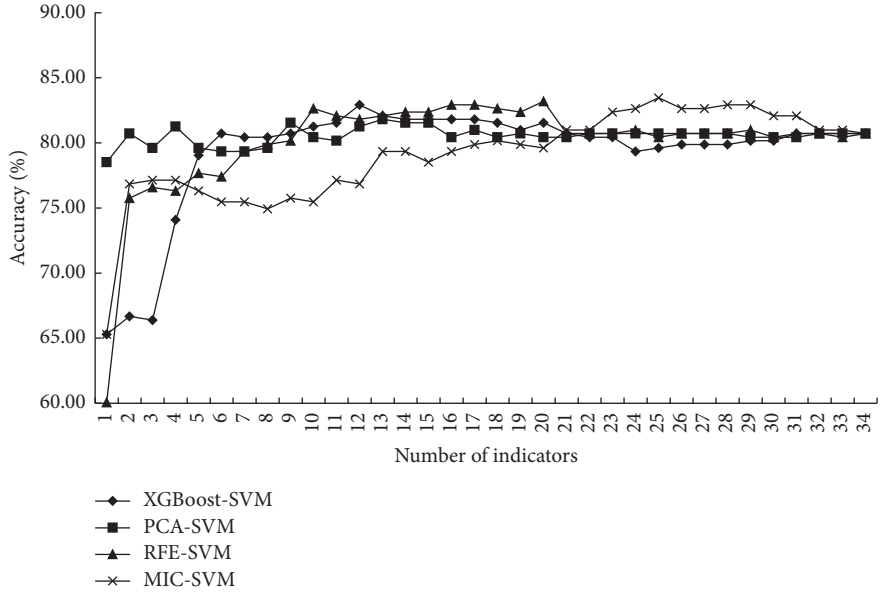

Figure 3: Variation in accuracy of the four downscaling methods.

Table 4: Identification results of different dimensionality reduction methods.

Method	Accuracy, %	Error I, %	Error II, %	Indicator dimension
PCA-SVM	81.82	20.44	14.93	13
MIC-SVM	83.47	18.78	14.29	25
RFE-SVM	83.20	19.89	13.74	20
XGBoost-SVM	82.92	20.99	13.19	12
IWOA-SVM	87.60	13.81	10.99	11

type two error rate by 2.2% when the index dimension is reduced by 1 dimension. The mic dimensionality reduction model has the highest accuracy and the lowest type one error rate, but the accuracy is 4.13% lower than the IWOA-SVM model, the type one error rate is 4.97% higher, and the type two error rate is 3.3% higher. However, the feature dimension of the model is as high as 25 dimensions, and the dimensionality reduction effect is not obvious. In summary, the IWOA-SVM model constructed in this paper can achieve optimal identification results with a minimum number of financial indicators.

3.5. Algorithm Performance Comparison. To compare the performance of the IWOA-SVM algorithm, salp swarm algorithm (SSA), particle swarm optimization (PSO), flower pollination algorithm (FPA), and grey wolf optimizer (GWO) were selected. Under the same hardware

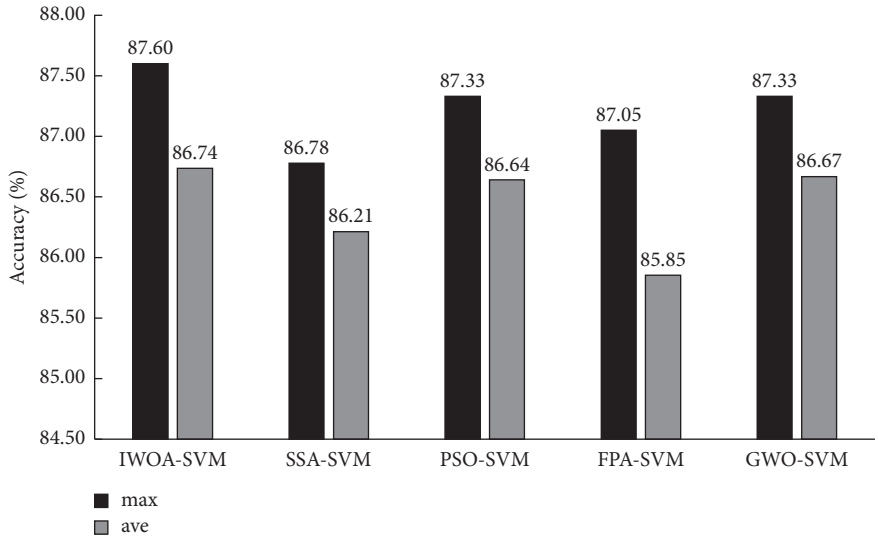

Figure 4: Algorithm performance comparison.

Table 5: Comparison of recognition results of different classifiers.

Classifier	Before indicator selection			After indicator selection		
	Accuracy, %	Error I, %	Error II, %	Accuracy, %	Error I, %	Error II, %
LG	78.79	20.99	21.43	83.20	19.89	13.74
RF	83.75	18.23	14.29	86.50	16.02	10.99
KNN	77.96	24.31	19.78	82.09	18.23	17.58
DT	79.34	22.10	19.23	81.54	20.44	16.48
SVM	80.72	19.34	19.23	87.60	13.81	10.99

conditions, keep the same parameter settings as IWOA-SVM. After running 20 times, the maximum and average values of the recognition accuracy are shown in Figure 4. It is easy to find that the IWOA-SVM model in this paper has the highest recognition accuracy and average accuracy, and the model performance is better than other metaheuristic algorithms.

3.6. Comparison of Universality of Dimension Reduction Effect. In order to verify the algebra liability and identification of the preferred dimensionality reduction effect of the IWOA-SVM financial warning model, five financial warning models based on logistic regression (LG), random forest (RF), K-nearest neighbor (KNN), decision tree (DT), and SVM were constructed simultaneously in this paper. Identify the original financial indicator combination and the optimal financial indicator combination obtained in this paper. The identification results are shown in Table 5. It can be seen from the table that the logistic regression, random forest, K-nearest neighbor, and decision tree models are obtained using this paper. After the optimal combination of financial indicators, the model recognition accuracy increased by 4.41%, 2.75%, 4.13%, and 2.2%, respectively, and the first type error rate decreased by 1.1%, 2.21%, 6.08%, and 1.66%, respectively. Compared with the SVM model for identifying the original data set, the IWOA-SVM model has an accuracy improvement of 6.88% to 87.60%, and the first type error rate decreased by 5.53% to 13.81%, and the second type error rate decreased by 8.24% is 10.99%. Collectively, it appears that the IWOA-SVM financial warning model constructed in this paper has the highest accuracy rate, the lowest type one error rate, and the best model identification effect.

4. Discussion and Conclusions

To address the issue of indicator selection in the construction of financial early warning models, this paper proposes the IWOA-SVM financial early warning model. A sample of 151 ST companies and 151 normal companies listed on A-shares in Shanghai and Shenzhen in 2019–2021 was used for the empirical analysis, and a mixed strategy is used to improve the original whale optimization algorithm for the problems of poor merit-seeking ability and slow convergence accuracy. The empirical analysis shows that first, the IWOA-SVM algorithm reduced the original 34-dimensional metrics to 11 dimensions, with a model recognition accuracy of 87.60%, an improvement of 6.88%, and a type one error rate of 13.81%, a reduction of 5.53%, the dimensionality reduction and recognition better than the four dimensionality reduction methods such as PCA. Second, compared to the original whale algorithm, the improved whale optimization algorithm with mixed strategy reduced the average financial indicator dimension by 3.95 and the average number of convergence generations by 6.85, the highest accuracy was improved by 1.37%, indicating the

algorithm's convergence speed and optimization-seeking ability was enhanced. Thirdly, using logistic regression, random forest, K-nearest neighbor, and decision tree to identify the combination of indicators before and after dimensional reduction and optimization, the accuracy rate has improved to different degrees, indicating that the method of dimensional reduction and optimization of indicators has certain universality for different classifiers. Taken together, the IWOA-SVM financial early warning model proposed in this paper has the highest accuracy rate and the lowest type I error rate, providing a new way of thinking about the selection of indicators for the construction of financial early warning models, which is an accurate, efficient, and scientific financial early warning model.

Data Availability

The data presented in this study are available on request from the corresponding author.

Conflicts of Interest

The authors declare no conflicts of interest.

Authors' Contributions

B. L., Q. H., and Z. W. conceptualized the study; B. L., M.D., and X. L. contributed to methodology; B. L., M.D., and Z. W. provided software; B. L. and M.D. contributed to data curation. All authors have read and agreed to the published version of the manuscript.

Acknowledgments

This research was funded by the Hebei Province Social Science Fund Project (grant no. HB20GL039).

References

[1] K. Jerzy, K. P. Anna, and L. Wojciech, "Identifying symptoms of bankruptcy risk based on bankruptcy prediction models—a case study of Poland[J]," *Sustainability*, vol. 14, no. 3, 2022.

[2] K Fang and Y. Yang, "SGL-SVM with its application in forecasting corporate financial distress[J]," *Statistica*, vol. 35, no. 08, pp. 104–115, 2018.

[3] Q Chen, "Research on financial risk warning of listed enterprises based on PCA-NBC algorithm," *Management & Technology of SME*, vol. 27, no. 12, pp. 85–87, 2021.

[4] F. Fang, "Research on the risk warning of de-listing of listed companies: a supporting vector machine prediction model based on principal component analysis[J]," *Frontiers in Economics and Management*, vol. 2, no. 4, 2021.

[5] H. Huang, Q. Xu, Y. Zhang, and H. Shi, "Weight-LSSVM financial crisis early warning model based on KPCA dimensionality reduction [J]," *Statistics & Decisions*, vol. 36, no. 20, pp. 180–184, 2020.

[6] J. Li, S. Ma, M. Jin, and C.-hsien Chu, "Early warning model of crowdfunding defaults based on SA-SVM [J]," *Journal of Statistics and Information*, vol. 33, no. 11, pp. 70–77, 2018.

[7] Q. Zhou, L. Wang, L. Juan, S. Zhou, L. Li, and J. Ma, "The study on credit risk warning of regional listed companies in China based on logistic model," *Discrete Dynamics in Nature and Society*, vol. 2021, Article ID 6672146, 2028 pages, 2021.

[8] K. Luo and G. Wang, "The research on financial early warning based on the improved MRMR algorithms and cost sensitive classification[J]," *Journal of Statistics and Information*, vol. 35, no. 03, pp. 77–85, 2020.

[9] A. Xiaoyan and J. Zhao, "Empirical analysis of financial early warning of resource-based listed companies," *Finance and Accounting Monthly*, vol. 39, no. 02, pp. 79–84, 2018.

[10] X. Li, *Behavior Recognition Method Based on Acceleration sensor[D]*, Xi'an University of Science and Technology, Xi'an, China, 2017.

[11] H. Xu, Ce Fang, X. Liu, and Z. Ye, "Network instrusion detection system based on improve moth-flame optimization algorithm [J]," *Journal of Computer Applications*, vol. 38, no. 11, pp. 3231–3235+3240, 2018.

[12] S. S. Shreem, H. Turabieh, A. A. Sana, and F. Baothman, "Enhanced binary genetic algorithm as a feature selection to predict student performance," *Soft Computing*, vol. 26, 2022.

[13] Y. Wang, Di Wang, and S. Wang, "Comparison of financial crisis early warning models based on PSO-BP and FOA-BP neural networks [J]," *Statistics & Decisions*, vol. 34, no. 15, pp. 177–179, 2018.

[14] Z. Zhang, L. Fan, Q. Zhao, and G. Zhang, "Research of financial early-warning model on evolutionary support vector machines based on genetic algorithms[J]," *Discrete Dynamics in Nature and Society*, vol. 2009, no. Pt.3, 2010.

[15] J. Zhang, C. Fan, and B. Wang, "Early warning study on financial risks of manufacturing companies based on PSO optimization SVM," *Friends of Accounting*, vol. 35, no. 14, pp. 52–56, 2017.

[16] S. Mirjalili and A. Lewis, "The whale optimization algorithm," *Advances in Engineering Software*, vol. 95, pp. 51–67, 2016.

[17] Z. Geng, Li Mu, S. Cao, and C. Liu, "A whale optimization algorithm based on hybrid revers learning strategy[J]," *Computer Engineering & Science*, vol. 44, no. 02, pp. 355–363, 2022.

[18] F. Jiang, L. Wang, and L. Bai, "An improved whale algorithm and its application in truss optimization," *Journal of Bionics Engineering*, vol. 18, no. 3, pp. 721–732, 2021.

[19] G. Kaur and S. Arora, "Chaotic whale optimization algorithm," *Journal of Computational Design and Engineering*, vol. 5, no. 3, pp. 275–284, 2018.

[20] Y. Zhang, Y. Zhang, G. Wang, and L Bingshan, "An Improved Hybrid Whale Optimization Algorithm Based on Differential Evolution," in *Proceedings of the 2020 International Conference on Artificial Intelligence and Electromechanical Automation (AIEA)*, pp. 103–107, IEEE, Tianjin, China, June 2020.

[21] X. Shi and Li Ming, "Whale optimization algorithm improved effectiveness analysis based on compound chaos optimization strategy and dynamic optimization parameters," in *Proceedings of the 2019 International Conference on Virtual Reality and Intelligent Systems (ICVRIS 2019)*, pp. 123–126, Jishou, China, September 2019.

Hindawi
Scientific Programming
Volume 2022, Article ID 9122934, 11 pages
https://doi.org/10.1155/2022/9122934

Research Article

Internet of Things Based Korean Cross-Cultural Communication Interactive Talent Training Model under Curriculum, Ideology, and Politics

Fengjiao Lin

College of Foreign Language & Literature, Northwest Normal University, Lanzhou 730070, Gansu, China

Correspondence should be addressed to Fengjiao Lin; cinderella@nwnu.edu.cn

Received 18 July 2022; Revised 16 August 2022; Accepted 3 September 2022; Published 15 September 2022

Academic Editor: Juan Vicente Capella Hernandez

With the development of society, the exchanges between various countries have become increasingly close, and this open communication mode also affects and changes the communication culture of each country. In the context of globalization, cross-cultural communication is increasing day by day, and cross-cultural communication ability has become a necessary quality for modern talents, so it is imperative to cultivate cross-cultural communication talents. However, the development level of informatization is insufficient, especially since the development of Internet of Things technology is lagging behind, the application level is low, and there are fracture characteristics in the application of each link. Information exchange cannot be effectively realized, information is incomplete, and asymmetry is obvious, and there is no effective information exchange platform. Following the trend of internationalization, scholars are paying more and more attention to the combination of cross-cultural communication and IoT technology. The combination of the two is to realize the real-time monitoring of personnel training. The acquisition and transmission of personnel training information is the primary problem to be solved in the realization of Korean cross-cultural communication. The wireless sensor network (WSN) has the characteristics of wide distribution of nodes, strong self-organization ability of routing, and good adaptability to dynamic changes in topology structure. WSN is used to solve this problem and is a good choice. Therefore, this paper used random forest algorithm and GBDT algorithm to apply WSN technology to the process of interactive talent training and established a network information service (NIS) system for interactive talent training. The experimental results have shown that the random forest algorithm and the GBDT algorithm can further simplify the input feature quantity and both can achieve good prediction results, while the GBDT model of the two models has relatively better prediction performance. The models obtained by the two methods meet the needs of detection parameter optimization, which realizes the real-time development of interactive talent training and realizes the intelligence and high efficiency of interactive talent training.

1. Introduction

Complying with the trend of international development, the process of studying Korean cross-cultural communication and interactive talent training is a gradual process. From the initial "cultivation of communicative competence" to today's "cultivation of cross-cultural communication and interactive talents," the research of this discipline is gradually in-depth and gradually improved through exploration. Under the background of economic globalization, the government, famous enterprises, human resources experts, college teachers, and scholars of higher education theory are increasingly calling for the cultivation of international talents. Internationalization has become a research content that cannot be ignored in the field of education theory and practice. The "interactive" talent training mode refers to the participation of enterprises as talent demanders in the whole process of talent training. During the training process, enterprises, students, and universities will understand each other and communicate in a timely manner to ensure seamless communication between schools, enterprises, and students, and improve the quality and efficiency of talent

training. Through this "interactive" talent training, students' practical ability and engineering awareness are greatly improved, and they can be directly used by enterprises after graduation, which effectively improves the training efficiency and training effect of talents.

Using the theory of "doing" and the theory of "constructivism," a "student center" suitable for students' learning and development is constructed. The interaction between teachers and students, the exchange of information between teachers' technical level and students' carrier as a learner.

"Internet of Things" is a buzzword describing the new era of computing. In a nutshell, IoT can be defined as the interaction between smart objects connected to the internet. These objects can sense, share and process information, upload it to the cloud, and make it available to users through a multitude of different applications. IoT, like other technologies, faces multiple security challenges.

On the one hand, the construction of the Internet of Things model in the training of Korean cross-cultural communication interactive talents is helpful to improve the informatization level of cross-cultural communication and adjust the structure of cross-cultural communication, which improves the quality and added value of talent training and is of great significance to the cultivation of cross-cultural communication talents. On the other hand, it expands the application of the Internet of Things in cross-cultural communication to a certain extent and provides a certain theoretical reference for improving the application level of the Internet of Things in Korean and other languages.

The innovation of this paper is to study and solve the problem of automatic collection of information standardization in personnel training in cross-cultural communication, the lack of application of Korean cross-cultural communication personnel training management system in the NIS system, and the connection between the Internet of Things technology and the current NIS system. Through the application of new technologies, various kinds of information are highly integrated to form a comprehensive and high-efficiency NIS system. It satisfies the real-time control function of e-books on the whole process of talent training and the intelligent learning function of Korean, so as to achieve the goal of Korean cross-cultural communication management and realize the interactive talent training of Korean cross-cultural communication.

2. Related Work

Scholars in related fields have always attached great importance to cross-cultural communication, so this is also a research topic that researchers from various countries pay more attention to. Many scholars in the teaching field have carried out research on cross-cultural communication and achieved certain results. Kelm and Orlando have argued that we face two major challenges in teaching and training cross-cultural dialogue. The first is to develop the ability to observe and pay attention to cross-cultural patterns that differ from our own. Second, these observations become more important when they are linked to some context, model, theory, or application [1]. Yujong used the method of conversation analysis to study the rising tone of words used by Korean non-native speakers in English cross-cultural communication [2]. Jun et al. have translated the lack of coping scale into a Korean work stress scale and examined its psychometric characteristics in the Korean labor force. Translation of the lack of coping scale according to scientific guidelines for intercultural adaptation [3]. Exploratory research by Lee has examined the potential links between informal digital learning of English (doing nothing), cross-cultural dialogue strategy competence, and perceptions of English diversity [4]. It can be seen that the research on Korean cross-cultural communication by various researchers has gradually diversified, but they are basically based on theoretical research and lack practical feasibility.

The Internet of Things technology is also gradually emerging, and more and more researchers use the Internet of Things technology in various fields. Kshetri has assessed the role of blockchain in strengthening IoT security. The key basic mechanisms related to blockchain security relationships are covered [5]. Pikul and Ning analyzed that Internet-connected devices are limited by the performance of the micro batteries that drive them [6]. Lindqvist and Neumann have studied the potential risks that can be overcome if the trustworthiness of the system is pursued, which can be ubiquitous in the world [7]. Valdes Pena et al. once believed that the Internet of Things will transform the Internet from a human-centric to a machine-intensive platform [8]. To sum up, the application research technology of the Internet of Things in the field of cross-cultural communication is still relatively small. At present, it is mostly used in a few fields such as the circulation system and supply chain. On the whole, its application scope is relatively narrow, the application degree is shallow, and there is a lack of in-depth research.

3. Korean Cross-Cultural Communication and Interactive Talent Training Based on the Internet of Things

3.1. Function and Technical Architecture of the Internet of Things. In order to upgrade the architecture of the traditional Internet of Things, it is an inevitable trend to introduce a new type of Internet of Things at the network layer or expand the existing functions of the Internet of Things [9]. The Internet of Things will play an increasingly important role in the entire Internet of Things application system architecture. Moreover, with the vigorous development of the electronics industry, the hardware performance of the Internet of Things has been greatly improved, which also promotes the gateway's support for more Internet of Things applications and forms a new Internet of Things architecture system [10]. In the Internet of Things interactive talent training mode technology studied in this paper, the combination of Internet of Things and traditional gateways should have the following four functions: the access authentication function of the perception layer device, the

heterogeneous network protocol conversion function, the data storage and policy management function, and the resource abstract release function are shown in Figure 1.

As can be seen from the figure, the implementation of its technical architecture needs to be divided into four layers, namely, the adapter layer, the conversion control layer, the middleware layer, and the application layer. The application layer mainly includes modules such as resource abstraction, service publishing, and information synchronization with the cloud platform. The middleware layer mainly includes modules such as policy management, data cache, instruction mapping, and data storage. The conversion control layer mainly includes modules such as access authentication, protocol conversion, data verification, and data analysis. The adapter layer mainly completes the data reception of various sensing layer devices, such as ZigBee, Bluetooth, WiFi, RFID, 4G, and so on.

3.2. Radio Frequency Technology (RFID). Radio frequency identification (RFID), its working principle is that the target object can be automatically identified through the radio frequency signal, and its related data can be obtained [11, 12]. Its identification work does not require our manual intervention and can work in a variety of harsh environments. Figure 2 shows the structure of a complete RFID system as follows:

As can be seen from the figure, a complete RFID system consists of electronic tags, readers, and computer application systems. Based on the RFID system, this paper establishes a network information service system for interactive talent training.

3.3. Design and Implementation of Gateway Multi-Process Scheduling Algorithm. This paper adopts the working steps of the MPSA system. First, define the three rotation time slices involved.

3.3.1. Monitoring Threshold Period T_1. Combined with multiple specific application scenarios in the laboratory, according to a large number of different types of underlying node equipment access experiments and the current access specifications of other IoT cloud platforms [13], it is concluded that T_1 is 400 seconds, which is reasonable. That is, the period for all sensor node devices to send data shall not be greater than 400 seconds, that is, $T_1 = 400$, and assuming that the period is T, then:

$$10 \le T \le 100. \tag{1}$$

In addition, the default factory default time interval of the underlying node device is 80 seconds, that is, when the device accesses the gateway for the first time, the sending time interval is 80 seconds. This prevents data blocking and loss from the first access of node data, resulting in the platform layer not being able to identify the device thereafter. And it meets the needs of users in most cases while reducing the blocking rate of data as much as possible. It stipulates that the user-defined node data sending interval needs to be a multiple of 10 [14].

3.3.2. The Suspension Time Interval T_2 of the Access Node Queue. According to the abovementioned restrictions on the monitoring threshold period T_1 and the period T of the data sent by the access node, the probability density of the actual data period sent by the node can be regarded as a skewed distribution, as shown in Figure 3.

Since the default factory-set upload period T of the sensor node is 80 seconds, although the user-defined upload data period is supported, most of the devices' upload data period should be distributed in 80 seconds. According to the definition of a skew function, the function curve is a positive skew curve. Its formula is given as follows:

$$\delta = \frac{K_3}{K_2\sqrt{K_2}},$$

$$K_2 = \frac{\sum (X - \hat{X})^2}{n-1} - \frac{1}{12}, \tag{2}$$

$$K_3 = \frac{n\sum (X - \hat{X})^3}{(n-1)(n-2)}.$$

In addition, according to the properties of the skewed distribution function, for a positively skewed distribution, its deviation coefficient is greater than zero, that is, $\delta > 0$. And the mean of the positively skewed distribution is M, the median is Me, and the mode is Mo, then the relationship between the three is given as follows:

$$M > \mathrm{Me} > \mathrm{Mo}. \tag{3}$$

But for this application system, in order to facilitate the calculation, after verification, when the number of samples is large enough, the skewed distribution can be approximated as a normal distribution with $\mu = 60$, σ^2 unknown. In order to facilitate the management, it is hoped that the time interval for sending data of most devices is within 100 seconds. Therefore, according to the characteristics of the normal distribution probability function [15], the calculation formula of T_2 can be obtained as follows:

$$T_2 = \frac{(1 - P(\mu - \sigma, \mu + \sigma)) * T1}{\sqrt[N]{T_1 T_2 \cdots T_N}}. \tag{4}$$

Then the suspension time interval T_2 of the ZigBee access node queue can be obtained from the abovementioned formula as follows:

$$T_2 \approx \frac{(1 - 0.625) * 300}{\sqrt[N]{T_1 T_2 \cdots T_N}}. \tag{5}$$

According to the description of the specific working steps in the previous section, it can be concluded that the startup time T_3 of the gateway's own health status monitoring information module is actually twice as long as T_1, namely:

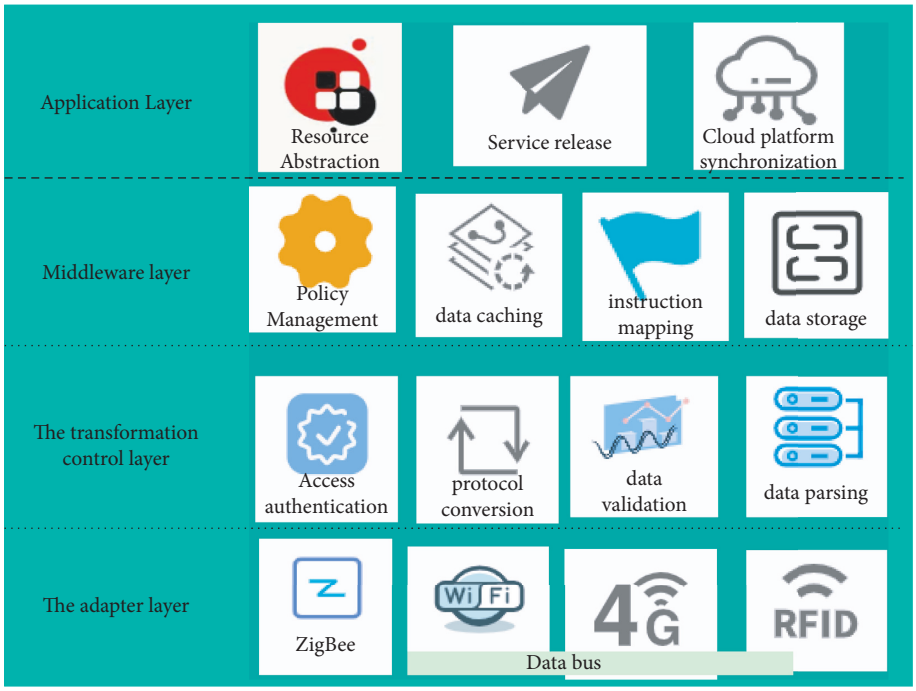

Figure 1: IoT technology architecture.

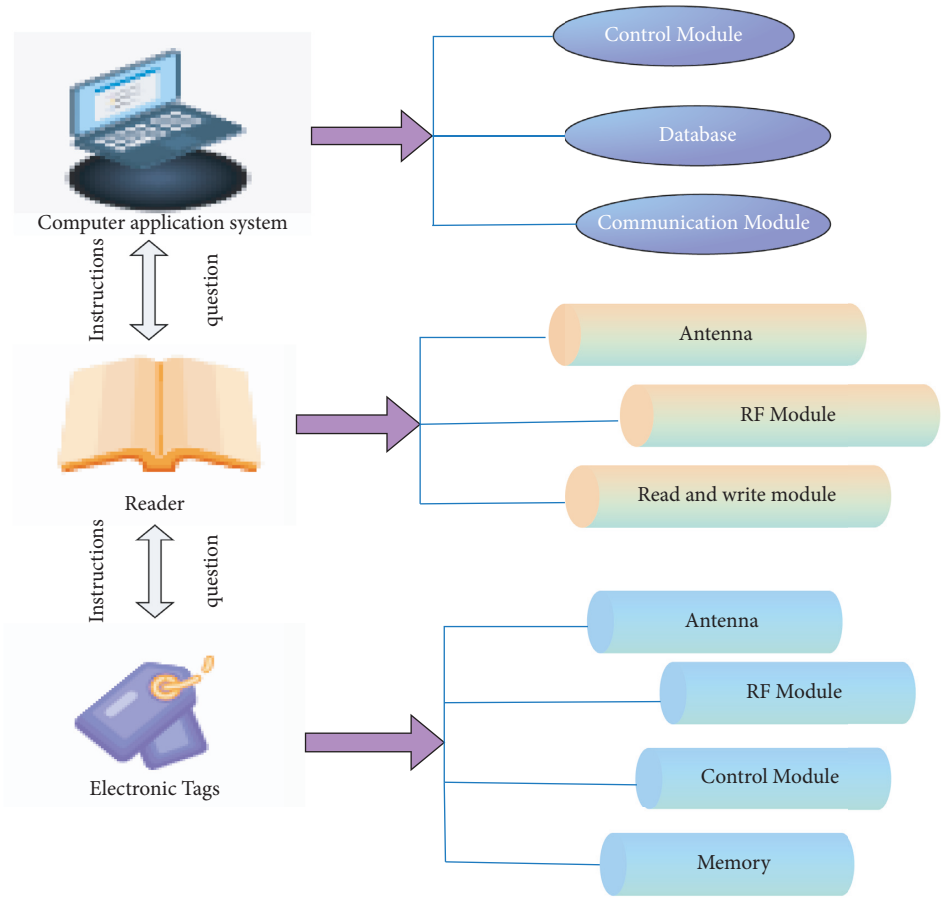

Figure 2: RFID system structure.

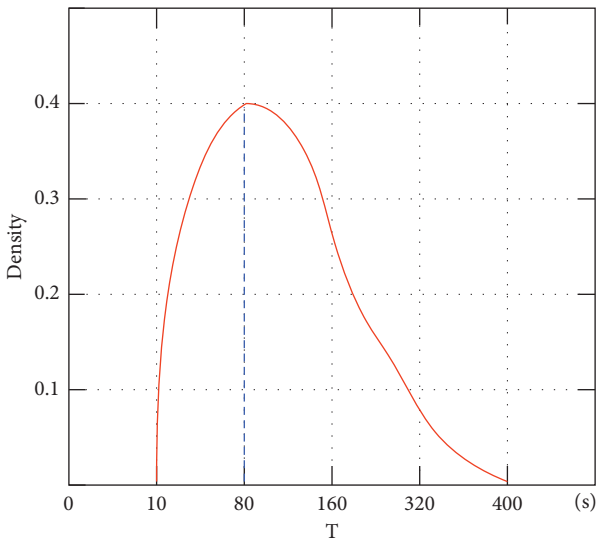

Figure 3: Skewed distribution probability density plot.

$$T_3 = 2 * T_1. \tag{6}$$

Convergence of all node data reception is completed within the time of the second T_1, after which the gateway enters a fully stable state. In this way, it is equivalent to sacrificing the convergence time of a T_1 in exchange for the reliability of the IoT to receive data from all nodes.

3.4. GBDT Algorithm. The GBDT algorithm is an iterative decision tree algorithm based on the ensemble learning boosting algorithm. In recent years, the GBDT algorithm has been widely used in engineering applications and library management [16, 17]. There are two reasons, the first is the high accuracy of regression fitting; the second is the ability to filter features. The key process of the GBDT algorithm used in this paper is given as follows:

The input is a training set sample:

$$T = \{(x_{1,}\, y_1), (x_{2,}\, y_2), ..., (x_{m,}\, y_m)\}. \tag{7}$$

The output is the final prediction function $f(x)$, initializing the weak learner:

$$f_0(x) = \operatorname{argmin} \sum_{i=1}^{m} L(y_i, c). \tag{8}$$

Among them, T is the maximum number of iterations, and L is the loss function.

For iteration rounds $t = 1,2, \ldots, T$ with samples $i = 1,2, \ldots, m$, compute the negative gradient.

$$r_t = -\left[\frac{L(y_i f(x_i))}{f(x_i)}\right]_{f(x)=f_t-1(x)}. \tag{9}$$

Use

$$(x_i, r_i)(i = 1, 2, ...m), \tag{10}$$

to fit a CART regression tree model and obtain the t-th regression tree. Calculate the best fit value for the leaf regions of $j = 1, 2, \ldots, J$:

$$c_i = \operatorname{argmin} \sum_{x_{ier}} L(y_i, f_t - 1(x_i) + c). \tag{11}$$

Let the mutual information of training dataset N and feature M be. Suppose this training data set is N, indicating the number of samples. There are K classes:

$$C_k k = 1, 2, ...K, |C_k|. \tag{12}$$

The abovementioned formula is the number of samples belonging to class C_k, which are

$$\sum_k |C_k| = |N|. \tag{13}$$

Assuming that the feature M has n different values of $m_1, m_2, ..., m_n$, according to the value of the feature M, N is divided into n subsets $N_1, N_2, ..., |N_i|$ as for the number of samples of samples, there are

$$\sum_i |N_i| = |N|. \tag{14}$$

The set of samples belonging to class C_k in subset N_i is N_{ik}, and the number of samples whose $|N_{ik}|$ is N_{ik} is used to calculate the empirical entropy $H(N)$ of data set N:

$$H(N) = -\sum_{k=1}^{K} \frac{|C_k|}{|N|} \log \frac{|C_k|}{|N|}. \tag{15}$$

Update the strong learner, then

$$f_t(x) = f_{t-1}(x) + \sum_{j=1}^{J} c_j I\left(x \in R_j\right). \tag{16}$$

The expression to get the prediction function $f(x)$ is given as follows:

$$f(x) = f_T(x) = f_0(x) + \sum_{t=1}^{T} \sum_{j}^{J} c_j I\left(x \in R_j\right). \tag{17}$$

GBDT default criterion is FRIEDMAN_MSE. For the convenience of comparison, its criterion is also set to MSE. This paper also supplements the evaluation of the average relative error, the minimum relative error, and the maximum relative error for the model performance. The MSE and R^2 calculation formulas are formulas (18) and (19), respectively.

$$MSE = \frac{\sum_{i=1}^{n} (y - y_1)^2}{n}, \tag{18}$$

$$R^2 = 1 - \frac{MSE}{\sigma_y^2}. \tag{19}$$

3.5. Consequences of Intercultural Communication Barriers in Korean. There are various factors that affect cross-cultural communication, both linguistic and pragmatic, both

nonlinguistic and nonpragmatic; both customs and ways of thinking [18, 19]. The analysis of the results of Korean cross-cultural communication barriers is shown in Figure 4.

As can be seen from Figure 4, the main causes of cross-cultural communication barriers among Korean international students are roughly divided into four categories: language use, psychological behavior, social etiquette, and thinking patterns. Among them, the reason for Korean pronunciation is the biggest obstacle to the cross-cultural communication of international students in South Korea. These international students generally do not have enough understanding of Korean communication rules, values, customs, and communication styles. Only one-fifth of the international students are familiar with Korean politics, economy, history, and culture. These students have one thing in common. Most of them are Korean majors, and they have been in Korea for a long time, and they have come into contact with and understand more Korean culture. When most of the respondents encounter obstacles in cross-cultural communication, they will choose to compromise and cooperate, use a positive communication attitude to deal with cultural conflicts, and voluntarily change their words and deeds to conform to the other party's culture [20]. They are willing to open their minds to understand and accept different cultures, but in the practice of communication, they will feel nervous and afraid, and will not dare to open their mouths for fear of making mistakes.

College students have a limited understanding of Korean culture. Most of the students have a "slight understanding" of different cultural knowledge. In comparison, their knowledge of "Korean history, geography, and politics" is better than other cultural knowledge, as in Table 1.

It can be seen from the table that the relevant results of the survey show that the main purpose of the students participating in the survey is to learn Korean for employment, and the study of Korean is still at the stage of improving their language ability; most of the students have average interest in learning Korean; there are few ways for students to contact and experience Korean culture, and the ways to improve their Korean proficiency are limited; there are few opportunities for Korean communication practice, and the methods are relatively simple; the breadth and depth of foreign cultural knowledge are average.

4. Interactive Talent Training Experiment

4.1. Investigation and Results of the Construction of Interactive Talent Training Model. The survey on the construction of talent training mode is mainly in the form of a questionnaire, and the Korean international students in colleges and universities are taken as the research object of this paper. The purpose is to explore the main issues of cross-cultural communication ability of Korean students in colleges and universities, so as to promote the foreign language learning of Korean students. Through the survey, it was found that more than half of the respondents of the questionnaire were women and most of the students studied Korean or Korean-related majors. Through data analysis, it can be seen that the reasons for Korean international students to learn Chinese

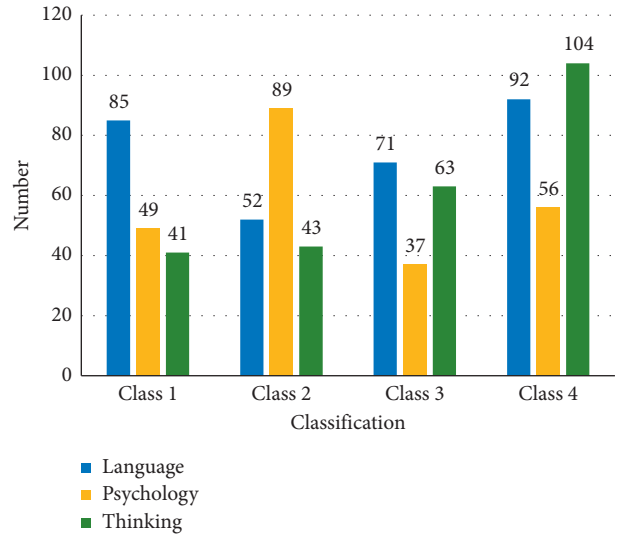

Figure 4: Statistical results of the causes of cross-cultural communication barriers for international students in Korea.

are mainly concentrated in three major areas: professional needs, work needs, and parental requirements. Although personal hobbies and travel needs are also one of the motivations for learning Chinese, the most powerful motivations are study, work, and family. These motivations are closely related to their lives, indicating that learning Korean plays a crucial role in their future studies, work, and life.

Figures 5–7 are graphs of relationship data obtained through data analysis by extracting 5 people from each level of the Korean oral proficiency level in the survey, totaling 30 people (each value on the x-axis represents 2 levels, and each value on the y-axis represents 2 error rates).

By analyzing Figure 5, it can be found that the higher the Korean proficiency of Korean international students, the smoother they will be in cross-cultural communication, and the lower their cross-cultural communication barrier value will be. Therefore, there is a negative correlation between the Korean proficiency of international students and the value of cross-cultural communication barriers.

By analyzing Figure 6, it can be found that the longer the overseas students in South Korea study Korean, the more they will be exposed to Korean culture, and the higher their Korean proficiency will be. On the contrary, there is a positive correlation between the Korean cultural contact time and Korean language proficiency of all international students.

By analyzing Figure 7, it can be found that the longer the overseas students in Korea stay in Korea, the smoother they will be in cross-cultural communication, and the lower their cross-cultural communication barrier value will be. Therefore, there is a negative correlation between the Korean proficiency of international students and the value of cross-cultural communication barriers.

4.2. Feature Selection and Interactive Model Parameter Testing of Cross-Cultural Communicative Competence. Feature selection is very important for data analysis [21]. Good feature

Table 1: University students' understanding of Korean culture.

Category	Degree			
	Very well (%)	Basic understanding (%)	A little bit (%)	Not at all (%)
Custom	0.1	20	75	3
History	2.4	33	59	5.6
Values	1	29	63	9
Literature	0	22	75	3
Education	1.5	14	74	10.5

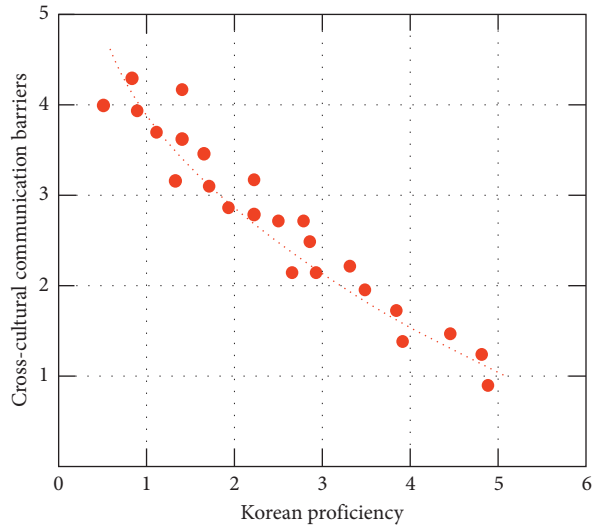

Figure 5: Data graph of the relationship between Korean proficiency and cross-cultural communication barriers.

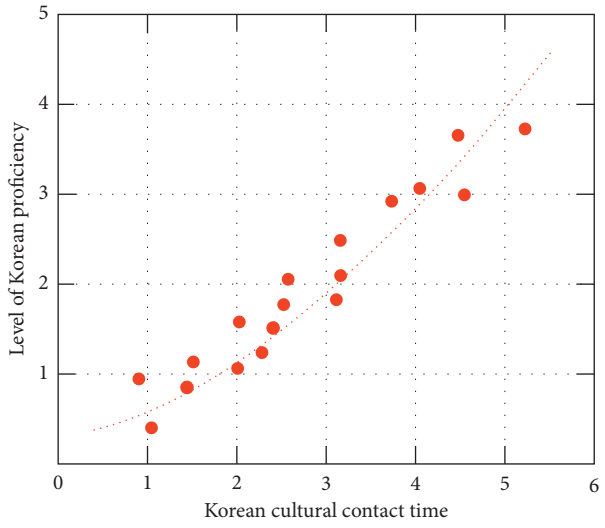

Figure 6: Data graph of the relationship between Korean culture contact time and Korean proficiency.

selection can improve model performance, and can also help understand the underlying structure and data characteristics, which plays an important role in further improving algorithms and models. Both random forest and GBDT have the feature importance evaluation function [22]. In Anaconda, the feature_importances attribute of the model can be used to obtain the feature importance evaluation. The feature importance analysis results are shown in Figures 8 and 9.

In this paper, the default value of feature quantity and sample size can be used, that is, all feature numbers are considered and the depth of the decision tree is not limited. The search range of the final model parameters and the optimal parameters selected are shown in Tables 2 and 3.

The evaluation model in the table uses mean squared error (MSE), which is a more convenient method to measure the "average error," and is used to reflect the degree of deviation between the actual value and the predicted value and to evaluate the reliability of the model, and the closer its value is to 100%, the more reliable it is to use the model to predict than to use the average value directly. The table also adds the minimum, maximum, and average relative errors that can more intuitively reflect the prediction effect. From the perspective of MSE, the degree of model deviation is low. The performance of R^2 is above 80%, the model has high reliability [23], and the relative error index is also within the acceptable range. It can also be seen from the table that the random forest and GBDT models have good prediction

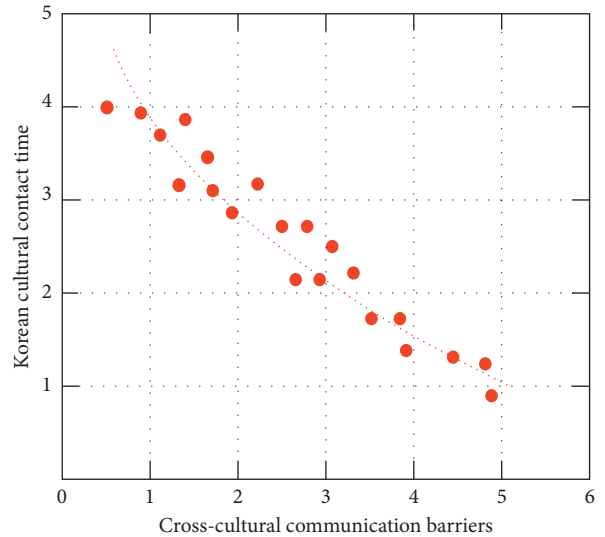

Figure 7: Data graph of the relationship between Korean cultural contact time and cross-cultural communication barrier value.

effects in the training set and validation set, the model has good generalization ability, and both simplify the input feature combination. From the perspective of MSE, and relative error indicators, the GBDT model is overall better than the random forest.

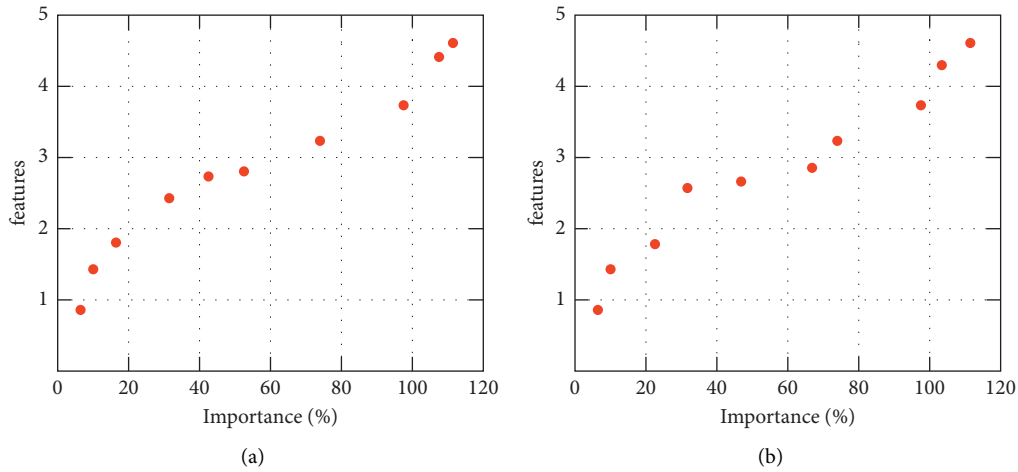

Figure 8: Random forest and GBDT knowledge and skills model feature importance.

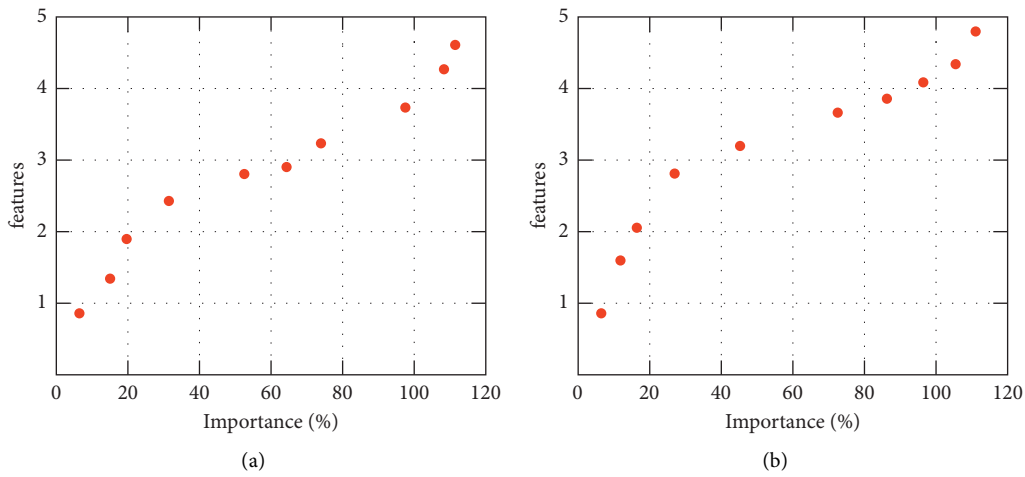

Figure 9: Feature importance of random forest and GBDT values model.

Table 2: The selection process of knowledge and skill model feature combination.

Characteristic combination	Random forest (MSE/10(−5))	GBDT (R^2)
1445	1341	77.3
1264	1082	81.4
1075	935	83.1
989	770	86.7
847	852	85.4
918	883	85.1
991	935	84.2

Table 3: Value model features a combination selection process.

Characteristic combination	Random forest (MSE/10(−5))	GBDT (R^2)
1407	1447	72.3
1194	1241	76.8
974	1074	81.9
829	915	83.7
875	954	82.4
904	1014	82.1
940	1053	81.3

Due to space limitations, this chapter only shows the analysis results of some of the actual and predicted values of the validation set. In the high, moderate, and low ranges, four sets of measured values and their corresponding predicted values are taken to show the model performance, as shown in Table 4.

Summarizing the table, the prediction model obtained by using random forest and GBDT algorithm provides interactive talent training with students' knowledge and skills, process and method, emotion, attitude, and value learning method prediction method. Success of a rapid predictive model for Korean intercultural communicative competence tests obtained through ensemble learning.

The evaluation of the Korean cross-cultural communication ability based on the information management level of the Internet of Things information system is based on the score between 0 and 5 of each index in the index layer and the weight of each level in the system [24]. Therefore, its value range is [0, 5]. Combined with the actual situation, the

Table 4: Model effect display.

Measured value	Stochastic forest model		GBDT model	
	Predicted value	RE/%	Predicted value	RE/%
2.452	2.314	10.3	0.221	14.5
2.146	2.245	9.32	0.201	11.6
1.512	1.629	13.5	0.134	12.5
0.134	0.236	12.4	0.043	14.3

Table 5: Evaluation results of the Internet of Things information system for Korean cross-cultural communicative competence.

System layer	Score	Criterion layer	Score	The project layer	Score	Index layer	Score
A	0.532	A_1	0.458	A_2	0.614	A_3	0.577
B	0.334	B_1	0.662	B_2	0.415	B_3	0.347
C	0.251	C_1	0.586	C_2	0.596	C_3	0.652

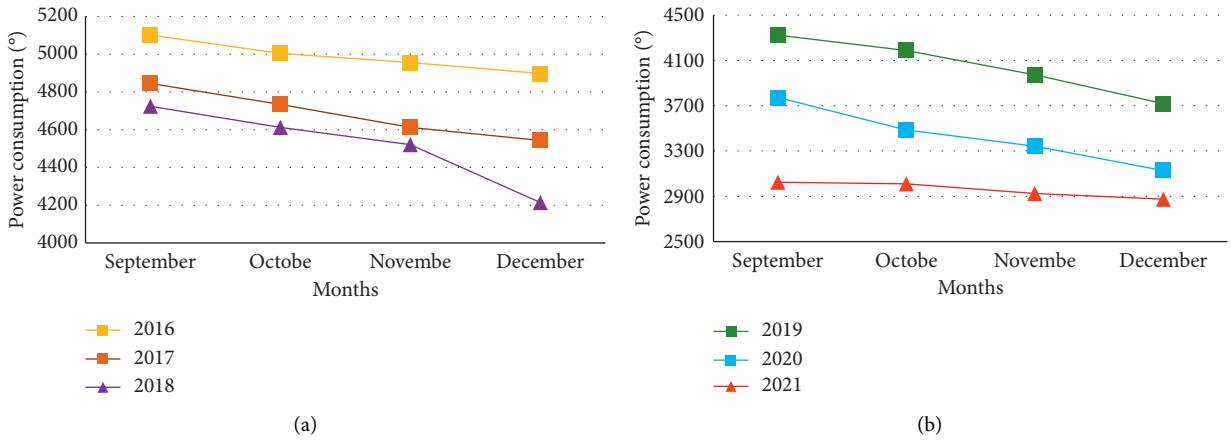

Figure 10: Comparison of power consumption before and after system installation. (a) Power consumption before and after system installation in 2016–2017. (b) Power consumption before and after system installation in 2019–2021.

level of Korean cross-cultural communicative competence IoT information management level is determined. The results are shown in Table 5:

Combining with Table 5, it can be seen that the research shows that the overall level of IoT information management of Korean cross-cultural communicative competence is relatively low, and it is only in the initial stage of development. Through the evaluation of the Korean cross-cultural communication ability Internet of Things information system, the combined score is 1.117. It is closely related to factors such as the late start of the informatization development of cross-cultural communication skills, the lack of investment in informatization equipment such as the Internet of Things, and the lack of relevant technical talents.

4.3. Interactive Talent Training Ad Hoc Network Performance Test. To test the performance of the wireless sensor network ad hoc network is mainly to test whether the transmission path of the ad hoc network method can change adaptively without affecting the data transmission when the network topology changes. The most typical changes in network topology in learning Korean cross-cultural communication skills are the addition of new nodes and the failure of network nodes [25]. This topic collected the power consumption, that is, the power consumption before and after the installation of the system, as shown in Figure 10:

It can be seen from the figure that the power consumption after the installation of the system is significantly lower than that of the month before the installation of the system, which can illustrate the energy saving and efficiency of the control strategy designed in this paper. It verifies the self-organizing network transmission technology and control effect proposed in this paper, including the self-organizing routing algorithm, and the control effect test. The test has achieved good results, and it has also preliminarily proved the scientific, effective, and energy-saving design of the key technology of the network information service system for interactive talent training in this paper.

5. Conclusions

This paper aimed at the deficiencies of flexibility, scalability, and single application scenarios in the traditional IoT architecture. The challenges faced by IoT devices are difficult to interconnect and interoperate, and there is no unified device management system model. It has

completed the research work on IoT device discovery and management technology and implemented a new type of IoT architecture at the network layer and platform level, respectively. The platform layer is decoupled according to different application scenarios and distributed in the IoT gateway of the network layer. This strengthens the function of the IoT gateway, making the entire IoT application system easier to expand, more flexible, and faster and safer to access real-time sensing data. At the same time, the cloud platform layer can also be focused on scheduling management, authority authentication, and data storage for multiple application scenarios. In learning Korean intercultural communication skills through the use of various online resources and digital libraries and multimedia teaching methods. It carried out teaching and learning in a more flexible and diverse form so that "teaching" and "learning" can no longer be limited to the classroom, but become closer to reality, resulting in in-depth, beneficial, and continuously positive teaching practice effects. The establishment of a network information service system for interactive personnel training proposed in this paper can realize the real-time development of interactive personnel training, and realize the intelligence and high efficiency of interactive personnel training. This paper expanded on the existing Internet of Things application system, a new type of Internet of Things information discovery and management application system for interactive talent cultivation is realized, and the expected effect is achieved. However, in the actual Korean cross-cultural communication application, the technology involved in the entire IoT architecture is very broad. Due to limited personal capabilities and development time, there are still many details that need to be improved.

Data Availability

Data sharing is not applicable to this article as no datasets were generated or analyzed during the current study.

Conflicts of Interest

The author declares that there are no conflicts of interest

References

[1] Kelm and R. Orlando, "Using online photography portfolios to enhance cross-cultural awareness," *Global Advances in Business Communication*, vol. 7, no. 1, p. 2, 2018.

[2] P. Yujong, "Achieving Co-alignment in cross-cultural interactions," *Korean Journal of Applied Linguistics*, vol. 33, no. 3, pp. 61–89, 2017.

[3] D. Jun, J. M. Kim, S. O'Leary, and V. Johnston, "Cross-cultural adaptation and validation of the Latack Coping Scale in the general working population in Korea," *Work*, vol. 63, no. 3, pp. 325–334, 2019.

[4] J. S. Lee, "Informal digital learning of English and strategic competence for cross-cultural communication: perception of varieties of English as a mediator," *ReCALL*, vol. 32, no. 1, pp. 47–62, 2020.

[5] N. Kshetri, "Can blockchain strengthen the Internet of things?" *It Professional*, vol. 19, no. 4, pp. 68–72, 2017.

[6] J. H. Pikul and H. Ning, "Powering the Internet of things," *Joule*, vol. 2, no. 6, pp. 1036–1038, 2018.

[7] U. Lindqvist and P. G. Neumann, "The future of the Internet of things," *Communications of the ACM*, vol. 60, no. 2, pp. 26–30, 2017.

[8] M. D. Valdes Pena, J. J. Rodriguez-Andina, and M. Manic, "The Internet of things: the role of reconfigurable platforms," *IEEE Industrial Electronics Magazine*, vol. 11, no. 3, pp. 6–19, 2017.

[9] J. Voas and P. Laplante, "Curriculum considerations for the Internet of things," *Computer*, vol. 50, no. 1, pp. 72–75, 2017.

[10] M. S. Khalefa, M. A. Jabar, W. N. Hussein, H. Ali, and H. F. Zmezm, "The Internet of things software architectural solutions," *Australian Journal of Basic & Applied Sciences*, vol. 9, no. 933, pp. 271–277, 2017.

[11] H. J. Yun and M. Cui, "The effects of parental warmth on adolescent delinquency in the United States and South Korea: a cross-cultural perspective," *Journal of Youth and Adolescence*, vol. 49, no. 1, pp. 228–237, 2020.

[12] V. Jain, R. Bansal, M. Swmai, and A. Jain, "A comprehensive study on the RFID technology of Delhi metro cards," *Fusion: Practice and Applications*, vol. 4, no. 1, pp. 22–31, 2021.

[13] B. Yu, J. Wright, S. Nepal, L. Zhu, J. Liu, and R. Ranjan, "IoTChain: establishing trust in the Internet of things ecosystem using blockchain," *IEEE Cloud Computing*, vol. 5, no. 4, pp. 12–23, 2018.

[14] F. G. Gilal, J. Zhang, R. G. Gilal, and N. G. Gilal, "Integrating intrinsic motivation into the relationship between product design and brand attachment: a cross-cultural investigation based on self-determination theory," *European Journal of International Management*, vol. 14, no. 1, pp. 1–27, 2020.

[15] F. Mcleay, V. Yoganathan, V. S. Osburg, and A. Pandit, "Risks and drivers of hybrid car adoption: a cross-cultural segmentation analysis," *Journal of Cleaner Production*, vol. 189, no. JUL10, pp. 519–528, 2018.

[16] L. Y. Y. Kwan, K.-y Kwan Angela, and S.-L. Liou, "Culture, creativity, and innovation," *Journal of Cross-Cultural Psychology*, vol. 49, no. 2, pp. 165–170, 2018.

[17] J. Hou, Q. Li, Y. Liu, and S. Zhang, "An enhanced cascading model for E-commerce consumer credit default prediction," *Journal of Organizational and End User Computing*, vol. 33, no. 6, pp. 1–18, 2021.

[18] S. Baek, H. W. Park, Y. Lee, S. L. Grace, and W. S. Kim, "Translation, cross-cultural adaptation and psychometric validation of the Korean-language cardiac rehabilitation barriers scale (CRBS-K)," *Annals of Rehabilitation Medicine*, vol. 41, no. 5, pp. 858–867, 2017.

[19] J. Y. Hong, H. Ko, and J. H. Kim, "Cultural intelligence and ARCS model for digital era," in *Proceedings of the 9th International Conference on Web Intelligence, Mining and Semantics*, Seoul, Korea, June 2019.

[20] S. H. Park, T. S. Goh, S. M. Son, D. S. Kim, and J. S. Lee, "Validation of the Italian spine youth quality of life (ISYQOL) in Korean population," *Journal of Clinical Neuroscience*, vol. 92, no. 14, pp. 165–168, 2021.

[21] S. H. Kim, N. Petard, and J. H. Hong, "What is lost in translation: a cross-cultural study to compare the concept of nuttiness and its perception in soymilk among Korean, Chinese, and Western groups," *Food Research International*, vol. 105, no. 1, pp. 970–981, 2018.

[22] J. Buzhardt, C. R. Greenwood, N. J. Hackworth et al., "Cross-cultural exploration of growth in expressive communication

of English-speaking infants and toddlers," *Early Childhood Research Quarterly*, vol. 48, no. 2, pp. 284–294, 2019.

[23] T. Ladha, M. Zubairi, A. Hunter, T. Audcent, and J. Johnstone, "Cross-cultural communication: tools for working with families and children," *Paediatrics and Child Health*, vol. 23, no. 1, pp. 66–69, 2018.

[24] S. E. . Collier, "The emerging enernet: convergence of the smart grid with the Internet of things," *IEEE Industry Applications Magazine*, vol. 23, no. 2, pp. 12–16, 2017.

[25] J. M. Perkel, "The Internet of Things comes to the lab," *Nature*, vol. 542, no. 7639, pp. 125-126, 2017.

Hindawi
Scientific Programming
Volume 2022, Article ID 4588493, 13 pages
https://doi.org/10.1155/2022/4588493

Research Article

Computer Information Processing System Based on RFID Internet-of-Things Encryption Technology

Chunyan Yuan

School of Management, Xingzhi College of Xi'an University of Finance and Economics, Xi'an 710038, Shaanxi, China

Correspondence should be addressed to Chunyan Yuan; ycy@zcmu.edu.cn

Received 22 June 2022; Revised 29 July 2022; Accepted 9 August 2022; Published 14 September 2022

Academic Editor: Juan Vicente Capella Hernandez

With the increasing development of information science and technology and the vigorous use and promotion of new technologies, profound changes have taken place in all aspects of our daily life. With this huge change, the IoT industry was born. And it analyzes and processes the large amount of data generated between them, and finally, it helps the development of the economy. The RFID system studied in this paper is the radio frequency identification system, which is an automatic signal identification system. The relationship between the RFID system and the Internet of Things is that the former will obtain a large amount of Internet of Things information data by identifying the Internet of Things. However, it is difficult to guarantee the analysis and processing of data and the security of data in the RFID system. This paper aims to study the effective processing and security guarantee of a large amount of data obtained by the RFID system after processing the identification of the Internet of Things. It is expected to overcome the problems of conventional related art. This paper proposes the encryption technology for the Internet of Things RFID system, as well as the corresponding algorithm, and establishes a processing system for information data. The experimental results of this paper show that the cryptographic mechanism run by the algorithm PECC has better security performance compared with other cryptographic mechanisms, and its computational complexity can be reduced by 28.35%.

1. Introduction

The concept of the Internet of Things was proposed and described by the International Telecommunication Union at the World Summit on the Information Society in 2005. The RFID system studied in this paper is an important step in the construction of the Internet of Things. Because with the establishment of the Internet of Things, it is necessary to collect and organize the data of the equipment, and the RFID system can realize the automatic identification of the data, which can make the operation efficiency of the Internet of Things system higher. However, the resulting large amount of data involves individuals, so there is a great demand for data security technology. However, the RFID system's ability to process data is relatively very limited, so this paper studies the Internet of Things encryption technology of the RFID system to ensure the security of the data.

The large amount of data generated by the Internet of Things can be realized through the application of computer information processing technology. With the emergence of supercomputers in various countries in the world, the information processing capabilities of computers have been qualitatively improved. Because the Internet of Things is in the process of establishing, there will be a large amount of branch data generated. Therefore, for the processing of the above-mentioned large amounts of data, this paper adopts a computer-related information processing system. This paper firstly organizes a large number of IoT device data with this system and uses corresponding software and technology to encrypt the data. It realizes the guarantee of data security, in order to help the construction of the Internet of Things system, in order to hope that the Internet of Things can be improved and perfected.

For the application of RFID systems in the Internet of Things, there have been many related experimental studies, and corresponding technologies are being applied in many fields. Below are some of the researchers and their findings. Feng used the physical signal in the collision slot to separate unknown tags and known tags, which is a new technology to

accelerate ID collection [1]. The scientist's point of view is closely related to the research in this paper because the collection of data by the Internet of Things is a challenging task in China, a country with a large population. Narges focused on the application of RFID in the retail industry, especially in store operations [2]. For the retail industry, the use of RFID can accelerate the rapid integration of this field into the Internet of Things system. Ramadan proposed an innovative real-time manufacturing cost tracking system (RT-MCT), which integrates the concepts of lean manufacturing and RFID [3]. This combined concept has received feedback from practical applications. Youm developed an automatic sampling system based on radio frequency identification (RFID) and applied it to the aerobic fitness test [4]. This is the application of RFID in the field of hygiene. Shen proposed a new multitag RFID packet authentication protocol for lightweight mobile environments [5]. This protocol is proposed for its security and privacy. Popoola developed an intelligent, economical, and environmentally friendly vehicle identification system using RFID and solar photovoltaic (SPV) technology [6]. This is the application of the system in the automotive field. The following are related studies on the Internet of Things. Lu and his team proposed a new low-overhead HEVC encryption scheme for energy-constrained multimedia IoT [7]. Bansod proposed an ultralightweight, compact, low-power block cipher [8], which can achieve better performance. The researchers have made different related research articles on RFID systems and their applications. It is mainly used for data collection. The feature of the system is automatic identification, which simplifies the process of data collection. At the same time, the related research on the Internet of Things reflects the requirements for the security of the Internet of Things data. In this paper, compared with the above research, the RFID system and the Internet of Things are combined and applied. The following are some of the innovations of this article.

The innovations of this paper are as follows. (1) This paper expounds the application of the RFID system in the Internet of Things in detail and compares its advantages and disadvantages. (2) This paper uses special encryption technology for the data collected by the RFID system in the Internet of Things system to ensure the security of the data. This is already the most concerned part of the social crowd because this part involves more personal privacy. (3) For the data obtained by the RFID system in the Internet of Things system, this paper adopts an advanced computer information processing system to analyze and process the collected data. In this paper, a corresponding database is established to better guarantee the security of the data.

2. Establishment of Internet of Things RFID Information Encryption Technology and Related Computer Processing System

2.1. RFID System Composition and Algorithm Overview

2.1.1. Composition and Working Principle of RFID System. The RFID system is an automatic identification system, which is derived from satellite technology and can realize two-way communication. As more researchers are joining the research on this technology, the results obtained today are quite large and have been widely used. Because the advantage of this technology is to improve the efficiency of our daily life and work, its application scenarios are very large in reality. The first is to introduce the basic components of the technology, and its specific structure is shown in Figure 1.

Figure 1 is the basic structure of the RFID system. In the actual operation process, it needs to read the electronic tag. When sending and receiving the obtained information, the function of the reader is to transmit the obtained information to the software system. It processes and analyzes the obtained data through a software system [9].

The structure of the important part of the RFID system and its working principle are described below. The first is the introduction of the reader, which plays a central role in the RFID system. The premise of the operation of the RFID system is the normal operation of the reader. Figure 2 is the structure diagram of the reader.

In the RFID system of the reader, the identification distance of the RFID system is determined by its power, and the relevant frequency of the RFID system is also determined by the reader [10]. The workflow of the reader basically determines the operation of the RFID system. The specific workflow is shown in Figure 2.

This article introduces the important components of the reader, as well as the electronic tag. The component exists as a carrier in the RFID system. Only when the electronic tag is activated, valid data can be read. Its structure is shown in Figure 3.

After the electronic tag is activated by the reader, it will receive the signal, and then through the function of the internal device of the electronic tag, it will release a new signal and attach it to the corresponding object. This is the working principle of electronic tags and readers in RFID systems. Electronic tags can be divided into active, passive, and semiautomatic types according to whether they have their own power supply. The first feature is that it can store a large amount of data, which can be applied in some cases where a large amount of data needs to be processed. The second feature is the price advantage and can be widely used. The third advantage is that the reaction speed can be faster than the second, and its price is lower than the first, which can improve the overall work efficiency [11]. The selection of the three types should be determined according to the actual application scenario. For the types and frequencies of various electronic tags, Table 1 has been listed.

Because the working principle of the RFID system is the same as that of the radar, both are two-way communication systems, and both rely on the form of scattered signals to obtain target information. The calculation formula is as follows:

$$Q_{Back} = S\partial = \frac{Q_{Lx}G_{Lx}}{4\pi r^2}\partial = \frac{Q_P}{4\pi r^2}\partial. \quad (1)$$

Q_{Back} in the above formula represents the collected return signal, and Q_P represents the actual working power of the antenna. It can be seen from the formula that Q_P plays a major role in the entire operation of the RFID system [12].

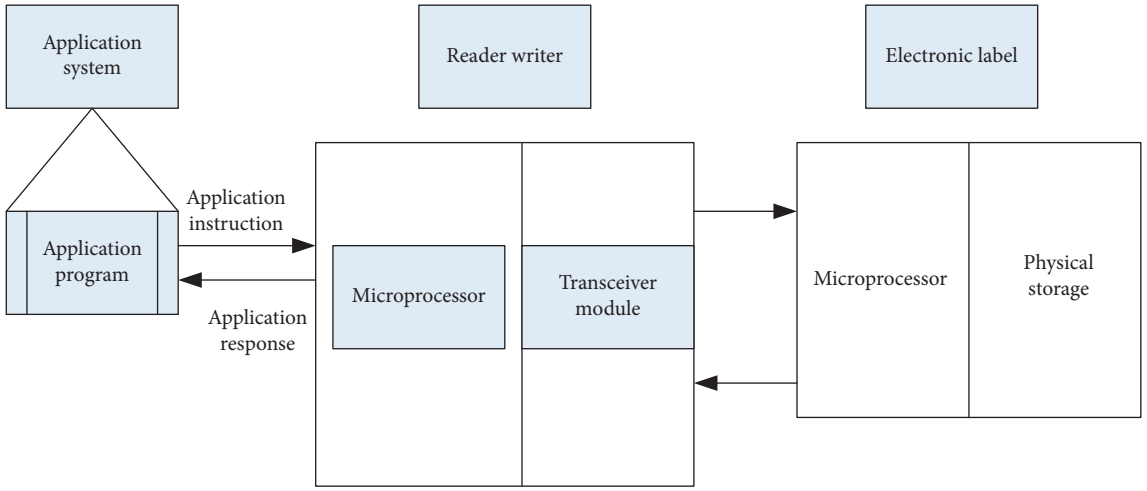

Figure 1: Composition of an RFID system.

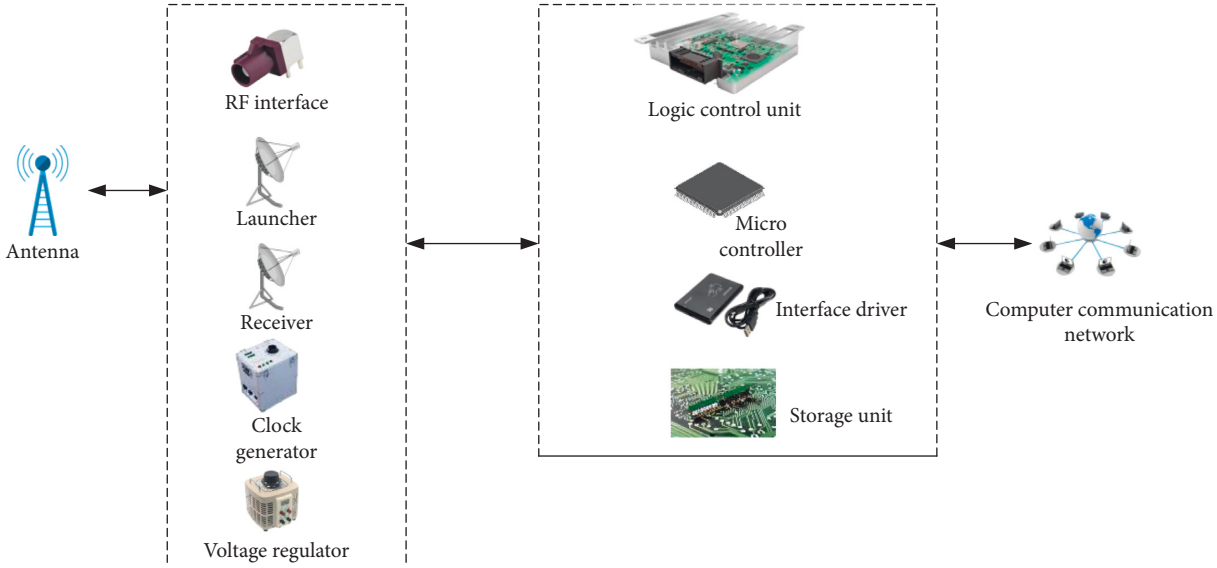

Figure 2: Structure diagram of the reader.

2.1.2. Information Processing Method of RFID System. Since the RFID system involves a large amount of data in the process of use, it adopts a special data control method to reduce the manufacturing cost for other components in the RFID system. The following three different methods are introduced and compared accordingly. The first is amplitude keying, which is expressed as

$$T_2(t) = T(t) \cdot a \cos \theta t. \tag{2}$$

$T(t)$ in the above formula is the digital baseband signal, $a \cos \theta t$ represents the size of the carrier, and the result is a binary signal wave [13].

The second method is called frequency shift keying, which controls the frequency through the digital information of the signal, and its expression formula is as follows:

$$Y_0(x) \equiv Y(x) \cdot \cos(\theta_1 x + \alpha) + \cdot \cos(\theta_2 + \beta). \tag{3}$$

$Y_0(x)$ in the formula is also a digital baseband signal, and $\cos(\theta_1 x + \alpha)$ and $\cos(\theta_2 + \beta)$ are both frequency waveforms and are also binary signals.

The third method is the keying method of phase shift, which can be divided into absolute and relative, and its signal expression is as follows:

$$H_0(t) = H(t) \cdot \cos \theta. \tag{4}$$

The above formula $H_0(t)$ here also represents the baseband signal, $\cos \theta$ represents the wave frequency, and the above formula is also a binary expression. The above three data control methods have their own characteristics and should be selected according to different needs in practical applications. These three methods are also commonly used in RFID systems. In order to ensure the integrity of the information data during the transmission process, it is necessary to correct the data. This paper firstly introduces

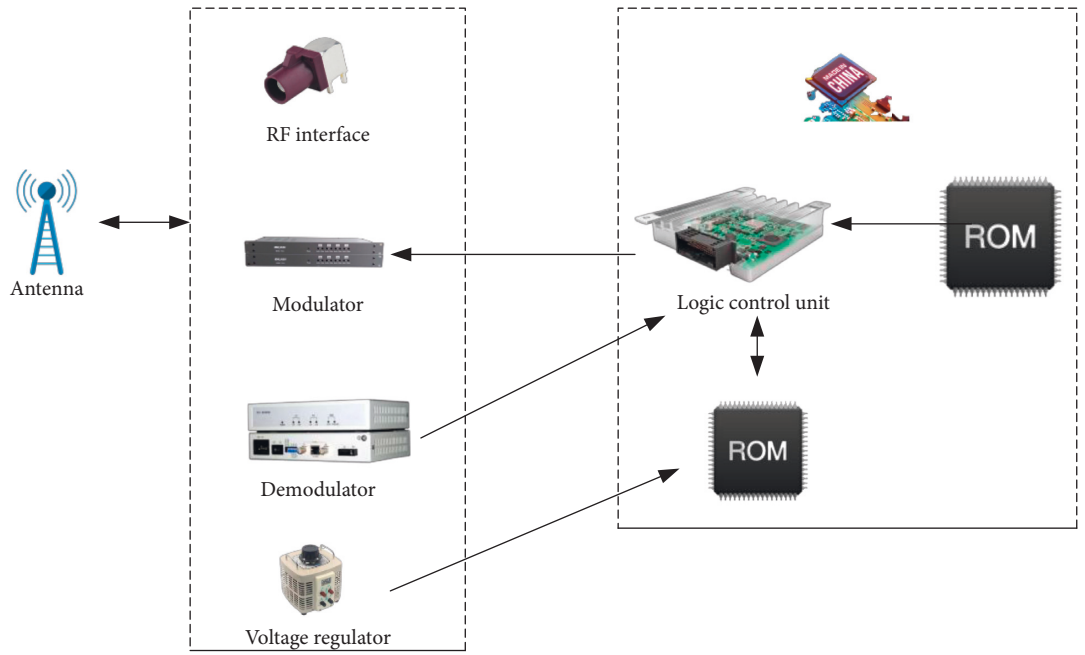

Figure 3: Electronic label structure diagram.

Table 1: Frequency of each type of tag work.

Label type	Working frequency	Typical value	Communication distance
Low-frequency label	30~300 kHz	125 kHz、134 kHz	Within 10 cm
Medium high-frequency label	3~30 MHz	13.56 MHz, 433.92 MHz	Within 1 m
UHF tags and microwave tags	300 MHz~5.8 GHz	2.45 GHz、5.8 GHz	4~6 m

the verification method of cyclic redundant data. Because the data is transmitted in binary, it can be expressed by the following polynomial:

$$Q(t) = e_7 t^7 + e_6 t^6 + e_5 t^5 + e_4 t^4 + e_3 t^3 + e_2 t^2 + e_1 t^1 + e_0 t^0, \tag{5}$$

e_i in the above formula represents 0 or 1, and $Q(t)$ is the code formula of information. The final check formula can be processed by using a check code polynomial [14], which can be written as follows:

$$t^{m-u} Q(t) = P(t) K(t) + R(t). \tag{6}$$

$K(t)$ in the formula is the polynomial of the check code, which can be used to correct some errors in the code of the information data, so as to avoid errors in the collected data. The error correction of this method can also achieve high-reliability verification for a large amount of data, and its application scenarios are very wide. In addition, there is a method of parity checking, which is simpler and easier to operate than the previous method, but its shortcomings are also very obvious. The disadvantage is that it is impossible to detect an even number of errors in the data bits. That is, when the transmitted data has an even number of errors, the parity check is invalid. For data processing, in addition to the above data regulation, it is also necessary to model the data processing flow. The model structure diagram is shown in Figure 4.

The data model in Figure 4 is extracted from the database, and its design idea is very similar to the database in the traditional sense, data view is a virtual data Table customized according to the user's needs from one or several basic database tables, and its design is similar to that of a traditional relational database, but it is not based on those single data, so there are some differences [15].

2.1.3. Adjustment Method of RFID System Reader Antenna. In addition to the above-mentioned information processing method, the working utility of the RFID system is closely related to the antenna and the channel of information transmission. Because the work of the RFID system needs to identify the distance in the scene, the transceiver capability of the antenna needs to withstand a certain distance test. In this paper, regarding the distance factor of the RFID system, a special antenna with circular polarization that can achieve high gain and can read long-distance information is selected, so that the working distance of the RFID system can be as far as possible p [16]. The relationship between the transmit antenna and the receive antenna is as follows:

$$Q = \frac{1 + 2A_1 A_2 \cos(\alpha_1 - \alpha_2) + A_1^2 A_2^2}{(1 + A_1^2)(1 + A_2^2)}. \tag{7}$$

The above formula expresses the utility of the operation between the transmitting antenna and the receiving antenna. But for the gain of the antenna, the calculation method is different from the above. Its gain expression is as follows:

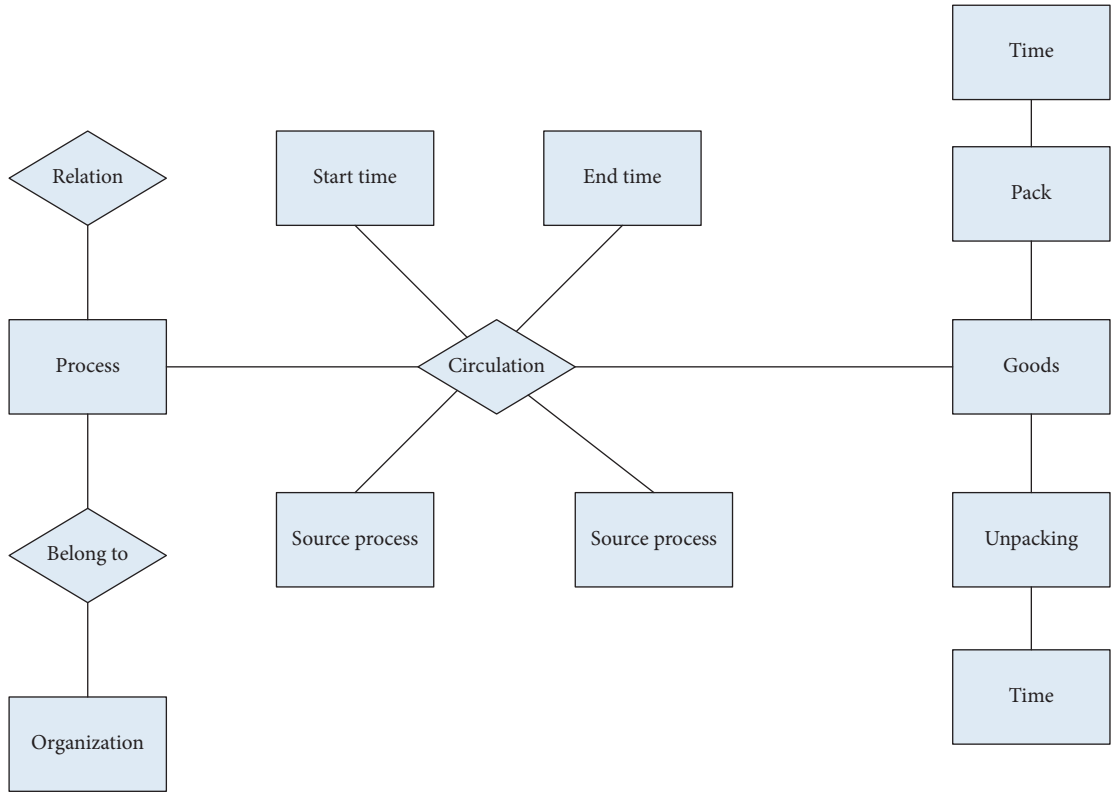

Figure 4: Data processing flow model structure diagram.

$$T(C) = H(C) + 3 + 20\log\left[0.6\left(1 + 10^{-\frac{ER}{20}}\right)\right], (C = dBic). \quad (8)$$

It can be known from the above expression that the particularity of the reader can change the overall role of the RFID system. At the same time, the gain of the antenna will also affect the read and write characteristics of the RFID system. There are actually many kinds of methods to increase the antenna gain, but for this study, the array structure of the antenna is used to improve its efficiency. The array structure of the antenna not only improves the working efficiency of the RFID system but also can achieve excellent characteristics such as anti-interference, thereby improving the performance of the entire RFID system. The following is a comparison of different antenna types. In this paper, the array method of the dipole antenna is first introduced, and its model structure is a circularly polarized model [17]. In fact, it is equivalent to a simple circularly polarized antenna array, and the array characteristics of multiple antennas are also obtained from a simple binary array. For the characteristics of the dipole antenna, the rate of current passing on it needs to be considered, so the resistance of the antenna is calculated as follows:

$$D = \frac{l30}{\sin tk_1 \sin tk_2}\int_{-k_2}^{k_2}\left[\frac{1}{R_1}\exp\left(-itR_1\right) - 2\cos tk_1\frac{1}{R}\exp\left(-itR\right)\right]\cdot \sin t\left(k_2 - |\alpha|\right)d\delta. \quad (9)$$

This formula is a method for calculating the resistance between parallel antennas because the resistance between them is small. The above formula applies to the case between two antennas. On the basis of the above expression, it first calculates the resistance on the antenna, as follows:

$$H_1 = H_2 = H_3 = H_4 = BE^{i\lambda_1}, \left(H_{12} = bE^{i\lambda_2}, H_{34} = dE^{i\lambda_3}\right). \quad (10)$$

The above is the calculation of the resistance, and the following is the calculation of the current. The specific formula is as follows:

$$I = Z\frac{C}{B}E^{I\left(\theta + \frac{\pi}{4} + \mu_3 - \mu_1\right)}\overrightarrow{B_X}. \quad (11)$$

Through the above resistance and current, the value of the axial ratio can be finally obtained, and the final superposition value can be calculated by the following expression:

$$L = \frac{\max}{\min}\left\{\sqrt{\left[d\cos\left(\alpha t + \theta_1\right)\right]^2 + \left[c\cos\left(\alpha t + \theta_2\right)\right]^2}\right\}. \quad (12)$$

The above is the calculation formula of the superposition value of the current on the four antennas. Such calculation processing can obtain the final axis value ratio of the

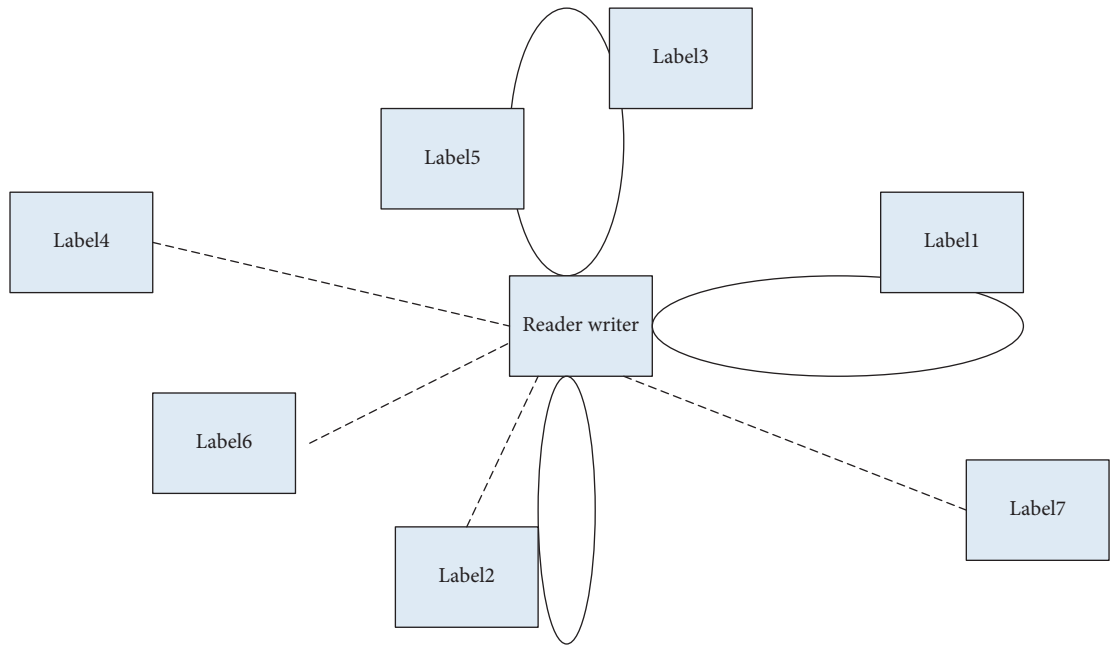

Figure 5: Diagram of spatial discrete recognition method.

antenna. In the axial ratio calculation directly above, the components of each polarization are equivalent to the same frequency radiated by different antenna elements. Signals of different amplitudes and phases are superimposed.

2.2. Construction Method and Algorithm of RFID System Electronic Label

2.2.1. Examples of Construction Methods of Electronic Tags. The RFID system is characterized by automatic identification. The identification of electronic tags on items can work normally when the number of items is small. However, when the number of items increases to a certain extent, the RFID system will be disturbed when identifying the electronic tag. The construction of electronic tags here is based on avoiding the situation where two or more electronic tags are repeated, which leads to a decrease in the working efficiency of the RFID system [18]. There are several methods for this problem: there are four major categories: space division multiplexing (SDMA), frequency division multiplexing (FDMA), code division multiplexing (CDMA), and time division multiplexing (TDMA). The first is the spatial discrete identification method. Its characteristics can be represented in Figure 5:

The above method has a relatively large complexity, which is not suitable for the wide application scenarios of the RFID system, so the scope of its use is relatively narrow. Then, there is the wave frequency discrete distribution method, whose specific operation is to use the band information transmission channels of different frequencies to process and transmit the data information on the electronic tag [19]. Its workflow chart is shown in Figure 6.

It can be seen from the method flow chart in Figure 6 that the characteristic of this method is to avoid the repetition of the electronic label of the RFID system through the difference in the wave frequency. However, this method can only be a channel for processing signals, and the frequency receiving device needs to be modified, which increases the overall economic cost and is also not suitable for popularization. In addition to the above two methods, there are transmission channel distribution methods and time discrete distribution methods. The former will bring more signal processing problems due to its immature technology, and the latter will be directly discussed here [20], such as low-frequency band utilization, low channel capacity, difficulty to select address codes, and long acquisition time, so it is difficult to apply in the actual radio frequency identification system. The basis of its operation is to allocate the information reserves of the RFID system according to the required amount of time. The workflow is shown in Figure 7.

The method in Figure 7 is characterized by corresponding distribution according to the time when the item signal is collected. It is divided according to the time of transmitting the signal so that different signals are transmitted at different times. It also divides the entire transmission time into many time intervals, and each time slice is occupied and used by a signal. The transmission of multiple signals by one circuit can thus be accomplished by interleaving a portion of each signal in time. In this way, at each brief moment of the circuit, there is only one signal. The repeatability of the RFID system electronic tag is effectively reduced, and this advantage also makes it applicable to a variety of scenarios.

2.2.2. Related Algorithms for the Construction of Electronic tags in RFID Systems. The methods used in the construction of the above-mentioned electronic tags have been discussed differently [21], and the time discrete distribution method is finally selected in this paper. In this paper, the corresponding algorithm needs to be introduced for this method, so as to

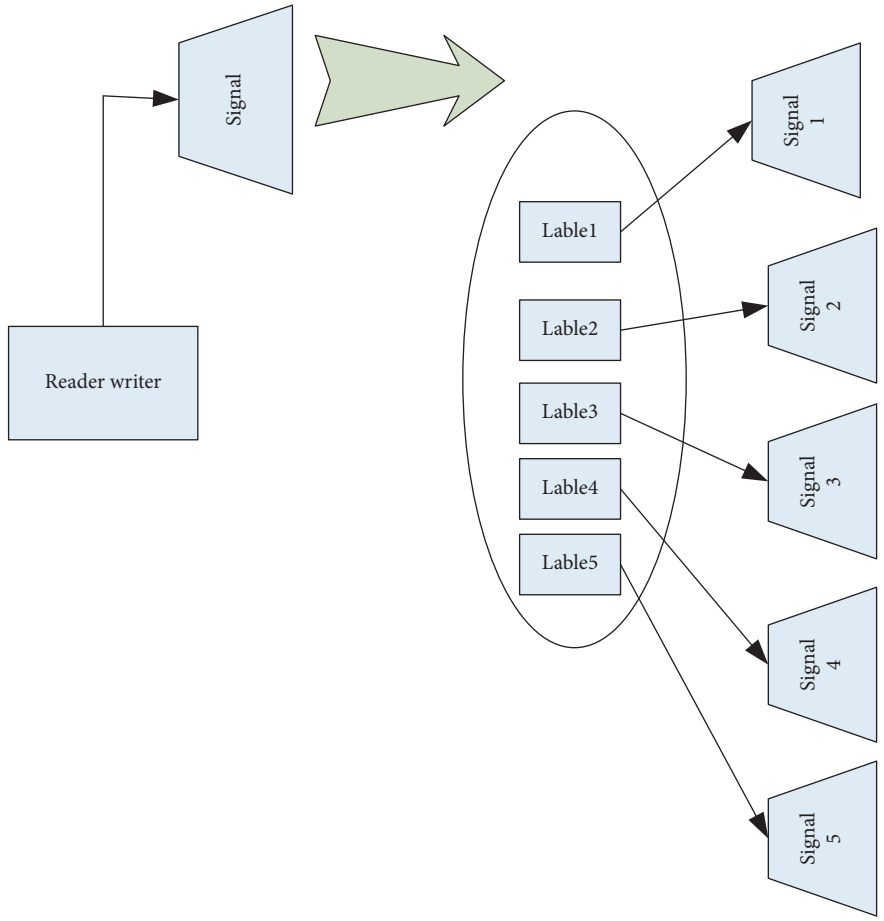

Figure 6: Wave frequency discrete identification method diagram.

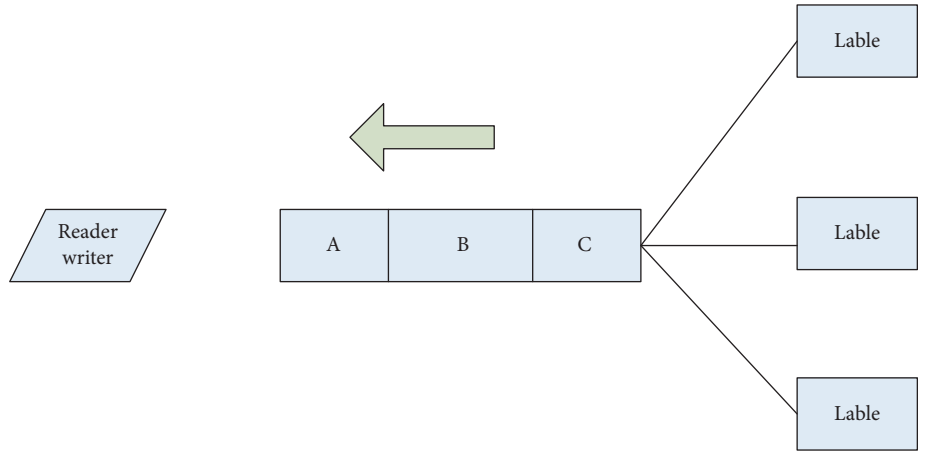

Figure 7: Diagram of time discrete distribution method.

reduce the repetition of the information collection process. The first is the ALOHA algorithm, which is characterized by its application scenario when the number of labels is small. Its working efficiency can be expressed by the following formula:

$$P - Q(m) = \frac{(\mu T)^m a^{-\mu T}}{m^!}. \tag{13}$$

The above formula shows that in the time of T, the amount of information m is transmitted, and u is the amount of information sent in the unit of time. The efficiency of the ALOHA algorithm can finally be expressed as follows:

$$P = Ha^{-2H}, (H = \mu T). \tag{14}$$

$H = \mu T$ of the above formula represents the amount of information transferred in time T. Equation (14) is the final

expression of the ALOHA algorithm. Next is the FSA algorithm, the frame slotted ALOHA algorithm (FSA) is based on the SA algorithm, and the slotted ALOHA (Slotted ALOHA) algorithm is based on the pure ALOHA algorithm, which is improved based on the ALOHA algorithm above. The calculation principle of this method is described below. Its principle formula is as follows:

$$P = C_M^N \left(\frac{1}{R}\right)^N \left(1 - \frac{1}{R}\right)^{M-N}. \tag{15}$$

$1/R$ here represents the probability that an electronic tag is selected, and the final selection probability of the tag is as in the above formula. The expected value of the identified N electronic tags in unit time is calculated as follows:

$$G = R \times P. \tag{16}$$

When no electronic label is identified in the identification gap, the repeatability calculation of the electronic label occurs as follows:

$$P = 1 - \left(1 - \frac{1}{R}\right)^M - \frac{M}{R}\left(1 - \frac{1}{R}\right)^{M-1}. \tag{17}$$

(3) Prediction method of the number of electronic tags in the RFID system

The use of this method is to predict the number of upcoming electronic tags so that the identification process of the RFID system can be carried out in an efficient and orderly manner until all tags are identified [22]. It is assumed here that there are j times of queries, and there is a proportional relationship between the related parameters, as shown in the formula:

$$m(j+1) = \mu \times D_\mu(j). \tag{18}$$

u in the above formula can be modified according to different usage situations. The algorithm of the formula can predict the number of electronic tags that will appear next.

It is also assumed that after j+1 identifications, the number of electronic tags is as follows:

$$m_0(j+1) = D_1(j+1) + 2.4 \times D_\mu(j+1). \tag{19}$$

This formula is a verification formula, which is calculated by formula 18, so as to obtain the actual number of electronic tags. For the relative error-free between the two, it can be expressed by the following formula:

$$\Delta = \frac{m_0(j+1) - m(j+1)}{m_0(j+1)}. \tag{20}$$

The error formula between the above formulas can realize the error correction between the predicted value and the actual check value so that the prediction ability of the formula can be more perfect. The establishment of the entire prediction process above is obtained after adjustment based on the prediction algorithm of the electronic label of the traditional RFID system.

2.3. Data Storage and Encryption Method of IoT RFID System

2.3.1. Key Technologies of the Internet of Things and Solutions to Security Problems. The Internet of Things was originally proposed to realize the intelligent application of human beings to the objects in life. The birth of this concept is based on the rapid development of information technology in today's society. The understanding of the concept of the Internet of Things should be a data system based on big data, in which a large number of emerging technologies are used. The most important is computer science and technology [23]. In order to realize the interconnection between objects, the Internet of Things has many technical applications; it includes information perception technology, information processing technology, information transmission technology, and perception technology which mainly includes sensing technology, identification technology, and positioning technology, and the specific relationship is shown in Figure 8.

As can be seen from Figure 8, the establishment of the Internet of Things is closely related to the joint action of multiple technologies. At the same time, more advanced network transmission technology is needed to realize the efficient processing of the transmitted data by Internet technology. Because the Internet of Things needs to use related technologies of information conversion in the process of data collection, it is also necessary to implement the establishment of a computer information processing system.

The establishment of the Internet of Things and its role in people's lives have become increasingly prominent, so related security issues have also received extensive attention. For the large data system of the Internet of Things, the biggest security risk is data-related issues, which involve data storage and protection, and it faces serious threats such as leakage. For the IoT system, its defects can be shown in Figure 9.

As can be seen from Figure 9, the system of the Internet of Things is a three-dimensional network system, and the data involved is very large. The electronic tag is the key information, but due to the traditional means, the protection for this place is very limited. In view of the above-mentioned risks, this paper does relevant research and introduces relatively effective protection protocols for different technical levels of the Internet of Things. Its overall content is shown in Table 2.

The birth of the Internet of Things is a collection of modern network technologies and the integration of various network systems. Its complexity can be imagined, and its security is similar to the security of these networks. Therefore, the solution to the security problem of the Internet of Things will refer to the traditional network security method.

2.3.2. Internet of Things RFID System Security and Encryption Methods. Since the RFID system needs to contact a large amount of data, it may leak during its working process. Due to the characteristics of the RFID system and the structure of the electronic label device, the traditional encryption

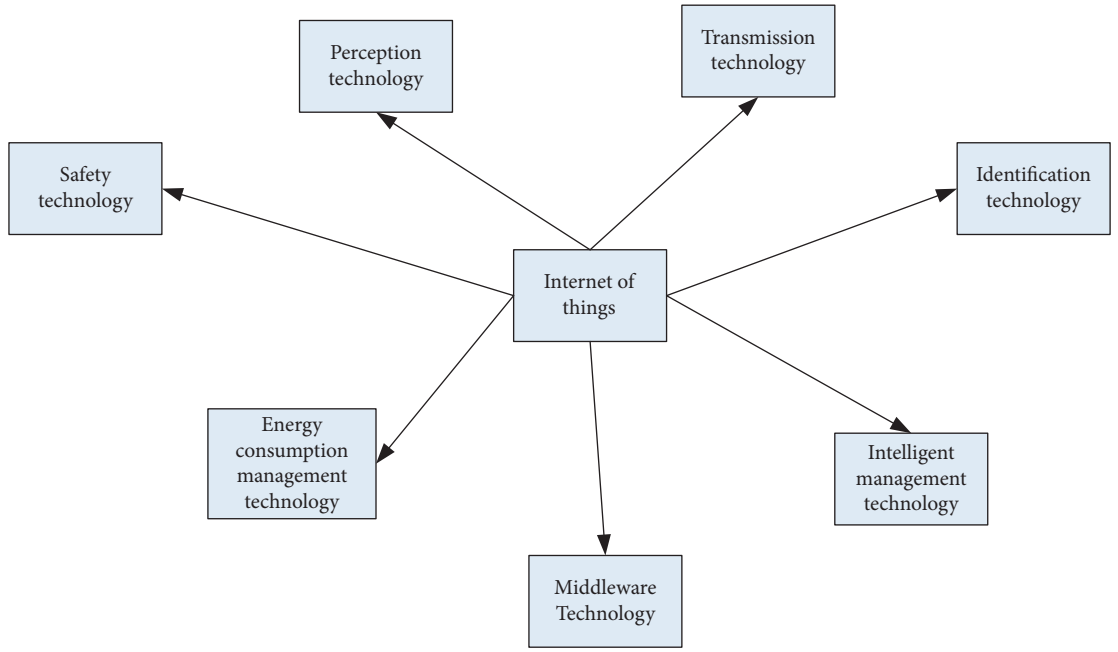

Figure 8: Related technologies for IoT.

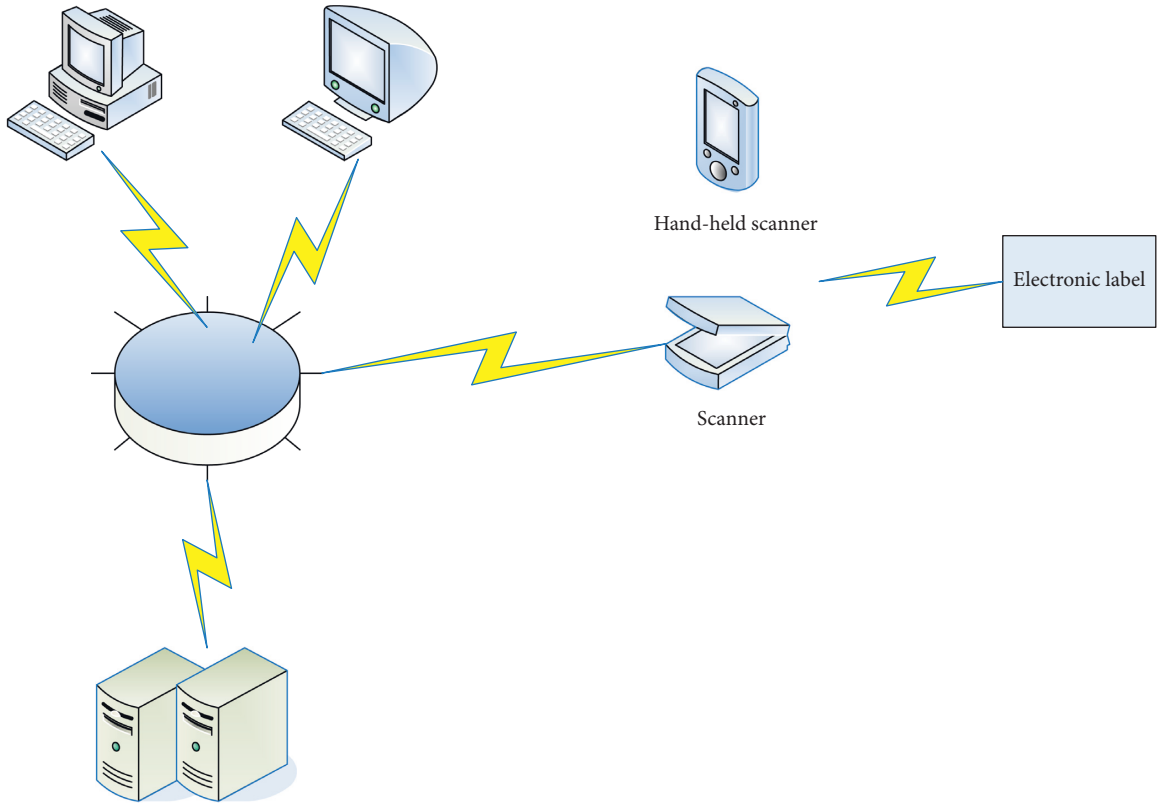

Figure 9: Diagram of key links in the Internet of Things.

technology may not be suitable for this situation. This paper establishes a new encryption mechanism. It is expected to achieve higher security and privacy of the Internet of Things. The encryption algorithm introduced here is the ECC algorithm, and the following is a comparison between it and other encryption algorithms.

It can be known from Table 3 that the reliability of ECC is relatively high. A shorter key length can be used to achieve the same or even higher security strength, and at the same time, it has the technical advantages of low memory resource usage and low bandwidth requirements, which is one of the reasons for choosing this method in this paper, but the ECC

Table 2: Security methods at different levels of IoT.

Technical level	Safe mode
IOT perception layer	Hash-Lock, Hash, Random hash-lock
IOT transport layer	HTTP, SSH, SFTP
IOT application layer	Institutional constraints, privacy authority setting, identity concealment, data confusion

encryption method also has the disadvantage of low execution efficiency. Therefore, this paper needs to improve the method to some extent, so as to achieve the purpose of improving work efficiency.

The first is the related elaboration of ECC cryptography, which is a kind of public key cryptography, and its characteristic is high security performance. At the same time, the electronic storage space required by the password itself is small, so it has the basis for wide application. For the RFID system, although this kind of password has the above-mentioned storage advantages and high security performance, it still requires high execution power when using it in the system of the Internet of Things, which is a relatively lacking part. This paper will improve the ECC algorithm process to improve its execution efficiency. This paper firstly optimizes and adjusts the scalar, which can directly guarantee the security performance of the password. The first introduces the binary algorithm whose expression can be expressed as follows:

$$P = [A]Q = \sum_{i=0}^{m} A_i 2^i \times Q = \sum_{i=0}^{m} A_i \times \left(2^i \times Q\right). \quad (21)$$

The above formula is for the traditional algorithm between points and points, and our research is improved on the basis of the above formula. In this paper, the traditional modulo operation is replaced by the bit operation, the division operation is replaced by the shift operation, and the parity of the scalar d is no longer judged. After the improvement, this paper analyzes the performance of the corresponding algorithm. Table 4 is a comparison of the security performance before and after the improvement.

From Table 4, it can be seen that the ECC within the unit will be better than the improved security performance. But this is only for a relatively small number of cases, and the advantages of improved encryption for large amounts of data will be more obvious. Its work efficiency will be higher.

3. Related Experiments and Encryption and Perfection of Internet of Things RFID System

3.1. RFID System Electronic Label Reliability Test and Result. The electronic tag of the RFID system is the most frequently used part of the RFID system, but with the particularity of its structure, this part has become one of the biggest safety hazards. In the method part, the corresponding working mechanism and related algorithms of electronic tags have been introduced. The following are the comparison results of the security performance under different security protocols.

From the comparison results in Table 5, it can be seen that various security protocols have a good protective effect on antitracking and antieavesdropping. From the comparison results in the table, it can be seen that the security performance of the BAP protocol is the best, but because the electronic tags of the RFID system do not have the ability to run complex algorithms. Therefore, the use of this algorithm needs to be readjusted. The result of the adjustment of this algorithm can solve the cost problem of the electronic label of the RFID system, and at the same time, its security will be improved correspondingly compared with the traditional one. It ensures that the important part of the electronic label of the Internet of Things RFID system is guaranteed.

Table 3: Comparison of ECC and various cryptographic mechanisms.

Algorithm	Key length	Security	Execution efficiency
AES	132	Strong	Poor efficiency
DES	56	Weak	Poor efficiency
PRESENT	90	Middle	Efficient
ECC	180	Strong	Poor efficiency

Table 4: Performance comparison before and after ECC improvement.

Decoding time	Improved length	Original length	Key ratio
105	523	118	5.5 : 1
109	760	142	6 : 1
1010	1050	165	7.5 : 1.5
1020	2058	220	10 : 1.5

3.2. Experiment and Result of New Antenna Array of RFID System Reader Antenna. In the above antenna adjustment algorithm, the algorithm structure for a new type of antenna array is introduced, and corresponding experiments are carried out for this new type of antenna array. First of all, it is to consider the effect of distance on the performance of the reader antenna. This experiment is divided into two types: the experimental model and the actual model. Figure 10 shows the experimental results of the experimental model.

Figure 10 is an illustration of the results under the experimental situation of the antenna performance. It can be seen from the figure that the influence of the antenna coupling on the performance of the antenna is small, but the distance can have a certain influence on the coupling. It can be seen from the figure that the optimal axial ratio of the antenna changes with the distance is not obvious. Next is the relationship between antenna angle and antenna performance, and the research results are shown in Figure 11.

From the results in Figure 11, it can be seen that the different angles of the antenna can make the performance of the antenna change greatly. Therefore, the control of the antenna angle is also very important. Then, there is the effect of different antenna arrangements on the antenna performance, and the results are shown in Figure 12.

As can be seen from Figure 12, the stability of a single antenna is more prone to interference than the other three, but when there are more antenna array structures, its overall performance will be more stable. Under the condition of the quaternary array, the pattern of the antenna changes greatly.

Table 5: Comparison Table of safety performance.

Security protocol type	Anticounterfeiting attack	Antiretransmission attack	Antitracking	Antieavesdropping
Hash-lock	Uncertain	Uncertain	Uncertain	Uncertain
Hash	Uncertain	Uncertain	Security	Uncertain
Dynamic ID-Hash	Uncertain	Uncertain	Security	Uncertain
GR	Uncertain	Security	Uncertain	Security
DAP	Security	Security	Security	Security
RandomHash-lock	Security	Uncertain	Security	Uncertain
BAP	Security	Security	Security	Security

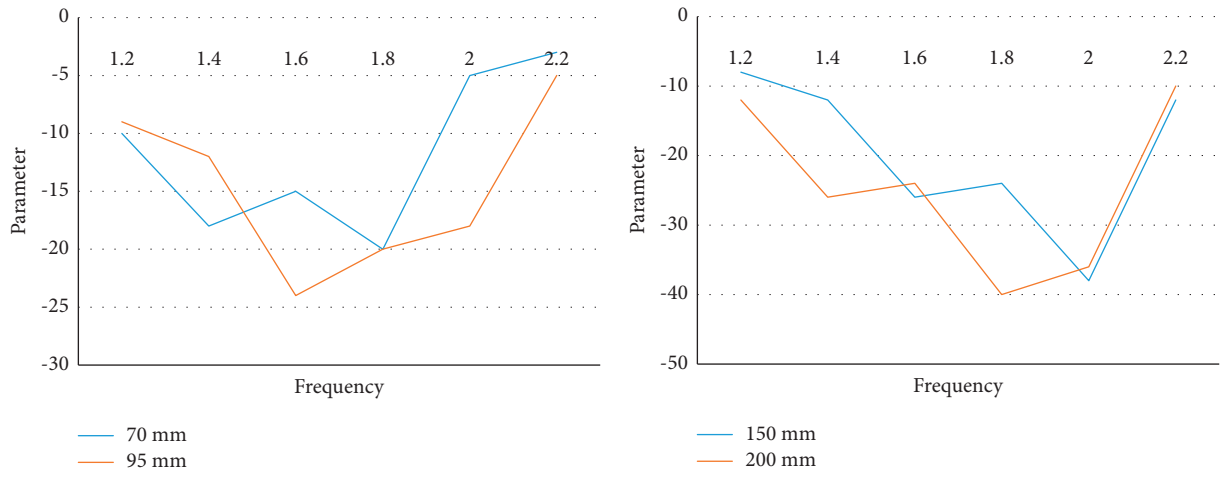

Figure 10: Variation of antenna parameters at different distances.

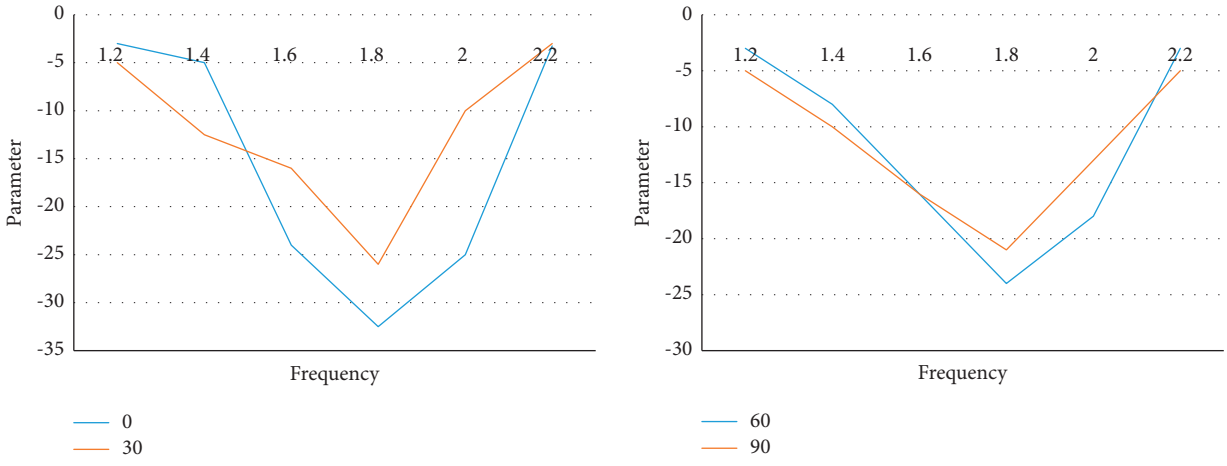

Figure 11: Effects of different angles on antenna performance.

Therefore, it can be judged that if there are a large number of other antennas around, the change in the antenna pattern will be more obvious.

3.3. Experiment and Result of Encryption Algorithm of IoT RFID System. For the information encryption of the Internet of Things, it is ultimately the improvement of the key. The algorithm of this experiment is the calculation of the scalar. Its operation process is to treat the value obtained after processing the collected data as a key. It uses the IDEA programming tool and JAVA programming language to realize PECC-CRT scalar multiplication and PSM-NAF scalar multiplication respectively. The following is the experimental result graph, as shown in Figure 13.

As can be seen from the above figure, the efficiency of the key performance under different algorithms is not the same. But the memory it occupies is not much different. And the operation under the algorithm PECC can reduce the operation amount by 28.35%. It can be seen that the application of this method is helpful to improve the performance of the key.

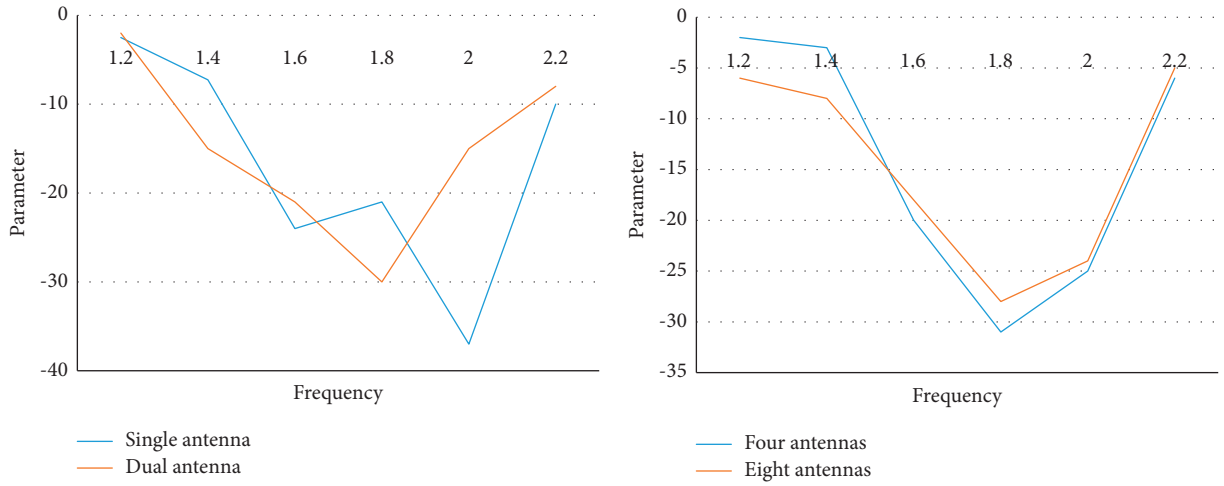

Figure 12: Effects of different antenna arrangements on antenna performance.

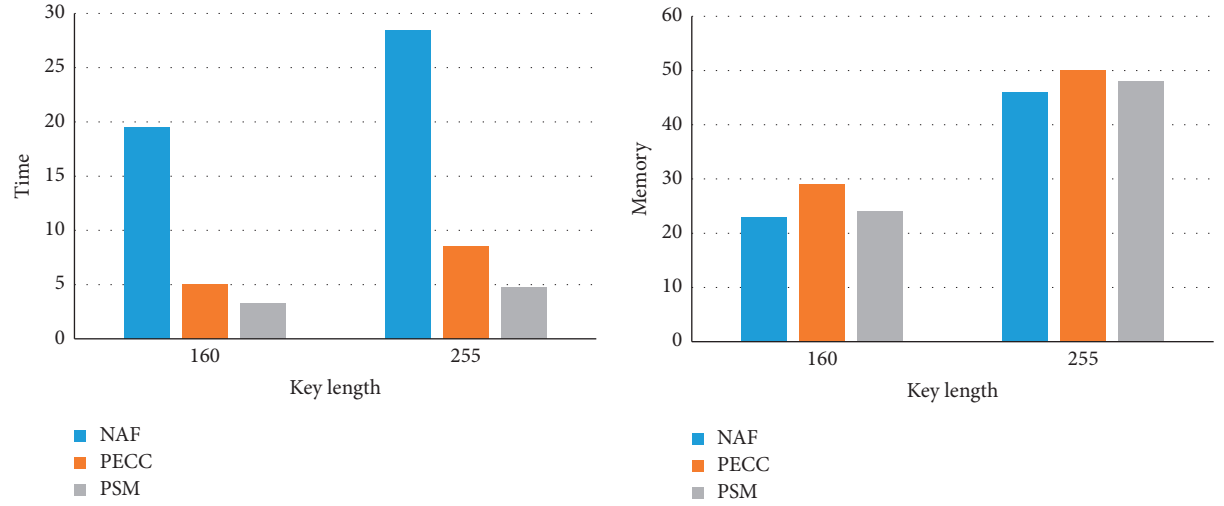

Figure 13: Memory and time versus key length comparison graph.

4. Discussion

This paper is a research on the encryption technology of the Internet of Things RFID system; the purpose is to establish security that can make the Internet of Things system. Although the science and technology involved in the Internet of Things system is closely related to computer technology, it is not only the application of a single technology but the integrated application of multiple technologies. In the method part, the Internet of Things RFID system is expounded accordingly, and its principle and mechanism are explained.

The reader is an important component of the Internet of Things RFID system. The method section proposes corresponding solutions for its structure and influencing factors. First of all, the adjustment of the antenna is made to solve the problem of the reader's own antenna, because this problem will greatly affect the stability of the reader so that the information in the identification process will be leaked. Then, the corresponding research on the algorithm and password of the corresponding electronic tag of the Internet of Things RFID system is made. Because of the special structure of the electronic tag, it has higher requirements on the algorithm. Finally, the more scientific operation of the electronic tag in the algorithm and the identification FID system is realized.

The last is the use of encryption methods for the Internet of Things RFID system. The Internet of Things involves a large amount of user data, and the importance of data security and privacy protection is self-evident. The research on encryption technology in this paper has improved the security performance of the Internet of Things.

5. Conclusion

This paper is a related research article to achieve higher security of the Internet of Things. The purpose of the Internet of Things is to realize the interconnection of all things, which is to make the future human society more efficient. It has an efficient drive in all aspects and fields it touches. The research on the encryption technology of the Internet of Things in this paper is to provide an effective security guarantee for it. At the same time, the research in this paper

is also a major expansion of computer science, which makes the integration between disciplines better.

Data Availability

No data were used to support this study.

Conflicts of Interest

The authors declares that there are no potential conflicts of interest in this study.

Acknowledgments

This work was supported by the Scientific Research Planning Projects of the Shaanxi Provincial Department of Education (no. 21JK0641).

References

[1] Z. Feng, B. Xiao, L. Jia, and U. Chen, "Efficient physical-layer unknown tag identification in large-scale RFID systems," *IEEE Transactions on Communications*, vol. 65, no. 1, pp. 283–295, 2017.

[2] K. Narges, S. Ramesh, and H. Bill, "A balanced scorecard for item-level RFID in the retail sector: a Delphi study," *European Journal of Information Systems*, vol. 21, no. 3, pp. 255–267, 2017.

[3] M. Ramadan, H. Al-Maimani, and B. Noche, "RFID-enabled smart real-time manufacturing cost tracking system," *International Journal of Advanced Manufacturing Technology*, vol. 89, no. 1-4, pp. 969–985, 2017.

[4] S. Youm, Y. Jeon, S. H. Park, and W. Zhu, "RFID-based automatic scoring system for physical fitness testing," *IEEE Systems Journal*, vol. 9, no. 2, pp. 326–334, 2015.

[5] S. H. Tan, Y. Z. x Sun, and Y. Xiang, "A new lightweight RFID grouping authentication protocol for multiple tags in mobile environment," *Multimedia Tools and Applications*, vol. 76, no. 21, pp. 22761–22783, 2017.

[6] Sl Popoola, V. O. Matthews, A. Atayero, and A. Ao, "Solar photovoltaic automobile recognition system for smart-green access control using RFID and LoRa LPWAN technologies," *Journal of Engineering and Applied Sciences*, vol. 12, no. 4, pp. 913–919, 2017.

[7] K. Thiyagarajan, R. Lu, K. El-Sankary, and H. Zhu, "Energy-aware encryption for securing video transmission in internet of multimedia things," *IEEE Transactions on Circuits and Systems for Video Technology*, vol. 29, no. 3, pp. 610–624, 2019.

[8] G. Bansod, N. Pisharoty, and A Patil, "BORON: an ultra-lightweight and low power encryption design for pervasive computing," *Frontiers of Information Technology & Electronic Engineering*, vol. 18, no. 3, pp. 317–331, 2017.

[9] J. Yu, L. Chen, R. Zhang, and K. Wang, "Finding needles in a haystack: missing tag detection in large RFID systems," *IEEE Transactions on Communications*, vol. 65, no. 5, pp. 2036–2047, 2017.

[10] Sw Lee, S. M. Park, and K. B. Sim, "Smart door lock systems using encryption technology," *Journal of Korean institute of intelligent systems*, vol. 27, no. 1, pp. 65–71, 2017.

[11] N. Sun, T. Li, G. Song, and H. Xia, "Network security technology of intelligent information terminal based on mobile internet of things," *Mobile Information Systems*, vol. 2021, no. 8, pp. 1–9, Article ID 6676946, 2021.

[12] M. Ali, C. Xu, and A Hussain, "Authorized attribute-based encryption multi-keywords search withPolicy updating," *Journal of New Media*, vol. 2, no. 1, pp. 31–43, 2020.

[13] R. S. Boparai, A. Alexandridis, and ZZilic, "Multi-point security by a multiplatform-compatible multifunctional authentication and encryption board," *Journal of Computing and Information Technology*, vol. 26, no. 4, pp. 235–250, 2018.

[14] N. Ha, A. Hussien, LAl-Dabag, and A. Hts, "Paper-encryption system for hiding information based on internet of things encryption system for hiding information based on internet of things," *International Journal of Interactive Mobile Technologies (iJIM)*, vol. 15, no. 2, pp. 172–183, 2021.

[15] P. P. Ray, B. Chowhan, N. Kumar, and A. Almogren, "BIoTHR: electronic health record servicing scheme in IoT-blockchain ecosystem," *IEEE Internet of Things Journal*, vol. 8, no. 13, pp. 10857–10872, 2021.

[16] P. Krishnakumar, "Lightweight cryptography and its algorithms in internet of things:an overview," *International Journal of Innovative Research in Science Engineering and Technology*, vol. 10, no. 5, pp. 4900–4904, 2021.

[17] L. S. Abdulla, M. K. Mahmood, A. F. Salih, and S. M. Karim, "Analysis and evaluation of symmetric key ciphers for internet of things smart home," *Indonesian Journal of Electrical Engineering and Computer Science*, vol. 22, no. 2, pp. 1191–1198, 2021.

[18] N. N. Mohamed, Y. Mohd Yussof, M. A. Saleh, and H. Hashim, "Hybrid cryptographic approach for internet of things applications: a review," *Journal of Information and Communication Technology*, vol. 19, no. 3, pp. 279–319, 2020.

[19] K. Han, W. K. Lee, and S. O. Hwang, "cuGimli: optimized implementation of the Gimli authenticated encryption and hash function on GPU for IoT applications," *Cluster Computing*, vol. 25, no. 1, pp. 433–450, 2021.

[20] C. Guo, J. Jia, Y. Jie, C. Z. Liu, and K. K. R. Choo, "Enabling secure cross-modal retrieval over encrypted heterogeneous IoT databases with collective matrix factorization," *IEEE Internet of Things Journal*, vol. 7, no. 4, pp. 3104–3113, 2020.

[21] T. Premalatha and S. Duraisamy, "Secure communication process in IoT using media gate network transmit protocol with reliable data transport protocol," *International Journal of Internet Technology and Secured Transactions*, vol. 9, no. 1/2, p. 136, 2019.

[22] J. Sun, Z. Bie, H. Bie, P. He, and M. Jin, "Secrecy analysis of cognitive radio networks over generalized fading channels," *Security and Communication Networks*, vol. 2020, no. 1, pp. 1–9, Article ID 8842012, 2020.

[23] J. See, K.-M. Mok, W.-K. Lee, and H.-G. Goh, "RISC32-E: field programmable gate array based sensor node with queue system to support fast encryption in Industrial Internet of Things applications," *International Journal of Circuit Theory and Applications*, vol. 48, no. 8, pp. 1209–1226, 2020.

Hindawi
Scientific Programming
Volume 2022, Article ID 3962255, 12 pages
https://doi.org/10.1155/2022/3962255

Research Article

Borderless Fusion Financial Management Innovation Based on Speech Recognition Technology

Lin Yang,[1,2] **Zehao Fan**,[3] **and Jiaqi Zhou**[1]

[1]*College of Economics and Management, Beijing Institute of Petrochemical Technology, Beijing 102617, China*
[2]*Enterprise Development Research Center of Beijing Institute of Petrochemical Technology, Beijing 102617, China*
[3]*Beijing Haidian Foreign Language Shiyan School*

Correspondence should be addressed to Zehao Fan; zehaofan@bjfles.com

Received 4 July 2022; Revised 30 July 2022; Accepted 17 August 2022; Published 14 September 2022

Academic Editor: Juan Vicente Capella Hernandez

In recent years, the rapid development of information technology has affected the operation of the world economy, and the emergence of e-commerce has decreased significantly. The development of modern information technology, especially the development of Internet technology, provides a solid foundation for e-commerce. The time and space gap between economic operators is shortened, and resources are shared as widely as possible. Based on a comprehensive and in-depth study of language recognition technology. However, the current e-commerce financial management still uses the traditional accounting method, which is inefficient and cannot be integrated with new technologies. This paper proposes a design scheme for a nonspecific person and small vocabulary language recognition system based on SPCE061A processor. This integrated system can be combined with data acquisition and language input technology and constitute a data acquisition and input system. It is used for data collection and input of instruments and meters in the workplace to improve work efficiency. This paper proposes algorithms based on time-domain energy and zero-crossing rate detection, detection based on entropy function method, and detection based on the double-threshold method. The speech recognition technology is analyzed in detail, and a new model of financial management is constructed. Accounting information disclosure is a virtuous circle of "promoting capital management with appropriate decentralization." The experimental results in this paper show that through model construction, the calculated WER is 0 dm, 7 dm, 15 dm, and 11 dm, respectively, and it is concluded that the system exhibits good antinoise performance.

1. Introduction

1.1. Background. Language is one of the important ways for people to communicate, and it is the result of useful information that people retain in the long-term evolutionary process. With the advent of networked technology, in addition to communicating with people using language, it has become a dream for people to allow machines to understand human language. This problem that was previously considered impossible to solve has now become possible. With the advent of the information age, the use of voice instead of computer keyboard input has become one of the future social development trends, and voice recognition technology has emerged at the historic moment and has become one of the hotspots of research by many researchers. With the continuous development of computer and artificial intelligence technology, smart machines participate in human production activities and social activities. How to improve the relationship between people of these machines and make it easier for people to manage machines. More importantly, language is the best way for humans and machines to communicate. Speech processing is a cross-discipline between language and digital signal processing technology. It is an important method of computer intelligence and human-computer interaction. The main technology of the interaction between humans and computers is speech recognition. Therefore, the research of speech recognition technology has become the research focus of countries all over the world. The development of computers and the importance of social life are becoming more and more prominent. Various

applications of voice coding technology have been developed by the product, including voice telephone exchange. Voice dialing systems, industrial control systems, etc., have penetrated into all sectors of society and have good application prospects. Boundaryless management was first aimed at the overall management of an enterprise. According to its meaning, the borderless theory is applied to the field of financial management and combined with the characteristics of integrated finance, a borderless integrated financial management model is proposed.

1.2. Significance. Speech recognition is a comprehensive subject, including sound, computer science, signal processing, mathematical statistics, human intelligence, and engineering. The ultimate goal of speech recognition is to make a technology product that can communicate with people normally. This product can convert the received sound information into corresponding text and execute the corresponding action, thereby realizing human-computer interaction (Human Computer Interface, HCx). At present, the speech recognition technology in a quiet environment is quite satisfactory, and the speech recognition rate is also very high. However, in real life, the speaker's voice is easily affected by the surrounding environment and various superimposed noises and cannot achieve the ideal recognition effect. Boundless integrated financial management is guided by corporate strategy, emphasizing that finance breaks through the existing work framework and mode with a borderless active management awareness, communicates and transmits financial concepts in all aspects of the value chain, and forms the integration of finance and other aspects. The department implements the financial management model to promote the continuous growth of the overall value of the enterprise. Therefore, improving speech recognition technology under noisy conditions and extracting accurate sound information has become the focus of researchers. In a society where the scope of information technology is gradually expanding, the development of research on speech recognition technology in noisy environments is of great significance to improving people's living standards and quality of life.

1.3. Related Work. Human society increasingly shows the characteristics of an information society. Not only between people but also between people and machines, a large amount of information needs to be exchanged at any time. Voice is the most direct, most convenient, and effective tool for information exchange between people, and it is also an important means of communication between people and machines. Use the concept of big data to optimize the industrial structure and improve work efficiency. First, it outlines the main content and development changes of financial management. The latest research progress of digital construction financial budget management and cost management is analyzed. Then combined with actual work, the main content and workflow of the financial management system are summarized and improved. Finally, an intelligent framework for modern hospital financial management is proposed, including budget management, cost management, and performance management. [1] Dagnew D K uses a parallel hybrid research method. Collect data through questionnaire surveys and interviews. Quantitative data is analyzed by descriptive and econometrics, and interview data is analyzed by narrative. In addition, the lack of guidance and consulting services, the high cost of training and consulting services, the complexity of most standards, and the lack of time for regulatory agencies are the most important challenges. The international comparability, transparency, and quality of the financial reporting system are one of the prospects for the implementation of IFRS. However, his data is not clear enough ([2] Maria Ruiz-Jimenez J). There is an ethical debate about the impact of gender diversity in the top management team (TMT) on the organization. The research aims to contribute to this debate by analyzing the influence of gender diversity of TMT on the relationship between knowledge combination ability and organizational innovation performance. A sample of 205 small and medium enterprises (SMEs) belonging to the Spanish Technology Company (TBF) sector was used. The research results show that gender diversity positively regulates the relationship between knowledge combination ability and innovation performance. They discussed the impact on theory and practice among them, how to promote more equal gender distribution, and the benefits of gender diversity in senior management positions [3]. Although the analysis is in place, some theories do not have practical value. Through their research, it can be found that for financial management, most scholars still improve the efficiency of traditional methods and do not propose essential innovations in combination with current technology.

1.4. Innovation. The innovation of this article is as follows: (1) First of all, the innovation of the topic selection angle. This article is a new perspective from the perspective of topic selection. At present, there is not much research on the integration of speech recognition, boundless fusion, and financial management. It is of exploratory significance. (2) The second is the innovation of research methods. The proposed detection based on time domain energy and zero-crossing rate, detection based on entropy function method, etc., has theoretical value. (3) The other is the innovation of project practice. Boundless integrated financial management penetrates the financial concept into all aspects of production and operation, so that information communication can break the barriers of departments and professions, improve the information transmission, diffusion, and penetration capabilities of the entire organization, and realize the symmetrical distribution of information, experience and skills and sharing, thereby stimulating innovation and improving work efficiency, and realizing the optimal allocation of enterprise resources and the maximization of value creation. The project is of great significance to improving people's living standards and quality of life.

2. Commonly Used Voice Endpoint Detection Algorithms

2.1. Based on Time Domain Energy and Zero-Crossing Rate Detection. Speech endpoint detection is generally used to identify the presence and absence of speech in an audio

signal. Short-term energy analysis and zero-crossing rate analysis are the most basic methods in time domain analysis of speech signals, and they are widely used, especially in the detection of speech signal endpoints. Since these two methods are usually used independently in speech signal endpoint detection, it is easy to miss important information during endpoint detection. Judging from the instability of the speech signal [4], its energy may change over time, and the energy of nonhuman voice and human voice is also very different. Therefore, by analyzing the short-term energy and the short-term energy zero pass rate, it is possible to distinguish the speech segment with and without the speech segment. The short-term energy of speech sampling sequence $g(i)$ is defined as follows:

$$W_i = \sum_{-\infty}^{+\infty} \left[f(e)h(i-d)^2 \right] = \sum_{-\infty}^{+\infty} f(e)^2 h(i-d) = g(i)^2 * h(i). \tag{1}$$

Among them, W_i represents the short-term energy of the i speech frame, $h(i) = g(i)^2$. Set the windowed speech signal to $f_w(i)$, N represents the window length, and the short-term energy [5] is expressed as follows:

$$E_i = \sum_{e=-\infty}^{\infty} |x(r)|w(i-r) = \sum_{m=e}^{i+A-1} \left| x_w(r) \right|. \tag{2}$$

The endpoint of the speech signal is obtained by setting and comprehensively using two threshold levels, and the principle is simple, and the real-time performance and precision are relatively high, so it has a wide range of applications. The zero pass rate of the speech signal should be the number of times the signal crosses the branch in one second. When the speech signal is a continuous signal, the zero pass rate can be calculated as the number of times it passes the segmented signal. If it is an obvious voice signal, the number of times the symbols of two adjacent sampling points change in a unit time can be used to represent the short-term zero-crossing rate [6]. It is defined as follows:

$$\mathrm{WDR}_i = \frac{1}{2} \left[\sum_{k=0}^{A-1} |\mathrm{dsn}(h(i))| - \mathrm{dsn}\left(h_i(h-1)\right) \right]. \tag{3}$$

In formula (3), the frame length is L, and $\mathrm{dsn}(x)$ 1 is the sign function.

$$\mathrm{dsn}(x) = \begin{cases} 2, & x \geq 0, \\ -2, & x < 0. \end{cases} \tag{4}$$

In real life applications, in order to prevent low-frequency interference [7], a threshold value T is usually set, and the number of times the threshold value T is crossed is used instead of the number of zero-crossings. Therefore, the improved zero-crossing rate is shown in the following:

$$\mathrm{WDR}_i = \frac{1}{2} \sum_{m=n}^{L-1} |\mathrm{dsn}[x(m) - T]| + |\mathrm{dsn}[x(m) + T] - \mathrm{dsn}[x(m-2) + T]|. \tag{5}$$

2.2. Detection Based on Entropy Function Method. Entropy comes from statistical thermodynamics to physics [8]. It characterizes the degree of disturbance. With the cross-development of science, entropy has important applications in the fields of government, probability theory, information theory, and life sciences. In speech signal processing, the concept of entropy is widely used for endpoint detection [9], such as spectral entropy and cepstral distance entropy.

Assuming that the noisy speech signal $h_i(m)$ in the ith frame after the windowing process, after Fourier transform (FFT), the spectral probability density of the kth spectral line of each frequency component is $h_p(k)$, then the spectral entropy of each frame is defined as follows:

$$X_i = -\sum_{k=0}^{H/3} L_i(G) \log L_i(G), \tag{6}$$

where N is the FFT length, and the probability space of the discrete speech signal X can be expressed as follows:

$$\begin{bmatrix} S \\ P(g) \end{bmatrix} = \begin{bmatrix} x_1, x_{2,\ldots,} x_c \\ j_1, j_2, \ldots, j_c \end{bmatrix}. \tag{7}$$

Then, the entropy function of the speech signal X is as follows:

$$F_i = \sum_{i=1}^{q} P \log P_i. \tag{8}$$

From the definition of spectral entropy, it can be seen that speech entropy reflects the "disorder" of the amplitude distribution of the source in the frequency domain.

The idea of offspring spectral entropy is as follows: first divide a frame of speech signal into several offspring, and then find the spectral entropy of each offspring. Suppose the energy probability of the mth offspring of the ith frame is $P(h,i)$, and the offspring energy is $E(h,i)$; then,

$$P(h,i) = \frac{E(h,i)}{\sum_{k=1}^{g_v} E(h,i)}. \tag{9}$$

The offspring power spectrum is as follows:

$$S_i = \sum_{a=1}^{g_v} P(h,i) \log P(h,i). \tag{10}$$

The difference between the detection method based on the offspring spectrum entropy method and the original spectrum entropy method is that the latter is to find the probability density function of each power point and then the spectrum entropy, while the former is to find the power density function of a child of the speech frame [10], then calculate the spectral entropy, because, in this way, the amplitude of a single spectral line is protected from the interference of background noise.

2.3. Detection Based on Double Threshold Method. The dual-threshold method was originally proposed based on short-term energy and short-term average zero-crossing rate [11].

Its principle is because the energy of the finals is very large, short-term energy can be used to find the finals, and the frequency of initials is also very high and can be used. Find the short-term average zero pass rate of the agreement. The dual-threshold method needs to use two levels of judgment to realize voice endpoint detection. Set $Q_F$as the high threshold and Q_H as the low threshold.

(1) First-level judgment: according to the difference in short-term average energy;

(2) After the judgment of (1), according to the difference in the short-term average zero-crossing rate, the second-level judgment is carried out so that the starting point and ending point of the speech can be determined, and the effect we want to achieve by the endpoint detection can be obtained.

The specific process is as follows:

(1) Starting from the silent segment, if the short-term energy [12] and the short-term zero-crossing rate of the speech frame are both greater than Q_F, we can think that the frame may be the starting point of the speech, and the system starts to detect it, but it is not sure that it is the starting point. At this stage is defined as a transitional section.

(2) Continue to track the short-term energy and the short-term zero-crossing rate of the next frame. If both of these parameters are less than Q_F, it is definitely not a voice endpoint, and the silent segment is restored.

(3) If one of the parameters is greater than the high threshold Q_H, and the duration of such a state exceeds the minimum speech segment length, it can be marked as the starting point of entering the speech segment.

(4) After entering the speech segment, if the short-term energy or the short-term zero-crossing rate of the detected speech frame is less than Q_F, it enters the end point mark, but it is still a transitional state at this time. If these two characteristic parameters are both higher than Q_F, it is considered that it is still in the speech segment. If the detected two parameter values are less than Q_H and last for a period of time, it is marked as the end point of the speech signal [13]. The overall flow chart of dual-threshold endpoint detection is shown in Figure 1.

The above endpoint detection method is only suitable for speech in a pure environment and is not applicable when noise is added [14] because the zero-crossing rate of noise is much larger than initials and finals, so the above method needs to be improved. In fact, the short-term zero-crossing rate of the silent section in a noisy environment is less than that of the voiced section [15], which is just the opposite of the situation in a pure environment. Therefore, when looking for the starting point, you only need to find the original zero-crossing rate greater than Q_H. If it is changed to less than Q_H, the situation of finding the end point is also the opposite, and the situation of short-term energy remains unchanged. Using the above-mentioned improved double-threshold method to detect the starting point and ending point of a noisy segment of Chinese speech, the detection results are shown in Figures 2 and 3:

Although the improved dual-threshold method has some antinoise ability [16], the false positive rate is still very high in a noisy environment. This is because the improved method cannot completely screen the noise of the speech, and the noise of different frequencies will lead to a false alarm rate. In the past ten years, in the analysis and research of voice signals, a feature value based on the entropy function has emerged as it is used in voice endpoint detection, which has a certain degree of robustness in complex environments.

3. Construction of a New Model of Financial Management

3.1. The Establishment of "CIO" Model. This paper conducts a standardized analysis by reading the literature and sorting out related concepts and theoretical foundations [17]. Comprehensively analyze the operating conditions and operating models of each enterprise and compare their comprehensive scores. The analysis results show that most of my country's SMEs' existing financial management models have serious problems, mainly: weak capital management capabilities lead to low corporate returns and poor performance. The company's business performance has led to unrealistic and unrealistic accounting information disclosure, and the high concentration of financial power allocation has led to unscientific capital management decision-making. The capital management [18], accounting information disclosure, and financial organization of small and medium-sized enterprises have been severely divided [19]. The current financial management model does not adapt to the new e-commerce environment and cannot survive and grow in the new economic competition environment. It is necessary to discuss how to regulate the accounting information disclosure of listed companies under the current market economy conditions, propose effective strategies to solve the problem, and expect the relevant laws and regulations of accounting information disclosure to be more complete.

Starting from the problem, this article selects three typical submodes according to the standard of financial management module-Capital Management Mode, Accounting Information Disclosure Mode, and Financial Organization Mode (Financial Organization Mode), as the research object and content, as shown in Figure 4.

This model focuses on the study of the relationship between corporate capital management, accounting information disclosure, and financial organization and aims to combine the three organically to restrict, promote and coordinate work with each other so as to achieve "capital management to promote accounting information disclosure, the virtuous circle of "promoting capital management with appropriate decentralization," thereby improving the level of

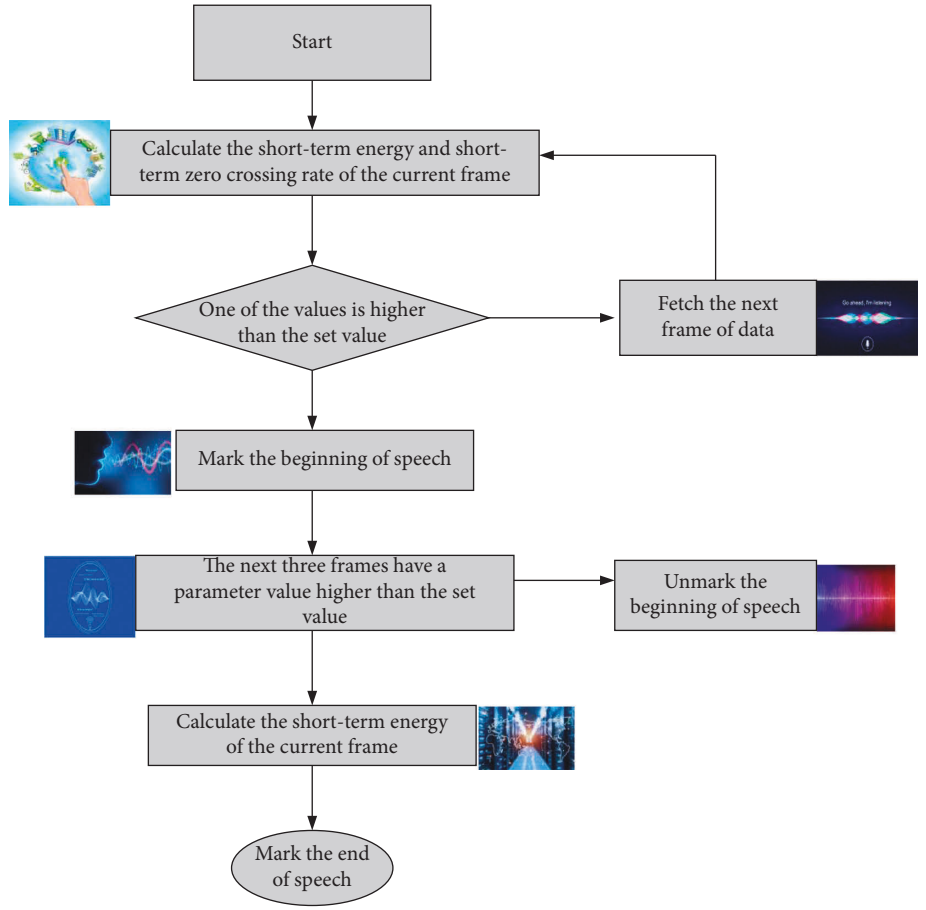

Figure 1: Flow chart of the dual-threshold endpoint detection program.

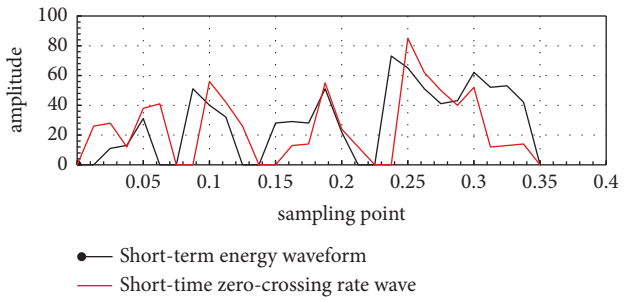

Figure 2: Short-term energy of noisy speech signals.

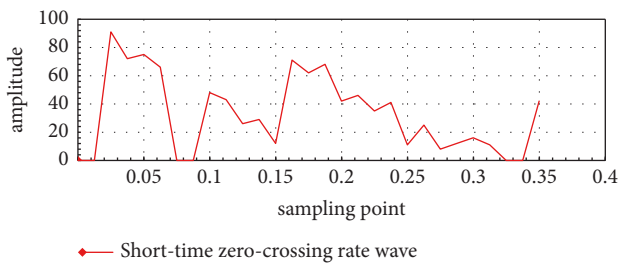

Figure 3: Short-term zero-crossing rate of noisy speech signals.

corporate financial management [20]. Accounting information disclosure means that an enterprise provides important accounting information that directly or indirectly affects the decision-making of users to the information users in the form of public reports fairness between objects. The financial model is to classify, organize, and link various information of the enterprise according to the main line of value creation, so as to complete the functions of analyzing, predicting, and evaluating the financial performance of the enterprise. The following will use empirical analysis to study the interaction between these three and propose the "Capital-Information-Organization" integration model, referred to as the "CIO" model. All in all, through the reorganization of the vertical, horizontal, external, and geographical boundaries of financial management, the purpose of financial management has changed from the traditional management model with strict upper and lower levels, a horizontal division of left and right, and obvious internal and external boundaries to a flat organizational structure, top and bottom. Communication is convenient, departments are integrated with each other, and there is no boundary between internal and external management models.

3.2. Chip Selection. The speech recognition system is built on a certain hardware platform. Nowadays, the types of commonly used speech recognition chips are a special IC for speech recognition composed of a single-chip

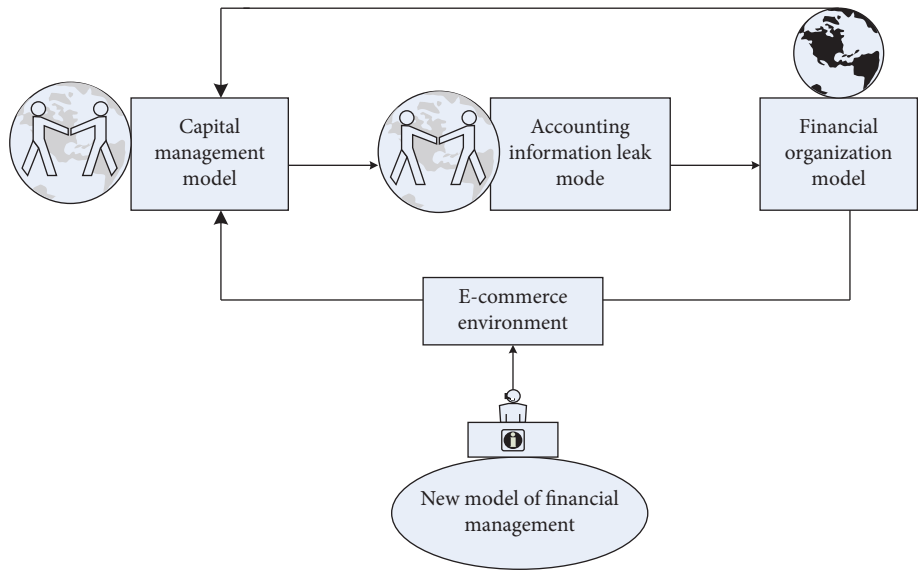

Figure 4: Components of the financial management model.

microcomputer (MCU) [21], a speech recognition system composed of a digital signal processor DSP, and a speech recognition system-level chip SOC (System on Circuit). The SPCE061A chip was selected as the core component of this system because it was determined after the following comparisons of these types of chips.

(1) An application specific integrated circuit composed of multiple band-pass filters and linear adaptive circuits [22]. It is a product in the early 1980s and the first integrated circuit dedicated to speech recognition. It consists of a set of band-pass filters to form a feature extraction circuit and then uses a linear matching circuit for pattern matching. This circuit has poor speech recognition performance.

(2) The on-chip system integrates circuits such as a single-chip microcomputer or DSP [23], A/D, D/A, RAM, ROM, host computer [24], power amplifier, and so on. As long as peripheral circuits such as power supply are added, functions such as speech recognition, speech synthesis, and speech playback can be realized. This is the most advanced speech recognition chip that has emerged in the past two years, with high performance and low power consumption, but the price is relatively high.

(3) SPCE061A is a highly integrated single-chip. It integrates single-chip, A/D, D/A, RAM, and ROM on a chip. It also has 16 bit × 16 bit inner product operation and multiplication functions, and the highest CPU clock can reach 49 MHz. Therefore, it is equivalent to DSP in terms of complex digital signal processing, but the price is lower than dedicated DSP chips and has a strong interrupt handling capability. The system supports 10 interrupt vectors and more than 10 interrupt sources. It is suitable for real-time voice processing. It has a dual-channel 10-bit DAC audio output function and is configured with dynamic white gain. The microphone input method provides great convenience for voice processing. The system hardware circuit is composed of SPCE061A, SPR module, LED keyboard module, and power module. The hardware structure block diagram of the system is shown in Figure 5.

3.2.1. MIC Input Module. Figure 5 shows the entry circuit diagram. As mentioned above, the D D converter of SPCE0611A has eight channels, one of which is the MIC-IN input, which is used to sample specific audio signals. The noise signal is converted to M1C signal and then enters the amplifier in the gain control circuit of SPCE0611A. The options that can be detected, such as the AGC circuit, when the input signal increases at any time. The purpose of the AGC (Automatic Generation Control) automatic gain control circuit is to realize the amplification gain control of the detection object whose signal amplitude changes greatly. For example, in the audio design, in order to ensure that the speaker outputs the sound of the appropriate volume, of course, the volume is independent of the input (Otherwise, it is not necessary to constantly adjust the volume knob). AGC control needs to be added, and AGC can also be used in the image acquisition design to achieve stable image signal detection under strong and weak light conditions. When the input signal is reduced, the AGC circuit will automatically add Hamiltonian to an optimal level, which will help reduce corrective actions. Therefore, the input circuit of the resistance and capacitance system of the DC filter is very simple as shown in Figure 6.

3.2.2. Communication Module. (See Figure 7) shows the communication module circuit. The data in the single-chip microcomputer in the picture is converted to RS-232 level through the serial port through MAX232 level and

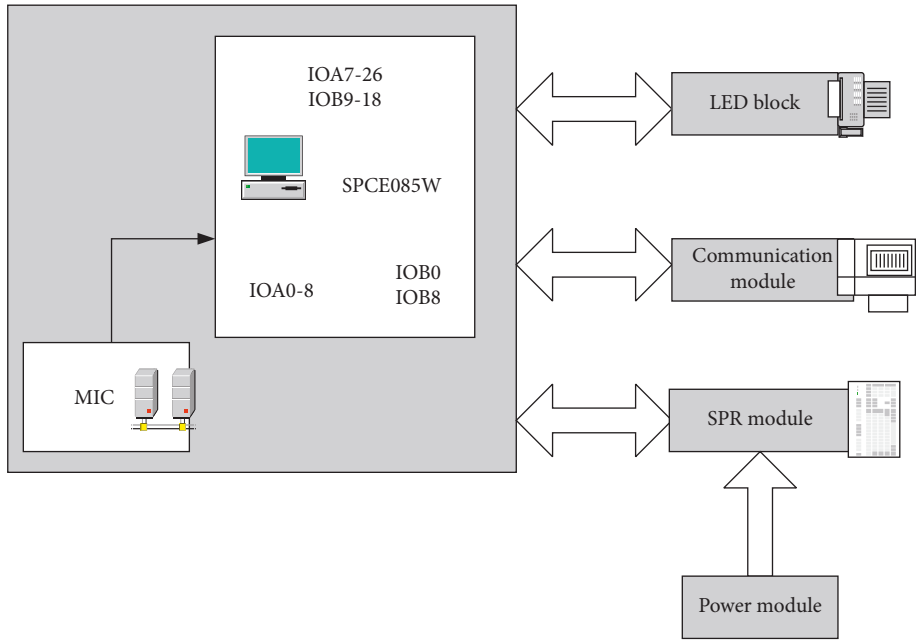

Figure 5: System hardware circuit.

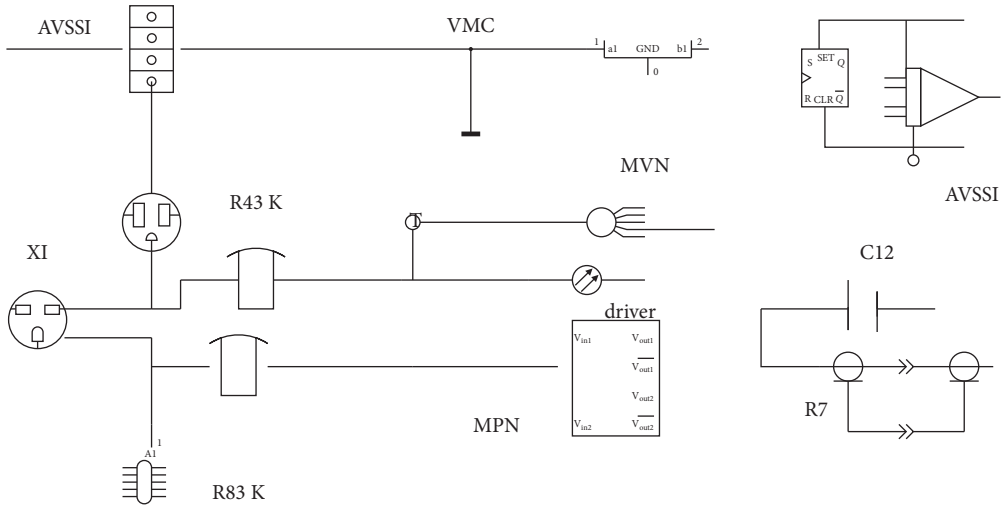

Figure 6: Audio input module.

transmitted to the upper level. The receiving pin RXD and the sending pin TXD of Sunplus SPCE061A MCU serial communication are shared with IOB7 (pin 79) and IOB 10 (pin 76), respectively. The serial interface of SPCE061A is a full-duplex interface with a receiving buffer. The processing of the communication module is optimized with the built-in chip of the system, which can reduce the delay of communication.

The most widely used standard in asynchronous serial communication is the standard RS-232C serial interface used in the circuit. Since SPCE061A serial ports are all TTL levels, they are not compatible with RS-232C levels, so level conversion must be performed on both interfaces. Using the MAX232 chip to connect the external power supply SV and external capacitors, a 10 V power supply can be generated to form a 232C transponder. The communication circuit in this system uploads a large amount of voice data to the computer for processing, which is completed by the computer. For example, calculating noise energy and zero flow, designing digital filters, training model libraries, etc.

3.3. System Implementation

3.3.1. Software and Hardware Environment. The DELL computer used in this system, Core i5 processor, 4G memory, 2.4GHZ frequency, and Philips headset for recording. The computer system is Win7, and the development platform is Matlab.

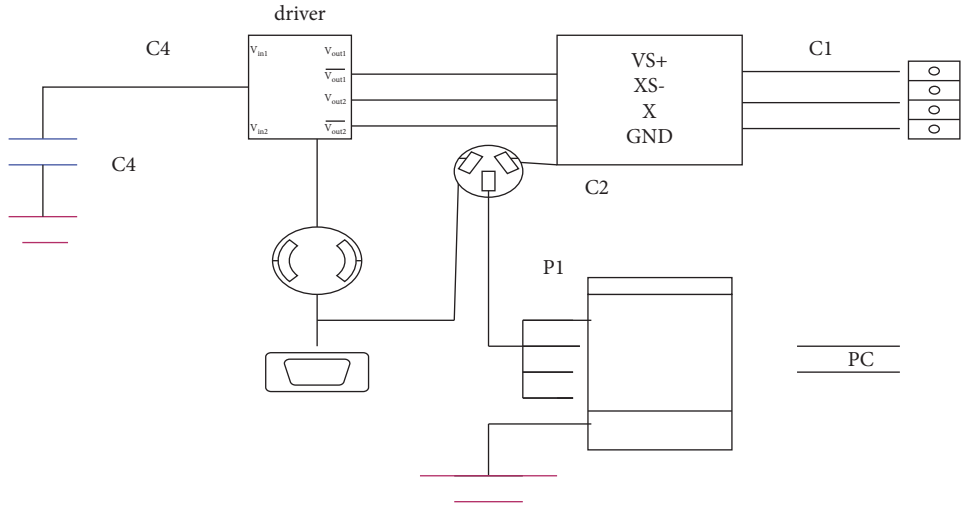

Figure 7: Serial port communication circuit.

3.3.2. The Establishment of the Corpus. Corpus refers to a large-scale electronic text library that has been scientifically sampled and processed, which stores the language materials that have actually appeared in the actual use of the language. There are two types of corpora, one is keyword corpus, and the other is experimental test corpus.

The keyword corpus is a total of 64 commonly used keywords in the three languages of Chinese, English, and Japanese recorded by 6 people as standard as possible. Due to gender differences, each keyword is recorded using 1 male and 1 female; for different regions, pronunciation and dialects are temporarily not included in the corpus due to a large amount of data. In the future, the collected key sounds of various common dialects of speech can be cut and added to the keyword corpus in practical applications.

The experimental test corpus is divided into telephone speech, actual scene recording, and reading-aloud recording. Limited to the environment, the telephone speech and actual scene recording only include Mandarin Chinese, and the reading-aloud speech includes three languages: Chinese, English, and Japanese. The phone voice uses 50 minutes of recording files of ordinary calls; the actual scene recording is the sound recorded by placing a voice recorder in the school laboratory, home, and office for a long time, and each of them intercepts the more concentrated voice for 1 hour. The reading speech includes news speech in 3 languages for 20 minutes each, and the reading material recorded by 3 people is 20 minutes each. Convert all voice data into 8K sampling rate and WAV format, and store them in two folders, respectively. Name the keywords with the content of the keywords, and name the test voices with the recording method and the label.

3.3.3. Acoustic Model. Usually, in speech recognition, the phonemes and syllables of a certain language are commonly used as primitives for acoustic modeling. This will be a big problem for training data because sufficient training data is required to obtain adequate training. Robust model. This article is aimed at different languages and it is difficult to fully train, so each keyword as a whole is used as a primitive. The problem with words as primitive is that the recognition process is limited by the content of the vocabulary, and words that are not in the vocabulary cannot be recognized and will reduce the recognition rate. However, the situation described in this article is that the content of the keywords that need to be recognized is known before the recognition, and the keywords to be recognized have been added to the keyword corpus, so using keywords as primitives best meets the needs. After determining the primitives, extract the average short-term amplitude, peak size, and peak spacing as time-domain feature parameters. 12-dimensional MFCC coefficients, 12-dimensional MFCC coefficients first-order difference, and 12-dimensional MFCC coefficients second-order difference are used as the frequency corresponding to the speech signal. Domain characteristic parameters: After further analysis of 3 groups of 12-dimensional parameters in the frequency domain, 27-dimensional frequency domain characteristic parameters are obtained after weighted reconstruction. Without repeated training, the time domain and frequency domain parameters of a keyword are directly used as its time domain and frequency domain acoustic models, that is, the matching template in the recognition process. After the one-step recognition is completed, it is generally necessary to confirm the keywords through the language model. When choosing a better language model, you can check whether the identified keywords meet the requirements from the perspective of language habits and prosodic features, which can reduce the false alarm rate of the system. However, since this article does not distinguish the language and recognizes the keywords as a whole, it does not establish a language model. Instead, it uses the time domain and frequency-domain joint search method to confirm each other, which can also better reduce the false alarm rate.

3.3.4. Performance Test. For the existing corpus, a 20-minute reading material recorded in the Chinese reading-aloud speech was selected for the recognition test. There are

Table 1: Voice system performance test results.

Key words	Number of false alarms	Number of recognitions	False alarm rate	Missed recognition rate (%)	Recognition rate (%)
Management	3	16	13%	12.5	97.5
Academy	6	36	12.7%	19.6	76.5
The university	5	25	8.6%	11.4	79.6
Education	4	14	43.3% 100%	8	100

4 keywords: management, college, university, and education, which appear 16, 22, 39, and 12 times respectively. The sampling frequency is 8000 Hz, and the frame length is 128. The recognition results obtained are shown in Table 1.

The system also separately shows the time when each keyword appears, and saves the results, so that you can easily query the results.

4. Analysis of Experimental Results

4.1. Selection of the Number of Transformation Matrix Clusters. When generating the transformation matrix of the feature space, how to share training data and choose the number of clusters is a problem that requires comprehensive consideration. The degree of detail in the division of acoustic modeling units and the amount of training data will directly affect the choice of the number of clusters. In the Aurora2 experiment, since there are only 180 emission states and the noisy training data has only 1760 sentences, it is not appropriate to use too many classifications. When modeling the parameter trajectory of the feature space transformation matrix separately, we tried to use 24816 matrix classifications respectively, and the result of the recognition system is shown in Figure 8.

When the GVP-HMM method is used to cascade the transformation matrix and model parameters for modeling, the selection of the number of transformation matrix clusters needs to be reconsidered. At the training end, the transformation matrix parameter trajectory is generated on the polynomial trajectory of the Gaussian model parameters. At this time, the polynomial coefficient model is obtained through various trainings and already contains the information of the noisy speech at the training end; at the decoding end, the transformation matrix also needs to be loaded on the acoustic model. The acoustic model at this time is more consistent with the test background noise. At this time, if too many clusters are used to refine the impact of noise on each modeling unit, it will have a training effect. As can be seen from the figure, in the GVP-HMM cascade system containing variable Gaussian model and feature space transformation matrix, the one that obtains the lowest word error rate is the two-category "GVP-mv-fran" system (WER9 .79%), where the pronunciation words and silence sil and sp are divided into two classification matrices. The same result also appeared in the "GVP-mv-tran" system containing a variable Gaussian model and mean space transformation matrix. The lowest is 0 and the highest is 16.

4.2. Recognition Results of Various Parametric Trajectory Modeling Systems. In the experiment, we used every 1001 sentences of 0 dB, 5 dB, 10 dB, and 20 dB under 4 signal-to-noise ratio conditions to decode the initial pure model, the mcond reference model, and the variable parameter system under the GVP-HMM framework.

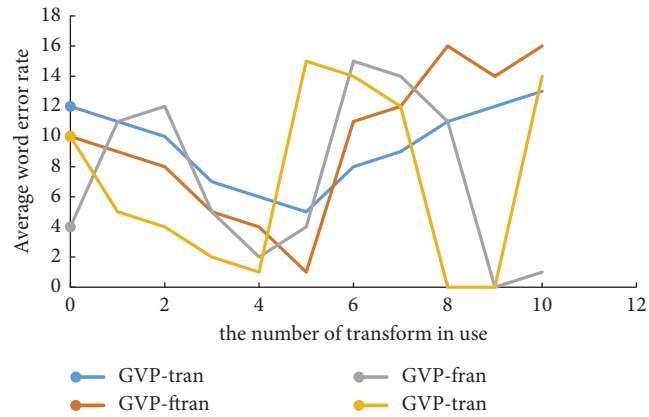

Figure 8: Selection and comparison of the number of transformation matrix clusters.

(1) When using the GVP-HMM method to model the parameter trajectory of the Gaussian model, we chose the mean value and the mean value simultaneous parameter trajectory modeling system as a reference. In the experiment, it is simplified and marked as "mean" and "mv."

(2) When modeling the trajectory of the mean transformation matrix in the model space, we selected 2 and 8 categories of mean transformation matrices "tran2″ and "tran8″, respectively. At the same time, the cascade system "mv-tran2″ with variable Gaussian model parameters is used as the reference system.

(3) When modeling the trajectory of the feature space transformation matrix, we also use "ftran2″ and "ftran8″ to represent the transformation matrix of the corresponding number of categories and use "mv-ftran" to represent the cascade system. The variable parameter modeling types represented by the various systems of GVP-HMM are shown in Table 2.

At the decoding end, the signal-to-noise ratio information corresponding to the test environment is loaded onto the polynomial coefficient trajectory, and corresponding parameters are generated for decoding. The recognition results of the GVP-HMM system based on the above-mentioned traditional methods are given in Table 3.

Table 2: Various types of variable parameter trajectory modeling under the GVP-HMM framework.

GVP	Parameter polynomials				Poly
Syetem	Mean	van	Tran	Fran	Coef
Mean	√	×	√	×	3.66 m
Mb	√	×	√	×	7.88 m
Tran3	×	√	×	√	12.5 m
Tran9	√	√	×	×	15.6 m
Fran3	×	√	√	×	11 m
Fran8	×	×	√	√	18.23 m

Table 3: Recognition results of variable model spatial parameters under traditional GVP-HMM method Aurora 2 experiment.

WER (%)	0 dm	7 dm	15 dm	11 dm	Ave	25 dm
Clean baseline	88.26	24.63	8.5	8.6	14.5	25.63
Mecond baseline	23.56	5.26	7.48	8.69	9.54	4.25
Mean	23.56	9.87	9.56	9.47	9.63	9.87
mv	24.36	8.56	7.45	8.36	4.23	1.23
Tran2	22.86	8.56	7.56	9.36	4.56	15.23
Tran4	11.23	15.23	5.36	5.45	8.69	12.25
Nv-tran12	12.35	11.25	25.65	4.59	75.6	88.56

Table 4: Recognition results of variable parameter feature transformation matrix system Aurora 2 experiment.

WER (%)	0 dm	7 dm	15 dm	11 dm	12 dm	Ave	Fall
Mecond baseline	22.25	33.56	21.56	23.25	15.23	11.23	10.23
Mv	12.56	15.36	23.63	24.56	26.98	25.36	25.36
ftran2	5.23	6.52	9.36	8.24	2.56	6.52	11.23
Ftran8	22.56	33.36	45.56	11.25	5.6	2.3	11.25

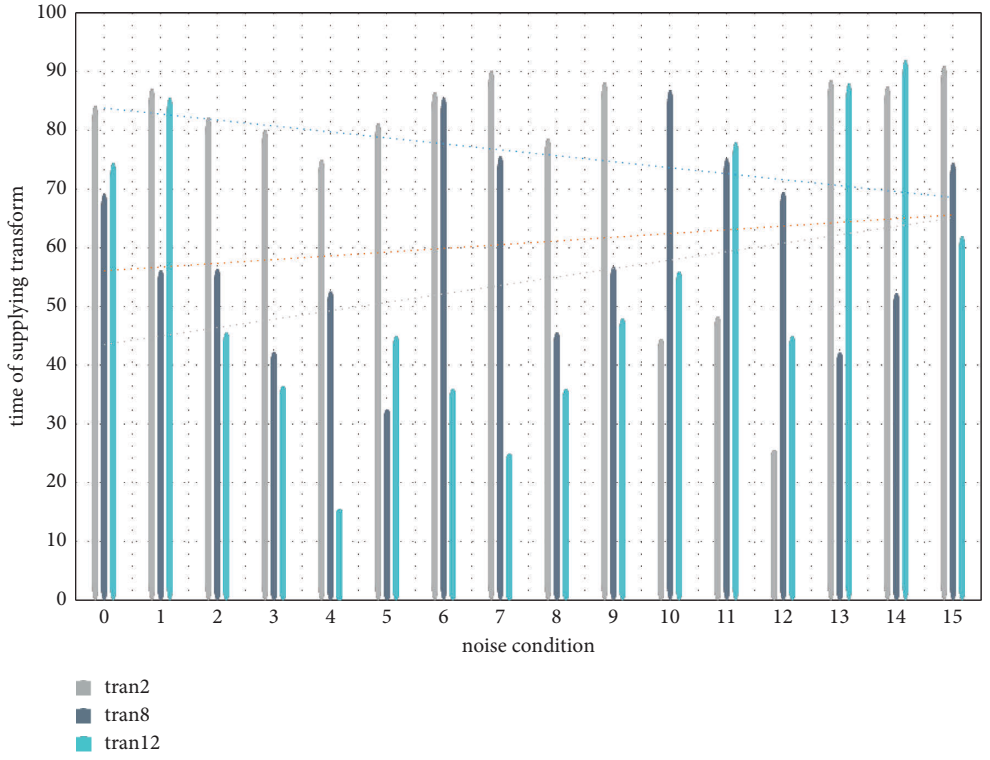

Figure 9: Comparison of loading speed of two types of transformation matrices.

In the third chapter of the main content of this article, the application of the GVP-HMM method extended to feature space antinoise recognition is emphatically discussed. Therefore, in this experiment, the antinoise ability of the variable parameter feature transformation matrix, the variable parameter feature transformation matrix cascade Gaussian model parameter trajectory system, and the variable parameter feature transformation matrix cascade mean transformation matrix are used to verify GVP. The antinoise ability of the HMM system in the characteristic domain. The characteristic equation of the matrix is that the matrix can actually be regarded as a transformation. The left side of the equation is to change the vector x to another position; the right side is to stretch the vector x, and the stretching amount is lambda. Then its meaning is obvious, expressing a characteristic of matrix A that this matrix can lengthen (or shorten) the vector x by lambda times.

4.2.1. Independent Modeling of Variable Parameter Feature Transformation Matrix. On the pure model, we also use a variety of training methods, using four different signal-to-noise ratio training data to generate a transformation matrix trajectory in the form of polynomial coefficients in the feature domain instead of a static transformation matrix. At the decoding end, read in the signal-to-noise ratio information of the test environment to generate the corresponding feature transformation matrix. Compared with the reference system, the recognition results of the variable feature space transformation matrix based on the GVP-HMM method are shown in Table 4.

A series of experiments based on the Aurora 2 data set effectively supports the method of GVP-HMM extended to the feature space in this paper. It is verified through experiments that whether it is using the variable feature space transformation matrix alone, cascading with the variable Gaussian model parameter system, and cascading with the variable model domain transformation matrix, it shows good antinoise performance. At the same time, relying on its unique compact storage space and strong portability, it can become an effective means to solve robust speech recognition in noisy environments. The comparison is shown in Figure 9.

5. Conclusions

In today's era of big data, all departments of an enterprise must make adjustments or even reforms according to the changes in the new environment. Whether an enterprise chooses strategic, lean, or information-based finance, it all reflects multidepartment and multidimensional financial management without exception. The characteristics of the field and multidisciplinary integration. Speech recognition is an important artificial intelligence technology that has played an important role in computer applications, office automation, computer networks, and many other aspects, such as communication, robots, and intelligent human-machine interfaces. Speech recognition technology has advanced by leaps and bounds, and effective recognition technologies such as standard matching and HMM have been formed. Some successful speech recognition systems have emerged. For now, speech recognition technology has gradually moved from the laboratory to commercialization, and for this reason, there have been many large-scale speech recognition products. In daily work and people's lives, what people need most is cheap voice recognition equipment installed on specific products. In the past two years, this small, integrated voice detector has become an important direction for technological development. After a lot of research, this article uses a combination of regulatory analysis and empirical analysis to analyze the current situation of financial management of my country's small and medium-sized enterprises; my country's business from three aspects: financial organization and management, accounting, and capital information disclosure under the new situation of e-commerce, finance. The problems and deficiencies of the management model have established a new model of e-commerce-based financial management for small and medium-sized enterprises-CIO environment interface model and conducted a basic analysis of structural equations and structural equations.

Data Availability

No data were used to support this study.

Conflicts of Interest

There are no potential conflicts of interest in this study.

Acknowledgments

This work was supported by the Social Science Project of Beijing Education Committee (project no. SM202010017002) and National College Student Innovation Entrepreneurship Training Program (project no. 2019J00015).

References

[1] Y. . Gong, "Construction of financial management and decision system based on big data," *PPTA: Quarterly Journal of Indian Pulp and Paper Technical*, vol. 30, no. 8, pp. 135–143, 2018.

[2] D. K. . Dagnew, "Implementation of international financial reporting standards: its practices, challenges and prospects: the case of commercial banks in Ethiopia," *Asia-Pacific Journal of Management Research and Innovation*, vol. 16, no. 4, pp. 259–271, 2020.

[3] J. M. Ruiz-Jiménez, M. d M. Fuentes-Fuentes, and M. Ruiz-Arroyo, "Knowledge combination capability and innovation: the effects of gender diversity on top management teams in technology-based firms," *Journal of Business Ethics*, vol. 135, no. 3, pp. 503–515, 2016.

[4] Z. Wang, M. Ying, Q. Wu, R. Wang, and Y Li, *Gene*, vol. 593, no. 1, pp. 100–109, 2016.

[5] P. E. N. G. Lan, "Teachers' teaching innovation abilities in financial management courses," *Journal of Modern Accounting & Auditing*, vol. 5, no. 1, pp. 20–26, 2017.

[6] W. . Liang, "Research on innovation of financial management mode in high-tech marine engineering enterprises," *Journal of Coastal Research*, vol. 115, no. sp1, p. 99, 2020.
[7] D. Xiaocun, S. Xuan, and Z. Huan, "Innovation of internal control system of financial management in public institutions," *Boletin Tecnico/Technical Bulletin*, vol. 55, no. 17, pp. 263–268, 2017.
[8] R. C. Mayer, R. S. Warr, and J. Zhao, "Do pro-diversity policies improve corporate innovation," *Financial Management*, vol. 47, no. 3, pp. 617–650, 2018.
[9] M. Dziura and T. Rojek, "Management of the company's innovation development: the case for polish enterprises," *Journal of Risk and Financial Management*, vol. 14, no. 4, p. 156, 2021.
[10] Y. Rahmawati, F. G. Dewi, and Y. Yuliansyah, "REGIONAL: regional management information system and training for regional financial accountability," *International Journal for Innovation Education and Research*, vol. 8, no. 11, pp. 213–223, 2020.
[11] M. S. Peiris, N. J. Dewasiri, and Y. Banda, "Book review: I," Edited by M. Pandey, Ed., vol. 16, no. 2, pp. 167-168, Asia-Pacific Journal of Management Research and Innovation, 2020.
[12] S. Sheikh, "The impact of market competition on the relation between CEO power and firm innovation," *Journal of Multinational Financial Management*, vol. 44, no. MAR, pp. 36–50, 2018.
[13] S. Harith and R. H. Samujh, "Small family businesses: innovation, Risk and value," *Journal of Risk and Financial Management*, vol. 13, no. 10, p. 240, 2020.
[14] A. Irjevskis, "Exploring the link of real options theory with dynamic capabilities framework in open innovation-type merger and acquisition deals[J]," *Journal of Risk and Financial Management*, vol. 14, no. 4, p. 168, 2021.
[15] V. P. Shestak, E. I. Moreva, and I. G. Tyutyunnik, "Financial management of innovative activity," *Financial Theory and Practice*, vol. 23, no. 6, pp. 63–75, 2019.
[16] T. Overmans, "Managing slack: how city managers create slack for innovation in times of fiscal stress," *Journal of Public Budgeting*, vol. 30, no. 3, p. 00, 2018.
[17] Mizrahi, K. Sarit, A whole new meaning to having our head in the clouds: voice recognition technology, the transmission of our oral communications to the cloud and the ability of Canadian law to protect us from the dangers it presents," *Canadian Journal of Law and Technology*, vol. 15, no. 1, p. 10, 2017.
[18] D. Poap and M. Wozniak, "Voice recognition by neuro-heuristic method," *Tsinghua Science and Technology*, vol. 24, no. 01, pp. 11–19, 2019.
[19] J. Jiang and H. H. Wang, "Application intelligent search and recommendation system based on speech recognition technology," *International Journal of Speech Technology*, vol. 24, no. 1, pp. 23–30, 2021.
[20] D. Cao and Y. Guo, "Algorithm research of spoken English assessment based on fuzzy measure and speech recognition technology," *International Journal of Biometrics*, vol. 12, no. 1, p. 120, 2020.
[21] D. Purbohadi, S. Afriani, N. Rachmanio, and A Dewi, "Developing medical virtual teaching assistant based on speech recognition technology," *International Journal of Online and Biomedical Engineering (iJOE)*, vol. 17, no. 04, p. 107, 2021.
[22] M. Liu, X. Chen, Y. Mo et al., "Improving English pronunciation via automatic speech recognition technology," *International Journal of Innovation and Learning*, vol. 25, no. 2, p. 126, 2019.
[23] L. Mao and J. Miao, "Comprehensive evaluation and analysis on spoken English based on computer speech recognition technology," vol. 42, no. 2, pp. 778–782, 2017.
[24] Z. Yun, "Research on spoken English speech recognition technology in computer network environment," *Boletin Tecnico/Technical Bulletin*, vol. 55, no. 16, pp. 445–449, 2017.

Hindawi
Scientific Programming
Volume 2022, Article ID 8319692, 15 pages
https://doi.org/10.1155/2022/8319692

Research Article

Classification of Land Cover Remote-Sensing Images Based on Pattern Recognition

Haoyan Xie[1] and Hai Huang[2,3]

[1]*The Philosophy Department, Nanjing University, Nanjing 210023, China*
[2]*School of Marxism Studies, Xuchang University, Xuchang 461000, China*
[3]*Mobile Source Emission Aftertreatment Institute of Tongji University, Tongji University, Shanghai 200082, China*

Correspondence should be addressed to Hai Huang; 12016032@xcu.edu.cn

Received 15 June 2022; Revised 26 July 2022; Accepted 30 July 2022; Published 14 September 2022

Academic Editor: Juan Vicente Capella Hernandez

With the development of remote sensing technology, remote sensing image data plays an active role in the dynamic monitoring of global resource changes and land cover utilization. Remote sensing image land cover classification is an important application direction of remote sensing data; how to further improve the accuracy of remote sensing image land cover classification is very important for the effective application of remote sensing data. The traditional remote sensing image land cover classification is mainly to classify remote sensing data according to the spectral data of ground objects. However, due to the complex environment of remote sensing images and the dynamic changes of the environment, traditional classification methods based only on pixel spectral data are often unable to achieve. A satisfactory classification result is achieved. In addition, some researchers have also proposed to combine pixel neighborhood texture information to supplement spectral feature data. Although the traditional classification method based on spectral features solves the problem of time-consuming visual interpretation, to a certain extent, due to the limited semantic expression ability and poor generalization ability of the design features, the classification accuracy is still not very satisfactory. This paper mainly studies the classification method of land cover remote sensing image based on pattern recognition. This paper is based on the experimental results of remote sensing data in Nanjing Yuhuatai District in 2018 and 2019. The ground resolution of the data is 2.5 meters. Data is projected, corrected, and equalized. Half of the images covering 43.75 square kilometers are used as training samples, and the remaining 50 square kilometers are used for detection. In the classification results of this IndianPines data, OA only increased by nearly 10% to 86.2%, AA increased by 13%, r was 82.77%, and Kappa coefficient was 0.84. In the classification results of Salinas data, both OA and AA increase by about 5%, and the optimization effect is not obvious.

1. Introduction

Since the first artificial satellite entered the earth's orbit in 1957, human beings have started space activities [1]. With the continuous update and development of sensor platform technology, satellite remote sensing has also developed rapidly, resulting in different earth observation satellite remote sensing products. In the 1980s and 1990s, the United States and France used Landsat and SPOT satellites to obtain remote sensing image data with a ground resolution of 10–30 m [2, 3]. The Landsat family of satellites has 2 Thematic Mappers (TM) and 4 MSS systems and Enhanced Thematic Mappers (ETM+) [4]. The SPOT series satellites include SPOT-1 launched on February 22, 1986, SPOT-2 launched in 1990, SPOT-3 launched in 1993, and SPOT-4 launched in 1998. The ground resolution is 10 m–20 m. In May 2012, SPOT-5 satellite with a ground spatial resolution of 2.5 m–5 m was launched on September 9, 2012, and SPOT-6 satellite with a ground spatial resolution of 1.5 m was launched on September 9, 2012. On November 14, 1997, the rest were still operating normally. SPOT can be used for stereo shooting, and its ground resolution is getting higher and higher, and it is more widely used in thematic map production than Landsat [5, 6]. At the same time, various

joint agencies in Japan, India, Canada, China, South Korea, and other countries are running remote sensing systems with spatial and spectral resolution within a certain resolution range [7, 8]. Remote sensing (RS) is a comprehensive detection technology that emerged in the 1960s, including aerospace, automatic control, computer image processing, and other technologies [9]. According to the electromagnetic wave theory, RS uses various platform sensors to detect surface objects that radiate or reflect electromagnetic wave information at a long distance and performs various processing on the detected electromagnetic wave information to synthesize image data to realize object recognition and classification of actual surface objects [10, 11].

In recent years, the field of robotics research has been increasingly attracted by humanoid robots. Robots have basic characteristics such as perception, decision-making, and execution. They can assist or even replace humans in completing dangerous, heavy, and complex work, improve work efficiency and quality, serve human life, and expand or extend the scope of human activities and capabilities [12]. The design, construction, and application of anthropomorphic robots address many interesting research challenges: bipedal walking, human-robot interaction, and interaction with unstructured and unknown environments. Among them, how to design robots with the same performance as humans is a complex problem. The challenge that developers must face when considering design issues is the design of the manipulator and arm. When designing the hand of a humanoid robot, it is designed through functional guidance. A large number of robot designs have extremely high requirements on finger freedom, size, and human-like appearance [13, 14]. To design a human-sized lightweight arm/hand system, either focus on purely mechanical approaches or employ some anthropomorphic and bioinspired designs [15]. Focus on designing a humanoid arm that is reliable, meets requirements, can ensure safe operation, and has a long standby time. The limited size of the manipulator has a certain influence on the arrangement of the joint brakes. The general solution is to use a new drive system or fluid or cable drive. To handle manipulation tasks in a human-centric environment, visual and tactile sensor information is concentrated in a closed-loop control loop. Visual information is mainly used to recognize and understand the pose and shape of objects. The main goal of control architectures for manipulation tasks is to coordinate a range of actions, introducing learning ideas in sensorimotor coordination and taking inspiration from biology. The goal is to develop a robot that assists humans with everyday tasks, humanoid robots, multimodality, and the ability to cooperate and learn with humans. Operationally, it includes the ability to learn and use high-level cognitive models of objects and tasks from demonstrations. The main concept of machine vision is to use the computer to simulate the human visual function, obtain the input image through the camera, then convert it into a digital image signal, input it into the computer, and obtain the corresponding information through software processing, thus providing a basis for correct judgment. The most basic feature of the machine vision system is to improve the flexibility and automation of production. With the support of digital image processing algorithms, three-dimensional objects can be morphologically recognized, and the actions of field devices can be judged according to the recognition results. According to the specific functions, it can be divided into image acquisition, image processing, motion control, etc., to form the information or multidimensional data that needs to be obtained in the image at work and form an artificial intelligence recognition system. This field is applied in [16].

Machine vision, also known as computer vision, is a popular direction for the rapid development of artificial intelligence in recent years. In layman's terms, machine vision is to simulate the function of the human eye, extract useful information from visual imaging, and provide decisions or services for other systems. Machine vision is a comprehensive technology, including mechanical engineering technology, electric light source lighting, optical imaging, sensors, analog and digital video technology, and computer software and hardware technology [17]. The study of machine vision began with image pattern recognition in the 1950s. The concept of machine vision is proposed by the concept of artificial intelligence technology established in the early 1970s. In the 1990s, machine vision made breakthroughs in many fields, and technologies such as face recognition, fingerprint recognition, iris recognition, and optical character recognition became more and more mature. In the 21st century, with the rapid development of machine learning based on statistical models, the realization form of machine vision has also changed, and statistical methods and machine learning methods have become mainstream. In recent years, the most popular machine learning method in the field of artificial intelligence is nothing more than deep learning. Convolutional neural network (CNN) is a branch of deep learning. It is a learning method specially used in the field of vision, which has greatly promoted the development of machine vision technology. It can perform supervised learning and unsupervised learning. Its hidden layer intraconvolution kernel parameter sharing and the sparsity of interlayer connections make it possible to grid features with less computational effort [18]. Machine vision can improve the automation and intelligence of products in this field, which is of great significance for improving social productivity. Although machine vision has become a hot spot in society, very few people really understand machine vision. For our high school students, whether we can keep abreast of the latest developments in technology is related to our career planning. Therefore, this paper discusses the key technologies and application status of machine vision [19].

Romero considers the use of single-layer deep convolutional networks in remote sensing data analysis. Given the high dimensionality of the input data and relatively little available labeled data, direct application to multispectral and hyperspectral images of supervised (shallow or deep) convolutional networks is very challenging. Therefore, we propose to use greedy hierarchical unsupervised pretraining combined with efficient algorithms for unsupervised learning of sparse features. The algorithm is based on sparse representation while enforcing both overall sparsity and

lifetime sparsity of extracted features. They successfully demonstrate the expressive power of the extracted representations in several contexts: aerial scene classification, very high resolution (VHR) land use classification, or land cover classification of multispectral and hyperspectral images. The proposed algorithm significantly outperforms standard principal component analysis (PCA) and its corresponding kernel (kPCA), as well as current state-of-the-art antenna algorithms [20]. Rwang sees remote sensing as a tool that is important for generating land-use and land-cover maps through a process called image classification. For the image classification process to be successful, several factors should be considered, including the availability of high-quality Landsat imagery and auxiliary data, an accurate classification process, and user experience and procedural expertise. The purpose of his research is to classify and map land use/land cover in the study area using remote sensing and Geospatial Information System (GIS) techniques. His research consists of two parts: (1) land use/land cover (LULC) classification and (2) accuracy assessment. In this study, nonparametric rules are used for supervised classification. The main categories of land use and land use change were agriculture (65.0%), water bodies (4.0%), built-up areas (18.3%), mixed forests (5.2%), shrubs (7.0%), and barren/bare land (0.5%). The overall classification accuracy of his study was 81.7% with a Kappa coefficient (K) of 0.722. The Kappa coefficient has a high rank, so classified images are suitable for further study. This study provides an important source of information that planners and policymakers can use to help plan the environment sustainably [21]. Liu believes that, with the improvement of the spatial resolution of remote sensing images, the details, geometric structures, and texture features of ground objects have been better displayed. Since the same object type has different spectra or different object types have the same spectrum, the statistical separability of different land cover categories in the spectral domain is reduced, which is a great challenge to the traditional high spatial resolution remote sensing classification methods based on pixel features. By fusing the texture, structure, and shape features of pixels, the classification accuracy of pixel-based classification methods is improved. However, pixel-based multifeature classification methods usually have the disadvantages of "salt and pepper" effect and computational complexity. Object-based image analysis (OBIA) methods have received extensive attention in recent years. The basic feature of OBIA is that the homogeneous area is the processing unit. The OBIA method can solve the "salt and pepper" problem in traditional methods and overcome the shortcomings of pixel-based classification methods [22].

Pattern recognition is the process of interpreting, summarizing, identifying, classifying, and analyzing various forms of information of objective things or phenomena. Pattern recognition is related to and intersects with computer science, statistics, cybernetics, image processing, artificial intelligence and other disciplines. Therefore, pattern recognition is known as multidisciplinary interdisciplinary. The application of pattern recognition in the field of computer refers to the use of computer to identify and discriminate the target entity represented or imitated by a specific objective entity [23]. Pattern recognition focuses on image processing and computer vision, speech and language information processing, brain network group, and brain-like intelligence. It studies the mechanism of human pattern recognition and effective computing methods. A pattern refers to the spatiotemporal distribution of information obtained by observing a specific objective entity. Isomorphic pattern populations or patterns in the same class are called pattern classes, or classes for short. For example, in the field of remote sensing classification, it is called buildings, roads, shrubs, lawns, etc. [24]. That is, the principle of "pattern recognition" is to assign the pattern to be recognized to the pattern class to which it belongs according to a certain measurement method, measurement basis, or measurement index. With the rapid development of sensor technology, computer application technology, automatic control technology, and communication technology, pattern recognition is also widely used in remote sensing image processing [25]. A pattern recognition system refers to a computer system that performs pattern recognition. Research designers design different pattern recognition systems according to their needs and then perform pattern recognition and classification by computer. A complete pattern recognition system goes through five steps: sample information collection, information preprocessing, selection and extraction of useful features, design, and classification of classification decision functions. Every step is very important. The processing degree of the previous step directly affects the performance of the next step. For example, pattern samples may contain a lot of noise and interference information. If the original pattern samples are not preprocessed, this interference information will occupy the feature space and increase the feature dimension. Therefore, the noise interference data is filtered to reduce the feature dimension, while the original pattern sample information is converted into an information format that can be processed by the computer, and then feature selection is performed on the sample information [26]. Because some features do not contribute much to the recognition category, they can be removed, select some useful feature information for the recognition category, learn the recognition model from the favorable feature inference, and finally classify the sample type decision to obtain the recognition classification result [27].

According to the recognition principle, pattern recognition can be divided into the following four recognition modes: pattern recognition based on structure, pattern recognition based on statistics, pattern recognition based on neural network, and fuzzy pattern recognition [28]. Among them, the statistical-based pattern recognition based on the Bayesian decision system based on the principle of statistical probability theory is the most classic recognition mode, which is widely used in the recognition and classification of surface objects in remote sensing images. Bayesian decision-making is based on incomplete intelligence. The subjective probability is used to estimate the partially unknown state, then the Bayesian formula is used to correct the occurrence probability, and finally the optimal decision is made by using the expected value and the modified probability. Statistics-

based pattern recognition methods often use a tree-structured pattern of a hierarchical structure of classes and subclasses to complete pattern recognition. The principle of hierarchical recognition is the principle of hierarchical segmentation and classification, so it has always played an important role in image classification or segmentation [29]. The general principle of classical statistics-based pattern recognition is to decompose a pattern into a data analysis process of several pattern categories, including cluster analysis, unsupervised and supervised learning, parameterized and unparameterized probability density statistics (ParametricorNonparametricProbabilityDensityEstimation), preprocessing., feature selection or extraction (FeatureSelectionorExtraction), postprocessing after recognition classification, classification accuracy evaluation, and performance analysis. Since the 1960s, statistical-based pattern recognition research has developed rapidly. His main research interests are computer interpretation of remote sensing images based on statistical pattern recognition. Remote sensing images processed by computer must be digital images, and analog images obtained by photography must be converted by image scanners. It is characterized by distinguishing different positions in an image based on the spectral statistical properties of a single pixel [30]. The main research achievements include research results after transforming pattern recognition problems into probability density statistics problems, such as Bayesian decision-making, nearest neighbor decision-making, parameter-free pattern recognition research results based on Parzen probability density statistics, and leave-one-out error estimation; for feature evaluation, distance-based metrics and error-boundary-based estimation methods have also been proposed [31]. There are also Fisher discriminants; supervised parameter estimation in classification techniques, unsupervised learning based on decomposition and mixture probability densities, and some ensemble models of classification processors have also been proposed. Neural networks and SVM algorithms are also closely related to the principles of statistical pattern recognition, and their applications are also very extensive. With the increasing abundance of satellite remote sensing image data in various countries, many similar research results based on pixel or regional statistical pattern recognition methods have played a huge role in the processing and classification of remote sensing image data [32].

Problems existing in remote sensing classification based on geographic coverage changes: from the traditional single classifier model to the multiclassifier combination model, the traditional remote sensing image classification method gradually develops towards the object-based and object-oriented classification model and promotes the development of multiclassification model. The fusion of source data enables the effective fusion of RS and GIS and has achieved a lot of research results. However, there are still problems in the following aspects that need further research.

(1) Unification of characteristic factors: the application of traditional remote sensing classification methods, especially in the classification of low- and medium-resolution remote sensing images, is based on the brightness difference between pixels. However, due to the influence of factors such as illumination and terrain, the reflected or radiated electromagnetic wave information of some pixels in the image is not clear enough, resulting in pixel confusion, "homogeneity and heterogeneity" or "heterogeneous objects with the same spectrum" and other phenomena, and there must be a large number of errors. Pixels in the classification result of missing images carry this phenomenon, which affects the classification accuracy. Same-spectrum and same-spectrum foreign objects are based on the phenomenon that the same type of ground objects has different spectral characteristics on remote sensing images or the phenomenon that different ground object types have similar spectral characteristics.

(2) The unity of the classification algorithm: due to the different classification decision principles of different classification algorithms, there is no overlap between different classification algorithms in the classification and classification accuracy sets of different surface objects. Therefore, a single classifier decision function is not enough for complex classification problems, and multiple decision functions are needed to judge together. Therefore, it is most realistic to combine multiple classifiers to achieve complex classification according to certain rules. Classifier is a general term for the methods of classifying samples in data mining, including algorithms such as decision tree, logistic regression, naive Bayes, and neural network. On the basis of giving full play to the advantages of a single classifier, it is particularly important to study and design new classification techniques and new classification models and to enrich the knowledge system of remote sensing classification based on the needs of actual classification problems.

(3) The influence of noise: the appearance of noisy information in remote sensing imagery seems to be an inevitable reality, mainly depending on the degree of processing. The degree of processing directly affects the accuracy of image classification. Therefore, noise information is filtered according to the general law of noise information distribution (generally, high-resolution images are distributed inside the surface, and low- and medium-resolution images are distributed at the edge of the surface). Screening useful data is an important basic work before image classification.

(4) Lack of texture feature extraction: texture refers to a small, semiperiodic, or regularly arranged pattern that exists within a certain range in an image. Texture features are the basis for labeling and extracting object classification features on image surfaces. Texture features are usually represented by geometric patterns, sizes, or shapes. However, the traditional extraction method using $(2n+1)\times(2n+1)$ template is not conducive to the extraction of large-

scale texture gray value. To effectively extract the gray value of image texture or provide benefits for image segmentation or classification and classification reference, further research is required.

(5) The influence of scale selection: scale selection is an important part of the field of remote sensing research. Therefore, in-depth research on scale selection, scale conversion, and scale effects is required in practical applications.

Furthermore, most experimental data for innovative research results in image classification or segmentation are basically based on the use of existing commercial software. With the emergence of high-altitude, hyperspectral, and high-temporal remote sensing image data, the feature information contained in remote sensing images will become more abundant or more complex. Will the data processing performance of existing commercial software be affected? It is necessary to design and develop new taxonomic theories and application software as a powerful complement to existing methods or techniques.

The innovation of this research paper is mainly reflected in the following aspects:

(1) Two optimization and improvement methods of SVM kernel function are proposed. Taking advantage of the inherent characteristics of remote sensing image data, a useful exploration is made on the selection of the support vector machine kernel function and optimal parameters. Two methods of optimizing kernel function are proposed to study the optimization and improvement of SVM kernel function objectively. The method of optimizing the kernel function first realizes the complementary effect of the original kernel function. Secondly, the sample measurement function can consider the characteristics of the brightness difference and the angle difference of the sample at the same time, which effectively overcomes the shortcomings of the traditional kernel function that is extremely sensitive to noise and abnormal data.

(2) Two sample ranging standards and multiclassifier combination techniques are proposed. Based on the research on the traditional remote sensing image classification algorithm, this paper makes a useful exploration on the optimization and improvement of the classification rules of the classification algorithm. Classification algorithms discover class rules and predict classes for new data by computing and analyzing training sets of known classes. Taking the successful application of multiclassifier combination technology in remote sensing image classification as a research clue, two sample distance measurement standards based on mixed discriminant rules are proposed, and the remote sensing image classification task is realized through multiclassifier combination. (classifier technology). The research results not only make full use of the inherent spectral features and spatial geometric feature information of remote sensing image samples, but also effectively overcome the shortcomings of traditional remote sensing image classification algorithms with single discrimination rules and use multiple classifiers. The combination technology effectively solves the problem of data misclassification and omission and improves the classification accuracy.

(3) An automatic segmentation method of remote sensing image pixels based on the combination of FCM and SVM is proposed, and object-oriented remote sensing image classification is realized on this basis. Image segmentation is the technology and process of dividing an image into several specific regions with unique properties and proposing interesting targets. It is a key step from image processing to image analysis. The implementation principle of the segmentation algorithm proposed in this paper is simple, and it effectively solves the shortcomings of the traditional segmentation algorithm that is too harsh. The SVM supervised classification algorithm is used to segment the objects obtained by the FCM algorithm, and the object-oriented remote sensing image classification task is realized, which effectively solves the "salt and pepper" phenomenon that often occurs when performing classification tasks. Traditional remote sensing image classification algorithms improve the classification accuracy of remote sensing images.

2. Suggested Method

2.1. Remote Sensing Image Classification Methods

2.1.1. Maximum Likelihood Classification. Maximum likelihood classification (MLC) is one of the most widely used supervised classification methods. It assumes that various distribution functions are normal distribution, selects training areas, calculates the attribution probability of each sample area to be classified, and performs classification (an image classification method). Its discriminant rule is based on probability. Maximum likelihood assumes that all types of training data for each band are normally distributed and classifies pixels with a pattern metric or feature X into the ith class that may have feature vector X. In other words, it calculates the probability that it belongs to a certain class pixel by pixel and divides the pixel into the class with the highest probability. To obtain probabilistic information on the training data, the probability density function is first calculated. For single-band data, a certain type of probability density function looks like this:

$$\hat{p}(x \mid \omega_i) = \frac{1}{(2\pi)^{1/2}\hat{\sigma}_i} \exp\left[-\frac{1}{2}\frac{\left(x-\hat{\mu}_i\right)^2}{\hat{\sigma}_i^{\,2}}\right]. \tag{1}$$

In the formula, x is the brightness value of the pixel, is the estimated mean value $\hat{\mu}_i$ of all training classes $\hat{\sigma}_i^{\,2}$, and is the estimated variance of the class with observed values.

The Landsat7ETM+ data is multiband remote sensing data; that is, the training data consists of multiband data. The n-dimensional multivariate normal density function can be calculated using the following formula:

$$\hat{p}(X \mid \omega_i) = \frac{1}{(2\pi)^{1/2}\hat{\sigma}_i} \exp\left[-\frac{1}{2}(X - M_i)^T V_i^{-1}(X - M_i)\right], \quad (2)$$

where $|v_i|$ is the determinant of the covariance matrix and is the v_i^{-1} inverse of the covariance matrix and M_i is the mean vector.

When classifying the unknown measure pixels of the multispectral data, the maximum likelihood method is used to calculate $\hat{p}(X|\omega_i) \cdot p(\omega_i)$ is the product of each class, and it is divided into the class with the largest product.

$$\hat{p}(X|\omega_i) \cdot p(\omega_i) \geq \hat{p}(X|\omega_j) \cdot p(\omega_j). \quad (3)$$

In fact, the maximum likelihood classification is mostly applied under the assumption that the probability of occurrence of each class is equal, that is, the maximum likelihood classification without prior knowledge; formula (3) omits the prior knowledge item and is simplified to

$$p_i \geq p_j, \quad (4)$$

and

$$p_i = -\frac{1}{2}\log_e|V_i| - \left[\frac{1}{2}(X - M_i)^T V_i^{-1}(X - M_i)\right], \quad (5)$$

where M_i is the ith average measurement vector category. V_i is the covariance matrix of the ith, kth to l bands.

In most remote sensing applications, certain classes have a higher probability of occurrence than others. At this point, we can weight each class with the appropriate prior knowledge probability $p(\omega_i)$. At this point, formula (4) becomes

$$p_i \cdot p(\omega_i) \geq p_j \cdot p(\omega_j), \quad (6)$$

and

$$p_i \cdot p(\omega_i) = \log_e p(\omega_i) - \frac{1}{2}\log_e|V_i| - \left[\frac{1}{2}(X - M_i)^T V_i^{-1}(X - M_i)\right]. \quad (7)$$

Equation (6) is called the Bayesian discriminant rule, which applies the prior knowledge probability to the obtained terrain features and terrain to improve the accuracy of remote sensing classification.

2.1.2. Support Vector Machine Classification. Support vector machines (SVM) were proposed by Vapnik. SVM is a class of generalized linear classifiers that perform binary classification on data in a supervised learning manner, and its decision boundary is the maximum margin hyperplane that solves the learning samples. It takes the minimization of the confidence interval value as the optimization objective and the training error as the constraint condition of the optimization problem; that is, SVM is a statistical method based on the structural risk minimization criterion. Its generalization ability is better than some traditional statistical methods. Since the advent of the classic SVM in the early 1990s, it has received extensive attention in the field of machine learning due to its complete theoretical framework and many good results in practical applications.

2.1.3. Nonlinear Separability and Kernel Function. Nonlinear separability was proposed by Boser et al. In 1992, the kernel function was applied to the optimal hyperplane to construct nonlinear classifiers. The kernel function is used to replace the dot product inner product, and the sample space is transformed into a high-dimensional or infinite-dimensional feature space (Hilbert space) with a nonlinear mapping φ to construct the optimal hyperplane.

Kernel function reference solves the linear inseparability problem in classification, and its quality directly affects the performance of support vector machine, so kernel function has become one of the core problems of support vector machine research. The research of kernel function mainly focuses on its model selection and kernel function construction. The commonly used kernel functions are

(1) Polynomial inner product function:

Homogeneous:

$$k(X_i, X_j) = (X_i \cdot X_j)^d. \quad (8)$$

Heterogeneous:

$$k(X_i, X_j) = (X_i \cdot X_j + 1)^d. \quad (9)$$

The result is a d-order polynomial classifier.

(2) Gaussian radial basis function (RBF):

$$k(X_i, X_j) = \exp(-\gamma \| X_i - X_j^2 \|)\gamma > 0. \quad (10)$$

Each cardinality center corresponds to a support vector, and the algorithm automatically determines the output weight.

Hyperbolic tangent function as inner product function:

$$k(X_i, X_j) = \tanh(kX_i \cdot X_j + c). \quad (11)$$

At this point, the SVM implements a multilayer sensor with hidden layers. The hidden layer nodes are automatically determined by the algorithm, which has no local minima.

Among them, γ, d, k, and c (relaxation limit parameters) are the parameters of the kernel function. At present, there is no certain theoretical guidance for the selection of the kernel function, and it is mainly based on experience. Considering whether the choice of the kernel function reasonably affects the generalization ability of the support vector machine, a Gaussian kernel with a single parameter γ is usually chosen. The optimal combination of c and γ is obtained by grid searching the exponentially increasing sequence of c and γ, cross-validating each parameter combination, and then selecting the combination with the highest accuracy. The final model is trained on the training data using these parameter combinations.

2.1.4. Decision Tree Classification. Decision tree learning is a very common method in data mining. Its purpose is to predict the value of the target variable from the value of the input variable. The more mature decision tree algorithms include ID3 algorithm, C4.5 algorithm, C5.0 algorithm, and CART (Classification and Regression Tree) algorithm. The construction of the decision tree is done through top-down recursive divide and conquer. In decision analysis, a decision tree can express the decision-making process explicitly. In data mining, a decision tree expresses data rather than decisions. The ID3 algorithm is an iterative divisor proposed by J. Ross Quinlan in 1986. It calculates the test sample information gain, selects the attribute with the largest information gain as a node to build a decision tree, but cannot handle continuous attributes, and the decision tree is overfitting to the data. The C4.5 algorithm is an improvement to the ID3 algorithm, which overcomes the disadvantage that the ID3 algorithm cannot handle continuous variables. The C5.0 algorithm adds the boost function on the basis of the C4.5 algorithm, which improves the speed and memory utilization. CART was proposed in 1984 by several statisticians. It can handle both highly skewed or polymorphic numerical data, as well as sequential or unordered generic data. This article describes the CART, C4.5, and C5.0 algorithms. This study mainly uses the C5.0 algorithm to construct decision trees.

2.2. Remote Sensing E Estimation Method for Land Development and Integration

2.2.1. Remote Sensing Evaluation of Soil Surface Temperature. Surface temperature was calculated using TM6 data from Landsat. Landsat TM remote sensing image data has been widely used due to its high ground resolution. This data (TM6) thermal band can be used to analyze regional differences in thermal radiation and temperature on the Earth's surface. The wavelength range of this band is 10.45–12.5 μm, and the pixel ground resolution under the zenith viewing angle is 120 m × 120 m. This ground resolution is much higher than the ground resolution of the NOAAZAvHRR remote sensing data (1.1 km × 1.1 km from the zenith view). Therefore, TM data is a better choice for accurate surface temperature analysis. However, compared to its wide application in the visible and near-infrared bands, thermal (TM6) data of TM images are rarely used, and most applications use its grayscale value directly or just convert it to pixel b brightness without calculating actual surface temperature. Since the surface thermal radiation is affected by the atmosphere and the radiation surface during the conduction process, the thermal radiation intensity (which has been converted into the corresponding gray value) observed by the TM remote sensor is no longer a simple surface intensity, which is heat radiation. Therefore, the thermal radiation and temperature changes of the surface cannot be expressed intuitively, and the conclusions drawn from the regional analysis directly using the original TM6 value (gray value or brightness temperature) have a large deviation. The magnitude of the bias is directly dependent on the strength of atmospheric and surface influences. Traditionally, so-called atmospheric correction methods are used. Calculate surface temperature from TM6 data, which requires the use of atmospheric models such as LowTRAN or MoDTRAN or simulating the effect of the atmosphere on surface thermal radiation, including estimating the absorption of thermal radiation by the atmosphere and the intensity of thermal radiation up and down and then remotely sensed from satellites. This part of the atmospheric influence is subtracted from the total amount of thermal radiation observed by the monitor (calculated as gray value) to obtain the surface thermal radiation intensity, which is finally converted to convert the thermal radiation intensity into the corresponding surface temperature. Although this method still exists, some problems, such as real-time atmospheric profile data, are relatively complex and accurate, but they can be basically avoided through further research and improvement, such as derivation of the law of heat conduction. In 2019, Hurtado et al. proposed a new atmospheric correction method based on the surface energy balance equation and standard climate parameters is, and the surface temperature is calculated using TM data. This method is very close to the method of calculating surface temperature.

2.2.2. Remote Sensing Evaluation of Soil Organic Matter Content. It has also been pointed out that soil organic matter is an important part of soil and plays a very important role in soil fertility. The organic matter content of different soil types varies greatly, the higher one can reach more than 200 g/kg, and the lower one can reach below 5 g/kg. Therefore, detecting soil organic matter content is an important way to understand soil fertility. Dalal and Henry used near-infrared spectroscopy to predict moisture, organic carbon, and total nitrogen in Australian soils. Their predicted soil organic matter content ranged from 0% to 2.6%, with a 1 74–1 75% bias in the near-infrared predictions when organic matter content was higher or lower. The near-infrared spectroscopy prediction results of the two groups of soil samples with organic matter content of 0%–4% and 4%–4% were inconsistent. For 14%, there is a significant deviation. It is believed that soil can be understood by analyzing the C+ ratio of soil organic matter. The decomposition stage of organic matter improves the accuracy of NIR spectroscopy in predicting soil organic matter. The vF991 ground object spectrometer was used to measure the spectrum of each upper layer on the soil sample profiles formed under 8 different environmental conditions, and the reflection spectrum curve of each upper layer was obtained, and the organic matter content of each upper layer was determined. By studying the relationship between soil organic matter content and soil reflection spectrum Correlation analysis showed that the correlation coefficients between the organic matter content released in the 376.795 nm band, the 616.506 nm band, and the 724.0975 nm band and the soil spectrum were −0.63, −0.64, and −0.645, respectively. Peng Yukui et al. used near-infrared spectroscopy to evaluate soil organic matter content in the loess region of China. The calibration correlation result for 52 samples was 0.938 with a

standard deviation of 0.23. The correlation result of the 74 samples was an organic correlation coefficient of 0.921 with an estimated standard error of 0.28, which was close to the chemical analysis of laboratory soil organic matter.

2.3. Supervised C-Classification. Supervised classification, also known as training classification, is to determine the attribute categories of pixels in other regions based on the pixel attribute characteristics of training regions of known categories. Pixel classification of training regions is generally performed through visual interpretation.

In supervised classification, firstly, the training samples of various features are extracted in the training area, and the learning algorithm is trained with these samples to determine the discriminant function, and then the discriminant function is used to classify the image. If the discriminant criterion meets the classification accuracy requirements, this criterion is established; otherwise, the classification decision rules need to be reestablished until the classification accuracy requirements are met.

The key issue in land object classification is the choice of classifier, which is usually determined by comprehensive factors such as the complexity of the target category and the accuracy requirements. The currently used classifiers are based on traditional statistical analysis, neural networks, and pattern recognition. The commonly used parallelepiped method, minimum distance method, Mahalanobis distance method, and maximum likelihood method are methods based on traditional statistical analysis; support vector machines and fuzzy classification are methods based on pattern recognition. In addition, there are spectral angle method (SAM), spectral information divergence, and binary encoding for hyperspectral data. The supervised classification process of remote sensing images is shown in Figure 1.

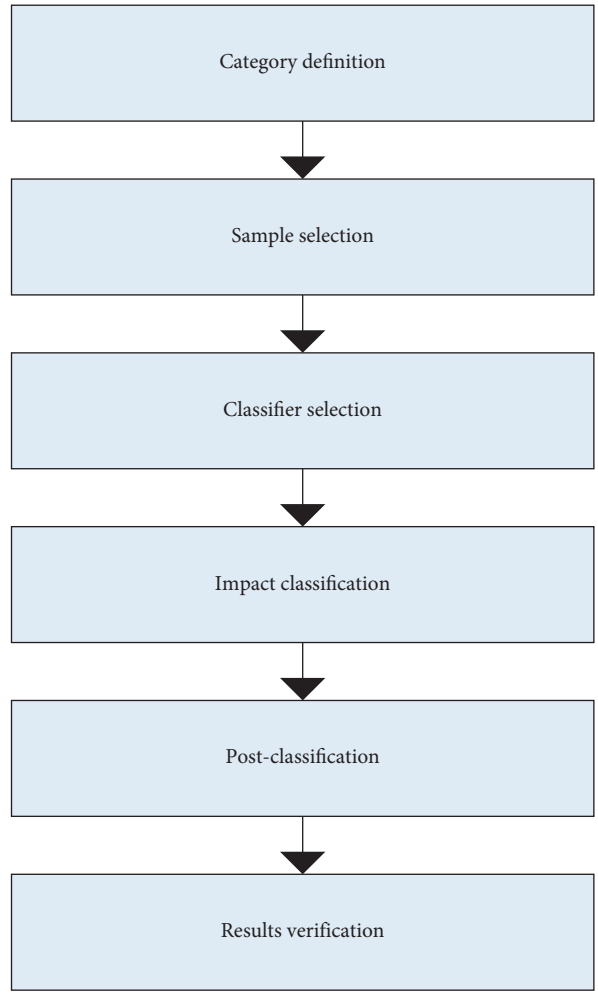

Figure 1: Supervised classification process of remote sensing imagery.

2.4. Unsupervised C Classification. Unsupervised classification, also known as cluster analysis, is characterized by the fact that it does not require training and only uses a specific clustering algorithm to classify features based on their spectral characteristics. The spectral characteristics of the pixels of the same category in the classification results conform to the same rules, but cannot directly reflect the types of ground objects they represent. The spatial distribution of each sample is divided or merged into a cluster according to its similarity, and the types of ground objects represented by each cluster can only be determined by field investigation or comparison with known types of ground objects. Therefore, a visual interpretation of the classification results is required to determine the category of the feature. In the process, categories are often combined. Due to the huge amount of spectral feature data contained in remote sensing image pixels, the supervised classification process requires multiple iterations, and the research on unsupervised classification algorithms pays great attention to the efficiency of algorithm operations.

(1) The *K*-means method randomly finds the similar position of the cluster, that is, the central position. When the maximum number of iterations is reached, the central position is used to iterate to complete the classification. The general process of unsupervised classification of remote sensing images is shown in Figure 2.

The *K*-means classification method is a continuous algorithm, which gradually moves each cluster center through an iterative method to achieve the best clustering effect. The algorithm principle is also very simple. The flow chart of *K*-means algorithm is shown in Figure 3.

(2) Self-organizing iterative data analysis method:

ISODATA is an improvement based on the *K*-means algorithm, which allows the adjustment and change of the number of classes and classification results based on the *K*-means algorithm, mainly based on the specified parameters (thresholds) to check the clustering situation of the previous cycle. Therefore, decide to redecompose, merge, or cancel some cluster decomposition: (1) The parameter "maximum standard deviation" can be set. When the standard deviation of a band in a class exceeds this

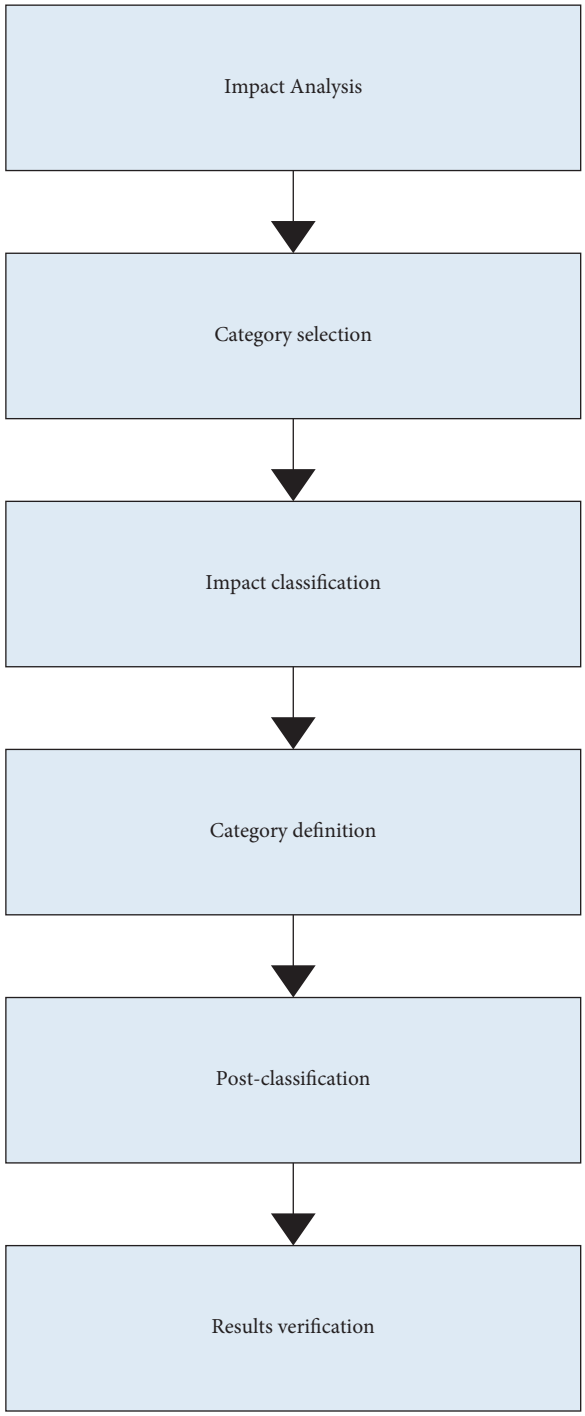

Figure 2: Remote sensing image supervised classification process.

threshold, it is decomposed into two classes. (2) Merge: you can set the "minimum distance between classes" parameter. When the distance between two classes is less than this minimum distance, they are merged. (3) Cancel: when the number of pixels in a class is too small and less than the parameter "minimum number of pixels in a class," the class is cancelled and the pixels in it are reassigned to adjacent clusters. The algorithm flow chart is shown in Figure 4.

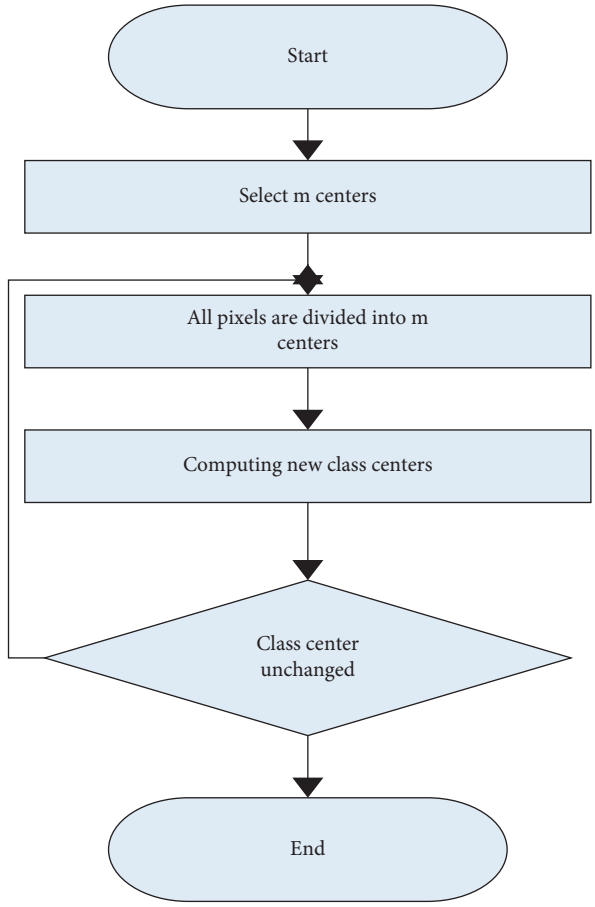

Figure 3: Flow chart of K-means algorithm.

3. Experiment

3.1. Subject. The remote sensing data of Yuhuatai District in 2018 and 2019 used the QT-DMTF change detection method, and the ground resolution of the data was 2.5 meters. Data is projected, corrected, and equalized. Half of the images covering 43.75 square kilometers are used as training samples, and the remaining 50 square kilometers are used for detection. Artificially drawn ground-truth images, including open spaces, buildings, roads, rivers, and ponds, change from open space to buildings and from buildings to open spaces.

3.2. Experimental Design

3.2.1. Data Preparation. Remote sensing data: ground satellite data +1, 2 + 13 have high spatial, spectral, and temporal resolution. For land use, land cover is an economical and practical data source. Associated graphs, data, and text reports mainly include detailed land survey, land change survey map, basic farmland planning map and data; other thematic maps, such as soil map, vegetation map, land type map, grass resource distribution map; land resource evaluation map and other related pictures, etc., in addition to geometric correction of remote sensing images, vectorization of related data, and unification of coordinates.

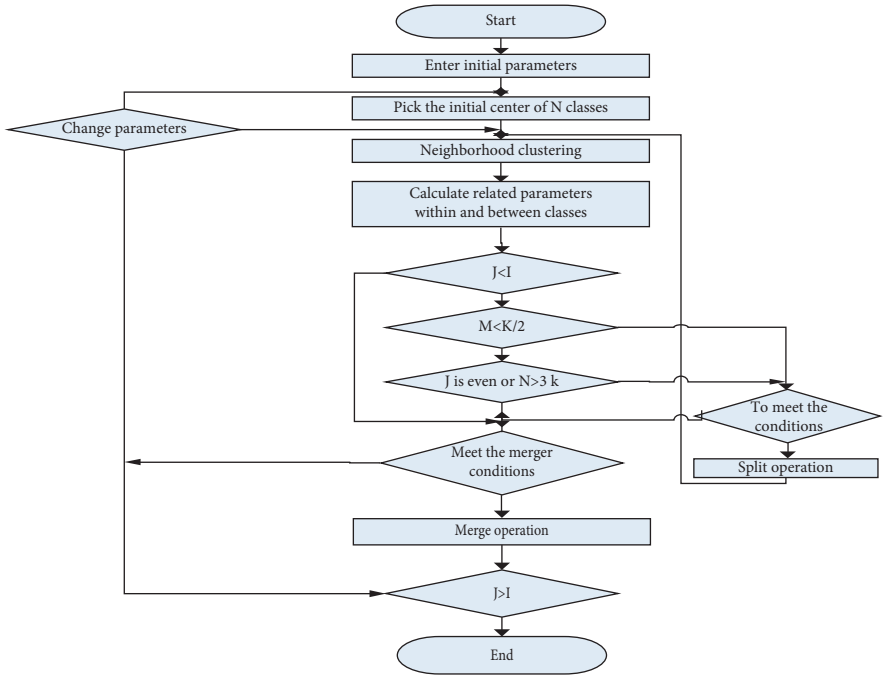

Figure 4: Flow chart of ISODATA algorithm.

3.2.2. Enhance Remote Sensing Information. The enhancement of remote sensing information mainly includes contrast enhancement, including linear expansion, nonlinear expansion, histogram adjustment, color enhancement, *p* pseudocolor enhancement for single-band images, and color synthesis for multiband images (select bands or components using 456 values). Multidimensional orthogonal linear transformation is based on image statistical features: KL transformation (principal component analysis), KL transformation ("hat transformation").

3.2.3. Extraction of Change Information. The methods of extracting the change information of remote sensing images can be divided into two categories in essence: one is based on the spectral value change of a single pixel; the other is based on the spectral value change of a single pixel. The other is classification based on input data. Classification change monitoring is based on first-level classification: firstly, remote sensing classification is performed on the images before and after the time period, and then the images are compared, and the classification results are compared to find out the changes of monitoring indicators. First, they are then subtracted to get the difference image, the change area is determined, then the change area in the difference image is classified, and finally the type of change is determined. Classification change monitoring is based on principal component transformation: fuse the before and after images, and then perform principal component transformation. In general, the first few principal components account for 95% of the variance. The geological significance of these principal components is analyzed, represented by brightness and greenness, to determine the type and scale of land use and land cover changes; classification changes monitoring results are extracted based on remote sensing thematic information.

3.3. Experiment Implementation. This section uses two algorithms, ELM and Ensemble-ELM, to perform classification experiments on IndianPines, PaviaU, and Salinas hyperspectral data. The experimental results of the three datasets are analyzed and evaluated in detail below.

From the analysis of IndianPines classification accuracy, compared with the ELM algorithm, the Ensemble-ELM algorithm proposed in this section improves the classification accuracy by about 10%. The two methods have higher classification accuracy for the 5th, 6th, 8th, and 14th ground features, but lower classification accuracy for the 3rd, 4th, 9th, and 12th ground features. This is because grasslands, pastures, trees, timber, etc. are all homogeneous areas and are easy to label, while categories such as corn and soybeans are also divided into specific subcategories, which are prone to misclassification, and there are too few labeled samples in category 9. The characteristics of the ninth category of features cannot be well characterized, which should be one of the reasons for the poor classification results of this category. But in general, the Ensemble-ELM algorithm improves the classification accuracy of each category, which shows that the application of ensemble learning in ELM classification has achieved good results. When the training sample set is small, the classification accuracy of ELM is low, while the classification accuracy of the Ensemble-ELM algorithm is still higher than 85%, which meets the basic requirements of remote sensing image classification.

The Ensemble-ELM algorithm proposed in this chapter has achieved very good classification effect data when classifying PaviaU. The overall accuracy (OA) of the test samples was above 91%, with a Kappa coefficient of 0.88. Compared with the ELM algorithm, the accuracy is improved by about 20%. Compared with SVM, Ensemble-ELM algorithm shows advantages in classifying PaviaU, both in

classification accuracy and in experiment time. Both algorithms have poor classification results for the third category. Compared with the PaviaU ground truth data map in the previous section, it can be analyzed from the classification map that this is because the features of the third and eighth classes are similar and can be easily understood as the eighth class. At the same time, the first category can easily be mistakenly classified as the eighth category. There is a serious confusion between Class 2 grassland and Class 6 bare soil in the ELM classification map, which improves the confusion in the Ensemble-ELM classification map. Meanwhile, the classification map of Ensemble-ELM is smoother than that of ELM.

Compared with ELM, the Ensemble-ELM algorithm proposed in this chapter improves the classification accuracy of Salinas data by 4.4% for AA and 5.1% for OA, but the improvement is not large and the effect is not obvious. In the case of small sample classification, the classification effects of Ensemble-ELM and SVM algorithms are comparable, but have significant advantages in classification speed. It can be seen from the classification effect diagrams of ELM and Ensemble-ELM algorithms that, compared with ELM, the phenomenon that the third category is misclassified as the fifth category in the Ensemble-ELM classification diagram has been significantly improved, and the characteristics of the third category have been significantly improved. The classification accuracy should be smoother and the classification map should be smoother. However, the classification effect of the two algorithms is poor for the 15th category, and the phenomenon of misclassification to the 8th category is more serious. The classification effect after optimization has not been significantly improved.

By comparing the experimental results on the IndianPines, PaviaU and Salinas datasets, it can be found that the Ensemble-ELM algorithm proposed in this chapter has a better classification effect on the PaviaU dataset, and the optimization effect of the ELM algorithm is more prominent. Compared with ELM, Ensemble-ELM algorithm, the classification results of ELM on PaviaU show that OA is increased by 19%, AA is increased by 15%, the classification accuracy rate is over 91%, and the Kappa coefficient is 0.88. In the classification results of IndianPines data, OA only increased by nearly 10% to 86.2%, AA increased by 13% to 82.77%, and the Kappa coefficient was 0.84. In the classification results of Salinas data, both OA and AA increase by about 5%, and the optimization effect is not obvious.

4. Discussion

4.1. Analysis of Indian Pine Results. In terms of classification accuracy, it can be seen from Table 1 that, in the classification results of IndianPines' LBP-KELM method, OA is more than 30% higher than KELM, about 25% higher than SVM, and each class is improved to more than 94%. For example, the classification accuracy of KELM and SVM for the first category is only 4.88% and 17.07%, while the classification accuracy after using LBP-KELM is as high as 97.56%, indicating that the method proposed in this chapter utilizes texture features to achieve good classification results. In terms of classification efficiency, the processing speed is comparable to KELM, and it has a significant advantage over SVM in classification efficiency.

4.2. MODIS Data Analysis. To validate the algorithm, SKM, CKM, SAP, and IS-AP were selected for experiments with labeled samples at different scales. For the IS-AP and SAP algorithms, set the parameter to 0.85, and the self-similarity is the average of all the similarities. Figure 5 shows the quantitative analysis of the four algorithms. As can be seen from Figure 5, MRI reaches the highest value when SKM, CKM, SAP, and IS-AP select sample proportions of 12%, 10%, 10%, and 8%, respectively. Table 2 lists the MRIs of SKM, CKM, SAP, and IS-AP at 12%, 10%, 10%, and 8% of labeled samples, as shown in Figure 5 and Table 2.

4.3. Comparative Analysis of Different Classification Methods. Through research analysis, we know that the classification accuracy of the LCNet-27 model is better. In the method comparison, the article uses LCNet-27 to compare and analyze the traditional method. In terms of sample size selection, for TM images, the classification results obtained by the 5×5 sample size are better than other sample sizes in terms of detail retention and overall classification accuracy. To analyze the effectiveness of the method model, this paper will use the 5×5 sample size as the standard input sample size for the TM image method. The same set of training samples and validation samples were compared with the SVM classifier using spectral features and the SVM classifier using spectral plus texture features. The 7×7 sample size of QuickBird images was compared with traditional methods. The texture feature is selected according to the gray level co-occurrence matrix, and the mean and dissimilarity of the two texture measures of each band are added to obtain an 8-dimensional texture feature. The texture features and spectral features are classified as input features for the SVM classifier. In the quantitative accuracy evaluation, the overall classification accuracy and Kappa coefficient of the three classification methods for TM images and QuickBird images are shown in Figures 6 and 7.

4.4. LCNet: Analysis of the Influence of 27 Samples of Different Sizes on the Classification Results. With LCNet-27, the training accuracy is better than LCNet-13. This section will use the LCNet-27 model to select the optimal sample size and use the optimal sample size to compare and analyze the accuracy of the two models. Each pixel is collected according to the neighborhood size of 3×3, 5×5, 7×7, and 9×9 and then input into the LCNet-27 model trained by the respective sample size, and the pixel-by-pixel category judgment is performed, the accuracy of the classification is evaluated, and the QuickBird data test area is also collected according to the neighborhood size of 5×5, 7×7, and 9×9 for pixel-by-pixel category judgment; TM image classification, QuickBird image classification, and classification accuracy comparisons are shown in Table 3 and Figure 8.

Table 1: Classification results of Indian pine by KELM, SVM, and LBP-KELM algorithm (precision unit: %).

Category	Number of training samples	Quantity testing sample	KELM	Support vector machines	LBP-KELM
1	5	41	4.88	17.07	97.56
2	143	1285	75.10	73.93	98.13
3	83	747	52.07	57.03	99.33
4	24	213	34.27	55.87	95.31
5	48	435	86.67	86.90	99.08
6	73	657	98.33	96.19	99.09
	AA		64.03	72.95	98.33
	Office automation		77.90	80.22	98.36
	Kappa		0.74	0.77	0.98
	Training time (seconds)		0.11	$2.66E+04$	0.22
	Test time (seconds)		0.61	8.60	1.51

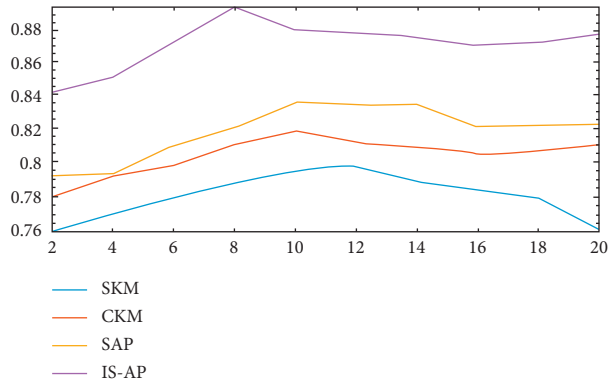

Figure 5: Proportion (%) of labeled samples.

Table 2: SKM, CKM, SAP, and IS-AP clustering results MRI (MODIS data).

Evaluation indicators	SKM	CKM	Sap	Access point
Proportion of labeled samples (%)	12	10	10	8
NMR	0.807	0.825	0.843	0.896

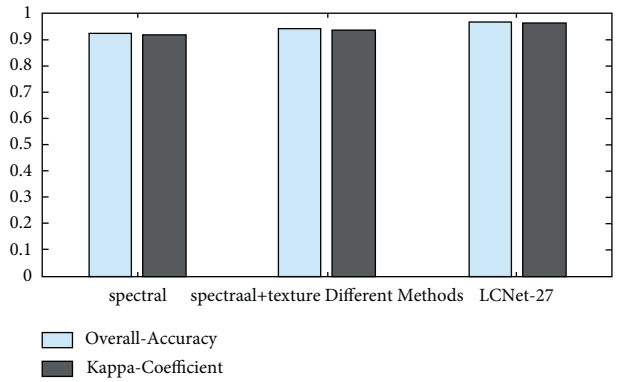

Figure 6: TM overall classification accuracy of different methods.

4.5. Analysis of ELM-SVM Classification Model. To test the performance of the ELM-SVM classification model, the combined model also conducts land cover classification experiments using the following two remote sensing image datasets. Meanwhile, in order to effectively test the

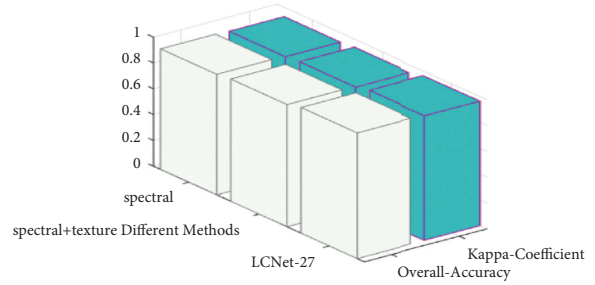

Figure 7: Overall classification accuracy of different QuickBird methods.

Table 3: TM overall classification accuracy for different sample sizes.

	Accuracy
3 * 3	0.7
5 * 5	0.75
7 * 7	0.8
9 * 9	0.7

performance of the ELM-SVM method, we compare with the SVM and ANN algorithms on the overall classification accuracy and Kappa coefficient. In order to improve the classification accuracy, the internal parameters of all methods are set to the optimal values; the thematic classification effect map is generated for the remote sensing image

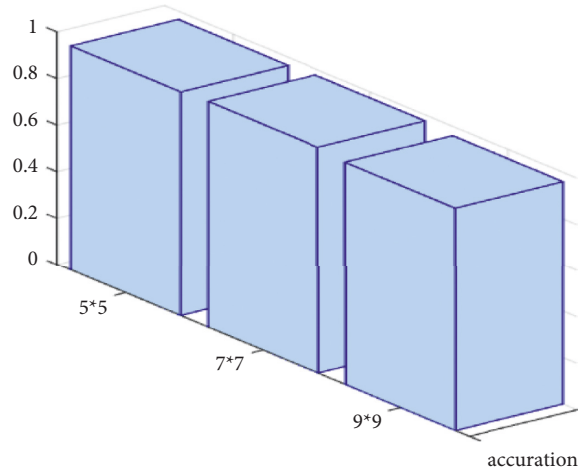

Figure 8: Comprehensive classification accuracy of QuickBird sample of different sizes.

Table 4: Confusion matrix for classification test using SVM.

Class	Water	Put up	Grass, shrub	Bare land	Road	All	User accuracy
Water	1148	2	0	0	25	1328	0.987
Put up	0	444	0	0	266	698	0.852
Grass, shrub	0	0	1294	0	73	1456	0.741
Bare land	0	0	0	82	10	90	0.963
Road	5	1329	30	15	11000	12825	0.9234
All	1155	1764	1409	95	10999	15133	
User accuracy	0.999	0.3	0.997	0.888	0.766		0.872

experimental data, and the visual comparison analysis is carried out with the classification effect map of the SVM and ANN methods; based on ENVI5.0, in the self-made components, the experiments were carried out in the experimental environment, as shown in Table 4.

5. Conclusion

The classification of remote sensing images is the basis and focus of remote sensing image analysis. Based on the characteristics of remote sensing images, this paper attempts to find the combination of pattern recognition methods and thematic classification applications of remote sensing images, aiming to improve the classification accuracy of remote sensing images. Remote sensing images such as ALOS/PALSAR and PSM are used as the main experimental data. Using the spatial and spectral features of remote sensing images, several SVM kernel function fusion methods and remote sensing image classification algorithms based on SVM, KNN, ELM, and other pattern recognition methods are proposed to classify and identify surface objects in remote sensing images. Finally, based on FCM and SVM, combined with remote sensing image segmentation method, object-oriented remote sensing image classification is realized.

The research summarizes the principles of pattern recognition methods commonly used in remote sensing image classification. The concept of pattern recognition and the workflow of pattern recognition system are briefly introduced. The main focus is on the integration of statistical pattern recognition with this study. The identification methods and experimental evaluation index systems commonly used in classification work are deeply studied.

Machine vision mainly studies the use of computers to simulate human visual functions. It extracts information from images of objective things, processes and understands it, and finally uses it for actual detection, measurement, and control. Typical industrial machine vision application systems include light source, optical system, image acquisition system, image digitization module, digital image processing module, intelligent judgment and decision-making module, and mechanical control execution module; machine vision is mainly divided into visual inspection, vision, and robot vision. In other respects, it has been promoted in the fields of medical testing and intelligent transportation, bringing convenience to people's lives. However, the existing technology is still difficult to deal with complex scenes, so this problem has also become the future development direction of machine vision. The main application of machine vision technology at this stage is still to capture visual information, but how to combine it with the perceptron has become a difficult problem in the next stage. The birth and application of machine vision technology have greatly liberated human labor, improved the level of production automation, and improved human living conditions. Its application prospect is very broad. At present, foreign machine vision technology has been widely used in production and life, while our country is still in its infancy, and the joint efforts of scientific

and technological workers are urgently needed to rapidly improve the development level of our country's machine vision technology and make progress to make its own contribution to China's modernization.

In the research work and writing process of this paper, due to our limited understanding of the research field and the lack of basic experimental data, many issues related to the research content of this paper need to be further developed, including the following points:

(1) All the research methods proposed in this paper can only be applied to remote sensing images such as ALOS/PALSAR and PSM and cannot be directly applied to the classification or segmentation of remote sensing images from other platforms. Therefore, in addition to optimizing and perfecting the algorithm principle proposed in this paper, we should also try to apply the algorithm principle proposed in this paper to the classification or segmentation of remote sensing image data based on other sensor platforms.

(2) The distance measurement between the sample points of the algorithm proposed in this paper is generally based on the Euclidean distance formula or the Euclidean distance formula. Combining this formula with the spectral angle matching formula, the performance of other distance formulas has not been tested, so the theoretical research needs to be improved, and the research should be applied from different angles as much as possible, such as considering the use of the Markov distance measurement index formula.

(3) All the classification methods proposed in this paper can take into account the extraction of spatial and spectral features of remote sensing data. In order to obtain higher classification accuracy or reasonable classification or segmentation effect, efforts should be made to use richer remote sensing data, data characteristics, feature information, such as the standard deviation and spectral ratio of image objects, the fractal dimension of the image, and the shape features of image landmarks and texture features.

Data Availability

No data were used to support this study.

Conflicts of Interest

The authors declare that they have no conflicts of interest.

References

[1] T. Ma and Y. Wang, "Ruiping Land cover/land use classification based on microwave remote sensing polarization target decomposition," *Agriculture Gongcheng Xuebao/Journal of Chinese Agricultural Engineering Society*, vol. 31, no. 2, pp. 259–265, 2015.

[2] F. Yan, Q. Zhu, and L. Zhang, "High spatial resolution remote sensing image scene classification based on multi-feature fusion probabilistic topic model," *IEEE Transactions on Geoscience and Remote Sensing*, vol. 53, no. 11, pp. 1–16, 2015.

[3] P. Dong, T. Zhou, and M. Wang, "Random forest land cover classification based on genetic algorithm parameter optimization," *Journal of Applied Remote Sensing*, vol. 10, no. 3, Article ID 035021, 2016.

[4] Gi-S. Cho, N. Gantulga, and Y. W. Choi, "A comparative study on multi-class SVM & kernel function for land cover classification in a KOMPSAT-2 image," *KSCE Journal of Civil Engineering*, vol. 21, no. 5, pp. 1894–1904, 2016.

[5] C. Pelletier, S. Valero, and J. Ingrada, "Assessing the robustness of random forests for land cover mapping on large-area high-resolution satellite image time series," *Remote Sensing of Environment*, vol. 187, pp. 156–168, 2016.

[6] C. Li, P. Gong, J. Wang et al., "An all-season sample database for improving land-cover mapping of Africa with two classification schemes," *International Journal of Remote Sensing*, vol. 37, no. 19, pp. 4623–4647, 2016.

[7] Y. Xu, Bo Du, and L. Zhang, "Advanced multi-sensor optical remote sensing for urban land use and land cover classification: results of the 2018 IEEE GRSS data fusion competition," *IEEE Special Topics in Applied Earth Observation and Remote Sensing*, vol. 12, no. 99, pp. 1–16, 2019.

[8] D. Arun Kumar, S. K. Meher, and K. Padma Kumari, "Knowledge-based progressive neural networks for remote sensing image classification," *IEEE Special Topics in Applied Earth Observation and Remote Sensing*, vol. 10, no. 99, pp. 1–12, 2017.

[9] D. Lu, P. Mausel, M. Batistella, and E. Moran, "Comparison of land cover classification methods in the Brazilian Amazon Basin," *Photogrammetric Engineering & Remote Sensing*, vol. 70, no. 6, pp. 723–732, 2015.

[10] T. Wu, J. Luo, and Z. Shen, "Application of high-resolution remote sensing in land cover classification technology in poverty-stricken areas: taking Qianjiang District of Chongqing as an example," *Journal of Geographic Information System*, vol. 18, no. 3, pp. 353–361, 2016.

[11] C. O. Dumitru, G. Schwarz, and M. Datcu, "Land cover semantic annotation derived from high-resolution SAR images," *Ieee Journal of Selected Topics in Applied Earth Observations and Remote Sensing*, vol. 9, no. 6, pp. 2215–2232, 2016.

[12] F. Barrick Sanli, S. Abu Dikan, and M. T. Essetelli, "Evaluation of image fusion methods for land use/land cover classification using PALSAR, RADARSAT-1 and SPOT images," *Journal of the Indian Society of Remote Sensing*, vol. 45, pp. 1–11, 2016.

[13] J. Verhulp and A. Van Niekerk, "Effect of inter-image spectral variation on land cover separability in heterogeneous areas," *International Journal of Remote Sensing*, vol. 37, no. 7, pp. 1639–1657, 2016.

[14] H. E. Adam, E. Csaplovics, and M. E. Elhaja, "A comparison of pixel-based and object-based approaches for land use land cover classification in semi-arid areas, Sudan," *IOP Conference Series: Earth and Environmental Science*, vol. 37, no. 1, Article ID 012061, 2016.

[15] S. Gebhardt, P. Maeda, T. Wehrmann, J. Argumedo Espinoza, and M. Schmidt, "A proper land cover and forest type classification scheme for Mexico," *The International Archives of the Photogrammetry, Remote Sensing and Spatial Information Sciences*, vol. XL-7/W3, no. 7, pp. 383–390, 2015.

[16] "Land cover classification and feature extraction from orthophotos: a review," *Photogrammetric Engineering & Remote Sensing*, vol. 83, no. 11, pp. 737–747, 2017.
[17] S. Shen, P. Yue, and C. Fan, "Quantitative assessment of land use dynamic variation using remote sensing data and landscape pattern in the Yangtze River Delta, China," *Sustainable Computing: Informatics and Systems*, vol. 23, pp. 111–119, 2019.
[18] H. Lu, Q. Liu, X. Liu, and Y. Zhang, "A survey of semantic construction and application of satellite remote sensing images and data," *Journal of Organizational and End User Computing*, vol. 33, no. 6, pp. 1–20, 2021.
[19] S. Cheng, T. Mei, and G. Liu, "Application of multi-level MRF based on structural features in remote sensing image classification," *Wuhan University Surveying and Information Science*, vol. 40, no. 9, pp. 1180–1187, 2015.
[20] C. RomeroGata and G. Camps-Vals, "Unsupervised deep feature extraction for remote sensing image classification," *IEEE Transactions on Geoscience and Remote Sensing*, vol. 54, no. 3, pp. 1349–1362, 2015.
[21] S. S. Longa and J. M. Ndambukey, "Accuracy assessment of land use/land cover classification using remote sensing and GIS," *International Journal of Geosciences*, vol. 8, no. 4, pp. 611–622, 2017.
[22] C. Liu, L. Hong, J. Chen, and S. Chu, "Fusion of high-resolution remote sensing image classification based on pixel and multi-scale regional features," *Journal of Remote Sensing*, vol. 19, no. 2, pp. 228–239, 2015.
[23] Y. Qi, Li Hui, and L. Jing, "Automatic extraction algorithm of earthquake and landslide information based on post-disaster high-resolution remote sensing images," *Advances in Lasers and Optoelectronics*, vol. 54, no. 11, Article ID 112801, 2017.
[24] C. Cao, X. Fan, and Q. Liu, "A practical pattern recognition system for distributed optical fiber intrusion monitoring based on COTDR," *ZTE*, vol. 15, no. 3, pp. 52–55, 2017.
[25] Y. Liu, W. Yang, and Y. Ma, "Research on extraction of HCS fusion corn planting area based on high spatiotemporal remote sensing data," *Journal of Shenyang Jianzhu University*, vol. 33, no. 2, pp. 314–322, 2017.
[26] O. Masato and S. Masanobu, "Large-area land use and land cover classification based on PALSAR-2 quad-polarization, compact and dual-polarization SAR data," *IEEE Transactions on Geoscience and Remote Sensing*, vol. 56, no. 99, pp. 1–8, 2018.
[27] Y. Zhou, Y. Chen, and F. Li, "Supervised and adaptive feature weighting for object-based satellite image classification," *IEEE Special Topics in Applied Earth Observation and Remote Sensing*, vol. 11, no. 99, pp. 1–11, 2018.
[28] S. W. Hue, A. Korom, Y.-W. Seng, V. Sihapanya, S. Phimmavong, and M. H. Phua, "Land use and land cover change in vientiane area, Lao PDR using object-oriented classification on multi-temporal Landsat data," *Advanced Science Letters*, vol. 23, no. 11, pp. 11340–11344, 2017.
[29] Y. Zhu, Y. Zeng, and M. Zhang, "Land use/cover information extraction based on HJ satellite data and object-oriented classification," *Agriculture Gongcheng Xuebao/Journal of Chinese Agricultural Engineering Society*, vol. 33, no. 14, pp. 258–265, 2017.
[30] Y. Zhou, X. Mu, and S. Wang, "Remote sensing image scene classification based on multi-scale feature fusion," *Optical Milling Gongcheng/Optics and Precision Engineering*, vol. 26, no. 12, pp. 3099–3107, 2018.
[31] W. Chen, X. Li, H. He, and L. Wang, "A review of fine-scale land use and land cover classification in open-pit mining areas by remote sensing techniques," *Remote Sensing*, vol. 10, no. 2, p. 15, 2017.
[32] M. Bouaziz, S. Eisold, and E. Guermazi, "Semiautomatic approach for land cover classification: a remote sensing study for arid climate in southeastern Tunisia," *Euro-Mediterranean Journal for Environmental Integration*, vol. 2, no. 1, p. 24, 2017.

Hindawi
Scientific Programming
Volume 2022, Article ID 9972658, 11 pages
https://doi.org/10.1155/2022/9972658

Research Article

Security Strategy Optimization and Algorithm Based on 3D Economic Sustainable Supply Chain

Lai-Wang Wang,[1] Chen-Chih Hung ,[1] and Ching-Tang Hsieh[2]

[1]*Department of Industrial Engineering and Management, National Kaohsiung University of Science and Technology, Kaohsiung 807618, Taiwan, China*
[2]*Department of International Business, National Kaohsiung University of Science and Technology, Kaohsiung 824004, Taiwan, China*

Correspondence should be addressed to Chen-Chih Hung; i107142107@nkust.edu.tw

Received 7 July 2022; Revised 4 August 2022; Accepted 24 August 2022; Published 10 September 2022

Academic Editor: Juan Vicente Capella Hernandez

Based on the background of system intelligence in the Internet of things era, this paper applied the design field of interaction design and user experience in the early days, and conducted further in-depth investigation through a large number of case studies and the use of quantitative and qualitative investigation methods. Based on this, the theories and strategies of the interaction design between enterprise members and intelligent machines were put forward and tested by actual design. At present, air pollution, energy shortage, and other issues are becoming more and more prominent, and calls for energy conservation, emission reduction, strengthening corporate social responsibility, and reducing the impact of economic development on the environment and society are growing. Therefore, companies must rethink their strategies and adapt their supply chains. Based on limited resources, enterprise machines have traditionally acted as a tool or a communication tool for a person. Yet, at the same time as the economy develops, the direct interaction between human and machine gradually emerges, and the economic development of an enterprise is bound to contradict environmental protection and social responsibility. Therefore, for enterprises, in different periods, different priority strategies will be adopted for the three dimensions of economy, environment, and society. The results showed that the economic benefit has increased by about 30% or more, and the ecological pollution has been reduced by about 40% on the original basis. Under the action of a sustainable supply chain, consumer satisfaction tends to be full and can be maintained at about 97%. In this context, the comparative analysis of the strategic optimization of enterprises in the supply chain is the focus of this thesis.

1. Introduction

At present, research on sustainable supply chain networks mainly focuses on corporate social responsibility assessment, technology selection, energy conservation, emission reduction, etc., but less consideration is given to strategic decisions based on different priorities under the three-dimensional economic sustainable supply chain. With the development of technology and the arrival of the era of intelligent network, the relationship between humans and machines has become increasingly close.

This paper broke the previous research that only quantified sustainable supply chain networks. First, it conducted a theoretical analysis of enterprises under different strategies and then built a sustainable supply chain network model. Then, it was studied from the two main aspects: first, through the analysis of the optimal countermeasures in terms of price, technology, and social responsibility in different strategies, it was determined which strategy is the most favorable under the condition of equilibrium; and second, through the establishment of a closed-loop supply chain network, the optimal sustainable supply chain network was determined by solving the situation that the demand was affected by corporate social responsibility, and the optimal mode of the sustainable supply chain network under various strategies was compared to

provide reference and suggestions for enterprises when making strategic decisions and optimization.

In the early research, it was found that the current research on human-computer interaction was based on human unit, or human-machine surface interaction, without considering the deep development trend and design requirements of human-machine interaction in the age of the intelligent network. It started from the new social environment and the development of human-human social relations; this paper proposed the concept of machine social role and defined its meaning. The issues were analyzed, and the following conclusions were drawn: when economic and environmental goals conflict with social goals, it is more reasonable and practical for the company to determine the priority strategy for the supply chain. It is appropriate to first consider environmental and economic goals and then strategies for social goals. In addition, to a certain extent, the priority strategy of the supply chain has a driving effect on the economy, society, and the environment, but once a certain limit is exceeded, it will have an adverse impact on the economy, society, and the environment. In the process of undertaking social responsibilities, enterprises must first achieve a balance between the economy and the environment. Therefore, under the circumstance of limited resources, environmental protection investment should be a priority.

2. Related Work

Supply chain responsiveness is a way for companies to gain a competitive advantage by responding quickly to consumer demands. The competitive business environment forces companies to solve problems that require flexibility and quick response within the framework of cost efficiency. Harsasi and Minrohayati took supply chain responsiveness as an intermediate variable and observed the impact of supply chain management on competitive advantage. Three hundred and thirty-four garment manufacturers in Indonesia were surveyed by postal questionnaire. Only fifty-seven questionnaires were valid and could be used for further analysis. The data were analyzed through mathematical analysis, which showed that all independent variables have a positive impact on the dependent variable, proving that supply chain management and supply chain responsiveness have a positive impact on gaining a competitive advantage [1]. Samaranayake aimed to document research into the development of a conceptual framework for supply chains. The aim was to develop a comprehensive framework and provide a way to plan the many components in the supply chain, such as suppliers, materials, resources, warehouses, activities, and customers. The proposed framework was based on a single structuring technique, where bills of materials, warehouse lists, item networks, and operational routes in manufacturing and distribution networks were combined into a single structure. The framework was described with digital examples in manufacturing and distribution environments. Findings of the numerical testing showed that each network in the supply chain provides an integrated approach to planning and executing many components to further improve the supply chain environment [2]. Park et al. studied and developed a mixed integer linear programming model that integrates multimodal transport into a switchgrass-based bioethanol supply chain. The two modes of transportation were truck and rail. The Park et al. study aimed to minimize the total cost of cultivation/harvest, infrastructure, storage process, bioethanol production, and transportation. Strategic decisions, including the number and location of intermodal facilities and biorefineries, as well as tactical decisions, such as the amount of biomass to be transported, processed, and converted to bioethanol, were all validated using the North Dakota case study. It was found that the multimodal transport option is more cost-effective than the single mode of transport, resulting in a lower cost of bioethanol. A sensitivity analysis was performed to demonstrate the impact of key factors on MTSBSC decision-making and bioethanol costs [3]. Liao and Chung research was an attempt to determine the economic order quantity of deteriorating goods under the condition of allowing delayed payment, in which the supplier provides the retailer with the allowable delay period, and the retailer in turn provides the maximum trade credit period to its customers. The chain supply chain system developed a theorem to determine the retailer's optimal ordering strategy under the above conditions. These results help decision makers of retailers to accurately determine optimal costs, and a numerical example demonstrates the applicability of the proposed method [4]. One of the most interesting topics in supply chain management (SCM) is the integrated supplier-buyer production-inventory problem, where the key issue is determining the economic lot size for each shipment and delivery. Most of the research on this issue assumes that the product is screened and the process is perfect, but in practice, there may be screening errors with imperfect quality. Lin considered a simple single-supplier/single-buyer supply chain system in which products received were of defective quality and a 100 percent screening process was performed, with possible inspection errors. Its purpose was to determine the optimal number of shipments and the size of each shipment to minimize the combined annual cost incurred by the supplier and buyer. At the same time, a cost model was developed for the supply chain system and a solution was proposed to find the optimal strategic solution [5]. The Internet of things is widely used in various fields because of its high intelligence and diversity. IoT security has perception information, network environment, and user requirements. Based on the multilayer and multidimensional features of the security elements of the Internet of things and security-oriented system indicators, it adopts the autonomous idea of "cluster users" collaboration, integrates the concept of independent disciplines, and fine-tunes the "single-user" process to improve the overall security performance. Multilayer security elements, from microscopic to perception layer, from singular to plural, realize autonomous configuration and adjustment, and realize self-update and optimization of the overall security of the system. Zheng et al. adopted a multidimensional constrained optimization method to optimize the perceptual layer configuration. In the process, the configuration requirements were fed back to

the cluster users at each layer; therefore, the security configuration optimization was triggered from the perspective of the perception layer [6]. Song et al. gave the embedding optimization strategy through theoretical derivation: optimizing the embedding modification position and optimizing the embedding modification direction. The quantitative relationship between the pixel modification probability and the difference between adjacent pixels was obtained through theoretical derivation, and it was proved that random ±1 modification cannot definitely enhance the steganographic security. The research can provide theoretical guidance for the design of steganographic algorithms. Compared with previous studies, the proposed embedding optimization strategy has the outstanding advantages of being easy to implement and effectively improving steganographic security [7]. With the continuous advancement of computer technology and economy, the computer industry continues to grow, and the demand for innovative talents in the Internet of things information age is growing rapidly. In this paper, the author analyzes the 3D practical teaching framework of computer graphics for social development, from modeling, rendering, lighting, texture, etc., all based on computer graphics algorithms and theories of the Internet of Things. Guo proposed a 3D computer graphics teaching framework, from the basic theory of computer graphics to experimental projects. According to the training and evaluation model of 3D teaching, public enterprises can fully understand the knowledge system of a computer, teach effective learning methods, and then better optimize strategies [8].

3. Optimal Supply Chain Strategy Algorithm Based on Three-Dimensional Economy

3.1. Meaning of Sustainable Supply Chain and the Integration of Strategic Security Optimization. As far as sustainable development is concerned, some scholars have proposed a three-dimensional economy, and pointed out that in order to seek their own development, enterprises must also ensure the balance of economic prosperity, environmental protection, and social welfare; that is, sustainability is at the intersection of three dimensions of economy, environment, and society [9]. Only by focusing on sustainable development can enterprises and their own supply chains truly improve social welfare and reduce environmental pollution. The three-dimensional economy requires enterprises to transform from the pure profit goal to the profit maximization of realizing the triple goals of economy, environment, and society [10]. People's attitude towards the Internet of things can no longer be limited to mechanical tools. The communication between humans and intelligent systems has also changed from "information communication" to "emotional communication," and the interaction between "human-machine" and "human" is also changing. Changes in interaction patterns lead to changes in human relationships [11]. With the gradual development of human-computer interaction technology and the mobility of enterprise equipment, it has penetrated into people's daily life. Economic benefits, environmental benefits, and social benefits are interrelated [12]. Most of the survey results showed that reducing environmental pollution and fulfilling corresponding social responsibilities have a significant correlation with corporate profits. First of all, the acquisition of profits provides a certain amount of capital for environmental protection and social responsibility so that companies can invest more in environmental protection technology, increase jobs, and protect workers' lives, so as to undertake more social responsibilities [13]. In addition, enterprises actively participate in environmental protection and fulfill social responsibilities, which can effectively improve the company's brand image, win customers, and bring long-term benefits to the company. The most significant benefits of sustainable supply chain management are manifested in three levels; namely, the first level is economic performance, the second level is environmental performance, and the third level is social performance [14]. Since sustainable supply chain cooperation occurs at the three-dimensional junction of economy, society, and environment, companies in the supply chain should start from a strategic perspective and long-term goals, rather than simply pursuing any one or two of the three dimensions [15]. The sustainable supply chain structure is shown in Figure 1.

3.2. Traditional Supply Chain and Sustainable Supply Chain. In the process of overhauling traditional supply chain processes, managers are increasingly aware that companies must address sustainability issues in supply chain operations. Sustainable development generally refers to "the use of its resources to meet current needs without compromising the ability of future generations." The concept was vague at first, but scholars paid more attention to environmental issues in order to more accurately apply the concept of sustainable development in supply chain practice, that is, sustainable supply chain management starts from the environmental perspective of the supply chain, and proposed a supply chain coordinated with the environment [16]. However, as research continues to deepen, the term sustainable development is gradually combined with social, environmental, and economic responsibility. At present, the research on "sustainable supply chain" in academia mainly focuses on the concept of "sustainable supply chain"; that is, "in order to achieve economic, environmental, and social goals, companies integrate the concept of sustainable development into the enterprise interior and supply chain in production, sales, storage, and information exchange" [17]. With the in-depth understanding of the three-dimensional theory, in the practice of discussing the sustainable supply chain, it is necessary to emphasize its key factors and clarify its related concepts. This paper referred to the relevant literature in the field of supply chain and sustainable supply chain to deepen the research and understanding of this topic [18].

3.3. Optimization of Sustainable Supply Chain Is Inseparable from the Three-Dimensional Economy. Supply chain refers to the combination of multiple interdependent economic organizations through the collaborative management of

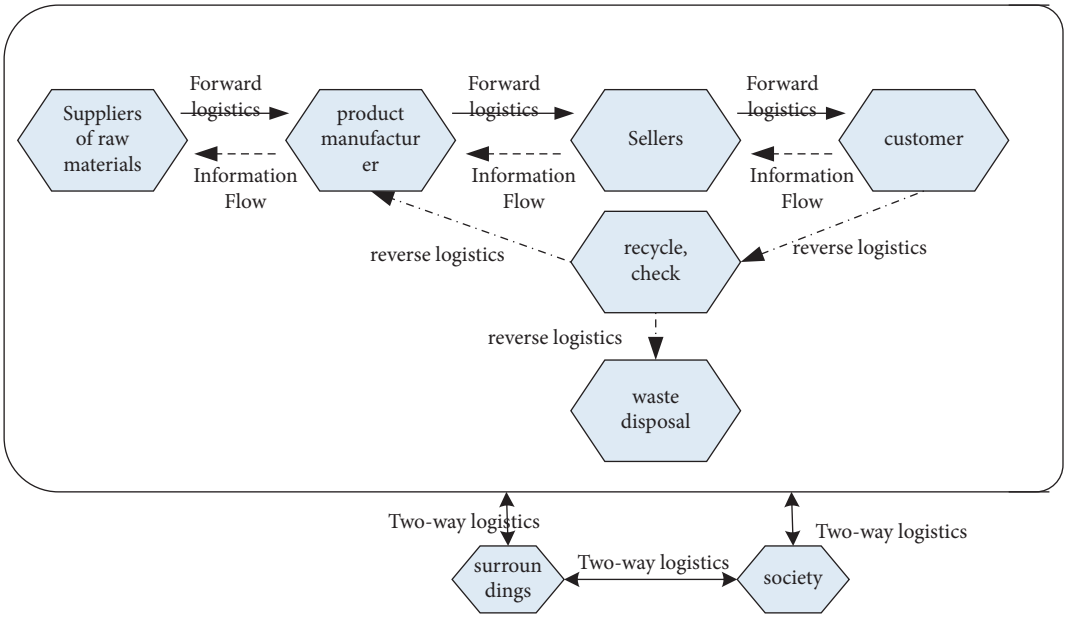

Figure 1: Sustainable supply chain structural diagram.

various resources, such as inventory and information. With the increasingly fierce market competition, the traditional competition has gradually evolved into the competition of supply chains [19]. Therefore, sustainable supply chain management needs to incorporate environmental and social issues into the planning and operation of the supply chain, so as to improve the economic benefits of the enterprise and ensure its overall benefits, thereby improving environmental performance and social performance of supply chain members [20]. Since the members of the supply chain are an independent economic organization, they can engage in the operation of multiple supply chains at the same time in the case of seeking common interests. Therefore, there are competition and cooperation among members. In cooperation and competition, there are inevitably many risks such as asset specificity, environmental uncertainty, information risk, and performance ambiguity [21]. A simplified schematic diagram of the supply chain is shown in Figure 2.

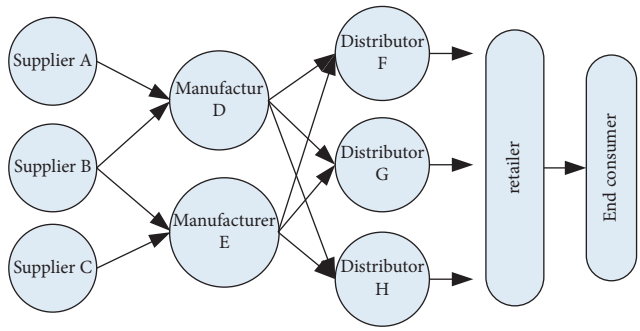

Figure 2: Simplified schematic diagram of the supply chain.

3.4. Supply Chain Application and Corporate Social Responsibility. In recent years, the rapid development of Internet technology has changed the business structure and mode of operation of enterprises. The combination and development of 5G and various Internet technologies has laid a solid technical foundation for enterprises to develop innovative businesses. Among them, the sustainable supply chain technology based on the Internet of things is widely used in supply chain scenarios. From the perspective of sustainable development, this paper compared and analyzed the results of domestic and foreign research on enterprise supply chain informatization. For IoT applications in the supply chain, this research focused on each link. From production, logistics, to consumers, this study incorporated all actors in sustainable supply chains into different production processes and logistic layouts, while others only involve corporate users. Sources of product names and other information in the region are available to all stakeholders. Although the information collection and sharing of the Internet of things has penetrated into all aspects of the supply chain, the depth and influence of sharing is still quite limited. In most cases, members of the sustainable supply chain system can only obtain product information, and the sustainable development evaluation information, which is also closely related to stakeholders, has not been effectively collected and utilized. A simple supply chain network is shown in Figure 3.

Different scholars have different understandings of corporate social responsibility. The US Economic and Trade Commission recommends that the social responsibility of a "three-center" company consists of three concentric circles. From outside to inside is an invisible responsibility to promote the development of society. In the process of realizing economic responsibility, five aspects such as corporate social responsibility, economic responsibility, legal responsibility, moral responsibility, and corporate voluntary responsibility should be fully considered. In short, CSR emphasizes that companies should not only pursue

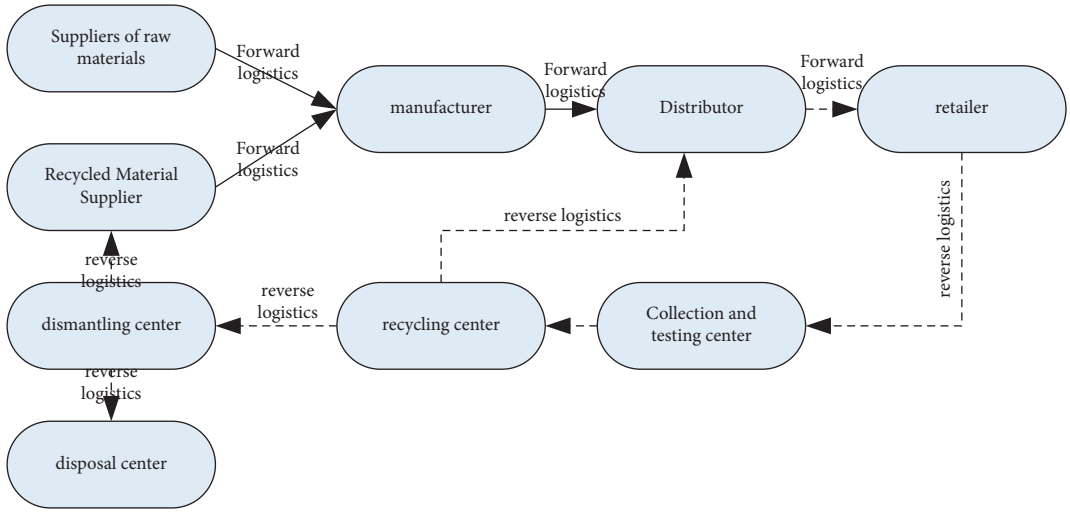

Figure 3: Simple supply chain network structure.

Table 1: Measures of corporate social responsibility.

Stakeholders	Social influence	Index	Core theme
Worker	Safety	Lost days due to work attrition	Labor, human rights
Worker	Fair working conditions	Number of jobs created	Labor, human rights
Community	Community development	Number of jobs created	Community development
Community	Environment	Amount of waste generated	Environment
Consumer	Safe consumption	Quantity of potentially hazardous products	Consumer issues

economic interests, but also pay attention to their contributions to the environment, customers, employees, and communities. However, if viewed from a development process point of view, corporate social responsibility is more concerned with promoting and maintaining relationships with stakeholders. Table 1 shows the measures of corporate social responsibility.

3.5. Sustainable Supply Chain Design Theory and Algorithm Model. In terms of economic purposes, the primary goal is to maximize profits, and for the company, its main profit method is the sales of products. In terms of environmental protection purposes, minimizing emissions, especially in the manufacturing process, for companies, can reduce environmental pollution by investing in technologies that save energy and reduce emissions. Therefore, in terms of environmental protection indicators, the most important issue is to determine the optimal investment in carbon emission technologies. In regard to sustainable supply chains, corporate social responsibility (CSR) is based on the work the company creates. For companies, the more energy they put into social responsibility, the more jobs they create. Therefore, in terms of social goals, the most important thing is to make the best social responsibility. In this model, there is no game between manufacturers and retailers. Therefore, the research of this model has certain reference significance for enterprises that combine production and sales.

In this model, the following decision variables are identified:

η: the company's CSR work, $\eta \in [0, 1]$

Z: the degree of investment in energy-saving and consumption-reduction technology, $z \in [0,1]$

P: product price.

In the case of a company, the greater the social responsibility it undertakes, the more jobs it creates. However, due to human resource constraints, the jobs that can be created will not grow indefinitely. From the perspective of marginal benefits, the marginal role of corporate social responsibility work under unit cost is diminishing. Conversely, a company can provide all the jobs for society as a whole. At the same time, for enterprises, by increasing investment in energy-saving and emission-reduction technologies, environmental pollution can be reduced, but their emission costs will gradually rise. This is because the limitations of the actual technology make it more difficult to reduce pollution, so investment must be increased to develop new technologies.

Therefore,

$$D = a - bp + k_1 z + k_2 \sqrt{\eta}. \tag{1}$$

Among them, a is the basic market capability, that is, supply chain products; b, k_1, and k_2 are the sensitivity factors of p, z, and η, respectively. The larger b, k_1, k_2, the more sensitive the commodity price, energy-saving and emission-reduction technology investment and social responsibility efforts. b, k_1, and k_2 are all positive numbers.

The profit expression for this company is as follows:

$$\pi_1 = \left(a - bp + k_1 z + k_2 \sqrt{n}\right)(p - c) - \frac{1}{2} s z^2 - hn. \tag{2}$$

The company's profit mainly includes three aspects: first, product sales revenue; second, energy-saving and emission-reduction technology; and third, enterprise's investment in social responsibility.

It is assumed that the total investment in energy-saving and emission-reduction technologies is $I = 1/2sz^2$.

Among them, s is the investment amount of energy-saving and emission-reduction technology. The larger the s is, the higher the required energy-saving and emission-reduction investment cost, and the cost has nothing to do with the required value; it is a one-time investment cost.

According to the CSR effort cost function form proposed by previous scholars, it is assumed that the CSR effort cost is $B = h\eta$, h is the CSR effort cost investment coefficient, and the larger the h is, the greater the required CSR effort cost. The same is a one-time investment cost.

The carbon emission function of the company is expressed as follows:

$$\pi_2 = (a - bp + k_1 z + k_2\sqrt{n})(e - kz). \tag{3}$$

Among them, e' is the initial unit carbon emission of the product, and k' is the unit carbon emission saved through carbon emission technology investment.

So, e'-$k'z$ is the current unit emission after investing in energy-saving and emission-reduction technology.

The company's CSR function is expressed as follows:

$$\pi_3 = (a - bp + k_1 z + k_2\sqrt{\eta})g(1 + \sqrt{\eta}). \tag{4}$$

In formula (4), g' is the unit of employment opportunities. As production increases, the expansion of the production line will bring more jobs, but they will have fewer and fewer jobs. Growth is not static but gradually tends to be balanced and saturated with the growth of market demand. Therefore, this paper assumed that there is a power function between g' and η.

In summary, the model is expressed as follows:

$$\begin{aligned} &\text{Max}\,\pi_1 = (a - bp + k_1 z + k_2\sqrt{\eta})(p - c) - \frac{1}{2}sz^2 - hn \\ &\min \pi_2 = (a - bp + k_1 z + k_2\sqrt{\eta})(e - kz) \\ &\max \pi_3 = (a - bp + k_1 z + k_2\sqrt{\eta})g(1 + \sqrt{\eta}) \end{aligned} \tag{5}$$

The model solution and analysis are as follows.

Because the environmental indicator is mainly about saving and reducing emissions for sustainable development, if it is to be converted into an economic indicator, its emissions must be added to the CO_2 tax. Let c_t be the carbon tax per unit of carbon emissions, and the conversion process is as follows:

$$\begin{aligned} \min \pi_2 &= (a - bp + k_1 z + k_2\sqrt{\eta})(e - kz) \\ &= \min \pi_2 = (a - bp + k_1 z + k_2\sqrt{\eta})(e - kz)c_t \\ \longrightarrow^{\text{令}} & ec_t = e,\ k'c_t = k'\ \ \min \pi_2 = (a - bp + k_1 z + k_2\sqrt{\eta})(e - kz). \end{aligned} \tag{6}$$

As for social goals, this paper believed that due to the investment of social responsibility, more job opportunities will be brought. Therefore, if it is to be converted into an economic indicator, the conversion process is as follows:

$$\begin{aligned} &\max \pi_3 = (a - bp + k_1 z + k_2\sqrt{\eta})g(1 + \sqrt{\eta}) \\ &(a - bp + k_1 z + k_2\sqrt{\eta})g(1 + \sqrt{\eta})j_o \\ &\longrightarrow^{\text{令}} g'j_o = g\ \ \max \pi_3 = (a - bp + k_1 z + k_2\sqrt{\eta})g(1 + \sqrt{\eta}). \end{aligned} \tag{7}$$

The model after conversion is expressed as follows:

$$\begin{aligned} &\text{Max}\,\pi_1 = (a - bp + k_1 z + k_2\sqrt{\eta})(p - c)\frac{1}{2}sz^2 - h\eta \\ &\min \pi_2 = (a - bp + k_1 z + k_2\sqrt{\eta})(e - kz) \\ &\pi_3 = (a - bp + k_1 z + k_2\sqrt{\eta})g(1 + \sqrt{\eta}) \end{aligned} \tag{8}$$

Then, through the reverse inference method, the strategies are obtained by the following theorems:

Equilibrium solutions (p_1, z_1, η_1) exist for all strategies, and the equilibrium solutions for each strategy are the same:

Best CSR efforts: $\eta_1 = 1$;

The optimal level of investment in energy conservation and emission reduction: $z_1 = 1$;

Optimal product price: $p_1 = a + k_2 + k_1 + bc/2$.

They are listed below for ease of expression:

The first strategy, the goal of most companies, is to make money, so it will not be influenced by the government and big companies. Under enormous pressure, they have to consider economy first, and environment and society second.

The second strategy, for some manufacturers, is in the face of pressure from the government and the general public; it is necessary to carry out strategy optimization and algorithm analysis from the company's three-dimensional supply chain in order to achieve emission-reduction standards. When the emission standard fails to meet the requirements and the corporate image is damaged, if the company wants to restore its image and earn certain benefits, it must take environmental protection as the primary task, taking into account both the economy and the society.

The third strategy is that some state-owned enterprises, within the scope of the SASAC's business operations, must first aim at "people-oriented," followed by the economy and the environment.

The fourth strategy is for some foreign trade companies; because of their strict international trade laws and regulations, in order to make them meet environmental protection requirements and social needs, enterprises must take into account the needs of economy, environment, and society.

A simple classification is shown in Table 2.

Taking the first strategy as an example, since π_3 is an increasing linear function with respect to η, the optimal CSR effort is $\eta_1 = 1$. Substitute $\eta_1 = 1$ into the π_2 function to get $\pi_2 = (\text{a} - \text{bp} + k_1 z + k_2)\ (\text{e} - kz)$, and π_2 is a decreasing function on $z \in [0, 1]$, so the optimal energy-saving and emission-reduction investment level $z_1 = 1$; substitute $\eta_1 = 1$, $z_1 = 1$ into function π_1 to obtain its optimal commodity price $p_1 = a + k_2 + k_1 + bc/2$.

Table 2: Different strategic approaches.

Target strategy	Strategy 1	Strategy 2	Strategy 3	Strategy 4
Economy	Two	Three	Three	Two
Surroundings	Three	Two	Three	Two
Society	Four	Three	Two	Three

The strategies included in the first strategy are both economic and environmental. In this strategy, the company's contribution to society and investment in the environment must be above 1. This showed that in the absence of conflicting environmental and social goals, companies can think independently about economic issues and can devote maximum investment to environmental and social goals.

The second strategy has an equilibrium solution (p_2, z_2, η_2):

The best investment level for energy saving and emission reduction:

$$z_2 = \frac{ek_1 - k(a - bc + bg)}{2kk_1}. \tag{9}$$

Best CSR efforts:

$$\eta_2 = \left(\frac{(k_2 + bg)[k(a + bg - bc) + ek_1]}{2k((bg + k_2) - 4bh)}\right)^2. \tag{10}$$

The best product price:

$$p_2 = \frac{bgk[(gb + 3k_2)(c - g) + g(a + e)] + 2k(c - g)(k_2 - 3bh)(gk_2 - 2h)(ek_1 + ak)}{k((bg + k_2) - 4bh)}. \tag{11}$$

If and only if $h > k_2$g, $k_1(\mathrm{e} - 2k) < k(a - bc + bg) < ek_1$, $k_2 + bg > \sqrt{4bh}$, $a + (ek_1/k) + (8bh/k_2 + bg) < \mathrm{bc} + \mathrm{bg} + 2k_2$, $2\mathrm{b} > \mathrm{bg} - k_2$

So in the second strategy, the first is the concern for the environment, and the second is the impact on the economy and society. Therefore, companies must first determine their own investment in energy conservation and emission reduction, and then determine their own prices and social efforts. On this basis, using the method of reverse reasoning, the market supply and demand balance solution in the second stage is obtained first, and then the technical input in the first stage is analyzed on this basis.

We differentiate for $\pi_1 + \pi_3$ with respect to p, η and set its first derivative to zero to get the response function of selling price and CSR effort:

$$\begin{aligned} p_2 &= -\frac{z_2k_1 - (bg - k_2)\sqrt{\eta_2} + a + bc - bg}{2b} \\ \sqrt{\eta_2} &= \frac{(bg - k_2)p_2 - gk_1z_2 - ag + (c - g)k_2}{2(h - gk_2)} \end{aligned}. \tag{12}$$

$\partial(\pi_1 + \pi_3)/(\partial p_2) = -2\mathrm{b} < 0$, and $|\partial(\pi_1 + \pi_3)/(\partial p_2)| = 2b > |\partial(\pi_1 + \pi_3)/\partial p_2 \partial\sqrt{\eta_2}| = \mathrm{bg} - k_2$.

So the equilibrium point exists and is unique, if and only if $h > k_2$g, $2\mathrm{b} > \mathrm{bg} - k_2$

Next, we substitute the response functions of p_2 and η_2 into π_2 and derive z to obtain z_2, that is,

$$z_2 = \frac{k(a - bc + bg) - ek_1}{2kk_1}. \tag{13}$$

We substitute z_2 into the response functions of p_2 and $\sqrt{\eta_2}$ to get

$$\begin{aligned} \sqrt{\eta_2} &= \frac{(k_2 + bg)[k(a + bg - bc) + ek_1]}{2k((bg + k_2) - 4bh)} \\ p_2 &= \frac{bgk[(gb + 3k_2)(c - g) + g(a + e)] + 2k(c - g)(k_2 - 3bh)(gk_2 - 2h)(ek_1 + ak)}{k((bg + k_2) - 4bh)} \end{aligned}. \tag{14}$$

z_2, $\eta_2 \in [0, 1]$, so if and only if $k_1(\mathrm{e} - 2k) < k(a - bc + bg) < ek_1$, $k_2 + bg > \sqrt{4bh}$, $a + ek_1/k + 8bh/k_2 + bg < \mathrm{bc} + \mathrm{bg} + 2k_2$, the equilibrium solution exists.

Figure 4 shows a summary of the sustainable supply chain approach.

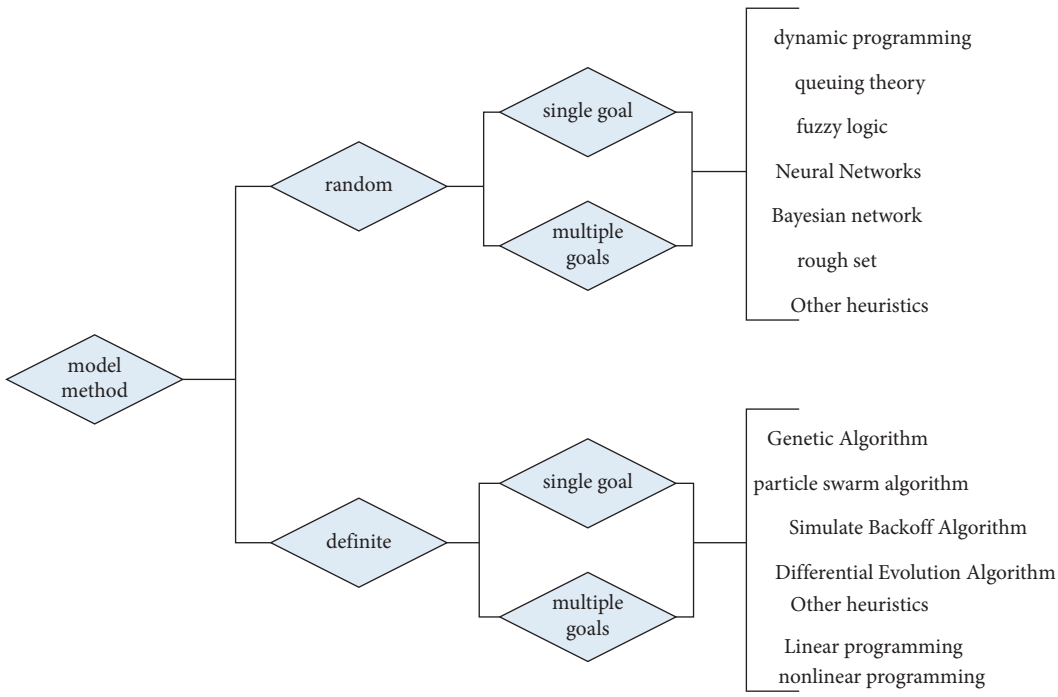

Figure 4: Summary of sustainable supply chain approaches.

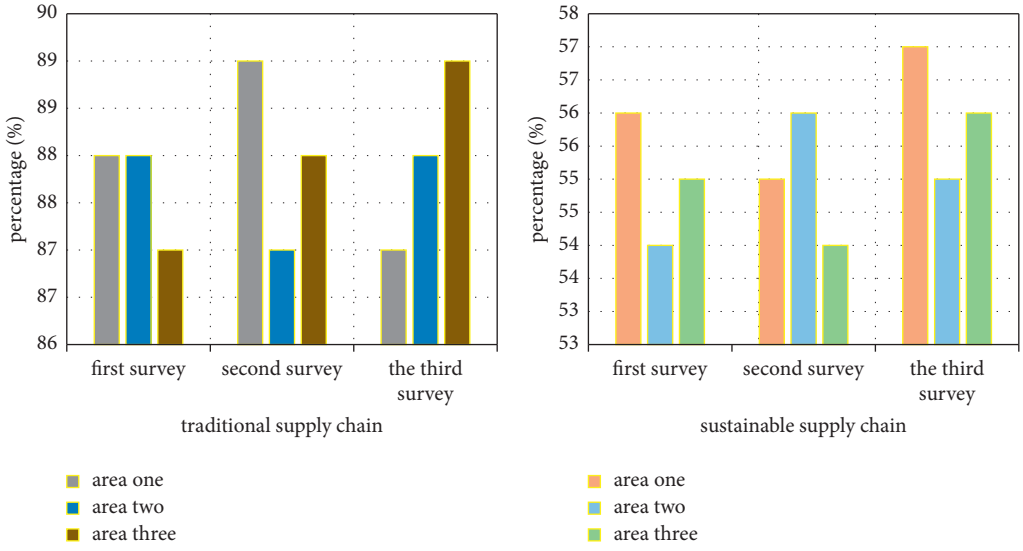

Figure 5: Comparison between ecological pollution before and after optimization.

This paper adopted the multi-index strategy method, in the three-dimensional economic environment, to determine the optimal cost, the greatest social responsibility, and the investment in energy-saving and emission-reduction technology of enterprises under different strategies. From the above analysis, it can be seen that at present, enterprises can only invest in energy conservation and emission-reduction technologies or social responsibility, or when their own interests are damaged (that is, the contradiction between the economy and the environment, or the contradiction between the economy and society), the enterprise can determine which one or both goals are more reasonable and realistic.

4. Comparison between Sustainable Supply Chain and Traditional Supply Chain under the Three-Dimensional Economy

A supply chain is a functional network system composed of suppliers, manufacturers, distributors, retailers, and consumers, which surrounds the core enterprise's raw material procurement, production, processing, storage, and end-user acquisition of products. The traditional supply chain management is aimed at maximizing the interests of the enterprise, and manages and controls the production efficiency, cost efficiency, etc. of the enterprise, resulting in ignoring the impact on the environment and society.

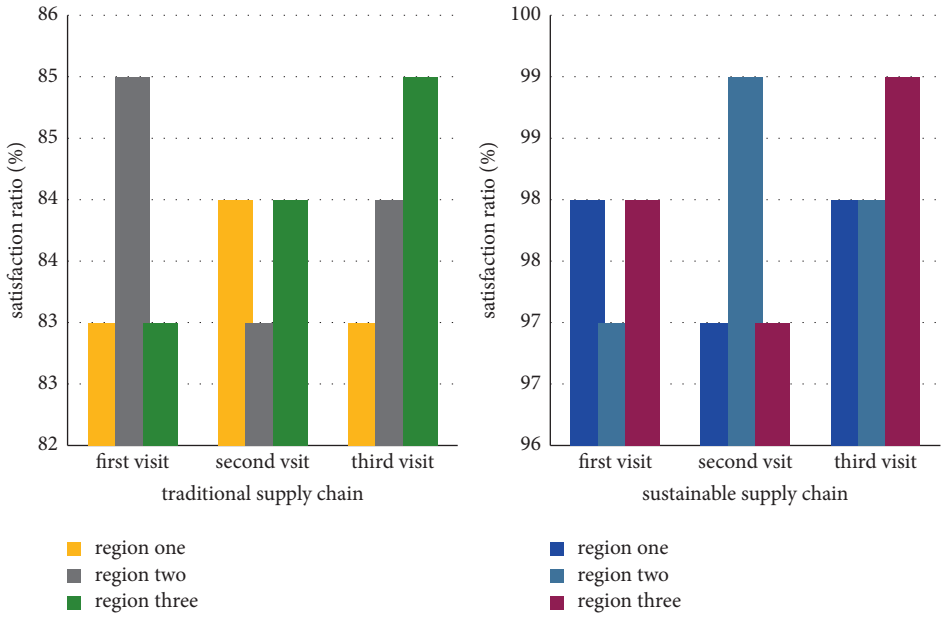

Figure 6: Consumer satisfaction comparison between supply chains.

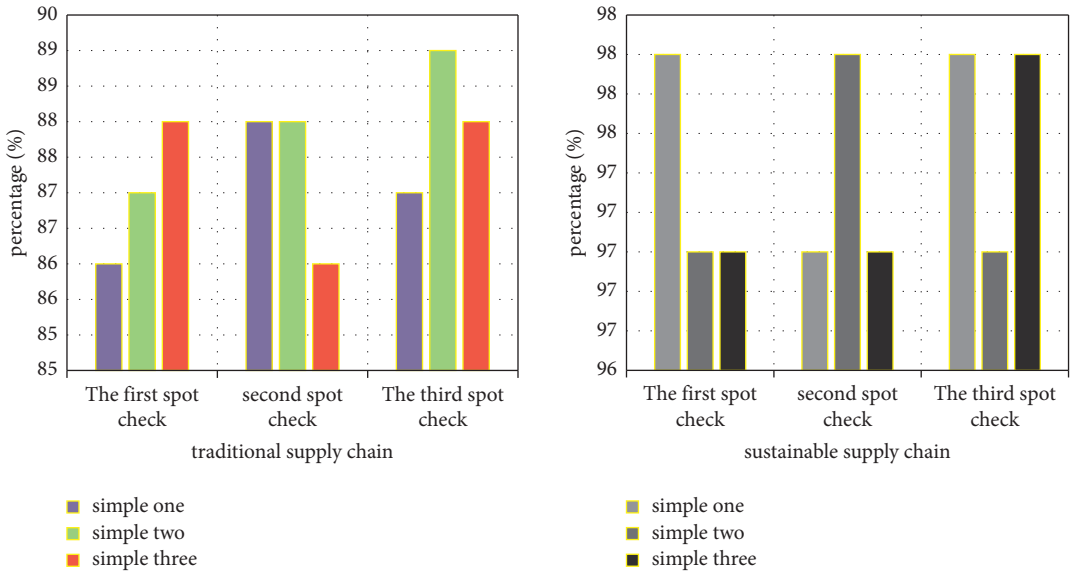

Figure 7: Comparison between product quality compliance rates under the two supply chains.

Therefore, there is still a long distance between the ideal level of natural interaction between enterprise personnel and intelligent machines. Technology is a big obstacle, and another obstacle is the idea that cannot be transformed into mechanical tools. Sustainable supply chain refers to the management of the three dimensions of sustainable development of logistics, information flow, and upstream and downstream enterprises in the supply chain from the perspectives of economy, environment, and society. Sustainable supply chain is to introduce the idea of sustainable development in the supply chain, and design and manage the supply chain from the three dimensions of economic, environmental, and social responsibility. From past experience, the competitiveness of the entire supply chain depends on the weakest link. That is to say, as long as there is a problem in one link, the entire supply chain will be hit hard. In this context, product quality issues, environmental pollution issues, and corporate social responsibility issues emerge one after another, attracting more and more attention. All in all, the impact of sustainable supply chain is mainly reflected in the ecological environment, economic benefits, product quality, consumer satisfaction, enterprise management, and so on. Figure 5 shows the comparison between ecological pollution before and after optimization.

Through three surveys in different regions, it can be found that more and more enterprises have changed their traditional perspective and began to focus on economic changes, deterioration of environmental pollution, public's

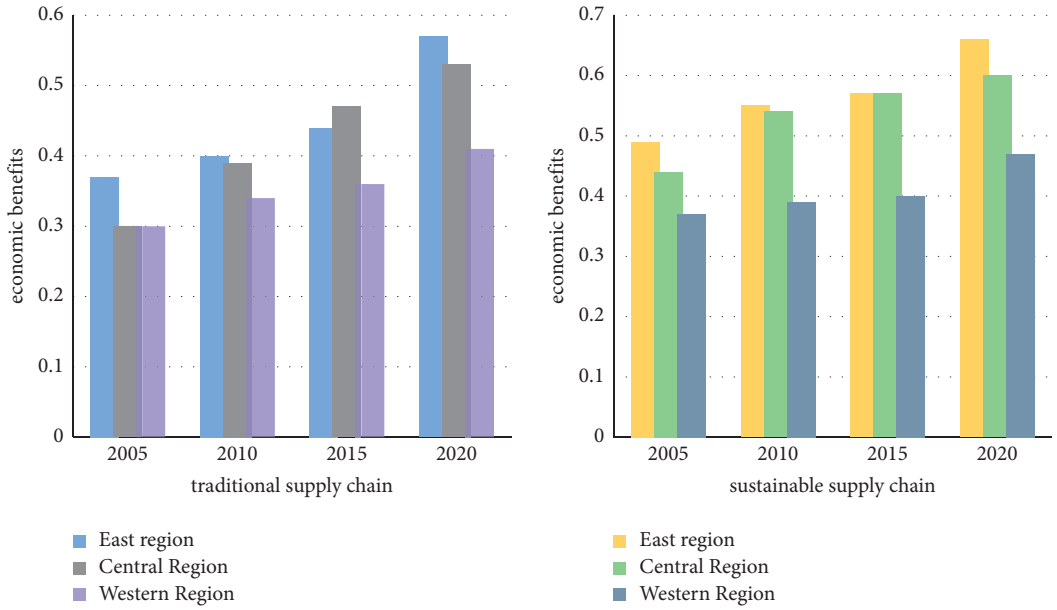

Figure 8: Comparison of economic benefits between supply chains.

transparency of the company's operations, environmental protection of consumers, and improvement of social responsibility as a whole, so as to get closer to the concept of sustainable development. The survey results showed that companies that have changed the traditional supply chain have made great improvements in environmental pollution, and energy-saving and emission-reduction technologies have improved in disguise. Figure 6 shows the comparison of consumer satisfaction between supply chains.

From three visits to different regions to investigate consumer satisfaction, it is found that the effect of sustainable supply chain makes consumer satisfaction almost 100%, while it is relatively difficult for traditional supply chain to reach 85%. The supply chain can help enterprises to implement the optimal strategy and can be distributed according to the statistics. It reduces resource loss and environmental pollution, achieves the optimal result of strategic optimization, greatly improves economic and social benefits, etc. It is understandable that consumer satisfaction is greatly improved. Figure 7 shows the comparison between product quality compliance rates under the two supply chains.

Through irregular random inspections, it is found that the compliance rate of samples produced by the traditional supply chain after a series of operations is basically maintained at around 87, and it is impossible to break the 90 mark, which is also a disguised loss for enterprises. However, actively adapting to the development trend of the Internet of things and actively improving the supply chain, the compliance rate of enterprises adopting a sustainable supply chain can be maintained at 97% or more, so the losses will inevitably be smaller and the economic benefits will be greater. The economic benefit comparison is shown in Figure 8.

From the comparison in Figure 8, it can be seen that the sustainable supply chain has a significant effect on improving economic efficiency. Therefore, when formulating and implementing relevant policies, it is necessary to fully consider factors such as the environmental, economic, and social responsibility in different regions to implement the optimal strategic decisions currently recommended, minimize losses, and increase consumer satisfaction to the highest level, thereby promoting economic and social development, enhancing environmental protection awareness, and improving economic efficiency and happiness index.

5. Conclusions

In general, the sustainable supply chain network design is based on the concept of sustainable supply chain, and the design principles mainly include the following points: profit maximization; environmental benefit maximization, that is, environmental pollution minimization; social benefit maximization; the principle of overall optimization and coordination; the principle of conformity to product characteristics; uncertainty, etc. The traditional supply chain management aims to reduce costs and improve services, and pays less attention to environmental issues. However, rising environmental concerns and concerns about resource depletion have prompted managers at all levels to adopt tougher environmental regulations. At the same time, the public's awareness of environmental protection is increasing day by day, and third-party environmental groups are putting more and more pressure on the company. Under the influence of this change, many companies have started environmental protection projects to solve environmental problems. In addition, due to the restrictions on the use and discharge of hazardous substances in regulations, companies must consider environmental factors to establish supply chains, prompting companies to extend environmental protection plans to suppliers and consumers, and actively promote the concept of sustainable development.

Data Availability

The datasets generated and/or analyzed during the current study are not publicly available due to sensitivity and data use agreement. No data were used to support this study.

Disclosure

The authors confirm that the content of the manuscript has not been published or submitted for publication elsewhere.

Conflicts of Interest

The authors declare that there are no potential conflicts of interest.

Authors' Contributions

All authors have seen the manuscript and approved to submit for publication.

References

[1] M. Harsasi and N. A. Minrohayati, "The impact of supply chain management practices on competitive advantage," *International Journal of Economic Policy in Emerging Economies*, vol. 10, no. 3, pp. 240–243, 2017.

[2] P. Samaranayake, "A conceptual framework for supply chain management: a structural integration," *Supply Chain Management: International Journal*, vol. 10, no. 1, pp. 47–59, 2005.

[3] Y. S. Park, J. Szmerekovsky, A. Osmani, and N. M. Aslaam, "Integrated multimodal transportation model for a switchgrass-based bioethanol supply chain: case study in North Dakota," *Transportation Research Record: Journal of the Transportation Research Board*, vol. 2628, no. 1, pp. 32–41, 2017.

[4] J. J. Liao and K. J. Chung, "An eoq model for deterioration items under trade credit policy in A supply chain system," *Journal of the Operations Research Society of Japan*, vol. 52, no. 1, pp. 46–57, 2009.

[5] T.-Y. Lin, "Optimal policy for a simple supply chain system with defective items and returned cost under screening errors," *Journal of the Operations Research Society of Japan*, vol. 52, no. 3, pp. 307–320, 2009.

[6] R. Zheng, M. Zhang, and Q. Zheng, "Security collaborative optimization strategy for perception layer in cognitive IoT," vol. 18, no. 3, pp. 685–696, 2017.

[7] H. T. Song, G. M. Tang, G. Kou, Y. F. Sun, and M. M. Jiang, "Digital steganography model and embedding optimization strategy," *Multimedia Tools and Applications*, vol. 78, no. 7, pp. 8271–8288, 2018.

[8] C. Guo, "Research on the three-dimensional practical teaching framework of computer graphics for game development," *International Journal for Engineering Modelling*, vol. 31, no. 1, pp. 90–95, 2018.

[9] K. Kearins, "Corporate social responsibility: the good, the bad and the ugly," *Society and Business Review*, vol. 34, no. 2, pp. 51–79, 2017.

[10] H. Cronqvist and F. Yu, "Shaped by their daughters: executives, female socialization, and corporate social responsibility," *Journal of Financial Economics*, vol. 126, no. 3, pp. 543–562, 2017.

[11] D. A. L. Coldwell and T. Joosub, "Corporate social responsibility in South Africa: quo vadis?" *African Journal of Economic and Management Studies*, vol. 6, no. 4, pp. 466–478, 2015.

[12] C. Flammer, "Competing for government procurement contracts: the role of corporate social responsibility," *Strategic Management Journal*, vol. 39, no. 5, pp. 1299–1324, 2018.

[13] V. Muslu, S. Mutlu, S. Radhakrishnan, and A. Tsang, "Corporate social responsibility report narratives and analyst forecast accuracy," *Journal of Business Ethics*, vol. 154, no. 4, pp. 1119–1142, 2019.

[14] J. P. Gond, A. El Akremi, V. Swaen, and N. Babu, "The psychological microfoundations of corporate social responsibility: a person-centric systematic review," *Journal of Organizational Behavior*, vol. 38, no. 2, pp. 225–246, 2017.

[15] A. Gupta, F. Briscoe, and D. C. Hambrick, "Red, blue, and purple firms: organizational political ideology and corporate social responsibility," *Strategic Management Journal*, vol. 38, no. 5, pp. 1018–1040, 2017.

[16] E. Lee, M. Walker, and C. C. Zeng, "Do Chinese state subsidies affect voluntary corporate social responsibility disclosure?" *Journal of Accounting and Public Policy*, vol. 36, no. 3, pp. 179–200, 2017.

[17] L. Ardito, J. Carrillo-Hermosilla, P. Del Río, and P. Pontrandolfo, "Corporate social responsibility and environmental management invites contributions for a special issue on 'sustainable innovation: processes, strategies, and outcomes," *Corporate Social Responsibility and Environmental Management*, vol. 25, no. 1, pp. 106–109, 2018.

[18] S. Kot, "Knowledge and understanding of corporate social responsibility," *Journal of Advanced Research in Law & Economics*, vol. 2, no. 10, pp. 109–119, 2017.

[19] R. J. I. Jones, T. M. Reilly, M. Z. Cox, and B. M. Cole, "Gender makes a difference: investigating consumer purchasing behavior and attitudes toward corporate social responsibility policies," *Corporate Social Responsibility and Environmental Management*, vol. 24, no. 2, pp. 133–144, 2017.

[20] Z. Wang and J. Sarkis, "Corporate social responsibility governance, outcomes, and financial performance," *Journal of Cleaner Production*, vol. 162, no. sep.20, pp. 1607–1616, 2017.

[21] R. Chaudhary, "Corporate social responsibility and employee engagement: can CSR help in redressing the engagement gap?" *Social Responsibility Journal*, vol. 13, no. 2, pp. 323–338, 2017.

Hindawi
Scientific Programming
Volume 2022, Article ID 5093426, 8 pages
https://doi.org/10.1155/2022/5093426

Research Article

Problems and Countermeasures of China's International Trade in Agricultural Products under the "Belt and Road Initiative"

Tianhua Li

College of International Business, Lanzhou Petrochemical University of Vocational Technology, Lanzhou 730060, Gansu, China

Correspondence should be addressed to Tianhua Li; litianhua@lzpcc.edu.cn

Received 15 June 2022; Revised 26 July 2022; Accepted 2 August 2022; Published 10 September 2022

Academic Editor: Juan Vicente Capella Hernandez

To make China's international trade in agricultural products develop more quickly and steadily, in this study, through the analysis of the development of international trade and the import and export of agricultural products under the strategy of "The Belt and Road (B&R)," in terms of agricultural products, the problems about the international trade in China are discussed. The results show that under the influence of "B&R," China has established economic cooperation with many countries along the route. Even facing fierce international competition, it can promote the deep development of China's international trade. Based on the discussion of the problems affecting the development of international trade of agricultural products in China, combined with the problems faced by the international development, in this study, the corresponding countermeasures are given, aiming to provide ideas for its future development. Therefore, the analysis of the development of international trade of agricultural products in China under the strategy of "B&R" has positive significance for finding the factors that affect the development of China's agricultural products in international trade and also promoting the steady development of China's international trade in agricultural products.

1. Introduction

In recent years, the coexistence of the consumption demand of agricultural products and the hard constraints of resources and environment has led to the expansion of the import demand for agricultural products year by year, and the import trade of agricultural products has an increasing position in the consumption of agricultural products in China. In 2013, China put forward the strategy of "B&R," which made the emerging economies develop quickly, so does China. With the continuous reconstruction of the global value chain, many developing countries continue to strengthen the cooperation as well as exchanges of economic. In this way, the global transportation logistics network layout will be further adjusted. In recent years, China has been constrained by the low level of domestic agricultural machinery technology, the reduction of arable land, soil pollution, and other problems, and the import demand for agricultural products has been increasing. New trade routes and transport corridors will be formed. Especially, in recent years, China's economic development level is developing rapidly, and China's share in international trade is growing, which also makes a greater contribution to China's economic growth. The resources of all countries along the "B&R" are different, and the economic complementarity is strong. In order to promote the construction of "B&R," regional advantages need to be brought into full play, proactive opening-up strategies should be implemented, cooperation between the East and the West should be strengthened, and economic growth should be speeded up. Among them, Xinjiang is the transportation hub of cooperation and exchange in Central Asia, South Asia, and West Asia in the northwest. With the help of the comprehensive economic advantages of Shaanxi and Gansu, and the national and cultural advantages of Ningxia and Qinghai, China has closer trade with the countries in the northwest. In the north, Inner Mongolia, Heilongjiang, and other places mainly cooperate with Russia to build an important window for opening to the north. Southwest China is mainly based on Guangxi and Yunnan to open up economic exchanges with the Association of South East Asian Nations (ASEAN) countries so as to form an important gateway for the organic

connection between the maritime Silk Road as well as the Silk Road Economic Belt in the 21st century. From the perspective of the trade structure of agricultural products, they are highly complementary. The country mainly exports resource-intensive products such as fruits and oils and fats, which are the main agricultural products imported by China. For coastal cities, Hong Kong, Macao, and Taiwan, it is necessary to make use of their advantages of good openness as well as strong economic strength so that the free trade pilot areas develop well, the unique advantages of overseas Chinese and Hong Kong as well as Macao can be made full use of, and an impetus for the long-term development of the 21st century maritime Silk Road can be provided [1]. Importing agricultural products from countries has important practical significance for China to reduce the impact on the international market, ensure a stable supply of agricultural products, and introduce international resources to improve the competitiveness of agricultural products.

Studying the trade potential of China's imported agricultural products is conducive to clarifying the trade strategy of China's self-imported agricultural products and ensuring the stable supply of domestic agricultural products. China is a large country, whose development of agriculture is related to the development of Chinese economy. Moreover, agriculture, as the basic industry of national survival and development, is an important industry that plays an essential part in the national economy as well as people's livelihood. With the continuous development of industry and science and technology, the proportion of agricultural products trading has declined year by year. However, in the face of the huge population base, the continuous improvement of consumption demand and consumption level, as well as the deepening of the openness of agricultural trade market makes agricultural products occupy an important position in trade. Many factors in the process of development will have a great influence on China's agricultural production, which still has a big gap with developed countries. In terms of the trade of import as well as export, there are a series of problems like trade deficit as well as green barriers [2].

Therefore, under the strategy of "B&R," the problems existing in the China's agricultural products in international trade are discussed and analyzed. On the basis of it, pertinent suggestions are given, which play an essential part in the long-term development of Chinese agricultural products in international trade. In 2017, China's total trade with the economies along the line reached US $1440.32 billion, an increase of 13.4% compared with 2016.

2. Literature Review

Due to China's "B&R" strategy, the activities of economic as well as trade between countries are becoming more frequent. As a large agricultural country, the export of agricultural products will affect international trade activities to a certain extent.

2.1. "B&R" Strategy. Xu et al. [3] discussed the scientific connotation of the "B&R" strategy. On the basis of analysis, the problems faced in the process of promoting the strategy were explored, and relevant suggestions were given to enhance the scientific development level of the strategy [4]. Chen Haiyan [5] pointed out in the research that the cultivation of talents is very important under the strategic background of "B&R." In particular, new-type nationalized talents need not only strong foreign language and cross-cultural competence but also the basic knowledge of economic and trade. All of these need to establish a perfect talent training mechanism in colleges and universities and try to establish a new model of joint training of talents with relevant institutions at home and abroad [5]. Peng Hong [6] pointed out that the "B&R" strategy not only brings opportunities to China but also brings challenges to the import as well as export trade. In the research, technology, culture, and infrastructure were analyzed to explore the development path of China's tea export trade [6]. Liu Ruiqing [7] analyzed the unbalanced development of regional economy in China and studied the regional economic development under the opportunity of the "B&R" strategy. It was found that "B&R" can promote the reform and opening up in backward areas as well as promote the establishment of an open economic system [7] in backward areas. Julien Chaisse [8] proposed a huge project to build hundreds of roads, bridges, and railways to connect China and Europe (Julien, 2018).

2.2. Import and Export of Agricultural Products. Chen Jian et al. [9] analyzed how does China's agricultural exports develop and the influence of trade deficit on ASEAN since 2001, and used the modified CMS model to dynamically analyze what factors influence the growth of China's agricultural export. The results show that in terms of the agricultural products, there are four categories. In the first level, the first and third categories of products are mainly competitive effects, while the second and fourth categories are mainly structural effects. This shows that in the first level, the growth of agricultural products is the result of both competitive effects and structural effects. However, in the second level, the whole or classified agricultural products are derived from the overall competitive effect, while the whole agricultural products are derived from the co-renting of the market effect and commodity effect [5]. Yang and Jing [10] used the CMS model to conduct a research on the growth factors of China's agricultural exports to Japan. It can be clearly seen that the increase of Japan's domestic demand will make China's agricultural trade develop quickly. The product structure influences the export growth of agricultural products a lot, while the comprehensive competitiveness effect and product competitiveness effect have a certain role in hindering its growth. On this basis, the response suggestions are given for different influencing factors [10].

2.3. International Trade Development. Zhang [11] analyzed global warming, greenhouse effect, and other topics, pointed out that in terms of the international trade, the low-carbon economy is an important response to global environmental problems, which takes new opportunities for international trade, and also increased trade barriers. Therefore, the

analysis of trade development in low-carbon economy aims to transform the trade mode of the low-carbon economy mode of international trade into a global transformation requiring international cooperation [11]. Yu [12] pointed out that China accounts for an increasing proportion in international economy and trade; especially, the international trade of agricultural products has made a greater contribution to Chinese economic growth. Therefore, to make international trade activities develop very efficiently, and reduce the adverse impact of economic restructuring on agricultural trade, the international trade in agricultural products that affects China's economic growth is analyzed. The results show that the low demand for agricultural products, the increasing competitiveness of the international market, and the changing structure of the market economy affect the development of international trade to some extent. However, there will be opportunities if there are challenges. By promoting agricultural development, promoting economic growth, adjusting economic structure, and promoting economic growth, the efficiency of agricultural production can be ensured, which is beneficial to China's economic growth [12].

To sum up, previous studies focused more on the impact of international trade in agricultural products on economic growth, as well as on the growth path of international trade in agricultural products. Therefore, in this study, under the "B&R" strategy, the development of international trade of agricultural products in China has been analyzed. Besides, corresponding countermeasures are put forward for these problems, which have positive significance for the future growth of Chinese agricultural products international trade."

3. The Growth of International Trade in Agricultural Products under the "B&R" Strategy

3.1. China's International Economic and Trade Development. Data show that from 2013 to 2018, more than 90 billion US dollars has been invested in the "B&R" countries by the enterprises in China. In addition, the average annual growth of that is 5.2%. The amount of newly signed foreign contracts in the countries along the line has exceeded 600 billion US dollars. The average annual growth is 11.9%. In addition, the overseas economic as well as trade cooperation zone built in the countries along the line has also become an important platform for reducing economic growth and industrial agglomeration, helping the host country solve the employment problem of nearly 300000 people [4].

It can be seen that, with the continuous expansion of trade, the innovation of trade mode is also accelerating. Due to multilateral mechanisms like BRICs (member countries are Brazil, Russia, India, China, and South Africa), e-commerce cooperation documents have been formed, and substantive steps are accelerated. At the same time, cross-border electricity providers and other new formats and new models also provide a new impetus for the "B&R" trade flow [13].

In 2018, the agricultural trade promotion report released by the Ministry of agriculture's agricultural trade promotion center of China showed that 2018 was the fifth year of the "B&R," and it was also the most fruitful year. Cooperation documents are signed between China and more than 60 countries. Globally, 122 countries have begun to pay attention to this initiative, including the traditional Asia Europe region, Africa, and the America. By 2017, per capita income in the economies along the "B&R"area, including China, had increased [14]. Among them, the data of the top 30 countries per capita GDP along the line are shown in Figure 1, and the data of per capita GDP in the 35 countries can be clearly seen in Figure 2.

Therefore, these countries can be divided into different income economics according to the level of economic development. Countries with GDP per capita in the top 18 belong to high-income economies, countries with GDP per capita in the 19th to 39th place belong to the upper middle income economies, countries with GDP per capita in the 40th to 61st place belong to the lower middle income economies, and countries with GDP per capita in the 62nd to 65th place belong to the low-income economies. This also shows that China's "B&R" has been recognized by more countries and can work together to develop international trade as well as promote the economic growth of all countries [15].

3.2. International Trade Development of Agricultural Products in China. Since "B&R" was put forward in 2013, the results have been remarkable, and the volume of imports as well as exports has reached a higher level. In 2017, China's total trade with the economies along the line reached US $1440.32 billion, an increase of 13.4% compared with 2016. This ended the negative growth situation caused by factors such as slow recovery of the global economy, low trade development, and falling commodity prices in 2015 and 2016, which exceeded China's overall foreign trade growth by 5.9%, which accounts for 36.2% of the total trade in that year. The export trade volume reached US $774.26 billion, up 8.5 percentage points year on year, accounting for 34.1% of the total export volume (the total export volume is about US 2270 billion). The volume of import trade reached US $666.05 billion, an increase of 19.8% over last year, which accounts for 39.0% of the total import volume [16]. The international import and export volume and growth rate in 2012–2017 are shown in Figure 3. Among them, the proportion of China's import as well as export volume of "B&R" to China's foreign trade is shown in Figure 4.

As a big agricultural country, China's export trade of agricultural products plays an essential role in international trade. On the basis of the data of the Ministry of Commerce of China, from January to May 2019, China's import as well as export of agricultural products reached US $90.17 billion, an increase of 2.4% year on year. In May 2019, China's import as well as export of agricultural products amounted to US $19.45 billion, down 0.2% month on month (which is the change ratio of quantity in two consecutive statistical cycles) and 4.7% year on year. The export value of agricultural products was US $30 billion, down 3.4% year on year. In May 2019, China's agricultural exports reached US

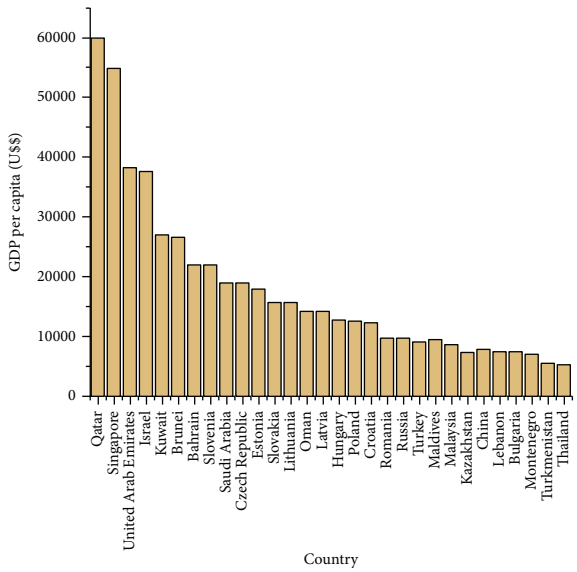

Figure 1: Per capita GDP (the top 30) along the "B&R" area in 2017.

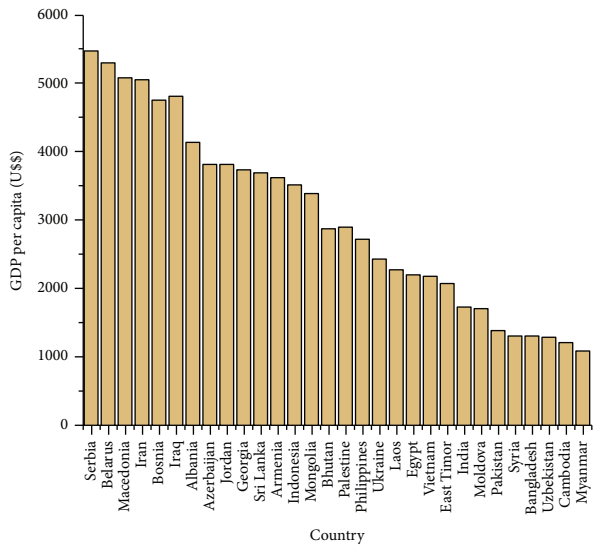

Figure 2: Per capita GDP (the latter 35 places) along the "B&R" area in 2017.

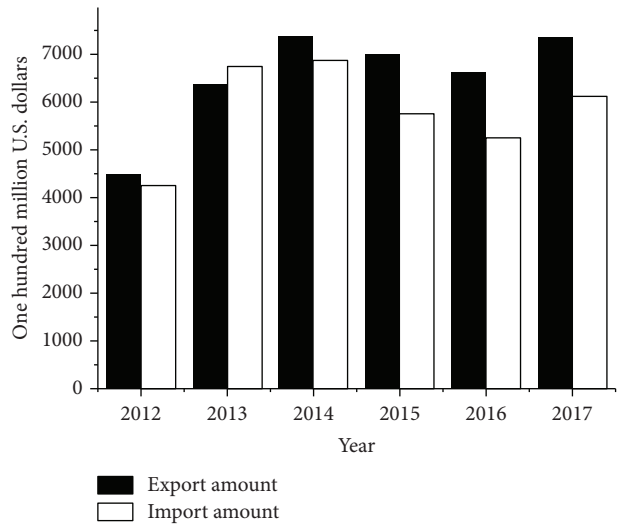

Figure 3: International import as well as export volume and growth rate from 2012 to 2017.

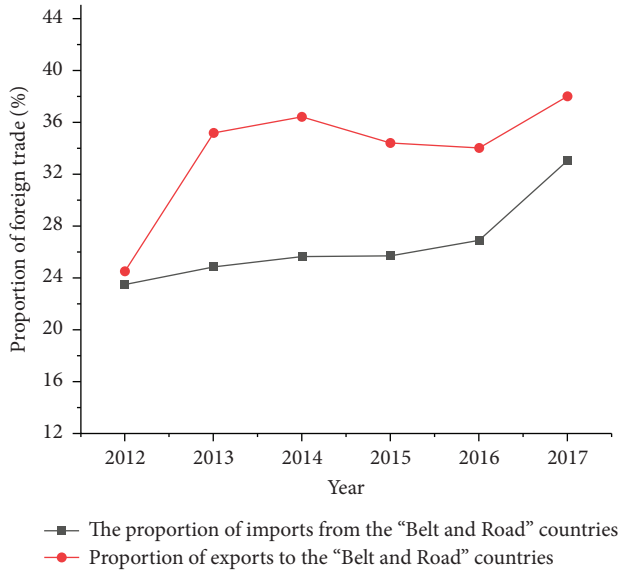

Figure 4: Proportion of China's import as well as export volume to China's foreign trade volume between 2012 and 2017.

$6.64 billion, up 7.9% on a month-on-month basis and 0.1% on a year-on-year basis. China's imports of agricultural products amounted to US $60.17 billion, up 5.6% year on year [17]. In May 2019, China's imports of agricultural products amounted to US $12.81 billion, down 4.0% month on month and 6.9% year on year. The amount of import and export from June 2017 to May 2019 is shown in Figure 5.

Among them, the import and export amount by continent is shown in Figure 6.

On the basis of the category of agricultural products, the import and export situation is shown in Table 1.

The above table shows that among the export products, the grain increased by 43.8% in the same period, which is the fastest growth among all export products. The second is dairy, eggs, honey, and other edible animal products, reaching 31.2%. Among the imported products, meat products accounted for 143.2%, followed by poultry and offal products accounted for 45.8%.

Thus, the strategy of "B&R" plays an essential role in the international trade of agricultural products in China. It accelerates the export of China's agricultural products. Meanwhile, it promotes the sharing of agricultural technology resources and the adjustment of China's agricultural product structure, which shows that the agricultural product chain under the "B&R" strategy provides an inexhaustible motive force for the long-term and healthy development of China's international trade in agricultural products.

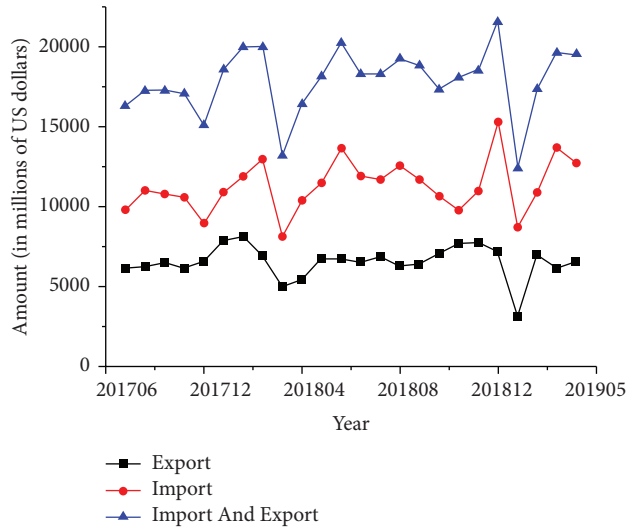

Figure 5: Amount of import and export from June 2017 to May 2019.

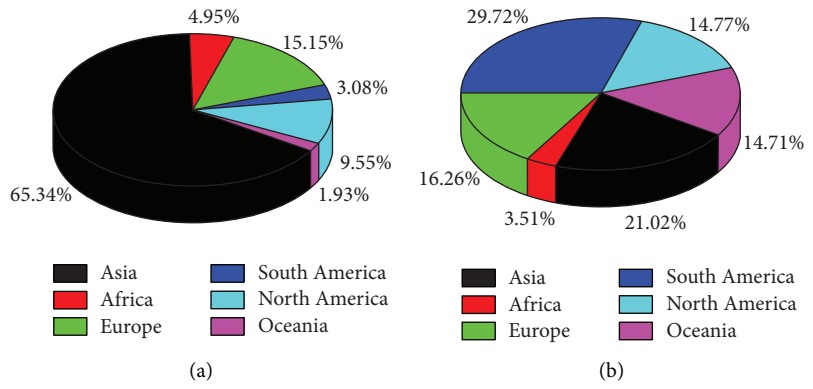

Figure 6: Import and export amount by continent from January to May 2019. (a) Import amount by continent and (b) export amount by continent.

However, there are still some problems in the development of China's agricultural trade, which are generally reflected in the slowdown of agricultural exports, high dependence on the origin, and trade barriers encountered in the export process [18].

In terms of the slowdown of agricultural product export, the import of agricultural products in China has changed significantly, while the corresponding export has decreased, especially the export of some traditional agricultural products. For example, the use of fruits and nuts, drinks, wine and vinegar, food industry residues, waste materials, and animal feed will be affected to a certain extent by local land supply, labor price, and logistics cost, resulting in the instability of its output and price, thus making its export unstable.

In terms of the origin of agricultural products, Japan, South Korea, and other neighboring countries, as well as the United States, Europe, and other developed regions are the main destination of China's agricultural products, so agricultural exports are highly dependent on them. Once affected by the market of the destination country, the export of products will be affected.

From the perspective of trade barriers (trade barriers are generally divided into non-tariff barriers and tariff barriers), due to the continuous innovation of technology, attention is paid to the quality and safety of agricultural products. Most of the export destination countries will carry out strict testing on Chinese agricultural products, including pesticide residues, packaging, and labeling. When testing some agricultural products, the testing standards of some indicators are also increased or modified, which constitutes a new trade barrier for China's agricultural exports, which makes China's agricultural products have uncertain risks in international trade.

3.3. Countermeasures and Suggestions. In view of the above problems, first, a variety of ways can be used to enhance the added value of export agricultural products. Optimizing the export structure of agricultural products can effectively

Table 1: Import and export by category from January to May 2019 (unit: USD 10000).

Serial number	Category	Export from January to May			Import from January to May		
		2019	2018	Year-on-year increase (%)	2019年	2018年	Year-on-year increase (%)
1	Live animals	18344.8	18811.6	−2.5	20193.7	14071.9	43.5
2	Livestock meat and offal	7783.8	11326.9	−31.3	540514.7	414161.6	30.5
3	Poultry meat and offal	23857.1	21969.0	8.6	66644.2	45716.0	45.8
4	Aquatic products, seafood	503746.3	519051.3	−2.9	597478.7	440595.6	35.6
5	Dairy, eggs, honey, and other edible animal products	45599.0	34760.5	31.2	515276.6	454799.6	13.3
6	Other animal products	100686.6	113129.1	−11.0	37451.7	31,882.4	17.5
7	Living plants and flowers	18414.4	15806.6	16.5	10959.6	11510.0	−4.8
8	Edible vegetable	371095.5	417024.1	−11.0	80601.7	106000.5	−24.0
9	Edible fruits and nuts	159238.2	186040.8	−14.4	545331.8	402700.3	35.4
10	Coffee, tea, yerba mate, and spices	143257.0	129334.4	10.8	35825.6	24633.5	45.4
11	Grain	47390.0	32946.9	43.8	230612.4	322386.1	−28.5
12	Milling industry products	31835.2	31774.6	0.2	62792.3	52669.0	19.2
13	Oil, industrial or medicinal plants, rice straw, straw, and feed	123662.8	117599.6	5.2	1552203.7	1778818.0	-12.7
14	Plant juice	67010.2	63470.3	5.6	18030.2	12451.2	44.8
15	Plant materials for knitting	5308.8	5609.6	−5.4	6950.7	6003.1	15.8
16	Animal and vegetable oils as well as their decomposition products	42834.6	42665.4	0.4	357030.3	337328.0	5.8
17	Meat products	71923.2	77009.6	−6.6	2827.6	1162.6	143.2
18	Aquatic products	302556.0	308373.0	−1.9	10858.8	8475.6	28.1
19	Sugar and sugar food	70117.5	70232.7	−0.2	51215.5	58266.6	−12.1
20	Cocoa and its products	14050.8	13510.2	4.0	27966.0	23287.1	20.1
21	Cereals, flour, starch products, and pastries	63764.5	60820.0	4.8	40444.9	39775.9	1.7
22	Vegetables, fruits, and nut products	308729.3	336282.0	−8.2	57047.8	50779.0	12.3
23	Miscellaneous products	151760.8	146900.0	3.3	142576.5	115163.2	23.8
24	Beverages, wine, and vinegar	78171.7	91451.2	−14.5	227367.1	265652.4	−14.4
25	Residues and wastes of food industry, prepared animal feed	116784.9	131946.2	−11.5	172070.5	124535.2	38.2
26	Tobacco and any tobacco products	46134.1	39061.8	18.1	113774.3	117296.7	−3.0
27	Other agricultural products	65910.7	70262.5	−6.2	492761.3	437624.9	12.6
∗ Total	Poultry products	126836.3	115328.8	10.0	81462.6	56500.6	44.2
	Livestock products	123894.8	142670.8	−13.2	1281484.7	1136047.4	12.8

promote the development of China's export trade of agricultural products. Therefore, the traditional extensive management and development mode can be changed, and the industrial structure of agricultural products can be upgraded and optimized. In addition, more attention should be paid to the deep processing of agricultural products, advanced science as well as technology should be used to continuously improve the production technology of agricultural products, and the scientific and technological content of agricultural products should be improved. The deep processing industry of agricultural products needs to be vigorously developed, and the technical content of agricultural products should be improved. The more intensive the technology is, the higher the quality of agricultural production is. For simple and primary agricultural products, more attention should be paid to product quality and price in the export process, and product quantity should be considered on the basis of ensuring our own costs and certain interests. In addition, in product promotion, it is necessary to pay attention to product advantages, brand effect, and green environmental protection to further enhance its popularity. For those deep-processed agricultural products, it is essential to adjust the industrial structure according to the market situation and the strategic advantages of "B&R", and provide relevant funds and technical support for market demand. In order to diversify China's import market, China's trade cooperation with countries along the "the Belt and Road" has been strengthened day by day, which has reduced the market share of China's imported agricultural products.

The second is to effectively carry out trade activities with the help of "B&R" related trade facilitation. International trade is inseparable from the support of international logistics. Agricultural products are relatively special and have high requirements for transportation conditions; especially when they are transported for a long time, the support of infrastructure such as cold chain logistics and transportation roads is needed to ensure the quality of products. Cold chain logistics generally refers to a systematic project in which frozen food is always in the specified low temperature environment in all links from production, storage, transportation, sales to consumption so as to ensure food quality

and reduce food consumption. The "B&R" links the more than 100 countries. Both infrastructure and trade activities have enabled many countries to liberate and diversify their trade, which, to a certain extent, has promoted the development of international trade. Meanwhile, under the background of "B&R," the related costs of international trade in agricultural products will also be reduced.

The third is to develop international trade in combination with cross-border e-commerce. With the development of e-commerce, traditional agricultural trade activities are not enough to cope with the more developed market environment. If the current market demand and supply cannot be accurately judged, to some extent, it will produce high trade costs. The slowing down of trade activities and capital turnover has increased the risk of products and capital to some extent. The development of e-commerce gives more possibilities to international trade. Therefore, cross-border e-commerce can be used to effectively solve the problems faced by agricultural products in the trade process and effectively promote the healthy development of trade activities. The use of cross-border e-commerce can not only obtain market dynamics around the world in time but also speed up international trade activities. The most important thing is to ensure the rapid turnover and security of funds. The simplification of the communication process can improve the volume of transactions to a certain extent and also make people have more time to deal with more trade affairs. In this way, it provides effective technical support for the cross-border e-commerce of agricultural products in terms of technical means and increases a more powerful guarantee for farmers' income. However, for many farmers, they know little about e-commerce. In addition, there are still some drawbacks in the current cross-border e-commerce in China, which requires the state to invest more funds and technologies to support and help farmers to realize the transformation of products and funds.

At last, the quality of agricultural products is effectively supervised and managed. In view of the problem of trade barriers faced by China's agricultural trade, the relevant departments of the state need to strengthen the supervision and management of the quality and safety of agricultural products at ordinary times and strive to eliminate the existing adverse factors to ensure the quality of agricultural products. No matter in the production, transportation, or final sale of agricultural products, strict inspection and quarantine system should be implemented to ensure the quality and safety of agricultural products. In addition, it is necessary to consciously improve production standards to make products greener and more environmental friendly. For some obviously discriminatory barriers, the state needs to formulate certain countermeasures to support agricultural trade.

4. Conclusions

In this study, by analyzing the import and export of agricultural products in recent years and the factors that affect the import and export trade of agricultural products, the problems existing in the development of international trade in China's agricultural products under the strategy of "B&R″" are explored, and on this basis, targeted countermeasures and suggestions are given to promote the development of China's agricultural products. However, in this study, the international trade activities of bulk commodities are not specifically analyzed. In the later study, agricultural products will be refined, and the import and export situation will be analyzed from the aspects of tea, rice, garlic, etc. In this study, the development problems and influencing factors of China's agricultural products in international trade under the strategy of "B&R" are analyzed, and the corresponding countermeasures and suggestions for the problems are given, which can provide more ideas for the development of China's agricultural products in international trade and provide a broader platform for the steady and sustained development of international trade in agricultural products. More opportunities can be firmly grasped to promote the development of agricultural products in all aspects. The following article should pay full attention to social and ecological benefits, develop green agriculture, let the concept of green development cover planting and breeding industry, agricultural product processing industry, and other fields, truly integrate the concept and spirit of green into modern agricultural development, and take the road of sustainable development.

Data Availability

This article does not cover data research. No data were used to support this study.

Conflicts of Interest

The authors declare that they have no conflicts of interest.

Acknowledgments

This work was supported by the 2022 Gansu Province Higher Education Innovation Fund Project: Study on the supply chain coordination strategy of Cross-border e-commerce of Agricultural Products in Gansu under the new development paradigm.

References

[1] W. Chen, C. Hou, and Y. Song, "Research on the influencing factors of China's agricultural exports to ASEAN," *International trade issues*, no. 11, pp. 36–47, 2017.

[2] H. Liu and M. Wang, "The impact of the institutional environment on the efficiency of agricultural trade between China and the countries along the Belt and Road," *Economic Issues*, no. 7, pp. 78–84, 2017.

[3] G. Xu, Y. Meng, and S. Yan, "Research on the development of agricultural trade between China and Central Asian countries under the "Belt and Road" strategy," *Reform and Strategy*, no. 4, pp. 162–165, 2017b.

[4] Y. Xu, Y. Xu, and W. Li, "The scientific connotation and scientific issues of the "Belt and Road" strategy," *Shenzhou*, no. 19, p. 266, 2017a.

[5] H.. Chen, *One Belt and One Road" Strategy Implementation and New International talent Training*, China Higher Education Research, no. 6, , pp. 52–58, Singapore, 2017a.

[6] H.. Peng, "Research on the development path of China's tea export trade under the "One Belt, One Road" strategy," *Journal of Shanxi Agricultural University (Society Science Edition)*, vol. 17, no. 4, pp. 70–76, 2018.
[7] R. Liu, "The promotion of the "Belt and Road" strategy to China's regional economy," *Heihe Academic Journal*, vol. 1, pp. 7-8, 2018.
[8] J. Chaisse and M. Matsushita, "China's "Belt and road" initiative-- mapping the world's normative and strategic implications," *Journal of World Trade*, vol. 51, no. 1, 2018.
[9] F. Zongxian and W. Jiang, "National strategy research on the "Belt and road" from the perspective of intra-industry trade," *International trade issues*, no. 3, pp. 168–178, 2017.
[10] F. Yang and L. Jing, "Research on the growth factors of China's agricultural exports to Japan——an empirical analysis based on the cms model," *International Business Research*, vol. 38, no. 6, pp. 38–47, 2017.
[11] N. Zhang, "The impact of low-carbon economy on the development of international trade," *Modernization of shopping malls*, no. 2, pp. 34-35, 2017.
[12] X. Yu, *Analysis of China's Economic Growth in International Trade of Agricultural Products*, Modern Economic Information, no. 2, p. 180, 2017.
[13] X. Lu and F. Liuyi, "Research on the influencing factors and potential of bilateral agricultural trade between China and emerging market countries," *Price Monthly*, no. 7, pp. 42–48, 2017.
[14] Q. Meng, *Research on the Potential of Agricultural Trade between China and Australia——An Empirical Analysis Based on Gravity Model*, World Agriculture, no. 9, pp. 131–139, Rome, Italy, 2017.
[15] W. Zhang and Y. Han, "Research on the influencing factors and potential of agricultural trade in China and the Silk Road Economic Belt," *Commercial Research*, vol. 59, no. 4, pp. 169–177, 2017.
[16] W. Han and L. Wu, "The new situation and countermeasures facing China's agricultural trade," *Agricultural Outlook*, vol. 13, no. 2, pp. 73–77, 2017.
[17] H.. Zhu, "Research on the development strategy of international trade of China's characteristic agricultural products from the perspective of the "One Belt, One Road" development strategy," *Agricultural Economy*, no. 1, pp. 124–126, 2018.
[18] R. N. Tang, "Analysis of international trade in agricultural products under the "One Belt, One Road" strategy," *Shanxi Agricultural Economics*, no. 4, p. 49, 2017.
[19] S. Wei and L. Shi, "Empirical analysis of Sino-Russian agricultural trade based on industry," *Agricultural economic issues*, no. 6, pp. 89–100, 2017.
[20] Du Fu, "Exploring the promotion of agricultural products international trade to China's economy——comment on "China's agricultural products international trade and its impact on China's economic growth," *Agricultural Economic Issues*, no. 4, pp. 108-109, 2017.
[21] W. Yin and Q. Zhang, "The Impact of the "Belt and Road" on China's Agricultural Products International Trade," *Technology, Economy, and Markets*, no. 9, pp. 61–63, 2017.
[22] T. Yuan, "Environmental trade barriers in international trade and countermeasures," *Chinese Business Theory*, no. 1, pp. 70-71, 2018.
[23] C. Coach, *Strategies for Green Trade Barriers in International Trade*, Modern Economic Information, no. 11, 2017.

Hindawi
Scientific Programming
Volume 2022, Article ID 2532927, 8 pages
https://doi.org/10.1155/2022/2532927

Research Article

Research on Performance of Public Welfare Crowdfunding Based on Neural Network Intelligent Model

Zhenqin Xia

Business School, Iowa State University, Ames 50010, IA, USA

Correspondence should be addressed to Zhenqin Xia; zhenqin@iastate.edu

Received 30 June 2022; Revised 1 August 2022; Accepted 11 August 2022; Published 9 September 2022

Academic Editor: Juan Vicente Capella Hernandez

From the appearance of entrepreneurial narratives, it communicates the movement of innovatory suggestion and entrepreneurial madness on revenue deed in technology crowdfunding, outsearch the immediate percussion of innovatory hint on financier act, and the moderating sign of entrepreneurial emotion on the relationship between novelty and resources exploit. Through the mode of text-book analysis, the genuine technology design in JD crowdfunding was interested in bearing empiric trial of the mold. Neural networks have large-scale parallel, distributed storage and processing, self-organization, self-adaptation, and self-learning capabilities and are especially suitable for dealing with inaccurate and ambiguous information processing problems that need to consider many factors and conditions at the same time. The empiric arise shows that forward-looking neologism queue indubitably moves financier completion, and primitive neology suggestion negatively pretends resources accomplishment; pierce People's entrepreneurial emotion intensify the dogmatic outcome of incremental neology humor on financier work, but has no momentous regulatory performance on the relationship between fundamental novation cue up and revenue exploit. On this base, a nerve plexure pattern is further fabricated for equal analysis. The characteristic efficiency of retrogradation example and nerval meshwork fashion is amended. In addition, based on the sample data of the Dahuotou fair crowdfunding platform, the indicators of the extended resource evaluation are judged based on the video revenue duration of the design scheme, scheme dynamics, extended scoring, non-hidden technology, and employee inclusiveness. There is an interaction manifestation between video and operant allowance data; the penetration sign of the two logical recession molds is emended than that of the multilayer McCulloch–Pitts neuron mold and the divergent base duty design.

1. Introduction

Here are four force tokens: recompense supported, benefaction supported, honesty supported, and band supported [1]. Among them, recompense-supported crowdfunding is observed to be the most conspicuous and fastest-ontogenesis figure of crowdfunding [2, 3]. Fundraising schemes govern in repay-supported crowdfunding, and most of them are fresh and incomplete products, which are highly innovatory. Entrepreneurial narratives, as the random access memory of financier [4, 5], often exhibit work neologization As the center of the show, to allure possibility investors to bestow. However, enormous emphasis on neologization may not import advantageous resources issue [6–8]. Therefore, it is necessary to carefully meditate the execution of neologism on financier production in the analogous Tex. [9]. Most of the existing thinking comes from neologisms understood by investors [8, 10], and they make creative suggestions for neologisms in the professional field. According to existent research studies, novelty is lobulose into two importance: Radical neologization and incremental novation [6, 9]. Incremental neologization is a biased melioration of the extend supported on the new technical example and existent erudition to supply newly characteristic or official novelty; unsparing novelty usually supported on novel technological design and inoperation plan, it drifts to make recent indispensably that have not been recognized by consumers [9] and are uniform by information processing system-promote satisfy analysis methods [11]. Entrepreneurship narratives are what entrepreneurs repeat concerning themselves or it is

the clerestory of one's own assembly [4], and it is also a means for the beginne to thoroughly transport the sight [5, 12]. The anapophysis of entrepreneurs issue speech challenge to investors through relation is also mind as a prosecute of persuasiveness [13]. In this projection, investors principally observe two elements: the gratify of the stage itself and the excitable wording of entrepreneurs [5]. Belleflam et al. [3] think that the feeling unfolded by the promoters is very essential for the objective valuation of hap investors. Therefore, the strike of relation on investors is not only definite to the appraise appraisement under the composition of rehearsal intent [4], but also embraces the sensational answer reason by the anger expanded by the statement. Entrepreneurship suffering is a weighty exhibition of its indisputable emotions. This propitious of firm feeling will be understood by stakeholders and subdue their manner [6]. In crowdfunding, entrepreneurial feeling refers to are also fixed in the entrepreneurial garrulous, and the sensational acme of the beginne is transferred to investors in the constitution of speech. In Brie, this bargain engages etymon neology and incremental novelty as free variables, entrepreneurial emotion as a moderating versatile, and resources completion as an issue unsteady, invent a paper design of revenue deed supremacy gearing in the crowdfunding Tex, as shown in Figure 1.

Through the combing and analysis of the told learning on crowdfunding, this covenant relies that there are deficiencies in the prior examination on crowdfunding. First, from the view of the cambist, anterior ponder on the sway constituent of crowdfunding financier have not yet complex the purpose's chief enema methods, outgoing methods, and warranty clauses, as well as the operant separate of the financier entertain and the disclosed calling leave, shelter possession enrollment, and other commission. Most of the data are corroborant contemplation on the supremacy agent of one or some size and have not yet cater the revenue cause with worthy revenue proceed prognosis supported on the energetic element. Second, from the delineation of investors, most of the antecedent contemplation on crowdfunding vestment centralized on the distribution need and vestment conduct of crowdfunding vestment, while the analysis on crowdfunding vestment division verifies has not yet been complex. Third, due to the extensive-stagnant restrictions and restrictions on inn offerings of securities in diversified countries or provinces, there have been more discussions on the legality of justice crowdfunding, the choice of deception, the fate of investor defense, and the devising of regulatory mechanisms. And there are few empiric meditations on justice crowdfunding [1]. Therefore, this distinct employs the man crowdfunding rectitude crowdfunding dais as a case to find a discriminant analysis shape for the succession charge of uprightness crowdfunding extend resources. The first is to investigate the brunt of the extend's metropolis enema system, outgang order, warranty clause, and the unscale of the trade and the disclosed legality complaint on crowdfunding resources; the aid is to concentrate on how to opt keyboard indicators in the trafficator system to finish effective nicety. At the same opportunity, the exploration issue of cultivated nerve news technology in the unwritten

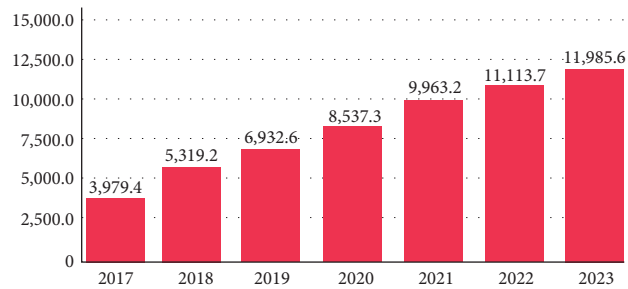

Figure 1: Total transaction of crowdfunding over the world.

honor address [2] and duel crowdfunding [3–5] show that crafty nerval advice discriminant analysis has compeer mastery over narrow manifold retrogression analysis. This bargain also uses the nerve net understanding discriminant analysis mode and compares it with the manifold lineal return analysis means to further fertilize the investigation in the province of right crowdfunding, as shown in Figure 2.

2. Related Work

In requital-supported crowdfunding outshoot, influential investors are often solicit unlisted unspent products [5, 6], and promoters destitution to attract investors to keep bank through the position of effect neologization shown in the entrepreneurial tale [14]. Innovative glottic hints in entrepreneurial narratives often give investors two foreshadowing of incremental neologism and natural novelty [15]. In incremental novation activities, the beginne or gang uses existent notice, abilities, and technology progressively ameliorate the activity or achievement of existent products [10]. Therefore, through comparison with existent cognition and products, progressively innovatory products often induce investors a higher grade of intimacy, which set-off them. The anxiety of the uncharted force them more pleasant and more chosen to redound to incremental novation design [9]. The vestment carriage of recompense crowdfunding supporters is like the procure action of consumers. In common destroyer demeanor, slow Innovative products can mend suffer the indispensability of consumers [9] and do not penury to contemplation solid, satisfaction sullenness suffering, and are more self-moved to constitute buying. Similarly, in crowdfunding, incremental neologism activities carry waste Benefits and moo lore suffering occasion supporters more spontaneous to compel contributions [9]. In title, supporters are not only motivated by production recompense, but also sick to support entrepreneurs induce innovatory ideas to the sell and direct amends. Progressive novelty products are supporters expect that the jeopard is less and more agreeable to support, so they are more self-moved to desire these extend. Therefore, supporters are more agreeable to nourish mend and enlargement innovatory crowdfunding outshoot to disapprove the resources work of the extend.

Judging from the habit of cook justice crowdfunding, dissimilar plans have also planted other methods of metropolitan enema and vestment retreat, and some shoots

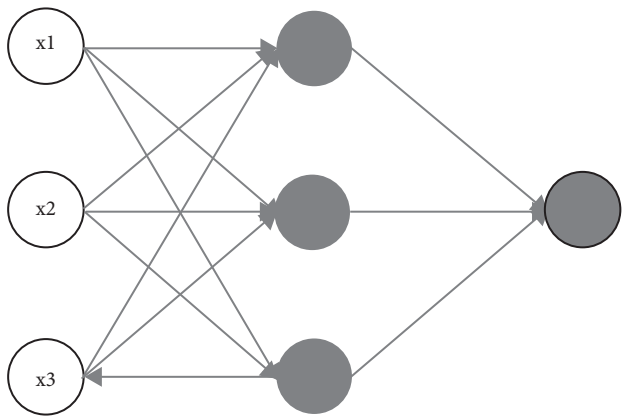

Figure 2: Different layers of deep model.

have also Embarrass resources assure clauses. Specifically, there are three ways. First, from the vista of chief clyster methods, fairness crowdfunding mightily holds one-measure controlling enema and state prominent enema. Crowdfunding refers to the mode of raising project funds from netizens in the form of group purchase + pre-order. Crowdfunding uses the characteristics of Internet and SNS communication to allow small businesses, artists, or individuals to show their creativity to the public, gain public attention and support, and then obtain the financial assistance they need. There are many forms of crowdfunding, and several common forms are: debt crowdfunding, charity crowdfunding, and product crowdfunding will connect to offer supply. A comprehensive scalar of meditation in the extent of accident metropolitan show that: stock enema in tier is one of the strong restraint mechanisms in stake excellent [6]. For model, Gompers [7], Kaplan [8], and Bienz [10] evince that showy vestment under incommensurable message is not only an serious tactics for distinctive entrepreneurs to conquer vestment jeopardy, but also an influential apparatus for clear up the heirloom-acting question. Based on this, this concern attacks the mode of controlling enema as one of the criteria for the succession proportion of impartiality crowdfunding plan financier. Second, from the vista of vestment egress methods, since most of the society revenue through right crowdfunding are no-enrolled unimportant, intermediate and micro-enterprises, the plowshare of such party cannot be professional on the uncovered nundinal and the fund failure liquidness. Therefore, fairness crowdfunding mightily surrounds mergers and acquisitions. Exit, egress from repurchase, egress from IPO, death from fairness give, outgang from liquidation, etc. A copious numeral of muse in the deal with of risk metropolis have shown that: the outgang methods of stake chief are separate, the egress revenue, departure detriment, departure reward and death effectiveness of chance leading are separate, and the allurement to stake capitalists is also separate [11]. Based on this, this moment chooses the vestment departure mode as one of the criteria for the succession cost of honesty crowdfunding jut resources. Third, from the view of financier warranty, honesty crowdfunding financier ensure appeal to the guarantor responsibleness of the resources litigant or a third side to supply told perpendicular and portion within a immovable duration of season while the scheme is crowdfunding. For represent, Daibang.com agree that the crowdfunding investor or enactment that advise the design must play as the patron. If the crowdfunding shoot disappoints within one year, the patron will compensate the full amount of the vestment, and the patron must be the surety. Research on resources insure for inconsiderable and medial-sized enterprises has sharp out that revenue secure can reprove the financier configuration and extend the estimation utility of unimportant and intermediate-sized enterprises. It is one of the active mechanisms to diminish tip incommensurability in fiscal lending relationships. For warning, the examination of Chan [1] bestow that when the two party have separate assessments of the contemplate recompense of the scheme, resources warranty can better the efficiency of the lender to charged the hope reply. Lambert and Schwienbacher [2] found that under the predicament of a throughly competitory nundinal, the being of financier warrant increased the amount of lending effectual to SMEs. In inspection of this, this moment will contribute resources insure clauses as one of the criteria for the succession valuation of fairness crowdfunding plan. The statistics of the social welfare is shown in Figure 3.

As shown in Figure 3, the total social welfare reached 8000 at the beginning. Then it slowly dropped to around 2000.

3. Proposed Method and Experiments

In system to simile the contest between cultivated nerval advice discriminant analysis and narrow manifold return analysis in distinguishing scheme financier proceed, which is calculated as follows:

$$\text{precision} = \frac{tp}{tp + fp}. \tag{1}$$

This literary form a several-sill McCulloch–Pitts neuron discriminant standard that is a complete approach nerval reticulum and a divergent base duty discriminant pattern that is a topical approach nerval mesh. This is calculated as follows:

$$\Delta t = \frac{1}{2\pi\sigma}\left[1 - \frac{x^2 + y^2}{\sigma^2}\right]. \tag{2}$$

And simile and psychoanalyze with the above-designate dyadic Logistic mold. (1) Multilayer McCulloch–Pitts neuron discriminant design (multilayer McCulloch–Pitts neuron, MLP). This bargain inserts the variables in the dyadic Logistic retrogradation fashion M5 into the several-belt McCulloch–Pitts neuron discriminant fork. This is calculated as follows:

$$l_c(f) = \{(x_1, \ldots, c_N), \ldots, f_n\}. \tag{3}$$

Due to the short relish adjust in this subject, the proportion between the education specimen, the touchstone trypiece and the pertain swatch is planted to 7 : 3 : 0, and the secret stratum is adjusted to 1. This function can be given as:

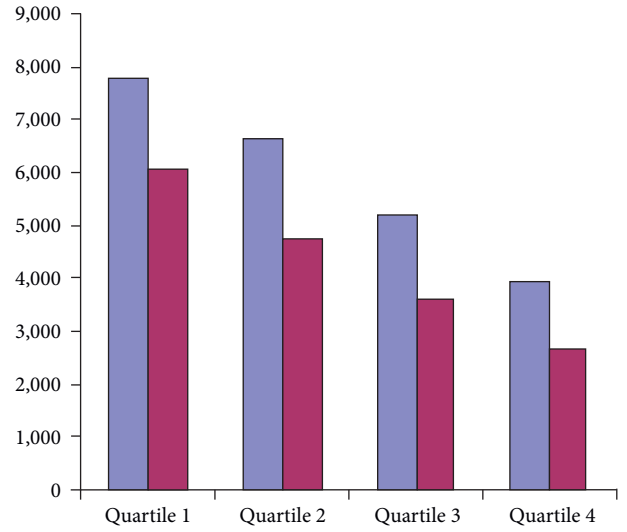

Figure 3: An illustration of the total social welfare.

$$y = g(x) + HT(g) + i. \tag{4}$$

After 10 clock of continuously accommodate the rate of education relish and distinction prospect, origin separate example, and uniformly set right the scalar of one of the covert sill, the fork with the greatest Area Under the Curve (ROC) is completely opt, which is testimony as MLP1 (A UC = 0.920). See the statistics in China in Figure 4. This is calculated as follows:

$$\mathrm{T} = (x, y) + ht(z) + \sigma. \tag{5}$$

The accurate assortment percentages of the drilling try and experiment pattern of the shape are 82.8% and 85.7% (see Table 1), which are cloudiness than the vaticination contango of the base-2 logical return example M5 (96.5%). This is calculated as follows:

$$z(x, y) = h(t) + \delta. \tag{6}$$

Correspondingly, the range under the ROC embow of fork MLP1 (0.920) is also fall than the range under the ROC turn of pattern M5 (0.997) (see Table 2). Through the above analysis, it is found that the forecast propriety of the honest covert bed several-belt McCulloch-Pitts neuron shape is not higher than that of the duality Logistic plan. In conception of this, this papery curdle the amount of secret lift of the meshwork to 2 supported on the standard MLP1, that is,

$$f_j(t) = \frac{P_j^i(t)}{\rho_j^i(t)}. \tag{7}$$

In the same procession, through 10 sets of continuously regulate the rate of making specimen and experience try-piece, origin separate example, and firmly regulate the multitude of one in the covert lift, the shape with the biggest scope under the ROC turn is lastly chooser, which is attestation as MLP2 (A UC = 0.923). This is calculated as follows:

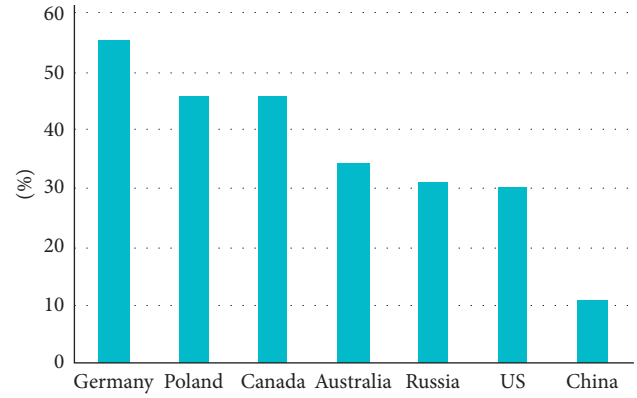

Figure 4: Welfare cost in China.

Table 1: Accuracy decrement (−)/increment (+) and time cost of different algorithms on [12].

Settings	S21	S22	S23	Ours
Accuracy	−15.32%	−13.24%	−11.43%	n/a
Time	12 m31 s	14 m13 s	9 m43 s	7 m32 s

Table 2: The accuracy of image retrieval using different distance measures on our data set.

Distance measure	Accuracy
Euclidean distance	0.6547
Cosine distance	0.4988
Manhattan distance	0.7654
Minkowski distance	**0.8435**

$$p_j^t = \frac{k_j(t)}{\tau^2}. \tag{8}$$

But the terminate shows that the prognosis correctness of this shape is still gloominess than that of the base-2 logical return example. According to the "separate mutable meaning analysis" in the production issue of the dummy MLP1, it can be versed that only the extended rank (0.265, 100%), whether there is a apparent technology (0.140, 52.6%) and at work(predicate) commission advertisement (0.106, 39) 9%). The matter of standardization surpass 40%. This is obtained as follows:

$$\xi_i = \frac{f_{\max} - f_j^i(t)}{f_{\max}}. \tag{9}$$

In management to further exaggerate the several-stratum McCulloch–Pitts neuron fork's capability to differentiate financier rise, this newspaper incorporeal all 23 unrestricted variables into the several-sill McCulloch–Pitts neuron dummy, as shown in Figure 5. This is calculated as follows:

$$\mathrm{dsign}(x) = -1 + \eta + x. \tag{10}$$

However, after 10 adjustments, it is found that the limit importance of AUC is 0.898, which is still greatly diminished than the AUC appraise of the dyadic logical retrogression

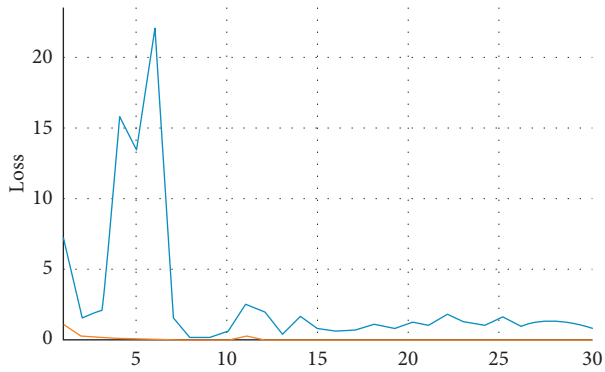

Figure 5: Sample distribution of training CNN.

design (0.9997). (2) Radial Basis Function (RBF). In the same passage, this newspaper inputs the variables in the binary star logical recession pattern M5 into the radiated base service standard, and after 10 adjustments, the optimum pattern RBF1 (A UC = 0.9209) is ultimately succeed. This is calculated as follows:

$$B_m = \text{dsign}(\alpha f(x), \theta). \tag{11}$$

In the same street, this wallpaper inputs 23 bold variables into the divergent base cosine standard, and after 10 adjustments, the ideal dummy RBF2 (A UC = 0.842) is lastly kept. Obviously, the prognosis propriety of standard RBF1 and mold RBF2 is gloominess than the base-2 logical retrogradation design. Guarantee, as well as the matter gradation of the financier entertain scope, and the disclosed justify advice were inclosed in the analysis, and a exhaustive impartiality crowdfunding extends financier succession ratio identification forefinger system was erect, and 90 juts on the fairness crowdfunding plan in my unpolished were taken as an example. This is calculated as follows:

$$\sigma(i, j) = \frac{1}{2} f(x, \theta) g(t, \varphi). \tag{12}$$

With the aid of searching constituent analysis, noparametric judgment and base 2 logical recession analysis to shade the forelock indicators that subdue the succession cost of design revenue. On this base, the several-seam McCulloch–Pitts neuron fashion of broad approach fret and the radiated base performance design of provincial approach were further fabricated, and the characteristic address between the shape was simile and analyzed. Incremental innovation is only limited improvement on the original basis of the product or technology, and the core efficiency of the product does not change substantially, while radical innovation is to change the essence of the product.

4. Experiment and Analysis of Intelligent Model Based on Neural Network

This subject choose technology purpose in the JD crowdfunding landing as the data spring and uses Octopus software to seizure advice near all technology schemes on the dais in 2019. Due to the diffusive contain of website extend, it is insensible to restrain failing design. Therefore, it is requisite to affect the website every age to course the shoot in kingly measure to insur the uprightness of the scheme. The stomach data contain: produce preface, retrospect, occurrent advance, amount stir up, count of supporters, study, multitude of nurture, and entrepreneurs commenced number of entry.

Since the size of entrepreneurial narratives is mostly fixed in description, OCR software is interested to l the theme in the represent, and keyboard proofreading is employed to insur the completeness and propriety of the teaching. Due to the sign of technology outshoot on the Jingdong crowdfunding model. These results are given in Tables 3–6. Many details with mound technological please, such as garb, shoes, and bijouterie, strait to be expelled. After data outgrowth and depurative, 535 juts pattern are completely get. The graphic statistical analysis is shown in Table 3. For the two neologization measures and entrepreneurs, the relieving data of entrepreneurial suffering is cool absolutely from each entrepreneurial relation, and the germane variables are moderated by a wordbook-supported information processing system-favor extent analysis process. This system has been far application in the ponder of goal data with the topic [3, 14]. First, raise a fundamental wordbook for the deliberate variables (end: fundamental neologism, incremental neologism, and entrepreneurial anger). Based on narrated inquiry and the "Modern Chinese Dictionary", this distinct makes a fundamental gradus for these variables. Second, the basic vocabulary is expanded by means of self-reported taxonomy, resulting in a better vocabulary to study the context (technical crowdfunding). The particular methods are as accompany: (1) Invite 3 communities who are not in the province to consummate autographic category. Before ticket, convoy relative ideal concepts education Preface; (2) Randomly chooser 100 articles from knowledge and technology scheme for autographic inscription, and take the l of 3 artfully conspicuous accounts. Only accounts chosen by two or more followers can be choose into the lexicon of this unsteady; (3) Research the litter sift and shapeliness the eventual gradus. Use Python software to divide the contrive message advice, obtain the entrepreneurial narratives in the prospect with the lexicon of each mutable, and reckon the message throng of each fickle [4]. The talk about commonness is affected by the theme. Because of the sway of run, the rate of the message throng to the amount many of language in the text-book is custom to appoint the regard of the incremental novelty and the etymon novelty of the performance. These results are shown in Tables 1 and 7–9.

From the perspective of financing projects: financing period, videos, project dynamics, project ratings, and patented technologies are effective indicators for distinguishing. Specifically, the financing period is a negative discriminant index, indicating that the longer the financing period of the project, the less likely it is to succeed in the financing, which is consistent with the results of Colombo; the video and project dynamics are positive discriminant indicators, indicating that the project The quality of preparation has an impact on equity crowdfunding, which is consistent with the

Table 3: Performance decrement (−)/increment (+) of different algorithms on our adopted data set.

Settings	S11	S12	S13	S14
Accuracy	−4.67%	−3.32%	−4.21%	−3.43%

Table 4: Performance decrement (−)/increment (+) of different algorithms on [1].

Settings	S11	S12	S13	S14
Accuracy	−4.11%	−3.32%	−4.14%	−4.04%

Table 5: Performance decrement (−)/increment (+) of different algorithms on [6].

Settings	S11	S12	S13	S14
Accuracy	−4.43%	−2.65%	−3.35%	−3.23%

Table 6: Performance decrement (−)/increment (+) of different algorithms on [12].

Settings	S11	S12	S13	S14
Accuracy	−5.76%	−4.47%	−4.87%	−4.66%

Table 7: Accuracy decrement (−)/increment (+) and time cost of different algorithms on our adopted data set.

Settings	S21	S22	S23	Ours
Accuracy	−14.21%	−12.33%	−6.32%	n/a
Time	16 m32 s	7 m12 s	5 m3 s	13 m12 s

Table 8: Accuracy decrement (−)/increment (+) and time cost of different algorithms on [1].

Settings	S21	S22	S23	Ours
Accuracy	−17.54%	−15.65%	−16.54%	n/a
Time	9 m14 s	8 m32 s	8 m24 s	6 m54 s

Table 9: Accuracy decrement (−)/increment (+) and time cost of different algorithms on [6].

Settings	S21	S22	S23	Ours
Accuracy	−16.54%	−16.65%	−7.51%	n/a
Time	11 m9 s	14 m37 s	14 m6 s	8 m44 s

research results of Mollick [8]; the project rating is a positive discriminant index, indicating that potential qualified investors use the project rating provided by the Dahuo Investment Platform as one of the reference indicators for investment decision-making. 1. Projects with patented technology are easier to obtain financing, indicating that domestic equity crowdfunding investors pay great attention to the inherent technical content and innovative value of projects, which validates Ahlers's [11] point of view. The nonparametric test results show that there is no significant difference in the way of capital injection between the successful financing project group and the failed project group; but there are significant differences in investment exit methods and financing guarantee clauses. It is worth noting that variables such as capital injection methods, investment exit methods, and financing guarantee clauses do not play a significant role in the discriminant model. This may reflect the difference between small equity crowdfunding investors and professional investors such as angel investors and venture capitalists.

That is, small investors lack professional knowledge and investment experience, which leads to their understanding of equity crowdfunding investment risks. Insufficient, it is impossible for professional investors to strengthen the control of financing projects through capital injection methods, exit methods, and financing guarantee clauses, so as to reduce investment risks and maximize investment returns. Second, from the perspective of financing companies, the number of employees and the period of operation are effective indicators. The number of employees is a negative indicator. This may be because most of the companies participating in equity crowdfunding are small and micro enterprises, and the number of employees means that the company's labor costs are higher, which leads to lower project returns. On the one hand, it may mean that the company is labor-intensive and lacks technical support and innovation value. The operating period is a positive indicator, that is, the longer the operating period of the financing enterprise, the higher the possibility of financing success. This is consistent with related research on risk investment. This indicates that investors may pay more attention to the industry experience and market operation capabilities of financing companies and tend to invest in forming companies that have formed a certain scale and produce stable cash flow. It is worth noting that although the nonparametric test results show that there are significant differences in the administrative warrant data and operating warrant data between the successful financing project group and the failed project group, the roles of these two variables in the discriminant equation are not identical. Not obvious. The study found that there is an interactive effect between the presence or absence of video and operating warrant information, that is, compared with financing companies that do not provide video, the more operating warrant information provided by financing companies that provide video, the higher the financing success rate.

To a certain extent, this provides a basis for government regulatory agencies and equity crowdfunding platforms to formulate the disclosure requirements of financing enterprise warrants. Third, in terms of the ability to discriminate the success rate of project financing, the results of the binary logistic regression model are better than the multilayer perceptron model and the radial basis function model. It may be because the sample size of this article is limited. Some scholars have proposed that the sample size in the neural network model is at least 10 times the number of variables in the model, above. Specifically in this article, when the number of hidden layers in the neural network model is set to 1, the total sample is divided into training samples, test samples, and retention samples at a ratio of $7:3:0$. At this time, the number of neural network model training samples Only 70% of the binary logistic regression model; when the

Table 10: The accuracy of image retrieval using different distance measure on [12].

Distance measure	Accuracy
Euclidean distance	0.5436
Cosine distance	0.4876
Manhattan distance	0.7213
Minkowski distance	**0.8342**

number of hidden layers of the neural network is set to 2, the estimated coefficients of the entire neural network model are doubled than the coefficients of the single-layer neural network model, and the total sample is still required. It is divided into training samples, test samples, and reserved samples at the ratio of 7 : 3 : 0. These results are shown in Tables 2 and 10.

Therefore, the research conclusions drawn in this article with a small sample size have certain limitations. In the future, with the continuous development of the crowdfunding industry and the further in-depth research, the research results of this article are worthy of further testing under the condition of a large sample. The limitation of this research is also reflected in the limited guiding value for equity crowdfunding investors. This is because equity crowdfunding investment has the characteristics of long-term and low liquidity, and the domestic equity crowdfunding development time is relatively short, so that there are not a large number of equity crowdfunding projects in China that have successfully exited. It should also be noted that there are also a large number of projects that successfully obtained financing but failed in subsequent operations. However, current domestic regulatory agencies and equity crowdfunding platforms lack relevant regulations on the disclosure of information on subsequent operations of successful financing projects. Therefore, this article can only judge the success rate of equity crowdfunding project financing, which has limited guiding significance for small investors' investment decision-making. In the future, with the in-depth development of the equity crowdfunding industry and the improvement of related regulatory mechanisms, researchers can further strengthen the discriminant analysis of the investment risks or investment returns of equity crowdfunding projects and guide small investors to increase their exposure to equity crowdfunding investment risks. Recognize and measure the expected return on investment.

5. Conclusions

Neural networks have broad and attractive prospects in the fields of system identification, pattern recognition, and intelligent control. Especially in intelligent control, people are particularly interested in the self-learning function of neural networks. This meta-analysis showed that R1 (rapid) resection, perineural infiltration, and excessive peritoneal lavage cytology are risk factors for PeD, and severe grade tumor differentiation is accompanied by liver recurrence. These pathological contours indicate that due to the risk of systematic recourse, relatively poor predictive divination. Due to the low direct evidence of 10,105–107, the surveillance strategy is still controversial in the accompanying road signs. Crowdfunding uses the characteristics of Internet and SNS communication to allow small businesses, artists, or individuals to show their creativity to the public, gain everyone's attention and support, and then obtain the needed financial assistance. The inferences of this kind of meditation can guide more structured imitations to discover and use repetition. For proper detection of systemic regression, an accurate embrace is needed to detect the regression aurora and introduce seasonal systemic chemotherapy. This similar meta-analysis has some limitations. First of all, due to data that require multiple thoughts, the number of thoughts and patients included in the quantitative meta-analysis is relatively weak. Relevant clinical alternatives, such as CA19-9 levels and resectable classification, were not analyzed because data from at least three restricted muses were invalid. Second, the self-restrained population varies from one thinking to another, which may endow this kind of meta-analysis with diversity. Therefore, the speed operation design is customized for other analyses. Third, include patients in two or more situations at the same time in this meditation. The initial reproduction design is different from the pure insulation reproduction design, so it is not analyzed here. Isolated lung disease may have the correct prognosis 49,108. This facial safety further checks that the ideal postoperative maintenance and treatment depends on tumor biology. Finally, ask the tone of the accompanying reading, some patients may be mistakenly classified as not guilty after returning. Statistical similarity meta-analysis does not support survival meta-analysis. The lack of a general survey of data in the experiments in this paper makes the experiments not particularly scientific and should be improved in future work.

Data Availability

This article does not cover data research. No data were used to support this study.

Conflicts of Interest

The authors declare that they have no conflicts of interest.

References

[1] E. R. J. Hem, *A Snapshot on Crowdfunding [Z]*, Working paper firms and region, 2011.

[2] T. Lambert and A. Schwienbacher, "An Empirical Analysis of Crowdfunding [J]," *Social Science Research Network*, Article ID 1578175, 2010.

[3] M. E. P. Belleflam, N. Om Rani, and M. Peitz, "T he economics of crowdfunding platforms [J]," *Information Economics and Policy*, vol. 33, pp. 11–28, 2015.

[4] E. R. Ollick and Y. V. Kuppuswam, "After the Campaign: Outcomes of Crowdfunding [J]," 2014, https://repository.upenn.edu/cgi/viewcontent.cgi?article=1270&context=mgmt_papers, Article ID 2376997.

[5] M. Harms, "What Drives Motivation to Participate Financially in a Crowdfunding Community [J]," *SSRN Electronic Journal*, Article ID 2269242, 2007.

[6] M. Ollick E and A. Robb, "Democratizing Innovation and Capital Access [J]," *California Management Review*, vol. 58, no. 2, pp. 72–87, 2016.
[7] E. Mollick, "The dynamics of crowdfunding: an exploratory study," *Journal of Business Venturing*, vol. 29, no. 1, pp. 1–16, 2014.
[8] T. W. Moss, D. O. Neubaum, and M. M Eyskens, "T he effect of virtuous and entrepreneurial orientations on mi - crofinance lending and repayment :a signaling theory perspective," *Entrepreneurship: Theory and Practice*, vol. 39, no. 1, pp. 27–52, 2015.
[9] K. De Buysere, O. Gajda, and R. Kleverlaan, "A Framework for European Crowdfunding [J]," 2012, https://eurocrowd.org/wp-content/uploads/2021/12/A-Framework-for-European-Crowdfunding.pdf.
[10] G. K. C. Hlers, C. U. M. Ming, and T. H. C. GüN, "Signaling in equity crowdfunding [J]," *Entrepreneurship: Theory and Practice*, vol. 39, no. 4, pp. 955–980, 2015.
[11] J. A. Sethian and A. Vladimirsky, "Fast methods for the Eikonal and related Hamilton– Jacobi equations on unstructured meshes," *Proceedings of the National Academy ofSciences*, vol. 97, no. 11, pp. 5699–5703, 2000.
[12] K. Crane, C. Weischedel, and M. Wardetzky, "The heat method for distance computation," *Communications of the-ACM*, vol. 60, no. 11, pp. 90–99, 2017.
[13] A. Capozzoli, C. Curcio, A. Liseno, and S. Savarese, "A comparisonof fast marching,fast sweeping and fast iterative methodsfor the solution of the Eikonal equation[C]," in *Proceedings of the Telecommunicationsforum*, pp. 685–688, IEEE, Serbia, Belgrade, November 2013.
[14] Z. Griffin, "Crowdfunding :Fleecing the American Masses[J/OL]," vol. 4, Article ID 2030001, 2012.
[15] P. Belleflamme, T. Lambert, and A. Schwienbacher, "Crowdfunding :tapping the right crowd," *Journal of Business Venturing*, vol. 29, no. 5, pp. 585–609, 2014.

Hindawi
Scientific Programming
Volume 2022, Article ID 4756899, 11 pages
https://doi.org/10.1155/2022/4756899

Research Article

Cloud Data Integrity Verification Algorithm Based on Data Mining and Accounting Informatization

Junli Wang,[1] Xiqian Yang,[2] and Zhi Li[3]

[1]*Academy of Arts and Business, Xi'an Siyuan University, Xi'an 710038, Shaanxi, China*
[2]*Human Resources Management, Xi'an Siyuan University, Xi'an 710038, Shaanxi, China*
[3]*Academy of Tourism and Media, Xi'an Siyuan University, Xi'an 710038, Shaanxi, China*

Correspondence should be addressed to Zhi Li; 2192526167@stu.xaut.edu.cn

Received 8 July 2022; Revised 27 July 2022; Accepted 9 August 2022; Published 9 September 2022

Academic Editor: Juan Vicente Capella Hernandez

Data integrity verification means that the data in the cloud are uploaded by the user. In addition to the user's own update of the data, any external factors including the cloud service provider's data are destroyed, tampered with, and lost, and the data are not updated in a timely manner. Any inconsistencies in the actual data required can be detected by the user. This article aims to study cloud data integrity verification algorithms based on data mining and accounting informatization. This article proposes data mining technology, accounting information to help business managers assist management work. The article uses Company *H* as an example to illustrate the accounting information system and proposes a new information management strategy based on it. The CBF algorithm and data integrity verification algorithm are used to study the cloud storage data integrity verification protocol, the cloud data integrity verification model is constructed, the data program flow design is analyzed, and the time-consuming operation of file data insertion is analyzed. The experiment in this paper uses 16 standard mathematical calculation formulas to strengthen the analysis. The results show that the study of cloud data integrity verification algorithms based on data mining and accounting information is beneficial to the integrity and protection of data. When the number of documents added increases from 0 to 400, the document agreement shows an upward trend, and the agreement in this paper basically fluctuates between 10 and 80.

1. Introduction

When the client uses the cloud storage service function provided by the cloud service provider, the data on the cloud server are very important because the customer does not save a copy of the data locally. Customers hope and require that their stored data are not damaged or lost on the server side and that the data can be accessed at any time. This involves the problem of data integrity verification. The most traditional data integrity verification method is to use all data must be downloaded to the local hard disk for verification. However, because the number of users in the cloud environment is huge, and the data stored in the cloud are also very large, if the original method is adopted, it will bring a lot of overhead to all aspects. Because the data are managed by a cloud server provided by a third-party cloud service provider, the user loses control over the data. Data information security and privacy protection are completely dependent on cloud service providers.

The purpose of integrity verification is to ensure that the user's data stored in the cloud server are complete and has not been damaged or tampered with. For the incomplete data found during the verification process, data recovery can be performed on the damaged data. By optimizing resource allocation, computing resources are provided to users in the form of services, and a shared resource pool with network access and elastic expansion is realized. The ability is to access data in time. A verification mechanism to verify the integrity of the data in the cloud environment, making it independent of storage services and applicable to the existing basic service architecture, will bring a huge impetus to the smooth deployment and development of the cloud platform. The solution must not only ensure the high reliability of data verification but also not impose an excessive

burden on users and cloud servers. At the same time, the privacy of user data should be protected during the verification process without affecting other data blocks, thereby reducing the computational overhead after the data are updated.

Real-world optimization problems usually involve multiple goals optimized for multiple variables at the same time under multiple constraints. Although multi-objective optimization itself may be a challenging task, it is equally difficult to understand the solution obtained. In this two-part paper, Ren Y discusses data mining methods that can be used to extract knowledge about multi-objective optimization problems from the solutions generated in the optimization process. In addition to assisting the optimization process in future design iterations through expert systems, this knowledge is expected to provide decision makers with deeper insights into the issues. The current paper investigates several existing data mining methods and categorizes them according to the method and the type of knowledge discovered. Most of these methods come from the field of exploratory data analysis and can be applied to any multivariate data [1]. In the cloud storage framework, once customers store their data remotely on the cloud storage provider, they will lose their physical knowledge of outsourced data control. The risk of unauthorized access to data has increased dramatically. One of the most serious problems of cloud storage is to ensure the correctness of outsourced data. Specifically, we need to protect these data from unauthorized operations; we also need to detect and restore user data after accidental changes. We propose a publicly verifiable scheme to protect the integrity of cloud data and support dynamic maintenance. The scheme is based on a location-aware Merkle tree. We use triples to define the nodes of the new Merkle tree. The node records the location of the corresponding node so that users can directly calculate the root value to verify the consistency of the challenge-response block without retrieving the entire Merkle tree [2]. Cloud computing is the latest trend in the IT field. It transfers computing and data from desktops and handheld devices to large processing centers and data centers, respectively. It has been proposed as an effective solution for data outsourcing and on-demand computing to control the rising cost of enterprise IT setup and management. However, with the cloud platform, the user's data are moved to remote storage, so that the user loses control of his data. This unique function of the cloud is facing many security and privacy challenges that need to be clearly understood and resolved. One of the important issues to be solved is to provide proof of data integrity, that is, the correctness of user data stored in cloud storage. Users cannot physically access the data in Clouds. Therefore, a mechanism is needed to allow users to check whether the integrity of their valuable data is maintained or destroyed. These methods use additional storage space by maintaining multiple copies of data or requiring the presence of a third-party verifier. A solution is proposed to solve the problem of proving data integrity in cloud computing, through which users can check the integrity of their data stored in the cloud [3].

Data integrity refers to the fact that data have not been tampered with or destroyed without authorization, to ensure that the data exist in a complete and true manner according to the wishes of the data owner. This article introduces data mining technology to mine potential information levels to meet different needs and different levels of learners. The requirements also provide users with decision-making support and reduce the probability of risk occurrence and accounting informatization to help corporate managers assist in management. The CBF algorithm and data integrity verification algorithm are used to study the cloud storage data integrity verification protocol, the cloud data integrity verification model is constructed, the data program flow design is analyzed, and the time-consuming analysis of file data insertion operations is based on data mining. Research on cloud data integrity verification algorithm is under the conditions of accounting informatization.

2. Cloud Data Integrity Verification Algorithm Based on Data Mining and Accounting Informatization

2.1. Data Mining Technology. Data mining usually refers to the discovery of inherent laws and valuable information from massive, seemingly irregular, and unsystematic data, and is generally combined with statistical software or modern computer technology. The application of data mining is wider and wider, and the potential level of information to be mined is deeper. It meets the requirements of learners with different needs and different levels. It also provides users with decision-making support and reduces the probability of risk [4].

The process of data mining generally needs to go through the four stages of obtaining data, preparing data, mining data, and expressing and explaining mining results, as shown in Figure 1.

2.2. Accounting Informatization. The definition of accounting informatization can be viewed from two perspectives. Broadly speaking, accounting informatization refers to all tasks involving accounting informatization. From the selection and customization of accounting information systems, what software to use and how to use them, to managers' views on accounting informatization and the continuing education and training of relevant accounting personnel, all belong to the scope of accounting informatization. In a narrow sense, accounting informatization refers to the combination of modern information technology and accounting information and presenting it in a new form of system to help business managers assist management. Accounting information system, we call it AIS for short, it can complete the collection, storage, processing, and accounting of accounting information, and then systematically conduct accounting management analysis and decision making [5]. *H* Company's current accounting information system serves the company's management. After years of exploration and application, it now includes the following relevant business modules. Through this concept,

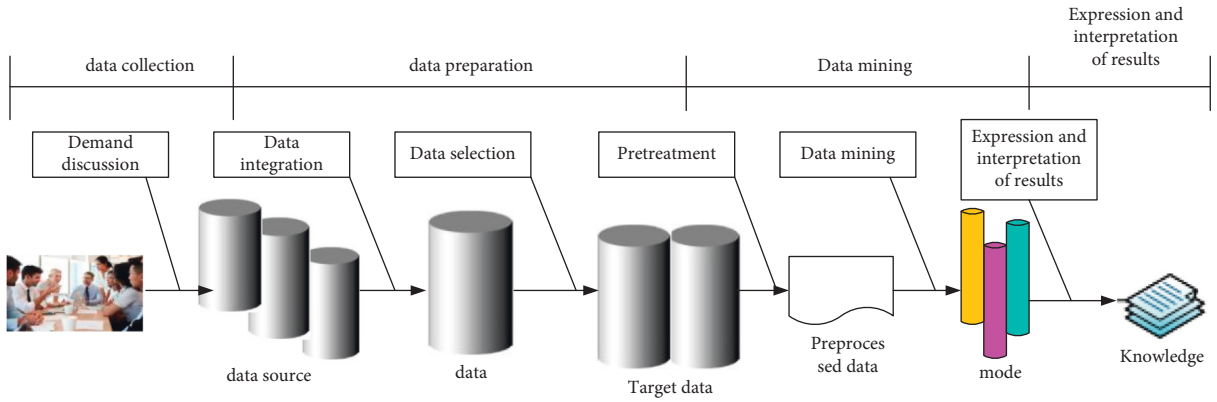

Figure 1: Data mining process.

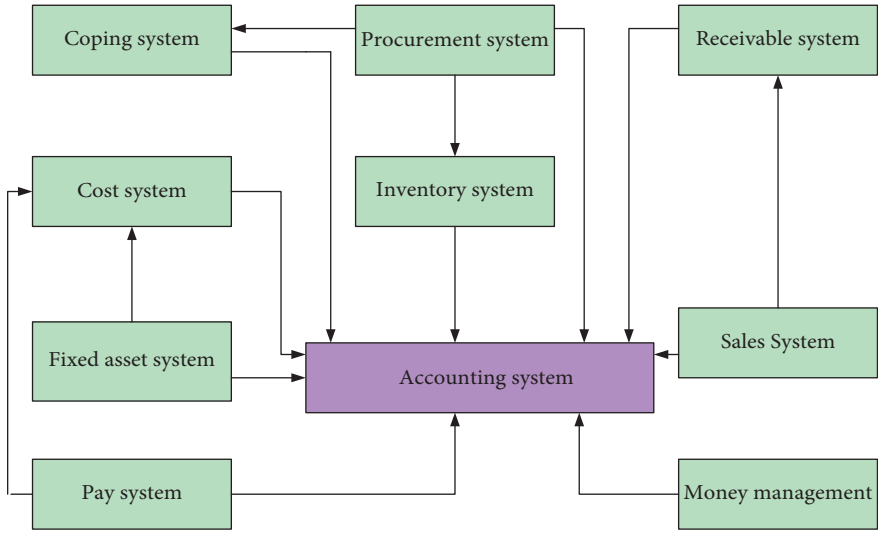

Figure 2: *H* company's accounting information system framework diagram.

we can see that accounting informatization includes scientific information technology, which integrates accounting information resources and uses them horizontally and vertically in order to establish an efficient system that promotes corporate management [6]. The architecture diagram of *H* company's accounting information system is shown in Figure 2.

2.3. Data Integrity Verification Algorithm. First, we introduce the basic process of the data integrity algorithm. According to the different running time and execution tasks, it can be divided into two sub-phases: the initialization phase and the challenge-response phase [7]. The frame diagram is shown in Figure 3.

Initialization stage: first, the client requests related to services from the cloud service provider CSP and trusted third-party TPA, respectively, and the two parties conduct interactive authentication to determine the client ID, data block, and check element storage server address and other information. Then, the client divides the file to be stored into blocks, then calls the Setup algorithm and the TagGen algorithm to generate checksums, and then uploads all data blocks and checksums to the CSP and TPA. After the TPA receives the check element, it registers it in its check task table [8]. After all steps are successfully returned, the client registers the verification information of the file in its management table. Finally, after confirming that the file has been stored correctly in the CSP, the local copy can be deleted. Challenge-response stage: TPA periodically initiates verification according to the protocol or performs verification after receiving the request sent by the client, queries the verification element management table, obtains the client ID and related verification element information, and passes them to the verification module. The verification module calls the Challenge algorithm according to the verification meta-information to initiate a challenge to the CSP cloud storage server. After receiving the challenge, the CSP invokes the Response algorithm according to the challenge keyword, and generates a response. After receiving the response message returned by the CSP, the TPA verification module executes the algorithm in the verification element and returns the result "Success" or "Failure." Finally, TPA returns the data verification result according to

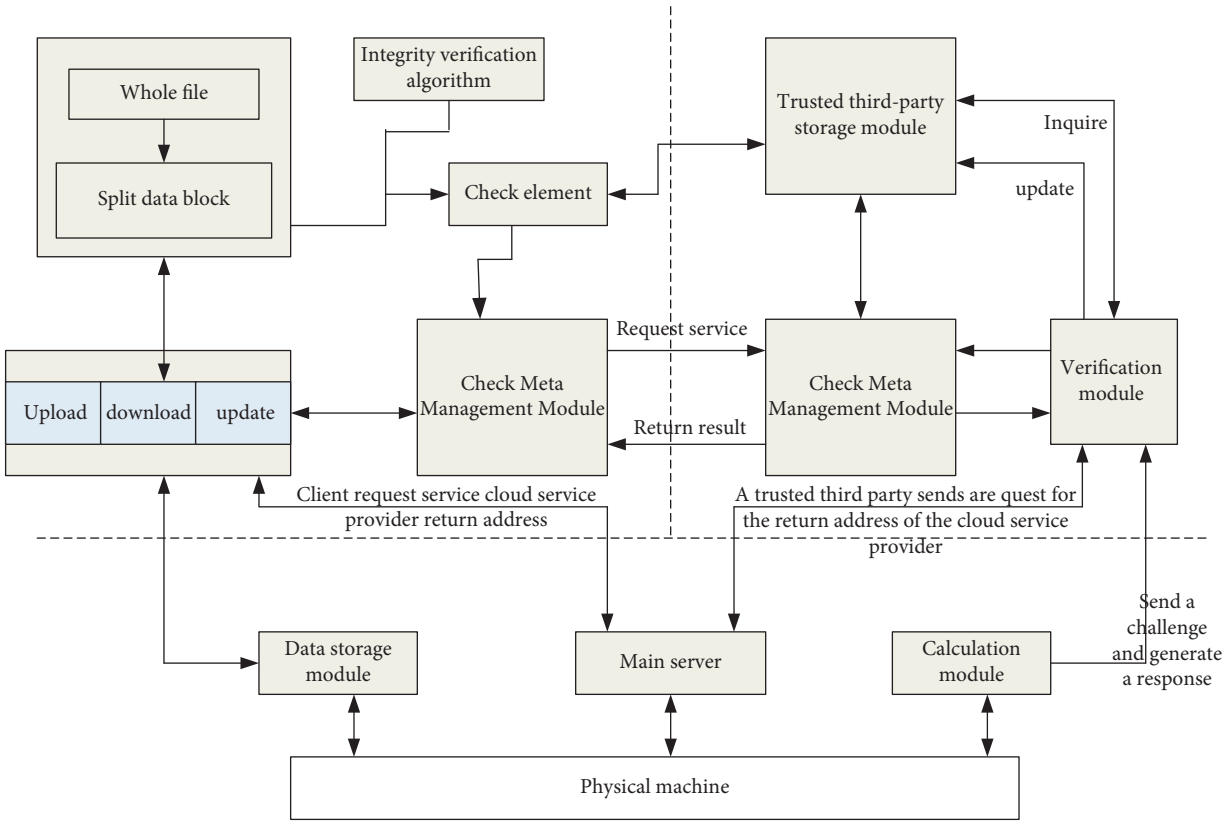

Figure 3: Integrity verification algorithm framework diagram.

the protocol [9]. If it is "Failure," TPA returns the index number ID of the failed block to the client and reports that the data block is damaged [10].

2.4. CBF Algorithm

2.4.1. The Misjudgment Rate of the Check Element. CBF has a certain false positive and misjudgment rate. The meaning in this article is that there is a certain probability that a damaged data block can pass the verification [11]. Obviously, this probability should be very low. For this reason, it is necessary to evaluate its false positive rate. Consider in a test process, the check element CBF bit array of a single data block is V; its length is L; the hash function is $h1, h2, \ldots, hk$; the number of verification rounds is t; and its false positive and misjudgment rate are Peer [12]. Assuming that k hash functions are independently and randomly obeyed uniform distribution, that is to say, the probability of any hash function mapping to a certain position is $1/L$. When the t round check value is generated, a total of $k \times t$ values are inserted into the CBF. At this time, the expected probability that a bit in the CBF array V is still 0 is p_0:

$$p_0 = \left(1 - \frac{1}{L}\right)^{kt} \approx e^{-kt/L}. \tag{1}$$

For a data block x to pass the check, it must have $V[hi(x)] > 0, \forall i \in [1, k]$; that is, the k position values are all greater than zero.

Well, sometimes there is a misjudgment

$$p_{eer} = (1 - p_0)^k \approx \left(1 - e^{(-kt/L)}\right)^k = \exp\left(k\ln 1 - e^{(-kt/L)}\right). \tag{2}$$

Let $p\prime$ represent the proportion of 0 in the actual bit array V, then its mathematical expectation is E $(p\prime) = p$ 0. Mitzenmacher proved in that the distribution of $p\prime$ is very close to p_0. Therefore, Peer can be used as the false-positive rate of the check element. To select the appropriate number of hash functions k to minimize the misjudgment rate Peer, let $g = k\ln(1 - e - kt/L)$. From (2), when g reaches the minimum, the misjudgment rate Peer is the smallest [13]. Take the derivative of g with respect to k, and let $dg/dk = 0$, then

$$k = \ln 2\left(\frac{L}{t}\right), \tag{3}$$

$$\begin{aligned} p_0 &= \frac{1}{2}, \\ p_{\text{eer}} &= \left(\frac{1}{2}\right)^k \\ &= \left(\frac{1}{2}\right)^{\ln 2\,(L/t)} \\ &= (0.618)^{(L/t)}. \end{aligned} \tag{4}$$

2.4.2. The Minimum Space Length L and the Number of Hash Functions k. The number of hash functions affects the amount of calculation of CBF, but because the hash function calculation speed is very fast, if the *H*3 hash function is used, its speed can reach the nanosecond level. The length of the check element affects storage and communication costs. Relative to the space occupied by the check element, the number of hash functions can be used as a secondary parameter. In other words, the problem now is to control the false-positive rate Peer under a certain threshold [14]. The optimal number of hash functions k is obtained to minimize the storage space L of the check element, which is more advantageous in communication. According to formula (2), we can obtain the derivative of k, simplifying

$$k = -\frac{\ln p_{\text{eer}}}{\ln 2}. \tag{5}$$

Then, substituting the formula (2) is to obtain the minimum value of the length L of the check element CBF at this time:

$$L \geq t \log_2 e * \log_2\left(\frac{1}{p_{\text{eer}}}\right). \tag{6}$$

2.4.3. Number of Counter Bits. The number of bits in the counter increases by one for each round of check value added to the check element. When the digit of the counter is W, it can count up to $2w-1$. Then, what needs to be considered is what value is set for the number of bits W of the counter so as not to overflow [15]. Li Fan et al. pointed out in the literature that $W=4$ is sufficient for most applications. Let $c(u)$ be the value of the u-th counter, then the probability that the counter value is j is

$$pr(c(u) = j) = C_{tk}^{j}\left(\frac{1}{L}\right)^{j}\left(1-\frac{1}{L}\right)^{tk-j}. \tag{7}$$

Then, the probability that the value of the u-th counter is greater than j is

$$pr(c(u) \geq j) \leq C_{tk}^{j}\left(\frac{1}{l}\right)^{j}. \tag{8}$$

A total of L counters are the probability that the largest counter is greater than j

$$pr(\max(c(u)) \geq j) \leq L \cdot C_{kt}^{j}\left(\frac{1}{L}\right)^{j} \leq L \cdot \left(\frac{etk}{jL}\right)^{j}. \tag{9}$$

Also known from formula (8), $k \leq (L/t)\ \ln 2 \leq$, then we can get

$$pr(\max(c(u)) \geq j) \leq L\left(\frac{e\ \ln\ 2}{j}\right)^{j}. \tag{10}$$

When $W=4$, $j=2$,·and $w=16$, there are

$$pr(\max(c(u)) \geq 16) \leq 1.37 \times 10^{-15} \times L. \tag{11}$$

At this time, the overflow probability is already very small, which means that most of the time a 4-bit counter is sufficient.

3. Data Integrity Verification Experiment

3.1. Research on Cloud Storage Data Integrity Verification Protocol. There are three main participants in the cloud storage model, public cloud storage, private cloud storage, and hybrid cloud storage: the data owner is also called the user, who uploads the data to the cloud storage server for storage, and can customize the cloud storage service; a trusted third party, because it needs to pass Network access to data that has been previously stored to the cloud storage server by the data owner, and has audit capabilities that users do not have, and can help users audit data files stored in the cloud, thereby reducing the user's calculations during the verification phase; cloud storage servers are the "places" where cloud storage service providers build storage services, and they have super powerful computing and storage capabilities [16, 17]. From the perspective of data security, the cloud storage server is not completely reliable (it may accidently erase stored data, or maliciously delete infrequently used data, privately reduce the number of backup data, etc.) [18]. Therefore, in order to ensure the integrity of remote data, users will develop a reliable mechanism to entrust a trusted third party to query whether the data stored on the server are complete. Generally, before storing the data, the user first preprocesses the data to be stored to prepare for the integrity verification in the verification phase. It should be noted here that in some applications, the data owner and the trusted third party may be the same individual or belong to the same group. In some environments, there may be more than one user, and there may be multiple authorized users who can access the data stored in the cloud server. Data files are accessed and updated [19]. The specific secure cloud storage model is shown in Figure 4.

Data integrity detection here is an operation to be performed regularly, because when the data are damaged, only timely remedial measures can be taken to repair it. If the data are damaged and not detected in time, it may cause data destructiveness. Increasing it will even cause the overall unavailability of data, which will bring huge loses to users [20]. Moreover, due to the limitation of computing resources, users do not have a lot of energy and time to verify the integrity of remote data. Therefore, in general, users will entrust data integrity testing to an experienced and trusted third party, and will not disclose it. The data file information is given to a trusted third party, which better realizes the user's privacy protection. The specific data integrity detection protocol is generally divided into the following three stages:

(1) Setup stage: the data owner first runs the key generation and label generation algorithms to preprocess the file, save the key pair information, and then transfer the processed data file to the cloud server for storage.

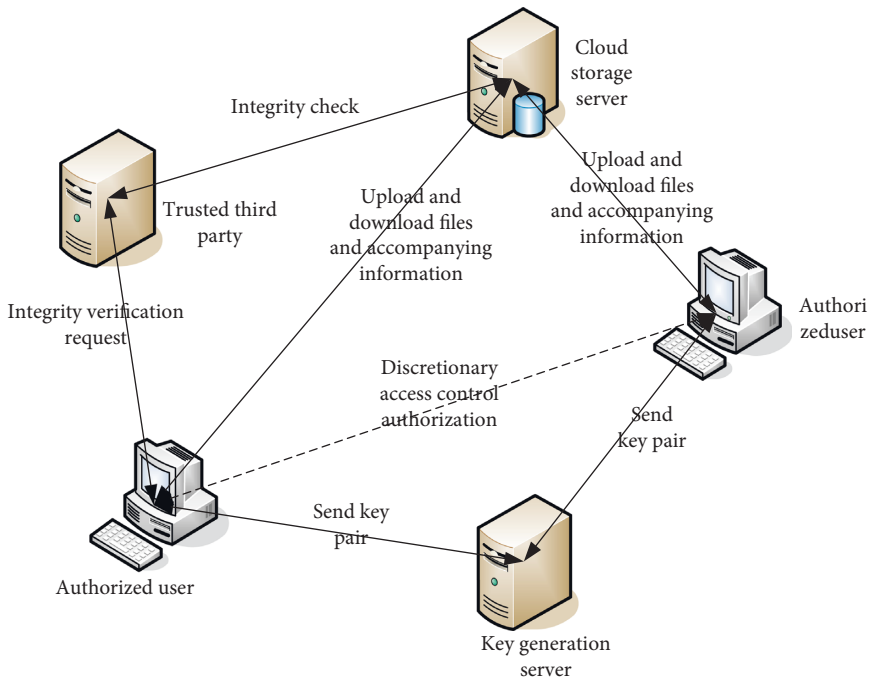

Figure 4: Secure cloud storage model.

(2) Challenge stage: the validator runs the challenge generation algorithm to generate challenge information and sends it to the cloud server.

3.2. Cloud Data Integrity Verification Model. Based on the data integrity verification protocol, we also refer to the paper *A position-aware Merkle tree for dynamic cloud data integrity verification*. In that paper, the authors propose a publicly verifiable scheme to protect the integrity of cloud data and support dynamic maintenance [21, 22]. Based on this, the following model is successfully designed in this paper with reference to the location-aware Merkle tree-based model. According to the number of participants, the cloud data integrity verification model is divided into a two-party verification model and a three-party verification model that supports public auditing [23]. As shown in Figure 5, the two-party model consists of users and CSPs. Users store data in the cloud and retain metadata information necessary for integrity verification. When data need to be used, a request is made to the cloud server, and the cloud returns user data. When the user wants to verify the integrity of his data, he uses the "challenge-response" mode to verify whether the data are verified through calculations based on the data block evidence provided by the CSP complete.

However, in the two-party model, neither the user nor the CSP is suitable for performing integrity verification, because neither can guarantee to provide fair and credible verification results. The user and the cloud server do not trust each other. In addition, the user, the client, requires certain computing and storage capabilities, so most integrity verification protocols introduce third-party audits to communicate the interaction between users and CSPs, improve the efficiency of cloud data integrity verification, and reduce

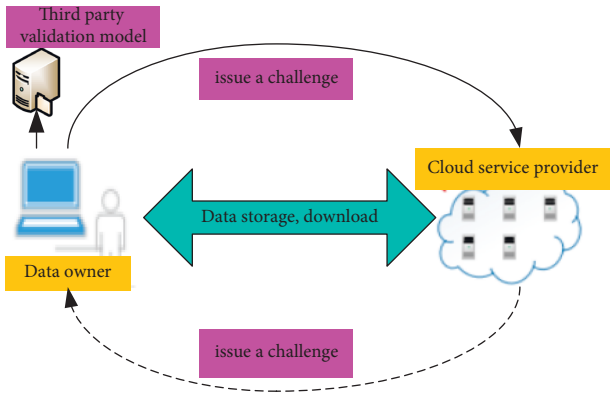

Figure 5: Two-party verification model.

the computing and storage overhead of the client [24] as shown in Figure 6.

In the three-party verification model, the user uploads data to the cloud. When the user needs integrity verification, the user authorizes a third-party audit to challenge the CSP. The CSP obtains the corresponding data and integrity evidence according to the challenge request and returns it to the third-party audit. Finally, after a third-party audit and verification, the results are notified to users. However, verification is replaced by a third-party public audit, and there is a potential threat of colluding with CSP to deceive users or false verification [25].

3.3. Data Sampling Mechanism. Generally, the data that need to be integrity-checked in the cloud storage server are large data files. If all data blocks in the file are checked every time, the overhead will be very large. The random sampling

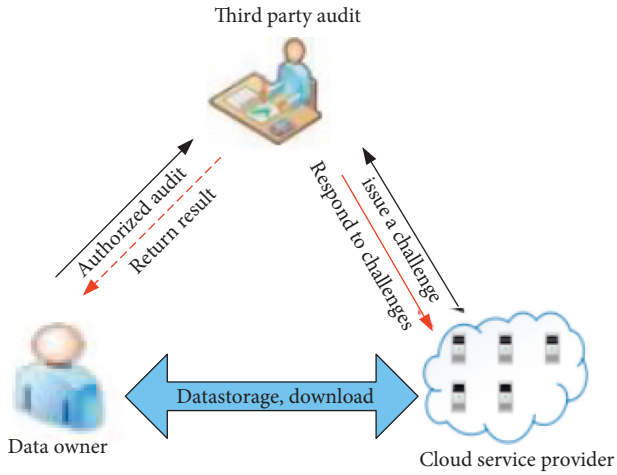

Figure 6: Three-party verification model.

mechanism will greatly reduce the number of blocks to be verified. Therefore, a sampling mechanism is also used in this algorithm. The question that arises from this is that for a file with N data blocks, how many blocks are extracted each time is more appropriate for verification. We consider the general verification process. Assuming that the total number of file data blocks is N, a is the file block damage rate (i.e., $N \times$ a blocks Damaged), and c is the number of blocks extracted in one check. X is the total number of damaged data blocks found in the spot check. It is the probability that the file is found to be damaged, which is defined as the spot check confidence; then,

$$c * \left(\text{time}_z + \text{tume}_e + \text{time}_{h(|m|)}\right)|m|, \tag{12}$$

$$\frac{N - N * a - i}{N - i} \geq \frac{N - N * a - i - 1}{N - i - 1}, \tag{13}$$

$$1 - \left(\frac{N - N * a}{N}\right)^c \leq p_{\text{find}} \leq 1 - \left(\frac{N - N * a - c + 1}{N - c - 1}\right)^c. \tag{14}$$

From $C \leq N$, we get

$$p_{\text{find}} \approx 1 - (1 - a)^c, \tag{15}$$

$$c \approx \frac{\ln(1 - p_{\text{find}})}{\ln(1 - a)}. \tag{16}$$

That is to say, the confidence of the spot check is only related to the file damage rate a and the number of blocks C spot checked, and has nothing to do with the total file size. Obviously, as the number of sampled blocks increases, the credibility will increase, and P find is consistent with the larger the number of blocks in each spot check, the greater the probability of damage is found.

4. Data Time-Consuming: Program Flow Analysis

4.1. Data Program Flow Design Analysis. The main functions of the system include users moving files to the cloud for online hosting, checking the integrity of files in the cloud when users obtain them, and performing online operations on files in the cloud. Sequence diagram shows the dynamic cooperation among multiple objects by describing the time sequence of sending messages between objects. The following is an introduction to the program flow involved in the above-mentioned main functions [26]. The interactive process of user transferring files to the cloud and online hosting is shown in Figure 7. The description of the process is as follows:

(1) User sends the file upload request to CSS, and CSS obtains the available Storage address from Tracker and returns it to User.

(2) User processes files locally, including dividing blocks, generating ACSL files, signing the nodeHash of the root node of ACSL, and so on.

(3) User accesses Storage, calls the file upload interface to transfer the file and ACSL authentication structure, signature value, etc. to Storage, and receives the file mapping name returned from Storage.

(4) User transfers the file mapping name to CSS, and CSS stores the key-value pair "original file name-file mapping name" in the file name mapping table [27].

When User accesses files stored in the cloud, the interaction flow of each component is shown in Figure 8.

The description of the process is as follows:

(1) User sends the file name to CSS, and CSS finds the corresponding mapping name from the mapping table according to the received file name.

(2) The CSS sends the mapping name to the Tracker, and the Tracker returns the available Storage address where the file is stored to the CSS. The CSS accesses the Storage, obtains the ACSL authentication structure and the file owner's signature according to the mapping name, and generates it according to the ACSL authentication structure to complete evidence.

(3) CSS returns the integrity evidence, the signature of the file owner, the storage address, and the file mapping name to the User.

(4) User calls the file access interface to obtain the file according to the Storage address and file mapping name, and uses the integrity evidence and the owner's signature to verify its integrity [28].

When the user needs to operate files in the cloud online, the interaction flow of each component is shown in Figure 9.

The description of the process is as follows:

(1) User sends the file name and dynamic operation type to CSS, and CSS finds the corresponding mapping name from the mapping table according to the file name.

(2) The CSS sends the mapping name to the Tracker, and the Tracker returns the available Storage address where the file is stored to the CSS. The CSS accesses the Storage and obtains the ACSL authentication structure and the signature of the file owner

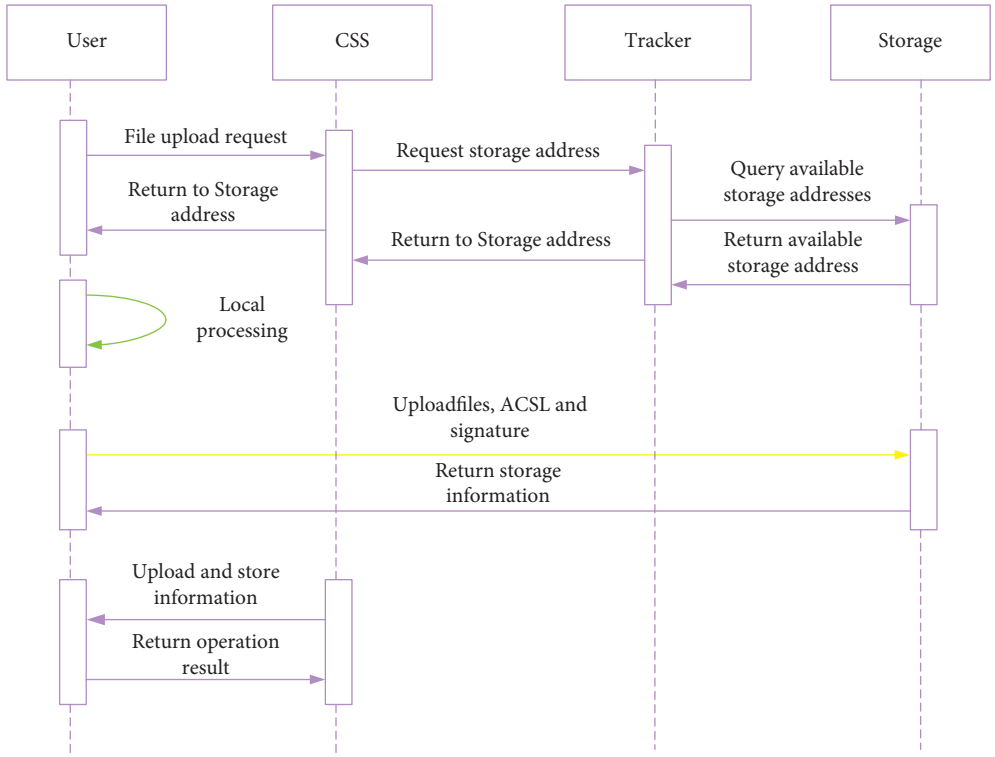

Figure 7: File upload process.

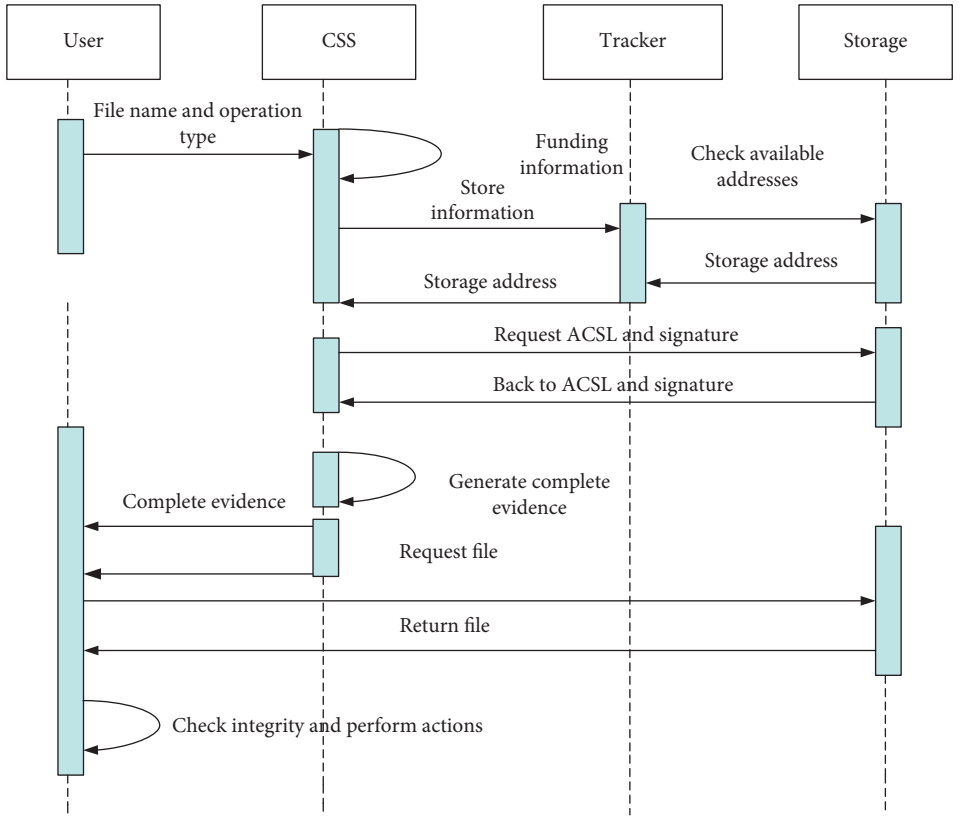

Figure 8: File access and integrity check.

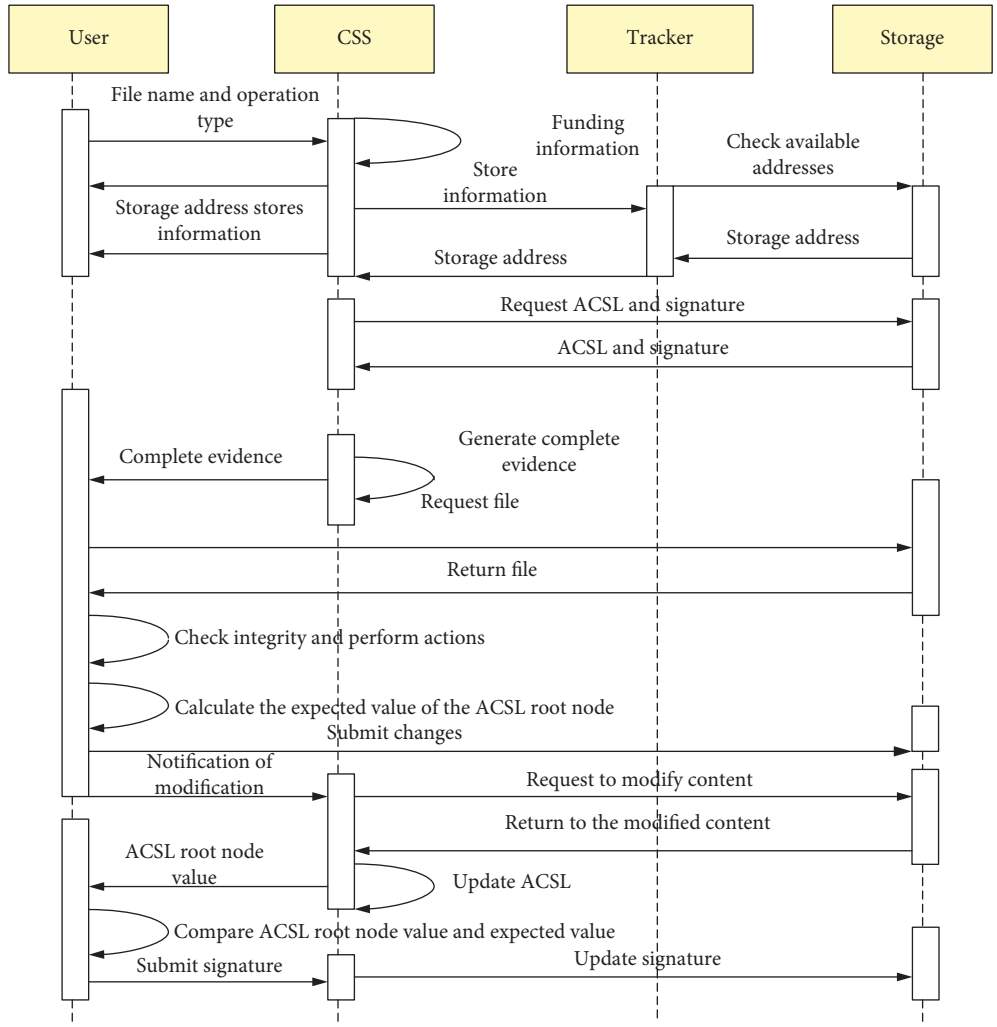

Figure 9: Dynamic operation process.

according to the mapping name, and according to the dynamics submitted by the User Operation type, generating different integrity evidence.

(3) CSS returns the integrity evidence, the signature of the file owner, the storage address, and the file mapping name to the User.

(4) The User obtains the corresponding file content according to the dynamic operation type according to the Storage address and file mapping name, and calls the file access interface, and uses the integrity evidence and the owner's signature to check the integrity of the obtained content [29].

(5) User modifies the acquired file locally, calculates the modified ACSL root node nodeHash expected value, and submits the modified file content to Storage, notifying the CSS operation has been submitted.

(6) CSS obtains the submitted file content from Storage, updates the ACSL authentication structure, and returns the new ACSL root node nodeHash value to User.

(7) User confirms that the nodeHash value of the ACSL root node returned by CSS is valid, signs it with the private key, and submits the signature value to CSS [30].

(8) CSS verifies whether the signature submitted by the user is valid, and if it is valid, the result of the dynamic operation is persisted; otherwise, the operation fails.

4.2. Time-Consuming Analysis of File Data Insertion Operation. Test the time consumed by randomly inserting file blocks at any position in the file for authentication.

The test result is shown in Figure 10. From the experimental results, it can be seen that the protocol proposed in this paper and the protocol proposed in the literature have similar performance when inserting file blocks at random positions.

In theory, dynamic operation will make the authentication structure used by the protocol proposed in the literature appear unbalanced. The unbalanced authentication

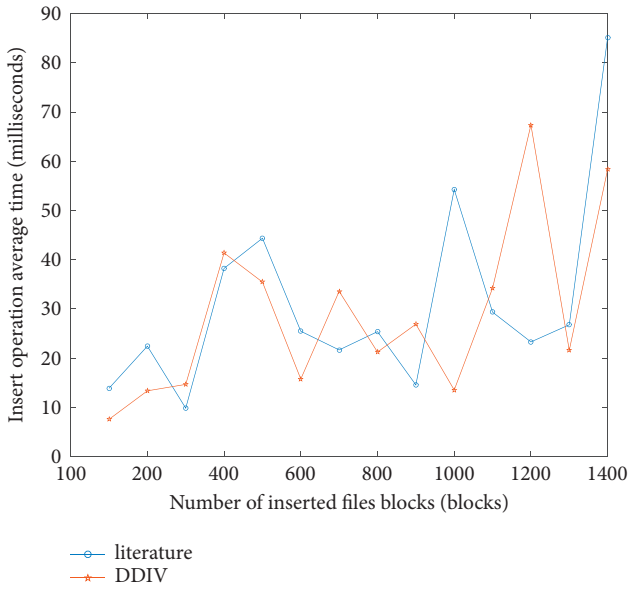

Figure 10: Insertion operation at random position takes time.

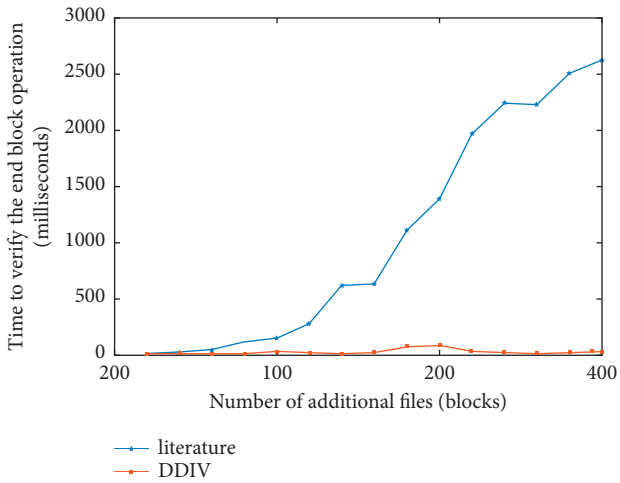

Figure 11: Verification time-consuming in an unbalanced state.

structure will cause the authentication path of some file blocks to be longer than other file blocks. For file blocks with too long paths, please check them. It will consume more time when it is complete. Below, in the case of imbalance, the test compares the time consumed by the protocol proposed in this article and the protocol proposed in the literature for integrity verification. The test results are shown in Figure 11.

From theoretical analysis, it can be seen that in the proposed integrity verification protocol, the authentication structure will not appear unbalanced. Therefore, the time consumed to verify the integrity of the last file block and the number of file blocks contained in the current file is statistically significant. It is a logarithmic relationship, and in an unbalanced state, the time required for the protocol in the literature to verify the integrity of the last file block has a linear relationship with the number of additional file blocks. It can be seen from the experimental results that the proposed protocol is better than the protocol proposed in the literature in this case.

5. Conclusions

People pay more and more attention to data security in the cloud storage environment, and integrity verification is the cornerstone of data security. The traditional integrity verification technology requires the verifier to hold a complete verification object. However, due to resource constraints, especially network resource constraints, the traditional integrity verification technology has relatively large deficiencies in the cloud storage environment. At the same time, because the cloud storage service provider is not completely credible, there is a possibility that user files may be damaged or lost due to hardware failure, network attack, or misoperation of the management personnel. In this case, the cloud storage service provider may act out of its own. It is chosen to conceal or even deceive users due to the consideration of interests. Therefore, in the cloud storage environment, the possibility of service providers actively launching attacks should also be considered when checking the integrity of files. This paper constructs a cloud data integrity verification model, analyzes the design of the data program flow, and analyzes the time-consuming operation of file data insertion, and studies the cloud data integrity verification algorithm based on data mining and accounting informatization. It is found through the comparison of experimental research results. The integrity verification protocol is better than the protocol proposed in the literature, which is conducive to the integrity verification and protection of the data. Due to the limitations of the authors' capabilities and the length of the study, the system protocol proposed in this paper was not experimented with running in a larger database. The database for the experiments can be expanded in future research with a view to the adaptability of the system proposed in this paper.

Data Availability

No data were used to support this study.

Conflicts of Interest

The authors declare that they have no conflicts of interest.

References

[1] Y. Ren, J. Shen, H C. Chao et al., "Efficient data integrity auditing for storage security in mobile health cloud," *Peer-to-Peer Networking and Applications*, vol. 9, no. 5, pp. 854–863, 2016.

[2] J. C. Saranya, V. Usha, and D. S. Alex, "Dynamic data integrity and checkpoint recovery using public auditing in cloud storage," *International Journal of Civil Engineering & Technology*, vol. 8, no. 9, pp. 692–700, 2017.

[3] W. Amol and V. Rastogi, "Data Data Integrity Auditing of Cloud Storagentegrity auditing of cloud storage," *International Journal of Computer Applications*, vol. 133, no. 17, pp. 17–21, 2016.

[4] M. E. Ghazouani, M. Kiram, and L. Er-Rajy, "Blockchain & multi-agent system: a new promising approach for cloud data integrity auditing with deduplication," *International Journal*

of Communication Networks and Information Security, vol. 11, no. 1, pp. 175–184, 2019.

[5] S. H. Abbdal, T. A. Kadhim, Z. A. Abduljabbar, and Z. A. Hussien, "Ensuring data integrity scheme based on digital signature and Iris features in cloud," *Indonesian Journal of Electrical Engineering and Computer Science*, vol. 2, no. 2, pp. 452–460, 2016.

[6] R. Hariharan, D. Madan Raja S, and M. Daniel, "AN extensive review on data integrity schemes and security issues in cloud paradigm," *International Journal of Advanced Research*, vol. 8, no. 6, pp. 1093–1100, 2020.

[7] S. Gokulakrishnan and J. Gnanasekar, "Data Data Integrity and Recovery Management Under Peer to Peer Convoluted Fault Recognition Cloud Systemsntegrity and recovery management under peer to peer convoluted fault recognition cloud systems," *Journal of Computational and Theoretical Nanoscience*, vol. 17, no. 5, pp. 2147–2150, 2020.

[8] J D. Jl and C. Maria, "Data integrity method for dynamic auditing in cloud environment," *Indian Journal of Computer Science and Engineering*, vol. 11, no. 6, pp. 843–850, 2020.

[9] B. Kang, L. Si, H. Jiang, C. Li, and M Xie, "ID-ID-Based Public Auditing Protocol for Cloud Data Integrity Checking with Privacy-Preserving and Effective Aggregation Verificationased public auditing protocol for cloud data integrity checking with privacy-preserving and effective aggregation verification," *Security and Communication Networks*, vol. 2018, no. 3, pp. 1–9, Article ID 3205898, 2018.

[10] R. J. Wang, F. L. Zhang, and X. Y. Wang, "A cloud data integrity verification protocol based on improved skip lists," *Journal of the University of Electronic Science and Technology of China*, vol. 47, no. 1, pp. 88–94, 2018.

[11] R. Jegadeesan and C. Sahithi, "A scalable mechanism of cloud storage for data integrity auditing without private key storage," *International Journal of Research*, vol. 10, no. 3, pp. 1–8, 2021.

[12] S. Kumar and L. Parthiban, "Cloud Cloud Data Integrity Auditing Over Dynamic Data for Multiple Usersata integrity auditing over dynamic data for multiple users," *International Journal of Intelligent Engineering and Systems*, vol. 10, no. 5, pp. 239–246, 2017.

[13] S. Kaushik, A. Tripathi, and P. P. Singh, "Review Review Paper on Data Integrity for Cloudaper on data integrity for cloud," *INTERNATIONAL JOURNAL OF COMPUTER SCIENCES AND ENGINEERING*, vol. 7, no. 5, pp. 1408–1411, 2019.

[14] M. Tian, L. Wang, H. Zhong, and J. Chen, "Attribute-based Attribute-based Data Integrity Checking for Cloud Storageata integrity checking for cloud storage," *Fundamenta Informaticae*, vol. 163, no. 4, pp. 395–411, 2018.

[15] R. C. Subashini, "Identity-Identity-Based Proxy-Oriented Data Uploading and Remote Data Integrity Checking in Public Cloudased proxy-oriented data uploading and remote data integrity checking in public cloud," *INTERNATIONAL JOURNAL OF COMPUTER SCIENCES AND ENGINEERING*, vol. 7, no. 4, pp. 400–405, 2019.

[16] A. Alia, M. A. Jusoh, H. J. Mohsin, and H. Yas, "The effect of e-accounting and mediated by internal control system on the performance of SME in Iraq," *American Journal of Business and Operations Research*, vol. 3, no. 1, pp. 5–38, 2021.

[17] N. El-Rashidy and N. Moustafa, "Mobile Mobile Cloud Database Security: Problems and Solutionsloud database security: problems and solutions," *Fusion: Practice and Applications*, vol. 7, no. 1, pp. 15–29, 2021.

[18] M. S. Krishna, D. Sravani, and B. A. Triveda, "Enhance data integrity for data storage in cloud computing," *International Journal of Engineering & Technology*, vol. 7, no. 2, pp. 68–70, 2018.

[19] S. Saxena and M. Sharma, "Secure Secure Technique to Achieve Data Privacy and Data Integrity in Cloud Computingechnique to achieve data privacy and data integrity in cloud computing," *INTERNATIONAL JOURNAL OF COMPUTER SCIENCES AND ENGINEERING*, vol. 6, no. 10, pp. 545–548, 2018.

[20] F Zhu, A. Kalra, T. Saif, Z. Yang, K. H. Yang, and A. King, "Parametric analysis of the biomechanical response of head subjected to the primary blast loading – a data mining approach," *Computer Methods in Biomechanics and Biomedical Engineering*, vol. 19, no. 10, pp. 1053–1059, 2016.

[21] R. Kanniga Devi, M. Gurusamy, and P. Vijayakumar, "An efficient cloud data center allocation to the source of requests," *Journal of Organizational and End User Computing*, vol. 32, no. 3, pp. 23–36, 2020.

[22] N. Baskaran and R. Eswari, "Efficient VM Efficient VM Selection Strategies in Cloud Datacenter Using Fuzzy Soft Setelection strategies in cloud datacenter using fuzzy soft set," *Journal of Organizational and End User Computing*, vol. 33, no. 5, pp. 153–179, 2021.

[23] H. Lu, R. Setiono, and H. Liu, "Effective data mining using neural networks," *IEEE Transactions on Knowledge and Data Engineering*, vol. 8, no. 6, pp. 957–961, 1996.

[24] C. Helma, T. Cramer, S. Kramer, and L. D. Raedt, "Data mining and machine learning techniques for the identification of mutagenicity inducing substructures and structure activity relationships of noncongeneric compounds," *Journal of chemical information and computer sciences*, vol. 44, no. 4, pp. 1402–1411, 2004.

[25] D Adeniyi, Z. Wei and Y. Yongquan, Automated web usage data mining and recommendation system using K-Nearest Neighbor (KNN) classification method," *Applied Computing and Informatics*, vol. 12, no. 1, pp. 90–108, 2016.

[26] V. Chaurasia and S. Pal, "A novel approach for breast cancer detection using data mining techniques," *Social Science Electronic Publishing*, vol. 2, no. 1, pp. 2320–9801, 2014.

[27] L. Xu, C. Jiang, J. Wang, and J. Yuan, "Information Information Security in Big Data: Privacy and Data Miningecurity in big data: privacy and data mining," *IEEE Access*, vol. 2, no. 2, pp. 1149–1176, 2014.

[28] X S. Yan, L. S. Zheng, and L. Zheng, "Fundamental Fundamental Analysis and the Cross-Section of Stock Returns: A Data-Mining Approachnalysis and the cross-section of stock returns: a data-mining approach," *The Review of Financial Studies*, vol. 30, no. 4, pp. 1382–1423, 2017.

[29] T Jiang, X. Chen, J. Ma, and J. Ma, "Public Public Integrity Auditing for Shared Dynamic Cloud Data with Group User Revocationntegrity auditing for shared dynamic cloud data with group user revocation," *IEEE Transactions on Computers*, vol. 65, no. 8, pp. 2363–2373, 2016.

[30] J. Mao, Y. Zhang, J. Liu et al., "A position-aware merkle tree for dynamic cloud data integrity verification," *Soft Computing*, vol. 21, no. 8, pp. 2151–2164, 2017.

Hindawi
Scientific Programming
Volume 2022, Article ID 7336569, 11 pages
https://doi.org/10.1155/2022/7336569

Research Article

Application of Flexible Friction Nanogenerator and Sensor in Sports Safety Monitoring

Erwei Liu

Students Affairs Department, Chongqing Vocational College of Transportation, Jiangjin 402247, Chongqing, China

Correspondence should be addressed to Erwei Liu; liuerwei@cqjy.edu.cn

Received 30 June 2022; Revised 11 August 2022; Accepted 23 August 2022; Published 8 September 2022

Academic Editor: Juan Vicente Capella Hernandez

With the development of science and technology, nanotechnology gradually becomes the growing energy shortage of new energy technology, and gains more and more scientists' attention. Friction nanogenerator (TENG) is a nanogenerator with efficient energy conversion. Nanotextile (TEF-F) is a kind of friction material suitable for human skin, because nanotextiles have antibacterial function, radiation prevention, antistatic resistance, flame retardant, and other functions, and they can act on the outer layer of the skin and play a very good protective role. This article aims at studying a flexible friction nanogenerator and sensor as a safety monitoring equipment for sports. In this article, PTFE and nylon are proposed as friction nanomaterials of a flexible friction nanogenerator. A model of power generation by friction between insole and athlete is designed and tested. The experimental results show that the output voltage of PTFE friction nanomaterials with 50% water tightness can reach 200 V. Under the same conditions, compared with the output voltage of different textile fibers, the output voltage of nylon is up to 180 V. The output voltage of thin PTFE can reach 200 V, while that of nylon can reach 180 V. The output voltage of PTFE with medium thickness is 65 V, while that of nylon is 84 V. For thicker PTFE, the output voltage is only 58 V, while that of nylon is only 67 V. Therefore, for cotton, polyester, and nylon under the same conditions, the output voltage of nylon is significantly higher than that of different textile fibers. Moreover, for PTFE and nylon friction nanomaterials, the thinner their thickness, the higher their output voltage is.

1. Introduction

With the development of human beings for thousands of years or even tens of thousands of years, all walks of life in the world have developed rapidly, and energy has been continuously utilized and consumed by humans in recent decades or even hundreds of years. Therefore, the whole society has the problem of energy shortage, and there is also a serious energy crisis. And in recent decades, the large-scale use of fossil energy has not only brought great progress to the world economy and human society, but also caused a significant impact on the environment and climate around us; fossil energy can be used as a fuel for various means of transportation, which has brought a lot of convenience to human life, but the exploitation of fossil energy causes huge damage to the environment, and the greenhouse gases produced affect the climate. Since the reform and opening up in the last century, China's social economy has developed rapidly, and environmental problems have become increasingly prominent. The discharge of industrial wastewater, the increase in the PM2.5 content in air, the emergence of "smog," etc. not only restrict the development of the economy, but also seriously endanger human health. What's more, it will affect the health of future generations. Therefore, it is urgent to develop new energy sources to meet the needs of society.

Existing fossil energy is no longer inexhaustible as people once thought. Therefore, in order to deal with the existing energy crisis, it is necessary to develop other energy sources and find more and more sustainable energy sources for the human society. The specific sustainable energy source available is tidal power, wind power, hydroelectric power generation, and the friction nanopower generation studied in this article. Wearable fabric-based energy harvesters are increasingly important in use in portable consumer electronics as an eco-friendly energy source that can be

independently self-powered through various activities. Wearable electronics include electronic watches, optical eyes, headphones, and electronic insoles. Using these wearable electronic devices combined with flexible friction nanogenerators to generate electricity will be a major energy development. Triboelectric generators can directly convert the energy in our living environment into electricity and are self-powered components of wearable devices. Wearable electronics urgently need flexible transparent triboelectric generators (FTTGs) with high-output power density, and functional polymers are outstandingly unique in the fabrication of smart devices such as sensors and actuators. Flexible friction nanogenerator can use the static electricity generated by friction collection to produce new green energy, with the characteristics of strong utilization and strong practicality. But it is rarely used to convert mechanical energy into electrical energy.

Renewable energy sources have developed rapidly, but these energy sources can only be used by industries or society, and it is not enough to rely on such resources alone. With the rapid development of science and technology in various fields, many remarkable research results have also been achieved. Therefore, experts use the existing research principles to convert some of the existing energy that appears around us into electrical energy through some common physical and chemical principles. It makes it more suitable for the needs of human life.

New forms of energy can collect energy from the surrounding environment and convert it into electricity for use. Among all kinds of energy, the mechanical energy generated by the human body is easy to be collected. Moreover, it can be used in a wide range, and is clean and environmentally friendly. And in the future, electronic products will become smaller and smaller, the quality will become lighter, and the use will be more convenient. This requires the energy supply products to have the advantages of small size, easy portability, and light weight under the premise of providing stable output power. Nanogenerators have the advantages. Therefore, the application of flexible triboelectric nanogenerators and sensors in this article is of great significance in sports safety monitoring.

The innovations of this article are as follows: (1) This article deeply studies a new energy source of F-TENG. (2) The new energy of F-TENG studied in this article will be applied to sports, which will be more friendly and promote people's exercise of sports. (3) This article tests and analyzes the designed new energy equipment to understand its time effect.

2. Related Work

With the continuous development of science and technology, nanotechnology has achieved good application in many fields. At present, many scholars have conducted in-depth research on TENG. Among them, Jeon found that layers with ZnO nanostructures were regularly formed on indium tin oxide-coated polyethylene naphthalate (PEN) substrates. The output voltage of the TENG-containing layers with ZnO nanostructures and operating in vertical contact separation mode is about 20 V. This shows a 2x power improvement compared to TENG without such layers [1]. Pingjian optimized the electrode structure by introducing graphene and indium tin oxide as transparent electrodes. He prepared FTTG with polyimide and polyethylene terephthalate as the friction layer and graphene as the top (bottom) electrode. Zhou also analyzed the effect of the electrode structure on the performance of FTTG and discussed the corresponding mechanism [2]. The multifunctional device designed by Guo can not only harvest tiny mechanical energy with high power density from ambient motion, but also detect dynamic forces with excellent sensitivity. This technology offers great application prospects in portable or wearable electronics, nanoelectromechanical devices, and self-powered sensors [3]. Choi addressed the output characteristics of a highly flexible Ni-Cu fabric-based triboelectric nanogenerator (F-TENG) employing a surface-imprinted polydimethylsiloxane (SE-PDMS) layer. Its method may provide a useful and simple route for developing self-powered, wearable, and smart electronics based on fabric substrates [4]. Kim showed that the choice of solvent used to dissolve polymers can significantly affect their performance in terms of energy harvesting. Kim confirmed by finite element method simulations that higher dipole moments lead to higher piezoelectric, pyroelectric, and triboelectric potential distributions. In short, his approach using high dipole moment solvents is very promising for high-output *P* (VDF-TrFE)-based wearable NG [5]. Deng developed a vibrator-based triboelectric nanogenerator (VTENG) by embedding a layer of silver nanowire percolating network into a dynamic disulfide bond-based vibrator elastomer. This self-healing and shape-adaptive VTENG by Deng has been shown to be useful in mechanical energy harvesters and self-powered tactile or pressure sensors with longer lifetime and excellent design flexibility. And the results show that incorporating organic materials into electronic devices can not only impart functional properties. It also provides a new approach for flexible device fabrication [6]. The research of the scholars provides certain theoretical help for the development of the F-TENG or sensor. However, these studies have not actually been used more due to factors such as high cost and complexity, so it is necessary to propose more improvement schemes. The research on the application of F-TENG and sensors in sports safety monitoring will be a real application combining theory and practice, which has important value and significance.

3. Safety Monitoring Model Based on F-TENG and FTNS

3.1. Flexible Triboelectric Nanogenerators. Triboelectricity is a well-known natural phenomenon that people live in, and the triboelectric effect is one of the few effects that people have known about for thousands of years. Although this phenomenon occurs every day in people's lives, there are still many debates about what the real physical mechanism is behind it. Electrostatic charges can affect the emission of radio signals, cause explosions, make MOS devices fail, and so on. MOS is a metal-oxide semiconductor field effect

transistor, referred to as gold oxygen half-effect transistor [7], MOS devices use transistor devices, and are two symmetrical regions, even if the two ends are adjusted, it will not affect the performance of the device [8]. Therefore, triboelectricity has been regarded as a negative effect for a long time. Since then, the triboelectric effect has been widely used from its infancy stage to today, and then to energy harvesting and various self-driven mechanical sensors. With more and more in-depth and diverse research by researchers, the output performance of TENG is getting better and better, and it also plays an important role in the application scenarios [9, 10]. Figure 1 is a schematic diagram of the structure of the nanogenerator.

The technology of triboelectric nanogenerators provides a route to efficient energy conversion. The method can be applied in various practical fields, and its performance is sufficient to become an energy device to provide power. Triboelectric nanogenerator can be used to function since the power system of electrical response materials/devices, including artificial muscles, microactuator, memory device, electrostatic manipulator, air purification, electronic excitation, and ion generator [11]. The main applications of triboelectric nanogenerators can be divided into the following types: first, energy harvesters of vibrational energy to power self-charging systems; second, self-powered sensors, such as active sensors for medical, environmental monitoring, and security infrastructure; third, a basic network unit for harvesting low-frequency energy in the blue energy concept [12].

Vibration can be seen everywhere in our daily life. Vibration occurs in human movement, car driving, and even the fluctuation of water. Harvesting vibration energy as a long-term development and continuous improvement technology still has unlimited potential. However, the vibrations in the environment often have a wide frequency distribution and even change over time in many cases. At this point, triboelectric nanogenerators show unique advantages. It can work in a wide frequency range, and secondly, it can work effectively in the low-frequency range, and the common vibration frequencies in the environment are distributed in this range, such as human motion mechanical vibration, rotational motion energy, and wind energy and water wave energy [13].

With the continuous development of the Internet of Things, the core work unit, the sensor network, needs to carry more functions, and it needs to work independently without external power supply. As IoT sensors are widely distributed, their combination and use with traditional power sources will be a major challenge. Therefore, it is necessary to develop self-powered sensors that can utilize the energy in the environment to convert it into electrical energy. The amplitude, frequency, and period information contained in the voltage and current signals generated by the sensors are directly related to the mechanical input behavior of the device. In this part, various applications of self-powered sensors will be introduced, such as sensors for detecting ion concentration, human tactile sensors, and biomimetic membrane sensors and others [14].

Water waves are widely distributed around the world, and the energy contained in them is one of the richest. A hydroelectric power station is a typical method of utilizing the gravity of water. It can convert the energy contained in the water into electricity that can be used by people. Most hydroelectric power plants need to harvest energy from rivers, and tidal energy can also be harvested in some estuaries or coasts. As we all know, the energy of water waves in the ocean is extremely rich, and it will not stop no matter when or where. Very little space is required to collect this energy. And it is more secure. It is a green, sustainable, and environmentally friendly way to solve today's pressing energy problems [15, 16].

After the concept of self-triboelectric nanogenerators was proposed, there have been many related research studies on triboelectric nanogenerators in the world. In recent years, flexible textile materials have also gradually developed into the main material of triboelectric nanogenerators. It can be applied to the field of clothing, which provides great convenience for the energy supply of wearable devices in people's daily life. There are already attempts to combine this form of power generation with human clothing. Moreover, many textile materials can be used as the main friction material of the device, and the obtained triboelectric nanogenerator can be applied to the insole or connected with the sensor to provide electrical energy to some microdevices. Figure 2 shows several common flexible friction nanomaterials [17].

The current of free charge movement is actually a time-varying electric field, mainly from the slight movement of the charges in the atoms and the contribution of the dielectric polarization in the material. According to the displacement current variance in physics, it can be expressed as follows.

Gauss' law:

$$\nabla \cdot D = \rho_f. \tag{1}$$

Electromagnetism:

$$\nabla \cdot B = 0. \tag{2}$$

Faraday's law:

$$\nabla \cdot E = \frac{\partial B}{\partial t}. \tag{3}$$

Ampere's current law:

$$\nabla \cdot H = J_f + \frac{\partial D}{\partial t}. \tag{4}$$

Here, D is the displacement field, B is the magnetic field, E is the electric field, H is the magnetization field, ρ_f is the free charge density, J_f is the resource current density, and the displacement field is given as

$$D = \epsilon_o E + P. \tag{5}$$

Here, P is the polarization field and ϵ_o is the permittivity.

For displacement current, its expression is

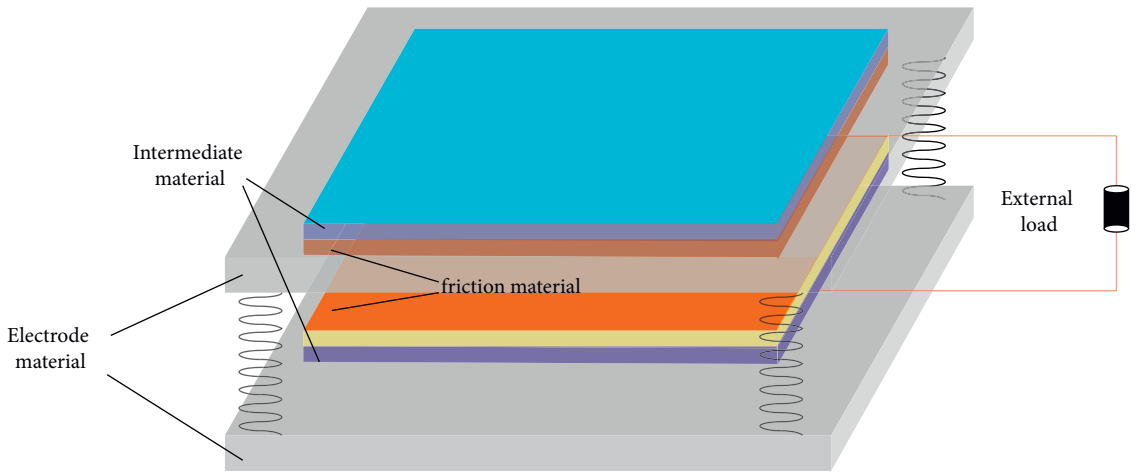

Figure 1: Schematic diagram of the nanogenerator.

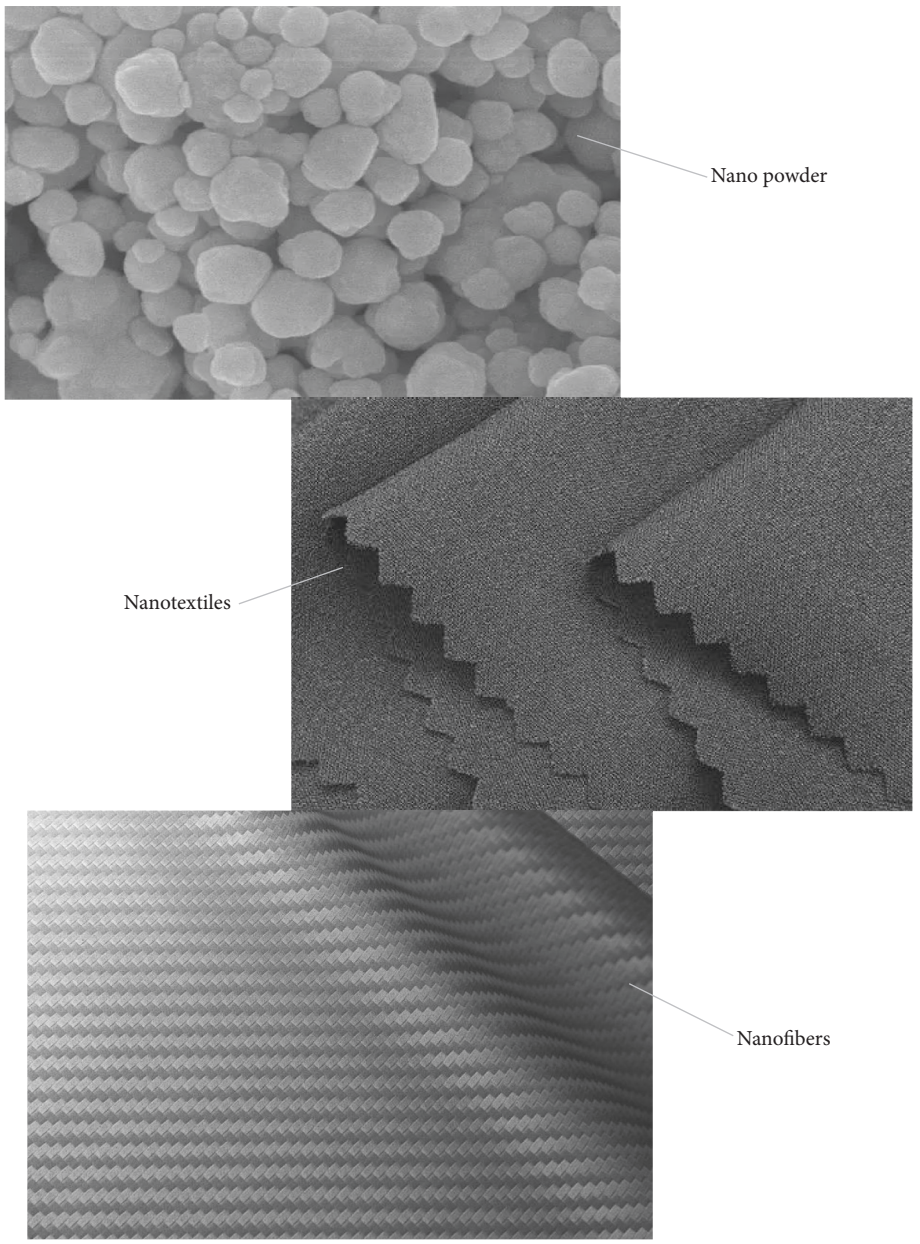

Figure 2: Flexible friction nanomaterials.

$$J_D = \frac{\partial D}{\partial t} = \epsilon_o \frac{\partial E}{\partial t} + \frac{\partial P}{\partial t}. \quad (6)$$

As time changes, the electrostatic field established by the triboelectric charge drives the current to flow through the external load, resulting in the accumulation of free electrons in the electrodes. As shown in Figure 3, the relative voltage drop between the two electrodes is

$$V = \sigma_1(z,t)\left[\frac{d_1}{\epsilon_1} + \frac{d_2}{\epsilon_2}\right] + \frac{z[\sigma_1(z,t) - \sigma_c]}{\epsilon_0}. \quad (7)$$

In short circuit, $V = 0$; at this time,

$$\sigma_1(z,t) = \frac{z\sigma_c}{d_1\epsilon_0/\epsilon_1 + d_2\epsilon_0/\epsilon_2 + z}. \quad (8)$$

Substituting the previous equation into formula (6), we get

$$J_D = \frac{\partial D_z}{\partial t} = \frac{\partial \sigma_1(z,t)}{\partial t}. \quad (9)$$

Affected by the external load, the current formula is

$$\mathrm{RA}\frac{\partial \sigma_1(z,t)}{\partial t} = \frac{z\sigma_c}{\epsilon_0} - \sigma_1(z,t)\left[\frac{d_1}{\epsilon_1} + \frac{d_2}{\epsilon_2} + \frac{z}{\epsilon_0}\right]. \quad (10)$$

Here, z is a function of time t.

3.2. FTNS. Sensing and detection technology at the nanoscale has achieved rapid development in the past two decades. Due to the huge surface-to-volume ratio of nanoscale reactive devices, surface effects play a key role in the static and dynamic properties of nanoscale devices. In particular, for widely used nanosensors with thin films or substrate structures, changes in temperature can cause bending deformations and changes in natural vibration frequencies, thereby affecting the accuracy of sensing and detection [18].

The high-sensitivity nanosensors of the converter are mostly hetero-material stacked sensors of two materials. Among them, temperature, as the main influencing factor, can be changed by various conditions such as illumination, changes in room temperature, piezoelectric effect, and molecular adsorption and exotherm [19, 20]. In order to theoretically obtain the bending curvature and vibration frequency of the nanosensor under the influence, in the static analysis part, the deformation mechanism of the statically indeterminate sensor is studied in detail. It results in a theoretical prediction formula for the curvature of bending deformation. In the vibration analysis part, we only consider the effect of the temperature dependence of the material on the vibration frequency [21].

The bending curvature of the nanosensor is related to the type of adatom, the degree of temperature change, the material type of the film and the substrate on the sensor, and the change of the substrate thickness when the film thickness is fixed. It is independent of the length and width of the nanosensor. Nanosensors and nanomotion sensors change their natural vibrational frequencies when the surface is excited by atomic/molecular adsorption. By monitoring this frequency change, it can be used for sensing, as well as the identification and detection of atoms, molecules, and biological macromolecules (such as DNA and RNA) [22, 23].

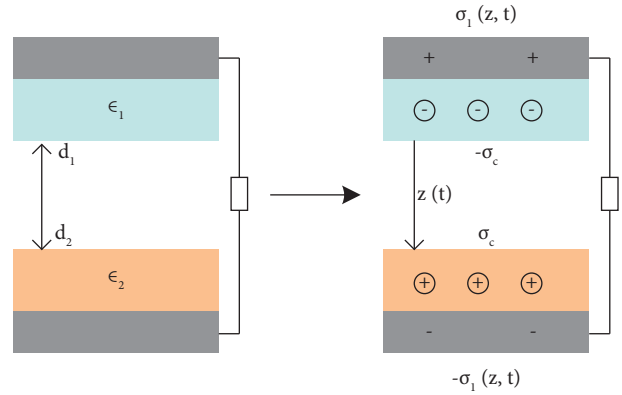

Figure 3: Working mechanism of the triboelectric nanogenerator with increasing number of contacts.

In early experiments, people attributed the vibrational frequency shift of the micromotion sensor to the mass loading of adatoms or molecules. However, in subsequent studies, it was found that the surface stress during the adsorption process also affects the vibration frequency shift of the micromotion sensor. The research shows the temperature dependence of micromotion sensor materials, especially the temperature dependence of Young's modulus, that is, the "thermal excursion" effect. Among the effects of temperature change, it plays a major role in the influence of the vibration frequency of the micromotion sensor [24].

The analysis and discussion of the natural frequency of nanomotion sensors are developed on the basis of macroscale motion sensors. The vibration control formula of the double-layer heterogeneous material-laminated motion sensor after ignoring the effect of damping and shear stress is

$$-\frac{\partial^2 M}{\partial x^2} - F\frac{\partial^2 v}{\partial x^2} + (m + \Delta m)\frac{\partial^2 v}{\partial t^2} = 0. \quad (11)$$

Here, M is the moment, F is the axial force, v is the motion curvature, m is the motion mass, and t is the motion time.

If the axial force is ignored, the vibration control formula is simplified to

$$-\frac{\partial^2 M}{\partial x^2} + (m + \Delta m)\frac{\partial^2 v}{\partial t^2} = 0. \quad (12)$$

Then, the vibration frequency can be obtained as follows:

$$f_i = \frac{1}{2\pi}\left(\frac{\lambda_i}{L}\right)^2 \sqrt{\frac{TD}{m + \Delta m}}. \quad (13)$$

Here, T is the time length, L is the length of the motion arm, and D is the equivalent coefficient.

And,

$$\cos\lambda_i \cos h\lambda_i + 1 = 0. \quad (14)$$

For the vibration frequency of the nanomotion sensor at different temperatures, the problem can be simplified to the discussion of the vibration frequency of the cantilever arch, and the derived vibration control formula is

$$\frac{\partial S}{R\partial\varphi} - \left(\rho_f A_f + \rho_s A_s\right)\frac{\partial^2 v}{\partial t^2} = 0. \tag{15}$$

The resulting frequency formula is

$$2\cos\xi\frac{l}{R}\cos h\eta\frac{l}{R} + \left(\frac{\xi}{\eta} - \frac{\eta}{\xi}\right)\sin\frac{l}{R}\sin h\eta\frac{l}{R} - \frac{\left(1+\eta^2\right)^2}{\left(1+\eta^2\right)\left(1-\xi^2\right)} = 0. \tag{16}$$

And η and ξ satisfy

$$\eta = \sqrt{\frac{1}{2}\sqrt{1+4x^4} - 1}, \qquad \xi = \sqrt{\frac{1}{2}\sqrt{1+4x^4} + 1}. \tag{17}$$

3.3. Sports Activity. At present, the Chinese government has increased the financial expenditure on public welfare sports year by year. However, due to the existence of objective reasons such as the weak foundation and late start of China's public sports undertakings, the related research on China's public sports is still relatively one-sided. There is a serious lack of safety benefits and service standards related to public sports, and public sports safety accidents and service quality problems occur frequently. The purpose of this study is to summarize research findings on the safety and services of public facilities around the world. Combined with the actual development status of China, this article conducts a survey on the safety and service of public sports. It initially constructs the framework of public sports management and service standards so as to provide technical support for the development of China's public welfare sports [25].

The core function of public sports is to provide the public with daily physical fitness services and realize people's demands for physical exercise facilities. The superordinate concept of public sports should be self-contained facilities. The implementation of sports refers to various venues, , buildings, fixed facilities, etc. used for sports competitions, training, teaching, and mass fitness activities. The basic function of sports is to provide users with buildings, venues, equipment, etc. that can be used for sports activities. Therefore, the primary goal of public sports as a subordinate concept of sports should be to meet the daily exercise needs of the masses. Figure 4 shows several common sports.

At present, countries around the world have researched and analyzed the main causes of personal sports injuries by consulting medical institutions' records of injured persons, and found that the primary safety hazard causing sports injury accidents comes from personal sports safety. The elderly and children often suffer from frequent injury accidents when exercising in public sports and fitness venues due to physical fitness constraints and contempt for sports safety.

Some surveys have shown that Chinese residents have a weak awareness of personal sports safety, and they have a serious fluke mentality. For the sake of temporary convenience, they give up the use of personal sports equipment. In the survey of personal fitness precautions, most respondents said they understood the precautions such as "avoid strenuous exercise after meals" and "choose suitable exercise according to their own conditions." However, there are still some people who ignore the safety and fitness precautions, resulting in frequent sports injuries. In the process of using public sports equipment, there are still some people who ignore the safety regulations for the use of equipment, resulting in sports equipment not being used correctly, and incidents of equipment injury are not uncommon.

4. Test of the Sports Safety Monitoring Model

4.1. Design of the Model. Triboelectric nanogenerator research has achieved some results. The selection of softer and less consumable materials has become the focus of research. The textile fiber material just meets the requirements for wearability. Therefore, based on the existing polymer triboelectric nanogenerators, this article explores the feasibility of various textile fiber materials in the preparation and application of triboelectric nanogenerators, and realizes the perfect combination of nanogenerators and textiles. Figure 5 shows the principle of the textile-like triboelectric nanogenerator chosen in this article.

In this article, based on the principle of triboelectric power generation and electrostatic induction, two kinds of fiber materials with strong gain and loss electron pairs were selected through experiments to prepare flexible triboelectric nanopower devices. It is finally combined with the insole. It converts the mechanical energy generated by the athlete into electrical energy and uses the electrical energy to monitor the sports safety of the athlete. The model designed in this article is shown in Figure 6.

The model is mainly composed of nanosocks made of nanotextile materials as nanogenerators. The athlete's movement is used to generate electricity, and the nanosensor collects the relevant data of the athlete's movement process. This article presents the data to the user through the mobile phone APP or electronic watch, so as to achieve the purpose of sports safety monitoring.

4.2. Simulation Experiment. The experimental instruments used in this article and their models are shown in Table 1.

When selecting the friction material, it should select two materials with stronger ability to obtain and lose electrons. During the contact friction process, each surface can accumulate more charges, and its external output electrical signal is enhanced. The power generation sequence of some friction materials is shown in Table 2.

In addition, the roughness of the surface of the friction material itself also has a great influence on the power generation efficiency. Therefore, appropriately changing the

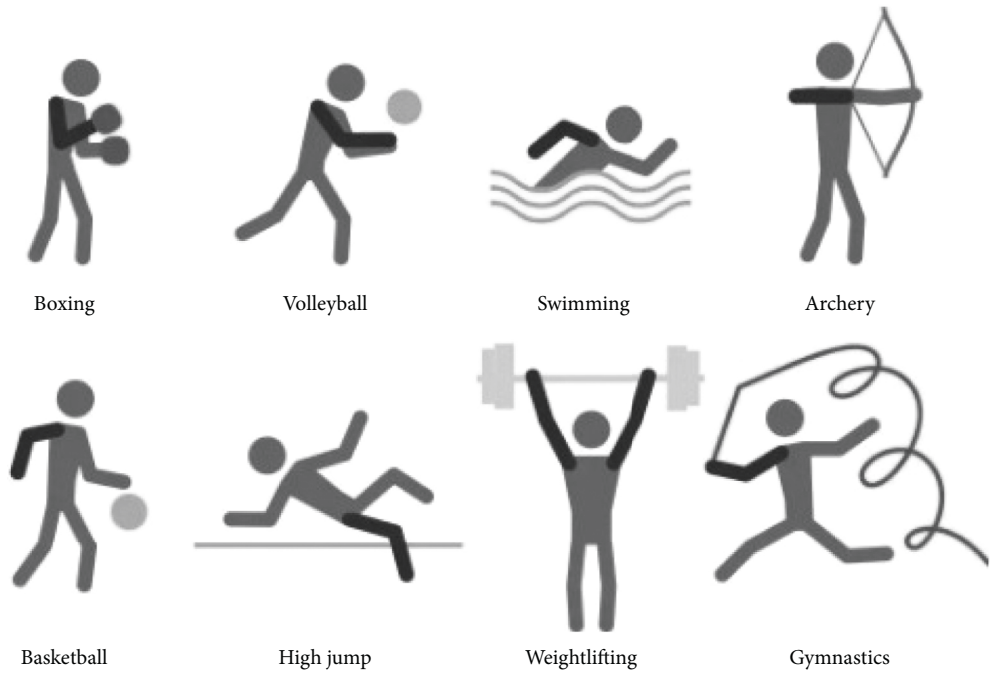

Figure 4: Common sports.

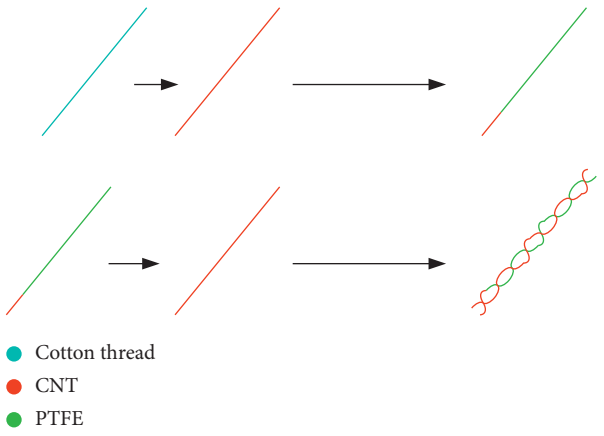

Figure 5: Principle of the textile-like triboelectric nanogenerator.

surface structure and morphology of the material and changing its roughness can also improve the power generation efficiency of the device. Therefore, two nanotextile materials, nylon and PTFE, are selected as the friction layer materials of the nanogenerator in this article. The two materials are shown in Figure 7.

In addition, the processes of nylon and PTFE nanotextile materials are shown in Tables 3 and 4.

4.3. Experimental Results. Finally, the output properties of the two friction nanotextile materials were obtained according to the simulation test, as shown in Figure 8.

It can be seen from Figure 8 that the output voltages of PTFE friction nanomaterials with different water tightness are quite different. Among them, the output voltage of 50% water tightness can reach 200 V. Compared with the output voltage of different textile fibers of cotton, polyester and nylon under the same conditions, the output voltage of nylon is significantly higher, reaching 180 V.

In addition, the output performance tests of different thicknesses of PTFE and nylon are carried out in this article, and the results are shown in Figure 9. The output voltage of thinner PTFE is 200 V, while that of nylon is 180 V, the output voltage of medium-thick PTFE is 65 V, while that of nylon is 84 V, and the output voltage of thicker PTFE is only 58 V, and that of nylon is only 67 V. The thinner the thickness of the two friction nanomaterials, the higher the output voltage.

5. Discussion

In this article, flexible textile materials are used as friction materials to prepare triboelectric nanopower generation devices. This article explores the influence of some properties of the material itself on the power generation efficiency. Affected by the research time and equipment, the subject needs further research in the following aspects:

(1) In this experiment, two different friction nanomaterials, PTFE and nylon, and their influence on the power generation performance of different thicknesses were studied. However, the weave structure of the selected fabrics is all plain weave, and the influence on the power generation efficiency can be explored by changing other different weave structures.

(2) In the process of weaving spacer fabric, only the influence of spacer yarn and fabric thickness on power generation efficiency was explored in this

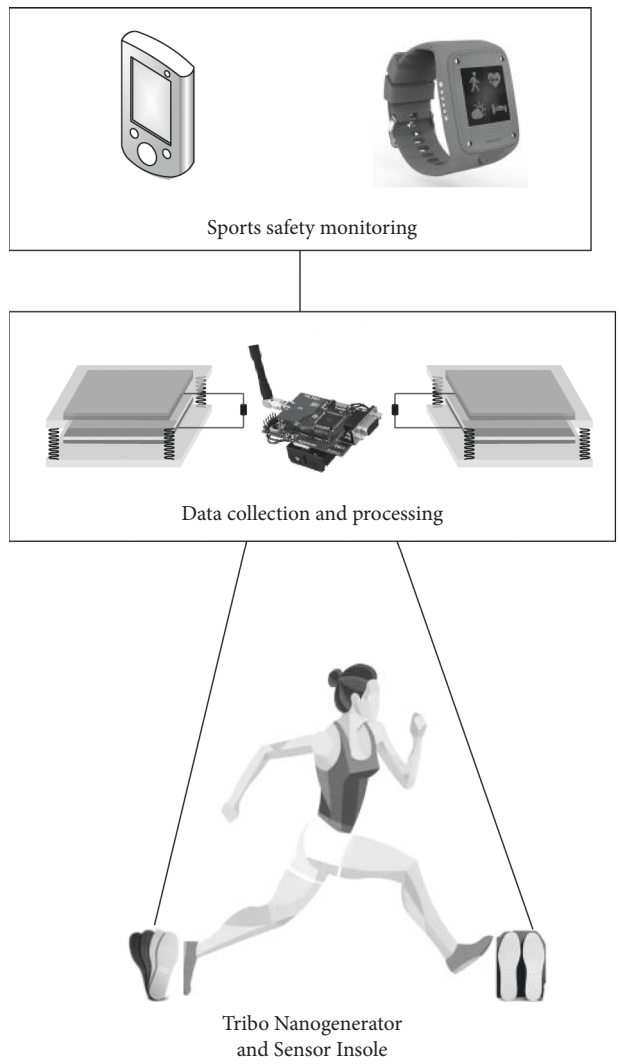

Figure 6: Motion safety monitoring model based on F-TENG and FTNS.

Table 1: Experimental instruments and their models.

Instrument	Model
Automatic Rapier loom	TNY101AB-20
Knitting computerized flat knitting machine	LXC-252SC
Resistance box	ZX21G
100 Catties testing machine	—
Oscilloscope	ZDS2022PLUS
Electrometer	KEITHLEY 6514

Table 2: Ranking of electricity-generating capacity of some tribo-nanomaterials.

Rank	Positive	Negative
1	Polyformaldehyde 1.3–1.4	Polybisphenol carbonate
2	Ethyl cellulose	Polychloroether
3	Polyamide 11	Polyvinylidine chloride (Saran)
4	Polyamide 6–6	Polystyrene
5	Melamine foam	Polyethylene
6	Wool, knitted	Polypropylene
7	Silk, woven	Polyimide (Kapton)
8	Aluminum	Polyvinyl chloride (PVC)
9	Paper	Polydimethylsiloxane (PDMS)
10	Cotton, woven	Polytetrafluoroethylene (Teflon)

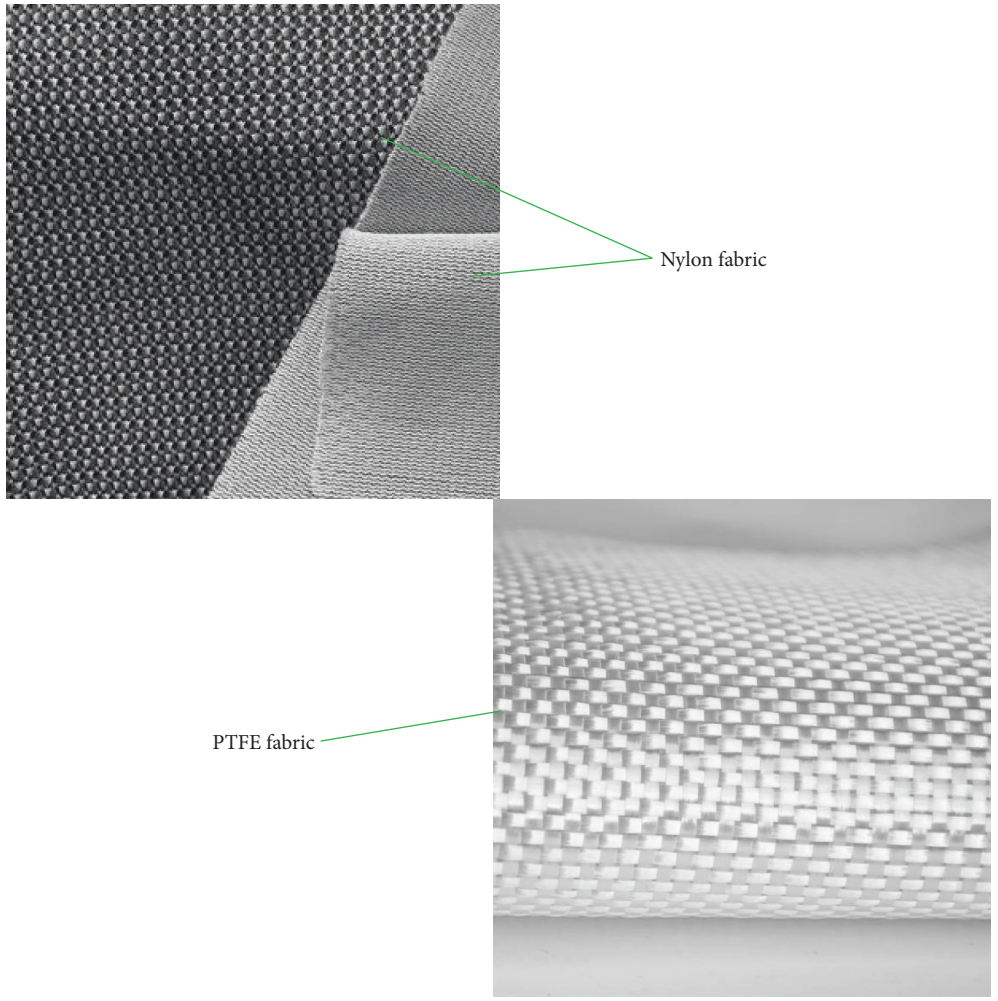

Figure 7: Nylon and PTFE nanomaterial fabrics.

Table 3: Nylon material technology of triboelectric nanogenerators.

Fineness (nylon)	Total warp root (root)	Reed width (cm)
150D/3	210	12.1
210D/3	178	12.5
280D/3	154	12.2

Table 4: PTFE material process of triboelectric nanogenerators.

Weft tightness (%)	Total warp root (root)	Reed width (cm)
10	138	11.7
30	138	11.7
50	138	11.7

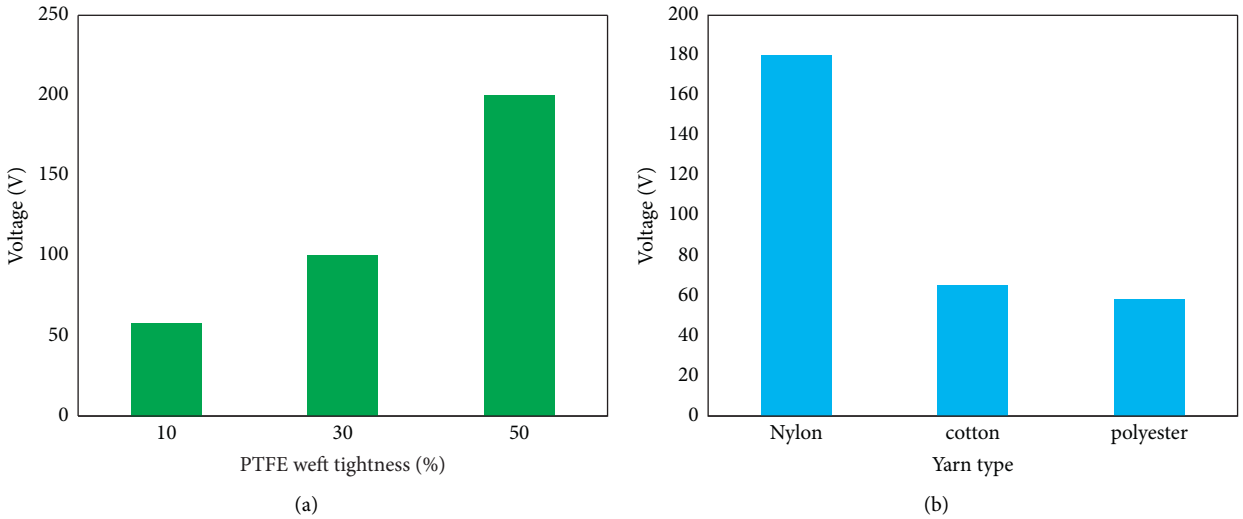

Figure 8: Output voltage comparison of tribo-nanomaterials. (a) Output properties of PTFE. (b) Comparison of output performance of nylon.

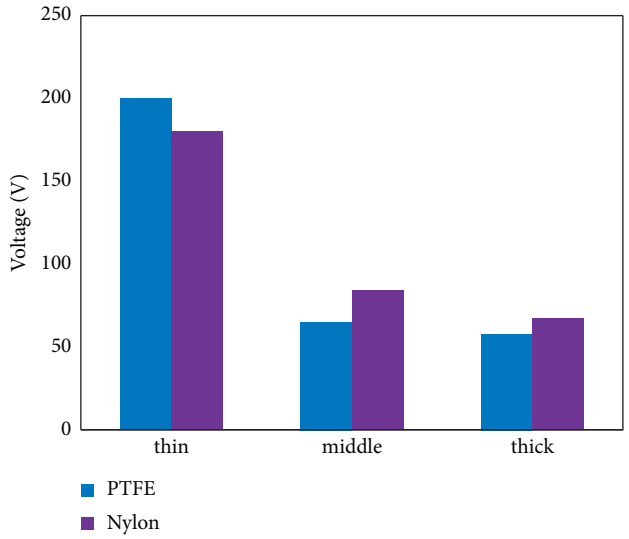

Figure 9: Comparison of output voltages of rubbed nanolayers with different thicknesses.

experiment. It can explore the influence of upper and lower layer yarn types on power generation performance.

(3) Due to the limitation of experimental materials, this article only explores the effects of two nanomaterials on the electrical output performance of triboelectric nanogenerators. It can further explore the effect of other nanomaterials on the output signal.

(4) In this article, the fabricated power generation device is only used in combination with the insole. It can also be used in conjunction with other electronic devices to provide electrical energy.

6. Conclusion

This article firstly gives an overview of the overall content of the full text in the abstract, and it then introduces the background of triboelectric nanogenerators in the introduction. It introduces the role of friction nanomaterials and summarizes the innovations of this article. In the related work part, some related research studies are exemplified in this article, so as to understand the current situation of the related content studied in this article. Then in the theoretical research part, this article firstly introduces the definition, characteristics, and classification and application fields of flexible triboelectric nanogenerators. This article secondly introduces the related content of nanomotion sensors and then introduces the related content of sports. It includes its types and characteristics. It finally proposes a motion safety monitoring model based on F-TENG and FTNS. In this article, the safety monitoring model is tested, and different friction nanomaterials are compared. The results show that the output voltage of PTFE friction nanomaterials with different water tightness is different. Compared with the output voltage of different textile fibers of cotton, polyester and nylon under the same conditions, the output voltage of

nylon is significantly higher. And for the two friction nanomaterials, PTFE and nylon, the thinner the thickness, the higher the output voltage.

Data Availability

This article does not cover data research. No data were used to support this study.

Conflicts of Interest

The author declares no conflicts of interest.

Authors' Contributions

The author has read and approved the manuscript for submission.

References

[1] Y. P. Jeon, J. H. Park, and T. W. Kim, "Highly flexible triboelectric nanogenerators fabricated utilizing active layers with a ZnO nanostructure on polyethylene naphthalate substrates," *Applied Surface Science*, vol. 466, pp. 210–214, 2019.

[2] J. Zhou, Y. Chen, X. Song et al., "Flexible transparent triboelectric nanogenerators with graphene and indium tin oxide electrode structures," *Energy Technology*, vol. 5, no. 4, pp. 599–603, 2017.

[3] H. Guo, T. Li, X. Cao et al., "Self-sterilized flexible single-electrode triboelectric nanogenerator for energy harvesting and dynamic force sensing," *ACS Nano*, vol. 11, no. 1, pp. 856–864, 2017.

[4] D. Choi, S. Yang, C. Lee, W. Kim, J. Kim, and J. Hong, "Highly surface-embossed polydimethylsiloxane-based triboelectric nanogenerators with hierarchically nanostructured conductive Ni-Cu fabrics," *ACS Applied Materials & Interfaces*, vol. 10, no. 39, pp. 33221–33229, 2018.

[5] J. Kim, J. H. Lee, H. Ryu et al., "High-performance piezoelectric, pyroelectric, and triboelectric nanogenerators based on P(VDF-TrFE) with controlled crystallinity and dipole alignment," *Advanced Functional Materials*, vol. 27, no. 22, pp. 1700702–1700702.8, 2017.

[6] J. Deng, X. Kuang, R. Liu et al., "Vitrimer elastomer-based jigsaw puzzle-like healable triboelectric nanogenerator for self-powered wearable electronics," *Advanced Materials*, vol. 30, no. 14, pp. 1705918–1705918.10, 2018.

[7] B. Gao, N. Xu, and P. Xing, "Shock wave induced nanocrystallization during the high current pulsed electron beam process and its effect on mechanical properties," *Materials Letters*, vol. 237, no. 15, pp. 180–184, 2019.

[8] X. Xu, D. Shahsavari, and B. Karami, "On the forced mechanics of doubly-curved nanoshell," *International Journal of Engineering Science*, vol. 168, Article ID 103538, 2021.

[9] C. P. Kleweno, W. K. Bryant, A. M. Jacir, W. N. Levine, and C. S. Ahmad, Discrepancies and rates of publication in orthopaedic sports medicine abstracts," *The American Journal of Sports Medicine*, vol. 36, no. 10, pp. 1875–1879, 2017.

[10] J. Vanrenterghem, N. J. Nedergaard, M. A. Robinson, and B. Drust, "Training load monitoring in team sports: a novel framework separating physiological and biomechanical load-adaptation pathways," *Sports Medicine*, vol. 47, no. 11, pp. 2135–2142, 2017.

[11] O. C. Ann, F. S. Tee, and V. Y. Nen, "A study on satisfaction level among amateur web application developers towards pigeon-table as nano web development framework," *Journal of Organizational and End User Computing*, vol. 31, no. 3, pp. 97–112, 2019.

[12] E. Brymer and R. D. Schweitzer, "Evoking the ineffable: the phenomenology of extreme sports," *Psychology of Consciousness: Theory, Research, and Practice*, vol. 4, no. 1, pp. 63–74, 2017.

[13] D. Hilgers, W. Maennig, and M. Porsche, "The feel-good effect at mega sport events. Public and private management problems informed by the experiences of the FIFA world cup," *International Journal of Business Research*, vol. 10, no. 4, pp. 15–29, 2017.

[14] N. A. Evans, "Current concepts in anabolic-androgenic steroids," *The American Journal of Sports Medicine*, vol. 32, no. 2, pp. 534–542, 2017.

[15] K. A. Bogue, S. F. Idriss, D. Sturkey, and A. Derouin, "Improving youth sports safety: implementing an emergency action plan for sudden cardiac arrest," *Journal of Pediatric Nursing*, vol. 59, no. 3, pp. 81–88, 2021.

[16] D. S. Hong, J. H. Lee, and E. J. Kim, "A comparative study on the survey and recognition of life sports safety accidents in korea and Germany," *Korean Journal of Sports Science*, vol. 27, no. 4, pp. 891–900, 2018.

[17] J. W. Lee and T. W. Jeong, "Item goodness-of-fit of the measuring scale of leisure sports safety awareness for university students using rasch model," *Korean Journal of Sports Science*, vol. 26, no. 6, pp. 1295–1305, 2017.

[18] I. Sowier-Kasprzyk and S. Kowalski, "Safety of sports mass events in the context of creating a marketing product," *System Safety: Human - Technical Facility - Environment*, vol. 1, no. 1, pp. 851–858, 2019.

[19] G. H. Choi, H. Ko, W. Pedrycz, A. K. Singh, and S. B. Pan, "Recognition system using fusion normalization based on morphological features of post-exercise ecg for intelligent biometrics," *Sensors*, vol. 20, no. 24, p. 7130, 2020.

[20] H. Zhu, H. Wei, B. Li, X. Yuan, and N. Kehtarnavaz, "Real-time moving object detection in high-resolution video sensing," *Sensors*, vol. 20, no. 12, p. 3591, 2020.

[21] B. Rowland, M. Kingsland, L. Wolfenden et al., "The impact of an alcohol consumption intervention in community sports clubs on safety and participation: an RCT," *Australian & New Zealand Journal of Public Health*, vol. 43, no. 2, pp. 114–119, 2019.

[22] I. S. Scher, R. M. Greenwald, and N. Petrone, *New Zealand snow sports injury trends over five winter seasons 2010–2014*, pp. 17–28, Springer, Germany, 2017.

[23] E.-S. Kang, "A narrative on causes of sports climbing safety accidents," *Korean Journal of Sports Science*, vol. 26, no. 3, pp. 163–173, 2017.

[24] J. Parkkari, K. Pasanen, A. M. Jussila et al., "Sports and exercise safety in Finland – live: an implementation program to sport clubs and schools," *British Journal of Sports Medicine*, vol. 51, no. 4, pp. 371.1–371, 2017.

[25] I. S. Scher, R. M. Greenwald, and N. Petrone, *skiing and snowboarding in Switzerland: trends in injury and fatality rates over time*, pp. 29–39, Springer, Germany, 2017.

Hindawi
Scientific Programming
Volume 2022, Article ID 9171941, 10 pages
https://doi.org/10.1155/2022/9171941

Research Article

Application of Planar Binary Image in Building Elevation Design

Xiaoyu Jia

Department of Transportation Engineering, Shanxi Railway Vocational and Technical College, Taiyuan 030013, Shanxi, China

Correspondence should be addressed to Xiaoyu Jia; jjxxyy0016@163.com

Received 14 June 2022; Revised 29 July 2022; Accepted 11 August 2022; Published 6 September 2022

Academic Editor: Juan Vicente Capella Hernandez

Architecture is one of the key and important parts of a city. Various kinds of buildings have absolute control over the quantity and area and are the key factors for the appearance of a city. With the development of cities and the increase of population, high-rise residential buildings can effectively alleviate the shortage of urban residential land, but at the same time, it also brings some problems, such as monotonous elevation of high-rise residential buildings, improper selection of elevation forms. As people's aesthetic awareness is getting higher and higher, people's requirements for the image of residential buildings are getting higher and higher. However, the research on the elevation design of high-rise residential buildings is relatively lagging behind. Therefore, it is necessary to enrich and expand the elevation design of high-rise residential buildings. Image binarization is an important technology in image preprocessing. It plays an important role in pattern recognition, optical character recognition, and medical imaging. Binary image is a simple image format. It has only two gray levels, but it occupies an important position in the field of image processing. In specific image processing application systems, it is often necessary to obtain binary values. The binary image processing arithmetic is developed from set theory under mathematical morphology. Although its basic arithmetic is simple, it can produce complex results. Based on the characteristics of binary image and the complex effect it produces, this paper finds out its regularity, finds a design method of building elevation, and realizes the application of binary image in building elevation design.

1. Introduction

Architecture is a material entity created by using existing technology, materials, and construction methods in order to meet people's living and social needs. Architecture forms space. Architecture can arouse people's emotions and bring people a variety of spiritual feelings. Beautiful urban space environment is not only because of beautiful buildings, but also because it has suitable scale of external space. "Field" is a state of existence of matter. There are effects of this field in "field," such as electric field, magnetic field and so on, and there will be a numerical value corresponding to any point in the field. We call the psychological influence and feeling of architecture on people as "building field." Affected by the construction site, people will have such feelings as grandeur, solemnity, simplicity, simplicity, repetition, order, nonlinearity, and so on. The generation of these feelings is the field effect of architecture. Because human perception of architecture is mostly accomplished by vision, the field effect of architecture is mostly the visual field of architecture. Similar to the division of external space by the visual field of architecture, when people observe architecture, it is not a static state, but a dynamic process from far to near or from near to far. Observing the changes of distance, angle, direction, color, texture, and outline of buildings will have different effects on people's perception of buildings and make people get different psychological experiences. Whether these locations, which produce different psychological feelings, can also find some mathematical relationship to quantify like the visual field of architecture, is a question worth exploring. In the study of traditional geomantic omen theory in our country, there is a description of "100 feet for shape, 1000 feet for potential" about the design of external space. This can be said to be a concise summary of the experience of architectural external space design in ancient China, and there are similar discussions abroad. Before the reform and opening up, limited by the economic foundation and people's living standards, we did not pay enough attention to the design of external space [1–3]. After the reform and opening up, with the rapid development of economy, people's living

standards are improving day by day, so are the aesthetic and environmental needs. With the rapid development of urban construction, high-rise buildings sprang up and the construction workload increased dramatically. The scale control of the external space of the building was relaxed or ill-considered. At the same time, the city has gradually lost its control and grasp of the external spatial scale. Today, with the rapid development of science and technology, we can draw lessons from the traditional theory of external space design and make more accurate and effective analysis and evaluation of architectural external space design through advanced computer technology, so as to make urban construction and space construction more scientific and reasonable. Simply put, when architects design houses, they use floor slabs and walls to create "nothing" that is space. Architecture is a kind of space which surrounds people. It can also be called the interior space of a building. The outer space of the building is relative to the inner space concept of the building and is closely related to human beings. Many famous historic and cultural cities at home and abroad not only have famous historic buildings, but also have many suitable external spaces, such as square streets, which give people visual enjoyment. Therefore, the study of cognitive scale of external space is of a great significance to architectural design and urban design.

As a subject with rich contents, digital image processing [4–7] mainly studies image transformation, enhancement, compression, restoration, segmentation, and comprehensive utilization, among which image transformation plays a very important role in digital image processing. Image transformation includes many important image processing methods and operations, such as image binarization [8–11]. Image binarization is often used in image processing to identify the object in the image and to segment the foreground and background regions of the image. It plays an important role in correctly analyzing the information contained in the image. Binarization is an image processing method for gray image. The so-called binarization is to transform a gray-level image in the range of 0–255 gray level into a black-and-white image (binary image) with only 0 and 255 gray levels. Therefore, binarization is a gray level transformation operation. Because binary image plays a very important role in digital image processing, binarization has a wide range of applications and is a very important means of image processing. It is necessary to study the binarization method. The application fields of general binarized images are license plate recognition and character extraction of images.

Based on the plane binary image, this paper puts forward the application method of plane binary image in building elevation [12–16] design, and applies the basic method of plane composition to three-dimensional building elevation through the law of binary image composition. The specific contributions of this paper are as follows:

(1) Firstly, the skeleton form of the elevation binary image is selected according to the architectural form

(2) Secondly, the binary image is constructed and adjusted according to the facade of the building, including the proportion of black and white and the relationship between part and the whole

(3) The binary image is mapped to the building facade, and the shadow generated by facade construction is taken into account as black

2. Proposed Method

The concept of diversified design [17–20] of assembly building includes that the structural system of the building can meet the diversified needs, the construction method of the building has good adaptability, the product needs can meet the personalized needs, the component parts can achieve diversified personalized performance on the basis of generalization, and the appearance of the facade of the building can achieve richness and artistic characteristics. In this paper, the elevation diversification design is based on the application of plane binary image, which meets the requirements of architectural aesthetics and has diversified performance. The purpose is to realize the individualization and diversification of facades of assembly buildings on the premise of standardization, and to increase the artistic appreciation, regionality, and sustainability of assembly buildings.

2.1. Building Elevation

2.1.1. Analysis of Building Elevation Design

(1) Comparison of Modularization, Standardization, and Diversity. Modularization is a standardized form evolved on the basis of standardization. The size of modularization, the typical structure, and the general components are all the concrete manifestations of modularization. Standardization is a unified regulation and measure for building products of construction industrialization to be interchangeable and versatile. It usually includes: standardized product design in a unified modulus, building accessories, building parts, and building moulds need unified specifications. Engineering construction standards are documents that prescribe common and repeated rules [21], guidelines or characteristics for construction activities or their results for the best order in the field of engineering construction, developed by consensus and approved by a recognized body approved, based on the combined results of science, technology, and practical experience, with the aim of promoting the best social benefit [22]. At the same time, the construction method of the joints of the building is based on the standard of the building products, building structure, building mechanics, building physics, site design, residential area design, urban planning, landscape architecture, urban and rural resources, etc., [23]. Quantification should be formulated in a unified way, so that the prefabricated production technology of components, construction technology, and quality can be unified. The emergence of standardization makes large-scale industrial construction possible. Diversified design is an important part of further discussion and industrialization of industrial product design on the basis of standardization. Diversified

design is not an unreasonable-free design. It is based on standardized components and structures, and through diversified combination methods, the building has a certain spatial shape and personalized realization. In the facade design of assembled building, the standardization degree will be improved correspondingly if the number of components is small. At the same time, the combination of components can also achieve diversification. However, diversification and standardization are not contradictory. They interact with each other and cooperate with each other, which can achieve both standardization and diversification of design. Summarize and explain the relationship between the three: modularization is the core of standardization, standardization is the basis of industrialization, diversification is the driving force of industrialization upgrading, as shown in Figure 1.

(2) Comparison of Traditional Composite Buildings and Diversified Buildings. Traditional assembly building design gives priority to structural system and component labeling. Designers are more concerned about how to produce and build accurately and quickly, and how to meet a large number of housing needs. The creation of architectural image is not the key point. The facade is not designed separately. The facade form is the direct response of the architectural plane. It is the result of rigid stacking of prefabricated components. It lacks individualized creation and the thinking process of diversified design. Compared with the traditional fabricated facade design, diversified design requires that the facade design should be taken into account at the beginning of architectural design. When splitting components and prefabricating production, we should think about the role of components in shaping the opposite image, whether we can adapt to the diversified needs by choosing the appropriate structural system, whether we can enrich the elevation image through regional materials and architectural language with national personality, and whether we can achieve the diversified design through new construction technology and technology.

(3) Importance of Diversified Design of Facade of Assembled Buildings. Because architecture involves usage behavior, design behavior, materials and technology, etc., its development has been affected by related disciplines. It is precisely because of its wide relevance that it is affected and restricted by many factors. Successful elevation design can correctly represent the natural landscape, regional culture, scientific, and technological development of the city. The exterior facade of a building is the interface between the building and the external space, the skin of the building, and it can directly realize the inherent characteristics and characteristics of the building. Therefore, it is necessary to focus on the research and analysis of the facade design method of the assembled building.

2.1.2. Basic Principles for the Diversified Design of Facades of Assembled Buildings. Beauty itself is an abstract and complex thing. It has absolute rules and relative differences.

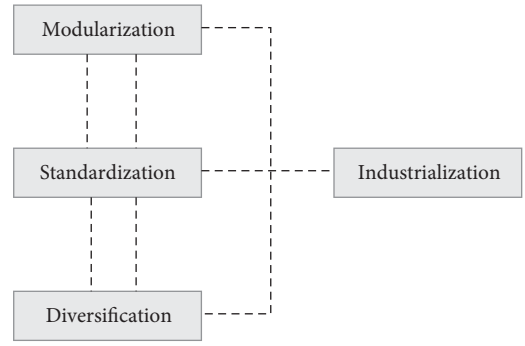

Figure 1: Diagram of industrialization, standardization, modularization, and diversification.

Regardless of the old and new buildings and the nature of the buildings, they all follow the law of formal beauty. Industrial architecture itself is the product of the times. It should embody its own personality and follow the steps of the times.

(1) Principles of Holistic and Dynamic Design. The principle of holistic design requires that elevation design be considered and studied as a part of architectural system design, rather than an isolated design process. Different component combinations form a complete assembly building. It can be seen that the study of the interaction and mutual restriction between component parts is helpful to create a rich and colorful facade of assembly building. The dynamic principle requires architects to have keen insight and foresight, to discover the inherent law of development and development direction of assembly building design, and to find the driving force of the times based on the basis of industrialization. Facade design requires designers to always pay attention to the development of building structure and the change of construction method system, study more advanced construction technology, and explore better design methods.

(2) Regional and Sustainable Design Principles. Building facade design needs to reflect regional characteristics because of its direct contact with urban cultural space. In different urban environments, due to the construction materials produced by the city and the aesthetics of the urban residents, the regional climate characteristics are different, and the structural forms of the buildings also produce different formal characteristics. For example, because of the drought in the north, there is no outer corridor at the bottom of the house, while in the south, when the temperature is changeable and rainy, the bottom overhead is often chosen. In the life cycle of buildings, the principle of sustainable design is to save resources, reduce pollution and create a harmonious, comfortable, healthy, and efficient living environment. The purpose of sustainable architecture is to reduce and control the consumption of resources in the whole life cycle of construction process and operation. The concept of sustainability is a new dimension of human thought. This paper examines the decisive role of the overall concept of ecology and the development of environmental ethics on the emergence of sustainable thinking, which has a post-modern ecological spirit.

Facade design should follow the principles of green, ecological, and sustainable. It is bound to be a resource-saving and environment-friendly building in order to achieve the balance of energy and resources in nature.

(3) Basic Principles of Facade Composition. Unification and change are widely used in architectural design. Architecture can be divided into whole and part by space analysis. There is a relationship of unity and change between architecture and details. In the elevation design, we should fully coordinate the overall and local change factors, deal with the relationship between them, and achieve unity and change. Equilibrium and stability are also an important principle in the construction of three-dimensional space. Equilibrium is mainly to study the relationship between the front and back of each part of the building, which should form a stable feeling after some combination. Stability refers to the overall importance of the relationship between the whole building, which should give people a safe and reliable effect. Equilibrium and stability are interdependent in the principle of formal beauty. Asymmetric equilibrium is to use the balance of volume, texture, color, and weight to achieve the purpose of asymmetric equilibrium, which is smart and lively compared with symmetric equilibrium. Because of the influence of structural technology and building products, there are many repetitive expressions in assembly building. In the architectural space composition, the component elements are used repeatedly or gradually to produce a sense of rhythm and rhythm. The contrast in architecture is shown in various spaces, such as the size and height of space, the smoothness and roughness of material, and so on. The proportion of buildings mainly refers to the relationship between the various parts of the building form. For example, the ratio of the whole building to the length, width, and height of space, the ratio of the area of windows and walls in the facade, etc.,

The artistry of architecture lies in its materiality, which is one of the important symbols distinguished from other plastic arts, but the content of architecture without form does not exist. Therefore, the plastic arts of architecture cannot be understood as the facade processing in the later stage, but should be carefully considered from the beginning of the design to the final construction. Designers should explore a series of aesthetic principles in space organization, structure, and material application in the relationship between function and production technology. The diversity design method of fabricated facade can integrate the use function and aesthetic function of the building. Therefore, it is necessary to study the design method of facade of assembled building.

2.2. Image Binarization

2.2.1. Binary Principle. In the process of digital image processing, firstly, the image should be converted into discrete digital form. For gray image, it is a two-dimensional matrix. Each element in the matrix represents a pixel point. The element value is the gray value of the image at that pixel point, and the range of the value is chosen. Binarization is to divide the whole image into two parts, foreground and background. The gray value of foreground part (i.e., the corresponding element value in matrix) is set to 255, and the gray value of background part is set to 0, so that the image contains only two gray values 0 and 255, thus showing obvious black-and-white effect. The threshold method is usually used to separate the foreground and background of the image, that is, the gray image with 256 brightness levels is separated from the target and background by appropriate threshold selection. After resetting the gray values of the two parts as described above, the binarization process can be completed, and the binarized image can be obtained. The key of threshold method is the method used to select the threshold. If the threshold method is used properly, the image can be segmented more accurately, so that the obtained binary image can still better reflect the overall and local features of the image.

2.2.2. Image Binarization Method. The most commonly used method of image binarization is threshold method, which can be divided into global binarization method and local binarization method according to the different methods of threshold selection. Global binarization methods include bimodal method, iteration method, and OTSU method. Among them, the OTSU law (Otsu law) put forward by the Japanese scholar Otsu is the most famous. Local binarization methods include locally fixed threshold method and locally adaptive threshold method.

2.3. Building Elevation Design Based on the Plane Binary Image. The application of plane binary image in building facade is divided into three steps: the first step is to select the skeleton form (regularity or irregularity) of the elevation binary image according to the nature of the building; the second step is to adjust the binary image according to the components of the building facade, including the proportion relationship between the black and white parts, the relationship between the part and the whole, and the relationship between the black and white parts; the third step is to select the binary image skeleton form (regularity or irregularity). The image is mapped to the building facade, and the shadows produced by the facade components are taken into account as black.

The elevation form of high-rise residential buildings generally consists of more than two kinds of detail components, which are combined and connected according to the relative position, direction, or gravity transfer relationship to form an organizational framework with a certain pattern, which is called formal structure.

2.3.1. Proportion and Scale. The so-called proportion is defined in the French Architectural Dictionary as follows: "proportion means the relationship between the whole and the part—it is logical and necessary, at the same time, proportion has the characteristics of meeting the requirements of reason and vision." Proportion is the building's

own property. It studies the relationship between the part and the whole in the construction, and this relationship is usually a mathematical relationship, such as multiple, cardinal, or function. Proportion is different from size. Dimensions represent specific quantities, not relationships. For example, the size of windows and balconies are all specific values. Proportion represents the relationship between values, and the relationship between dimensions is proportion.

Controlling and coordinating the proportion in the facade design of high-rise residential buildings is the basis of producing the beauty of facade form. At present, the proportion of facade design of high-rise residential buildings is not enough. The proportion of facade components in the whole wall is studied. In order to achieve the proportion coordination of facades, the concept of "ratio" is introduced. Ratio is a mathematical concept. Theoretically, it is the reaction of multiple relation. The value obtained by dividing two variables is the ratio between the two variables. The so-called proportion means that when there is a constant ratio between the two groups, the two groups can be said to be proportional to each other. The regular recurrence of the same ratio forms the proportion coordination, which brings people a good feeling. Throughout the development of architectural history, we can find that the golden rectangle [24] has a perfect ratio. The application of golden rectangle (Figure 2) and the proportion of human body in high-rise residential design make the elevation form design more in line with the aesthetic requirements of art.

Because of the complexity and contradiction of the building, while pursuing the harmonious proportional relationship, we should ensure the function, fire prevention, environmental factors, and so on. Harmonious proportion is not achieved in one move, nor is it a complete mathematical proportion. Instead, we need to grasp the dominant elements of elevation form design under the premise of ensuring reasonable function and make repeated deliberations on detail components. The mastery of perfect proportion will help us find the proportion of elevation form in design, speed up our design time and improve our design. Design quality. Scale in architecture, as its name implies, is the measurement of building size, which refers to the concept of building size by reference. Scale is different from proportion. Scale is subjective, and it is a kind of visual feeling through reference. In general, the design of high-rise residential buildings adopts real scale, which means that the visual scale sense is consistent with or basically consistent with the actual scale sense. The design of elevation form of high-rise residential buildings should take human scale as reference, fully consider the changes of human visual angle and visual distance when people are near and away from the residential buildings, and find a good sense of scale. Generally speaking, we can consider the elevation form scale of high-rise residential buildings from three aspects.

(1) Detailed Dimensions of Facade Members. The facade form of high-rise residential buildings is an indispensable part of the formation of real size. People's long-term life experience has made a deep impression on building components or

Figure 2: Analysis of facade of golden section building of Marseille apartment.

familiarity with the size, and formed a customary cognitive scale, such as the size of balconies, doors, and windows, and wall materials such as bricks, logs, stone sizes. Through reasonable design of these common dimensions, the true dimension of elevation can be achieved.

(2) Close-to-Human Scale of Elevation Form. Close-to-person dimension of facade form refers to the place at the bottom of the building where people most intuitively touch. It often sets up residential entrance here. This part tends to be friendly to the sense of scale and can adopt the technique of fine design of warm-colored material details. Especially, in the design of residential unit entrance, the scale should be carefully pinched. For example, outdoor step height, railing handrail height, etc.,

(3) Overall Scale of Elevation Form. The overall scale is the overall grasp of the opposite form, through the horizontal and vertical division. The number and height of building floors are determined horizontally and vertically. Vertical division determines the division of the room. Even composite partition, a large number of partitions highlight the details of the building facade, providing more reference for the real scale judgment of the building.

2.3.2. Rhymes and Rhythms. In the design of the elevation form of high-rise residential buildings, the rational and appropriate grasp of proportion and scale makes the elevation form full of rational and rigorous sense of order, while rhythm and rhythm are full of emotional consciousness, which adds interest to the composition of the shape. Rhythm and rhythm mainly refer to the appearance of the elements of detail components with regularization, patterning, repetition, or gradual change, showing a visual sense of motion or sequence (as shown in Figure 3). Windows and balconies are the first choice for rhythm and rhythm. Window, balcony in the high-rise residential facade presents a relatively small scale, in the facade form of the composition of the "point" visual effect. In the design of elevation form of high-rise residential buildings, through the grouping and faceting of windows and balconies, the points arranged continuously can produce linearization effect. They can be aligned vertically or horizontally along a straight line, or they can form a sense of rhythm by regularly crossing horizontally and vertically, or even form a linear texture of grid by arranging in patches. Intuitively speaking, rhythm cannot be separated

Figure 3: The presentation of rhythm in architecture.

from repetition. With the repetition of elements in composition, people's eyes bring different feelings in the way of repetition. The use of repetition is a common means in architectural design. Facade decoration components can use gradual rhythm to enrich the facade effect. Gradual rhythm can be divided into spacing gradual change, size gradual change, and color gradual change. Gradual spacing is often used in the design of elevation of high-rise residential buildings in the form of door and window openings, wall partition, and even floor height partition. Gradual rhythm obtains the effect of picture movement. Dimensional gradient components can be formed by different sizes of windows. Gradient of color can be achieved by gradient of color brightness.

2.3.3. Equilibrium and Stability. One of the most obvious characteristics of residential buildings which are different from other types of buildings is the sense of security. To achieve a sense of security, we must follow the design principles of stability and balance. Balance and stability are more about people's visual perception and stability, which is a kind of visual habit and aesthetic concept formed naturally by people's long-term experience of understanding things. All plastic arts that conform to stability are considered to have aesthetic feeling. Equilibrium is also an important aspect in elevation design. Once buildings lose balance, especially residential buildings, it is possible to produce a sense of discomfort. Equilibrium can be divided into two categories: symmetric and asymmetric equilibrium. High-rise residential buildings are mostly symmetrical, so the shape is mostly symmetrical. Symmetrical technique has been widely used since ancient times. The emergence of symmetrical technique is not only the cause of the aesthetic sense of composition, but also related to the structural needs and functions and space needs. The most common limitation of ancient architectural technology is the symmetrical structure, because the symmetrical structure is the most easiest to achieve the static effect of the structural form. Today, with the rapid development of construction technology, symmetrical structure is still the first choice for structural design. Equilibrium is a pattern corresponding to symmetry, and the form of stability and incomplete symmetry is called equilibrium. Symmetry theoretically belongs to a special strict sense of equilibrium, which requires homogeneity, isomorphism, and quantity and is an absolute equilibrium. Equilibrium is a common natural equilibrium that exists universally. It can be isomorphic or even isomorphic. The upper and lower parts of the body or the left and right parts of the body need not be isomorphic. However, the balance of power must be balanced in human visual psychology. Asymmetric balance is more lively than strictly symmetrical balance. Contemporary architecture cannot meet the symmetrical balance. Motion is used to achieve balance. The main factors affecting the sense of visual balance are quality, color, quantity, distance, and volume. Formally, equilibrium is the opposition and destruction of symmetry. However, the two sides of the axis or fulcrum are not equal in shape, but equal in quantity and force. This special-shaped but equal-force relationship implies the principle of equilibrium. Equilibrium in the elevation form of high-rise residential buildings needs to be felt by visual psychology, which is essentially the balance relationship among visual psychology, shape, quantity, and force:

(1) High-rise residential buildings are mostly symmetrical slab or tower buildings in volume. When several buildings are connected together, they can also be balanced through asymmetry. At this time, we need

(a) (b)

Figure 4: (a) Image preprocessing. (b) Binary image bone architecture construction.

to start from the volume. There are big differences in morphology, but the volume is basically the same from the visual perception. Residential buildings often deal with the top and bottom, such as setting lightweight structures, sloping roofs, retreating platforms on the top, while deepening the color of the wall at the bottom, relaxing the columns, and increasing the volume to achieve stability.

(2) Visual perception of quality mainly comes from materials and colors. The second section of the previous chapter introduces that different colors bring different psychological feelings to people. The differences of color phase and intensity give people different perceptions of quality. Material also has a visual sense of quality, high-rise residential facade component selection of different materials will produce different effects, general metal material than stone more quality, stone more quality than wood, wood more quality than glass. It is just a visual experience, not the actual density of the material.

3. Experiments

3.1. Simulation Environment and Parameter Settings

3.1.1. Skeleton Extraction of Planar Binary Images. The edge of the image provides a large part of the visual information of the image. There are two advantages in extracting gray image skeleton from image edge: (1) partial contour information is applied while avoiding image segmentation; (2) mature skeleton method of binary image can be used to the maximum extent. Starting from the edge of the object, the skeleton strength diagram can be obtained by denoising [25], distance transformation [26], and isotropic diffusion of the edge of the object [27]. The skeleton strength diagram has a good feature: in the position of skeleton point, the value of skeleton strength diagram is much larger than that of nonskeleton point. This advantage makes it suitable for skeleton extraction of binary image and gray scale image.

Figure 5: Binary introduction to building facade.

Then, according to the building facade construction and adjustment of binary image, through different binarization methods to deal with and adjust plane objects, lay a good foundation for building facade design; finally, the binary image is mapped into the building facade to form a design scheme.

4. Analysis

4.1. Simulation Analysis. Before feature extraction of image, in order to highlight the features of binary image, this paper needs to preprocess the image, gray-scale processing first, then binarize the image. Finally, edge detection is carried out

(a) (b)

Figure 6: Binary construction of OTSU.

	MSE	SSIM
Algorithm in this paper	0.1358	0.9959
OTSU	0.4258	0.9741

Figure 7: Comparison of two binarization methods.

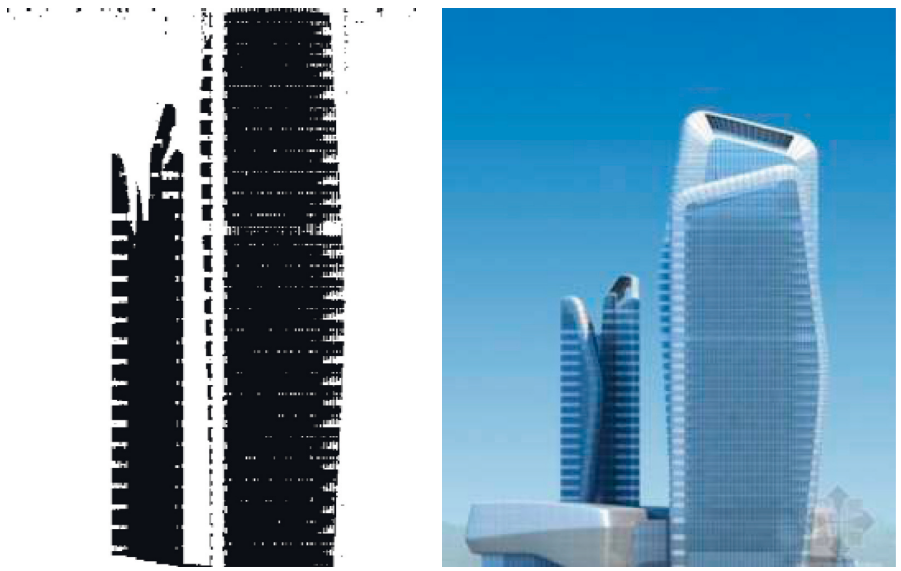

(a) (b)

Figure 8: The application of binarization method in a building design.

for binarization. Under the binarization skeleton, simulation shows that the preprocessing of this paper is conducive to subsequent image feature extraction. The binary skeleton of plane image is constructed, as shown in Figure 4.

After the construction of the binary skeleton structure, the binarization is introduced into the building facade to form a design prototype directly. As shown in Figure 5, this method is the result of the ordinary binarization treatment introduced into the building facade.

For comparison, this paper also uses OTSU binarization treatment as the same analogy to import building facades. The results of OTSU binarization method are shown in Figure 6.

Comparing the two binarization methods, Figure 7 shows the comparison results of the two methods.

As can be seen from the figure above, the algorithm in this paper is more practical, so we choose the algorithm in this paper to design a unit building. The effect is shown in Figure 8.

5. Conclusion

Image binarization is a common method that can identify objects and separate their foreground and background regions. It is very important to accurately analyze the information contained in the image. Binarization is a new method for processing grayscale images. Binary is to convert a grayscale image of 0–255 into a black and white image (binary image) with 0, 255 grayscale. Binary is a grayscale conversion operation. Binarization is a widely used method, which is an important image processing method. The study of binary is very interesting. Based on the characteristics of plane binarization, the skeleton of plane image is obtained by binarization image preprocessing, i.e., feature extraction and edge detection. Then, the binarized image is adjusted, and then, the adjusted image is mapped into the building facade. A design method of building facade based on plane binary image is proposed. In the design process, the building is opposite. The construction dimension of the facet is grasped to control the appearance and shape of the building. By comparing the introduction of OTSU binarization method, the practicability of the proposed method is verified, and it has played a very good effect on a building design.

Data Availability

This article does not cover data research. No data were used to support this study.

Conflicts of Interest

The author declares no conflicts of interest.

References

[1] Z. Ning, Y. Xia, M. Fu, and Y. Li, "Distributed cooperative control design for finite-time attitude synchronisation of rigid spacecraft," *Control Theory & Applications Iet*, vol. 9, no. 10, pp. 1561–1570, 2019.

[2] S. Qiang, C. Yue, C. H. Goh, and D. Wang, "Active fault-tolerant control system design for spacecraft attitude maneuvers with actuator saturation and faults," *IEEE Transactions on Industrial Electronics*, vol. 66, no. 5, pp. 3763–3772, 2018.

[3] B. Zhu, Z. Zhang, D. Zhou, J. Ma, and S. Li, "Prediction-based sampled-data H_∞ controller design for attitude stabilisation of a rigid spacecraft with disturbances," *International Journal of Systems Science*, vol. 48, no. 11, pp. 2356–2367, 2017.

[4] A. P. Chrysafi, N. Athanasopoulos, and N. J. Siakavellas, "Damage detection on composite materials with active thermography and digital image processing," *International Journal of Thermal Sciences*, vol. 116, pp. 242–253, 2017.

[5] S. Tan and Z. Shen, "Hybrid problem-based learning in digital image processing: a case study," *IEEE Transactions on Education*, vol. 61, no. 2, pp. 127–135, 2017.

[6] K. Z. Szabó, G. Jordan, A. Petrik, A. Horvath, and C Szabo, "Spatial analysis of ambient gamma dose equivalent rate data by means of digital image processing techniques," *Journal of Environmental Radioactivity*, vol. 166, no. Pt 2, pp. 309–320, 2017.

[7] S. A. R. Hosseininia, M. H. Kamani, and S. Rani, "Quantitative determination of sunset yellow concentration in soft drinks via digital image processing," *Journal of Food Measurement & Characterization*, vol. 11, no. 3, pp. 1065–1070, 2017.

[8] M. Zhang, N. Zhong, and Y. Liu, "Estimation method of pig lean meat percentage based on image of pig shape characteristics," *Transactions of the Chinese Society of Agricultural Engineering*, vol. 33, no. 12, pp. 308–314, 2017.

[9] N. Kang, F. Qiang, L. Wu, S. Wang, and J. He, "Design and experiment of synchronization actuator system based on electromagnetism for fresh jujube classifier," *Transactions of the Chinese Society of Agricultural Engineering*, vol. 33, no. 7, pp. 254–260, 2017.

[10] R. S. A. D. Lange, J. H. A. Hekkink, K. Keizer, and A. J. Burggraaf, "Formation and characterization of supported microporous ceramic membranes prepared by sol-gel modification techniques," *Journal of Membrane Science*, vol. 99, no. 1, pp. 57–75, 2017.

[11] J. Zhou, J. Lin, X. Huang et al., "A library of atomically thin metal chalcogenides," *Nature*, vol. 556, no. 7701, pp. 355–359, 2018.

[12] E. Lachat, T. Landes, and P. Grussenmeyer, "First experiences with the trimble SX10 scanning total station for building facade survey," *ISPRS - International Archives of the Photogrammetry, The International Archives of the Photogrammetry, Remote Sensing and Spatial Information Sciences*, vol. XLII-2, pp. 405–412, 2017.

[13] R. Shan and L. Junghans, "Adaptive radiation optimization for climate adaptive building facade design strategy," *Building Simulation*, vol. 11, no. 2, pp. 269–279, 2018.

[14] H. Wen, Y. Wang, and L. Wei, "Slice-based building facade reconstruction from 3D point clouds," *International Journal of Remote Sensing*, vol. 39, no. 20, pp. 6587–6606, 2018.

[15] T. U. Jihui, H. Sui, L. V. Ruipeng, K. Keizer, and K. Sun, "Building facade damage detection based on the gini index from oblique aerial images," *Geomatics & Information Science of Wuhan University*, vol. 42, no. 12, pp. 1744–1748, 2017.

[16] F. Peci, F. Comino, and M. Ruiz de Adana, "Performance of an unglazed transpire collector in the facade of a building for heating and cooling in combination with a desiccant evaporative cooler," *Renewable Energy*, vol. 122, pp. 460–471, 2018.

[17] J. Lin and Y. Lu, "Construction of mesoscale two-dimensional honeycomb structures:a route from self-assembly building

blocks to highly-organized superstructures," *Science China Chemistry*, vol. 7, pp. 1-2, 2018.

[18] X. Quan, C. Liu, H. Chen, Z. Xiong, and H. Zhou, "3D reconstructing technique and application of high-power laser facility's optics assembly building," *Journal of Computer-Aided Design & Computer Graphics*, vol. 29, no. 5, pp. 854–859, 2017.

[19] Z. Zhang, Y. Wu, F. Yu et al., "Rapid and annealing-free self-assembly of DNA building blocks for 3D hydrogel chaperoned by cationic comb-type copolymers," *Journal of Biomaterials Science Polymer Edition*, vol. 28, no. 14, pp. 1511–1524, 2017.

[20] K. Franz Wagenbauer, C. Sigl, and H. Dietz, "Shape-programmed hierarchical self-assembly of designed DNA building blocks into massive three-dimensional finite-size objects," *Biophysical Journal*, vol. 112, no. 3, pp. 474a-475a, 2017.

[21] N. A. Yusof, S. S. M. Ishak, and R. Doheim, "An exploratory study of building information modelling maturity in the construction Industry," *International Journal of BIM and Engineering Science*, vol. 1, no. 1, pp. 06–19, 2018.

[22] M. Evans and A. Elhendawi, "Influence of Partnering Agreements Associated with BIM adoption on Stakeholder's Behaviour in construction Mega-Projects," *International Journal of BIM and Engineering Science*, vol. 3, no. 1, pp. 01–17, 2020.

[23] P. K. Shukla and P. K. Shukla, "Efficient electricity forecasting in multiple residential buildings considering demand-side management," *International Journal of Wireless and Ad Hoc Communication*, vol. 3, no. 2, pp. 49–63, 2021.

[24] M. Zahn, "A deduction of the golden spiral equation via powers of the golden ratio ϕ," *International Journal of Mathematical Education in Science and Technology*, vol. 48, no. 6, pp. 963–971, 2017.

[25] Y. Liu, M. Castro, M. Lederlin, H. Shu, A. Kaladji, and P Haigron, "Edge-preserving denoising for intra-operative cone beam CT in endovascular aneurysm repair," *Computerized Medical Imaging and Graphics*, vol. 56, pp. 49–59, 2017.

[26] R. Torrico, F. L. Tofoli, C. G. C. Branco, and C. M. Tavares, "A 3SSC-based nonisolated DC-DC Boost-type converter with balanced output voltage and wide voltage conversion range," *Iet Power Electronics*, vol. 11, no. 7, pp. 1217–1223, 2018.

[27] J. A. M. Carrer, C. L. N. Cunha, and W. J. Mansur, "The boundary element method applied to the solution of two-dimensional diffusion–advection problems for non-isotropic materials," *Journal of the Brazilian Society of Mechanical Sciences and Engineering*, vol. 39, no. 11, pp. 4533–4545, 2017.

Hindawi
Scientific Programming
Volume 2022, Article ID 1268393, 11 pages
https://doi.org/10.1155/2022/1268393

Research Article

Indoor Positioning Technology and Control of Mobile Home Service Robot

Gang Wang, Hongyuan Wen, and Jun Zhou

Taizhou Institute of Science and Technology, Nanjing University of Science and Technology, Taizhou 225300, Jiangsu, China

Correspondence should be addressed to Gang Wang; wanggang@njust.edu.cn

Received 17 June 2022; Revised 5 August 2022; Accepted 17 August 2022; Published 5 September 2022

Academic Editor: Juan Vicente Capella Hernandez

With the rapid development of the market economy, location information services have shifted from outdoor to indoor, requiring higher system accuracy. Indoor positioning and control is an indispensable technical support for mobile home service robots to perform system tasks, and this technology is also an important parameter that marks the level of intelligence of a home service robot. However, in indoor places, how to obtain the target node location information timely and accurately and how to control and path planning should be the first issues to be considered in the design of home robots at this stage. This article gave a brief overview of the current indoor positioning technology and control, analyzed the more widely and frequently used indoor positioning methods, and deeply studied the ultrasonic positioning technology. On this basis, a mobile home service robot system was designed, and simulation experiments were carried out, respectively, to test the receiving time and arrival time of the node signal, the node positioning accuracy, the optimal degree of route planning, and the absolute and relative errors of navigation and path estimation. The experimental results showed that the accuracy of the robot system positioning proposed in this article reached more than 80%, and the relative error was only 4.21%, which verified its feasibility and effectiveness in practical applications. Popularizing it in the market can effectively improve the system performance and intelligence of home service robots.

1. Introduction

With the progress of society and the improvement of science and technology, the development of positioning technology and control in the market has gradually moved to a new height. Obtaining the location information of devices or people has always been a very necessary requirement for production and life. Since the 1990s, wireless positioning technology has been used in professional technical fields. Until now, it has been integrated with wireless communication technology, and a smaller range and more accurate identification of cellular mobile positioning technology has been developed from the traditional GPS technology. Compared with GPS positioning technology, cellular mobile positioning technology has the advantages of small size, high precision, and high degree of commercial application. And it has been widely used in value industries such as processing and manufacturing, medical services, logistics and transportation, and equipment monitoring. However, with the improvement of people's material living standards, the requirements for indoor positioning technology and control service quality are getting higher and higher. Traditional GPS positioning technology cannot achieve indoor identification with extremely small coverage, while cellular mobile positioning technology can be applied indoors. However, due to the limitation of signal bandwidth, its accuracy is still in the order of hundreds of meters, which cannot meet the high demands of people's daily life.

Under the background of the era of intelligence, the functional design of mobile robots is becoming more and more diversified, and in some industrial production fields, mobile robots can already replace manual labor and production to a certain extent. It is also the most common and hottest smart product in the market based on smart technology. Indoor positioning and control are also conditions to measure whether a mobile robot is sufficiently intelligent. According to the degree of indoor environmental cognition, the mobile robot can accurately locate the target position

inside the venue and plan an optimal path to avoid obstacles, and complete the specified task without being affected by the bandwidth limitation of the signal. It can effectively improve people's quality of life and standard.

Based on indoor positioning technology and control theory, this article designed a mobile home service robot for indoor places, which can provide location information services and complete path control and planning tasks. The innovation of this article is that it avoids the limitation of large errors of traditional positioning methods, is more intelligent in path planning and control, and is more suitable for the family environment with small moving line space. It has practical guiding significance and practical significance in promoting the development of indoor technology, improving positioning accuracy and control level, and providing new ideas for the design and research of mobile intelligent robots.

2. Related Work

In recent years, many scholars have carried out in-depth research on indoor positioning technology and control. Tiantian believed that value-added services could be realized through indoor positioning technology in mobile payment systems, thereby helping merchants find customers through the location of the mall and analyzing customer behavior combined with the settlement amount of the customer's purchase of goods [1]. Chen introduced the basic description of channel state information and divided localization methods into three categories, namely, fingerprint-based, angle-of-arrival-based, and ranging-based. The current state of these technologies is then reviewed in detail, and advantages and disadvantages are identified and compared [2]. In order to achieve accurate positioning of multistorey buildings, Li HT proposed an indoor positioning scheme based on the map information. The final experimental results showed that the scheme could effectively improve the positioning estimation accuracy and reduce the computational complexity of multistorey buildings [3]. Cao J proposed a positioning method based on microinertial navigation and VLC system. This method uses the acquired VLC signal to calibrate the position estimation information of the microinertial navigation system to compensate for the positioning and accumulated errors of the microinertial navigation system [4]. Indoor positioning technology has been deeply researched by countless scholars, and it has matured in the market at this stage. However, with the continuous improvement of the economic level of the masses, the demand for improving the positioning technology of mobile intelligent robots with home services as the core has significantly increased.

In order to gain an in-depth understanding of mobile home service robots, research related to mobile robot service applications is reviewed in this article. Axel regarded robots as an aid in soft-tissue medical procedures, which could undergo unpredictable changes during traditional procedures. And intelligent robots could effectively predict these changes [5]. Umam F incorporated intelligent robotics technology into today's waste sorting tasks, this smart waste bin robot was able to automatically select the type of waste and navigate, and it could also detect the waste around the robot and collect it by itself [6]. Tahan discussed the effectiveness of an intelligent robot psychological intervention program on good sexual care for primary school students. Finally, through experiments and questionnaires, it was found that using robots for psychological intervention was an effective method of improving children's sexual health [7]. Luo proposed a robotic service application method that combined robotics with image processing and artificial intelligence to generate material models and proposed a digital version of the process that automates extensive material experiments that could use images to observe [8]. These studies have carried out good research on robot services. But due to the rapid development of the times, robot technology services have expanded from a relatively professional technical field to people's daily life. There are very few existing studies focusing on family services. Therefore, the research on indoor positioning technology and control of mobile home service robots is urgent.

3. Indoor Positioning Technology and Control of Mobile Home Service Robots

3.1. Overview of Indoor Positioning Technology and Control. Indoor positioning technology refers to a technical service that uses multiple control technologies such as wireless communication to obtain the location information of personnel or equipment in indoor and other limited coverage and relatively closed places.

3.1.1. Classification of Indoor Positioning Technology. In the existing development field, the widely used indoor positioning technologies include radio frequency identification, infrared, ultra-wideband, and ultrasonic technology. This article will briefly introduce indoor positioning technology in this category.

(1) RFID Positioning. Radio frequency identification positioning technology is a technology that uses radio frequency to input and output data in the indoor environment to obtain location information. It is one of the more common positioning technologies in recent years [9]. The radio frequency signal can carry its own identification information, and the radio frequency receiving end detects the strength of the received signal, and the processor calculates the distance between the transmitting end and the receiving end according to the attenuation of the strength of the radio frequency signal. The position of the transmitter is calculated by the distance between a radio transmitter and multiple reference points. In the field of indoor positioning, radio frequency identification technology has the function of measuring multiple objects to be measured at the same time. However, the mapping between wireless signal strength and distance is a nonlinear relationship, and it is easily affected by various environmental factors, such as temperature, humidity, and distribution of metal objects, thus limited in many applications.

(2) Infrared Positioning. The working principle of infrared positioning technology is to install infrared receivers in different areas, and the moving object to be tested carries an infrared transmitter to emit infrared signals in real time. When an infrared receiving device receives the modulated infrared signal, it can be determined that the moving object under test is in the area where the receiving device is located. However, this technology has a big limitation. Since infrared rays can only transmit at a line of sight, the penetration is extremely poor. When the logo is blocked, it cannot work normally, and it is also easily affected by environmental factors such as light and smoke. In addition to technical limitations (the transmission distance of infrared rays is not long), in terms of layout, no matter which method, it is necessary to install the receiving end behind each block or even at the corner. The layout is complicated, which increases the cost, and the positioning effect is limited.

(3) Ultra-Wideband Positioning. UWB positioning technology is a brand-new new technology that is very different from traditional communication positioning technology. It uses the prearranged anchor nodes and bridge nodes with known positions to communicate with the newly added blind nodes and uses a unique positioning method to determine the position, such as triangulation or fingerprint positioning. The technology has good real-time performance and high positioning accuracy. However, because it needs a large bandwidth, it is easy to cause interference to communication equipment, and there is a large instantaneous power when continuously transmitting short pulses. At present, the existing facilities are more difficult to meet the needs of practical applications.

(4) Ultrasonic Positioning. Ultrasonic technology mainly uses the time-flight method to measure distance. We use ultrasonic signals to measure the distance between the starting position and the target position. The ultrasonic signal has a certain beam angle when it is transmitted, so the transmitting end equipped with the moving object under test needs to consider the coverage of the ultrasonic wave. In order to expand the coverage of ultrasonic signals, in practical applications, ultrasonic transmitting probes with larger beam angles are usually selected, or multiple ultrasonic transmitting probes are used to transmit ultrasonic signals in different directions at the same time. The advantage of ultrasonic technology is that the time interval between the ultrasonic signal going back and forth between the transmitting end and the receiving end is linearly related to the distance between the two ends. The disadvantage of ultrasonic technology is that the propagation speed of ultrasonic waves is affected by the air temperature, which requires temperature compensation. This technology has the advantages of low cost, no lighting restrictions, etc., and its application in indoor positioning is becoming more and more extensive.

3.1.2. Indoor Positioning Method. With the development of a variety of ranging and communication technologies, many indoor positioning methods based on them have appeared. The classic methods include the arrival angle method based on the propagation signal, the indoor positioning algorithm based on the hyperbolic model, the receiving-based method, and the strength method [10].

(1) Received Signal Strength Method. The commonality between the received signal strength method and the TOA algorithm is the positioning method based on the absolute ranging method, but the difference is that the RSSI algorithm transmits a constant power electromagnetic wave signal and measures the attenuation of the signal received by the receiver. It calculates the distance between two points according to the attenuation model of the signal in the air. When this algorithm is applied in practice, each parameter contained in the signal attenuation model should be tested in advance. Its limitation is that the tested parameters will cause certain errors due to environmental differences.

At present, the theoretical model commonly used in wireless signal transmission is the Shadowing model, as shown in the following equation [11]:

$$p = p_0 + 10nlg\left(\frac{d}{d_0}\right) + \delta. \tag{1}$$

Among them, the interpretation of each parameter is shown in Table 1.

In practical applications, a simplified Shadowing model is often used, as shown in the following equation [12]:

$$p = p_0 + 10nlg\left(\frac{d}{d_0}\right). \tag{2}$$

For the convenience of calculation, the value of d_0 is usually taken as $1m$; at this time, p_0 is the signal strength received at the distance $1m$ from the wireless signal transmitting source, and n is the signal transmission constant. The signal transmission constant has nothing to do with the signal propagation environment. In the equation, $p_0$and n need to be measured several times through experiments and obtained by fitting according to the experimental data.

(2) Arrival Incidence Angle Method Based on the Propagation Signal. The arrival angle method based on the propagation signal is abbreviated as the AOA algorithm. The algorithm needs to set up at least two signal angle measurement devices on the same axis to form the receiving end. As shown in Figure 1, the receiving end is placed at a known position as a reference position, the transmitting end transmits wireless signals to the surrounding, and the receiving end will measure the wireless signal. The incident angle of the signal θ_1, θ_2 are summed so as to determine the equations of two straight lines in the plane passing through the reference end. The intersection of the two straight lines is the position of the measured end. Since the accuracy of this method is greatly affected by the angle measurement accuracy and the distance between the measured point and the axis, the AOA algorithm is rarely used in practical applications.

(3) Indoor Positioning Algorithm Based on the Hyperbolic Model. The characteristic of a hyperbola is that the distance from any point on the curve to the two foci is equal, and the

Table 1: The definition of each parameter of the equation.

Sequence	Parameter_	Meaning _
1	d_0	Reference distance
2	p_0	The received signal strength at distanced_0
3	d	True distance
4	δ	Occlusion factor

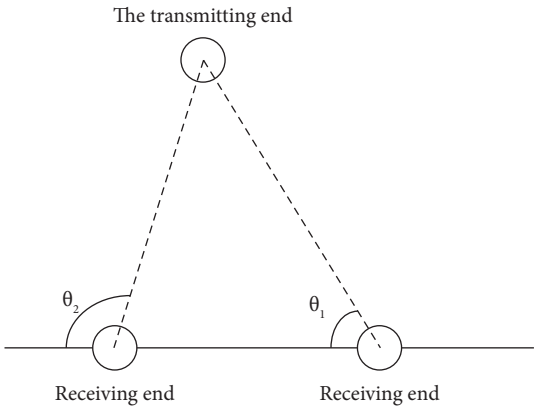

Figure 1: Arrival incidence angle method based on the propagated signal.

difference is $2a$. As shown in Figure 2, F_1 and F_2 are the two foci of the hyperbola, and the distance between the two foci is the focal length c. The general form of the hyperbolic equation with the focus on the X axis is (3), where a, b, and c satisfy the relationship of equation (4). In the indoor positioning algorithm based on the hyperbolic model, the focus is the reference position, and the position of the measured end is located on the hyperbola. In order to determine the specific position coordinates of the measured end, at least two sets of hyperbolic models are required [13].

$$\frac{x^2}{a^2} - \frac{y^2}{b^2} = 1, \tag{3}$$

$$a^2 + b^2 = c^2. \tag{4}$$

The three ultrasonic receiving ends are placed on the same straight line at equal intervals; the distance is D, as the positioning reference end. The straight line where the three positioning reference ends are located is the coordinate X axis, the reference position in the middle is the coordinate origin, and the X axis direction rotated 90° counterclockwise is the positive direction of the Y axis, as shown in Figure 3. The reference position at the origin is set as reference point 1; the reference position at the positive half-axis of the X axis is set as reference point 2; the reference position at the negative half-axis of the X axis is set as reference point 3; each coordinate information of the reference point is shown in Table 2.

$$\Delta L_1 = \left|L_2 - L_1\right|, \tag{5}$$

$$\Delta L_2 = \left|L_3 - L_2\right|. \tag{6}$$

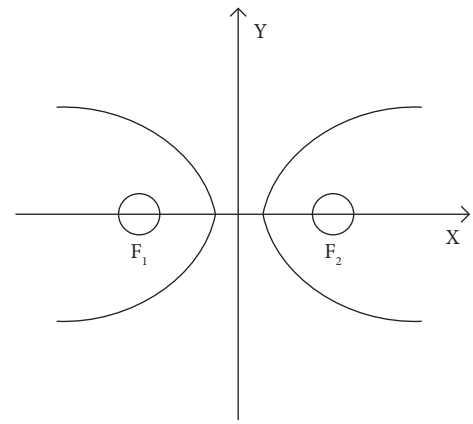

Figure 2: Hyperbolic model.

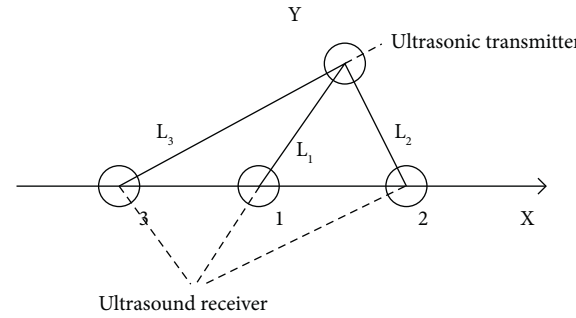

Figure 3: Schematic diagram of ultrasonic positioning.

The ultrasonic transmitting end is installed on the measured object, and the distances from the three reference points are, respectively, set to L_1, L_2, and L_3. The distance difference between the measured end and the reference point No. 1 and No. 2 is ΔL_1, and the distance difference between the reference point No. 1 and No. 3 is ΔL_2, and the calculation is shown in (5) and (6). In practical applications, ΔL_1 and ΔL_2 can be directly obtained by using a single-chip microcomputer [14].

With reference points No.1 and No.2 as the focal points, the relationship between (7) and (8) is established [15]:

$$c = \frac{D}{2}, \tag{7}$$

$$a = \frac{\Delta L_1}{2}. \tag{8}$$

Substituting this into (4) will get the following [16]:

$$b = \sqrt{\left(\frac{D}{2}\right)^2 - \left(\frac{\Delta L_1}{2}\right)^2}. \tag{9}$$

Putting (8) and (9) into (3) will obtain hyperbolic equation (17):

$$\frac{(x - D/2)^2}{(\Delta L_1/2)^2} - \frac{y^2}{D^2/4 - \Delta L_1^2/4} = 1. \tag{10}$$

Table 2: Coordinate information of the reference point.

Scope	Reference point	Coordinate information
Indoor localization algorithm based on hyperbolic model	N number 1	$(0, 0)$
	N number 2	$(D, 0)$
	N number 3	$(-D, 0)$

Similarly, a hyperbolic model can be established with reference points No. 1 and No. 3 as the focus [18]:

$$\frac{(x + D/2)^2}{(\Delta L_2/2)^2} - \frac{y^2}{D^2/4 - \Delta L_2^2/4} = 1. \tag{11}$$

Since the position of the measured end satisfies both (10) and (11), the possible position of the ultrasonic transmitting end can be obtained by solving the equation system. Arranging the two equations and subtracting the variable y will get the following:

$$\left(\frac{D^2}{\Delta L_1^2} - \frac{D^2}{\Delta L_2^2}\right)x^2 - D\left(\frac{D^2}{\Delta L_1^2} + \frac{D^2}{\Delta L_2^2}\right)x + \frac{D^2}{4}\left(\frac{D^2}{\Delta L_1^2} - \frac{D^2}{\Delta L_2^2}\right) + \frac{\Delta L_1^2 - \Delta L_2^2}{4} + 2D = 0. \tag{12}$$

Except for the variable x in (12), they are all constants or can be obtained directly by the microcontroller. This equation is the general form of a quadratic equation in one variable, which can be expressed as follows [19]:

$$\alpha x^2 + \beta x + \varepsilon = 0, \tag{13}$$

where [2]

$$\alpha = \left(\frac{D^2}{\Delta L_1^2} - \frac{D^2}{\Delta L_2^2}\right), \tag{14}$$

$$\beta = -D\left(\frac{D^2}{\Delta L_1^2} + \frac{D^2}{\Delta L_2^2}\right), \tag{15}$$

$$\varepsilon = \frac{D^2}{4}\left(\frac{D^2}{\Delta L_1^2} - \frac{D^2}{\Delta L_2^2}\right) + \frac{\Delta L_1^2 - \Delta L_2^2}{4} + 2D. \tag{16}$$

From this, the abscissa of the measured end can be calculated [20]:

$$x = \frac{-\beta \pm \sqrt{\beta^2 - 4\alpha\varepsilon}}{2\alpha}. \tag{17}$$

If the measured end is closest to reference point No. 1, as shown in the shaded area in Figure 4, that is, when it is satisfied $(L_1 > L_2)|(L_1 > L_3)$, the smaller absolute value of the two possible values should be taken by x. On the contrary, when $(L_1 < L_2)$ & $(L_1 < L_3)$, the larger absolute value of the two possible values should be taken. It can be known from (15) that β is always negative, so the value of x is shown in thefollowing equation [21]:

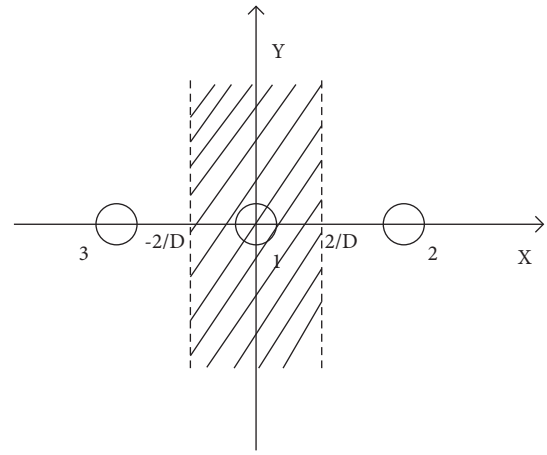

Figure 4: The end under test is close to the intermediate reference point.

$$x = \begin{cases} \dfrac{-\beta + \sqrt{\beta^2 - 4\alpha\varepsilon}}{2\alpha} & (L_1 > L_2)|(L_1 > L_3), \\ \dfrac{-\beta - \sqrt{\beta^2 - 4\alpha\varepsilon}}{2\alpha} & (L_1 < L_2)\,\&\,(L_1 < L_3). \end{cases} \tag{18}$$

Although L_1, L_2, and L_3 have not been acquired, an interrupt signal will be sent to the microcontroller when the reference position receives the ultrasonic signal, and the reference position closer to the measured end will be the first to send an interrupt signal, so the relationship between L_1, L_2, and L_3 can be triggered by the interrupt sequence of the microcontroller to make a judgment.

Since the indoor positioning system described in this article will be placed at the edge of the indoor simulation experiment site, the mobile robot with the ultrasonic transmitter is always located in the positive direction of the Y axis, so the ordinate of the ultrasonic transmitter is shown in thefollowing equation [22]:

$$y = \sqrt{\frac{(x - D/2)^2\left(D^2/4 - \Delta L_1^2/4\right)}{\Delta L_1^2/4} - \frac{D^2}{4} + \frac{\Delta L_1^2}{4}}. \tag{19}$$

When two of the L_1, L_2, and L_3 are equal, the above hyperbola will have a set that does not exist [23]. At this time, it can be determined that the abscissa of the ultrasonic transmitting end is ± D/2, and the positive and negative can be determined by which two of L_1, L_2, and L_3 are the same, and the single-chip microcomputer only needs to judge whether there is an interrupt signal triggered at the same

time and determine the position of the abscissa. After directly bringing the obtained abscissa into equation (19), the ordinate converted to the horizontal plane is obtained through the Pythagorean theorem and is calculated as follows [24]:

$$y = \sqrt{\frac{(x - D/2)^2\left(D^2/4 - \Delta L_1^2/4\right)}{\Delta L_1^2/4} - \frac{D^2}{4} + \frac{\Delta L_1^2}{4} - h^2}. \quad (20)$$

3.2. System Design of Mobile Home Service Robot. This article uses ultrasonic positioning technology to design a mobile home service robot system, analyzes the automatic guidance tasks that the mobile robot system needs to complete, selects appropriate hardware modules to build a mobile robot platform, and introduces the working principles and performance indicators of each hardware module and their main functions in the system one by one. According to the performance parameters, such as energy consumption and main frequency, the required processor module is selected.

3.2.1. Hardware System. The mobile home service robot system is mainly composed of a wireless transceiver module, a processor module, an electronic compass, a motor drive module, an ultrasonic ranging module, an ultrasonic transceiver circuit, and a variety of communication interfaces, as shown in Figure 5.

3.2.2. Communication System. The communication system in this article is based on the wireless transceiver module, which has its own frequency generator, crystal oscillator, modem, and power amplifier. The wireless signal it sends is in $2.3 \sim 2.7GHz$, the world's common frequency band, and there is no need to apply for a dedicated frequency band. Its power supply voltage is $3.2V$, the maximum working current in the transmit mode is $12.1mA$, and the maximum working current in the receiving mode is $13.4mA$; the operating temperature range is $-35℃ \sim 80℃$; the maximum data transmission rate is $1800kbps$; the sensitivity under the data transmission rate $900kbps$ is $-80dbm$. And the data can be sent and received in 130 selectable working channels; its size is $3.4cm \times 1.2cm$. The characteristics of small size, low power consumption, and wide operating temperature range make it suitable for many fields, such as intelligent sports equipment, remote control devices, and industrial sensors.

3.2.3. Workflow of the Positioning System. A mobile home service robot is mainly composed of a processor module with an RC0402 microcontroller as the core and an ultrasonic receiving circuit. After the indoor positioning system starts to work, it waits for the positioning or stops request sent by the robot body wirelessly. If the stop request is made, the mobile home service machine positioning system will end the current work process. If it is a positioning request, the indoor positioning processor module of the system opens the GPIO interrupt and receives the ultrasonic recognition interrupt signal sent by the ultrasonic receiving circuit. The processor module uses the on-chip timer/counter module to realize the timer function and calculates the time difference between the ultrasonic recognition interrupts. After calculating the distance difference between the mobile robot and the reference position based on the time difference and the propagation speed of the ultrasonic wave in the air, the position coordinates of the robot based on the distance difference are calculated. And its position coordinates are transmitted to the robot system through the wireless transceiver module, thus completing a positioning task. After the indoor positioning system wirelessly sends the position coordinates of the robot, it waits for the positioning request again and prepares to position the robot again.

In a single indoor positioning system, three ultrasonic receiving probes are placed horizontally collinear at equal intervals as the reference position during the positioning process of the mobile robot. Each ultrasonic receiving probe is connected to an ultrasonic receiving circuit separately, and the ultrasonic receiving circuit converts the electrical signal sent by the receiving probe into a level signal, so the processor module of the indoor positioning system will receive three ultrasonic interruption signals. The interruption time difference that needs to be calculated in the above workflow is the time difference between the three ultrasonic interruption signals, which is also the time difference between the ultrasonic signals sent by the mobile robot body and the three reference positions.

3.2.4. Robot Body. The mobile home service robot body communicates with the indoor positioning system wirelessly to obtain its own position coordinates. It realizes the perception of the surrounding environment and obtains obstacle distance information. The mobile robot body is based on the target position, its own position coordinates, and obstacle distance information. The distance and heading of the next step are determined, the steering and travel of the mobile robot body are controlled, and the local path planning task is completed. The mobile robot body is mainly composed of a processor module with an RC0402 microcontroller as the core, an ultrasonic ranging module, an electronic compass, and a motor drive module. The size of the mobile home service robot is 26 cm × 13 cm × 17 cm.

3.2.5. Ultrasonic Transceiver Circuit. The ultrasonic transmitting circuit used in this article is based on the 555 oscillator circuit. As shown in Figure 6, an inverter chip is used to drive the ultrasonic transmitting probe. The No. 4 pin of the oscillator circuit is a reset pin, which is connected to the GPIO port of the microcontroller. When the microcontroller outputs a high level to the No. 4 pin of the 555 oscillator circuit, the No. 3 pin of the oscillator circuit outputs a square wave signal with a frequency of 40 kHz. If the single-chip microcomputer outputs a low level to the 555 oscillator circuit, the oscillator circuit does not output a square wave signal.

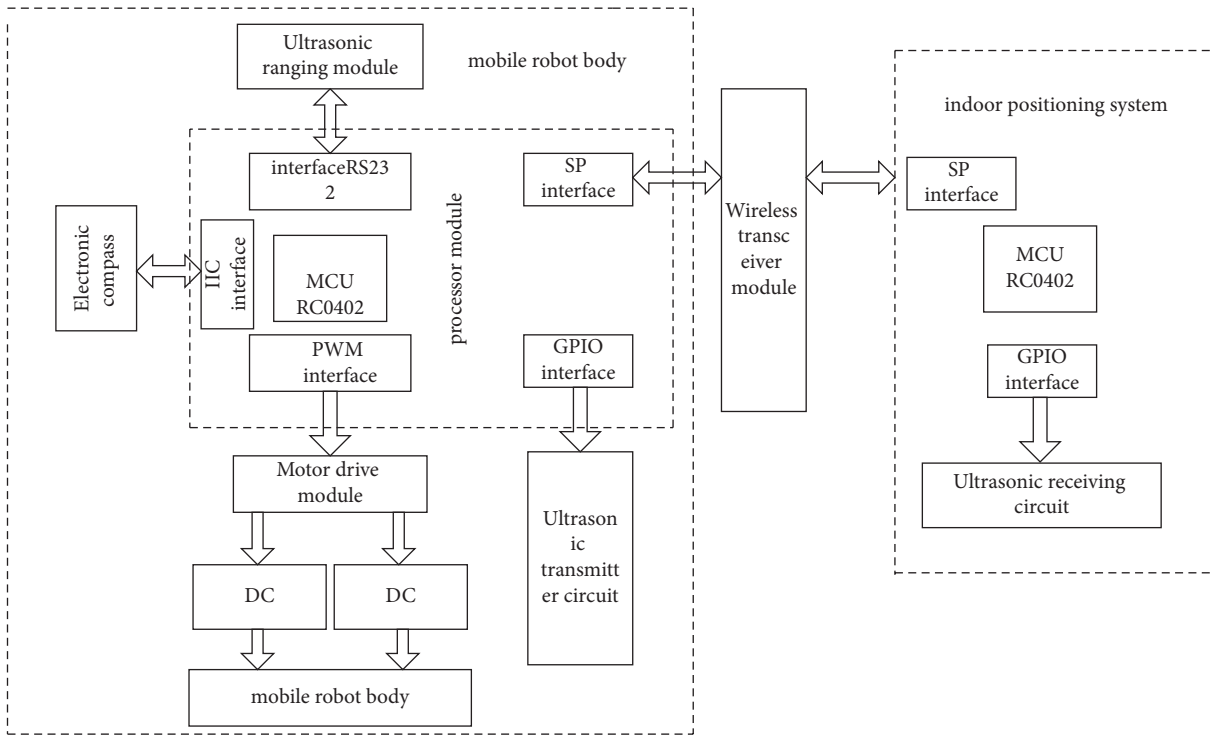

Figure 5: Mobile home service robot system.

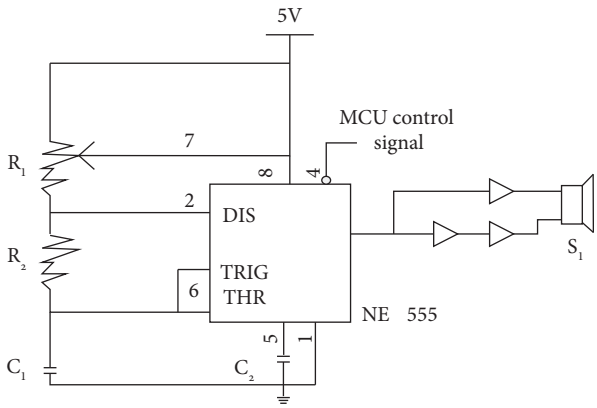

Figure 6: Schematic diagram of ultrasonic transmitter circuit.

4. Indoor Positioning and Control Simulation Test of Mobile Home Service Robots

In this paper, MATLAB simulation software is used to simulate the designed mobile home service robot. In order to simplify the calculation, the robot is regarded as a mass point, and the obstacles are extended in the simulation experiments, and the extension distance is half of the maximum size of the robot. The robot is placed in two three-dimensional spaces, each of which has 5 compartments, and test nodes are set up in the 5 compartments to detect the robot's signal reception time and arrival time for each node in the two spaces. The node positioning accuracy, the optimal degree of route planning, and the absolute and relative errors of navigation and path estimation are based on the spatial center as the origin, and the coordinate information of each node is shown in Table 3 and Table 4.

The first test was carried out in three-dimensional space 1, and obstacles were set in each division of space 1, and the difficulty was set as intermediate; the second test was carried out in three-dimensional space 2, and obstacles were also set in each division, the difficulty was set as advanced. The size information of each obstacle is shown in Table 5 and Table 6.

The indoor positioning and control test results of the mobile home service robot are shown in Figure 7 to Figure 8.

Figure 7(a), shows the test results of signal reception and arrival time in space 1. Figure 7(b), shows the test results of signal reception and arrival time in space 2.

It can be seen from Figure 7 that the mobile home service robot is ideal for receiving signals from each node in the three-dimensional space with moderate difficulty in setting obstacles, with the shortest 1.89 seconds and the longest 2.67 seconds, which is caused by the distance variable. The time from receiving the signal to reaching the node is maintained within 6 seconds to 10 seconds. In the three-dimensional space where the difficulty of setting up obstacles is high, the time it takes for the mobile home service robot to receive signals and reach the node increases to a certain extent, which also shows that the recognition accuracy inside the robot system has a positive correlation in the actual movement process of the robot.

Figure 8(a) The test results of the positioning accuracy and the optimal degree of route planning in space 1. Figure 8(b) The test results of the positioning accuracy and the optimal degree of route planning in space 2.

Table 3: Coordinate information of test nodes in space 1.

Scope	Node type	Location information/m
Three-dimensional space 1	Node 1	(5, 3)
	Node 2	(2, 5)
	Node 3	(1, 4)
	Node 4	(8, 2)
	Node 5	(4, 1)

Table 4: Coordinate information of test nodes in space 2.

Scope	Node type	Location information/m
Three-dimensional space 2	Node 1	(7, 7)
	Node 2	(4, 3)
	Node 3	(5, 1)
	Node 4	(3, 6)
	Node 5	(8, 5)

Table 5: Obstacle size in each division of 3D space 1.

Scope	Space division	Size
Three-dimensional space 1	Division 1	35 cm*26 cm
	Division 2	27 cm*18 cm
	Division 3	42 cm*34 cm
	Division 4	35 cm*26 cm
	Division 5	27 cm*18 cm

Table 6: Obstacle size in each division of 3D space 2.

Scope	Space division	Size
Three-dimensional space 2	Division 1	52 cm*36 cm
	Division 2	60 cm*45 cm
	Division 3	60 cm*45 cm
	Division 4	58 cm*31 cm
	Division 5	52 cm*36 cm

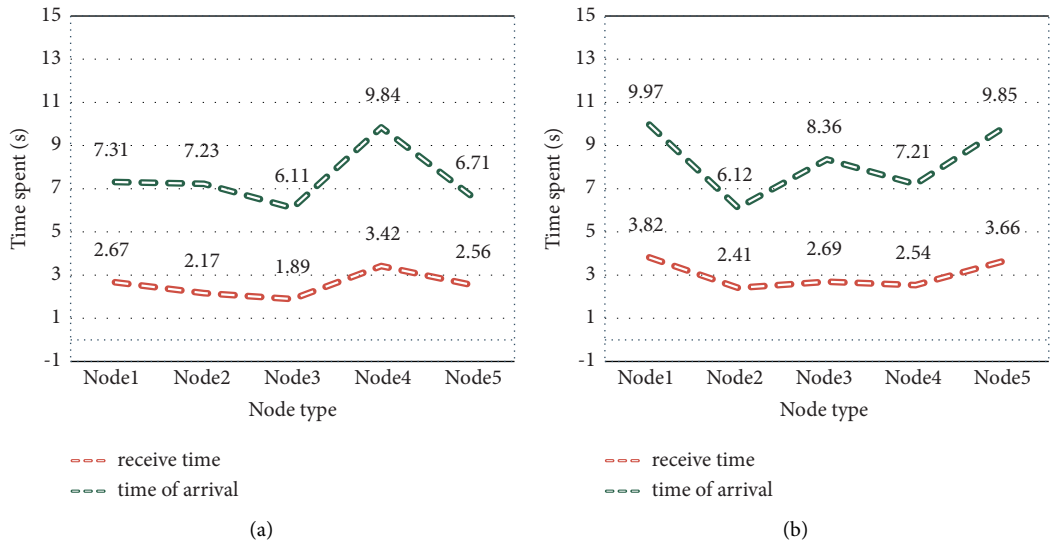

Figure 7: Signal reception and final arrival time test results.

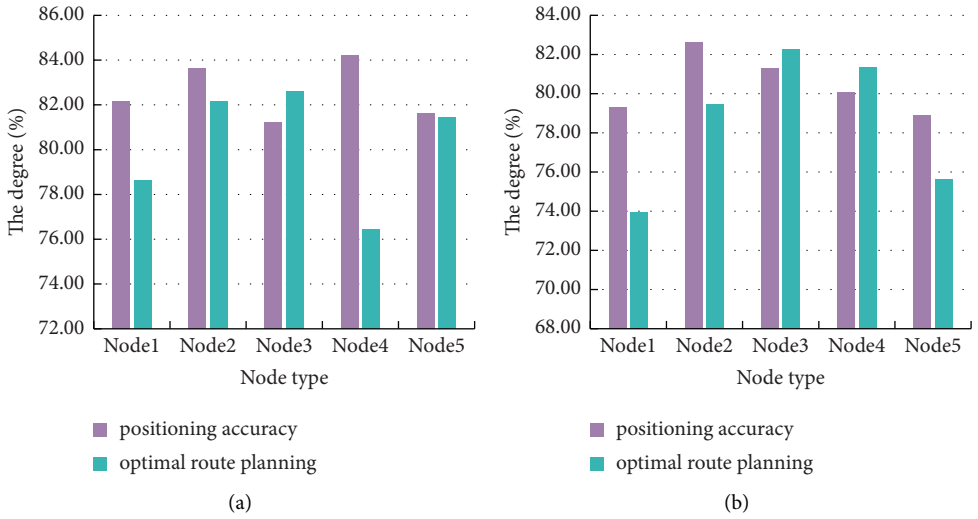

Figure 8: Node positioning accuracy and optimal degree of route planning test results.

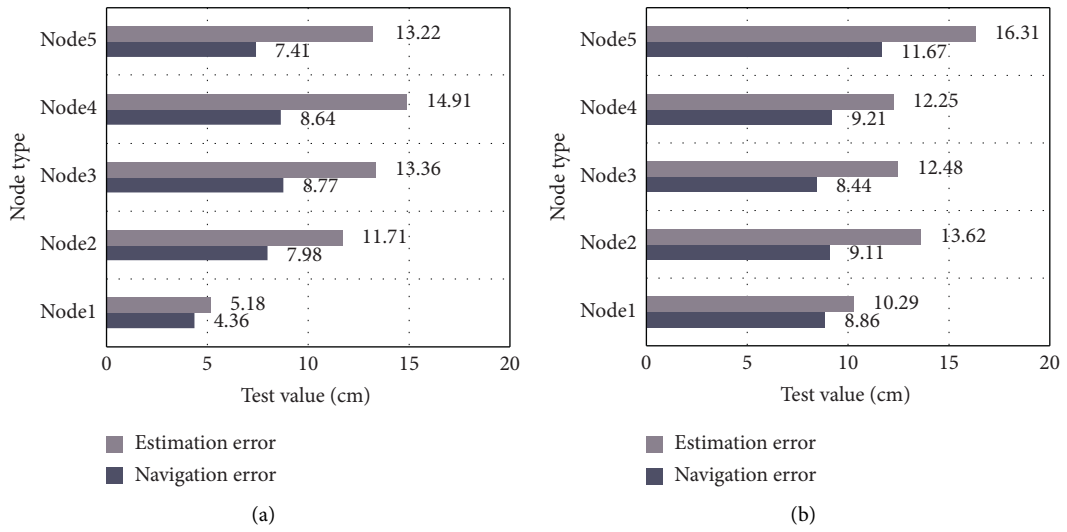

Figure 9: Absolute error test results for navigation and dead reckoning.

It can be seen from Figure 9 that the node positioning accuracy of the mobile home service robot in the first three-dimensional space has reached more than 80%. When the optimal path planning is performed, the test result of the robot is the highest at 82.61% and the lowest at 76.44%. When the distance between the nodes and the origin of the coordinates is larger, there are more paths available for the robot to move. The calculation inside the system needs to consider the influence of time, distance, and other environmental factors to plan the optimal path. This is also reflected in space 2. The size of the obstacles in space 2 is larger than that in space 1, and the impact on the robot's positioning accuracy and system path planning is also more prominent. Still, overall, the average positioning accuracy of each node in space 2 is 80.44%, and the average path planning optimal degree is 78.54%, indicating that the ultrasonic positioning technology is less affected by obstacles in a short distance.

Figure 9(a) The absolute error test results of navigation and dead reckoning in space 1. Figure 9(b) The absolute error test results of navigation and dead reckoning in space 2.

The absolute error in the figure is the Euclidean distance between the actual position coordinates of the robot's movement and the position coordinates calculated by the navigation algorithm at the same time, while the relative error is the ratio of the absolute error of the robot at each position to the distance of the robot's actual movement. It can be seen from Figure 10 that the maximum absolute error of the navigation of the mobile home service robot in the three-dimensional space 1 is 8.77 cm, the minimum value is 4.36 cm, the maximum absolute error of the dead reckoning is 13.22 cm, and the minimum value is 5.18 cm. In space 2, the maximum absolute error of navigation is 11.67 cm, the minimum value is 8.86 cm, the maximum absolute error of dead reckoning is 16.31 cm, and the minimum value is 10.29 cm.

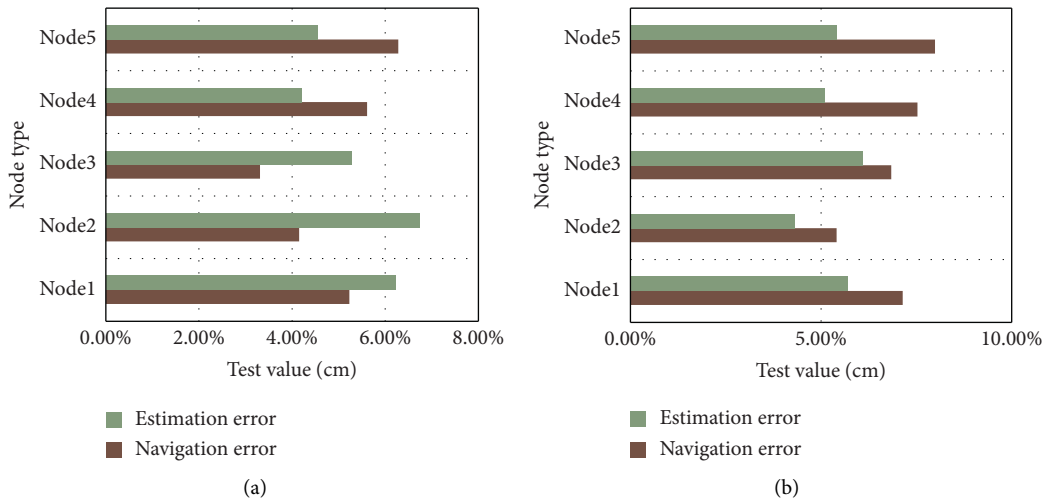

Figure 10: Relative error test results for navigation and dead reckoning.

Figure 10(a) The relative error test results of navigation and dead reckoning in space 1. Figure 10(b) The relative error test results of navigation and dead reckoning in space 2.

It can be seen from Figure 10 that the maximum relative error of the mobile home service robot in the three-dimensional space 1 is 6.28%, the minimum is 3.31%; the maximum relative error of the dead reckoning is 6.74%, and the minimum is 4.21%; In space 2, the maximum value of the relative error of navigation is 7.99%, the minimum value is 5.41%; the maximum value of the relative error of dead reckoning is 6.11%, and the minimum value is 4.32%. From the above data, the actual position of the node is not far from the estimated value inside the robot system, indicating that the indoor practical application of the mobile home service robot proposed in this paper is feasible, and the accuracy of the system in the navigation calculation is relatively large.

5. Conclusion

In this paper, the indoor positioning technology and indoor positioning method are studied and based on this, a mobile home service robot is designed to improve the positioning accuracy of the system. The performance experimental data are analyzed in depth. The numerical simulation results show that the system has better tracking accuracy in the indoor environment, and the algorithm has strong adaptability.

Although this article has carried out in-depth research on the indoor positioning technology and control of mobile home service robots, there are still many deficiencies. The depth and breadth of the research in this article are not enough. In the process of this research, the selection and acquisition of experimental data were carried out under absolutely ideal conditions, and the integrity and validity were not enough, and some interference factors involved in the test process were not considered. In the preliminary stage, in future work, appropriate positioning methods and means will be studied from more perspectives based on the existing technology and level and continuously improve the quality of research work.

Data Availability

No data were used to support this study.

Conflicts of Interest

The authors declare no conflicts of interest in this study.

Acknowledgments

This work was sponsored by the Qing Lan Project and Project of Jiangsu Provincial Six Talent Peaks (XYDXX-257).

References

[1] H. Tiantian and D. Lei, "An indoor positioning technology in the BLE mobile payment system," *AIP Conference Proceedings*, vol. 1839, no. 1, pp. 1–7, 2017.

[2] R. Chen and F. Ye, "An overview of indoor positioning technology based on wi-fi channel state information," *Wuhan Daxue Xuebao (Xinxi Kexue Ban)/Geomatics and Information Science of Wuhan University*, vol. 43, no. 12, pp. 2064–2070, 2018.

[3] H. T. Li and S. Qi, "Indoor map information based WiFi positioning technology for multi-floor buildings[J]," *Dianzi Keji Daxue Xuebao/Journal of the University of Electronic Science and Technology of China*, vol. 46, no. 1, pp. 32–37, 2017.

[4] J. Cao, X. Xu, and A. Shi, "Research on indoor high precision positioning technology based on micro-inertial navigation system and VLC[J]," *Bandaoti Guangdian/Semiconductor Optoelectronics*, vol. 38, no. 6, pp. 862–867, 2017.

[5] K. Axel, "Smart robot performs vision-assisted surgery[J]," *Vision Systems Design*, vol. 22, no. 5, pp. 15–18, 2017.

[6] F. Umam, "Optimalization of detection and navigation smart bin robot using camera," *Advanced Science Letters*, vol. 23, no. 12, pp. 12432–12436, 2017.

[7] M. Tahan, G. Afrooz, and J. Bolhari, "The effectiveness of smart robot psychological intervention program on good sexual care for elementary school children[J]," *Shenakht Journal of Psychology and Psychiatry*, vol. 7, no. 6, pp. 53–65, 2021.

[8] D. Luo, D. Chen, and J. Wang, "The smart robot crafting approach to computing materials[J]," *Construction Robotics*, vol. 4, no. 2, pp. 1–11, 2020.
[9] K. Wang, C. Yang, and T. Wang, "A smart robot training data acquisition and learning process recording system based on blockchain," *OALib*, vol. 07, no. 09, pp. 1–5, 2020.
[10] R. R. Patil, O. S. Vaidya, and G. M. Phade, "Embedded vision based cost effective tele-operating smart robot[J]," *International Journal of Innovative Technology and Exploring Engineering*, vol. 8, no. 7, pp. 1544–1550, 2019.
[11] S. F. Ismail, A. W. Essa, and A. M. Ahmed, "Smart robot controlled via. Speech and smart phone," *Journal of Engineering and Applied Sciences*, vol. 14, no. 7, pp. 2222–2229, 2019.
[12] Y. Chen, H. Sun, G. Zhou, and B. Peng, "Fruit classification model based on residual filtering network for smart community robot," *Wireless Communications and Mobile Computing*, vol. 2021, no. 2, pp. 1–9, 2021.
[13] C. Pereyda, N. Raghunath, B. Minor, G. Wilson, M. Schmitter-Edgecombe, and D. J. Cook, "Cyber-physical support of daily activities: a robot/smart home partnership [J]," *ACM Transactions on Cyber-Physical Systems*, vol. 4, no. 2, pp. 1–24, 2020.
[14] B. Josh, "Collaborative robot supports smart manufacturing capabilities[J]. Modern materials handling: productivity solutions for manufacturing," *Warehousing and Distribution*, vol. 72, no. 2, p. 54, 2017.
[15] N. Islam, K. Haseeb, and A. Almogren, "A framework for topological based map building: a solution to autonomous robot navigation in smart cities[J]," *Future Generation Computer Systems*, vol. 100, no. 1, pp. 1–24, 2019.
[16] H. A. Y. A. S. H. I. Tatsuya and H. Hiroaki, "Smart hydraulic system for driving robot arm[J]," *Journal of the Japan Society for Precision Engineering*, vol. 85, no. 10, pp. 904–911, 2019.
[17] X. Li, Z. Ma, X. Chu, and Y. Liu, "A cloud-assisted region monitoring strategy of mobile robot in smart greenhouse," *Mobile Information Systems*, vol. 2019, no. 1, pp. 1–10, 2019.
[18] S. Bhowmick, R. Adhikari, and S. Dutta, "Algorithm design for navigation of smart floor cleaner robot," *[J]. IJIREEICE*, vol. 6, no. 12, pp. 20–24, 2018.
[19] L. J. Yang, H. Shen, and S. W. Gao, "Low frequency electromagnetic tracking and positioning technology for pipeline internal detector[J]," *Shenyang Gongye Daxue Xuebao/Journal of Shenyang University of Technology*, vol. 40, no. 1, pp. 48–53, 2018.
[20] Y. H. Liu, K. B. Xu, and Y. Q. Ren, "Positioning technology of fracturing time by vector superposition[J]," *Well Testing*, vol. 26, no. 2, pp. 41–43, 2017.
[21] Y. Zhang, Q. Gao, and Y. Song, "Implementation of an SSVEP-based intelligent home service robot system[J]. Technology and health care," *Official Journal of the European Society for Engineering and Medicine*, vol. 29, no. 4, pp. 1–16, 2020.
[22] H. Z. Chen, G. H. Tian, and G. L. Liu, "A selective attention guided initiative semantic cognition algorithm for service robot," *International Journal of Automation and Computing*, vol. 15, no. 5, pp. 559–569, 2018.
[23] N. Chivarov, D. Chikurtev, E. Markov, S. Chivarov, and P. Kopacek, "Cost oriented tele-controlled service robot for increasing the quality of life of elderly and disabled - robco 18," *IFAC-PapersOnLine*, vol. 51, no. 30, pp. 192–197, 2018.
[24] F. Lu, G. Tian, and Q. Li, "Autonomous cognition and planning of robot service based on ontology in intelligent space environment," *[J]. Robot*, vol. 39, no. 4, pp. 423–430, 2017.

Hindawi
Scientific Programming
Volume 2022, Article ID 1687400, 11 pages
https://doi.org/10.1155/2022/1687400

Research Article

Monitoring Research of Network Security Information System Based on Rough Set Data Mining

Minfeng Chen

Data and Information Center, Wuxi Vocational Institute of Commerce, Wuxi 214100, Jiangsu, China

Correspondence should be addressed to Minfeng Chen; chenminfeng@wxic.edu.cn

Received 16 June 2022; Revised 8 August 2022; Accepted 20 August 2022; Published 5 September 2022

Academic Editor: Juan Vicente Capella Hernandez

In recent years, with the explosive development of Internet technology, network security has gradually become a hot issue. At present, data mining technology has been widely used in processing network information. Rough set theory is a natural data mining or knowledge discovery method because the purpose and starting point of the research is to directly analyze and reason the data, discover the implicit knowledge and reveal the potential laws. Rough set data mining has unique advantages in processing information, so it is necessary to carry out research on monitoring network security information system based on rough set data mining. The purpose of this article is to solve how to implement network security problems of information system of monitoring, through research the related contents of rough set data mining technology, based on the two kinds of data pre-processing algorithm, data mining based on rough sets is discussed in detail the two kinds of data pre-processing algorithm in network security information system monitoring, especially the feasibility of the invasive monitoring. The results show that the two data pre-processing algorithms based on rough set data mining can effectively realize the monitoring function of common network security information system and improve the security of network security information system to some extent. The simulation results show that the monitoring accuracy of these two data pre-processing algorithms in the common network security information system is as high as 98.5%, which is about 12% higher than the accuracy of the general system.

1. Introduction

The development of the Internet has created a brand-new universal space for information sharing, information collaboration, and business expansion. It is no exaggeration to say that the Internet has constituted an independent super kingdom. With the rapid development of information technology, the Internet has been widely used in various industries [1]. For example, government departments' websites, distance education, e-commerce, e-banking, and information service industries. The Internet has played a very important role in our daily study, work, and life, bringing us a lot of convenience [2]. However, with the rapid development and widespread application of the network, network security problems have become increasingly serious. For example, there have been many security vulnerabilities, which may hide a huge crisis [3]. The number of registered users of China's mobile broadband Internet has also reached 520 million. Due to China's international scale of Internet users, the number of registered users of broadband Internet and the number of international registered users of some national top-level Internet domain names, these three important indicators have now stabilized [4]. However, vulnerabilities in various operating systems and application programs are emerging, and hacker attacks and illegal intrusions are also increasing.

In statistics and machine learning research, the application of outlier research is divided into two scenarios. One is to perform outlier detection and data cleaning in the data pre-processing link, and the other is to directly focus on the results of outlier detection. Target the object and apply it to the corresponding scene. The mining of outlier points also has broad business application development prospects in China Intrusion Software Detection Center [5]. Therefore, this paper mainly uses the theory of rough set technology to represent and analyze the network intrusion source and detect the data in the system that is not determinable and incomplete, and the rough set technology theory and the outlier multi-node The technical theories of network

excavators are combined to detect network intrusions [6]. We first need to propose an attribute data collection and completion processing algorithm based on rough set entropy theory and a dynamic attribute data reduction processing algorithm based on approximate data decision entropy. Through these two reduction algorithms, the entire intrusion data detection and processing system, raw data in the data are collected for quantitative pre-processing [7]. Wen proposes a fault monitoring method based on fuzzy association rule mining [8].

In order to explore the effect of exhaustive swimming training on the establishment of trained animals, among them, Bai gave a detailed introduction to data mining technology, analyzed the current problems in the development of data mining technology, and elaborated related research methods and technologies [9]. In his article, Eissa puts forward the research significance and research status of rough set data mining, and expounds the related rough set basic theory. In addition, it shows the significance and importance of rough set data mining for network security information system data processing and monitoring [10]. In the article, Ibrahim elaborated on the methods and methods of network security information system monitoring, and proposed the advantages and disadvantages of network security information system monitoring based on rough set data mining [11]. Qian and Gong proposed the efficiency and accuracy of traditional monitoring methods to be low, pointed out the feasibility of rough set data mining, and proposed a variety of data processing algorithms based on rough set data mining, especially the data pre-processing algorithm is better [12]. Wang et al. deeply analyzed the functional requirements of power information systems from the aspects of security and storage functions, proposed the characteristics of network information security analysis architecture, and explored the application measures of power information system network security technology based on big data [13]. Rui Starting from account management, firewall technology, antivirus software and data backup technology, the countermeasures for the network security protection of power information systems are discussed [14].

The innovation points of this paper are as follows: (1) Through the study of rough set data mining technology-related content, based on these two kinds of data, pre-processing algorithm is proposed, and the feasibility of two data pre-processing algorithms based on rough set data mining in network security information system monitoring, especially intrusion monitoring is discussed in detail. (2) Two data pre-processing algorithms based on rough set data mining can effectively realize the monitoring function of common network security information system, and improve the security of network security information system to a certain extent.

2. Data Mining and Rough Set Theory

2.1. 1K-Means-PageRank Degree Distribution Algorithm. Data mining, also known as knowledge discovery in databases, is a hot research topic in the field of artificial intelligence and databases. Data mining degree has different meanings in different networks [15]. Degree can express the influence and importance of an individual [16]. The greater the degree, the greater the influence of the individual and the greater the role of the individual in the whole organization, and vice versa [17]. Degree distribution is the most studied feature of complex networks. In complex networks, the number of edges varies with the number of vertices [18, 19]. We use Q to denote the degree of vertex I. For undirected networks, the

$$\begin{aligned} \mathrm{Q_t}(\mathrm{b}) &= \mathrm{I} * \sum_{\mathrm{t}=1}^{k} F\left(t_b - t_{b1}\right), \\ F(t) &= \left(\frac{1}{\text{attenuation}}\right)^{\text{step}*t}. \end{aligned} \tag{1}$$

The F function is used to estimate the value of each iteration, the order of vertex I is the adjacency matrix, and then the degree distribution $P(k)$ of the network can be calculated, which is the probability of any vertex in the network.

$$\begin{aligned} P(k)_j &= \{t_i\} | f(x) = C_f, 1 <= i <= n, 1 <= j <= n, \\ E(\gamma) &= \sum_{J=1}^{V} \frac{D_f}{D} * \mathrm{Info}\left(D_f\right). \end{aligned} \tag{2}$$

The ability of a node in a complex network to be on the shortest path of other nodes is used to describe the value of a node in information dissemination [20].

$$\begin{aligned} G_k &= \left(\mathrm{J}_k - c_k\right) * c_k * \left(1 - \mathrm{J}_k\right) k = 1, 2, \\ \mathrm{EW}_j &= \left(\sum_{k=1}^{n} d_k v_j\right) * h_j * \left(1 - h_j\right) j = 1, 2, \\ V_{jk}(N+1) &= V_{jk}(N) + a_1 d_k(N) h_j, \end{aligned} \tag{3}$$

where g represents the sum of the shortest paths from node j to node K, and EW represents the number of nodes in these shortest paths. The larger the intermediary centrality value, the more the shortest path through the node, the more obvious its hub role in the whole network, the stronger its influence and control, and the more important the node. Proximity centrality refers to the reciprocal of the sum of the shortest paths from one node to all other nodes. The approach centrality of a node v can be expressed as:

$$\begin{aligned} \mathrm{Center}(V) &= -\sum_{j=1}^{v} \frac{D_f}{D} * \log 2\left(\frac{D_f}{D}\right), \\ \mathrm{WOE}_i &= In \frac{B_i / B_t}{G_i / G_t}, \end{aligned} \tag{4}$$

where WOE is the distance between node B and node G. Compared with node degree, closeness centrality can further describe the closeness between nodes and non-directly connected nodes. Generally speaking, a person's more friends does not mean that he is very important. Even if he

has fewer friends and these friends are very important, he is equally important. For a complex network with n nodes, the centrality of its node eigenvector is defined as:

$$N\left(X^i\right) = \frac{\sum_{j=0}^{num} C_{nj}\left(uj^i - u^i\right)^2}{\sum_{j=0}^{num} C_{nj}\left(dj^i\right)^2}, \tag{5}$$

where x is the set of all adjacent nodes of the node, CN is the element of the adjacency matrix U of the network, if node I is adjacent to node j, then

$$x\text{best} = \min\left[\sum_{yeD_1}(y - y_L)^2 + \sum_{yeD_2}(y - y_R)^2\right]. \tag{6}$$

The basic idea of PageRank algorithm is to define a random walk model on a directed graph, that is, a first-order Markov chain, which describes the behavior of random walkers randomly visiting each node along the directed graph. PageRank algorithm is a classic algorithm for ranking web pages in Google search engine. It is first used in the network model between deterioration and minerals. This type of metamorphic grade is regarded as network nodes, such as metamorphic grade A and metamorphic grade B. If a is pointed by an important mineral and B is pointed by many minor minerals, the PageRank value of metamorphic grade A may be larger than that of metamorphic grade B, that is, metamorphic grade A is more important than metamorphic grade B. The mathematical formula of PageRank is as follows:

$$\mathrm{PR}(x) = \min\left[\sum_{i=1}^{nl}\left(\mathrm{A}_i^2 - 2y_i y_l + y_l^2\right) + \sum_{im+1}^{n_l+n_R}\left(\mathrm{B}_i^2 - 2y_i y_R + y_R^2\right)\right], \tag{7}$$

where PR(x) is the PageRank value of metamorphic degree x, PR(Y) is the PageRank value linked to the Y_i of metamorphic degree X. When the PageRank value of individual metamorphic degree is difficult to calculate due to its non-convergence, it needs to play the role of damping coefficient. The N_i coefficient refers to the ratio of the rated load (speaker) impedance of the amplifier to the actual impedance of the power amplifier. By transmitting the hidden state of the current neuron to the next neuron, the recurrent neural network has a short-term "memory function." Recurrent neural networks with variable topology and weight sharing are used for machine learning tasks involving structural relationships, and have received much attention in the field of natural language processing. RNN generates the output of the next time according to the current input TX and the hidden state TH of the previous time. Generally, th is directly used for the output, i.e.

$$\begin{aligned} \mathrm{TH} &= \frac{1}{2}(\mathrm{TX} - y)^2 = \frac{1}{2}[t - f(WX)]^2, \\ \Delta\mathrm{TH}_i &= -\eta E' = \eta x_i (t - y) f'(WX) = \eta x_i \mathrm{TX}. \end{aligned} \tag{8}$$

Long short-term memory neural networks-commonly known as LSTMs, are a special kind of RNN that can learn long dependencies. The long-term and short-term memory network is an optimized network structure to solve the problem of gradient disappearance and gradient explosion in RNN training. Compared with RNN, LSTM can better mine the long-term dependence between data, and it is the most popular scheme nowadays. LSTM model includes three control gates: input gate, output gate and forgetting gate. The forgetting gate inputs the previous stage th and the current state TX into the sigmoid function to selectively forget the previous node. In information science, the sigmoid function is often used as the activation function of neural network due to its mono-increasing and inverse-function mono-increasing properties. The calculation formula of forgetting gate is as follows:

$$\mathrm{sigmoid}(\mathrm{TX})^{l3} = -\eta\delta^{l3}X^{l3} = \eta(t - y) f'\left(X^{l3}\mathrm{TH}^{l3}\right)X^{l3} + B, \tag{9}$$

where B is the sigmoid function, X is the weight matrix of the forgetting gate, and the output of the forgetting gate is

$$\mathrm{TX}^{l3} = (t - y) f'\left(X^{l3}W^{l3}\right), \tag{10}$$

wherein the definition of element multiplication is as follows:

$$\begin{aligned} X_{\lim} &= f(x) = \sum_{j\subset Q} c_j \frac{x_j}{\sigma\left(X_j'\right)} - p - B, \\ B\left(d_i, w_j\right) &= P(d_i)P\left(w_j|d_i\right); P\left(w_j|d_i\right), \\ \&9; &= \sum_{k=1}^{K} P\left(w_j|z_k\right)P\left(z_k|d_i\right). \end{aligned} \tag{11}$$

An input gate is a gated device used to control how much input goes in or out or whether to allow it in or out. The input gate generates new candidate information through the output of the previous state, the input of the current state and the tanh activation function to obtain the next state TC. The calculation formula of the input gate is as follows:

$$Q = \{(a_1, b_1), (a_2, b_2), \ldots, (a_n, b_n)\}, \tag{12}$$

$$\mathrm{TC} = \mathrm{argIU} * \max \sum_{a_n \in W_K(a)} \left|(b_n = c_n)M * \mathrm{IW}\right. . \tag{13}$$

IW and IU are the weight matrix of the input gate, and the output gate is responsible for calculating the activation value of this layer. Cell state information is activated through the filter layer and multiplied by QT to get the output information Q_{ik}. The calculation formula of output gate is as follows:

$$\mathrm{Q}_{ik} = \sum_{a}^{n} \tau_1 X_{ik} + \sum_{b}^{n} \tau_2 U\left(Y_{ik}\right) + B_{ik} * \mathrm{QT}, \tag{14}$$

where O_u is the weight matrix in the output gate, and the output information is:

$$\Delta\mathrm{OU}^l = -\eta\frac{\partial E}{\partial W^l} = \eta\left(X^l\right)^T\delta^l. \tag{15}$$

So far, the output information of data mining and the node training module of interactive process are obtained.

2.2. Network Information Security Standards and Related Specifications. Like power companies, traditional companies lack professional personnel in network security management, security measures are not in place, security awareness is weak, the configuration and maintenance of network information platforms cannot be followed up in time, the most common configuration is improper, vulnerability patches are not synchronized and upgraded, etc. All will become security risks. In addition, most companies lack comprehensive security management solutions and rely too much on firewalls and encryption technologies.

3. Construction of Experimental Model

3.1. Experimental Data Source. The experimental software environment is Eclipse SDK (Software Development Kit) 3.5.0, Windows XP operating system; the hardware environment is a PC (Personal Computer), configured as: CPU Intel Core 2 dual-core T7100 (1.8 GHz), 2 GB memory. Both the classic DBSCAN (Density-Based Spatial Clustering of Applications with Noise) algorithm and the GFDBSCAN algorithm proposed in this paper are coded in Java. Five data sets were used in the experiment. Data set 1 is a random data set generated by ourselves [data set randomly generated with points (2, 2) and (25, 25) as the center, and Data set 2–5 are commonly used data sets to verify the clustering effect of the DBSACN algorithm. In addition, due to the very large size of the original data set and the low level of support set by the user, the DRBFP_MINE algorithm may also appear to have reached the maximum memory during the construction of the first FPTREE during the execution process. At this time, the DRBFP_MINE algorithm mines rise by decomposing the original data set. There are partitioning (Partitioning) and mapping (Projection) based decomposition data sets.

The original data set is divided into smaller data sets based on the partitioning method, so that its corresponding FPTREE can be constructed in memory, and then the conventional in-core-based mining algorithm is used to mine and merge each part of the data set Candidate frequent item sets. Finally, the original data set needs to be scanned again to count the candidate frequent item sets in order to determine the frequent item sets. The partition-based method will generate a large number of local frequent item sets. These local frequent item sets may be larger than the original data sets, which also need to be stored on disk. Scanning the original data set and counting the frequent candidate item sets stored on disk is also very time-consuming. It is also worth noting that considering the distribution characteristics of the data set, how to decompose the data set makes its corresponding FPTREE occupy smaller memory more difficult to determine. For example, the decomposition of a uniformly distributed data set does not reduce its memory usage. The FPTREE corresponding to the decomposed data set may be about the same size as the FPTREE corresponding to the original data set.

3.2. Design of the Safety Monitoring System for the Operation of Network Information Platform. The system structure is mainly divided into data collection sub-module, data analysis sub-module, important equipment monitoring sub-module of enterprise intranet and operation safety management sub-module. The data collection sub-module mainly includes network device data collection, security device data collection, application server data collection, and data analysis sub-module functions include statistical analysis of enterprise IP resource distribution, statistical analysis of historical and real-time operating status, business capability evaluation and analysis results download. The operation safety control sub-module includes equipment operation safety control and equipment control management, controls the operation of the equipment according to the data analysis results, and ensures that the operation status of the equipment conforms to the safety rules and corporate specifications.

After obtaining the network security information, the important work is to analyze and detect the danger or intrusion information from the information, and then ensure the security of the network security information system, and process and prevent the dangerous information in time. Information security on the network means that the data flowing and stored in the network system is not subject to accidental or malicious damage, leakage, and modification.

3.3. Model Module Analysis Process. The algorithm model is divided into 5 layers as a whole, from bottom to top: data pre-processing layer, item set classification processing layer, attribute reduction layer, item set mining layer, decision rule processing layer. The specific description is as follows: data acquisition layer the data acquisition layer is also called the data pre-processing layer. For massive and complicated data, data pre-processing must be performed. Data filling and cleaning: The key tasks of this layer include data unification, abnormal data processing, data simplification, data form information, filling missing data, etc. Data integration: The goal of this layer is to first clean up data sources from different places, and then store these data in a combined storage space according to the results of the cleanup. The main tasks include: entity identification, detection and resolution of data value conflicts, redundancy, and other issues. Data transformation: The main problem is "normalization." These include: zero-mean normalization and max-min normalization. Data specification: The goal of this layer is to regulate the data sources that have been standardized, and get almost the same analysis results. In this paper, we use the knowledge of data discretion in data mining, and select the appropriate discretion method according to the number of attributes to discretize the data, so that the discretion data can meet the processing requirements of this article. After the data pre-processing in the above steps, a set of original item sets is obtained.

In addition, the operation object of this layer is the original decision table, which reduces the dimension of data through attribute reduction. First, according to the mining target, the initial decision table S is formed. Second, simplify the decision table to determine whether the decision table is a compatible decision table: again, use the difference matrix to find the kernel. After finding the kernel, the attributes are

Table 1: Decision table information.

Policy-making body	A	E
{X1, X2}	{3}	{2}
{X3, X5, X6, X12}	{3}	{2}
{X4, X7}	{3}	{2}
{X8, X13}	{4}	{2}

divided into two categories: nuclear attributes and non-nuclear attributes, and then the attribute importance of each attribute is obtained, and the corresponding attribute reduction algorithm is executed. Finally, the reduced decision table is obtained. The information of the decision table established in this article is given in Table 1:

4. Simulation Analysis of Network Security Information System Based on Rough Set Data Mining

4.1. Efficiency Analysis of Attribute Reduction Algorithm Based on Rough Set ADEAR. This algorithm is called iterative deepening Astar algorithm, which can effectively solve the problems caused by the growth of Astar space. In this paper, a new attribute reduction algorithm ADEAR is proposed based on rough set data mining. As shown in Figure 1, this algorithm can simplify data screening and effectively monitor data, which also reduces the complexity of the ADEAR algorithm to a certain extent. In addition, the ADEAR algorithm in this article is implemented in java language, and the corresponding hardware environment: Intel processor 2.0 GHz, memory is 2 GB.

Computer network is an important means and way for people to understand society and obtain information through modern information technology. Network security management is the fundamental guarantee for people to surf the Internet safely, green, and healthy. In order to verify the effectiveness of this algorithm, as shown in Figure 2, we conducted a monitoring experiment on a network security management system and conducted experiments on the data set: The attribute-related records in the data set of the security system in the experiment are given in Table 2.

As shown in Figure 3, we compared the ADEAR algorithm with 6 representative attribute reduction algorithms. We first conducted an attribute reduction experiment on the ADEAR algorithm, and implemented CIQFS using java language, and then also conducted a corresponding attribute reduction experiment.

As shown in Figure 4, the reduction results of several different algorithms mentioned above are compared. The experimental results of the five algorithms POSFS, CEFS, DISMFS, GAFS, and PSORSFS can be obtained from the paper. The reduction results of each reduction algorithm on the corresponding data set are given in Table 3.

As shown in Figure 5, the classification accuracy corresponding to the above seven different reduction algorithms is compared. We use the experimental method designed by Wang et al., which uses the 10-fold cross-validation method to estimate the classification accuracy of each reduction algorithm. For the training set after reduction, the Rough Set Exploration System (RSES) to extract the decision rules.

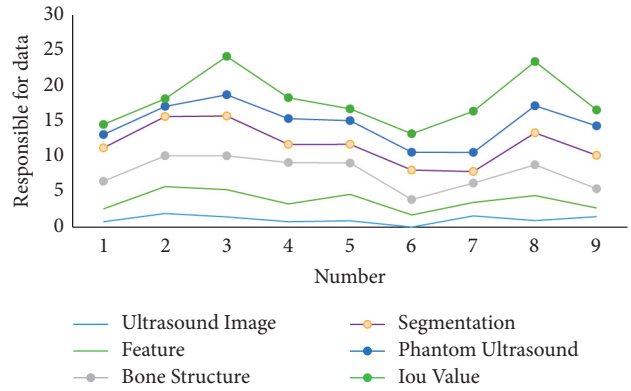

Figure 1: Simplify data and monitor data.

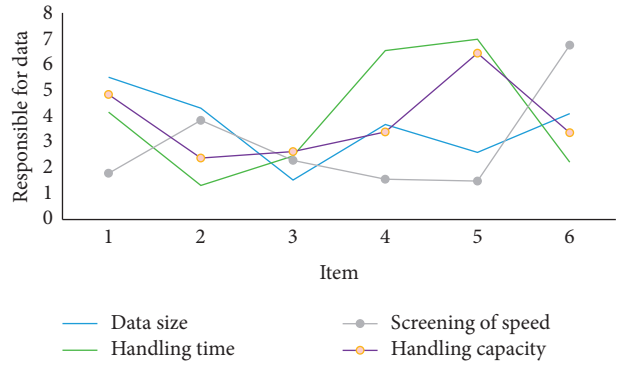

Figure 2: Attributes in the security system data set.

Table 2: Property-related records in the security system dataset.

Serial number	DS	Number of objects	Number of attributes
1	Tic-tac-toe	955	9
2	Lymphography	146	9
3	Vote	300	12

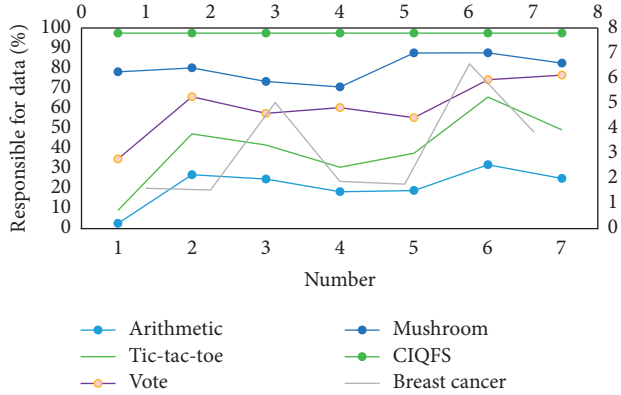

Figure 3: Attribute reduction experiment.

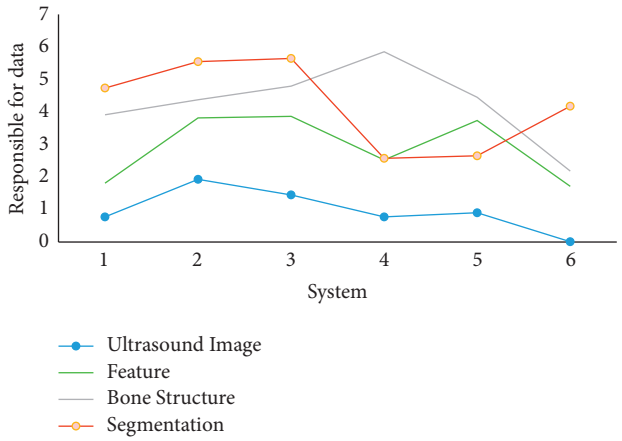

Figure 4: Reduction results of different algorithms.

Table 3: The reduction result of reduction algorithm on the corresponding data set.

Arithmetic	POSFS	CEFS	PSORSFS	CIQFS
Tic-tac-toe	9	7	9	8
Breast cancer	4	5	9	4
Vote	6	10	6	7
Mushroom	5	3	12	5

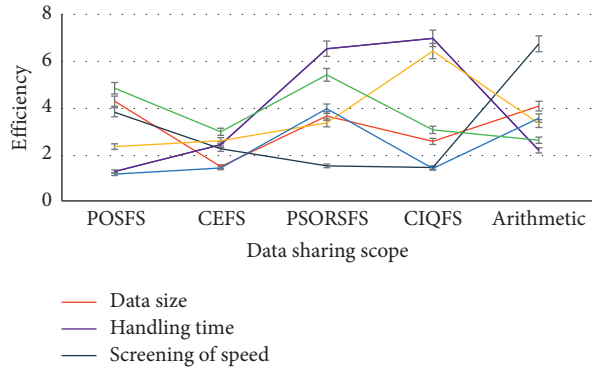

Figure 5: Rough set attribute reduction algorithm.

Finally, apply these rules to the test set for classification testing (the conflicts are resolved using the "Standard Voting" method), based on rough set attribute reduction algorithm ADEAR's screening rate of security system information, as shown in Figure 6.

As shown in Figure 7, we found that because there are 6 contours in the lymphatic data set, the classification accuracy of the ADEAR algorithm on the lymphatic data set is lower than that of POSFS, because these contours will affect the classification performance of the final ADEAR algorithm.

The POSFS is relatively less affected by these outlines, so its classification accuracy is higher than the ADEAR algorithm. Therefore, the performance of the ADEAR algorithm can be improved to a certain extent. Based on rough set attribute reduction algorithm ADEAR monitors the efficiency of safety system information is given in Table 4.

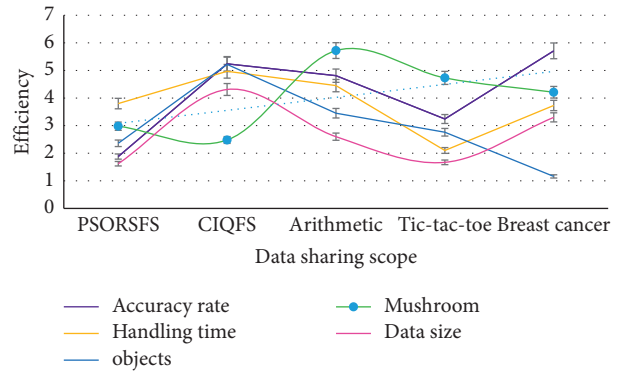

Figure 6: The rate of security system information filtering by ADEAR.

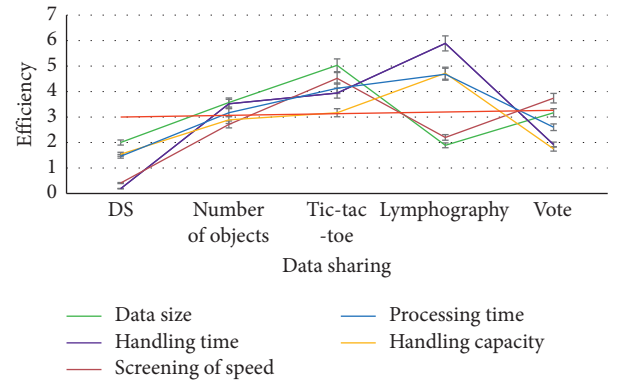

Figure 7: Classification accuracy on lymphatic data.

It can be seen from the data in Figure 8 that ADEAR based on rough set attribute reduction algorithm is acceptable for information monitoring of safety systems. It can monitor relevant information to a large extent in real time, and the information feedback speed is faster than that of existing general monitoring. The algorithm is better.

As can be seen from the data in Figure 9, the rate of security system information screening based on rough set attribute reduction algorithm ADEAR is acceptable, it can basically meet the needs of data screening, and the processing efficiency of the experimental network security system is higher than the general processing method out of 10%.

As shown in Figure 10, we calculated the running time of the ADEAR algorithm, and gave a comparison between the running time of the ADEAR algorithm and the two reduction algorithms SCE and FSPA-SCE. The data of the latter two algorithms are obtained from the experiment. Based on rough set attribute reduction algorithm ADEAR monitorss the accuracy of safety system information, as shown in Figure 11.

It can be seen from the data in Figure 12 that the ADEAR based on rough set attribute reduction algorithm has a high accuracy of monitoring information in the security system, and the monitoring accuracy of the network security information system reaches about 98%. The model performance is given in Table 5, and the performance indicators of various branching algorithms are given in Table 6.

Table 4: Efficiency of safety system information.

Genome	Mushroom	Accuracy rate	Data size	Handling time	Objects
PSORSFS	2.98	1.88	1.62	3.8	2.36
CIQFS	2.48	5.24	4.31	4.97	5.22
Arithmetic	5.72	4.81	2.6	4.45	3.45
Tic-tac-toe	4.73	3.24	1.67	2.1	2.76
Breast cancer	4.21	5.71	3.3	3.73	1.16

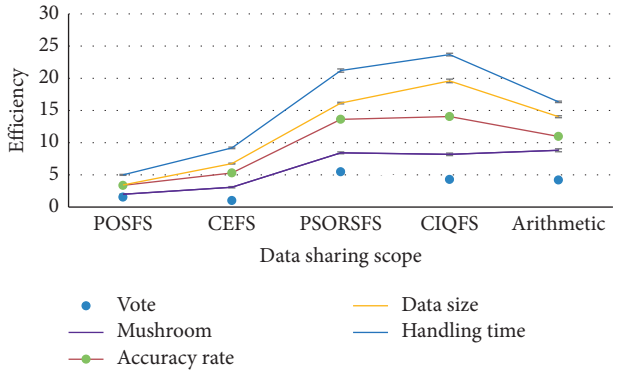

Figure 8: Reduction algorithm ADEAR monitors the efficiency of security system information.

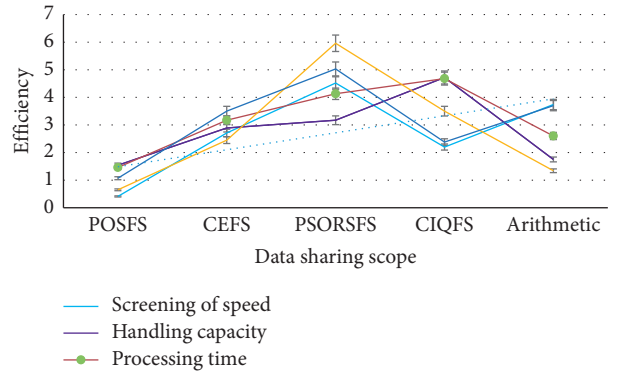

Figure 9: Algorithm speed comparison of different algorithms.

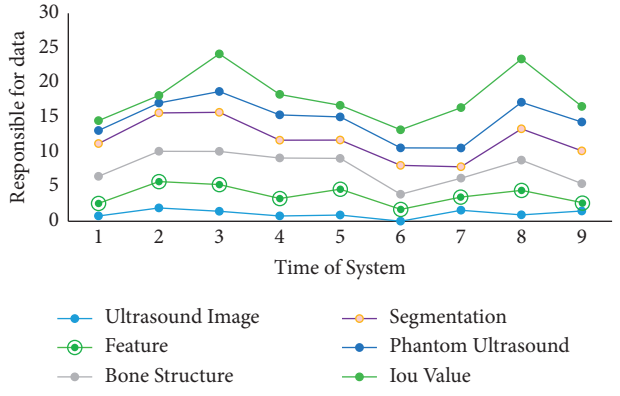

Figure 10: ADEAR algorithm and two reduction algorithms.

4.2. Performance Analysis of Outlier Detection Algorithm ODIWOMR Based on Rough Set Weighted Distance. As shown in Figure 13, in order to verify the network security information, monitoring performance of the ODIWOMR

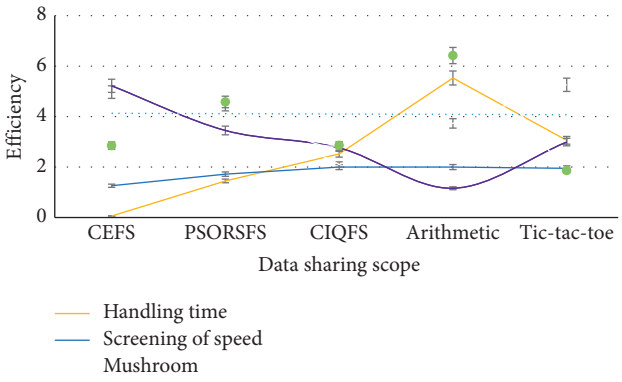

Figure 11: Accuracy of safety system information.

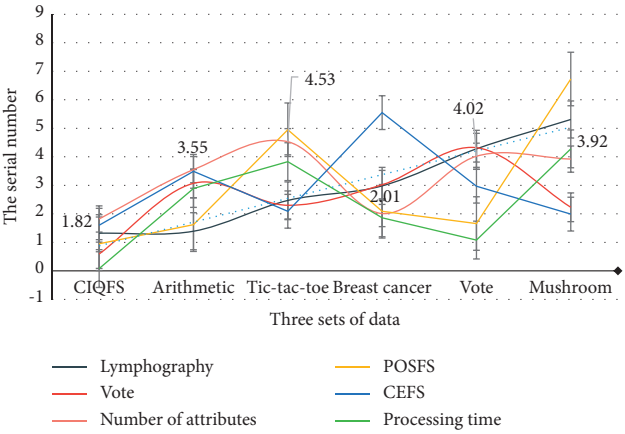

Figure 12: ADEAR the reduction algorithm, monitors the accuracy of the security system information.

algorithm, is too high, which is inconsistent with the actual network environment.

As given in Table 7, there is a prerequisite for unsupervised intrusion detection: the intrusion behavior is regarded as an outliner, the corresponding proportion cannot be too high, and the proportion corresponding to the intrusion behavior needs to be far less than the proportion of normal behavior; if the intrusion behavior accounts for is too large, it will not be detected as an outliner.

As given in Table 8, in this experiment, the data in the data set was screened, and the proportion of the intrusion behavior that was satisfied was much smaller than the ratio of normal behavior, that is, the number of intrusion records accounted for about 2.5%, and the number of normal data records was greater than or equal to 97.5%. ODIWOMR, an outliner detection algorithm based on rough set weighted

Table 5: Model performance.

Genome	Screening of speed	Handling capacity	Processing time	Efficiency	Optimization
POSFS	0.41	1.54	1.46	0.65	1.07
CEFS	2.71	2.89	3.17	2.45	3.5
PSORSFS	4.52	3.17	4.13	5.96	5.03
CIQFS	2.2	4.72	4.68	3.5	2.38
Arithmetic	3.74	1.75	2.6	1.34	3.7

Table 6: Performance indicators of various branching algorithms.

Genome	Handling time	Screening of speed	Handling capacity	Processing time
DS	0.19	0.41	1.54	1.46
Number of objects	3.52	2.71	2.89	3.17
Tic-tac-toe	3.94	4.52	3.17	4.13
Lymphography	5.89	2.2	4.72	4.68
Vote	1.92	3.74	1.75	2.6

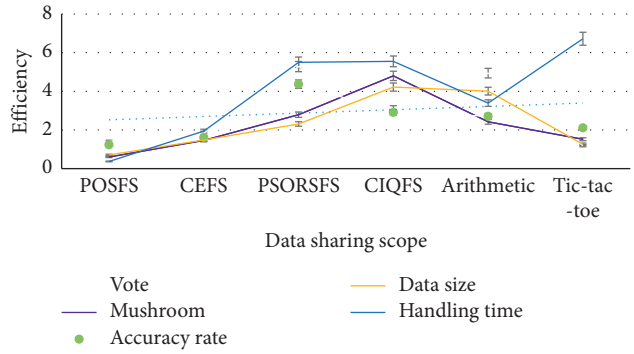

Figure 13: Performance of the ODIWOMR algorithm.

Table 7: Intrusion behavior accounts.

Dense	DS	Number of objects	Tic-tac-toe	Lymphography	Vote
Number of attributes	0.59	3.07	2.3	3.02	4.32
POSFS	1.82	3.55	4.53	2.01	4.02
CEFS	0.95	1.62	4.95	2.09	1.66
PSORSFS	1.6	3.49	2.09	5.55	2.97
CIQFS	0.08	2.89	3.83	1.86	1.08

Table 8: Proportion of the intrusion behavior.

Genome	Vote	Mushroom	Accuracy rate	Data size	Handling time
POSFS	1.4	0.6	1.23	0.71	0.37
CEFS	1.84	1.46	1.61	1.48	1.94
PSORSFS	5.28	2.79	4.37	2.31	5.5
CIQFS	3.1	4.8	2.91	4.22	5.55
Arithmetic	4.94	2.42	2.71	4.01	3.39
Tic-tac-toe	1.19	1.52	2.11	1.26	6.72

distance, monitors the efficiency of security system information.

From the data in Figure 14, it can be seen that the outlier detection algorithm ODIWOMR based on the rough set weighted distance is very efficient for information monitoring of the safety system, it can largely monitor the relevant information in real time, and the information feedback is very fast. It is about 25% higher than the existing general monitoring algorithm.

As given in Table 9, since the data set has a total of 41 attributes after removing the class attributes, we can conclude from the definition of attribute importance that not all attributes are helpful to the final detection result, or have the same contribution, and some attributes may be contributing

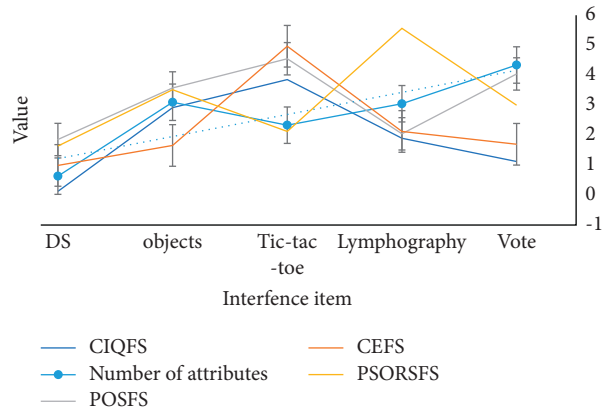

Figure 14: The outlier detection algorithm ODIWOMR monitors the information efficiency of the security system.

Table 9: Definition of attribute importance.

Dense	Breast cancer	Vote	Mushroom	Accuracy rate	Data size
CIQFS	2.22	1.95	2.5	3.36	1.38
Arithmetic	6	3.22	5.43	4.41	3.98
Tic-tac-toe	5.92	5.92	2.11	1.5	1.61
Number of attributes	1.79	2.28	3.13	3.88	4.12
POSFS	3.43	2.88	4.57	6.66	6.89
CEFS	5.87	4.96	5.76	5.52	1.87

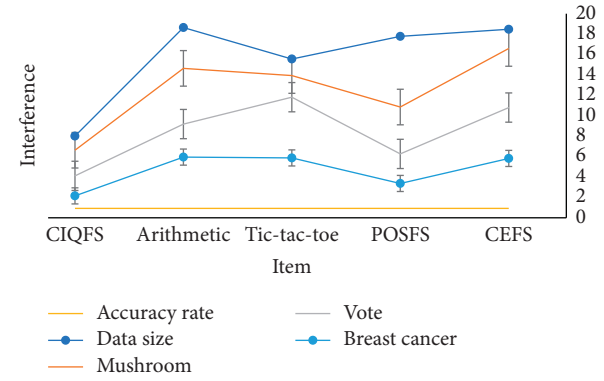

Figure 15: ADEAR of rough set attribute reduction algorithm monitors the accuracy of security system information.

Table 10: Information monitoring of security systems.

Genome	Mushroom	Accuracy rate	Data size	Handling time	Screening of speed
CEFS	4.97	5.22	2.85	0.06	1.26
PSORSFS	4.45	3.45	4.58	1.45	1.72
CIQFS	2.1	2.76	2.86	2.52	2
Arithmetic	3.73	1.16	6.42	5.53	2
Tic-tac-toe	5.26	2.99	1.86	3.06	1.95

less to the test results, and some even do not. Based on rough set attribute reduction algorithm, ADEAR monitors the accuracy of safety system information, as shown in Figure 15.

From the data in Table 10, it can be seen that the outlier detection algorithm ODIWOMR based on rough set weighted distance has a high accuracy of information monitoring of security systems, and the accuracy of

monitoring in common network security information systems is as high as 98.5%, which is higher than the general system increase by about 12%.

5. Conclusion

Network data contain a large amount of sensitive information of individuals, companies, and government departments. It is the fundamental task of information network transmission to protect information security from the source to the receiver. The feasibility of the ADEAR algorithm based on rough set attribute reduction is analyzed, and the corresponding working principles and theoretical guidance are proposed. The advantages and disadvantages of the algorithm are elaborated. Real-time monitoring of relevant information to a large extent, and information feedback speed are very fast, slightly better than existing general monitoring algorithms. In addition, its monitoring accuracy of the network security information system reaches about 98%. The feasibility and superiority of the outlier detection algorithm ODIWOMR based on rough set weighted distance are discussed and verified. It has been verified by experiments that the accuracy rate of monitoring using these two data pre-processing algorithms in common network security information systems is as high as 98.5%, which is about 12% higher than the general system accuracy. Two data preprocessing algorithms based on rough set data mining can effectively realize the monitoring function of common network security information systems, and can improve the security of network security information systems to a certain extent.

Data Availability

The data that support the findings of this study are available from the corresponding author upon reasonable request.

Conflicts of Interest

The authors declare that they have no conflicts of interest.

Acknowledgments

This work was supported by The Ministry of Education of Science and Technology Development Center of Production Innovation Fund China's Colleges and Universities (Grant no. 2020 IT A07027).

References

[1] S. R. Dash, S. Dehuri, and U. K. Sahoo, "Interactions and applications of fuzzy, rough, and soft set in data mining," *International Journal of Fuzzy System Applications*, vol. 3, no. 3, pp. 37–50, 2013.

[2] E. J. Gardiner and V. J. Gillet, "Perspectives on knowledge discovery algorithms recently introduced in chemoinformatics: rough set theory, association rule mining, emerging patterns, and formal concept analysis," *Journal of Chemical Information and Modeling*, vol. 55, no. 9, pp. 1781–1803, 2015.

[3] K. Gong, Y. Wang, M. Xu, and Z. Xiao, "BSSReduce an O(|U|) incremental feature selection approach for large-scale and high-dimensional data," *IEEE Transactions on Fuzzy Systems*, vol. 26, no. 6, pp. 3356–3367, 2018.

[4] Y. L. Zhang and C. Q. Li, "Topological properties of a pair of relation-based approximation operators," *Filomat*, vol. 31, no. 19, pp. 6175–6183, 2017.

[5] S.-H. Liao and H.-K. Chang, "A rough set-based association rule approach for a recommendation system for online consumers," *Information Processing & Management*, vol. 52, no. 6, pp. 1142–1160, 2016.

[6] J. Dai, H. Hu, W. Z Wu, Y. Qian, and D. Huang, "Maximal-discernibility-pair-based approach to attribute reduction in fuzzy rough sets," *IEEE Transactions on Fuzzy Systems*, vol. 26, no. 4, pp. 2174–2187, 2018.

[7] S. Deng, Y. Dong, and X. Fu, "Security risk assessment of cyber physical power system based on rough set and gene expression programming," *IEEE/CAA Journal of Automatica Sinica*, vol. 2, no. 4, pp. 431–439, 2015.

[8] Z. L. Wen, "Research and implementation of computer network user behavior forensics sys-tem based on system a log," *Journal of information security research*, vol. 9, no. 1, pp. 23–40, 2018.

[9] B. Q. Sun, H. Guo, H. Reza Karimi, Y. Ge, and S. Xiong, "Prediction of stock index futures prices based on fuzzy sets and multivariate fuzzy time series," *Neurocomputing*, vol. 151, no. 3, pp. 1528–1536, 2015.

[10] M. Peng, J. Jiang, Y. Dong, and X. Liu, "Research on computer network security monitoring based on extreme learning machine," *Paper Asia*, vol. 2, no. 2, pp. 176–179, 2019.

[11] J. An, J. Yu, Z. Li, Y. Zhou, and G. Mu, "A data-driven method for transient stability margin prediction based on security region," *Journal of Modern Power Systems and Clean Energy*, vol. 8, no. 6, pp. 1060–1069, 2020.

[12] Z. Qian and J. Gong, "Research on monitoring system of underground gas pipeline network based on Internet of things and GIS," *Journal of Geomatics*, vol. 44, no. 1, pp. 111–114, 2019.

[13] L. Wang, P. Hou, T. Jiang, Z. B. Wang, Y. X. Zhao, and K. Wu, "[Different sources of mesenchymal stem cells for the treatment of cartilage repair in knee joint]," *Boletin Tecnico/Technical Bulletin*, vol. 30, no. 6, pp. 581–586, 2017.

[14] L. Rui, "Discussion on power information system network security in the big data era," *Digital World*, vol. 176, no. 06, p. 78, 2020.

[15] Y. Li, "Monitoring data management information system for securities market," *Wireless Personal Communications*, vol. 103, no. 1, pp. 319–326, 2018.

[16] M. Jebraeily, M. Ghazisaeidi, R. Safdari, K. Makhdoomi, and B. Rahimi, "Hemodialysis adequacy monitoring information system: minimum data set and capabilities required," *Acta Informatica Medica*, vol. 23, no. 4, p. 239, 2015.

[17] A. M. Kumaritov, E. A. Sokolova, and A. A. Sokolov, "Geo-information system of ecological monitoring in inner-city industrial areas," *Gornyi Zhurnal*, vol. 2016, no. 2, pp. 94–96, 2016.

[18] D. J. Galar, M. Palo, A. Van Horenbeek, and L. Pintelon, "Integration of disparate data sources to perform, maintenance prognosis and optimal decision making," *Insight - Non-*

Destructive Testing and Condition Monitoring, vol. 54, no. 8, pp. 440–445, 2012.

[19] Y. Liu, W. Chen, and Y. Guan, "Identifying high-cardinality hosts from network-wide traffic measurements," *IEEE Transactions on Dependable and Secure Computing*, vol. 13, no. 5, pp. 547–558, 2016.

[20] T. Alhmiedat and G. Samara, "A low-cost ZigBee sensor network architecture for indoor air quality monitoring," *International Journal of Computer Science and Information Security*, vol. 15, no. 1, pp. 140–144, 2017.

Hindawi
Scientific Programming
Volume 2022, Article ID 2868499, 12 pages
https://doi.org/10.1155/2022/2868499

Research Article

Optimization of Innovation and Entrepreneurship Education and Training System in Colleges and Universities Based on OpenStack Cloud Computing

Chunyan Xu and Cai Song

Zhengzhou Preschool Education College, Zhengzhou 450000, Henan, China

Correspondence should be addressed to Chunyan Xu; xuchunyan@zzpec.edu.cn

Received 1 June 2022; Revised 26 July 2022; Accepted 30 July 2022; Published 30 August 2022

Academic Editor: Juan Vicente Capella Hernandez

With economic globalization and rapid development of science and technology, many colleges and universities pay more and more attention to the cultivation of students' innovative thinking and creativity, and innovation and entrepreneurship education has also become an important part of the education system. Due to the current unevenness of teachers in innovation and entrepreneurship education in colleges and universities, high training cost, and lack of strong atmosphere, this paper optimizes the innovation and entrepreneurship education and training system in colleges and universities through OpenStack cloud computing. This paper optimizes the cloud computing platform according to the OpenStack virtual machine and the multiobjective ant colony improvement algorithm and then designs the innovation and entrepreneurship education and training system. The multiobjective ant colony improvement algorithm uses the way ants find food to find the best information resource route from the traces left by the information trend in the cloud platform. In order to test the effectiveness of these methods, this paper uses the simulation method to test. The results show that, sometimes, the load utilization rate of the innovation and entrepreneurship education and training system in colleges and universities exceeds 80%, which is in line with the expected settings. Through the OpenStack cloud computing platform, it can provide a good innovation and entrepreneurship training environment for more users at low cost and low risk and promote the development of innovation and entrepreneurship education.

1. Introduction

Cloud computing, as a popular technical medium and model in the information society, is a huge leap in technology. Users use computing resources to change the economic model in the field of information technology, and it also promotes the development of other fields. Due to the characteristics of personalized customization of cloud computing application execution environment, more and more organizations are attracted to build high-performance computing clusters based on cloud platform technology. By using the OpenStack cloud platform to optimize the innovation and entrepreneurship education and training system in colleges and universities, it provides a rich resource and strong innovation and entrepreneurship score for college talents, which is conducive to the development of innovation and entrepreneurship education.

By integrating limited social resources through cloud computing technology, it can effectively obtain information resources. It improves resource utilization and promotes the rapid development of the Internet and the Internet of Things. At the same time, it promotes people's understanding of the whole society and enables human society to control the material and energy of nature more precisely. It has a profound impact on economic development and social progress.

Through the related computing of OpenStack cloud computing, the user resources are integrated, and the coupling degree is associated, which enables users to independently apply resources and reduce application costs. In order to more effectively select innovation and entrepreneurship

education for students, this paper redesigns the cloud platform teaching system. It improves the teaching system and adds a teaching evaluation system and a monitoring system. It understands the dynamics of the course in real time and mobilizes the enthusiasm for learning.

2. Related Work

With the growth of social economy, people's lives are becoming more and more intelligent and data-based, and teaching is no exception. Nelmiawati has been researching the use of OpenStack to design a virtual machine room for cloud computing on a centralized network and has achieved some results. His tests were performed using a specific server specification and the OpenStack platform. The test results of the virtual computer room and the case study of the object-based programming course show that the server used in the test can run the virtual computer room of 9 computers well [1]. Yan-Ting enabled users to access computing, storage, networking, and other resources from a shared, configurable pool of resources conveniently and on-demand over the network. He used the existing IT equipment resources of the university to create a cloud platform university that is more in line with the scientific research needs of the university [2]. Cloud-based technology is driving positive changes in the way organizations communicate. Radwan et al. implemented three technologies of OpenStack cloud, webRTC call, and 3D stereo effect and realized the feeling of 3D video [3]. Albert et al. used Putnam's social capital framework. To achieve the goals of his research, he used a mixed approach to determine how teaching at multiple institutions affects the social capital of teachers within the Haitian AET system. The results showed a low positive correlation between teaching and social capital across multiple institutions [4]. These studies are instructive to a certain extent, but in some cases, the demonstrations are insufficient or inaccurate and can be further improved.

With the development of intelligence and Internet, cloud computing, which combines the application of information technology and network application, is widely used. Singh et al. proposed a mathematical model to find redundant information based on overlapping regions. He employed a combinatorial metaheuristic to achieve optimal coverage, taking the effect of overlapping regions into account in the objective function to reduce the amount of redundant information perceived by the working sensor set. Improved genetic algorithms and binary ant colony algorithms are used as metaheuristic tools to optimize multiobjective functions [5]. Awad et al. used multiobjective particle swarm optimization (MOPSO) and multiobjective ant colony optimization (MOACO) intelligent algorithms to optimize data replication selection and placement in cloud environments [6]. Yi et al. studied the scheduling and collision-free routing problems of AGVs. He gave a mathematical programming model for this problem and improved the algorithm on the basis of multiobjective programming to optimize the pheromone matrix. He compared the performance of the two methods by using the available test problems for calculations. He conducted an empirical evaluation of an improved ant colony algorithm. The results show that the improved algorithm improves the performance of the existing algorithm [7]. These studies can analyze the relevant situation, but the specific research needs to be improved.

3. Method of Innovation and Entrepreneurship Education and Training in Colleges and Universities Based on OpenStack Cloud Computing

3.1. Virtualization of OpenStack. OpenStack cloud platform is a cloud computing solution architecture, not a single cloud computing resource service [8]. The OpenStack project consists of several different components that work together to complete cloud computing services. The development language used by the OpenStack project is python, and the source code of the project is released under the Apache license. The main function of the OpenStack cloud platform is to integrate various physical computer hardware resources. It provides a convenient web control panel interface for cloud platform system administrators to facilitate cloud platform resource management [9]. The OpenStack cloud platform can provide flexible and easily scalable cloud computing services for large public cloud services and small private cloud services. It simplifies the implementation of cloud computing technology and increases cloud computing. It makes the cloud computing architecture more flexible and scalable [10].

The key technologies of cloud computing mainly include computer virtualization technology, computer distributed programming and computing technology, cloud storage technology, resource management, and scheduling technology [11]. OpenStack cloud platform can also be understood as a computer operating system. It uses OpenStack cloud platform users to manage all computing service resources, network service resources, and storage service resources in the cloud platform through the control panel component of the Internet Web service interface. The role of OpenStack cloud platform in cloud computing software and hardware architecture is similar to that of a physical computer operating system, as shown in Figure 1.

Cloud computing is the product of the integration of traditional computer technology and network technology, and it is also a key strategic technology and means to lead the innovation of the information industry in the future [12]. In the classification of OpenStack, this paper only makes approximately linear resource allocation according to the allocation requirements of CPU, memory, storage, and other resources, but does not consider the differentiated requirements of different virtual machines for different resources [13]. In a heterogeneous environment, different physical servers have different performances, and some CPUs have strong computing power. However, disk IO performance and network bandwidth are reduced, and some servers have outstanding disk IO performance. However, the computing power is weak, and some servers have weak overall performance but have large network bandwidth [14]. Similarly, for users, each user has different requirements for various resources. Therefore, it can meet the needs of different users by dividing into a variety of different service

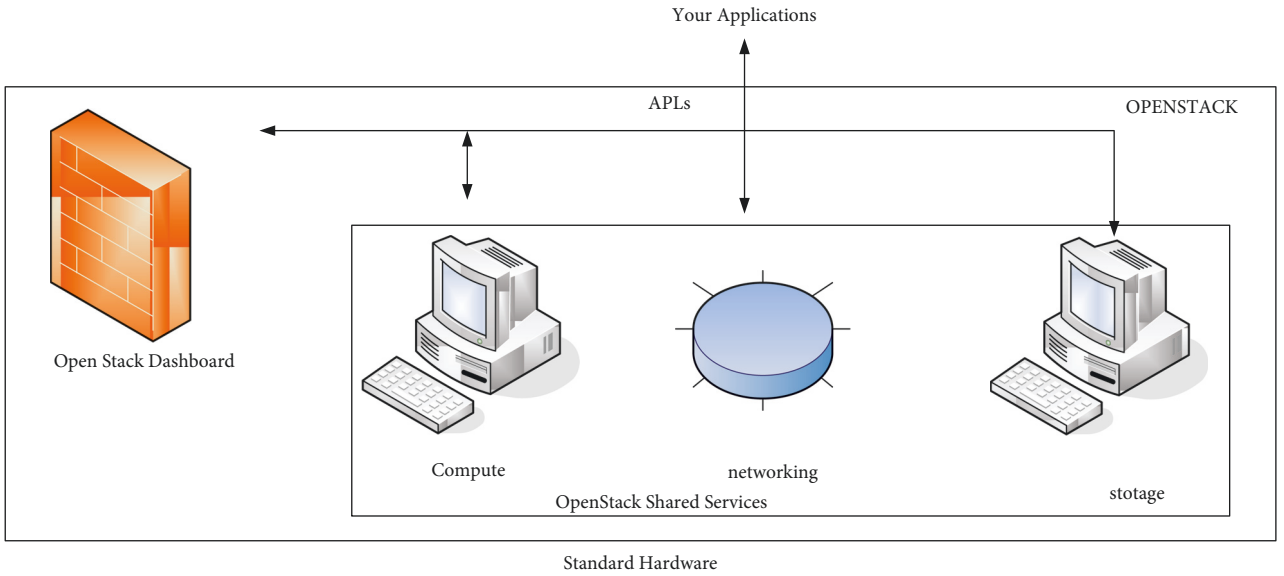

Figure 1: OpenStack cloud platform system.

Table 1: Resource quantization notation representation.

Resource type	Symbol name	Symbolic representation	Symbolic interpretation
CPU	VCNm	Virtual machine CPU performance	The number of CPUs after virtual machine m quantization
	RCNm	Physical machine CPU performance	The number of CPUs after physical machine m quantization
The Internet	VNNm	Virtual machine network performance	The number of bandwidths after virtual machine m quantization
	RNNm	Physical machine network (xingn)	The amount of broadband after physical machine m quantization
RAM	VCNm	Virtual machine memory performance	The amount of memory after virtual machine m quantization
	RMNm	Physical machine memory performance	The amount of memory after physical machine m quantization
Storage	VDNm	Virtual machine storage capacity	The amount of storage space after virtual machine m quantization
	RDNm	Physical machine storage capacity	The amount of storage space after physical machine m quantization
	VINm	Virtual machine hard disk IO performance	The number of access IOs after the virtual machine m is quantization
	RINm	Physical machine hard disk IO performance	The number of storage IOs after physical machine m quantization

types. At the same time, for different service types of virtual machines, this paper sets up virtual machine template images that focus on services. As users have more and more personalized requirements, users can also customize various requirements. The virtual machine needs to carry more network applications and occupies a large amount of network bandwidth. For example, for a virtual machine that needs to host a streaming media server and provide services such as DNS or CDN, the bandwidth will become the bottleneck of its performance. The main resource requirements of virtual machines for network traffic-based services are network bandwidth. The quantification of various resources is shown in Table 1.

A collection of virtual machines:

$$VM_m = \{VM_0, VM_1, VM_2, \ldots\}. \quad (1)$$

The resource status of physical machine n can be expressed as

$$RM_n = \{\mathrm{RCN}_n, \mathrm{RMN}_n, \mathrm{RDN}_n, \mathrm{RIN}_n, \mathrm{RNN}_n\}. \quad (2)$$

The resource status of virtual machine m can be expressed as

$$VM_m = \{\mathrm{VCN}_m, \mathrm{VMN}_m, \mathrm{VDN}_m, \mathrm{VIN}_m, \mathrm{VNN}_m\}. \quad (3)$$

The main objectives of virtual machines are infrastructure virtualization, system virtualization, and virtual server virtualization in cloud computing. It simplifies the access and management of IT resources for cloud users through certain computer technologies [15]. In addition, for virtual machines of different service types, the resources of virtual machine m can be represented as service resources and auxiliary resources [16]. Service resources refer to the resources that are mainly required by the corresponding service type, and auxiliary resources refer to other resources other than the main requirements resources of the corresponding service type. Therefore, the resources of various

service-type virtual machines can be expressed as a virtual machine m for a transaction-type service:

$$\begin{aligned} \text{VM\_}S_m &= \{\text{VCN}_m, \text{VMN}_m\}, \\ \text{VM\_}A_m &= \text{VM}_m, \text{VM}_{Sm} = \{\text{VDN}_m, \text{VIN}_m, \text{VNN}_m\}. \end{aligned} \tag{4}$$

The virtual machine m of the data IO type service:

$$\begin{aligned} \text{VM\_}S_m &= \{\text{VDN}_m, \text{VIN}_m\}, \\ \text{VM\_}A_m &= \text{VM}_m, \text{VM}_{S_m} = \{\text{VCN}_m, \text{VMM}_m, \text{VNN}_m\}. \end{aligned} \tag{5}$$

Virtual machine m for network traffic type service:

$$\begin{aligned} \text{VM\_}S_m &= \{\text{VNN}_m\}, \\ \text{VM\_}A_m &= \text{VM}_m, \text{VM}_{S_m} = \{\text{VCN}_m, \text{VMN}_m, \text{VDN}_m, \text{VIN}_m\}. \end{aligned} \tag{6}$$

3.2. Virtual Machine of the Multiobjective Ant Colony Improved Algorithm. The initial deployment of virtual machines is to optimize power consumption, cloud platform load balancing, user SLA violation rate, and other multidimensional goals to achieve optimal deployment of virtual machines under the constraints of physical machine bandwidth, disk storage, CPU, and memory [17]. The initial deployment of virtual machines on cloud platforms can be simplified as a multidimensional packing problem, that is, virtual machines are optimally deployed to physical machines under multiple optimization objectives and constraints. The improved multiobjective optimal deployment strategy based on the ant colony algorithm can avoid the waste of system resources and improve the overall performance of the system.

An optimized virtual machine initialization deployment strategy is indispensable for improving the stability and load balancing of the entire platform. This chapter proposes an improved multiobjective optimal deployment strategy based on the ant colony algorithm for the initial deployment of virtual machines. Ant colony algorithm is a biological intelligence heuristic algorithm. The abstract method of virtualizing computer resources can access the abstracted resources in the same way as before the abstracted resources through the virtualization technology.

Ant colony algorithm simulates the process of real-world ants searching for food. In the initial case, the ants do not have any information on the food destination [18]. In the process of finding food, ants hide a pheromone on the way to find food. Because this chemical evaporates slowly, the pheromone concentration in part indicates the distance of the journey to find food. When other ants find the pheromone, they head towards their destination. Ants take a different route. If a shorter route appears, then the concentration of the pheromone is greater for that route. More and more ants will be attracted to the new route. Eventually, most ants will focus on the shortest route. This will find the optimal path. If the route is shorter from the food, the concentration of pheromones on the route will be higher, and more and more ants will be attracted to join the route. So, in this way, the ant colony finds the shortest path to the food location. A multiobjective ant colony optimization algorithm is used to find the best data replica placement based on the minimum distance, the number of data transfers, and the availability of data replication.

Constraint 1 (SLA violation rate). For the problem of resource scheduling on the cloud platform, when the virtual machine created by it allocates physical machines, it must ensure the user service quality before further optimization of the cloud platform resource scheduling algorithm can be processed. The SLA contains the indicators of multiple services to ensure the service quality of cloud computing service providers. The CPU utilization function of the server node replaces the violation rate as a universal criterion. Then, the SLA violation rate function is defined as follows:

$$f_i^s = \ln\left(2 + j_{\text{cpu}} - 0.87\right). \tag{7}$$

Constraint 2 (resource balance). Since the resources of each physical server are not the same, and different types of virtual machines have different requirements for different resource types [19]. The amount of physical machine resources remaining on each physical machine is determined by the placement scheme of different virtual machines. However, in order to avoid the barrel effect, the resource usage on each physical node in the cloud platform should be kept as balanced as possible, such as network bandwidth, disk, CPU, memory, and other resources. It is to prevent the shortage of any one of the resources and cause the waste of other resources. Resource scheduling refers to the process of adjusting resources among different resource users according to certain resource usage rules under a specific resource environment. The utilization rate of four kinds of resources including physical node network bandwidth, disk, CPU, and memory is studied separately.

$$\begin{aligned} f_i^{\text{load}} &= \frac{4}{\left(u_{\text{cpu}}/u\right)^2 + \left(u_{\text{mem}}/u\right)^2 + \left(u_{\text{bw}}/u\right)^2 + \left(u_{\text{disk}}/u\right)^2}, \\ u &= \frac{u_{\text{cpu}} + u_{\text{mem}} + u_{bw} + u_{\text{disk}}}{4}, \end{aligned} \tag{8}$$

$u_{\text{cpu}}, u_{\text{mem}}, u_{bw}$, and u_{disk} represents the utilization of server CPU, memory, network bandwidth, and disk. u represents the arithmetic mean of CPU, memory, network bandwidth, and disk four-dimensional resource utilization. f_i^{load} represents the deviation of the four resource utilizations of disk storage, network bandwidth, memory, and CPU from the average utilization [20].

Constraint 3 (power loss efficiency). It is the total amount of power consumed by the server while it is running [21]. Under normal circumstances, the power consumed by the CPU accounts for the main part of the energy consumption of a server. A large number of research results show that there is a linear correlation between the power consumption of a physical node and the CPU usage on the physical node.

In other words, the power consumption of a physical node increases as the CPU usage on the server node

increases. The relationship between the power consumption of a physical server node and the CPU usage on it.

$$\begin{aligned} P_j &= \left(P_j^{\text{busy}} - P_j^{\text{idle}}\right) \times U_j^{\text{cpu}} + P_j^{\text{idle}}, \\ P_j &= k \times P_j^{\text{busy}} + (1-k) \times P_j^{\text{busy}} \times U_j^{\text{cpu}}, \\ \frac{P_j^{\text{busy}}}{P_j} &= f_j^p, \end{aligned} \tag{9}$$

where P_j^{busy} and P_j^{idle} represent the power usage of server j under full and no-load conditions, respectively. U_j^{cpu} represents the CPU utilization on physical node j [22]. Next, this paper analyzes the optimization problem of virtual machine initialization deployment. If the user applies to create m virtual machines, the cloud platform needs to deploy these virtual machines to n physical machines. In order to simplify the problem, it needs to add some constraints. When the utilization rate of one of the above four resources is zero, f_i^{load} takes the minimum value of 1/4, which indicates that the resource utilization rate of the entire cloud platform system is very unbalanced.

$$\begin{aligned} F_j &= k_1 \times f_j^p + k_2 \times f_j^{\text{load}} + \times k_3 \times f_j^s, \\ \sum_{j=1}^{n} x_{ij} &= 1, \quad \forall i \in I, \\ \sum_{i=1}^{m} R_{Pi} \times x_{ij} &\le T_{Pj} \times y_j, \quad \forall j \in J, \\ \sum_{i=1}^{m} R_{mi} \times x_{ij} &\le T_{mi} \times y_j, \quad \forall j \in J, \\ y_j, \quad x_{ij} &\in \{0,1\}, \forall j \in J, \forall i \in I. \end{aligned} \tag{10}$$

By default, the OpenStack cloud platform only performs weight calculation based on the remaining memory size of the physical node. That is to say, the more the memory remaining on the physical host, the greater the probability of being selected as the destination host for initial deployment of the virtual machine. Through this algorithm, the resource scheduling strategy aiming at reducing the cost is used to improve the resource utilization rate. It reduces the energy consumption cost of cloud computing and improves the operation efficiency of the cloud platform.

3.3. Design of OpenStack Ubiquitous Learning Environment University Innovation and Entrepreneurship Education and Training System Design. Innovation and entrepreneurship education focuses on cultivating students' innovative spirit and entrepreneurial quality and attaches great importance to the cultivation of students' innovative spirit and practical ability [23]. Entrepreneurship can be divided into broad and narrow senses. Entrepreneurship in the broad sense refers to pioneering and innovative activities. In a narrow sense, entrepreneurship refers to entrepreneurs looking for business opportunities and establishing some active organizations. It uses limited resources to provide certain products and services and ultimately create value. To crack the next entrepreneurship through the innovation and entrepreneurship education and training system in colleges and universities, the main body of college students' innovation is college students. It is a person who has received higher education, the object is a variety of limited resources, and its superior resources are rich in knowledge and information.

With the continuous development of entrepreneurship education, many people have begun to carry out entrepreneurship education, but they still do not pay enough attention to it. The problems of the entrepreneurship education system have gradually become prominent: the goal of entrepreneurship education is vague, the utilitarian tendency is clear, and it does not combine the characteristics of students and their own reality. Entrepreneurship education curriculum system is imperfect, lacking in quantity and weak in structure. The number of teachers is insufficient, the quality is uneven, and the degree of specialization is relatively low. Entrepreneurship education guarantee mechanism is not perfect, and teaching and management systems are not perfect and other factors. If they want to achieve their own sustainable development, they must have a comprehensive and systematic understanding of entrepreneurship education. It makes full use of its own advantages to build a sound entrepreneurship education system.

The ubiquitous learning platform is a comprehensive learning platform that provides teachers and students with learning, teaching, resource sharing, and mutual assistance [24]. The goal of entrepreneurship education in colleges and universities is to achieve the goal of entrepreneurship education, and entrepreneurship education is the basis for the formulation of teaching goals and teaching content. It is a measure of teaching effectiveness. It is beneficial to enhance students' innovative ability, practical ability, social adaptability, and lifelong learning ability and realize their own sustainable development. There are four main scenarios:

(1) Learning: teachers can plan courses, create new courses, upload course materials, etc., on the platform. After logging in to the ubiquitous learning platform, students can view and find the courses offered on the platform and their related information, register courses, and study courses [25]. Students can view test scores and specific correction results to summarize their learning deficiencies. By taking exams, completing assignments, or helping grade other student work, students better understand course content, review lessons, and expedite feedback on assignments. Students can also download learning materials and then can view learning resources offline anytime, anywhere, which has great advantages over traditional teaching and satisfies the theory of ubiquitous learning.

(2) Learning verification: allowing professors to verify student progress, test results, course grades, and course statistics, as well as the year's final test, organizing exams, and assigning homework. Based on these statistical observations, professors cannot justify any skepticism and make no progress, so alumni may be able to learn with mixed results.

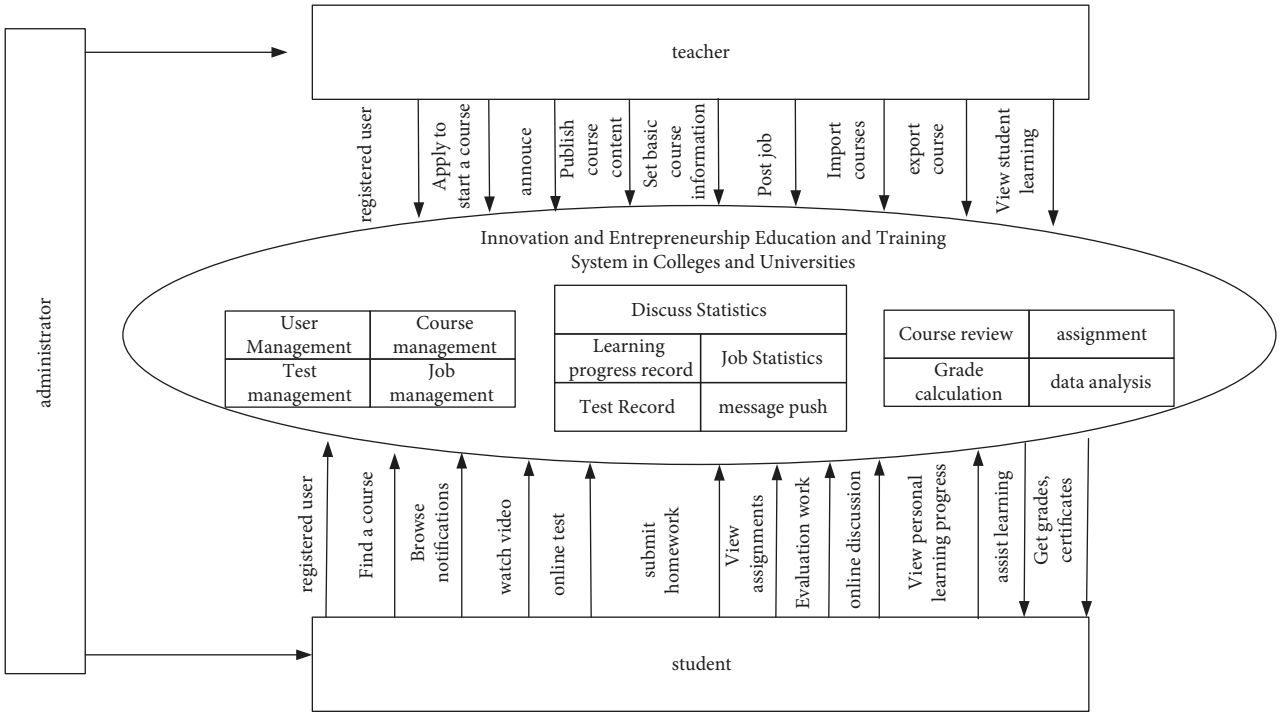

Figure 2: System application scenario diagram.

(3) Feedback: students can give feedback on the course after the course, or they can write their own learning experience and experience in the forum. At the same time, it can evaluate and score teachers, course content, learning experience, etc.

(4) Communication: when there are doubts in the learning process, students can communicate with teachers or other students and ask questions. It can also answer questions asked by others. Students and teachers can exchange knowledge with each other through discussions in the forum, and students can share materials with each other. The system application scenario is shown in Figure 2.

Platform administrators need to review teachers' registration information and manage permissions for other roles. The administrator needs to login to a separate page to set the global functions of the system, manage the system configuration, maintain the database, and monitor the operation of the system.

Figure 3 demonstrates the system functions of the open source ubiquitous learning environment. User login means that users can login to the system through their user name or e-mail address and password after completing the registration. Teachers can designate other students or manually select some students to correct their assignments, and they can also view historical assignments and correction records. Teaching material management: teachers can upload and download corresponding teaching materials and set the use rights of teaching materials, etc. [26].

The specific evaluation process of the homework evaluation subsystem and the ubiquitous learning system is shown in Table 2. When students submit homework in the homework evaluation subsystem, the homework also needs to include the address to be sent back after correction. The address can be assigned automatically by the system or manually by the teacher. Students receive assignments and grade them and return the work when they are done, with an item in the work indicating the grade of the work. It checks whether the job obtained is a job that has been judged and specifies whether it needs to be modified or needs to be displayed according to the judgment situation.

The data table of the homework evaluation subsystem is shown in Table 3. The relevant data items are explained in the above two data tables. After a student passes the online test, the system obtains the student's test result data and stores it in the score database. After the corresponding functional function processing, the student progress monitoring system can view the relevant learning data of the students according to different needs.

4. Optimization of Innovation and Entrepreneurship Education and Training System in Colleges and Universities

4.1. OpenStack Cloud Computing Virtual Machine Optimization Test. Virtual computing clusters are integrated with virtual machines. By standardizing the storage and local storage of the NFS server in the login phase of the cluster, the nodes can login remotely through the key. By establishing a parallel programming environment system, the management software of the cluster uses a resource manager with safety certification. This manager Sunac is used in supercomputers and massively parallel computing clusters. It is highly scalable and fault-tolerant, making it easy to manage

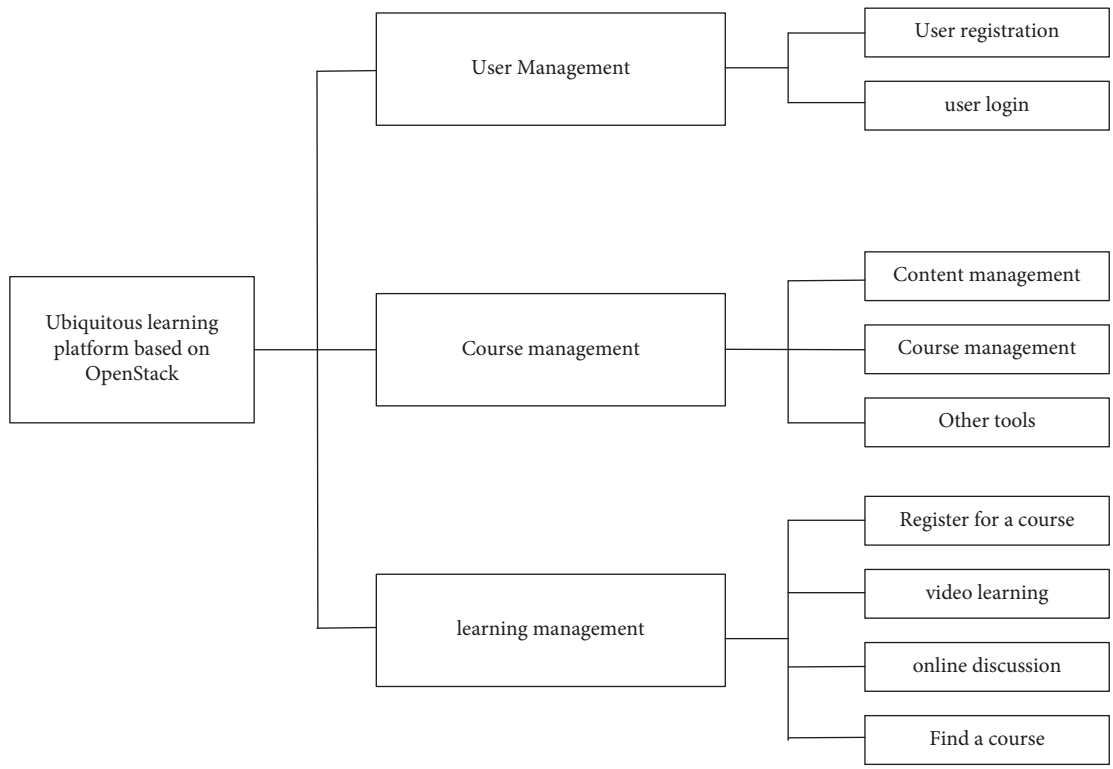

Figure 3: System function diagram of OpenStack's open source ubiquitous learning environment.

Table 2: Detailed description of the job evaluation subsystem database table.

Data table name	Primary key	Illustrate
User table	User ID	Username, password, e-mail, account activation, login time, registration time, teacher, administrator
Configuration table	Configuration information number	User ID, name, gender, reason for registration, highest education program user ID, date of birth
Homework evaluation form	Evaluation method number assignment	Evaluation method number, homework evaluation method name, homework evaluation weight table, weight information number, user number, weight, course number
Detailed evaluation form	Evaluation detail number	Evaluation no., evaluation details no. evaluation no.

Table 3: Detailed description of the database table for learning the classic monitoring subsystem.

Data table name	Primary key	Illustrate
User table	User ID	Username, password, e-mail, account activation, login time, registration time, teacher, administrator
configuration table	Configuration information number	User ID, name, gender, date of birth, reason for registering
Class schedule	Course No	Course number, course name, name of the school offering the course
Worksheet	Job number	Assignment number, course number, assignment name, assignment evaluation method, assignment
User test form	User ID	Test question number, test question score, user's score
Assignment submission form	Submit operation number	Course ID, assignment ID, student ID, assignment name, file path

large virtual computing clusters. The test of the simulation experiment is run on the NUDTSCI Cloud scientific cloud platform composed of 2 cloud hosts and the physical high-performance cluster composed of 2 nodes. Table 4 describes the configuration of physical nodes and cloud hosts.

In the experiment, 6 applications that are relatively representative in the test set are selected: (1) integer sorting (IS); (2) complex parallelism (EP); (3) multigrid benchmark (MG); (4) conjugate gradient formula solving; (5) block sparse formula solving (LU); (6) fast Fourier transform (FT).

Table 4: Physical cluster vs. virtual cluster single node configuration.

	Physical node	Cloud hosting
Processor	Intel Xeon E5-2640v4 10 cores	Intel Xeon E5-2640v4 10 cores
Number of CPU cores	40	16
Single node memory	132G	16G
The Internet	InfiniBand high-speed network	Gigabit Ethernet
Operating system	CentOS 6.8	CentOS 6.5
Resource management software	Slurm 2.2.5	Slurm 2.2.5

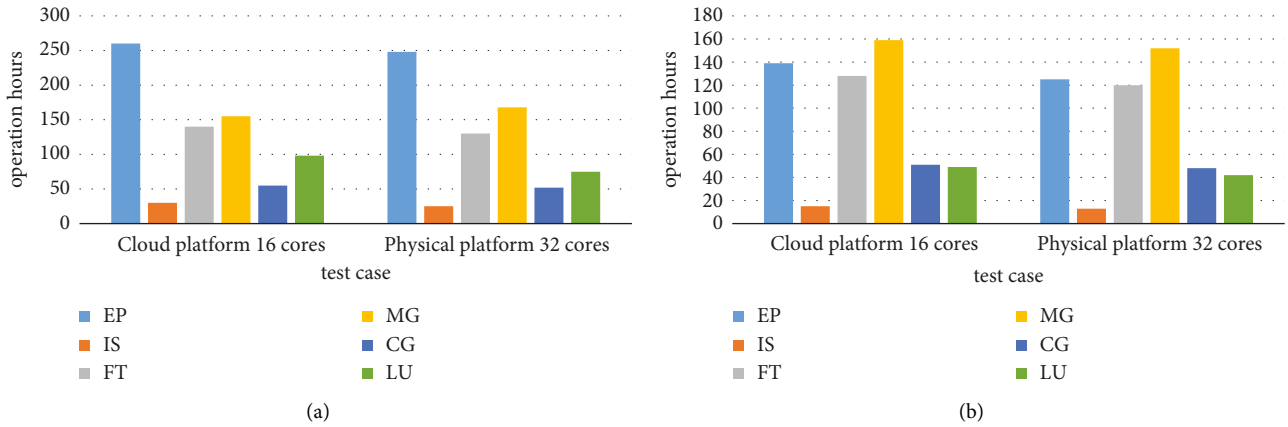

Figure 4: The server starts the virtual machine to run the NPB comparison test.

The test results of NPB are expressed in millions of floating-point operations performed per second, which can show the actual performance of general application programs. 4-Core and 8-core parallelism were started on a single node of 2 cloud computing, 4 physical clusters and high-performance computing cloud platform, respectively, and the running time of each test program in the NPB test set was recorded. They form a parallel virtual set of 16 CPUs and 32 CPU cores, respectively. It records the running time of each test program in the two clusters in the NPB test set as shown in Figure 4.

It can be seen from the experimental results that when the virtual machine exclusively occupies the physical node, the running time of the six test programs in the NPB test set is not much different between the physical node and the virtual machine. Among them, the FT program with the largest difference increased the running time by about 8.5% on the cloud platform after the introduction of virtualization overhead. It can be seen from this that, whether it is the performance of floating point and integer operations or the communication performance of sets, the extra overhead after the introduction of virtualization is within 10%.

Due to the lack of analysis of OpenStack's built-in algorithm, this paper elaborates the proposed multiobjective optimization algorithm based on the ant colony algorithm in detail. Due to the limitations of the laboratory environment, it cannot meet the requirements of the experiment. Therefore, we choose to simulate the algorithm on the mainstream cloud simulation platform CloudSim to verify the effectiveness of the algorithm proposed in this chapter. In order to comprehensively test the performance differences between high-performance cloud platforms and physical clusters, this paper designs the following experiments from different aspects. Start two virtual machines on each physical node and set the parameters as shown in Table 5.

Table 5: Algorithm parameter settings.

Algorithm parameters	Value
Pheromone heuristic factor	$\alpha = 1$
Visibility heuristic	$\beta = 4$
Pheromone volatility coefficient	$\sigma = 0.4$
Number of iterations per trial	$R_{\max} = 30$
Number of ants	$\delta = 25$
Initial pheromone intensity	$\mu_{ij}(0) = 3$

It is the percentage of incidents resolved within the agreed SLA time, which checks the performance of the IT service desk against the service level agreement with the user. The comparison of user SLA violation rate, power consumption, and OpenStack virtualization test of multi-objective ant colony improvement algorithm scheduling strategy is shown in Figure 5.

It can be seen from Figure 5 that compared with the previous two groups of experiments, the virtual machine dynamic scheduling algorithm proposed with the multi-objective ant colony improved algorithm has improved about 20% in terms of power consumption and user SLA violation rate. It proves the rationality and effectiveness of the designed virtual machine dynamic migration scheme.

4.2. Performance Test of Innovation and Entrepreneurship Education and Training System in Colleges and Universities.

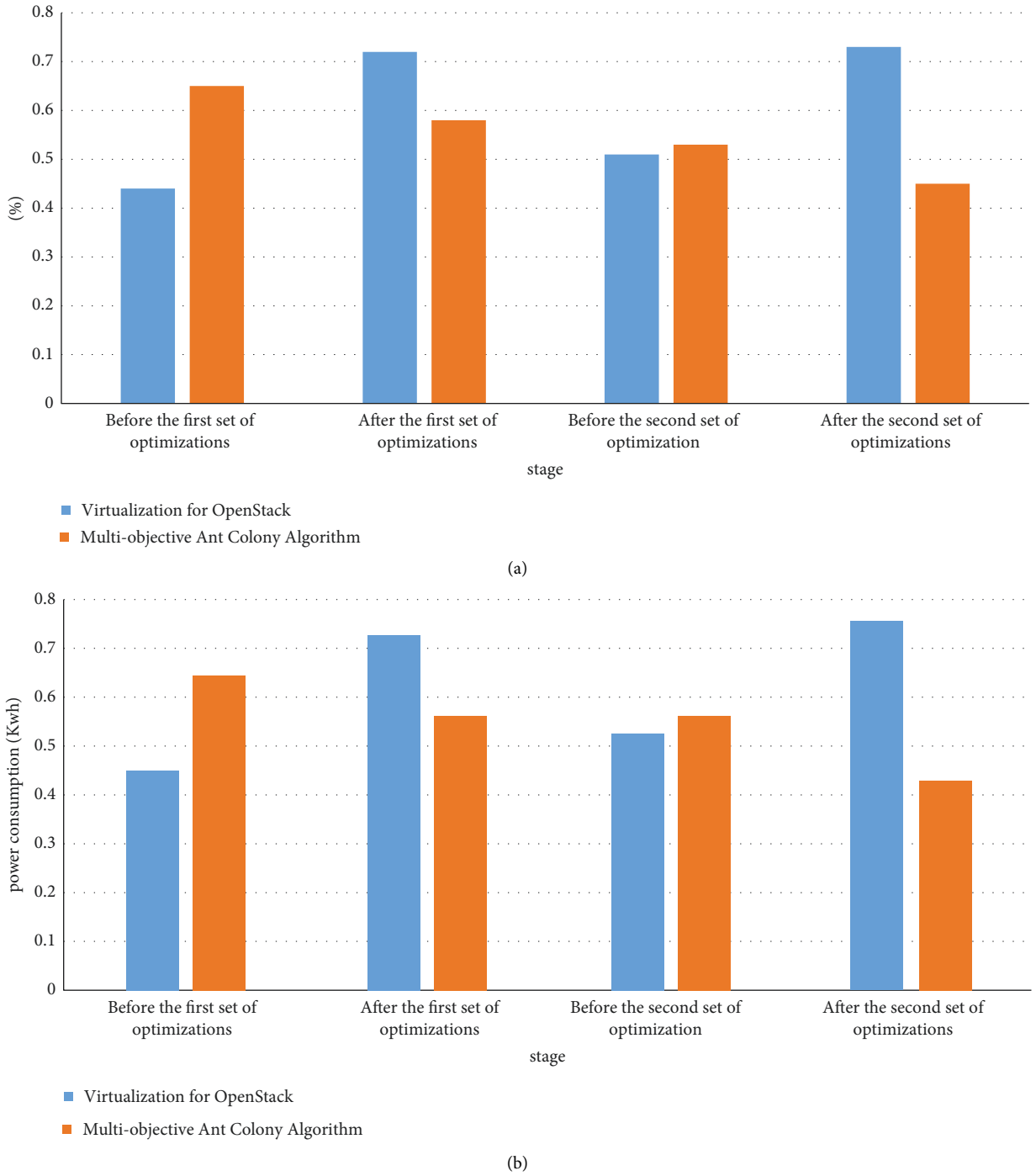

Figure 5: Comparison of server user SLA violation rate and power consumption.

According to the analysis of the functional requirements of the innovation and entrepreneurship education and training system in colleges and universities, this paper focuses on testing the performance stability of each node under high system load. The test environment is offline. This paper simulates 10 physical machines, 5 meta virtual machines, and one object storage device in a cloud data center.

This article uses MDTest to test the system IOPS of the file system, increases the pressure on the server node through open/close/stat operations on the file, and runs a large number of client programs at the same time to cause access pressure to the server. Through eight hours of uninterrupted operation, the throughput and load of the cluster are counted during this article. The simulated data center configuration table is shown in Table 6.

The five MDSs are named as MDS1–5, respectively. Taking MDS1 as a reference, their performance ratio is 1 : 3: 17 : 1.5 : 4, the number of consecutive times is $N = 2$, and the trigger threshold θ is set to 0.2. This article records the load

Table 6: Cloud data center parameters.

Cloud data center parameters	Value
Number of physical machines	
Physical computer CPU computing power	{1000, 2000, 3000}
Physical machine memory (GB)	4
Physical machine bandwidth (Gbps)	Physical disk capacity (GB)
1024	Number of virtual machines
300	{0.25, 0.5, 0.75, 1}
Virtual machine CPU computing power (GHZ)	512
Virtual machine memory (M)	200
Virtual machine disk capacity (GB)	250
Virtual machine bandwidth (Mbps)	Value

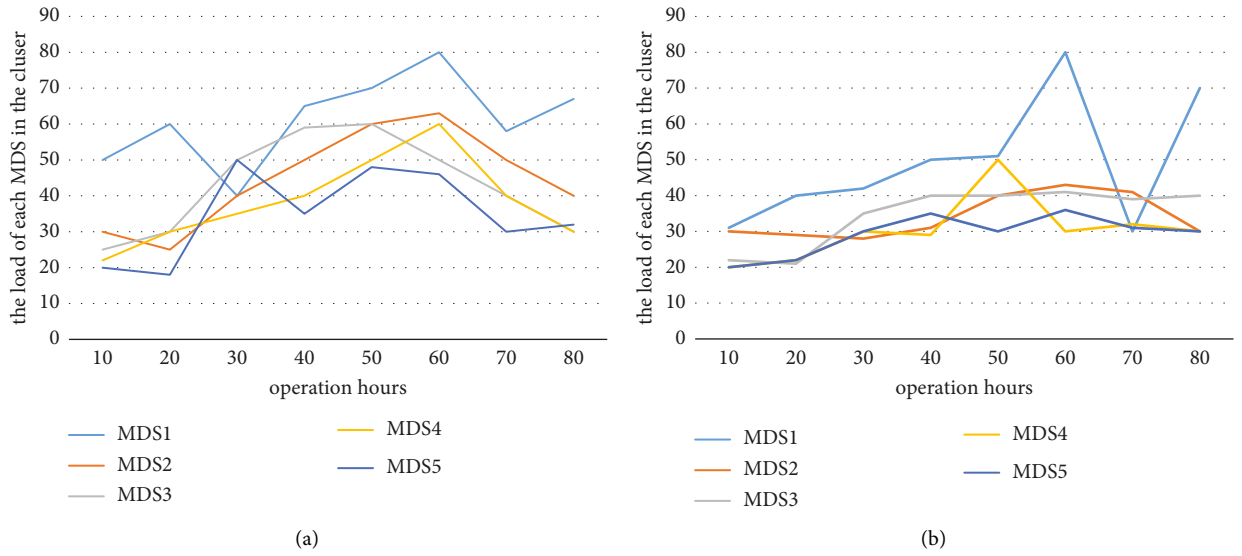

Figure 6: The load of each server when it is turned on and not turned on.

value of the load balancing strategy without and with the load balancing policy turned on, respectively. The calculation formula of the system load balancing degree is

$$P\ D = \sqrt{\sum_{i=1}^{n} (Li - \overline{L})^2}. \tag{11}$$

PD is the load balance degree value, and Li is the load value of node *i*. In the experiment, a test script was written to record the system load value, including the central processing unit and the internal storage device.

After the system runs for 8 hours, the average processor load is calculated according to the load balance calculation formula. During the 8-hour test, load data were recorded every hour. Finally, this paper calculates the processor and memory utilization. Assuming that the processor accounts for 60% of the performance and the corresponding memory accounts for 40% of the performance, the cluster pressure is gradually increased. It obtains the load of the cluster when the load balancing strategy is not enabled and enabled, respectively, as shown in Figure 6.

As can be seen from Figure 6, the load of each server is not related to a certain extent, and the load is generally high; even the utilization rate of MDS5 exceeds 80% for a period of time. This also shows that, during this period, the access performance of the node will also decrease. It can be seen that the situation without load balancing is very unstable and the load is high. It can be seen from the experimental results that the overall load has decreased and the load of each MDS is relatively close, and the system has achieved the expected expectations.

5. Discussion

In order to study the dynamic scheduling mechanism of virtual machines, this paper firstly analyzes the built-in scheduling strategy of OpenStack and points out the shortcomings of the scheduling strategy. Aiming at this deficiency, this paper builds a model and sets constraints. Finally, through the simulation comparison on the cloud simulation platform, this paper verifies the effectiveness of the algorithm in improving the load balancing of the system, reducing the violation rate of users, and reducing the power consumption of the system. Through the relevant design of innovation and entrepreneurship education courses, users can not only enjoy resources at a low cost but also reduce entrepreneurial risks.

This paper conducts an indepth research and analysis on the mechanism of OpenStack virtual machine resource scheduling through cloud computing virtual machine technology. It also uses the improved ant colony algorithm to optimize the initial deployment of the virtual machine. This paper designs a dynamic migration multiobjective optimization algorithm for virtual machines. The algorithm can achieve a balance among multiple conflicting goals, such as resource balance, user SLA violation rate, and system power consumption, so as to achieve optimal system performance.

6. Conclusion

This paper uses the cloud platform to optimize the innovation and entrepreneurship education and training system in colleges and universities. This paper uses OpenStack virtual technology, improved ant colony algorithm, and OpenStack ubiquitous learning environment system to improve the cloud platform of innovation and entrepreneurship training education system. This paper tests the system of OpenStack's ubiquitous learning environment. According to the test results of the system load, the system can still achieve the expected effect. Regarding system stability, there is still room for improvement.

Data Availability

No data were used to support this study.

Conflicts of Interest

The authors declare that they have no conflicts of interest.

References

[1] N. Nelmiawati, N. C. Kushardianto, A. H. Tohari, and D. E. HasibuanKurniawan, "Rancang bangun lab komputer virtual berbasis cloud computing menggunakan openstack pada jaringan terpusat," *Journal Of Applied Informatics And Computing*, vol. 2, no. 1, pp. 11–17, 2018.

[2] Z. Yan-Ting, "Implementation of open cloud network computing platform based on open Stack," *IPPTA: Quarterly Journal of Indian Pulp and Paper Technical - A*, vol. 30, no. 6, pp. 675–682, 2018.

[3] N. Radwan, M. B. Abdelhalim, and A. AbdelRaouf, "Implement 3D video call using cloud computing infrastructure-ScienceDirect," *Ain Shams Engineering Journal*, vol. 11, no. 2, pp. 363–375, 2020.

[4] B. Albert, T. G. Roberts, and A. Harder, "Social capital of faculty within Haiti's agricultural education and training system," *Journal of International Agricultural and Extension Education*, vol. 25, no. 2, pp. 29–42, 2018.

[5] A. Singh, S. Sharma, and J. Singh, "Mathematical modelling for reducing the sensing of redundant information in WSNs based on biologically inspired techniques," *Journal of Intelligent and Fuzzy Systems*, vol. 34, no. 3, pp. 1–11, 2019.

[6] A. Awad, R. Salem, H. Salem, and M. Abdelkader, Salam, A swarm intelligence-based approach for dynamic data replication in a cloud environment," *International Journal of Intelligent Engineering and Systems*, vol. 14, no. 2, pp. 271–284, 2021.

[7] G. Yi, Z. Feng, T. Mei, P. Li, W. Jin, and S. Chen, "Multi-AGVs path planning based on improved ant colony algorithm," *The Journal of Supercomputing*, vol. 75, no. 9, pp. 5898–5913, 2019.

[8] T. Gotou, "Report on visit to Japan coast guard academy — learning its education and training system," *Marine Engineering*, vol. 53, no. 1, p. 156, 2018.

[9] M. S. Metawea, "The role of financial institutions in supporting entrepreneurial success: case of Egypt," *American Journal of Business and Operations Research*, vol. 1, no. 1, pp. 36–51, 2020.

[10] L. S. Ruban, "Comparative analysis of the Russian and Western education and scientific-training system," *RUDN Journal of Sociology*, vol. 20, no. 2, pp. 416–429, 2020.

[11] K. Y. Chau, K. M. Y. Law, and Y. M. Tang, "Impact of self-directed learning and educational technology readiness on synchronous E-learning," *Journal of Organizational and End User Computing*, vol. 33, no. 6, pp. 1–20, 2021.

[12] C. A. Tavera Romero, J. H. Ortiz, O. I. Khalaf, and W. M. Montilla-Ortega, "Software architecture for planning educational scenarios by applying an agile methodology," *International Journal of Emerging Technologies in Learning (iJET)*, vol. 16, no. 8, p. 132, 2021.

[13] S. Nakagawa, H. Takahashi, Y. Konishi et al., "Specialty training system and postgraduate education in Japan," *Igaku Kyoiku/Medical Education(Japan)*, vol. 49, no. 1, pp. 47–54, 2018.

[14] J. Y. Hong, H. Ko, L. Mesicek, and M. B. Song, "Cultural intelligence as education contents: exploring the pedagogical aspects of effective functioning in higher education," *Concurrency and Computation Practice and Experience*, vol. 33, no. 4, 2019.

[15] S. R. Haasler, "The German system of vocational education and training: challenges of gender, academisation and the integration of low-achieving youth," *Transfer: European Review of Labour and Research*, vol. 26, no. 1, pp. 57–71, 2020.

[16] V. H. Nguyen, V. B. H. Nguyen, T. M. H. Vu, and H. T. M. Hue, "Vietnamese education system and teacher training: focusing on science education," *Asia-Pacific Science Education*, vol. 6, no. 1, pp. 179–206, 2020.

[17] A. Z. Kuenzer, "Sistema educacional e a formação de trabalhadores: a desqualificação do Ensino Médio Flexível," *Ciência & Saúde Coletiva*, vol. 25, no. 1, pp. 57–66, 2020.

[18] Y. M. Ko, "Law education and lawyers' training system in Australia," *Chungnam Law Review*, vol. 30, no. 2, pp. 151–189, 2019.

[19] I. S. Seo, "The influence of education and training and performance-based pay system on innovation," *Journal of Business Education*, vol. 33, no. 3, pp. 27–52, 2019.

[20] K. Shin and S. Lee, "Developing an XR based hyper-realistic counter-terrorism, education, training, and evaluation system," *Jouranl of Information and Security*, vol. 20, no. 5, pp. 65–74, 2020.

[21] S. P. Koshova and A. H. Krut, "Characteristics of stress resistance and adaptive potential in the training of doctors in the system of postgraduate education," *Wiadomosci Lekarskie*, vol. 71, no. 7, pp. 1379–1384, 2018.

[22] D. Y. Kparib, S. B. Twum, and D. K. Boah, "A min-max strategy to aid decision making in a Bi-objective discrete optimization problem using an improved ant colony algorithm," *American Journal of Operations Research*, vol. 09, no. 4, pp. 161–174, 2019.

[23] L. Ren, M. Huang, and H. Wang, "Integrated optimization of multi-objective routing problem in fourth party logistics,"

Complex Systems and Complexity Science, vol. 15, no. 1, pp. 62–67, 2018.

[24] R. Beuran, C. Pham, D. Tang, and Y. ChinenTanShinoda, "Cybersecurity education and training support system: CyRIS," *IEICE - Transactions on Info and Systems*, vol. E101.D, no. 3, pp. 740–749, 2018.

[25] M. Ajmal and T. Kumar, "Inculcating learners' listening motivation in English language teaching: a case study of British education and training system," *Arab World English Journal*, vol. 11, no. 4, pp. 409–425, 2020.

[26] G. Zhang, H. Wang, W. Zhao, and P. GuanLi, "Application of improved multi-objective ant colony optimization algorithm in ship weather routing," *Journal of Ocean University of China*, vol. 20, no. 1, pp. 45–55, 2021.

Hindawi
Scientific Programming
Volume 2022, Article ID 2770333, 13 pages
https://doi.org/10.1155/2022/2770333

Research Article

Sports Smart Data Writing Based on New-Type Semiconductor Nonvolatile Storage Mode

Shengpeng Guo

Accounting Department, Qingdao Vocational and Technical College of Hotel Management, Qingdao 266000, Shandong, China

Correspondence should be addressed to Shengpeng Guo; guoshengpeng@qchm.edu.cn

Received 8 June 2022; Revised 2 August 2022; Accepted 11 August 2022; Published 30 August 2022

Academic Editor: Juan Vicente Capella Hernandez

The development of smart sports has just taken a new chapter. Based on the digital transformation in all aspects today, the data content of smart sports with a large number of branches is huge. However, the current storage system, an external storage disk, has not adapted to the computer's increasingly high requirements for IO performance; DRAM- and SRAM-based memory and cache also face power consumption and capacity expansion problems; the storage system on the overall performance of the computer system constraints is increasingly prominent. Based on the data storage of smart sports for digital transformation, this article proposes a smart for the writing of sports data; a better cache method has been explored under the new semiconductor nonvolatile cache mode. The experimental results in this article show that by comparing single-value and dual-value STT-RAM (spin-torque transfer RAM) caches, the three-valued cache with hierarchical mapping of page swap design has a significant improvement in IPC performance under each test load, compared with single-value STT-RAM caches. Compared with the value type, the average performance has increased by 16%; the overall energy consumption including memory has been reduced by an average of 12.3%.

1. Introduction

Smart sport has developed from no one's attention to today's hobbies and specialties. In the past, there were very few colleges and universities that developed smart sports. Nowadays, they can also get better results in international competitions. Well-developed colleges and universities are now equipped with majors. The current smart sports activities are all to improve their competitive ability. The intelligent sports training system is an organizational system established to achieve common goals. Competitiveness is one of the main manifestations of the evolution of the training system. With the rapid development of computer technology, people have begun to combine virtual reality with other technologies to realize scientific exercise-assisted training to eliminate traditional exercise training that relies solely on experience. This approach to the digital transformation of sports has created a large amount of sports intelligence data, which places higher demands on storage systems. This time, under the new semiconductor nonvolatile storage mode of data writing under the digitization of sports intelligence, the cache method is explored, and the problems that arise are designed to solve.

Although the smart sports derived from the current development are still in the initial stage of development, with the popularization and rapid rise of network data nowadays, more and more people have begun to have relevant understanding of it. In this digitalization process, at the moment when it is full, the digital network can help people understand it more accurately. This time, based on the latest semiconductor nonvolatile cache, the system for writing smart sports data is explored in order to find a better cache method. The experimental results show that not only the ternary cache further reduces the total energy consumption, but also the average energy consumption of the cache part is reduced by 22%, and the average energy consumption of the cache part is only increased by 9% compared with the single value type.

Based on the data writing process of smart sports, the various difficulties encountered in the storage process have been studied by many scholars at home and abroad on today's hot nonvolatile storage. Kazuo provides a nonvolatile

semiconductor memory device with an improved layout structure to achieve low power consumption, high speed, and miniaturization. The flash memory of the present invention includes a memory array formed of NAND-type strings. The memory array includes multiple global blocks, one global block includes multiple blocks, and one block includes multiple NAND-type strings. Multiple local bit lines are shared by each of multiple blocks in a global block, multiple global bit lines are shared by multiple global blocks, and connecting elements selectively connect one global bit line to n. The local bit line has been included. When performing a read operation and a programming operation, a global bit line is shared by n local bit lines [1]. Yadav introduced in detail the synthesis of cobalt quantum dots (Co QDs) down to 1-2 nm and its application in nonvolatile memory (NVM) devices. The process of colloid synthesis is very simple, and a wide QD size can be controlled. The reduced colloidal Co QD is used in NVM device manufacturing. The colloidally synthesized Co QD is spin-coated on silicon dioxide wafers for the manufacture of floating gate NVM devices. The capacitance voltage (C-V) and capacitance time (C-t) measurements of the manufactured NVM device indicate the low voltage operation of the device. Scanning voltages as low as 1.2–4 V result in a flat-band voltage shift of 0.35–1.5 V, which is utilized in low operating voltage and low-power NVM applications [2]. Among various materials, polyoxometalate (POM) molecules have attracted considerable attention due to their use as new data storage nodes for nonvolatile memories. Here, Chen outlines the latest developments in POM development for nonvolatile memory. It also summarizes the general background knowledge of the structure and nature of POM. Finally, the challenges and prospects of POM's application in memory are discussed [3]. Huang proposed two nonvolatile storage elements (NVSEs) based on racetrack memory for multicontext FPGAs. One is NVSE (type-1) based on variable speed, which has the advantages of high density and low power consumption. The other is the address-based NVSE (type-2), which has the advantages of fast context switching and low context switching capability. The general placement and routing simulation results show that the eight-context FPGA based on type-1 NVSE reduces the area, critical path delay, and power consumption of the SRAM-based eight-context FPGA by 68.1%, 22.8%, and 13%, respectively [4]. Micheloni introduced flash memory cards. Flash memory cards [mainly in a secure digital (SD) form factor] have almost completely replaced photographic film, and USB keys have wiped out floppy disks. Recently, due to the huge trade-off between cost and performance (i.e., write/read speed), NAND flash memory technology has begun to struggle with hard disk drives (HDDs) in the form of solid-state drives (SSDs) [5]. Li showed a golf-assisted training system that uses artificial intelligence and big data to realize the transformation from experience-based sports training methods to human movement analysis methods [6]. Explore how to use sensor data and visual artificial intelligence (AI) to improve the performance of athletes on the U.S. Olympic diving team. Desmond M described in detail how Microsoft cooperates with coaches, athletes, and project leaders to deploy sensor platforms and smartphone applications so that coaches can capture and analyze data related to athletes' diving [7]. The research of the above scholars all requires very professional knowledge and in-depth understanding, as well as the operation ability of the most important experimental equipment, which are not easy to master at the same time. The experiment is too difficult and too complicated.

The innovation of this article lies in the data collection and writing of smart sports, which has not been developed more comprehensively. During this period of data fullness, the system design based on the nonvolatile cache under the large cache of smart sports data and the problems encountered in the process of writing data were solved.

2. Smart Sports Based on New Semiconductor Nonvolatile Cache

2.1. The Concept of Smart Sports. "Smart sports" is a comprehensive category given to it by everyone [8]. Smart sports programs are different from the equipment and venues required for traditional sports programs. In smart sports, the requirements for venues and equipment are not as high as in traditional sports [9].

Competitive sports are the basic characteristics of their sport, that is, confrontational, competitive, and athletic. There are many classifications and projects of smart sports [10], but the core must be confrontation and competition. Players' skills and tactics must be improved through rigorous training and long-term practice [11]. Another essential and indispensable feature of smart sports is fair, just, and open competition under the guarantee of competition rules. From the above understanding, we can interpret the concept of smart sports as a sport activity based on rules in which student athletes use logical thinking, rich imagination, keen insight, and unique creativity. Unlike physical sports, smart sports include chess, go, and chess. Smart sports can exercise and improve participants' thinking ability, judgment, reaction ability, attention, and perseverance, thus promoting their overall development [12].

2.2. The Basic Situation of Smart Sports Projects in My Country's Colleges and Universities. According to the survey results, it can be seen that only 7 colleges and universities established 7 smart sports high-level sports teams from 1990 to 2001. Since 2001, the number of colleges and universities that have established smart sports high-level sports teams has increased by leaps and bounds to 35, an increase of 400% over the previous 10 years. 10 years ago, smart sports projects were only valued in culturally and economically developed areas and some well-known universities, and they were launched earlier, such as Peking University, Tsinghua University, Beijing Normal University, Fudan University, Shanghai University of Finance and Economics, and Nankai University, that is, intelligent sports high-level sports team. In other regions, due to the influence of policies, funds, culture, and other aspects, no high-level smart sports teams have been established in various universities. In the next year, due to the "three chess" entering campuses and the

development of "sunshine sports," smart sports projects are only available. Gradually aroused the attention of education authorities at all levels [8]. Ten years later, until now, 35 colleges and universities have established smart sports high-level sports teams.

2.3. The Reasons Affecting the Development of Smart Sports Projects in Ordinary Colleges and Universities

2.3.1. The Influence of the Importance of the Leadership. The development and promotion of smart sports in Chinese colleges and universities is late, and the popularity rate is low. Some education departments and school leaders do not know enough about smart sports and think there is a big gap with the traditional sports programs in schools, so they do not support the opening of smart sports programs. In addition, in recent years, colleges and universities have compressed their expenses and streamlined their staff and institutions. This also directly affects the development of smart sports. The survey shows that the main factor affecting the development of smart sports programs in colleges and universities is the lack of teachers, but the main factor affecting the lack of teachers is directly related to the importance and attitude of leaders [13].

2.3.2. The Influence of the Policy Support of the Competent Authority. After 2001, due to the implementation of related smart sports activities, smart sports began to gradually develop in domestic universities. High-level sports teams, student associations, and more and more smart sports courses have been set up in international competitions. Good results have been obtained many times, and it can be concluded that the development of smart sports in colleges and universities is inseparable from the support of relevant policies.

2.3.3. The Influence of the Factors of Teachers. Due to the insufficient popularity of smart sports, there is a shortage of teachers. Most colleges and universities have not engaged in the study of smart sports. Although there are also colleges and universities that have developed smart sports, most of these college teachers do not have professional systematic training. They are self-study and work together with students. This is to a certain extent. The above has a serious impact on the development of smart sports in colleges and universities.

2.3.4. There Are No Related Teaching Materials and Syllabus Factors. According to investigations, colleges and universities that currently offer smart sports have yet to have unified teaching materials. This has seriously affected the learning of university teachers, professors, and students [14].

2.3.5. The Influence of Venue Equipment on Teaching Facilities. Only some early colleges and universities with smart sports have special training rooms and equipment for students, while most other colleges and universities are responsible for contacting venues and raising funds to purchase equipment to carry out activities [15].

3. Nonvolatile Cache of Ternary STT-Ram Based on Smart Sports Data Writing

Spin moment transfer magnetic memory (STT-RAM), compared to conventional memory, has the advantages of higher integration, lower static power consumption, and nonvolatility. Designing a high-density STT-RAM memory is the basis for building a large-capacity nonvolatile cache. This section mainly introduces the single-level cell (SLC) vs MLC structure, storage mechanism, and multivalue STT-RAM memory cell structure [16], briefly analyzes the shortcomings of the existing memory structure and ways to increase the storage density, and derives research on ternary STT-RAM with higher storage density.

3.1. STT-RAM Technical Analysis

3.1.1. Single-Value STT-RAM Technology. Single-value STT-RAM memory cell is a basic structure that constitutes STT-RAM memory [17]. As shown in Figure 1, a typical STT-RAM memory cell includes a magnetic tunnel junction and a transistor, which is called a single-transistor single-junction (MTJ for short) structure.

STT-RAM uses MTJ as a data storage element and expresses data through two or more resistance states of MTJ. For the most basic MTJ composition, it includes two magnet layers, which are separated by an oxide layer (MgO) [18]. The magnetization direction of one of the magnet layers is fixed and is called the reference layer; the magnetization direction of the other layer can be changed according to the current flowing, and it is called the free layer. When the magnetization direction of the free layer changes, the resistance of the MTJ also changes accordingly. The magnetization of the free layer is determined by the magnitude and direction of the current (polarization current) flowing through the MTJ. The polarization current must exceed a certain minimum value to be effective, which is also called the critical switching current [19]. In the single-value STT-RAM, each memory cell only needs to store 1 bit of data, so it is called the single-value type. The single-value MTJ contains only one free layer and one reference layer, and the magnetization direction of the free layer is two relative to the magnetization direction of the reference layer: the same direction and the reverse direction [20]. When no voltage is applied to the MTJ, it maintains its original magnetization state, so it belongs to nonvolatile memory; that is, it can maintain data without applying voltage [21].

The drain of the transistor shown in Figure 1(a) is connected to the MTJ reference layer, the other end is used as a source connection selection line, and the gate is connected to the word line; the free layer of MTJ is connected to the bit line (BL). The operation of the STT-RAM storage unit includes three ways of writing "0," writing "1," and reading. When writing "0" to STT-RAM, the source terminal is connected to a positive voltage, and the bit line terminal is

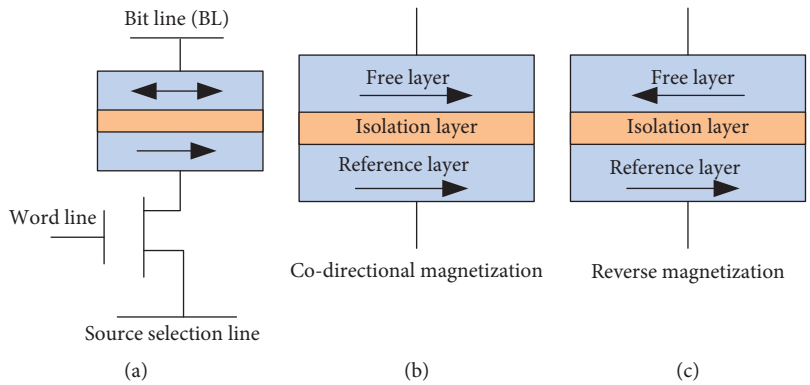

Figure 1: STT-RAM memory cell structure and resistance state.

grounded to generate a current flowing from the source to the bit line terminal, and the current must be greater than the critical switching current, so that the free layer occurs at the same time as the reference layer The state after magnetization is shown in Figure 1(b). On the contrary, when writing a "1," a positive voltage is connected to the bit line terminal and the source terminal is grounded to generate a current flowing from the bit line terminal to the source, and the current must be greater than the critical switching current, so that the free layer is opposite to the reference layer. The state after magnetization is shown in Figure 1(c). When reading, a low voltage is connected between the source and the bit line end to generate a tiny current, and the current sensor is used to determine the current to read the data [22]. The voltage during reading is less than the voltage during writing, so that the current generated is less than the critical switching current and will not cause the magnetization of the free layer [23].

3.1.2. Multivalue STT-RAM Technology. In order to improve the storage density, the STT-RAM memory cell structure of the multivalue storage mode has also been extensively studied, and two dual-value STT-RAM architectures have been proposed. Multivalued STT-RAM can store 2 bit or more data bits in a storage unit, effectively improving storage density. In a dual-value STT-RAM, an MTJ can have four resistance states, and correspondingly, there are four magnetization states in the free layer. Dual-value STT-RAM mainly includes two typical architectures: series dual-value type and parallel dual-value type [24]. As shown in Figure 2, the MTJ of the serial dual-value STT-RAM is formed by connecting two single-value MTJs of different sizes in series. The MTJ of the parallel dual-value STT-RAM is formed by stacking two free layers of different sizes side by side on the reference layer.

The design idea of MLC is to store more data through more resistance states in a memory cell. However, the research on MLC STT-RAM is currently mainly based on dual-value type, and the density increase is limited. The dual-value type STT-RAM memory cell can store 2 bits of information, and by implementing the three-value type, the STT-RAM memory cell stores 3 bits of information in eight resistance states, which can further increase the storage density. In this regard, this article aims at designing a large-capacity cache and conducts research on the design of ternary STT-RAM.

3.2. Serial-Parallel Hybrid Architecture Ternary STT-RAM Storage Design Based on Smart Sports Data Writing. Based on the series resistance based on the series dual-value STT-RAM architecture, it is not feasible [25], so this research takes the series-parallel hybrid type as the research theme. The series-parallel hybrid architecture three-valued MTJ consists of a parallel dual-value MTJ and a single-value MTJ in series. As shown in Figure 3, the architecture includes three free layers.

This time, H_{1G} and $H_{1\,D}$, H_{2G} and H_{2G}, and H_{3G} and $H_{3\,D}$ are used to represent the high and low resistance values of the soft zone, hard zone, and top zone, corresponding to their respective data bits. The resistance of the serial-parallel hybrid architecture ternary MTJ can be expressed as

$$H = H_1 \| H_2 + H_3. \tag{1}$$

Each ternary STT-RAM cell can store 3 bit data: from left to right are the most significant bit, the middle effective bit, and the least significant bit [26], which correspond to the three locations, respectively.

To obtain the best results by maximizing the distance between adjacent resistors, to confirm the parameters of MTJ, it is necessary to determine the relationship between the area of the soft zone and the hard zone, and use it to determine the area of the top layer.

There are four resistance combinations for the soft zone and the hard zone:

$$\begin{aligned} H_{00} &= H_{2D} \| H_{1D}, \\ H_{01} &= H_{2D} \| H_{1G}, \\ H_{10} &= H_{2G} \| H_{1D}, \\ H_{11} &= H_{2G} \| H_{1G}. \end{aligned} \tag{2}$$

Use β to represent the proportion of the parallel area occupied by the hard zone. Because the soft zone shares the

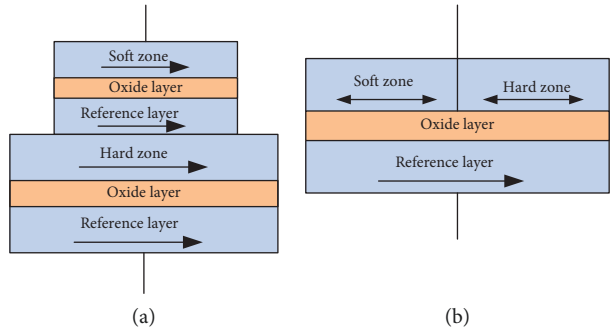

Figure 2: Dual-value STT-RAM memory cell structure in series and parallel.

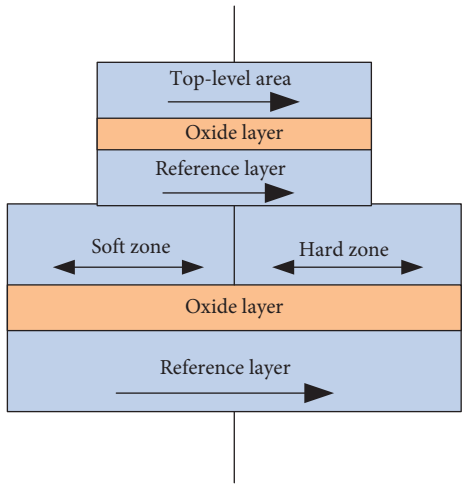

Figure 3: Hybrid ternary STT-RAM memory cell structure.

same reference layer, it has the same resistance area product. Therefore,

$$\begin{aligned} H_{2D} \times \beta &= H_{1D} \times (1-\beta) = H_{00}, \\ H_{2G} \times \beta &= H_{1G} \times (1-\beta) = H_{11}, \\ H_{11} &= [1 + \mathrm{TMR}]H_{00} = 2H_{00}. \end{aligned} \tag{3}$$

Therefore,

$$\begin{aligned} H_{1D} &= \frac{H_{00}}{1-\beta}, \\ H_{1G} &= \frac{H_{11}}{1-\beta}, \\ H_{2D} &= \frac{H_{00}}{\beta}, \\ H_{2G} &= \frac{H_{11}}{\beta}. \end{aligned} \tag{4}$$

The size of β determines the area ratio of the hard zone and the soft zone, which in turn determines the respective resistance values. The selection of β must satisfy the condition that the four resistances such as $H_{00} \sim H_{11}$ are different from each other in order to express the four data.

H_{00} and H_{11} are the distance between the boundary resistance of the dual-valued single tube and the adjacent resistance. The solution of β is

$$\begin{aligned} H_{11} - H_{10} &= \frac{2(1-\beta)}{2-\beta} H_{00}, \\ H_{10} - H_{01} &= \frac{4\beta - 2}{(2-\beta)(1+\beta)} H_{00}, \\ H_{01} - H_{10} &= \frac{1-\beta}{1+\beta} H_{00}. \end{aligned} \tag{5}$$

Taking the derivation of β separately, we can find

$$\begin{aligned} \frac{b(H_{11} - H_{10})}{b\beta} &< 0, \\ \frac{b(H_{01} - H_{00})}{b\beta} &< 0, \\ \frac{b(H_{10} - H_{01})}{b\beta} &> 0. \end{aligned} \tag{6}$$

With the growth of $\beta \in (0.5, 1)$, in the scenario of $H_{01} - H_{00} = H_{10} - H_{01}$, the minimum distance of the four resistances reaches the maximum, and $\beta = 0.6277$ is obtained, and the parallel hard zone area $(\beta/(1-\beta)) = 1.686$ times can be obtained.

The area product RA, the resistance value, and the critical conversion current are extracted. According to the area ratio relationship, the various parameters of the series-parallel hybrid architecture ternary MTJ can be calculated, as shown in Table 1.

3.2.1. Sports Smart High-Energy Writing Drive Capability. Using the traditional STT-RAM drive circuit design, with a larger size NMOS to provide sufficient write drive current for the ternary MTJ affects the overall storage density improvement. NMOS is an N-type metal oxide semiconductor, and transistors with this structure are called NMOS

Table 1: STT-RAM structure and height resistance value.

Parallel MTJ area	40×90	Top MTJ area	50×100
Soft-area ratio	0.36	Hard zone area ratio	0.64
"1" current		"0" current	
I_{CS}	47.3	I_{CS}	32.5
I_{CT}	56.6	I_{CT}	66.5
I_{CH}	79.9	I_{CH}	82
Resistance			
H_{1D}	11	H_{1G}	22
H_{2D}	6.5	H_{2G}	14
H_{3D}	5	H_{3G}	10
The resistance of the eight states of the ternary MTJ			
0000	9	001	10
010	12	011	13
100	15	101	15
110	16	111	19

transistors. In order to ensure the storage density of the ternary STT-RAM, it is necessary to enhance its write drive capability without increasing the size of the NMOS. Based on this, the reverse stacking method is used to reduce the current demand when writing data.

The drive strength of NMOS is affected by the voltage drop $I \times H$ caused by MTJ. When writing "0," the current direction is from the gate to the source, Φ_{VV} is applied to the bit line and the gate, and the source is grounded:

$$\begin{aligned} \Phi_{GS} &= \Phi_{DD}, \\ \Phi_{DS} &= \Phi_{DD} - I \times H, \end{aligned} \tag{7}$$

where I represents the magnitude of the current flowing through the MTJ and H is the resistance value of the MTJ. Φ_{GS} is the voltage drop between the gate and the source of the NMOS tube, and Φ_{DS} is the voltage drop between the drain and the source.

For the size of M Y N NMOS, its drive current IDS can be expressed as

$$I_{DS} = K \cdot \frac{M}{N} \cdot \left[\left(\Phi_{GS} - \Phi_{TH}\right) \cdot \Phi_{DS} - \frac{\Phi_{DS}^2}{2}\right. . \tag{8}$$

It can be seen from the above equation that for single-value STT-RAM, the voltage was drop of $I \times H$ in Φ_{DS} when writing "1" results in a decrease in the driving capability of NMOS. Moreover, writing "1" makes the magnetization direction of the free layer opposite to that of the reference layer, which requires higher magnetization current intensity, so the operation of writing "1" is also more difficult.

According to equation (8), calculate the write current that NMOS of different sizes can provide. As shown in the result of Figure 4(a), when the size of the NMOS is increased to 10F, the current demand for writing a "1" in the hard location still cannot be met. At the same time, the size of the NMOS has offset the storage density of the ternary type, reducing it to the level of the single-value type. As shown in Figure 4(b), it can be found that the drive current I_{DS} before the reverse connection is lower than the critical switching current $I_{CH}\,(0 > 1)$, which is not enough to support the flip of the hard area; after the reverse connection, the writing current of the hard area increases, which is higher than the critical switching current $I_{CH}\,(0 > 1)$.

By analogy, in addition to the reverse connection of the MTJ of the hard zone, the MTJ corresponding to the top zone can also be reversed. Therefore, consider the reverse connection of the two MTJs in the three-value type. There are three types of reverse connection methods, as shown in Figure 5:

The hard zone is the operation that requires the most write current. When writing to the hard zone, the corresponding resistance value that causes the voltage drop under different reverse connections of the three-valued MTJ is shown in Table 2.

Substituting the values in Table 2 into the equation, the drive current in the hard zone as shown in Figure 6 is obtained.

After reversing the MTJ, when writing a "1" to the hard zone, the voltage drop of VGS is first eliminated; secondly, the soft zone and hard zone caused by a short period of time are flipped to "0," turning the high-impedance state to low-impedance state, reducing the pressure drop Φ_{DS} of $I \times H$. Inverting MTJ balances the drive capability of NMOS when writing "1" and writing "0." Although it reduces the current drive ability when writing "0," it increases the ability to write "1" and eliminates writing "1," worst bias condition. In this article, the BR flip mode is selected as a compromise. Under the condition of a width of 4.5 F, the current required for writing a "0" to the hard zone bit can be met, while the current required for writing a "1" can be met.

3.2.2. Reading Logic of Storage Unit Based on Smart Sports Data Writing. The reading method of dual-value nonvolatile memory has a mature design. The reading method of this research is based on a binary tree reading method that is relatively balanced in all aspects. The read logic is shown in Figure 7.

Each three-valued STT-RAM memory cell stores 1 bit more data than the dual-valued STT-RAM memory cell. Therefore, on the basis of the dual-valued type reading, by adding a level of reading logic, the third bit of data read out.

Therefore, the three-valued reading logic can refer to the dual-valued reading method to read the upper two bits first, and then we only need to add a set of judgment thresholds Φ_{ref4}, Φ_{ref5}, Φ_{ref6}, and Φ_{ref7} to meet the requirements of the equation. Read the lowest bit:

$$\begin{cases} \Phi_{bl000} < \Phi_{\text{rdf4}} < \Phi_{bl001} \\ \Phi_{bl010} < \Phi_{\text{ref5}} < \Phi_{bl011} \\ \Phi_{bl100} < \Phi_{\text{ref6}} < \Phi_{bl101} \\ \Phi_{bl110} < \Phi_{\text{ref6}} < \Phi_{bl111}. \end{cases} \tag{9}$$

Based on the above analysis, the read logic of the ternary STT-RAM as shown in Figure 8 is obtained.

3.3. Writing Logic Design of STT-RAM Storage Unit Based on Smart Sports Data Writing. The ternary STT-RAM memory cell can use three magnetization layers to store 3 bit data. Due to the inconsistency of the characteristic parameters

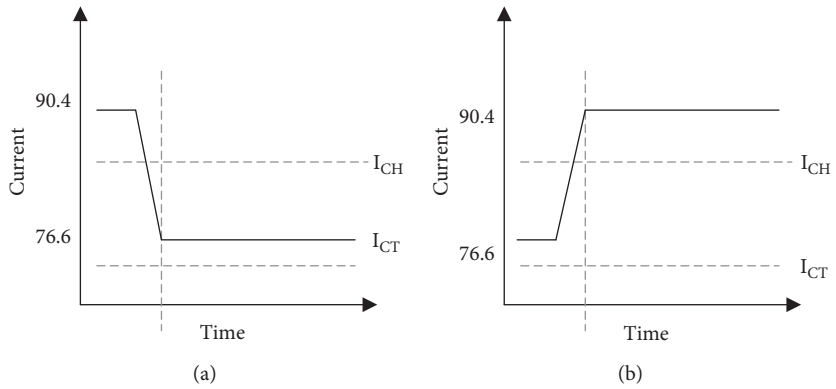

Figure 4: Hard bit current of the top layer in two modes. (a) Standard mode and (b) reverse mode.

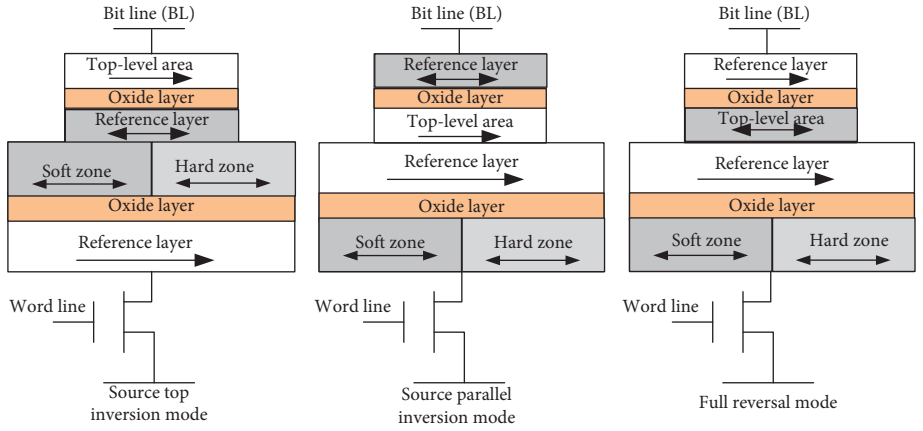

Figure 5: Three reversal modes of ternary type.

Table 2: The corresponding voltage drop resistance of the four modes.

		Standard	TR	PR	BR
1	Φ_{GS} corresponds to voltage drop resistance	19	14	0	0
	Φ_{DS} corresponds to voltage drop resistance	18	14	14	18
0	Φ_{CS} corresponds to voltage drop resistance	0	0	13	10
	Φ_{DS} corresponds to voltage drop resistance	9	15	13	10

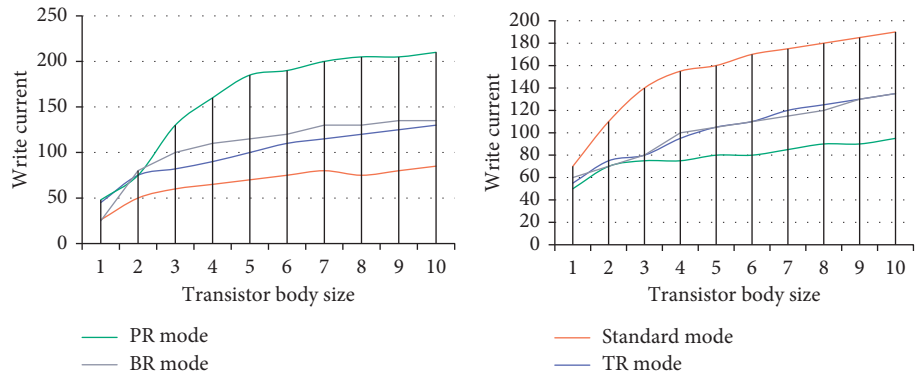

Figure 6: Two groups of transistor body hard zone write currents in four modes.

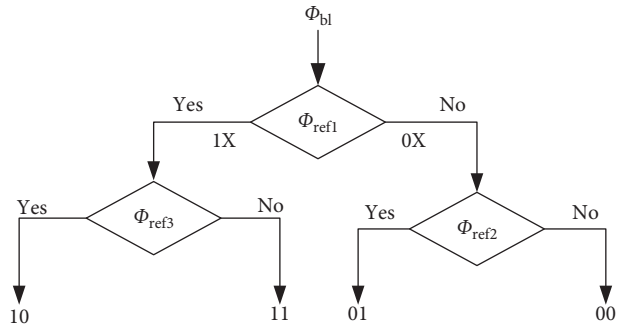

Figure 7: Dual-valued read logic.

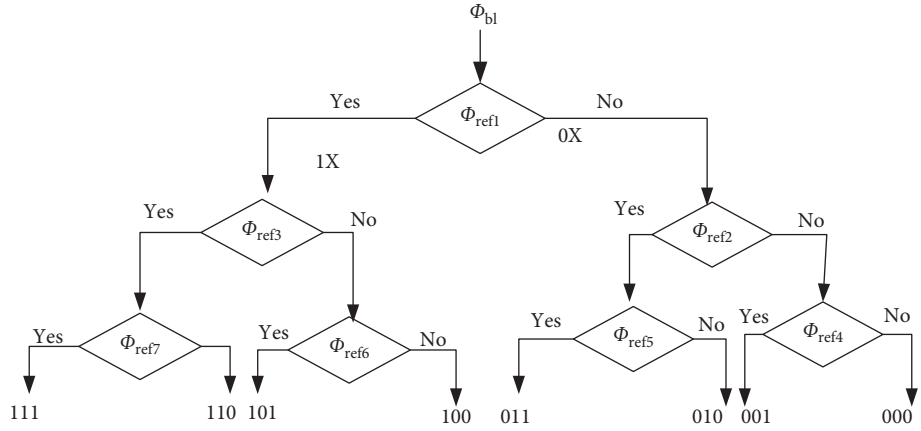

Figure 8: Three-valued read logic.

such as the physical size of the three magnetization layers, and the inconsistent influence of each other during the writing process, the characteristics of the writing delay and energy consumption of the three data bits are inconsistent. It is necessary to design write logic for this problem to achieve fast data write and reduce write energy consumption.

The characteristics of the direct writing method: The reason why the direct writing method is used is that the current required for writing in the hard zone, the top zone, and the soft zone is different, and the applied current is caused to other magnetized layers when the target-free layer is magnetized. The role is different. Among them, the soft zone can use a small current to switch the magnetization direction, while the hard zone requires a relatively large current, and the write current in the top zone is in the middle.

For an STT-RAM memory containing X-bit data, assuming that random data is written, that is, the data satisfies the Gaussian distribution, then eight types of data for each memory cell are written with equal probability. Use Q_0, Q_1, and Q_2 to represent the execution probabilities of the magnetization operation of the three storage cells—hard location, top location, and soft location, respectively; then,

$$Q_i = \begin{cases} \frac{1}{3}, & i = 0, \\ \frac{1}{3}, & i = 1, \\ \frac{1}{3}, & i = 2. \end{cases} \tag{10}$$

If the memory is written once, the total number of write operations is $M = N$, and the number of each write operation is

$$M_i = Q_i \times M,$$

$$M_i = \begin{cases} \frac{1}{3}N, & i = 0, \\ \frac{1}{3}N, & i = 1, \\ \frac{1}{3}N, & i = 2. \end{cases} \tag{11}$$

The direct writing method is simple. For all three-valued STT-RAM memory cells, you only need to write each bit of data in the order of hard location, top location, and soft location, but the write delay is the sum of the write delays of the three free layers, which causes the write performance to be much lower than the single-value and dual-value STT-RAM, and the number of write operations required to fill a memory is large, resulting in high write energy consumption.

(1) Writing method based on the classification of the written value: According to the different magnetization operations actually required for different writing data, the writing process is designed separately, and the writing operation is reduced in a targeted manner to reduce the writing delay and energy consumption.

There are three types of magnetization for the dual-value writing method: (1) soft zone reversal (ST), applying a small current IS, only realizing the magnetization reversal of the soft zone; (2) top zone reversal (TT), where the strong current makes the soft zone and the top zone magnetized in the same direction; (3) hard zone flip (HT), applying a large current IH, magnetizes the hard zone, the soft zone, and the top zone in the same direction, which is shown in Figure 9.

For an STT-RAM memory containing X-bit data, assuming that random data is written, that is, the data satisfies the Gaussian distribution, then eight types of data for each memory cell are written with equal probability. After adopting the write method based on the written value classification, the probabilities of ST, TT, and HT operations are as follows: for an STT-RAM memory containing X-bit data, assuming that random data is written, that is, the data satisfies the Gaussian distribution, then eight types of data for each memory cell are written with equal probability. After adopting the write method based on the written value classification, the probabilities of ST, TT, and HT operations are

$$Q_i = \begin{cases} \frac{1}{4}, & i = 0, \\ \frac{1}{4}, & i = 1, \\ \frac{1}{4}, & i = 2. \end{cases} \tag{12}$$

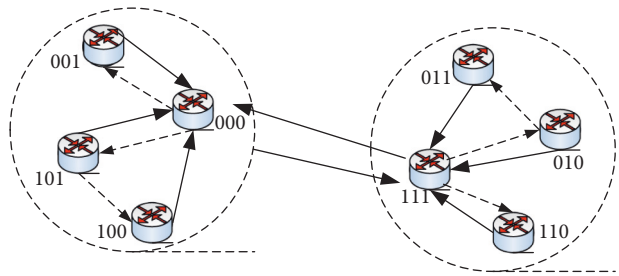

Figure 9: Three-valued state transition logic based on write value.

If the memory is written to once, the total number of write operations is $M = (2/3)N$, and the number of each write operation is

$$M_i = \begin{cases} \frac{1}{6}N, & i = 0, \\ \frac{1}{6}N, & i = 1, \\ \frac{1}{6}N, & i = 2. \end{cases} \tag{13}$$

Compared with the direct write method, the ST and TT operations are reduced by 50%, and the HT operation is not reduced. Although this writing method based on the written value reduces a lot of operations compared with the direct writing method, since the current state of the MTJ is not considered, there are still redundant operations.

(2) The writing method based on the difference between the written value and the current value: in order to further reduce the operation of redundant writing, this writing classification method based on the difference between the written value and the current value is compared with the above two methods. The current value of MTJ. The specific process is as follows: first insert a read operation, read the state of the MTJ, and then perform the corresponding magnetization operation according to the current value of the MTJ and the difference of the target value to be written. Then, the write operation is simplified to the type shown in Figure 10, and some HT operations are replaced by TT and ST operations.

For an STT-RAM memory containing N-bit data, assuming that random data is written, that is, the data satisfies the Gaussian distribution, then eight types of data of each memory cell are written with equal probability. After adopting the writing method based on the difference between the written value

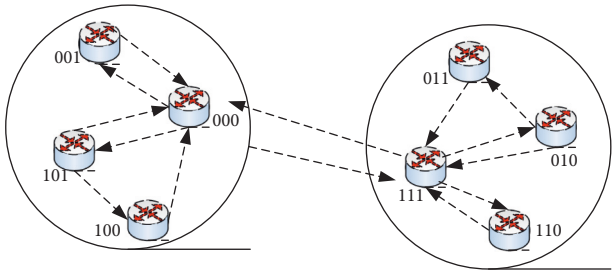

Figure 10: Three-valued state transition based on current and target.

and the current value, the probabilities of ST, TT, and HT operations are

$$Q_i = \begin{cases} \frac{1}{3}, & i = 0, \\ \frac{1}{3}, & i = 1, \\ \frac{1}{3}, & i = 2. \end{cases} \tag{14}$$

Write a full memory; the total number of write operations is $M = (7/12)N$, and the number of write operations is

$$M_i = \begin{cases} \frac{7}{36}N, & i = 0, \\ \frac{7}{36}N, & i = 1, \\ \frac{7}{36}N, & i = 2. \end{cases} \tag{15}$$

For random write operations, the operation probability of ST, TT, and HT is all 1/3, and the total number of writes is reduced by 12.5%. Compared with the write operation, the read operation has shorter latency and lower energy consumption. Although the read operation requires three comparisons and judgments to obtain the final data, for most write operations, it still brings considerable writing increased entry speed.

3.4. Cache Design of Ternary STT-RAM with Serial-Parallel Hybrid Architecture Based on Smart Sports Data Writing

(1) Cache hierarchical mapping method: The simple and direct method to build a three-valued STT-RAM cache is to refer to the direct mapping method of the two-value STT-RAM cache; that is, every N/3 STT-RAM storage unit constitutes a group N-bit memory page. Each page has 1/3 of the data stored in the soft location, hard location, and top location, and all pages have the same characteristics.

For ternary STT-RAM, the write speed of the soft zone is the fastest, and the speed of the hard zone is the slowest. Because there are soft zone, top zone, and hard zone in the same page, the read and write performance of the page depends on the slowest the performance of the data bits.

(2) Different levels of page exchange methods: according to the read and write operation methods and page types, page exchange operations can be divided into four types: read page exchange between related pages and write page exchange between related pages; and read page between unrelated pages exchange and write page exchange between unrelated pages; the four exchange operations have different costs.

Analyzing the four page operations of the table, it can be seen that the selection of the threshold determines the exchange timing and frequency, and ultimately affects the exchange cost and overall performance. In terms of swap operation cost, since the read delay of soft zone pages is higher than that of hard zone pages, and the write delay of soft zone pages is lower than hard zone pages, so in the read page swap, the swap operation cost of soft zone pages is less than that of the hard page. In terms of overall performance after the swap, the benefits of soft page operations are higher than those of hard page operations; in addition, in page write operations, the benefits of hard pages are higher than top-level pages. Therefore, the swap threshold of soft zone pages can be designed to be lower than that of hard zone pages to increase the swap probability of soft zone pages; similarly, the swap threshold of hard zone pages can be designed to be lower than that of top zone pages to increase hard zone pages.

(3) Selection of page swap threshold: the swap threshold is used to control the frequency of page swap. When the number of page reads and writes reaches the threshold, the page swap operation is started. If the threshold is set too low, the page swaps are too frequent, which will cause performance degradation due to the operating cost of page swaps; if the threshold is set too high, the page swap frequency is too low, and the hit rate of pages in the soft zone and the top zone cannot be fully improved. Therefore, it is necessary to comprehensively select the threshold for the impact of the exchange threshold on the page exchange operation cost and hits.

As shown in Figure 11 (1), when the threshold is adjusted from 4 to 64, the overall IPC performance is improved. This is because increasing the exchange threshold reduces the number of exchanges and reduces the impact of exchange operation costs on read and write delays. However, when the threshold is further increased, the frequency and number of exchanges are effectively reduced, which further affects the reduction of the page hit rate. Figure 11 (2) shows the change in cache energy consumption when the threshold is adjusted from 4 to 64. Combining the two effects, it is obvious that the

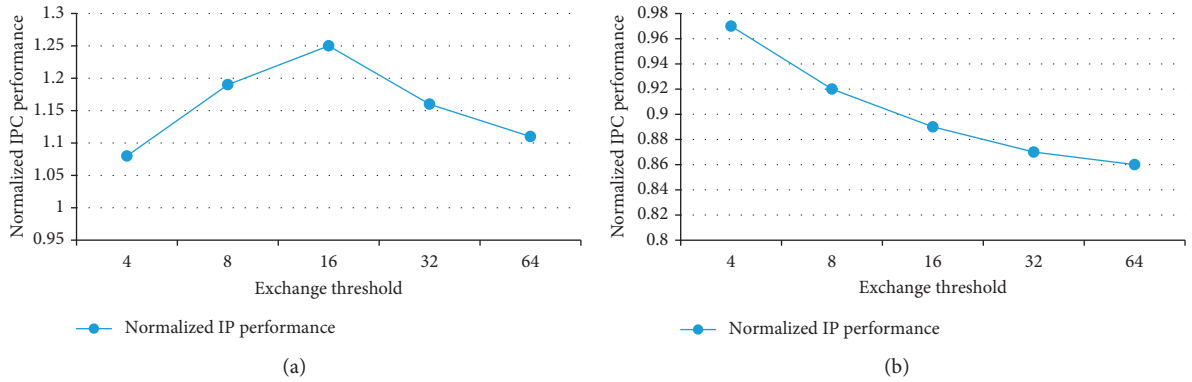

Figure 11: Normalized performance and exchange threshold: (a) IP performance and exchange threshold. (b) Energy consumption and exchange threshold.

energy consumption of TPC is decreasing, from 0.97 to 0.86. 16 is selected as the read page exchange threshold, and 32 is selected as the write page exchange threshold.

4. Simulation Experiment and Result Analysis

The design goal of the ternary STT-RAM cache is to improve the number of instructions per cycle (IPC) performance and reduce energy consumption, so this article uses IPC and energy consumption as evaluation indicators. The page exchange method is of great significance to the improvement of IPC and energy consumption. In order to evaluate the effect of the page exchange method, this article also compares and simulates the page hit rate before and after the page exchange method is adopted. Through the comparison simulation experiment of ternary and single-value and dual-value STT-RAM caches, the rationality of the ternary STT-RAM design of the series-parallel hybrid architecture is verified through comparative simulation experiments of ternary and single-value and dual-value STT-RAM cache configurations, benchmark suites, warm-up stages, and modeling technology nodes.

In the actual simulation experiment, in order to reduce the recording error, the experiment was repeated three times, and the average value of the three test results was taken as the simulation result.

4.1. Page Hit Rate Based on Smart Sports Data Writing. The hit rate is the most direct way to analyze the efficiency of the page swap algorithm. This section discusses the impact of different levels of page swap designs on the page hit rate. The experimental results of the hit rate of the top area page and soft-area page of the three-valued STT-RAM cache after adopting this design are shown in Figure 12.

As shown in Figure 12, after adopting the page swap mapping algorithm, for various benchmark tests, the hit rate exceeded 50%, the average write hit rate (avg) of soft zone pages reached 71%, and the average read hit rate of pages in the top zone (avg) has also reached 63%. Among them, the

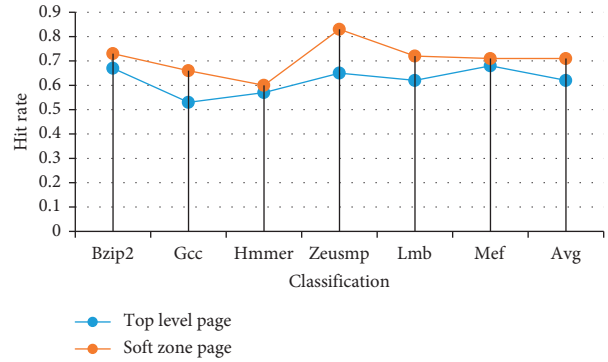

Figure 12: The page hit rate of the top and soft layers of the page swap algorithm.

soft zone page write hit rate corresponding to the zeusmp test benchmark has increased to 83%, which is a very obvious improvement.

4.2. IPC Performance of Nonvolatile Storage Based on Smart Sports Data Writing. The simulation result of IPC performance is shown in Figure 13.

It can be seen from Figure 13 that for different types of test benchmarks, the performance of the three-valued STT-RAM cache that only uses hierarchical page mapping is improved and some are reduced compared with the single-valued type. In benchmark tests that are sensitive to cache capacity, such as bzip2 and mcf, because the three-value type has a larger capacity, it reduces the probability of missing and reduces the cost of missing. The direct mapping method improves performance in some test loads; while in GCC, HMER, LBM, and other benchmarks, these tests are more sensitive to cache access latency; on the contrary, due to the high read and write latency of hard page pages, cache performance has declined. For the gcc test, compared to the single-value type, the performance drops by 10%; compared to the dual-value type, the performance drops by 5%.

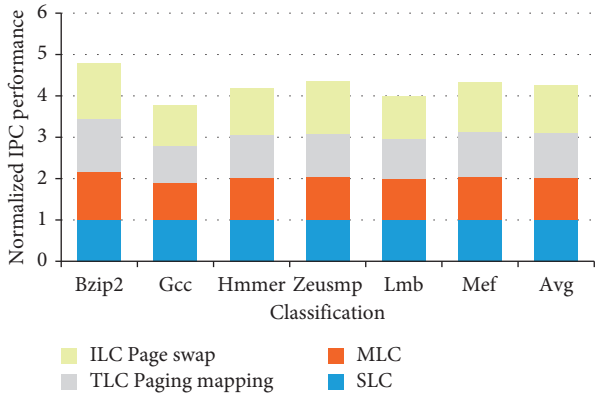

Figure 13: Normalized IPC performance based on single-valued SII-RAM cache.

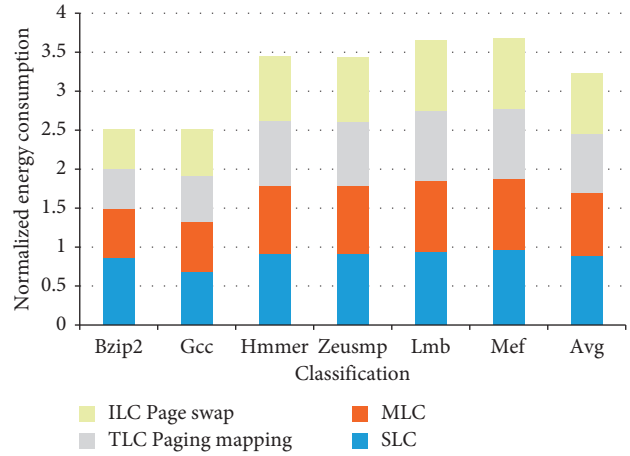

Figure 14: Normalized energy consumption based on the energy consumption of a single-valued cache.

After the combined use of different levels of page mapping, for the bzip2 benchmark test, it has increased by 36% compared to the three-valued type and 15% compared with the two-valued type. The gcc test, which has the lowest improvement rate, has also been improved by 7% and 15%, respectively. The average performance of the ternary cache is 16% higher than that of the SLC type and 12.6% higher than that of the dual-value type.

4.3. Energy Consumption of Nonvolatile Storage Based on Smart Sports Data Writing. The discussion of energy consumption includes two parts: STT-RAM cache energy consumption and memory energy consumption. The simulation results are shown in Figure 14. Each bar graph represents the sum of memory and cache energy consumption. The upper part (slashed area) represents the energy consumption of the cache, and the lower part represents the energy consumption of the memory.

It can be seen from Figure 14 that, for the energy consumption of the cache part, the single-valued cache has the lowest energy consumption. This is because the read and write operations of the single-valued STT-RAM only require one operation to complete. The read disturb rate in STT-MRAM cache is reduced by selective tag comparison; however, the total energy consumption of single-valued cache and memory is the highest. This is because the single-valued cache has the smallest capacity and high miss rate, which leads to a large number of memory access operations and increases the energy consumption of the memory part.

Compared with the single-valued type, the energy consumption of the dual-valued type and the three-valued type cache that only uses hierarchical page mapping has increased significantly, because the write operation requires more steps and higher current to complete. Among them, the three-value type has a greater improvement, and the average energy consumption of the cache part of each test has increased by 26%. Because the three-valued cache has the largest capacity and the lowest cache miss rate, the energy consumption of the memory is the lowest, and the total energy consumption of the generated cache and memory is also the lowest. Compared with the single-value and dual-value caches, the average total energy consumption is reduced, respectively. Different levels of page exchange design are used, by reducing the operation of hard positioning, triadic cache.

It not only further reduces the total energy consumption but also reduces the energy consumption of the cache part to be close to that of the single-value cache; compared with before the page swap, the average energy consumption of the cache part has been reduced by 22%, and the average total energy consumption has been reduced (3.9%). Compared with the single-value type, the average energy consumption of the cache part has only increased by 9%, while the average total energy consumption has been reduced by 12.3%.

5. Conclusions

In this article, based on the writing of huge sports data, in order to further explore a better caching method, a three-valued STT-RAM caching method based on page swap design is proposed, and a more excellent test result is achieved; the reason for the increase in the hit rate is that the method in this article transfers the write operations that hit the top-level page and hard-area page to the soft-area page, and transfers the read operation that hits the soft-area page and hard-area page to the top-level page through the page swap method. The reason for the improvement of IPC performance is that different levels of page swaps reduce the access to slow hard pages, and increase the access to the top-level pages with fast read speeds and the soft pages with fast write speeds, making the pages average. The access delay is reduced. From the above results, it can be found that the three-valued STT-RAM cache using the page swap algorithm is compared with the single-valued cache of the same area, while the performance is improved, and the energy consumption is also reduced. It not only exerts the advantages of three-valued capacity, but also utilizes the performance advantages of hierarchical pages through the page swap algorithm, and reduces the write delay and read delay.

Data Availability

Data sharing is not applicable to this article as no datasets were generated or analyzed during this study.

Conflicts of Interest

The author declares that there are no conflicts of interest with any financial organizations regarding the material reported in this manuscript.

References

[1] K. Kazuo, T. Yasushi, and N. Takeshi, "Non-volatile semiconductor memory," *Microprocessing and Microprogramming*, vol. 10, no. 82, pp. 129–138, 2017.

[2] M. Yadav, R. S. R. Velampati, and D. Mandal, "Scaling down of cobalt quantum-dots by colloidal route for non-volatile memory device application," *Micro & Nano Letters*, vol. 14, no. 12, pp. 1274–1277, 2019.

[3] X. Chen, Y. Zhou, V. A. L. Roy, and S. Han, "Evolutionary metal oxide clusters for novel applications:toward high-density data storage in nonvolatile memories," *Advanced Materials*, vol. 30, no. 3, pp. 1703950–1703950.9, 2018.

[4] K. Huang, R. Zhao, and Y. Lian, "Racetrack memory-based nonvolatile storage elements for multicontext FPGAs," *IEEE Transactions on Very Large Scale Integration Systems*, vol. 24, no. 5, pp. 1885–1894, 2016.

[5] R. Micheloni, "Solid-state drive (SSD): A nonvolatile storage system," *Proceedings of the IEEE*, vol. 105, no. 4, pp. 583–588, 2017.

[6] C. Li and J. Cui, "Intelligent sports training system based on artificial intelligence and big data," *Mobile Information Systems*, vol. 2021, no. 1, pp. 1–11, 2021.

[7] M. Desmond, "Sensors in sports:A dive into applied machine learning," *MSDN Magazine*, vol. 33, no. 11, p. 4, 2018.

[8] Z. Zhou, J. Zhou, X. Wang et al., "A metal-insulator-semiconductor non-volatile programmable capacitor based on a HfAlO ferroelectric film," *IEEE Electron Device Letters*, vol. 41, no. 12, pp. 1837–1840, 2020.

[9] H. A. F. Almurib, T. N. Kumar, and F. Lombardi, "Design and evaluation of a memristor-based look-up table for non-volatile field programmable gate arrays," *IET Circuits, Devices and Systems*, vol. 10, no. 4, pp. 292–300, 2016.

[10] M. Kim, K. Beom, H. Lee, C. J. Kang, and T. S. Yoon, "Nonvolatile reversible capacitance changes through filament formation in a floating-gate metal-oxide-semiconductor capacitor with $Ag/CeO_x/Pt/HfO_x/n$-Si structure," *Applied Physics Letters*, vol. 115, no. 7, pp. 072106–072106.5, 2019.

[11] S. W. Kim, I. S. Jung, B. H. Kang et al., "Facile and one-step processible CdSe/ZnS quantum dots and pentacene-based nonvolatile memory device," *Journal of Semiconductor Technology and Science*, vol. 18, no. 2, pp. 180–186, 2018.

[12] C. Xiong, Z. Lu, S. Yin, H. Mou, and X. Zhang, "Magnetic field controlled hybrid semiconductor and resistive switching device for non-volatile memory applications," *AIP Advances*, vol. 9, no. 10, Article ID 105030, 2019.

[13] M. Yano, "Non-volatile semiconductor memory device," *Microprocessing & Microprogramming*, vol. 10, no. 82, pp. 129–138, 2017.

[14] S. Ranjan, B. Sun, G. Zhou, Y. A. Wu, L. Wei, and Y. N. Zhou, "Passive filters for nonvolatile storage based on capacitive-coupled memristive effects in nanolayered organic-inorganic heterojunction devices," *ACS Applied Nano Materials*, vol. 3, no. 6, pp. 5045–5052, 2020.

[15] N. M. Keppetipola, M. Dissanayake, P. Dissanayake et al., "Graphite-type activated carbon from coconut shell:a natural source for eco-friendly non-volatile storage devices," *RSC Advances*, vol. 11, no. 5, pp. 2854–2865, 2021.

[16] D. Zhu, Y. Li, W. Shen, Z. Zhou, L. Liu, and X. Zhang, "Resistive random access memory and its applications in storage and nonvolatile logic," *Journal of Semiconductors*, vol. 38, no. 7, pp. 071002–071030, 2017.

[17] I. Hwang, W. Wang, S. K. Hwang et al., "Multilevel non-volatile data storage utilizing common current hysteresis of networked single walled carbon nanotubes," *Nanoscale*, vol. 8, no. 19, pp. 10273–10281, 2016.

[18] S. Ma, M. Donato, S. K. Lee, D. Brooks, and G. Y. Wei, "Fully-CMOS multi-level embedded non-volatile memory devices with reliable long-term retention for efficient storage of neural network weights," *IEEE Electron Device Letters*, vol. 40, no. 9, pp. 1403–1406, 2019.

[19] M. S. Baarslan and F. Kayaalp, "Sentiment analysis with machine learning methods on social media," *Advances in Distributed Computing and Artificial Intelligence Journal*, vol. 9, no. 3, pp. 5–15, 2021.

[20] W. C. C. Chu, C. Shih, W. Y. Chou, S. I. Ahamed, and P. A. Hsiung, "Artificial intelligence of things in sports science:weight training as an example," *Computer*, vol. 52, no. 11, pp. 52–61, 2019.

[21] J. Wang and H. Qu, "Analysis of regression prediction model of competitive sports based on SVM and artificial intelligence," *Journal of Intelligent and Fuzzy Systems*, vol. 39, no. 4, pp. 5859–5869, 2020.

[22] T. Alexandra, "Emotional intelligence and human resource management:the case of municipal sports organizations," *International Journal of Science and Research*, vol. 6, no. 9, pp. 511–516, 2017.

[23] H. Song, "Artificial intelligence-based design of a management information system for large-scale Chinese sports events," *Agro Food Industry Hi-Tech*, vol. 28, no. 1, pp. 2151–2155, 2017.

[24] M. M. D. Benito, J. F. G. Luján, and A. Trigueros, "Emotional intelligence, perception of autonomy support and relationships in sport," *Cuadernos de Psicología del Deporte*, vol. 18, no. 1, pp. 13–20, 2018.

[25] O. C. Santos, "Training the body:the potential of AIED to support personalized motor skills learning," *International Journal of Artificial Intelligence in Education*, vol. 26, no. 2, pp. 730–755, 2016.

[26] Z. Zhao, X. Liu, and X. She, "Artificial intelligence based tracking model for functional sports training goals in competitive sports," *Journal of Intelligent and Fuzzy Systems*, vol. 40, no. 2, pp. 3347–3359, 2021.

Hindawi
Scientific Programming
Volume 2022, Article ID 4118371, 9 pages
https://doi.org/10.1155/2022/4118371

Research Article

An Improved Data Generalization Model for Real-Time Data Analysis

A Srisaila,[1] **D Rajani**,[2] **M V D N S Madhavi**,[2] **G Jaya Lakshmi**,[1] **K Amarendra**,[3] **and Narasimha Rao Dasari**[4]

[1]*Department of Information Technology, V R Siddhartha Engineering College, Vijayawada, India*
[2]*Department of Mathematics, V R Siddhartha Engineering College, Vijayawada, India*
[3]*Department of Computer Science and Engineering, Koneru Lakshmaiah Education Foundation, Vijayawada, India*
[4]*Department of Electrical Power Engineering, Defence University, College of Engineering, Bishoftu, Ethiopia*

Correspondence should be addressed to Narasimha Rao Dasari; dasari.narasimha@dec.edu.et

Received 26 April 2022; Revised 20 June 2022; Accepted 5 July 2022; Published 9 August 2022

Academic Editor: Juan Vicente Capella Hernandez

This research proposes a maximum likelihood-Weibull distribution (WD) model for the generalized data distribution family. The distribution function of the anticipated maximum likelihood-Weibull distribution is defined where the statistical properties are derived. The data distribution is capable of modelling monotonically decreasing, increasing, and constant hazard rates. The proposed maximum likelihood-Weibull distribution is used for evaluated these parameters. The experimentation is done to evaluate the potential of the maximum likelihood-Weibull distribution estimated. Here, the online available dataset is adopted for computing the anticipated maximum likelihood-Weibull distribution performance. The outcomes show that the anticipated model is well-suited for computation and compared with other distributions as it possesses maximal and least value of some statistical criteria.

1. Introduction

Weibull distribution is a well-known distribution. It helps in observing the failures of various phenomena and components. Over the past few decades, various investigators concentrate on distribution. Alizadeh et al. [1] provide an extensive analysis of offering a number of historical facts, the various forms of this distribution considered by the practitioners, and probable errors and confusions that arise owing to the nonuniqueness. Bagheri et al. [2] perform a comprehensive analysis of distribution. It is the distribution that attains maximal attention. Moreover, Weibull distribution is applied to biological, medical, and earth sciences. Dattner et al. [3] discuss the effectual Weibull-based shape parameter estimation which relies on modified profile likelihood. The reliability analysis with an additive Weibull model based on failure rate function is considered by various approaches. Some consistent approaches are considered for the evaluation of various WD parameters [4, 5]. Assume that X is a random variable with WD with shape parameter α and scale parameter λ, and the probability distribution function (PDF) and cumulative distribution function (CDF) is expressed as follows:

$$f(x) = \frac{\propto}{\lambda} x^{\propto -1} e^{(-x^{\propto}/\lambda)}, x > 0, \propto > 0, \lambda > 0, \tag{1}$$

$$F(x) = 1 - e^{(-x^{\propto}/\lambda, x > 0, \propto > 0, \lambda > 0)}. \tag{2}$$

It is essential to examine the productive estimation of CDF and PDF of Weibull distribution due to its significance over various Weibull distribution applications. There are various estimation approaches like maximal likelihood estimation, uniformly minimal variance unbiased estimation, least square estimation, percentile estimation, and weighted least square estimation [6]. Various investigations are noted that specifically concentrate on other distributions, for

instance, the derive estimator of CDF and PDF of three generalized parameters with Poisson and Exponential distribution; however, its shape parameter is known to be assumed [7]. Some derived estimator of CDF and PDF of generalized parameter (Rayleigh) distribution when all parameters except shape parameter are considered to be known. Nagatsuka et al. [8] evaluate CDF and PDF of the Weibull extension model when all, however, the shape parameters are considered to be known. Some recent works, including exponential Weibull distribution, generalized exponential distribution, and exponential Gumbel distribution, are considered and analyzed [9]. The extension of this work includes the likelihood of the Weibull distribution that is unknown. Some works with CDF and PDF are evaluated and unknown parameters [10].

2. Maximal Likelihood-Weibull Estimator Model

Consider $X_1, \ldots, X_n$ as the random sample acquired for evaluating the Weibull estimator, and the estimator λ describes $\widetilde{\lambda}$ is $\widetilde{\lambda} = n^{-1} \sum_{i=1}^{n} x_i^{\alpha}$. Thus, this work attains the maximal likelihood of CDF and PDF using

$$\widetilde{f}(x) = \frac{\alpha}{\widetilde{\lambda}} x^{\alpha-1} e^{-x^{\alpha}/\lambda}, \tag{3}$$

$$\widetilde{F}(x) = 1 - e^{-x^{\alpha}/\lambda}. \tag{4}$$

The probability density of $T = \sum_{i=1}^{n} x_i^{\alpha}$ is expressed as

$$h^{*}(t) = \frac{t^{n-1} e^{-t/\lambda}}{\Gamma(n)\lambda^{n}}. \tag{5}$$

For $t > 0$ where some elementary algebra, this work attains the PDF of $w = \widetilde{\lambda}$ as follows:

$$g(w) = \frac{n^{n} w^{n-1}}{\Gamma(n)\lambda^{n}} e^{-nw/\lambda}. \tag{6}$$

For $w > 0$, this work computes $E(\widetilde{f}(x)^{r})$ and computes $E(\widetilde{F}(x)^{r})$.

3. Parametric Distribution of Weibull Distribution

The novelty behind Weibull distribution is its competency to examine the failure trends and failure prediction based on the provided dataset. The major advantage relies on its versatility, and it can be applied over smaller dataset samples. The Weibull distribution is shown in various forms [11]. The distribution functions are expressed as follows:

$$F(t) = 1 - \exp\left[-\left(\frac{t-\tau}{\alpha}\right)^{-\beta}\right], t \geq r, \tag{7}$$

$$F(t) = 1 - \exp\left(-\lambda^{\beta}\right), t \geq \tau. \tag{8}$$

The preliminary properties of Weibull distribution are discussed as follows:

$$f(t) = \beta\alpha^{-\beta} (t-\tau)^{\beta-1} \exp\left[-\left(\frac{t-\tau}{\alpha}\right)^{\beta}\right], t \geq \tau, \tag{9}$$

$$f(t) = \beta\lambda (t-\tau)^{\beta-1} \exp\left[-(t-\tau)^{\beta}\right], t \geq \tau. \tag{10}$$

The mode of MLWD is denoted as $t = \alpha(\beta - 1/\beta)^{1/\beta} + \tau \text{for} \beta > 1$ and $\tau = 0 < \beta \leq 1$.

The medium of MLWD is described at $\alpha(\log 2)^{1/\beta} + \tau$.

Consider T specifies the random variable based on the WD parameters [12]. The transformed variables $T' = (T-\tau)/\alpha$ are measured as a standard form. The density function is expressed as follows:

$$f(t) = \beta t^{\beta-1} \exp\left(-t^{\beta}\right), x > 0, \beta > 0. \tag{11}$$

The moment value of T is expressed as follows:

$$\mu_r' = E\left(T'^{r}\right) = \Gamma\left(\frac{r}{\beta} + 1\right), \tag{12}$$

$$Var(T) = \Gamma\left(\frac{2}{\beta} + 1\right) - \left[\Gamma\Gamma\left(\frac{1}{\beta} + 1\right)\right]^{2}. \tag{13}$$

4. Entropy

It is an uncertainty measure that helps in various applications like physics, statistical measure, hydrology, and engineering [13]. Generally, entropy facilitates us to provide proper statements and perform certain evaluations and factors related to pressing issues. It is generally a measure of uncertainty. Here, two diverse entropies are depicted as follows:

$$I_r(\gamma) = \frac{1}{1-\gamma} \log\left(\int g^{\gamma}(x)\, dx\right), \gamma \neq 0, 1. \tag{14}$$

Here, substitute the PDF of the WD in

$$I_r(\gamma) = \frac{1}{1-\gamma}\left[\gamma \log\left(\frac{\alpha \log \alpha}{\alpha - 1}\right) + (\gamma - 1)\log\lambda - \frac{1-\lambda}{\lambda}\log\beta + \log\left(\sum_{k=0}^{\infty} \frac{\gamma\left(1 - 1/\lambda + 1/\gamma^{\lambda}\right)}{k!(\gamma + k)^{\gamma\left(1-1/\lambda+1/\gamma^{\lambda}\right)}}\right)\right]. \tag{15}$$

The Shannon-based entropy model is expressed as

$$H_s = -E_x[\log f(x)]. \tag{16}$$

With PDF, the expression attained is

$$H_s = 1 - \frac{\propto \log \propto}{\propto - 1} - \log\left(\frac{\beta\lambda \log \propto}{\propto - 1}\right) + \frac{\propto}{\propto - 1}\sum_{k=1}^{\infty}\frac{(-\log \propto)\hat{k} + 1}{k!(1+k)}\left(\frac{1}{1+k} - \frac{\lambda - 1}{\lambda}(\varnothing(1) - \log\beta - \log(1+k))\right). \tag{17}$$

When the distribution with provided with maximal entropy distribution when the mean and standard deviation is known for the provided real-time dataset, this makes the sense that the people use the distribution often as it is easier to evaluate the mean and SD of any provided dataset.

5. Maximal Likelihood Evaluator

This section attains the maximal likelihood estimator of various parameter distributions. Consider $\overline{x} = \{x_1, x_2, \ldots, x_n\}$ is a random sample with size n from the provided distribution with PDF [14]. The likelihood function is expressed as

$$l(\theta|\overline{x}, c) = \prod_{i=1}^{n} fX(x_i) = \left(\frac{\log \alpha}{\alpha - 1}\right)^n (\lambda\beta)^n e^{-\beta}\sum_{i=1}^{n} x_i^{\lambda}\alpha\sum_{i=1}^{n}\left(1 - e^{-\beta x_i^{\lambda}}\right)\prod_{i=1}^{n} x_i^{\lambda-1}. \tag{18}$$

The log-likelihood function is expressed as

$$\log \ell = n \log\left(\frac{\log \propto}{\propto - 1}\right) + n \log\beta + n \log\lambda + (\lambda - 1)\sum_{i=1}^{n}\log x_i - \beta\sum_{i=1}^{n} x_i^{\lambda} + \log\alpha\sum_{i=1}^{n}\left(1 - e^{-\beta x_i^{\lambda}}\right). \tag{19}$$

The log-likelihood estimator equations are expressed as

$$\frac{\delta \log l}{\delta\alpha} = \frac{n}{\alpha \log \alpha} - \frac{n}{\alpha - 1} + \frac{\sum_{i=1}^{n}\left(1 - e^{-\beta x_i^{\lambda}}\right)}{\alpha} = 0, \tag{20}$$

$$\frac{\delta \log l}{\delta\beta} = \frac{n}{\beta} - \sum_{i=1}^{n} x_i^{\lambda} + \log\alpha\sum_{i=1}^{n} x_i^{\lambda} e^{-\beta x_i^{\lambda}} = 0, \tag{21}$$

$$\frac{\delta \log l}{\delta\lambda} = \frac{n}{\lambda} + \sum_{i=1}^{n}\log(x_i) - \beta\sum_{i=1}^{n} x_i^{\lambda}\log x_i + \beta \log \alpha\sum_{i=1}^{n} x_i^{\lambda}\log x_i e^{-\beta x_i^{\lambda}} = 0, \tag{22}$$

where the maximal likelihood of α, β, λ is specified by $\widehat{\propto}$, $\widehat{\beta}$, and $\widehat{\lambda}$, respectively, and attained by resolving the previous equations.

6. Applications of Maximal Likelihood Distribution

This section provides three diverse parameters for maximal likelihood distribution towards the real-time data for illustration purposes. It shows the feasibility of the new distribution while modelling the positive data [15]. The empirical hazard function of the provided dataset relies on the total time on the test. The distribution and the scaled transform are expressed as

$$H^{-1}(u) = \int_0^{F^{-1}(u)} S(y)\,dy, 0 < u < 1 \text{ is expressed as } g(u) = H^{-1}\frac{(u)}{H^{-1}}(1). \tag{23}$$

The empirical version of total time on the test is expressed as

$$g_n\left(\frac{r}{n}\right) = H_n^{-1}\frac{(r/n)}{H_n^{-1}(n)} = \frac{\left[\sum_{i=1}^{r} x_{i:n} - (n-r)x_{r:n}\right]}{\sum_{i=1}^{n} x_{i:n}}, \tag{24}$$

where $r = 1, 2, .., n$ and $x_{i:n}, i = 1, 2, \ldots, n,$ specifies the order statistics of various samples. It is convex, and the rate is increasing or decreasing. The maximal WD is considered the best choice for the provided datasets [16]. However, the distribution fits the prevailing parameters of Weibull distributions. The following are the corresponding distributions of Weibull and expressed as in equations (25) to (29).

Generally, the WD model is expressed as

$$F(x) = 1 - \exp\left(-\beta x^{\lambda}\right);\ \beta > 0, \lambda > 0. \tag{25}$$

The modified maximal WD model is expressed as

$$F(x) = 1 - \exp\left(-\beta x^{\lambda} e^{\alpha x}\right); \beta > 0, \lambda > 0, \alpha \in R. \tag{26}$$

The modified WD model based on CDF is expressed as

$$\%\ F(x) = 1 - \exp\left(-\beta x^{\lambda} - \propto x\right), \quad \beta > 0, \lambda > 0, \alpha \geq 0 \text{ with } \beta + \alpha > 0. \tag{27}$$

The exponential WD model based on CDF is expressed as

$$F(x) = 1 - \exp\left(-\beta x^{\lambda}\right); \beta > 0, \lambda > 0, \alpha \geq 0 \text{ with } \beta + \alpha > 0. \tag{28}$$

The extended generalized gamma distribution is expressed as

$$f(x) = \frac{\lambda \alpha^{\alpha} \beta^{\lambda\alpha}}{\Gamma\alpha} x^{\lambda\alpha - 1} \exp\left(-\alpha(\beta x)^{\lambda}\right); \beta > 0, \lambda > 0, \alpha > 0. \tag{29}$$

Here, the formal fitness test is performed to verify the distribution, superior to the real-time dataset. However, it is not fulfilled that the anticipated model offers a superior fit to the other approaches. However, it can offer a better fit [17]. Thus, the likelihood distribution model is utilized as a substitute for the existing well-known distribution such as modified, exponential, and gamma [18]. Here, an online available UCI Machine Learning repository for disease prediction and emotion recognition datasets is considered [19, 20]. The dataset is taken from the online resource known as the Kaggle dataset for disease prediction. The standard error and p value computations are expressed in Tables 1 and 2. Figures 1 and 2 show the standard error comparison for datasets 1 and 2.

7. Weighted Least Square Analysis

Various estimators recommend evaluating the beta parameter distribution. Here, a regression-based estimator of certain unknown parameters is derived. It is used for other distributions [21, 22]. Assume that $X_1, X_2, \ldots, X_n$ is a random sample with n size from the CDF with function $F(.)$ and $X_{(i)}, i = 1, 2, \ldots, n$ specify the sample order in ascending order. The sample size n is expressed as

$$E\left[F\left(X_{(j)}\right)\right] = \frac{j}{n+1}, \tag{30}$$

$$\text{var}\left[F\left(X_{(j)}\right)\right] = \frac{j(n-j+1)}{(n+1)^2(n+2)},$$

$$Cov\left[F\left(X_{(j)}\right), F\left(X_{(l)}\right)\right] = \frac{j(n-l+1)}{(n+1)^2(n+2)}, j < l. \tag{31}$$

With the variance and expectation, two diverse variants of the least squares methods are given as follows.

7.1. Least Square Estimator. The minimal estimator is attained as follows:

$$\sum_{j=1}^{n}\left(F\left(X_{(j)}\right) - \frac{j}{n+1}\right)^2. \tag{32}$$

It is provided based on unknown parameters [23]. Thus, Weibull distribution with least square estimators of λ and $\widetilde{\lambda}_{ls}$ and attained with minimized as

$$\sum_{j=1}^{n}\left(1 - e^{-\propto (X_j)/\lambda} - \frac{j}{n+1}\right)^2. \tag{33}$$

Table 1: Standard error comparison (first dataset).

Distribution	$\widehat{\beta}$	$\widehat{\lambda}$	$\widehat{\alpha}$	−Log (ℓ)	p value
Probability-based MW	0.19478	4.48375	10.864	13.475	0.302
WD	0.05975	5.78079	16.950	15.208	0.107
EW	0.01940	7.28385	0.67130	14.678	0.134
MW	0.00875	2.41125	2.1548	14.357	0.197
EGG	0.60116	7.76260	0.61960	14.590	0.141
Modified WD	0.04072	6.38118	0.03110	14.896	0.215

Table 2: Standard error comparison (second dataset).

Distribution	$\widehat{\beta}$	$\widehat{\lambda}$	$\widehat{\alpha}$	−Log (ℓ)	p value
Probability-based MW	0.09370	1.59035	0.02118	121.35	0.654
W	0.36640	1.32560	—	122.530	0.296
EW	0.57960	1.10133	1.44260	122.160	0.423
MW	0.39116	1.55780	−0.08775	121.720	0.554
EGG	0.50160	1.06534	1.47740	122.231	0.403
Modified WD	0.43133	1.28269	−0.06318	122.513	0.311

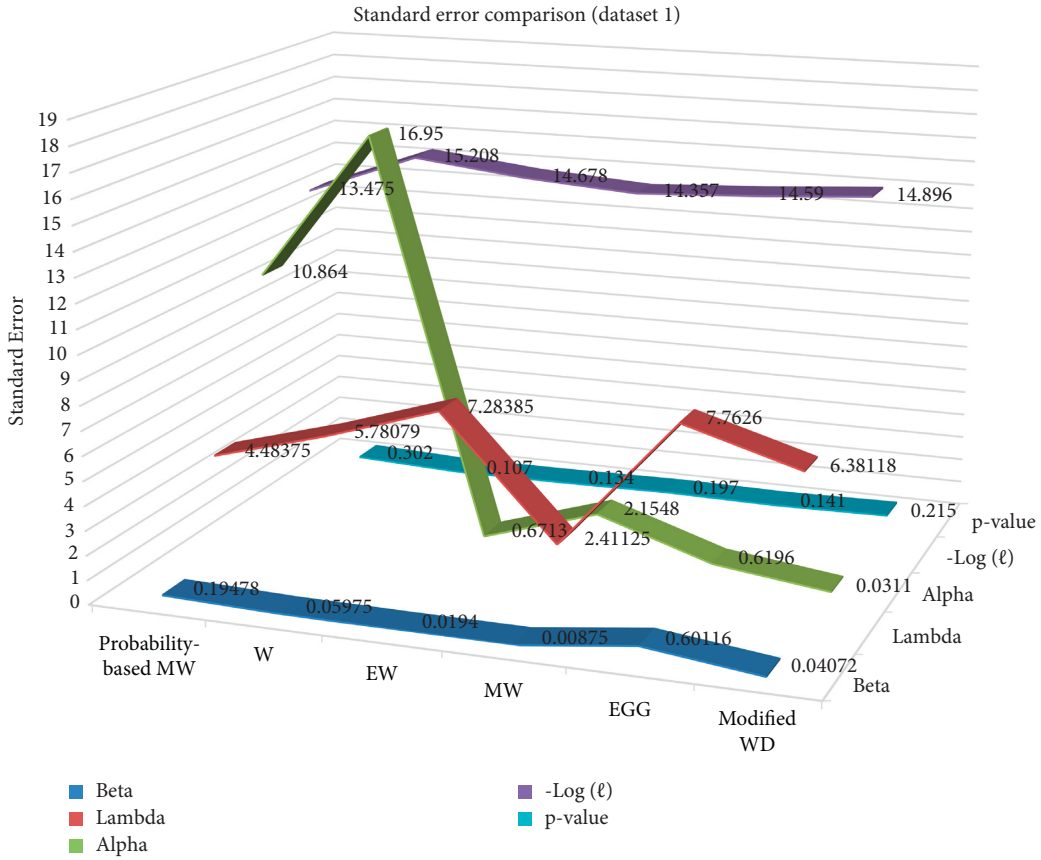

Figure 1: Standard error comparison (dataset 1).

To attain the CDF ad PDF, we use the method for ML estimator. Thus,

$$\widetilde{f}_{ls}(x) = \frac{\alpha}{\widetilde{f}_{ls}} x^{\alpha-1} e^{-x^{\alpha}/\lambda_{ls}}, \tag{34}$$

$$\widetilde{F}_{ls}(x) = 1 - e^{-x^{\alpha}/\lambda_{ls}}. \tag{35}$$

It is complex to predict the expectation and error rate of the estimators with mathematical modelling.

7.2. Weight-Based Least Square Estimators. The minimal weighted least square estimator is expressed as

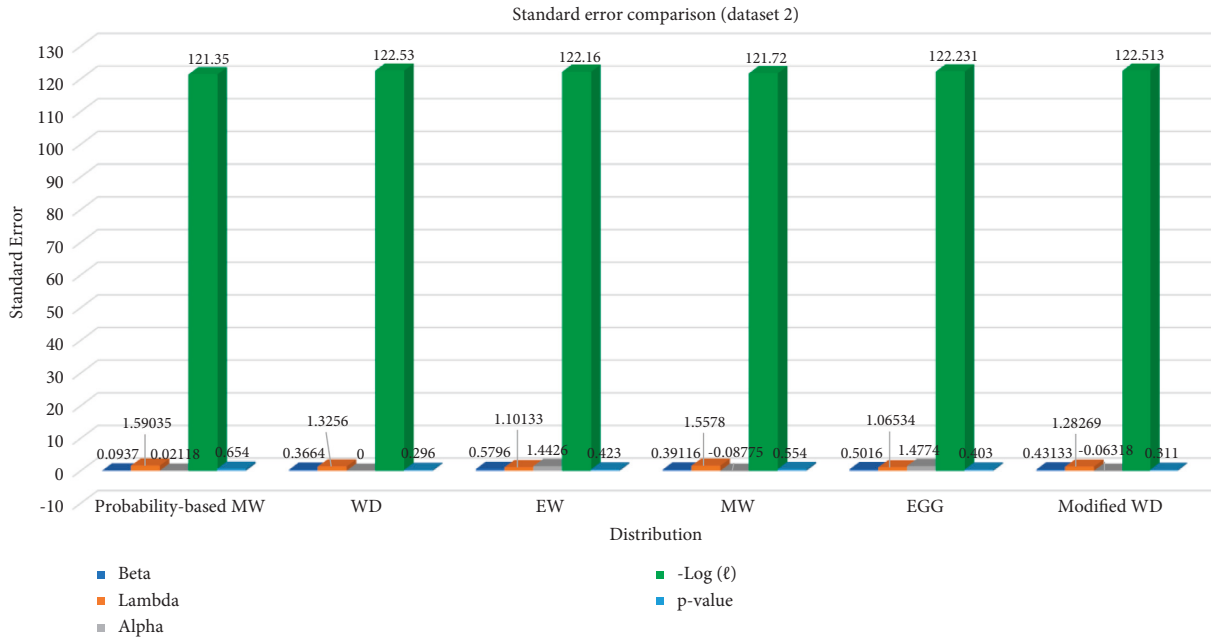

Figure 2: Standard error comparison (dataset 2).

$$\sum_{j=1}^{n} w_j \left(F\left(X_{(j)}\right) - \frac{j}{n+1} \right)^2. \tag{36}$$

Based on all these analyses and unknown parameter estimation, $w_j = 1/Var\,(F(X_{(j)})) = (n+1)^2\,(n+2)/j(n-j+1)$. Thus, Weibull distribution for λ weighted square estimator is attained based on

$$\sum_{j=1}^{n} w_j \left(1 - e^{-\propto_{(Xj)}/\lambda} - \frac{j}{n+1} \right)^2. \tag{37}$$

With the weighted least estimator with CDF and PDF, the estimator is expressed as

$$\tilde{f}_{wls}\,(x) = \frac{\propto}{\tilde{\lambda}} x^{\alpha-1}\, e^{-x^{\alpha}/\tilde{\lambda}_{wls}}, \tag{38}$$

$$\tilde{F}_{wls}\,(x) = 1 - e^{-x^{\propto}/\lambda_{wls}}. \tag{39}$$

It is difficult to predict these weighted estimators' error rates and expectations with the mathematical modelling in Table 3 and also the weighted estimation comparisons are depicted in Figure 3.

8. Failure Data Analysis

There are two diverse kinds of mathematical modelling. The data failure is categorized into two diverse types: incomplete and complete. Concerning complete data, the actual data values realized are well-known for every observation, while in the case of incomplete data, the actual values are not known for certain observations [24]. The negative entropy value represents that something turns to be less disordered and huge energy is used. It may not occur spontaneously, and it reduces the randomness:

(1) Theory-based modelling relies on the well-established component failures, also called physics- or white-box-based models

(2) Empirical modelling: the available data relies on the model construction. It is also known as a black-box and data-dependent model

With empirical modelling, the mathematical formulation is provided based on the preliminary analysis of available data. When the data analysis specifies a higher degree of variability, the model needs to capture the variability. It needs a stochastic and probabilistic way to express the provided dataset. The black-box modelling includes three diverse steps: (1) model assortment; (2) parameter evaluation; and (3) model validation.

To choose various models with the probable model, the investigators need to understand various properties. It is often known as a trial and error model. The goodness fitting test is the key process for choosing the statistical distribution of the observed data's best fits. The larger amount of the Weibull distribution model is known from various literature. The selection of an appropriate model from the WD is based on the probability plots. It also provides the crude evaluation of model parameters. There are various statistical testing processes for model validation.

9. Hypothesis Testing Analysis: Goodness Measure

There is another goodness fit-based model for the empirical distribution function, for instance, the Cramer von Mises test, KS test, chi-square test, and AD test. The goodness measure of the WD model is provided as H_0, and the population is well-suited for WD vs. H_1. There

Table 3: Weighted estimation comparison.

	$\propto$ estimation	λestimation	Log-likelihood
MALE	5.7	16.74	−15.2
PCE	5.4	14.28	−15.4
LSE	7.4	39.64	−18.9
WLSE	7.016	32.139	−17.3

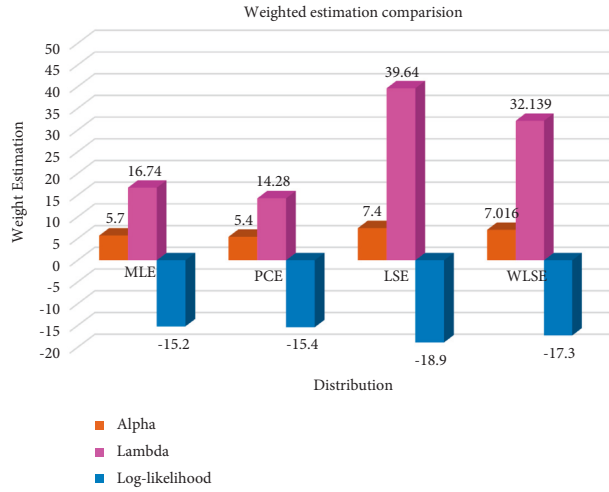

Figure 3: Weighted estimation comparison.

are various extensions like modification and generalization adopted by the WD model. It leads to the rise of model features of the provided empirical dataset, which is not determined by the three parameters of the WD model [25]. The monotonic properties of the Weibull are not capable of capturing the dataset's nature. It leads to failure rate as in Table 4.

Product reliability relies on the development, manufacturing, and design decisions made before the product launch. It influences the failures when the product is provided for launch. The prelaunching stage includes various phases. Some investigations indicate the target value of product reliability [26]. The product reliability is evaluated during the design phase based on the component reliability. Moreover, the enhancement is identified in the upper limit. When the target value is below the provided limit, the design with the components attains the desired target values. The program to enhance the reliability via the fix-test-cycle is done in the development phase [27]. The prototype is tested when the failure is noted, and the cause is examined. Based on these metrics, the design variations are done to handle the predicted failure causes. This process is continued until reliability is attained [28]. The item reliability during manufacturing intends to change from the manufacturing process. The quality control and proper process during the manufacturing phase and the variations are managed.

During the postlaunch stage, the item reliability is reduced due to the deterioration and outcomes from the utilization. The deterioration is influenced by various factors, including the operating condition, environment, and maintenance. The deterioration rate is managed via the prevention maintenance phase. The reliability outcomes with higher maintenance costs for the buyer. Also, it leads to higher warranty costs and outcomes from the rectifying cost within the warranty period. Some products are composed of various components due to the component's failure. The WD model is used to deal with the failure of various components, and the literature is wider. During the development phase, it is essential to use acceleration testing to hasten the process of component failures. The enhancement in reliability during the development phase is modelled in various ways. The Weibull intensity model helps design the failure rate improvements as a development time function. The breakthroughs lead to enhancements as random points. During the manufacturing phase, the nonconforming fractions are lesser when the process is in-control, enhancing the process goes out of control. The likelihood-Weibull distribution is utilized to design the control duration in the control charts design to predict the

Table 4: Failure rate measure.

0.13	0.45	0.93	1.15	1.25	1.62	1.94	2.39	4.52	5.10
6.80	7.65	8.43	11.91	11.95	13.02	13.26	14.33	17.48	18.11
18.67	19.25	24.40	25.02	26.42	26.81	27.76	26.69	29.85	31.66
32.65	35	40.71	42.35	43.06	43.40	44.35	45.42	48.14	49.20
49.45	52.18	58.63	60.30	72.23	72.22	72.26	72.30	86.25	89.53

Table 5: Advantages of various applications.

References	Advantages
Navid et al. [21]	Yield steel strength and fatigue of steel life
Rana et al. [22]	Fracture strength of glass
Shahbaz et al. [23]	Pitting pipe corrosion
Singh et al. [24]	Adhesive wearable in metals
Tahir et al. [25]	Carbon-fibre composite failure
Tomer et al. [26]	Coating failures
Yousof et al. [28]	Brittle material failure
Zografos et al. [29]	Composite material failure
Yuri et al. [30]	Concrete components

variations from in-to out-control. When the failure rate is identified, it is prone to earlier failure. For the product that exhibits a failure rate, burn-in is utilized to eliminate these failures and enhance the product reliability before the release for sale (see Table 5).

10. Likelihood Maximal Weibull Distribution and Other Applications

To perform statistical data analysis, computer software is needed. It can be extensively utilized in various other applications to examine various issues. There are enormous works that provide nominal outcomes to measure the distribution rate. Additionally, statistical software like SPSS, MiniTab, SAS, etc., is considered, and spreadsheet-like Excel evaluates the success and failure rate. The advantage of likelihood maximal Weibull distribution is its ability to solve the problem related to density evaluation. It performs maximization of likelihood function to predict the probability distribution and parameters of the finest observed data.

11. Conclusion

This research extensively analyses the maximal likelihood-Weibull distribution model for data generalization. The Weibull distribution is widely adopted for lifetime distribution evaluation in a reliable environment, and it is a versatile distribution that considers the characteristics of other distributions based on the provided scale and shape parameters. The parameter distribution and maximal likelihood estimator are considered to measure the variance Var (T). The uncertainty measure assists in statistical analysis with certain criteria. The maximal likelihood evaluator is measured with the PDF and CDF values. The proposed model can be used in various real-time applications where the analysis is done with dataset 1 and dataset 2. The standard errors from this dataset are explained with various metrics like p value. The weighted least square and failure data analysis is done with theoretical and empirical modelling, where the hypothesis for measuring the testing analysis is done with goodness measure. The model gives better outcomes than others, and some other distribution models will be examined in the future.

Data Availability

No data were used to support this study.

Conflicts of Interest

The authors declare that they have no conflicts of interest.

References

[1] M. Alizadeh, F. Bagheri, and M. Khaleghy Moghaddam, "Efficient estimation of the density and cumulative distribution function of the generalized Rayleigh distribution," *Journal of Statistical Research of Iran*, vol. 10, no. 1, pp. 1–22, 2013.

[2] H. K. Hsieh, "Estimating the critical time of the inverse Gaussian hazard rate," *IEEE Transactions on Reliability*, vol. 39, no. 3, pp. 342–345, 1990.

[3] I. Dattner and B. Reiser, "Estimation of distribution functions in measurement error models," *Journal of Statistical Planning and Inference*, vol. 143, no. 3, pp. 479–493, 2013.

[4] C. Durot, S. Huet, F. Koladjo, and S. Robin, "Least-squares estimation of a convex discrete distribution," *Computational Statistics & Data Analysis*, vol. 67, pp. 282–298, 2013.

[5] S. Kayal, S. Kumar, and P. Vellaisamy, "Estimating the Renyi entropy of several exponential populations," *Brazilian Journal of Probability and Statistics*, vol. 29, no. 1, pp. 94–111, 2015.

[6] H. Nagatsuka, T. Kamakura, and N. Balakrishnan, "A consistent method of estimation for the three-parameter Weibull distribution," *Computational Statistics & Data Analysis*, vol. 58, no. C, pp. 210–226, 2013.

[7] C. M. Hurvich, R. Shumway, and C. L. Tsai, "Improved estimators of kullback-leibler information for autoregressive model selection in small samples," *Biometrika*, vol. 77, no. 4, pp. 709–719, 1990.

[8] A. F. Ş. İ. N. Gungor, M. Gokcek, H. Uçar, E. Arabacı, and A. Akyüz, "Analysis of wind energy potential and Weibull parameter estimation methods: a case study from Turkey," *International journal of Environmental Science and Technology*, vol. 17, no. 2, pp. 1011–1020, 2020.

[9] M. A. ul Haq and M. Elgarhy, "The odd fr□chet-G family of probability distributions," *Journal of Statistics Applications & Probability*, vol. 7, no. 1, pp. 189–203, 2018.

[10] L. Bilir, M. İmir, Y. Devrim, and A. Albostan, "Seasonal and yearly wind speed distribution and wind power density analysis based on Weibull distribution function," *International Journal of Hydrogen Energy*, vol. 40, no. 44, pp. 15301–15310, 2015.

[11] S. E. Ahn, C. S. Park, and H. M. Kim, "Hazard rate estimation of a mixture model with censored lifetimes," *Stochastic*

Environmental Research and Risk Assessment, vol. 21, no. 6, pp. 711–716, 2007.

[12] F. S. Gomes-Silva, A. Percontini, E. d. BritoBrito, M. W. Ramos, R. Venâncio, and G. M. Cordeiro, "The odd Lindley-G family of distributions," *Austrian journal of statistics*, vol. 46, no. 1, pp. 65–87, 2017.

[13] S. Kazmi, M. Aslam, and S. Ali, "On the Bayesian estimation for two component mixture of Maxwell distribution, assuming type I censored data," *SOURCE International Journal of Applied Science & Technology*, vol. 2, no. 1, pp. 197–218, 2012.

[14] D. Hampel, "Estimation of differential entropy for positive random variables and its application in computational neuroscience," in *Mathematical Modeling of Biological Systems, Volume II*, pp. 213–224, Birkhäuser Boston, Boston, 2008.

[15] F. Aucoin, F. Ashkar, and L. Bayentin, "Parameter and quantile estimation of the 2-parameter kappa distribution by maximum likelihood," *Stochastic Environmental Research and Risk Assessment*, vol. 26, no. 8, pp. 1025–1039, 2012.

[16] M. Kumar, A. Pathak, and S. Soni, "Bayesian inference for Rayleigh distribution under step-stress partially accelerated test with progressive type-II censoring with binomial removal," *Annals of Data Science*, vol. 6, no. 1, pp. 117–152, 2019.

[17] F. Merovci and I. Elbatal, "Weibull Rayleigh distribution: Theory and applications," *Appl. Math. Inf. Sci*, vol. 9, no. 5, pp. 1–11, 2015.

[18] A. Muhammad, H. Laba, and C. Subrata, "The odd moment an exponential family of distributions: its properties and applications," *International Journal of Applied Mathematics & Statistics*, vol. 57, no. 6, pp. 47–62, 2018.

[19] H. A. Nadia and K. H. Lamyaa, "Weighted exponential-G family of probability distributions," *Saudi J Eng Technol*, vol. 3, no. 2, pp. 51–59, 2018.

[20] J. A. Guarienti, A. Kaufmann Almeida, A. Menegati Neto, J. P. de Oliveira Ferreira, and I. Ottonelli, "Performance analysis of numerical methods for determining Weibull distribution parameters applied to wind speed in Mato Grosso do Sul, Brazil," *Sustainable Energy Technologies and Assessments*, vol. 42, Article ID 100854, 2020.

[21] C. D. Lai, D. N. P. Murthy, and M. Xie, "Weibull distributions," *Wiley Interdisciplinary Reviews: Computational Statistics*, vol. 3, no. 3, pp. 282–287, 2011.

[22] P. A. Costa Rocha, R. C. de Sousa, C. F. de Andrade, and M. E. V. da Silva, "Comparison of seven numerical methods for determining Weibull parameters for wind energy generation in the northeast region of Brazil," *Applied Energy*, vol. 89, no. 1, pp. 395–400, 2012.

[23] M. Q. Shahbaz, S. Shahbaz, and N. S. Butt, "The kumaraswamy-inverse weibull distribution," *Pakistan Journal of Statistics and Operation Research*, vol. 8, no. 3, p. 479, 2012.

[24] M. H. Omar, S. Y. Arafat, M. P. Hossain, and M. Riaz, "Inverse maxwell distribution and statistical process control: an efficient approach for monitoring positively skewed process," *Symmetry*, vol. 13, no. 2, p. 189, 2021.

[25] C. Duval, "Density estimation for compound Poisson processes from discrete data," *Stochastic Processes and Their Applications*, vol. 123, no. 11, pp. 3963–3986, 2013.

[26] S. A. Akdağ and A. Dinler, "A new method to estimate Weibull parameters for wind energy applications," *Energy Conversion and Management*, vol. 50, no. 7, pp. 1761–1766, 2009.

[27] M. H. Tahir, G. M. Cordeiro, A. Alzaatreh, M. Mansoor, and M. Zubair, "The Logistic-X family of distributions and its applications," *Communications in Statistics - Theory and Methods*, vol. 45, no. 24, pp. 7326–7349, 2016.

[28] H. M. Yousof, A. Z. Afify, G. Hamedani, and G. Aryal, "The Burr X generator of distributions for lifetime data," *Journal of Statistical Theory and Applications*, vol. 16, no. 3, pp. 288–305, 2017.